ENANTIOSELECTIVE REACTIONS OF PALLADIUM ENOLATES AND PROGRESS TOWARD MITOMYCIN B

Thesis by

Christian Santiago Strong

In Partial Fulfillment of the Requirements for

the Degree of

Doctor of Philosophy

CALIFORNIA INSTITUTE OF TECHNOLOGY
Pasadena, California

2026
(Defended April 27, 2026)

© 2026

Christian Santiago Strong
ORCID: 0000-0003-1349-302X

to my family

ACKNOWLEDGEMENTS

As I near the completion of this document, my degree, and my time at Caltech I have become increasingly reflective on the myriad individuals who have had a positive influence on me throughout my training, education, and life. I am writing this section to thank many of these people who have been instrumental in enabling me to have such an enjoyable path to (and through) this program.

At the front of my mind as I compile this document, is (perhaps not surprisingly) my primary academic advisor, Professor Brian M. Stoltz. I feel incredibly fortunate that Brian allowed me to join his group, and the time I've spent within his group represent some of the most intellectually stimulating and fun years of my life. Brian suggested to us during our first-year orientation that the Ph.D. should represent the academic journey of a lifetime, and I think this is equally wise and useful advice that I've tried to live by during my time here. Brian's optimism and excitement about science, teaching, and mentorship is quite infectious and really helped keep me motivated during my studies. Above all, Brian is uncommonly kind and supportive which I think are qualities that lend to him being an excellent advisor and role model. Thank you so much Brian, you really are a rare sort.

Beyond my advisor, I have been fortunate to have an excellent committee made up of Profs. Greg Fu (who is my chair), Sarah Reisman, Linda Hsieh-Wilson, and Bill Goddard. I'd like to thank Greg for being an excellent committee chair who guided discussions during my annual meetings in a useful manner and provided a lot of meaningful feedback. I also appreciate that you've been willing to meet and chat outside of my annual meetings to provide more general advice and support. Given that the Stoltz and Reisman Groups host joint group meetings, many folks within our lab state how Sarah is really like a second

advisor to us, and I'd like to echo this notion. In addition to being a very attentive and helpful member of my committee, Sarah has also provided me with a lot of very useful scientific recommendations and career advice in less formal venues throughout my Ph.D. Linda has similarly been a great member of my committee, especially in terms of emphasizing the importance of communicating the value of a research direction to folks outside of a given subfield. Lastly, I'd like to thank Bill for serving on my committee and being an excellent collaborator throughout the years.

One thing that makes Caltech an excellent place to do research are the staff members who keep the institute running. I have benefitted verily from their hard work and am thankful to each of them. I'd like to thank Dr. Scott Virgil, who is the director of our catalysis center and mass spec facility, and has been an excellent resource on the third floor. Scott keeps many of the instruments we most rely upon running and is very generous with his time. Thank you, Scott, for being so friendly and helpful! I'd also like to thank Dr. David VanderVelde, Dr. Rajan Paranji, Dr. Mona Shahgholi, Dr. Jay Barbor, and Dr. Mike Takase for their expertise and maintenance of their respective instrumentation facilities over the years I've been here. Additionally, I'd like to thank Beth Marshall, Tomomi Kano, Alison Ross, Suri Pourmodheji, Allison Kinard, Joe Drew, Allen Lee, Greg Rolette, Armando Villasenor, Elyse Garlock, Rebecca Fox, Grace Liang-Franco, and Leslie Corado for all of their individual contributions to keeping Caltech running!

Beyond the lab I've had the unique opportunity to be a resident associate (RA) in one of the undergraduate residence halls (Bechtel) for the past four years. I was lucky to be hired by my current supervisor, Emily Sanger, who has become a mentor and role model for me in terms of how to interact with students that are struggling. I'd like to thank Emily for

being a very kind and accommodating boss who provided support to me when I've been in need and ensured that my academics could remain my top priority. Additionally, I'd like to thank some of my fellow RAs from Bechtel: Chris, Melissa, Yuping, Federico, Jose, Dominic, Cat, Jedi, and Jordan, for being such great team members and fun folks to work with! I also extend my thanks to other folks from housing including Vanessa, Felicia, Mahlet, Luciano, Steven, Julissa, and all the other members of the SFE team for being so welcoming and kind. Additionally, I'd like to thank all of the Bechtelians for being such a great group of kiddos! Being an RA has been one of the most fun experiences I've had while at Caltech and I am so fortunate to have participated!

Being a part of the Stoltz Group has also been very special to me. I'd like to thank all of the PhD students, postdocs, alumni, and visitors we've had while I've been here. Firstly, I'd like to thank my first mentors within the group, Kali Flesch and Alex "Cus" Cusumano. In addition to thanking you for letting me join y'all on the [4+2] project, I also wanted to say how much I appreciate all the work you did in onboarding me into the lab in general. Thank you each for also staying connected with me and continuing to give advice after you graduated! I look forward to our continued interactions. Next, I'd like to thank Ruby, who joined the [4+2] project at about the same time and who has gone on to be a close collaborator throughout the duration of my Ph.D. It has been so much fun working with you and I've learned a lot from you. Thanks for being a great team member and friend!

Another great mentor of mine from the Stoltz lab has been Kevin Gonzalez. I think one of the best decisions I've made while at Caltech has been to join Kevin's total synthesis project during the end of my 1st year. Not only has it been incredibly fun to work on our molecule together, but Kevin has been an excellent role model and mentor for me.

Additionally, Kevin has served as a sounding board and a thoughtful scientific critic throughout my Ph.D. which has positively influenced how I think about chemistry. Kevin has also been a great friend outside of lab and I am excited to stay in touch and see how his career develops over the coming years. Good luck as you continue your research at Stanford! I'd also like to thank other team members that have worked with us on our synthesis including Lulu Kwan, Michael Hamm, Prof. Nasri Nesnas, and Bryce Gaskins. Nasri was such a joy to have in the lab and a repository of useful and interesting information. It was so much fun to share a fume hood with you and I am so happy that you chose to return to the Stoltz group for your recent sabbatical. I am sure our paths will cross again (hopefully sooner than later)! I am so excited that Bryce is willing to carry the torch for our synthesis! Bryce is a very talented experimentalist and is incredibly hardworking. I can't wait to learn what he decides to pursue after finishing up at Caltech!

Adrian "little buster" de Almenara has been an excellent addition to the Stoltz lab and it has been a lot of fun getting to know him. I value Adrian's friendship and I also admire his strong work ethic and scientific rigor. I'd also like to thank Chloe Cerione for being an excellent former hood mate and friend! I've really enjoyed our wide-ranging conversations over the years, and I am excited to see what you'll be up to next. I'd also like to thank Cami Suarez and Kim Sharp for all of their help and assistance over the years. Y'all have been great fellow cohort members and it has been a lot of fun going through our Ph.D.'s at the same time. You've always seemed to have the answers regarding different requirements and deadlines and been a great support mechanism when we've been going through candidacy, props, and thesis writing which has helped me out a lot.

Another group within the Stoltz lab I'd like to recognize are some of the Denksport folks including Zack Sercel, Nick Hafeman, Tyler Fulton, Elliot Hicks, Samir Rezgui, Kevin Gonzalez, Ben Gross, and Hao Yu. Outside of my coursework, I found these informal sessions to be some of the most important learning experiences for me in graduate school. Each of you taught me a lot and I am very thankful for the sessions you each hosted. Samir was my "big sib" when I first came to Caltech, and he introduced me to the Stoltz group shortly after I arrived by inviting me to lunch. Thanks, Samir, for making me feel welcome, I really appreciate it. I'd also like to mention my rotation mentor, Jay Barbor, who taught me a lot during and following my rotation with him. Thank you to Ally Stanko, an excellent bay mate that taught me a method for column chromatography I still use today and for being such a fun person to be around.

I've been fortunate to work with many great visitors and undergraduates while in the Stoltz group. This includes Profs. Kyung-Ho Roh and Nasri Nesnas, who were each visiting on their sabbaticals. As someone who aspires to be an academic one day, it was very nice learning from your experiences and philosophies on mentorship. More recently, I've been able to work with Ilaria Di Stefano and Suhyun Ji who are visiting from the University of Bologna and Sogang University, respectively. It has been so much fun chatting and bouncing ideas together with y'all and I really value each of your approaches to science. I also mentored Sanzhar Bissenali and Daood Hashmi, two Caltech undergrads. Each of you are so uniquely talented and I am really grateful you decided to work with me. It is so exciting to see y'all become increasingly independent young scientists and I can't wait to hear from y'all going forward regarding what you decide to pursue next! I'd also like to thank the

visiting researcher Liam Hunt for being a great desk neighbor and for the many helpful discussions.

There are many other Stoltz lab members who I'd like to thank briefly. This includes some of the older students and postdocs including Stephen Sardini, Veronica Hubble, Alex Rand, Adam Zoll, Melissa Ramirez, Vaishnavi Nair, Melinda Chan, Alexia Kim, Tyler Casselman, Farbod Moghadam, and Adrian Samkian. I would also like to wish good luck to some of the younger folks such as Jonathan Farhi, Madison Patch, Sara Siddiqui, Eli Gonzalez, Sean Corman, and Weicheng Xu! It has been fun getting to know all of you and I wish you good luck! I've had other mentors outside of the Stoltz group while at Caltech who have also helped me out a lot. This includes Stanna Dorn, a talented postdoc in the Reisman group. Thank you for all of the conversations, advice, and edits on some of my fellowship applications; I really appreciate your perspective. Also, good luck with your independent career, I am so excited to see how the Dorn lab develops! I'd also like to thank Gino Occhialini, Sojung Kim, Hayden Carder, Mike Zott, and John Ovian who similarly helped me as I navigated applying for postdocs and fellowships.

A unique experience that I was able to participate in was the Manabiya international research exchange at Hokkaido University (Hokudai) at the Institute for Chemical Reaction Design and Discovery (ICReDD). Thank you, Brian, for being supportive of me participating in this program as it ended up being a really great opportunity. I would also like to thank my hosts: Prof. Hajime Ito and Prof. Koji Kubota as well as my mentor in the group, Keisuke Kondo. Hokudai is an excellent research environment and I was so happy to be a visitor in the Ito laboratory. Prof. Ito was a very generous host, and I also appreciate how attentive and friendly Prof. Kubota has been to me before, during, and after my exchange in Sapporo. It

was a lot of fun working with Keisuke and I was very impressed by his strong work ethic and scientific curiosity. I would also like to thank all the excellent staff members of ICReDD for being so helpful in organizing my stay. I would be remiss if I did not also thank Prof. Simon Cooper, who was previously a postdoc at Caltech in the Reisman group who also helped me prepare my application materials for this program. I strongly recommend this program to any graduate students interested!

Beyond Caltech, I'd also like to recognize all the other folks that have helped me along my path up to this point starting with those from the University of Texas at San Antonio (UTSA). I look back very fondly upon the years I spent at UTSA as an undergraduate. I was lucky to be a part of the Top Scholar program which connected me to a lot of great peers, faculty, and staff members at UTSA. Thank you, Kristi Meyer, for being such an excellent director of that program and helping me reach goals that I set. I'd also like to thank some of the older students in the program who served as positive role models such as Linda McNulty Perez, Cameron Nguyen, and Sara Dibrell! Also, I'd like to thank Andrew Chapman in the Honors College for his help with some of the applications I prepared for graduate school and several other programs. I would also like to thank members of the chemical engineering department at UTSA. When I joined UTSA, I was fortunate to be part of the first class of chemical engineers to graduate as this program was newly established. As such, I became close to many of my peers as well as the great faculty members! I'd like to thank Caleb Watson and Spencer Funkhouser, two good friends of mine who were fellow ChemE's at UTSA. I'd also like to thank Profs. Nehal Abu-Lail, Gary Jacobs, Abelardo Ramirez-Hernandez, and Gabriela Romero Uribe for being such excellent educators and mentors to

me. Even though I've ventured away from chemical engineering, I still carry many of the lessons y'all gave to me.

Although I studied chemical engineering at UTSA, it was Prof. Doug Frantz's organic chemistry course which helped me discover that I have a deep interest in synthetic chemistry. I am so grateful to Prof. Frantz for his continued mentorship and advice over the years and I am very lucky that I met him while at UTSA. I am also very grateful to the advice Sara Dibrell gave me during the end of my first year when she suggested that I enroll in Prof. Frantz's section of organic chemistry, in hindsight some of the most impactful advice I received as an undergraduate. I'd also like to thank Dr. Robynne Neff, the TA for this course who encouraged me to talk with Prof. Frantz about joining his research group. Working in Prof. Frantz's lab was a very fun and special experience for me and I continue to use daily the lessons I took from it. Thanks so much Prof. Frantz for all your help and advice. I look forward to the next time we are able to see each other in person. I'd also like to thank some of the folks I overlapped with in your group including Melissa Cadena, Nicholas Clanton, Eli Ortiz, Taylor Spiller, Roberto Villatoro, Charissa Munteanu, and Emerson Thomas. You really cultivate a great group of people in your group, and it was so fun to be a part of it. It has also been very exciting that Josh Belfield is now at Caltech in Prof. Reisman's lab! Briefly, I'd like to thank some other folks in chemistry at UTSA who helped me out along my path including Profs. Hector Aguilar, Michael Doyle, Zachary Tonzetich, and Hadi Arman. During the summer of 2019, I was able to participate in the MIT Summer Research Program (MSRP) as an intern in the lab of Prof. Timothy Jamison. My mentor, Katie McGeough, was very influential on my decision to go to graduate school in chemistry. She

was really an excellent mentor, and I lucked out working with her. I would also like to thank Tim for letting me work in his group and chat with him about my long-term interests.

Before I made the decision to attend UTSA as a chemical engineer, I went to high school at the Science Academy of South Texas in Mercedes, Texas. This relatively small public magnet school ended up being the ideal environment for me as a young student as I had some amazing teachers and mentors during this time. Thank you, Mary Pat Strong, for suggesting that I attend SciTech, and thanks Annie Strong for also helping me get home from school during those times. Some folks from SciTech that come to mind include Mr. and Mrs. Gamboa, Mr. Ramirez, Mr. Lal, Mr. Cortez, and Mrs. Rodriguez, Mr. Rodriguez, and Mrs. Houston. I would also like to thank my chemistry and biology teachers Mr. and Mrs. Overton in particular as they encouraged me to pursue a career in the sciences. I also want to thank my close friend, Abriella Corker, for all of the fun and conversations over the years. I was also lucky to participate in a summer internship program at my local university, the University of Texas, Rio Grande Valley where I joined the synthetic chemistry lab of Prof. Shizue Mito as a high schooler. I was mentored by Benjamin Garcia and Marian Anabila, two undergraduates in Prof. Mito's lab. This ended up being a really fun summer where I was introduced to some of the fundamentals of laboratory technique which have proven invaluable since. I really enjoyed the opportunity that Prof. Mito gave me, and it really helped plant the seed regarding my interest in organic chemistry. Thank you Prof. Mito and I am glad that we have stayed in touch over these years.

Lastly, I'd like to thank my family for their support throughout my life. This includes my maternal and paternal grandparents: Altagracia "Coca" Iluminada Rodriguez Tejada and Jose Angel Fernandez as well as Patricia Marion and Charles Richard Strong. It also includes

all their children such as my parents, aunts, and uncles. My parents, Isabel Altagracia and John David Strong deserve special recognition for being wonderful and encouraging me to pursue my interests. I am so happy to know each of you and I cherish our conversations. I'd also like to recognize my three brothers, Charles, Tommy, and Jacobo for each individually teaching me many useful lessons and serving as great role models. Each step of the way they have been there for me and I really appreciate their unconditional help. Additionally, I have been happy to get to know my three sisters-in-law, Pratista, Elin, and Yamilet who have made substantial and positive contributions to our family and are excellent parents to my nieces (Maya, Soliel, and Romy) and my nephew (Mateo). I love you all very much and couldn't imagine a better family. Thank you for always providing helpful advice and assistance whenever I've been in need. I'd like to end by saying that a common theme I've noticed throughout my life is that I've been surrounded by kind and talented people who have time and again helped me with incredible patience and care. Thank you all.

ABSTRACT

Research within the Stoltz group encompasses the total synthesis of natural products and the development of useful enantioselective transformations. This thesis overlaps with these domains in that it describes: 1) the development of several stereoselective reactions of Pd enolates and 2) progress toward the total synthesis of mitomycin B. Specifically, Chapter 1 provides historical context for the development of enantioselective reactions of Pd enolates beyond allylic alkylation within our group. Chapter 2 details the development of an enantioselective [4+2] cycloaddition of Pd enolates generated from prenyl β-ketoesters. Additionally, it describes experimental and computational mechanistic investigations related to the origins of stereoselectivity and the mechanism of catalyst turnover in this transformation. Chapter 3 discloses an enantioselective Michael spirocyclization reaction of Pd enolates as well as a stereoselective intramolecular enone difunctionalization. This method leverages lessons learned from the [4+2] cycloaddition and enables access to a diverse library of stereochemically rich polycycles. Chapter 4 presents our ongoing progress toward the total synthesis of mitomycin B via an isomitomycin approach. Our current strategy involves a key intramolecular nitrile oxide cycloaddition that rapidly constructs a complex framework en route to mitomycin B.

PUBLISHED CONTENT AND CONTRIBUTIONS

1. Flesch, K. N.‡; Cusumano, A. Q.‡; Chen, P.-J.; Strong, C. S.; Sardini, S. R.; Du, Y. E.; Bartberger, M. D.; Goddard, W. A. III; Stoltz, B. M. Divergent Catalysis: Catalytic Asymmetric [4+2] Cycloaddition of Palladium Enolates. *J. Am. Chem. Soc.* **2023**, *145*, 11301–11310. DOI: 10.1021/jacs.3c02104

   C.S.S. carried out experimental work, data analysis, and manuscript preparation.

2. Chen, P.-J.‡; Cusumano, A. Q.‡; Flesch, K. N.; Strong, C. S.; Goddard, W. A. III; Stoltz, B. M. Molecular Dynamics Investigations of Dienolate [4+2] Reactions. *J. Am. Chem. Soc.* **2024**, *146*, 12758–12765. DOI: 10.1021/jacs.4c02681

   C.S.S. participated in manuscript preparation.

3. Strong, C. S.; Chen, P.-J.; Bissenali, S.; Goddard, W. A. III; Stoltz, B. M. Enantioselective Michael Spirocyclization of Palladium Enolates. *ACS. Catal.* **2025**, *15*, 12231–12237. DOI: 10.1021/acscatal.5c02758

   C.S.S. carried out reaction optimization, experimental work, data analysis, and manuscript preparation.

TABLE OF CONTENTS

Dedication iii
Acknowledgements iv
Abstract xiv
Published Content and Contributions xv
Table of Contents xvi
List of Figures xx
List of Tables xlviii
List of Abbreviations lii

CHAPTER 1 **1**
Development of Asymmetric Reactions of Palladium Enolates Beyond Allylic Alkylation

1.1 Introduction 1
1.2 Development of Asymmetric Reactions of Palladium Enolates 7
1.2.1 Asymmetric Protonation of Palladium Enolates 8
1.2.2 Asymmetric Difunctionalization of Alkenes Using Palladium Enolate 10
1.2.3 Asymmetric Aldol Cyclization of Palladium Enolates 12
1.2.4 Complete Catalytic Cycle 35
1.3 Conclusions and Outlook 15
1.6 References and Notes 17

CHAPTER 2 **23**
Asymmetric [4+2] Cycloaddition of Pd Enolates

2.1 Introduction 23
2.2 Results and Discussion 25
2.2.1 Reaction Design and Optimization 25
2.2.2 Proposed Mechanism 30
2.2.3 Substrate Scope 31
2.2.4 [4+2] Cycloaddition 36
2.2.5 Catalyst Turnover 38
2.2.6 Additional Developments 39
2.2.7 Product Derivatization 41
2.3 Conclusions 43
2.4 Experimental Section 43
2.4.1 Materials and Methods 43
2.4.2 Experimental Procedures and Spectroscopic Data 45
2.4.3 Determination of Absolute Stereochemistry by VCD Spectroscopy . 147
2.4.4 2D NMR Analysis of Select Compounds 171
2.4.5 General Computational Details 177
2.5 References and Notes 186

APPENDIX 1 **198**
Spectra Relevant to Chapter 2

CHAPTER 3 **430**
Asymmetric Michael Spirocyclization of Pd Enolates

3.1 Introduction 430

3.2 Results and Discussion 432
3.3 Conclusions 441
3.4 Experimental Section 441
3.4.1 Materials and Methods 442
3.4.2 Experimental Procedures and Spectroscopic Data 444
3.4.3 Quantum Mechanics Calculations 501
3.4.4 2D NMR Analysis of Select Compounds 510
3.4.5 Preliminary Experimental Mechanistic Investigations 516
3.5 References and Notes 521

APPENDIX 2 **536**
Spectra Relevant to Chapter 3

APPENDIX 3 **649**
X-Ray Crystallography Reports Relevant to Chapter 3

CHAPTER 4 **704**
Progress Toward Mitomycin B

4.1 Introduction 704
4.2 Retrosynthetic Analysis 710
4.3 Results and Discussion 711
4.3.1 Synthesis of the Arene and Epoxide Fragments 711
4.3.2 Selective Aniline Alkylation and Aziridine Formation 714
4.3.3 Intramolecular Nitrile Oxide Cycloaddition 715
4.3.4 Investigations of Isoxazoline N–O Bond Cleavage 716
4.4 Conclusions and Future Directions 722
4.5 Experimental Section 723
4.5.1 Materials and Methods 723
4.5.2 Experimental Procedures and Spectroscopic Data 725

4.6 References and Notes 754

APPENDIX 4 **760**
Spectra Relevant to Chapter 4

APPENDIX 5 **806**
X-Ray Crystallography Reports Relevant to Chapter 4

APPENDIX 6 **836**
Notebook Cross-Reference for New Compounds

ABOUT THE AUTHOR **841**

LIST OF FIGURES

CHAPTER 1

Development of Asymmetric Reactions of Palladium Enolates Beyond Allylic Alkylation

Figure 1.1 The Wacker Process summarized and the Development of Pd-mediated C–C bond formation 3

Figure 1.2 Decarboxylative allylic alkylation of β-ketoesters and related reactions. 5

Figure 1.3 Joint experimental and computational mechanistic picture of allylic alkylation 6

Figure 1.4 Enantioselective protonation of Pd-enolates 8

Figure 1.5 Enantioselective difunctionalization of alkenes using Pd-enolates 11

Figure 1.6 Enantioselective aldol spirocyclization 13

Figure 1.7 Enantioselective isocyanate spirocyclization of Pd-enolates 15

CHAPTER 2

Asymmetric [4+2] Cycloaddition of Pd Enolates

Figure 2.1 Asymmetric reactivity of Pd-enolates and this reasearch..... 24

Figure 2.2 Desired cycloaddition reactivity of Pd enolates and Modifying allyl group to influence reductive elimination 26

Figure 2.3 Alternative catalyst turnover strategies 27

Figure 2.4 Proposed catalytic cycle with undesired pathways in gray. 30

Figure 2.5 Eyring analysis of product ratios (115/123) for propylene and butylene tethered substrates 34

Figure 2.6 Thermodynamics of C–C bond formation and Origins of enantioenduction. 36

Figure 2.7 Two low energy pathways for catalyst turnover. 39

Figure 2.8 Leveraging KIE to slow proton transfer and Modification of prenyl ester. 40

Figure 2.9 Derivatization of [4+2] cycloaddition products 42

Figure 2.10 Three diastereomers **115a**, **115q**, and **115q'**to be compared to spectra computed from all eight possible stereoisomers. 149

Figure 2.11 Comparison of experimental VCD and IR spectra for product **115a** to computed spectra for A endo-trans.[a] 150

Figure 2.12 Overlayed experimental and calculated VCD spectra for **115a** – assigned as **ent-A_endo-trans**. 150

Figure 2.13 Comparison of experimental VCD and IR spectra for product **115a** to computed spectra for **A_exo-trans**.[a] 151

Figure 2.14 Comparison of experimental VCD and IR spectra for product **115a** to computed spectra for **A_endo-cis**.[a] 152

Figure 2.15 Comparison of experimental VCD and IR spectra for product **115a** to computed spectra for **A_exo-cis**.[a] 153

Figure 2.16 Comparison of experimental VCD and IR spectra for product **115q** to computed spectra for **A_endo-trans**.[a] 154

Figure 2.17 Comparison of experimental VCD and IR spectra for product **115q** to computed spectra for **A_exo-trans**.[a] 155

Figure 2.18 Comparison of experimental VCD and IR spectra for product **115q** to computed spectra for **A_endo-cis**.[a] 156

Figure 2.19 Overlayed experimental and calculated VCD spectra for **115q** – assigned as **ent-A_endo-cis**. 156

Figure 2.20 Comparison of experimental VCD and IR spectra for product **115q** to computed spectra for **A_exo-cis**.[a] 157

Figure 2.21 Comparison of experimental VCD and IR spectra for product **115q'** to computed spectra for **A_endo-trans**.[a] 158

Figure 2.22 Comparison of experimental VCD and IR spectra for product **115q'** to computed spectra for **A_exo-trans**.[a] 159

Figure 2.23 Comparison of experimental VCD and IR spectra for product **115q'** to computed spectra for **A_endo-cis**.[a] 160

Figure 2.24 Comparison of experimental VCD and IR spectra for product **115q'** to computed spectra for **A_exo-cis**.[a] 161

Figure 2.25 Overlayed experimental and calculated VCD spectra for **115q'** – assigned as **ent-A_exo-cis**. 161

Figure 2.26 Three diastereomers **115k**, **115k'**, and **115k''** to be compared to spectra computed from all eight possible stereoisomers. 162

Figure 2.27 Experimental VCD and IR spectra for product **115k** compared to computed spectra for **B_endo-trans**.[a] 162

Figure 2.28 Overlayed experimental and calculated VCD spectra for **115k** – assigned as **B_endo-trans**. 163

Figure 2.29 Experimental VCD and IR spectra for product **115k** compared to computed spectra for **B_exo-trans**.[a] 163

Figure 2.30 Experimental VCD and IR spectra for product **115k** compared to computed spectra for **B_endo-cis**.[a] 164

Figure 2.31 Experimental VCD and IR spectra for product **115k** compared to computed spectra for **B_exo-cis**.[a] 165

Figure 2.32 Experimental IR spectrum for product **115k'** compared to computed spectra for **B_endo-trans** (top left), **B_exo-trans** (top right), **B_endo-cis** (bottom left), **B_exo-cis** (bottom right).[a] 166

Figure 2.33 Experimental VCD and IR spectra for product **115k''** compared to computed spectra for **B_endo-trans**.[a] 167

Figure 2.34 Experimental VCD and IR spectra for product **115k''** compared to computed spectra for **B_exo-trans**.[a] 168

Figure 2.35 Experimental VCD and IR spectra for product **115k''** compared to computed spectra for **B_endo-cis**.[a] 169

Figure 2.36 Overlayed experimental and calculated VCD spectra for **115k''** – assigned as **B_endo-cis**. 169

Figure 2.37 Experimental VCD and IR spectra for product **115k''** compared to computed spectra for **B_exo-cis**.[a] 170

Figure 2.38 ^{1}H-^{1}H COSY NMR spectrum of **115a** (400 MHz, $CDCl_3$)..... 171

Figure 2.39 ^{1}H-^{13}C HSQC NMR spectrum of **115a** (400 MHz, $CDCl_3$). 172

Figure 2.40 ^{1}H-^{1}H NOESY NMR spectrum of **115a** (400 MHz, $CDCl_3$). 172

Figure 2.41 ^{1}H-^{1}H COSY NMR spectrum of **115p** (400 MHz, $CDCl_3$). 173

Figure 2.42 ^{1}H-^{13}C HSQC NMR spectrum of **115p** (400 MHz, $CDCl_3$). 173

Figure 2.43 ^{1}H-^{1}H NOESY NMR spectrum of **115p** (400 MHz, $CDCl_3$). 174

Figure 2.44 ^{1}H-^{1}H COSY NMR spectrum of **115q** (400 MHz, $CDCl_3$). 174

Figure 2.45 ^{1}H-^{13}C HSQC NMR spectrum of **115q** (400 MHz, $CDCl_3$). 175

Figure 2.46 ^{1}H-^{1}H NOESY NMR spectrum of **115q** (400 MHz, $CDCl_3$). 175

Figure 2.47 ^{1}H-^{1}H COSY NMR spectrum of **115q'** (400 MHz, $CDCl_3$). 176

Figure 2.48 ^{1}H-^{13}C HSQC NMR spectrum of **115q'** (400 MHz, $CDCl_3$). 176

Figure 2.49 ^{1}H-^{1}H NOESY NMR spectrum of **115q'** (400 MHz, $CDCl_3$). 177

Figure 2.50 Relative free energies for various inner-sphere reductive elimination transition states from allyl (**189**), cinnamyl (**190**), and prenyl (**191**) complexes.[a] 181

Figure 2.51 Relative free energies for various proton transfer transition states from post-cycloaddition enolate **130**.[a] 182

Figure 2.52 Relative free energies for various proton transfer transition states from pre-cycloaddition enolate **129**.[a] 183

Figure 2.53 IBO analysis of N-detached inner-sphere mechanism and corresponding derived arrow-pushing mechanism..... 184

Figure 2.54 Computed pKa values of cationic π-allyl Pd complex **192** and ketones **123a** and **115a**. 185

Figure 2.55 Comparison of internal versus external dienophile approach to both enantiotopic diene faces. 186

APPENDIX 1

Spectra Relevant to Chapter 2

Figure A1.1. ^{1}H NMR (400 MHz, $CDCl_3$) of compound **115a**. 199

Figure A1.2. Infrared spectrum (Thin Film, NaCl) of compound **115a** 200

Figure A1.3. ^{13}C NMR (100 MHz, $CDCl_3$) of compound **115a**..... 200

Figure A1.4. ^{1}H NMR (400 MHz, $CDCl_3$) of compound **115b** 201

Figure A1.5. Infrared spectrum (Thin Film, NaCl) of compound **115b**. 202

Figure A1.6. ^{13}C NMR (100 MHz, $CDCl_3$) of compound **115b** 202

Figure A1.7. ^{1}H NMR (400 MHz, $CDCl_3$) of compound **115c**. 203

Figure A1.8. Infrared spectrum (Thin Film, NaCl) of compound **115c**. 204

Figure A1.9. ^{13}C NMR (100 MHz, $CDCl_3$) of compound **115c**..... 204

Figure A1.10. ^{1}H NMR (400 MHz, $CDCl_3$) of compound **115d** 205

Figure A1.11. Infrared spectrum (Thin Film, NaCl) of compound **115d**. 206

Figure A1.12. ^{13}C NMR (100 MHz, $CDCl_3$) of compound **115d**. 206

Figure A1.13. ^{1}H NMR (400 MHz, $CDCl_3$) of compound **115f**. 207

Figure A1.14. Infrared spectrum (Thin Film, NaCl) of compound **115f**. 208

Figure A1.15. ^{13}C NMR (100 MHz, $CDCl_3$) of compound **115f**. 208

Figure A1.16. ^{1}H NMR (400 MHz, $CDCl_3$) of compound **115j**. 209

Figure A1.17. Infrared spectrum (Thin Film, NaCl) of compound **115j**. 210

Figure A1.18. ^{13}C NMR (100 MHz, $CDCl_3$) of compound **115j**. 210

Figure A1.19. ^{1}H NMR (400 MHz, $CDCl_3$) of compound **115k**. 211

Figure A1.20. Infrared spectrum (Thin Film, NaCl) of compound **115k**. 212

Figure A1.21. ^{13}C NMR (100 MHz, $CDCl_3$) of compound **115k**..... 212
Figure A1.22. ^{1}H NMR (400 MHz, $CDCl_3$) of compound **115k**. 213
Figure A1.23. Infrared spectrum ($CDCl_3$ solution) of compound **115k'**..... 214
Figure A1.24. ^{13}C NMR (100 MHz, $CDCl_3$) of compound **115k'**..... 214
Figure A1.25. ^{1}H NMR (400 MHz, $CDCl_3$) of compound **115k**. 215
Figure A1.26. Infrared spectrum ($CDCl_3$ solution) of compound **115k''**..... 216
Figure A1.27. ^{13}C NMR (100 MHz, $CDCl_3$) of compound **115k''**..... 216
Figure A1.28. ^{1}H NMR (400 MHz, $CDCl_3$) of compound **115l**. 217
Figure A1.29. Infrared spectrum (Thin Film, NaCl) of compound **115l**..... 218
Figure A1.30. ^{13}C NMR (100 MHz, $CDCl_3$) of compound **115l**. 218
Figure A1.31. ^{1}H NMR (400 MHz, $CDCl_3$) of compound **115m**. 219
Figure A1.32. Infrared spectrum (Thin Film, NaCl) of compound **115m**..... 220
Figure A1.33. ^{13}C NMR (100 MHz, $CDCl_3$) of compound **115m**. 220
Figure A1.34. ^{1}H NMR (400 MHz, $CDCl_3$) of compound **115m**. 221
Figure A1.35. Infrared spectrum (Thin Film, NaCl) of compound **115m'**..... 222
Figure A1.36. ^{13}C NMR (100 MHz, $CDCl_3$) of compound **115m'**. 222
Figure A1.37. ^{1}H NMR (400 MHz, $CDCl_3$) of compound **115n**. 223
Figure A1.38. Infrared spectrum (Thin Film, NaCl) of compound **115n**..... 224
Figure A1.39. ^{13}C NMR (100 MHz, $CDCl_3$) of compound **115n**. 224
Figure A1.40. ^{1}H NMR (400 MHz, $CDCl_3$) of compound **115o**. 225
Figure A1.41. Infrared spectrum (Thin Film, NaCl) of compound **115o**..... 226
Figure A1.42. ^{13}C NMR (100 MHz, $CDCl_3$) of compound **115o**. 226
Figure A1.43. ^{1}H NMR (400 MHz, $CDCl_3$) of compound **115o**. 227
Figure A1.44. Infrared spectrum (Thin Film, NaCl) of compound **115o'**..... 228
Figure A1.45. ^{13}C NMR (100 MHz, $CDCl_3$) of compound **115o'**. 228
Figure A1.46. ^{1}H NMR (400 MHz, $CDCl_3$) of compound **115p**. 229
Figure A1.47. Infrared spectrum (Thin Film, NaCl) of compound **115p**..... 230
Figure A1.48. ^{13}C NMR (100 MHz, $CDCl_3$) of compound **115p**. 230

Figure A1.49. ^{1}H NMR (400 MHz, $CDCl_3$) of compound **115p**. 231
Figure A1.50. Infrared spectrum (Thin Film, NaCl) of compound **115p'**. 232
Figure A1.51. ^{13}C NMR (100 MHz, $CDCl_3$) of compound **115p'**. 232
Figure A1.52. ^{1}H NMR (400 MHz, $CDCl_3$) of compound **115q**. 233
Figure A1.53. Infrared spectrum (Thin Film, NaCl) of compound **115q**..... 234
Figure A1.54. ^{13}C NMR (100 MHz, $CDCl_3$) of compound **115q**. 234
Figure A1.55. ^{1}H NMR (400 MHz, $CDCl_3$) of compound **115q**. 235
Figure A1.56. Infrared spectrum (Thin Film, NaCl) of compound **115q'**. 236
Figure A1.57. ^{13}C NMR (100 MHz, $CDCl_3$) of compound **115q'**. 236
Figure A1.58. ^{1}H NMR (400 MHz, $CDCl_3$) of compound **115r**. 237
Figure A1.59. Infrared spectrum (Thin Film, NaCl) of compound **115r**. 238
Figure A1.60. ^{13}C NMR (100 MHz, $CDCl_3$) of compound **115r**. 238
Figure A1.61. ^{1}H NMR (400 MHz, $CDCl_3$) of compound **115s**. 239
Figure A1.62. Infrared spectrum (Thin Film, NaCl) of compound **115s**. 240
Figure A1.63. ^{13}C NMR (100 MHz, $CDCl_3$) of compound **115s**. 240
Figure A1.64. ^{1}H NMR (400 MHz, $CDCl_3$) of compound **115t**. 241
Figure A1.65. Infrared spectrum (Thin Film, NaCl) of compound **115t**. 242
Figure A1.66. ^{13}C NMR (100 MHz, $CDCl_3$) of compound **115t**. 242
Figure A1.67. ^{1}H NMR (400 MHz, $CDCl_3$) of compound **115t**. 243
Figure A1.68. Infrared spectrum (Thin Film, NaCl) of compound **115t'**. 244
Figure A1.69. ^{13}C NMR (100 MHz, $CDCl_3$) of compound **115t'**. 244
Figure A1.70. ^{1}H NMR (400 MHz, $CDCl_3$) of compound **115u**. 245
Figure A1.71. Infrared spectrum (Thin Film, NaCl) of compound **115u**. 246
Figure A1.72. ^{13}C NMR (100 MHz, $CDCl_3$) of compound **115u**. 246
Figure A1.73. ^{1}H NMR (400 MHz, $CDCl_3$) of compound **D-115f**. 247
Figure A1.74. Infrared spectrum (Thin Film, NaCl) of compound **D-115f**. 248
Figure A1.75. ^{13}C NMR (100 MHz, $CDCl_3$) of compound **D-115f**. 248
Figure A1.76. ^{2}H NMR (61 MHz, $CDCl_3$) of compound **D-115f**. 249

Figure A1.77. ^{1}H NMR (400 MHz, $CDCl_3$) of compound **118**. 250
Figure A1.78. Infrared spectrum (Thin Film, NaCl) of compound **118**. 251
Figure A1.79. ^{13}C NMR (100 MHz, $CDCl_3$) of compound **118**. 251
Figure A1.80. ^{1}H NMR (400 MHz, $CDCl_3$) of compound **114a**. 252
Figure A1.81. Infrared spectrum (Thin Film, NaCl) of compound **114a**. 253
Figure A1.82. ^{13}C NMR (100 MHz, $CDCl_3$) of compound **114a**..... 253
Figure A1.83. ^{1}H NMR (400 MHz, $CDCl_3$) of compound **114b**. 254
Figure A1.84. Infrared spectrum (Thin Film, NaCl) of compound **114b**. 255
Figure A1.85. ^{13}C NMR (100 MHz, $CDCl_3$) of compound **114b**. 255
Figure A1.86. ^{1}H NMR (400 MHz, $CDCl_3$) of compound **114c**. 256
Figure A1.87. Infrared spectrum (Thin Film, NaCl) of compound **114c**. 257
Figure A1.88. ^{13}C NMR (100 MHz, $CDCl_3$) of compound **114c**..... 257
Figure A1.89. ^{1}H NMR (400 MHz, $CDCl_3$) of compound **114d**. 258
Figure A1.90. Infrared spectrum (Thin Film, NaCl) of compound **114d**. 259
Figure A1.91. ^{13}C NMR (100 MHz, $CDCl_3$) of compound **114d**. 259
Figure A1.92. ^{1}H NMR (400 MHz, $CDCl_3$) of compound **114e**. 260
Figure A1.93. Infrared spectrum (Thin Film, NaCl) of compound **114e**. 261
Figure A1.94. ^{13}C NMR (100 MHz, $CDCl_3$) of compound **114e**..... 261
Figure A1.95. ^{1}H NMR (400 MHz, $CDCl_3$) of compound **114f**..... 262
Figure A1.96. Infrared spectrum (Thin Film, NaCl) of compound **114f**..... 263
Figure A1.97. ^{13}C NMR (100 MHz, $CDCl_3$) of compound **114f**. 263
Figure A1.98. ^{1}H NMR (400 MHz, $CDCl_3$) of compound **D-114f**. 264
Figure A1.99. Infrared spectrum (Thin Film, NaCl) of compound **D-114f**..... 265
Figure A1.100. ^{13}C NMR (100 MHz, $CDCl_3$) of compound **D-114f**. 265
Figure A1.101. ^{2}H NMR (61 MHz, $CDCl_3$) of compound **D-114f**. 266
Figure A1.102. ^{1}H NMR (400 MHz, $CDCl_3$) of compound **114g**. 267
Figure A1.103. Infrared spectrum (Thin Film, NaCl) of compound **114g**. 268
Figure A1.104. ^{13}C NMR (100 MHz, $CDCl_3$) of compound **114g**..... 268

Figure A1.105. ^{1}H NMR (400 MHz, $CDCl_3$) of compound **114h**. 269
Figure A1.106. Infrared spectrum (Thin Film, NaCl) of compound **114h**. 270
Figure A1.107. ^{13}C NMR (100 MHz, $CDCl_3$) of compound **114h**. 270
Figure A1.108. ^{1}H NMR (400 MHz, $CDCl_3$) of compound **114i** 271
Figure A1.109. Infrared spectrum (Thin Film, NaCl) of compound **114i**. 272
Figure A1.110. ^{13}C NMR (100 MHz, $CDCl_3$) of compound **114i**. 272
Figure A1.111. ^{1}H NMR (400 MHz, $CDCl_3$) of compound **114j**. 273
Figure A1.112. Infrared spectrum (Thin Film, NaCl) of compound **114j**. 274
Figure A1.113. ^{13}C NMR (100 MHz, $CDCl_3$) of compound **114j**. 274
Figure A1.114. ^{1}H NMR (400 MHz, $CDCl_3$) of compound **114k**. 275
Figure A1.115. Infrared spectrum (Thin Film, NaCl) of compound **114k**. 276
Figure A1.116. ^{13}C NMR (100 MHz, $CDCl_3$) of compound **114k**..... 276
Figure A1.117. ^{1}H NMR (400 MHz, $CDCl_3$) of compound **114l**. 277
Figure A1.118. Infrared spectrum (Thin Film, NaCl) of compound **114l**. 278
Figure A1.119. ^{13}C NMR (100 MHz, $CDCl_3$) of compound **114l** 278
Figure A1.120. ^{1}H NMR (400 MHz, $CDCl_3$) of compound **114m**. 279
Figure A1.121. Infrared spectrum (Thin Film, NaCl) of compound **114m**. 280
Figure A1.122. ^{13}C NMR (100 MHz, $CDCl_3$) of compound **114m**. 280
Figure A1.123. ^{1}H NMR (400 MHz, $CDCl_3$) of compound **114n**. 281
Figure A1.124. Infrared spectrum (Thin Film, NaCl) of compound **114n**. 282
Figure A1.125. ^{13}C NMR (100 MHz, $CDCl_3$) of compound **114n**. 282
Figure A1.126. ^{1}H NMR (400 MHz, $CDCl_3$) of compound **114o**. 283
Figure A1.127. Infrared spectrum (Thin Film, NaCl) of compound **114o**. 284
Figure A1.128. ^{13}C NMR (100 MHz, $CDCl_3$) of compound **114o**. 284
Figure A1.129. ^{1}H NMR (400 MHz, $CDCl_3$) of compound **173**. 285
Figure A1.130. Infrared spectrum (Thin Film, NaCl) of compound **173**. 286
Figure A1.131. ^{13}C NMR (100 MHz, $CDCl_3$) of compound **173**. 286
Figure A1.132. ^{1}H NMR (400 MHz, $CDCl_3$) of compound **114p**. 287

Figure A1.133. Infrared spectrum (Thin Film, NaCl) of compound **114p**. 288
Figure A1.134. ^{13}C NMR (100 MHz, $CDCl_3$) of compound **114p**. 288
Figure A1.135. ^{1}H NMR (400 MHz, $CDCl_3$) of compound **114q**. 289
Figure A1.136. Infrared spectrum (Thin Film, NaCl) of compound **114q**. 290
Figure A1.137. ^{13}C NMR (100 MHz, $CDCl_3$) of compound **114q**. 290
Figure A1.138. ^{1}H NMR (400 MHz, $CDCl_3$) of compound **114r**. 291
Figure A1.139. Infrared spectrum (Thin Film, NaCl) of compound **114r**. 292
Figure A1.140. ^{13}C NMR (100 MHz, $CDCl_3$) of compound **114r**. 292
Figure A1.141. ^{1}H NMR (400 MHz, $CDCl_3$) of compound **114s**. 293
Figure A1.142. Infrared spectrum (Thin Film, NaCl) of compound **114s**. 294
Figure A1.143. ^{13}C NMR (100 MHz, $CDCl_3$) of compound **114s**. 294
Figure A1.144. ^{1}H NMR (400 MHz, $CDCl_3$) of compound **114t**. 295
Figure A1.145. Infrared spectrum (Thin Film, NaCl) of compound **114t**. 296
Figure A1.146. ^{13}C NMR (100 MHz, $CDCl_3$) of compound **114t** 296
Figure A1.147. ^{1}H NMR (400 MHz, $CDCl_3$) of compound **114u**. 297
Figure A1.148. Infrared spectrum (Thin Film, NaCl) of compound **114u**. 298
Figure A1.149. ^{13}C NMR (100 MHz, $CDCl_3$) of compound **114u**. 298
Figure A1.150. ^{1}H NMR (400 MHz, $CDCl_3$) of compound **116**. 299
Figure A1.151. Infrared spectrum (Thin Film, NaCl) of compound **116**. 300
Figure A1.152. ^{13}C NMR (100 MHz, $CDCl_3$) of compound **116**. 300
Figure A1.153. ^{1}H NMR (400 MHz, $CDCl_3$) of compound **121**. 301
Figure A1.154. Infrared spectrum (Thin Film, NaCl) of compound **121**. 302
Figure A1.155. ^{13}C NMR (100 MHz, $CDCl_3$) of compound **121**. 302
Figure A1.156. ^{1}H NMR (400 MHz, $CDCl_3$) of compound **137** 303
Figure A1.157. Infrared spectrum (Thin Film, NaCl) of compound **137**. 304
Figure A1.158. ^{13}C NMR (100 MHz, $CDCl_3$) of compound **137**. 304
Figure A1.159. ^{1}H NMR (400 MHz, $CDCl_3$) of compound **138**. 305
Figure A1.160. Infrared spectrum (Thin Film, NaCl) of compound **138**. 306

Figure A1.161. ^{13}C NMR (100 MHz, $CDCl_3$) of compound **138**. 306
Figure A1.162. ^{1}H NMR (400 MHz, $CDCl_3$) of compound **139** 307
Figure A1.163. Infrared spectrum (Thin Film, NaCl) of compound **139**. 308
Figure A1.164. ^{13}C NMR (100 MHz, $CDCl_3$) of compound **139**. 308
Figure A1.165. ^{1}H NMR (400 MHz, $CDCl_3$) of compound **140**. 309
Figure A1.166. Infrared spectrum (Thin Film, NaCl) of compound **140** 310
Figure A1.167. ^{13}C NMR (100 MHz, $CDCl_3$) of compound **140**. 310
Figure A1.168. ^{1}H NMR (400 MHz, $CDCl_3$) of compound **141**. 311
Figure A1.169. Infrared spectrum (Thin Film, NaCl) of compound **141**. 312
Figure A1.170. ^{13}C NMR (100 MHz, $CDCl_3$) of compound **141**. 312
Figure A1.171. ^{1}H NMR (400 MHz, $CDCl_3$) of compound **175**. 313
Figure A1.172. Infrared spectrum (Thin Film, NaCl) of compound **175**. 314
Figure A1.173. ^{13}C NMR (100 MHz, $CDCl_3$) of compound **175**. 314
Figure A1.174. ^{1}H NMR (400 MHz, $CDCl_3$) of compound **176**. 315
Figure A1.175. Infrared spectrum (Thin Film, NaCl) of compound **176**. 316
Figure A1.176. ^{13}C NMR (100 MHz, $CDCl_3$) of compound **176**. 316
Figure A1.177. ^{1}H NMR (400 MHz, $CDCl_3$) of compound **159**. 317
Figure A1.178. Infrared spectrum (Thin Film, NaCl) of compound **159**. 318
Figure A1.179. ^{13}C NMR (100 MHz, $CDCl_3$) of compound **159**. 318
Figure A1.180. ^{1}H NMR (400 MHz, $CDCl_3$) of compound **160**. 319
Figure A1.181. Infrared spectrum (Thin Film, NaCl) of compound **160**. 320
Figure A1.182. ^{13}C NMR (100 MHz, $CDCl_3$) of compound **160**. 320
Figure A1.183. ^{1}H NMR (400 MHz, $CDCl_3$) of compound **D-160**. 321
Figure A1.184. Infrared spectrum (Thin Film, NaCl) of compound **D-160**. 322
Figure A1.185. ^{13}C NMR (100 MHz, $CDCl_3$) of compound **D-160**. 322
Figure A1.186. ^{2}H NMR (61 MHz, $CHCl_3$) of compound **D-160**. 323
Figure A1.187. ^{1}H NMR (400 MHz, $CDCl_3$) of compound **161**. 324
Figure A1.188. Infrared spectrum (Thin Film, NaCl) of compound **161**. 325

Figure A1.189. ^{13}C NMR (100 MHz, $CDCl_3$) of compound **161**. 325
Figure A1.190. ^{1}H NMR (400 MHz, $CDCl_3$) of compound **167**. 326
Figure A1.191. Infrared spectrum (Thin Film, NaCl) of compound **167**. 327
Figure A1.192. ^{13}C NMR (100 MHz, $CDCl_3$) of compound **167**. 327
Figure A1.193. ^{1}H NMR (400 MHz, $CDCl_3$) of compound **162**. 328
Figure A1.194. Infrared spectrum (Thin Film, NaCl) of compound **162**. 329
Figure A1.195. ^{13}C NMR (100 MHz, $CDCl_3$) of compound **162**. 329
Figure A1.196. ^{1}H NMR (400 MHz, $CDCl_3$) of compound **163**. 330
Figure A1.197. Infrared spectrum (Thin Film, NaCl) of compound **163**. 331
Figure A1.198. ^{13}C NMR (100 MHz, $CDCl_3$) of compound **163**. 331
Figure A1.199. ^{1}H NMR (400 MHz, $CDCl_3$) of compound **164**. 332
Figure A1.200. Infrared spectrum (Thin Film, NaCl) of compound **164** 333
Figure A1.201. ^{13}C NMR (100 MHz, $CDCl_3$) of compound **164**. 333
Figure A1.202. ^{1}H NMR (400 MHz, $CDCl_3$) of compound **165**. 334
Figure A1.203. Infrared spectrum (Thin Film, NaCl) of compound **165**. 335
Figure A1.204. ^{13}C NMR (100 MHz, $CDCl_3$) of compound **165**. 335
Figure A1.205. ^{1}H NMR (400 MHz, $CDCl_3$) of compound **166**. 336
Figure A1.206. Infrared spectrum (Thin Film, NaCl) of compound **166**. 337
Figure A1.207. ^{13}C NMR (100 MHz, $CDCl_3$) of compound **166**. 337
Figure A1.208. ^{1}H NMR (400 MHz, $CDCl_3$) of compound **168**. 338
Figure A1.209. Infrared spectrum (Thin Film, NaCl) of compound **168**. 339
Figure A1.210. ^{13}C NMR (100 MHz, $CDCl_3$) of compound **168**. 339
Figure A1.211. ^{1}H NMR (400 MHz, $CDCl_3$) of compound **169**. 340
Figure A1.212. Infrared spectrum (Thin Film, NaCl) of compound **169**. 341
Figure A1.213. ^{13}C NMR (100 MHz, $CDCl_3$) of compound **169**. 341
Figure A1.214. ^{1}H NMR (400 MHz, $CDCl_3$) of compound **170**. 342
Figure A1.215. Infrared spectrum (Thin Film, NaCl) of compound **170**. 343
Figure A1.216. ^{13}C NMR (100 MHz, $CDCl_3$) of compound **170**. 343

Figure A1.217. ^{1}H NMR (400 MHz, $CDCl_3$) of compound **171**. 344
Figure A1.218. Infrared spectrum (Thin Film, NaCl) of compound **171**. 345
Figure A1.219. ^{13}C NMR (100 MHz, $CDCl_3$) of compound **171**. 345
Figure A1.220. ^{1}H NMR (400 MHz, $CDCl_3$) of compound **172**. 346
Figure A1.221. Infrared spectrum (Thin Film, NaCl) of compound **172**. 347
Figure A1.222. ^{13}C NMR (100 MHz, $CDCl_3$) of compound **172**. 347
Figure A1.223. ^{1}H NMR (400 MHz, $CDCl_3$) of compound **174**. 348
Figure A1.224. Infrared spectrum (Thin Film, NaCl) of compound **174**. 349
Figure A1.225. ^{13}C NMR (100 MHz, $CDCl_3$) of compound **174**. 349
Figure A1.226. ^{1}H NMR (400 MHz, $CDCl_3$) of compound **D-174**. 350
Figure A1.227. Infrared spectrum (Thin Film, NaCl) of compound **D-174**. 351
Figure A1.228. ^{13}C NMR (100 MHz, $CDCl_3$) of compound **D-174**. 351
Figure A1.229. ^{2}H NMR (61 MHz, $CHCl_3$) of compound **D-174**. 352
Figure A1.230. ^{1}H NMR (400 MHz, $CDCl_3$) of compound **177**. 353
Figure A1.231. Infrared spectrum (Thin Film, NaCl) of compound **177**. 354
Figure A1.232. ^{13}C NMR (100 MHz, $CDCl_3$) of compound **177**. 354
Figure A1.233. ^{1}H NMR (400 MHz, $CDCl_3$) of compound **179**. 355
Figure A1.234. Infrared spectrum (Thin Film, NaCl) of compound **179**. 356
Figure A1.235. ^{13}C NMR (100 MHz, $CDCl_3$) of compound **179**. 356
Figure A1.236. ^{1}H NMR (400 MHz, $CDCl_3$) of compound **180**. 357
Figure A1.237. Infrared spectrum (Thin Film, NaCl) of compound **180**. 358
Figure A1.238. ^{13}C NMR (100 MHz, $CDCl_3$) of compound **180**. 358
Figure A1.239. ^{1}H NMR (400 MHz, $CDCl_3$) of compound **181**. 359
Figure A1.240. Infrared spectrum (Thin Film, NaCl) of compound **181**. 360
Figure A1.241. ^{13}C NMR (100 MHz, $CDCl_3$) of compound **181**. 360
Figure A1.242. ^{1}H NMR (400 MHz, $CDCl_3$) of compound **187**. 361
Figure A1.243. Infrared spectrum (Thin Film, NaCl) of compound **187**. 362
Figure A1.244. ^{13}C NMR (100 MHz, $CDCl_3$) of compound **187**. 362

Figure A1.245. ^{1}H NMR (400 MHz, $CDCl_3$) of compound **178**. 363
Figure A1.246. Infrared spectrum (Thin Film, NaCl) of compound **178**. 364
Figure A1.247. ^{13}C NMR (100 MHz, $CDCl_3$) of compound **178**. 364
Figure A1.248. ^{1}H NMR (400 MHz, $CDCl_3$) of compound **182**. 365
Figure A1.249. Infrared spectrum (Thin Film, NaCl) of compound **182**. 366
Figure A1.250. ^{13}C NMR (100 MHz, $CDCl_3$) of compound **182**. 366
Figure A1.251. ^{1}H NMR (400 MHz, $CDCl_3$) of compound **183**. 367
Figure A1.252. Infrared spectrum (Thin Film, NaCl) of compound **183**. 368
Figure A1.253. ^{13}C NMR (100 MHz, $CDCl_3$) of compound **183**. 368
Figure A1.254. ^{1}H NMR (400 MHz, $CDCl_3$) of compound **184**. 369
Figure A1.255. Infrared spectrum (Thin Film, NaCl) of compound **184**. 370
Figure A1.256. ^{13}C NMR (100 MHz, $CDCl_3$) of compound **184**. 370
Figure A1.257. ^{1}H NMR (400 MHz, $CDCl_3$) of compound **185**. 371
Figure A1.258. Infrared spectrum (Thin Film, NaCl) of compound **185**. 372
Figure A1.259. ^{13}C NMR (100 MHz, $CDCl_3$) of compound **185**. 372
Figure A1.260. ^{1}H NMR (400 MHz, $CDCl_3$) of compound **186**. 373
Figure A1.261. Infrared spectrum (Thin Film, NaCl) of compound **186** 374
Figure A1.262. ^{13}C NMR (100 MHz, $CDCl_3$) of compound **186**. 374
Figure A1.263. ^{1}H NMR (400 MHz, $CDCl_3$) of compound **123a**. 375
Figure A1.264. Infrared spectrum (Thin Film, NaCl) of compound **123a**. 376
Figure A1.265. ^{13}C NMR (100 MHz, $CDCl_3$) of compound **123a**..... 376
Figure A1.266. ^{1}H NMR (400 MHz, $CDCl_3$) of compound **123d** 377
Figure A1.267. Infrared spectrum (Thin Film, NaCl) of compound **123d**. 378
Figure A1.268. ^{13}C NMR (100 MHz, $CDCl_3$) of compound **123d**. 378
Figure A1.269. ^{1}H NMR (400 MHz, $CDCl_3$) of compound **123e**. 379
Figure A1.270. Infrared spectrum (Thin Film, NaCl) of compound **123e**. 380
Figure A1.271. ^{13}C NMR (100 MHz, $CDCl_3$) of compound **123e**..... 380
Figure A1.272. ^{1}H NMR (400 MHz, $CDCl_3$) of compound **123f** 381

Figure A1.273. Infrared spectrum (Thin Film, NaCl) of compound **123f**. 382
Figure A1.274. ^{13}C NMR (100 MHz, $CDCl_3$) of compound **123f**. 382
Figure A1.275. ^{1}H NMR (400 MHz, $CDCl_3$) of compound **D-123f**. 383
Figure A1.276. Infrared spectrum (Thin Film, NaCl) of compound **D-123f**. 384
Figure A1.277. ^{13}C NMR (100 MHz, $CDCl_3$) of compound **D-123f**. 384
Figure A1.278. ^{2}H NMR (61 MHz, $CHCl_3$) of compound **D-123f**. 385
Figure A1.279. ^{1}H NMR (400 MHz, $CDCl_3$) of compound **123g**. 386
Figure A1.280. Infrared spectrum (Thin Film, NaCl) of compound **123g**. 387
Figure A1.281. ^{13}C NMR (100 MHz, $CDCl_3$) of compound **123g**. 387
Figure A1.282. ^{1}H NMR (400 MHz, $CDCl_3$) of compound **123h**. 388
Figure A1.283. Infrared spectrum (Thin Film, NaCl) of compound **123h**. 389
Figure A1.284. ^{13}C NMR (100 MHz, $CDCl_3$) of compound **123h**. 389
Figure A1.285. ^{1}H NMR (400 MHz, $CDCl_3$) of compound **123i**. 390
Figure A1.286. Infrared spectrum (Thin Film, NaCl) of compound **123i**. 391
Figure A1.287. ^{13}C NMR (100 MHz, $CDCl_3$) of compound **123i**. 391
Figure A1.288. ^{1}H NMR (400 MHz, $CDCl_3$) of compound **123m**. 392
Figure A1.289. Infrared spectrum (Thin Film, NaCl) of compound **123m**. 393
Figure A1.290. ^{13}C NMR (100 MHz, $CDCl_3$) of compound **123m**. 393
Figure A1.291. ^{1}H NMR (400 MHz, $CDCl_3$) of compound **123r**. 394
Figure A1.292. Infrared spectrum (Thin Film, NaCl) of compound **123r**. 395
Figure A1.293. ^{13}C NMR (100 MHz, $CDCl_3$) of compound **123r**. 395
Figure A1.294. ^{1}H NMR (400 MHz, $CDCl_3$) of compound **123t**. 396
Figure A1.295. Infrared spectrum (Thin Film, NaCl) of compound **123t**. 397
Figure A1.296. ^{13}C NMR (100 MHz, $CDCl_3$) of compound **123t**. 397
Figure A1.297. ^{1}H NMR (400 MHz, $CDCl_3$) of compound **123u**. 398
Figure A1.298. Infrared spectrum (Thin Film, NaCl) of compound **123u**. 399
Figure A1.299. ^{13}C NMR (100 MHz, $CDCl_3$) of compound **123u**. 399
Figure A1.300. ^{1}H NMR (400 MHz, $CDCl_3$) of compound **157** 400

Figure A1.301. Infrared spectrum (Thin Film, NaCl) of compound **157**. 401
Figure A1.302. ^{13}C NMR (100 MHz, $CDCl_3$) of compound **157**. 401
Figure A1.303. ^{1}H NMR (400 MHz, $CDCl_3$) of compound **158**. 402
Figure A1.304. Infrared spectrum (Thin Film, NaCl) of compound **158**. 403
Figure A1.305. ^{13}C NMR (100 MHz, $CDCl_3$) of compound **158**. 403
Figure A1.306. ^{1}H NMR (400 MHz, $CDCl_3$) of compound **133**. 404
Figure A1.307. Infrared spectrum (Thin Film, NaCl) of compound **133**. 405
Figure A1.308. ^{13}C NMR (100 MHz, $CDCl_3$) of compound **133**. 405
Figure A1.309. ^{1}H NMR (400 MHz, $CDCl_3$) of compound **142**. 406
Figure A1.310. Infrared spectrum (Thin Film, NaCl) of compound **142**. 407
Figure A1.311. ^{13}C NMR (100 MHz, $CDCl_3$) of compound **142**. 407
Figure A1.312. ^{1}H NMR (400 MHz, $CDCl_3$) of compound **188**. 408
Figure A1.313. Infrared spectrum (Thin Film, NaCl) of compound **188**. 409
Figure A1.314. ^{13}C NMR (100 MHz, $CDCl_3$) of compound **188**. 409
Figure A1.315. ^{1}H NMR (400 MHz, $CDCl_3$) of compound **143**. 410
Figure A1.316. Infrared spectrum (Thin Film, NaCl) of compound **143**. 411
Figure A1.317. ^{13}C NMR (100 MHz, $CDCl_3$) of compound **143**. 411
Figure A1.318. ^{1}H NMR (400 MHz, $CDCl_3$) of compound **144**. 412
Figure A1.319. Infrared spectrum (Thin Film, NaCl) of compound **144**. 413
Figure A1.320. ^{13}C NMR (100 MHz, $CDCl_3$) of compound **144**. 413
Figure A1.321. ^{1}H NMR (400 MHz, $CDCl_3$) of compound **149**. 414
Figure A1.322. Infrared spectrum (Thin Film, NaCl) of compound **149**. 415
Figure A1.323. ^{13}C NMR (100 MHz, $CDCl_3$) of compound **149**. 415
Figure A1.324. ^{1}H NMR (400 MHz, $CDCl_3$) of compound **150**. 416
Figure A1.325. Infrared spectrum (Thin Film, NaCl) of compound **150**. 417
Figure A1.326. ^{13}C NMR (100 MHz, $CDCl_3$) of compound **150**. 417
Figure A1.327. ^{1}H NMR (400 MHz, $CDCl_3$) of compound **151**. 418
Figure A1.328. Infrared spectrum (Thin Film, NaCl) of compound **151**. 419

Figure A1.329. ^{13}C NMR (100 MHz, $CDCl_3$) of compound **151**. 419
Figure A1.330. ^{1}H NMR (400 MHz, $CDCl_3$) of compound **152** 420
Figure A1.331. Infrared spectrum (Thin Film, NaCl) of compound **152**. 421
Figure A1.332. ^{13}C NMR (100 MHz, $CDCl_3$) of compound **152**. 421
Figure A1.333. ^{1}H NMR (400 MHz, $CDCl_3$) of compound **153**. 422
Figure A1.334. Infrared spectrum (Thin Film, NaCl) of compound **153**. 423
Figure A1.335. ^{13}C NMR (100 MHz, $CDCl_3$) of compound **153**. 423
Figure A1.336. ^{1}H NMR (400 MHz, $CDCl_3$) of compound **154**. 424
Figure A1.337. Infrared spectrum (Thin Film, NaCl) of compound **154**. 425
Figure A1.338. ^{13}C NMR (100 MHz, $CDCl_3$) of compound **154**. 425
Figure A1.339. ^{1}H NMR (400 MHz, $CDCl_3$) of compound **155**. 426
Figure A1.340. Infrared spectrum (Thin Film, NaCl) of compound **155**. 427
Figure A1.341. ^{13}C NMR (100 MHz, $CDCl_3$) of compound **155**. 427
Figure A1.342. ^{1}H NMR (400 MHz, $CDCl_3$) of compound **156**. 428
Figure A1.343. Infrared spectrum (Thin Film, NaCl) of compound **156**. 429
Figure A1.344. ^{13}C NMR (100 MHz, $CDCl_3$) of compound **156**. 429

CHAPTER 3

Asymmetric Michael Spirocyclization of Pd Enolates

Figure 3.1 Pd-catalyzed enantioselective [4+2] cycloaddition and Racemic Pd-catalyzed Michael spirocyclization reported by Tsuji et al 431
Figure 3.2 Generic reaction scheme and Scope of spirocycles formed via Michael spirocyclization reaction. 434
Figure 3.3 Application of this reaction system to asymmetric enone difunctionalization and Product derivatizations toward versatile functional groups and diverse tricycles. 436
Figure 3.4 Proposed catalytic cycle. 437

Figure 3.5 Computational evaluation of the four possible Michael addition transition states leading to the formation of stereoisomers. 440

Figure 3.6 Relative free energies for transition states explored for the Michael addition process. 504

Figure 3.7 Relative free energies for Pd intermediates explored. Gibbs free energies in kcal/mol. 506

Figure 3.8 Relative free energies for proton transfer pathways studied. Gibbs free energies in kcal/mol 507

Figure 3.9 Proposed reaction pathway for Michael addition and proton transfer and the computed relative energies of relevant intermediates and transition states..... 509

Figure 3.10 ^{1}H–^{1}H COSY NMR spectrum of **202** (400 MHz, $CDCl_3$)..... 510

Figure 3.11 ^{1}H–^{13}C HSQC NMR spectrum of **202** (400 MHz, $CDCl_3$) 511

Figure 3.12 ^{1}H–^{13}C HMBC NMR spectrum of **202** (400 MHz, $CDCl_3$)..... 512

Figure 3.13 ^{1}H–^{1}H COSY NMR spectrum of **206** (400 MHz, $CDCl_3$)..... 513

Figure 3.14 ^{1}H–^{13}C HSQC NMR spectrum of **206** (400 MHz, $CDCl_3$) 514

Figure 3.15 ^{1}H–^{13}C HMBC NMR spectrum of **206** (400 MHz, $CDCl_3$)..... 515

Figure 3.16 ^{31}P spectra of various relevant mixtures (400 MHz, toluene-d_8). 517

Figure 3.17 ^{1}H spectra timecourse over ~ 5 hours (400 MHz, toluene-d_8)..... 519

Figure 3.18 ^{1}H NMR timecourse plot of integration vs time. 520

APPENDIX 2

Spectra Relevant to Chapter 3

Figure A2.1. ^{1}H NMR (600 MHz, $CDCl_3$) of compound **197a**. 537

Figure A2.2. Infrared spectrum (Thin Film, NaCl) of compound **197a**. 538

Figure A2.3. ^{13}C NMR (100 MHz, $CDCl_3$) of compound **197a**..... 538

Figure A2.4. ^{1}H NMR (400 MHz, $CDCl_3$) of compound **197b**. 539

Figure A2.5. Infrared spectrum (Thin Film, NaCl) of compound **197b**. 540

Figure A2.6. ^{13}C NMR (100 MHz, $CDCl_3$) of compound **197b**. 540
Figure A2.7. ^{1}H NMR (400 MHz, $CDCl_3$) of compound **197c**. 541
Figure A2.8. Infrared spectrum (Thin Film, NaCl) of compound **197c**. 542
Figure A2.9. ^{13}C NMR (100 MHz, $CDCl_3$) of compound **197c**..... 542
Figure A2.10. ^{1}H NMR (400 MHz, $CDCl_3$) of compound **197d**. 543
Figure A2.11. Infrared spectrum (Thin Film, NaCl) of compound **197d**. 544
Figure A2.12. ^{13}C NMR (100 MHz, $CDCl_3$) of compound **197d**. 544
Figure A2.13. ^{1}H NMR (400 MHz, $CDCl_3$) of compound **197e** 545
Figure A2.14. Infrared spectrum (Thin Film, NaCl) of compound **197e**. 546
Figure A2.15. ^{13}C NMR (100 MHz, $CDCl_3$) of compound **197e**..... 546
Figure A2.16. ^{1}H NMR (400 MHz, $CDCl_3$) of compound **197f**. 547
Figure A2.17. Infrared spectrum (Thin Film, NaCl) of compound **197f**..... 548
Figure A2.18. ^{13}C NMR (100 MHz, $CDCl_3$) of compound **197f**. 548
Figure A2.19. ^{1}H NMR (400 MHz, $CDCl_3$) of compound **197g**. 549
Figure A2.20. Infrared spectrum (Thin Film, NaCl) of compound **197g**..... 550
Figure A2.21. ^{13}C NMR (100 MHz, $CDCl_3$) of compound **197g**..... 550
Figure A2.22. ^{1}H NMR (400 MHz, $CDCl_3$) of compound **197h (d1)**..... 551
Figure A2.23. Infrared spectrum (Thin Film, NaCl) of compound **197h (d1)**. 552
Figure A2.24. ^{13}C NMR (100 MHz, $CDCl_3$) of compound **197h (d1)**..... 552
Figure A2.25. ^{1}H NMR (400 MHz, $CDCl_3$) of compound **197h (d2)**..... 553
Figure A2.26. Infrared spectrum (Thin Film, NaCl) of compound **197h (d2)**. 554
Figure A2.27. ^{13}C NMR (100 MHz, $CDCl_3$) of compound **197h (d2)**..... 554
Figure A2.28. ^{1}H NMR (400 MHz, $CDCl_3$) of compound **197i (d1)**..... 555
Figure A2.29. Infrared spectrum (Thin Film, NaCl) of compound **197i (d1)** 556
Figure A2.30. ^{13}C NMR (100 MHz, $CDCl_3$) of compound **197i (d1)**..... 556
Figure A2.31. ^{1}H NMR (600 MHz, $CDCl_3$) of compound **197i (d2)**..... 557
Figure A2.32. Infrared spectrum (Thin Film, NaCl) of compound **197i (d2)**. 558
Figure A2.33. ^{13}C NMR (100 MHz, $CDCl_3$) of compound **197i (d2)**..... 558

Figure A2.34. ^{1}H NMR (600 MHz, $CDCl_3$) of compound **197j**. 559
Figure A2.35. Infrared spectrum (Thin Film, NaCl) of compound **197j**. 560
Figure A2.36. ^{13}C NMR (100 MHz, $CDCl_3$) of compound **197j**. 560
Figure A2.37. ^{1}H NMR (400 MHz, $CDCl_3$) of compound **197k**. 561
Figure A2.38. Infrared spectrum (Thin Film, NaCl) of compound **197k**. 562
Figure A2.39. ^{13}C NMR (100 MHz, $CDCl_3$) of compound **197k**..... 562
Figure A2.40. ^{1}H NMR (400 MHz, $CDCl_3$) of compound **199**. 563
Figure A2.41. Infrared spectrum (Thin Film, NaCl) of compound **199**..... 564
Figure A2.42. ^{13}C NMR (100 MHz, $CDCl_3$) of compound **199**. 564
Figure A2.43. ^{1}H NMR (400 MHz, $CDCl_3$) of compound **216a**. 565
Figure A2.44. Infrared spectrum (Thin Film, NaCl) of compound **216a**. 566
Figure A2.45. ^{13}C NMR (100 MHz, $CDCl_3$) of compound **216a**..... 566
Figure A2.46. ^{1}H NMR (400 MHz, $CDCl_3$) of compound **216b**. 567
Figure A2.47. Infrared spectrum (Thin Film, NaCl) of compound **216b**. 568
Figure A2.48. ^{13}C NMR (100 MHz, $CDCl_3$) of compound **216b**. 568
Figure A2.49. ^{1}H NMR (400 MHz, $CDCl_3$) of compound **216c**. 569
Figure A2.50. Infrared spectrum (Thin Film, NaCl) of compound **216c**. 570
Figure A2.51. ^{13}C NMR (100 MHz, $CDCl_3$) of compound **216c**..... 570
Figure A2.52. ^{1}H NMR (600 MHz, $CDCl_3$) of compound **216d**. 571
Figure A2.53. Infrared spectrum (Thin Film, NaCl) of compound **216d**. 572
Figure A2.54. ^{13}C NMR (100 MHz, $CDCl_3$) of compound **216d**. 572
Figure A2.55. ^{1}H NMR (600 MHz, $CDCl_3$) of compound **201a**. 573
Figure A2.56. Infrared spectrum (Thin Film, NaCl) of compound **201a**. 574
Figure A2.57. ^{13}C NMR (100 MHz, $CDCl_3$) of compound **201a**..... 574
Figure A2.58. ^{1}H NMR (400 MHz, $CDCl_3$) of compound **201b**. 575
Figure A2.59. Infrared spectrum (Thin Film, NaCl) of compound **201b**. 576
Figure A2.60. ^{13}C NMR (100 MHz, $CDCl_3$) of compound **201b**. 576
Figure A2.61. ^{1}H NMR (400 MHz, $CDCl_3$) of compound **196a**. 577

Figure A2.62. Infrared spectrum (Thin Film, NaCl) of compound **196a**. 578
Figure A2.63. ^{13}C NMR (100 MHz, $CDCl_3$) of compound **196a**..... 578
Figure A2.64. ^{1}H NMR (400 MHz, $CDCl_3$) of compound **196b**. 579
Figure A2.65. Infrared spectrum (Thin Film, NaCl) of compound **196b**. 580
Figure A2.66. ^{13}C NMR (100 MHz, $CDCl_3$) of compound **196b**. 580
Figure A2.67. ^{1}H NMR (400 MHz, $CDCl_3$) of compound **196c**. 581
Figure A2.68. Infrared spectrum (Thin Film, NaCl) of compound **196c**. 582
Figure A2.69. ^{13}C NMR (100 MHz, $CDCl_3$) of compound **196c**..... 582
Figure A2.70. ^{1}H NMR (400 MHz, $CDCl_3$) of compound **196d** 583
Figure A2.71. Infrared spectrum (Thin Film, NaCl) of compound **196d**. 584
Figure A2.72. ^{13}C NMR (100 MHz, $CDCl_3$) of compound **196d**. 584
Figure A2.73. ^{1}H NMR (400 MHz, $CDCl_3$) of compound **196e**. 585
Figure A2.74. Infrared spectrum (Thin Film, NaCl) of compound **196e**. 586
Figure A2.75. ^{13}C NMR (100 MHz, $CDCl_3$) of compound **196e**..... 586
Figure A2.76. ^{1}H NMR (400 MHz, $CDCl_3$) of compound **196f** 587
Figure A2.77. Infrared spectrum (Thin Film, NaCl) of compound **196f**. 588
Figure A2.78. ^{13}C NMR (100 MHz, $CDCl_3$) of compound **196f** 588
Figure A2.79. ^{1}H NMR (400 MHz, $CDCl_3$) of compound **196g**. 589
Figure A2.80. Infrared spectrum (Thin Film, NaCl) of compound **196g**. 590
Figure A2.81. ^{13}C NMR (100 MHz, $CDCl_3$) of compound **196g**..... 590
Figure A2.82. ^{1}H NMR (400 MHz, $CDCl_3$) of compound **196h**. 591
Figure A2.83. Infrared spectrum (Thin Film, NaCl) of compound **196h**. 592
Figure A2.84. ^{13}C NMR (100 MHz, $CDCl_3$) of compound **196h**. 592
Figure A2.85. ^{1}H NMR (400 MHz, C_6D_6) of compound **198**. 593
Figure A2.86. Infrared spectrum (Thin Film, NaCl) of compound **198**. 594
Figure A2.87. ^{13}C NMR (100 MHz, C_6D_6) of compound **198**..... 594
Figure A2.88. ^{1}H NMR (400 MHz, $CDCl_3$) of compound **196i** 595
Figure A2.89. Infrared spectrum (Thin Film, NaCl) of compound **196i**. 596

Figure A2.90. ^{13}C NMR (100 MHz, $CDCl_3$) of compound **196i**. 596
Figure A2.91. ^{1}H NMR (400 MHz, $CDCl_3$) of compound **218**. 597
Figure A2.92. Infrared spectrum (Thin Film, NaCl) of compound **218**. 598
Figure A2.93. ^{13}C NMR (100 MHz, $CDCl_3$) of compound **218**. 598
Figure A2.94. ^{1}H NMR (400 MHz, $CDCl_3$) of compound **196j**. 599
Figure A2.95. Infrared spectrum (Thin Film, NaCl) of compound **196j**. 600
Figure A2.96. ^{13}C NMR (100 MHz, $CDCl_3$) of compound **196j**. 600
Figure A2.97. ^{1}H NMR (400 MHz, $CDCl_3$) of compound **196k**. 601
Figure A2.98. Infrared spectrum (Thin Film, NaCl) of compound **196k**. 602
Figure A2.99. ^{13}C NMR (100 MHz, $CDCl_3$) of compound **196k**..... 602
Figure A2.100. ^{1}H NMR (400 MHz, $CDCl_3$) of compound **215a**. 603
Figure A2.101. Infrared spectrum (Thin Film, NaCl) of compound **215a**. 604
Figure A2.102. ^{13}C NMR (100 MHz, $CDCl_3$) of compound **215a**..... 604
Figure A2.103. ^{1}H NMR (400 MHz, $CDCl_3$) of compound **215b**. 605
Figure A2.104. Infrared spectrum (Thin Film, NaCl) of compound **215b**. 606
Figure A2.105. ^{13}C NMR (100 MHz, $CDCl_3$) of compound **215b**. 606
Figure A2.106. ^{1}H NMR (400 MHz, $CDCl_3$) of compound **215c** 607
Figure A2.107. Infrared spectrum (Thin Film, NaCl) of compound **215c**. 608
Figure A2.108. ^{13}C NMR (100 MHz, $CDCl_3$) of compound **215c**..... 608
Figure A2.109. ^{1}H NMR (400 MHz, $CDCl_3$) of compound **215d**. 609
Figure A2.110. Infrared spectrum (Thin Film, NaCl) of compound **215d**. 610
Figure A2.111. ^{13}C NMR (100 MHz, $CDCl_3$) of compound **215d**. 610
Figure A2.112. ^{1}H NMR (400 MHz, $CDCl_3$) of compound **200a**. 611
Figure A2.113. Infrared spectrum (Thin Film, NaCl) of compound **200a**. 612
Figure A2.114. ^{13}C NMR (100 MHz, $CDCl_3$) of compound **200a**..... 612
Figure A2.115. ^{1}H NMR (400 MHz, $CDCl_3$) of compound **200b**. 613
Figure A2.116. Infrared spectrum (Thin Film, NaCl) of compound **200b**. 614
Figure A2.117. ^{13}C NMR (100 MHz, $CDCl_3$) of compound **200b**. 614

Figure A2.118. ^{1}H NMR (400 MHz, $CDCl_3$) of compound **217a**. 615
Figure A2.119. Infrared spectrum (Thin Film, NaCl) of compound **217a**. 616
Figure A2.120. ^{13}C NMR (100 MHz, $CDCl_3$) of compound **217a**..... 616
Figure A2.121. ^{1}H NMR (400 MHz, $CDCl_3$) of compound **217b** 617
Figure A2.122. Infrared spectrum (Thin Film, NaCl) of compound **217b**. 618
Figure A2.123. ^{13}C NMR (100 MHz, $CDCl_3$) of compound **217b**. 618
Figure A2.124. ^{1}H NMR (400 MHz, $CDCl_3$) of compound **217c**. 619
Figure A2.125. Infrared spectrum (Thin Film, NaCl) of compound **217c**. 620
Figure A2.126. ^{13}C NMR (100 MHz, $CDCl_3$) of compound **217c**..... 620
Figure A2.127. 1H NMR (400 MHz, CDCl3) of compound **217d**. 621
Figure A2.128. Infrared spectrum (Thin Film, NaCl) of compound **217d**. 622
Figure A2.129. ^{13}C NMR (100 MHz, $CDCl_3$) of compound **217d**. 622
Figure A2.130. ^{1}H NMR (400 MHz, $CDCl_3$) of compound **217e**. 623
Figure A2.131. Infrared spectrum (Thin Film, NaCl) of compound **217e**. 624
Figure A2.132. ^{13}C NMR (100 MHz, $CDCl_3$) of compound **217e**..... 624
Figure A2.133. ^{1}H NMR (400 MHz, $CDCl_3$) of compound **217f**..... 625
Figure A2.134. Infrared spectrum (Thin Film, NaCl) of compound **217f**..... 626
Figure A2.135. ^{13}C NMR (100 MHz, $CDCl_3$) of compound **217f**. 626
Figure A2.136. ^{1}H NMR (400 MHz, $CDCl_3$) of compound **217g**. 627
Figure A2.137. Infrared spectrum (Thin Film, NaCl) of compound **217g**. 628
Figure A2.138. ^{13}C NMR (100 MHz, $CDCl_3$) of compound **217g**..... 628
Figure A2.139. ^{1}H NMR (400 MHz, $CDCl_3$) of compound **217h** 629
Figure A2.140. Infrared spectrum (Thin Film, NaCl) of compound **217h**. 630
Figure A2.141. ^{13}C NMR (100 MHz, $CDCl_3$) of compound **217h**. 630
Figure A2.142. ^{1}H NMR (400 MHz, $CDCl_3$) of compound **217i**. 631
Figure A2.143. Infrared spectrum (Thin Film, NaCl) of compound **217i**. 632
Figure A2.144. ^{13}C NMR (100 MHz, $CDCl_3$) of compound **217i**. 632
Figure A2.145. ^{1}H NMR (600 MHz, $CDCl_3$) of compound **217j**. 633

Figure A2.146. Infrared spectrum (Thin Film, NaCl) of compound **217j**..... 634
Figure A2.147. ^{13}C NMR (100 MHz, $CDCl_3$) of compound **217j**. 634
Figure A2.148. ^{1}H NMR (400 MHz, $CDCl_3$) of compound **202**. 635
Figure A2.149. Infrared spectrum (Thin Film, NaCl) of compound **202**. 636
Figure A2.150. ^{13}C NMR (100 MHz, $CDCl_3$) of compound **202**. 636
Figure A2.151. ^{1}H NMR (400 MHz, $CDCl_3$) of compound **204**. 637
Figure A2.152. Infrared spectrum (Thin Film, NaCl) of compound **204**. 638
Figure A2.153. ^{13}C NMR (100 MHz, $CDCl_3$) of compound **204**. 638
Figure A2.154. ^{1}H NMR (400 MHz, $CDCl_3$) of compound **205**. 639
Figure A2.155. Infrared spectrum (Thin Film, NaCl) of compound **205**. 640
Figure A2.156. ^{13}C NMR (100 MHz, $CDCl_3$) of compound **205**. 640
Figure A2.157. ^{1}H NMR (400 MHz, $CDCl_3$) of compound **203**. 641
Figure A2.158. Infrared spectrum (Thin Film, NaCl) of compound **203**. 642
Figure A2.159. ^{13}C NMR (100 MHz, $CDCl_3$) of compound **203**. 642
Figure A2.160. ^{1}H NMR (400 MHz, $CDCl_3$) of compound **206**. 643
Figure A2.161. Infrared spectrum (Thin Film, NaCl) of compound **206**..... 644
Figure A2.162. ^{13}C NMR (100 MHz, $CDCl_3$) of compound **206**. 644
Figure A2.163. ^{1}H NMR (400 MHz, $CDCl_3$) of compound **207**. 645
Figure A2.164. Infrared spectrum (Thin Film, NaCl) of compound **207**. 646
Figure A2.165. ^{13}C NMR (100 MHz, $CDCl_3$) of compound **207**. 646
Figure A2.166. ^{1}H NMR (400 MHz, $CDCl_3$) of compound **208**. 647
Figure A2.167. Infrared spectrum (Thin Film, NaCl) of compound **208**. 648
Figure A2.168. ^{13}C NMR (100 MHz, $CDCl_3$) of compound **208**. 648

APPENDIX 3

X-Ray Crystallography Reports Relevant to Chapter 3

Figure A3.2.1 X-Ray Coordinates of Compound **197a** (V25038) 650

Figure A3.3.1 X-Ray Coordinates of Compound **197b** (V25125) 668

Figure A3.4.1 X-Ray Coordinates of Compound **201a** (V24254) 679

Figure A3.5.1 X-Ray Coordinates of Compound **205** (V25146) 692

CHAPTER 4

Progress Toward Mitomycin B

Figure 4.1 Members of the mitomycin family of natural products. 705

Figure 4.2 Proposed mechanism of DNA cross-linking by mitomycin C. 706

Figure 4.3 Introduction to mitomycin B. 707

Figure 4.4 Summary of Kishi's total synthesis of the mitomycins. 708

Figure 4.5 The mitomycin rearrangement. 709

Figure 4.6 Summary of Fukuyama's synthesis of mitomycin C. 710

Figure 4.7 Retrosynthetic analysis of mitomycin B. 711

Figure 4.8 Synthesis of functionalized aniline and enantioenriched epoxide.... 713

Figure 4.9 Selective aniline alkylation and aziridine formation. 714

Figure 4.10 Synthesis of O-silyl hydroxamic acid and Intramolecular nitrile oxide cycloaddition using Carreira's protocol. 716

Figure 4.11 Challenges remaining in the synthesis and two proposed strategies. 717

Figure 4.12 Initial investigations into N–O bond cleavage. 718

Figure 4.13 Potential advantages and synthesis of primary amine. 719

Figure 4.14 Attempted N–O bond cleavage and undesired retro-aldol decomposition. 720

Figure 4.15 Reduction with nickel boride and subsequent oxidation with N-tert-butylphenylsulfinimidoyl chloride. 721

Figure 4.16 Attempts to hydrolyze enecarbamate and alternative substrate for investigation. 722

Figure 4.17 Proposed route for the completion of the synthesis of mitomycin B. 723

APPENDIX 4

Spectra Relevant to Chapter 4

Figure A4.1. ^{1}H NMR (400 MHz, $CDCl_3$) of compound **269**. 761

Figure A4.2. Infrared spectrum (Thin Film, NaCl) of compound **269**. 762

Figure A4.3. ^{13}C NMR (100 MHz, $CDCl_3$) of compound **269**. 762

Figure A4.4. ^{1}H NMR (400 MHz, $CDCl_3$) of compound **271**. 763

Figure A4.5. Infrared spectrum (Thin Film, NaCl) of compound **271**. 764

Figure A4.6. ^{13}C NMR (100 MHz, $CDCl_3$) of compound **271**. 764

Figure A4.7. ^{1}H NMR (400 MHz, $CDCl_3$) of compound **272**. 765

Figure A4.8. Infrared spectrum (Thin Film, NaCl) of compound **272**. 766

Figure A4.9. ^{13}C NMR (100 MHz, $CDCl_3$) of compound **272**. 766

Figure A4.10. ^{1}H NMR (400 MHz, $CDCl_3$) of compound **273**. 767

Figure A4.11. Infrared spectrum (Thin Film, NaCl) of compound **273**. 768

Figure A4.12. ^{13}C NMR (100 MHz, $CDCl_3$) of compound **273**. 768

Figure A4.13. ^{1}H NMR (400 MHz, $CDCl_3$) of compound **274**. 769

Figure A4.14. Infrared spectrum (Thin Film, NaCl) of compound **274**. 770

Figure A4.15. ^{13}C NMR (100 MHz, $CDCl_3$) of compound **274**. 770

Figure A4.16. ^{1}H NMR (400 MHz, $CDCl_3$) of compound **275**. 771

Figure A4.17. Infrared spectrum (Thin Film, NaCl) of compound **275**. 772

Figure A4.18. ^{13}C NMR (100 MHz, $CDCl_3$) of compound **275**. 772

Figure A9.14. ^{1}H NMR (400 MHz, $CDCl_3$) of compound **267**. 773

Figure A4.20. Infrared spectrum (Thin Film, NaCl) of compound **267**. 774

Figure A4.21. ^{13}C NMR (100 MHz, $CDCl_3$) of compound **267**. 774

Figure A4.22. ^{1}H NMR (400 MHz, $CDCl_3$) of compound **277**. 775

Figure A4.23. Infrared spectrum (Thin Film, NaCl) of compound **277**. 776

Figure A4.24. ^{13}C NMR (100 MHz, $CDCl_3$) of compound **277**. 776

Figure A4.25. ^{1}H NMR (400 MHz, $CDCl_3$) of compound **278**. 777

Figure A4.26. Infrared spectrum (Thin Film, NaCl) of compound **278**. 778
Figure A4.27. ^{13}C NMR (100 MHz, $CDCl_3$) of compound **278**. 778
Figure A4.28. ^{1}H NMR (400 MHz, $CDCl_3$) of compound **279**. 779
Figure A4.29. Infrared spectrum (Thin Film, NaCl) of compound **279**. 780
Figure A4.30. ^{13}C NMR (100 MHz, $CDCl_3$) of compound **279**. 780
Figure A4.31. ^{1}H NMR (400 MHz, $CDCl_3$) of compound **280**. 781
Figure A4.32. Infrared spectrum (Thin Film, NaCl) of compound **280**. 782
Figure A4.33. ^{13}C NMR (100 MHz, $CDCl_3$) of compound **280**. 782
Figure A4.34. ^{1}H NMR (400 MHz, $CDCl_3$) of compound **281**. 783
Figure A4.35. Infrared spectrum (Thin Film, NaCl) of compound **281**. 784
Figure A4.36. ^{13}C NMR (100 MHz, $CDCl_3$) of compound **281**. 784
Figure A4.37. ^{1}H NMR (400 MHz, $CDCl_3$) of compound **266**. 785
Figure A4.38. Infrared spectrum (Thin Film, NaCl) of compound **266**. 786
Figure A4.39. ^{13}C NMR (100 MHz, $CDCl_3$) of compound **266**. 786
Figure A4.40. ^{1}H NMR (400 MHz, $CDCl_3$) of compound **282**. 787
Figure A4.41. Infrared spectrum (Thin Film, NaCl) of compound **282**. 788
Figure A4.42. ^{13}C NMR (100 MHz, $CDCl_3$) of compound **282**. 788
Figure A4.43. ^{1}H NMR (600 MHz, $CDCl_3$) of compound **283**. 789
Figure A4.44. Infrared spectrum (Thin Film, NaCl) of compound **283**. 790
Figure A4.45. ^{13}C NMR (100 MHz, $CDCl_3$) of compound **283**. 790
Figure A4.46. ^{1}H NMR (400 MHz, $CDCl_3$) of compound **284**. 791
Figure A4.47. Infrared spectrum (Thin Film, NaCl) of compound **284**. 792
Figure A4.48. ^{13}C NMR (100 MHz, $CDCl_3$) of compound **284**. 792
Figure A4.49. ^{1}H NMR (400 MHz, $CDCl_3$) of compound **295**. 793
Figure A4.50. Infrared spectrum (Thin Film, NaCl) of compound **295**. 794
Figure A4.51. ^{13}C NMR (100 MHz, $CDCl_3$) of compound **295**. 794
Figure A4.52. ^{1}H NMR (400 MHz, $CDCl_3$) of compound **295a**. 795
Figure A4.53. Infrared spectrum (Thin Film, NaCl) of compound **295a**. 796

Figure A4.54. ^{13}C NMR (100 MHz, $CDCl_3$) of compound **295a**..... 796
Figure A4.55. ^{1}H NMR (600 MHz, $CDCl_3$) of crude compound **290**. 797
Figure A4.56. ^{1}H NMR (400 MHz, $CDCl_3$) of compound **298**. 798
Figure A4.57. Infrared spectrum (Thin Film, NaCl) of compound **298**. 799
Figure A4.58. ^{13}C NMR (100 MHz, $CDCl_3$) of compound **298**. 799
Figure A4.59. ^{1}H NMR (600 MHz, $CDCl_3$) of compound **300**. 800
Figure A4.60. Infrared spectrum (Thin Film, NaCl) of compound **300**. 801
Figure A4.61. ^{13}C NMR (100 MHz, $CDCl_3$) of compound **300**. 801
Figure A4.62. ^{1}H NMR (400 MHz, $CDCl_3$) of compound **301**. 802
Figure A4.63. Infrared spectrum (Thin Film, NaCl) of compound **301**. 803
Figure A4.64. ^{13}C NMR (100 MHz, $CDCl_3$) of compound **301**. 803
Figure A4.65. ^{1}H NMR (400 MHz, $CDCl_3$) of compound **305**. 804
Figure A4.66. Infrared spectrum (Thin Film, NaCl) of compound **305**. 805
Figure A4.67. ^{13}C NMR (100 MHz, $CDCl_3$) of compound **305**. 805

APPENDIX 5

X-Ray Crystallography Reports Relevant to Chapter 4

Figure A5.2.1 X-Ray Coordinates of Compound **266** (V23354) 808
Figure A5.3.1 X-Ray Coordinates of Compound **284** (V24001) 825

LIST OF TABLES

CHAPTER 2

Asymmetric [4+2] Cycloaddition of Pd Enolates

Table 2.1 Optimization of Reaction Conditions 29

Table 2.2 Substrate Scope of the [4+2] Reaction 32

CHAPTER 3

Asymmetric [4+2] Cycloaddition of Pd Enolates

Table 3.1 Optimization of Reaction Conditions 433

APPENDIX 3

X-Ray Crystallography Reports Relevant to Chapter 3

Table A3.2.1 Crystal data and structure refinement for V25038. 651

Table A3.2.2 Atomic coordinates (x 10^4) and equivalent isotropic displacement parameters ($Å^2$x 10^3) for V25038. U(eq) is defined as one third of the trace of the orthogonalized U^{ij} tensor. 652

Table A3.2.3 Bond lengths [Å] and angles [°] for V25038. 653

Table A3.2.4 Anisotropic displacement parameters ($Å^2$x 10^3) for V25038. The anisotropic displacement factor exponent takes the form: $-2p^2[h^2 a^{*2}U^{11} + ... + 2 h k a^* b^* U^{12}]$ 661

Table A3.2.5 Hydrogen coordinates (x 10^4) and isotropic displacement parameters ($Å^2$x 10^3) for V25038. 663

Table A3.2.6 Torsion angles [°] for V25038. 664

Table A3.3.1 Crystal data and structure refinement for V25125. 668

Table A3.3.2 Atomic coordinates (x 10^4) and equivalent isotropic displacement parameters ($Å^2$x 10^3) for V25125. U(eq) is defined as one third of the trace of the orthogonalized U^{ij} tensor. 670

Table A3.3.3 Bond lengths [Å] and angles [°] for V25125. 670

Table A3.3.4 Anisotropic displacement parameters ($Å^2$x 10^3) for V25125. The anisotropic displacement factor exponent takes the form: $-2p^2[h^2 a^{*2}U^{11} + ... + 2 h k a^* b^* U^{12}]$ 675

Table A3.3.5 Hydrogen coordinates (x 10^4) and isotropic displacement parameters ($Å^2$x 10^3) for V25125..... 676

Table A3.3.6 Torsion angles [°] for V25125..... 677

Table A3.4.1 Crystal data and structure refinement for V24254..... 680

Table A3.4.2 Atomic coordinates (x 10^4) and equivalent isotropic displacement parameters ($Å^2$x 10^3) for V24254. U(eq) is defined as one third of the trace of the orthogonalized U^{ij} tensor. 681

Table A3.4.3 Bond lengths [Å] and angles [°] for V24254. 682

Table A3.4.4 Anisotropic displacement parameters ($Å^2$x 10^3) for V24254. The anisotropic displacement factor exponent takes the form: $-2p^2[h^2 a^{*2}U^{11} + ... + 2 h k a^* b^* U^{12}]$ 687

Table A3.4.5 Hydrogen coordinates (x 10^4) and isotropic displacement parameters ($Å^2$x 10^3) for V24254..... 688

Table A3.4.6 Torsion angles [°] for V24254..... 690

Table A3.5.1 Crystal data and structure refinement for V25146..... 693

Table A3.5.2 Atomic coordinates (x 10^4) and equivalent isotropic displacement parameters ($Å^2$x 10^3) for V25146. U(eq) is defined as one third of the trace of the orthogonalized U^{ij} tensor. 694

Table A3.5.3 Bond lengths [Å] and angles [°] for V25146. 695

Table A3.5.4 Anisotropic displacement parameters ($Å^2$x 10^3) for V25146. The anisotropic displacement factor exponent takes the form: $-2p^2[h^2 a^{*2}U^{11} + ... + 2 h k a^* b^* U^{12}]$ 699

Table A3.5.5 Hydrogen coordinates (x 10^4) and isotropic displacement parameters ($Å^2$x 10^3) for V25146..... 700

Table A3.5.6 Torsion angles [°] for V25146..... 701

Table A3.5.7 Hydrogen bonds for V25146 [Å and °]..... 703

APPENDIX 5

X-Ray Crystallography Reports Relevant to Chapter 4

Table A5.2.1 Crystal data and structure refinement for V23354..... 808

Table A5.2.2 Atomic coordinates (x 10^4) and equivalent isotropic displacement parameters ($Å^2$x 10^3) for V23354. U(eq) is defined as one third of the trace of the orthogonalized U^{ij} tensor. 809

Table A5.2.3 Bond lengths [Å] and angles [°] for V23354. 811

Table A5.2.4 Anisotropic displacement parameters ($Å^2$x 10^3) for V23354. The anisotropic displacement factor exponent takes the form: $-2p^2[h^2 a^{*2}U^{11} + ... + 2 h k a^* b^* U^{12}]$ 816

Table A5.2.5 Hydrogen coordinates (x 10^4) and isotropic displacement parameters ($Å^2$x 10^3) for V23354..... 818

Table A5.2.6 Torsion angles [°] for V23354..... 820

Table A5.3.1 Crystal data and structure refinement for V24001..... 825

Table A5.3.2 Atomic coordinates (x 10^4) and equivalent isotropic displacement parameters ($Å^2$x 10^3) for V24001. U(eq) is defined as one third of the trace of the orthogonalized U^{ij} tensor. 826

Table A5.3.3 Bond lengths [Å] and angles [°] for V24001. 828

Table A5.3.4 Anisotropic displacement parameters ($Å^2$x 10^3) for V24001. The anisotropic displacement factor exponent takes the form: $-2p^2[h^2 a^{*2}U^{11} + ... + 2 h k a^* b^* U^{12}]$ 830

Table A5.3.5 Hydrogen coordinates (x 10^4) and isotropic displacement parameters ($Å^2$x 10^3) for V24001..... 832

Table A5.3.6 Torsion angles [°] for V24001..... 833

APPENDIX 6

Notebook Cross-Reference for New Compounds

Table A6.1 Notebook Cross-Reference for Chapter 2. 837

Table A6.2 Notebook Cross-Reference for Chapter 3. 839

Table A6.3 Notebook Cross-Reference for Chapter 4.. 840

LIST OF ABBREVIATIONS

$[\alpha]_D$	specific rotation at wavelength of sodium D line
ºC	degrees Celsius
Å	Angstrom
Aq	aqueous
Ar	aryl
atm	atmosphere
Bn	benzyl
Boc	*tert*-butyloxycarbonyl
bp	boiling point
br	broad
Bz	benzoyl
c	concentration for specific rotation measurements
calc'd	calculated
cm^{-1}	wavenumer(s)
d	doublet
D	deuterium
dba	dibenzylideneacetone
DMF	*N,N*-dimethylformamide
dr	diastereomeric ratio
ee	enantiomeric excess
equiv	equivalent(s)

ESI	electrospray ionization
Et	ethyl
EtOAc	ethyl acetate
G	grams
GC	gas chromatography
h	hours
HPLC	high-performance liquid chromatography
HRMS	high-resolution mass spectrometry
Hz	hertz
IPA	isopropanol
IR	infrared (spectroscopy)
J	coupling constant (NMR), exchange coupling constant (diradicals)
K	Kelvin (absolute temperature)
kcal	kilocalorie
KHMDS	potassium hexamethyldisilazide
L	liter; ligand
LDA	lithium diisopropylamide
m/z	mass to charge ratio
Me	methyl
mg	milligram(s)
MHz	megahertz
min	minutes
mol	mole(s)

n-Bu	*n*-butyl
NMR	nuclear magnetic resonance
Pd/C	palladium on carbon
Ph	phenyl
PHOX	phosphinooxazoline (ligand)
ppm	parts per million
R	generic for any atom or functional groups
Ra/Ni	Raney Nickel
SCF	self-consistent field
SFC	supercritical fluid chromatography
t-Bu	*tert*-butyl
TBAF	tetrabutylammonium fluoride
TBDPS	*tert*-butyldiphenylsilyl
TBS	*tert*-butyldimethylsilyl
Tf	trifluoromethanesulfonyl (trifyl)
TFA	trifluoroacetic acid
THF	tetrahydrofuran
XRD	x-ray diffraction

CHAPTER 1

Development of Asymmetric Reactions of Palladium Enolates Beyond Allylic Alkylation†

1.1 INTRODUCTION

Palladium (Pd), the 46th element of the periodic table and a member of the 'platinum group metals' (PGMs), is named after the asteroid Pallas (⚴), which was discovered shortly before the element was isolated in pure form in 1802.[1] Pallas, in turn is an epithet of the Greek Goddess of reason, wisdom, and war, Athena, who supposedly took this name to honor a mythologic friend she inadvertently killed who shared this name.[2] According to legend and as a further symbol of her remorse, Pallas Athena constructed a statue likeness of her late friend known as 'the Palladium' which was supposedly imbued with protective powers.

As alluded to above, Pd the pure element has been known for some two centuries after first being successfully isolated from crude platinum ore imported from South America by an Englishman, William Wollaston.[1] Confoundingly, instead of publishing a traditional article on his discovery (as he did shortly thereafter on his discovery of Rhodium), Wollaston initially disclosed the discovery of this new element by advertising samples of it for sale in London through an anonymized flyer. These strange circumstances understandingly caused some controversy at the time, but ultimately, Wollaston's 'New

†This review was written in collaboration with Peng-Jui Chen, Dr. Alex Q. Cusumano, Dr. William A. Goddard III, and Dr. Brian M. Stoltz.

Silver' became recognized as an authentic element and was eventually assigned the symbol 'Pd'.[1]

Although discovered in the 19th century, the chemistry of Pd (especially in a homogeneous sense) matured significantly throughout the second half of the 20th century.[3] One example that foreshadowed the upcoming proliferation of organometallic methods reliant on Pd catalysts is the Wacker Process, named for the chemical company whose scientists discovered it in 1956.[4] Specifically, this process converts ethylene to acetaldehyde in the presence of Pd and Cu halide cocatalysts, stoichiometric oxygen, and water (Figure 1.1A). According to one simplified mechanistic picture, water and ethylene displace two halides from Pd(II) species **1** to form intermediate **2**.[5] This is then proposed to undergo an inner sphere migratory insertion to **3**, which, upon β-hydride elimination generates the enol tautomer of acetaldehyde bound to Pd (see **4**). Subsequent isomerization and loss of HCl occurs, followed by Cu mediated reoxidation of Pd by oxygen.[5]

Inspired by this work, Tsuji and Takahashi (at the time industrial chemists at the basic research laboratories of Toyo Rayon Corporation) questioned whether carbon-based nucleophiles could similarly attack a Pd-olefin complex to construct a C–C bond.[6] Ultimately, they published their findings in a classic 1965 communication article in which they report the reaction $PdCl_2$(cod) (**5**) with the sodium enolate of diethylmalonate, generating Pd dimer **6** (Figure 1.1B). Treatment with additional base (such as the dimsyl anion) causes a subsequent deprotonation to **7**, which ultimately generates cyclopropane **8** and metallic Pd.

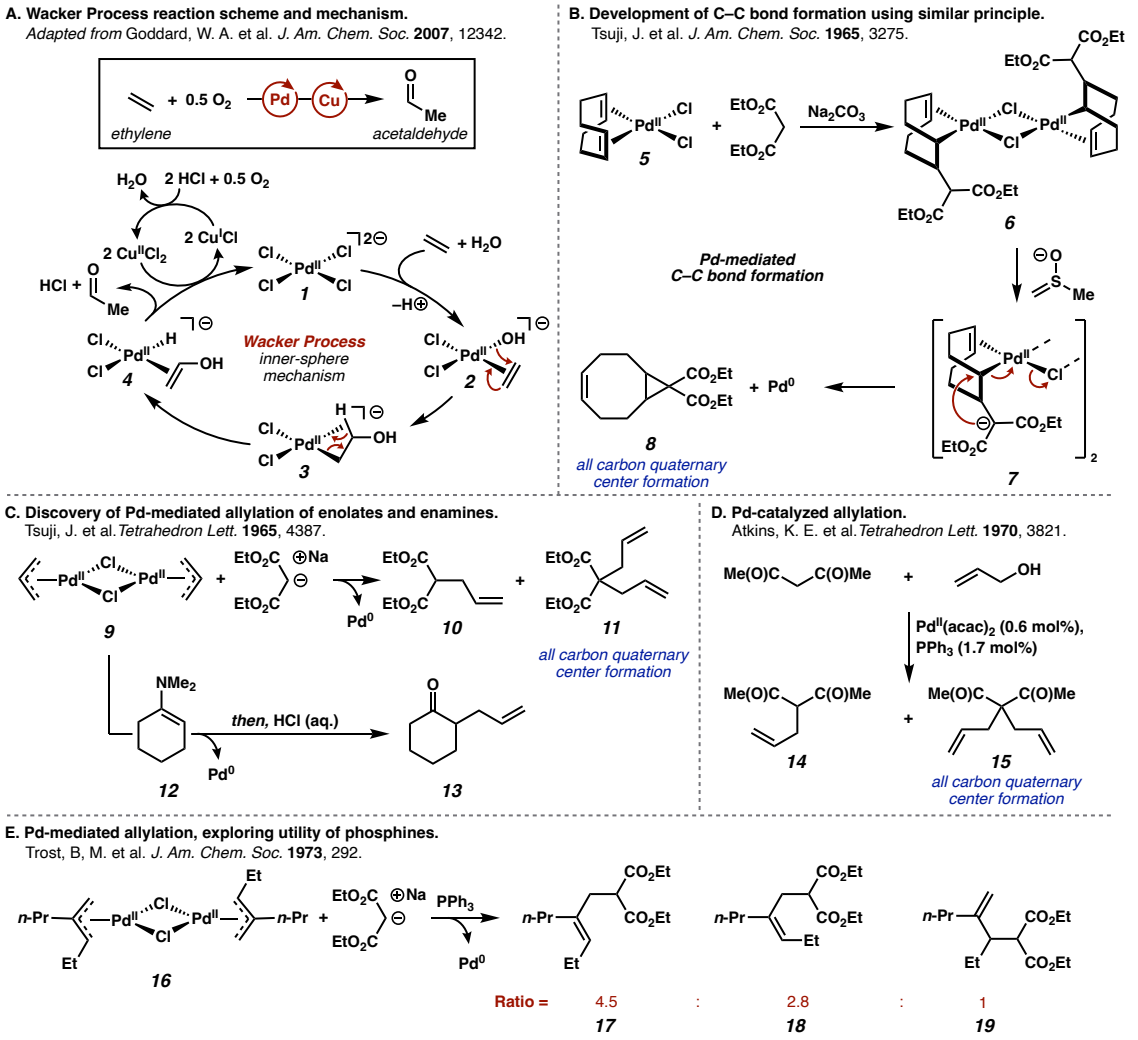

Figure 1.1 *(A) Wacker Process summarized. (B) Development of Pd-mediated C–C bond formation. (C) Pd-mediated allylation of carbon nucleophiles. (D) Pd-catalyzed allylic alkylation. (E) Pd-mediated allylation, exploring utility of phosphines.*

Interested in expanding this to other Pd-olefin complexes, Tsuji and coworkers attempted a similar reaction on $[Pd(allyl)Cl]_2$, which generated metallic Pd alongside two allylated products (**10** and **11**, Figure 1.1C).[6] In addition to sodium enolates, enamine **12** was also a compatible nucleophile leading to **13**. Shortly thereafter, several groups reported

early catalytic variants of this general transformation class (e.g. Figure 1.1D). Pd-mediated reactions between various π-allyl electrophile precursors and nucleophiles have come to be known as Tsuji–Trost allylations for Tsuji's pioneering discoveries and Trost's subsequent extensive contributions ranging from stoichiometric studies to catalytic asymmetric variants (for an example of Trost's contributions, see Figure 1.1E).[7]

Throughout the course of Tsuji's investigations into Pd π-allyl chemistry (and during his time at the Tokyo Institute of Technology), he discovered a Pd-catalyzed variant of the Carroll Rearrangement of allyl esters which proceeds under milder conditions than the uncatalyzed version (**20** to **23**, Figure 1.2A).[8, 9] The authors speculated that this transformation proceeded via initial oxidative addition and decarboxylation to generate a Pd-enolate intermediate (either **21** or **22**, potentially in equilibrium).

On the basis of this hypothesis, Tsuji went on to develop a suite of related reactions over the ensuing years including dehydrogenation (**24**), deacetoxylation (**25**), protonation (**26**), aldol cyclization (**27**), and Michael cyclization (**28**) of the postulated intermediate.[10] One notable feature of several of these transformations is that they readily generate all-carbon quaternary centers. These motifs can be challenging to install due to the steric encumbrance associated with bringing four carbon substituents to a single carbon center.

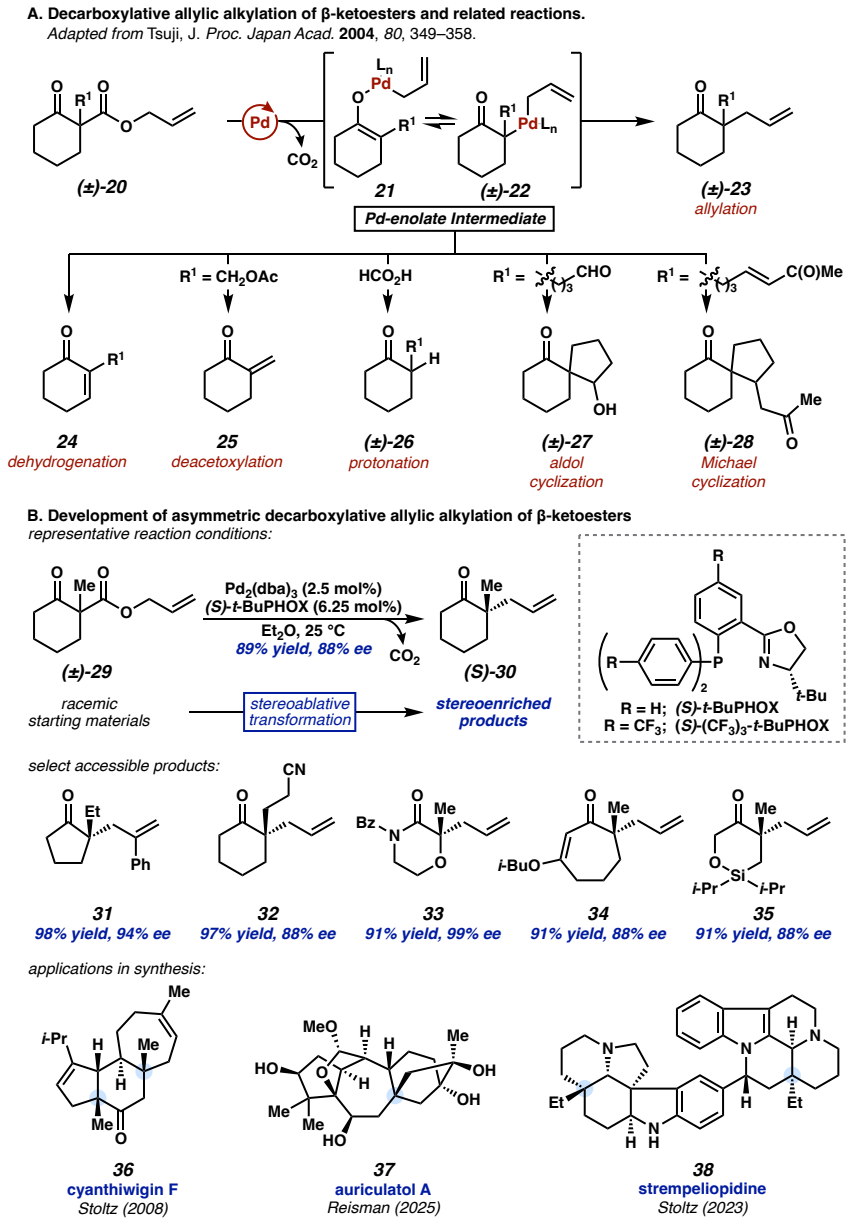

Figure 1.2 *(A) Decarboxylative allylic alkylation of β-ketoesters and related reactions. (B) Development of asymmetric decarboxylative allylic alkylation of β-ketoesters.*

In the mid 2000's, the Stoltz group (in the course of our investigations toward the total synthesis of the zoanthamine alkaloids that bear several all-carbon quaternary stereogenic centers) developed an enantioselective variant of this transformation (**29** to **30**,

Figure 1.2B).[11] This reaction employs a Pd (0 or II) precatalyst in the presence of a Pfaltz-type phosphinooxazoline chiral ligand (commonly either *(S)-t*-BuPHOX or *(S)*-$(CF_3)_3$-*t*-BuPHOX) to transform initially racemic or prochiral starting materials to stereoenriched products. Over the ensuing years, our group has expanded this reaction methodology to access a growing library of enantioenriched products (see select examples **31**–**35**). Additionally, our group and others have applied this reaction strategically to construct all-carbon quaternary centers in the context of natural product total synthesis (e.g. **36**–**38**).[12]

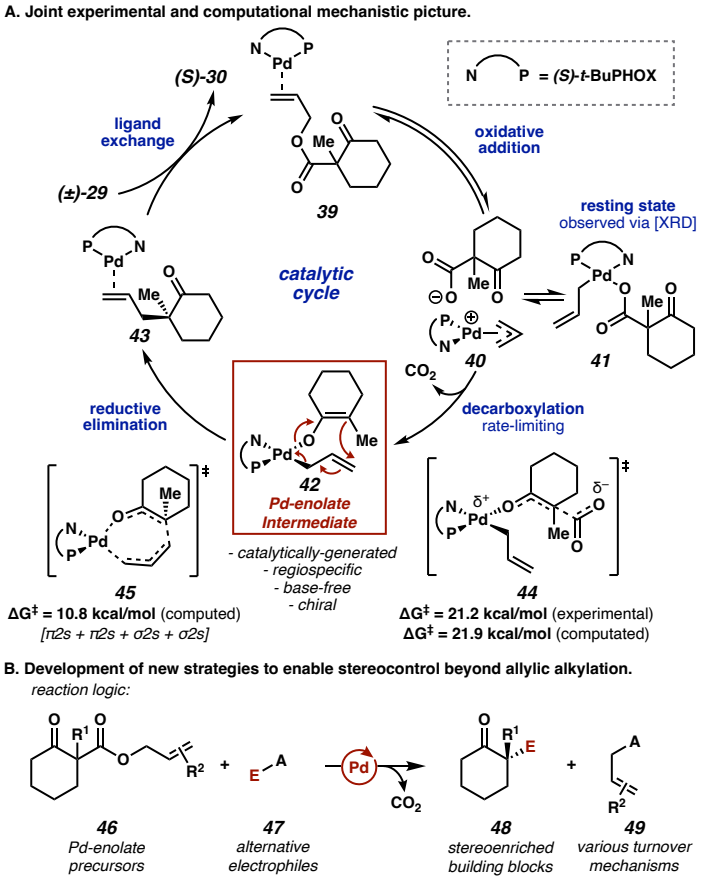

Figure 1.3 *(A) Joint experimental and computational mechanistic picture. (B) Development of new strategies to enable stereocontrol beyond allylic alkylation.*

Since this time, we (alongside excellent collaborators in the Goddard group) have invested considerable effort to develop a mechanistic proposal which is consistent with all of our experimental and computational observations (Figure 1.3A).[13] Namely, this begins with coordination of Pd(0) to the vinyl portion of racemic allyl β-ketoester **29** to form **39** that then undergoes an oxidative addition toward charge separated species **40**. This interconverts with the resting state (**41**) that we can observe as a mixture of diastereomers via SCXRD.[14] This then undergoes a turnover limiting decarboxylation (for TS model see **44**) to generate the computed *O*-bound Pd enolate intermediate **42**. This then undergoes an enantiodetermining inner-sphere [π2s + π2s + σ2s + σ2s] pericyclic reductive elimination (see **45**) that generates **43**. Upon ligand exchange, the catalyst is regenerated and stereoenriched product (**30**) is released.

Given the high stereoselectivity and apparent generality of this class of reaction, we questioned whether this Pd-enolate intermediate might have other utility in the context of asymmetric reactions. These intermediates are attractive because they are catalytically-generated chiral enolates, the formation of which occurs in a regiospecific fashion and in the absence of harsh base. That said, a key challenge associated with utilizing these intermediates toward reactions beyond allylic alkylation is that inner-sphere allylation is a very facile process ($\Delta G^{\ddagger}$ = 10.8 kcal/mol). Despite this, we have developed several distinct approaches that realize the potential of this chiral enolate in reactions beyond allylic alkylation (Figure 1.3B).

1.2 DEVELOPMENT OF ASYMMETRIC REACTIONS OF PALLADIUM ENOLATES

1.2.1 Asymmetric protonation of palladium enolates.

The simplest reaction of an enolate is its protonation, although this is not generally a desired transformation, as many enolates are themselves generated through the reverse deprotonation reaction. That said, by generating an enolate, the stereochemical information present α to the corresponding carbonyl starting material is ablated, which opens the door to a stereoselective protonation. Given the mild conditions under which these Pd-enolates can be generated, this reaction proved a fertile testing ground for an enantioselective interception of such an intermediate.[15]

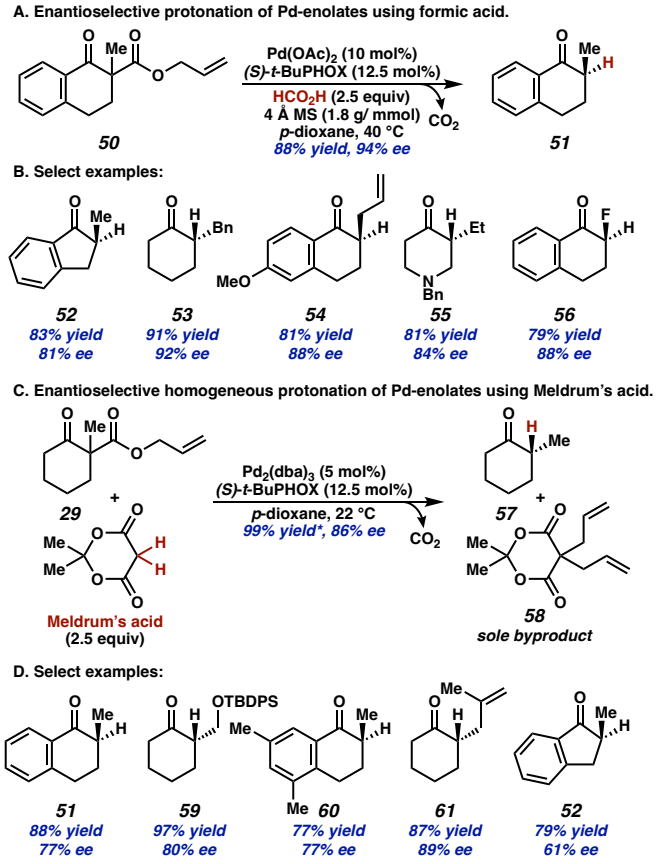

Figure 1.4 *(A) Enantioselective protonation of Pd-enolates using formic acid. (B) Select examples of this transformation. (C) Enantioselective homogeneous*

protonation of Pd-enolates using Meldrum's acid. (D) Select examples of this transformation.

Inspired by non-asymmetric conditions developed by Tsuji and coworkers, we began our development using formic acid as a stoichiometric acid and allyl scavenger (Figure 1.4A). We found that the inclusion of 4 Å MS is required to maintain good levels of enantioselectivity across a range of fused aryl and cyclohexanone derivatives (**51**–**56**, Figure 1.4B). Interestingly, the absolute configuration of products varied by substrate class upon comparison of the optical rotation values to compounds known in the literature. When utilizing HCO_2D under the reaction conditions, a maximum of 35% deuterium incorporation was observed in the corresponding products. Conversely, when DCO_2H was used, <1% deuterium incorporation was observed. When the allyl β-ketoester starting material was exchanged for either an allyl enol carbonate or silyl enol ether Pd-enolate precursor (which generally behave similarly under related asymmetric allylic alkylation conditions), poor selectivity was observed in the former case and sluggish conversion was seen in the latter case.

In the interest of developing a homogeneous variant of this reaction that might prove more amenable to mechanistic investigations, we next explored other classes of proton donor/ allyl scavengers.[15] Ultimately, Meldrum's acid (and related derivatives) were found to be effective proton donors and allyl scavengers in the absence of molecular sieves (**29** to **57**, Figure 1.4C). Interestingly, under the reaction conditions only diallylated Meldrum's acid (**58**) was observed as a byproduct. That said, these mild conditions are similarly effective in the generation of enantioenriched tertiary centers (**51**, **52**, **59**–**61**,

Figure 1.4D). In accord with the heterogeneous conditions, opposite enantiomeric series are observed between the fused aryl and cyclohexanone derived substrates, hinting that a similar mechanistic picture might encompass both of these related reactions.

1.2.2 Asymmetric difunctionalization of alkenes using palladium enolates.

Interested in expanding to electrophiles beyond the proton, our subsequent endeavors have focused on the formation of C–C bonds to our Pd enolate. In order to realize this however, a strong C-based electrophile had to be identified that could outcompete the facile reductive elimination of the inner-sphere allyl group. Initially, we identified highly electrophilic benzylidenemalononitriles (**63**, Figure 1.5A), which in the presence of an appropriate Pd-enolate precursor (**62**) could undergo a Pd-catalyzed stereoselective net alkene difunctionalization that is effectively an intercepted allylic alkylation reaction.[16] Gratifyingly, a diverse range of products are accessible utilizing this reaction methodology (although substrate identity does influence enantio- and diastereoselectivity). Some substrate classes in particular (1,4-piperidinones for instance, **64** and **68**) work very well in this reaction leading to highly enantio- and diasteroenriched products in excellent yields. Generally speaking, reactions that form vicinal quaternary and tertiary stereocenters in a single step are uncommon and this initial success hints at the potential of these Pd-systems to display broad utility and generality in asymmetric catalysis. Intriguingly, the absolute configuration of the products with respect to the stereocenter α to the carbonyl (determined via SCXRD) is the same as the cyclohexanone-derived protonation products. This is also the opposite stereochemical series of the inner-sphere allylation products.

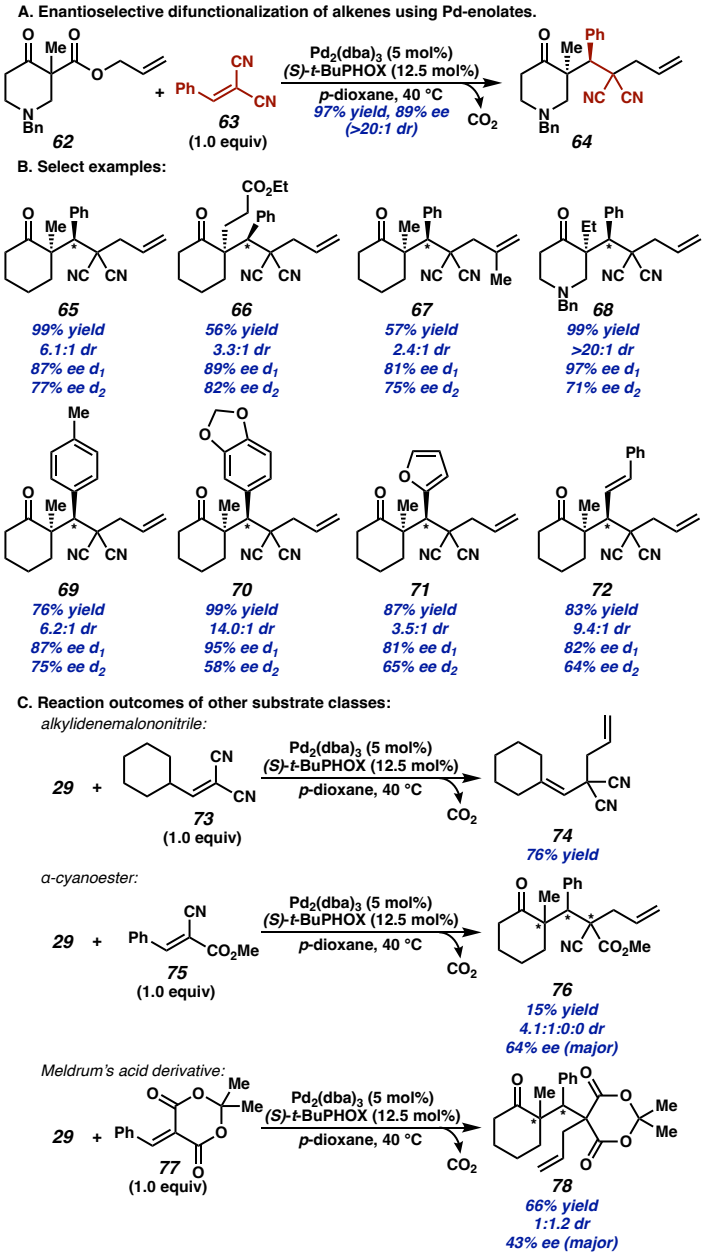

Figure 1.5 *(A) Enantioselective difunctionalization of alkenes using Pd-enolates. (B) Select examples of this transformation. (C) Reaction outcomes of other substrate classes.*

Notably, this intermolecular coupling is generally limited to arylidene- and vinylidenemalononitriles as no target product is observed when alkylidenemalononitriles (**29** and **73** to **74**) are employed (Figure 1.5C). When the malononitrile is replaced by an α-cyanoester (**29** and **75** to **76**) or a Meldrum's acid derivative (**29** and **77** to **78**), target difunctionalized products are observed in diminished yield and low diastereo/ enantioselectivities.

1.2.3 Asymmetric aldol cyclization of palladium enolates.

An orthogonal strategy to intercept a short-lived Pd-enolate intermediate is to intramolecularly tether an electrophile to a Pd-enolate precursor, enabling weaker classes of electrophile to be effectively intercepted. As alluded to previously (see Figure 1.2A), Tsuji displayed that this is an effective strategy in several non-asymmetric examples.[10] Inspired by this approach, we developed an enantioselective aldol spirocyclization reaction that couples Pd-enolates to tethered aldehydes to generate various carbo- and heterospiranes (Figure 1.6A).[17] This reaction utilizes a protic allyl scavenger such as 3,5-dimethylphenol, which enables protonolysis of the postulated Pd-aldolate providing **80** and traps the allyl group (see **81**). For the optimal substrate this reaction proceeds in high yield and good enantio- and diastereoselectivity.

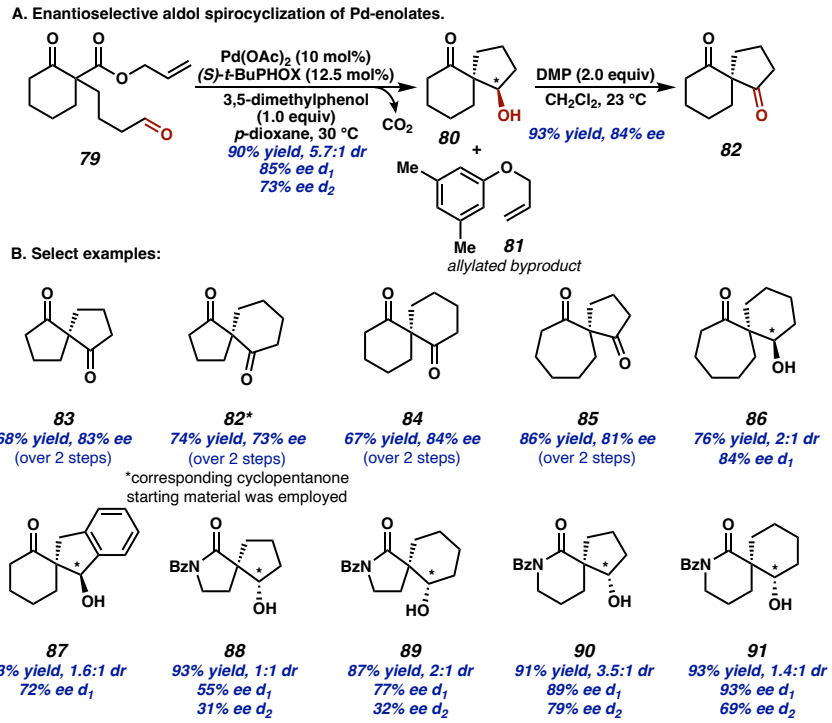

Figure 1.6 *(A) Enantioselective aldol spirocyclization. (B) Select examples of this transformation.*

Beyond the initial substrate, a range of other carbospirocycles can be accessed (**83**–**87**) in good yield and ee in general. Many of these substrates are subsequently oxidized to yield the corresponding 1,3-diketones as the diastereomers of some of the secondary alcohols were challenging to separate chromatographically. In addition to carbocycles, heterocycles are also accessible via this methodology (**88**–**91**) in moderate to good diastereo- and enantioselectivities, but generally high yields. This reaction represents compelling proof-of-principle for stereoselective intramolecular Pd-enolate cyclizations and hints at the complexity of controlling selectivity at multiple stereocenters and across various classes of substrates. The quaternary center formed in these transformations is once

again in the same stereochemical series as is observed for enantioselective protonation of cyclohexanone derivatives (and by extension the asymmetric alkene difunctionalizations). Interestingly, it appears as though the α-stereogenic center derived from the Pd-enolate is the dominant stereo-determining element as opposed to the facial bias of the pendant aldehyde.

1.2.4 Asymmetric isocyanate cyclization of palladium enolates.

Interested in broadening the generality of Pd-enolate chemistry, we next investigated the nucleophilic attack of these intermediates on tethered isocyanates, generated through a Curtius rearrangement from acyl azides (Figure 1.7A).[18] Unlike our previous reactions, this reactivity was not precedented for Pd-enolates in a non-asymmetric fashion. Following extensive screening and optimization, we developed a highly stereoselective cyclization forming spirocyclic γ-lactams (**92** to **94** to **95**) in excellent yield and ee. This chemistry utilized a spirocyclic derivative of Meldrum's acid (**93**) inspired by our prior asymmetric protonation chemistry, which served as a proton source for the resulting lactam and acted as an allyl scavenger, enabling catalyst turnover (see **96**).

Further substitution of the arene (particularly with electron donating substituents) is well tolerated (**97**, **98**), although electron withdrawing substituents can be better accommodated by modification of ligand electronics (i.e., **99**). Heteroaryl derivatives are accessible, albeit in diminished enantioselectivity (**100**). This can by modulated, however, by incorporating an electron donating group (**101**). Oxygen heterocycles are also accessible in good yields and high ee's (**102**, **103**). In addition to 6/5 spiranes, 5/5 and 7/5 derivatives (**104** and **105** respectively) can also be synthesized, with the latter formed in diminished

selectivity. Preliminary mechanistic experiments revealed the importance of utilizing a Pd(II) source as a precatalyst in maintaining high levels of enantioselectivity. Furthermore, a negative nonlinear effect was observed, which is indicative of higher-order Pd species being catalytically relevant. Interestingly, the absolute configuration of products formed in this reaction is consistent with the protonation products observed for tetralone derivatives.

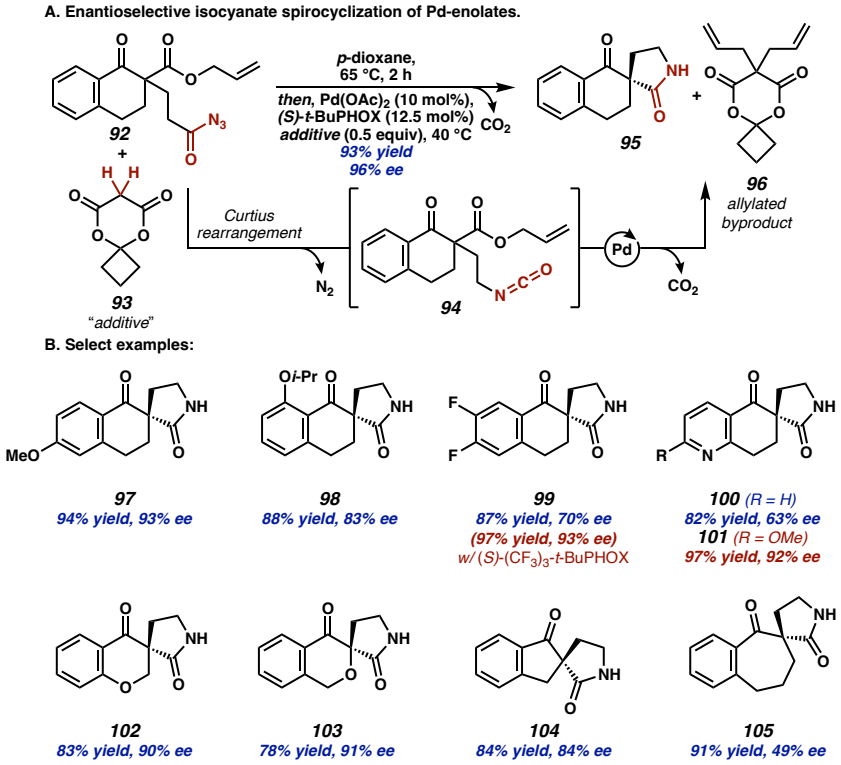

Figure 1.7 *(A) Enantioselective isocyanate spirocyclization of Pd-enolates. (B) Select examples of this transformation.*

1.3 CONCLUSIONS AND OUTLOOK

Taken together, these investigations describe the true utility of Pd-enolates as intermediates in a diverse range of enantioselective transformations beyond allylic alkylation. We have shown the feasibility of both inter- and intramolecular reactions and

the potential to impart control over multiple stereocenters generated in a single step. Many of these enantioselective variants represent expansions upon reported non-asymmetric reactions with notable modifications being required to enable enantioselectivity. Unlike our studies of Pd-catalyzed decarboxylative allylic alkylation, we have yet to construct a fully coherent overarching mechanistic picture that is consistent with all of the observations in these studies. Generally, the reactivity observed is consistent with our hypothesized Pd-enolate intermediate, but the fine details separating different reaction classes and substrates hints that there are multiple distinct but related mechanisms that can be operable. Based on the transformations developed, it seems in general that cyclohexanone vs. tetralone derivatives tend to produce products in opposite enantiomeric series and that cyclohexanone products are formed in the opposing series as allylic alkylation products. Interestingly, we have found empirically that the inclusion (and identity) of proton sources/ allyl scavengers apparently has a large influence on the productivity and selectivity of these transformations. Some classes of reaction (such as the alkene difunctionalization) work well without them, whereas others (such as the isocyanate cyclization) rely upon them for maintained selectivity.

Understanding the observed reactivity trends across these disparate systems holds the potential to establish a set of rational design principles that will allow further developments. The ensuing chapters seek to: 1) gain new insights into the origins of stereocontrol in these processes, 2) develop additional strategies to enable catalytic turnover in these systems, and 3) elucidate design heuristics that will expedite future reaction discovery and optimization.

1.4 REFERENCES AND NOTES

(1) (a) Tikkanen, A. Palladium. *Encyclopedia Britannica*, Britannica Editors; Encylopedia Britannica Inc., 2026. (b) Griffith, W. P. Bicentenary of Four Platinum Group Metals. Part I: Rhodium and Palladium – Events Surrounding their Discoveries. *Platinum Metals Rev.* **2003**, *47*, 175–183.

(2) Roy, G. Athena. *Encyclopedia Britannica*, Britannica Editors; Encyclopedia Britannica Inc., 2026.

(3) (a) Suzuki, A. Cross-Coupling Reactions of Organoboranes: an Easy Way to Construct C–C Bonds (Nobel Lecture). *Angew. Chem. Int. Ed.* **2011**, *50*, 6723–6737. (b) Negishi, E.-i. Magical Power of Transition Metals: Past, Present, and Future (Nobel Lecture). *Angew. Chem. Int. Ed.* **2011**, *50*, 6738–6764.

(4) (a) Jira, R. Acetaldehyde from Ethylene – a Retrospective on the Discovery of the Wacker Process. *Angew. Chem. Int. Ed.* **2009**, *48*, 9034–9037. (b) Mhaldar, S. N.; Gaikwad, M. M.; Tilve, S. G. Wacker Oxidation: a Powerful Tool for Natural Product Synthesis. *Asian J. Org. Chem.* **2025**, *14*, e202500117.

(5) This reaction has been the subject of extensive experimental and computational investigations. The mechanism presented above is a simplified picture of what is believed to be one of multiple potential pathways. For three articles exploring this reaction's mechanism in more depth, see: (a) Keith, J. A.; Nielsen, R. J.; Oxgaard, J.; Goddard III, W. A. Unraveling the Wacker Oxidation Mechanisms. *J. Am. Chem. Soc.* **2007**, *129*, 12342–12343. (b) Keith, J. A.; Henry, P. M. The Mechanism of the

Wacker Reaction: A Tale of Two Hydroxypalladations. *Angew. Chem. Int. Ed.* **2009**, *48*, 9038–9049. (c) Stirling, A.; Nair, N. N.; Lledós, A.; Ujaque, G. Challenges in Modelling Homogeneous Catalysis: New Answers from Ab Initio Molecular Dynamics to the Controversy over the Wacker Process. *Chem. Soc. Rev.* **2014**, *43*, 4940–4952.

(6) (a) Smidt, J.; Hafner, W. Eine Reaktion von Palladiumchlorid mit Allylalkohol. *Angew. Chem.* **1959**, *71*, 284. (b) Tsuji, J. Organopalladium Chemistry in the '60s and '70s. *New. J. Chem.* **2000**, *24*, 127–135. (c) Tsuji, J.; Takahashi, H. Organic Syntheses by Means of Noble Metal Compounds. XII. Reaction of the Cyclooctadiene–Palladium. Chloride Complex with Ethyl Malonate. *J. Am. Chem. Soc.* **1965**, *87*, 3275–3276. (d) Tsuji, J.; Takahashi, H.; Morikawa, M. Organic Syntheses by Means of Noble Metal Compounds XVII. Reaction of π-Allylpalladium Chloride with Nucleophiles. *Tetrahedron Lett.* **1965**, *49*, 4387–4388. (e) Tsuji, J. Carbon–Carbon Bond Formation via Palladium Complexes. *Acc. Chem. Res.* **1969**, *2*, 144–152.

(7) (a) Atkins, K. E.; Walker, W. E.; Manyik, R. M. Palladium Catalyzed Transfer of Allylic Groups. *Tetrahedron Lett.* **1970**, *43*, 3821–3824. (b) Hata, G.; Takahashi, K.; Miyake, A. Palladium-Catalysed Exchange of Allylic Groups of Ethers and Esters with Active-Hydrogen Compounds. *Chem. Commun.* **1970**, 1392–1393. (c) Trost, B. M. Metal Catalyzed Allylic Alkylation: its Development in the Trost Laboratories. *Tetrahedron* **2015**, *71*, 5708–5733. (d) Trost, B. M.; Fullerton, T. J.

New Synthetic Reactions. Allylic Alkylation. *J. Am. Chem. Soc.* **1973**, *95*, 292–293.

(8) Carroll, M. F. Addition of αβ-Unsaturated Alcohols to the Active Methylene Group. Part I. The Action of Ethyl Acetoacetate on Linalool and Geraniol. *J. Chem. Soc.* **1940**, 704–706.

(9) (a) Shimizu, I.; Yamada, T.; Tsuji, J. Palladium-Catalyzed Rearrangement of Allylic Esters of Acetoacetic Acid to Give ɣ,δ-Unsaturated Methyl Ketones. *Tetrahdron Lett.* **1980**, *21*, 3199–3202. (b) Tsuda, T.; Chujo, Y.; Nishi, S.-i.; Tawara, K.; Saegusa, T. *J. Am. Chem. Soc.* **1980**, *102*, 6381–6384. (c) Tsuji, J.; Minami, I.; Shimizu, I. Palladium-Catalyzed Allylation of Ketones and Aldehydes via Allyl Enol Carbonates. *Tetrahedron Lett.* **1983**, *24*, 1793–1796.

(10) Tsuji, J. Development of β-Keto Ester and Malonate Chemistry. Palladium-Catalyzed New Reactions of their Allylic Esters. *Proc. Japan Acad.* **2004**, *80*, 349–358.

(11) (a) Behenna, D. C.; Stoltz, B. M. The Enantioselective Tsuji Allylation. *J. Am. Chem. Soc.* **2004**, *126*, 15044–15045. (b) Mohr, J. T.; Behenna, D. C.; Harned, A. M.; Stoltz, B. M. Deracemization of Quaternary Stereocenters by Pd-Catalyzed Enantioconvergent Decarboxylative Allylation of Racemic β-Ketoesters. *Angew. Chem. Int. Ed.* **2005**, *44*, 6924–6927. (c) Mohr, J. T.; Stoltz, B. M. Enantioselective Tsuji Allylations. *Chem. Asian. J.* **2007**, *2*, 1476–1491. (d) Liu, Y.; Han, S.-J.; Liu, W.-B.; Stoltz, B. M. Catalytic Enantioselective Construction of Quaternary

Stereocenters: Assembly of Key Building Blocks for the Synthesis of Biologically Active Molecules. *Acc. Chem. Res.* **2015**, *48*, 740–751.

(12) (a) Enquist, J. A.; Stoltz, B. M. The Total Synthesis of (–)-Cyanthiwigin F by Means of Double Catalytic Enantioselective Alkylation. *Nature* **2008**, *453*, 1228–1231. (b) Thompson, J. K.; Youngblood, K. C.; Teh, Y. H. S.; Farley, C. M.; Zhang, Z.; Virgil, S. C.; Reisman, S. E. Enantioselective Synthesis of (+)-Auriculatol A. *J. Am. Chem. Soc.* **2025**, *147*, 42170–42174. (c) Rand, A. W.; Gonzalez, K. J.; Reimann, C. E.; Virgil, S. C.; Stoltz, B. M. Total Synthesis of Strempeliopidine and Non-Natural Stereoisomers through a Convergent Petasis Borono–Mannich Reaction. *J. Am. Chem. Soc.* **2023**, *145*, 7278–7287.

(13) (a) Keith, J. A.; Behenna, D. C.; Mohr, J. T.; Ma, S.; Marinescu, S. C.; Oxgaard, J.; Stoltz, B. M.; Goddard, W. A. The Inner-Sphere Process in the Enantioselective Tsuji Allylation Reaction with (S)-t-Bu-phosphinooxazoline Ligands. *J. Am. Chem. Soc.* **2007**, *129*, 11876–11877. (b) Keith, J. A.; Behenna, D. C.; Sherden, N.; Mohr, J. T.; Ma, S.; Marinescu, S.; Nielsen, R. J.; Oxgaard, J.; Stoltz, B. M.; Goddard, W. A. The Reaction Mechanism of the Enantioselective Tsuji Allylation: Inner-Sphere and Outer-Sphere Pathways, Internal Rearrangements, and Asymmetric C−C Bond Formation. *J. Am. Chem. Soc.* **2012**, *134*, 19050–19060. (c) Cusumano, A. Q.; Stoltz, B. M.; Goddard, W. A. Reaction Mechanism, Origins of Enantioselectivity, and Reactivity Trends in Asymmetric Allylic Alkylation: A Comprehensive Quantum Mechanics Investigation of a $C(sp^3)$−$C(sp^3)$ Cross-Coupling. *J. Am.*

Chem. Soc. **2020**, *142*, 13917–13933. (d) Cusumano, A. Q.; Goddard, W. A.; Stoltz, B. M. The Transition Metal Catalyzed [π2s + π2s + σ2s + σ2s] Pericyclic Reaction: Woodward−Hoffmann Rules, Aromaticity, and Electron Flow. J. Am. Chem. Soc. 2020, 142, 19033–19039. (e) McPherson, K. E.; Croatt, M. P.; Morehead, A. T.; Sargent, A. L. DFT Mechanistic Investigation of an Enantioselective Tsuji−Trost Allylation Reaction. *Organometallics* **2018**, *37*, 3791–3802.

(14) Sherden, N. H.; Behenna, D. C.; Virgil, S. C.; Stoltz, B. M. Unusual Allylpalladium Carboxylate Complexes: Identification of the Resting State of Catalytic Enantioselective Decarboxylative Allylic Alkylation Reactions of Ketones. *Angew. Chem. Int. Ed.* **2009**, *48*, 6840–6843.

(15) (a) Mohr, J. T.; Nishimata, T.; Behenna, D. C.; Stoltz, B. M. Catalytic Enantioselective Decarboxylative Protonation. *J. Am. Chem. Soc.* **2006**, *128*, 11348–11349. (b) Marinescu, S. C.; Nishimata, T.; Mohr, J. T.; Stoltz, B. M. Homogeneous Pd-Catalyzed Enantioselective Decarboxylative Protonation. *Org. Lett.* **2008**, *10*, 1039–1042. (c) Tsuji, J.; Nisar, M.; Shimizu, I. Facile Palladium-Catalyzed Decarboxylation Reaction of Allylic β-Keto Esters. *J. Org. Chem.* **1985**, *50*, 3416–3417. (d) Mandai, T.; Imaji, M.; Takada, H.; Kawata, M.; Nokami, J.; Tsuji, J. Facile Transformation of Substituted Allyl Malonates to Monocarboxylic Acids and Esters by the Reaction with Ammonium Formate Catalyzed by Palladium Complexes. *J. Org. Chem.* **1989**, *54*, 5395–5397.

(16) (a) Streuff, J.; White, D. E.; Virgil, S. C.; Stoltz, B. M. A Palladium-Catalyzed Enolate Alkylation Cascade for the Formation of Adjacent Quaternary and Tertiary Stereocentres. *Nat. Chem.* **2010**, *2*, 192–196. (b) Patil, N. T.; Yamamoto, Y. Palladium-Catalyzed Cascade Reactions of Highly Activated Olefins. *Synlett* **2007**, *13*, 1994-2005.

(17) (a) Inanaga, K.; Wollenburg, M.; Bachman, S.; Hafeman, N. J.; Stoltz, B. M. Catalytic Enantioselective Synthesis of Carbocyclic and Heterocyclic Spiranes via a Decarboxylative Aldol Cyclization. *Chem. Sci.* **2020**, *11*, 7390–7395. (b) Nokami, J.; Mandai, T.; Watanabe, H.; Ohyama, H.; Tsuji, J. The Palladium-Catalyzed Directed Aldol Reaction of Aldehydes with Ketone Enolates Generated by the Decarboxylation of Allyl β-Keto Carboxylates under Neutral Conditions. *J. Am. Chem. Soc.* **1989**, *111*, 4126–4127.

(18) Barbor, J. P.; Flesch, K. N.; Chan, M.; Ang, H. R.; Stoltz, B. M. Enantioselective Spirocyclization of Pd-Enolates and Isocyanates. *Angew. Chem. Int. Ed.* **2025**, *64*, e202502583.

CHAPTER 2

Asymmetric [4+2] Cycloaddition of Pd Enolates†

2.1 INTRODUCTION

The enantioselective construction of all-carbon quaternary stereocenters represents a central and ongoing challenge in synthetic organic chemistry.[1] Asymmetric allylic alkylation of enolate nucleophiles represents a powerful strategy to access such motifs.[2] A notable aspect of the Pd-catalyzed allylic alkylation methodology developed by our group is the inner-sphere reductive elimination that occurs from an *O*-bound Pd enolate intermediate (**106**), yielding enantioenriched ketones (**23**) (Figure 2.1A).[3, 4] This intermediate can be catalytically generated from achiral or racemic enolate precursors, such as allyl enol carbonates and β-ketoesters (**20**).[5, 6] This enolate is accessed in the absence of harsh base, under mild and neutral conditions, in a regiospecific fashion, and under catalytic conditions. Other canonical conditions for enolate formation are often plagued by regioselectivity challenges and typically require the application of a strong base or Lewis acid. Given the advantages offered by Pd enolates, we sought to exploit their reactivity toward more general asymmetric transformations.

As proof of principle, our group demonstrated the enantioselective protonation of Pd enolates as a successful strategy to access ketones with an adjacent tertiary stereocenter (**107**).[7] Subsequently, we have developed methods to construct quaternary centers via

†This research was performed in collaboration with Flesch, K. N.; Cusumano, A. Q.; Chen, P.-J.; Sardini, S. R.; Du, Y. E.; Portions of this chapter have been reproduced with permission from Stoltz, et al. *J. Am. Chem. Soc.* **2023**, *145*, 11301–11310. © 2023 American Chemical Society.

enantioselective intermolecular alkene difunctionalization (**108**), intramolecular aldol spirocyclization (**109**), and intramolecular spirocylization of in-situ generated isocyanates (**110**).[8, 9] Taken together, these advances display the feasibility of employing Pd enolates as nucleophiles in enantioselective reactions beyond allylic alkylation.

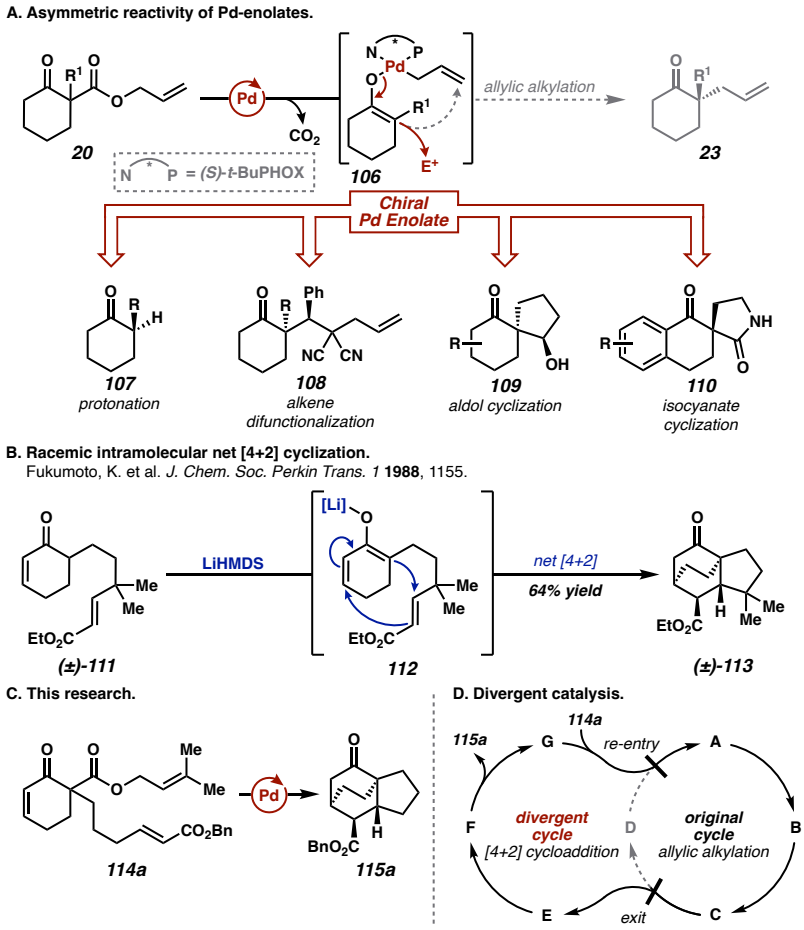

Figure 2.1 *(A) Asymmetric reactivity of Pd-enolates. (B) Racemic intramolecular net [4+2] cyclization. (C) This reasearch. (D) Divergent catalysis.*

Interestingly, Fukumoto and coworkers reported a unique reaction of Li enolates, a formal [4+2] reaction from an in situ generated conjugated lithium enolate (**112**), forging tricyclic product **113** in a racemic fashion (Figure 2.1B).[10] Inspired, we envisioned an

analogous asymmetric transformation could be tractable from a chiral, conjugated Pd enolate derived from the decarboxylation of unsaturated β-ketoester **114a** (Figure 2.1C). To realize this complex transformation, we sought to develop a conceptual framework that would leverage our prior mechanistic understanding and enable us to expand the utility of Pd enolates. We refer to this strategy as 'divergent catalysis' (see Figure 2.1D), where the point of divergence is the common Pd enolate intermediate (**C**), with the desired alternative reactivity occurring through a series of alternative steps (see **E**–**G**). This is followed by subsequent reentry into the original catalytic cycle, allowing for regeneration of the catalyst.

Applying this strategy, we developed a catalytic decarboxylative asymmetric intramolecular [4+2] cycloaddition of conjugated Pd enolates. Subsequently, we performed mechanistic investigations including quantum mechanics calculations, Eyring analysis, and KIE studies that offer insight into the reaction's mechanism. This transformation enables access to tricyclic scaffolds bearing 4–5 contiguous stereocenters with 1–2 being quaternary.

2.2 RESULTS AND DISCUSSION

2.2.1 Reaction design and optimization.

Employing unsaturated β-ketoester **116** as a precursor for conjugated Pd enolate **117**, we hypothesized that the precented allylic alkylation forming **118** could be interrupted by a [4+2] cycloaddition, generating **119** (Figure 2.2A). Subsequent reductive elimination of transposed enolate **119**, will enable catalyst turnover and forge tricyclic product **120**. In practice however, the rate of premature allylic alkylation of enolate **117** supersedes the desired divergent reactivity as subjection of **116** to our standard conditions produces ketone

118 in 98% yield and 84% ee (Figure 2.2B). According to our design framework (Figure 2.1D), this required us to modify our exit strategy. In principle, this could be tuned by increasing the rate of the desired cycloaddition via modification of the diene or dienophile, or addition of an exogenous Lewis acid. In practice, however, we felt these approaches might limit the reaction's scope.

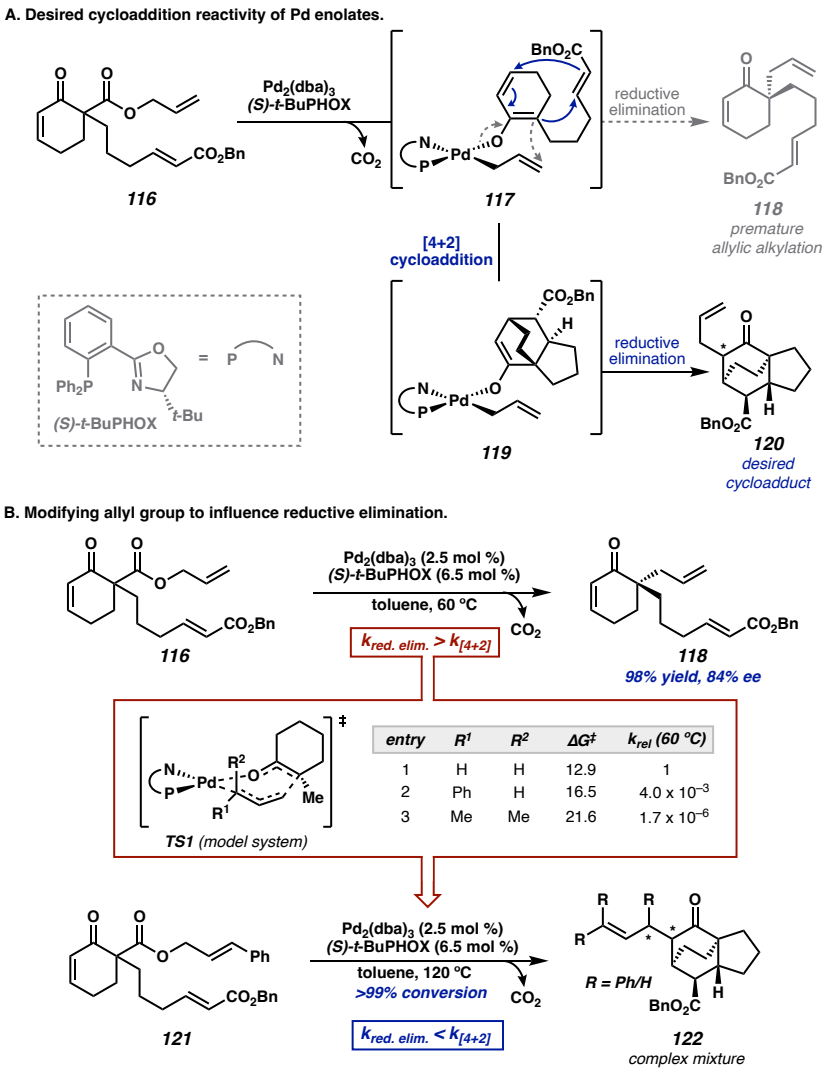

Figure 2.2 *(A) Desired cycloaddition reactivity of Pd enolates. (B) Modifying allyl group to influence reductive elimination.*

Alternatively, we sought to impede the rate of allylic alkylation through substitution of the allyl group. We have previously observed that terminal substitution of the allyl group slows down the rate of conversion in these reactions. A computational investigation of a model system (**TS1**) suggested that introduction of terminal substitution on the allyl group raises the barrier to reductive elimination, decreasing the rate of allylic alkylation (see experimental section for computational details).[11] For example, phenyl substitution (entry 2) slows the rate of inner-sphere reductive elimination by about 3 orders of magnitude. Inspired by these computational and experimental results, we explored the experimental efficacy of cinnamyl ester substrate **121** in the [4+2] reaction. In alignment with our hypothesis, the desired tricyclic core was observed (**122**), albeit as a complex mixture of isomers, thereby hampering the synthetic utility. To address this, we sought to develop an alternative strategy for catalyst turnover that could simplify the product outcome.

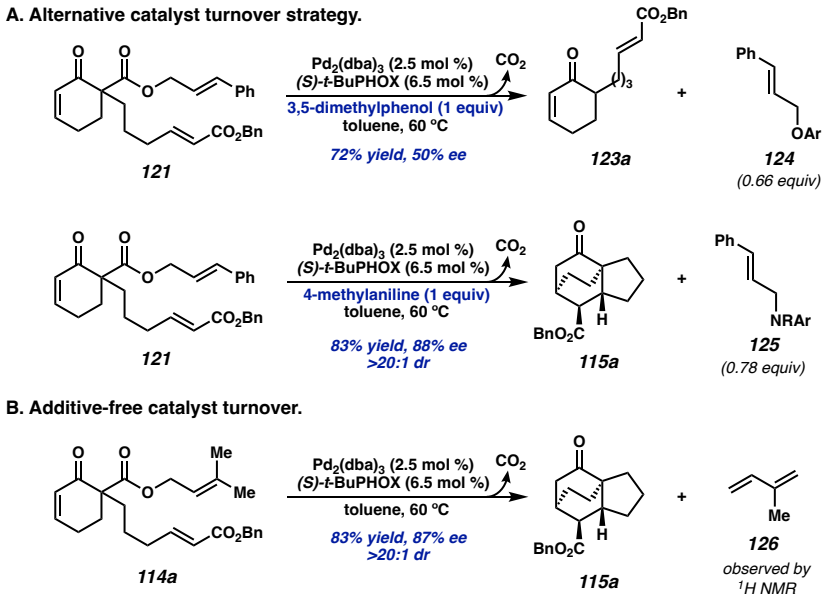

Figure 2.3 *(A) Alternative catalyst turnover strategy. (B) Additive-free catalyst turnover.*

Building upon prior findings from our group, we sought to employ stoichiometric protic allyl scavengers to enable catalyst turnover. These exogenous acids serve the dual role of protonating the transposed enolate (such as **119**) and enabling turnover of the catalyst by reductively deallylating palladium. Addition of 3,5-dimethylphenol[9] exclusively yielded premature protonation product **123a** alongside the corresponding aryl ether (**124**, Figure 2.3A). Gratifyingly, exchange of the phenol additive with 4-methylaniline afforded the desired *endo* [4+2] adduct **115a** as a single diastereomer in 83% yield and 88% ee. In an effort to further improve the reaction yield, the competency of β-ketoester **114a**, derived from the commodity chemical prenol, was explored. According to our computational investigation, a substrate bearing a di-substituted allyl moiety would similarly hinder premature allylic alkylation by raising the barrier to reductive elimination (entry 3, Figure 2.2B). Perplexingly, while the desired tricyclic product **115a** was generated in 73% isolated yield and 88% ee, no alkylated 4-methylaniline (**125**) was observed as a byproduct (entry 8, Table 1.1). When a control reaction excluding 4-methyl aniline was carried out, tricycle **115a** was formed in 83% yield and 87% ee (Figure 2.3B), suggestive that an alternative catalyst turnover mechanism is operative. Further NMR investigation revealed the stoichiometric evolution of isoprene (**126**) accompanying the formation of product **115a**. Intrigued by this serendipitous result and the outstanding reaction profile, we pursued optimization of additive-free reaction conditions.

The reaction proceeds in THF or benzene albeit in slightly diminished yield and enantioselectivity (entries 2–3, Table 2.1). Employing 1,4-dioxane as the solvent, protonation product **123a** was obtained as the major product in 63% yield and 49% ee,

while cycloadduct **115a** was observed in a mere 12% yield (entry 4). Lowering the temperature to 40 °C slightly improved the ee to 89% at the cost of slower conversion (entry 5). Modification of the electronic properties of the PHOX ligand had a deleterious effect on product distribution (entries 6–7). Phenol or aniline additives do not improve the reaction (entries 8–10).

Table 2.1 *Optimization of reaction conditions.*[a]

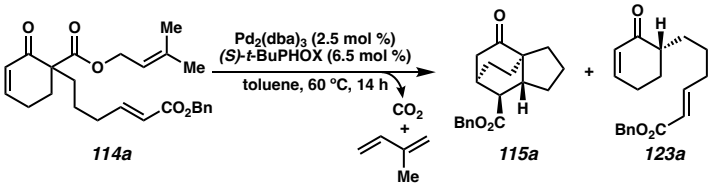

Entry	Deviation from standard conditions	Yield *115a* (%)[b]	ee *115a* (%)	Yield *123a* (%)[b]	ee *123a* (%)
1	none	96 (83)	87 (87)	–	–
2	THF	86	81	–	–
3	benzene	92	87	–	–
4	1,4-dioxane	12	–	63	49
5	40 °C	51	89	–	–
6	*(S)*-$(CF_3)_3$-*t*-BuPHOX	12	89	66	62
7	*(S)*-$(OMe)_3$-*t*-BuPHOX	40	88	26	65
8	4-methylaniline (1 equiv)	93 (73)	87 (88)	–	–
9	4-methylaniline (2 equiv)	78	87	–	–
10	3,5-dimethylphenol (1 equiv)	0	–	100	71

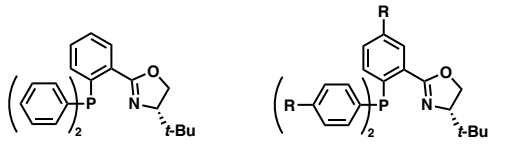

(S)-*t*-BuPHOX

R = CF_3: *(S)*-$(CF_3)_3$-*t*-BuPHOX
R = OMe: *(S)*-$(OMe)_3$-*t*-BuPHOX

[a] Conditions: 0.02 mmol **114a**, 2.5 mol % $Pd_2(dba)_3$, 6.5 mol % ligand, in 1.0 mL of solvent (0.02 M). [b] Yields determined by ^1H NMR with respect to 1,3,5-trimethoxybenzene as internal standard. Isolated yields on 0.2 mmol scale in parentheses.

Therefore, optimal reaction conditions were determined to be additive free with *(S)*-*t*-BuPHOX in toluene and at 60 °C. Under these conditions the reaction affords **115a**, a bridged bicycle with a pendant fused 5-membered ring in 83% isolated yield and 87% ee.

This transformation enables the simultaneous construction of four contiguous stereocenters one of which being an all-carbon quaternary center. The reaction can also be carried out with reduced catalyst loading (0.625 mol%) on 1.0 mmol scale to afford **115a** in 59% yield and 89% ee. The major enantiomer of product is determined by vibrational circular dichroism (VCD) spectroscopy (see experimental section for details). The ability to efficiently and enantioselectively construct a complex molecular framework on scale highlights the potential synthetic utility of this reaction.

2.2.2 Proposed mechanism.

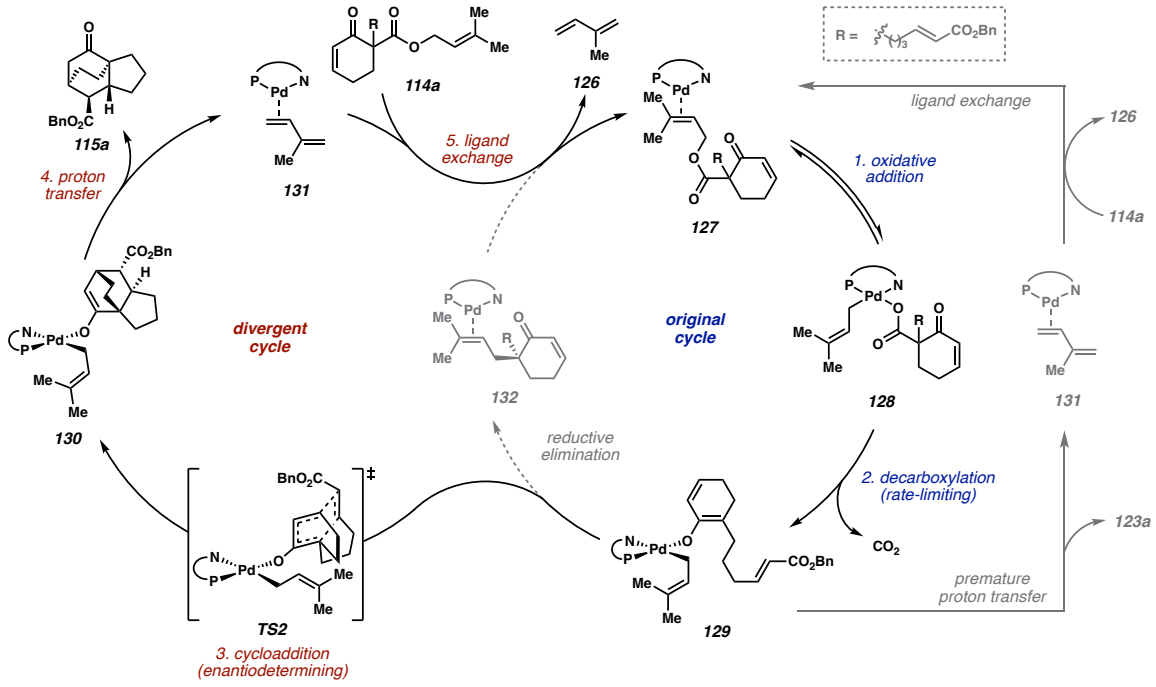

Figure 2.4 *Proposed catalytic cycle with undesired pathways in gray.*

Based on these exciting results, we sought to construct a mechanistic model to inform subsequent reaction design. Based on our previous investigations of Pd-catalyzed decarboxylative asymmetric allylic alkylation reactions, we propose that oxidative addition

of Pd(0) to β-ketoester **114a** proceeds through complex **127** to afford the η^1-allyl carboxylate **128**, which has been shown in related systems to be the resting state (Figure 2.4).[12] Decarboxylation then ensues, affording *O*-bound Pd enolate **129**. This chiral, conjugated enolate then serves as the diene in an endo selective [4+2] cycloaddition (**TS2**) with the pendant dienophile to form tricyclic enolate **130**. From the standpoint of stereochemistry, the dienolate facial bias is opposite to that of the canonical allylic alkylation, suggesting a transition state for the cycloaddition that resembles **TS2**. Subsequent proton transfer generates **115a** concomitant with isoprene generation (see **131**). Ligand exchange releases isoprene and turns over the catalyst. Alternatively, we posit that formation of undesired ketone **123a** could occur via an off-cycle pathway, where catalyst turnover occurs prior to cycloaddition via premature proton transfer to **129**.

2.2.3 Substrate scope.

With our mechanistic hypothesis in hand, we sought to draw additional insights by using substrate design to explore the limitations of this transformation. Considering the inverse relationship between diene ring size and Diels–Alder reaction rate, we explored whether this trend effects the generality of this reaction.[2, 13] When cyclopentenone substrate **114c** was employed, a decrease in yield and ee was observed when compared to the parent substrate **114a** (Table 2.2). Compared to five- and six-membered rings, seven-membered cyclic dienes require increased distortion energy to reach the desired [4+2] transition state. Despite this, substrate **114d** leads to high yield and improved ee. Accordingly, this reaction represents a powerful methodology to synthesize a range of bicyclic cores fused to a pendant five-membered ring.

Table 2.2 *Substrate scope of the [4+2] reaction.*[a]

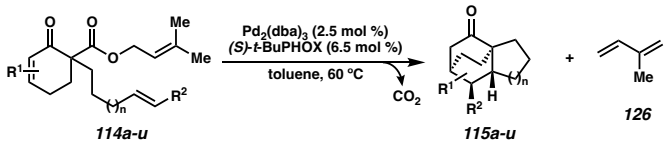

Substrate	Product(s)
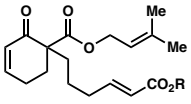 R = Bn ***114a*** R = Et ***114b***	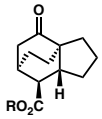 ***115a (endo)*** 83% yield, 87% ee ***115b (endo)*** 85% yield, 88% ee
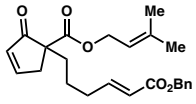 ***114c***	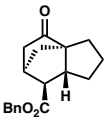 ***115c (endo)*** 65% yield, 65% ee
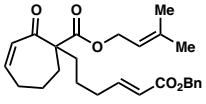 ***114d***	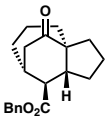 ***115d (endo)*** 83% yield, 97% ee
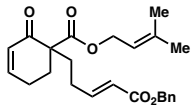 ***114e***	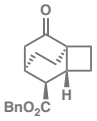 ***115e (endo)*** (not observed) 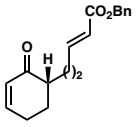 ***123e*** 81% yield, 47% ee
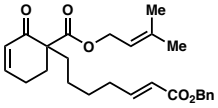 ***114f***	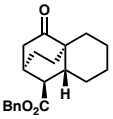 ***115f (endo)*** 42% yield, 92% ee 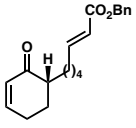 ***123f*** 45% yield, 51% ee
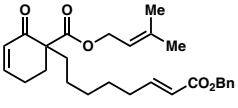 ***114g***	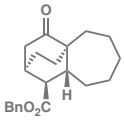 ***115g (endo)*** (not observed) 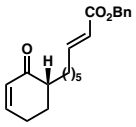 ***123g*** 74% yield, 56% ee

Substrate	Product(s)	
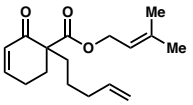 ***114h***	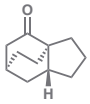 ***115h (endo)*** (not observed)	***123h*** 33% yield, 58% ee
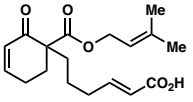 ***114i***	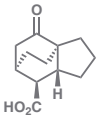 ***115i (endo)*** (not observed)	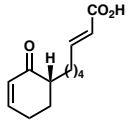 ***123i*** 80% yield, 7% ee
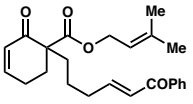 ***114j***	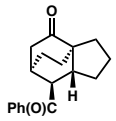 ***115j (endo)*** 50% yield, 87% ee	
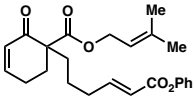 ***114k***	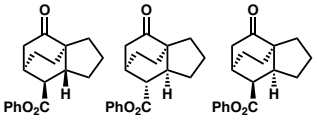 ***115k (endo) 115k' (exo) 115k'' (other)*** 82% yield, 10.4:1.4:1 dr, 88% ee (endo)	
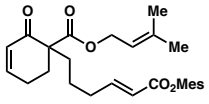 ***114l***	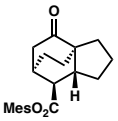 ***115l (endo)*** 90% yield, 89% ee	
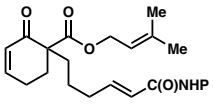 ***114m***	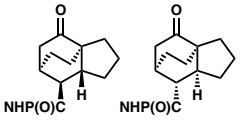 ***115m (endo) 115m' (exo)*** 65% yield, 1.4:1 dr[b] 62% ee (endo), 62% ee (exo)	

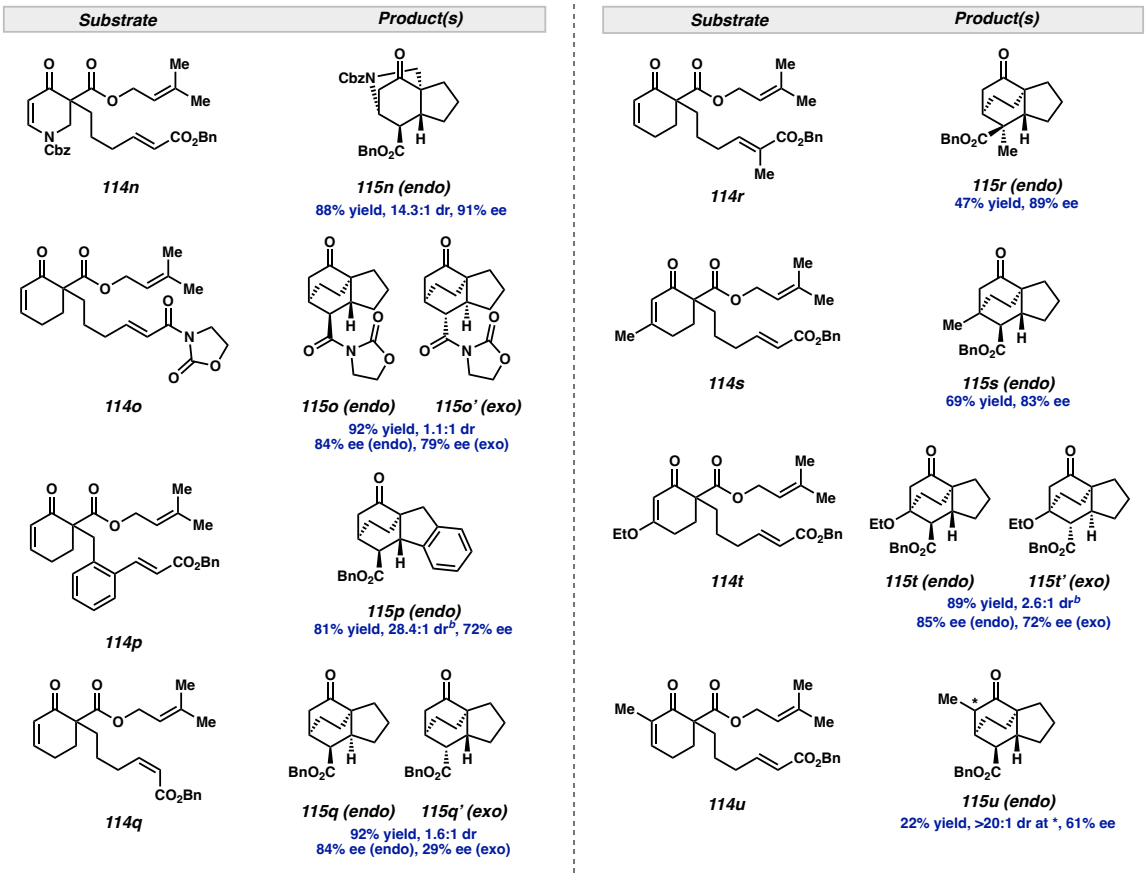

[a] Conditions: 0.2 mmol **114**, 2.5 mol % $Pd_2(dba)_3$, 6.5 mol % ligand, in toluene (10 mL, 0.02 M), isolated yields, dr determined by ^1H NMR analysis of reaction crude. [b] dr determined by isolated yields of endo/exo products.

Subsequently, the dienophile tether length was modulated to investigate its influence on product distribution. Ethylene tethered substrate **114e** solely yields the premature protonation product **123e**, likely due to insurmountable ring strain in the postulated [4+2] transition state. In contrast to the propylene tethered substrate (**114a**), butylene tethered substrate **114f** leads to near equivalent distribution of desired cycloadduct **115f** (42% yield, 92% ee) and undesired protonation byproduct **123f** (45% yield). In line

with this trend, the pentylene tethered substrate **114g** leads only to protonation product **123g**.

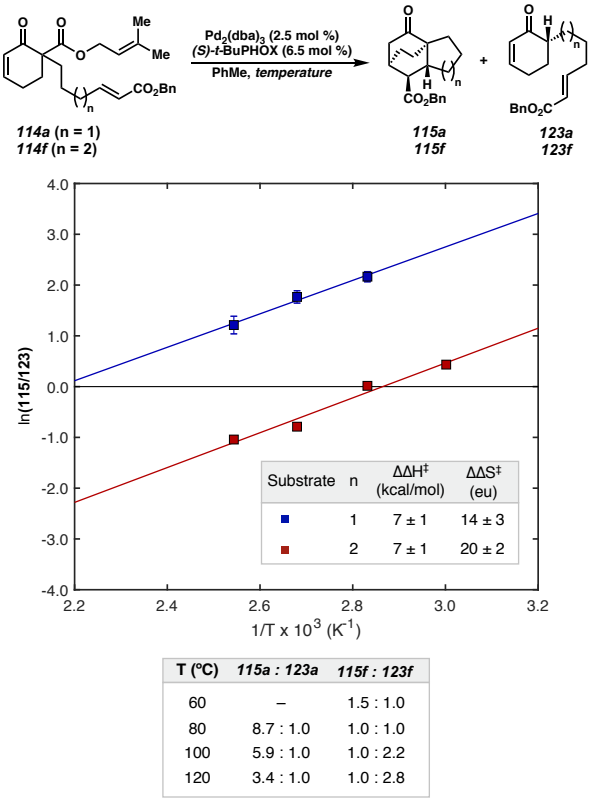

T (°C)	*115a : 123a*	*115f : 123f*
60	–	1.5 : 1.0
80	8.7 : 1.0	1.0 : 1.0
100	5.9 : 1.0	1.0 : 2.2
120	3.4 : 1.0	1.0 : 2.8

Figure 2.5 *Eyring analysis of product ratios (115/123) for propylene and butylene tethered substrates* ***114a*** *and* ***114f****. All data points collected in triplicate, error bars and ranges reflect a 95% confidence interval.*[14]

To rationalize this phenomenon, we propose that elongating the tether increases the conformational flexibility and therefore imposes a greater entropic penalty to the highly organized [4+2] transition state. In contrast, the length of the tether is effectively inconsequential to the protonation process. Eyring analysis of product distributions from reactions of **114a** and **114f** further support the hypothesis of an entropic preference for the formation of **123a/f** over **115a/f** (Figure 2.5). With **114a**, cycloaddition (toward **115a**) is

enthalpically favored ($\Delta\Delta H^{\ddagger}$ = 7 kcal/mol) but entropically disfavored ($\Delta\Delta S^{\ddagger}$ = 14 eu) over protonation (toward **123a**). As anticipated, increasing the tether length to four methylene units (see **114f**) further increases the entropic penalty for cycloaddition ($\Delta\Delta S^{\ddagger}$ = 20 eu), while the differential enthalpy of activation remails similar ($\Delta\Delta H^{\ddagger}$ = 7 kcal/mol). Apparently, entropy differences associated with the tether length lead to the formation of differential amounts of undesired ketones **123a** and **123f**.

Subsequently, we surveyed the scope of functional groups that are tolerated in this transformation (Table 1.2). The cycloaddition doesn't proceed in the absence of a π-acceptor (**114h**), and carboxylic acid **114i** exclusively generates undesired ketone **123i**. Gratifyingly, a variety of other functional groups are compatible including ethyl ester **114b**, phenyl ketone **114j**, phenyl ester **114k**, mesityl ester **114l**, N-hydroxyphthalimido (NHP) ester **114m**, enecarbamate **114n**, and *N*-acyl oxazolidinone **114o**. Additionally, the further conjugated cinnamic ester dienophile **114p** affords tetracycle **115p**. The majority of the substrate scope is reflective of a stereospecific process, yielding *endo* and *exo* diastereomers. We sought to exploit this property by employing *(Z)*-olefin dienophile **114q** resulting in desired cycloadducts **115q** (*endo*) and **115q'** (*exo*) are furnished in a 1.6:1 ratio with a 92% combined yield (and in 84% and 29% ee respectively). Trisubstituted dienophile **114r** furnished cycloadduct **115r**, featuring two all-carbon quaternary centers in 47% yield and 90% ee. β-Methyl (**114s**) and ethoxy (**114t**) substitution of the enone is also tolerated, forging additional tetrasubstituted bridgehead stereocenters. Finally, α-methyl substituted enone **114u** was employed resulting in product **115u** being formed, bearing five contiguous stereocenters. In summary, the transformation described herein

represents a versatile method for the preparation of several enantioenriched polycyclic scaffolds. Intrigued by the good selectivity, we sought to explore the origins of enantioinduction and study the mechanism through which catalyst turnover is achieved.

2.2.4 [4+2] Cycloaddition.

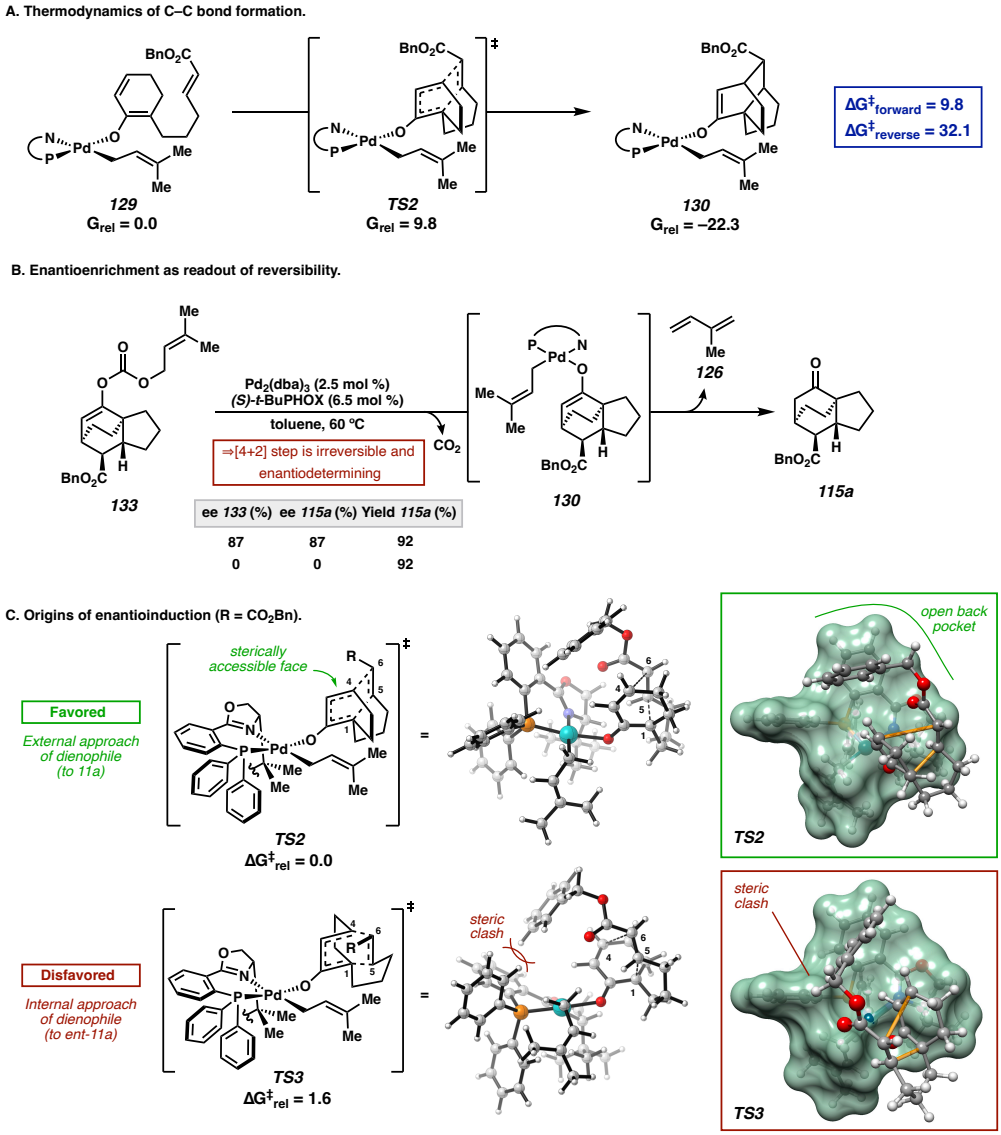

Figure 2.6 *(A) Thermodynamics of C–C bond formation. (B) Enantioenrichment as a readout of cycloaddition reversibility. (C) Origins of enantioenduction.*

In order to probe these origins, we first sought to elucidate the enantiodetermining step of the catalytic cycle. We postulated that either the cycloaddition is irreversible and therefore dictates the stereochemical outcome, or the cycloaddition is reversible and is coupled to a subsequent enantiodetermining step. To probe this, we initially investigated the energetics of the [4+2] computationally and found the cycloaddition of conjugated enolate **129** toward transposed enolate **130** via **TS2** proceeds with a $\Delta G^{\ddagger}$ of 9.8 and ΔG of –22.3 kcal/mol (Figure 2.6A). The reverse barrier of 32.1 kcal/mol implies the cycloaddition is irreversible at the reaction conditions, suggesting the cycloaddition step to be enantiodetermining.

To assess this hypothesis experimentally, a product of the reaction (**115a**) was converted to its corresponding prenyl enol carbonate (**133**). Under standard reaction conditions, Pd(0) presumably undergoes oxidative addition with **133**, which (following decarboxylation) affords common intermediate **130** (Figure 2.6B). No stereochemical resolution in resulting product **115a** is observed from racemic enol carbonate **133**, suggesting that a process post-cycloaddition is not responsible for enantioinduction. In addition to the implication that the cycloaddition is irreversible, these experiments also support the viability of enolate **130** as an intermediate in the catalytic cycle.

Considering this step to be enantiodetermining, the specific origin of this enantioinduction was subsequently investigated computationally. The lowest energy *endo* transition structures giving rise to each enantiomer of **115a** were evaluated (Figure 2.6C). Both minimum energy pathways feature transition structures in which the dienophile tether is *syn* to the *t*-Bu substituent of the PHOX ligand (in accord with prior computational

models for the inner-sphere allylic alkylation).[3, 15] From this arrangement, the dienophile preferentially approaches the externally-exposed enantiotopic face of the diene to avoid steric clash between the benzyl ester of the substrate and phenyl group of the PHOX ligand. A 1.6 kcal/mol preference for external (**TS2**) over internal (**TS3**) approach is calculated, in agreement with the experimentally observed 87% ee.[16] The major enantiomer of product **115a** that is predicted by these computations agrees with the absolute configuration assigned by VCD (see experimental section for details). In summary, our experimental and computational investigations are consistent with C–C bond formation being irreversible and enatiodetermining.

2.2.5 Catalyst turnover.

The aforementioned [4+2] reaction is apparently rendered catalytic via reduction of Pd(II) to Pd(0) that occurs concomitant to the formation of isoprene (**126**) and ketone **115a**. Intrigued by the mechanism underlying this process, we sought to investigate it computationally. Of the mechanisms explored, the minimum energy pathway involves isomerization of **130** to an *N*-detached π-allyl Pd species (**134**), which undergoes subsequent inner-sphere proton transfer via **TS4** (Figure 2.7). Alternatively, a pathway involving outer-sphere proton transfer via **TS5** was also located, which is apparently competitive for catalyst turnover. These two processes present very similar free energy barriers of 22.3 and 22.4 kcal/mol respectively and are readily surmountable at 60 °C. A single favored pathway cannot be identified as the energy difference between these two mechanisms is within the margins of computational error. Regardless, subsequent ligand exchange of isoprene (**126**) for starting material **114a** completes the catalytic cycle.

Interestingly, analysis of the intrinsic bonding orbitals (IBOs) along the reaction coordinate suggests these processes are best conceptualized as the transfer of a proton (as opposed to a hydride) to the Pd enolate.[17,18] Analogous mechanisms were found to be operative from pre-cycloaddition enolate **129**, giving rise to premature protonation product **123a**.

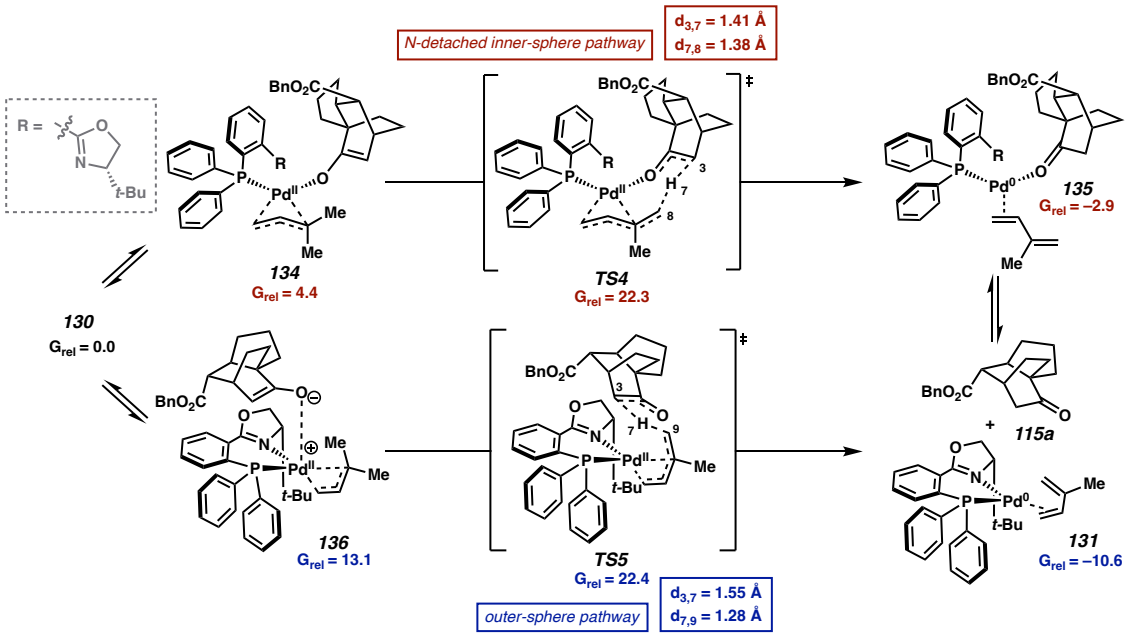

Figure 2.7 *Two low energy pathways for catalyst turnover.*

2.2.6 Additional developments.

While this method allows access to an array of complex scaffolds, premature protonation remains an outstanding challenge we sought to address. Toward this end, we turned our attention to butylene tethered substrate **114f** given its approximately equivalent yield of desired **115f** (44%) and byproduct **123f** (42%). Initially, we postulated that introducing a kinetic isotope effect could effectively slow down the undesired protonation process. Excitingly, employing hexa-deutero prenyl ester **D-114f** (Figure 2.8A) increased the yield of desired cycloadduct **D-115f** to 66% with 91% ee.[19] Interested in further

exploring the influence of the prenyl group, we synthesized several cyclic analogs of prenyl ester **114f** (Figure 2.8B). Seven-membered exocycle **140** affords a product distribution which closely mirrors that of parent substrate **114f** (entry 5). Contracting this ring by one methylene (**139**), however, shifts the distribution favorably toward **115f** (entry 4, 3:1 ratio of **115f**:**123f**). Further contraction toward five- and four-membered exocycles (**138** and **137**), as well as acyclic bis-benzylic allylic ester **141**, afford unfavorable product distributions. Taken together, the prenyl group is evidently an effective handle to modulate product distribution.

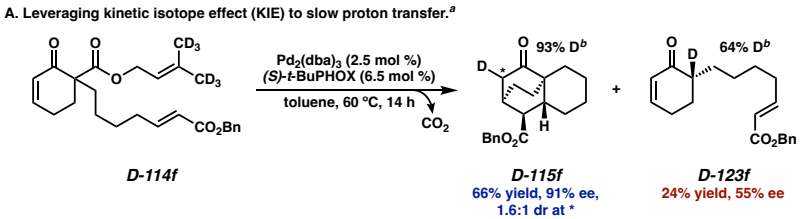

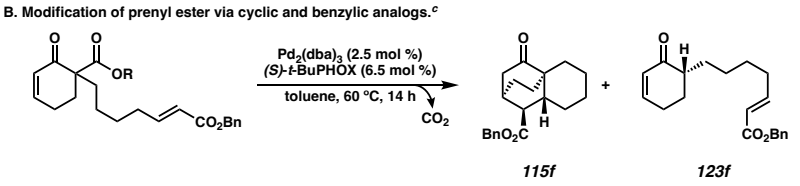

Entry	R		Yield 115f (%)	ee 115f (%)	Yield 123f (%)	ee 123f (%)
1	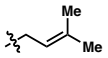	*(114f)*	44	91	42	40
2[d]	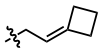	*(137)*	25	92	44	46
3	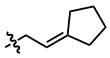	*(138)*	8	–	89	48
4	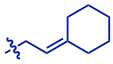	*(139)*	63	92	21	44
5	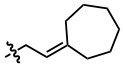	*(140)*	48	92	46	38
6[e]	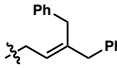	*(141)*	14	94	86	60

Figure 2.8 *(A) Leveraging KIE to slow proton transfer. (B) Modification of prenyl ester.*

[a] Conditions: 0.20 mmol **D-114f**, 2.5 mol % $Pd_2(dba)_3$, 6.5 mol % ligand, in 10 mL of solvent (0.02 M). [b] Deuterium incorporation determined by HRMS. [c] Conditions: 0.02 mmol substrate, 2.5 mol % $Pd_2(dba)_3$, 6.5 mol % ligand, in 1.0 mL of solvent (0.02 M). Yield determined by ^1H NMR with respect to 1,3,5-trimethoxybenzene as internal standard. [d] 21% of allylic alkylation product was also observed. [e] The corresponding benzylic diene was also observed (see 1.4 Experimental Section for details).

2.2.7 Product derivatization.

To assess the utility of the cycloadducts prepared in this study, we investigated their subsequent derivatization (Figure 2.9A). Beginning from **115a**, we could successfully perform a 1,2-reduction (**142**), a Beckmann rearrangement (**143**), or a Baeyer–Villiger oxidation (**144**) altering the oxidation state of the initial ketone and forming several heterocycles. Next, we turned our eye to the derivatization of ring expanded product **115f** as this carbon framework mapped onto several natural products (**145**–**148**, Figure 2.9B). We successfully performed a hydrogenolysis followed by persulfate-mediated radical decarboxylation of **115f** to afford ketone **149**.[20] Additionally, we could perform aldol condensations toward enones **150** and **151**. Enone **151** was subsequently subjected to dihydroxylation conditions to yield diol **152** in modest yield.[21, 22] Alternatively, we could perform a Riley oxidation of **115f** to generate diketone **153** which can be differentiated via selective acetalization (**154**).[23, 24] Directed C–H oxidation of **115f** (followed by subsequent oxime deprotection) results in acetate **156**.[25]

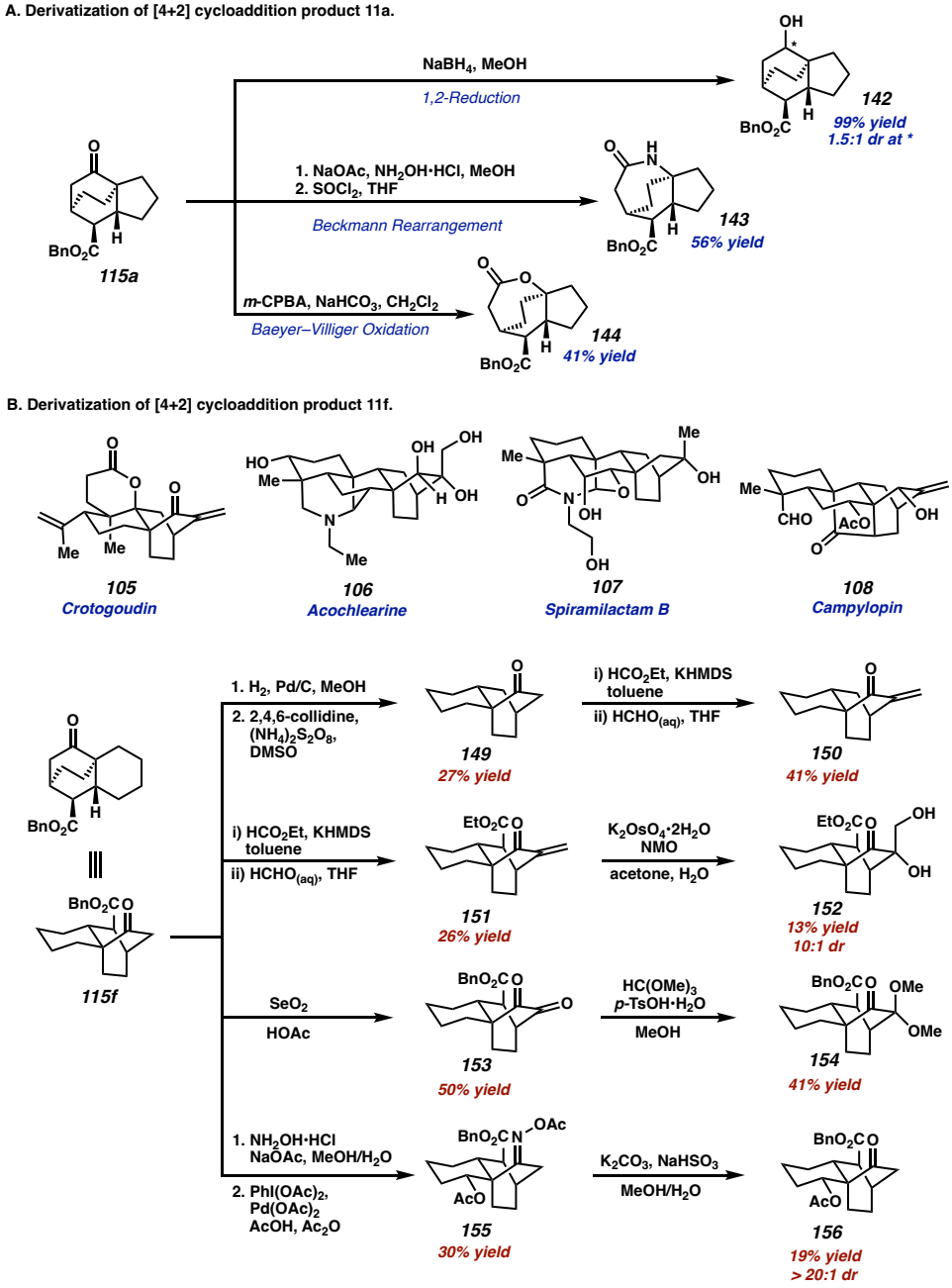

Figure 2.9 *(A) Derivatization of [4+2] cycloaddition product 115a. (B) Derivatization of [4+2] cycloaddition product 115f.*

2.3 CONCLUSIONS

We have developed an asymmetric decarboxylative [4+2] cycloaddition employing a catalytically-generated chiral Pd enolate intermediate (analogous to those implicated in inner-sphere allylic alkylation reactions). To enable this cyclization, we first systematically modified the allyl moiety to disfavor undesired allylic alkylation. This allows the conjugated Pd enolate to instead engage in [4+2] cycloaddition with the pendant dienophile. Computational and experimental investigations support the role of a C–C bond formation as the enantiodetermining step. Further computational studies reveal that catalyst turnover occurs via a proton transfer from the prenyl group to the transposed enolate, forming the desired product and releasing isoprene. Building upon these mechanistic insights, we were able to further favor the desired [4+2] cycloaddition over premature protonation for challenging substrates relevant to natural products. In summary, our approach serves as a powerful framework for rational design in asymmetric catalytic reactions. Studies applying this strategy more broadly in other synthetically relevant transformations are currently under investigation.

2.4 EXPERIMENTAL SECTION

2.4.1 Materials and methods.

Unless otherwise stated, reactions were performed in flame-dried glassware under an argon or nitrogen atmosphere using dry, deoxygenated solvents. Solvents were dried by passage through an activated alumina column under argon.[26] Reaction progress was monitored by thin-layer chromatography (TLC) or Agilent 1290 UHPLC-MS. TLC was performed using E. Merck silica gel 60 F254 precoated glass plates (0.25 mm) and

visualized by UV fluorescence quenching or $KMnO_4$ staining. Silicycle Silia*Flash*® P60 Academic Silica gel (particle size 40–63 nm) was used for flash chromatography. ^{1}H NMR spectra were recorded on a Bruker 400 MHz spectrometer and are reported relative to residual $CHCl_3$ (δ 7.26 ppm). ^{13}C NMR spectra were recorded on a Bruker 400 MHz spectrometer (100 MHz) and are reported relative to $CDCl_3$ (δ 77.16 ppm). ^{2}H NMR spectra were recorded on a Bruker 400 MHz (61 MHz) spectrometer and are reported relative to residual $CDCl_3$ (δ 7.26 ppm). Data for ^{1}H NMR are reported as follows: chemical shift (δ ppm) (multiplicity, coupling constant (Hz), integration). Multiplicities are reported as the peaks appear as follows: s = singlet, d = doublet, t = triplet, q = quartet, p = pentet, sept = septuplet, m = multiplet, br s = broad singlet, br d = broad doublet. Data for ^{13}C NMR are reported in terms of chemical shifts (δ ppm). Some reported spectra include minor solvent impurities of water (δ 1.56ppm), ethyl acetate (δ 4.12, 2.05, 1.26 ppm), methylene chloride (δ 5.30 ppm), acetone (δ 2.17 ppm), grease (δ 1.26, 0.86 ppm), and/or silicon grease (δ 0.07 ppm), which do not impact product assignments. ^{13}C NMR spectra of deuterated compounds are complicated by the low intensity of peaks of deuterium-substituted carbon atoms. IR spectra were obtained by use of a Perkin Elmer Spectrum BXII spectrometer or Nicolet 6700 FTIR spectrometer using thin films deposited on NaCl plates and reported in frequency of absorption (cm^{-1}). Optical rotations were measured with a Jasco P-2000 polarimeter operating on the sodium D-line (589 nm), using a 100 mm path-length cell. Analytical SFC was performed with a Mettler SFC supercritical CO_2 analytical chromatography system utilizing Chiralpak (AD-H or IC) or Chiralcel (OD-H, OJ-H, or OB-H) columns (4.6 mm x 25 cm) obtained from Daicel Chemical Industries, Ltd.

High resolution mass spectra (HRMS) were obtained from the Caltech Mass Spectral Facility using a JEOL JMS-600H High Resolution Mass Spectrometer in Field Desorption (FD+) mode. Absolute stereochemical assignments were made by vibrational circular dichroism analysis for select compounds with related compounds assigned by analogy. Reagents were purchased from commercial sources and used as received unless otherwise stated. Ligands were prepared according to literature procedures.[27] List of Abbreviations: ee – enantiomeric excess, SFC – supercritical fluid chromatography, TLC – thin-layer chromatography, IPA – isopropanol, VCD – vibrational circular dichroism.

2.4.2 Experimental procedures and spectroscopic data.

Pd-Catalyzed Decarboxylative Cycloadditions

General Procedure A: Asymmetric Pd-Catalyzed Decarboxylative Cycloadditions.

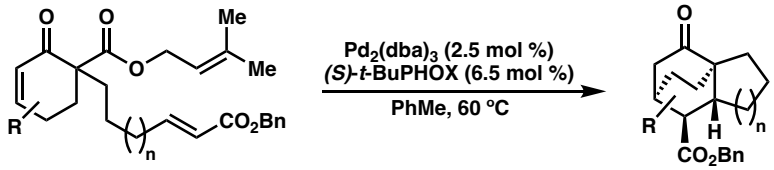

114 ***115***

In a nitrogen filled glovebox, an oven-dried 20 mL vial was charged with a stir bar, $Pd_2(dba)_3$ (4.6 mg, 0.005 mmol, 2.5 mol %), *(S)-t*-BuPHOX (5.0 mg, 0.013 mmol, 6.5 mol %), and toluene (5 mL). The catalyst solution was stirred at 23 ºC for 20 min. A solution of substrate **114** (0.2 mmol, 1 equiv) in toluene (5 mL) was added to the vial. The resultant solution was then heated to 60 ºC for 14 h. The solution was then cooled to 23 ºC and concentrated under reduced pressure. The crude reaction mixture was loaded directly onto a flash column and the product (**115**) was isolated by silica gel flash column chromatography.

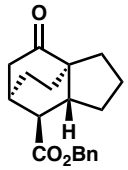

115a

benzyl (3a*R*,6*R*,7*S*,7a*R*)-4-oxooctahydro-3a,6-ethanoindene-7-carboxylate (115a)

Prepared from **114a** following General Procedure A. Purification by flash column chromatography (0–35% EtOAc/hexanes) afforded the title compound as a colorless oil (49.7 mg, 0.167 mmol, 83% yield, 87% ee). Absolute and relative stereochemistry were assigned by VCD (vida infra). 2D NMR studies independently confirm the relative stereochemistry (vida infra).

^{1}H NMR (400 MHz, $CDCl_3$): δ 7.40 – 7.31 (m, 5H), 5.14 (d, *J* = 1.6 Hz, 2H), 2.54 (dt, *J* = 18.8, 2.3 Hz, 1H), 2.51 – 2.47 (m, 2H), 2.21 (dddd, *J* = 10.6, 8.7, 7.2, 1.7 Hz, 1H), 2.14 – 2.04 (m, 3H), 1.86 (ddd, *J* = 13.0, 11.1, 6.8 Hz, 1H), 1.81 – 1.72 (m, 2H), 1.70 – 1.52 (m, 3H), 1.44 (ddt, *J* = 12.9, 10.9, 1.8 Hz, 1H), 1.22 (ddd, *J* = 13.9, 9.2, 4.9 Hz, 1H).

^{13}C NMR (100 MHz, $CDCl_3$): δ 215.1, 174.7, 136.0, 128.8, 128.5, 128.2, 66.7, 54.2, 47.5, 43.3, 41.3, 32.9, 29.1, 27.4, 26.5, 25.1, 22.6.

IR (Neat Film, NaCl): 2947, 2873, 1726, 1455, 1267, 1160 cm^{-1}.

HRMS (MM: FD+): *m/z* calc'd for $C_{19}H_{22}O_3$ $[M]^+$: 298.1564, found 298.1576.

Optical Rotation: $[\alpha]_D^{21}$ –20.3 (c 1.00, $CHCl_3$).

SFC conditions: 15% IPA, 2.5 mL/min, Chiralpak AD-H column, λ = 210 nm, t_R (min): minor = 4.21, major = 5.30

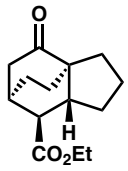

115b

ethyl (3a*R*,6*R*,7*S*,7a*R*)-4-oxooctahydro-3a,6-ethanoindene-7-carboxylate (115b)

Prepared from **114b** following General Procedure A. Purification by flash column chromatography (5–30% EtOAc/hexanes) afforded the title compound as a colorless oil (39.9 mg, 0.169 mmol, 84% yield, 88% ee).

^{1}H NMR (400 MHz, $CDCl_3$): δ 4.15 (q, *J* = 7.1 Hz, 2H), 2.55 (dt, *J* = 18.8, 2.6 Hz, 1H), 2.49 – 2.44 (m, 1H), 2.42 (d, *J* = 8.6 Hz, 1H), 2.23 – 2.14 (m, 1H), 2.15 – 2.04 (m, 3H), 1.91 – 1.71 (m, 3H), 1.71 – 1.52 (m, 3H), 1.50 – 1.40 (m, 1H), 1.26 (t, *J* = 7.1 Hz, 3H), 1.21 (dt, *J* = 9.2, 4.9 Hz, 1H).

^{13}C NMR (100 MHz, $CDCl_3$): δ 215.2, 174.9, 60.8, 54.2, 47.5, 43.3, 41.3, 32.9, 29.1, 27.4, 26.5, 25.1, 22.6, 14.4.

IR (Neat Film, NaCl): 2947, 2873, 1725, 1270, 1170 cm^{-1}.

HRMS (MM: FD+): *m/z* calc'd for $C_{14}H_{20}O_3$ $[M]^+$: 236.1412, found 236.1415.

Optical Rotation: $[\alpha]_D^{21}$ –34.2 (c 1.00, $CHCl_3$).

Enantiomeric excess determined by converting ethyl ester to benzyl ester through saponification and Steglish esterification.

SFC conditions: 15% IPA, 2.5 mL/min, Chiralpak AD-H column, λ = 210 nm, t_R (min): minor = 4.21, major = 5.30

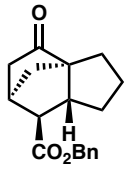

115c

benzyl (3a*R*,6*R*,7*S*,7a*R*)-4-oxooctahydro-3a,6-methanoindene-7-carboxylate (115c)

Prepared from **114c** following General Procedure A. Purification by flash column chromatography (0–30% EtOAc/hexanes) afforded the title compound as a colorless oil (37.0 mg, 0.130 mmol, 65% yield, 65% ee).

^{1}H NMR (400 MHz, $CDCl_3$): δ 7.42 – 7.29 (m, 5H), 5.13 (dd, *J* = 12.3, 7.9 Hz, 2H), 2.96 (t, *J* = 4.2, 1H), 2.92 (ddd, *J* = 5.2, 3.7, 1.4, 1H), 2.42 – 2.35 (m, 1H), 2.22 – 2.17 (m, 1H), 2.16 – 2.05 (m, 3H), 1.95 (ddtd, *J* = 12.9, 8.4, 5.1, 2.2 Hz, 1H), 1.90 – 1.80 (m, 2H), 1.66 (dt, *J* = 10.6, 1.6 Hz, 1H), 1.52 – 1.37 (m, 2H).

^{13}C NMR (100 MHz, $CDCl_3$): δ 213.9, 173.3, 136.0, 128.8, 128.5, 128.3, 67.8, 66.6, 52.4, 48.5, 41.8, 40.6, 40.5, 32.2, 27.5, 22.1.

IR (Neat Film, NaCl): 2960, 2358, 1739, 1164, 730, 668 cm^{-1}.

HRMS (MM: FD+): *m/z* calc'd for $C_{18}H_{20}O_3$ $[M]^+$: 284.1414, found 284.1407.

Optical Rotation: $[\alpha]_D^{21}$ +20.0 (c 1.00, $CHCl_3$).

SFC conditions: 15% IPA, 2.5 mL/min, Chiralpak AD-H column, λ = 210 nm, t_R (min): minor = 3.97, major = 4.33.

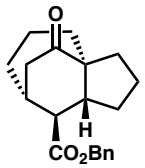

115d

benzyl (3a*R*,7*R*,8*S*,8a*R*)-10-oxooctahydro-1*H*-3a,7-ethanoazulene-8-carboxylate (115d)

Prepared from **114d** following General Procedure A. Purification by flash column chromatography (0–35% EtOAc/hexanes) afforded the title compound as a colorless oil (51.8 mg, 0.166 mmol, 83% yield, 97% ee).

^{1}H NMR (400 MHz, $CDCl_3$): δ 7.40 – 7.31 (m, 5H), 5.16 (d, *J* = 12.4 Hz, 1H), 5.12 (d, *J* = 12.3 Hz, 1H), 2.70 – 2.63 (m, 2H), 2.64 – 2.56 (m, 1H), 2.25 (ddd, *J* = 18.5, 2.0, 1.0 Hz, 1H), 2.08 (td, *J* = 10.5, 7.8 Hz, 1H), 2.03 – 1.94 (m, 1H), 1.93 – 1.79 (m, 3H), 1.78 – 1.60 (m, 4H), 1.59 – 1.43 (m, 4H).

^{13}C NMR (100 MHz, $CDCl_3$): δ 215.7, 175.8, 136.0, 128.8, 128.5, 128.3, 66.7, 58.0, 50.2, 45.4, 41.0, 35.7, 33.6, 33.3, 32.0, 28.0, 21.8, 21.2.

IR (Neat Film, NaCl): 2934, 2873, 1727, 1713, 1455, 1161 cm^{-1}.

HRMS (MM: FD+): *m/z* calc'd for $C_{20}H_{24}O_3$ $[M+H]^+$: 312.1720, found 312.1734.

Optical Rotation: $[\alpha]_D^{21}$ +21.4 (c 1.00, $CHCl_3$).

SFC conditions: 15% IPA, 2.5 mL/min, Chiralpak AD-H column, λ = 210 nm, t_R (min): minor = 4.70, major = 6.23.

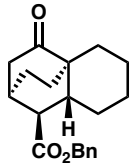

115f

benzyl (1*S*,2*R*,4a*R*,8a*R*)-4-oxooctahydro-2*H*-2,4a-ethanonaphthalene-1-carboxylate (115f).

Prepared from **114f** following General Procedure A. Purification by flash column chromatography (0–35% EtOAc/hexanes) afforded the title compound as a colorless oil (26.3 mg, 0.084 mmol, 42% yield, 92% ee).

^{1}H NMR (400 MHz, $CDCl_3$): δ 7.39 – 7.29 (m, 5H), 5.16 (d, *J* = 12.4 Hz, 1H), 5.10 (d, *J* = 12.2 Hz, 1H), 2.47 (dt, *J* = 17.0, 2.8 Hz, 2H), 2.28 – 2.19 (m, 2H), 2.14 (ddd, *J* = 19.7, 3.8, 1.8 Hz, 1H), 2.01 (dddd, *J* = 11.8, 6.8, 4.5, 1.7 Hz, 1H), 1.87 (ddtd, *J* = 12.8, 4.5, 3.4, 1.6 Hz, 1H), 1.83 – 1.71 (m, 1H), 1.71 – 1.56 (m, 4H), 1.51 – 1.11 (m, 5H).

^{13}C NMR (100 MHz, $CDCl_3$): δ 216.3, 174.5, 136.0, 128.7, 128.4, 128.2, 66.7, 49.8, 45.1, 40.5, 37.1, 30.9, 30.0, 28.9, 26.2, 25.6, 21.7, 21.1.

IR (Neat Film, NaCl): 2928, 2856, 1721, 1170 cm^{-1}.

HRMS (MM: FD+): *m/z* calc'd for $C_{20}H_{24}O_3$ $[M]^+$: 312.1720, found 312.1732.

Optical Rotation: $[\alpha]_D^{21}$ –15.5 (c 1.00, $CHCl_3$).

SFC conditions: 15% IPA, 2.5 mL/min, Chiralpak AD-H column, λ = 210 nm, t_R (min): minor = 4.70, major = 6.23.

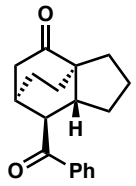

115j

(3a*R*,6*R*,7*S*,7a*R*)-7-benzoylhexahydro-3a,6-ethanoinden-4(1*H*)-one (115j)

Prepared from **114j** following General Procedure A. Purification by flash column chromatography (0–30% EtOAc/hexanes) afforded the title compound as a colorless oil (27.1 mg, 0.101 mmol, 50% yield, 87% ee).

^{1}H NMR (400 MHz, $CDCl_3$): δ 7.97 – 7.94 (m, 2H), 7.61 – 7.56 (m, 1H), 7.51 – 7.46 (m, 2H), 3.42 (d, *J* = 8.5 Hz, 1H), 2.58 – 2.50 (m, 2H), 2.41 – 2.38 (m, 1H), 2.16 (ddd, *J* = 13.7, 11.1, 6.2 Hz, 1H), 2.08 – 1.87 (m, 4H), 1.82 – 1.74 (m, 1H), 1.70 – 1.50 (m, 4H), 1.25 (ddd, *J* = 14.0, 9.2, 5.1 Hz, 1H).

^{13}C NMR (100 MHz, $CDCl_3$): δ 214.9, 201.0, 136.4, 133.4, 128.9, 128.5, 54.2, 49.4, 41.4, 40.8, 34.1, 28.9, 27.8, 26.5, 25.6, 22.7.

IR (Neat Film, NaCl): 2945, 2871, 1720, 1677, 1447, 1217 cm^{-1}.

HRMS (MM: FD+): *m/z* calc'd for $C_{18}H_{20}O_2$ $[M]^+$: 268.1463, found 268.1463.

Optical Rotation: $[\alpha]_D^{21}$ –32.7 (c 1.00, $CHCl_3$).

SFC conditions: 30% IPA, 2.5 mL/min, Chiralpak AD-H column, λ = 210 nm, t_R (min): minor = 2.55, major = 3.40.

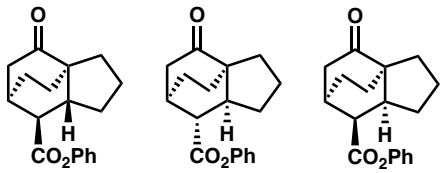

115k ***(endo-trans)*** ***115k'*** ***(exo-cis)*** ***115k"*** ***(endo-cis)***

phenyl (3a*R*,6*R*,7*S*,7a*R*)-4-oxooctahydro-3a,6-ethanoindene-7-carboxylate (115k, 115k' and 115k'')

Prepared from **114k** following General Procedure A. Purification by flash column chromatography (0–35% EtOAc/hexanes) afforded the title compound as a colorless oil (47.2 mg, 0.166 mmol, 83% yield, 14.8:1.6:1.0 *endo-trans*/*endo-cis*/*exo-trans*, 88% ee (*endo-trans*)). Crude analysis by ^{1}H NMR affords a 10.4:1.4:1.0 ratio of *endo-trans*/*exo-trans/endo-cis*. The diastereomers were subsequently separated by preparative HPLC (15% IPA/hexanes, 25 mL/min, Chiralpak AD-H column) for independent characterization. Absolute and relative stereochemistry were assigned/confirmed by VCD where applicable (vida infra) in addition to 2D NMR.

115k (endo-trans):

^{1}H NMR (400 MHz, $CDCl_3$): δ 7.41 – 7.34 (m, 2H), 7.25 – 7.20 (m, 1H), 7.09 – 7.04 (m, 2H), 2.70 (d, *J* = 8.7 Hz, 1H), 2.67 – 2.60 (m, 2H), 2.31 (dddd, *J* = 10.6, 8.8, 7.3, 1.7 Hz, 1H), 2.23 – 2.09 (m, 3H), 1.97 – 1.76 (m, 3H), 1.67 (ddddd, *J* = 13.5, 11.1, 9.0, 6.2, 4.5 Hz, 3H), 1.50 (ddt, *J* = 12.5, 10.6, 1.7 Hz, 1H), 1.31 – 1.17 (m, 1H).

^{13}C NMR (100 MHz, $CDCl_3$): δ 214.8, 173.4, 150.7, 129.6, 126.0, 121.5, 54.2, 47.5, 43.4, 41.2, 32.9, 29.1, 27.3, 26.5, 25.0, 22.5.

IR (Neat Film, NaCl): 2948, 2872, 1750, 1721, 1592, 1492, 1192, 1144 cm^{-1}.

HRMS (MM: FD+): *m/z* calc'd for $C_{18}H_{20}O_3$ $[M]^+$: 284.1412, found 284.1411.

Optical Rotation: $[\alpha]_D^{21}$ –16.7 (c 0.20, $CHCl_3$). *(single major enantiomer of 11j)*

SFC conditions: 15% IPA, 2.5 mL/min, Chiralpak AD-H column, λ = 210 nm, t_R (min): minor = 4.09, major = 6.08.

115k' (exo-trans):

^{1}H NMR (400 MHz, $CDCl_3$): δ 7.39 – 7.34 (m, 2H), 7.25 – 7.19 (m, 1H), 7.06 – 7.01 (m, 2H), 3.30 (dt, *J* = 12.0, 2.3 Hz, 1H), 3.08 (dt, *J* = 19.5, 2.8 Hz, 1H), 2.58 (h, *J* = 2.8 Hz, 1H), 2.47 – 2.33 (m, 2H), 2.21 (dt, *J* = 19.6, 2.4 Hz, 1H), 2.08 – 2.01 (m, 2H), 1.93 – 1.71 (m, 5H), 1.70 – 1.59 (m, 1H), 1.04 (ddd, *J* = 12.8, 11.4, 6.7 Hz, 1H).

^{13}C NMR (100 MHz, $CDCl_3$): δ 215.2, 171.8, 150.6, 129.6, 126.0, 121.7, 54.6, 45.8, 44.0, 40.1, 31.4, 28.4, 28.2, 27.0, 26.3, 21.8.

IR ($CDCl_3$ solution): 2951, 2870, 1751, 1717, 1194, 1163, 1146 cm^{-1}.

HRMS (MM: FD+): *m/z* calc'd for $C_{18}H_{20}O_3$ $[M]^+$: 284.1412, found 284.1417.

115k'' (endo-cis):

^{1}H NMR (400 MHz, $CDCl_3$): δ 7.43 – 7.36 (m, 2H), 7.27 – 7.22 (m, 1H), 7.12 – 7.07 (m, 2H), 2.76 – 2.67 (m, 1H), 2.58 (dt, *J* = 8.3, 1.7 Hz, 1H), 2.48 – 2.33 (m, 4H), 2.12 – 2.01 (m, 2H), 1.91 – 1.63 (m, 5H), 1.10 (ddd, *J* = 13.0, 11.2, 6.5 Hz, 1H), 1.01 (ddd, *J* = 12.4, 9.5, 2.8 Hz, 1H).

^{13}C NMR (100 MHz, $CDCl_3$): δ 215.1, 172.9, 150.9, 129.6, 126.1, 121.6, 53.8, 49.4, 46.0, 44.2, 32.7, 32.0, 28.6, 27.4, 22.6, 21.5.

IR ($CDCl_3$ solution): 2945, 2872, 1751, 1717, 1194, 1163, 1130 cm^{-1}.

HRMS (MM: FD+): *m/z* calc'd for $C_{18}H_{20}O_3$ $[M]^+$: 284.1412, found 284.1407.

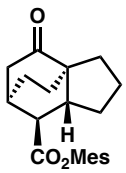

115l

mesityl (3a*R*,6*R*,7*S*,7a*R*)-4-oxooctahydro-3a,6-ethanoindene-7-carboxylate (115l)

Prepared from **114l** following General Procedure A. Purification by flash column chromatography (0–35% EtOAc/hexanes) afforded the title compound as a colorless oil (58.6 mg, 0.180 mmol, 90% yield, 89% ee).

^{1}H NMR (400 MHz, $CDCl_3$):) δ 6.87 (s, 2H), 2.75 (d, *J* = 8.8 Hz, 1H), 2.72 – 2.65 (m, 2H), 2.36 (dddd, *J* = 10.6, 8.9, 7.3, 1.6 Hz, 1H), 2.26 (s, 3H), 2.24 – 2.09 (m, 3H), 2.08 (s, 6H), 1.98 – 1.78 (m, 3H), 1.75 – 1.61 (m, 3H), 1.55 – 1.48 (m, 1H), 1.31 – 1.24 (m, 1H).

^{13}C NMR (100 MHz, $CDCl_3$): δ 214.8, 172.8, 145.9, 135.6, 129.5, 129.5, 54.2, 47.4, 43.5, 41.3, 33.2, 29.2, 27.5, 26.5, 25.1, 22.6, 20.9, 16.4.

IR (Neat Film, NaCl): 2946, 2873, 1747, 1723, 1485, 1458, 1189, 1137 cm^{-1}.

HRMS (MM: FD+): *m/z* calc'd for $C_{21}H_{26}O_3$ $[M]^+$: 326.1877, found 326.1886.

Optical Rotation: $[\alpha]_D^{21}$ –25.8 (c 1.00, $CHCl_3$).

SFC conditions: 15% IPA, 2.5 mL/min, Chiralpak AD-H column, λ = 210 nm, t_R (min): minor = 4.06, major = 4.33.

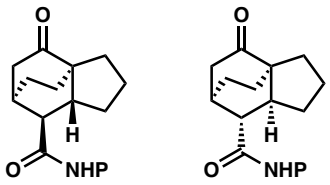

115m **(endo)** **115m'** **(exo)**

1,3-dioxoisoindolin-2-yl(3a*R*,6*R*,7*S*,7a*R*)-4-oxooctahydro-3a,6-ethanoindene-7-carboxylate (115m and 115m')

Prepared from **114m** following General Procedure A. Purification by flash column chromatography (0–35% EtOAc/hexanes) afforded the title compounds as colorless oils

(**Endo**: 37.7 mg, 0.106 mmol, 53% yield, 62% ee; **Exo**: 8.6 mg, 0.024 mmol, 12% yield, 62% ee).

115m (endo):

^{1}H NMR (400 MHz, $CDCl_3$): δ 7.92 – 7.85 (m, 2H), 7.83 – 7.75 (m, 2H), 2.84 (dd, *J* = 8.7, 1.3 Hz, 1H), 2.71 (m, 1H), 2.64 (dt, *J* = 18.9, 2.5 Hz, 1H), 2.46 – 2.28 (m, 1H), 2.28 – 2.18 (m, 2H), 2.13 (m, 1H), 1.98 – 1.76 (m, 3H), 1.76 – 1.60 (m, 3H), 1.56 – 1.48 (m, 1H), 1.34 – 1.19 (m, 1H).

^{13}C NMR (100 MHz, $CDCl_3$): δ 214.0, 171.4, 162.1, 135.0, 129.0, 124.2, 54.1, 44.8, 43.3, 41.0, 33.2, 28.9, 27.2, 26.4, 24.9, 22.4.

IR (Neat Film, NaCl): 2948, 2873, 1782, 1742, 1718, 1466, 1362, 1185 cm^{-1}.

HRMS (MM: FD+): *m/z* calc'd for $C_{20}H_{19}NO_5$ $[M]^+$: 353.1263, found 353.1251.

Optical Rotation: $[\alpha]_D^{21}$ –0.2 (c 1.00, $CHCl_3$).

SFC conditions: 30% IPA, 2.5 mL/min, Chiralpak IC column, l = 210 nm, t_R (min): minor = 4.03, major = 3.00

115m' (exo):

^{1}H NMR (400 MHz, $CDCl_3$): δ 7.90 (dd, *J* = 5.5, 3.1 Hz, 2H), 7.81 (dd, *J* = 5.5, 3.1 Hz, 2H), 2.77 (tt, *J* = 3.9, 2.2 Hz, 1H), 2.73 (d, *J* = 8.4 Hz, 1H), 2.47 – 2.28 (m, 4H), 2.19 – 2.02 (m, 2H), 1.92 – 1.71 (m, 4H), 1.71 – 1.61 (m, 1H), 1.11 (ddd, *J* = 13.1, 11.2, 6.6 Hz, 1H), 1.08 – 0.95 (m, 1H).

^{13}C NMR (100 MHz, $CDCl_3$): δ 214.2, 170.8, 162.1, 135.0, 129.1, 124.2, 53.7, 46.7, 46.0, 44.1, 32.9, 31.8, 28.4, 27.2, 22.5, 21.2.

IR (Neat Film, NaCl): 2947, 2868, 1809, 1784, 1743, 1717, 1466, 1362, 1185 cm^{-1}.

HRMS (MM: FD+): *m/z* calc'd for $C_{20}H_{19}NO_5$ $[M]^+$: 353.1263, found 353.1261.

Optical Rotation: $[\alpha]_D^{21}$ –13.6 (c 0.81, $CHCl_3$).

SFC conditions: 30% IPA, 2.5 mL/min, Chiralpak IC column, l = 210 nm, t_R (min): minor = 4.98, major = 4.29.

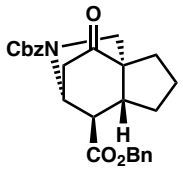

115n

dibenzyl (3aR,4R,5R,7aS)-7-oxooctahydro-5,7a-(epiminomethano)indene-4,9-dicarboxylate (115n)

Prepared from **114n** following General Procedure A. Purification by flash column chromatography (0–40 % EtOAc/hexanes) afforded the title compound as a colorless oil (76.1 mg, 0.176 mmol, 88% yield, 14.3:1 endo/exo, 91% ee (endo)).

^{1}H NMR (400 MHz, $CDCl_3$): δ 7.35 (dd, *J* = 7.1, 4.9 Hz, 10H), 5.21 – 5.07 (m, 4H), 4.90 – 4.74 (m, 1H), 3.49 (dd, *J* = 12.1, 5.8 Hz, 1H), 3.40 – 3.27 (m, 1H), 2.88 (t, *J* = 8.9 Hz, 1H), 2.66 – 2.42 (m, 2H), 2.30 (p, *J* = 9.3 Hz, 1H), 2.23 – 2.10 (m, 2H), 1.91 – 1.56 (m, 3H), 1.33 – 1.14 (m, 1H).

^{13}C NMR (100 MHz, $CDCl_3$): δ 210.1, 209.7, 172.2, 154.4, 136.3, 135.5, 128.9, 128.7, 128.7, 128.4, 128.4, 128.4, 128.3, 128.2, 128.1, 67.6, 67.2, 55.9, 55.8, 50.4, 50.0, 48.8, 48.6, 45.7, 45.6, 42.6, 42.6, 41.7, 41.6, 29.0, 28.9, 24.1, 22.9.

IR (Neat Film, NaCl): 3399, 2963, 2874, 2357, 1729, 1700, 1652, 1414, 1288, 1156, 1115, 748, 681 cm^{-1}.

HRMS (MM: FD+): *m/z* calc'd for $C_{26}H_{27}NO_5$ $[M]^+$: 433.1889, found 433.1874.

Optical Rotation: $[\alpha]_D^{21}$ –39.8 (c 0.75, $CHCl_3$).

SFC conditions: 15% IPA, 2.5 mL/min, Chiralpak AD-H column, l = 210 nm, t_R (min): minor = 9.19, major = 11.59.

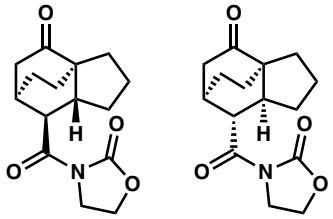

115o (endo) ***115o' (exo)***

3-((3a*R*,6*R*,7*S*,7a*R*)-4-oxooctahydro-3a,6-ethanoindene-7-carbonyl)oxazolidin-2-one (115o and 115o')

Prepared from **114o** following General Procedure A. Purification by flash column chromatography (0–90 % EtOAc/hexanes) afforded the title compound as a colorless oil (51.2 mg, 0.185 mmol, 92% yield, 1.1:1 endo/exo (ratio from crude ^{1}H NMR analysis), 84% ee (endo), 79% ee (exo)).

115o (endo):

^{1}H NMR (400 MHz, $CDCl_3$): δ 4.43 (t, *J* = 8.1 Hz, 2H), 4.15 – 4.00 (m, 2H), 3.54 – 3.47 (m, 1H), 2.66 (ddd, *J* = 12.4, 8.3, 6.9 Hz, 1H), 2.52 – 2.25 (m, 4H), 1.92 – 1.68 (m, 5H), 1.67 – 1.53 (m, 2H), 1.08 (ddd, *J* = 12.9, 11.2, 6.4 Hz, 1H), 0.89 (tt, *J* = 12.3, 9.5 Hz, 1H).

^{13}C NMR (100 MHz, $CDCl_3$): δ 215.5, 173.8, 153.4, 62.1, 53.7, 48.3, 44.1, 44.0, 43.1, 33.8, 31.3, 28.7, 27.3, 22.8, 20.8.

IR (Neat Film, NaCl): 2942, 2867, 1775, 1714, 1693, 1387, 1267, 1222, 1040 cm^{-1}.

HRMS (MM: FD+): *m/z* calc'd for $C_{15}H_{19}NO_4$ $[M]^+$: 277.1314, found 277.1321.

Optical Rotation: $[\alpha]_D^{21}$ –39.5 (c 1.00, $CHCl_3$).

SFC conditions: 20% IPA, 2.5 mL/min, Chiralpak AD-H column, λ = 210 nm, t_R (min): minor = 4.15, major = 5.17.

115o' (exo):

^{1}H NMR (400 MHz, $CDCl_3$): δ 4.43 (t, *J* = 8.1 Hz, 2H), 4.13 – 3.97 (m, 2H), 3.71 (d, *J* = 8.8 Hz, 1H), 2.59 – 2.41 (m, 2H), 2.35 (dd, *J* = 3.5, 2.3 Hz, 1H), 2.19 – 1.84 (m, 5H), 1.81 – 1.41 (m, 6H), 1.27 – 1.18 (m, 1H).

^{13}C NMR (100 MHz, $CDCl_3$): δ 214.9, 174.6, 153.5, 62.13, 54.1, 45.6, 43.1, 41.2, 40.6, 34.5, 28.4, 27.3, 26.5, 25.3, 22.7.

IR (Neat Film, NaCl): 2949, 2872, 1775, 1718, 1692, 1387, 1221,1040, 759 cm^{-1}.

HRMS (MM: FD+): *m/z* calc'd for $C_{15}H_{19}NO_4$ $[M]^+$: 277.1314, found 277.1317.

Optical Rotation: $[\alpha]_D^{21}$ –5.8 (c 1.00, $CHCl_3$).

SFC conditions: 15% IPA, 2.5 mL/min, Chiralpak AD-H column, λ = 210 nm, t_R (min): minor = 6.80, major = 6.38.

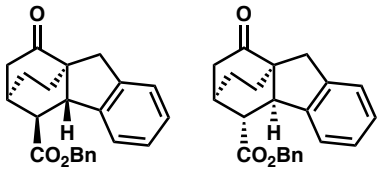

115p (endo) ***115p' (exo)***

benzyl (3*R*,4*S*,4a*S*,9a*S*)-1-oxo-1,2,3,4,4a,9-hexahydro-3,9a-ethanofluorene-4-carboxylate (115p and 115p')

Prepared from **114p** following General Procedure A. Purification by flash column chromatography (0–35% EtOAc/hexanes) afforded the title compounds as colorless oils (**Endo**: 56.8 mg, 0.156 mmol, 78% yield, 72% ee; **Exo**: 2.0 mg, 5.48 μmol, 3% yield).

115p (endo):

^{1}H NMR (400 MHz, $CDCl_3$): δ 7.28 – 7.20 (m, 5H), 7.14 – 7.05 (m, 4H), 5.13 (d, *J* = 2.4 Hz, 2H), 3.53 (dd, *J* = 9.4, 1.0 Hz, 1H), 3.16 (d, *J* = 15.7 Hz, 1H), 2.74 (dt, *J* = 9.3, 1.1 Hz, 1H), 2.61 (dt, *J* = 18.8, 2.4 Hz, 1H), 2.51 (ttd, *J* = 3.5, 2.2, 1.1 Hz, 1H), 2.31 (d, *J* = 15.8 Hz, 1H), 2.11 (ddd, *J* = 18.8, 3.5, 1.2 Hz, 1H), 1.70 – 1.56 (m, 2H), 1.54 – 1.45 (m, 1H), 1.42 – 1.34 (m, 1H).

^{13}C NMR (100 MHz, $CDCl_3$): δ 214.0, 174.6, 142.3, 140.6, 135.8, 128.8, 128.6, 128.4, 127.3, 127.0, 125.5, 124.3, 67.1, 56.6, 47.8, 45.6, 42.1, 35.0, 33.2, 27.0, 24.8.

IR (Neat Film, NaCl): 2942, 2869, 1726, 1457, 1164 cm^{-1}.

HRMS (MM: FD+): *m/z* calc'd for $C_{23}H_{22}O_3$ $[M+H]^+$: 346.1564, found 346.1571.

Optical Rotation: $[\alpha]_D^{21}$ +1.4 (c 1.00, $CHCl_3$).

SFC conditions: 15% IPA, 2.5 mL/min, Chiralpak AD-H column, λ = 210 nm, t_R (min): minor = 6.74, major = 6.28.

115p' (exo):

^{1}H NMR (400 MHz, $CDCl_3$): δ 7.41 – 7.34 (m, 5H), 7.24 (d, *J* = 7.1 Hz, 1H), 7.14 – 7.07 (m, 3H), 5.30 (d, *J* = 12.3 Hz, 1H), 5.25 (d, *J* = 12.3 Hz, 1H), 3.85 (d, *J* = 9.4 Hz, 1H), 3.46 (d, *J* = 14.7 Hz, 1H), 2.75 (d, *J* = 9.3 Hz, 1H), 2.69 – 2.65 (m, 1H), 2.44 (d, *J* = 14.9 Hz, 1H), 2.37 (dd, *J* = 18.7, 2.1 Hz, 1H), 2.19 (ddd, *J* = 18.6, 3.4, 2.1 Hz, 1H), 2.15 – 2.07 (m, 2H), 1.90 – 1.84 (m, 1H), 1.81 – 1.76 (m, 1H).

^{13}C NMR (100 MHz, $CDCl_3$): δ 213.5, 174.0, 143.8, 142.7, 135.9, 128.8, 128.6, 128.4, 127.2, 126.6, 124.8, 122.5, 67.1, 56.4, 49.9, 48.3, 44.1, 35.3, 31.9, 27.5, 21.8.

IR (Neat Film, NaCl): 2918, 1727, 1161 cm^{-1}.

HRMS (MM: FD+): *m/z* calc'd for $C_{23}H_{22}O_3$ $[M+H]^+$: 346.1569, found 346.1568.

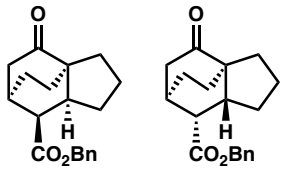

115q (endo) *115q' (exo)*

benzyl (3a*R*,6*R*,7*S*,7a*S*)-4-oxooctahydro-3a,6-ethanoindene-7-carboxylate (115q and 115q')

Prepared from **114q** following General Procedure A. Purification by flash column chromatography (0–35% EtOAc/hexanes) afforded the title compound as a colorless oil (54.9 mg, 0.183 mmol, 92% yield, 1.6:1 endo/exo, 84% ee (endo), 29% ee (exo)). The *endo* (**115q**) and *exo* (**115q'**) diastereomers were subsequently separated by preparative TLC (25% EtOAc/hexanes) for independent characterization. Absolute and relative stereochemistry were assigned/confirmed by VCD (see below).

115q (endo):

^{1}H NMR (400 MHz, $CDCl_3$): δ 7.39 – 7.31 (m, 5H), 5.13 – 5.02 (m, 2H), 3.10 – 2.99 (m, 2H), 2.47 (h, *J* = 2.9 Hz, 1H), 2.36 – 2.21 (m, 2H), 2.15 (dt, *J* = 19.3, 2.3 Hz, 1H), 1.86 – 1.63 (m, 6H), 1.56 – 1.48 (m, 1H), 1.06 – 0.92 (m, 2H).

^{13}C NMR (100 MHz, $CDCl_3$): δ 215.5, 172.9, 135.9, 128.7, 128.7, 128.5, 66.3, 54.4, 45.9, 44.0, 40.2, 31.4, 28.3, 28.1, 27.0, 26.4, 21.8.

IR (Neat Film, NaCl): 2940, 2868, 1728, 1456, 1174, 1166, 1146 cm^{-1}.

HRMS (MM: FD+): *m/z* calc'd for $C_{19}H_{22}O_3$ $[M]^+$: 298.1564, found 298.1578.

Optical Rotation: $[\alpha]_D^{21}$ –32.4 (c 1.00, $CHCl_3$).

SFC conditions: 15% IPA, 2.5 mL/min, Chiralpak AD-H column, λ = 210 nm, t_R (min): minor = 5.44, major = 6.53.

115q' (exo):

^{1}H NMR (400 MHz, $CDCl_3$): δ 7.40 – 7.31 (m, 5H), 5.14 (d, *J* = 12.3 Hz, 1H), 5.09 (d, *J* = 12.2 Hz, 1H), 3.01 (ddd, *J* = 11.7, 3.3, 1.4 Hz, 1H), 2.46 (h, *J* = 3.3 Hz, 1H), 2.35 – 2.25 (m, 3H), 2.14 (tdd, *J* = 11.6, 7.9, 1.6 Hz, 1H), 2.07 – 1.94 (m, 2H), 1.88 – 1.69 (m, 3H), 1.63 – 1.57 (m, 1H), 1.47 – 1.34 (m, 2H), 1.16 (ddd, *J* = 13.9, 9.1, 5.0 Hz, 1H).

^{13}C NMR (100 MHz, $CDCl_3$): δ 215.5, 173.1, 136.0, 128.8, 128.5, 128.5, 66.3, 53.6, 45.4, 42.7, 41.2, 32.0, 26.4, 25.3, 24.4, 22.3, 21.8.

IR (Neat Film, NaCl): 2946, 2847, 1720, 1457, 1154 cm^{-1}.

HRMS (MM: FD+): *m/z* calc'd for $C_{19}H_{22}O_3$ $[M]^+$: 298.1564, found 298.1578.

Optical Rotation: $[\alpha]_D^{21}$ –5.1 (c 1.00, $CHCl_3$).

SFC conditions: 15% IPA, 2.5 mL/min, Chiralpak IC column, λ = 210 nm, t_R (min): minor = 7.01, major = 7.42.

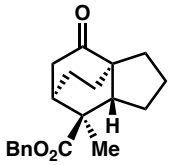

115r

benzyl (3a*R*,6*R*,7*S*,7a*S*)-7-methyl-4-oxooctahydro-3a,6-ethanoindene-7-carboxylate (115r)

Prepared from **114r** following General Procedure A. Purification by flash column chromatography (0–30% EtOAc/hexanes) afforded the title compound as a colorless oil (29.4 mg, 0.094 mmol, 47% yield, 89% ee).

^{1}H NMR (400 MHz, $CDCl_3$): δ 7.39 – 7.29 (m, 5H), 5.16 (d, *J* = 12.4 Hz, 1H), 5.10 (d, *J* = 12.4 Hz, 1H), 2.49 – 2.38 (m, 2H), 2.32 (dt, *J* = 18.9, 2.8 Hz, 1H), 2.19 – 2.10 (m, 2H),

2.01 – 1.92 (m, 1H), 1.85 – 1.66 (m, 4H), 1.65 – 1.55 (m, 1H), 1.49 – 1.31 (m, 5H), 1.13 (ddd, *J* = 14.5, 9.1, 6.0 Hz, 1H).

^{13}C NMR (100 MHz, $CDCl_3$): δ 215.2, 177.8, 136.1, 128.7, 128.4, 128.0, 66.8, 54.37, 45.8, 44.7, 43.4, 37.3, 26.5, 24.4, 24.1, 22.7, 22.4, 20.8.

IR (Neat Film, NaCl): 2951, 2875, 1723, 1454, 1239, 1212, 1106 cm^{-1}.

HRMS (MM: FD+): *m/z* calc'd for $C_{20}H_{24}O_3$ $[M]^+$: 312.1725, found 312.1732.

Optical Rotation: $[\alpha]_D^{21}$ –15.3 (c 1.00, $CHCl_3$).

SFC conditions: 40% IPA, 2.5 mL/min, Chiralpak IC column, λ = 210 nm, t_R (min): minor = 2.68, major = 3.51.

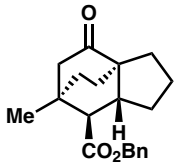

11s

benzyl (3aR,6R,7R,7aR)-6-methyl-4-oxooctahydro-3a,6-ethanoindene-7-carboxylate (115s)

Prepared from **114s** following General Procedure A. Purification by flash column chromatography (0–25% EtOAc/hexanes) afforded the title compound as a colorless oil (43.6 mg, 0.140 mmol, 69% yield, 83% ee).

^{1}H NMR (400 MHz, $CDCl_3$): δ 7.42 – 7.29 (m, 5H), 5.13 (d, *J* = 1.1 Hz, 2H), 2.86 (dd, *J* = 18.5, 3.5 Hz, 1H), 2.37 (dd, *J* = 8.8, 1.4 Hz, 1H), 2.29 – 2.15 (m, 1H), 2.15 – 2.04 (m, 1H), 2.01 – 1.70 (m, 3H), 1.84 (dd, *J* = 18.7, 1.4 Hz, 1H), 1.68 – 1.36 (m, 4H), 1.30 – 1.15 (m, 2H), 0.94 (s, 3H).

^{13}C NMR (100 MHz, $CDCl_3$): δ 214.5, 174.9, 135.9, 128.8, 128.5, 128.5, 66.7, 54.2, 52.6, 47.0, 44.9, 38.0, 36.0, 28.7, 26.3, 26.0, 23.8, 22.8.

IR (Neat Film, NaCl): 2949, 2873, 1750, 1498, 1454, 1384, 1324, 1155, 1114, 977, 754, 698, 678, 556 cm^{-1}.

HRMS (MM: FD+): *m/z* calc'd for $C_{20}H_{24}O_3$ $[M]^+$: 312.1703, found 312.1720.

Optical Rotation: $[\alpha]_D^{21}$ –68.2 (c 0.75, $CHCl_3$).

SFC conditions: 15% IPA, 2.5 mL/min, Chiralpak IC column, λ = 210 nm, t_R (min): minor = 10.23, major = 12.31.

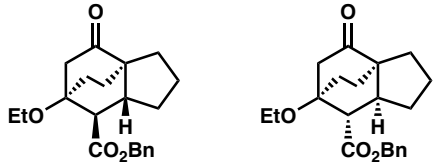

115t (endo) ***115t' (exo)***

benzyl (3a*R*,6*S*,7*R*,7a*R*)-6-ethoxy-4-oxooctahydro-3a,6-ethanoindene-7-carboxylate (115t and 115t')

Prepared from **114t** following General Procedure A. Purification by flash column chromatography (0–50% EtOAc/hexanes) afforded the title compounds as colorless oils (**Endo**: 44.0 mg, 0.128 mmol, 64% yield, 85% ee; **Exo**: 17.0 mg, 0.050 mmol, 25% yield, 72% ee). Absolute and relative stereochemistry were assigned/confirmed by VCD (see below).

115t (endo):

^{1}H NMR (400 MHz, $CDCl_3$): δ 7.38 – 7.28 (m, 5H), 5.16 (d, *J* = 1.5 Hz, 2H), 3.55 – 3.32 (m, 2H), 3.17 (dd, *J* = 18.5, 3.1 Hz, 1H), 2.86 (dd, *J* = 8.5, 1.5 Hz, 1H), 2.38 – 2.25 (m,

2H), 2.16 – 2.02 (m, 1H), 2.02 – 1.86 (m, 3H), 1.87 – 1.39 (m, 5H), 1.20 (ddd, J = 14.1, 9.1, 5.1 Hz, 1H), 1.03 (t, J = 7.0 Hz, 3H).

^{13}C NMR (100 MHz, $CDCl_3$): δ 210.8, 173.7, 136.0, 128.7, 128.4, 128.3, 78.2, 66.8, 58.0, 54.2, 51.9, 45.1, 45.1, 30.7, 28.8, 25.8, 24.8, 22.9, 15.8.

IR (Neat Film, NaCl): 2944, 2875, 1726, 1458, 1390, 1320, 1282, 1153, 1110, 1039, 746, 700 cm^{-1}.

HRMS (MM: FD+): *m/z* calc'd for $C_{21}H_{26}O_4$ $[M]^+$: 342.1832, found 342.1826.

Optical Rotation: $[\alpha]_D^{21}$ –47.4 (c 0.75, $CHCl_3$).

SFC conditions: 15% IPA, 2.5 mL/min, Chiralpak AD-H column, λ = 210 nm, t_R (min): minor = 4.73, major = 5.13.

115t' (exo):

^{1}H NMR (400 MHz, $CDCl_3$): δ 7.42 – 7.28 (m, 5H), 5.19 (d, J = 1.1 Hz, 2H), 3.57 – 3.35 (m, 2H), 2.69 (dd, J = 7.8, 1.7 Hz, 1H), 2.60 – 2.47 (m, 1H), 2.47 – 2.44 (m, 2H), 2.39 (ddd, J = 12.5, 7.9, 6.9 Hz, 1H), 2.28 (ddd, J = 13.5, 9.4, 4.6 Hz, 1H), 1.92 – 1.78 (m, 3H), 1.77 – 1.66 (m, 1H), 1.67 – 1.58 (m, 1H), 1.11 (ddd, J = 11.3, 6.6, 3.7 Hz, 1H), 1.03 (t, J = 6.9 Hz, 3H), 0.89 (tt, J = 12.4, 9.6 Hz, 1H).

^{13}C NMR (100 MHz, $CDCl_3$): δ 211.5, 173.4, 136.0, 128.7, 128.4, 128.3, 66.9, 58.1, 54.1, 52.8, 47.5, 46.8, 31,0, 27.7, 26.5, 25.9, 23.1, 15.7.

IR (Neat Film, NaCl): 2946, 1721, 1451, 1390, 1328, 1154, 1117, 767, 698 cm^{-1}.

HRMS (MM: FD+): *m/z* calc'd for $C_{21}H_{26}O_4$ $[M]^+$: 342.1833, found 342.1826.

Optical Rotation: $[\alpha]_D^{21}$ +1.8 (c 0.75, $CHCl_3$).

SFC conditions: 15% IPA, 2.5 mL/min, Chiralpak IC column, λ = 210 nm, t_R (min): minor = 3.29, major = 4.04.

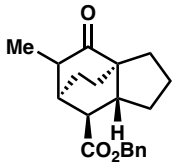

115u

benzyl (3a*R*,6*R*,7*S*,7a*R*)-5-methyl-4-oxooctahydro-3a,6-ethanoindene-7-carboxylate (115u)

Prepared from **114u** following General Procedure A. Purification by flash column chromatography (0–25% EtOAc/hexanes) afforded the title compound as a colorless oil (13.6 mg, 0.044 mmol, 22% yield, 61% ee).

^{1}H NMR (400 MHz, $CDCl_3$): δ 7.39 – 7.32 (m, 5H), 5.14 (ddd, *J* = 17.8, 12.2 Hz, 2H), 2.61 (dd, *J* = 3.7, 2.1 Hz, 1H), 2.45 – 2.30 (m, 3H), 2.21 – 2.06 (m, 4H), 1.90 – 1.63 (m, 3H), 1.61 – 1.35 (m, 2H), 1.32 – 1.16 (m, 1H), 0.97 (d, *J* = 7.7 Hz, 3H).

^{13}C NMR (100 MHz, $CDCl_3$): δ 217.7, 174.8, 135.9, 128.7, 128.6, 128.5, 66.8, 54.2, 48.3, 46.9, 42.2, 38.1, 29.7, 28.9, 26.6, 24.1, 22.5, 15.8.

IR (Neat Film, NaCl): 2943, 2873, 1718, 1455, 1197, 1171 cm^{-1}.

HRMS (MM: FD+): *m/z* calc'd for $C_{20}H_{24}O_3$ $[M]^+$: 312.1725, found 312.1730.

Optical Rotation: $[\alpha]_D^{21}$ +10.9 (c 0.75, $CHCl_3$).

SFC conditions: 15% IPA, 2.5 mL/min, Chiralpak AD-H column, λ = 210 nm, t_R (min): minor = 5.84, major = 5.43.

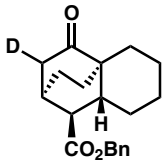

***D*-115f**

benzyl (1*S*,2*R*,4a*R*,8a*R*)-4-oxooctahydro-2*H*-2,4a-ethanonaphthalene-1-carboxylate-3-*d* (*D*-115f)

Prepared from ***D*-114f** following General Procedure A. Purification by flash column chromatography (0–30% EtOAc/hexanes) afforded the title compound as a colorless oil (41.3 mg, 0.132 mmol, 66% yield, 91% ee).

^{1}H NMR (400 MHz, $CDCl_3$): δ 7.39 – 7.30 (m, 5H), 5.16 (d, *J* = 12.4 Hz, 1H), 5.11 (d, *J* = 12.2 Hz, 1H), 2.51 – 2.41 (m, 1.6H), 2.36 – 2.10 (m, 2.7H), 2.02 (dddd, *J* = 11.8, 9.1, 5.3, 2.9 Hz, 1H), 1.91 – 1.83 (m, 1H), 1.82 – 1.71 (m, 1H), 1.70 – 1.55 (m, 4H), 1.52 – 1.11 (m, 5H).

^{13}C NMR (100 MHz, $CDCl_3$): δ 216.4, 174.5, 136.0, 128.8, 128.4, 128.2, 77.5, 77.2, 76.8, 66.7, 49.9, 45.1, 40.5, 37.1, 31.0, 30.9, 30.8, 30.0, 28.9, 26.2, 25.6, 21.8, 21.2.

**Partial deuteration complicates ^{13}C NMR spectrum. Peaks are listed as they appear.*

^{2}H NMR (61 MHz, $CHCl_3$): δ 2.46, 2.14.

**Trace D-exchanged water observed in spectrum.*

IR (Neat Film, NaCl): 2928, 2858, 1723, 1169 cm^{-1}.

HRMS (MM: FD+): *m/z* calc'd for $C_{20}H_{23}DO_3$ $[M+H]^+$: 313.1783, found 313.1795.

Optical Rotation: $[\alpha]_D^{21}$ –21.3 (c 1.00, $CHCl_3$).

SFC conditions: 15% IPA, 2.5 mL/min, Chiralpak AD-H column, λ = 210 nm, t_R (min): minor = 5.07, major = 6.38.

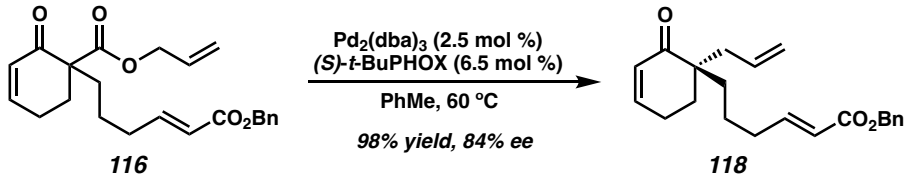

116 ***118***

benzyl (*S*,*E*)-6-(1-allyl-2-oxocyclohex-3-en-1-yl)hex-2-enoate (118)

Prepared from **116** (0.02 mmol) following General Procedure A. Purification by preparatory thin layer chromatography (25% EtOAc/hexanes) afforded the title compound as a colorless oil (10.1 mg, 0.0196 mmol, 98% yield, 84 % ee).

^{1}H NMR (400 MHz, $CDCl_3$): δ 7.40 – 7.29 (m, 5H), 6.97 (dt, *J* = 15.6, 6.9 Hz, 1H), 6.85 (dt, *J* = 10.1, 3.9 Hz, 1H), 5.91 (dt, *J* = 10.0, 2.0 Hz, 1H), 5.85 (dt, *J* = 15.7, 1.6 Hz, 1H), 5.69 (ddt, *J* = 16.6, 10.5, 7.3 Hz, 1H), 5.17 (s, 2H), 5.09 – 5.00 (m, 2H), 2.41 – 2.29 (m, 3H), 2.26 – 2.13 (m, 3H), 1.87 (t, *J* = 6.1 Hz, 2H), 1.63 – 1.23 (m, 4H).

^{13}C NMR (100 MHz, $CDCl_3$): δ 202.9, 166.6, 149.6, 148.7, 136.3, 134.0, 129.0, 128.7, 128.3, 128.3, 121.4, 118.3, 66.2, 47.6, 39.1, 33.9, 32.9, 30.8, 23.1, 22.4.

IR (Neat Film, NaCl): 2936, 2358, 1718, 1669, 1262, 992 cm^{-1}.

HRMS (MM: FD+): *m/z* calc'd for $C_{22}H_{26}O_3$ $[M]^+$: 338.1881, found 338.1877.

Optical Rotation: $[\alpha]_D^{21}$ –0.69 (c 0.62, $CHCl_3$).

SFC conditions: 15% IPA, 2.5 mL/min, Chiralpak IC column, λ = 210 nm, t_R (min): minor = 14.49, major = 11.94.

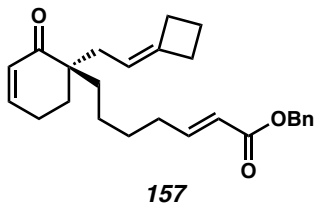

157

benzyl (*E*)-7-(1-(2-cyclobutylideneethyl)-2-oxocyclohex-3-en-1-yl)hept-2-enoateenoate (157)

Prepared from **137** following General Procedure A, with the modification of being on 0.1 mmol scale. Purification by preparatory thin layer chromatography (20% EtOAc/hexanes) afforded the title compound as a clear oil (2.4 mg, 0.006 mmol, 6% yield).

^{1}H NMR (400 MHz, $CDCl_3$): δ 7.41 – 7.29 (m, 5H), 6.99 (dt, *J* = 15.6, 6.9 Hz, 1H), 6.83 (dt, *J* = 10.0, 3.9 Hz, 1H), 5.92 – 5.81 (m, 2H), 5.17 (s, 2H), 5.01 – 4.92 (m, 1H), 2.67 – 2.54 (m, 3H), 2.40 – 2.30 (m, 2H), 2.27 – 1.99 (m, 4H), 1.96 – 1.82 (m, 3H), 1.63 – 1.49 (m, 3H), 1.49 – 1.36 (m, 3H), 1.32 – 1.13 (m, 2H).

^{13}C NMR (100 MHz, $CDCl_3$): δ 203.6, 166.6, 150.1, 148.5, 143.1, 136.3, 129.1, 128.7, 128.3, 128.3, 121.1, 115.4, 66.2, 48.3, 34.1, 33.1, 32.3, 31.2, 30.8, 29.6, 28.8, 23.6, 23.2, 17.1.

IR (Neat Film, NaCl): 2929, 1720, 1670, 1185 cm^{-1}.

HRMS (MM: FD+): *m/z* calc'd for $C_{26}H_{32}O_3$ $[M]^+$: 392.2351, found 392.2341.

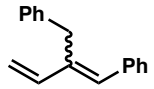

158

(2-vinylprop-1-ene-1,3-diyl)dibenzene (158)

Prepared from **141** following General Procedure A, with the modification of being on 0.1 mmol scale. Purification by flash column chromatography (0–35% EtOAc/hexanes) afforded the title compound as a colorless oil (6.5 mg, 0.03 mmol, 29% yield).

^{1}H NMR (400 MHz, $CDCl_3$): δ 7.39 – 7.18 (m, 11.5H), 6.91 – 6.80 (m, 1.15H), 6.56 (ddd, *J* = 17.4, 10.8, 0.9 Hz, 0.15H), 6.45 (s, 1H), 5.42 – 5.33 (m, 1H), 5.19 – 5.13 (m, 1.15H), 5.11 – 5.06 (m, 0.15H), 3.90 (s, 0.3H), 3.73 (s, 2H).

**Isolated as an apparent 1:0.15 mixture of alkene isomers.*

^{13}C NMR (100 MHz, $CDCl_3$): δ 140.5, 140.2, 139.9, 137.7, 137.5, 137.3, 134.2, 133.8, 131.8, 129.6, 128.9, 128.8, 128.7, 128.5, 128.2, 128.2, 127.3, 127.0, 126.2, 126.1, 116.4, 114.8, 40.3, 33.2.

**Isolated as an apparent 1:0.15 mixture of alkene isomers.*

IR (Neat Film, NaCl): 3060, 3023, 2919, 1601, 1493, 1455, 1165, 1074 cm^{-1}.

HRMS (MM: FD+): *m/z* calc'd for $C_{17}H_{16}$ $[M]^+$: 220.1252, found 220.1257.

Preparation of Unsaturated β-Ketoester Starting Materials

General Procedure B: Horner–Wadsworth–Emmons Olefination

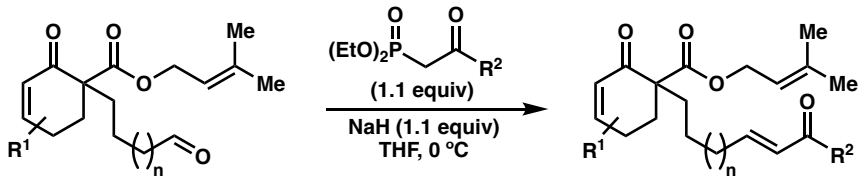

159 ***114***

To a suspension of NaH (60% by weight in mineral oil, 1.1 equiv) in THF (0.5 M) at 0 ºC was dropwise added a solution of the appropriate phosphonate ester (1.1 equiv) in THF (1.0 M). Stirred at 0 ºC was continued for 30 minutes. To the reaction was then dropwise added a solution of aldehyde **159** (1.0 equiv) in THF (0.5 M). Upon complete consumption of starting material (as determined by TLC), the reaction mixture was diluted with a saturated solution of $NaHCO_3$ and extracted with EtOAc (3x). The combined organic layers

were dried over Na_2SO_4, filtered, and concentrated under reduced pressure. The product (**114**) was purified by silica gel flash column chromatography.

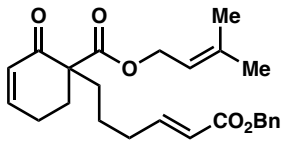

114a

3-methylbut-2-en-1-yl (*E*)-1-(6-(benzyloxy)-6-oxohex-4-en-1-yl)-2-oxocyclohex-3-ene-1-carboxylate (114a)

Prepared from **159** and benzyl 2-(diethoxyphosphoryl)acetate [28] following General Procedure B. Purification by flash column chromatography (20% EtOAc/hexanes) afforded the title compound as a colorless oil (0.410 g, 1.00 mmol, 67 % yield).

^{1}H NMR (400 MHz, $CDCl_3$): δ 7.38 – 7.29 (m, 5H), 6.98 (dt, *J* = 15.7, 6.9 Hz, 1H), 6.90 – 6.84 (m, 1H), 6.02 (ddd, *J* = 10.1, 2.5, 1.5 Hz, 1H), 5.87 (dt, *J* = 15.6, 1.6 Hz, 1H), 5.31 – 5.24 (m, 1H), 5.17 (s, 2H), 4.58 (dt, *J* = 7.2, 1.0 Hz, 2H), 2.55 – 2.41 (m, 2H), 2.37 – 2.27 (m, 1H), 2.22 (qd, *J* = 7.3, 1.6 Hz, 2H), 1.97 – 1.86 (m, 2H), 1.77 – 1.69 (m, 4H), 1.67 (d, *J* = 1.4 Hz, 3H), 1.55 – 1.38 (m, 2H).

^{13}C NMR (100 MHz, $CDCl_3$): δ 196.3, 171.6, 166.5, 149.3, 149.3, 139.7, 136.3, 129.4, 128.7, 128.3, 128.3, 121.5, 118.3, 66.2, 62.3, 57.0, 33.5, 32.7, 30.5, 25.8, 23.9, 23.2, 18.2.

IR (Neat Film, NaCl): 3034, 2938, 1723, 1684, 1653, 1455, 1384, 1246, 1174, 1166 cm^{-1}.

HRMS (MM: FD+): *m/z* calc'd for $C_{25}H_{30}O_5$ $[M]^+$: 410.2088, found 410.2097.

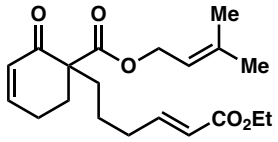

114b

3-methylbut-2-en-1-yl (*E*)-1-(6-(benzyloxy)-6-oxohex-4-en-1-yl)-2-oxocyclohex-3-ene-1-carboxylate (114b)

Prepared from **159** and ethyl 2-(diethoxyphosphoryl)acetate following General Procedure B. Purification by flash column chromatography (20% EtOAc/hexanes) afforded the title compound as a colorless oil (0.291 g, 0.835 mmol, 47 % yield).

^{1}H NMR (400 MHz, $CDCl_3$): δ 6.97 – 6.85 (m, 2H), 6.02 (ddd, *J* = 10.0, 2.6, 1.5 Hz, 1H), 5.81 (dt, *J* = 15.6, 1.6 Hz, 1H), 5.31 – 5.24 (m, 1H), 4.64 – 4.54 (m, 2H), 4.18 (q, *J* = 7.1 Hz, 2H), 2.55 – 2.41 (m, 2H), 2.37 – 2.27 (m, 1H), 2.21 (qd, *J* = 7.3, 1.6 Hz, 2H), 1.98 – 1.87 (m, 2H), 1.78 – 1.69 (m, 4H), 1.68 (s, 3H), 1.55 – 1.37 (m, 2H), 1.28 (t, *J* = 7.1 Hz, 3H).

^{13}C NMR (100 MHz, $CDCl_3$): δ 196.3, 171.6, 166.8, 149.3, 148.5, 139.7, 129.4, 121.8, 118.3, 62.3, 60.3, 57.0, 33.5, 32.6, 30.5, 25.8, 23.9, 23.3, 18.2, 14.4.

IR (Neat Film, NaCl): 2934, 1714, 1682, 1168 cm^{-1}.

HRMS (MM: FD+): *m/z* calc'd for $C_{20}H_{28}O_5$ $[M]^+$: 348.1937, found 348.1943.

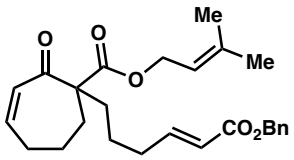

114d

3-methylbut-2-en-1-yl (*E*)-1-(6-(benzyloxy)-6-oxohex-4-en-1-yl)-2-oxocyclohept-3-ene-1-carboxylate (114d)

Prepared from cyclohept-2-en-1-one following General Procedures B–D. Note that inseparable impurities plagued the β-ketoester and aldehyde intermediates. Fortunately, these intermediates could be brought through the sequence in sub-optimal purity to still afford the title compound **114d** as a colorless oil (265 mg, 0.62 mmol, 3.2% yield from cyclohept-2-en-1-one) after a final purification by flash column chromatography (20% EtOAc/hexanes).

^{1}H NMR (400 MHz, $CDCl_3$): δ 7.39 – 7.30 (m, 5H), 6.97 (dt, *J* = 15.6, 6.9 Hz, 1H), 6.36 (ddd, *J* = 12.3, 5.5, 3.9 Hz, 1H), 5.98 (ddd, *J* = 12.3, 2.4, 1.4 Hz, 1H), 5.86 (dt, *J* = 15.6, 1.6 Hz, 1H), 5.28 (ddp, *J* = 8.6, 5.7, 1.4 Hz, 1H), 5.17 (s, 2H), 4.57 (d, *J* = 7.2 Hz, 2H), 2.47 – 2.27 (m, 3H), 2.19 (qd, *J* = 7.2, 1.6 Hz, 2H), 1.99 – 1.79 (m, 3H), 1.77 – 1.69 (m, 4H), 1.69 – 1.61 (m, 4H), 1.43 – 1.32 (m, 2H).

^{13}C NMR (100 MHz, $CDCl_3$): δ 201.1, 172.9, 166.5, 149.3, 143.2, 139.7, 136.3, 131.6, 128.7, 128.3, 128.3, 121.5, 118.2, 66.2, 63.9, 62.2, 36.5, 32.6, 32.3, 31.2, 25.8, 24.3, 23.0, 18.2.

IR (Neat Film, NaCl): 2927, 1720, 1686, 1453, 1162 cm^{-1}.

HRMS (MM: FD+): *m/z* calc'd for $C_{26}H_{32}O_5$ $[M]^+$: 424.2244, found 424.2241.

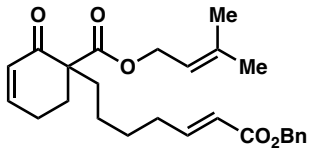

114f

3-methylbut-2-en-1-yl (*E*)-1-(7-(benzyloxy)-7-oxohept-5-en-1-yl)-2-oxocyclohex-3-ene-1-carboxylate (114f)

Prepared from **160** and benzyl 2-(diethoxyphosphoryl)acetate[28] following General Procedure B. Purification by flash column chromatography (15–20% EtOAc/hexanes) afforded the title compound as a colorless oil (652 mg, 1.54 mmol, 69% yield).

^{1}H NMR (400 MHz, $CDCl_3$): δ 7.39 – 7.30 (m, 5H), 6.99 (ddd, *J* = 15.5, 7.3, 6.3 Hz, 1H), 6.90 – 6.84 (m, 1H), 6.01 (d, *J* = 10.1 Hz, 1H), 5.85 (d, *J* = 15.6 Hz, 1H), 5.30 – 5.25 (m, 1H), 5.17 (s, 2H), 4.58 (d, *J* = 6.6 Hz, 2H), 2.55 – 2.40 (m, 2H), 2.36 – 2.26 (m, 1H), 2.24 – 2.16 (m, 2H), 1.96 – 1.86 (m, 2H), 1.77 – 1.65 (m, 7H), 1.47 (p, *J* = 7.4 Hz, 2H), 1.38 – 1.24 (m, 2H).

^{13}C NMR (100 MHz, $CDCl_3$): δ 196.2, 171.6, 166.5, 149.7, 149.2, 139.4, 136.2, 129.2, 128.6, 128.2, 128.2, 121.1, 118.2, 66.0, 62.1, 56.9, 33.5, 32.0, 30.2, 28.4, 25.7, 24.2, 23.7, 18.1.

IR (Neat Film, NaCl): 2932, 2861, 1722, 1684, 1653, 1456, 1263, 1181 cm^{-1}.

HRMS (MM: FD+): *m/z* calc'd for $C_{26}H_{32}O_5$ $[M]^+$: 424.2244, found 424.2247.

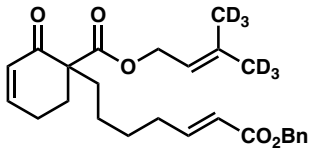

***D*-114f**

3-(methyl-d_3)but-2-en-1-yl-4,4,4-d_3 (*E*)-1-(7-(benzyloxy)-7-oxohept-5-en-1-yl)-2-oxocyclohex-3-ene-1-carboxylate (*D*-114f)

Prepared from ***D*-160** and benzyl 2-(diethoxyphosphoryl)acetate[28] following General Procedure B. Purification by flash column chromatography (15–20% EtOAc/hexanes) afforded the title compound as a colorless oil (201 mg, 0.467 mmol, 48 % yield).

^{1}H NMR (400 MHz, $CDCl_3$): δ 7.39 – 7.30 (m, 5H), 6.99 (dt, *J* = 15.6, 6.9 Hz, 1H), 6.90 – 6.85 (m, 1H), 6.01 (ddd, *J* = 10.1, 2.6, 1.5 Hz, 1H), 5.85 (dt, *J* = 15.6, 1.5 Hz, 1H), 5.27 (t, *J* = 7.1 Hz, 1H), 5.17 (s, 2H), 4.58 (dd, *J* = 7.2, 1.7 Hz, 2H), 2.55 – 2.41 (m, 2H), 2.36 – 2.27 (m, 1H), 2.25 – 2.15 (m, 2H), 1.98 – 1.85 (m, 2H), 1.73 (ddd, *J* = 13.6, 11.2, 5.3 Hz, 1H), 1.51 – 1.42 (m, 2H), 1.37 – 1.25 (m, 2H).

^{13}C NMR (100 MHz, $CDCl_3$): δ 196.4, 171.7, 166.6, 149.8, 149.3, 139.4, 136.3, 129.4, 128.7, 128.3, 128.3, 121.2, 118.4, 66.2, 62.3, 57.0, 33.6, 32.2, 30.3, 28.5, 24.3, 23.9.

^{2}H NMR (61 MHz, $CHCl_3$): δ 1.69, 1.65.

IR (Neat Film, NaCl): 2930, 1720, 1683, 1264, 1167 cm^{-1}.

HRMS (MM: FD+): *m/z* calc'd for $C_{26}H_{26}D_6O_5$ $[M]^+$: 430.2621, found 430.2622.

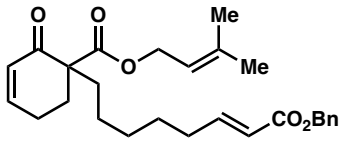

114g

3-methylbut-2-en-1-yl (*E*)-1-(8-(benzyloxy)-8-oxooct-6-en-1-yl)-2-oxocyclohex-3-ene-1-carboxylate (114g)

Prepared from **161** and benzyl 2-(diethoxyphosphoryl)acetate[28] following General Procedure B. Purification by flash column chromatography (10–25% EtOAc/hexanes) afforded the title compound as a colorless oil (773 mg, 1.76 mmol, 65 % yield).

^{1}H NMR (400 MHz, $CDCl_3$): δ 7.40 – 7.29 (m, 5H), 6.99 (dt, *J* = 15.6, 6.9 Hz, 1H), 6.89 – 6.84 (m, 1H), 6.01 (ddd, *J* = 10.0, 2.5, 1.5 Hz, 1H), 5.85 (dt, *J* = 15.6, 1.6 Hz, 1H), 5.28 (ddp, *J* = 8.6, 5.7, 1.4 Hz, 1H), 5.17 (s, 2H), 4.63 – 4.53 (m, 2H), 2.55 – 2.40 (m, 2H), 2.36

– 2.26 (m, 1H), 2.19 (qd, *J* = 7.1, 1.6 Hz, 2H), 1.98 – 1.84 (m, 2H), 1.77 – 1.69 (m, 4H), 1.67 (s, 3H), 1.49 – 1.41 (m, 2H), 1.36 – 1.23 (m, 4H).

^{13}C NMR (100 MHz, $CDCl_3$): δ 196.5, 171.7, 166.6, 150.1, 149.3, 139.5, 136.3, 129.4, 128.7, 128.3, 128.3, 121.2, 118.4, 66.2, 62.2, 57.1, 33.7, 32.3, 30.3, 29.6, 27.8, 25.8, 24.4, 23.9, 18.2.

IR (Neat Film, NaCl): 2929, 2858, 1721, 1684, 1654, 1456, 1264, 1168 cm^{-1}.

HRMS (MM: FD+): *m/z* calc'd for $C_{27}H_{34}O_5$ $[M]^+$: 438.2401, found 438.2396.

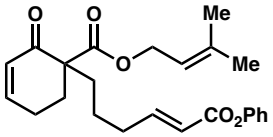

114k

3-methylbut-2-en-1-yl (*E*)-2-oxo-1-(6-oxo-6-phenoxyhex-4-en-1-yl)cyclohex-3-ene-1-carboxylate (114k)

Prepared from **159** and benzyl 2-(diethoxyphosphoryl)acetate [29] following General Procedure B. Purification by flash column chromatography (20% EtOAc/hexanes) afforded the title compound as a colorless oil (409 mg, 1.03 mmol, 57 % yield).

^{1}H NMR (400 MHz, $CDCl_3$): δ 7.38 (t, *J* = 8.0 Hz, 2H), 7.22 (t, *J* = 7.4 Hz, 1H), 7.18 – 7.10 (m, 3H), 6.91 – 6.87 (m, 1H), 6.05 – 6.00 (m, 2H), 5.29 (tt, *J* = 7.1, 1.3 Hz, 1H), 4.61 (d, *J* = 7.1 Hz, 2H), 2.56 – 2.44 (m, 2H), 2.37 – 2.27 (m, 3H), 2.00 – 1.92 (m, 2H), 1.82 – 1.73 (m, 4H), 1.69 (s, 3H), 1.63 – 1.46 (m, 2H).

^{13}C NMR (100 MHz, $CDCl_3$): δ 196.3, 171.6, 165.1, 150.9, 150.9, 149.3, 139.7, 129.5, 129.4, 125.8, 121.8, 121.1, 118.3, 62.4, 57.0, 33.6, 32.8, 30.5, 25.8, 23.9, 23.2, 18.2.

IR (Neat Film, NaCl): 2930, 1732, 1684, 1652, 1458, 1245, 1195 cm^{-1}.

HRMS (MM: FD+): *m/z* calc'd for $C_{24}H_{28}O_5$ $[M]^+$: 396.1931, found 396.1945.

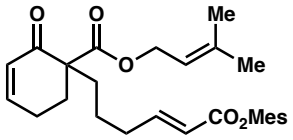

114l

3-methylbut-2-en-1-yl (*E*)-1-(6-(mesityloxy)-6-oxohex-4-en-1-yl)-2-oxocyclohex-3-ene-1-carboxylate (114l)

Prepared from **159** and mesityl 2-(diethoxyphosphoryl)acetate [30] following General Procedure B. Purification by flash column chromatography (20% EtOAc/hexanes) afforded the title compound as a colorless oil (597 mg, 1.36 mmol, 76% yield).

^{1}H NMR (400 MHz, $CDCl_3$): δ 7.17 (dt, *J* = 15.7, 6.8 Hz, 1H), 6.92 – 6.84 (m, 3H), 6.09 – 6.01 (m, 2H), 5.32 – 5.26 (m, 1H), 4.61 (d, *J* = 5.6 Hz, 2H), 2.57 – 2.43 (m, 2H), 2.39 – 2.27 (m, 3H), 2.26 (s, 3H), 2.09 (s, 6H), 2.01 – 1.92 (m, 2H), 1.79 (ddd, *J* = 13.6, 11.9, 4.8 Hz, 1H), 1.73 (s, 3H), 1.69 (s, 3H), 1.64 – 1.46 (m, 2H).

^{13}C NMR (100 MHz, $CDCl_3$): δ 196.3, 171.6, 164.6, 150.7, 149.3, 146.0, 139.7, 135.3, 130.0, 129.4, 129.3, 120.7, 118.3, 62.4, 57.0, 33.6, 32.8, 30.5, 25.8, 23.9, 23.2, 20.9, 18.2, 16.4.

IR (Neat Film, NaCl: 2920, 1733, 1684, 1458, 1248, 1192, 1140 cm^{-1}.

HRMS (MM: FD+): *m/z* calc'd for $C_{27}H_{34}O_5$ $[M]^+$: 438.2401, found 438.2401.

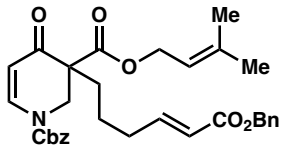

114n

1-benzyl 3-(3-methylbut-2-en-1-yl) (*E*)-3-(6-(benzyloxy)-6-oxohex-4-en-1-yl)-4-oxo-3,4-dihydropyridine-1,3(2*H*)-dicarboxylate (114n)

Prepared from **162** and benzyl 2-(diethoxyphosphoryl)acetate[28] following General Procedure B. Purification by flash column chromatography (20-30% EtOAc/hexanes) afforded the title compound as a colorless oil (181.3 mg, 0.332 mmol, 55% yield).

^{1}H NMR (400 MHz, $CDCl_3$): δ 7.79 (s, 1H), 7.44 – 7.28 (m, 10H), 6.94 (dt, *J* = 15.5, 6.8 Hz, 1H), 5.85 (dt, *J* = 15.7, 1.6 Hz, 1H), 5.42 – 5.21 (m, 4H), 5.17 (s, 2H), 4.67 – 4.51 (m, 3H), 3.71 (d, *J* = 13.6 Hz, 1H), 2.20 (q, *J* = 7.3 Hz, 2H), 2.07 – 1.92 (m, 1H), 1.69 – 1.58 (m, 1H), 1.71 (s, 3H), 1.66 (s, 3H), 1.49 – 1.40 (m, 2H).

^{13}C NMR (100 MHz, $CDCl_3$): δ 190.5, 169.5, 166.4, 148.7, 142.7, 140.1, 136.2, 135.0, 129.0, 128.9, 128.7, 128.6, 128.4, 128.3, 121.7, 118.0, 106.5, 69.4, 66.2, 62.8, 55.3, 48.3, 32.4, 31.3, 25.8, 23.0, 18.2.

IR (Neat Film, NaCl): 2938, 2338, 1726, 1676, 1604, 1456, 1388, 1303, 1201, 975 cm^{-1}.

HRMS (MM: FD+): *m/z* calc'd for $C_{32}H_{35}NO_7$ $[M]^+$: 545.2414, found 545.2408.

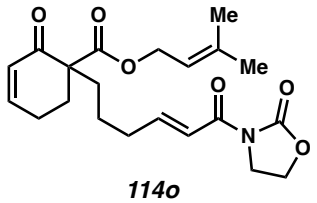

114o

3-methylbut-2-en-1-yl (*E*)-2-oxo-1-(6-oxo-6-(2-oxooxazolidin-3-yl)hex-4-en-1-yl)cyclohex-3-ene-1-carboxylate (114o)

Prepared from **159** and diethyl (2-oxo-2-(2-oxooxazolidin-3-yl)ethyl)phosphonate [31] following General Procedure B. Purification by flash column chromatography (0-80%

EtOAc/hexanes) afforded the title compound as a colorless oil (275.1 mg, 0.706 mmol, 71% yield).

^{1}H NMR (400 MHz, $CDCl_3$): δ 7.23 (d, *J* = 15.6 Hz, 1H), 7.12 (dt, *J* = 15.4, 6.7 Hz, 1H), 6.87 (ddd, *J* = 7.8, 6.0, 3.9 Hz, 1H), 6.01 (dt, *J* = 10.3, 2.0 Hz, 1H), 5.28 (tt, *J* = 7.2, 1.3 Hz, 1H), 4.62 – 4.54 (m, 2H), 4.41 (dd, *J* = 8.5, 7.6 Hz, 2H), 4.11 – 4.02 (m, 2H), 2.55 – 2.40 (m, 2H), 2.38 – 2.25 (m, 3H), 2.00 – 1.86 (m, 2H), 1.82 – 1.69 (m, 2H), 1.73 (s, 3H), 1.68 (s, 3H), 1.50 (dtd, *J* = 17.3, 12.4, 7.6 Hz, 2H).

^{13}C NMR (100 MHz, $CDCl_3$): δ 196.3, 171.6, 165.3, 153.6, 150.9, 149.4, 139.6, 129.3, 120.5, 118.3, 62.3, 62.2, 57.0, 42.8, 33.4, 33.1, 30.3, 25.8, 23.9, 23.3, 18.2.

IR (Neat Film, NaCl): 2927, 1774, 1724, 1684, 1636, 1385, 1359, 1222, 1042 cm^{-1}.

HRMS (MM: FD+): *m/z* calc'd for $C_{21}H_{27}NO_6$ $[M]^+$: 389.1838, found 389.1827.

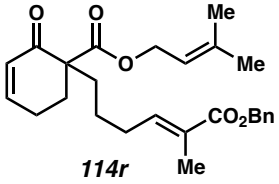

114r

3-methylbut-2-en-1-yl (*E*)-1-(6-(benzyloxy)-5-methyl-6-oxohex-4-en-1-yl)-2-oxocyclohex-3-ene-1-carboxylate (114r)

Prepared from **159** and benzyl 2-(diethoxyphosphoryl)propanoate[32] following General Procedure B. Purification by flash column chromatography (0–30% EtOAc/hexanes) afforded the title compound as a colorless oil (220 mg, 0.518 mmol, 29% yield).

^{1}H NMR (400 MHz, $CDCl_3$): δ 7.39 – 7.29 (m, 5H), 6.87 (dddd, *J* = 10.1, 4.9, 3.0, 1.1 Hz, 1H), 6.78 (tq, *J* = 7.5, 1.5 Hz, 1H), 6.01 (ddd, *J* = 10.1, 2.5, 1.5 Hz, 1H), 5.31 – 5.24 (m, 1H), 5.18 (s, 2H), 4.58 (d, *J* = 6.9 Hz, 2H), 2.55 – 2.41 (m, 2H), 2.36 – 2.26 (m, 1H), 2.19

(qd, *J* = 7.5, 1.1 Hz, 2H), 1.98 – 1.87 (m, 2H), 1.85 (s, 3H), 1.79 – 1.69 (m, 4H), 1.67 (s, 3H), 1.53 – 1.37 (m, 2H).

^{13}C NMR (100 MHz, $CDCl_3$): δ 196.3, 171.6, 168.0, 149.3, 142.3, 139.6, 136.5, 129.3, 128.6, 128.2, 128.1, 128.1, 118.3, 66.3, 62.3, 57.0, 33.7, 30.4, 29.2, 25.8, 23.9, 23.9, 18.2, 12.6.

IR (Neat Film, NaCl): 2930, 1711, 1686, 1452, 1265, 1180 cm^{-1}.

HRMS (MM: FD+): *m/z* calc'd for $C_{26}H_{32}O_5$ $[M]^+$: 424.2250, found 424.2250.

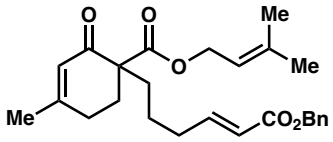

114s

3-methylbut-2-en-1-yl (*E*)-1-(6-(benzyloxy)-6-oxohex-4-en-1-yl)-4-methyl-2-oxocyclohex-3-ene-1-carboxylate (114s)

Prepared from **163** and benzyl 2-(diethoxyphosphoryl)acetate[28] following General Procedure B. Purification by flash column chromatography (15–20–25% EtOAc/hexanes) afforded the title compound as a colorless oil (827.2 mg, 2.16 mmol, 64% yield).

^{1}H NMR (400 MHz, $CDCl_3$): δ 7.39 – 7.28 (m, 5H), 6.98 (dt, *J* = 15.6, 6.8 Hz, 1H), 5.87 (dq, *J* = 2.7, 1.3 Hz, 1H), 5.86 (dt, *J* = 15.6, 1.6 Hz, 1H), 5.27 (tp, *J* = 7.1, 1.4 Hz, 1H), 5.16 (s, 2H), 4.64 – 4.51 (m, 2H), 2.52 – 2.36 (m, 2H), 2.28 – 2.14 (m, 3H), 1.98 – 1.83 (m, 5H), 1.72 (s, 4H), 1.67 (s, 3H), 1.54 – 1.34 (m, 2H).

^{13}C NMR (100 MHz, $CDCl_3$): δ 195.9, 171.7, 166.5, 161.4, 149.3, 139.6, 136.3, 128.7, 128.3, 128.3, 126.1, 121.5, 118.4, 66.2, 62.3, 55.9, 33.5, 32.7, 30.2, 28.8, 25.8, 24.2, 23.3, 18.2.

IR (Neat Film, NaCl): 3032, 2938, 1723, 1674, 1438, 1379, 1264, 1212, 1168, 1013, 741, 698 cm^{-1}.

HRMS (MM: FD+): *m/z* calc'd for $C_{26}H_{32}O_5$ $[M]^+$: 424.2235, found 424.2244.

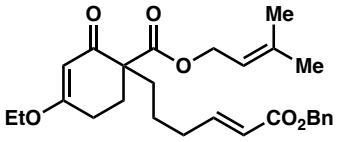

114t

3-methylbut-2-en-1-yl (*E*)-1-(6-(benzyloxy)-6-oxohex-4-en-1-yl)-4-ethoxy-2-oxocyclohex-3-ene-1-carboxylate (114t)

Prepared from **164** and benzyl 2-(diethoxyphosphoryl)acetate[28] following General Procedure B. Purification by flash column chromatography (30% EtOAc/hexanes) afforded the title compound as a colorless oil (814.7 mg, 1.79 mmol, 88% yield).

^{1}H NMR (400 MHz, $CDCl_3$): δ 7.40 – 7.28 (m, 5H), 6.98 (dt, *J* = 15.6, 6.8 Hz, 1H), 5.86 (dt, *J* = 15.7, 1.6 Hz, 1H), 5.34 (d, *J* = 1.2 Hz, 1H), 5.28 (dddt, *J* = 7.0, 5.6, 2.8, 1.4 Hz, 1H), 5.16 (s, 2H), 4.66 – 4.52 (m, 2H), 3.89 (qd, *J* = 7.1, 1.6 Hz, 2H), 2.61 (dddd, *J* = 17.9, 10.1, 4.9, 1.2 Hz, 1H), 2.46 – 2.27 (m, 2H), 2.21 (qd, *J* = 7.3, 1.6 Hz, 2H), 2.02 – 1.83 (m, 2H), 1.82 – 1.72 (m, 1H), 1.71 (s, 3H), 1.67 (s, 3H), 1.45 (dddd, *J* = 13.3, 11.2, 6.4, 2.7 Hz, 2H), 1.35 (t, *J* = 7.0 Hz, 3H).

^{13}C NMR (100 MHz, $CDCl_3$): δ 195.8, 176.6, 171.8, 166.5, 149.4, 139.5, 136.3, 128.7, 128.3, 128.3, 121.4, 118.5, 102.3, 66.2, 64.5, 62.3, 56.0, 33.8, 32.7, 28.7, 26.6, 25.8, 23.3, 18.2, 14.3.

IR (Neat Film, NaCl): 2939, 1721, 1655, 1608, 1446, 1380, 1314, 1242, 1190, 1026, 736 cm^{-1}.

HRMS (MM: FD+): *m/z* calc'd for $C_{27}H_{34}O_6$ $[M]^+$: 454.2349, found 454.2350.

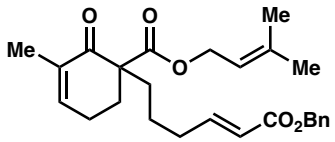

114u

3-methylbut-2-en-1-yl (*E*)-1-(6-(benzyloxy)-6-oxohex-4-en-1-yl)-3-methyl-2-oxocyclohex-3-ene-1-carboxylate (114u)

Prepared from **165** and benzyl 2-(diethoxyphosphoryl)acetate[28] following General Procedure B. Purification by flash column chromatography (10–25% EtOAc/hexanes) afforded the title compound as a colorless oil (1176.8 mg, 2.77 mmol, 71% yield).

^{1}H NMR (400 MHz, $CDCl_3$): δ 7.41 – 7.26 (m, 5H), 6.98 (dt, *J* = 15.6, 6.8 Hz, 1H), 6.59 (ddt, *J* = 4.7, 3.1, 1.3 Hz, 1H), 5.87 (dt, *J* = 15.6, 1.6 Hz, 1H), 5.27 (tdq, *J* = 7.1, 2.8, 1.5 Hz, 1H), 5.17 (s, 2H), 4.57 (d, *J* = 6.7 Hz, 2H), 2.50 – 2.36 (m, 2H), 2.33 – 2.16 (m, 3H), 1.98 – 1.83 (m, 2H), 1.78 (q, *J* = 1.7 Hz, 3H), 1.77 – 1.64 (m, 1H), 1.72 (s, 3H), 1.67 (s, 3H) 1.61 – 1.34 (m, 3H).

^{13}C NMR (100 MHz, $CDCl_3$): δ 197.0, 171.9, 166.5, 149.4, 143.8, 139.6, 136.3, 135.4, 128.7, 128.3, 128.3, 121.5, 118.3, 66.2, 62.2, 56.9, 33.6, 32.7, 30.9, 25.8, 23.6, 23.4, 18.2, 16.6.

IR (Neat Film, NaCl): 2921, 1721, 1677, 1450, 1377, 1248, 1168, 728 cm^{-1}.

HRMS (MM: FD+): *m/z* calc'd for $C_{26}H_{32}O_5$ $[M]^+$: 424.2244, found 424.2244.

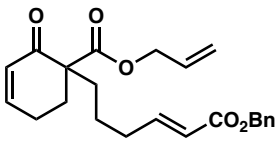

116

allyl (*E*)-1-(6-(benzyloxy)-6-oxohex-4-en-1-yl)-2-oxocyclohex-3-ene-1-carboxylate (116)

Prepared from **166** and benzyl 2-(diethoxyphosphoryl)acetate[28] following General Procedure B. Purification by flash column chromatography (20–25% EtOAc/hexanes) afforded the title compound as a colorless oil (599.1 mg, 1.41 mmol, 46% yield).

^{1}H NMR (400 MHz, $CDCl_3$): δ 7.41 – 7.26 (m, 5H), 6.98 (dt, *J* = 15.6, 6.9 Hz, 1H), 6.89 (dddd, *J* = 10.1, 4.8, 3.1, 1.0 Hz, 1H), 6.03 (ddd, *J* = 10.1, 2.5, 1.6 Hz, 1H), 5.93 – 5.77 (m, 2H), 5.27 (dq, *J* = 17.2, 1.5 Hz, 1H), 5.21 (dq, *J* = 10.4, 1.3 Hz, 1H), 5.17 (s, 2H), 4.60 (dq, *J* = 5.6, 1.6 Hz, 2H), 2.57 – 2.42 (m, 2H), 2.39 – 2.27 (m, 1H), 2.22 (qd, *J* = 7.3, 1.6 Hz, 2H), 2.02 – 1.87 (m, 2H), 1.77 (ddd, *J* = 13.7, 11.7, 5.2 Hz, 1H), 1.57 – 1.40 (m, 2H).

^{13}C NMR (100 MHz, $CDCl_3$): δ 196.0, 171.2, 166.5, 149.5, 149.1, 136.2, 131.7, 129.3, 128.7, 128.3, 128.3, 127.8, 127.1, 121.6, 118.7, 66.2, 65.9, 57.0, 33.4, 32.6, 30.3, 23.8, 23.2.

IR (Neat Film, NaCl): 2937, 2357, 1723, 1684, 1456, 1262, 1165, 992 cm^{-1}.

HRMS (MM: FD+): *m/z* calc'd for $C_{23}H_{27}O_5$ $[M]^+$: 383.1871, found 383.1853.

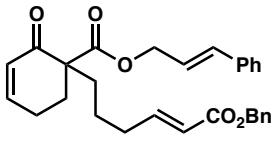

121

cinnamyl 1-((*E*)-6-(benzyloxy)-6-oxohex-4-en-1-yl)-2-oxocyclohex-3-ene-1-carboxylate (121)

Prepared from **167** and benzyl 2-(diethoxyphosphoryl)acetate[28] following General Procedure B. Purification by flash column chromatography (20% EtOAc/hexanes) afforded the title compound as a colorless oil (569 mg, 1.24 mmol, 67% yield).

^{1}H NMR (400 MHz, $CDCl_3$): δ 7.37 – 7.34 (m, 6H), 7.34 – 7.29 (m, 3H), 7.27 – 7.24 (m, 1H), 6.97 (dt, *J* = 15.6, 6.9 Hz, 1H), 6.89 (dddd, *J* = 10.1, 4.8, 3.1, 1.0 Hz, 1H), 6.62 (d, *J* = 15.9 Hz, 1H), 6.22 (dt, *J* = 15.9, 6.4 Hz, 1H), 6.04 (ddd, *J* = 10.1, 2.5, 1.6 Hz, 1H), 5.86 (dt, *J* = 15.7, 1.6 Hz, 1H), 5.16 (s, 2H), 4.76 (dt, *J* = 6.4, 1.4 Hz, 2H), 2.56 – 2.45 (m, 2H), 2.37 – 2.28 (m, 1H), 2.22 (ddd, *J* = 7.4, 7.4, 1.6 Hz, 2H), 1.95 (ddt, *J* = 16.8, 7.9, 5.7 Hz, 2H), 1.78 (ddd, *J* = 13.7, 11.7, 5.0 Hz, 1H), 1.56 – 1.42 (m, 2H).

^{13}C NMR (100 MHz, $CDCl_3$): δ 196.0, 171.4, 166.5, 149.5, 149.1, 136.2, 136.2, 134.7, 129.3, 128.7, 128.7, 128.3, 128.3, 126.8, 122.6, 121.6, 66.2, 65.9, 57.0, 33.4, 32.6, 30.3, 23.8, 23.2.

IR (Neat Film, NaCl): 3034, 2942, 1718, 1700, 1684, 1247, 1166 cm^{-1}

HRMS (MM: FD+): *m/z* calc'd for $C_{29}H_{30}O_5$ $[M]^+$: 458.2088, found 458.2082.

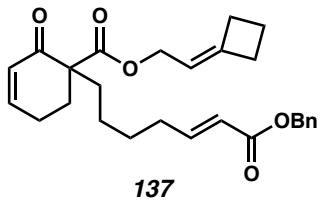

137

22-cyclobutylideneethyl (*E*)-1-(7-(benzyloxy)-7-oxohept-5-en-1-yl)-2-oxocyclohex-3-ene-1-carboxylatecarboxylate (137)

Prepared from **168** and benzyl 2-(diethoxyphosphoryl)acetate[28] following General Procedure B. Purification by flash column chromatography (5–60% EtOAc/hexanes) afforded the title compound as a colorless oil (354 mg, 0.81 mmol, 39.8% yield).

^{1}H NMR (400 MHz, $CDCl_3$): δ 7.40 – 7.29 (m, 5H), 6.99 (dt, *J* = 14.9, 1.0 Hz, 1H), 6.91 – 6.84 (m, 1H), 6.02 (d, *J* = 1.2 Hz, 1H), 5.86 (d, *J* = 15.7 Hz, 1H), 5.24 – 5.13 (m, 3H), 4.51 – 4.41 (m, 2H), 2.75 – 2.62 (m, 4H), 2.56 – 2.39 (m, 2H), 2.36 – 2.27 (m, 1H), 2.25 – 2.16 (m, 2H), 2.02 – 1.84 (m, 4H), 1.73 (ddd, *J* = 13.6, 11.2, 5.3 Hz, 1H), 1.47 (p, *J* = 7.5 Hz, 2H), 1.40 – 1.23 (m, 2H).

^{13}C NMR (100 MHz, $CDCl_3$): δ 196.4, 171.6, 166.6, 149.8, 149.3, 148.8, 136.3, 129.4, 128.7, 128.3, 128.3, 121.2, 114.0, 66.2, 62.3, 57.1, 33.6, 32.2, 31.2, 30.3, 29.6, 28.5, 24.3, 23.9, 17.1.

IR (Neat Film, NaCl): 2945, 1722, 1687, 1446, 1169 cm^{-1}.

HRMS (MM: FD+): *m/z* calc'd for $C_{27}H_{32}O_5$ $[M]^+$: 436.2250, found 436.2222.

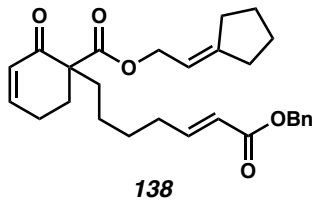

138

2-cyclopentylideneethyl (*E*)-1-(7-(benzyloxy)-7-oxohept-5-en-1-yl)-2-oxocyclohex-3-ene-1-carboxylate (138)

Prepared from **169** and benzyl 2-(diethoxyphosphoryl)acetate[28] following General Procedure B. Purification by flash column chromatography (10–60% EtOAc/hexanes) afforded the title compound as a colorless oil (1.40 g, 4.41 mmol, 38.9% yield).

^{1}H NMR (400 MHz, $CDCl_3$): δ 7.40 – 7.28 (m, 5H), 6.99 (dt, *J* = 15.6, 6.9 Hz, 1H), 6.91 – 6.83 (m, 1H), 6.01 (ddd, *J* = 10.1, 2.6, 1.5 Hz, 1H), 5.85 (dt, *J* = 15.6, 1.6 Hz, 1H), 5.37 (tp, *J* = 7.0, 2.2 Hz, 1H), 5.17 (s, 2H), 4.60 – 4.53 (m, 2H), 2.56 – 2.39 (m, 2H), 2.37 –

2.15 (m, 7H), 1.98 – 1.85 (m, 2H), 1.78 – 1.54 (m, 5H), 1.53 – 1.41 (m, 2H), 1.40 – 1.22 (m, 2H).

^{13}C NMR (100 MHz, $CDCl_3$): δ 196.4, 171.7, 166.6, 151.1, 149.8, 149.3, 136.3, 129.4, 128.7, 128.3, 128.3, 121.2, 113.8, 66.2, 63.7, 57.1, 33.9, 33.6, 32.2, 30.3, 29.0, 28.5, 26.4, 26.2, 24.3, 23.9.

IR (Neat Film, NaCl): 2946, 1719, 1686, 1457, 1165 cm^{-1}.

HRMS (MM: FD+): *m/z* calc'd for $C_{28}H_{34}O_5$ $[M]^+$: 450.2406, found 450.2394.

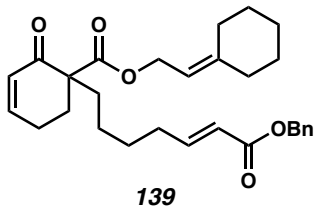

139

2-cyclohexylideneethyl (*E*)-1-(7-(benzyloxy)-7-oxohept-5-en-1-yl)-2-oxocyclohex-3-ene-1-carboxylate (139)

Prepared from **170** and benzyl 2-(diethoxyphosphoryl)acetate[28] following General Procedure B. Purification by flash column chromatography (10–60% EtOAc/hexanes) afforded the title compound as a colorless oil (81 mg, 0.17 mmol, 32.9% yield).

^{1}H NMR (400 MHz, $CDCl_3$): δ 7.41 – 7.27 (m, 5H), 6.99 (dt, *J* = 15.6, 6.9 Hz, 1H), 6.87 (dddd, *J* = 10.1, 5.2, 2.5, 1.1 Hz, 1H), 6.01 (ddd, *J* = 10.1, 2.6, 1.5 Hz, 1H), 5.85 (dt, *J* = 15.6, 1.6 Hz, 1H), 5.23 (tp, *J* = 7.3, 1.2 Hz, 1H), 5.17 (s, 2H), 4.59 (d, *J* = 7.2 Hz, 2H), 2.56 – 2.39 (m, 2H), 2.36 – 2.26 (m, 1H), 2.25 – 2.13 (m, 4H), 2.12 – 2.03 (m, 2H), 1.98 – 1.84 (m, 2H), 1.78 – 1.66 (m, 1H), 1.63 – 1.42 (m, 8H), 1.41 – 1.21 (m, 2H).

^{13}C NMR (100 MHz, $CDCl_3$): δ 196.4, 171.6, 166.6, 149.8, 149.3, 147.7, 136.3, 129.4, 128.7, 128.3, 128.3, 121.2, 114.9, 66.2, 61.5, 57.0, 37.1, 33.6, 32.2, 30.4, 29.2, 28.5, 28.5, 27.9, 26.7, 24.3, 23.9.

IR (Neat Film, NaCl): 2929, 2853, 1723, 1681, 1456, 1385, 1266, 1184 cm^{-1}.

HRMS (MM: FD+): *m/z* calc'd for $C_{29}H_{36}O_5$ $[M]^+$: 464.2563, found 464.2543.

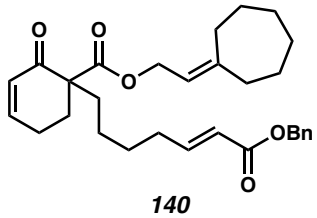

140

2-cycloheptylideneethyl (*E*)-1-(7-(benzyloxy)-7-oxohept-5-en-1-yl)-2-oxocyclohex-3-ene-1-carboxylate (140)

Prepared from **171** and benzyl 2-(diethoxyphosphoryl)acetate[28] following General Procedure B. Purification by flash column chromatography (5–70% EtOAc/hexanes) afforded the title compound as a colorless oil (135 mg, 0.28 mmol, 30% yield).

^{1}H NMR (400 MHz, $CDCl_3$): δ 7.43 – 7.29 (m, 5H), 6.99 (dt, *J* = 15.7, 6.9 Hz, 1H), 6.91 – 6.82 (m, 1H), 6.01 (ddd, *J* = 10.2, 2.6, 1.5 Hz, 1H), 5.85 (dt, *J* = 15.6, 1.6 Hz, 1H), 5.27 (tt, *J* = 7.1, 1.3 Hz, 1H), 5.17 (s, 2H), 4.59 (d, *J* = 7.1 Hz, 2H), 2.57 – 2.39 (m, 2H), 2.36 – 2.16 (m, 7H), 1.98 – 1.84 (m, 2H), 1.73 (ddd, *J* = 13.6, 11.3, 5.2 Hz, 1H), 1.61 – 1.43 (m, 10H), 1.31 (dddd, *J* = 13.2, 11.8, 8.6, 6.2 Hz, 2H).

^{13}C NMR (100 MHz, $CDCl_3$): δ 196.4, 171.7, 166.6, 149.8, 149.3, 149.0, 136.3, 129.4, 128.7, 128.3, 128.3, 121.2, 118.4, 66.2, 62.0, 57.0, 37.7, 33.6, 32.2, 30.4, 30.2, 29.8, 29.1, 28.9, 28.5, 27.3, 24.3, 23.9.

IR (Neat Film, NaCl): 2919, 2361, 1722, 1682, 1651, 1443, 1234, 1187 cm^{-1}.

HRMS (MM: FD+): *m/z* calc'd for $C_{30}H_{38}O_5$ $[M]^+$: 478.2719, found 478.2716.

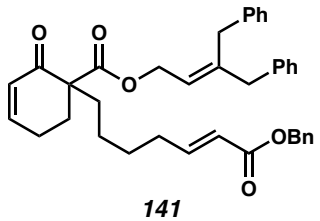

141

3-benzyl-4-phenylbut-2-en-1-yl (*E*)-1-(7-(benzyloxy)-7-oxohept-5-en-1-yl)-2-oxocyclohex-3-ene-1-carboxylate (141)

Prepared from **172** and benzyl 2-(diethoxyphosphoryl)acetate[28] following General Procedure B. Purification by flash column chromatography (5–70% EtOAc/hexanes) afforded the title compound as a colorless oil (205 mg, 0.36 mmol, 39% yield).

^{1}H NMR (400 MHz, $CDCl_3$): δ 7.39 – 7.24 (m, 9H), 7.23 – 7.17 (m, 2H), 7.09 (dd, *J* = 11.6, 7.3 Hz, 4H), 6.98 (dt, *J* = 15.6, 6.9 Hz, 1H), 6.89 – 6.80 (m, 1H), 6.02 (d, *J* = 10.1 Hz, 1H), 5.85 (d, *J* = 16.1 Hz, 1H), 5.51 (t, *J* = 7.2 Hz, 1H), 5.17 (s, 2H), 4.83 – 4.69 (m, 2H), 3.36 (s, 2H), 3.23 (s, 2H), 2.55 – 2.40 (m, 2H), 2.37 – 2.24 (m, 1H), 2.18 (q, *J* = 7.2 Hz, 2H), 2.00 – 1.85 (m, 2H), 1.75 (ddd, *J* = 13.5, 11.1, 5.2 Hz, 1H), 1.46 (p, *J* = 7.4 Hz, 1H), 1.38 – 1.22 (m, 2H).

^{13}C NMR (100 MHz, $CDCl_3$): δ 196.2, 171.6, 166.6, 149.8, 149.3, 144.8, 139.0, 138.8, 136.3, 129.4, 129.3, 128.8, 128.7, 128.7, 128.5, 128.3, 128.3, 126.5, 126.4, 121.7, 121.3, 66.2, 61.9, 57.1, 42.9, 35.8, 33.6, 32.1, 30.3, 28.5, 24.3, 23.9.

IR (Neat Film, NaCl): 3027, 2931, 1722, 1682, 1493, 1387, 1264, 1165 cm^{-1}.

HRMS (MM: FD+): *m/z* calc'd for $C_{38}H_{40}O_5$ $[M]^+$: 576.2876, found 576.2857.

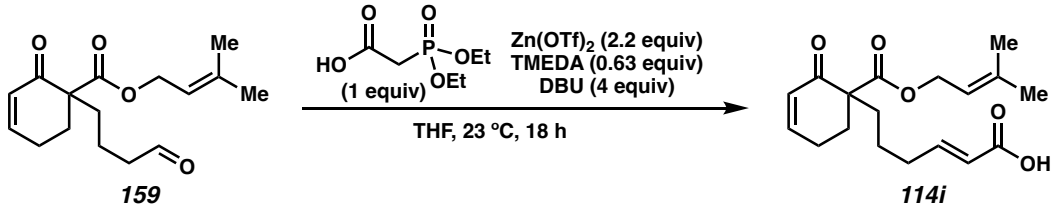

(*E*)-6-(1-(((3-methylbut-2-en-1-yl)oxy)carbonyl)-2-oxocyclohex-3-en-1-yl)hex-2-enoic acid (114i)[33]

To a suspension of $Zn(OTf)_2$ (6.6 mmol, 2.2 equiv) in THF (15 mL) was added (diethoxyphosphinyl)acetic acid (3 mmol, 1 equiv), followed by the addition of TMEDA (1.89 mmol, 0.63 equiv), DBU (12 mmol, 4 equiv), and then a solution of aldehyde **159** (3 mmol, 1 equiv) in THF (2 mL). The solution was stirred at 23 ºC for 18 h, and the reaction was diluted with 1 M HCl and extracted with dichloromethane (4x). The combined organic layers were dried over Na_2SO_4, filtered, and concentrated under reduced pressure. Purification by silica gel flash column chromatography (35% EtOAc/hexanes with 3% AcOH) afforded the title compound as a white solid (137.4 mg, 0.43 mmol, 43% yield).

^{1}H NMR (400 MHz, $CDCl_3$): δ 7.04 (dt, *J* = 15.7, 6.8 Hz, 1H), 6.93 – 6.84 (m, 1H), 6.03 (ddd, *J* = 10.2, 2.6, 1.5 Hz, 1H), 5.83 (dt, *J* = 15.6, 1.6 Hz, 1H), 5.28 (tp, *J* = 7.2, 1.4 Hz, 1H), 4.66 – 4.53 (m, 2H), 2.58 – 2.40 (m, 2H), 2.37 – 2.28 (m, 1H), 2.25 (qd, *J* = 7.3, 1.6 Hz, 2H), 1.98 – 1.87 (m, 2H), 1.80 – 1.68 (m, 1H), 1.73 (s, 3H), 1.68 (s, 3H), 1.61 – 1.37 (m, 3H).

^{13}C NMR (100 MHz, $CDCl_3$): δ 196.3, 171.6, 170.2, 151.4, 149.3, 139.7, 129.4, 120.8, 118.3, 62.4, 57.0, 33.5, 32.7, 30.5, 25.8, 23.9, 23.1, 18.2.

IR (Neat Film, NaCl): 2929, 1725, 1694, 1424, 1384, 1236, 1171 cm^{-1}.

HRMS (MM: FD+): *m/z* calc'd for $C_{18}H_{24}O_5$ $[M]^+$: 320.1624, found 320.1636.

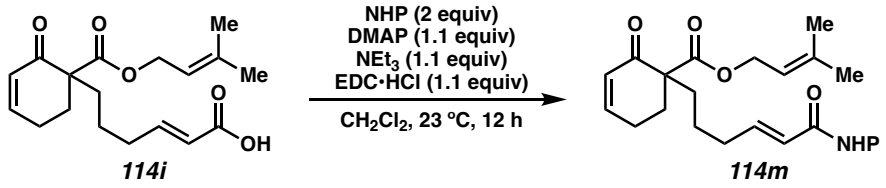

3-methylbut-2-en-1-yl (*E*)-1-(6-((1,3-dioxoisoindolin-2-yl)oxy)-6-oxohex-4-en-1-yl)-2-oxocyclohex-3-ene-1-carboxylate (114m)[34]

To a round bottom flask was added crude acid **114i** (assumed quantitative yield from previous reaction, 1 mmol, 1 equiv), DMAP (1.1 mmol, 1.1 equiv), NHP (2 mmol, 2 equiv), dichloromethane (9.5 mL), and triethylamine (1.1 mmol, 1.1 equiv). EDC·HCl (1.1 mmol, 1.1 equiv) was then added under N_2 atmosphere in a single portion, and the reaction was stirred vigorously at 23 ºC for 12 h. The reaction mixture was diluted with dichloromethane and washed with 0.5 N HCl, saturated aqueous $NaHCO_3$, and brine. The combined organic layers were dried over Na_2SO_4 and concentrated under reduced pressure. Purification by flash column chromatography (30–35% EtOAc/hexanes) afforded the title compound as a colorless oil (109.6 mg, 0.48 mmol, 24% yield over two steps).

^{1}H NMR (400 MHz, $CDCl_3$): δ 7.96 – 7.84 (m, 2H), 7.79 (dd, *J* = 5.5, 3.1 Hz, 2H), 7.30 (dd, *J* = 15.8, 6.7 Hz, 1H), 6.89 (dddd, *J* = 10.1, 4.9, 3.0, 1.1 Hz, 1H), 6.10 (dt, *J* = 15.8, 1.6 Hz, 1H), 6.04 (ddd, *J* = 10.1, 2.5, 1.5 Hz, 1H), 5.29 (tdt, *J* = 5.7, 2.8, 1.4 Hz, 1H), 4.67 – 4.55 (m, 2H), 2.58 – 2.40 (m, 2H), 2.35 (m, 3H), 2.03 – 1.89 (m, 2H), 1.87 – 1.74 (m, 1H), 1.74 (s, 3H), 1.69 (d, *J* = 1.3 Hz, 3H), 1.66 – 1.45 (m, 3H).

^{13}C NMR (100 MHz, $CDCl_3$): δ 196.2, 162.4, 162.2, 155.2, 149.3, 139.8, 134.8, 129.4, 129.1, 124.1, 118.3, 116.0, 62.4, 57.0, 33.5, 33.3, 30.6, 25.9, 23.9, 23.0, 18.3.

IR (Neat Film, NaCl): 1771, 1744, 1682, 1185 cm^{-1}.

HRMS (MM: FD+): *m/z* calc'd for $C_{26}H_{27}NO_7$ $[M]^+$: 465.1788, found 465.1779.

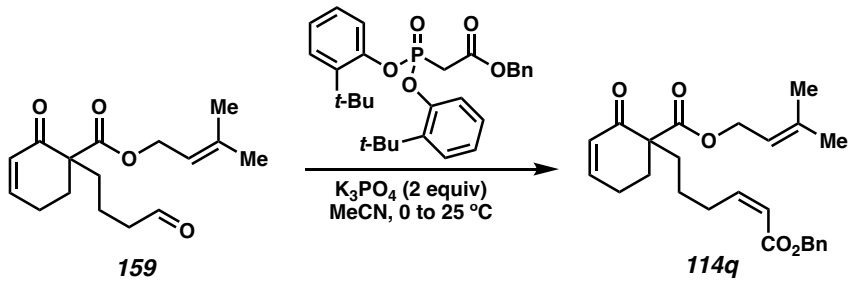

3-methylbut-2-en-1-yl (*Z*)-1-(6-(benzyloxy)-6-oxohex-4-en-1-yl)-2-oxocyclohex-3-ene-1-carboxylate (114q)

To a solution of benzyl 2-(bis(2-(*tert*-butyl)phenoxy)phosphoryl)acetate[35] (890 mg, 1.80 mmol, 1.00 equiv) in MeCN (18 mL, 0.1 M) was added K_2CO_3 (783 mg, 3.69 mmol, 2.05 equiv). The reaction was cooled to 0 ºC and a solution of **159** (500 mg, 1.80 mmol, 1.00 equiv) in MeCN (18 mL, 0.1 M) was dropwise added. The reaction was gradually warmed to 25 ºC and stirring was continued until consumption of **55** as determined by TLC (around 16 h). The reaction mixture was filtered through a plug of Celite® to remove solids and volatiles were removed in vacuo. Purification by flash column chromatography (0–40% EtOAc/hexanes) afforded the title compound as a colorless oil (482 mg, 1.17 mmol, 65 % yield).

^{1}H NMR (400 MHz, $CDCl_3$): δ 7.39 – 7.29 (m, 5H), 6.90 – 6.84 (m, 1H), 6.24 (dt, *J* = 11.5, 7.4 Hz, 1H), 6.01 (ddd, *J* = 10.1, 2.5, 1.6 Hz, 1H), 5.83 (dt, *J* = 11.5, 1.7 Hz, 1H), 5.28 (ddp, *J* = 8.6, 5.7, 1.4 Hz, 1H), 5.15 (s, 2H), 4.59 (d, *J* = 7.2 Hz, 2H), 2.68 (qd, *J* = 7.4, 1.8 Hz, 2H), 2.53 – 2.41 (m, 2H), 2.35 – 2.26 (m, 1H), 1.98 – 1.87 (m, 2H), 1.79 – 1.71 (m, 4H), 1.67 (s, 3H), 1.52 – 1.37 (m, 2H).

^{13}C NMR (100 MHz, $CDCl_3$): δ 196.4, 171.7, 166.2, 150.5, 149.3, 139.5, 136.3, 129.3, 128.7, 128.3, 128.3, 119.9, 118.4, 65.9, 62.3, 57.1, 33.4, 30.3, 29.4, 25.8, 24.2, 23.8, 18.2.

IR (Neat Film, NaCl): 2918, 1714, 1447, 1178, 1161 cm^{-1}.

HRMS (MM: FD+): *m/z* calc'd for $C_{25}H_{30}O_5$ $[M]^+$: 410.2093, found 410.2108.

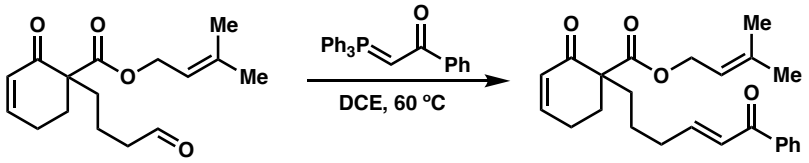

159 ***114j***

3-methylbut-2-en-1-yl (*E*)-2-oxo-1-(6-oxo-6-phenylhex-4-en-1-yl)cyclohex-3-ene-1-carboxylate (114j)

(2-oxo-2-phenylethyl)triphenylphosphonium bromide[36] (996 mg, 2.16 mmol, 1.2 equiv) was stirred in 26 mL of a 3:2 CH_2Cl_2/2 M aq. NaOH mixture for 30 minutes at 23 ºC. The layers were separated, and the aqueous layer was extracted twice with CH_2Cl_2. The combined organic layers were washed with brine, dried over Na_2SO_4, filtered, and solvent was removed in vacuo. To a solution of this crude ylide in DCE (22 mL, 0.1 M) was added aldehyde **159** (500 mg, 1.80 mmol, 1 equiv). The reaction was stirred at 65 ºC for 36 hours. Upon complete consumption of **159**, as determined by TLC, volatiles were removed in vacuo. Purification by flash column chromatography (30% EtOAc/hexanes) afforded the title compound as a colorless oil (330 mg, 0.867 mmol, 48% yield).

^{1}H NMR (400 MHz, $CDCl_3$): δ 7.95 – 7.90 (m, 2H), 7.60 – 7.51 (m, 1H), 7.46 (tt, *J* = 6.8, 1.5 Hz, 2H), 7.02 (dt, *J* = 15.4, 6.7 Hz, 1H), 6.93 – 6.85 (m, 2H), 6.03 (ddd, *J* = 10.2, 2.6, 1.5 Hz, 1H), 5.30 – 5.25 (m, 1H), 4.59 (d, *J* = 7.1 Hz, 2H), 2.55 – 2.43 (m, 2H), 2.38 – 2.27

(m, 3H), 2.01 – 1.91 (m, 2H), 1.80 (ddd, J = 13.6, 12.0, 4.7 Hz, 1H), 1.72 (s, 3H), 1.67 (s, 3H), 1.63 – 1.47 (m, 2H).

^{13}C NMR (100 MHz, $CDCl_3$): δ 196.3, 191.0, 171.6, 149.3, 149.1, 139.7, 138.1, 132.8, 129.4, 128.7, 128.7, 126.4, 118.3, 62.4, 57.0, 33.6, 33.2, 30.5, 25.8, 23.9, 23.4, 18.2.

IR (Neat Film, NaCl): 2931, 1724, 1671, 1619, 1447, 1229, 1177 cm^{-1}.

HRMS (MM: FD+): *m/z* calc'd for $C_{24}H_{28}O_4$ $[M]^+$: 380.1988, found 380.1982.

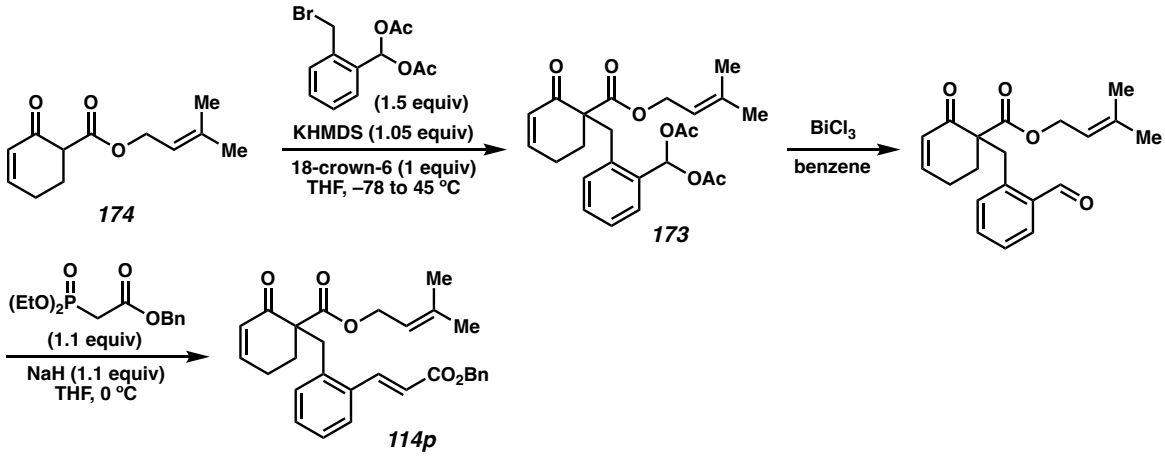

(2-((1-(((3-methylbut-2-en-1-yl)oxy)carbonyl)-2-oxocyclohex-3-en-1-yl)methyl)phenyl)methylene diacetate (173)

An oven dried round bottom flask was charged with KHMDS (837 mg, 4.20 mmol, 1.05 equiv), 18-crown-6 (1.06 g, 4.00 mmol, 1.0 equiv), and THF (21 mL). The mixture was cooled to –78 °C and a solution of enone **174** (830 mg, 4.00 mmol, 1.0 equiv) in THF (10 mL) was added. The reaction mixture was stirred for 15 minutes then (2-(bromomethyl)phenyl)methylene diacetate[37] (1.86 g, 6.00 mmol, 1.5 equiv) was added in a minimal amount of THF (*ca* 5 mL). The solution was slowly warmed to 45 °C and stirred for 14 h. Upon complete consumption of starting material (as determined by TLC), the solution was cooled to 23 °C, diluted with a saturated aqueous solution of NH_4Cl, and the

reaction mixture was extracted thrice with EtOAc. The combined organic layers were dried over Na_2SO_4, filtered, and concentrated under reduced pressure. Purification by flash column chromatography (20–60% EtOAc/hexanes) afforded the title compound as a colorless oil (1.00 g, 2.33 mmol, 58% yield).

^{1}H NMR (400 MHz, $CDCl_3$): δ 7.87 (s, 1H), 7.58 – 7.52 (m, 1H), 7.30 – 7.24 (m, 2H), 7.21 – 7.16 (m, 1H), 6.88 – 6.82 (m, 1H), 6.07 (ddd, *J* = 10.1, 2.8, 1.3 Hz, 1H), 5.24 (ddq, *J* = 8.6, 5.7, 1.4 Hz, 1H), 4.56 (d, *J* = 7.2 Hz, 2H), 3.52 (d, *J* = 14.8 Hz, 1H), 3.45 (d, *J* = 14.8 Hz, 1H), 2.53 – 2.41 (m, 1H), 2.36 (dddd, *J* = 13.6, 4.9, 2.6, 1.3 Hz, 1H), 2.29 – 2.19 (m, 1H), 2.12 (s, 3H), 2.10 (s, 3H), 1.86 (ddd, *J* = 13.6, 10.4, 5.3 Hz, 1H), 1.73 (s, 3H), 1.67 (s, 3H).

^{13}C NMR (100 MHz, $CDCl_3$): δ 195.4, 171.1, 168.8, 168.8, 149.6, 139.7, 135.5, 134.9, 131.5, 129.6, 129.5, 127.6, 127.2, 118.2, 88.4, 62.5, 58.2, 34.2, 30.2, 25.9, 24.1, 21.0, 21.0, 18.2.

IR (Neat Film, NaCl): 2935, 1759, 1731, 1682, 1447, 1371, 1236, 1206 cm^{-1}.

HRMS (MM: FD+): *m/z* calc'd for $C_{24}H_{28}O_7$ $[M]^+$: 428.1835, found 428.1833.

3-methylbut-2-en-1-yl (*E*)-1-(6-(benzyloxy)-6-oxohex-4-en-1-yl)-2-oxocyclohept-3-ene-1-carboxylate (114p)

To a solution of diacetate **173** (500 mg, 1.17 mmol, 1 equiv) in benzene (11.7 mL, 0.1 M) was added bismuth chloride (38 mg, 0.12 mmol, 0.1 equiv). The reaction mixture was heated to 35 ºC for 3 hours. Upon cooling to 25 ºC, the reaction mixture was diluted with water and the layers were separated. The aqueous layer was extracted twice with chloroform. The combined organic layers were washed with brine, dried over Na_2SO_4, and

volatiles were removed in vacuo. The crude aldehyde was used directly in the subsequent Horner–Wadsworth–Emmons olefination.

To a suspension of NaH (52 mg, 1.29 mmol, 60% by weight in mineral oil, 1.1 equiv) in THF (2.6 mL, 0.5 M) at 0 ºC was dropwise added a solution of benzyl 2-(diethoxyphosphoryl)acetate[28] (369 mg, 1.29 mmol, 1.1 equiv) in THF (1.3 mL, 1.0 M). Stirring at 0 ºC was continued for 30 minutes. To the reaction was then dropwise added a solution of the crude aldehyde in THF (2.4 mL, 0.5 M). Upon complete consumption of starting material (as determined by TLC), the reaction mixture was diluted with a saturated solution of $NaHCO_3$ and extracted with EtOAc (3x). The combined organic layers were dried over Na_2SO_4, filtered, and concentrated under reduced pressure. Purification by flash column chromatography (5–40% EtOAc/hexanes) afforded the title compound as a colorless oil (230 mg, 0.502 mmol, 43% yield).

^{1}H NMR (400 MHz, $CDCl_3$): δ 8.08 (d, *J* = 15.7 Hz, 1H), 7.57 (dd, *J* = 7.5, 1.9 Hz, 1H), 7.44 – 7.31 (m, 5H), 7.27 – 7.17 (m, 3H), 6.85 – 6.80 (m, 1H), 6.40 (d, *J* = 15.7 Hz, 1H), 6.06 (ddd, *J* = 10.1, 2.9, 1.2 Hz, 1H), 5.28 – 5.21 (m, 3H), 4.56 – 4.49 (m, 2H), 3.57 (d, *J* = 14.3 Hz, 1H), 3.31 (d, *J* = 14.4 Hz, 1H), 2.51 – 2.39 (m, 1H), 2.30 – 2.16 (m, 2H), 1.82 – 1.70 (m, 4H), 1.65 (s, 3H).

^{13}C NMR (100 MHz, $CDCl_3$): δ 195.1, 170.4, 166.7, 149.7, 143.2, 139.7, 136.7, 136.2, 134.7, 132.1, 130.0, 129.3, 128.7, 128.4, 128.3, 127.5, 126.8, 119.4, 118.2, 66.5, 62.5, 58.4, 35.4, 30.2, 25.9, 24.1, 18.2.

IR (Neat Film, NaCl): 3028, 2927, 1720, 1686, 1629, 1168 cm^{-1}.

HRMS (MM: FD+): *m/z* calc'd for $C_{29}H_{30}O_5$ $[M]^+$: 458.2088, found 458.2086.

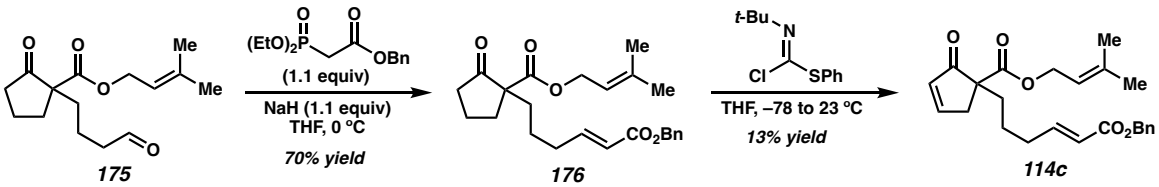

3-methylbut-2-en-1-yl (*E*)-1-(6-(benzyloxy)-6-oxohex-4-en-1-yl)-2-oxocyclopentane-1-carboxylate (176)

Prepared from **175** and benzyl 2-(diethoxyphosphoryl)acetate[28] following General Procedure B. Purification by flash column chromatography (15% EtOAc/hexanes) afforded the title compound as a colorless oil (1.40 g, 3.51 mmol, 70% yield).

^{1}H NMR (400 MHz, $CDCl_3$): δ 7.76 (dt, *J* = 5.6, 2.7 Hz, 1H), 7.42 – 7.26 (m, 5H), 6.95 (dt, *J* = 15.6, 6.9 Hz, 1H), 6.16 (dt, *J* = 5.8, 2.2 Hz, 1H), 5.85 (dt, *J* = 15.6, 1.6 Hz, 1H), 5.27 (tdq, *J* = 7.2, 2.9, 1.5 Hz, 1H), 5.16 (s, 2H), 4.59 (d, *J* = 7.1 Hz, 2H), 3.33 – 3.19 (m, 1H), 2.68 – 2.51 (m, 1H), 2.21 (qd, *J* = 7.3, 1.6 Hz, 2H), 1.99 (ddd, *J* = 13.7, 12.3, 4.5 Hz, 1H), 1.82 – 1.70 (m, 1H), 1.73 (s, 3H), 1.67 (s, 3H), 1.53 – 1.23 (m, 3H).

^{13}C NMR (100 MHz, $CDCl_3$): δ 205.7, 170.6, 166.4, 163.9, 148.9, 139.6, 136.2, 132.4, 128.7, 128.4, 128.3, 121.7, 118.3, 66.2, 62.7, 58.0, 39.5, 34.0, 32.4, 25.9, 23.2, 18.2.

IR (Neat Film, NaCl): 2932, 2356, 1715, 1263, 1164, 976, 754 cm^{-1}.

HRMS (MM: FD+): *m/z* calc'd for $C_{24}H_{28}O_5$ $[M]^+$: 396.1920, found 396.1931.

3-methylbut-2-en-1-yl (*E*)-1-(6-(benzyloxy)-6-oxohex-4-en-1-yl)-2-oxocyclopent-3-ene-1-carboxylate (114c)

A flame dried round bottom flask was charged with *i*-Pr_2NH (0.35 mL, 2.5 mmol, 1.25 equiv) and THF (8.0 mL, 0.25 M). The solution was cooled to –78 ºC and *n*-BuLi (0.96 mL, 2.4 mmol, 1.2 equiv) was added dropwise and the resultant solution was stirred for 30 min. Ketoester **176** (797 mg, 2.00 mmol, 1.0 equiv) in THF (8.0 mL, 0.25 M) was added dropwise and the mixture was stirred for 1 h. *N*-*tert*-Butylbenzenesulfinimidoyl chloride[38] (560.9 mg, 2.6 mmol, 1.3 equiv) in THF (4.0 mL, 0.5 M) was added dropwise and the solution was slowly warmed to 23 ºC. Upon complete consumption of starting material (as determined by TLC), the reaction mixture was diluted with saturated aqueous $NaHCO_3$ solution and extracted with Et_2O (25 mL x 3). The combined organic layers were dried with Na_2SO_4, filtered, and concentrated under reduced pressure. The crude product was purified by column chromatography (SiO_2, 0–40% EtOAc/Hexanes) to afford enone **114b** as a colorless oil (100 mg, 0.25 mmol, 13% yield).

^{1}H NMR (400 MHz, $CDCl_3$): δ 7.76 (dt, *J* = 5.6, 2.7 Hz, 1H), 7.42 – 7.26 (m, 5H), 6.95 (dt, *J* = 15.6, 6.9 Hz, 1H), 6.16 (dt, *J* = 5.8, 2.2 Hz, 1H), 5.85 (dt, *J* = 15.6, 1.6 Hz, 1H), 5.27 (tdq, *J* = 7.2, 2.9, 1.5 Hz, 1H), 5.16 (s, 2H), 4.59 (d, *J* = 7.1 Hz, 2H), 3.33 – 3.19 (m, 1H), 2.68 – 2.51 (m, 1H), 2.21 (qd, *J* = 7.3, 1.6 Hz, 2H), 1.99 (ddd, *J* = 13.7, 12.3, 4.5 Hz, 1H), 1.82 – 1.70 (m, 1H), 1.73 (s, 3H), 1.67 (s, 3H), 1.53 – 1.23 (m, 3H).

^{13}C NMR (100 MHz, $CDCl_3$): δ 205.7, 170.6, 166.4, 163.9, 148.9, 139.6, 136.2, 132.4, 128.7, 128.4, 128.3, 121.7, 118.3, 66.2, 62.7, 58.0, 39.5, 34.0, 32.4, 25.9, 23.2, 18.2.

IR (Neat Film, NaCl): 2932, 2356, 1715, 1263, 1164, 976, 754 cm^{-1}.

HRMS (MM: FD+): *m/z* calc'd for $C_{24}H_{28}O_5$ $[M]^+$: 396.1920, found 396.1931.

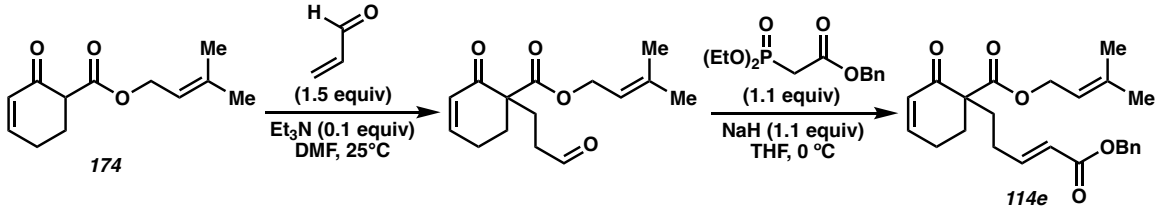

3-methylbut-2-en-1-yl (*E*)-1-(5-(benzyloxy)-5-oxopent-3-en-1-yl)-2-oxocyclohex-3-ene-1-carboxylate (114e)

To a solution of enone **174** (1.04 g, 5.00 mmol, 1.0 equiv) in DMF (10 mL, 0.5 M) at 25°C was added dropwise triethylamine (0.07 mL, 0.50 mmol, 0.1 equiv) followed by acrolein (0.50 mL, 7.50 mmol, 1.5 equiv). Upon consumption of starting material (as determined by TLC), the reaction mixture was diluted with water and extracted thrice with diethyl ether. The combined organic layers were washed with water followed by brine, dried over Na_2SO_4, and volatiles were removed in vacuo. The crude aldehyde was used directly in the subsequent Horner–Wadsworth–Emmons olefination. To a suspension of NaH (132 mg, 3.30 mmol, 60% by weight in mineral oil, 1.1 equiv) in THF (6 mL, 0.5 M) at 0 ºC was dropwise added a solution of benzyl 2-(diethoxyphosphoryl)acetate (945 mg, 3.30 mmol, 1.1 equiv) in THF (3.0 mL, 1.0 M). Stirred at 0 ºC was continued for 30 minutes. To the reaction was then dropwise added a solution of the crude aldehyde in THF (6.0 mL, 0.5 M). Upon complete consumption of starting material (as determined by TLC), the reaction mixture was diluted with a saturated solution of $NaHCO_3$ and extracted with EtOAc (3x). The combined organic layers were dried over Na_2SO_4, filtered, and concentrated under reduced pressure. Purification by flash column chromatography (10–20% EtOAc/hexanes) afforded the title compound as a colorless oil (490 mg, 1.24 mmol, 41% yield).

^{1}H NMR (400 MHz, $CDCl_3$): δ 7.41 – 7.29 (m, 5H), 6.99 (dt, *J* = 15.7, 6.8 Hz, 1H), 6.93 – 6.84 (m, 1H), 6.03 (ddd, *J* = 10.1, 2.5, 1.5 Hz, 1H), 5.88 (dt, *J* = 15.6, 1.6 Hz, 1H), 5.27 (ddt, *J* = 7.2, 5.8, 1.4 Hz, 1H), 5.17 (s, 2H), 4.59 (d, *J* = 7.1 Hz, 2H), 2.56 – 2.41 (m, 2H), 2.38 – 2.13 (m, 3H), 2.08 – 1.81 (m, 3H), 1.73 (s, 3H), 1.67 (s, 3H).

^{13}C NMR (100 MHz, $CDCl_3$): δ 196.0, 171.4, 166.4, 149.3, 148.9, 139.9, 136.2, 129.4, 128.7, 128.3, 121.5, 118.2, 66.2, 62.4, 56.6, 32.2, 30.7, 27.6, 25.8, 23.8, 18.2.

IR (Neat Film, NaCl): 3032, 2934, 1737, 1681, 1445, 1384, 1265, 1175, 1137 cm^{-1}.

HRMS (MM: FD+): *m/z* calc'd for $C_{24}H_{28}O_5$ $[M]^+$: 396.1937, found 396.1926.

Preparation of Aldehyde Precursors

General Procedure C: Alkylation of β-Ketoesters

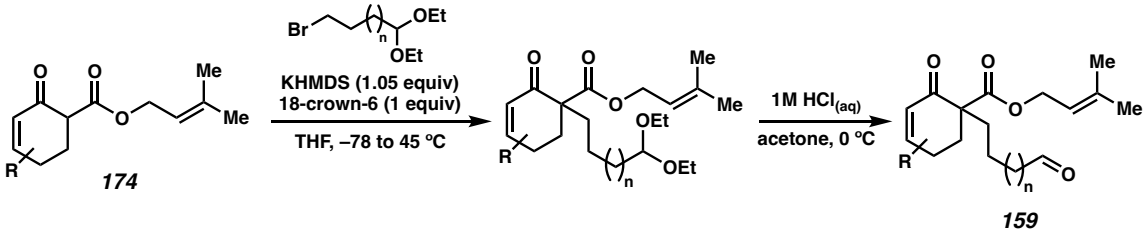

An oven dried round bottom flask was charged with KHMDS (1.05 equiv), 18-crown-6 (1.0 equiv), and THF (0.2 M with respect to KHMDS). The mixture was cooled to –78 ºC and a solution of acyclated enone **174** (1.0 equiv) in THF (0.4 M) was added. The reaction mixture was stirred for 15 minutes and then the appropriate alkyl bromide (1.5 equiv) was added neat dropwise. The solution was slowly warmed to 45 ºC and stirred for 14 h. Upon complete consumption of starting material (as determined by TLC), the solution was cooled to 23 ºC, diluted with a saturated aqueous solution of NH_4Cl and the reaction mixture was extracted thrice with EtOAc. The combined organic layers were dried over Na_2SO_4, filtered, and concentrated under reduced pressure to afford the crude diethyl acetal which was used

directly in the next step. A round bottom flask was charged with the crude acetal and acetone (0.5 M), then cooled to 0 ºC. Aqueous 1 M HCl (1:1 volume with respect to acetone) was added and stirring was continued for 1 h. Upon complete consumption of starting material (as determined by TLC), the reaction mixture was extracted with EtOAc (3x). The combined organic layers were washed with brine, dried over Na_2SO_4, filtered, and concentrated under reduced pressure. The crude product was purified by silica gel flash column chromatography to afford the respective aldehyde product (**159**).

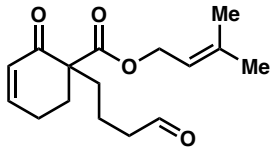

159

3-methylbut-2-en-1-yl 2-oxo-1-(4-oxobutyl)cyclohex-3-ene-1-carboxylate (159)

Prepared from **174** and 4-bromo-1,1-diethoxybutane[39] following General Procedure C. Purification by flash column chromatography (25% EtOAc/hexanes) afforded the title compound as a colorless oil (1.81 g, 6.50 mmol, 49% yield).

^{1}H NMR (400 MHz, $CDCl_3$): δ 9.75 (t, *J* = 1.5 Hz, 1H), 6.89 (dddd, *J* = 10.1, 4.4, 3.1, 1.1 Hz, 1H), 6.02 (ddd, *J* = 10.1, 2.5, 1.6 Hz, 1H), 5.31 – 5.25 (m, 1H), 4.59 (d, *J* = 6.8 Hz, 2H), 2.55 – 2.43 (m, 4H), 2.39 – 2.30 (m, 1H), 2.02 – 1.94 (m, 1H), 1.89 (ddd, *J* = 12.5, 11.7, 4.5 Hz, 1H), 1.78 (dd, *J* = 11.6, 4.9 Hz, 1H), 1.73 (s, 3H), 1.71 – 1.59 (m, 5H)

^{13}C NMR (100 MHz, $CDCl_3$): δ 202.2, 196.2, 171.5, 149.5, 139.7, 129.3, 118.3, 62.4, 57.0, 44.2, 33.2, 30.3, 25.8, 23.8, 18.2, 17.5.

IR (Neat Film, NaCl): 2942, 1732, 1716, 1456, 1180 cm^{-1}

HRMS (MM: FD+): *m/z* calc'd for $C_{16}H_{22}O_4$ $[M]^+$: 278.1518, found 278.1509.

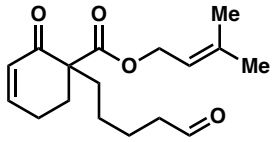

160

3-methylbut-2-en-1-yl 2-oxo-1-(5-oxopentyl)cyclohex-3-ene-1-carboxylate (160)

Prepared from **174** and 5-bromo-1,1-diethoxypentane[39] following General Procedure C. Purification by flash column chromatography (10–25% EtOAc/hexanes) afforded the title compound as a colorless oil (648 mg, 2.22 mmol, 38% yield).

^{1}H NMR (400 MHz, $CDCl_3$): δ 9.75 (s, 1H), 6.91 – 6.84 (m, 1H), 6.01 (ddd, *J* = 10.1, 2.6, 1.6 Hz, 1H), 5.27 (tdq, *J* = 7.1, 2.8, 1.4 Hz, 1H), 4.58 (d, *J* = 7.1 Hz, 2H), 2.54 – 2.40 (m, 4H), 2.36 – 2.27 (m, 1H), 1.98 – 1.86 (m, 2H), 1.78 – 1.60 (m, 10H), 1.40 – 1.26 (m, 2H).

^{13}C NMR (100 MHz, $CDCl_3$): δ 202.6, 196.4, 171.7, 149.4, 139.6, 129.3, 118.3, 62.3, 57.0, 43.7, 33.6, 30.4, 25.8, 24.3, 23.8, 22.5, 18.2.

IR (Neat Film, NaCl): 2941, 1733, 1717, 1456, 1219 cm^{-1}

HRMS (MM: FD+): *m/z* calc'd for $C_{16}H_{22}O_4$ $[M]^+$: 293.1747, found 293.1768.

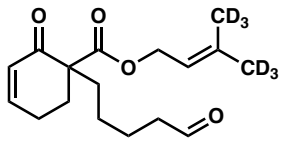

D-160

3-(methyl-d_3)but-2-en-1-yl-4,4,4-d_3 2-oxo-1-(5-oxopentyl)cyclohex-3-ene-1-carboxylate (*D*-160)

Prepared from ***D*-174** and 5-bromo-1,1-diethoxypentane[39] following General Procedure C. Purification by flash column chromatography (10–25% EtOAc/hexanes) afforded the title compound as a colorless oil (290 mg, 0.971 mmol, 42% yield).

^{1}H NMR (400 MHz, $CDCl_3$): δ 9.75 (t, *J* = 1.7 Hz, 1H), 6.90 – 6.85 (m, 1H), 6.01 (ddd, *J* = 10.1, 2.6, 1.6 Hz, 1H), 5.27 (t, *J* = 7.2 Hz, 1H), 4.58 (dd, *J* = 7.2, 1.8 Hz, 2H), 2.55 – 2.41 (m, 4H), 2.36 – 2.26 (m, 1H), 1.97 – 1.86 (m, 2H), 1.74 (ddd, *J* = 13.6, 11.6, 5.1 Hz, 1H), 1.68 – 1.60 (m, 2H), 1.40 – 1.24 (m, 2H).

^{13}C NMR (100 MHz, $CDCl_3$): δ 202.6, 196.4, 171.7, 149.4, 139.4, 129.3, 118.4, 62.3, 57.0, 43.7, 33.6, 30.4, 24.3, 23.9, 22.5.

^{2}H NMR (61 MHz, $CHCl_3$): δ 1.69, 1.65.

IR (Neat Film, NaCl): 2941, 1726, 1682, 1238, 1186 cm^{-1}

HRMS (MM: FD+): *m/z* calc'd for $C_{17}H_{18}D_6O_4$ $[M]^+$: 298.2051, found 298.2052.

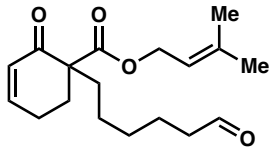

161

3-methylbut-2-en-1-yl 2-oxo-1-(6-oxohexyl)cyclohex-3-ene-1-carboxylate (161)

Prepared from **174** and 6-bromo-1,1-diethoxyhexane[39] following General Procedure C. Purification by flash column chromatography (10–25% EtOAc/hexanes) afforded the title compound as a colorless oil (838 mg, 2.73 mmol, 32% yield).

^{1}H NMR (400 MHz, $CDCl_3$): δ 9.75 (t, *J* = 1.8 Hz, 1H), 6.90 – 6.85 (m, 1H), 6.01 (ddd, *J* = 10.0, 2.5, 1.5 Hz, 1H), 5.30 – 5.25 (m, 1H), 4.62 – 4.55 (m, 2H), 2.54 – 2.39 (m, 4H), 2.36 – 2.27 (m, 1H), 1.98 – 1.84 (m, 2H), 1.73 (t, *J* = 1.2 Hz, 4H), 1.69 – 1.59 (m, 5H), 1.39 – 1.24 (m, 4H).

^{13}C NMR (100 MHz, $CDCl_3$): δ 202.8, 196.5, 171.7, 149.3, 139.5, 129.4, 118.4, 62.3, 57.1, 43.9, 33.6, 30.3, 29.6, 25.8, 24.4, 23.9, 21.9, 18.2.

IR (Neat Film, NaCl): 2934, 2864, 1733, 1717, 1684, 1456, 1220 cm^{-1}

HRMS (MM: FD+): *m/z* calc'd for $C_{18}H_{26}O_4$ $[M]^+$: 306.1831, found 306.1854.

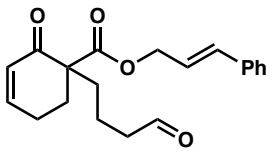

167

cinnamyl 2-oxo-1-(4-oxobutyl)cyclohex-3-ene-1-carboxylate (167)

Prepared from **177** and 4-bromo-1,1-diethoxybutane[39] following General Procedure C. Purification by flash column chromatography (10–25% EtOAc/hexanes) afforded the title compound as a colorless oil (0.607 g, 1.86 mmol, 49% yield).

^{1}H NMR (400 MHz, $CDCl_3$): δ 9.74 (t, *J* = 1.5 Hz, 1H), 7.38 – 7.35 (m, 2H), 7.35 – 7.30 (m, 2H), 7.28 – 7.24 (m, 1H), 6.91 (dddd, *J* = 10.1, 4.3, 3.1, 1.1 Hz, 1H), 6.63 (dt, *J* = 16.0, 1.4 Hz, 1H), 6.23 (dt, *J* = 15.8, 6.4 Hz, 1H), 6.05 (ddd, *J* = 10.1, 2.4, 1.7 Hz, 1H), 4.77 (dt, *J* = 6.5, 1.1 Hz, 2H), 2.57 – 2.45 (m, 4H), 2.42 – 2.32 (m, 1H), 2.05 – 1.98 (m, 1H), 1.93 (ddd, *J* = 13.2, 11.7, 5.1 Hz, 1H), 1.80 (ddd, *J* = 13.2, 11.1, 5.5 Hz, 1H), 1.73 – 1.63 (m, 2H).

^{13}C NMR (100 MHz, $CDCl_3$): δ 202.1, 196.0, 171.3, 149.7, 136.2, 134.7, 129.2, 128.8, 128.3, 126.8, 122.7, 66.0, 57.1, 44.1, 33.3, 30.1, 23.8, 17.5.

IR (Neat Film, NaCl): 2941, 1732, 1717, 1700, 1181, 734, 701 cm^{-1}

HRMS (MM: FD+): *m/z* calc'd for $C_{20}H_{22}O_4$ $[M]^+$: 326.1513, found 326.1510.

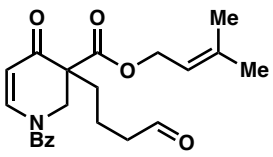

162

1-benzyl 3-(3-methylbut-2-en-1-yl) 4-oxo-3-(4-oxobutyl)-3,4-dihydropyridine-1,3(2*H*)-dicarboxylate (162)

Prepared from **178** and 4-bromo-1,1-diethoxybutane[39] following General Procedure C. Purification by flash column chromatography (15–30% EtOAc/hexanes) afforded the title compound as a colorless oil (603.9 mg, 1.46 mmol, 60% yield).

^{1}H NMR (400 MHz, $CDCl_3$): δ 9.73 (t, *J* = 1.4 Hz, 1H), 7.80 (s, 1H), 7.40 (d, *J* = 3.5 Hz, 5H), 5.27 (m, 4H), 4.61 (m, 3H), 3.78 (d, *J* = 13.6 Hz, 1H), 2.45 (tt, *J* = 6.8, 1.7 Hz, 2H), 2.03 – 1.90 (m, 1H), 1.72 (s, 3H), 1.67 (s, 3H), 1.70 – 1.60 (m, 1H).

^{13}C NMR (100 MHz, $CDCl_3$): δ 201.6, 190.5, 169.4, 142.7, 140.1, 135.0, 129.0, 128.9, 128.6, 118.0, 106.5, 69.4, 62.8, 55.4, 48.2, 43.9, 31.1, 25.8, 18.2, 17.2.

IR (Neat Film, NaCl): 2945, 2338, 1727, 1670, 1604, 1389, 1302, 1201, 932 cm^{-1}.

HRMS (MM: FD+): *m/z* calc'd for $C_{23}H_{27}NO_6$ $[M]^+$: 413.1838, found 413.1852.

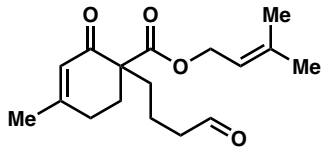

163

3-methylbut-2-en-1-yl 4-methyl-2-oxo-1-(4-oxobutyl)cyclohex-3-ene-1-carboxylate (163)

Prepared from **179** and 4-bromo-1,1-diethoxybutane[39] following General Procedure C. Purification by flash column chromatography (25–50% EtOAc/hexanes) afforded the title compound as a colorless oil (1141.4 mg, 3.90 mmol, 78% yield).

^{1}H NMR (400 MHz, $CDCl_3$): δ 9.74 (s, 1H), 5.87 (dt, *J* = 2.6, 1.2 Hz, 1H), 5.27 (tp, *J* = 7.1, 1.4 Hz, 1H), 4.58 (d, *J* = 7.2 Hz, 2H), 2.45 (ddd, *J* = 8.0, 4.8, 1.7 Hz, 4H), 2.29 – 2.18 (m, 1H), 1.92 (s, 3H), 2.00 – 1.84 (m, 2H), 1.72 (s, 3H), 1.67 (s, 3H), 1.79 – 1.54 (m, 3H).

^{13}C NMR (100 MHz, $CDCl_3$): δ 202.2, 195.9, 171.7, 161.6, 139.6, 126.0, 118.3, 62.3, 56.0, 44.2, 33.2, 30.0, 28.7, 25.8, 24.2, 18.2, 17.5.

IR (Neat Film, NaCl): 3426, 2936, 2730, 1725, 1672, 1637, 1440, 1380, 1348, 1311, 1272, 1233, 1214, 1177, 1104, 1050, 1016, 986, 939, 870, 842, 820, 776 cm^{-1}.

HRMS (MM: FD+): *m/z* calc'd for $C_{17}H_{24}O_4$ $[M]^+$: 292.1682, found 292.1669.

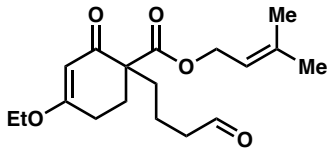

164

3-methylbut-2-en-1-yl 4-ethoxy-2-oxo-1-(4-oxobutyl)cyclohex-3-ene-1-carboxylate (164)

Prepared from **180** and 4-bromo-1,1-diethoxybutane[39] following General Procedure C. Purification by flash column chromatography (30–40% EtOAc/hexanes) afforded the title compound as a colorless oil (653.2 mg, 2.03 mmol, 21% yield).

^{1}H NMR (400 MHz, $CDCl_3$): δ 9.75 (t, *J* = 1.5 Hz, 1H), 5.34 (d, *J* = 1.1 Hz, 1H), 5.29 (tp, *J* = 7.2, 1.4 Hz, 1H), 4.66 – 4.53 (m, 2H), 3.86 (q, *J* = 7.18, 2H), 2.61 (dddd, *J* = 17.8, 10.3, 4.7, 1.3 Hz, 1H), 2.50 – 2.30 (m, 4H), 2.02 – 1.87 (m, 2H), 1.82 – 1.73 (m, 1H), 1.72 (s, 3H), 1.68 (s, 3H), 1.67 – 1.58 (m, 2H), 1.35 (t, *J* = 7.0 Hz, 3H).

^{13}C NMR (100 MHz, $CDCl_3$): δ 201.9, 195.5, 176.5, 171.5, 139.1, 118.1, 101.9, 64.3, 62.0, 55.7, 43.9, 33.1, 28.2, 26.3, 25.5, 17.9, 17.2, 13.9.

IR (Neat Film, NaCl): 2939, 2728, 1723, 1659, 1608, 1447, 1380, 1315, 1242, 1179, 1108, 1027, 942, 816, 769 cm^{-1}.

HRMS (MM: FD+): *m/z* calc'd for $C_{18}H_{26}O_5$ $[M]^+$: 322.1790, found 322.1775.

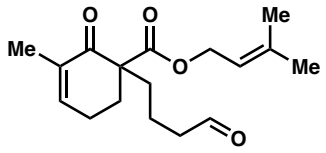

165

3-methylbut-2-en-1-yl 3-methyl-2-oxo-1-(4-oxobutyl)cyclohex-3-ene-1-carboxylate (165)

Prepared from **181** and 4-bromo-1,1-diethoxybutane[39] following General Procedure C. Purification by flash column chromatography (15–20% EtOAc/hexanes) afforded the title compound as a colorless oil (1.14 g, 3.90 mmol, 70% yield).

^{1}H NMR (400 MHz, $CDCl_3$): δ 9.75 (s, 1H), 6.64 – 6.57 (m, 1H), 5.27 (tt, *J* = 7.1, 1.4 Hz, 1H), 4.64 – 4.51 (m, 2H), 2.51 – 2.36 (m, 4H), 2.36 – 2.22 (m, 1H), 2.01 – 1.92 (m, 1H), 1.87 (m, 1H), 1.83-1.53 (m, 3H) 1.78 (s, 3H), 1.73 (s, 3H), 1.67 (d, *J* = 1.3 Hz, 3H).

^{13}C NMR (100 MHz, $CDCl_3$): δ 202.2, 196.9, 171.9, 143.9, 139.6, 135.3, 118.3, 62.2, 57.0, 44.2, 33.3, 30.7, 25.8, 23.5, 18.2, 17.7, 16.6.

IR (Neat Film, NaCl): 3500, 2925, 2333, 1725, 1681, 1449, 1361, 1182 cm^{-1}.

HRMS (MM: FD+): *m/z* calc'd for $C_{17}H_{24}O_4$ $[M]^+$: 292.1680, found 292.1669.

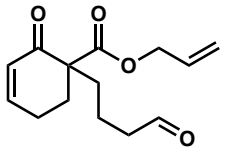

166

allyl 2-oxo-1-(4-oxobutyl)cyclohex-3-ene-1-carboxylate (166)

Prepared from allyl 2-oxocyclohex-3-ene-1-carboxylate [40] and 4-bromo-1,1-diethoxybutane[39] following General Procedure C. Purification by flash column chromatography (15–30% EtOAc/hexanes) afforded the title compound as a colorless oil (773.2 mg, 3.09 mmol, 21% yield).

^{1}H NMR (400 MHz, $CDCl_3$): δ 9.75 (t, *J* = 1.4 Hz, 1H), 6.91 (dddd, *J* = 10.1, 4.4, 3.1, 1.1 Hz, 1H), 6.03 (dt, *J* = 10.1, 2.0 Hz, 1H), 5.86 (ddt, *J* = 17.1, 10.2, 5.6 Hz, 1H), 5.28 (dq, *J* = 17.2, 1.6 Hz, 1H), 5.22 (dq, *J* = 10.4, 1.3 Hz, 1H), 4.60 (dq, *J* = 5.4, 1.6 Hz, 2H), 2.58 – 2.43 (m, 4H), 2.43 – 2.30 (m, 1H), 2.07 – 1.95 (m, 1H), 1.91 (ddd, *J* = 13.2, 11.6, 5.2 Hz, 1H), 1.79 (ddd, *J* = 13.2, 10.9, 5.6 Hz, 1H), 1.75 – 1.56 (m, 2H).

^{13}C NMR (100 MHz, $CDCl_3$): δ 202.1, 196.0, 171.2, 149.7, 131.7, 129.2, 118.7, 65.9, 57.1, 44.1, 33.1, 30.1, 23.7, 17.4.

IR (Neat Film, NaCl): 2947, 2732, 1726, 1680, 1238, 1184 cm^{-1}.

HRMS (MM: FD+): *m/z* calc'd for $C_{14}H_{19}O_4$ $[M]^+$: 251.1281, found 251.1278.

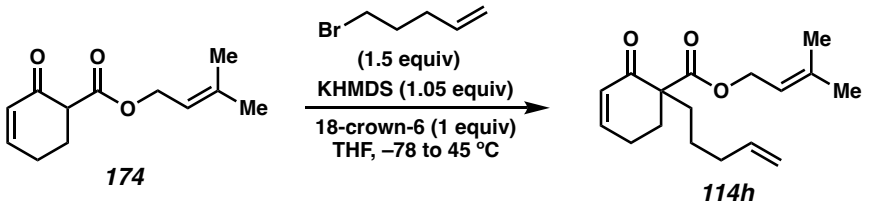

3-methylbut-2-en-1-yl 2-oxo-1-(pent-4-en-1-yl)cyclohex-3-ene-1-carboxylate (114h)

Prepared from **174** and 5-bromopent-1-ene following General Procedure C (without hydrolysis step). Purification by flash column chromatography (0-20% EtOAc/hexanes) afforded the title compound as a colorless oil (93.8 mg, 0.34 mmol, 23% yield).

^{1}H NMR (400 MHz, $CDCl_3$): δ 6.87 (dddd, *J* = 10.1, 4.8, 3.1, 1.1 Hz, 1H), 6.01 (ddd, *J* = 10.1, 2.5, 1.6 Hz, 1H), 5.78 (ddt, *J* = 16.9, 10.2, 6.6 Hz, 1H), 5.28 (tdq, *J* = 7.1, 2.9, 1.4 Hz,

1H), 5.00 (dq, *J* = 17.1, 1.6 Hz, 1H), 4.94 (ddt, *J* = 10.2, 2.2, 1.2 Hz, 1H), 4.59 (dd, *J* = 7.2, 3.7 Hz, 1H), 4.64 – 4.53 (m, 2H), 2.57 – 2.41 (m, 2H), 2.38 – 2.24 (m, 2H), 2.12 – 2.01 (m, 2H), 2.00 – 1.86 (m, 2H), 1.77 – 1.69 (m, 1H), 1.73 (s, 3H), 1.68 (s, 3H), 1.51 – 1.28 (m, 2H).

^{13}C NMR (100 MHz, $CDCl_3$): δ 196.5, 171.7, 149.3, 139.5, 138.4, 129.4, 118.4, 114.9, 62.2, 57.1, 34.2, 33.4, 30.3, 25.8, 24.0, 23.9, 18.2.

IR (Neat Film, NaCl): 2928, 1726, 1683, 1440, 1383, 1186, 912 cm^{-1}.

HRMS (MM: FD+): *m/z* calc'd for $C_{17}H_{24}O_3$ $[M]^+$: 276.1725, found 276.1718.

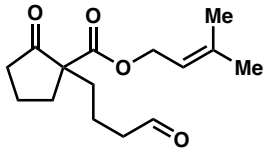

175

3-methylbut-2-en-1-yl 2-oxo-1-(4-oxobutyl)cyclopentane-1-carboxylate (175)

Prepared from 3-methylbut-2-en-1-yl 2-oxocyclopentane-1-carboxylate[41] and 4-bromo-1,1-diethoxybutane[39] following General Procedure C. Purification by flash column chromatography (20–25% EtOAc/hexanes) afforded the title compound as a colorless oil (1.86 g, 6.97 mmol, 87% yield).

^{1}H NMR (400 MHz, $CDCl_3$): δ 9.74 (t, *J* = 1.4 Hz, 1H), 5.29 (tp, *J* = 7.3, 1.4 Hz, 1H), 4.59 (d, *J* = 7.2 Hz, 2H), 2.58 – 2.47 (m, 1H), 2.44 (tt, *J* = 7.0, 1.5 Hz, 2H), 2.44 – 2.36 (m, 1H), 2.31 – 2.18 (m, 1H), 2.11 – 1.85 (m, 4H), 1.74 (s, 3H), 1.68 (s, 3H), 1.67 – 1.48 (m, 3H).

^{13}C NMR (100 MHz, $CDCl_3$): δ 214.8, 201.9, 171.0, 139.7, 118.2, 62.5, 60.4, 44.0, 38.0, 33.2, 33.0, 25.9, 19.8, 18.2, 17.6.

IR (Neat Film, NaCl): 3456, 2954, 2724, 1745, 1721, 1446, 1406, 1384, 1154, 953 cm^{-1}.

HRMS (MM: FD+): *m/z* calc'd for $C_{15}H_{22}O_4$ $[M]^+$: 266.1525, found 266.1513.

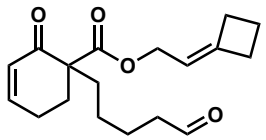

168

2-cyclobutylideneethyl 2-oxo-1-(5-oxopentyl)cyclohex-3-ene-1-carboxylate (168)

Prepared from **182** and 5-bromo-1,1-diethoxypentane[39] following General Procedure C. Purification by flash column chromatography (10–60% EtOAc/hexanes) afforded the title compound as a colorless oil (649 mg, 2.13 mmol, 29% yield).

^{1}H NMR (400 MHz, $CDCl_3$): δ 9.75 (t, *J* = 1.7 Hz, 1H), 6.94 – 6.83 (m, 1H), 6.02 (ddd, *J* = 10.1, 2.6, 1.5 Hz, 1H), 5.20 (tp, *J* = 7.1, 2.3 Hz, 1H), 4.46 (ddt, *J* = 7.4, 2.3, 1.1 Hz, 2H), 2.69 (dt, *J* = 16.0, 8.4 Hz, 4H), 2.56 – 2.40 (m, 4H), 2.37 – 2.26 (m, 1H), 2.03 – 1.84 (m, 4H), 1.75 (ddd, *J* = 13.6, 11.6, 5.1 Hz, 1H), 1.64 (p, *J* = 7.5 Hz, 2H), 1.42 – 1.26 (m, 2H).

^{13}C NMR (100 MHz, $CDCl_3$): δ 202.6, 196.4, 171.6, 149.4, 148.9, 129.4, 114.0, 62.3, 57.0, 43.7, 33.6, 31.2, 30.4, 29.6, 24.3, 23.9, 22.5, 17.1.

IR (Neat Film, NaCl): 2941, 1726, 1681, 1446, 1387, 1240, 1171, 1103 cm^{-1}.

HRMS (MM: FD+): *m/z* calc'd for $C_{18}H_{24}O_4$ $[M]^+$: 304.1675, found 304.1677.

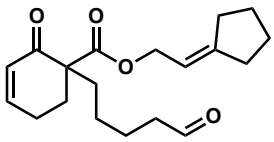

169

2-cyclopentylideneethyl 2-oxo-1-(5-oxopentyl)cyclohex-3-ene-1-carboxylate (169)

Prepared from **183** and 5-bromo-1,1-diethoxypentane[39] following General Procedure C. Purification by flash column chromatography (10–60% EtOAc/hexanes) afforded the title compound as a colorless oil (1.40 g, 4.40 mmol, 39% yield).

^{1}H NMR (400 MHz, $CDCl_3$): δ 9.75 (t, *J* = 1.7 Hz, 3H), 6.92 – 6.83 (m, 1H), 6.02 (ddd, *J* = 10.1, 2.6, 1.6 Hz, 1H), 5.41 – 5.32 (m, 1H), 4.64 – 4.50 (m, 2H), 2.56 – 2.39 (m, 4H), 2.37 – 2.20 (m, 5H), 1.99 – 1.83 (m, 2H), 1.80 – 1.57 (m, 7H), 1.45 – 1.22 (m, 2H).

^{13}C NMR (100 MHz, $CDCl_3$): δ 202.6, 196.4, 171.7, 151.1, 149.4, 129.4, 113.8, 63.8, 57.0, 43.7, 33.9, 33.6, 30.4, 29.0, 26.4, 26.2, 24.3, 23.9, 22.5.

IR (Neat Film, NaCl): 2947, 2725, 1729, 1697, 1456, 1356, 1215 cm^{-1}.

HRMS (MM: FD+): *m/z* calc'd for $C_{19}H_{26}O_4$ $[M]^+$: 318.1831, found 318.1809.

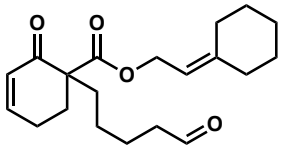

170

2-cyclohexylideneethyl 2-oxo-1-(5-oxopentyl)cyclohex-3-ene-1-carboxylate (170)

Prepared from **184** and 5-bromo-1,1-diethoxypentane[39] following General Procedure C. Purification by flash column chromatography (10–50% EtOAc/hexanes) afforded the title compound as a colorless oil (177 mg, 0.53 mmol, 25% yield).

^{1}H NMR (400 MHz, $CDCl_3$): δ 9.75 (t, *J* = 1.7 Hz, 1H), 6.93 – 6.83 (m, 1H), 6.02 (ddd, *J* = 10.1, 2.6, 1.6 Hz, 1H), 5.23 (tt, *J* = 7.2, 1.2 Hz, 1H), 4.60 (d, *J* = 7.2 Hz, 2H), 2.56 – 2.39 (m, 4H), 2.37 – 2.26 (m, 1H), 2.20 – 2.13 (m, 2H), 2.12 – 2.05 (m, 2H), 1.99 – 1.85 (m, 2H), 1.74 (ddd, *J* = 13.6, 11.7, 5.0 Hz, 1H), 1.64 (p, *J* = 7.5 Hz, 2H), 1.58 – 1.46 (m, 6H), 1.43 – 1.20 (m, 2H).

^{13}C NMR (100 MHz, $CDCl_3$): δ 202.6, 196.4, 171.6, 149.3, 147.7, 129.4, 114.8, 61.5, 57.0, 43.7, 37.1, 33.6, 30.4, 29.2, 28.5, 27.9, 26.7, 24.3, 23.9, 22.5.

IR (Neat Film, NaCl): 2929, 2858, 1731, 1446, 1170, 938 cm^{-1}.

HRMS (MM: FD+): *m/z* calc'd for $C_{20}H_{28}O_4$ $[M]^+$: 332.1988, found 332.1991.

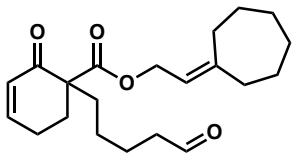

171

2-cycloheptylideneethyl 2-oxo-1-(5-oxopentyl)cyclohex-3-ene-1-carboxylate (171)

Prepared from **185** and 5-bromo-1,1-diethoxypentane[39] following General Procedure C. Purification by flash column chromatography (10–70% Et_2O/hexanes) afforded the title compound as a colorless oil (349 mg, 1.01 mmol, 15% yield).

^{1}H NMR (400 MHz, $CDCl_3$): δ 9.75 (t, *J* = 1.7 Hz, 1H), 6.91 – 6.84 (m, 1H), 6.02 (ddd, *J* = 10.1, 2.6, 1.6 Hz, 1H), 5.28 (tt, *J* = 7.1, 1.3 Hz, 1H), 4.60 (d, *J* = 7.1 Hz, 2H), 2.56 – 2.40 (m, 4H), 2.38 – 2.20 (m, 5H), 1.98 – 1.87 (m, 2H), 1.76 (ddd, *J* = 13.7, 12.0, 4.8 Hz, 1H), 1.65 (p, *J* = 7.5 Hz, 2H), 1.57 (q, *J* = 5.4 Hz, 4H), 1.50 (dt, *J* = 5.2, 2.4 Hz, 4H), 1.42 – 1.27 (m, 2H).

^{13}C NMR (100 MHz, $CDCl_3$): δ 202.6, 196.4, 171.7, 149.4, 149.0, 129.4, 118.4, 62.1, 57.0, 43.7, 37.7, 33.6, 30.4, 30.2, 29.8, 29.1, 28.9, 27.3, 24.3, 23.9, 22.5.

IR (Neat Film, NaCl): 2923, 2854, 1737, 1681, 1443, 1385, 1235, 1172 cm^{-1}.

HRMS (MM: FD+): *m/z* calc'd for $C_{21}H_{30}O_4$ $[M]^+$: 346.2144, found 346.2139.

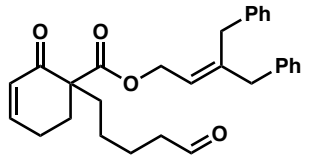

172

3-benzyl-4-phenylbut-2-en-1-yl 2-oxo-1-(5-oxopentyl)cyclohex-3-ene-1-carboxylate (172)

Prepared from **186** and 5-bromo-1,1-diethoxypentane[39] following General Procedure C. Purification by flash column chromatography (10–60% Et_2O/hexanes) afforded the title compound as a colorless oil (425 mg, 0.955 mmol, 18% yield).

^{1}H NMR (400 MHz, $CDCl_3$): δ 9.73 (t, *J* = 1.7 Hz, 1H), 7.32 – 7.27 (m, 4H), 7.21 (tt, *J* = 7.5, 2.3 Hz, 2H), 7.15 – 7.03 (m, 4H), 6.90 – 6.82 (m, 1H), 6.02 (ddd, *J* = 10.2, 2.5, 1.6 Hz, 1H), 5.51 (d, *J* = 7.4 Hz, 1H), 4.83 – 4.70 (m, 2H), 3.36 (s, 2H), 3.24 (s, 2H), 2.54 – 2.24 (m, 5H), 2.00 – 1.86 (m, 2H), 1.77 (ddd, *J* = 13.6, 11.6, 5.1 Hz, 1H), 1.63 (p, *J* = 7.5 Hz, 2H), 1.44 – 1.22 (m, 2H).

^{13}C NMR (100 MHz, $CDCl_3$): δ 202.5, 196.2, 171.6, 149.4, 144.8, 139.0, 138.8, 129.4, 129.3, 128.8, 128.7, 128.5, 126.5, 126.4, 121.7, 62.0, 57.0, 43.7, 42.9, 35.8, 33.6, 30.4, 24.3, 23.9, 22.5.

IR (Neat Film, NaCl): 2923, 1723, 1684, 1493, 1451, 1386, 1231 cm^{-1}.

HRMS (MM: FD+): *m/z* calc'd for $C_{29}H_{32}O_4$ $[M]^+$: 444.2301, found 444.2300.

β-Ketoesters Synthesis

General Procedure D: Prenyl β-ketoesters Synthesis through Acylation

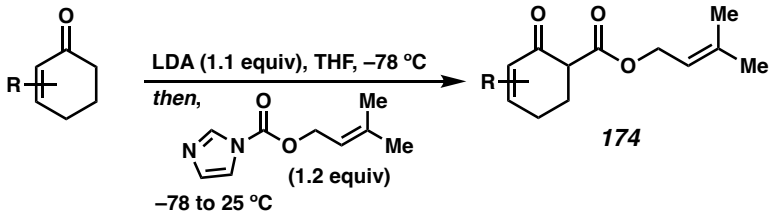

A flame dried round bottom flask was charged with iPr_2NH (1.1 equiv) and THF (1.75 M). The solution was cooled to 0 ºC and *n*-BuLi (2.5 M in hexanes, 1.05 equiv) was added dropwise. The resultant solution was stirred for 30 min at 0 ºC. The corresponding cyclohexenone (1.0 equiv) in THF (1.25 M) was added dropwise and stirring was continued at 0 ºC for 30 minutes. The solution was cooled to –78 ºC, and the appropriate N-acyl imidazole (1.2 equiv) in THF (3.25 M) was added dropwise. After 2 h, the reaction was gradually warmed to 23 ºC and diluted with 2 M aqueous HCl until reaching a pH < 7. The reaction mixture was extracted three times with EtOAc. The combined organic layers were washed with brine, dried over Na_2SO_4, filtered, and concentrated under reduced pressure. The crude product was purified by flash silica gel column chromatography to afford the corresponding acylated enone.

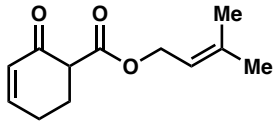

174

3-methylbut-2-en-1-yl 2-oxocyclohex-3-ene-1-carboxylate (174)

Prepared from 2-cyclohexen-1-one and 3-methylbut-2-en-1-yl 1H-imidazole-1-carboxylate [42] following General Procedure D. Purification by flash column

chromatography (25% EtOAc/hexanes) afforded the title compound as a colorless oil (6.65 g, 31.9 mmol, 41% yield).

^{1}H NMR (400 MHz, $CDCl_3$): δ 7.02 – 6.97 (m, 1H), 6.07 (dt, *J* = 10.2, 2.0 Hz, 1H), 5.37 – 5.32 (m, 1H), 4.65 (d, *J* = 7.1 Hz, 2H), 3.42 – 3.39 (m, 1H), 2.55 – 2.45 (m, 1H), 2.44 – 2.34 (m, 2H), 2.26 – 2.18 (m, 1H), 1.75 (s, 3H), 1.71 (s, 3H).

^{13}C NMR (100 MHz, $CDCl_3$): δ 194.1, 170.2, 150.7, 139.6, 129.3, 118.4, 62.3, 53.6, 25.9, 25.8, 24.5, 18.2.

IR (Neat Film, NaCl): 3033, 2934, 1736, 1682, 1447, 1387, 1302, 1233, 1159, 1123 cm^{-1}

HRMS (MM: FD+): *m/z* calc'd for $C_{12}H_{16}O_3$ $[M]^+$: 208.1099, found 208.1090.

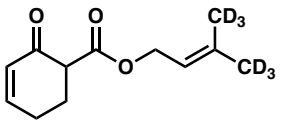

D-174

3-(methyl-*d*$_3$)but-2-en-1-yl-4,4,4-*d*$_3$ 2-oxocyclohex-3-ene-1-carboxylate (D-174)

Prepared from 2-cyclohexen-1-one and 3-(methyl-d_3)but-2-en-1-yl-4,4,4-d_3 1*H*-imidazole-1-carboxylate [43] following General Procedure D. Purification by flash column chromatography (25% EtOAc/hexanes) afforded the title compound as a colorless oil (1.00 g, 4.67 mmol, 37% yield). *Note that 1.0 equiv of the N-acyl imidazole can be employed.*

^{1}H NMR (400 MHz, $CDCl_3$): δ 6.99 (dt, *J* = 10.0, 3.7 Hz, 1H), 6.06 (dt, *J* = 10.2, 2.1 Hz, 1H), 5.34 (t, *J* = 7.2 Hz, 1H), 4.65 (d, *J* = 7.2 Hz, 2H), 3.40 (dd, *J* = 9.7, 5.0 Hz, 1H), 2.54 – 2.44 (m, 1H), 2.44 – 2.32 (m, 2H), 2.22 (ddt, *J* = 13.7, 8.8, 3.0 Hz, 1H).

^{13}C NMR (100 MHz, $CDCl_3$): δ 194.1, 170.2, 150.7, 139.4, 129.3, 118.4, 62.3, 53.6, 25.8, 24.5.

^{2}H NMR (61 MHz, $CHCl_3$): δ 1.72, 1.67.

IR (Neat Film, NaCl): 2942, 1736, 1681, 1388, 1164 cm^{-1}

HRMS (MM: FD+): *m/z* calc'd for $C_{12}H_{10}D_6O_3$ $[M]^+$: 214.1476, found 214.1476.

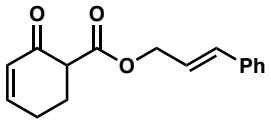

177

cinnamyl 2-oxocyclohex-3-ene-1-carboxylate (177)

Prepared from 2-cyclohexen-1-one and cinnamyl 1*H*-imidazole-1-carboxylate[42] following General Procedure D. Purification by flash column chromatography (15–25% EtOAc/hexanes) afforded the title compound as a colorless oil (0.98 g, 3.82 mmol, 39% yield).

^{1}H NMR (400 MHz, $CDCl_3$): δ 7.40 – 7.37 (m, 2H), 7.34 – 7.30 (m, 2H), 7.28 – 7.24 (m, 1H), 7.01 (dt, *J* = 10.3, 3.8 Hz, 1H), 6.67 (dt, *J* = 15.9, 1.3 Hz, 1H), 6.29 (dt, *J* = 15.9, 6.4 Hz, 1H), 6.09 (dt, *J* = 10.2, 2.0 Hz, 1H), 4.83 (d, *J* = 6.5 Hz, 2H), 3.47 (dd, *J* = 10.2, 4.9 Hz, 1H), 2.57 – 2.47 (m, 1H), 2.47 – 2.34 (m, 2H), 2.28 – 2.21 (m, 1H).

^{13}C NMR (100 MHz, $CDCl_3$): δ 193.9, 169.9, 150.8, 136.3, 134.6, 129.3, 128.7, 128.2, 126.8, 122.9, 65.9, 53.6, 25.8, 24.5.

IR (Neat Film, NaCl): 3024, 2940, 1734, 1676, 1304, 1223, 1157, 1123, 969 cm^{-1}

HRMS (MM: FD+): *m/z* calc'd for $C_{16}H_{16}NaO_3$ $[M+Na]^+$: 279.0997, found 279.0983.

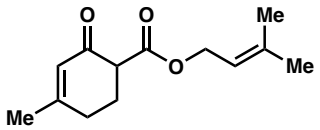

179

3-methylbut-2-en-1-yl 4-methyl-2-oxocyclohex-3-ene-1-carboxylate (179)

Prepared from 3-methylcyclohex-2-en-1-one and 3-methylbut-2-en-1-yl 1H-imidazole-1-carboxylate[42] following General Procedure D. Purification by flash column chromatography (10–20% EtOAc/hexanes) afforded the title compound as a colorless oil (2.95 g, 13.3 mmol, 17% yield).

^{1}H NMR (400 MHz, $CDCl_3$): δ 5.91 (h, *J* = 1.4 Hz, 1H), 5.35 (tp, *J* = 7.1, 1.6 Hz, 1H), 4.65 (d, *J* = 7.2 Hz, 2H), 3.37 – 3.27 (m, 1H), 2.48 – 2.24 (m, 3H), 2.21 – 2.15 (m, 1H), 1.97 (s, 3H), 1.75 (d, *J* = 1.3 Hz, 3H), 1.70 (s, 3H).

^{13}C NMR (100 MHz, $CDCl_3$): δ 193.9, 170.5, 163.0, 139.5, 126.0, 118.5, 62.3, 52.6, 29.5, 25.9, 25.7, 24.5, 18.2.

IR (Neat Film, NaCl): 2938, 1732, 1668, 1632, 1434, 1378, 1357, 1302, 1246, 1216, 1170, 1152, 1018 cm^{-1}.

HRMS (MM: FD+): *m/z* calc'd for $C_{13}H_{18}O_3$ $[M]^+$: 222.1257, found 222.1251.

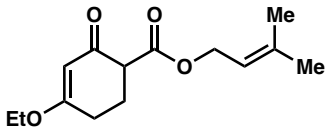

180

3-methylbut-2-en-1-yl 4-ethoxy-2-oxocyclohex-3-ene-1-carboxylate (76)

Prepared from 3-ethoxycyclohex-2-en-1-one and 3-methylbut-2-en-1-yl 1H-imidazole-1-carboxylate[42] following General Procedure D. Purification by flash column chromatography (25–30% EtOAc/hexanes) afforded the title compound as a colorless oil (2.84 g, 9.51 mmol, 19% yield).

^{1}H NMR (400 MHz, $CDCl_3$): δ 5.38 (s, 1H), 5.37 – 5.32 (m, 1H), 4.72 – 4.59 (m, 2H), 3.91 (qd, *J* = 7.0, 2.3 Hz, 2H), 3.36 – 3.27 (m, 1H), 2.56 (ddd, *J* = 16.6, 6.2, 4.5 Hz, 1H),

2.47 – 2.27 (m, 2H), 2.24 – 2.08 (m, 1H), 1.75 (s, 3H), 1.70 (s, 3H), 1.36 (t, J = 7.0 Hz, 3H).

^{13}C NMR (100 MHz, $CDCl_3$): δ 194.0, 177.7, 170.6, 139.4, 118.5, 102.3, 64.6, 62.3, 52.5, 27.5, 25.9, 24.3, 18.2, 14.2.

IR (Neat Film, NaCl): 2980, 2357, 1730, 1648, 1605, 1380, 1192, 1026, 668 cm^{-1}.

HRMS (MM: FD+): *m/z* calc'd for $C_{14}H_{20}O_4$ $[M]^+$: 252.1363, found 252.1356.

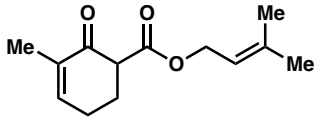

181

3-methylbut-2-en-1-yl 3-methyl-2-oxocyclohex-3-ene-1-carboxylate (181)

Prepared from 2-methylcyclohex-2-en-1-one[44] and 3-methylbut-2-en-1-yl 1H-imidazole-1-carboxylate[42] following General Procedure D. Purification by flash column chromatography (10–20% EtOAc/hexanes) afforded the title compound as a colorless oil (1.09 g, 4.90 mmol, 23% yield).

^{1}H NMR (400 MHz, $CDCl_3$): δ 6.78 – 6.69 (m, 1H), 5.35 (tdq, J = 7.2, 2.9, 1.5 Hz, 1H), 4.65 (d, J = 7.2 Hz, 2H), 3.42 – 3.36 (m, 1H), 2.48 – 2.11 (m, 5H), 1.79 (d, J = 1.6 Hz, 3H), 1.75 (s, 3H), 1.70 (s, 3H).

^{13}C NMR (100 MHz, $CDCl_3$): δ 194.7, 170.6, 145.5, 139.5, 135.4, 118.5, 62.2, 53.8, 26.3, 25.9, 24.6, 18.2, 16.2.

IR (Neat Film, NaCl): 2925, 1736, 1676, 1449, 1381, 1249, 1151 cm^{-1}.

HRMS (MM: FD+): *m/z* calc'd for $C_{13}H_{18}O_3$ $[M]^+$: 222.1255, found 222.1251.

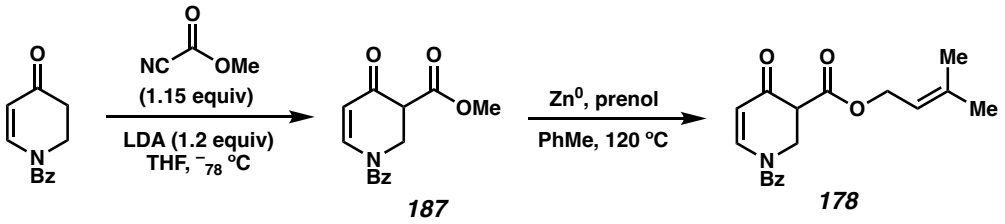

1-benzyl 3-methyl 4-oxo-3,4-dihydropyridine-1,3(2*H*)-dicarboxylate (187)

A flame dried round bottom flask was charged with *i*-Pr_2NH (2.52 mL, 18.0 mmol, 1.2 equiv) and THF (167 mL, 0.1 M). The solution was cooled to –78 ºC and *n*-BuLi (7.20 mL, 18.0 mmol, 1.2 equiv) was added dropwise. The resultant solution was slowly warmed to 0 ºC over 1 h and then cooled to – 78 ºC. The LDA solution was added dropwise to a solution of 1-benzoyl-2,3-dihydropyridin-4(1*H*)-one[45] (3.47 g, 15.0 mmol, 1.0 equiv) in THF (239 mL, 0.06 M) at –78 ºC. The resultant solution was stirred for 1 h. Then methyl cyanoformate (1.37 mL, 17.25 mmol, 1.15 equiv) was added dropwise. Upon complete consumption of starting material (as determined by TLC), the reaction was diluted with a saturated solution of NH_4Cl and the product was extracted with EtOAc (3 x 200 mL). The combined organic layers were dried over Na_2SO_4, filtered, and concentrated under reduced pressure. The crude product was purified by column chromatography (SiO_2, 20–30% EtOAc/Hexanes) to afford acylated enone **187** (1.17 g, 4.05 mmol, 27% yield).

^{1}H NMR (400 MHz, $CDCl_3$): δ 7.88 (s, 1H), 7.39 (d, *J* = 2.3 Hz, 5H), 5.40 (s, 1H), 5.28 (s, 1H), 4.39 (dd, *J* = 13.6, 8.9 Hz, 1H), 4.18 (dd, *J* = 13.6, 5.4 Hz, 1H), 3.76 (s, 3H), 3.51 (dd, *J* = 8.9, 5.4 Hz, 1H).

^{13}C NMR (100 MHz, $CDCl_3$): δ 187.8, 168.2, 143.6, 134.8, 129.1, 128.9, 128.8, 128.7, 106.8, 69.6, 52.9, 50.6, 44.4.

IR (Neat Film, NaCl): 2952, 2332, 1734, 1670, 1601, 1388, 1293, 1213 cm^{-1}.

HRMS (MM: FD+): *m/z* calc'd for $C_{15}H_{15}NO_5$ $[M]^+$: 289.0950, found 289.0948.

1-benzyl 3-(3-methylbut-2-en-1-yl) 4-oxo-3,4-dihydropyridine-1,3(2*H*)-dicarboxylate (178)

A flame dried round bottom flask equipped with a reflux condenser was charged with Zn^0 dust (51.5 mg, 0.787 mmol, 0.2 equiv), acylated enone **187** (1.14 g, 3.40 mmol, 1.0 equiv), and toluene (19.7 mL, 0.2 M). To the stirred solution, prenyl alcohol was added neat (2.00 mL, 19.68 mmol, 5.0 equiv). The resultant solution was heated to reflux for 3 days. The solution was cooled to 23 ºC, filtered through a celite plug and eluted with CH_2Cl_2, and concentrated under reduced pressure. The crude product was purified by column chromatography (SiO_2, 15–25% EtOAc/Hexanes) to afford acylated enone **178** (883 mg, 2.57 mmol, 65% yield).

^{1}H NMR (400 MHz, $CDCl_3$): δ 7.86 (s, 1H), 7.39 (m, 5H), 5.39 (s, 1H), 5.32 (tp, *J* = 7.3, 1.4 Hz, 1H), 5.27 (s, 2H), 4.65 (dd, *J* = 7.3, 2.9 Hz, 2H), 4.38 (dd, *J* = 13.6, 8.9 Hz, 1H), 4.17 (dd, *J* = 13.5, 5.4 Hz, 1H), 3.48 (dd, *J* = 9.1, 5.3 Hz, 1H), 1.74 (s, 3H), 1.69 (s, 3H).

^{13}C NMR (100 MHz, $CDCl_3$): δ 187.9, 167.8, 143.5, 140.1, 134.9, 129.0, 128.9, 128.8, 128.7, 118.0, 106.9, 69.5, 62.8, 50.8, 44.5, 25.9, 18.2.

IR (Neat Film, NaCl): 2965, 1727, 1676, 1599, 1388, 1293, 1209, 940 cm^{-1}.

HRMS (MM: FD+): *m/z* calc'd for $C_{19}H_{21}HO_5$ $[M]^+$: 343.1420, found 343.1420.

General Procedure E: Substituted β-Ketoesters Synthesis through Acylation[42]

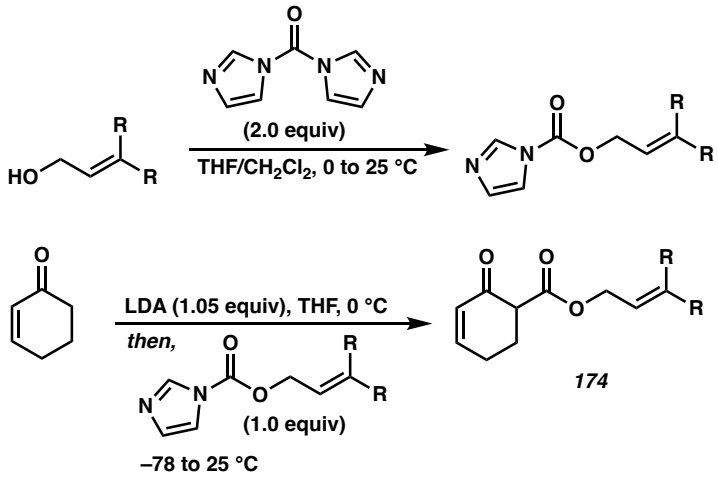

To a solution of di(1*H*-imidazol-1-yl)methanone (2.0 equiv) in THF (2.0 M) at 0 °C was added dropwise a solution of the corresponding alcohol (1.0 equiv) in CH_2Cl_2 (1.0 M). After 3 h, the reaction mixture was gradually warmed to 25 °C. Upon consumption of starting material (as determined by TLC), the reaction mixture was concentrated under reduced pressure then filtered through a silica plug and eluted with 50% EtOAc/Hexanes. The resulting solution was concentrated under reduced pressure.

A flame dried round bottom flask was charged with iPr_2NH (1.1 equiv) and THF (1.75 M). The solution was cooled to 0 ºC and *n*-BuLi (2.5 M in hexanes, 1.05 equiv) was added dropwise. The resultant solution was stirred for 30 min at 0 ºC. 2-cyclohexen-1-one (1.0 equiv) in THF (1.25 M) was added dropwise and stirring was continued at 0 ºC for 30 minutes. The solution was cooled to –78 ºC, and the corresponding crude 1*H*-imidazole-1-carboxylate (1.2 equiv) in THF (3.25 M) was added dropwise. After 2 h, the reaction was gradually warmed to 23 ºC and diluted with 2 M aqueous HCl until reaching a pH < 7. The reaction mixture was extracted three times with EtOAc. The combined organic layers were washed with brine, dried over Na_2SO_4, filtered, and concentrated under reduced pressure.

The crude product was purified by column chromatography to afford the corresponding acylated enone.

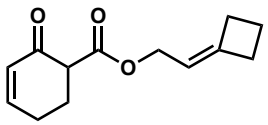

182

2-cyclobutylideneethyl 2-oxocyclohex-3-ene-1-carboxylate (182)

Prepared from 2-cyclohexen-1-one and 2-cyclobutylideneethan-1-ol[46] following General Procedure E. Purification by flash column chromatography (5–50% EtOAc/hexanes) afforded the title compound as a colorless oil (2.02 g, 9.19 mmol, 31.7% yield).

^{1}H NMR (400 MHz, $CDCl_3$): δ 7.00 (dt, *J* = 10.1, 3.7 Hz, 1H), 6.07 (dt, *J* = 10.2, 2.0 Hz, 1H), 5.27 (tp, *J* = 6.9, 2.2 Hz, 1H), 4.53 (d, *J* = 7.2 Hz, 2H), 3.45 – 3.36 (m, 1H), 2.80 – 2.65 (m, 4H), 2.56 – 2.31 (m, 3H), 2.28 – 2.15 (m, 1H), 1.98 (p, *J* = 8.0 Hz, 2H).

^{13}C NMR (100 MHz, $CDCl_3$): δ 194.1, 170.1, 150.7, 148.9, 129.3, 114.1, 62.3, 53.6, 31.2, 29.6, 25.8, 24.5, 17.1.

IR (Neat Film, NaCl): 2947, 1737, 1681, 1457, 1397, 1301, 1229, 1163, 1123 cm^{-1}.

HRMS (MM: FD+): *m/z* calc'd for $C_{13}H_{16}O_3$ $[M]^+$: 220.1099, found 220.1093.

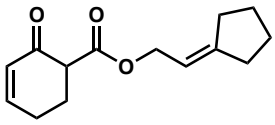

183

2-cyclopentylideneethyl 2-oxocyclohex-3-ene-1-carboxylate (183)

Prepared from 2-cyclohexen-1-one and 2-cyclopentylideneethan-1-ol[47] following General Procedure E. Purification by flash column chromatography (5–50% EtOAc/hexanes) afforded the title compound as a colorless oil (2.69 g, 11.46 mmol, 31.9% yield).

^{1}H NMR (400 MHz, $CDCl_3$): δ 6.99 (dt, *J* = 10.1, 3.8 Hz, 1H), 6.07 (dt, *J* = 10.2, 2.0 Hz, 1H), 5.50 – 5.40 (m, 1H), 4.64 (dt, *J* = 7.2, 1.1 Hz, 2H), 3.45 – 3.37 (m, 1H), 2.57 – 2.15 (m, 8H), 1.75 – 1.58 (m, 4H).

^{13}C NMR (100 MHz, $CDCl_3$): δ 194.1, 170.2, 151.2, 150.7, 129.3, 113.8, 63.8, 53.6, 34.0, 29.0, 26.4, 26.2, 25.8, 24.5.

IR (Neat Film, NaCl): 2946, 2869, 1782, 1681, 1455, 1387, 1304, 1224, 1156 cm^{-1}.

HRMS (MM: FD+): *m/z* calc'd for $C_{14}H_{18}O_3$ $[M]^+$: 234.1256, found 234.1255.

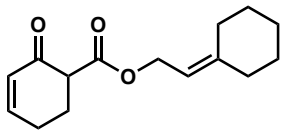

184

2-cyclohexylideneethyl 2-oxocyclohex-3-ene-1-carboxylate (184)

Prepared from 2-cyclohexen-1-one and 2-cyclohexylideneethan-1-ol[47] following General Procedure E, with the modification of 1.5 equiv of di(1*H*-imidazol-1-yl)methanone and 1.2 equiv of 2-cyclohexylideneethyl 1*H*-imidazole-1-carboxylate being used. Purification by flash column chromatography (5–30% EtOAc/hexanes) afforded the title compound as a colorless oil (535 mg, 2.15 mmol, 28% yield).

^{1}H NMR (400 MHz, $CDCl_3$): δ7.04 – 6.95 (m, 1H), 6.07 (dt, J = 10.1, 2.0 Hz, 1H), 5.29 (tt, J = 7.2, 1.2 Hz, 1H), 4.67 (d, J = 7.2 Hz, 2H), 3.45 – 3.36 (m, 1H), 2.56 – 2.30 (m, 3H), 2.27 – 2.15 (m, 3H), 2.14 – 2.08 (m, 2H), 1.60 – 1.48 (m, 6H).

^{13}C NMR (100 MHz, $CDCl_3$): δ 194.1, 170.2, 150.6, 147.5, 129.3, 115.0, 61.5, 53.6, 37.1, 29.2, 28.5, 27.9, 26.7, 25.8, 24.5.

IR (Neat Film, NaCl): 2930, 2852, 1735, 1683, 1447, 1388, 1298, 1169, 1122 cm^{-1}.

HRMS (MM: FD+): *m/z* calc'd for $C_{15}H_{20}O_3$ $[M]^+$: 248.1412, found 248.1418.

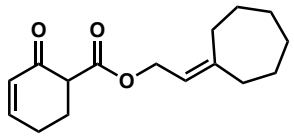

185

2-cycloheptylideneethyl 2-oxocyclohex-3-ene-1-carboxylate (185)

Prepared from 2-cyclohexen-1-one and 2-cycloheptylideneethan-1-ol[48] following General Procedure E. Purification by flash column chromatography (5–50% EtOAc/hexanes) afforded the title compound as a colorless oil (1.73 g, 5.43 mmol, 28.1% yield).

^{1}H NMR (400 MHz, $CDCl_3$): δ 6.99 (dt, *J* = 10.0, 3.8 Hz, 1H), 6.07 (dt, *J* = 10.1, 2.0 Hz, 1H), 5.34 (tt, *J* = 7.1, 1.3 Hz, 1H), 4.66 (d, *J* = 7.0 Hz, 2H), 3.45 – 3.37 (m, 1H), 2.57 – 2.15 (m, 8H), 1.63 – 1.44 (m, 8H).

^{13}C NMR (100 MHz, $CDCl_3$): δ 194.1, 170.2, 150.6, 148.8, 129.3, 118.5, 62.1, 53.6, 37.8, 30.2, 29.9, 29.1, 28.8, 27.3, 25.8, 24.5.

IR (Neat Film, NaCl): 2923, 2853, 1736, 1681, 1442, 1388, 1300, 1231, 1155, 1122, 1076 cm^{-1}.

HRMS (MM: FD+): *m/z* calc'd for $C_{26}H_{22}O_3$ $[M]^+$: 262.1569, found 262.1577.

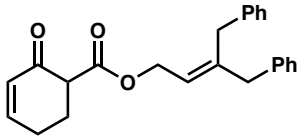

82

3-benzyl-4-phenylbut-2-en-1-yl 2-oxocyclohex-3-ene-1-carboxylate (82)

Prepared from 2-cyclohexen-1-one and 3-benzyl-4-phenylbut-2-en-1-ol [49] following General Procedure E. Purification by flash column chromatography (5–50% EtOAc/hexanes) afforded the title compound as a colorless oil (1.96 g, 5.43 mmol, 21.3% yield).

^{1}H NMR (400 MHz, $CDCl_3$): δ 7.33 – 7.25 (m, 4H), 7.24 – 7.18 (m, 2H), 7.17 – 7.07 (m, 4H), 7.03 – 6.97 (m, 1H), 6.08 (dt, *J* = 10.1, 2.0 Hz, 1H), 5.59 (tt, *J* = 7.1, 1.1 Hz, 1H), 4.86 – 4.80 (m, 2H), 3.48 – 3.35 (m, 3H), 3.26 (s, 2H), 2.55 – 2.32 (m, 3H), 2.30 – 2.15 (m, 1H).

^{13}C NMR (100 MHz, $CDCl_3$): δ 193.9, 170.1, 150.7, 144.4, 139.0, 138.9, 129.3, 129.3, 128.9, 128.7, 128.5, 126.5, 126.4, 121.9, 62.0, 53.6, 42.9, 35.9, 25.8, 24.5.

IR (Neat Film, NaCl): 3026, 2927, 1738, 1681, 1493, 1388, 1304, 1230, 1157, 1123 cm^{-1}.

HRMS (MM: FD+): *m/z* calc'd for $C_{24}H_{24}O_3$ $[M]^+$: 360.1725, found 360.17302.

Protonated Enone Byproducts

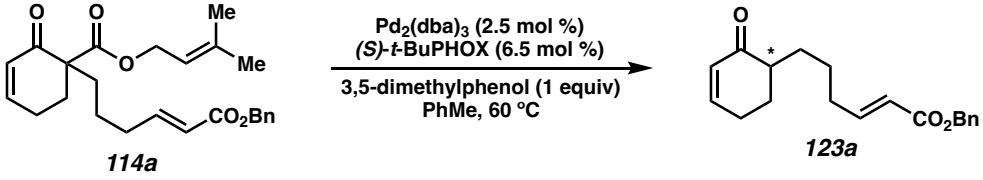

114a ***123a***

benzyl (*R*,*E*)-6-(2-oxocyclohex-3-en-1-yl)hex-2-enoate (123a)

In a nitrogen filled glovebox, an oven-dried 20 mL vial was charged with a stir bar, $Pd_2(dba)_3$ (0.46 mg, 0.50 μmol, 2.5 mol %), *(S)-t*-BuPHOX (0.50 mg, 1.3 μmol, 6.5 mol %), and toluene (0.5 mL). The catalyst solution was stirred at 23 ºC for 20 min. A solution of substrate **114a** (8.2 mg, 0.020 mmol, 1 equiv) and 3,5-dimethylphenol (2.4 mg, 0.020 mmol, 1 equiv) in toluene (0.5 mL) was added to the vial. The resultant solution was then heated to 60 ºC for 14 h. The solution was then cooled to 23 ºC and concentrated under reduced pressure. NMR analysis of the crude reaction mixture affords an NMR yield of 100% (with respect to 1,3,5-trimethoxybenzene as an internal standard). The sample was purified by preparatory TLC (25% EtOAc/hexanes) to afford **123a** (71% ee).

^{1}H NMR (400 MHz, $CDCl_3$): δ 7.39 – 7.29 (m, 5H), 7.01 (dt, *J* = 15.7, 6.9 Hz, 1H), 6.92 (dddd, *J* = 10.1, 4.5, 3.5, 0.9 Hz, 1H), 5.98 (ddd, *J* = 10.1, 2.3, 1.7 Hz, 1H), 5.88 (dt, *J* = 15.6, 1.6 Hz, 1H), 5.17 (s, 2H), 2.46 – 2.34 (m, 2H), 2.32 – 2.20 (m, 3H), 2.09 (dqd, *J* = 13.3, 4.8, 1.0 Hz, 1H), 1.89 – 1.80 (m, 1H), 1.75 (dddd, *J* = 13.3, 11.0, 8.4, 5.8 Hz, 1H), 1.55 – 1.35 (m, 3H).

^{13}C NMR (100 MHz, $CDCl_3$): δ 201.6, 166.6, 149.7, 149.6, 136.3, 129.7, 128.7, 128.3, 128.3, 121.4, 66.2, 46.5, 32.5, 29.0, 28.0, 25.6, 25.3.

IR (Neat Film, NaCl): 2921, 1712, 1673, 1257 cm^{-1}.

HRMS (MM: FD+): *m/z* calc'd for $C_{19}H_{22}O_3$ $[M]^+$: 298.1569, found 298.1565.

Optical Rotation: $[\alpha]_D^{21}$ +3.5 (c 0.20, $CHCl_3$).

SFC conditions: 40% IPA, 2.5 mL/min, Chiralpak IC column, λ = 210 nm, t_R (min): minor = 3.81, major = 4.34.

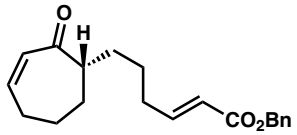

123d

benzyl (*R*,*E*)-7-(2-oxocyclohex-3-en-1-yl)hept-2-enoate (123d)

Isolated as a byproduct from the reaction of **114d** to **115d** as a colorless oil (10.4 mg, 0.0332 mmol, 17% yield, 67% ee).

^{1}H NMR (400 MHz, $CDCl_3$): δ 7.32 – 7.22 (m, 5H), 6.93 (dt, *J* = 15.7, 6.9 Hz, 1H), 6.53 (ddd, *J* = 12.0, 6.7, 4.0 Hz, 1H), 5.94 (ddd, *J* = 11.9, 2.5, 0.9 Hz, 1H), 5.80 (dt, *J* = 15.6, 1.6 Hz, 1H), 5.10 (s, 3H), 2.59 – 2.49 (m, 1H), 2.42 – 2.25 (m, 2H), 2.14 (tdd, *J* = 7.7, 4.8, 1.4 Hz, 2H), 1.90 – 1.48 (m, 5H), 1.44 – 1.29 (m, 4H).

^{13}C NMR (100 MHz, $CDCl_3$): δ 205.7, 166.5, 149.6, 146.0, 136.2, 132.8, 128.6, 128.2, 128.2, 121.2, 66.0, 51.7, 32.4, 31.1, 29.9, 29.5, 25.8, 25.4.

IR (Neat Film, NaCl): 2917, 1719, 1671, 1266, 1165 cm^{-1}.

HRMS (MM: FD+): *m/z* calc'd for $C_{20}H_{24}O_3$ $[M]^+$: 312.1720, found 312.1734.

Optical Rotation: $[\alpha]_D^{21}$ –0.6 (c 1.00, $CHCl_3$).

SFC conditions: 15% IPA, 2.5 mL/min, Chiralpak AD-H column, λ = 210 nm, t_R (min): minor = 8.23, major = 7.63.

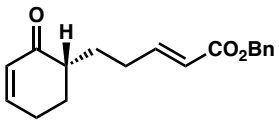

123e

benzyl (*S*,*E*)-5-(2-oxocyclohex-3-en-1-yl)pent-2-enoate (123e)

Isolated as the major byproduct from the reaction of **114e** to **115e**. Purification by flash column chromatography (0–45% EtOAc/hexanes) afforded the title compound as a colorless oil (46.1 mg, 0.16 mmol, 81% yield, 47% ee).

^{1}H NMR (400 MHz, $CDCl_3$): δ 7.42 – 7.28 (m, 5H), 7.01 (dt, *J* = 15.6, 6.9 Hz, 1H), 6.92 (dddd, *J* = 10.0, 4.4, 3.6, 1.0 Hz, 1H), 5.98 (dt, *J* = 10.0, 2.0 Hz, 1H), 5.90 (dt, *J* = 15.7, 1.6 Hz, 1H), 5.17 (s, 2H), 2.44 – 2.24 (m, 5H), 2.15 – 1.96 (m, 2H), 1.82 – 1.69 (m, 1H), 1.62 – 1.44 (m, 1H).

^{13}C NMR (100 MHz, $CDCl_3$): δ 201.3, 166.5, 149.6, 149.4, 136.2, 129.7, 128.7, 128.3, 128.3, 121.6, 66.2, 45.9, 29.7, 28.2, 27.8, 25.4.

IR (Neat Film, NaCl): 3032, 2932, 1719, 1675, 1455, 1386, 1265, 1171 cm^{-1}.

HRMS (MM: FD+): *m/z* calc'd for $C_{18}H_{20}O_3$ $[M]^+$: 284.1412, found 284.1407.

Optical Rotation: $[\alpha]_D^{21}$ +11.8 (c 1.00, $CHCl_3$).

SFC conditions: 10% IPA, 2.5 mL/min, Chiralpak AS-H column, λ = 210 nm, t_R (min): minor = 5.69, major = 6.54.

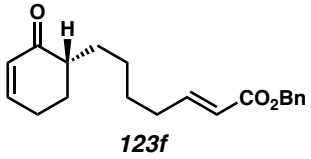

123f

benzyl (*R*,*E*)-7-(2-oxocyclohex-3-en-1-yl)hept-2-enoate (123f)

Isolated as a byproduct from the reaction of **114f** to **115f** as a colorless oil (28.1 mg, 0.090 mmol, 45% yield, 51% ee). Absolute stereochemistry proposed based on VCD analysis (vide infra).

^{1}H NMR (400 MHz, $CDCl_3$): δ 7.42 – 7.29 (m, 5H), 7.00 (dt, *J* = 15.6, 6.9 Hz, 1H), 6.90 (dddd, *J* = 10.0, 4.5, 3.5, 0.9 Hz, 1H), 5.97 (dt, *J* = 10.1, 2.0 Hz, 1H), 5.86 (dt, *J* = 15.6, 1.6 Hz, 1H), 5.17 (s, 2H), 2.42 – 2.33 (m, 2H), 2.29 – 2.18 (m, 3H), 2.08 (dqd, *J* = 13.3, 4.8, 0.9 Hz, 1H), 1.88 – 1.80 (m, 1H), 1.78 – 1.69 (m, 1H), 1.52 – 1.29 (m, 5H).

^{13}C NMR (100 MHz, $CDCl_3$): δ 201.8, 166.6, 150.0, 149.5, 136.3, 129.6, 128.6, 128.3, 128.3, 121.2, 66.1, 46.6, 32.2, 29.0, 28.2, 27.9, 26.6, 25.2.

IR (Neat Film, NaCl): 2927, 2859, 1716, 1675, 1652, 1262, 1172 cm^{-1}

HRMS (MM: FD+): *m/z* calc'd for $C_{20}H_{24}O_3$ $[M]^+$: 312.1725, found 312.1737.

Optical Rotation: $[\alpha]_D^{21}$ +4.1 (c 1.00, $CHCl_3$).

SFC conditions: 15% IPA, 2.5 mL/min, Chiralpak AD-H column, λ = 210 nm, t_R (min): minor = 7.77, major = 8.44.

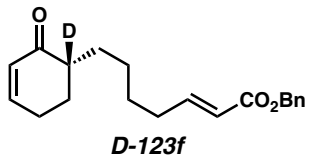

D-123f

benzyl (*R*,*E*)-7-(2-oxocyclohex-3-en-1-yl-1-*d*)hept-2-enoate (*D*-123f)

Isolated as a byproduct from the reaction of ***D*-114f** to ***D*-115f** as a colorless oil (14.9 mg, 0.0475 mmol, 24% yield, 55% ee).

^{1}H NMR (400 MHz, $CDCl_3$): δ 7.39 – 7.29 (m, 5H), 7.00 (dt, *J* = 15.6, 7.0 Hz, 1H), 6.91 (dddd, *J* = 10.1, 4.5, 3.5, 0.9 Hz, 1H), 5.97 (dddd, *J* = 10.0, 2.3, 1.6, 0.6 Hz, 1H), 5.86 (dt, *J* = 15.6, 1.6 Hz, 1H), 5.17 (s, 2H), 2.44 – 2.33 (m, 2H), 2.28 – 2.18 (m, 2.5H), 2.09 (ddt, *J* = 13.3, 5.8, 4.5 Hz, 1H), 1.87 – 1.70 (m, 2H), 1.53 – 1.27 (m, 5H).

^{13}C NMR (100 MHz, $CDCl_3$): δ 201.9, 166.6, 150.0, 149.6, 129.7, 129.7, 128.7, 128.3, 128.3, 121.2, 66.2, 46.6, 32.3, 29.0, 28.9, 28.2, 27.9, 27.8, 26.7, 26.6, 25.3, 25.2.

^{2}H NMR (61 MHz, $CHCl_3$): δ 2.25.

IR (Neat Film, NaCl): 2929, 2857, 1714, 1697, 1267, 1174 cm^{-1}.

HRMS (MM: FD+): *m/z* calc'd for $C_{20}H_{23}DO_3$ $[M+H]^+$: 313.1783, found 313.1788.

Optical Rotation: $[\alpha]_D^{21}$ +5.8 (c 0.50, $CHCl_3$).

SFC conditions: 15% IPA, 2.5 mL/min, Chiralpak AD-H column, λ = 210 nm, t_R (min): minor = 7.96, major = 8.67.

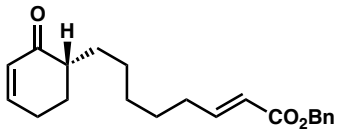

123g

benzyl (*R*,*E*)-8-(2-oxocyclohex-3-en-1-yl)oct-2-enoate (123g)

Isolated as the major product from the reaction of **114g** to **115g** as a colorless oil (50.5 mg, 0.155 mmol, 77% yield, 56% ee).

^{1}H NMR (400 MHz, $CDCl_3$): δ 7.40 – 7.29 (m, 5H), 7.01 (dt, *J* = 15.6, 6.9 Hz, 1H), 6.91 (dddd, *J* = 10.0, 4.5, 3.5, 0.9 Hz, 1H), 5.97 (dt, *J* = 10.0, 2.0 Hz, 1H), 5.86 (dt, *J* = 15.6, 1.6 Hz, 1H), 5.17 (s, 2H), 2.45 – 2.33 (m, 2H), 2.30 – 2.16 (m, 3H), 2.09 (dqd, *J* = 14.5, 5.0, 0.9 Hz, 1H), 1.86 – 1.70 (m, 2H), 1.51 – 1.42 (m, 2H), 1.41 – 1.28 (m, 5H).

^{13}C NMR (100 MHz, $CDCl_3$): δ 202.0, 166.7, 150.2, 149.5, 136.3, 129.7, 128.7, 128.3, 128.3, 121.1, 66.1, 46.6, 32.3, 29.3, 29.1, 28.0, 27.9, 26.8, 25.2.

IR (Neat Film, NaCl): 2927, 2859, 1718, 1677, 1555, 1450, 1257, 1165 cm^{-1}

HRMS (MM: FD+): *m/z* calc'd for $C_{21}H_{26}O_3$ $[M]^+$: 326.1877, found 326.1891.

Optical Rotation: $[\alpha]_D^{21}$ +7.0 (c 1.00, $CHCl_3$).

SFC conditions: 15% IPA, 2.5 mL/min, Chiralpak AD-H column, λ = 210 nm, t_R (min): minor = 9.70, major = 10.46.

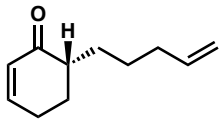

123h

6-(pent-4-en-1-yl)cyclohex-2-en-1-one (123h)

Isolated as the major product from the reaction of **114h** to **115h** as a colorless oil. Purification by flash column chromatography (0–15% EtOAc/hexanes) afforded the title compound as a colorless oil (11.0 mg, 0.067 mmol, 33% yield, 58% ee).

^{1}H NMR (400 MHz, $CDCl_3$): δ 6.91 (dddd, *J* = 10.1, 4.4, 3.5, 0.9 Hz, 1H), 5.97 (dt, *J* = 10.0, 2.1 Hz, 1H), 5.81 (ddt, *J* = 16.9, 10.2, 6.6 Hz, 1H), 5.01 (dq, *J* = 17.2, 1.8 Hz, 1H), 4.94 (dd, *J* = 10.1, 1.3 Hz, 1H), 2.45 – 2.24 (m, 3H), 2.16 – 1.98 (m, 2=3H), 1.95 – 1.69 (m, 2H), 1.55 – 1.31 (m, 3H).

^{13}C NMR (100 MHz, $CDCl_3$): δ 202.0, 149.5, 138.8, 129.7, 114.7, 46.6, 34.0, 28.8, 27.9, 26.4, 25.2.

IR (Neat Film, NaCl): 2925, 2859, 1677, 1639, 1456, 1387, 1215, 912 cm^{-1}.

HRMS (MM: FD+): *m/z* calc'd for $C_{11}H_{16}O$ $[M]^+$: 164.1201, found 164.1201.

Optical Rotation: $[\alpha]_D^{21}$ –111.5 (c 1.00, $CHCl_3$).

SFC conditions: 3% IPA, 2.5 mL/min, Chiralpak AD-H column, λ = 210 nm, t_R (min): minor = 4.41, major = 4.11.

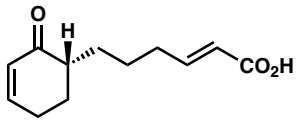

123i

(*E*)-6-(2-oxocyclohex-3-en-1-yl)hex-2-enoic acid (123i)

Isolated as the major product from the reaction of **114i** to **115i** as a colorless oil. Purification by flash column chromatography (35% EtOAc/hexanes with 3% AcOH) afforded the title compound as a white solid (33.2 mg, 0.16 mmol, 80% yield, 9% ee).

^{1}H NMR (400 MHz, $CDCl_3$): δ 7.07 (dtd, *J* = 15.5, 7.0, 1.5 Hz, 1H), 6.97 – 6.87 (m, 1H), 5.98 (dq, *J* = 10.1, 1.9 Hz, 1H), 5.84 (dt, *J* = 15.6, 1.6 Hz, 1H), 2.49 – 2.35 (m, 2H), 2.34 – 2.19 (m, 3H), 2.16 – 2.04 (m, 1H), 1.92 – 1.81 (m, 1H), 1.81 – 1.70 (m, 1H), 1.63 – 1.48 (m, 2H), 1.48 – 1.35 (m, 1H).

^{13}C NMR (100 MHz, $CDCl_3$): δ 201.7, 171.5, 151.9, 149.7, 129.7, 120.9, 46.5, 32.5, 29.0, 28.0, 25.5.

IR (Neat Film, NaCl): 2928, 2857, 1731, 1454, 1155 cm^{-1}

HRMS (MM: FD+): *m/z* calc'd for $C_{12}H_{17}O_3$ $[M]^+$: 209.1178, found 209.1168.

Optical Rotation: $[\alpha]_D^{21}$ 2.2 (c 1.00, $CHCl_3$).

SFC conditions: 30% IPA, 2.5 mL/min, Chiralpak IC column, l = 210 nm, t_R (min): minor = 3.30, major = 4.02

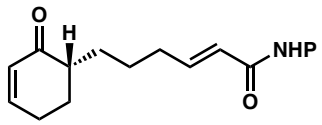

123m

1,3-dioxoisoindolin-2-yl (*E*)-6-(2-oxocyclohex-3-en-1-yl)hex-2-enoate (123m)

Isolated as a byproduct product from the reaction of **114m** to **115m** as a colorless oil. Purification by flash column chromatography (0–35% EtOAc/hexanes) afforded the title compound as a white solid (7.7 mg, 0.022 mmol, 11% yield).

^{1}H NMR (400 MHz, $CDCl_3$): δ 7.89 (dd, *J* = 5.5, 3.1 Hz, 2H), 7.79 (dd, *J* = 5.5, 3.1 Hz, 2H), 7.32 (dt, *J* = 15.8, 6.9 Hz, 1H), 6.93 (dddd, *J* = 10.1, 4.5, 3.5, 1.0 Hz, 1H), 6.10 (dt, *J* = 15.8, 1.6 Hz, 1H), 5.99 (ddd, *J* = 10.0, 2.3, 1.7 Hz, 1H), 2.50 – 2.25 (m, 5H), 2.12 (m, 1H), 1.95 – 1.84 (m, 1H), 1.78 (m, 1H), 1.59 (m, 2H), 1.45 (m, 1H).

^{13}C NMR (100 MHz, $CDCl_3$): δ 201.5, 162.5, 162.2, 155.6, 149.7, 134.9, 129.7, 129.1, 124.1, 115.9, 46.5, 33.2, 29.1, 28.1, 25.4, 25.3.

IR (Neat Film, NaCl): 2931, 1770, 1745, 1673, 1466, 1360, 1186 cm^{-1}.

HRMS (MM: FD+): *m/z* calc'd for $C_{20}H_{19}NO_5$ $[M]^+$: 353.1263, found 353.1242.

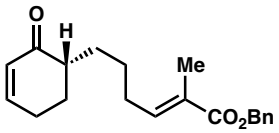

123r

benzyl (*R*,*E*)-2-methyl-6-(2-oxocyclohex-3-en-1-yl)hex-2-enoate (123r)

Isolated as a byproduct from the reaction of **114r** to **115r** as a colorless oil (23.2 mg, 0.0743 mmol, 37% yield, 59% ee).

^{1}H NMR (400 MHz, $CDCl_3$): δ 7.40 – 7.29 (m, 5H), 6.91 (dddd, *J* = 10.1, 4.5, 3.5, 0.9 Hz, 1H), 6.81 (td, *J* = 7.5, 1.5 Hz, 1H), 5.97 (dt, *J* = 10.0, 1.9 Hz, 1H), 5.18 (s, 2H), 2.45 – 2.34 (m, 2H), 2.32 – 2.17 (m, 3H), 2.09 (dqd, *J* = 13.4, 4.9, 1.0 Hz, 1H), 1.90 – 1.81 (m, 4H), 1.80 – 1.71 (m, 1H), 1.55 – 1.36 (m, 3H).

^{13}C NMR (100 MHz, $CDCl_3$): δ 201.7, 168.1, 149.6, 142.7, 136.6, 129.7, 128.6, 128.2, 128.1, 127.9, 66.3, 46.6, 29.2, 29.0, 28.0, 26.2, 25.2, 12.6.

IR (Neat Film, NaCl): 3033, 2932, 2861, 1710, 1677, 1256 cm^{-1}.

HRMS (MM: FD+): *m/z* calc'd for $C_{20}H_{24}O_3$ $[M]^+$: 312.1725, found 312.1729.

Optical Rotation: $[\alpha]_D^{21}$ +8.6 (c 1.00, $CHCl_3$).

SFC conditions: 15% IPA, 2.5 mL/min, Chiralpak AD-H column, λ = 210 nm, t_R (min): minor = 5.89, major = 6.22.

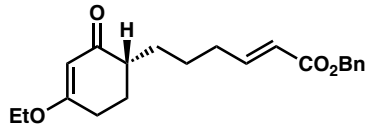

123t

benzyl (*E*)-6-(4-ethoxy-2-oxocyclohex-3-en-1-yl)hex-2-enoate (123t)

Isolated as a byproduct from the reaction of **114t** to **115t** as a colorless oil (5.2 mg, 0.015 mmol, 8% yield, 45% ee).

^{1}H NMR (400 MHz, $CDCl_3$): δ 7.41 – 7.27 (m, 5H), 7.01 (dt, *J* = 15.6, 6.9 Hz, 1H), 5.87 (dt, *J* = 15.6, 1.6 Hz, 1H), 5.31 (s, 1H), 5.17 (s, 2H), 3.88 (qd, *J* = 7.1, 1.4 Hz, 2H), 2.41 (dd, *J* = 7.2, 5.3 Hz, 2H), 2.29 – 2.13 (m, 3H), 2.06 (dq, *J* = 13.2, 5.2 Hz, 1H), 1.86 (ddt, *J* = 13.3, 11.1, 5.2 Hz, 1H), 1.78 – 1.64 (m, 1H), 1.59 – 1.37 (m, 3H), 1.35 (t, *J* = 7.0 Hz, 3H).

^{13}C NMR (100 MHz, $CDCl_3$): δ 201.4, 176.9, 166.6, 149.7, 136.3, 128.7, 128.3, 128.3, 121.3, 102.3, 66.1, 64.4, 45.1, 32.5, 29.3, 28.2, 26.4, 25.7, 14.3.

IR (Neat Film, NaCl): 2919, 1718, 1648, 1605, 1456, 1377, 1260, 1190, 732 cm^{-1}.

HRMS (MM: FD+): *m/z* calc'd for $C_{21}H_{26}O_4$ $[M]^+$: 342.1828, found 342.1826.

Optical Rotation: $[\alpha]_D^{21}$ –5.5 (c 0.34, $CHCl_3$).

SFC conditions: 15% IPA, 2.5 mL/min, Chiralpak AD-H column, λ = 210 nm, t_R (min): minor = 10.17, major = 11.69.

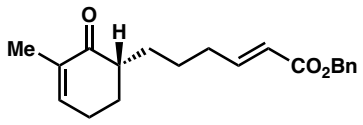

123u

benzyl (*E*)-6-(3-methyl-2-oxocyclohex-3-en-1-yl)hex-2-enoate (123u)

Isolated as a byproduct from the reaction of **114u** to **115u** as a colorless oil (23.6 mg, 0.075 mmol, 37% yield, 46% ee).

^{1}H NMR (400 MHz, $CDCl_3$): δ 7.41 – 7.28 (m, 5H), 7.01 (dt, *J* = 15.5, 6.9 Hz, 1H), 6.71 – 6.63 (m, 1H), 5.88 (dt, *J* = 15.6, 1.6 Hz, 1H), 5.17 (s, 2H), 2.33 (ddq, *J* = 6.3, 4.8, 2.0 Hz, 2H), 2.29 – 2.19 (m, 3H), 2.10 – 2.01 (m, 1H), 1.88 – 1.77 (m, 1H), 1.76 (q, *J* = 1.7 Hz, 3H), 1.74 – 1.69 (m, 1H), 1.56 – 1.34 (m, 3H).

^{13}C NMR (100 MHz, $CDCl_3$): δ 201.9, 166.6, 149.8, 144.5, 136.3, 135.3, 128.68, 128.3, 128.3, 121.3, 66.2, 46.6, 32.5, 29.2, 28.4, 25.7, 25.2, 16.3.

IR (Neat Film, NaCl): 2925, 1718, 1670, 1455, 1262, 1172, 1013 cm^{-1}.

HRMS (MM: FD+): *m/z* calc'd for $C_{20}H_{24}O_3$ $[M]^+$: 312.1725, found 312.1721.

Optical Rotation: $[\alpha]_D^{21}$ –14.7 (c 0.35, $CHCl_3$).

SFC conditions: 10% IPA, 2.5 mL/min, Chiralpak OJ-H column, λ = 210 nm, t_R (min): minor = 7.18, major = 7.62.

Product Derivatizations

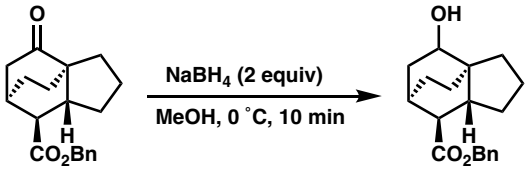

115a ***142***

benzyl (3a*R*,6*R*,7*S*,7a*R*)-4-hydroxyoctahydro-3a,6-ethanoindene-7-carboxylate (142)

To a solution of ketone **115a** (0.125 mmol, 1 equiv) in methanol (4.4 mL) was added $NaBH_4$ (0.25 mmol, 2 equiv) at 0 ºC. The reaction was allowed to stir for 10 min at 0 ºC and then was diluted with water. The aqueous layer was extracted with dichloromethane (3x), and the combined organic layers were dried over Na_2SO_4. Concentration under reduced pressure afforded the title compound as a colorless oil (37.6 mg, 0.125 mmol, 99% yield).

^{1}H NMR (400 MHz, $CDCl_3$): δ 7.42 – 7.30 (m, 5H), 5.19 – 5.05 (m, 2H), 3.76 (dd, *J* = 8.9, 5.3 Hz, 0.4H, minor), 3.69 (dt, *J* = 8.9, 1.5 Hz, 0.6H, major), 2.35 – 2.24 (m, 1H), 2.15 – 1.95 (m, 2H), 1.95 – 1.83 (m, br, 1H), 1.83 – 1.56 (m, 6H), 1.53 – 1.23 (m, 5H), 1.15 – 1.01 (m, 1H).

^{13}C NMR (100 MHz, $CDCl_3$): δ 175.8, 175.6, 136.3, 128.6, 128.2, 128.2, 128.0, 128.0, 75.6, 70.3, 66.3, 66.3, 49.21, 48.1, 44.5, 44.2, 43.2, 36.8, 35.0, 34.9, 34.0, 30.5, 30.3, 30.1, 29.6, 29.0, 26.7, 26.3, 22.8, 22.8, 20.3.

IR (Neat Film, NaCl): 3438, 3032, 2942, 2865, 1730, 1455, 1162 cm^{-1}

HRMS (MM: FD+): *m/z* calc'd for $C_{19}H_{24}O_3$ $[M]^+$: 300.1725, found 300.1730.

Optical Rotation: $[\alpha]_D^{21}$ –31.1 (c 1.00, $CHCl_3$).

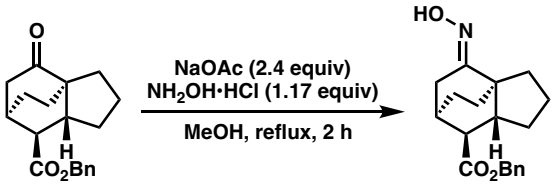

115a ***188***

benzyl (3a*R*,6*R*,7*S*,7a*R*,*E*)-4-(hydroxyimino)octahydro-3a,6-ethanoindene-7-carboxylate (188)

To a stirred solution of ketone **115a** (0.125 mmol, 1 equiv) in methanol (1.25 mL) was added NaOAc (0.3 mmol, 2.4 equiv), NH_2OH•HCl (0.15 mmol. 1.17 equiv), and water (0.05 mL). The reaction was brought to reflux for 2 h and was subsequently cooled to 23 ºC and concentrated under reduced pressure. The crude mixture was then diluted with water and extracted with EtOAc (3x), washed with a saturated aqueous solution of $NaHCO_3$ and brine, dried with Na_2SO_4, and concentrated under reduced pressure. The material was used in the next step without further purification assuming quantitative yield.

^{1}H NMR (400 MHz, $CDCl_3$): δ 7.42 – 7.28 (m, 5H), 5.20 – 5.06 (m, 2H), 2.52 – 2.46 (m, 2H), 2.43 – 2.39 (m, 1H), 2.39 – 2.36 (m, 1H), 2.15 (dtd, *J* = 10.2, 8.2, 1.8 Hz, 1H), 2.07 (ddt, *J* = 11.9, 8.3, 4.1 Hz, 1H), 1.98 (ddd, *J* = 13.0, 11.0, 8.0 Hz, 1H), 1.82 – 1.71 (m, 3H), 1.67 (ddd, *J* = 10.9, 3.6, 1.8 Hz, 1H), 1.48 (dddd, *J* = 12.5, 7.8, 6.5, 3.7 Hz, 2H), 1.36 (dddd, *J* = 23.6, 11.1, 8.8, 2.6 Hz, 2H).

^{13}C NMR (100 MHz, $CDCl_3$): δ 174.8, 165.4, 136.2, 128.7, 128.4, 128.2, 66.5, 48.2, 45.7, 44.4, 30.6, 29.2, 28.9, 28.1, 27.2, 25.5, 22.6.

IR (Neat Film, NaCl): 2945, 1731, 1161 cm^{-1}.

HRMS (MM: FD+): *m/z* calc'd for $C_{19}H_{23}NO_3$ $[M]^+$: 313.1678, found 313.1676.

Optical Rotation: $[\alpha]_D^{21}$ –22.0 (c 0.37, $CHCl_3$).

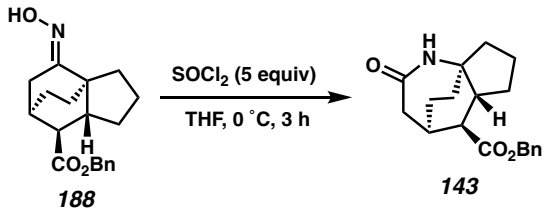

188 ***143***

benzyl (4*R*,5*S*,5a*R*,8a*R*)-2-oxooctahydro-1*H*-4,8a-ethanocyclopenta[*b*]azepine-5-carboxylate (143)

To a solution of **188** (0.125 mmol, 1 equiv) in THF (1.25 mL) at 0 ºC was added a solution of $SOCl_2$ (0.625 mmol, 5 equiv) in THF (0.23 mL). The reaction was stirred for 3 h at 0 ºC, followed by dilution with water. Aqueous solution NH_4OH was added to the reaction mixture until neutral, and the aqueous layer was extracted with dichloromethane (3x). The combined organic layers were washed with water and brine, dried over Na_2SO_4, and concentrated under reduced pressure. Purification by flash column chromatography (35% EtOAc/hexanes) afforded the title compound as a colorless oil (22 mg, 0.167 mmol, 56% yield over two steps).

^{1}H NMR (400 MHz, $CDCl_3$): δ 7.41 – 7.27 (m, 5H), 6.67 (s, 1H, br), 5.15 (q, *J* = 12.3 Hz, 2H), 2.73 (dt, *J* = 18.1, 1.6 Hz, 1H), 2.62 (tdd, *J* = 9.9, 8.0, 1.4 Hz, 1H), 2.48 (dd, *J* = 18.4, 6.9 Hz, 1H), 2.40 – 2.32 (m, 2H), 2.29 – 2.16 (m, 1H), 1.95 (dtd, *J* = 12.7, 8.7, 2.2 Hz, 1H), 1.82 – 1.62 (m, 7H), 1.62 – 1.52 (m, 1H), 1.44 – 1.30 (m, 1H).

^{13}C NMR (100 MHz, $CDCl_3$): δ 174.6, 174.2, 135.9, 128.8, 128.4, 128.3, 66.7, 59.9, 48.8, 48.5, 39.2, 33.3, 31.1, 29.8, 25.1, 23.3.

IR (Neat Film, NaCl): 3182, 3055, 2934, 1727, 1648, 1456, 1398, 1167 cm^{-1}.

HRMS (MM: FD+): *m/z* calc'd for $C_{19}H_{23}NO_3$ $[M]^+$: 313.1678, found 313.1678.

Optical Rotation: $[\alpha]_D^{21}$ –5.5 (c 0.89, $CHCl_3$).

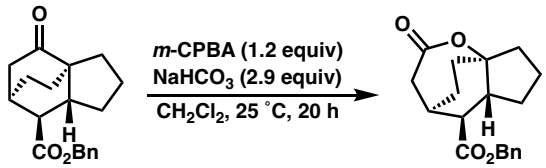

115a ***144***

benzyl (4*R*,5*S*,5a*R*,8a*R*)-2-oxooctahydro-4,8a-ethanocyclopenta[*b*]oxepine-5-carboxylate (144)

To a solution ketone **115a** (37 mg, 0.13 mmol, 1 equiv) in CH_2Cl_2 (1.25 mL, 0.1 M) at 0°C was added $NaHCO_3$ (30.8 mg, 0.37 mmol, 2.9 equiv). Subsequently, *m*-CPBA (31 mg, 0.15 mmol, 1.2 equiv) was added and the reaction was allowed to warm to 25 °C. Upon complete consumption of starting material (as determined by TLC), the reaction mixture was diluted with a saturated solution of $Na_2S_2O_3$ and extracted with Et_2O (3x). The combined organic layers were washed with a saturated solution of $NaHCO_3$ followed by brine, dried over Na_2SO_4, and volatiles were removed in vacuo. Purification by preparatory thin layer chromatography (30% EtOAc/hexanes) afforded the title compound as a clear oil (16 mg, 0.05 mmol, 41% yield).

^{1}H NMR (400 MHz, $CDCl_3$): δ 7.43 – 7.29 (m, 5H), 5.22 – 5.10 (m, 2H), 2.97 (ddd, *J* = 19.0, 2.5, 1.4 Hz, 1H), 2.83 – 2.61 (m, 2H), 2.41 – 2.32 (m, 2H), 2.28 – 2.09 (m, 3H), 2.05 – 1.93 (m, 1H), 1.81 – 1.56 (m, 5H), 1.40 – 1.26 (m, 1H).

^{13}C NMR (100 MHz, $CDCl_3$): δ 173.9, 172.9, 135.7, 128.8, 128.6, 128.3, 88.4, 66.9, 47.8, 46.5, 39.6, 39.1, 32.8, 30.4, 29.7, 24.9, 22.7.

IR (Neat Film, NaCl): 2943, 2873, 1722, 1255, 1189, 1167 cm^{-1}.

HRMS (MM: FD+): *m/z* calc'd for $C_{19}H_{22}O_4$ $[M]^+$: 314.1518, found 314.1521.

Optical Rotation: $[\alpha]_D^{21}$ –15.8 (c 1.00, $CHCl_3$).

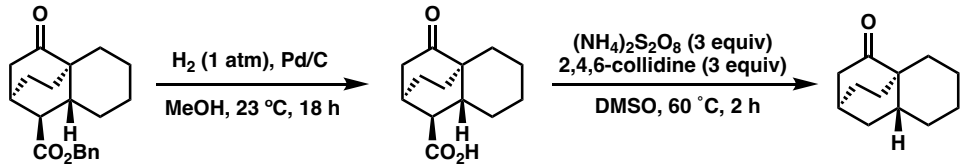

115f ***149***

(2*S*,4a*R*,8a*R*)-octahydro-2*H*-2,4a-ethanonaphthalen-9-one (149)

A vial containing ketone **115f** (0.72 mmol, 1 equiv) and Pd/C (10 wt. % with 67% H_2O, 0.072 mmol, 0.1 equiv) was evacuated and backfilled with H_2. Methanol (1.06 mL) was subsequently added, and the reaction was stirred at 23 ºC overnight. The crude reaction mixture was filtered through a silica plug and concentrated under reduced pressure to afford the corresponding acid as a white solid, which was used without further purification.

To a solution of the crude acid (0.62 mmol, 1 equiv) in DMSO (1.24 mL) was added $(NH_4)_2S_2O_8$ (1.86 mmol, 3 equiv) and 2,4,6-collidine (1.86 mmol, 3 equiv). The mixture was purged with N_2 for 5 min and was subsequently sealed and heated to 60 ºC for 2 h with stirring. The reaction mixture was diluted with dichloromethane, washed with brine (1x), and the aqueous layer was extracted with dichloromethane (3x). The combined organic layers were washed with brine (3x), dried over Na_2SO_4, and concentrated under reduced pressure. Purification by flash column chromatography (15% EtOAc/hexanes) afforded the title compound as a white solid (30.2 mg, 0.167 mmol, 27% yield).

^{1}H NMR (400 MHz, $CDCl_3$): δ 2.33 – 2.21 (m, 3H), 2.13 – 2.07 (m, 1H), 1.93 (dddd, *J* = 13.3, 10.6, 3.8, 2.8 Hz, 1H), 1.75 – 1.58 (m, 6H), 1.53 (dd, *J* = 13.6, 4.0 Hz, 1H), 1.47 – 1.38 (m, 2H), 1.38 – 1.28 (m, 1H), 1.27 – 1.17 (m, 1H), 1.17 – 1.05 (m, 2H).

^{13}C NMR (100 MHz, $CDCl_3$): δ 218.6, 44.9, 43.9, 34.5, 34.1, 30.6, 29.0, 27.7, 25.9, 25.9, 21.8, 21.4.

IR (Neat Film, NaCl): 2925, 1716 cm^{-1}

HRMS (MM: FI+): *m/z* calc'd for $C_{12}H_{18}O$ $[M]^+$: 178.1358, found 178.1359.

Optical Rotation: $[\alpha]_D^{21}$ –59.9 (c 0.89, $CHCl_3$).

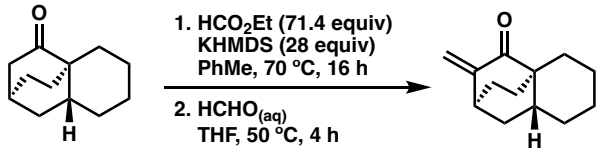

149 ***150***

(2*S*,4a*R*,8a*R*)-10-methyleneoctahydro-2*H*-2,4a-ethanonaphthalen-9-one (150)

To a solution of ketone **149** (0.056 mmol, 1 equiv) and ethyl formate (4 mmol, 71.4 equiv) in toluene (3.2 mL) was added a solution of KHMDS (0.5 M in toluene, 1.6 mmol, 28 equiv) at 23 ºC. The reaction mixture was stirred at 70 ºC for 16 h. Upon cooling to 0 ºC, THF (6.4 mL) and formalin (37% in water, 3.2 mL) was added, and then the reaction was heated to 50 ºC for 4 h. The reaction mixture was diluted with a saturated aqueous solution of NH_4Cl, extracted with EtOAc (3x), dried over Na_2SO_4, and concentrated under reduced pressure. Purification by preparatory thin layer chromatography (30% EtOAc/hexanes, 2x) afforded the title compound as a yellow oil (4.4 mg, 0.023 mmol, 41% yield).

^{1}H NMR (400 MHz, $CDCl_3$): δ 5.93 (d, *J* = 1.8 Hz, 1H), 5.15 (d, *J* = 1.8 Hz, 1H), 2.66 (p, *J* = 3.0 Hz, 1H), 2.39 – 2.19 (m, 1H), 1.98 (dddd, *J* = 13.2, 10.6, 3.9, 2.8 Hz, 1H), 1.81 – 1.61 (m, 6H), 1.51 – 1.42 (m, 2H), 1.41 – 1.31 (m, 2H), 1.23 – 1.15 (m, 2H), 1.11 (dt, *J* = 12.9, 3.6 Hz, 1H).

^{13}C NMR (100 MHz, $CDCl_3$): δ 205.3, 147.9, 116.3, 45.0, 36.1, 35.0, 34.7, 30.8, 29.0, 26.5, 26.0, 21.6, 21.3.

IR (Neat Film, NaCl): 2926, 2859, 1708, 1630, 1464, 1449 cm^{-1}

HRMS (MM: FD+): *m/z* calc'd for $C_{13}H_{18}O$ $[M]^+$: 190.1358, found 190.1353.

Optical Rotation: $[\alpha]_D^{21}$ –34.2 (c 0.29, $CHCl_3$).

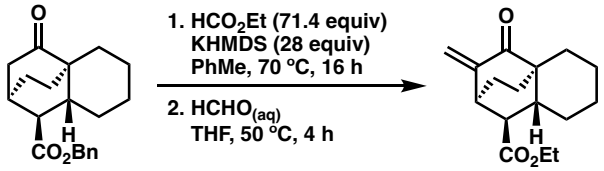

115f ***151***

ethyl (1*S*,2*S*,4a*R*,8a*R*)-3-methylene-4-oxooctahydro-2*H*-2,4a-ethanonaphthalene-1-carboxylate (151)

To a solution of **115f** (0.192 mmol, 1 equiv) and ethyl formate (13.71 mmol, 71.4 equiv) in toluene (11.1 mL) was added a solution of KHMDS (0.5 M in toluene, 5.49 mmol, 28 equiv) at 23 ºC. The reaction mixture was stirred at 70 ºC for 16 h. Upon cooling to 0 ºC, THF (22.2 mL) and formalin (37% in water, 11.1 mL) was added, and then the reaction was heated to 50 ºC for 4 h. The reaction mixture was diluted with a saturated aqueous solution of NH_4Cl, extracted with EtOAc (3x), dried over Na_2SO_4, and concentrated under reduced pressure. Purification by preparatory thin layer chromatography (30% EtOAc/hexanes, 2x) afforded the title compound as a yellow oil (13.1 mg, 0.05 mmol, 26% yield).

^{1}H NMR (400 MHz, $CDCl_3$): δ 5.99 (d, *J* = 1.7 Hz, 1H), 5.17 (d, *J* = 1.7 Hz, 1H), 4.21 – 4.01 (m, 2H), 3.04 (td, *J* = 3.1, 2.0 Hz, 1H), 2.27 (ddd, *J* = 14.2, 11.4, 5.4 Hz, 1H), 2.21

(dd, J = 6.8, 2.0 Hz, 1H), 2.01 (dddd, J = 11.6, 6.5, 4.4, 1.7 Hz, 1H), 1.92 – 1.75 (m, 3H), 1.73 – 1.65 (m, 2H), 1.56 – 1.50 (m, 1H), 1.47 – 1.31 (m, 2H), 1.29 – 1.16 (m, 6H).

^{13}C NMR (100 MHz, $CDCl_3$): δ 203.7, 173.8, 144.3, 119.0, 60.8, 51.1, 45.0, 39.1, 37.2, 30.3, 28.9, 26.2, 25.8, 21.3, 21.1, 14.4.

IR (Neat Film, NaCl): 2927, 2867, 1732, 1708, 1449, 1180 cm^{-1}.

HRMS (MM: FD+): *m/z* calc'd for $C_{16}H_{22}O_3$ $[M]^+$: 262.1569, found 262.1576.

Optical Rotation: $[\alpha]_D^{21}$ –3.9 (c 0.38, $CHCl_3$).

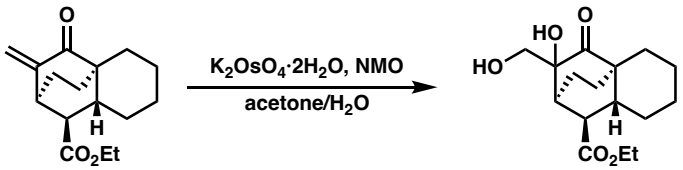

151 ***152***

ethyl (1*R*,2*S*,4a*R*,8a*R*)-3-hydroxy-3-(hydroxymethyl)-4-oxooctahydro-2*H*-2,4a-ethanonaphthalene-1-carboxylate (152)

A flame dried vial was charged with enone **151** (14.7 mg, 0.056 mmol, 1 equiv) and acetone (2.3 mL, 0.024 M) and water (0.6 mL, 0.094 M). NMO (50 wt. % in H_2O) (23 μL, 0.112 mmol, 2 equiv) was added and the solution was cooled to 0 ºC. $K_2OsO_4 \cdot 2H_2O$ (2.1 mg, 0.006 mmol, 0.1 equiv) was added to the solution. The resultant solution was slowly warmed to 23 ºC. Upon complete consumption of starting material (as determined by TLC), the reaction was quenched with a saturated solution of $Na_2S_2O_3$ and stirred for 30 min. The mixture was then diluted with CH_2Cl_2 and the product was extracted with CH_2Cl_2 (2 x). The combined organic layers were washed with brine, dried over Na_2SO_4, filtered, and concentrated under reduced pressure. Purification by preparatory thin layer chromatography (50% EtOAc/hexanes) afforded the title compound as a colorless oil (2.1

mg, 0.007 mmol,13% yield, 10:1 dr). In the ^{1}H NMR, peaks that correspond to the minor diastereomer closely resemble the major diastereomer. dr was determine through integration of ^{1}H NMR peaks 2.69 ppm (major) and 2.96 ppm (minor).

^{1}H NMR (400 MHz, $CDCl_3$): δ 4.15 (q, *J* = 7.1 Hz, 2H), 3.81 (dd, *J* = 11.8, 2.6 Hz, 1H), 3.54 (dd, *J* = 11.9, 2.7 Hz, 1H), 2.71 – 2.67 (m, 1H), 2.38 – 2.24 (m, 2H), 2.10 (d, *J* = 7.3 Hz, 1H), 1.94 – 1.64 (m, 7H), 1.47 – 1.18 (m, 9H).

^{13}C NMR (100 MHz, $CDCl_3$): δ 218.4, 174.8, 75.8, 65.8, 61.0, 48.9, 45.4, 37.3, 37.2, 30.3, 28.3, 25.6, 22.5, 21.0, 14.3.

IR (Neat Film, NaCl): 3468, 2930, 2355, 1716, 1197, 1033 cm^{-1}.

HRMS (MM: FD+): *m/z* calc'd for $C_{16}H_{24}O_5$ $[M]^+$: 296.1624, found 296.1619.

Optical Rotation: $[\alpha]_D^{21}$ 2.1 (c 0.24, $CHCl_3$).

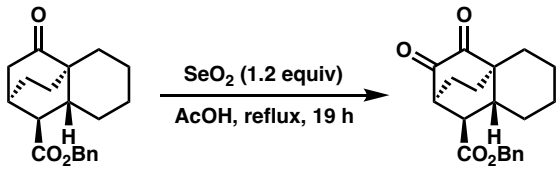

115f ***153***

benzyl (1*R*,2*S*,4a*R*,8a*R*)-3,4-dioxooctahydro-2*H*-2,4a-ethanonaphthalene-1-carboxylate (153)

To a solution of **115f** (0.064 mmol, 1 equiv) in glacial acetic acid (0.1 mL) was added SeO_2 (0.077 mmol, 1.2 equiv). The reaction was brought to reflux for 19 h. After cooling to 23 ºC, the reaction mixture was filtered and concentrated under reduced pressure. The resulting crude mixture was dissolved in EtOAc and washed with water (5x), dried over Na_2SO_4, and concentrated under reduced pressure. Purification by preparatory thin layer

chromatography (30% EtOAc/hexanes) afforded the title compound as a yellow oil (10.4 mg, 0.031 mmol, 48% yield).

^{1}H NMR (400 MHz, $CDCl_3$): δ 7.41 – 7.28 (m, 5H), 5.19 – 5.04 (m, 2H), 3.00 (m, 1H), 2.54 (dd, *J* = 6.4, 2.3 Hz, 1H), 2.40 (ddd, *J* = 14.6, 10.3, 6.9 Hz, 1H), 2.02 (m, 3H), 1.80 – 1.69 (m, 2H), 1.68 – 1.50 (m, 3H), 1.48 – 1.38 (m, 1H), 1.33 (dt, *J* = 13.4, 3.5 Hz, 1H), 1.29 – 1.15 (m, 2H).

^{13}C NMR (100 MHz, $CDCl_3$): δ 198.7, 196.1, 173.2, 135.4, 128.8, 128.6, 128.4, 67.4, 49.9, 48.0, 46.3, 37.9, 30.2, 28.3, 25.5, 22.7, 20.5, 20.2.

IR (Neat Film, NaCl): 2932, 2857, 1731, 1454, 1155 cm^{-1}.

HRMS (MM: FD+): *m/z* calc'd for $C_{20}H_{22}O_4$ $[M]^+$: 326.1518, found 326.1532.

Optical Rotation: $[\alpha]_D^{21}$ –49.2 (c 1.04, $CHCl_3$).

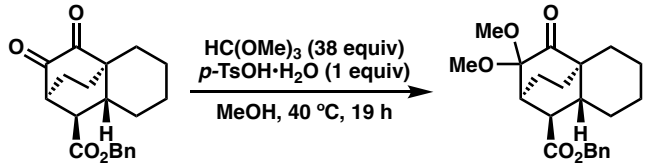

153 ***154***

benzyl (1*R*,2*S*,4a*R*,8a*R*)-3,3-dimethoxy-4-oxooctahydro-2*H*-2,4a-ethanonaphthalene-1-carboxylate (154)

To a solution of diketone **153** (0.031 mmol, 1 equiv) in methanol (0.13 mL) was added $HC(OMe)_3$ (1.2 mmol, 38 equiv) and *p*-TsOH•H_2O (0.031 mmol, 1 equiv). The reaction was stirred for 19 h at 40 ºC, followed by dilution with a saturated aqueous solution of $NaHCO_3$. The aqueous layer was extracted with EtOAc (4x), dried over Na_2SO_4, and concentrated under reduced pressure. Purification by preparatory thin layer

chromatography (30% EtOAc/hexanes) afforded the title compound as a yellow oil (4.7 mg, 0.013 mmol, 41% yield).

^{1}H NMR (400 MHz, $CDCl_3$): δ 7.42 – 7.29 (m, 5H), 5.26 (d, *J* = 12.3 Hz, 1H), 5.02 (d, *J* = 12.3 Hz, 1H), 3.20 (s, 3H), 3.06 (s, 3H), 2.93 (dt, *J* = 4.2, 2.2 Hz, 1H), 2.29 – 2.11 (m, 3H), 1.98 – 1.89 (m, 1H), 1.83 (dddd, *J* = 13.8, 11.4, 6.7, 2.4 Hz, 1H), 1.70 – 1.58 (m, 4H), 1.54 (d, *J* = 3.9 Hz, 1H), 1.31 (dd, *J* = 10.8, 2.4 Hz, 1H), 1.27 – 1.19 (m, 3H).

^{13}C NMR (100 MHz, $CDCl_3$): δ 209.0, 173.5, 136.5, 128.6, 128.5, 128.2, 97.4, 66.4, 50.4, 48.8, 48.4, 45.5, 36.4, 34.9, 30.0, 29.1, 25.5, 23.1, 21.0, 21.0.

IR (Neat Film, NaCl): 2933, 2855, 1736, 1449, 1172 cm^{-1}

HRMS (MM: FD+): *m/z* calc'd for $C_{22}H_{28}O_5$ $[M]^+$: 372.1937, found 372.1931.

Optical Rotation: $[\alpha]_D^{21}$ –26.2 (c 0.42, $CHCl_3$).

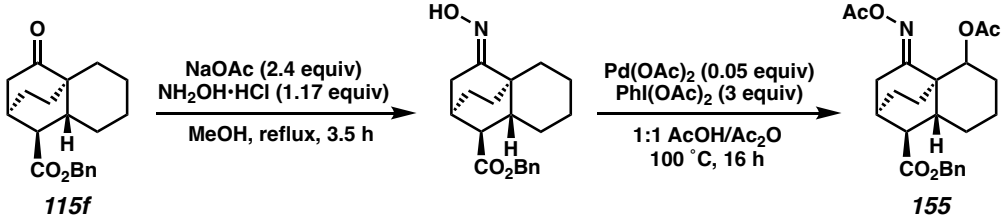

benzyl (1*S*,2*R*,4a*S*,8a*R*,*E*)-5-acetoxy-4-(acetoxyimino)octahydro-2*H*-2,4a-ethanonaphthalene-1-carboxylate (155)

To a stirred solution of ketone **115f** (0.096 mmol, 1 equiv) in methanol (0.93 mL) was added NaOAc (0.23 mmol, 2.4 equiv), NH_2OH•HCl (0.111 mmol, 1.17 equiv), and water (0.033 mL). The reaction was brought to reflux for 3.5 h and was subsequently cooled to 23 ºC and concentrated under reduced pressure. The crude mixture was then diluted with water and extracted with EtOAc (3x), washed with a saturated aqueous solution of $NaHCO_3$ and brine, dried with Na_2SO_4, and concentrated under reduced pressure. The

crude oxime was dissolved in a 1:1 mixture of AcOH/Ac_2O (0.78 mL). The reaction vessel was sealed and stirred at 23 ºC for 2 h. $Pd(OAc)_2$ (0.0048 mmol, 0.05 equiv) and $PhI(OAc)_2$ (0.288 mmol, 3 equiv) were subsequently added, and the reaction was heated to 100 ºC for 16 h. The reaction mixture was cooled to 23 ºC, filtered through a silica plug, and the filtrate was diluted with EtOAc. The organic layer was washed with a saturated solution of $NaHCO_3$ until not acidic, washed with brine, dried over Na_2SO_4, and concentrated under reduced pressure. Purification by preparatory thin layer chromatography (30% EtOAc/hexanes) afforded the title compound (**155**) as a yellow oil (12.3 mg, 0.0288 mmol, 30% yield over two steps).

^{1}H NMR (400 MHz, $CDCl_3$): δ 7.43 – 7.27 (m, 5H), 5.31 – 5.20 (m, 1H), 5.20 – 5.02 (m, 2H), 2.62 (dt, *J* = 20.2, 3.5 Hz, 1H), 2.40 – 2.29 (m, 2H), 2.27 – 2.17 (m, 1H), 2.14 (s, 3H), 2.02 (s, 3H), 1.89 (m, 1H), 1.83 – 1.69 (m, 4H), 1.62 (t, *J* = 2.8 Hz, 2H), 1.46 – 1.28 (m, 4H).

^{13}C NMR (100 MHz, $CDCl_3$): δ 173.9, 170.6, 170.4, 168.9, 135.9, 128.8, 128.5, 128.2, 71.7, 66.9, 49.6, 42.2, 39.1, 29.5, 28.9, 28.6, 26.9, 25.5, 23.0, 21.4, 20.2, 16.7.

IR (Neat Film, NaCl): 2930, 1764, 1731, 1456, 1371, 1248, 1210 cm^{-1}.

HRMS (MM: FD+): *m/z* calc'd for $C_{24}H_{29}NO_6$ $[M]^+$: 427.1995, found 427.2017.

Optical Rotation: $[\alpha]_D^{21}$ –27.6 (c 1.00, $CHCl_3$).

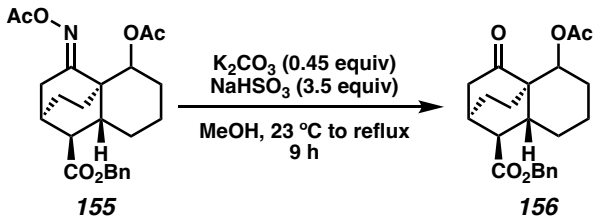

155 ***156***

benzyl (1*S*,2*R*,4a*R*,8a*R*)-5-acetoxy-4-oxooctahydro-2*H*-2,4a-ethanonaphthalene-1-carboxylate (156)

To a solution of **155** (0.029 mmol, 1 equiv) in methanol (0.06 mL) in a loosely capped vial was added K_2CO_3 (0.013 mmol, 0.45 equiv) at 23 ºC in three portions over 6 h. $NaHSO_3$ (0.1 mmol, 3.5 equiv) and water (0.06 mL) were subsequently added, and the vial was sealed and heated to 80 ºC for 3 h. The reaction mixture was diluted with $CHCl_3$, rinsed with 1 M HCl, and the aqueous layer was extracted with $CHCl_3$ (3x). The combined organic layers were neutralized with a saturated solution of $NaHCO_3$, washed with brine, dried over Na_2SO_4, and concentrated under reduced pressure. Purification by preparatory thin layer chromatography (35% EtOAc/hexanes) afforded the title compound as a colorless oil (1.8 mg, 0.0056 mmol, 19% yield).

^{1}H NMR (400 MHz, $CDCl_3$): δ 7.41 – 7.30 (m, 5H), 5.19 – 5.06 (m, 3H), 2.48 (m, 1H), 2.41 (dt, *J* = 19.2, 2.8 Hz, 1H), 2.29 (dt, *J* = 6.9, 2.0 Hz, 1H), 2.16 – 2.04 (m, 3H), 1.98 (s, 3H), 1.94 – 1.89 (m, 1H), 1.87 – 1.79 (m, 3H), 1.78 – 1.73 (m, 1H), 1.71 (m, 2H), 1.46 – 1.29 (m, 3H).

^{13}C NMR (100 MHz, $CDCl_3$): δ 212.2, 173.9, 170.2, 135.9, 128.8, 128.5, 128.3, 70.8, 66.9, 49.4, 48.5, 40.5, 37.9, 30.7, 29.0, 26.7, 25.8, 22.9, 21.3, 15.7.

IR (Neat Film, NaCl): 2928, 1781, 1375, 1246, 1173 cm^{-1}.

HRMS (MM: FD+): *m/z* calc'd for $C_{22}H_{26}O_5$ $[M]^+$: 370.1780, found 370.1774.

Optical Rotation: $[\alpha]_D^{21}$ –18.3 (c 0.18, $CHCl_3$).

Preparation of Additional Compounds

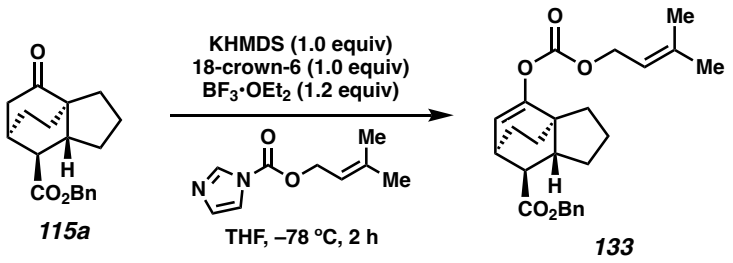

benzyl (3a*R*,6*R*,7*S*,7a*R*)-4-oxooctahydro-3a,6-ethanoindene-7-carboxylate (133)[42]

To a solution of KHMDS (40 mg, 0.20 mmol, 1.0 equiv) and 18-crown-6 (53 mg, 0.20 mmol, 1 equiv) in THF (2.0 mL) at –78 ºC was added a solution of **115a** (60 mg, 0.20 mmol, 1 equiv). Stirring was continued at –78 ºC for 30 minutes, then a pre-mixed solution of 3-methylbut-2-en-1-yl 1*H*-imidazole-1-carboxylate (43 mg, 0.24 mmol, 1.2 equiv) and boron trifluoride diethyl etherate (30 μL, 0.24 mmol, 1.2 equiv) in THF (1.2 mL) was added dropwise. After two additional hours of stirring at –78 ºC, EtOAc and saturated aqueous NH_4Cl were added. The layers were separated, and the aqueous layer was extracted twice with EtOAc. The combined organic layers were washed with brine, dried over Na_2SO_4, filtered, and solvent was removed in vacuo. The crude mixture was purified by silica gel flash column chromatography (0–40% EtOAc/hexanes) to afford enol carbonate **133** as a colorless oil (44 mg, 0.11 mmol, 55% yield).

^{1}H NMR (400 MHz, $CDCl_3$): δ 7.39 – 7.29 (m, 5H), 5.70 (d, *J* = 6.8 Hz, 1H), 5.42 – 5.36 (m, 1H), 5.09 (d, *J* = 3.6 Hz, 2H), 4.65 (d, *J* = 7.3 Hz, 2H), 3.08 – 2.96 (m, 1H), 2.25 (d, *J* = 5.6 Hz, 1H), 2.07 – 1.97 (m, 2H), 1.91 – 1.79 (m, 3H), 1.77 (s, 3H), 1.73 (s, 3H), 1.63 – 1.54 (m, 2H), 1.52 – 1.38 (m, 3H), 1.35 – 1.28 (m, 1H).

^{13}C NMR (100 MHz, $CDCl_3$): δ 174.9, 155.6, 153.5, 140.6, 136.4, 128.7, 128.2, 128.0, 117.9, 112.8, 66.3, 65.3, 51.3, 48.1, 48.1, 35.5, 28.4, 28.4, 27.3, 25.9, 24.6, 22.8, 18.3.

IR (Neat Film, NaCl): 2953, 2870, 1754, 1735, 1241, 1226, 1150 cm^{-1}

HRMS (MM: FD+): *m/z* calc'd for $C_{25}H_{30}O_5$ $[M]^+$: 410.2093, found 410.2094.

SFC conditions: 20% IPA, 2.5 mL/min, Chiralpak IC column, λ = 210 nm, t_R (min): minor = 3.05, major = 3.40.

2.4.3 Determination of absolute stereochemistry by VCD spectroscopy.

Experimental Protocol: A solution of the compound of interest (50 mg/mL) in $CDCl_3$ was loaded into a front-loading SL-4 cell (International Crystal Laboratories) possessing BaF_2 windows and a 100 mm path length. Infrared (IR) and VCD spectra were acquired on a BioTools ChiralIR-2X VCD spectrometer as a set of 24 one-hour blocks (24 blocks, 3120 scans per block) in dual PEM mode. A 15-minute acquisition of neat (+)-α-pinene control yielded a VCD spectrum in agreement with literature spectra. IR and VCD spectra were background corrected using a 30-minute block IR acquisition of the empty instrument chamber under gentle N_2 purge, and were solvent corrected using a 16-hour (16 blocks, 3120 scans per block) IR/VCD acquisition of $CDCl_3$ in the same 100 μm BaF2 cell. The reported spectra represent the result of block averaging.

Both enantiomers of compounds **11a**, **11q**, and **11q'** were prepared from the *(S)* and *(R)* enantiomers of the *t*-BuPHOX ligand. Data were collected for both enantiomers of compounds at identical concentration and the final reported VCD spectra are the half-difference of the spectra of the compounds derived from the *(S)* minus *(R)* enantiomer of

ligand. Due to limited sample size, spectra of cycloadducts **11k'** and **11k''** were collected at concentrations of 11.7 and 9.3 mg/mL, respectively.

Computational Protocol: An arbitrarily chosen enantiomer of the compound of interest was subjected to an exhaustive initial molecular mechanics-based conformational search (OPLS_2005 force field, $CHCl_3$ solvent, 10.0 kcal/mol cutoff, "Enhanced" torsional sampling) as implemented in MacroModel program.[50] The resulting ensemble of conformers was subsequently optimized using the B3PW91 functional, cc-pVTZ(-f) basis, and implicit PBF solvation model for chloroform using the Jaguar program.[51] Harmonic frequencies computed at the B3PW91/cc-pVTZ(-f)/PBF(chloroform) level were scaled by 0.98. The resultant structurally unique conformers possessing all positive Hessian eigenvalues were Boltzmann weighted by relative free energy at 298.15 K. The predicted IR and VCD frequencies and intensities of the retained conformers were convolved using Lorentzian line shapes (γ = 4 cm^{-1}) and summed using the respective Boltzmann weights to yield the final predicted IR and VCD spectra. The predicted VCD of the opposite enantiomer was generated by inversion of sign.

VCD Analysis for diastereomers 11a, 11q, and 11q'

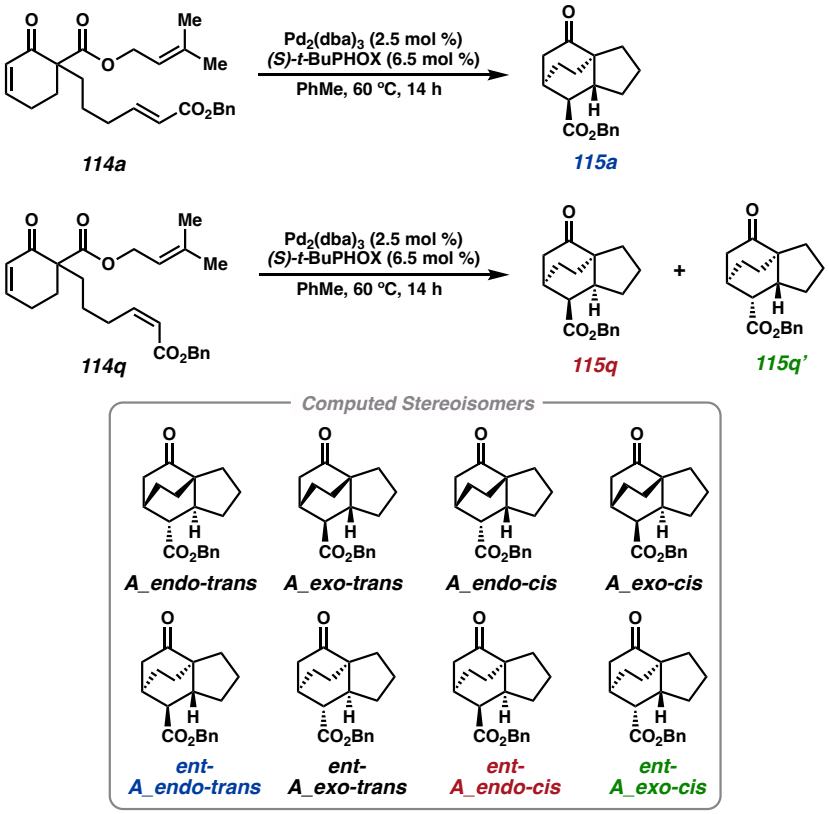

Figure 2.10 *Three diastereomers* ***115a***, ***115q***, *and* ***115q'*** *to be compared to spectra computed from all eight possible stereoisomers.*

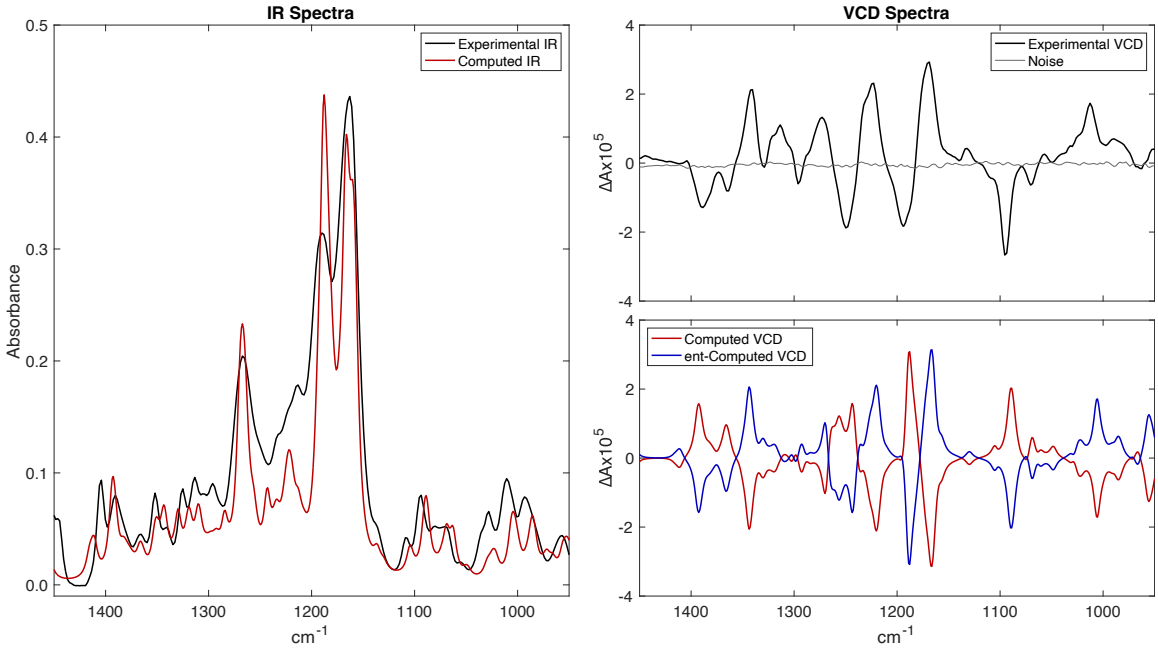

Figure 2.11 *Comparison of experimental VCD and IR spectra for product* ***115a*** *to computed spectra for A endo-trans.*[a]

[a] Experimental IR spectrum in good agreement with computed spectrum. Experimental VCD spectrum for **115a** is in excellent agreement with computed spectrum for ***ent*-A_endo-trans**.

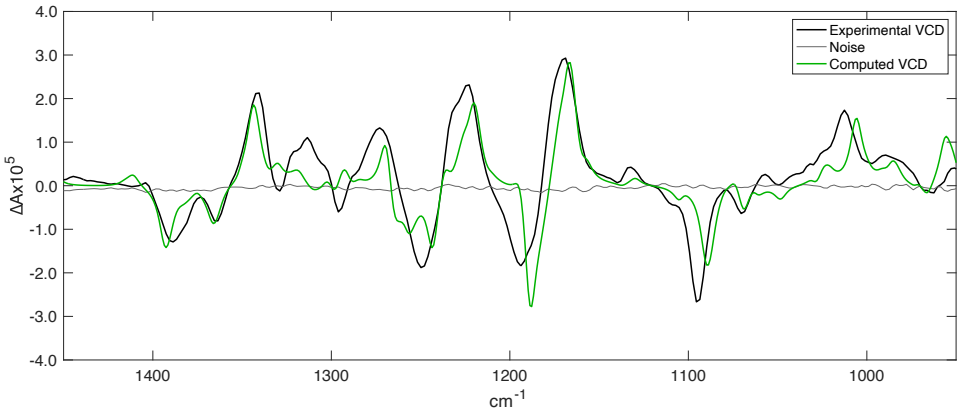

Figure 2.12 *Overlayed experimental and calculated VCD spectra for* ***115a*** *– assigned as* ***ent-A_endo-trans***.

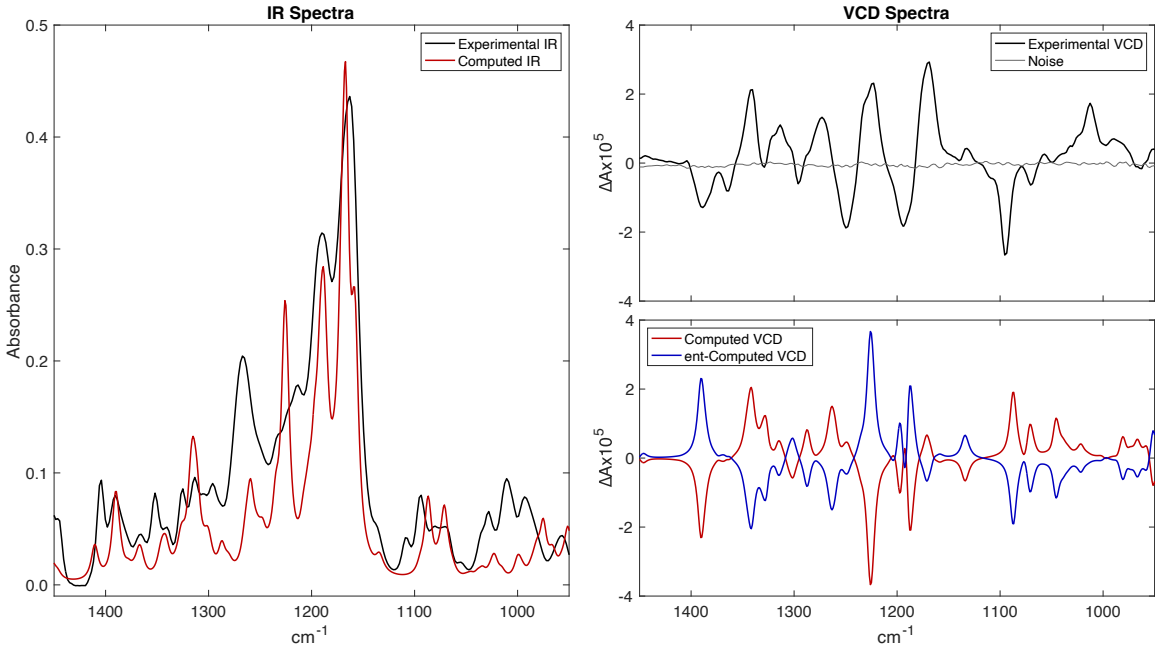

Figure 2.13 *Comparison of experimental VCD and IR spectra for product* ***115a*** *to computed spectra for* ***A_exo-trans****.*[a]

[a] A shift of –3 cm^{-1} along x-axis applied to computed spectra in fitting. Experimental data from **115a** do not match computed data of **A_exo-trans**.

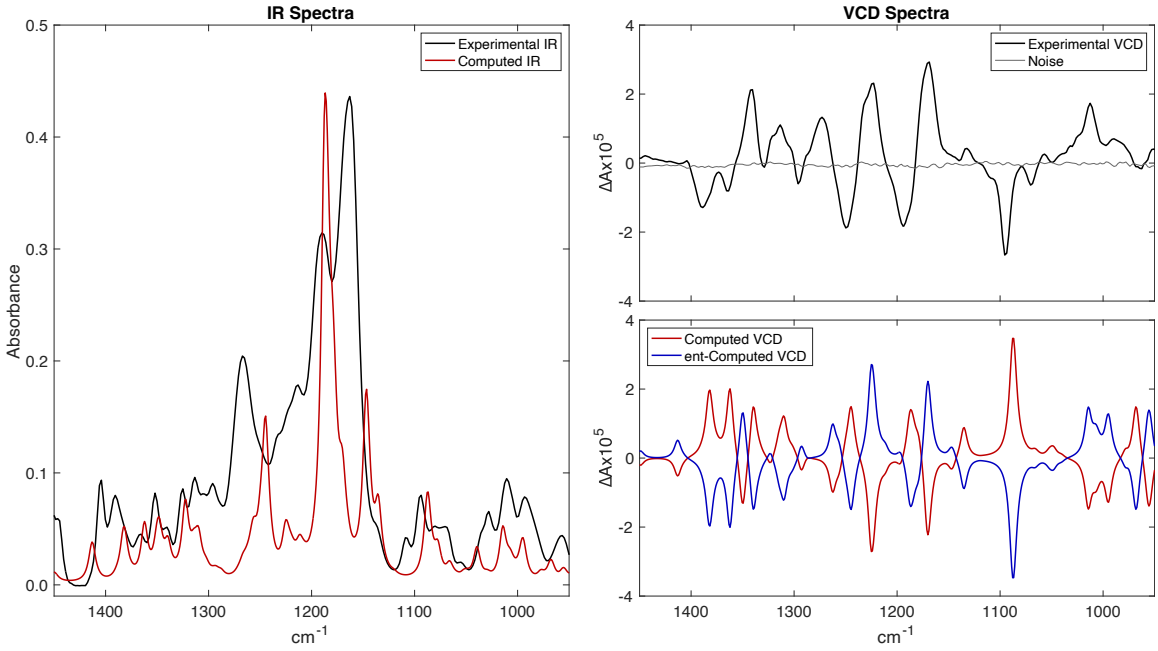

Figure 2.14 *Comparison of experimental VCD and IR spectra for product* ***115a*** *to computed spectra for* ***A_endo-cis****.*[a]

[a] Experimental data from **115a** do not match computed data of **A_endo-cis**.

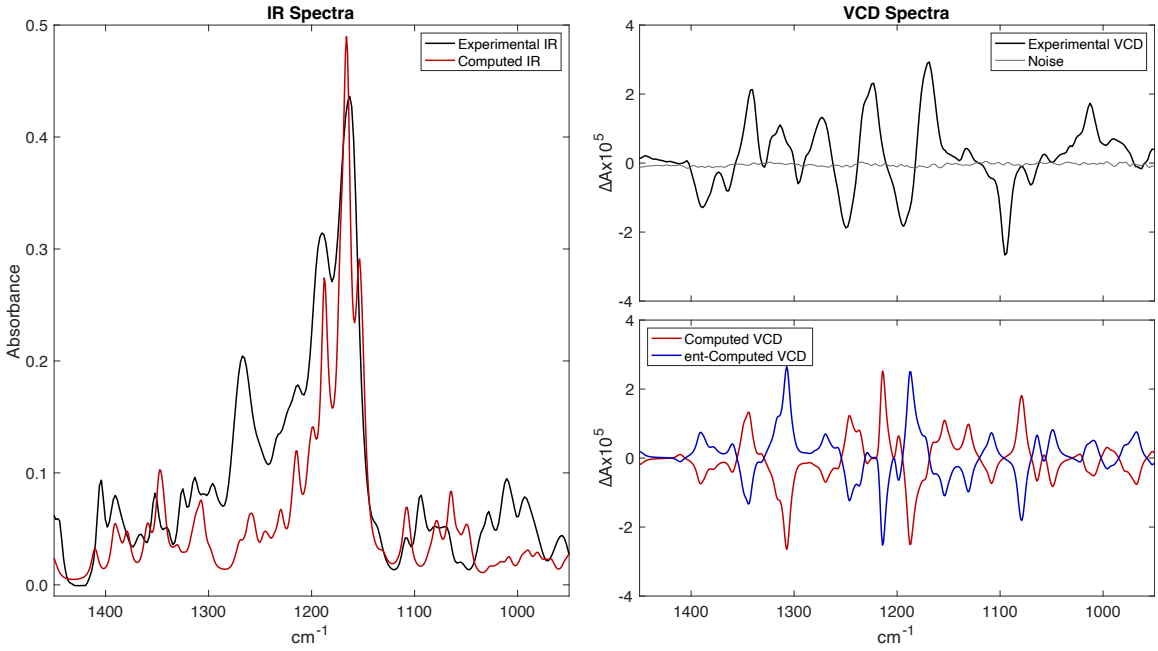

Figure 2.15 *Comparison of experimental VCD and IR spectra for product* ***115a*** *to computed spectra for* ***A_exo-cis****.*[a]

[a] A shift of –3 cm-1 along x-axis applied to computed spectra in fitting. Experimental data from **115a** do not match computed data of **A_exo-cis**.

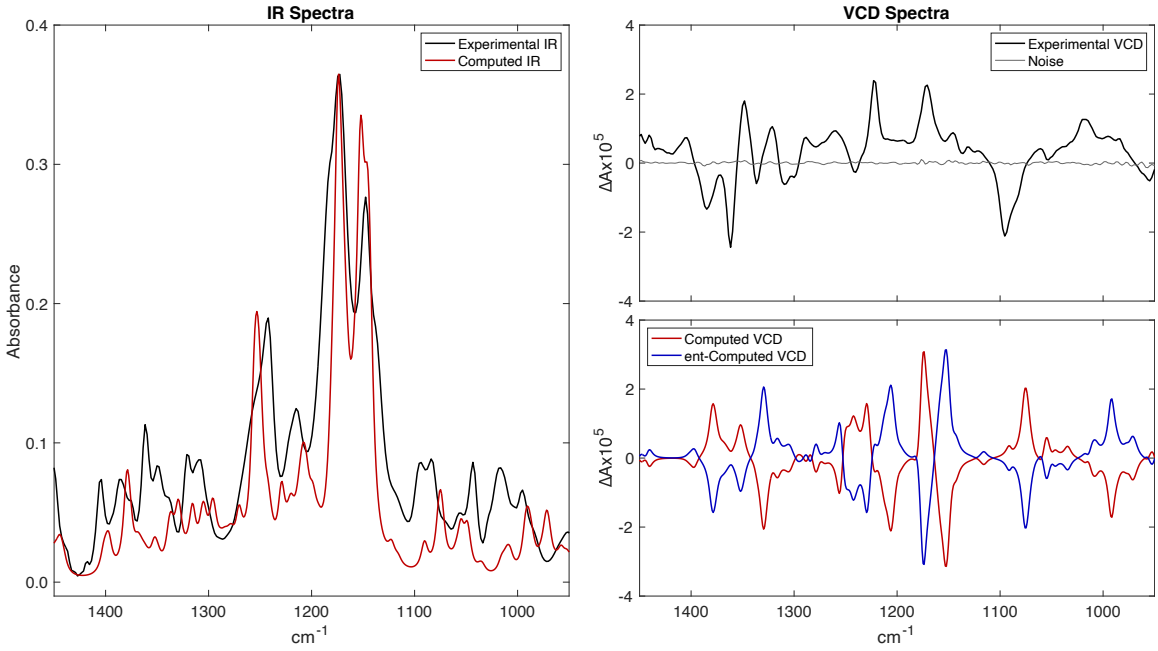

Figure 2.16 *Comparison of experimental VCD and IR spectra for product* ***115q*** *to computed spectra for* ***A_endo-trans***.[a]

[a] A shift of +14 cm^{-1} along x-axis applied to computed spectra in fitting. The IR spectrum of **115q** contains similar features to the calculated spectrum for **A_endo-trans**; however, the VCD spectrum displays large discrepancies at 1174, 1152, 1330, 1076, and 992 cm^{-1}. **115q** is <u>not</u> assigned as **A_endo-trans**.

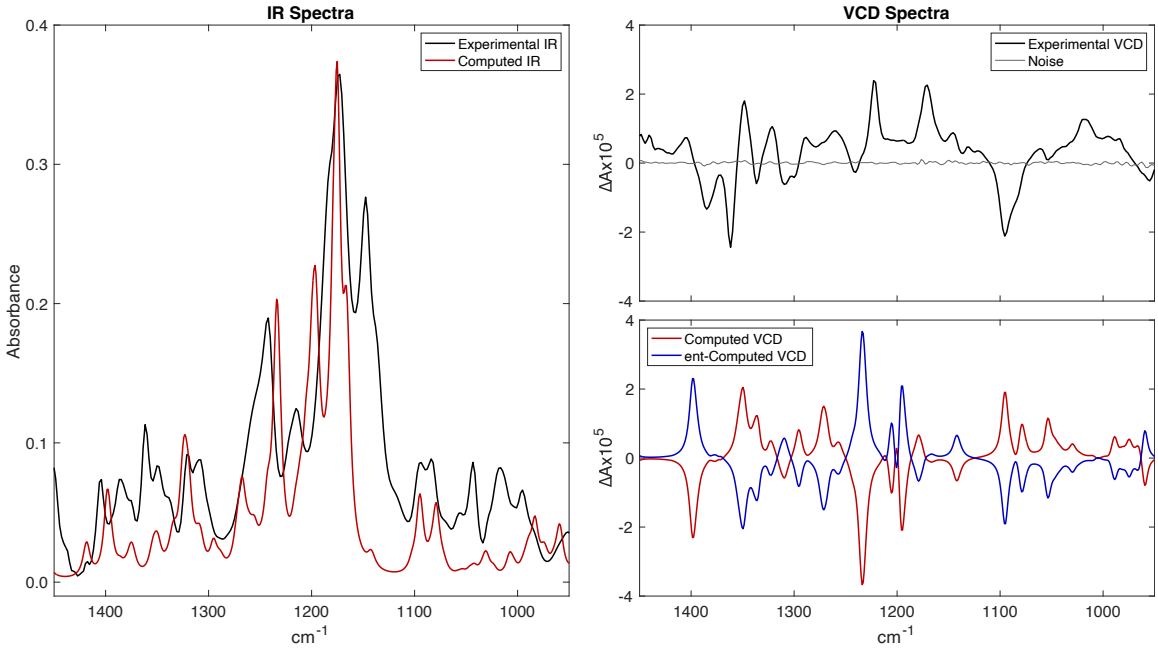

Figure 2.17 *Comparison of experimental VCD and IR spectra for product* ***115q*** *to computed spectra for* ***A_exo-trans***.[a]

[a] Experimental data from **115q** do not match computed data of **A_exo-trans**.

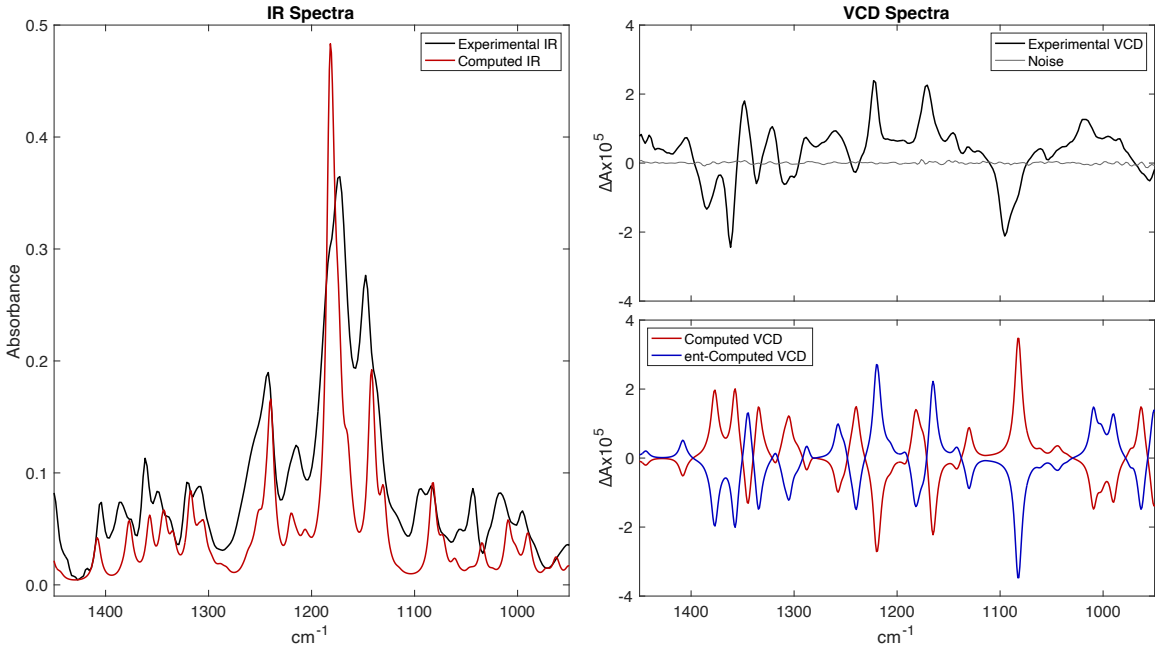

Figure 2.18 *Comparison of experimental VCD and IR spectra for product* ***115q*** *to computed spectra for* ***A_endo-cis****.*[a]

[a] A shift of +5 cm^{-1} along x-axis applied to computed spectra in fitting. The IR spectrum of **115q** is in good agreement with that of the computed IR spectrum of **A_endo-cis**. Experimental VCD spectrum for **115q** is in excellent agreement with computed spectrum for ***ent*-A_endo-cis**.

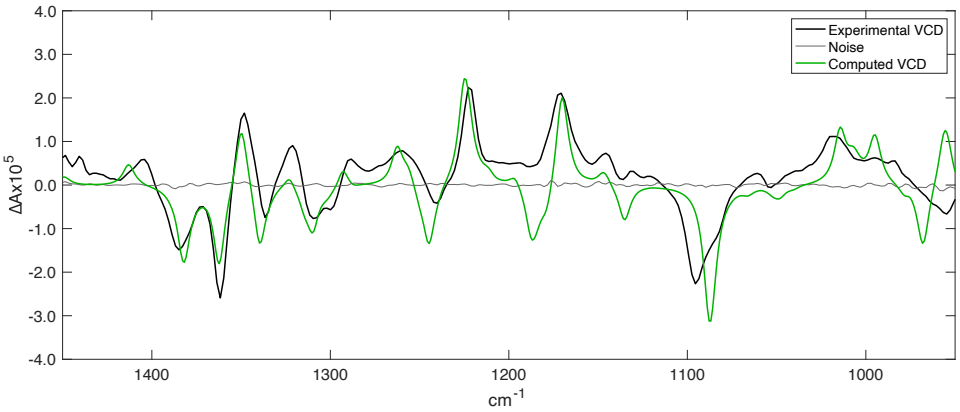

Figure 2.19 *Overlayed experimental and calculated VCD spectra for* ***115q*** *– assigned as* ***ent-A_endo-cis****.*

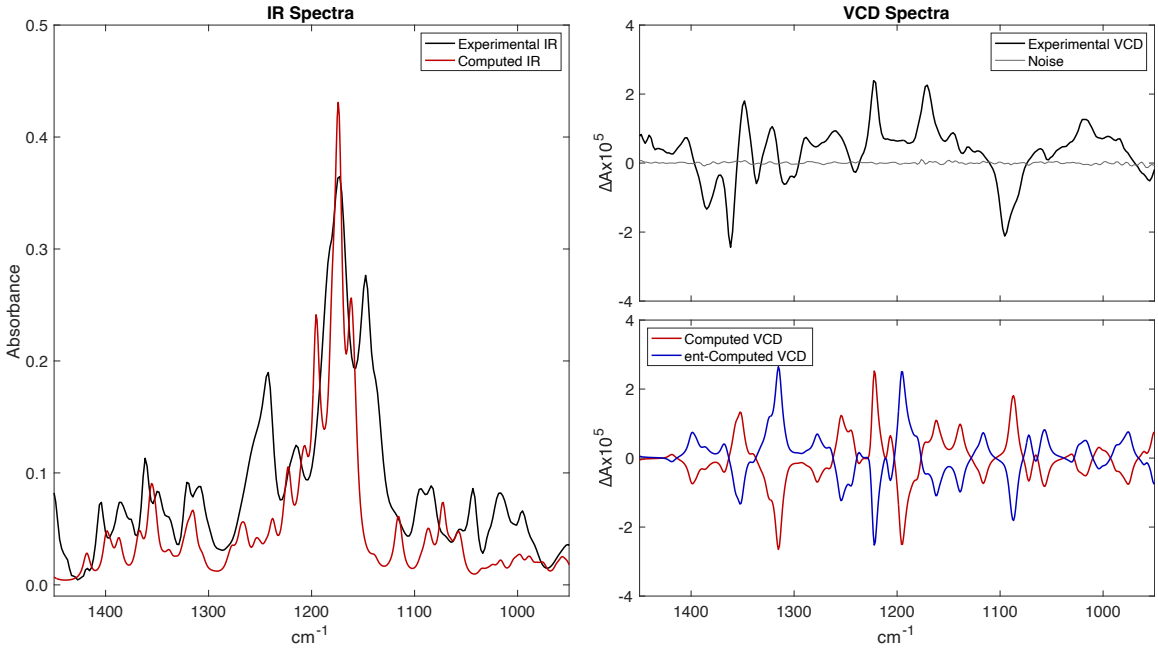

Figure 2.20 *Comparison of experimental VCD and IR spectra for product* ***115q*** *to computed spectra for* ***A_exo-cis****.*[a]

[a] Experimental data from **115q** do not match computed data of **A_exo-cis**.

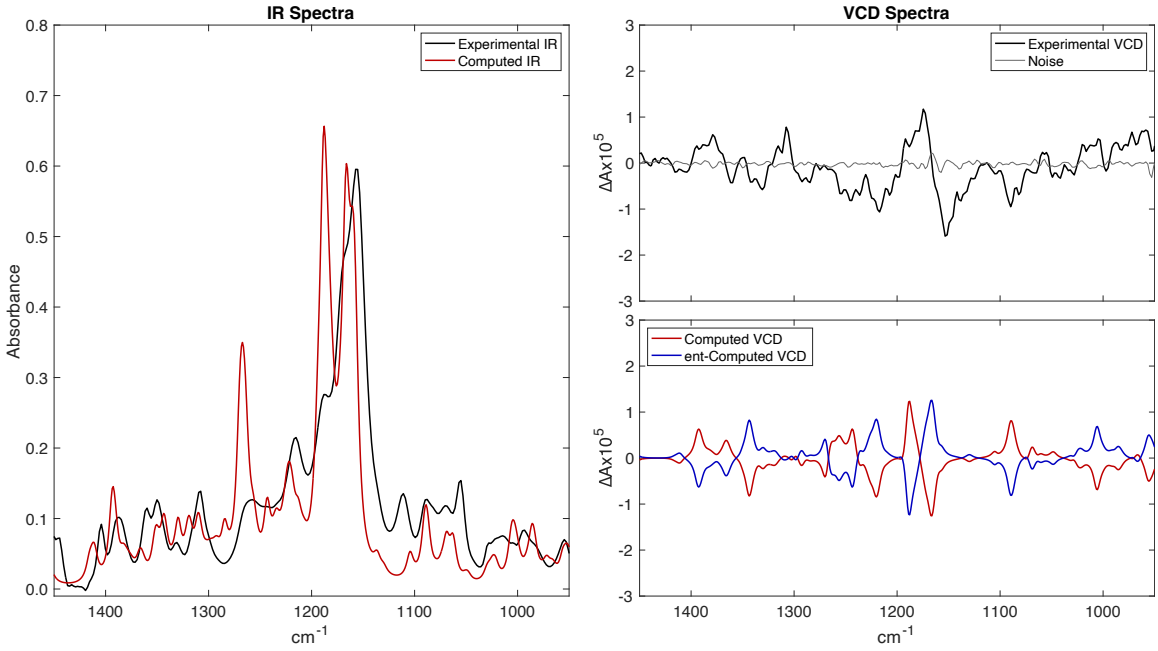

Figure 2.21 *Comparison of experimental VCD and IR spectra for product* ***115q'*** *to computed spectra for* ***A_endo-trans***.[a]

[a] The VCD spectrum was baseline-corrected with a shift of +7 cm^{-1} along y-axis. Experimental data from **115q'** do not match computed data of **A_endo-trans**.

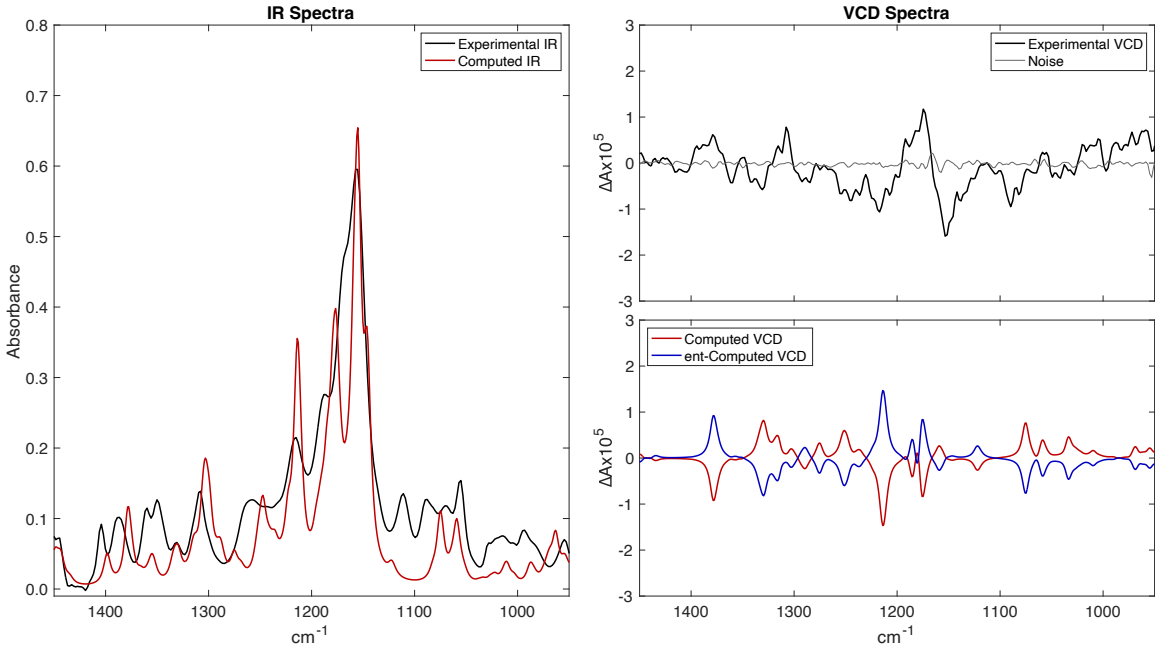

Figure 2.22 *Comparison of experimental VCD and IR spectra for product* ***115q'*** *to computed spectra for* ***A_exo-trans***.[a]

[a] The VCD spectrum of **115q'** was baseline-corrected with a shift of +7 cm^{-1} along y-axis. A shift of -15 cm^{-1} along x-axis applied to computed spectra in fitting. Experimental data from **115q'** do not match computed data of **A_exo-trans**.

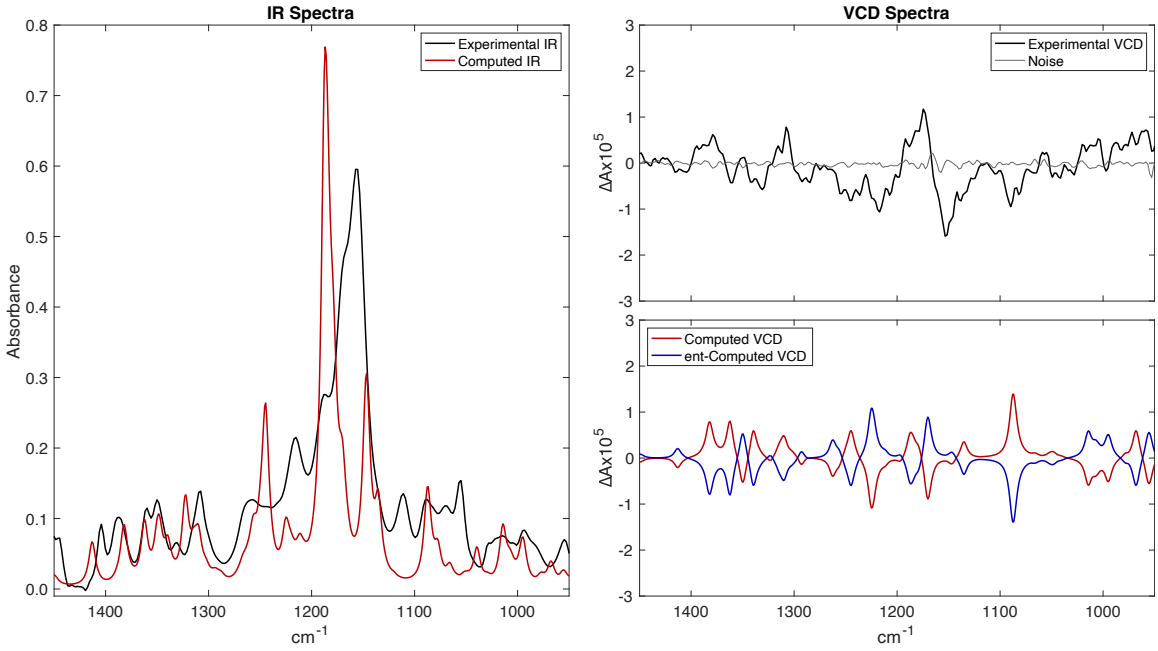

Figure 2.23 *Comparison of experimental VCD and IR spectra for product* ***115q'*** *to computed spectra for* ***A_endo-cis****.*[a]

[a] The VCD spectrum of **115q'** was baseline-corrected with a shift of +7 cm^{-1} along y-axis. Experimental data from **115q'** do not match computed data of **A_endo-cis**.

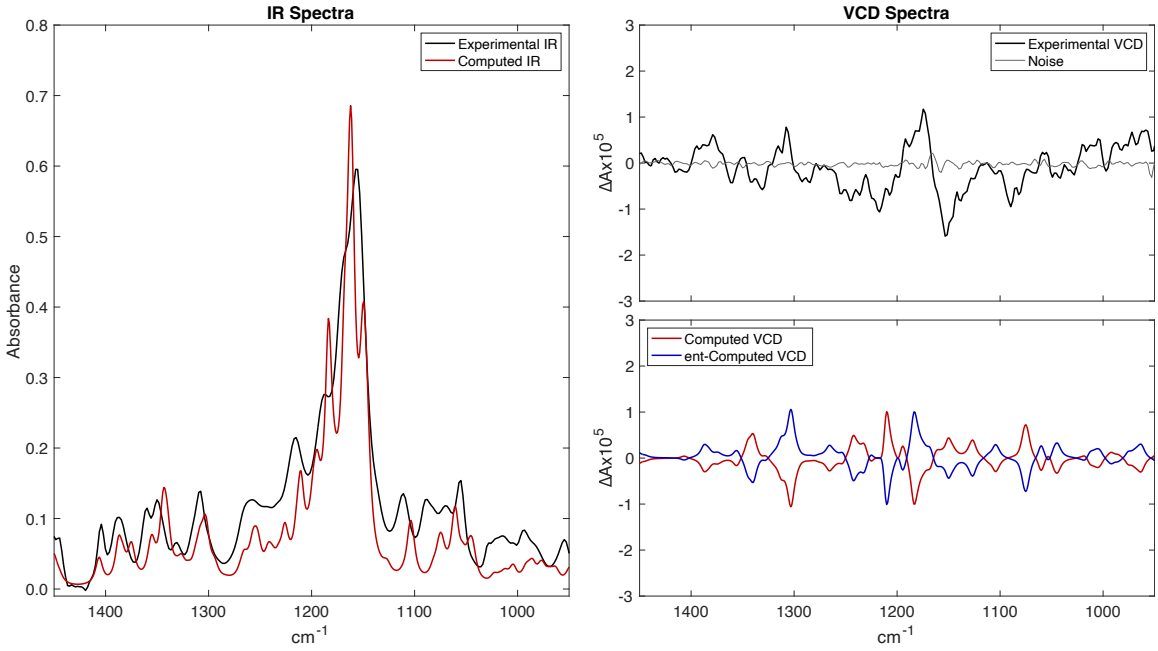

Figure 2.24 *Comparison of experimental VCD and IR spectra for product* ***115q'*** *to computed spectra for* ***A_exo-cis****.*[a]

[a] The VCD spectrum of **115q'** was baseline-corrected with a shift of +7 cm^{-1} along y-axis. A shift of +7 cm^{-1} along x-axis applied to computed spectra in fitting. Experimental VCD spectrum for **115q'** is in good agreement with computed spectrum for ***ent*-A_exo-cis**.

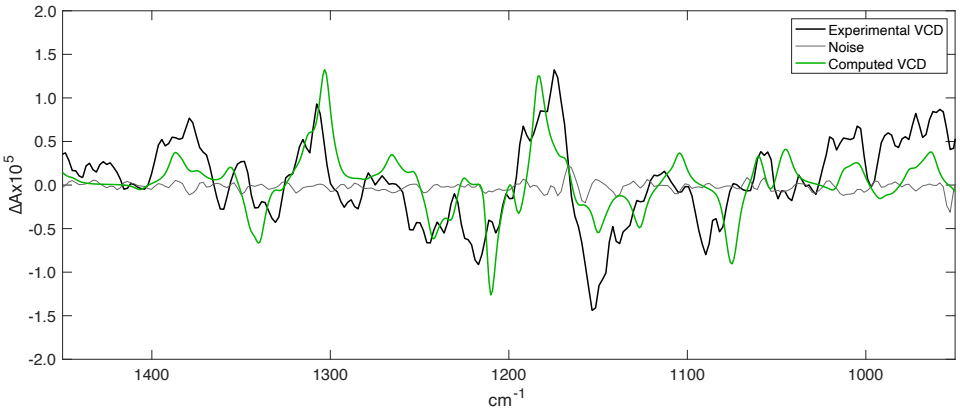

Figure 2.25 *Overlayed experimental and calculated VCD spectra for* ***115q'*** *– assigned as* ***ent-A_exo-cis****.*

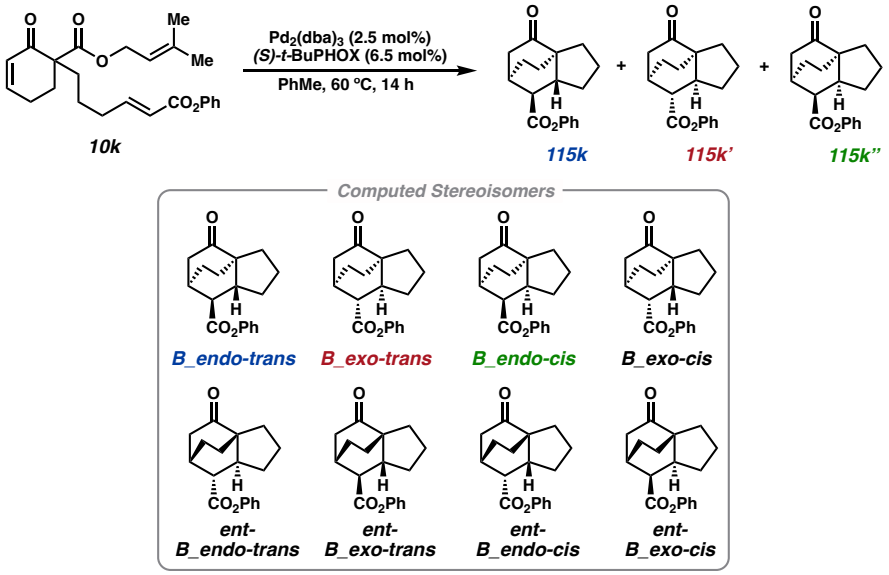

Figure 2.26 *Three diastereomers* ***115k***, ***115k'***, *and* ***115k''*** *to be compared to spectra computed from all eight possible stereoisomers.*

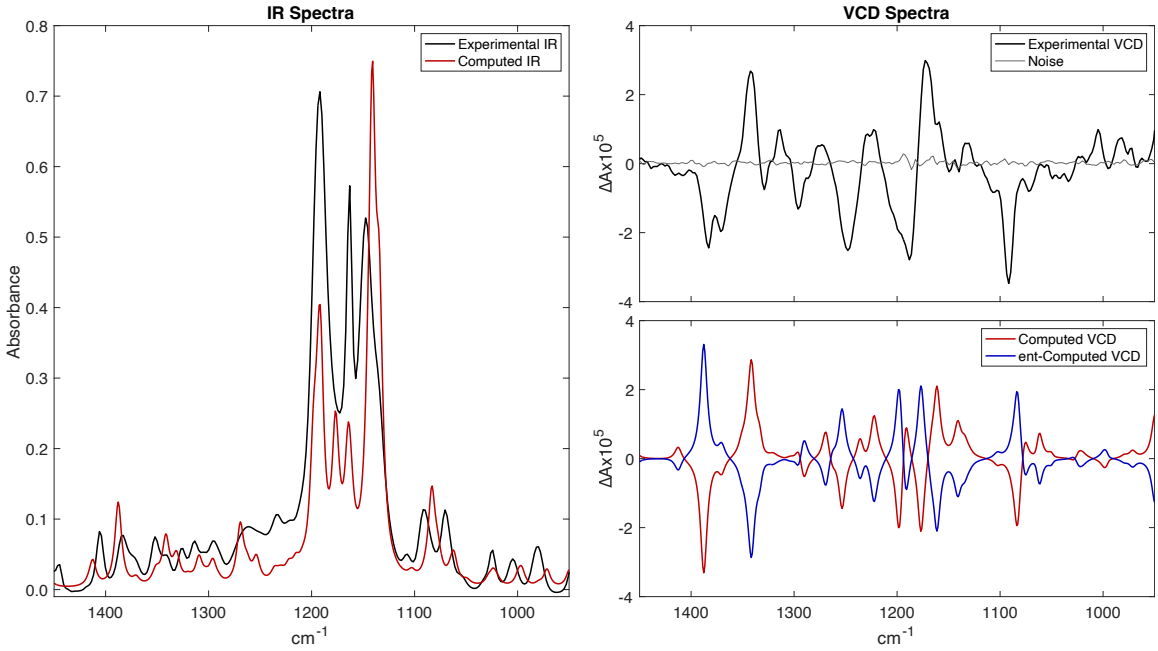

Figure 2.27 *Experimental VCD and IR spectra for product* ***115k*** *compared to computed spectra for* ***B_endo-trans***.[a]

[a] Experimental IR spectrum in good agreement with computed spectrum. Experimental VCD spectrum for **115k** is in excellent agreement with computed spectrum for **B_endo-trans**.

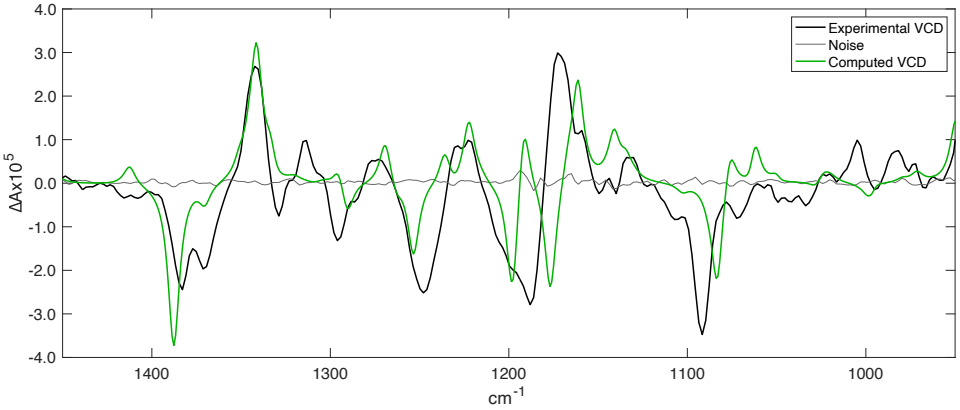

Figure 2.28 *Overlayed experimental and calculated VCD spectra for* ***115k*** *– assigned as* ***B_endo-trans****.*

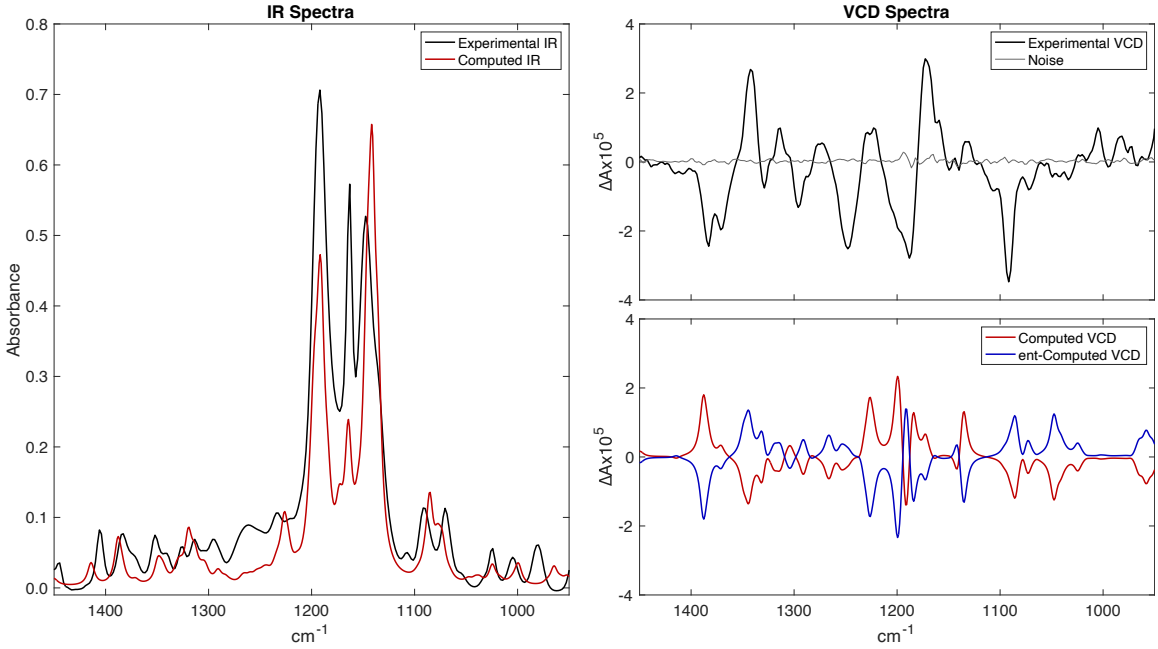

Figure 2.29 *Experimental VCD and IR spectra for product* ***115k*** *compared to computed spectra for* ***B_exo-trans****.*[a]

[a] Experimental IR spectrum in good agreement with computed spectrum. However, VCD spectrum contain key sign mismatches in regions around 1400 and 1100 cm^{-1}. Hence, **115k** is not assigned as **B_exo-trans**.

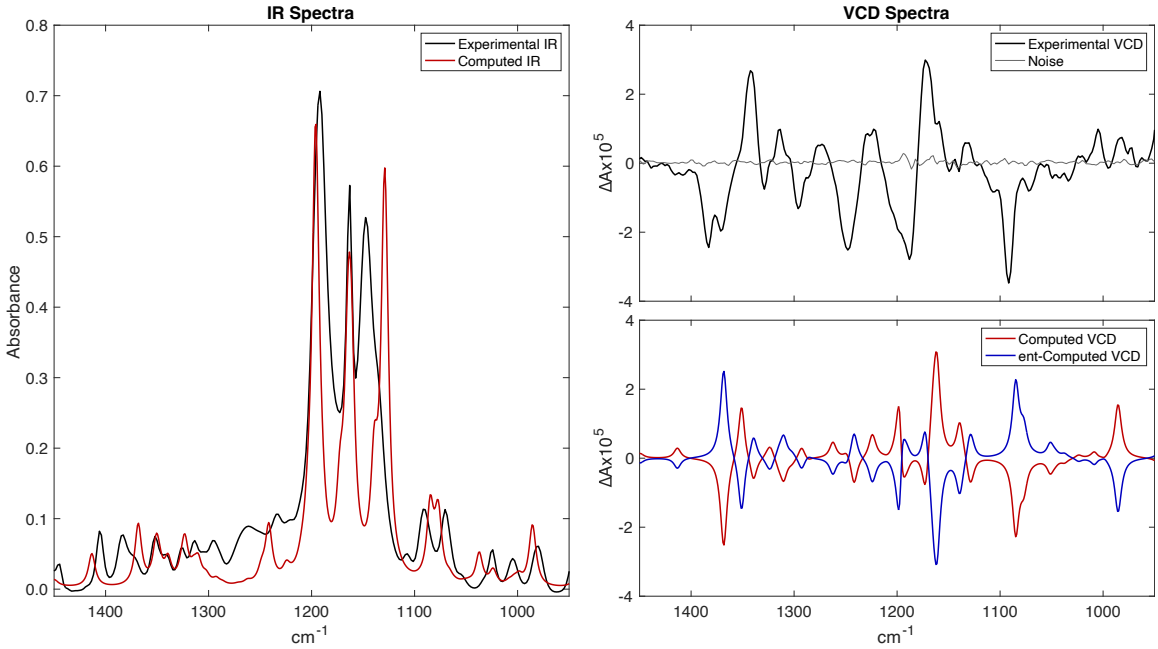

Figure 2.30 *Experimental VCD and IR spectra for product* ***115k*** *compared to computed spectra for* ***B_endo-cis****.*[a]

[a] Experimental data do not match computed data and **115k** is not assigned as **B_endo-cis**.

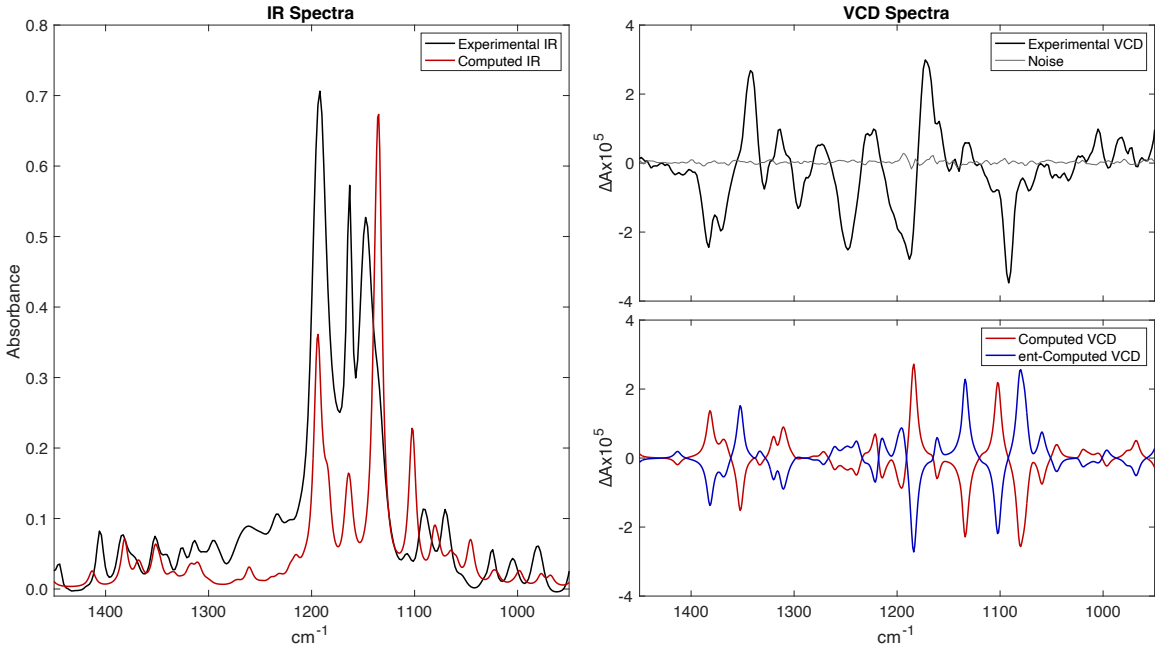

Figure 2.31 *Experimental VCD and IR spectra for product* ***115k*** *compared to computed spectra for* ***B_exo-cis***.[a]

[a] Experimental data do not match computed data and **115k** is not assigned as **B_exo-cis**.

Due to limited sample size (< 3 mg), useful VCD spectra of **115k'** were unable to be obtained. Enantiomeric series was assigned by analogy to the **115a**, **115q** and **115q'** series. The 1000–1500 cm^{-1} region of the IR spectra are still analyzed to support relative stereochemical assignments made by 2D NMR.

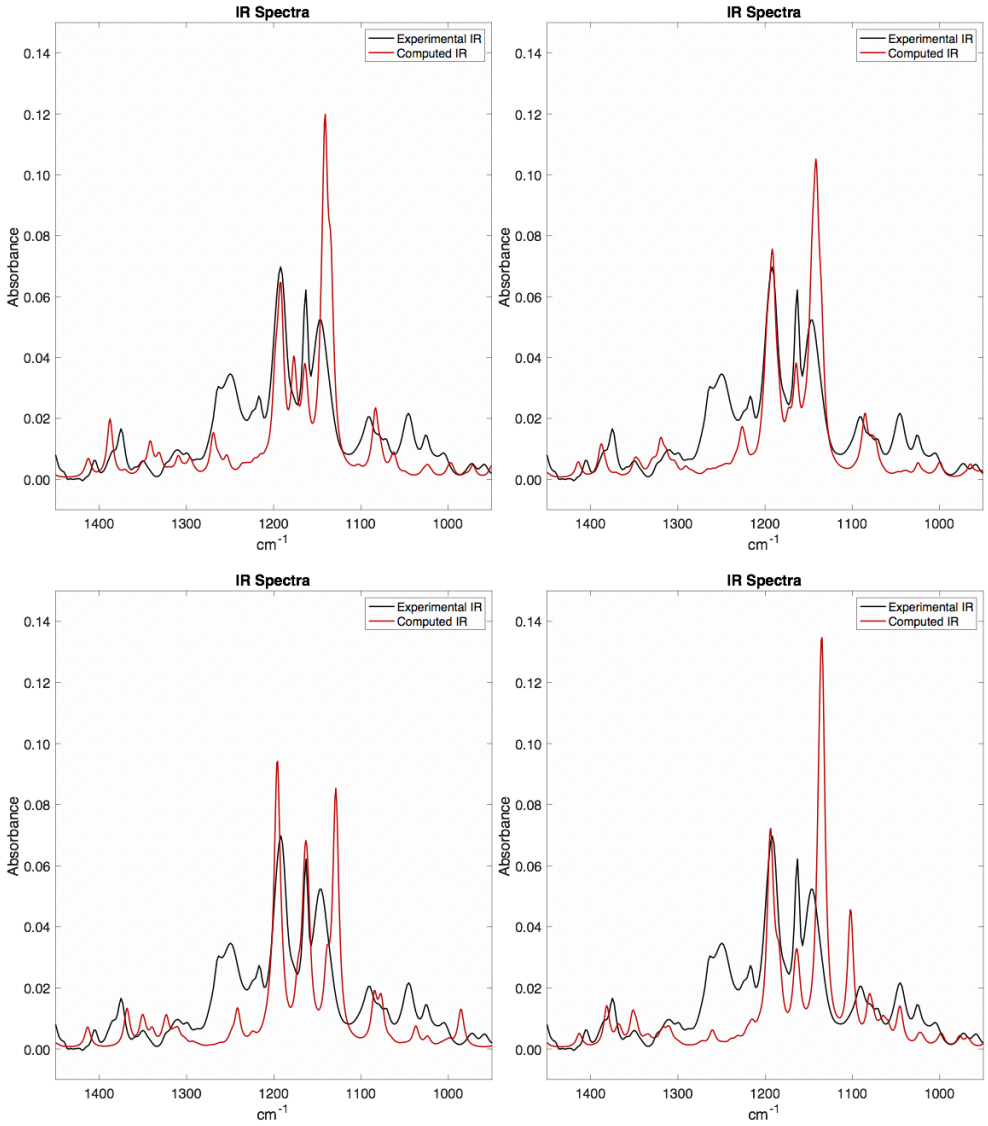

Figure 2.32 *Experimental IR spectrum for product* ***115k'*** *compared to computed spectra for* ***B_endo-trans*** *(top left),* ***B_exo-trans*** *(top right),* ***B_endo-cis*** *(bottom left),* ***B_exo-cis*** *(bottom right).*[a]

[a] The trans relationship is supported, in accord with 2D NMR data. In contrast to endo-cis and exo-cis, the computed IR spectra for both endo-trans and exo-trans are similar and do not offer key features for distinguishing the two. Given the trans stereochemistry, with **115k** known as **B_endo-trans**, **115k'** is assigned as **B_exo-trans** with absolute stereochemistry assigned based on analogy to **115q'**.

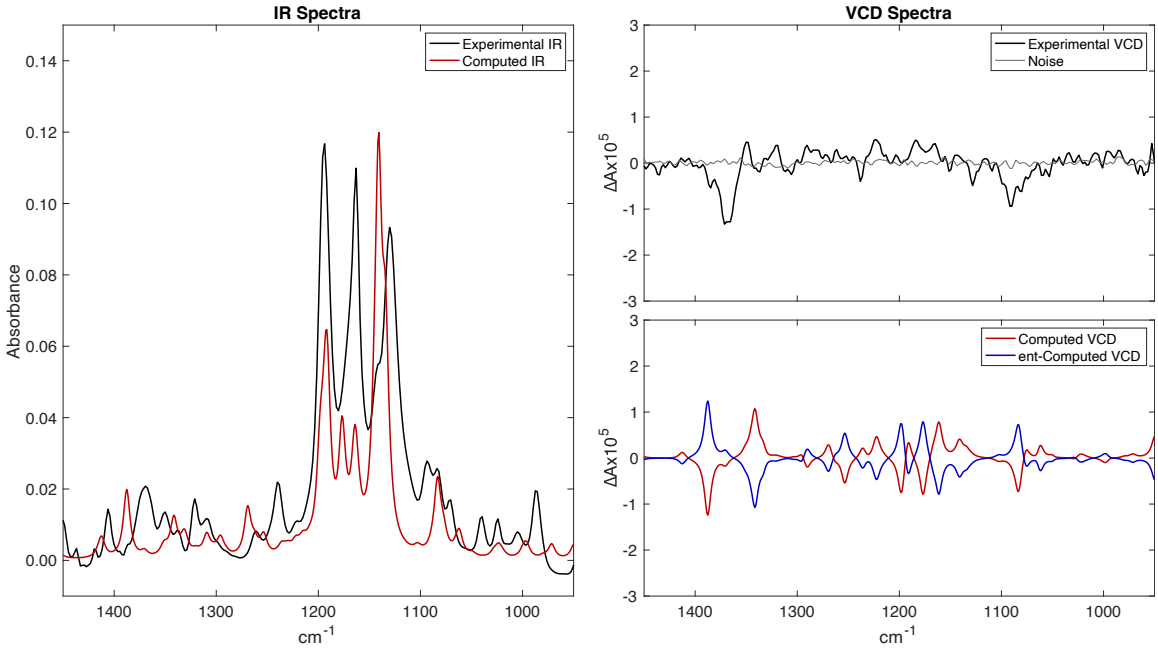

Figure 2.33 *Experimental VCD and IR spectra for product* ***115k″*** *compared to computed spectra for* ***B_endo-trans***.[a]

[a] Experimental data do not match computed data and **115k″** is not assigned as **B_endo-trans**.

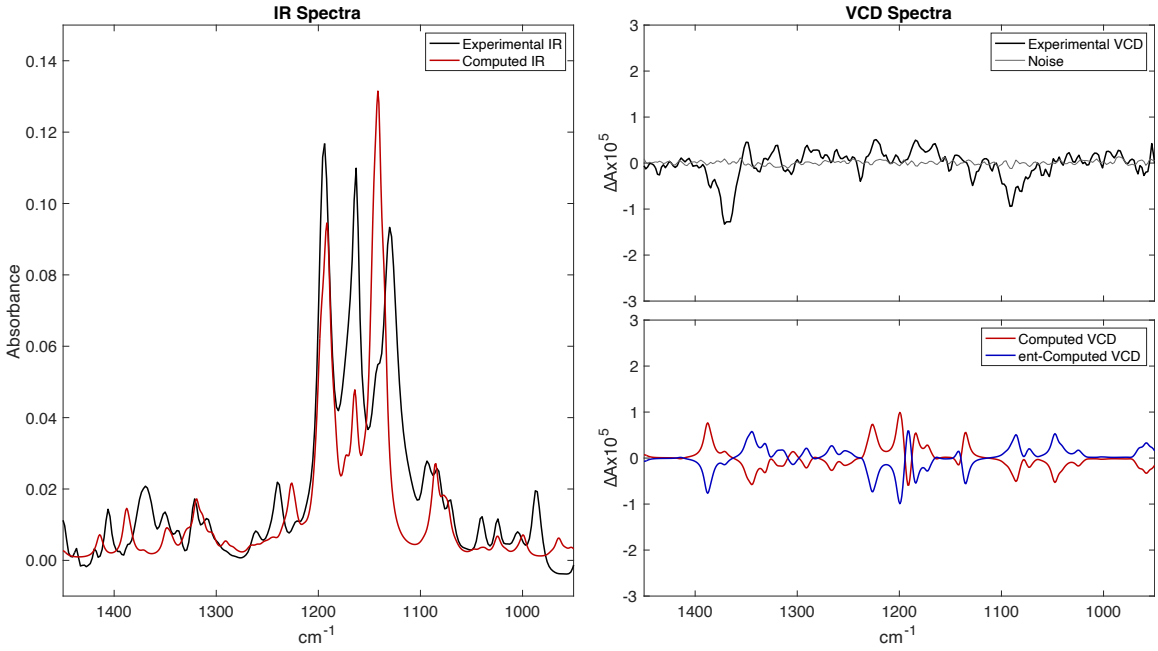

Figure 2.34 *Experimental VCD and IR spectra for product* ***115k″*** *compared to computed spectra for* ***B_exo-trans****.*[a]

[a] Experimental data do not match computed data and **115k″** is not assigned as **B_exo-trans**.

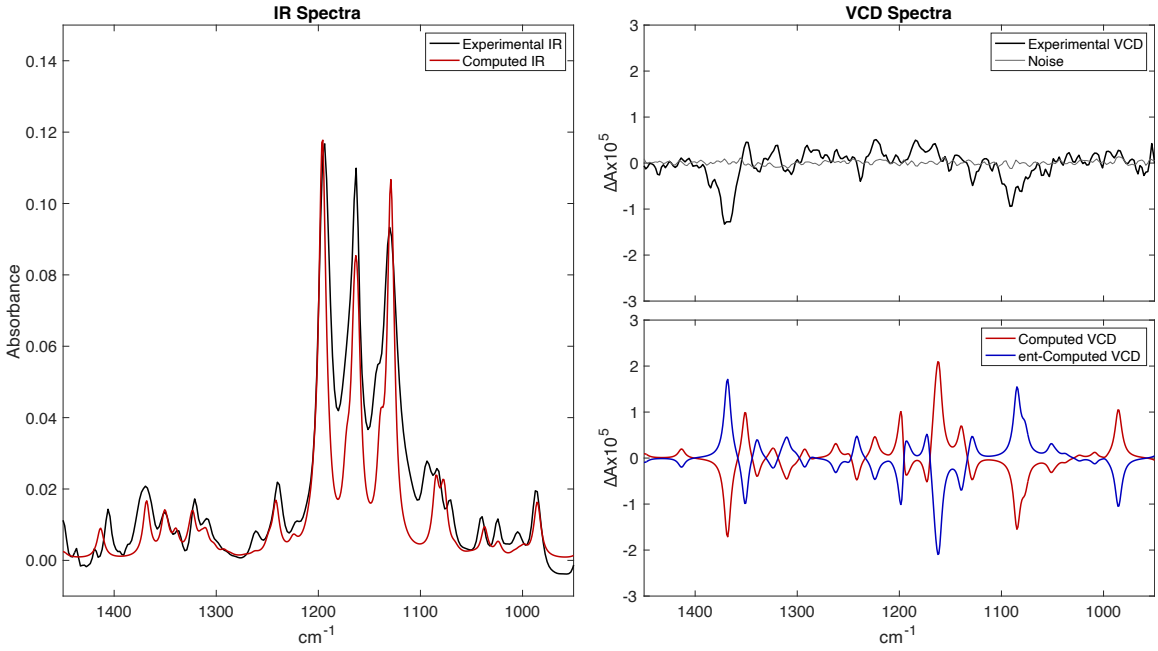

Figure 2.35 *Experimental VCD and IR spectra for product* ***115k″*** *compared to computed spectra for* ***B_endo-cis***.[a]

[a] Experimental IR spectrum is in agreement with the computed spectrum of **B_endo-cis**. Assignment of absolute stereochemistry is based the on the sign of the three most intense peaks in VCD spectrum, 1368, 1350, and 1085 cm^{-1}. These match **B_endo-cis**, the same enantiomeric series as **115k**.

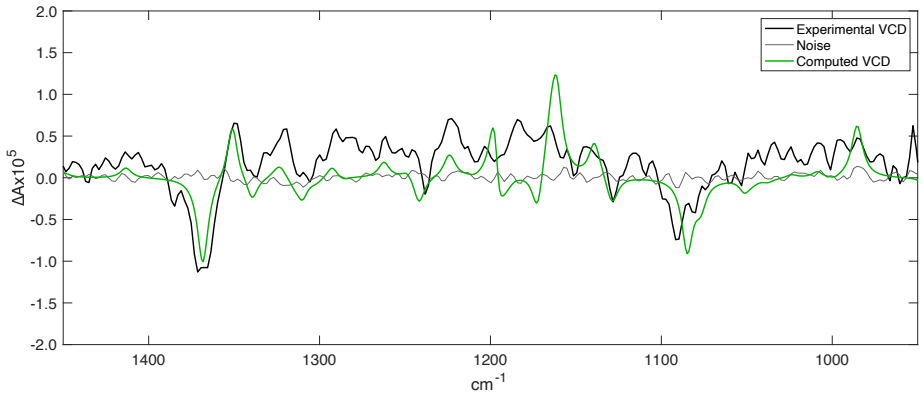

Figure 2.36 *Overlayed experimental and calculated VCD spectra for* ***115k″*** *– assigned as* ***B_endo-cis***.

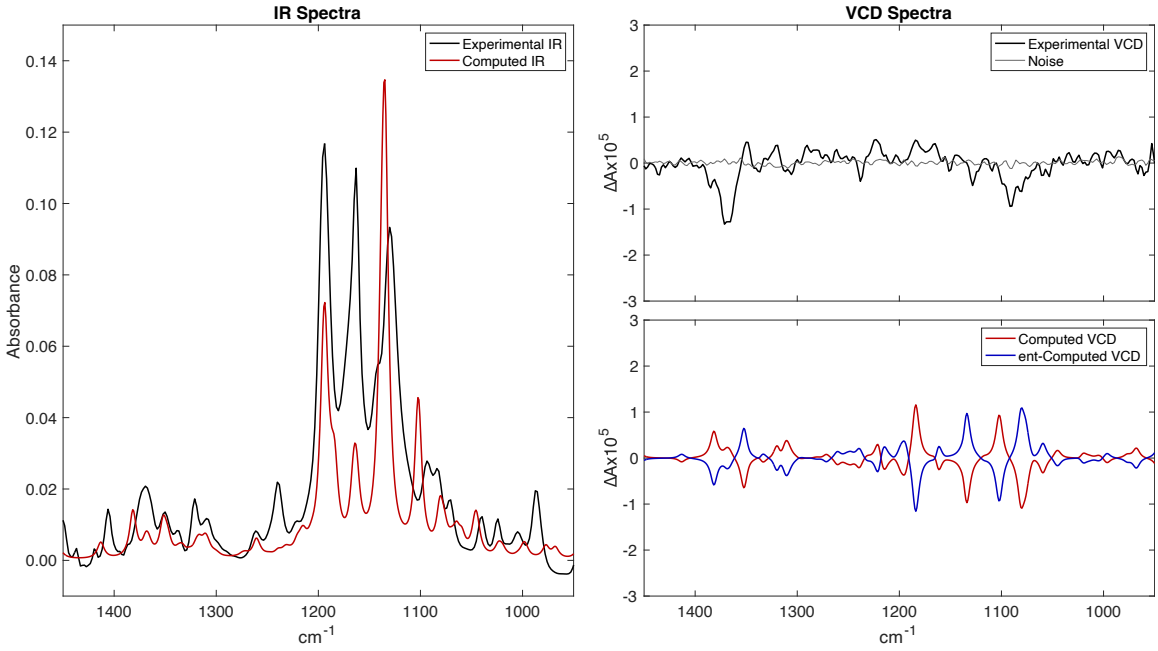

Figure 2.37 *Experimental VCD and IR spectra for product* ***115k″*** *compared to computed spectra for* ***B_exo-cis***.[a]

[a] Experimental data do not match computed data and **115k″** is not assigned as **B_exo-cis**.

2.4.4 2D nmr analysis of select compounds.

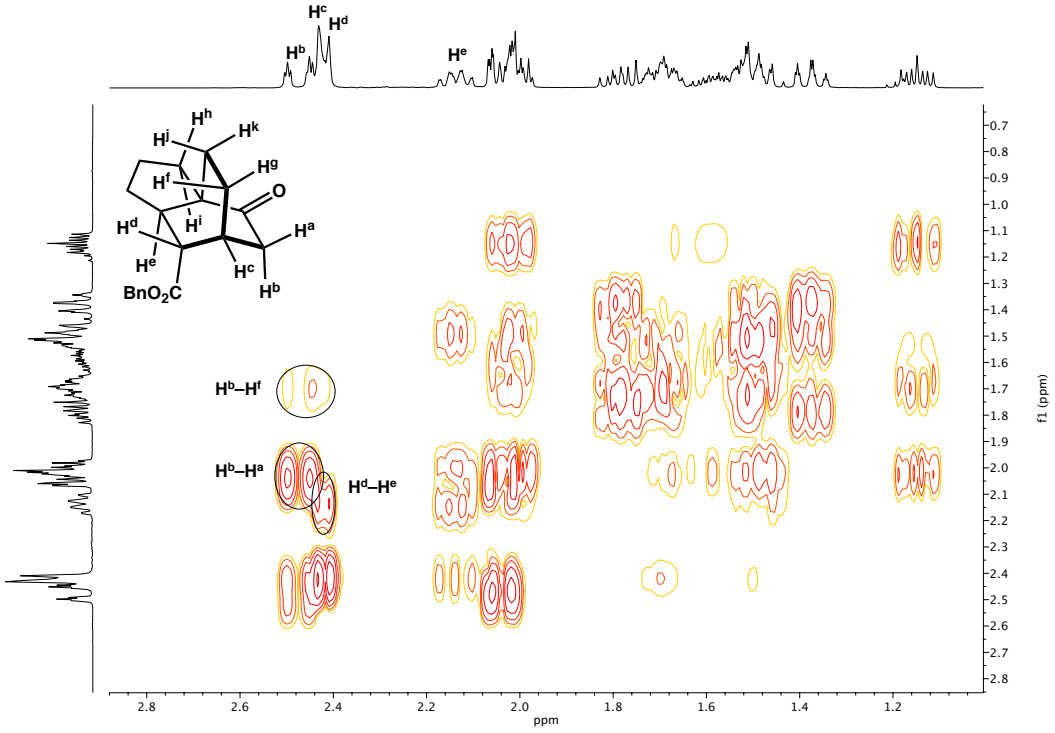

Figure 2.38 *^{1}H-^{1}H COSY NMR spectrum of* ***115a*** *(400 MHz, $CDCl_3$).*

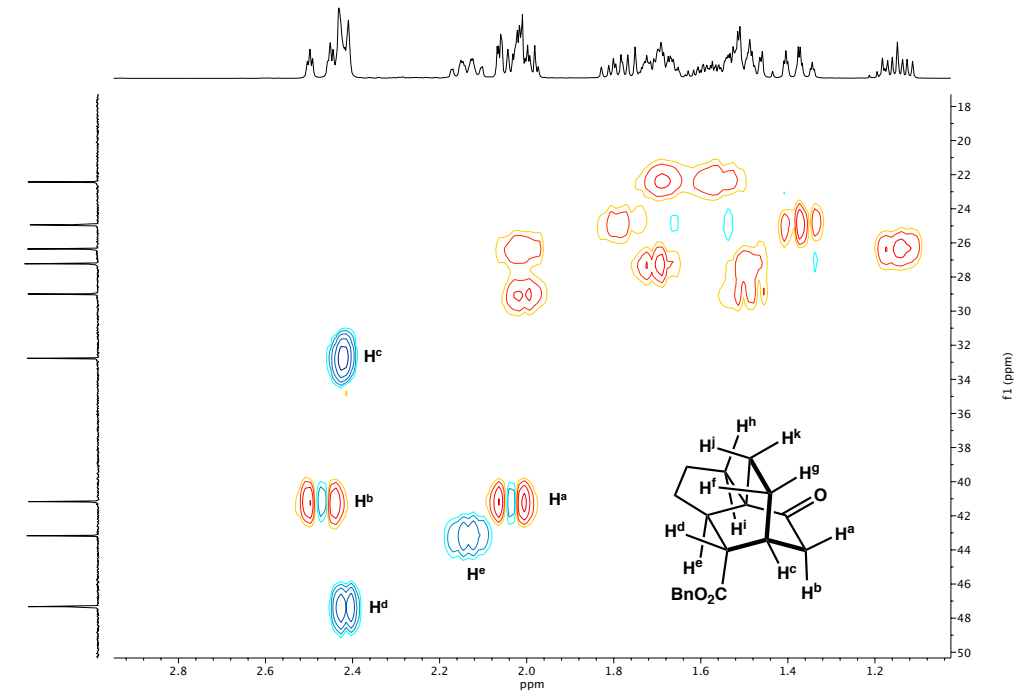

Figure 2.39 *^{1}H-^{13}C HSQC NMR spectrum of* ***115a*** *(400 MHz, $CDCl_3$).*

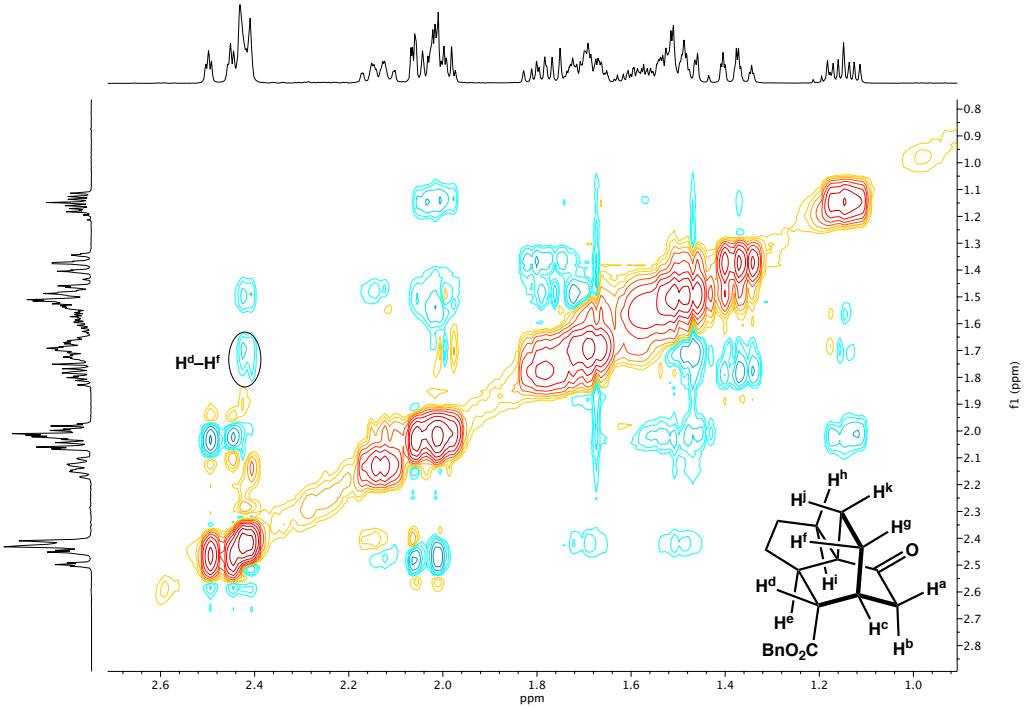

Figure 2.40 *^{1}H-^{1}H NOESY NMR spectrum of* ***115a*** *(400 MHz, $CDCl_3$).*

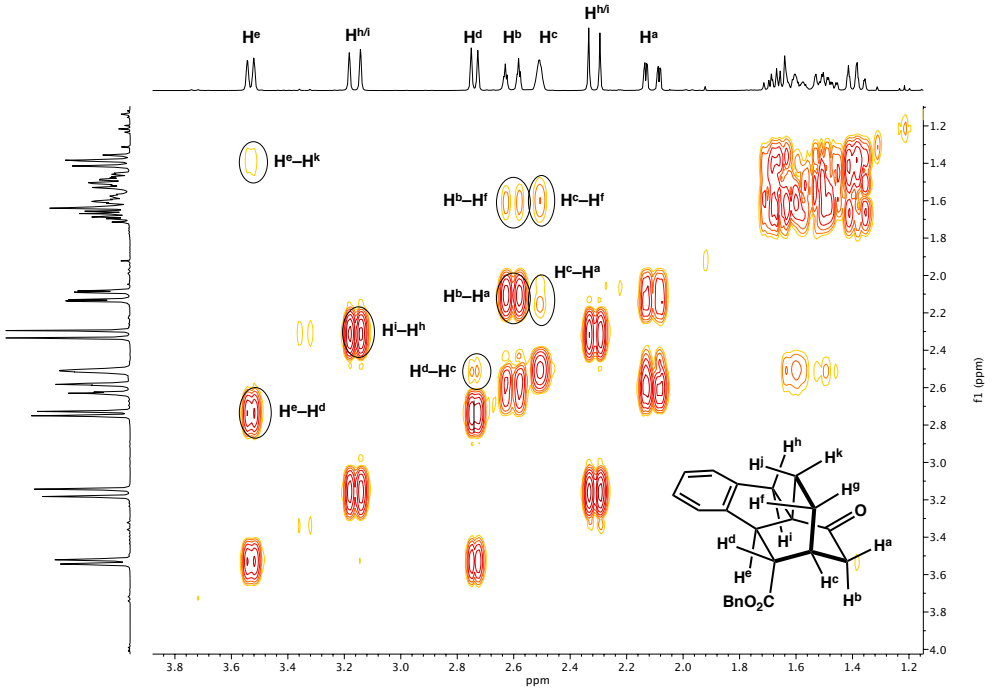

Figure 2.41 *^{1}H-^{1}H COSY NMR spectrum of* ***115p*** *(400 MHz, $CDCl_3$).*

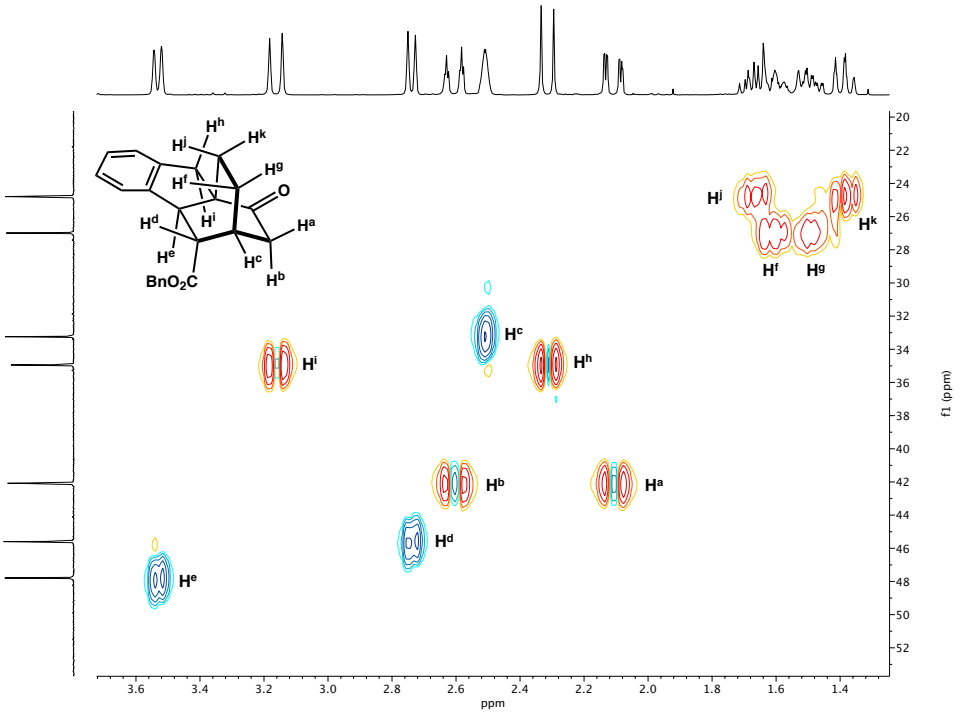

Figure 2.42 *^{1}H-^{13}C HSQC NMR spectrum of* ***115p*** *(400 MHz, $CDCl_3$).*

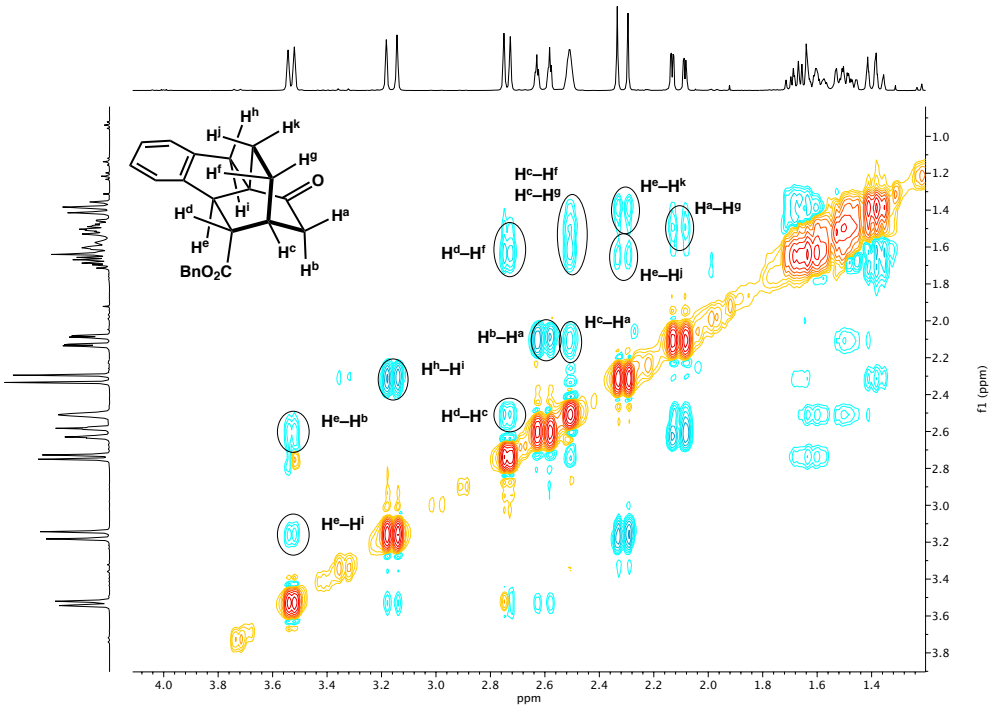

Figure 2.43 *^{1}H-^{1}H NOESY NMR spectrum of* ***115p*** *(400 MHz, $CDCl_3$).*

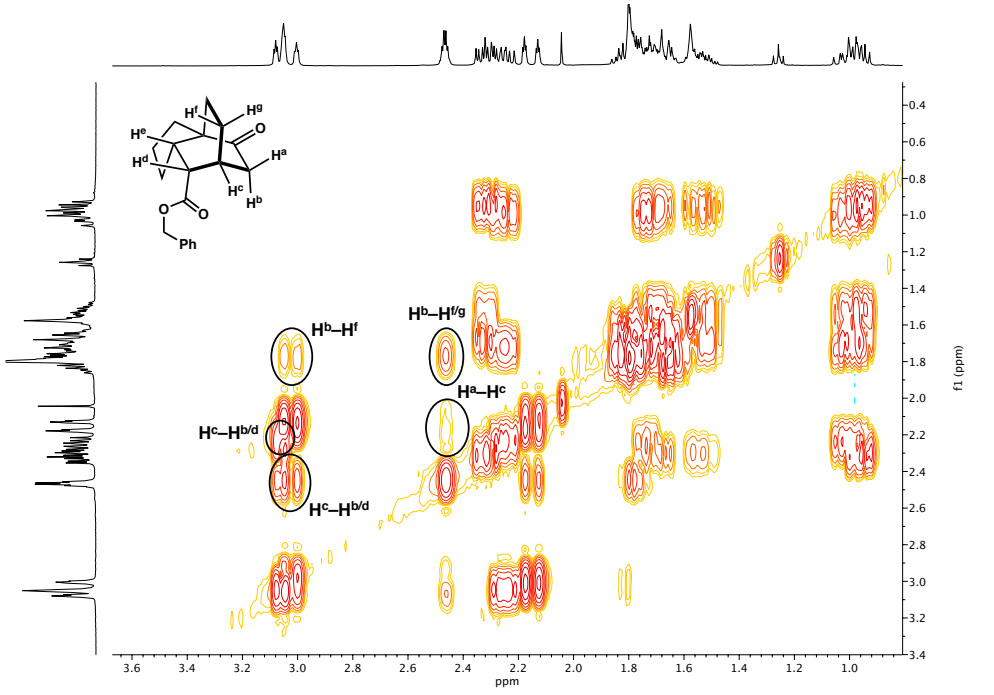

Figure 2.44 *^{1}H-^{1}H COSY NMR spectrum of* ***115q*** *(400 MHz, $CDCl_3$).*

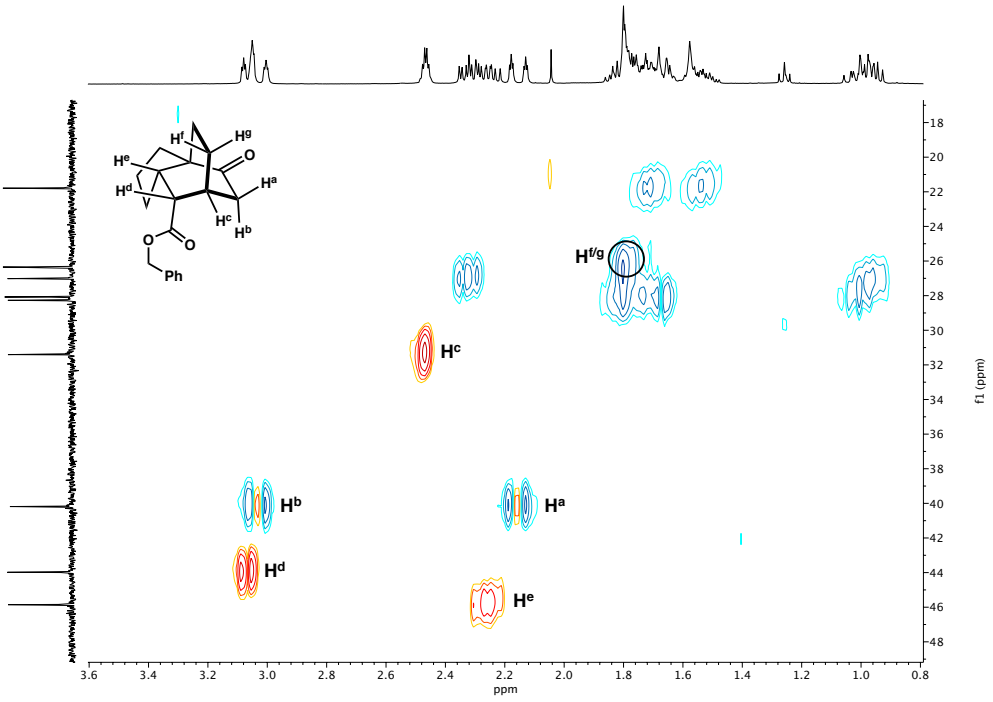

Figure 2.45 *^{1}H-^{13}C HSQC NMR spectrum of* ***115q*** *(400 MHz, $CDCl_3$).*

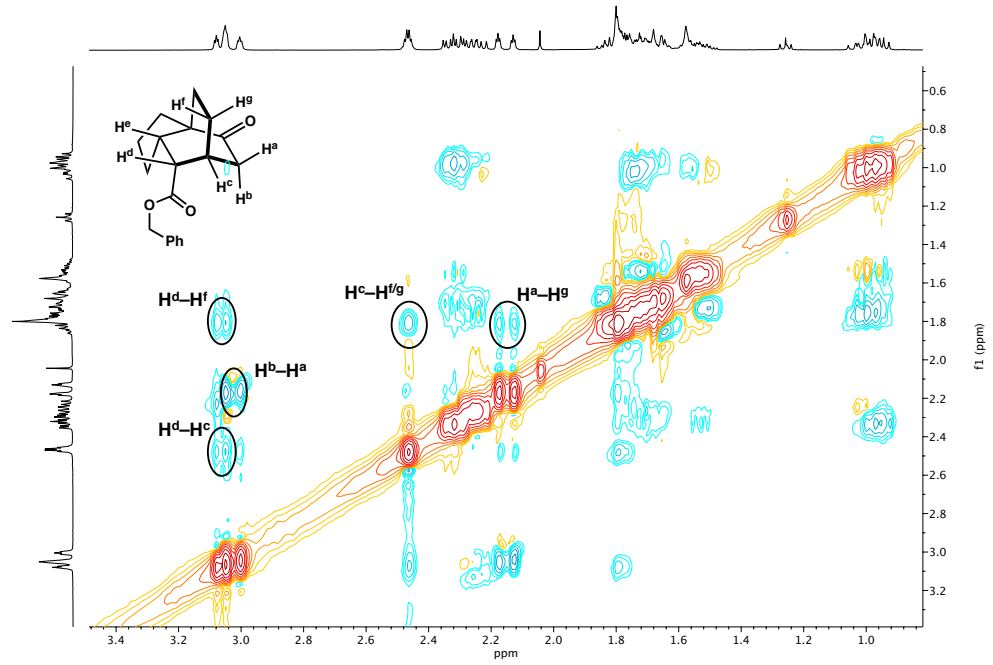

Figure 2.46 *^{1}H-^{1}H NOESY NMR spectrum of* ***115q*** *(400 MHz, $CDCl_3$).*

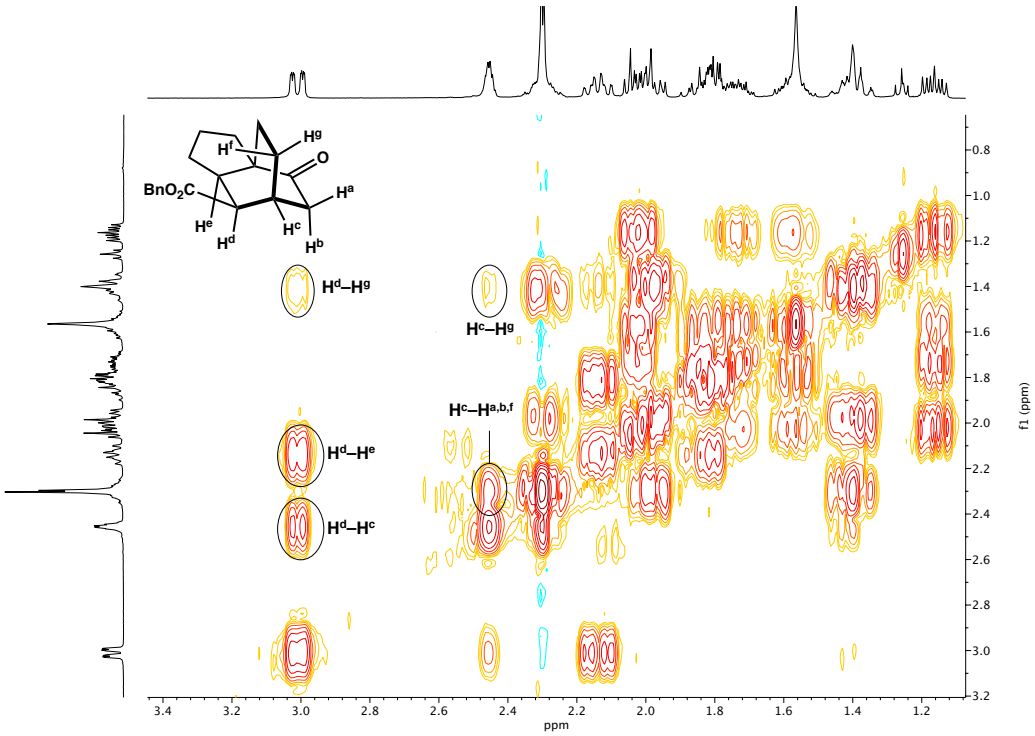

Figure 2.47 *^{1}H-^{1}H COSY NMR spectrum of* ***115q'*** *(400 MHz, $CDCl_3$).*

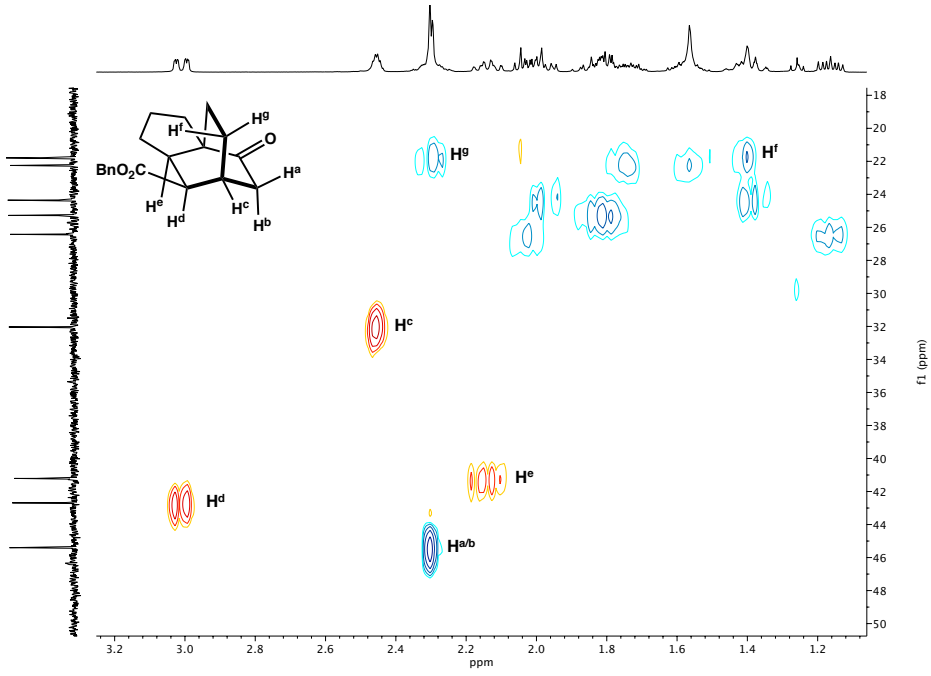

Figure 2.48 *^{1}H-^{13}C HSQC NMR spectrum of* ***115q'*** *(400 MHz, $CDCl_3$).*

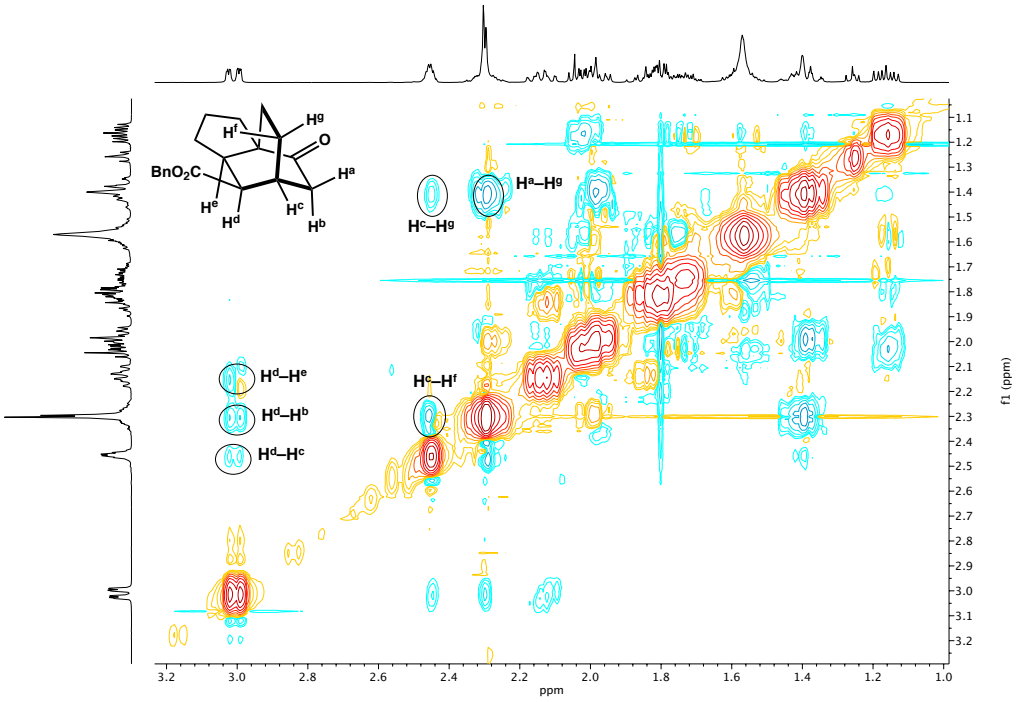

Figure 2.49 *^{1}H-^{1}H NOESY NMR spectrum of* ***115q'*** *(400 MHz, $CDCl_3$).*

2.4.5 General computational details.

General Notes

All quantum mechanics calculations were carried out with the ORCA program.[52] Geometry optimizations, harmonic frequency calculations, and single-point energy evaluations were carried out with density functional theory (DFT). The PBE0 functional[53] paired with Becke–Johnson damped D4 dispersion corrections[54], henceforth referred to as PBE0-D4, was used as it has proven a robust method for such systems in our prior studies.[55] For geometry optimization and harmonic frequency calculations, Pd is described by the def2-TZVP basis set[56] and the ECP28MWB small-core (18 explicit valence electrons) quasi-relativistic pseudopotential,[57] while C, H, N, and P are assigned the def2-SVP basis. Diffuse functions are added to oxygen (ma-def2-SVP). Herein, we refer to this composite

basis set as BS1. Geometry optimization and harmonic frequency calculations were carried out with the CPCM implicit solvation model for toluene (PhMe, $\varepsilon = 2.4$). For all calculations employing CPCM, surface charges are described by the improved Gaussian charge scheme of Neese and coworkers with a scaled Van der Waals cavity ($\alpha = 1.2$).[58] All Hessians were computed analytically. Stationary points are characterized by the correct number of imaginary vibrational modes (zero for minima and one for saddle points). Intrinsic reaction coordinate (IRC) analysis confirms the nature of transition states.[59] Cartesian coordinates of all optimized structures are included as ".xyz" files are available online in a compressed in a zip file format.

Electronic energies are further refined with single-point calculations employing the PBE0-D4 functional[60] and the def2-TZVPP basis set on all atoms (with the ECP28MWB pseudopotential for Pd) with additional diffuse functions on O (ma-def2-TZVPP). This mixed basis is henceforth referred to as BS2. Solvation was accounted for with CPCM as mentioned above (PhMe, $\varepsilon = 2.4$). Final Gibbs free energies were obtained by applying thermodynamic corrections obtained at the optimization level of theory to these refined electronic energies. Thermodynamic corrections from harmonic frequency calculations employ the quasi-ridged rotor harmonic oscillator approach to correct for the breakdown of the harmonic oscillator approximation at low vibrational frequencies.[61] Note that free energies are adjusted to a 1 M standard state. The translational (S_{trans}) and rotational entropy (S_{rot}) contributions to the Gibbs free energy calculated for a complex in condensed phase are *ca.* 40–60% of the values obtained assuming an ideal gas.[62] As suggested in the literature, S_{trans} and S_{rot} obtained by ideal gas treatment are scaled by a factor of 0.5 to

obtain the final condensed phase values.[63] Hence, the Gibbs free energy at 333.15 K is calculated as:

$$G^*_{solv} = E^{BS2}_{el,solv} + ZPE + E_{trans} + E_{rot} + E_{vib} + k_bT - T\left(S_{el} + S_{vib} + \frac{1}{2}S_{trans} + \frac{1}{2}S_{rot}\right) + \Delta G^{0\rightarrow *}$$

The resolution of identity (RI) and Chain-of-Spheres (COS) approximations are employed for efficient evaluation of Coulomb and exchange integrals, respectively.[64] The def2/J auxiliary basis[65] is employed for all atoms except oxygen, for which a suitable auxiliary was obtained via the automatic generation algorithm in the ORCA program (keyword: *AutoAux*). [66] Very fine grid settings are employed in all calculations (optimization/frequency calculations: DefGrid2, single point calculations: DefGrid3).

Conformer searching was carried out for each stationary point using the meta-dynamics-based CREST program (using GNF-FF) from the Grimme group. Duplicate conformers were removed, and low energy conformers were subsequently optimized and energies evaluated at the cheaper PBE0-D4/def2-TZVP (Pd), ma-def2-SVP (O), def2-SVP/CPCM(PhMe)//PBE-D4/def2-TZVP (Pd), ma-def2-SV(P) (O), def2-SV(P) level of theory. The final low energy conformers were further optimized at the level of theory mentioned prior. Note that for enantiodetermining transition states (such as TS2 and TS3) conformer searching also explicitly includes rotation about the Pd–O–C–C(enolate) dihedral, consideration of s-cis and s-trans ester conformations, as well as all permutations of the considered stereochemical elements.

Finally, conformational entropy [67] (entropy arising from multiple low energy thermally populated conformers) is accounted for by the *mixture of components* model of DeTar.[68] Conformational entropy (S_{conf}) is defined as:

$$S_{conf} = -R \sum \chi_i \ln (\chi_i)$$

where χ_i is the mole fraction (thermal population) of the ith conformer based on its relative free energy within the conformer ensemble. Given the computational demand for computing free energies for large ensembles of conformers, χ_i was derived from the free energies initially computed during the conformer screening process (PBE0-D4/def2-TZVP (Pd), ma-def2-SVP (O), def2-SVP/CPCM(PhMe)//PBE-D4/def2-TZVP (Pd), ma-def2-SV(P) (O), def2-SV(P))

$$G_{final} = G^*_{solv} - TS_{conf}$$

For the systems at hand, values of TS_{conf} (at 333.15 K) can be on the order of magnitude of a few kcal/mol.

Comparison of Barrier Heights to Inner-sphere Reductive Elimination

Employing cyclohexanone-derived Pd enolate as a model system (**189, 190, 191**), the barrier to inner-sphere reductive elimination was investigated while varying substitution on the allyl moiety (Figure 2.50).

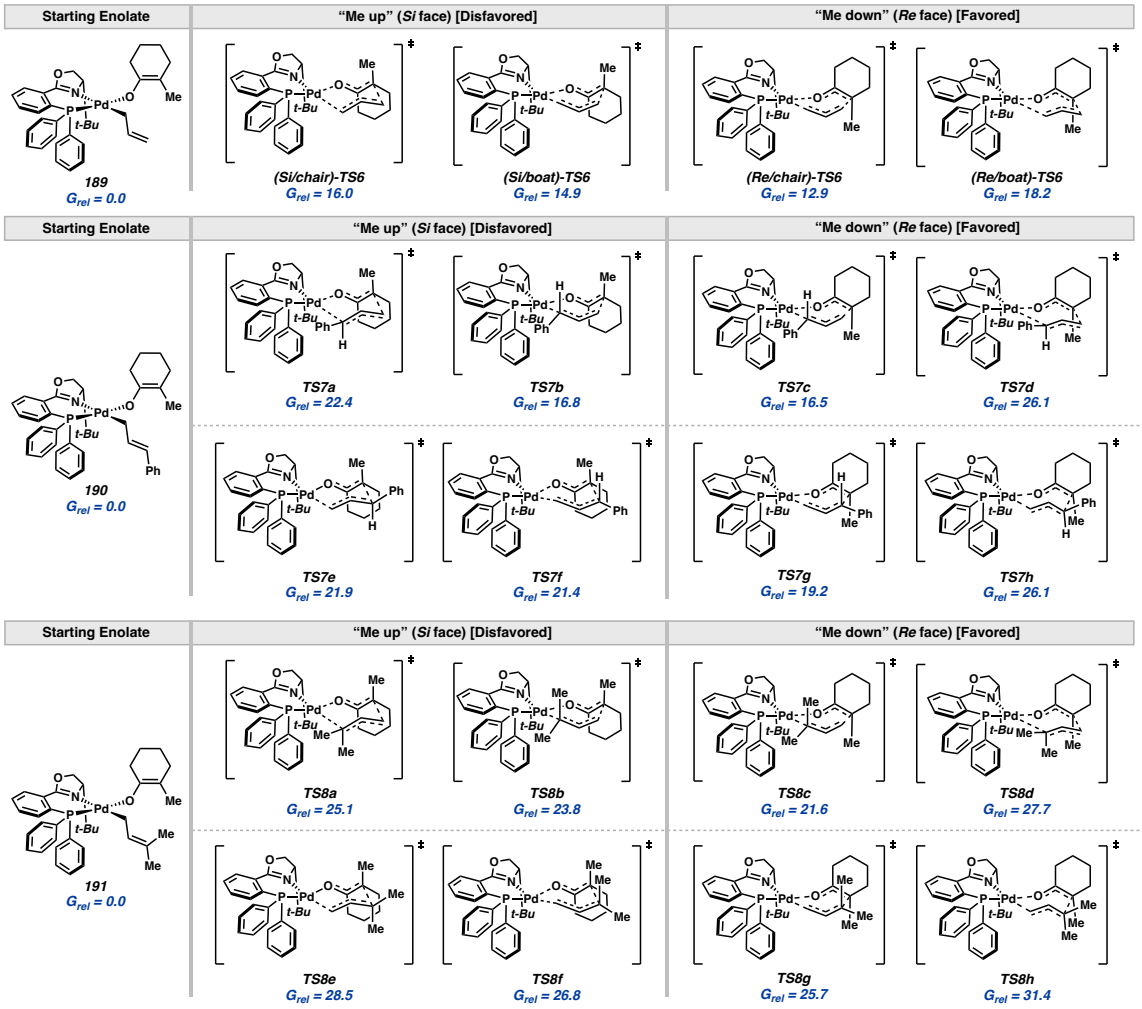

Figure 2.50 *Relative free energies for various inner-sphere reductive elimination transition states from allyl (**189**), cinnamyl (**190**), and prenyl (**191**) complexes.*[a]

[a] Gibbs free energies in kcal/mol computed at the PBE0-D4/BS2/CPCM(PhMe)//PBE0-D4/BS1/CPCM(PhMe) level of theory at 333.15 K.

Mechanism of Catalyst Turnover

Of all the sampled transition states, we found the outer-sphere and N-detached inner-sphere pathways to be highly competitive and lowest in energy. Additional transition states were

also explored, and the lowest energy pathway of each type of mechanism are shown in the following table.

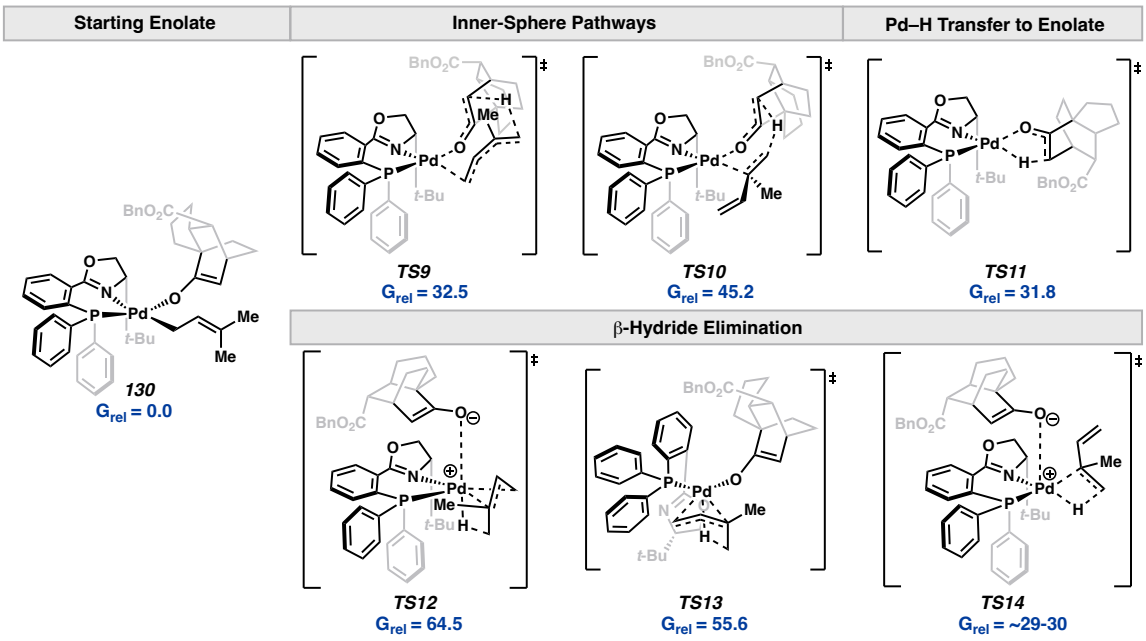

Figure 2.51 *Relative free energies for various proton transfer transition states from post-cycloaddition enolate* ***130****.*[a]

[a] Gibbs free energies in kcal/mol computed at the PBE0-D4/BS2/CPCM(PhMe)//PBE0-D4/BS1/CPCM(PhMe) level of theory at 333.15 K.

Mechanism of Premature Protonation

Analogous to the catalyst turnover mechanism, N-detached inner-sphere pathways were found to be lowest-energy for premature protonation. Of these transition states (**TS15a** and **TS15b**) that would yield enantiomeric protonation products, the lowest-energy **TS15a** provides the enantiomer consistent with the major reaction product. In addition, an outer-sphere pathway (**TS16**) was also found to be competitive.

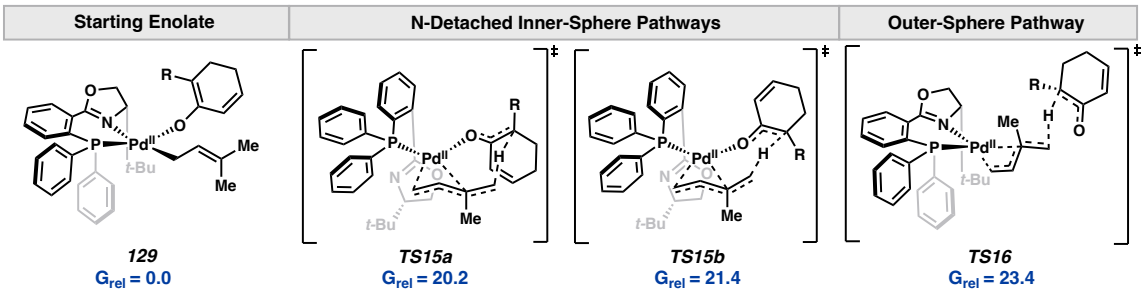

Figure 2.52 *Relative free energies for various proton transfer transition states from pre-cycloaddition enolate* ***129****.*[a]

[a] Gibbs free energies in kcal/mol computed at the PBE0-D4/BS2/CPCM(PhMe)//PBE0-D4/BS1/CPCM(PhMe) level of theory at 333.15 K.

Intrinsic Bonding Orbital (IBO) Analysis of Inner-sphere Proton Transfer

IBO analysis along the reaction coordinate of the N-detached inner-sphere proton transfer to post-cycloaddition enolate confirms the role of prenyl as a proton source.

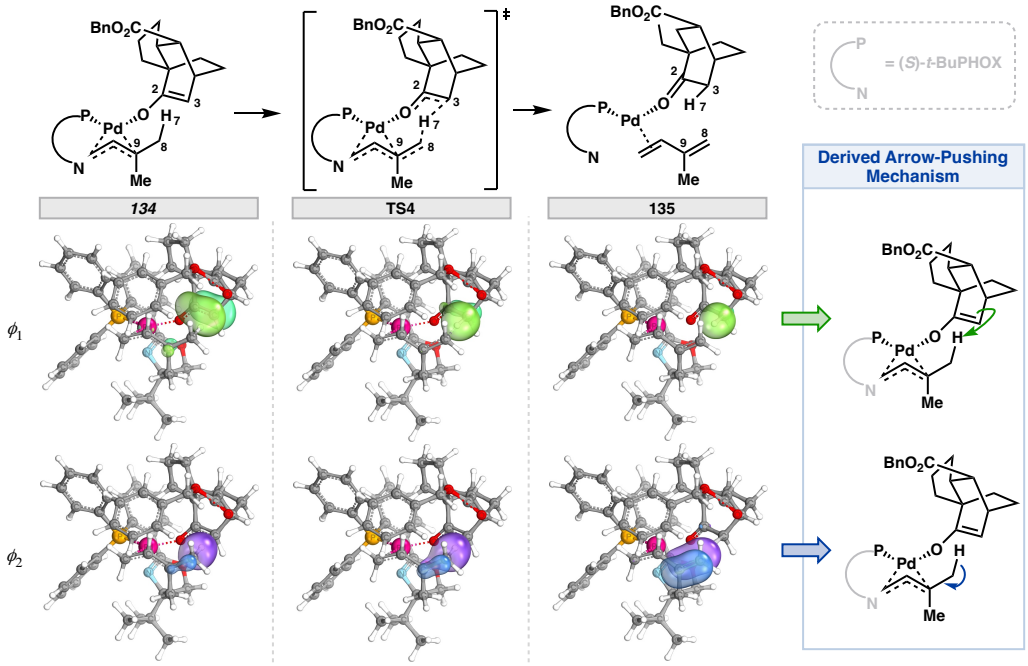

Figure 2.53 *IBO analysis of N-detached inner-sphere mechanism and corresponding derived arrow-pushing mechanism.*

pKa Calculations and Thermodynamics of Outer-Sphere Proton Transfer

The pK_a values of the π-allyl Pd complex **88** and ketones were calculated, and the results verify that the proton transfers to both pre- and post-cycloaddition enolates are thermodynamically favorable.

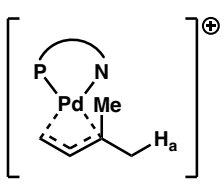

192

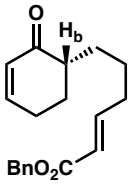

123a

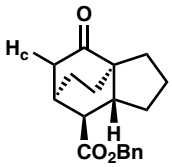

115a

Compound	Proton	pK_a in water	pK_a in DMSO
192	H_a	20.0	19.5
123a	H_b	30.1	30.3
115a	H_c	31.3	30.8

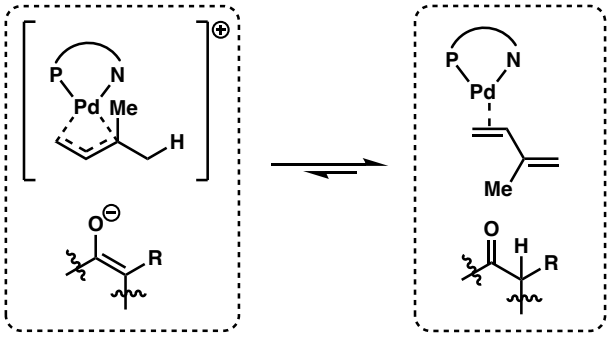

Figure 2.54 *Computed pKa values of cationic π-allyl Pd complex* ***192*** *and ketones* ***123a*** *and* ***115a****.*

Enantiodetermining [4+2] cycloaddition

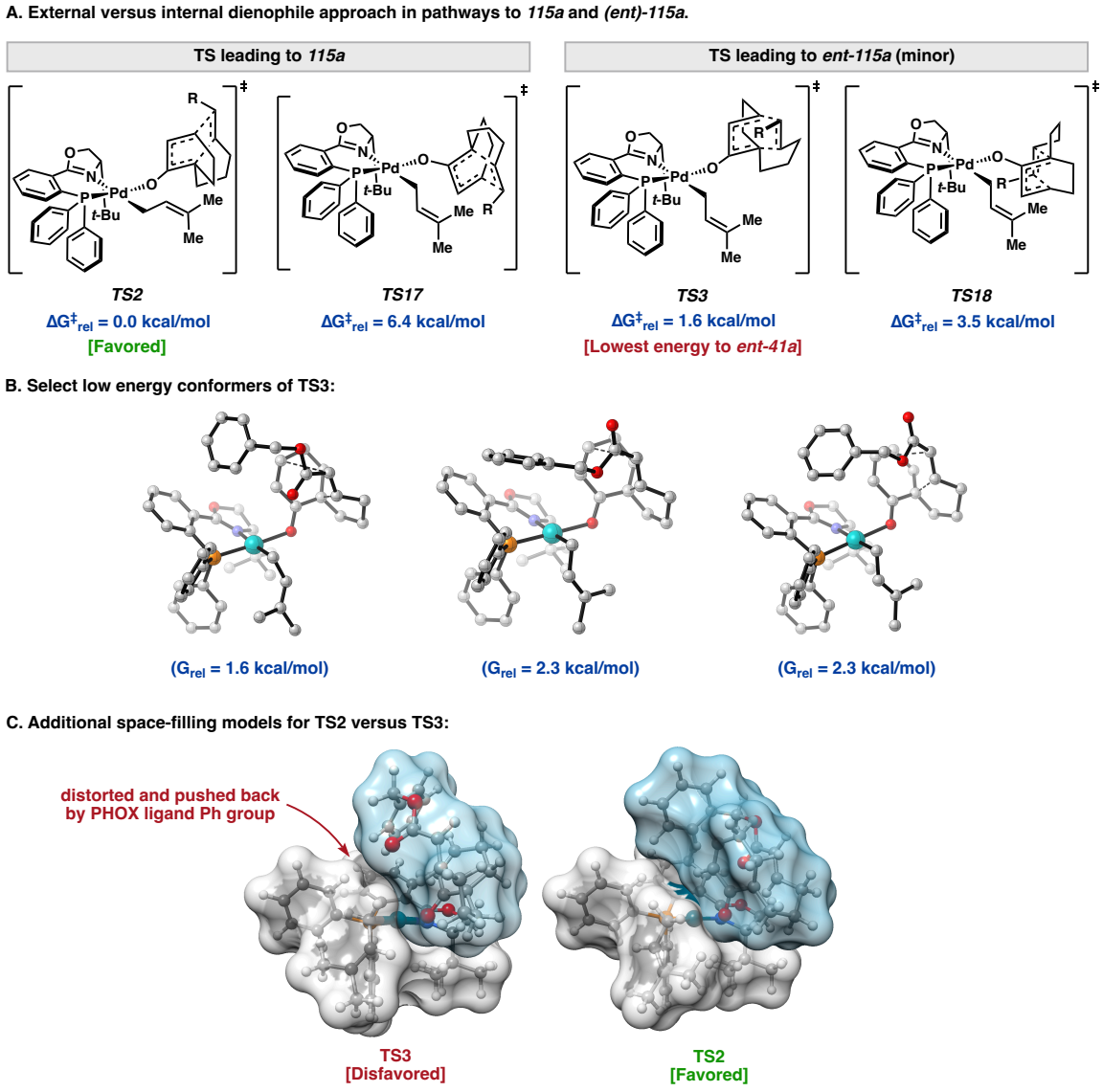

Figure 2.55 *(A) Comparison of internal versus external dienophile approach to both enantiotopic diene faces. (B) Select low energy conformers of* ***TS3*** *(allyl isomers not pictured). (C) Additional space-filling models for* ***TS2*** *and* ***TS3****.*

2.5 REFERENCES AND NOTES

(1) (a) Christoffers, J.; Mann, A. Enantioselective Construction of Quaternary Stereocenters. *Angew. Chem. Int. Ed.* **2001**, *40*, 4591–4597. (b) Douglas, C. J.; Overman, L. E. Catalytic Asymmetric Synthesis of All-Carbon Quaternary Stereocenters. *Proc. Natl. Acad. Sci. U.S.A.* **2004**, *101*, 5363–5367.

(2) (a) Liu, Y.; Han, S.-J.; Liu, W.-B.; Stoltz, B. M. Catalytic Enantioselective Construction of Quaternary Stereocenters: Assembly of Key Building Blocks for the Synthesis of Biologically Active Molecules. *Acc. Chem. Res.* **2015**, *48*, 740–751. (b) Trost, B. M.; Crawley, M. L. Asymmetric Transition-Metal-Catalyzed Allylic Alkylations: Applications in Total Synthesis. *Chem. Rev.* **2003**, *103*, 2921–2944.

(3) Cusumano, A. Q.; Stoltz, B. M.; Goddard, W. A. Reaction Mechanism, Origins of Enantioselectivity, and Reactivity Trends in Asymmetric Allylic Alkylation: A Comprehensive Quantum Mechanics Investigation of a C(sp3)–C(sp3) Cross-Coupling. J. *Am. Chem. Soc.* **2020**, *142*, 13917–13933.

(4) (a) Keith, J. A.; Behenna, D. C.; Mohr, J. T.; Ma, S.; Marinescu, S. C.; Oxgaard, J.; Stoltz, B. M.; Goddard, W. A. The Inner-Sphere Process in the Enantioselective Tsuji Allylation Reaction with (S)-t-Bu-Phosphinooxazoline Ligands. *J. Am. Chem. Soc.* **2007**, *129*, 11876–11877. (b) Keith, J. A.; Behenna, D. C.; Sherden, N.; Mohr, J. T.; Ma, S.; Marinescu, S. C.; Nielsen, R. J.; Oxgaard, J.; Stoltz, B. M.; Goddard, W. A. The Reaction Mechanism of the Enantioselective Tsuji Allylation: Inner-Sphere and Outer-Sphere Pathways, Internal Rearrangements, and Asymmetric C–C Bond Formation. *J. Am. Chem. Soc.* **2012**, *134*, 19050–19060. (C) McPherson,

K. E.; Croatt, M. P.; Morehead, A. T.; Sargent, A. L. DFT Mechanistic Investigation of an Enantioselective Tsuji–Trost Allylation Reaction. *Organometallics* **2018**, *37*, 3791–3802.

(5) Behenna, D. C.; Stoltz, B. M. The Enantioselective Tsuji Allylation. *J. Am. Chem. Soc.* **2004**, *126*, 15044–15045.

(6) Mohr, J. T.; Behenna, D. C.; Harned, A. M.; Stoltz, B. M. Deracemization of Quaternary Stereocenters by Pd-Catalyzed Enantioconvergent Decarboxylative Allylation of Racemic β-Ketoesters. *Angew. Chem. Int. Ed.* **2005**, *44*, 6924–6927.

(7) (a) Mohr, J. T.; Nishimata, T.; Behenna, D. C.; Stoltz, B. M. Catalytic Enantioselective Decarboxylative Protonation. *J. Am. Chem. Soc.* **2006**, *128*, 11348–11349. (b) Marinescu, S. C.; Nishimata, T.; Mohr, J. T.; Stoltz, B. M. Homogeneous Pd-Catalyzed Enantioselective Decarboxylative Protonation. *Org. Lett.* **2008**, *10*, 1039–1042.

(8) Streuff, J.; White, D. E.; Virgil, S. C.; Stoltz, B. M. A Palladium-Catalysed Enolate Alkylation Cascade for the Formation of Adjacent Quaternary and Tertiary Stereocentres. *Nature Chem* **2010**, *2*, 192–196.

(9) Inanaga, K.; Wollenburg, M.; Bachman, S.; Hafeman, N. J.; Stoltz, B. M. Catalytic Enantioselective Synthesis of Carbocyclic and Heterocyclic Spiranes via a Decarboxylative Aldol Cyclization. *Chem. Sci.* **2020**, *11*, 7390–7395.

(10) (a) Ihara, M.; Ishida, Y.; Abe, M.; Toyota, M.; Fukumoto, K.; Kametani, T. Stereocontrolled Synthesis of the CDF Part of Aconitum Alkaloids via Intramolecular Double Michael Reaction. *J. Chem. Soc., Perkin Trans. 1* **1988**, 5,

1155–1163. See also: (b) Ihara, M.; Makita, K.; Tokunaga, Y.; Fukumoto, K. Stereoselective Formation of Three Carbon-Carbon Bonds by Cascade Reaction with Enolate Anion: Synthesis of Tricyclo[6.2.2.$0^{1,6}$]Dodecane and Tricyclo[5.3.1.$0^{3,8}$]Undecane Derivatives. *J. Org. Chem.* **1994**, *59*, 6008–6013. (c) Ihara, M.; Toyota, M.; Fukumoto, K.; Kametani, T. Intramolecular Double Michael Reaction. Part II. Synthesis of Isoatisirene Type Compound. *Tetrahedron Lett.* **1984**, *25*, 3235–3238. (d) Ihara, M.; Suzuki, M.; Fukumoto, K.; Kabuto, C. Asymmetric Total Synthesis of Atisine via Intramolecular Double Michael Reaction. *J. Am. Chem. Soc.* **1990**, *112*, 1164–1171.

(11) All quantum mechanics calculations were carried out with the ORCA program. Neese, F. Software Update: The ORCA Program System—Version 5.0. *WIREs Computational Molecular Science* **2022**, *12*, e1606.

(12) Sherden, N. H.; Behenna, D. C.; Virgil, S. C.; Stoltz, B. M. Unusual Allylpalladium Carboxylate Complexes: Identification of the Resting State of Catalytic Enantioselective Decarboxylative Allylic Alkylation Reactions of Ketones. *Angew. Chem. Int. Ed.* **2009**, *48*, 6840–6843.

(13) Paton, R. S.; Kim, S.; Ross, A. G.; Danishefsky, S. J.; Houk, K. N. Experimental Diels–Alder Reactivities of Cycloalkenones and Cyclic Dienes Explained through Transition-State Distortion Energies. *Angew. Chem. Int. Ed.* **2011**, *50*, 10366–10368.

(14) Error bars are present for **114f** to **115f**/**123f** – they are smaller than the marker size in the figure.

(15) Bennett, N. B.; Duquette, D. C.; Kim, J.; Liu, W.-B.; Marziale, A. N.; Behenna, D. C.; Virgil, S. C.; Stoltz, B. M. Expanding Insight into Asymmetric Palladium-Catalyzed Allylic Alkylation of N-Heterocyclic Molecules and Cyclic Ketones. *Chem. Eur. J.* **2013**, *19*, 4414–4418.

(16) Unfortunately, attempts to further disfavor **TS3** by ortho-substitution of the PHOX ligand phenyl groups thwarted reactivity.

(17) (a) Knizia, G. Intrinsic Atomic Orbitals: An Unbiased Bridge between Quantum Theory and Chemical Concepts. *J. Chem. Theory Comput.* **2013**, *9*, 4834–4843. (b) Knizia, G.; Klein, J. E. M. N. Electron Flow in Reaction Mechanisms—Revealed from First Principles. *Angew. Chem. Int. Ed.* **2015**, *54*, 5518–5522.

(18) (a) Trost, B. M. When Is a Proton Not a Proton? *Chem. Eur. J.* **1998**, *4*, 2405–2412. See also: (b) Xu, L.; Hilton, M. J.; Zhang, X.; Norrby, P.-O.; Wu, Y.-D.; Sigman, M. S.; Wiest, O. Mechanism, Reactivity, and Selectivity in Palladium-Catalyzed Redox-Relay Heck Arylations of Alkenyl Alcohols. *J. Am. Chem. Soc.* **2014**, *136*, 1960–1967.

(19) Note that on smaller scales (0.02 mmol) the ratio of ***D*-115f** to ***D*-123f** is 6.7:1 – in accord with a primary KIE. We hypothesize this may arise from the highly temperature-dependent nature of the product distribution paired with less homogenous reaction solution temperature on larger scales.

(20) McLean, E. B.; Mooney, D. T.; Burns, D. J.; Lee, A.-L. Direct Hydrodecarboxylation of Aliphatic Carboxylic Acids: Metal- and Light-Free. *Org. Lett.* **2022**, *24* 686–691.

(21) Nishiyama, Y.; Han-ya, Y.; Yokoshima, S.; Fukuyama, T. Total Synthesis of (–)-Lepenine. *J. Am. Chem. Soc.* **2014**, *136*, 6598–6601.

(22) Kim, K. E.; Sakazaki, Y.; Stoltz, B. M. Synthesis of Non-Natural Cyanthiwigin–Gagunin Hybrids through Late-Stage Diversification of the Cyanthiwigin Natural Product Core. *Tetrahedron* **2020**, *76*, 130755.

(23) Yang, T.-F.; Chang, C.-Y.; Lin, W.-F. Rearrangement of Acyclic-Alkyl [3.2.1]Bicyclic Alcohols to Free Methylene Dimethyl Alkyl [2.2.2]Bicyclic Octanes: Application to Preparation of Stereospecific Novel Sesquiterpene and Terpenoids. *Tetrahedron Letters* **2015**, *56*, 801–804.

(24) Song, L.; Zhu, G.; Liu, Y.; Liu, B.; Qin, S. Total Synthesis of Atisane-Type Diterpenoids: Application of Diels–Alder Cycloadditions of Podocarpane-Type Unmasked *Ortho*- Benzoquinones. *J. Am. Chem. Soc.* **2015**, *137*, 13706–13714.

(25) Neufeldt, S. R.; Sanford, M. S. O-Acetyl Oximes as Transformable Directing Groups for Pd-Catalyzed C–H Bond Functionalization. *Org. Lett.* **2010**, *12*, 532–535.

(26) Pangborn, A. M.; Giardello, M. A.; Grubbs, R. H.; Rosen, R. K.; Timmers, F. J. Safe and Convenient Procedure for Solvent Purification. *Organometallics* **1996**, *15*, 1518–1520.

(27) McDougal, N. T.; Streuff, J.; Mukherjee, H.; Virgil, S. C.; Stoltz, B. M. Rapid synthesis of an electron-deficient *t*-BuPHOX ligand: cross-coupling of aryl bromides with secondary phosphine oxides. *Tetrahedron Lett.* **2010**, *51*, 5550–5554.

(28) Ando, K.; Narumiya, K.; Takada, H.; Teruya, T. Z-Selective Intramolecular Horner−Wadsworth−Emmons Reaction for the Synthesis of Macrocyclic Lactones. *Org. Lett.* **2010**, *12*, 1460–1463.

(29) Shelkov, R.; Nahmany, M.; Melman, A. Selective Esterifications of Alcohols and Phenols through Carbodiimide Couplings. *Org. Biomol. Chem.* **2004**, *2*, 397–401.

(30) Taguchi, T.; Sasaki, H.; Shibuya, A.; Morikawa, T. Regio- and Stereoselective Synthesis of Gem-Difluorocyclopropanes Using 4-Bromo-4,4-Difluorocrotonate. *Tetrahedron Lett.* **1994**, *35*, 913–916.

(31) Fornicola, R. S.; Subburaj, K.; Montgomery, J. A New Entry to the Isogeissoschizoid Skeleton. *Org. Lett.* **2002**, *4*, 615–617.

(32) Fillion, E.; Dumas, A. M. Synthesis of Fused 4,5-Disubstituted Indole Ring Systems by Intramolecular Friedel−Crafts Acylation of 4-Substituted Indoles. *J. Org. Chem.* **2008**, *73*, 2920–2923.

(33) Brandt, D.; Dittoo, A.; Bellosta, V.; Cossy, J. Synthetic Approach to Wortmannilactone C. *Org. Lett.* **2015**, *17*, 816–819.

(34) Fulton, T. J.; Cusumano, A. Q.; Alexy, E. J.; Du, Y. E.; Zhang, H.; Houk, K. N.; Stoltz, B. M. Global Diastereoconvergence in the Ireland–Claisen Rearrangement of Isomeric Enolates: Synthesis of Tetrasubstituted α-Amino Acids. *J. Am. Chem. Soc.* **2020**, *142*, 21938–21947.

(35) Touchard, F. P.; Capelle, N.; Mercier, M. Efficient and Scalable Protocol for the Z-Selective Synthesis of Unsaturated Esters by Horner–Wadsworth–Emmons Olefination. *Adv. Synth. Catal.* **2005**, *347*, 707–711.

(36) Romano, C.; Fiorito, D.; Mazet, C. Remote Functionalization of α,β-Unsaturated Carbonyls by Multimetallic Sequential Catalysis. *J. Am. Chem. Soc.* **2019**, *141*, 16983–16990.

(37) Sureshbabu, R.; Saravanan, V.; Dhayalan, V.; Mohanakrishnan, A. K. Lewis Acid Mediated One-Pot Synthesis of Aryl/Heteroaryl-Fused Carbazoles Involving a Cascade Friedel–Crafts Alkylation/Electrocyclization/Aromatization Reaction Sequence. *Eur. J. Org. Chem.* **2011**, 922–935.

(38) Mukaiyama, T.; Matsuo, J.; Yanagisawa, M. A New and Efficient Method for Oxidation of Various Alcohols by Using N-Tert-Butyl Phenylsulfinimidoyl Chloride. *Chem. Lett.* **2000**, *29*, 1072–1073.

(39) Inanaga, K.; Wollenburg, M.; Bachman, S.; Hafeman, N. J.; Stoltz, B. M. Catalytic Enantioselective Synthesis of Carbocyclic and Heterocyclic Spiranes via a Decarboxylative Aldol Cyclization. *Chem. Sci.* **2020**, *11*, 7390–7395.

(40) Mohr, J. T.; Behenna, D. C.; Harned, A. M.; Stoltz, B. M. Deracemization of Quaternary Stereocenters by Pd-Catalyzed Enantioconvergent Decarboxylative Allylation of Racemic β-Ketoesters. *Angew. Chem. Int. Ed.* **2005**, *44*, 6924–6927.

(41) Hierold, J.; Lupton, D. W. Synthesis of Spirocyclic γ-Lactones by Cascade Beckwith–Dowd Ring Expansion/Cyclization. *Org. Lett.* **2012**, *14*, 3412–3415.

(42) Trost, B. M.; Xu, J. The O-Acylation of Ketone Enolates by Allyl 1H-Imidazole-1-Carboxylate Mediated with Boron Trifluoride Etherate: A Convenient Procedure for the Synthesis of Substituted Allyl Enol Carbonates. *J. Org. Chem.* **2007**, *72*, 9372–9375.

(43) Prepared following ref. 42 with 3-(methyl-d_3)but-2-en-4,4,4-d_3-1-ol (Mosaferi, S.; Jelley, R. E.; Fedrizzi, B.; Barker, D. Scalable Synthesis of the Aroma Compounds D6-β-Ionone and D6-β-Cyclocitral for Use as Internal Standards in Stable Isotope Dilution Assays. *Tetrahedron Lett.* **2020**, *61*, 152642.

(44) Shimizu, I.; Tsuji, J. Palladium-Catalyzed Decarboxylation-Dehydrogenation of Allyl β-Oxo Carboxylates and Allyl Enol Carbonates as a Novel Synthetic Method for α-Substituted α,β-Unsaturated Ketones. *J. Am. Chem. Soc.* **1982**, *104*, 5844–5846.

(45) Knapp, S.; Yang, C.; Pabbaraja, S.; Rempel, B.; Reid, S.; Withers, S. G. Synthesis and Kinetic Analysis of the N-Acetylhexosaminidase Inhibitor XylNAc-Isofagomine. *J. Org. Chem.* **2005**, *70*, 7715–7720.

(46) Szczesńiak, P.; Pieczykolan, M.; Steck, S. The Synthesis of α,α-Disubstituted α-Amino Acids via Ichikawa Rearrangement. *J. Org. Chem.* **2016**, *81*, 1057–1074.

(47) Srikrishna, A.; Kumar, P.P. Claisen Rearrangement Based Methodology for the Spiroannulation of a Cyclopentane Ring. Formal Total Synthesis of (±)-Acorone and Isoacorones. *Tetrahedron* **2000**, *56*, 8189–8195.

(48) Yang, J.; Lu, K.; Li, C.; Zhao, Z.; Zhang, X.; Zhang, F.; Tu, Y. Chiral 1,2,3-Triazolium Salt Catalyzed Asymmetric Mono- and Dialkylation of 2,5-Diketopiperazines with the Construction of Tetrasubstituted Carbon Centers. *Angew. Chem. Int. Ed.* **2022**, *61*, e202114129.

(49) Hou, H.; Xu, Y.; Yang, H.; Chen, X.; Yan, C.; Shi, Y.; Zhu, S. Visible-Light Mediated Hydrosilylative and Hydrophosphorylative Cyclizations of Enynes and Dienes. *Org. Lett.* **2020**, *22*, 1748-1753.

(50) **Schrödinger Release 2021-4:** MacroModel, Schrödinger, LLC, New York, NY, 2021.

(51) Bochevarov, A.D.; Harder, E.; Hughes, T.F.; Greenwood, J.R.; Braden, D.A.; Philipp, D.M.; Rinaldo, D.; Halls, M.D.; Zhang, J.; Friesner, R.A., Jaguar: A high-performance quantum chemistry software program with strengths in life and materials sciences, *Int. J. Quantum Chem.*, **2013**, *113*, 2110-2142.

(52) (a) Neese, F. Software Update: The ORCA Program System, Version 4.0. *Wiley Interdiscip. Rev.: Comput. Mol. Sci.* **2018,** *8*, No. e1327. (b) Neese, F. The ORCA Program System. *Wiley Interdiscip. Rev.: Comput. Mol. Sci.* **2012**, *2*, 73−78.

(53) Adamo, C.; Barone, V. Toward Reliable Density Functional Methods without Adjustable Parameters: The PBE0 Model. *J. Chem. Phys.* **1999**, *110*, 6158−6170.

(54) (a) Caldeweyher, E.; Ehlert, S.; Hansen, A.; Neugebauer, H.; Spicher, S.; Bannwarth, C.; Grimme, S. A Generally Applicable Atomic-Charge Dependent London Dispersion Correction. *J. Chem. Phys.* **2019**, *150*, 154122. (b) Caldeweyher, E.; Bannwarth, C.; Grimme, S. Extension of the D3 Dispersion Coefficient Model. *J. Chem. Phys.* **2017**, *147*, 034112.

(55) Cusumano, A. Q.; Goddard, W. A. I.; Stoltz, B. M. The Transition Metal Catalyzed [σ2s + σ2s + π2s + π2s] Pericyclic Reaction: Woodward–Hoffmann Rules, Aromaticity, and Electron Flow. *J. Am. Chem. Soc.* **2020**, *142*, 19033–19039.

(56) Weigend, F.; Ahlrichs, R. Balanced Basis Sets of Split Valence, Triple Zeta Valence and Quadruple Zeta Valence Quality for H to Rn: Design and Assessment of Accuracy. *Phys. Chem. Chem. Phys.* **2005**, *7*, 3297–3305.

(57) Peterson, K. A.; Figgen, D.; Goll, E.; Stoll, H.; Dolg, M. Systematically Convergent Basis Sets with Relativistic Pseudopotentials. II. Small-Core Pseudopotentials and Correlation Consistent Basis Sets for the Post- *d* Group 16–18 Elements. *J. Chem. Phys.* **2003**, *119*, 11113–11123.

(58) Garcia-Ratés, M.; Neese, F. Effect of the Solute Cavity on the Solvation Energy and Its Derivatives within the Framework of the Gaussian Charge Scheme. *J. Comput. Chem.* **2020**, *41*, 922–939.

(59) Ishida, K.; Morokuma, K.; Komornicki, A. The Intrinsic Reaction Coordinate. An Ab Initio Calculation for HNC→HCN and H−+CH4→CH4+H−. *J. Chem. Phys.* **1977**, *66*, 2153−2156.

(60) Zhao, Y.; Truhlar, D. G. The M06 Suite of Density Functionals for Main Group Thermochemistry, Thermochemical Kinetics, Noncovalent Interactions, Excited States, and Transition Elements: Two New Functionals and Systematic Testing of Four M06-Class Functionals and 12 Other Functionals. *Theor. Chem. Account.* **2008**, *120*, 215–241.

(61) Grimme, S. Supramolecular Binding Thermodynamics by Dispersion-Corrected Density Functional Theory. *Chem. Eur. J.* **2012**, *18*, 9955–9964.

(62) Izato, Y.; Matsugi, A.; Koshi, M.; Miyake, A. A Simple Heuristic Approach to Estimate the Thermochemistry of Condensed-Phase Molecules Based on the Polarizable Continuum Model. *Phys. Chem. Chem. Phys.* **2019**, *21*, 18920–18929.

(63) Finkelstein, A. V.; Janin, J. The Price of Lost Freedom: Entropy of Bimolecular Complex Formation. *Protein Eng. Des. Sel.* **1989**, *3*, 1–3.

(64) Neese, F.; Wennmohs, F.; Hansen, A.; Becker, U. Efficient, Approximate and Parallel Hartree-Fock and Hybrid DFT Calculations. A 'Chain-of-Spheres' Algorithm for the Hartree-Fock Exchange. *Chem. Phys.* **2009**, *356*, 98–109.

(65) Weigend, F. Accurate Coulomb-Fitting Basis Sets for H to Rn. *Phys. Chem. Chem. Phys.* **2006**, *8*, 1057–1065.

(66) Stoychev, G. L.; Auer, A. A.; Neese, F. Automatic Generation of Auxiliary Basis Sets. *J. Chem. Theory Comput.* **2017**, *13*, 554–562.

(67) (a) Pracht, P.; Grimme, S. Calculation of Absolute Molecular Entropies and Heat Capacities Made Simple. *Chem. Sci.* **2021**, *12*, 6551–6568. (b) Gorges, J.; Grimme, S.; Hansen, A.; Pracht, P. Towards Understanding Solvation Effects on the Conformational Entropy of Non-Rigid Molecules. *Phys. Chem. Chem. Phys.* **2022**, *24*, 12249–12259.

(68) (a) DeTar, D. F. Theoretical Ab Initio Calculation of Entropy, Heat Capacity, and Heat Content. *J. Phys. Chem. A* **1998**, *102*, 5128–5141. See also: (b) Guthrie, J. P. Use of DFT Methods for the Calculation of the Entropy of Gas Phase Organic Molecules: An Examination of the Quality of Results from a Simple Approach. *J. Phys. Chem. A* **2001**, *105*, 8495–8499.

APPENDIX 1

Spectra Relevant to Chapter 2:

Asymmetric [4+2] Cycloaddition of Pd Enolates

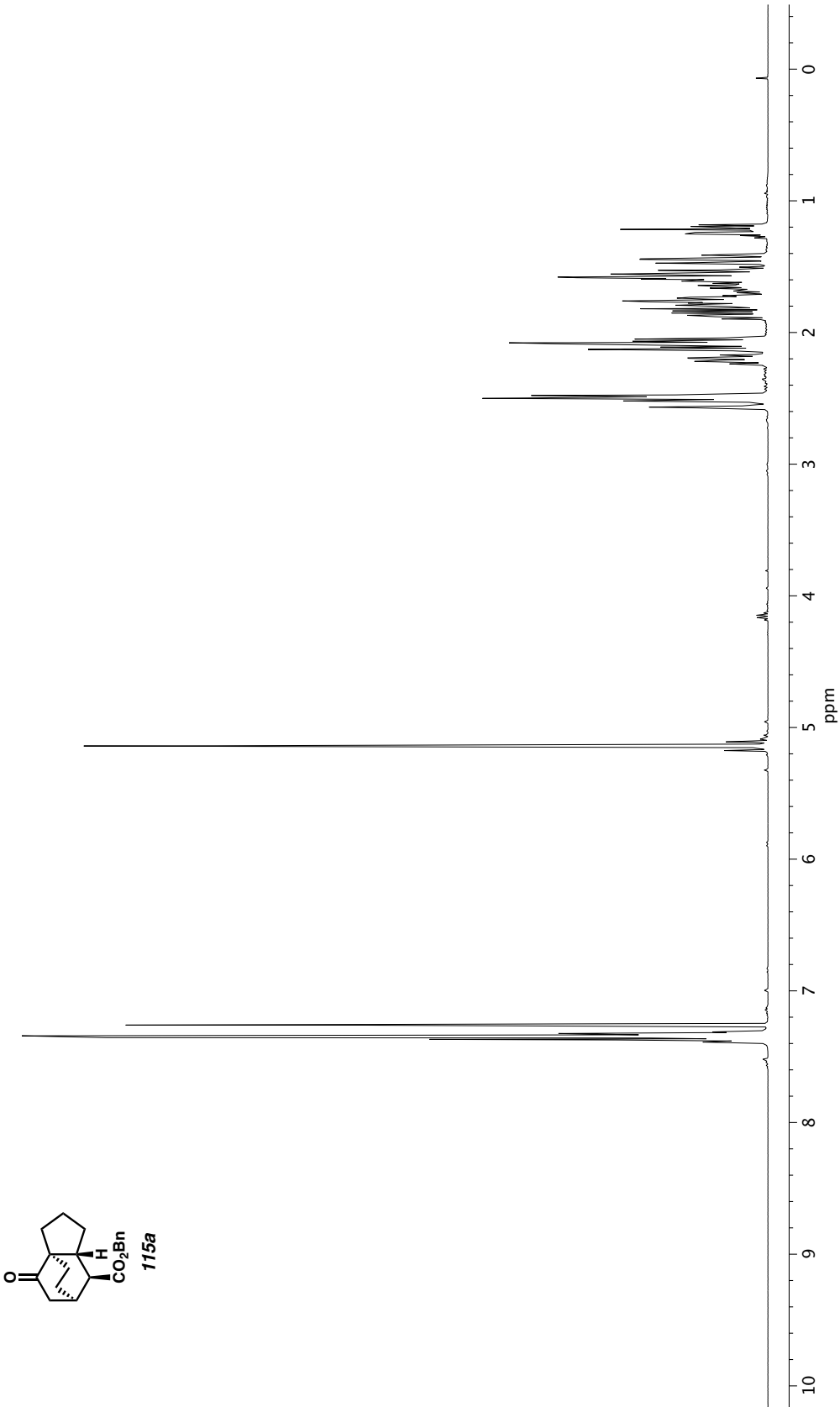

Figure A1.1. *^{1}H NMR (400 MHz, $CDCl_3$) of compound* ***115a.***

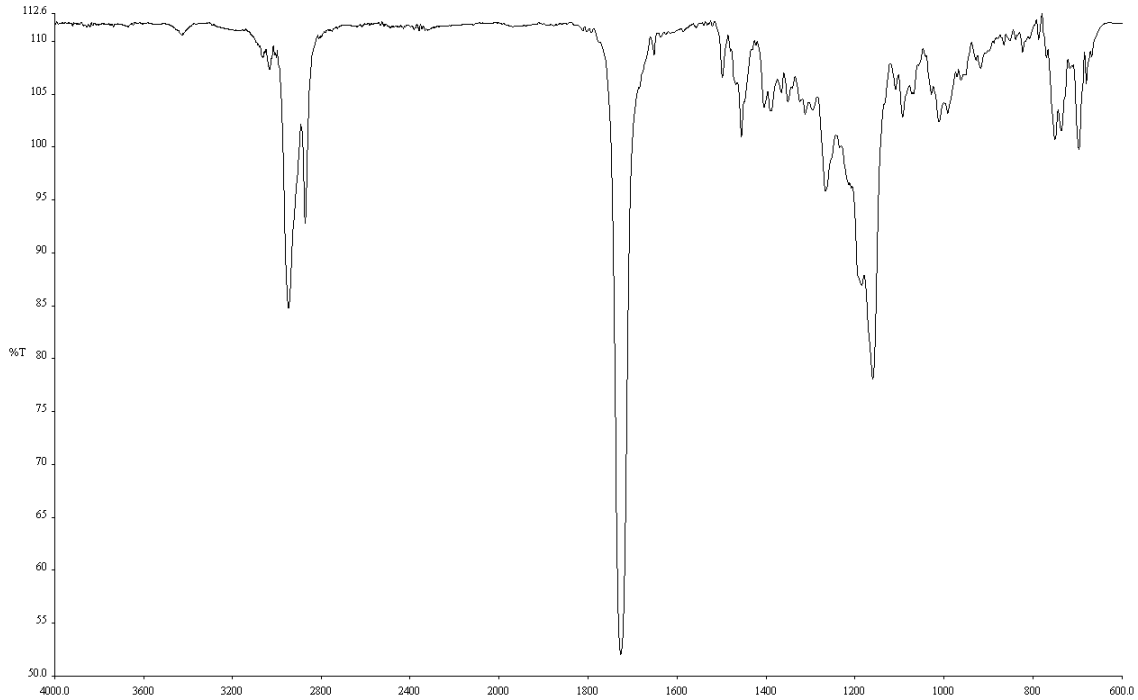

Figure A1.2. *Infrared spectrum (Thin Film, NaCl) of compound* ***115a.***

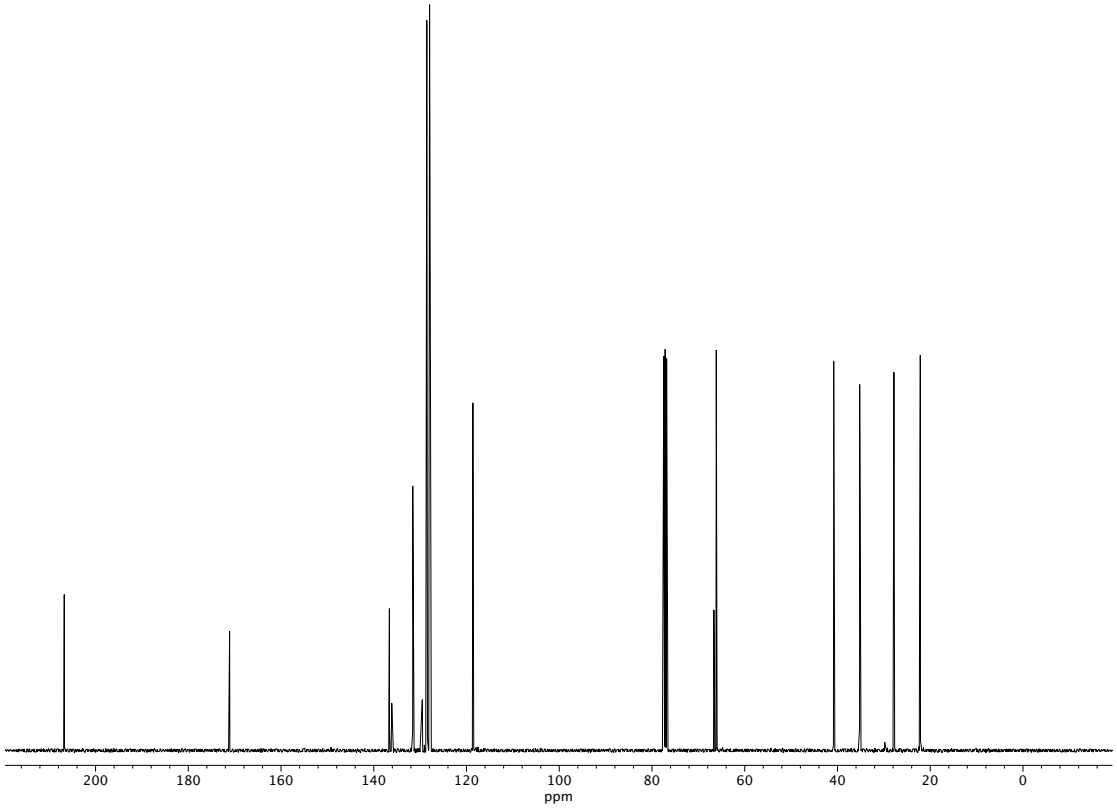

Figure A1.3. *^{13}C NMR (100 MHz, $CDCl_3$) of compound* ***115a.***

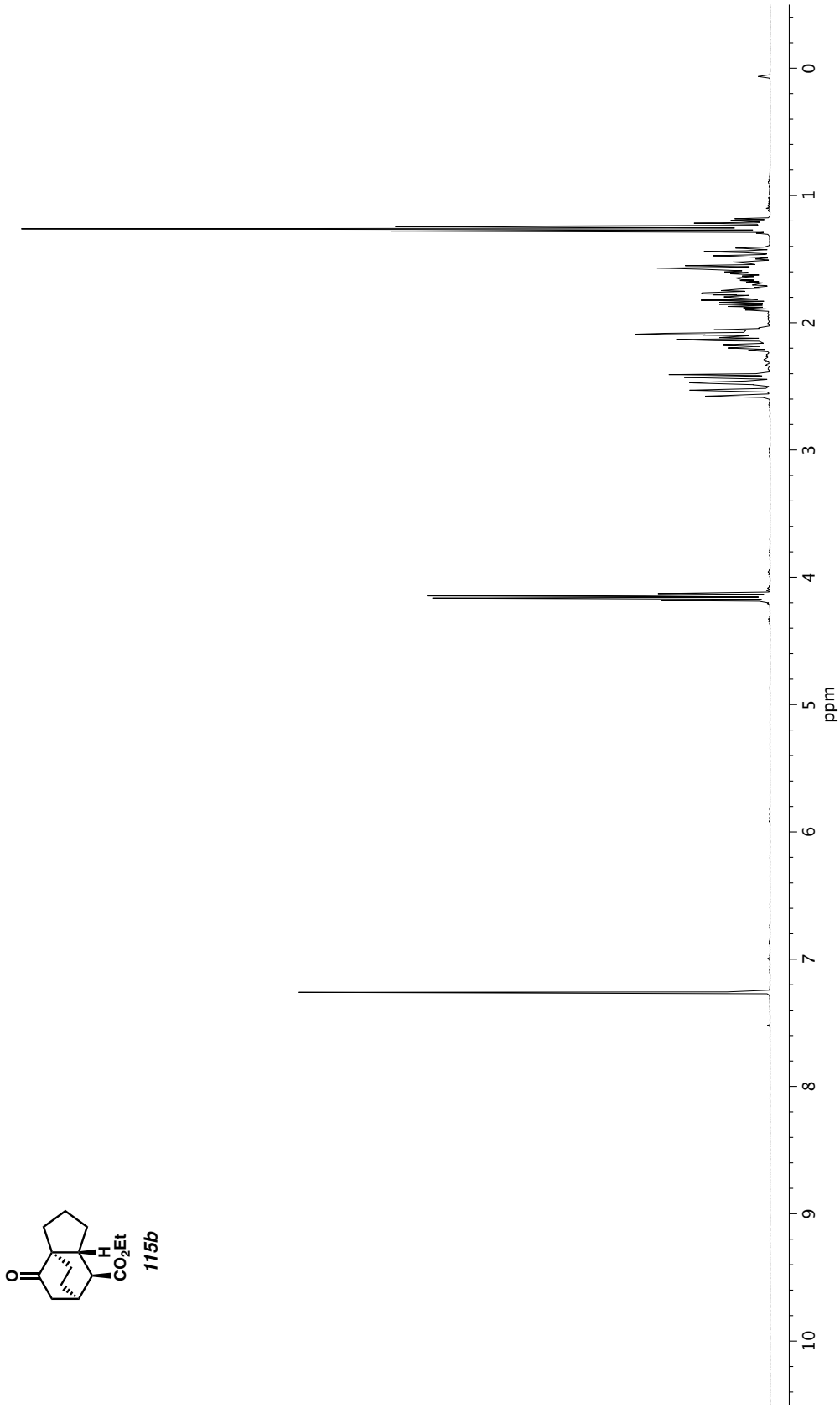

Figure A1.4. *^1H NMR (400 MHz, $CDCl_3$) of compound* ***115b.***

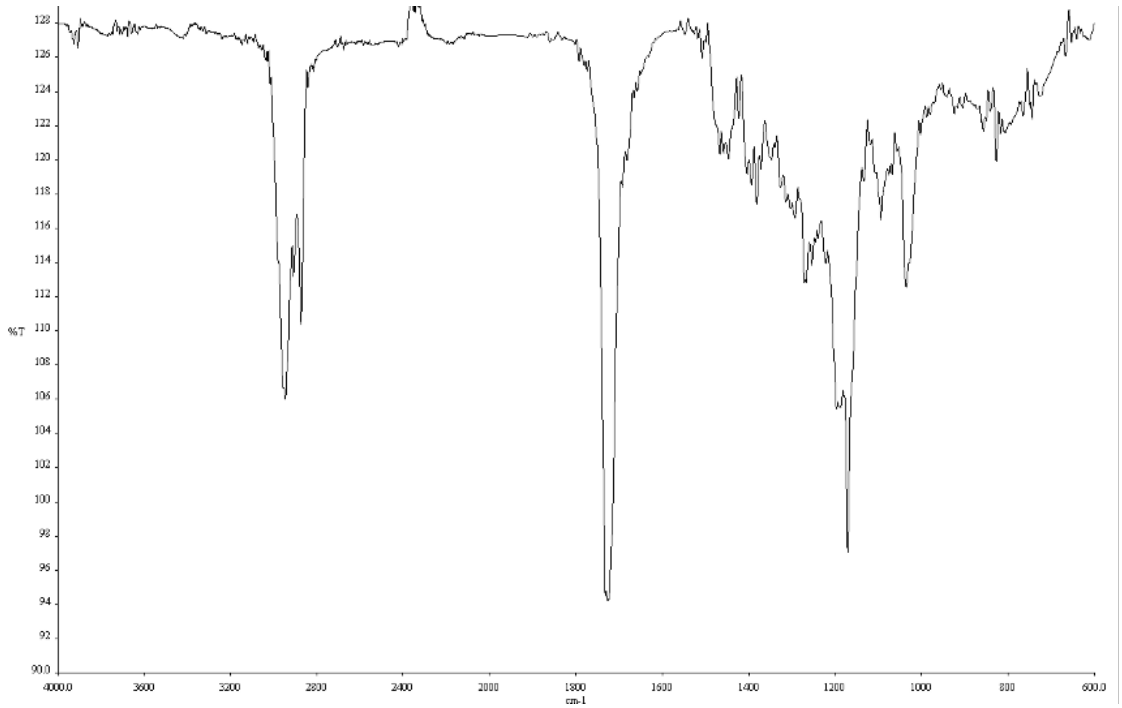

Figure A1.5. *Infrared spectrum (Thin Film, NaCl) of compound* ***115b.***

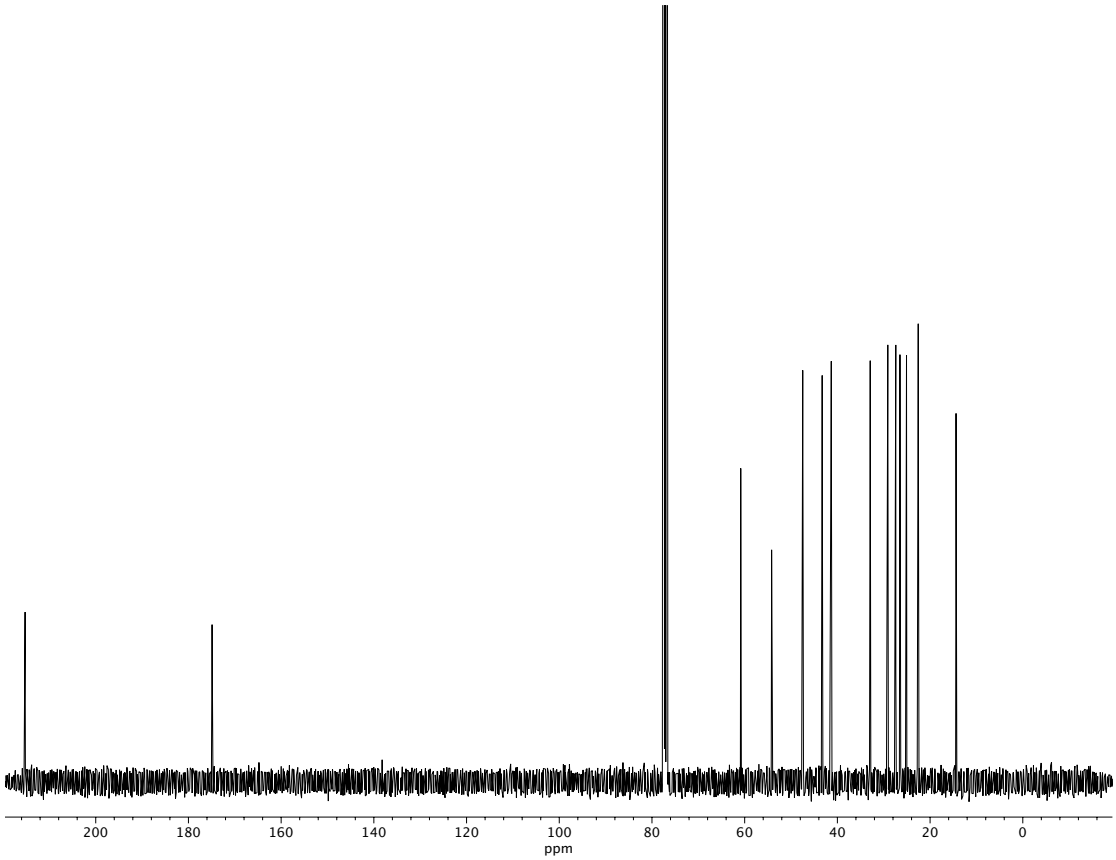

Figure A1.6. *^{13}C NMR (100 MHz, $CDCl_3$) of compound* ***115b.***

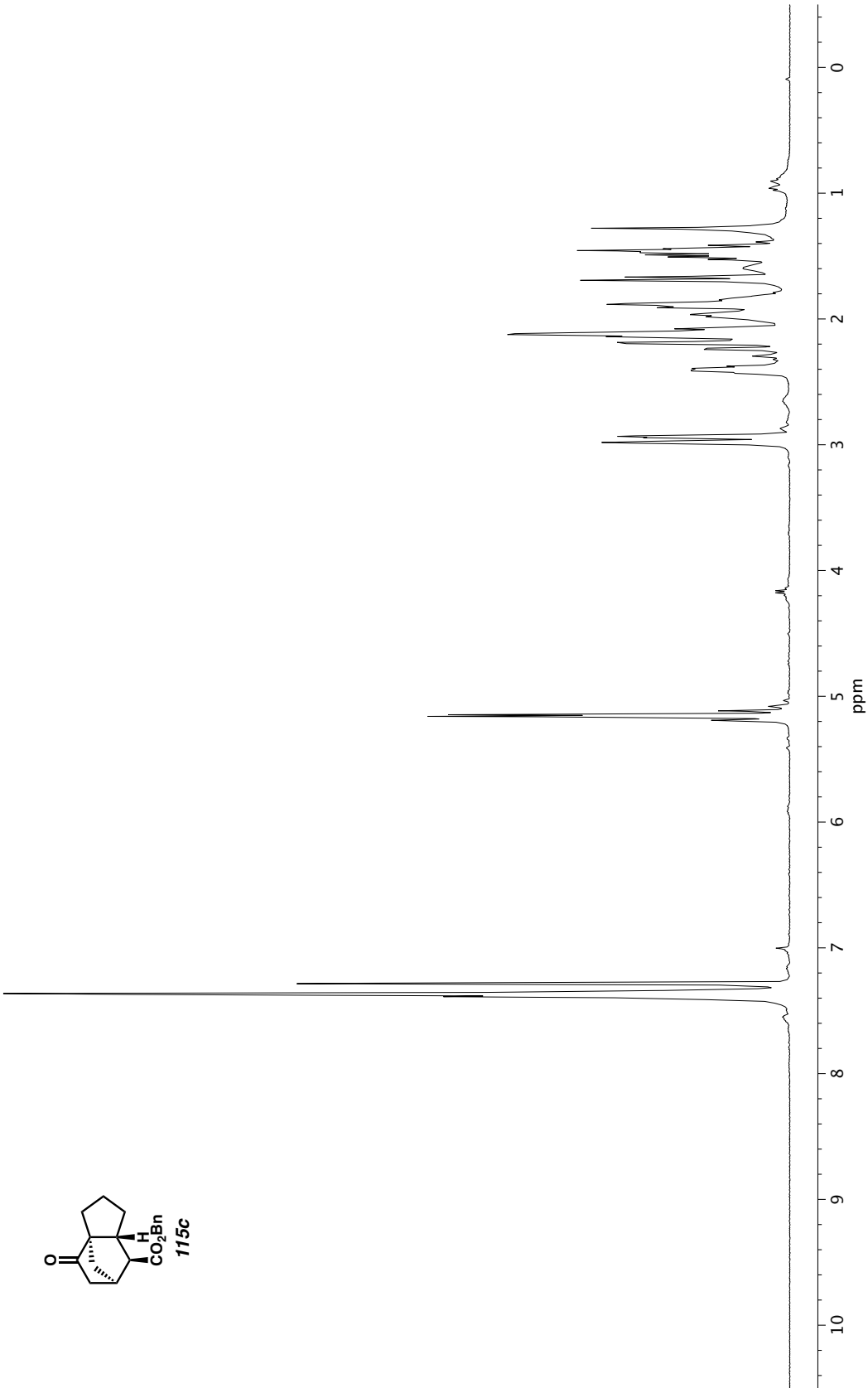

Figure A1.7. *^1H NMR (400 MHz, $CDCl_3$) of compound* ***115c.***

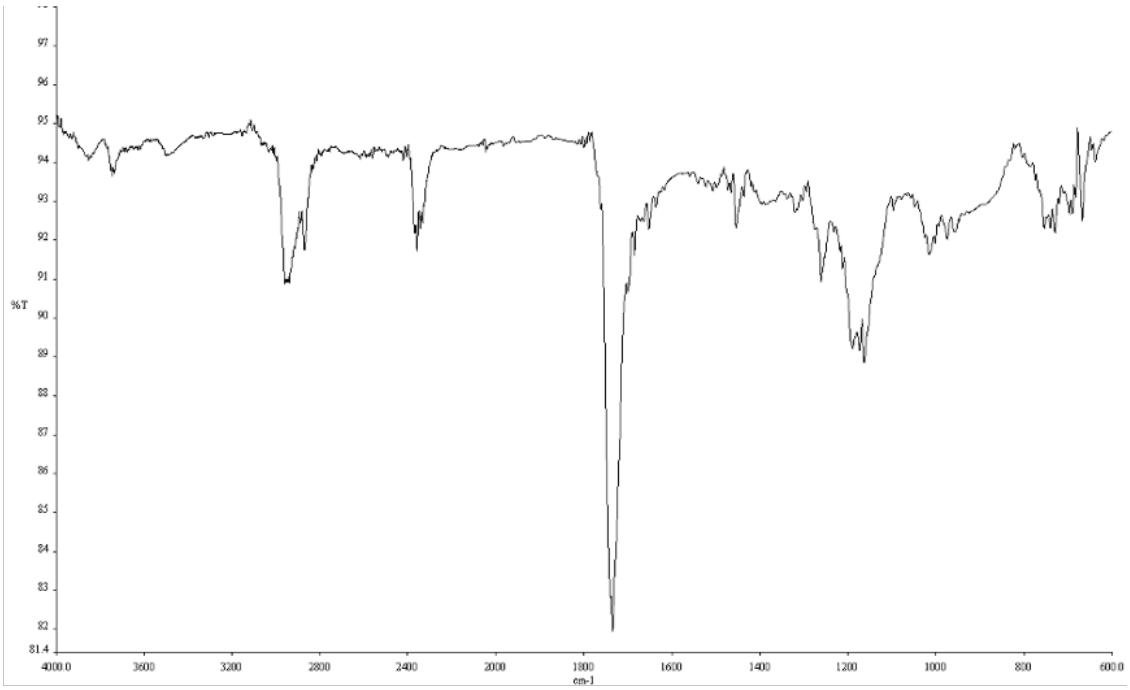

Figure A1.8. *Infrared spectrum (Thin Film, NaCl) of compound* ***115c.***

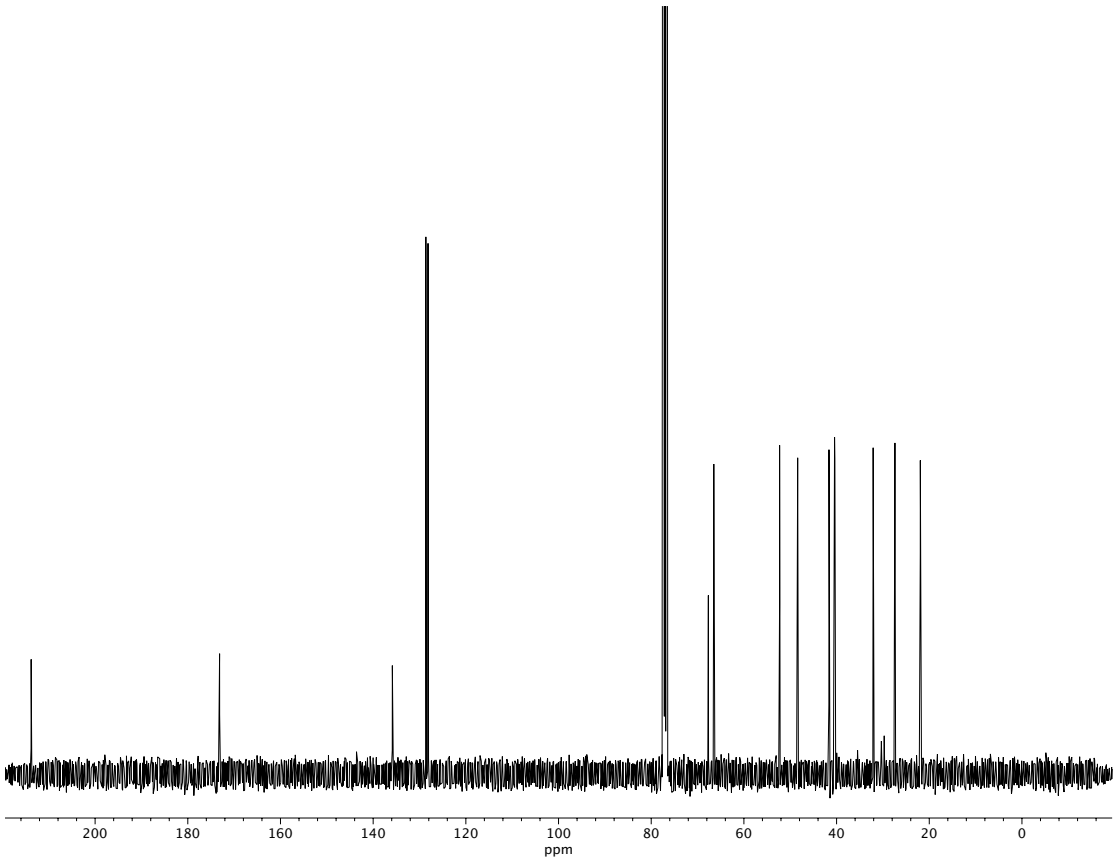

Figure A1.9. *^{13}C NMR (100 MHz, $CDCl_3$) of compound* ***115c.***

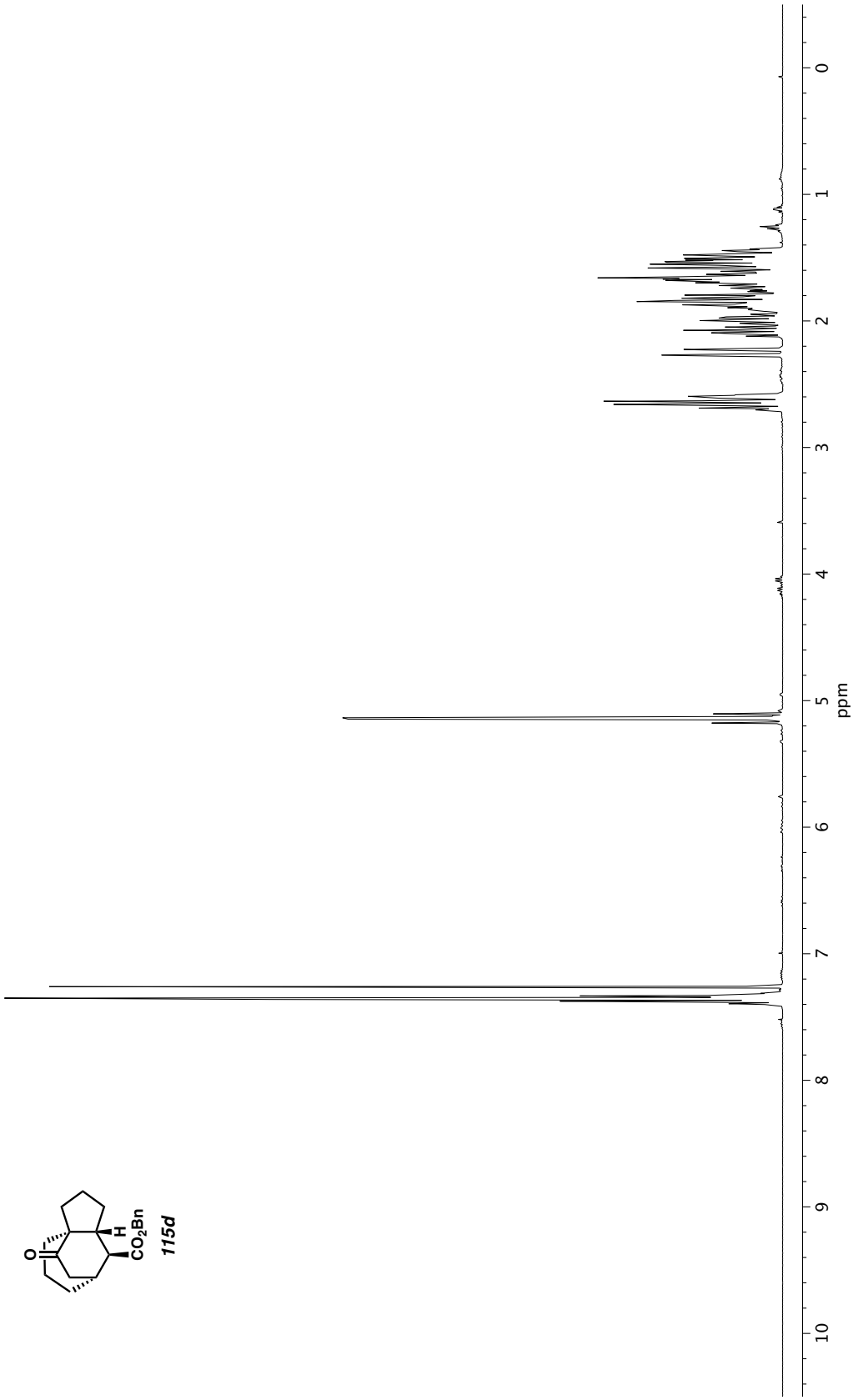

Figure A1.10. *^1H NMR (400 MHz, $CDCl_3$) of compound* ***115d.***

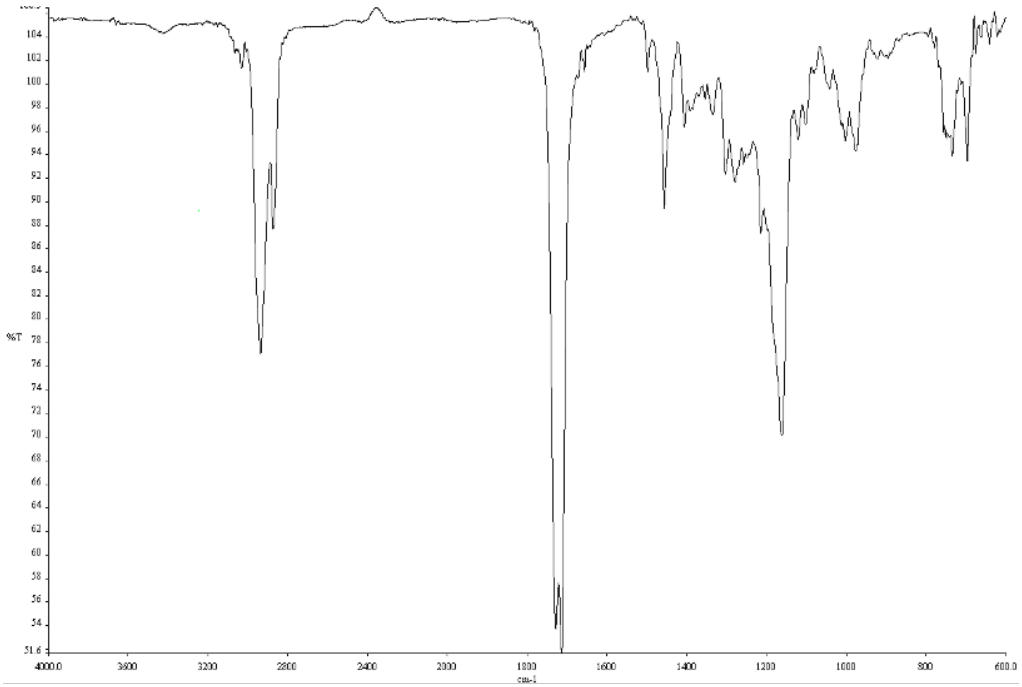

Figure A1.11. *Infrared spectrum (Thin Film, NaCl) of compound* ***115d.***

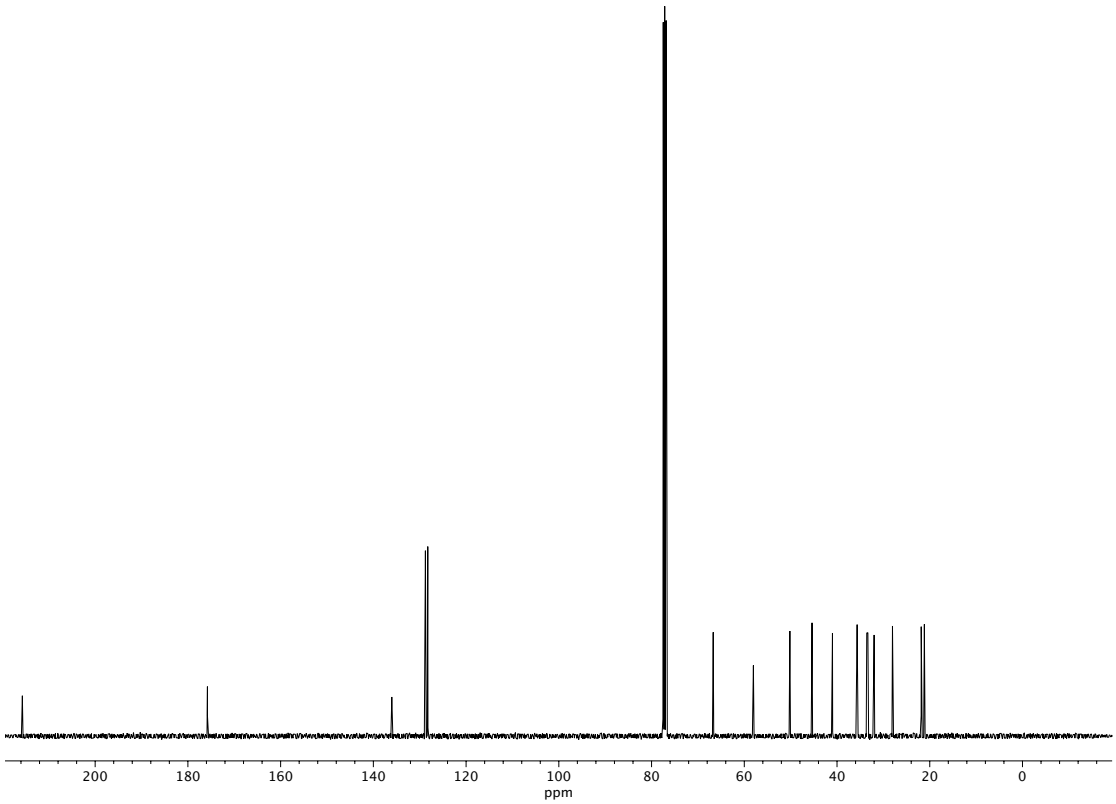

Figure A1.12. *^{13}C NMR (100 MHz, $CDCl_3$) of compound* ***115d.***

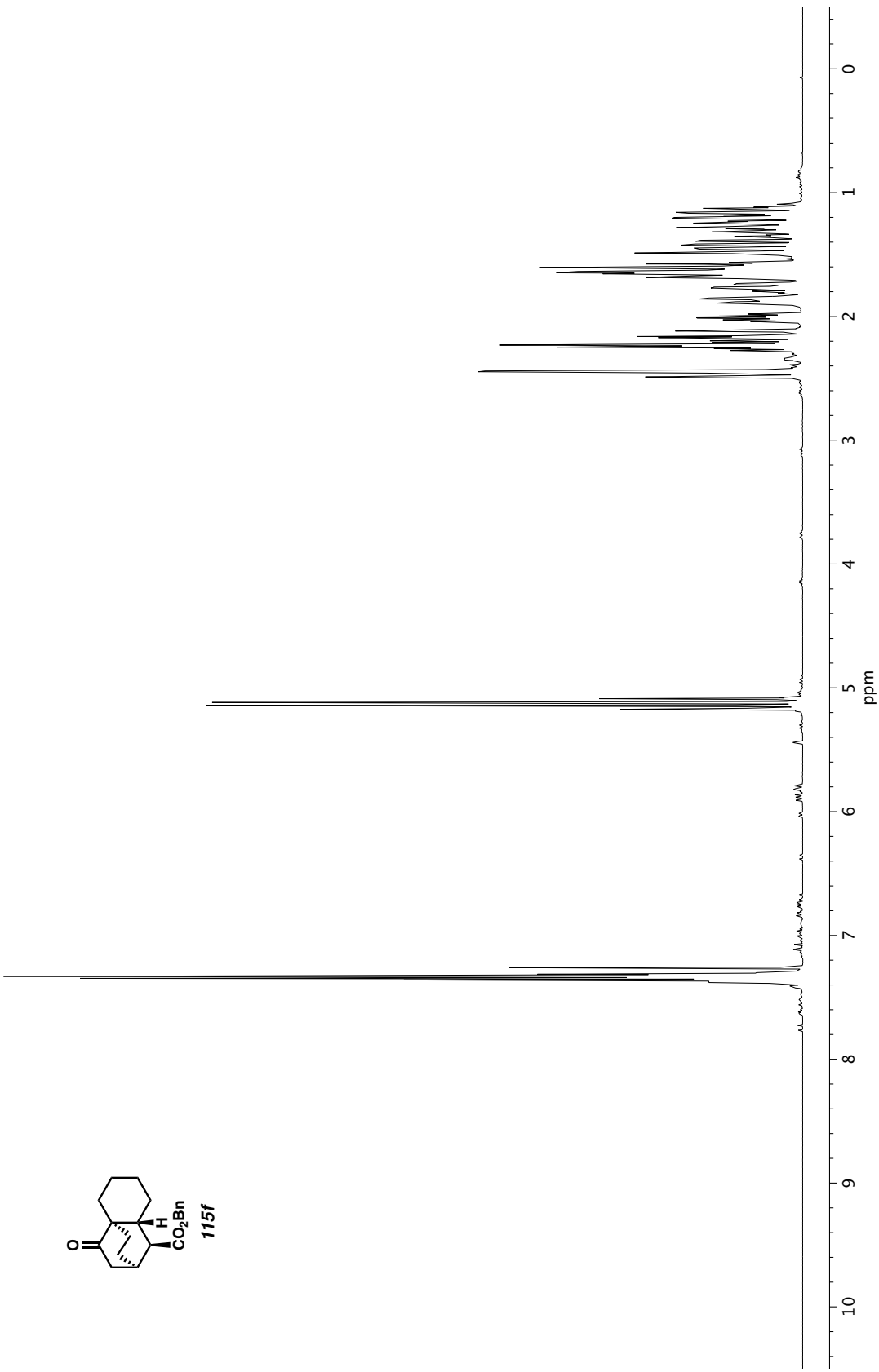

Figure A1.13. *^1H NMR (400 MHz, $CDCl_3$) of compound* ***115f.***

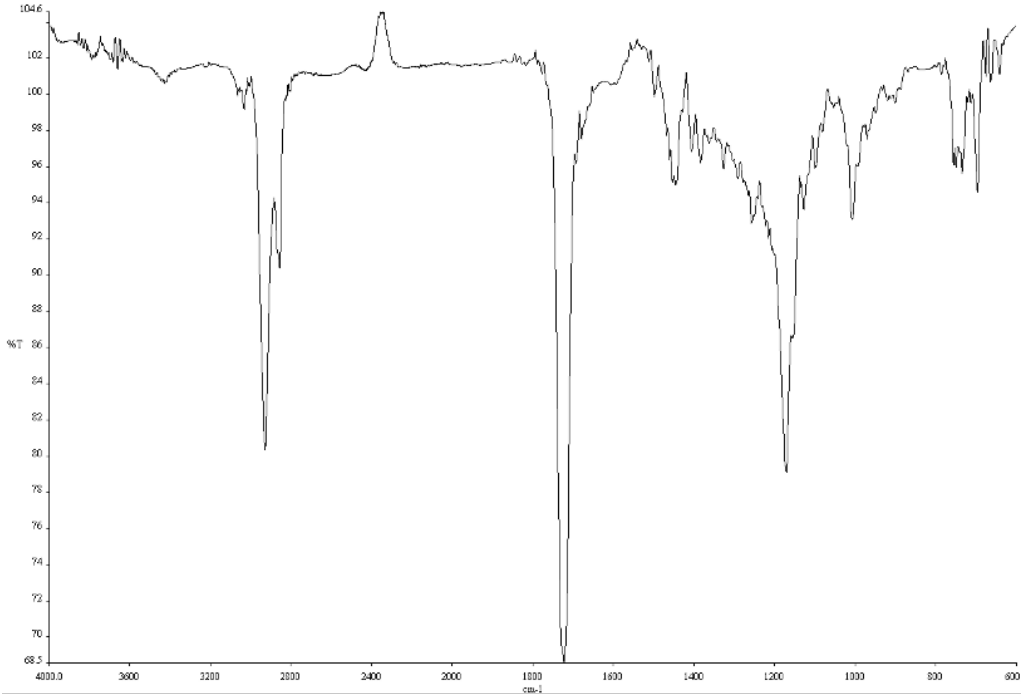

Figure A1.14. *Infrared spectrum (Thin Film, NaCl) of compound* ***115f.***

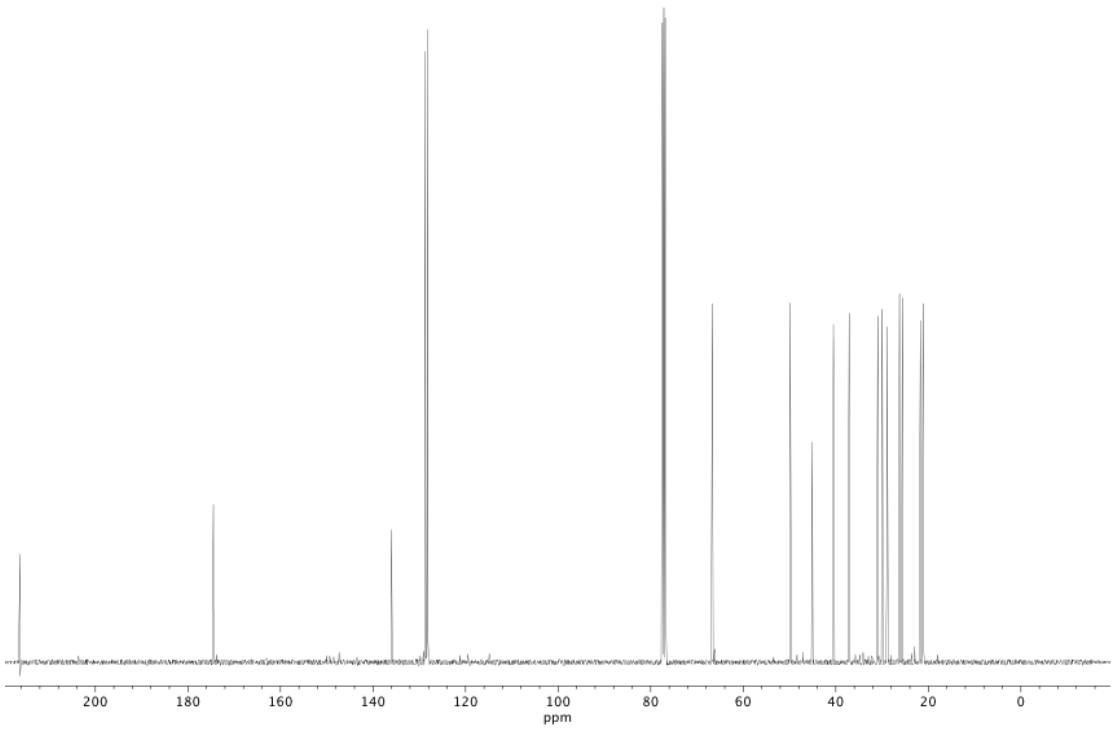

Figure A1.15. *^{13}C NMR (100 MHz, $CDCl_3$) of compound* ***115f.***

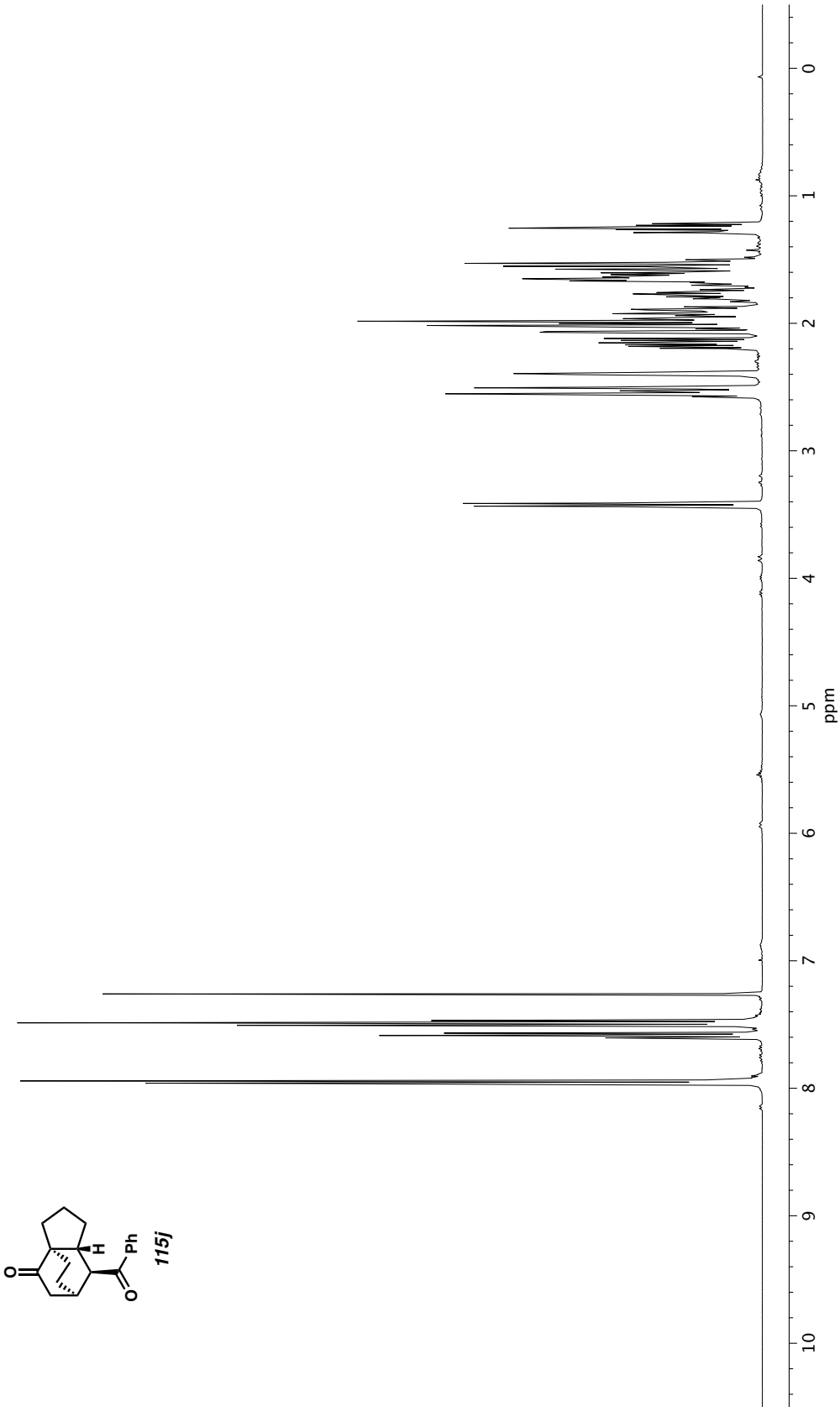

Figure A1.16. *^1H NMR (400 MHz, $CDCl_3$) of compound* ***115j.***

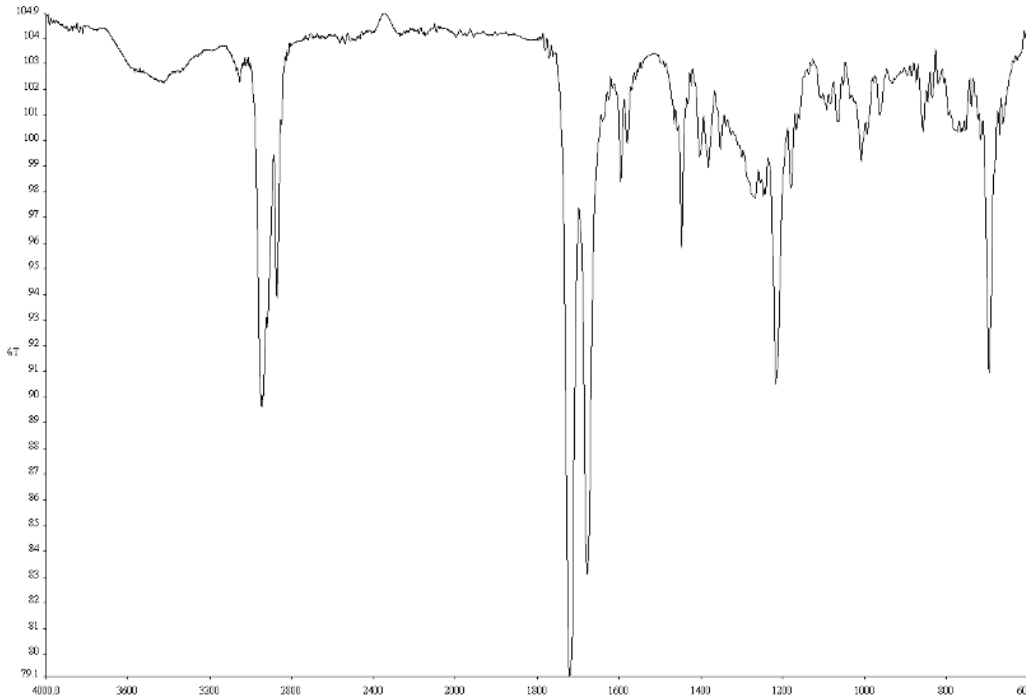

Figure A1.17. *Infrared spectrum (Thin Film, NaCl) of compound* ***115j.***

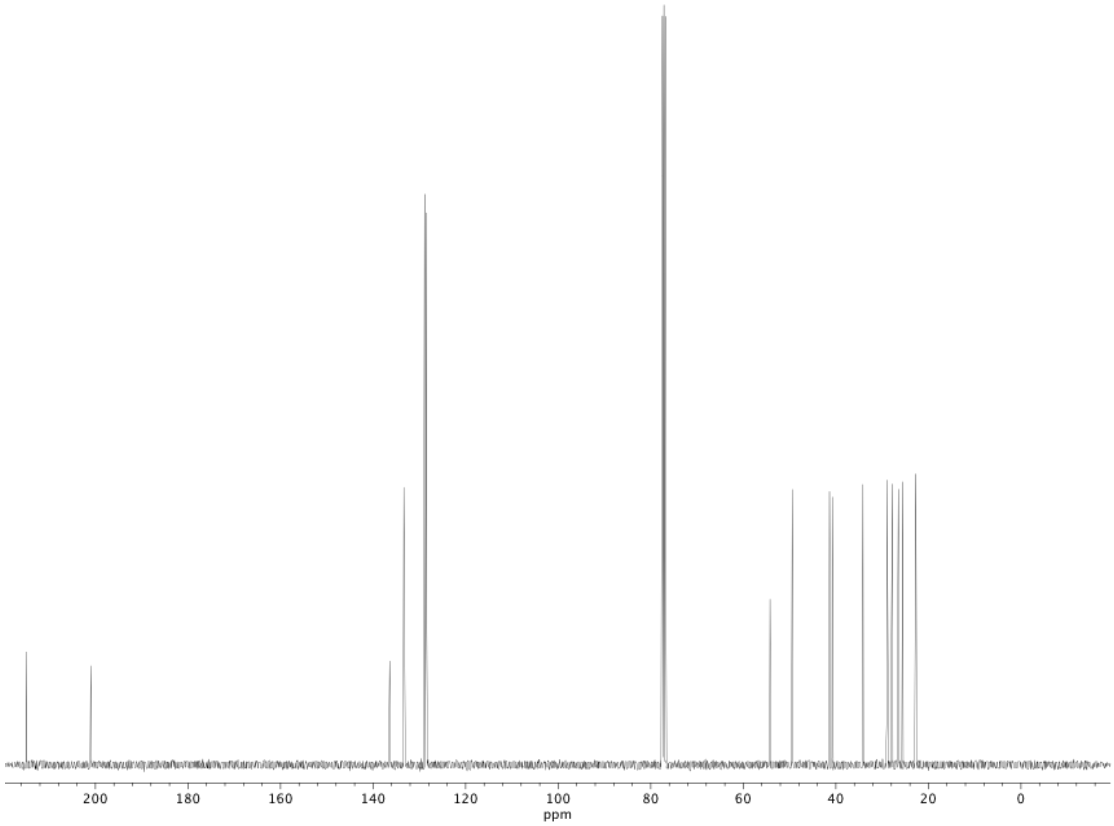

Figure A1.18. *^{13}C NMR (100 MHz, $CDCl_3$) of compound* ***115j.***

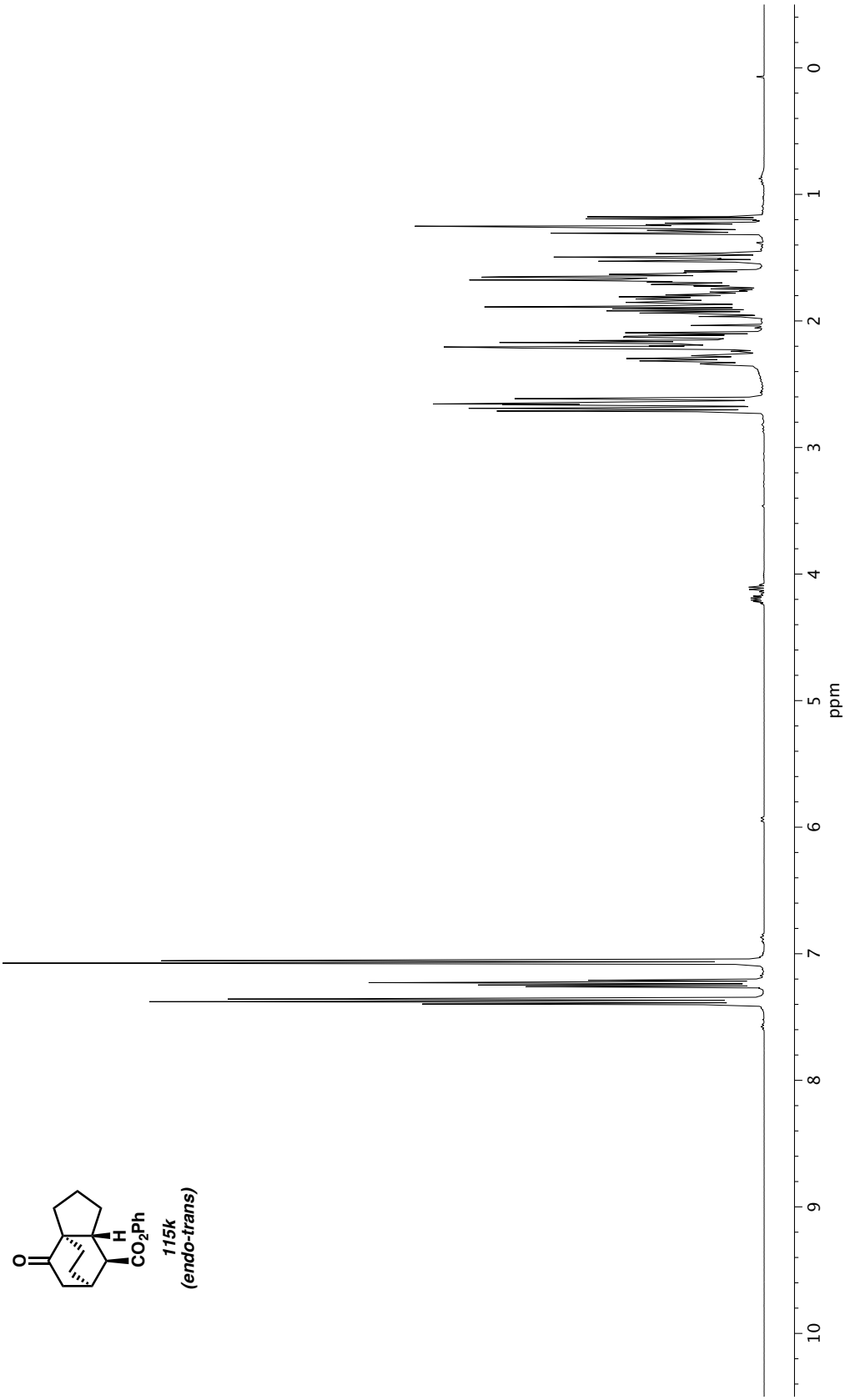

Figure A1.19. *^1H NMR (400 MHz, $CDCl_3$) of compound* ***115k.***

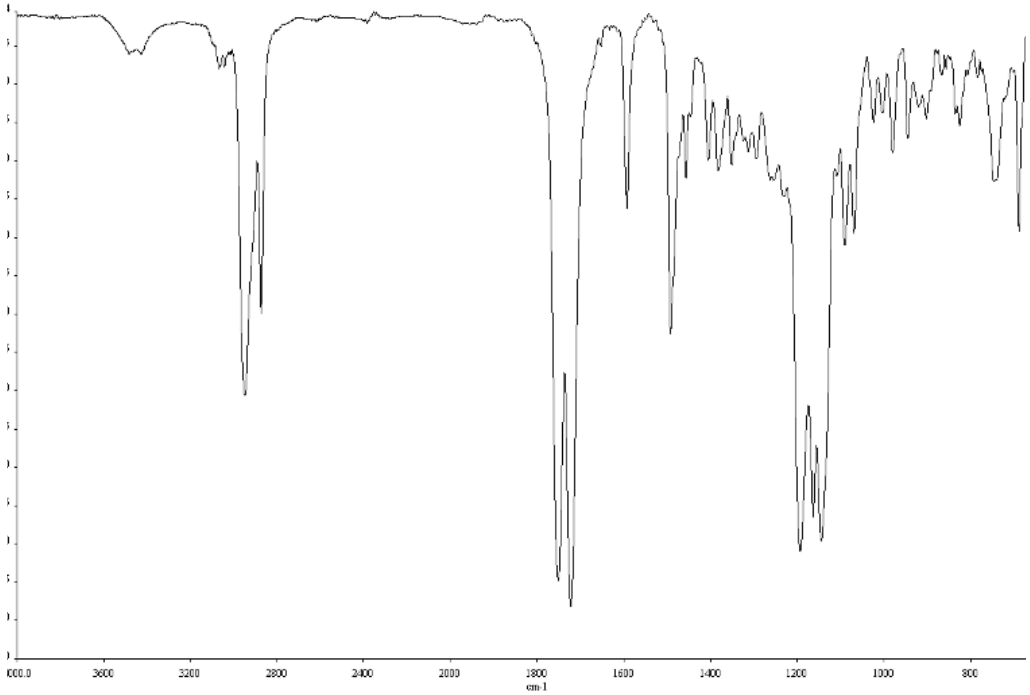

Figure A1.20. *Infrared spectrum (Thin Film, NaCl) of compound* ***115k.***

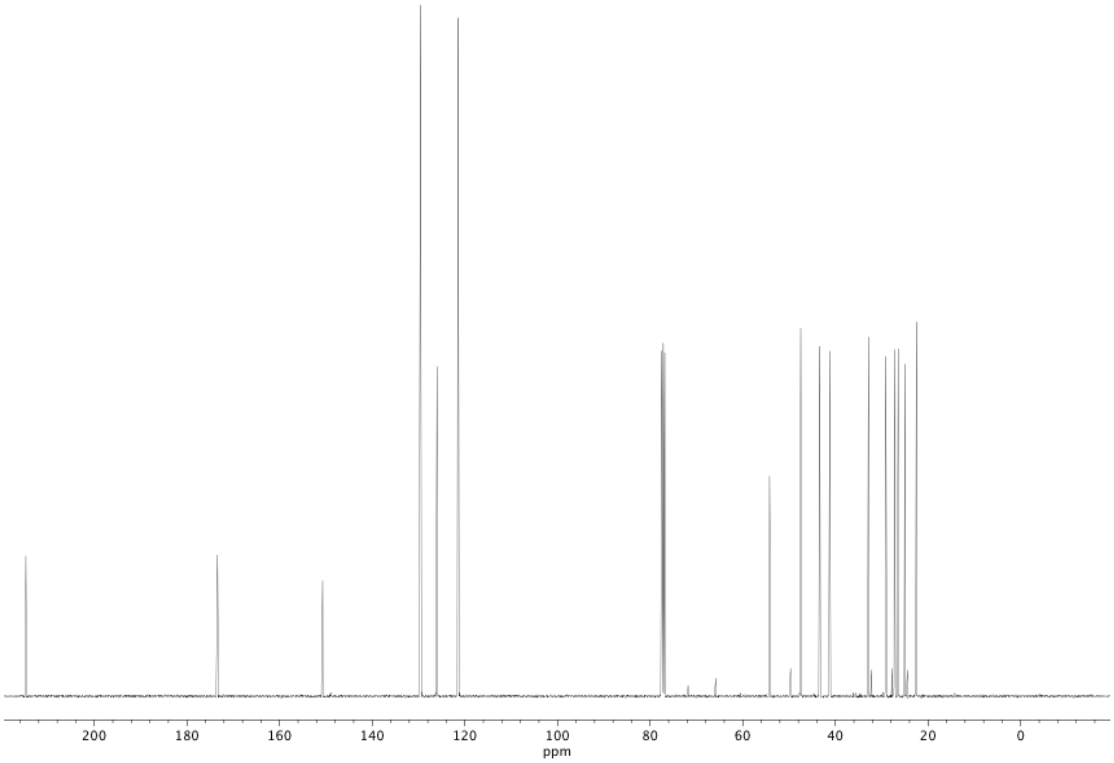

Figure A1.21. *^{13}C NMR (100 MHz, $CDCl_3$) of compound* ***115k.***

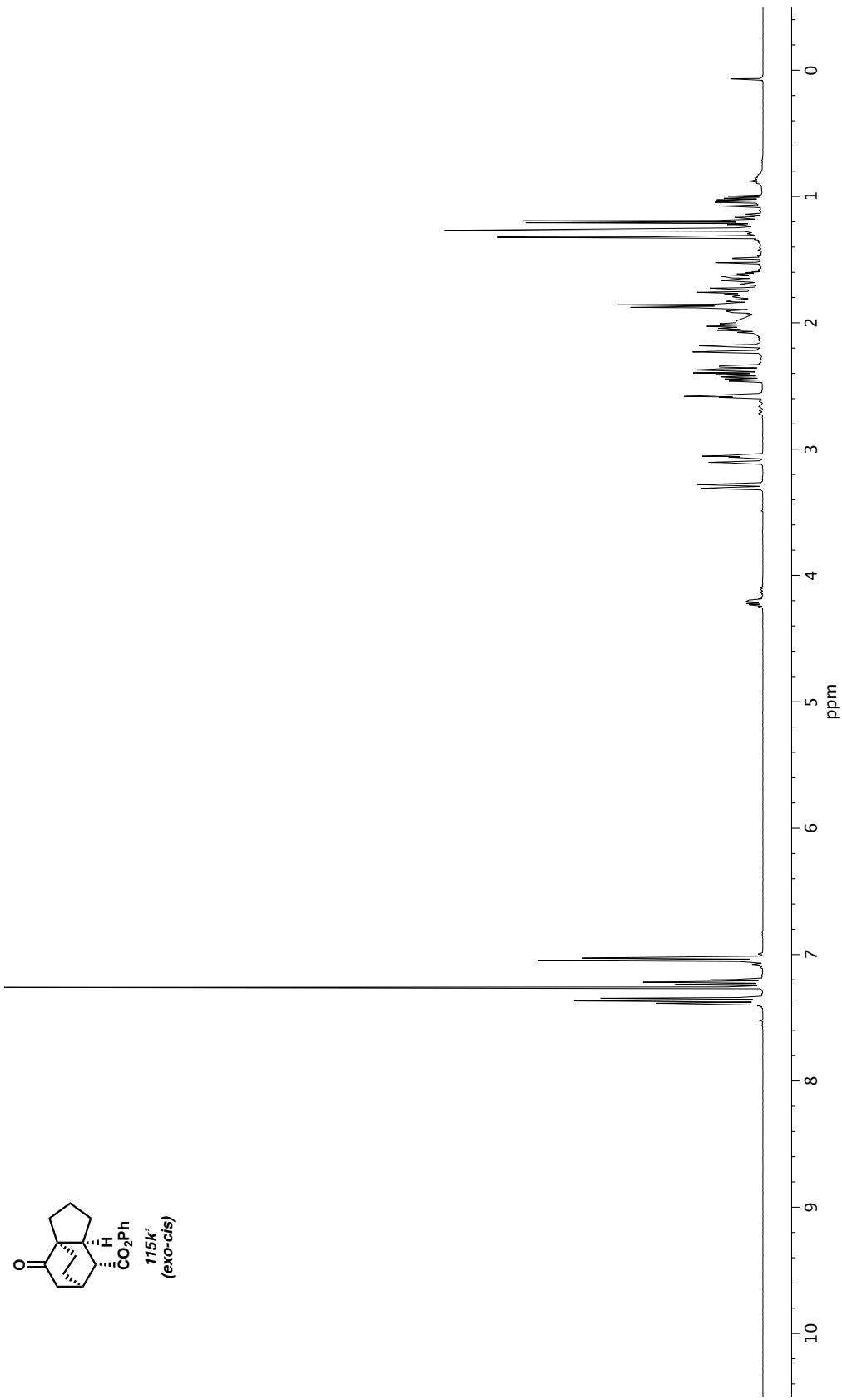

Figure A1.22. *^1H NMR (400 MHz, $CDCl_3$) of compound* ***115k.***

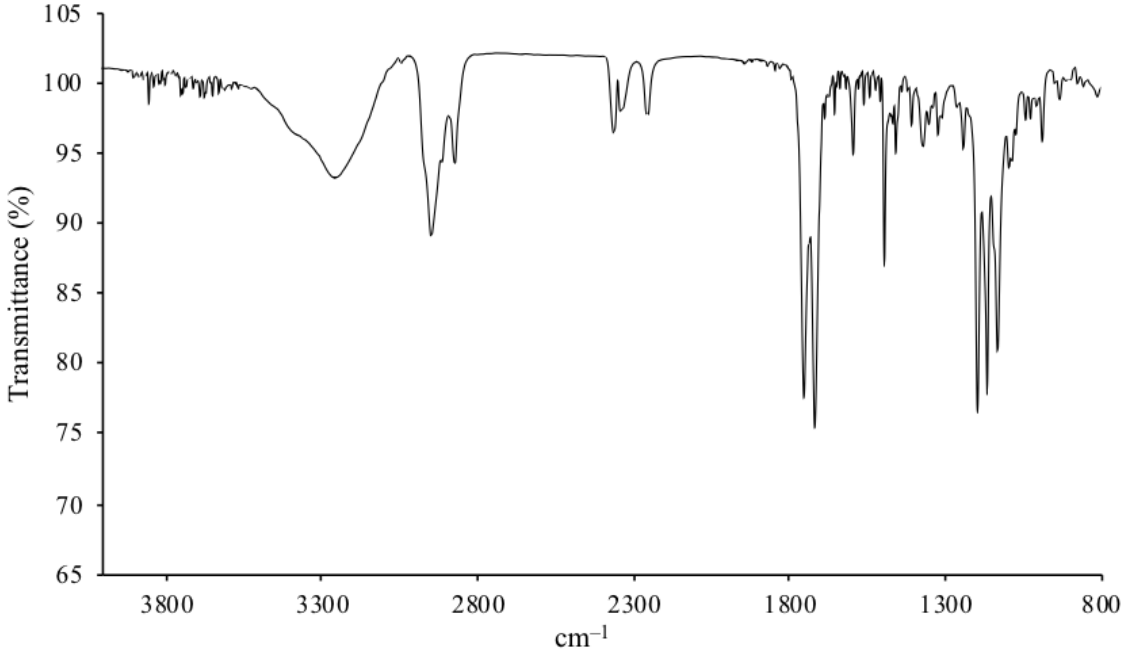

Figure A1.23. *Infrared spectrum ($CDCl_3$ solution) of compound* ***115k′.***

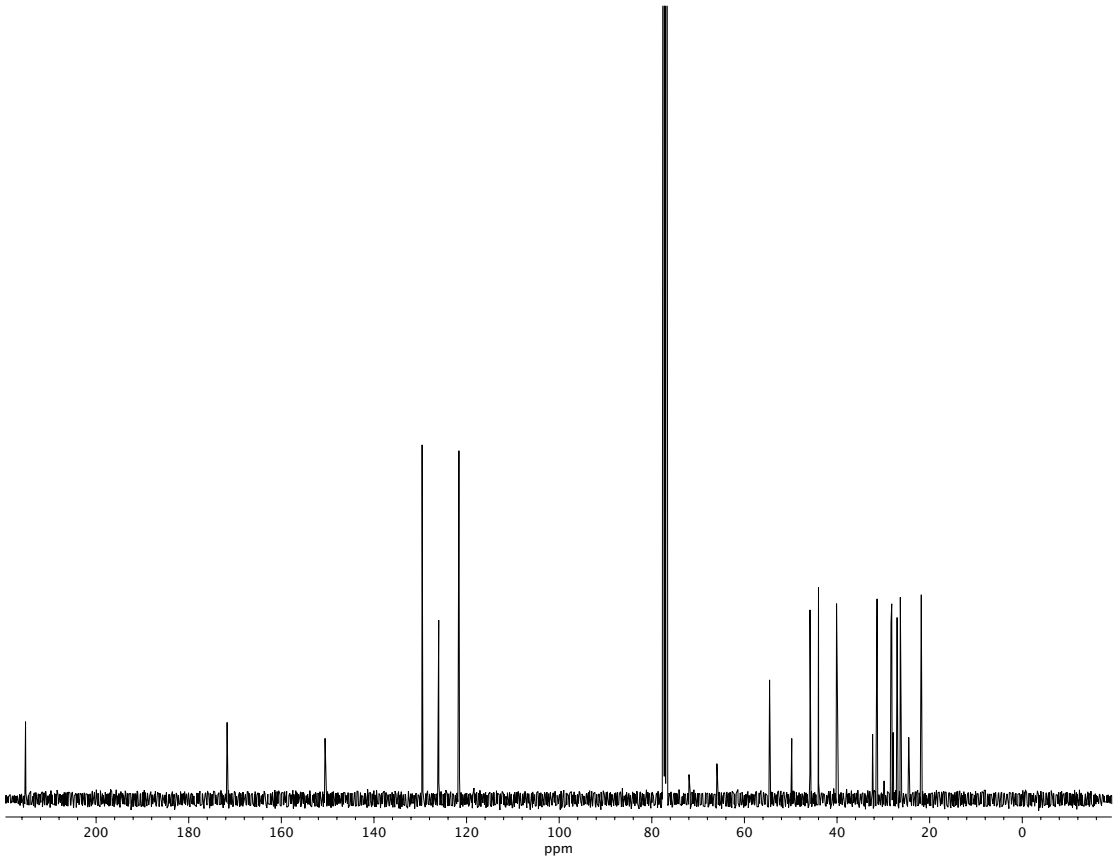

Figure A1.24. *^{13}C NMR (100 MHz, $CDCl_3$) of compound* ***115k′.***

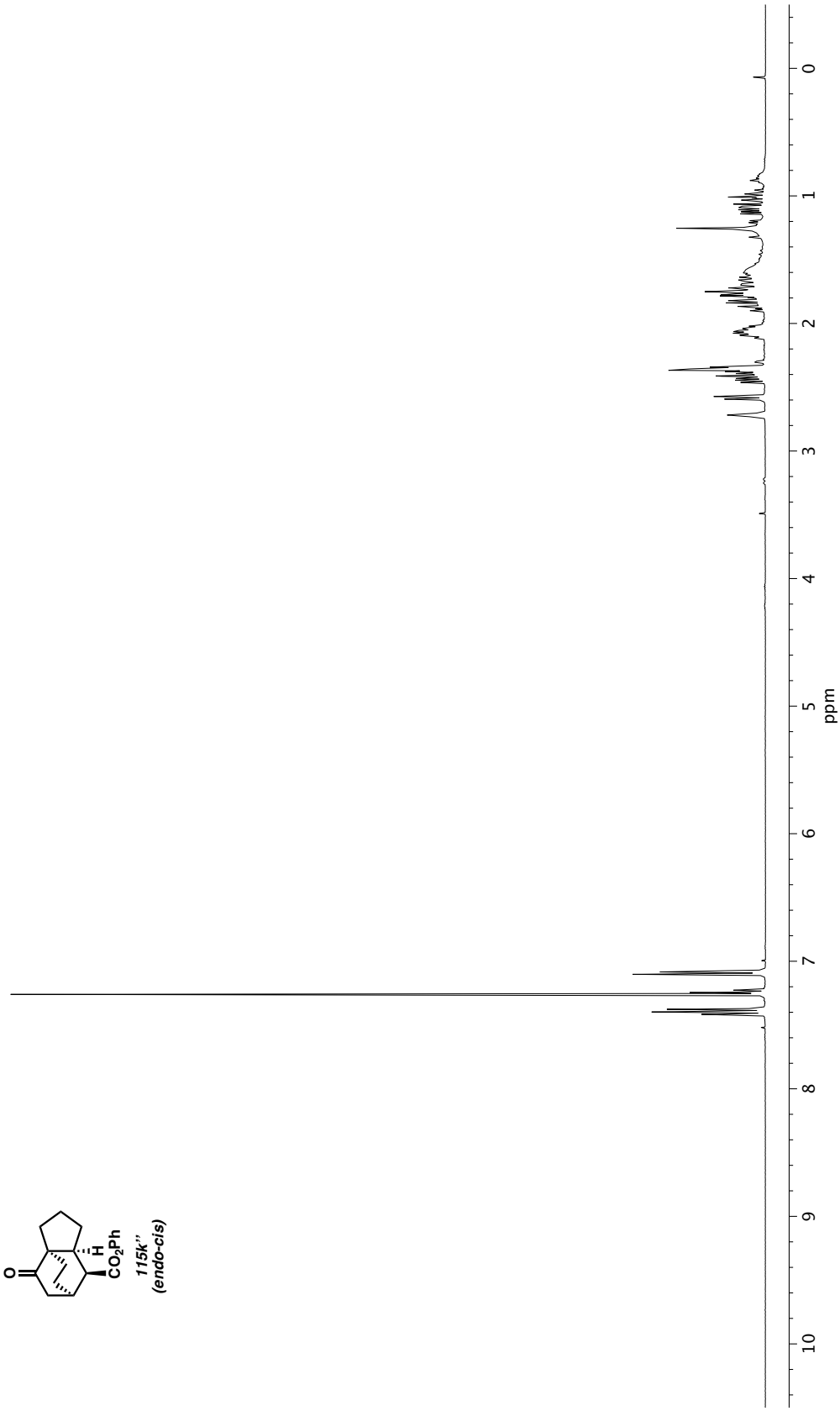

Figure A1.25. *^1H NMR (400 MHz, $CDCl_3$) of compound* ***115k.***

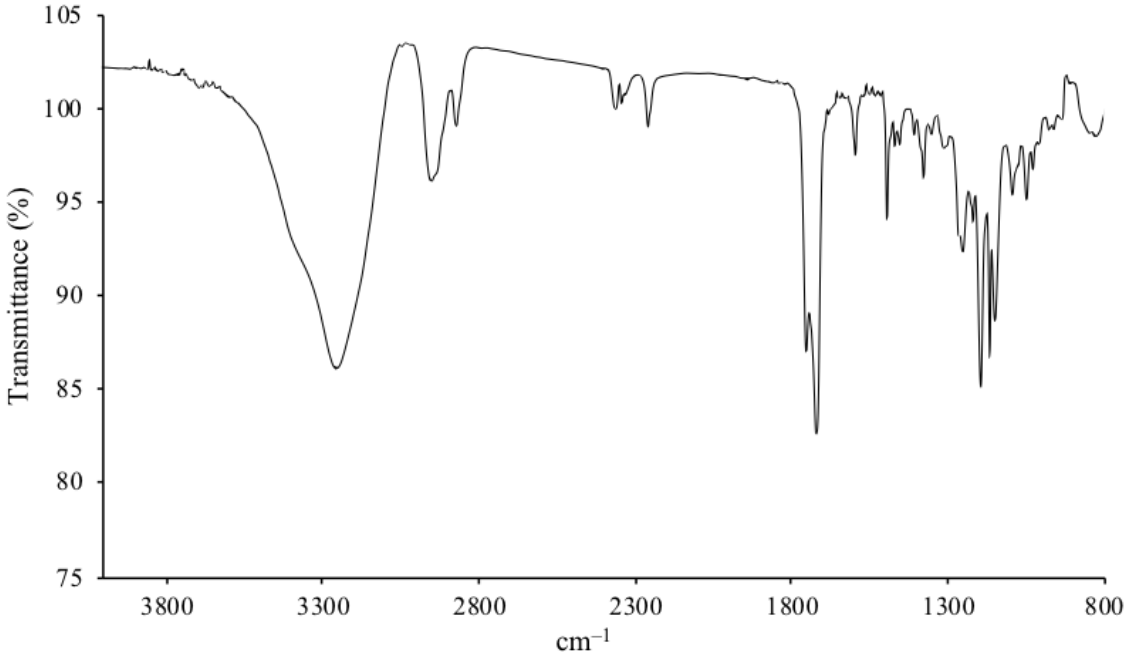

Figure A1.26. *Infrared spectrum ($CDCl_3$ solution) of compound* ***115k″.***

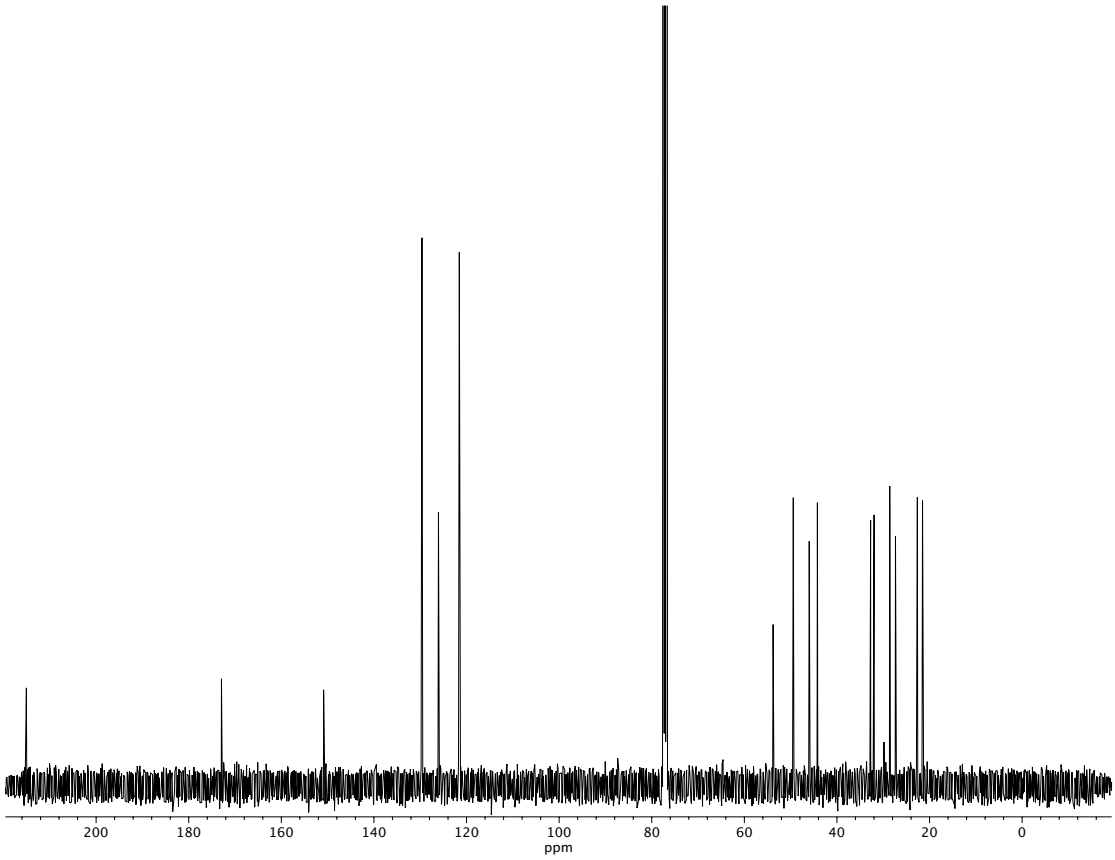

Figure A1.27. *^{13}C NMR (100 MHz, $CDCl_3$) of compound* ***115k″.***

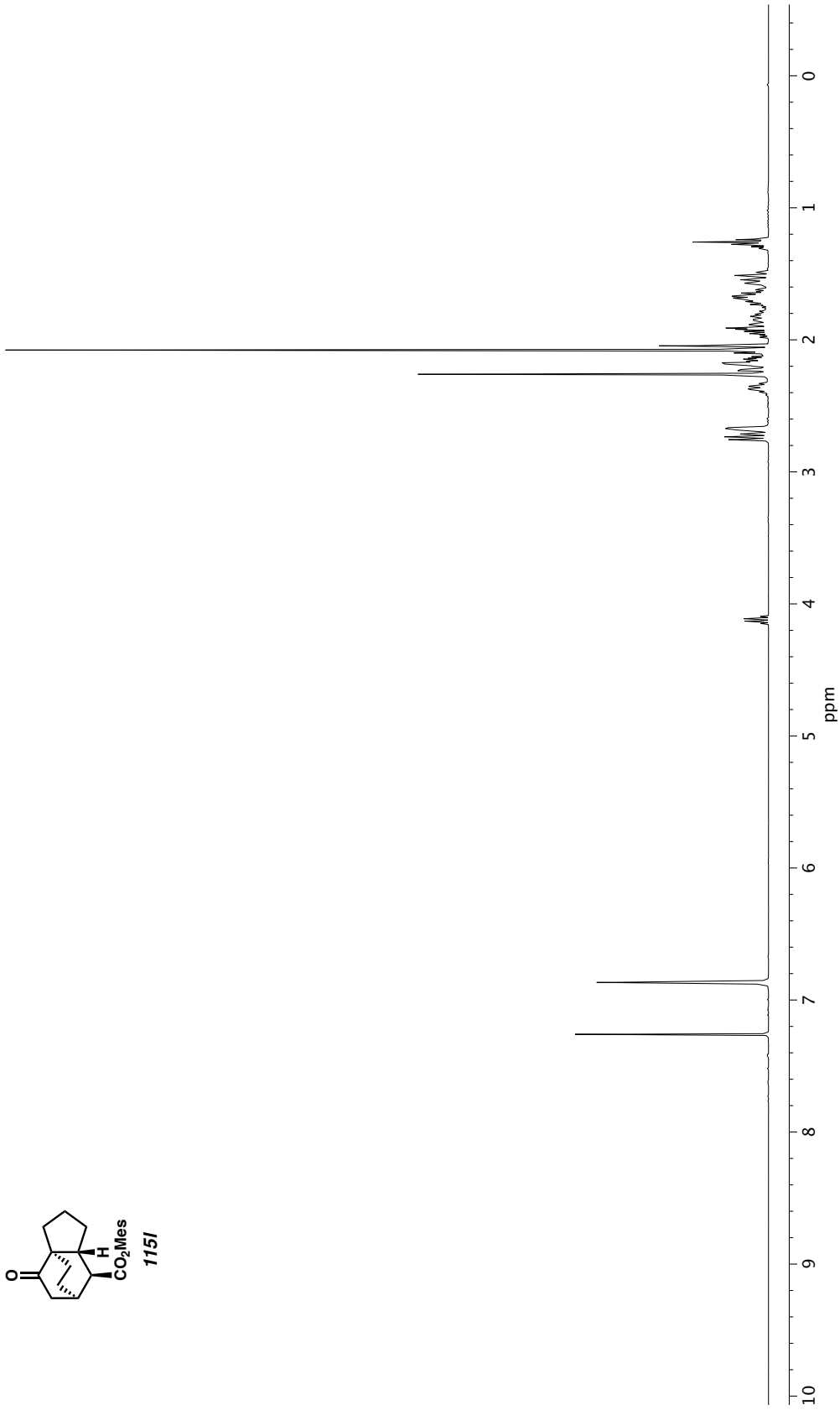

Figure A1.28. *^1H NMR (400 MHz, $CDCl_3$) of compound* ***115l.***

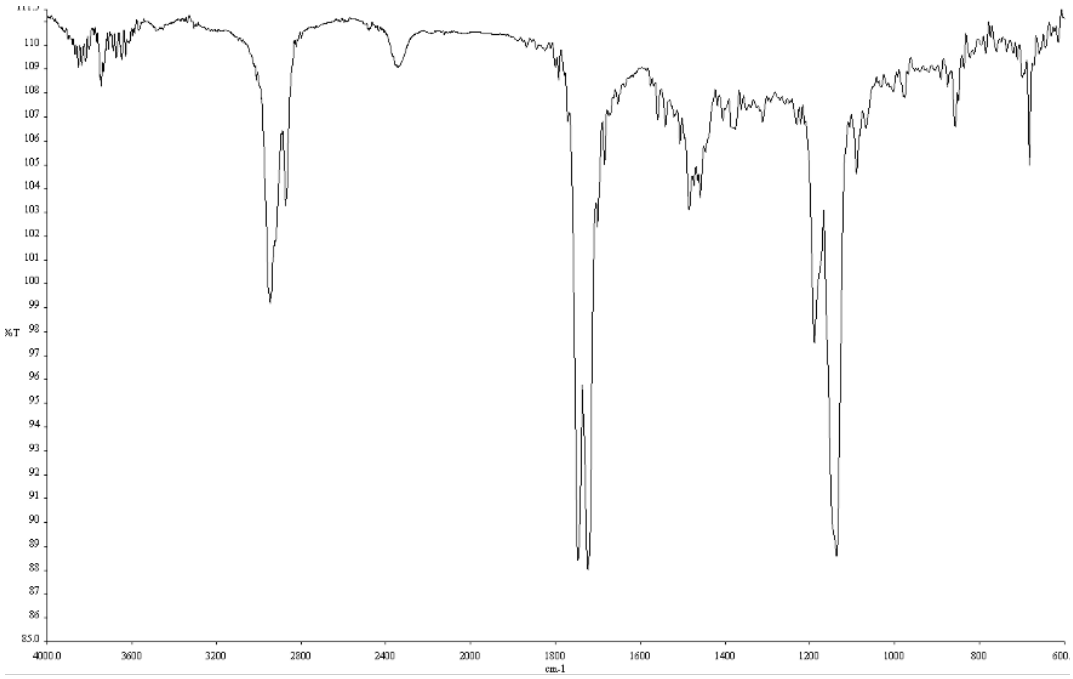

Figure A1.29. *Infrared spectrum (Thin Film, NaCl) of compound* ***115l.***

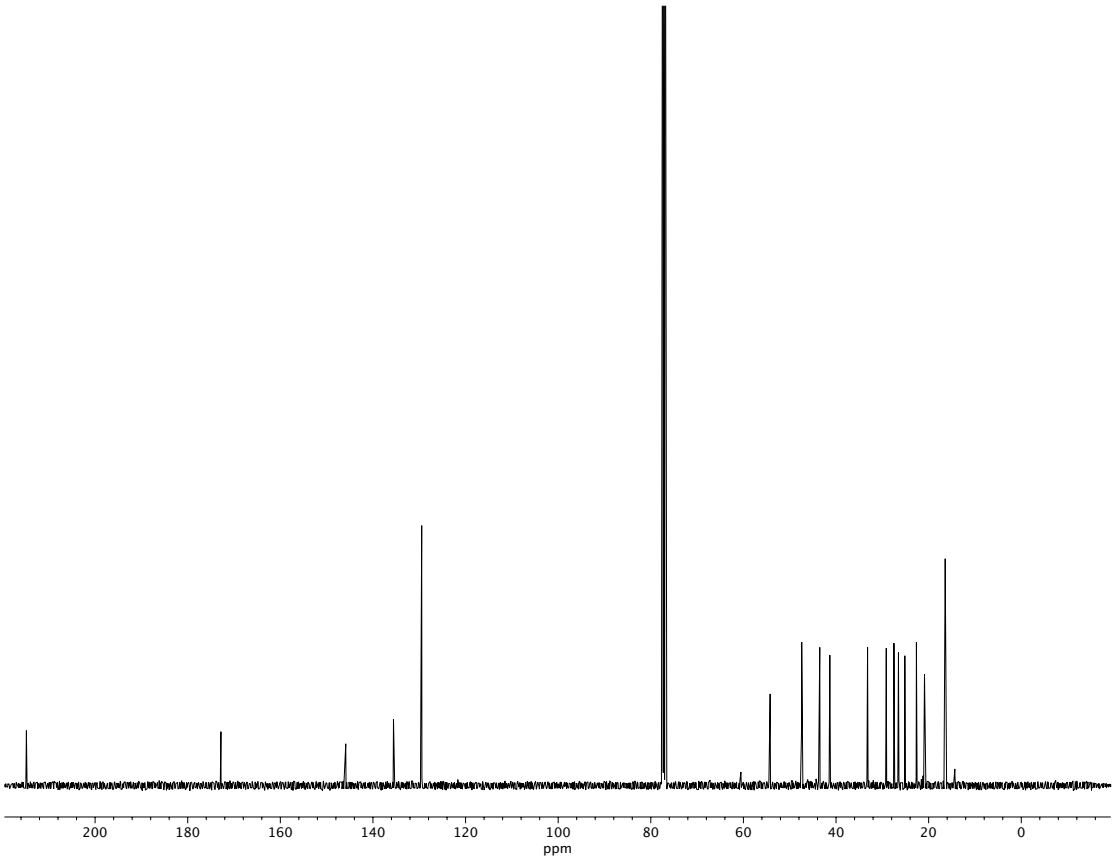

Figure A1.30. *^{13}C NMR (100 MHz, $CDCl_3$) of compound* ***115l.***

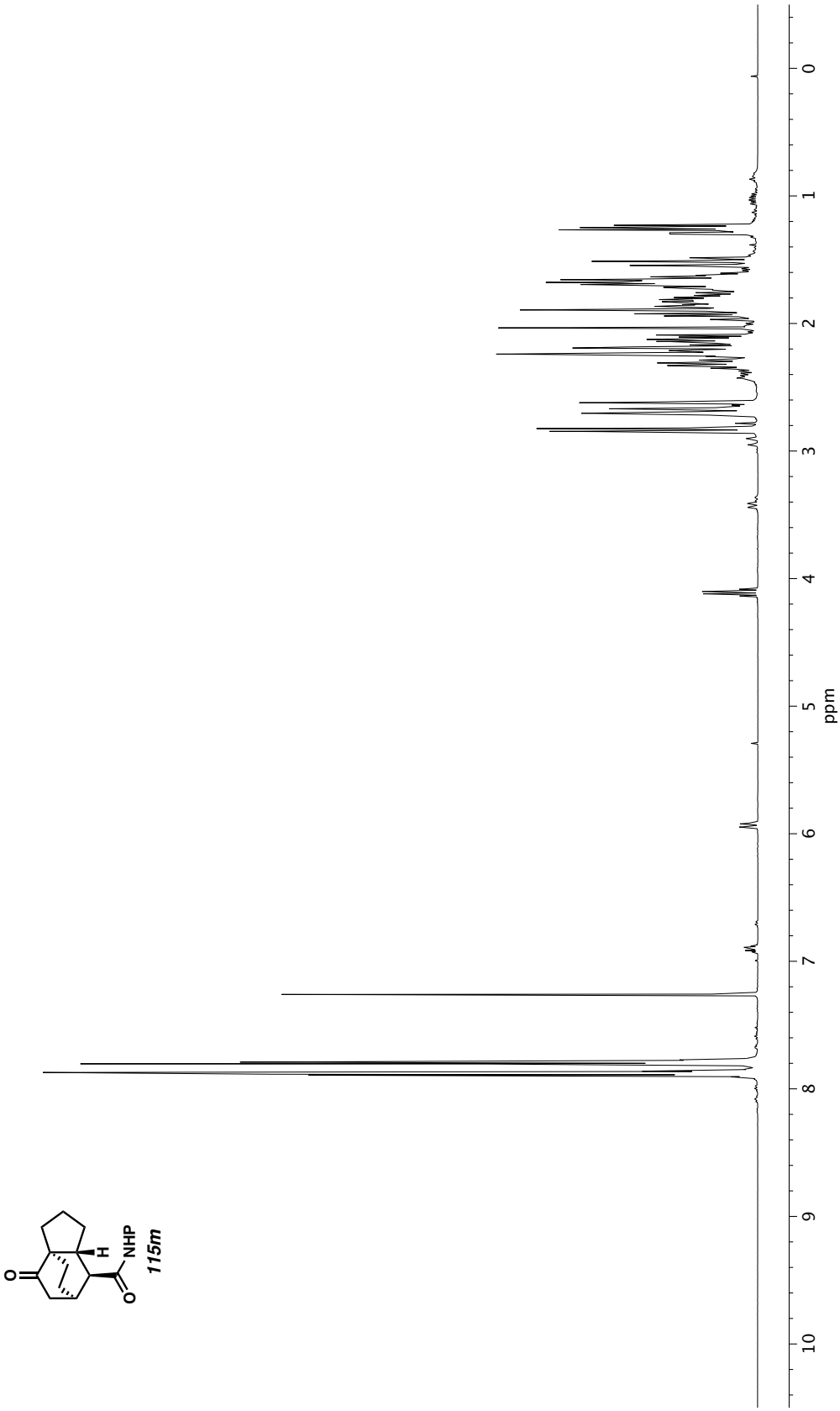

Figure A1.31. *^1H NMR (400 MHz, $CDCl_3$) of compound* ***115m.***

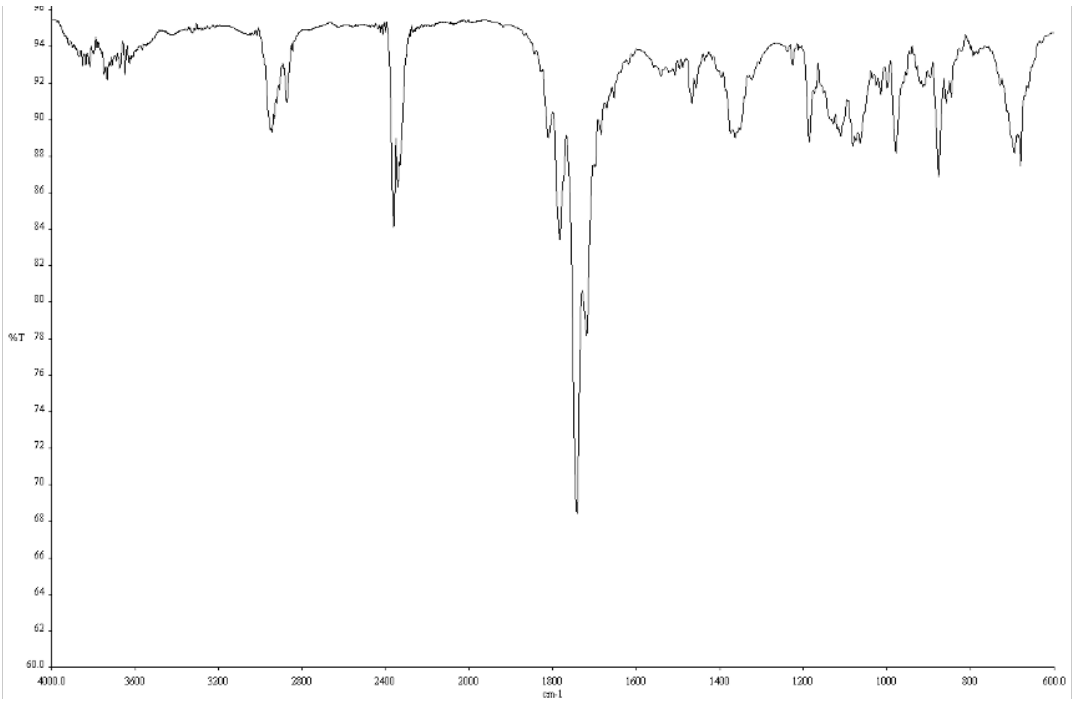

Figure A1.32. *Infrared spectrum (Thin Film, NaCl) of compound* ***115m.***

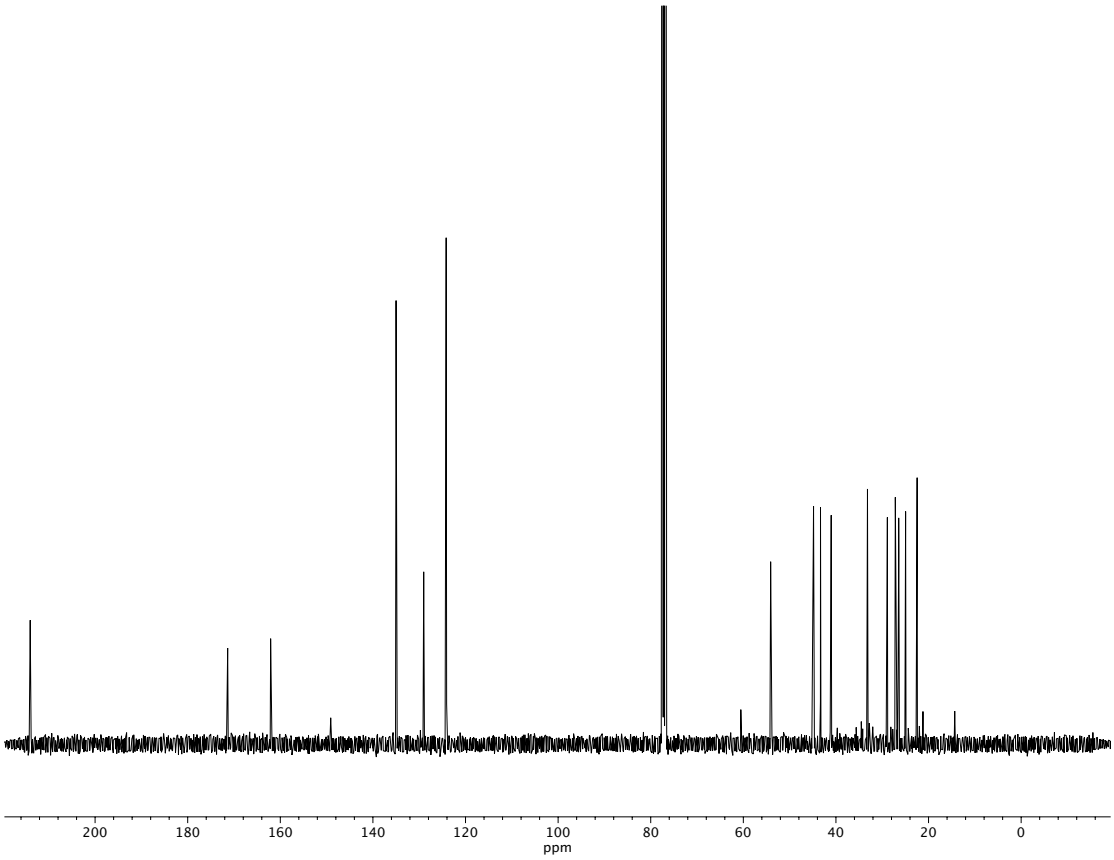

Figure A1.33. *^{13}C NMR (100 MHz, $CDCl_3$) of compound* ***115m.***

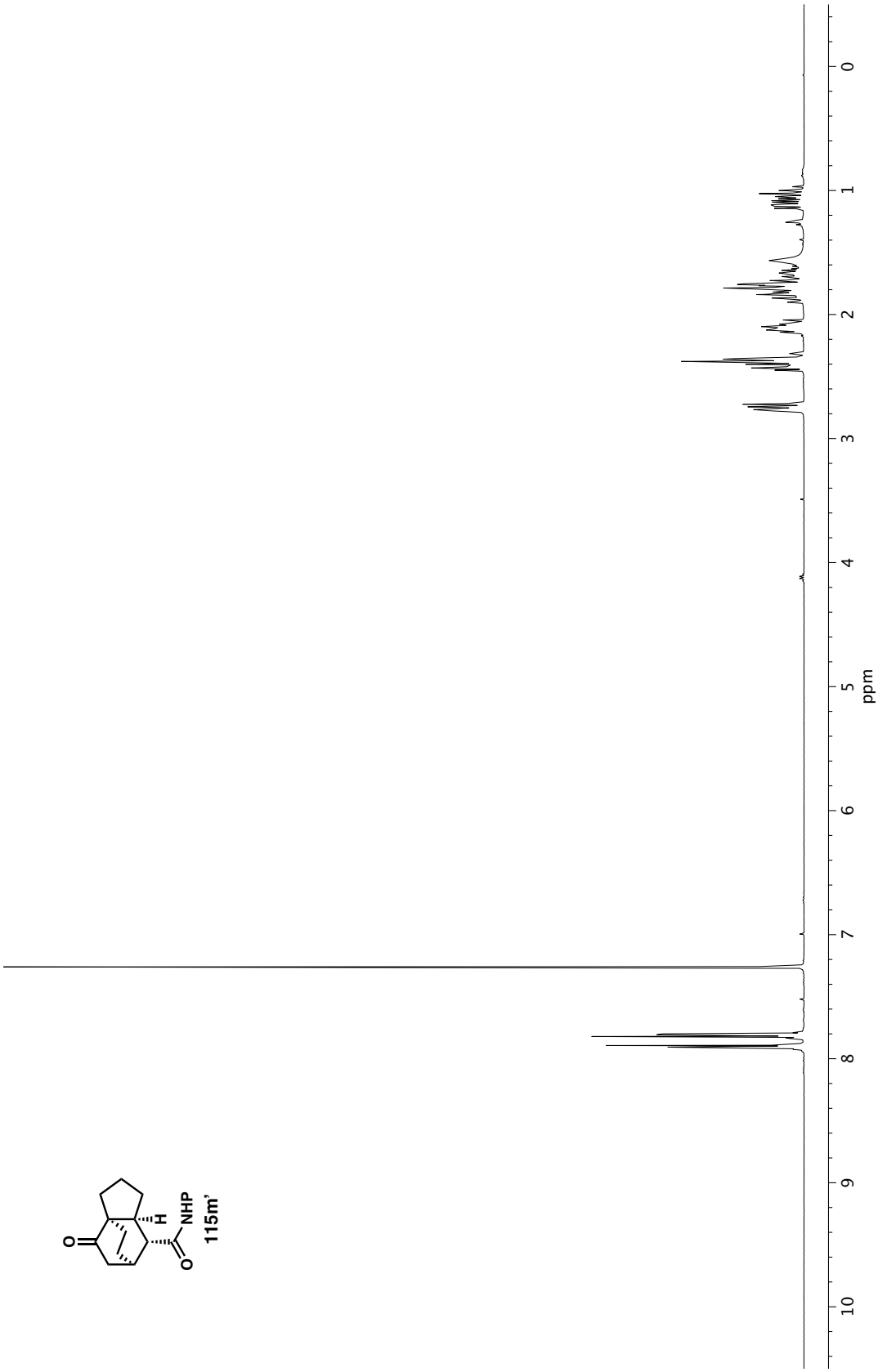

Figure A1.34. *^1H NMR (400 MHz, $CDCl_3$) of compound* ***115m.***

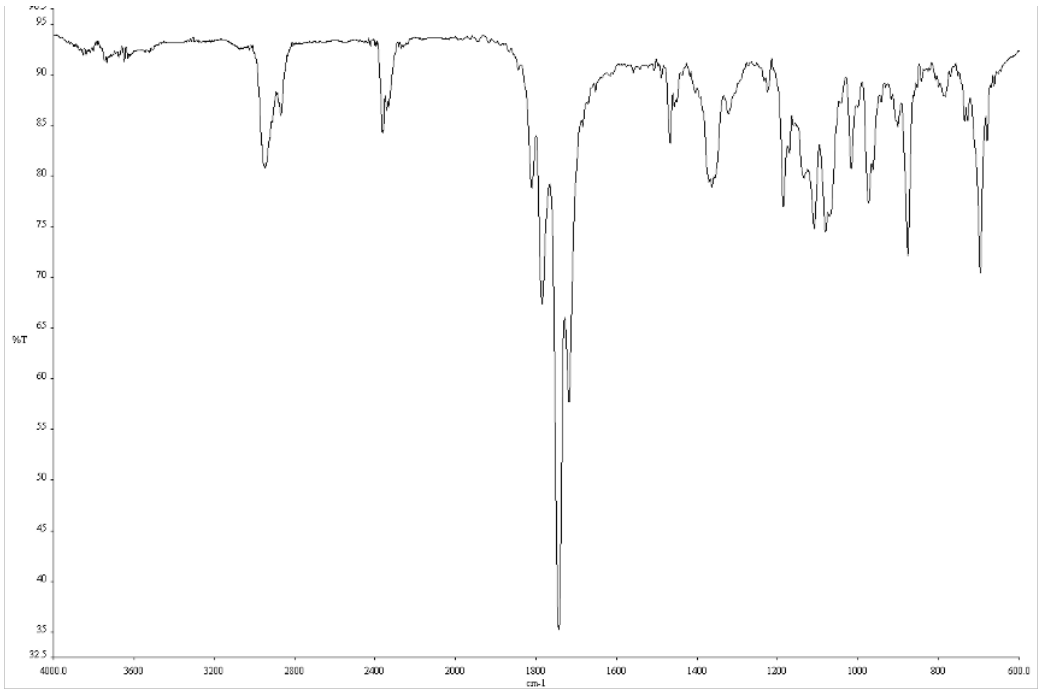

Figure A1.35. *Infrared spectrum (Thin Film, NaCl) of compound* ***115m′.***

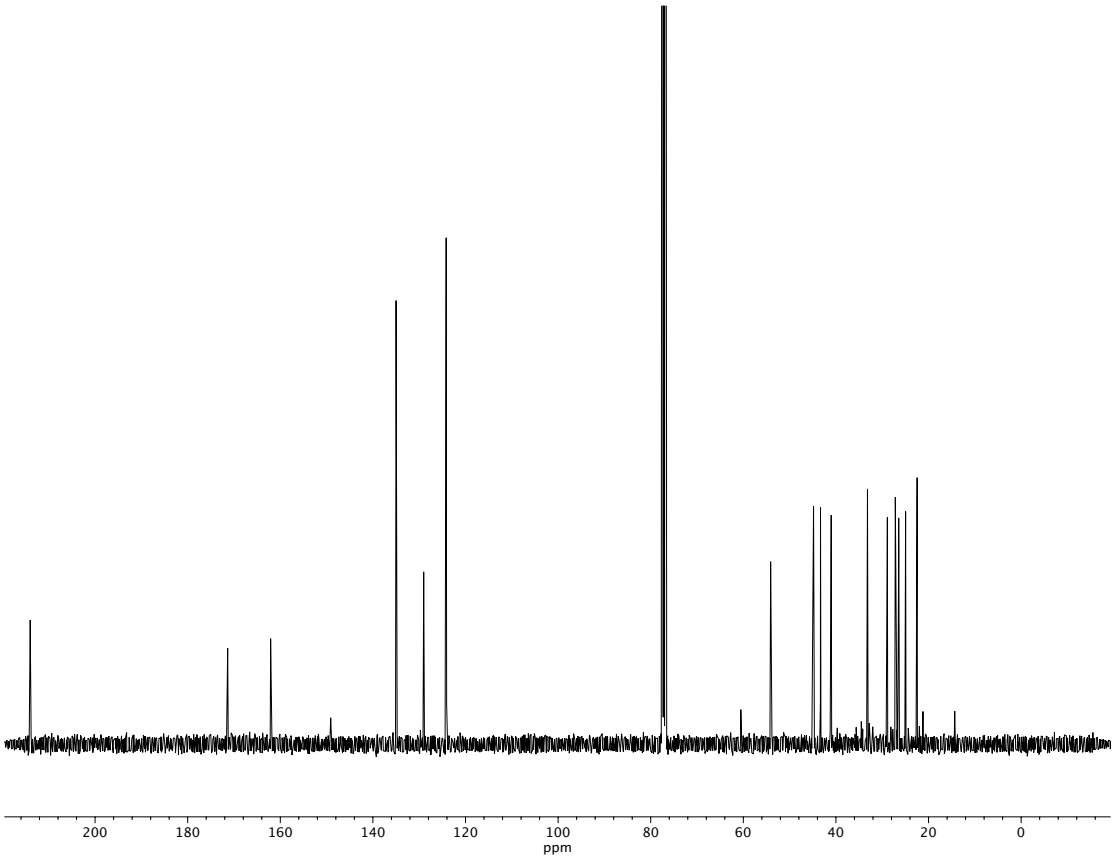

Figure A1.36. *^{13}C NMR (100 MHz, $CDCl_3$) of compound* ***115m′.***

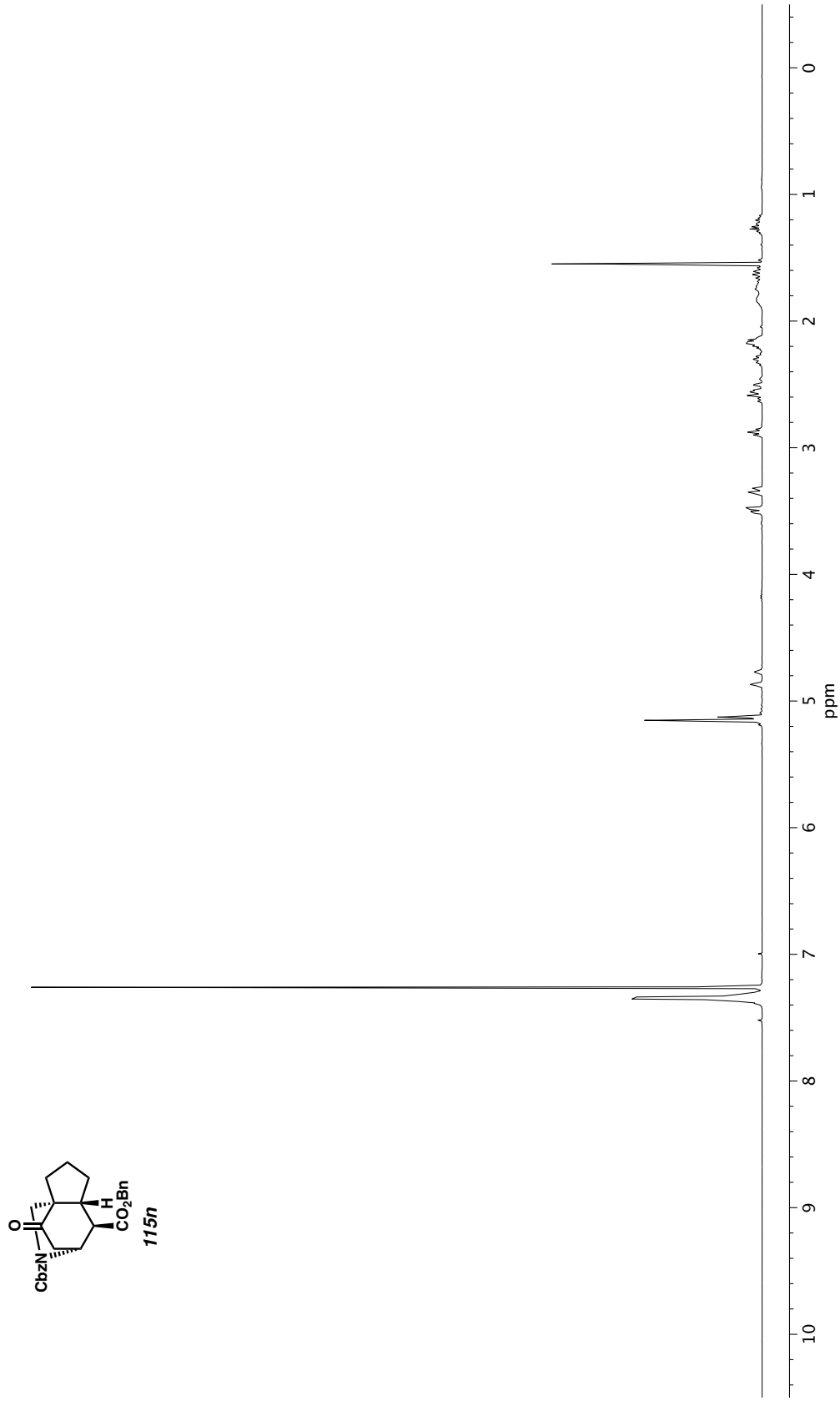

Figure A1.37. *^1H NMR (400 MHz, $CDCl_3$) of compound* ***115n.***

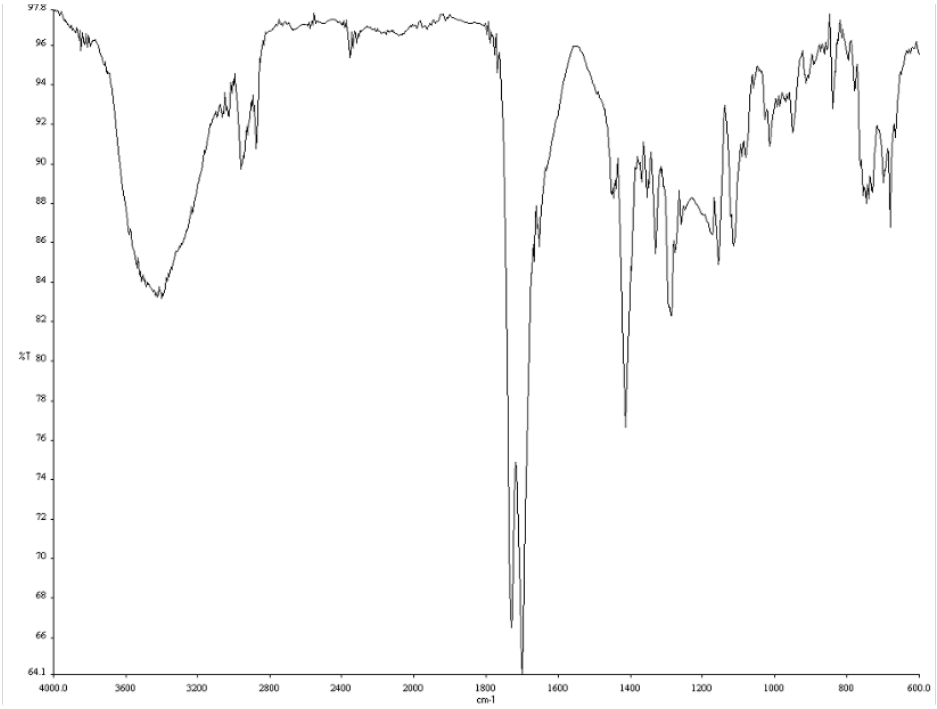

Figure A1.38. *Infrared spectrum (Thin Film, NaCl) of compound* ***115n.***

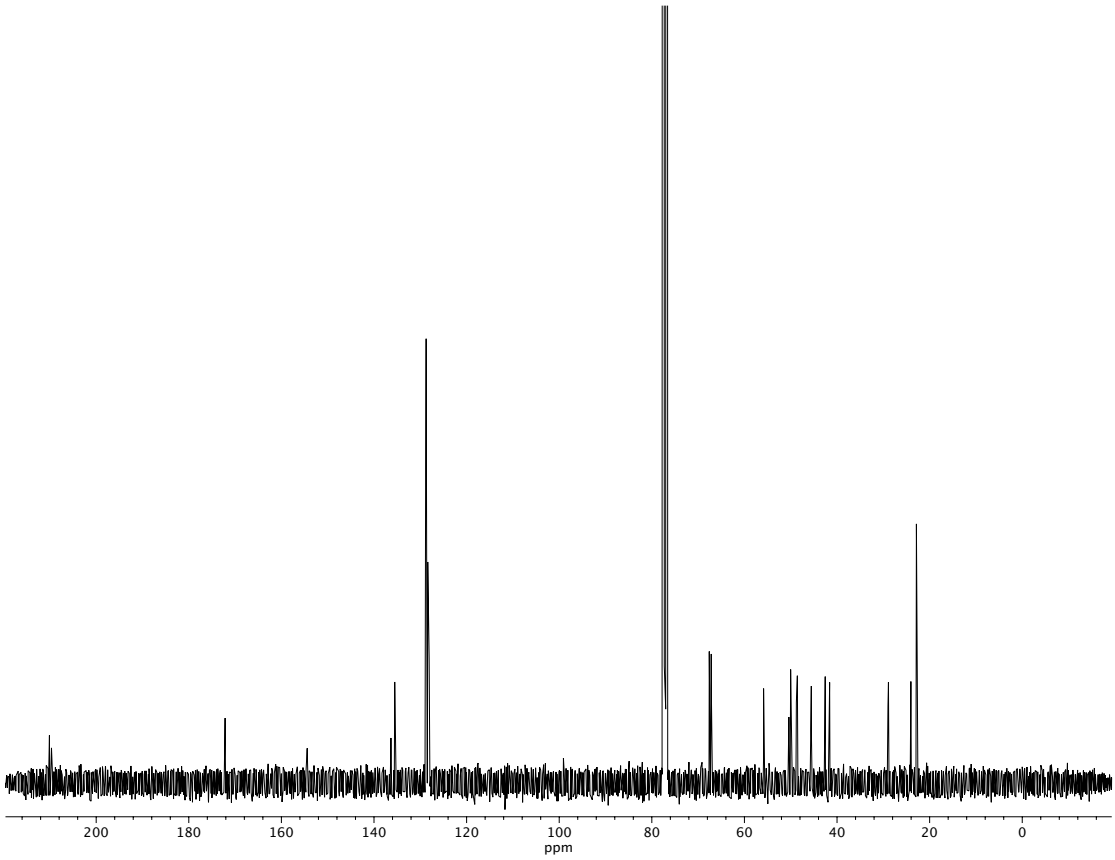

Figure A1.39. *^{13}C NMR (100 MHz, $CDCl_3$) of compound* ***115n.***

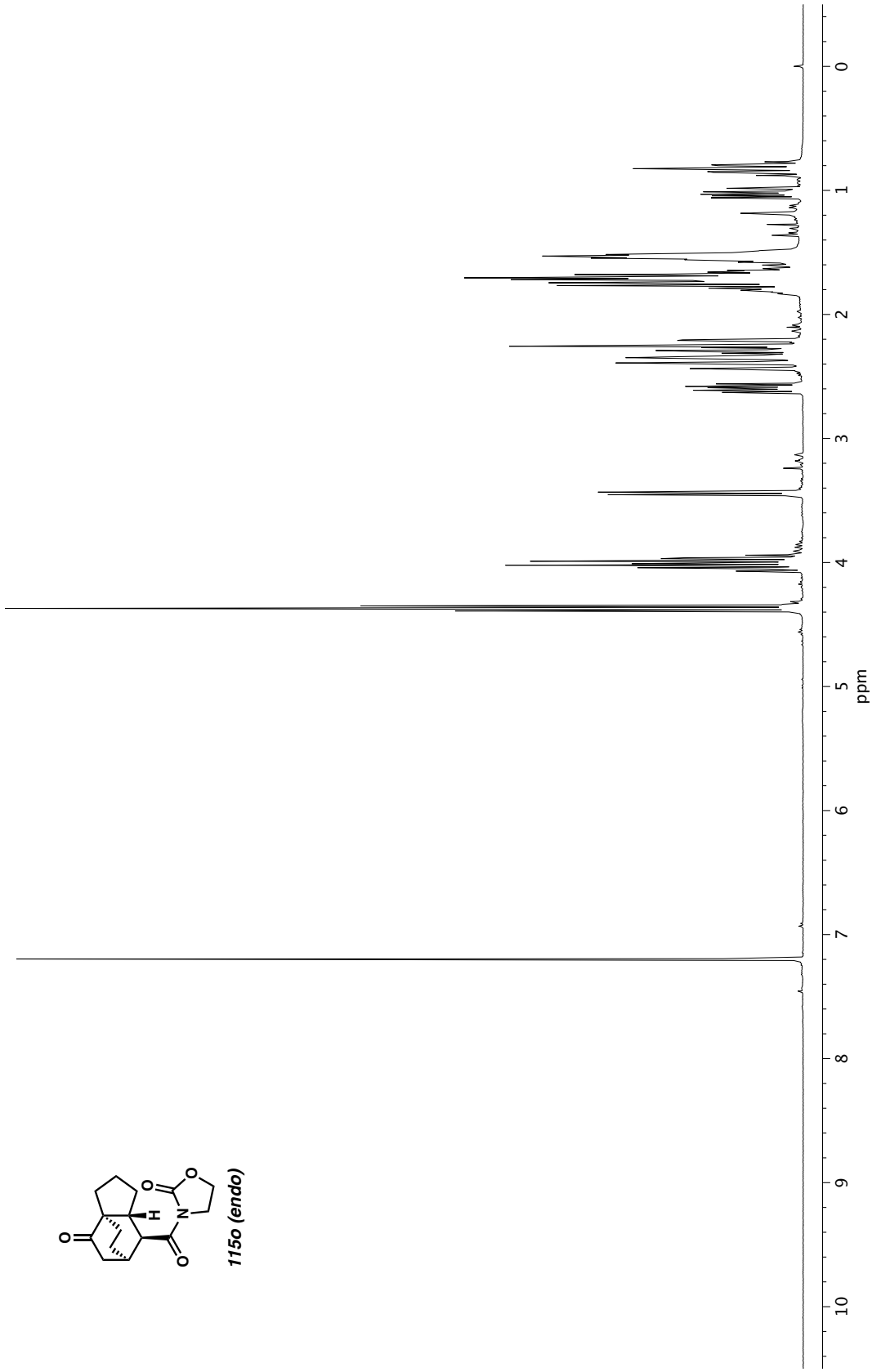

115o (endo)

Figure A1.40. *^1H NMR (400 MHz, $CDCl_3$) of compound* ***115o.***

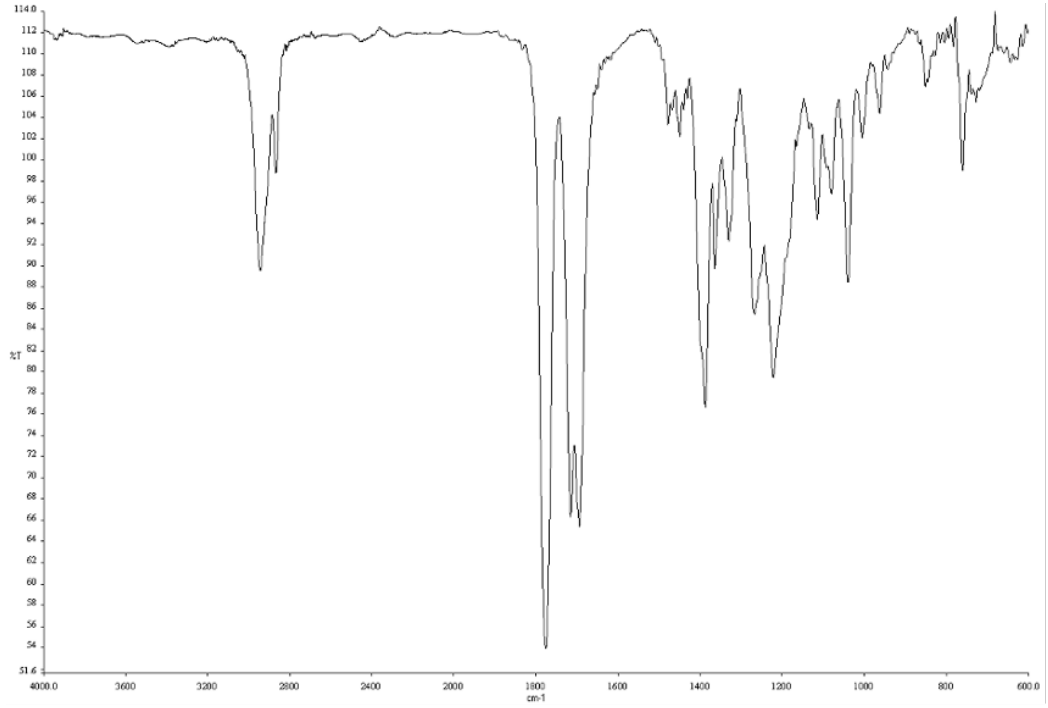

Figure A1.41. *Infrared spectrum (Thin Film, NaCl) of compound* ***115o.***

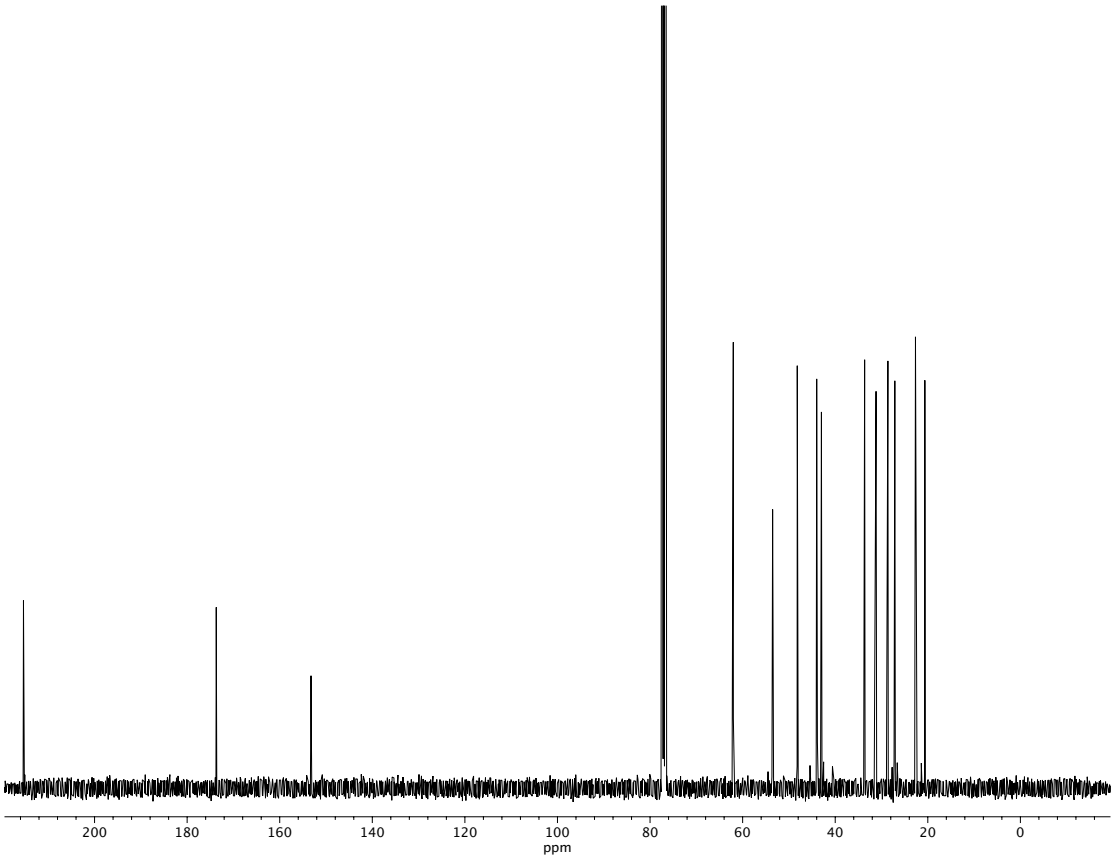

Figure A1.42. *^{13}C NMR (100 MHz, $CDCl_3$) of compound* ***115o.***

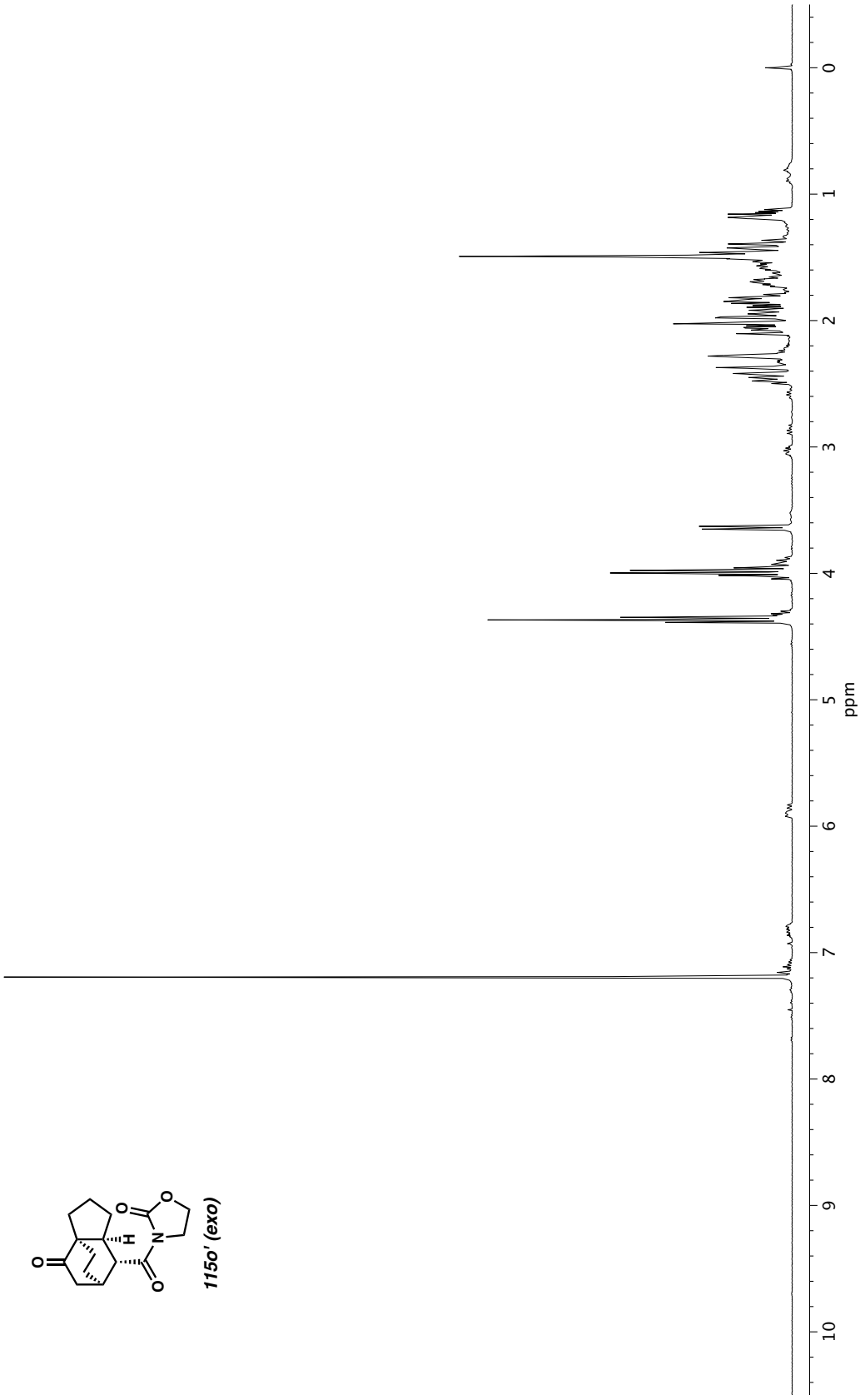

Figure A1.43. *^1H NMR (400 MHz, $CDCl_3$) of compound* ***115o.***

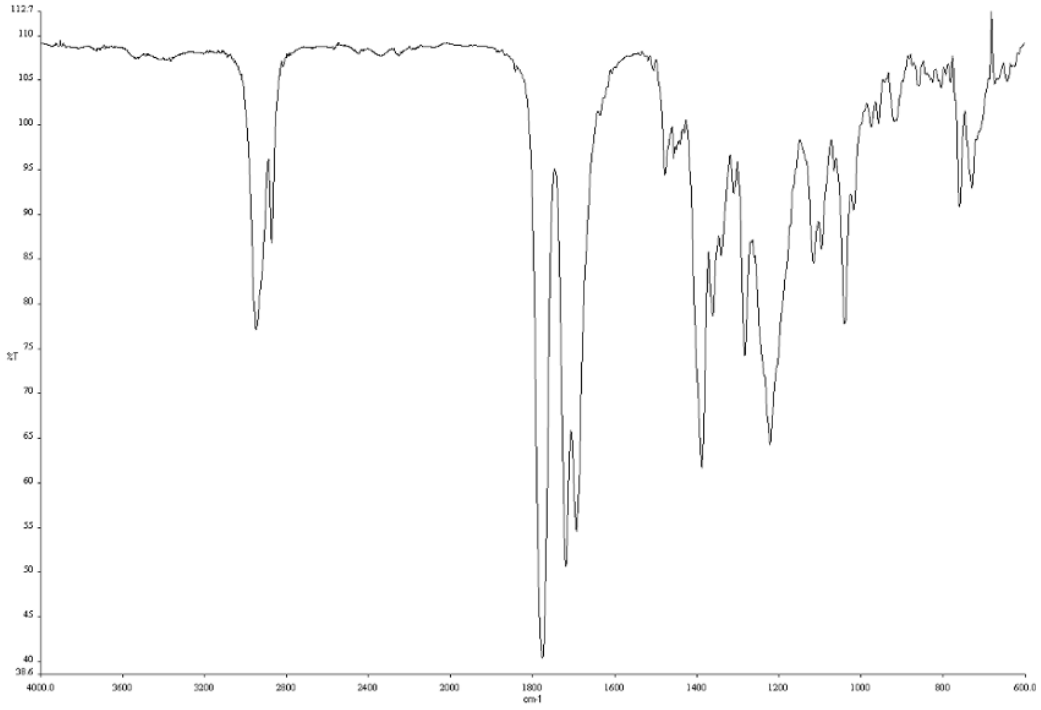

Figure A1.44. *Infrared spectrum (Thin Film, NaCl) of compound* ***115o′.***

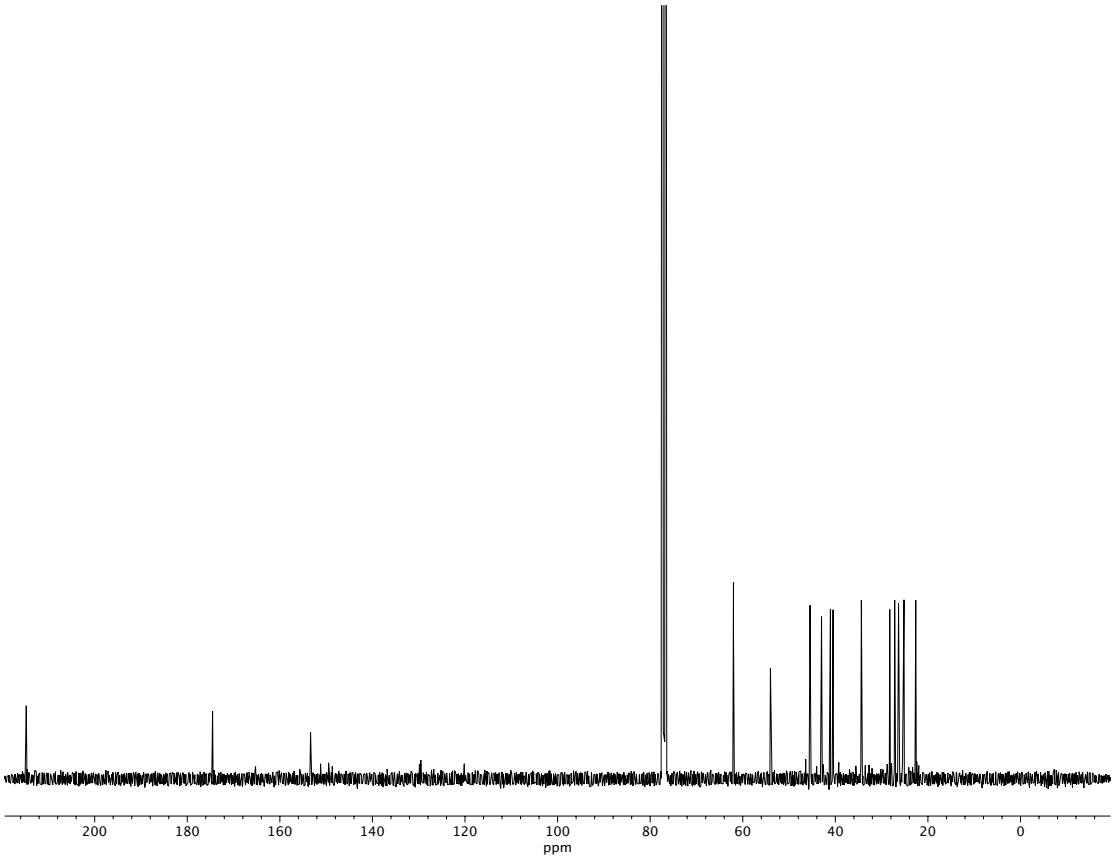

Figure A1.45. *^{13}C NMR (100 MHz, $CDCl_3$) of compound* ***115o′.***

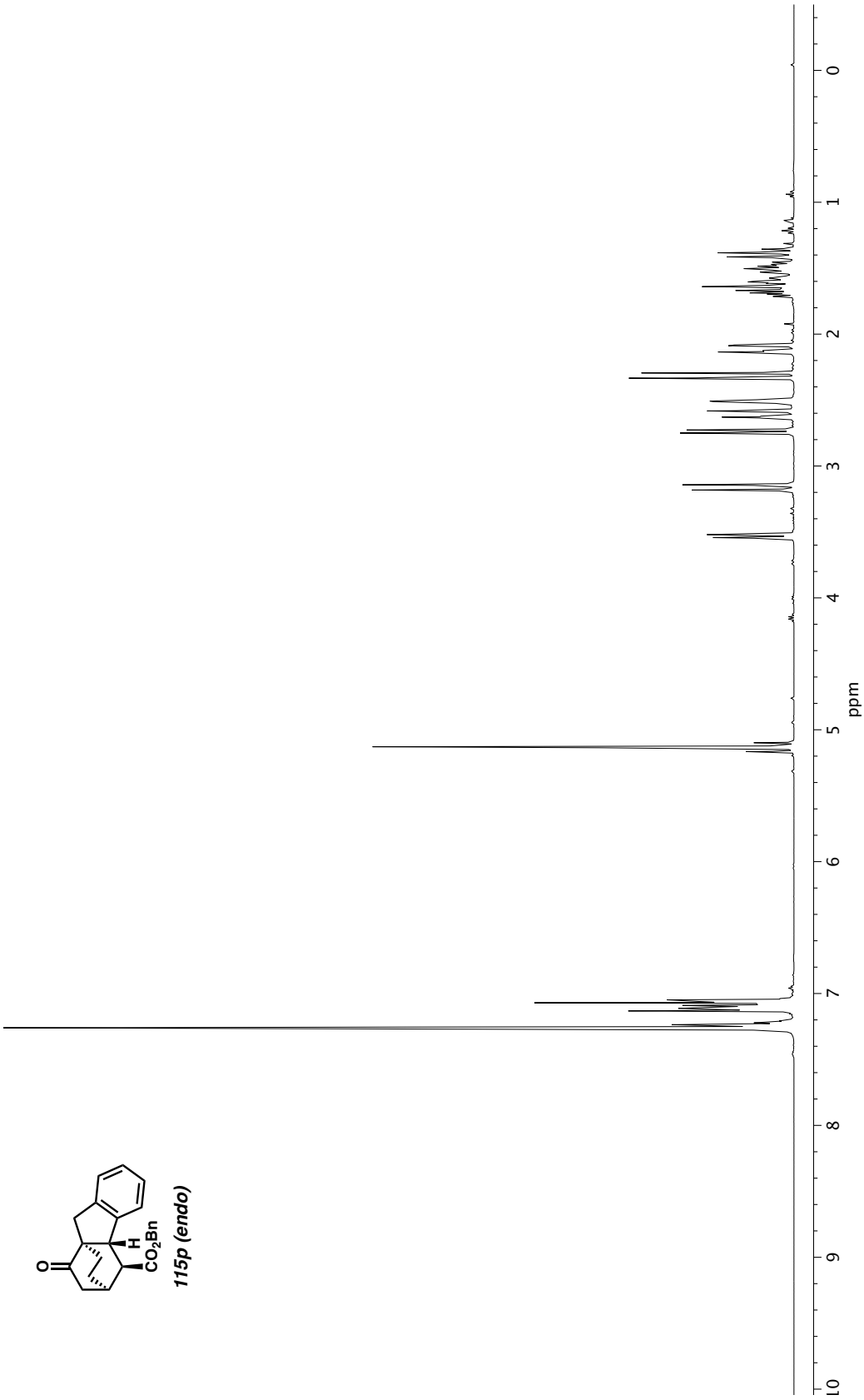

Figure A1.46. *^1H NMR (400 MHz, $CDCl_3$) of compound* ***115p.***

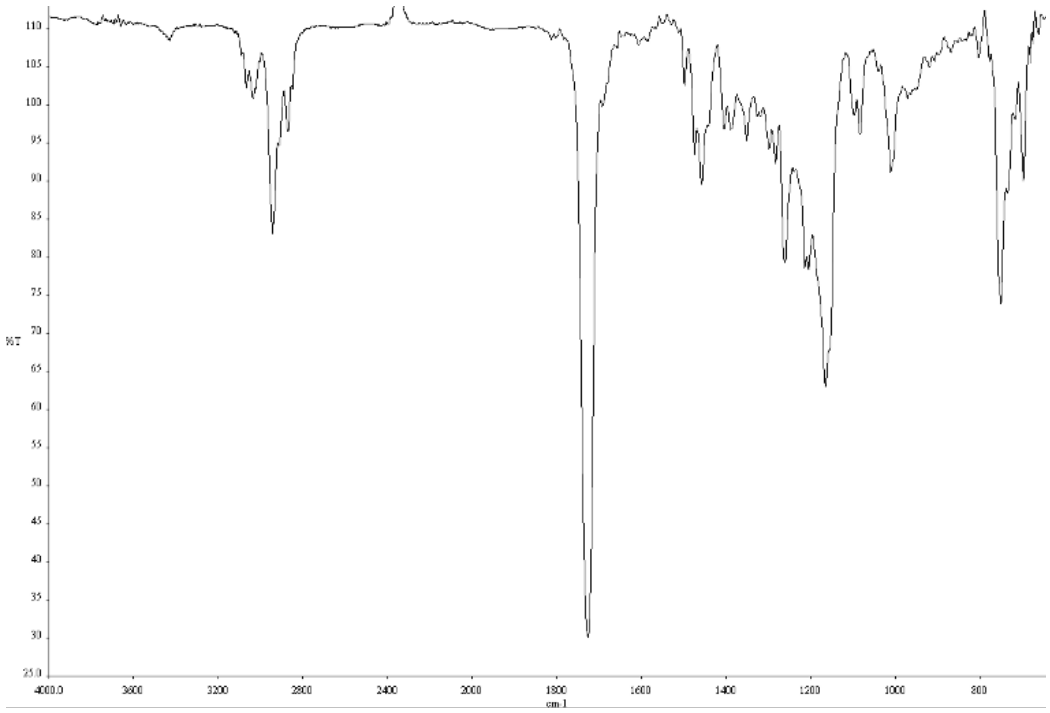

Figure A1.47. *Infrared spectrum (Thin Film, NaCl) of compound* ***115p.***

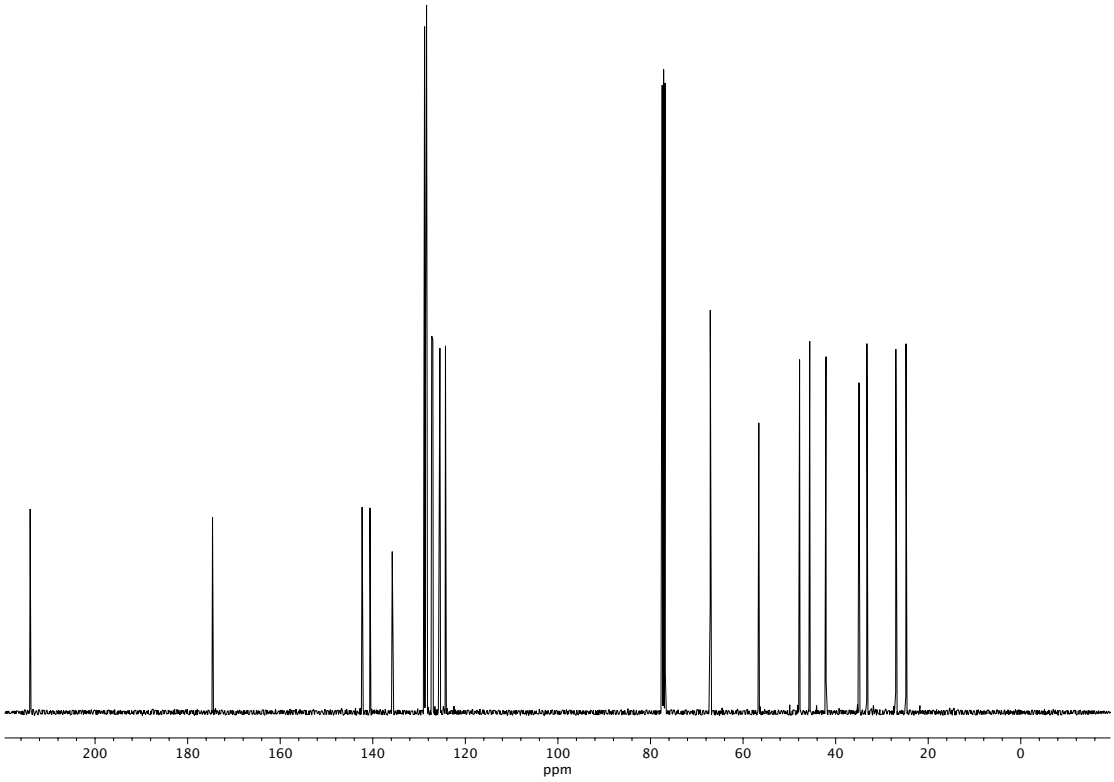

Figure A1.48. *^{13}C NMR (100 MHz, $CDCl_3$) of compound* ***115p.***

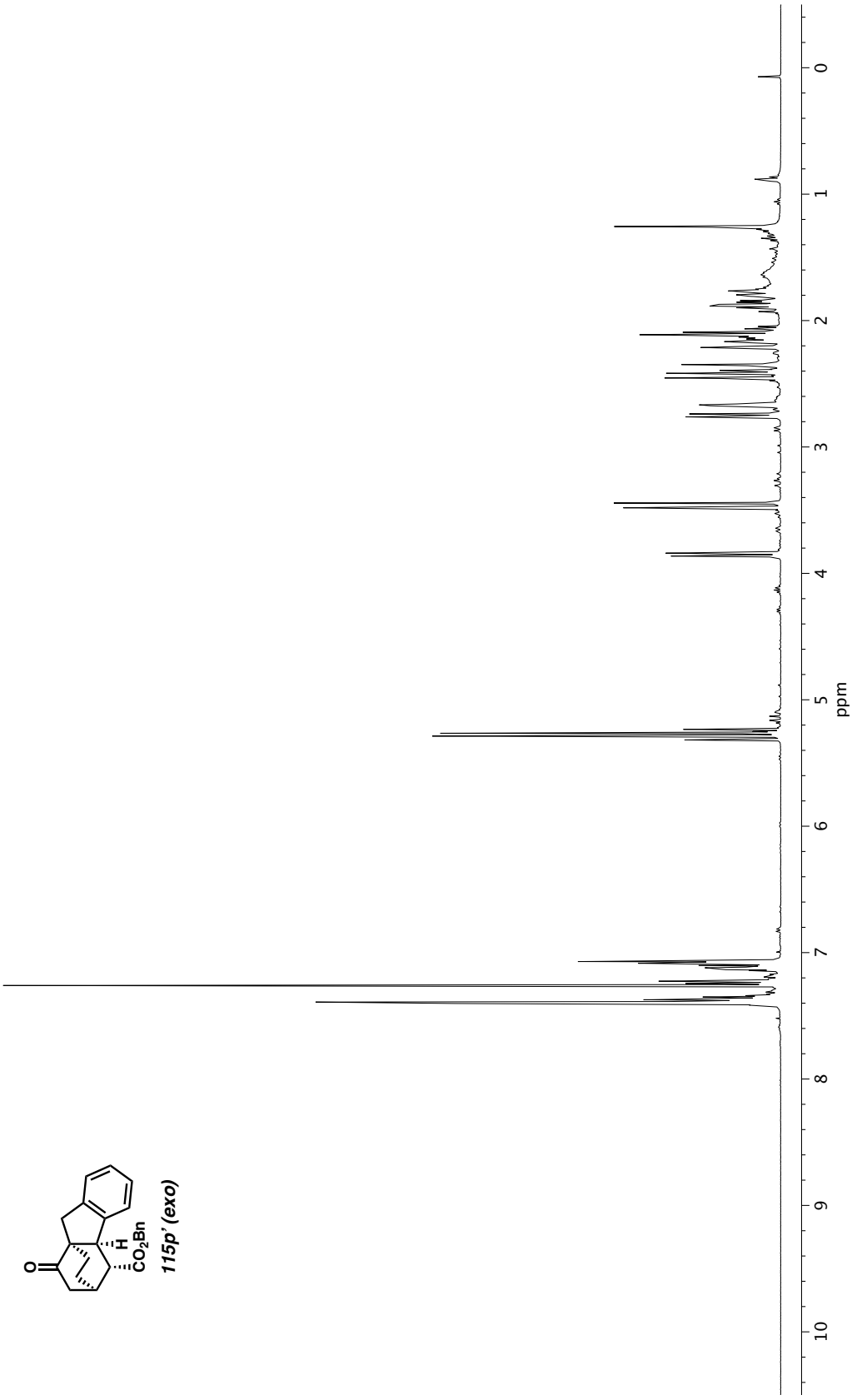

Figure A1.49. *^1H NMR (400 MHz, $CDCl_3$) of compound* ***115p.***

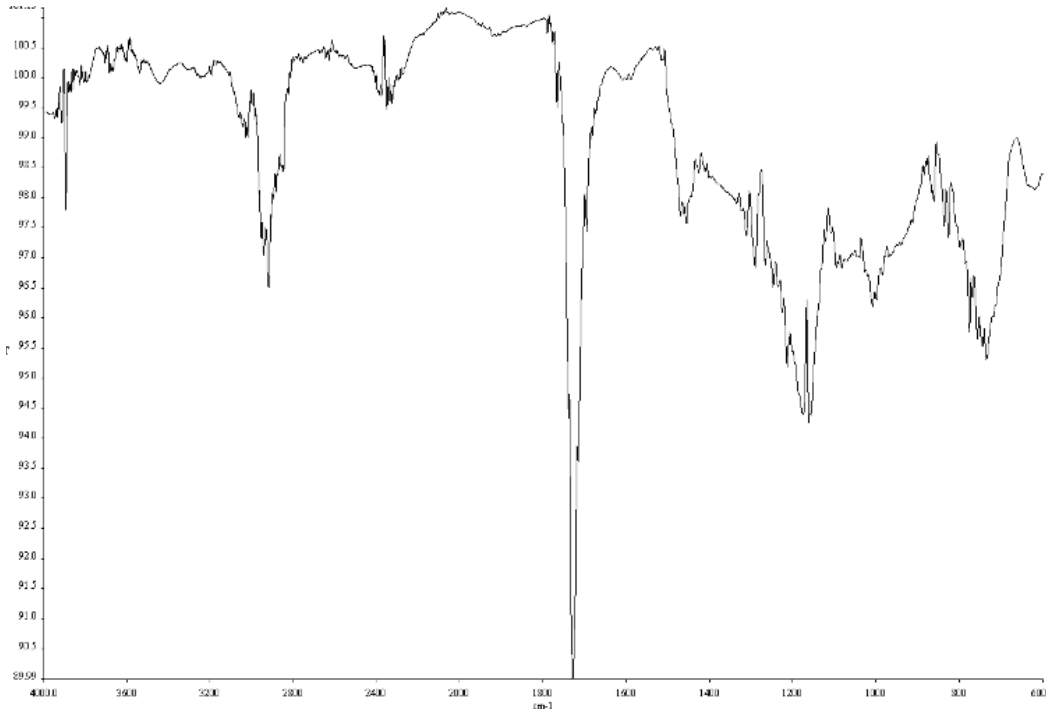

Figure A1.50. *Infrared spectrum (Thin Film, NaCl) of compound* ***115p′.***

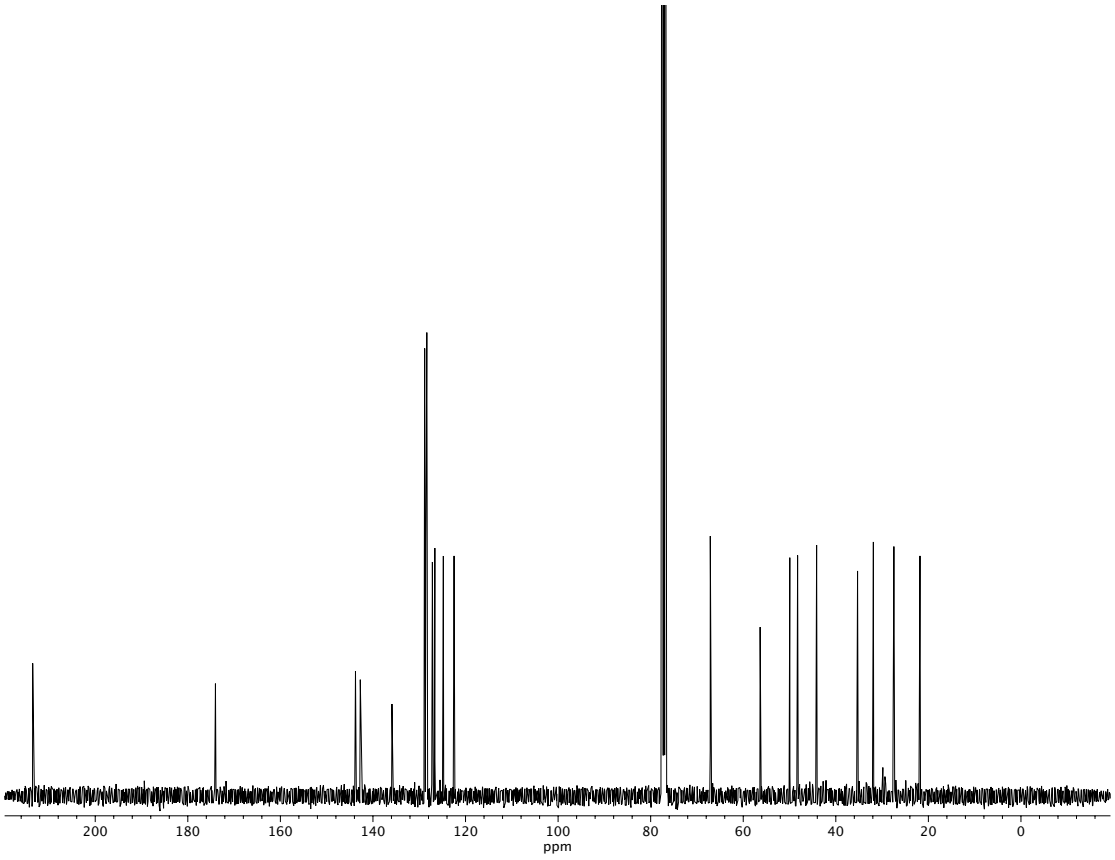

Figure A1.51. *^{13}C NMR (100 MHz, $CDCl_3$) of compound* ***115p′.***

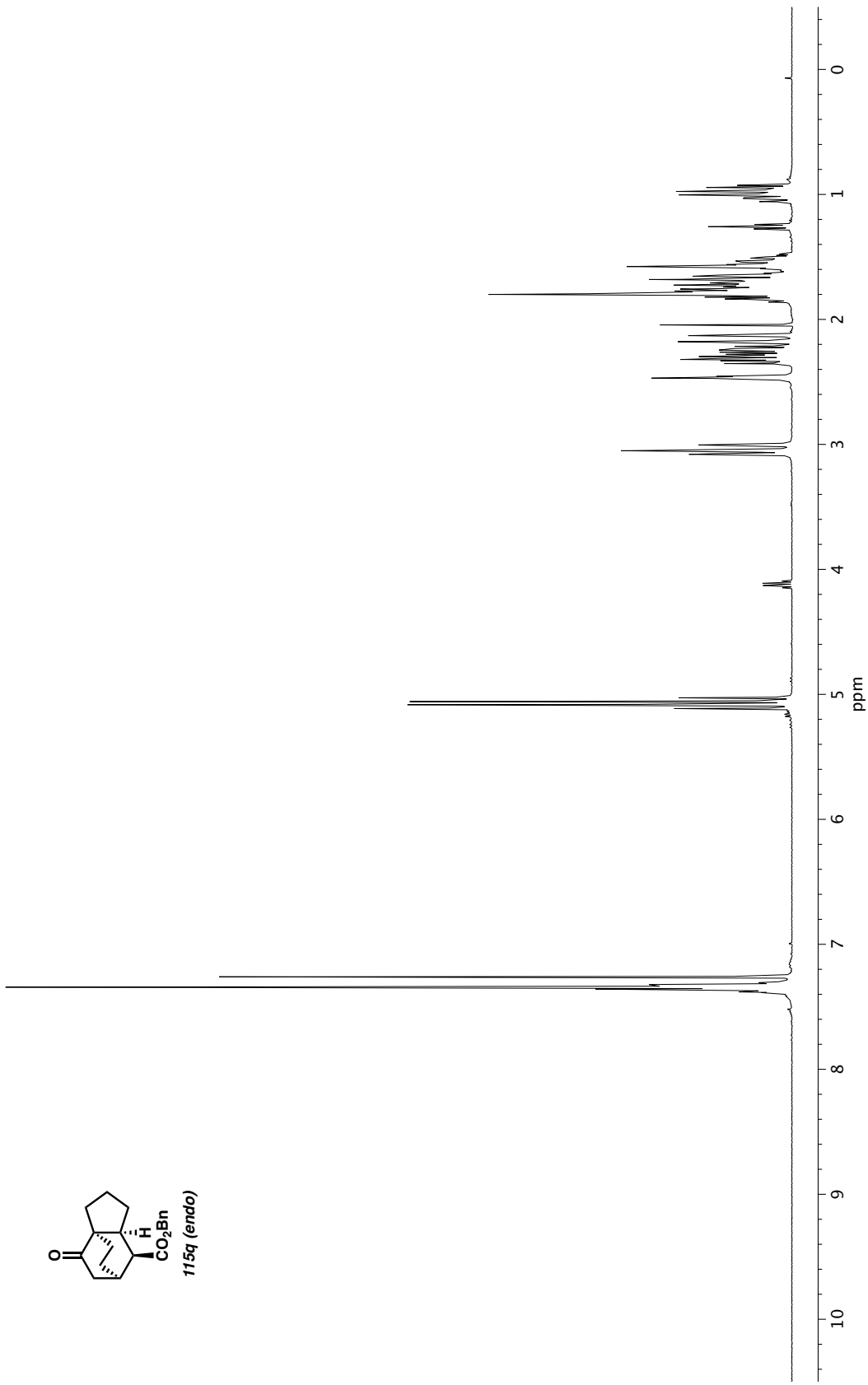

Figure A1.52. *^1H NMR (400 MHz, $CDCl_3$) of compound* ***115q.***

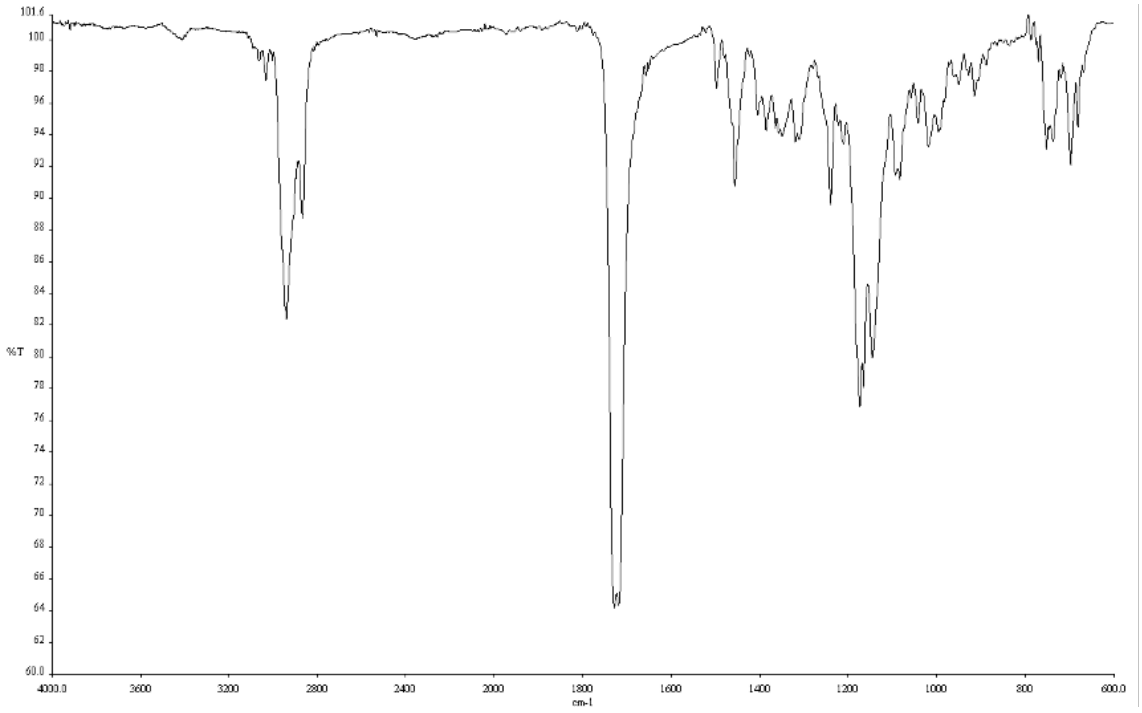

Figure A1.53. *Infrared spectrum (Thin Film, NaCl) of compound* ***115q.***

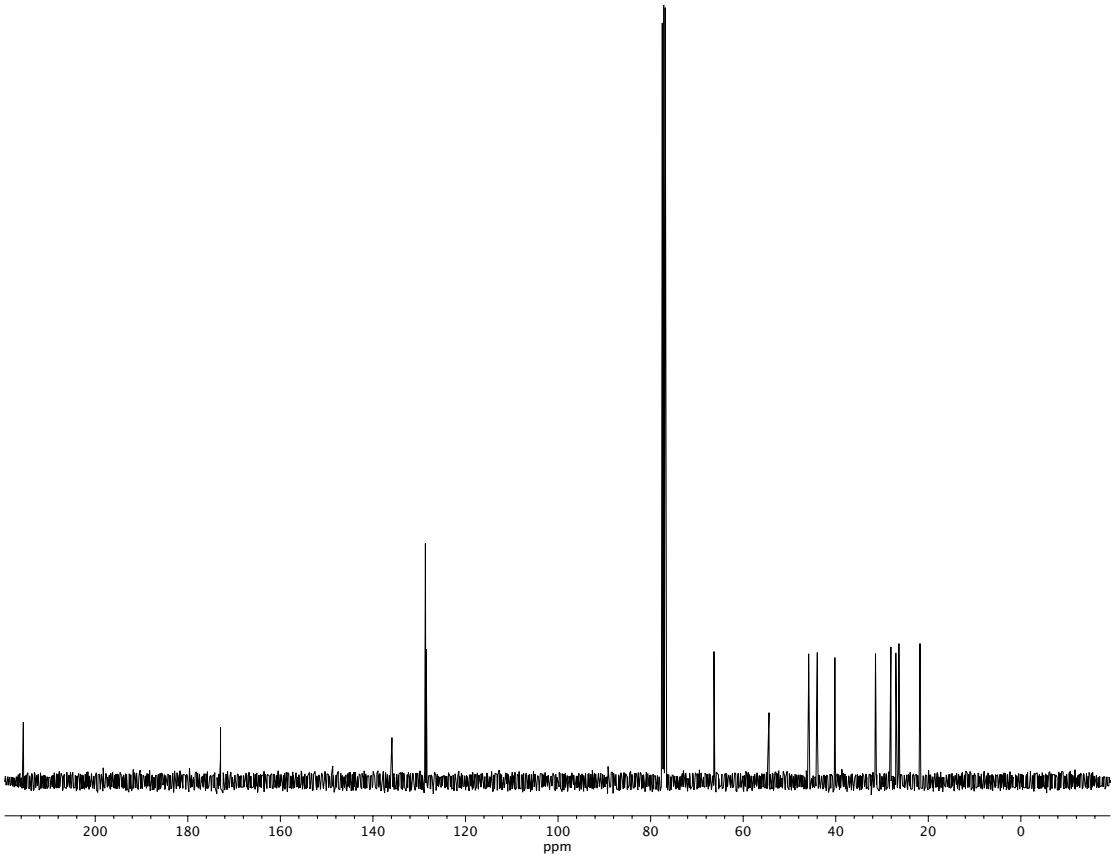

Figure A1.54. *^{13}C NMR (100 MHz, $CDCl_3$) of compound* ***115q.***

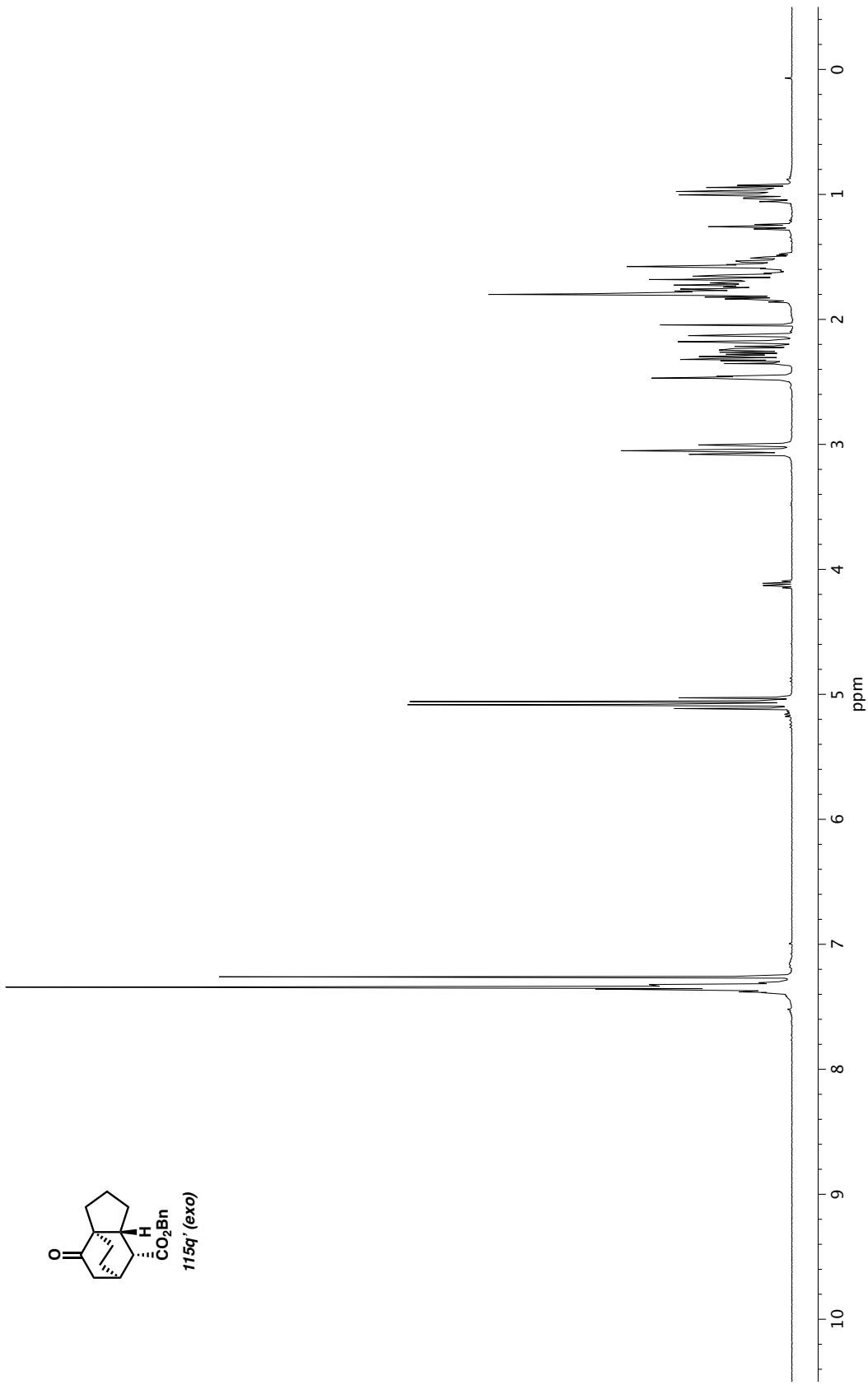

Figure A1.55. *^1H NMR (400 MHz, $CDCl_3$) of compound* ***115q.***

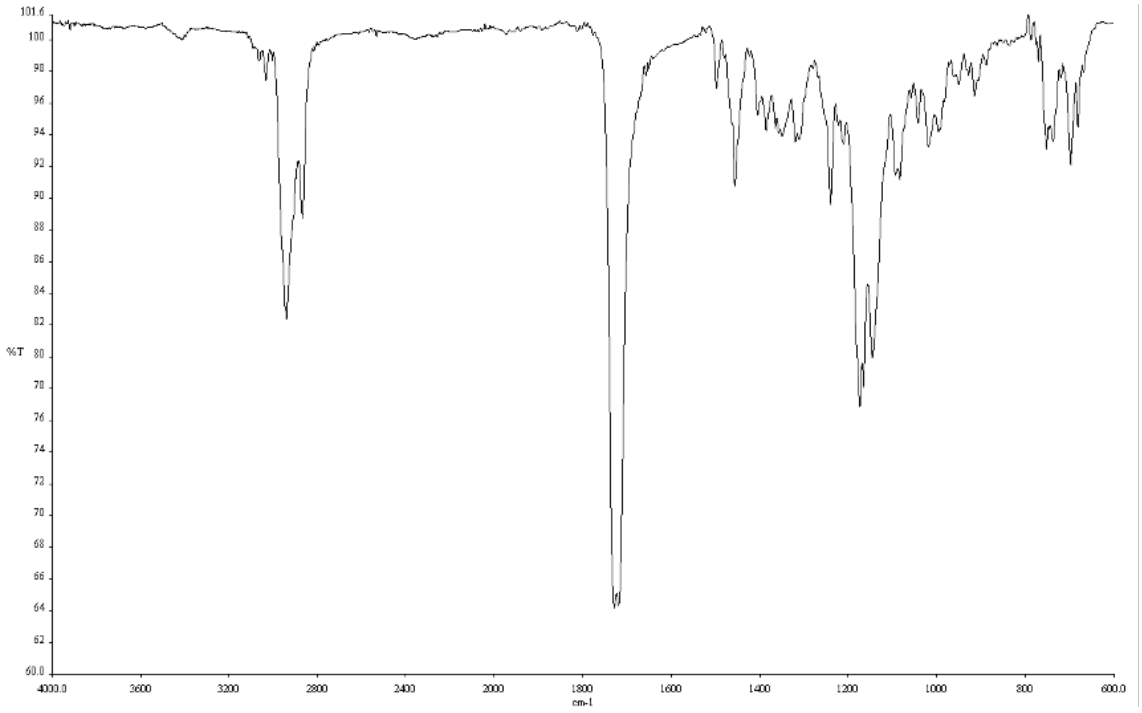

Figure A1.56. *Infrared spectrum (Thin Film, NaCl) of compound* ***115q'.***

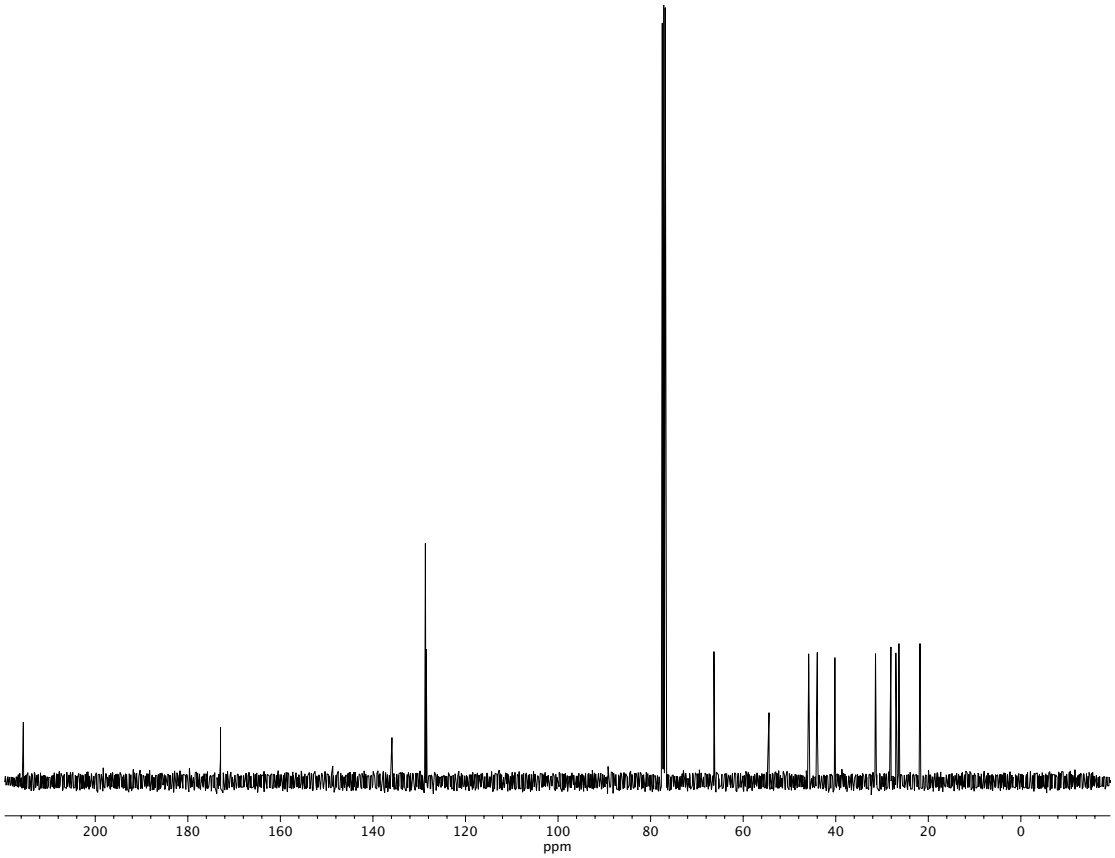

Figure A1.57. *^{13}C NMR (100 MHz, $CDCl_3$) of compound* ***115q'.***

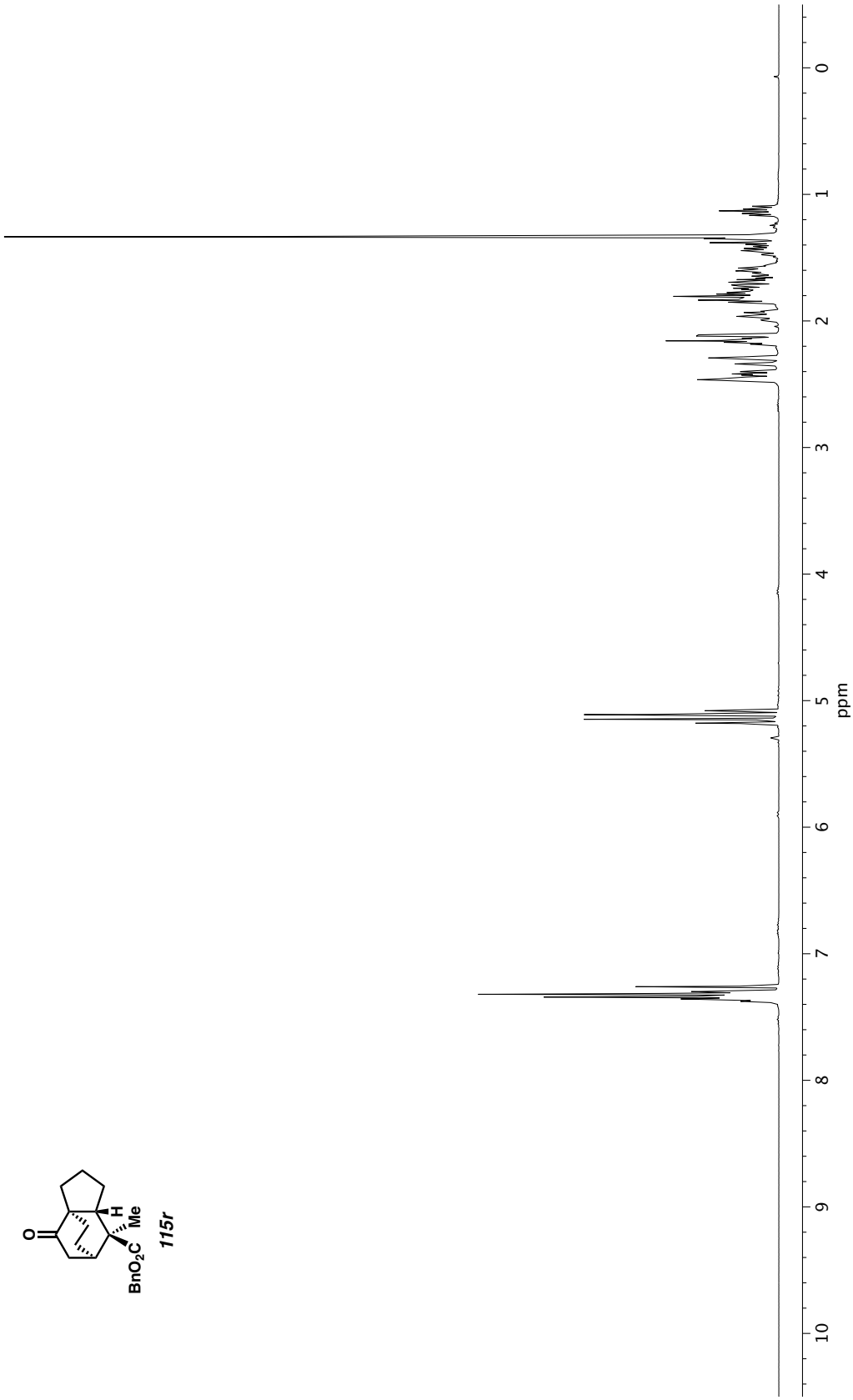

Figure A1.58. *^1H NMR (400 MHz, $CDCl_3$) of compound* ***115r.***

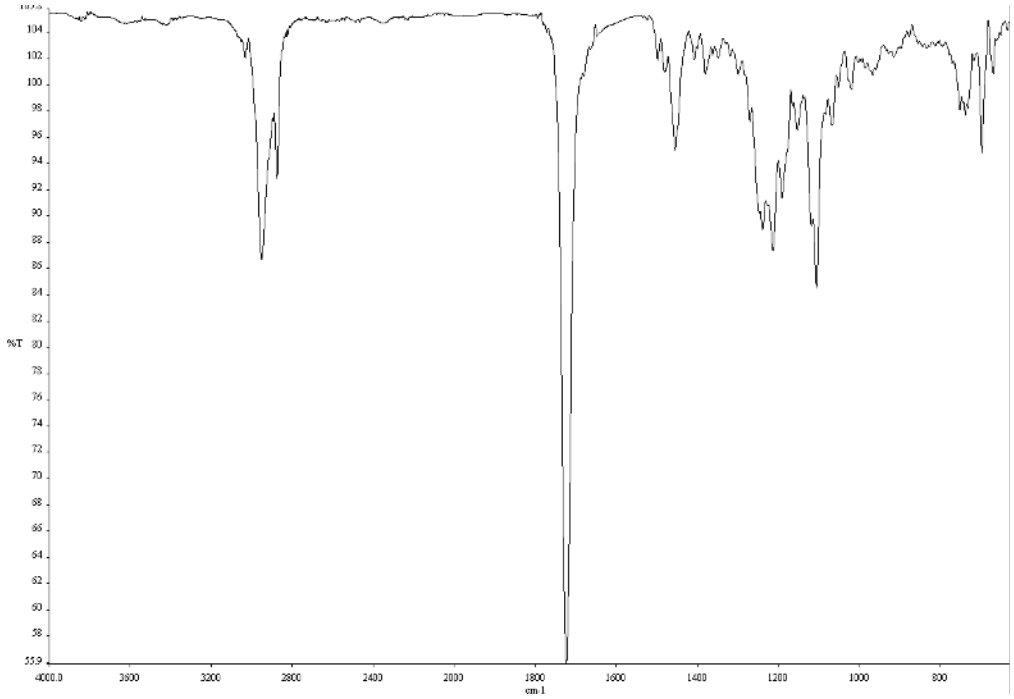

Figure A1.59. *Infrared spectrum (Thin Film, NaCl) of compound* ***115r.***

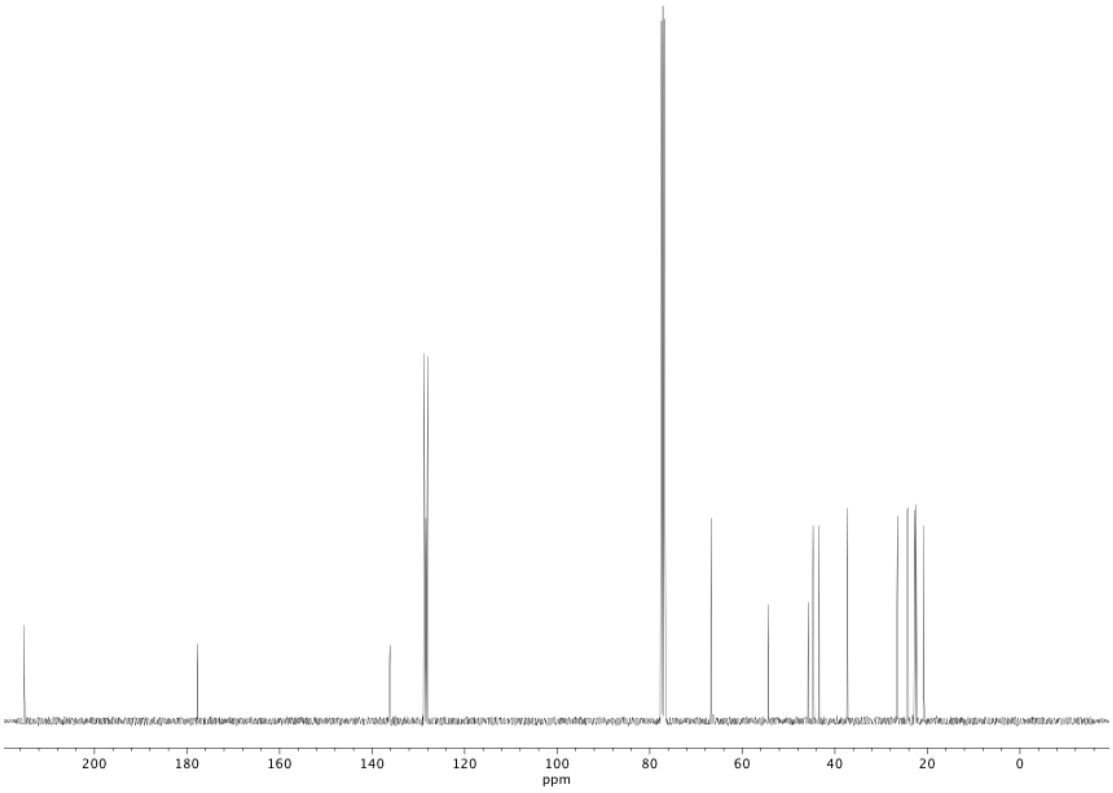

Figure A1.60. *^{13}C NMR (100 MHz, $CDCl_3$) of compound* ***115r.***

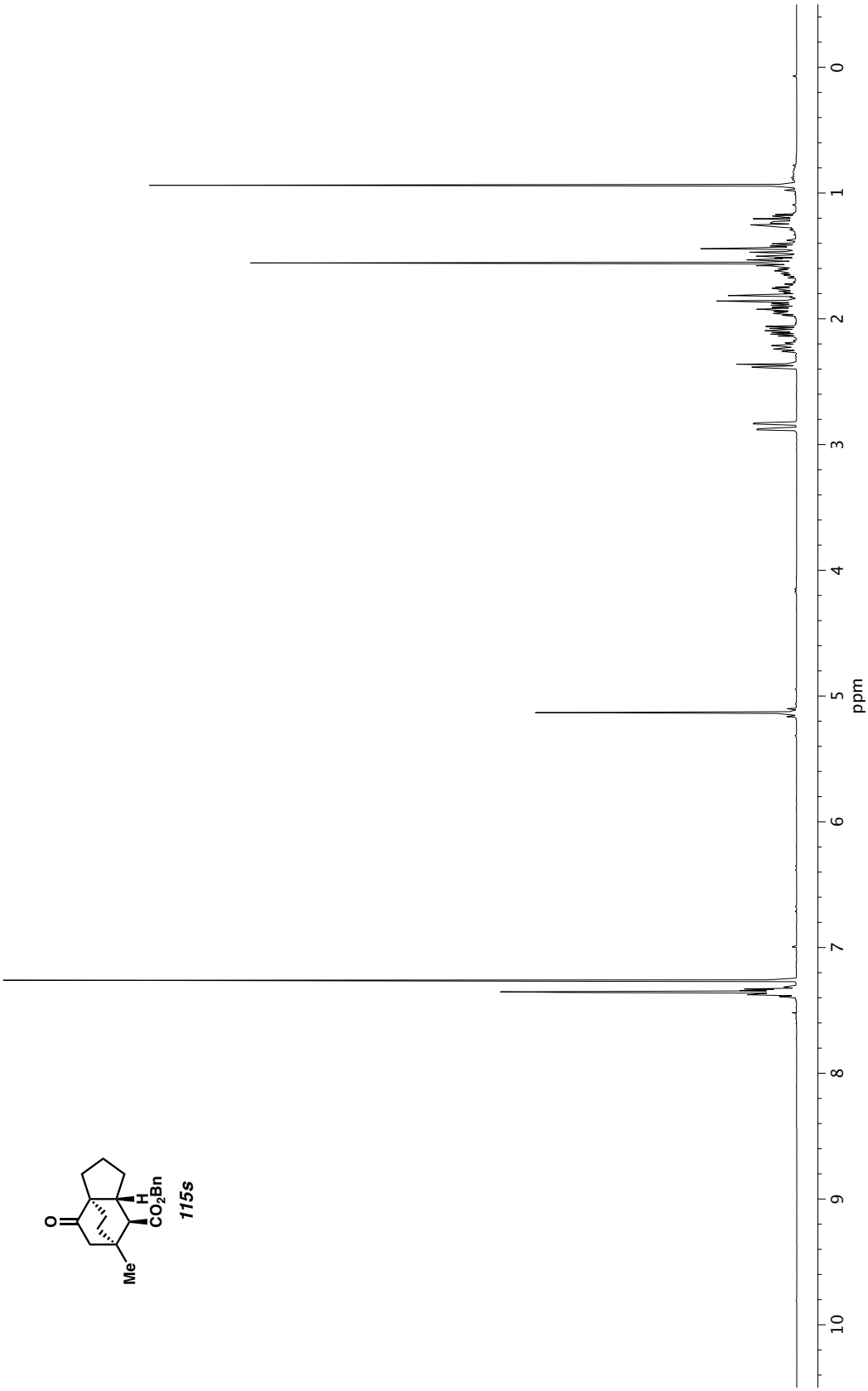

Figure A1.61. *^1H NMR (400 MHz, $CDCl_3$) of compound* ***115s.***

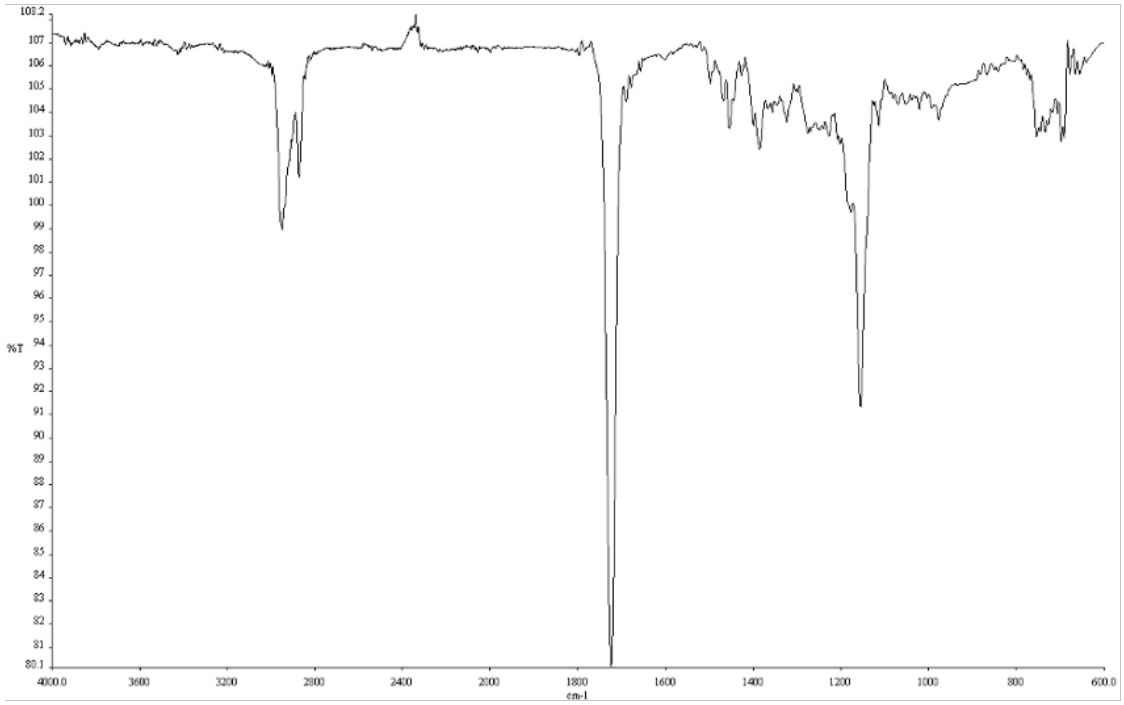

Figure A1.62. *Infrared spectrum (Thin Film, NaCl) of compound* ***115s.***

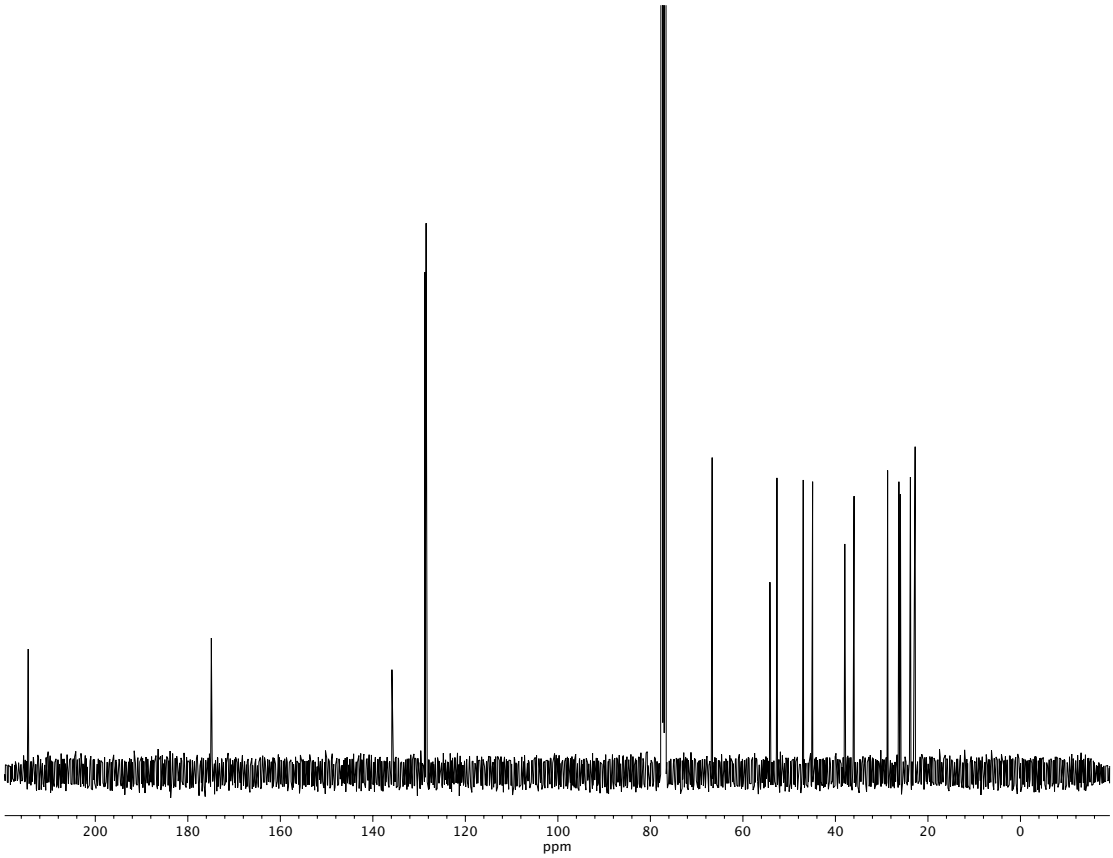

Figure A1.63. *^{13}C NMR (100 MHz, $CDCl_3$) of compound* ***115s.***

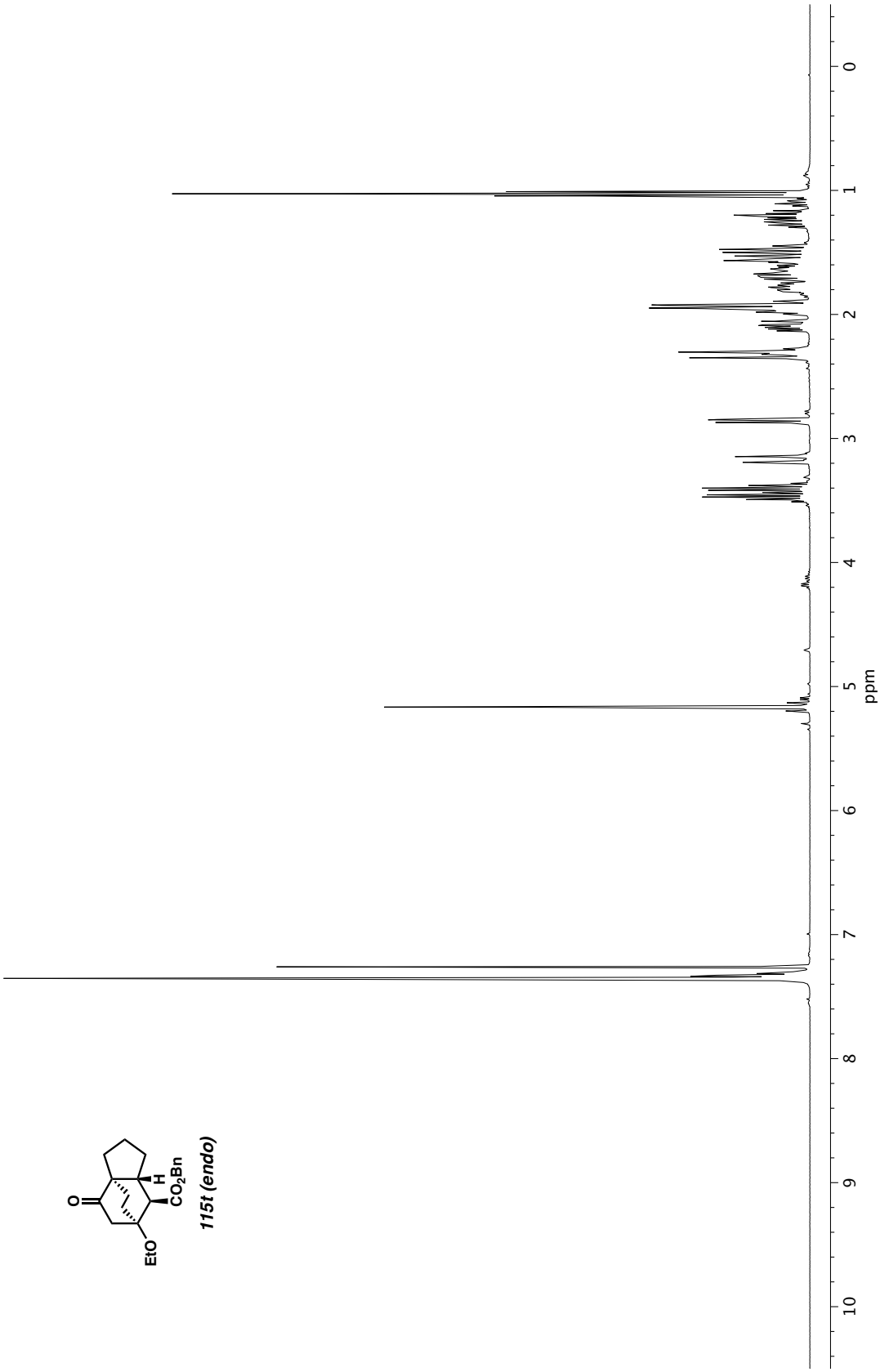

Figure A1.64. *^1H NMR (400 MHz, $CDCl_3$) of compound* ***115t.***

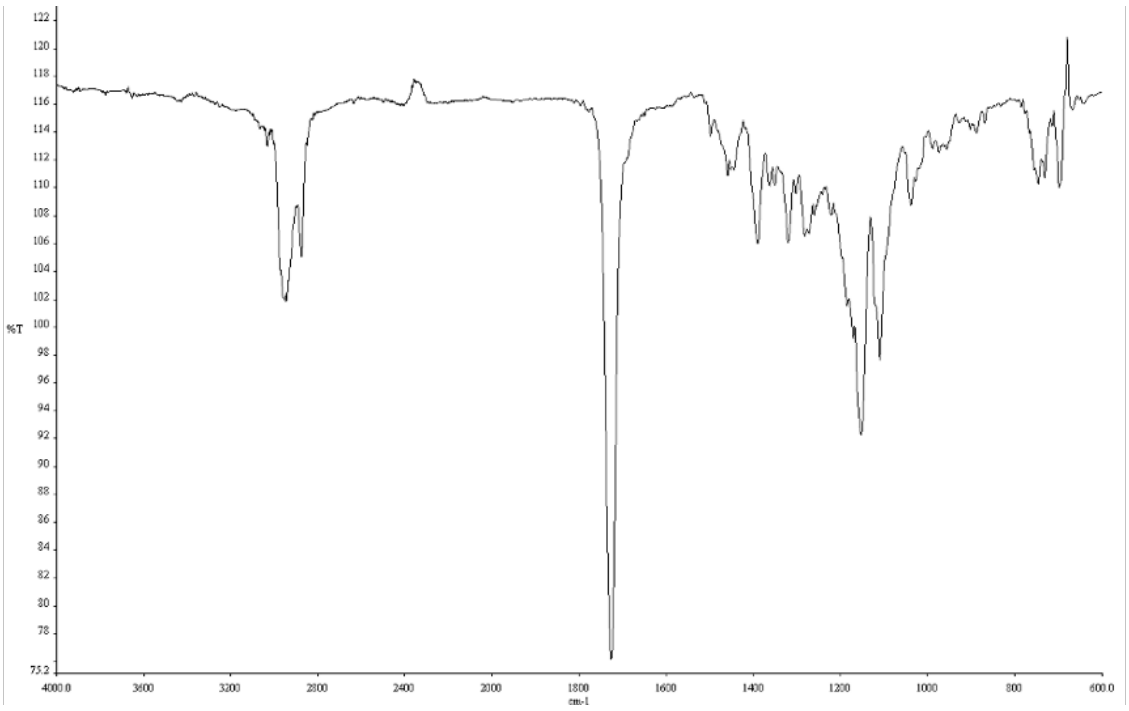

Figure A1.65. *Infrared spectrum (Thin Film, NaCl) of compound* ***115t.***

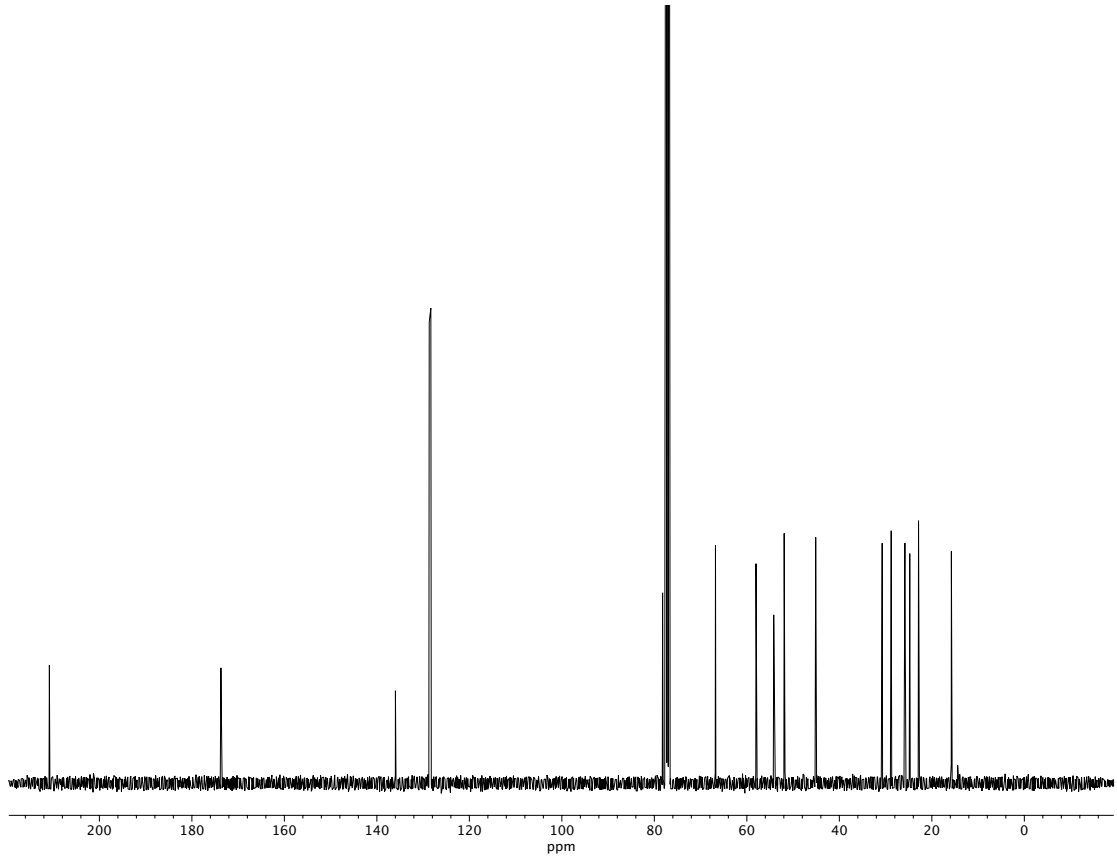

Figure A1.66. *^{13}C NMR (100 MHz, $CDCl_3$) of compound* ***115t.***

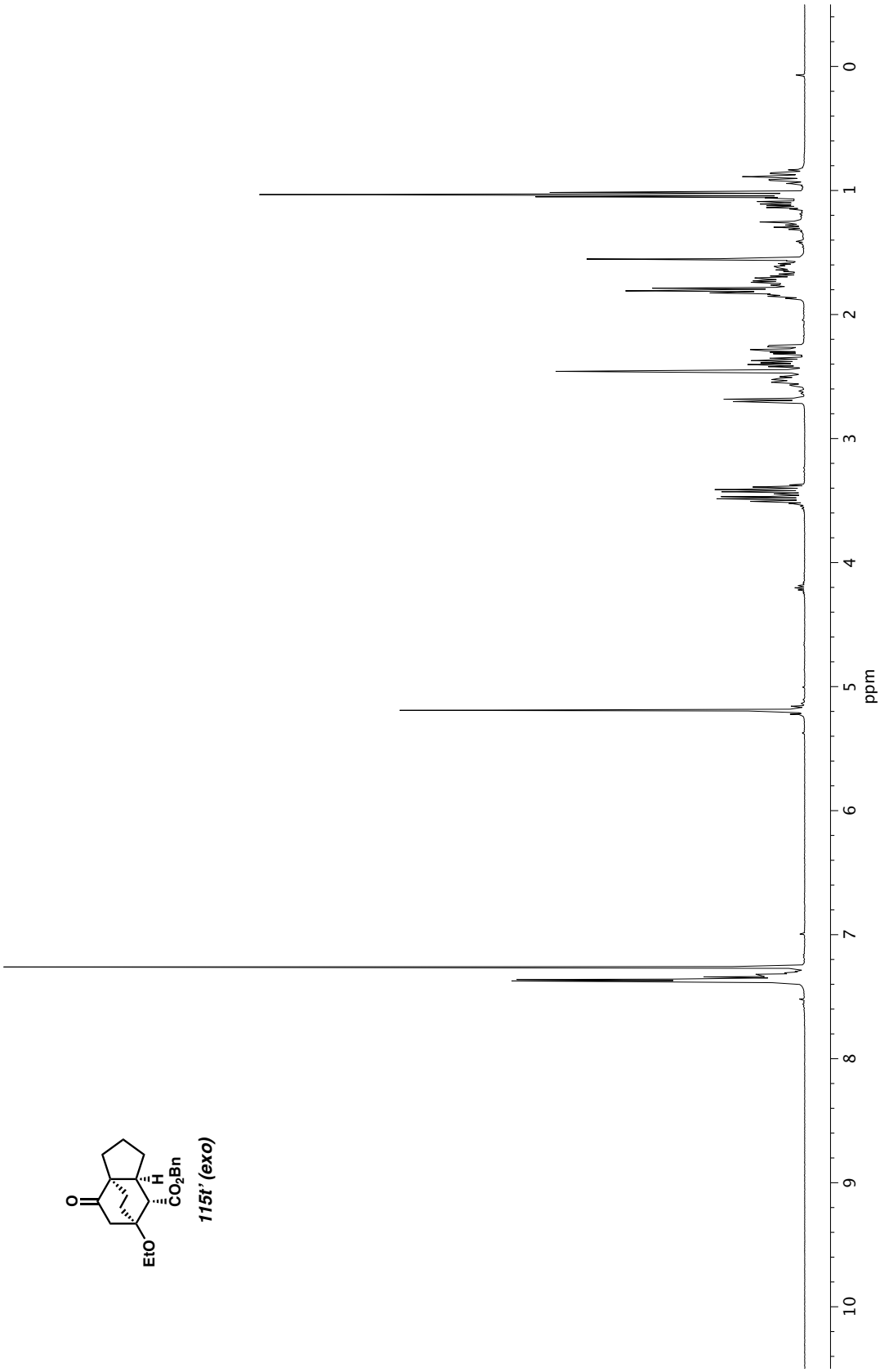

Figure A1.67. *^1H NMR (400 MHz, $CDCl_3$) of compound* ***115t.***

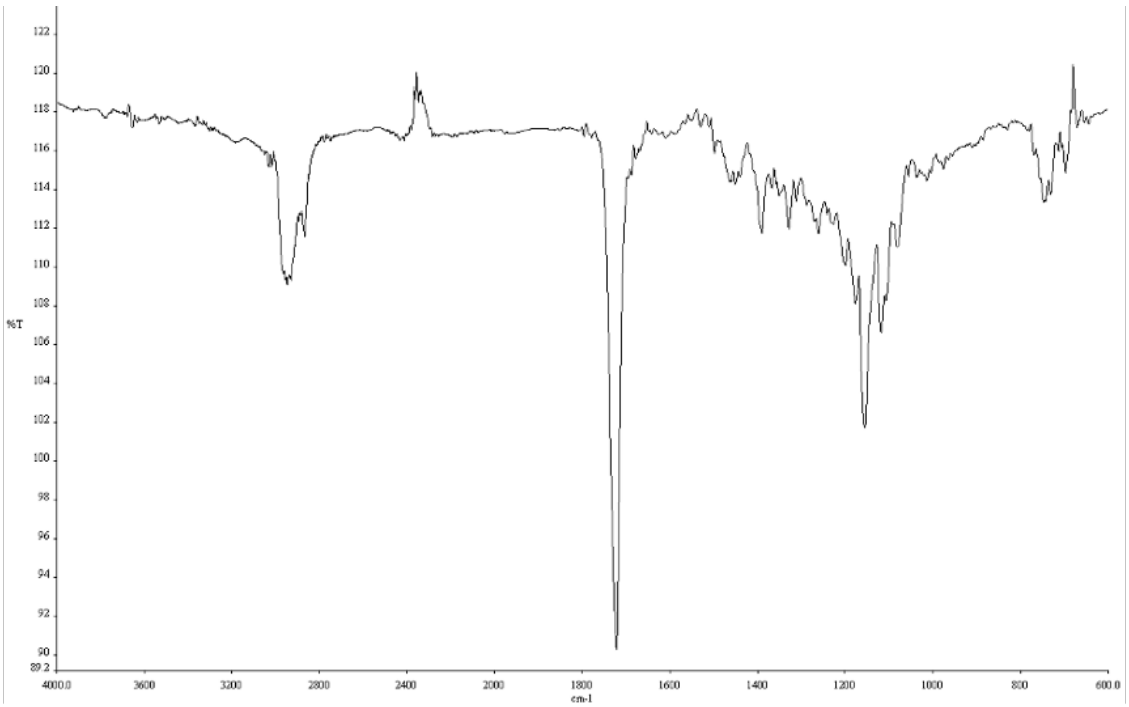

Figure A1.68. *Infrared spectrum (Thin Film, NaCl) of compound* ***115t′.***

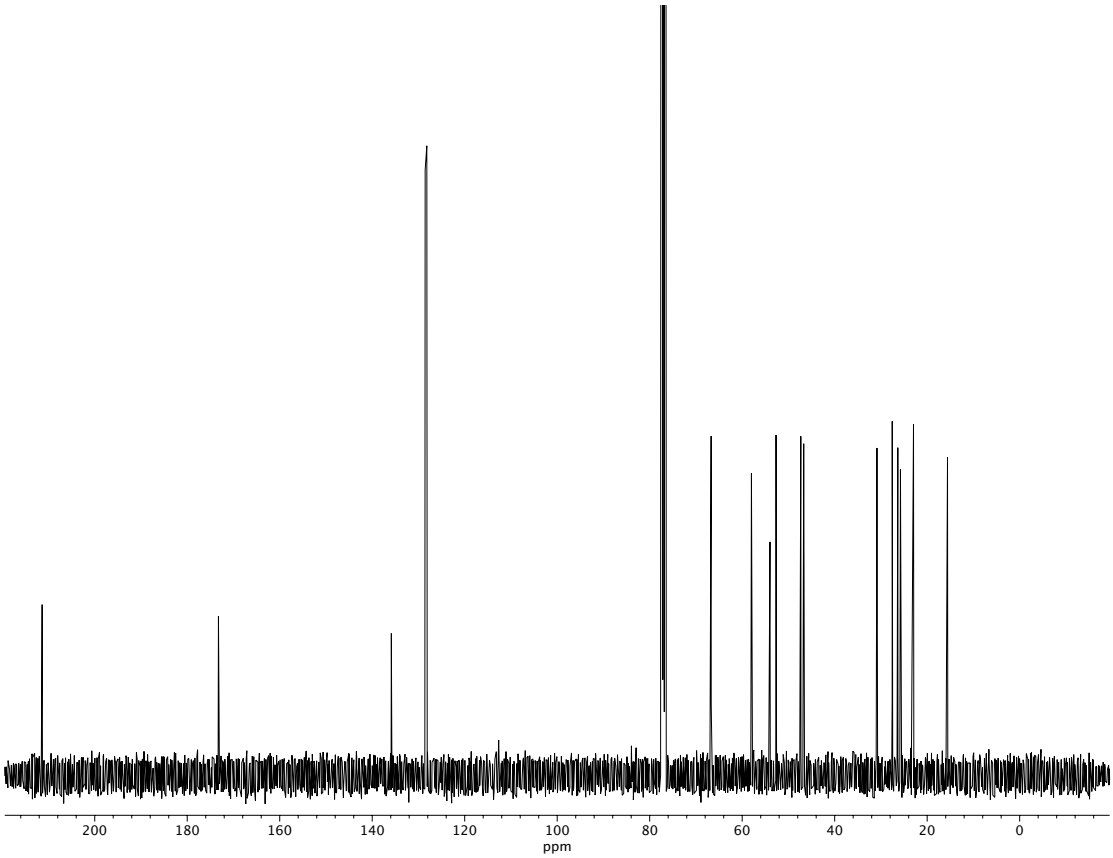

Figure A1.69. *^{13}C NMR (100 MHz, $CDCl_3$) of compound* ***115t′.***

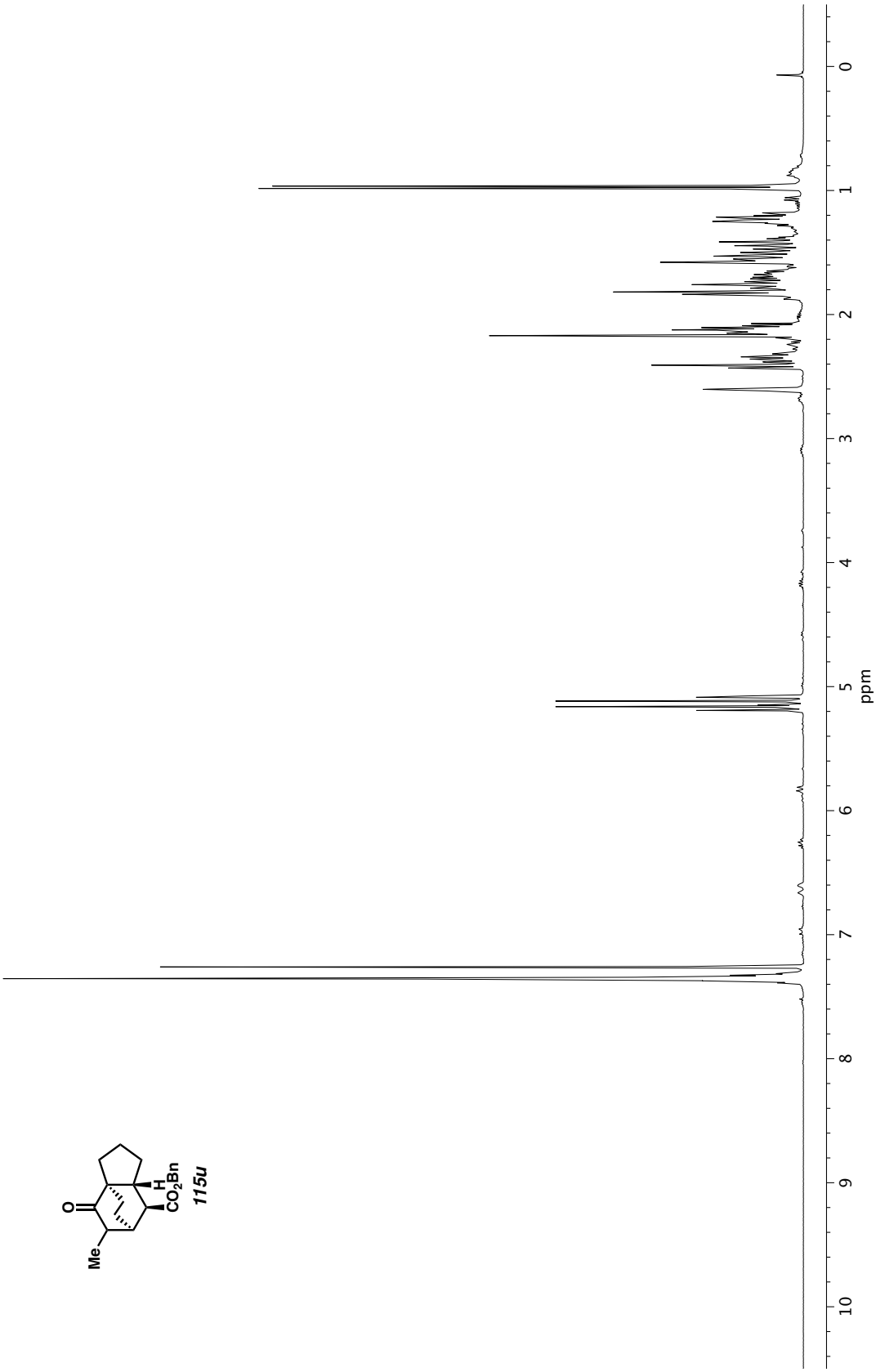

Figure A1.70. *^1H NMR (400 MHz, $CDCl_3$) of compound* ***115u.***

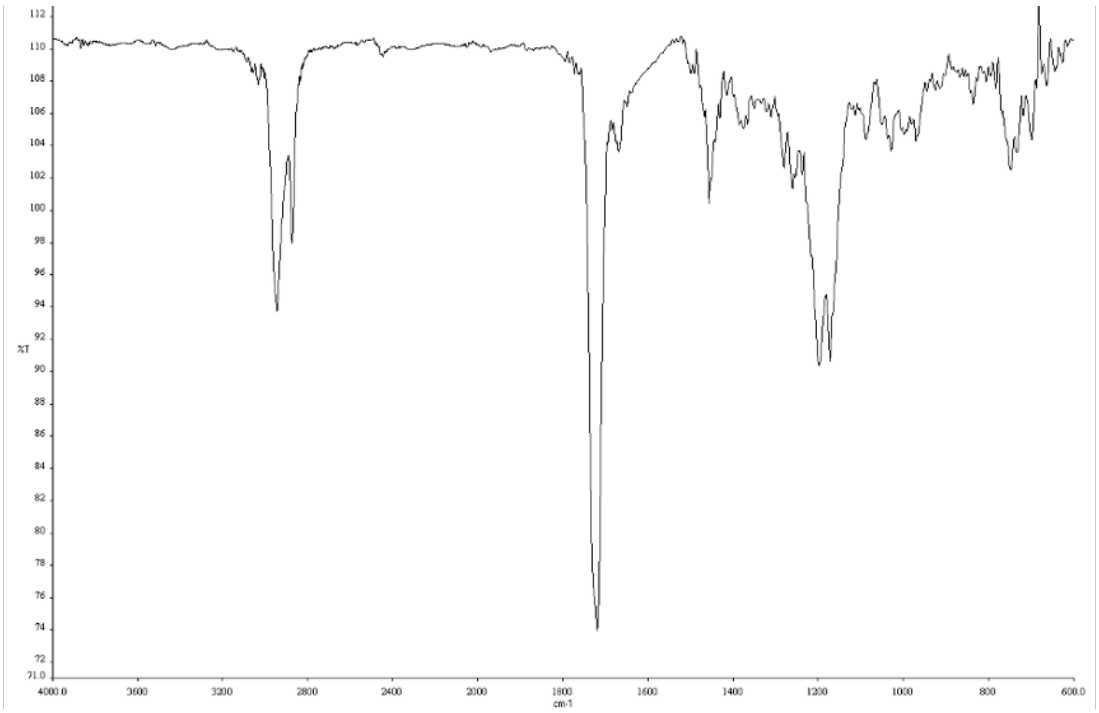

Figure A1.71. *Infrared spectrum (Thin Film, NaCl) of compound* ***115u.***

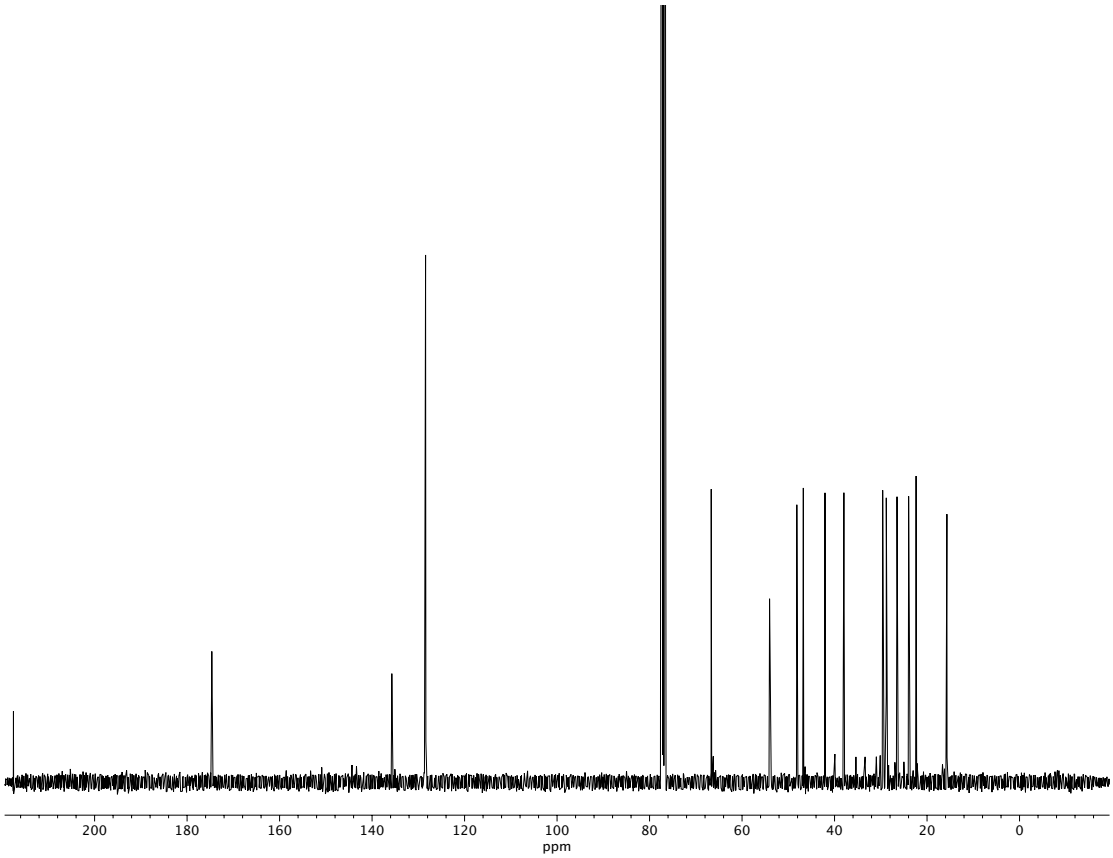

Figure A1.72. *^{13}C NMR (100 MHz, $CDCl_3$) of compound* ***115u.***

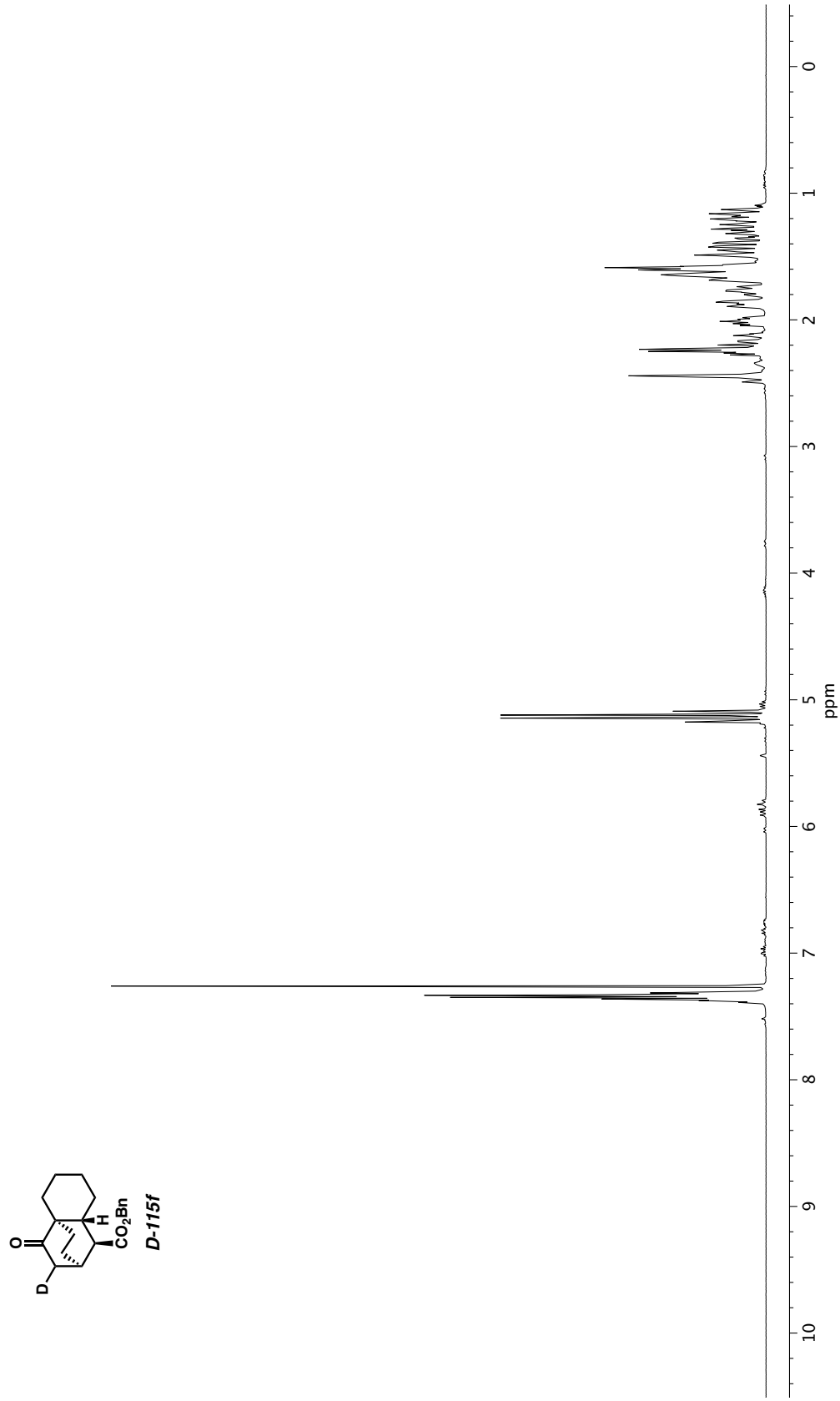

Figure A1.73. *^1H NMR (400 MHz, $CDCl_3$) of compound* ***D-115f.***

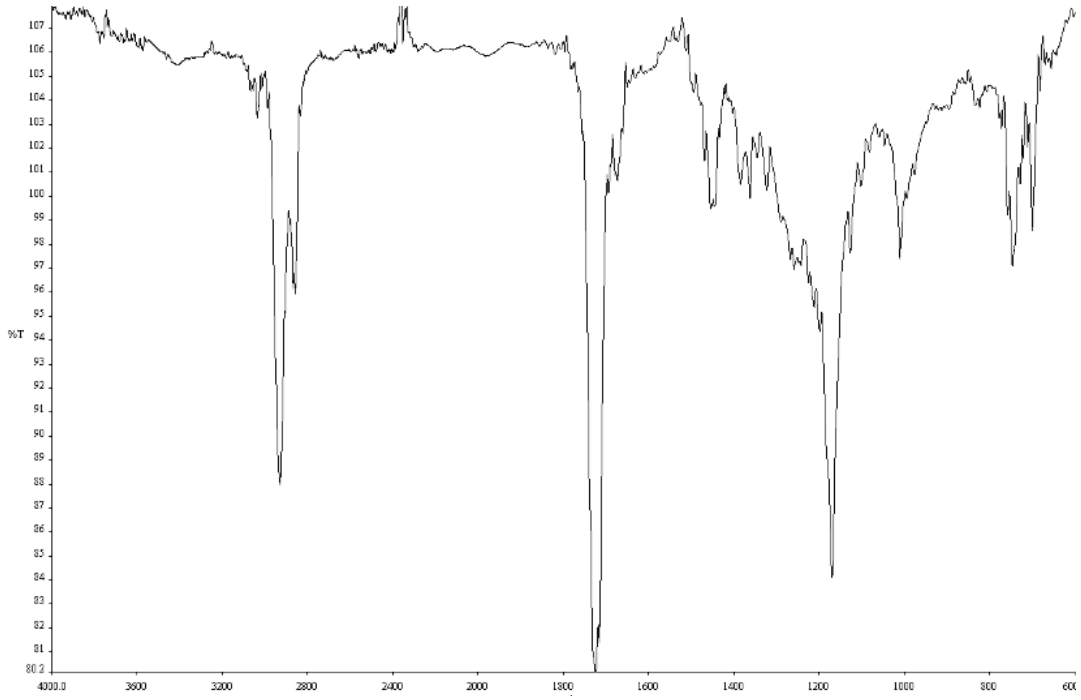

Figure A1.74. *Infrared spectrum (Thin Film, NaCl) of compound* ***D-115f.***

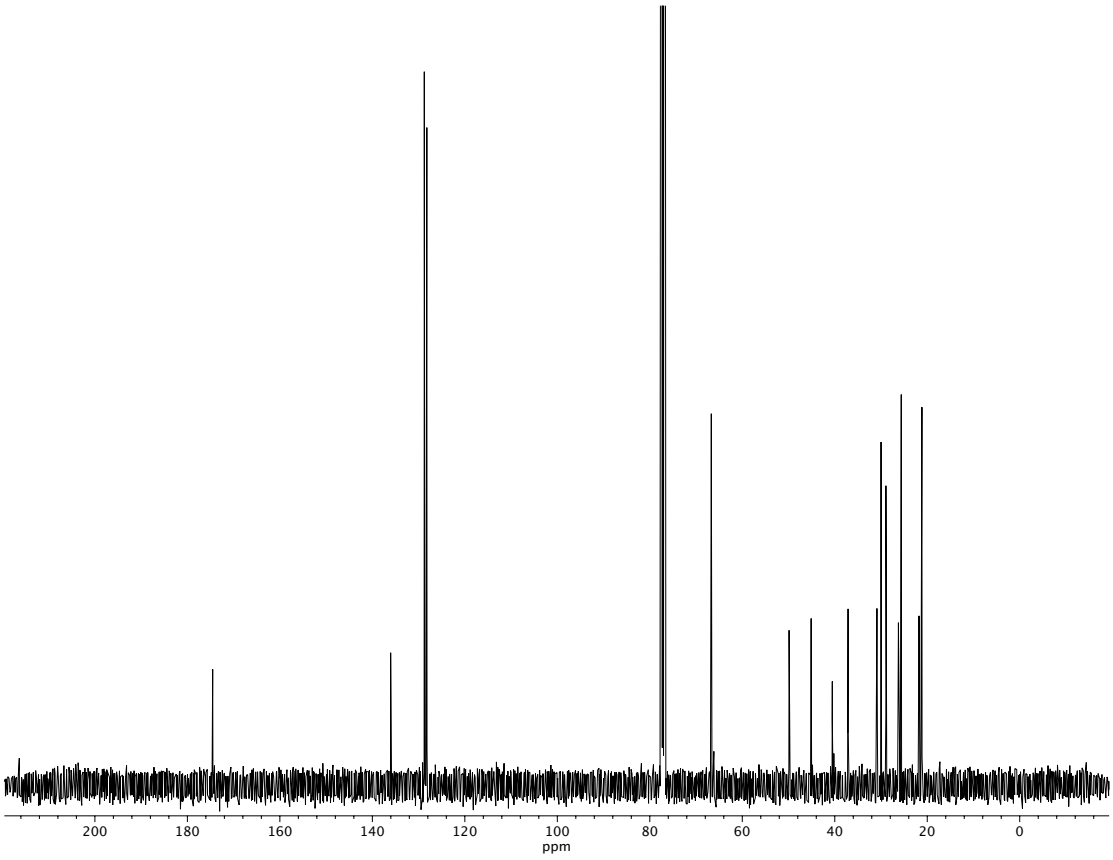

Figure A1.75. *^{13}C NMR (100 MHz, $CDCl_3$) of compound* ***D-115f.***

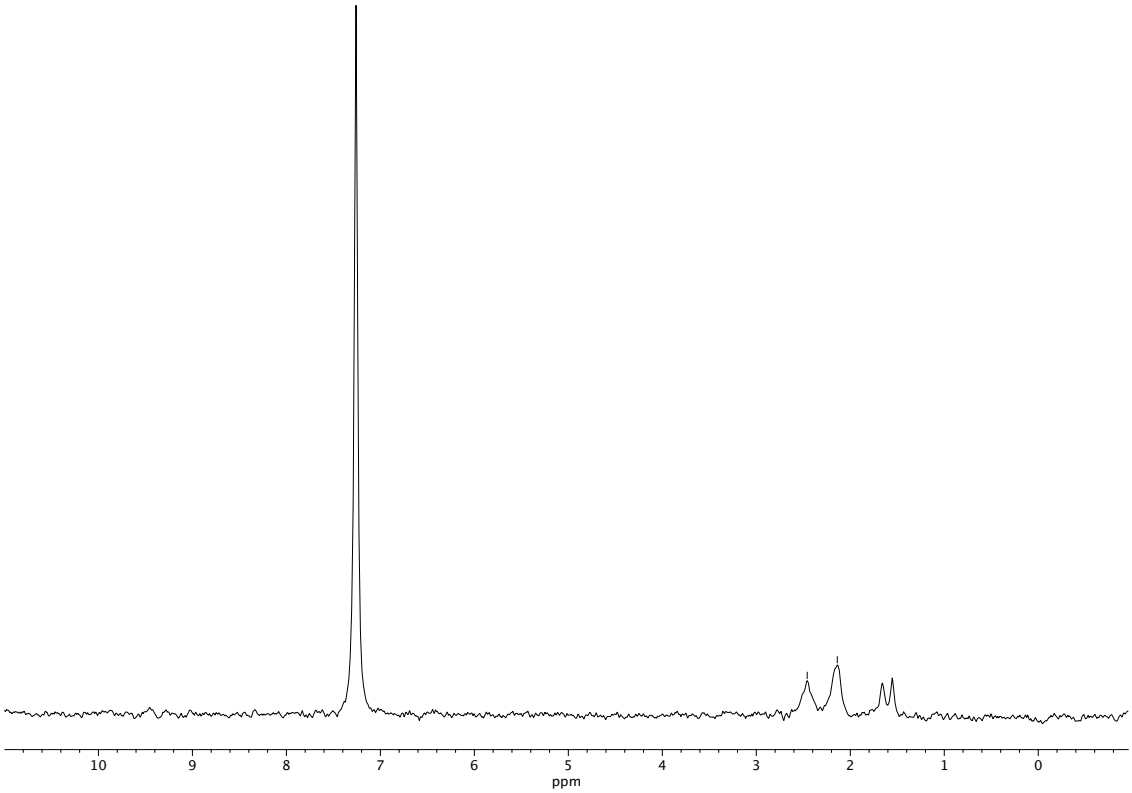

Figure A1.76. *^{2}H NMR (61 MHz, $CDCl_3$) of compound* ***D-115f.***

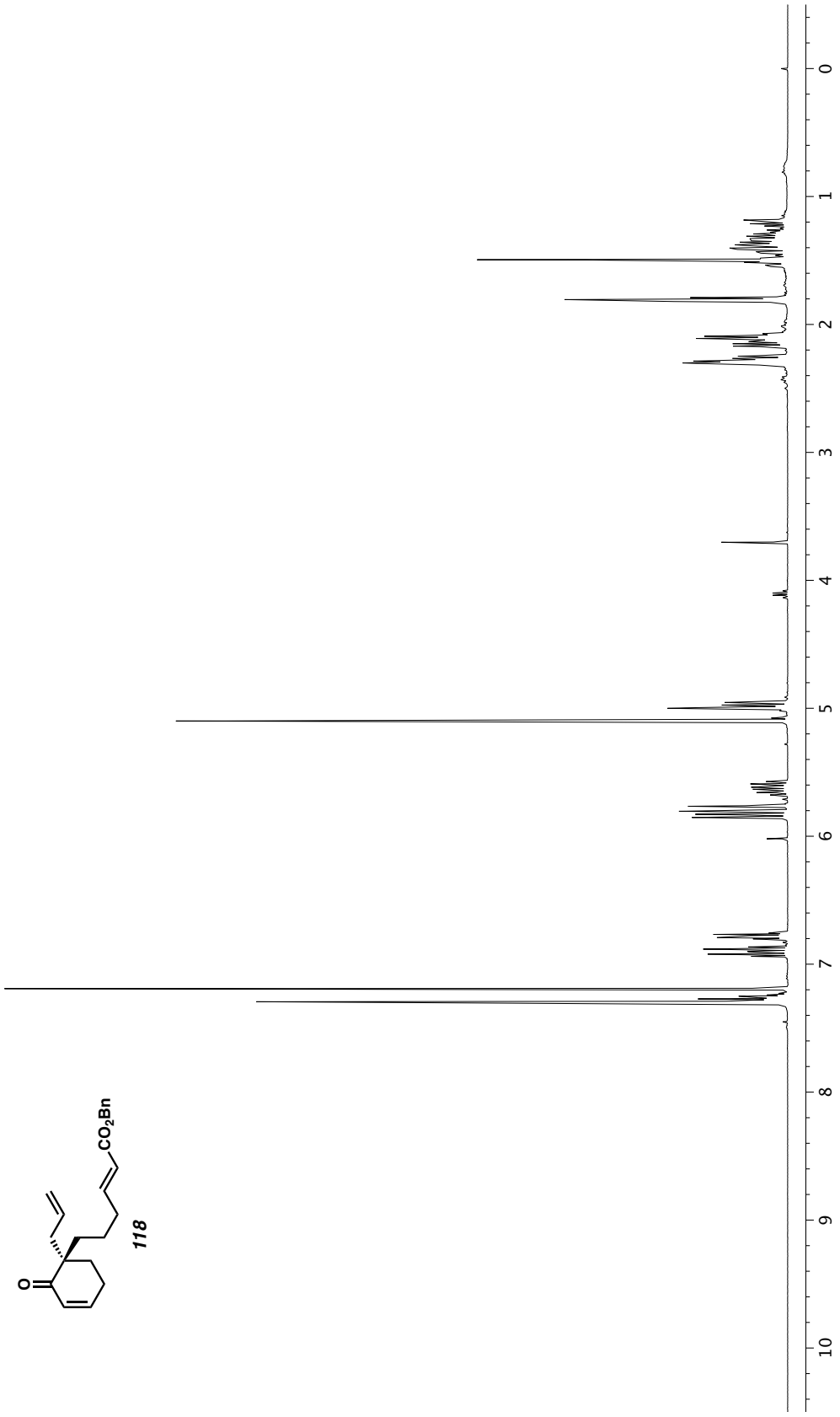

Figure A1.77. *^{1}H NMR (400 MHz, $CDCl_3$) of compound* ***118.***

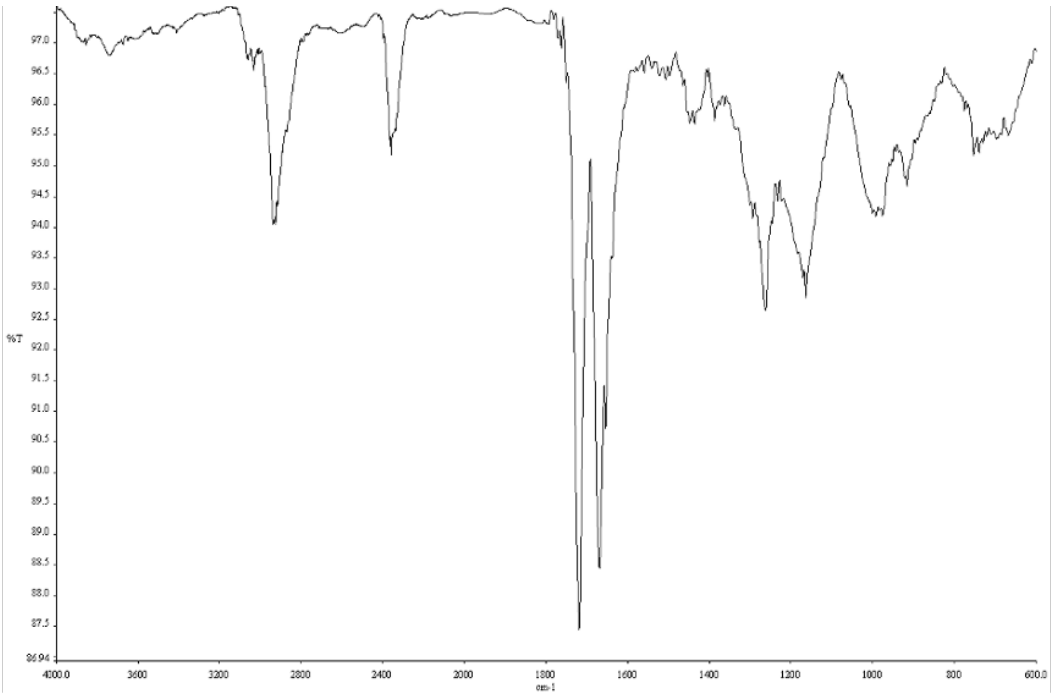

Figure A1.78. *Infrared spectrum (Thin Film, NaCl) of compound* ***118.***

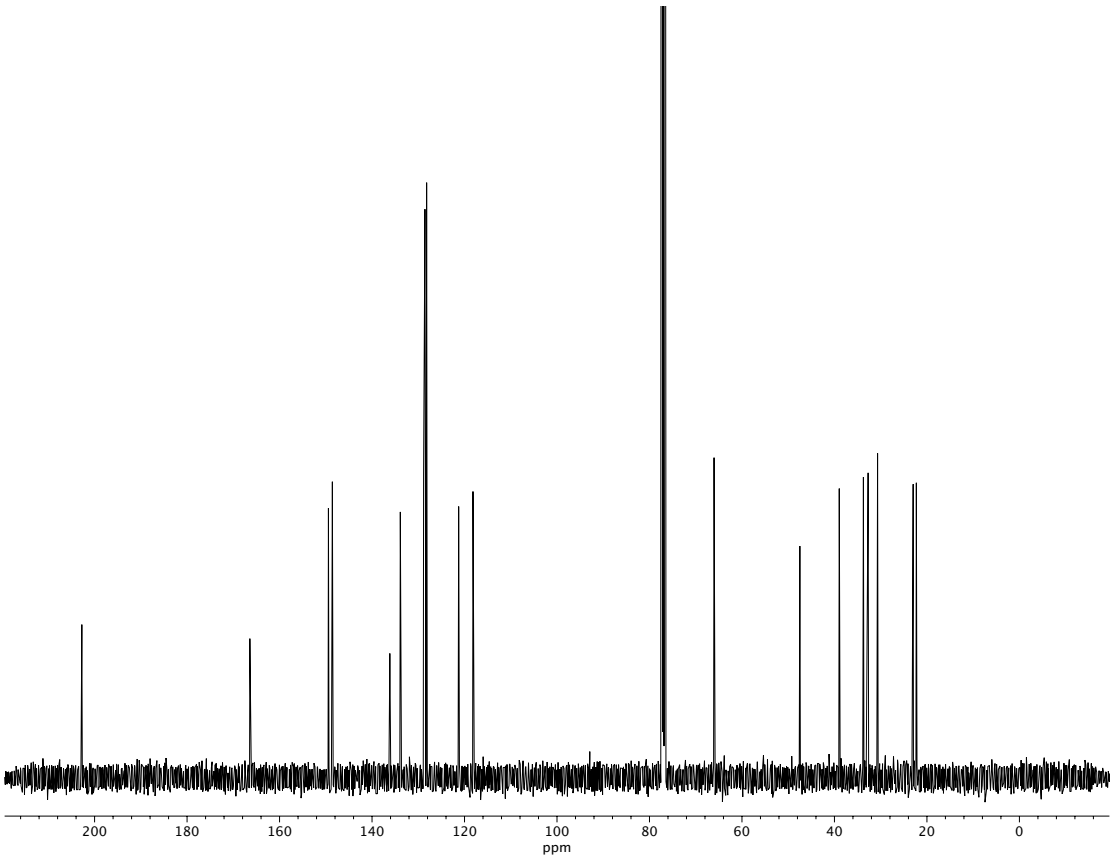

Figure A1.79. *^{13}C NMR (100 MHz, $CDCl_3$) of compound* ***118.***

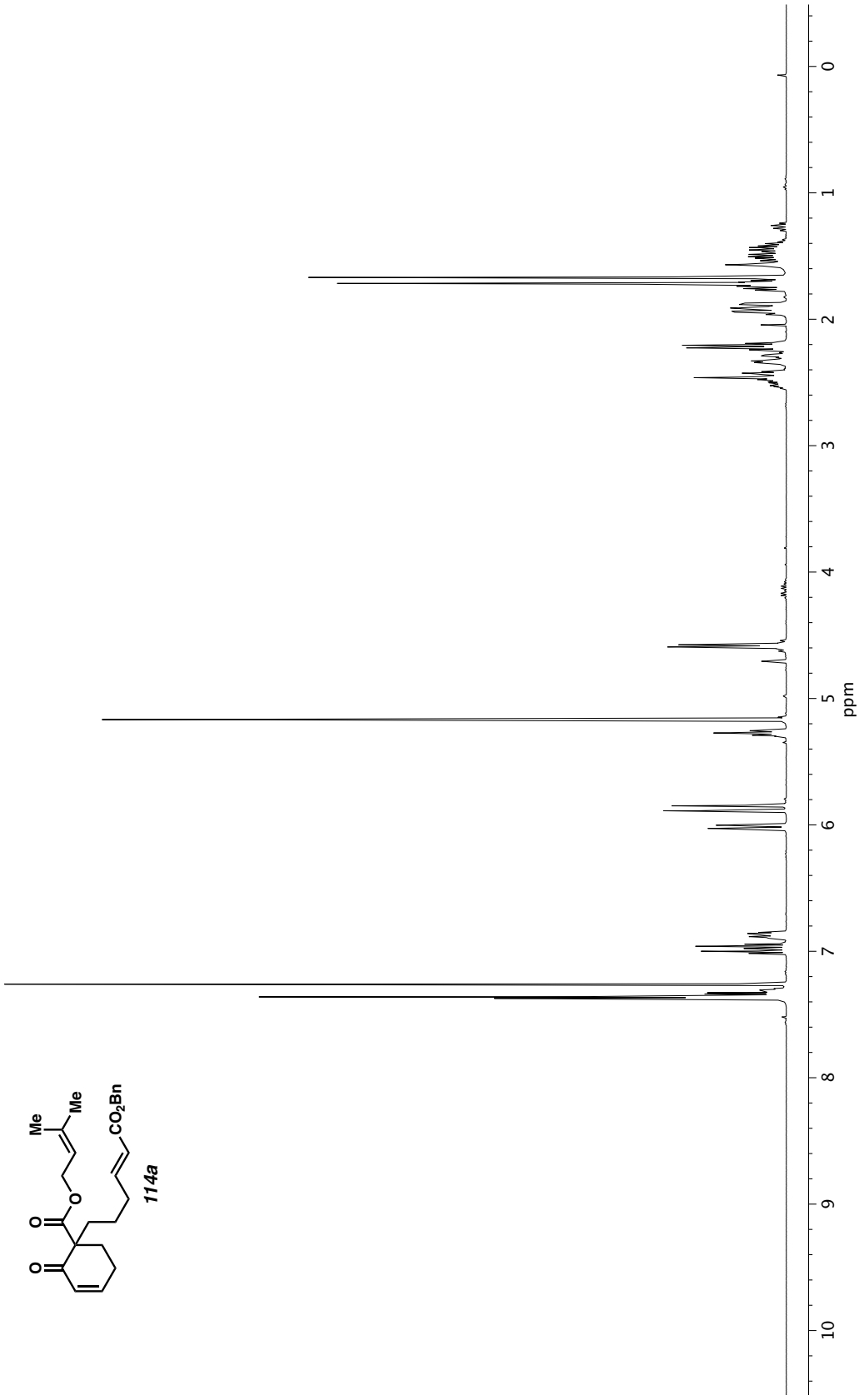

Figure A1.80. *^1H NMR (400 MHz, $CDCl_3$) of compound* ***114a.***

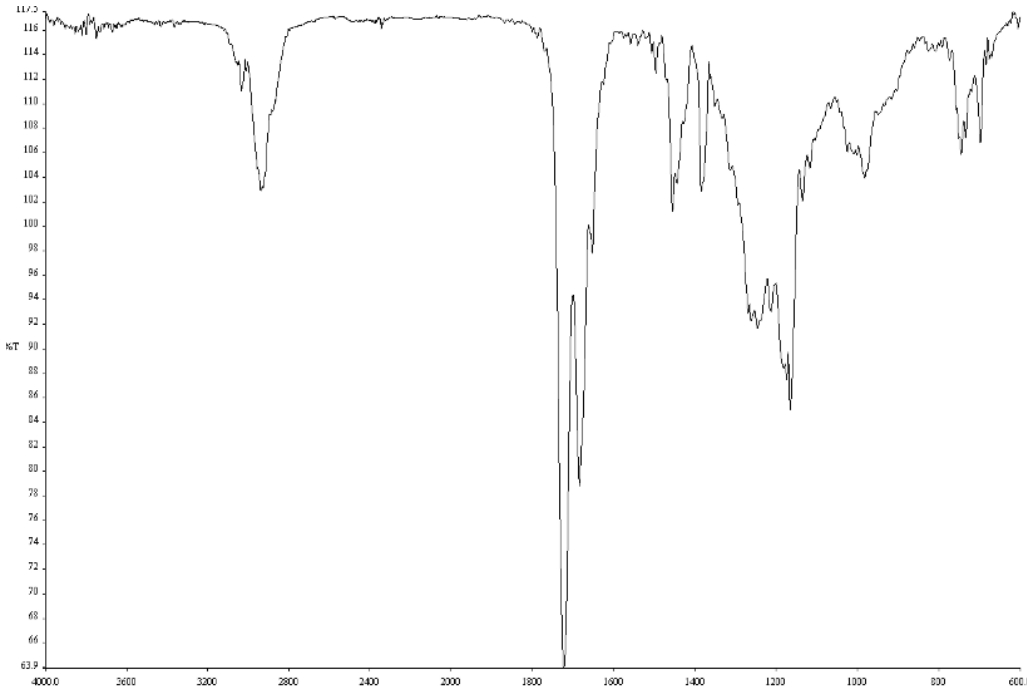

Figure A1.81. *Infrared spectrum (Thin Film, NaCl) of compound* ***114a.***

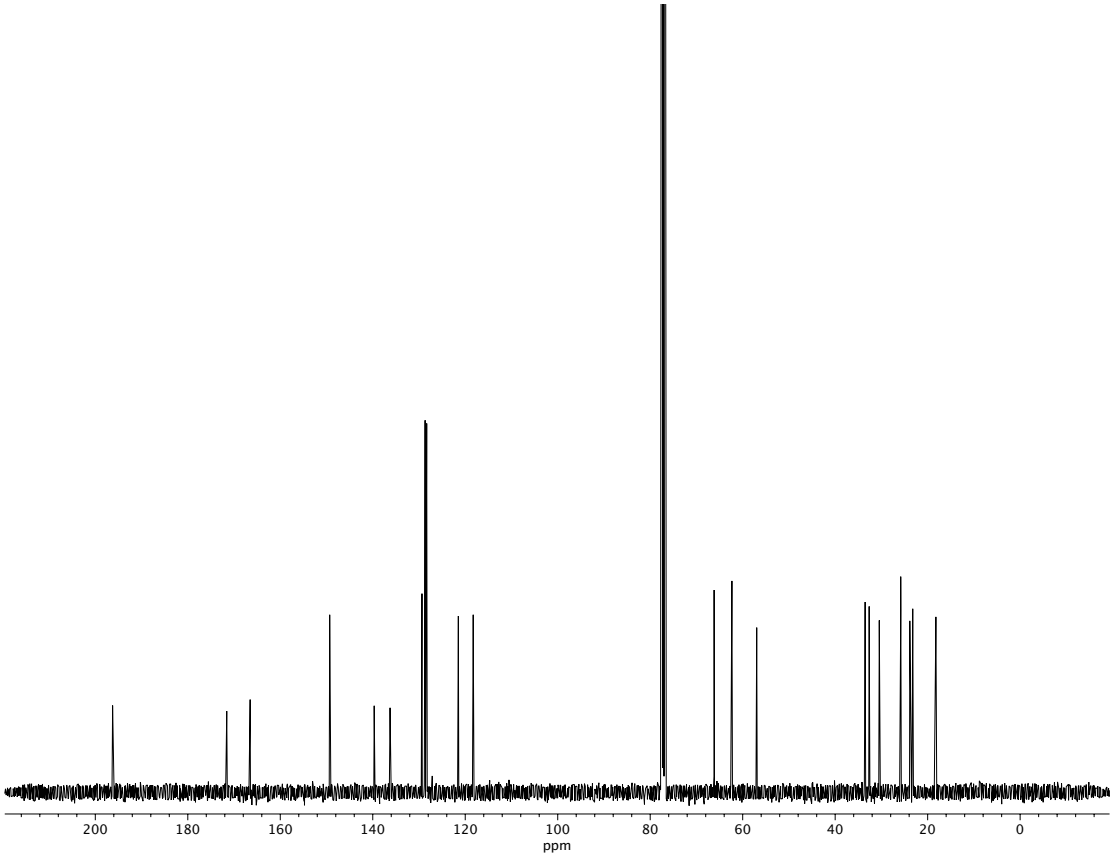

Figure A1.82. *^{13}C NMR (100 MHz, $CDCl_3$) of compound* ***114a.***

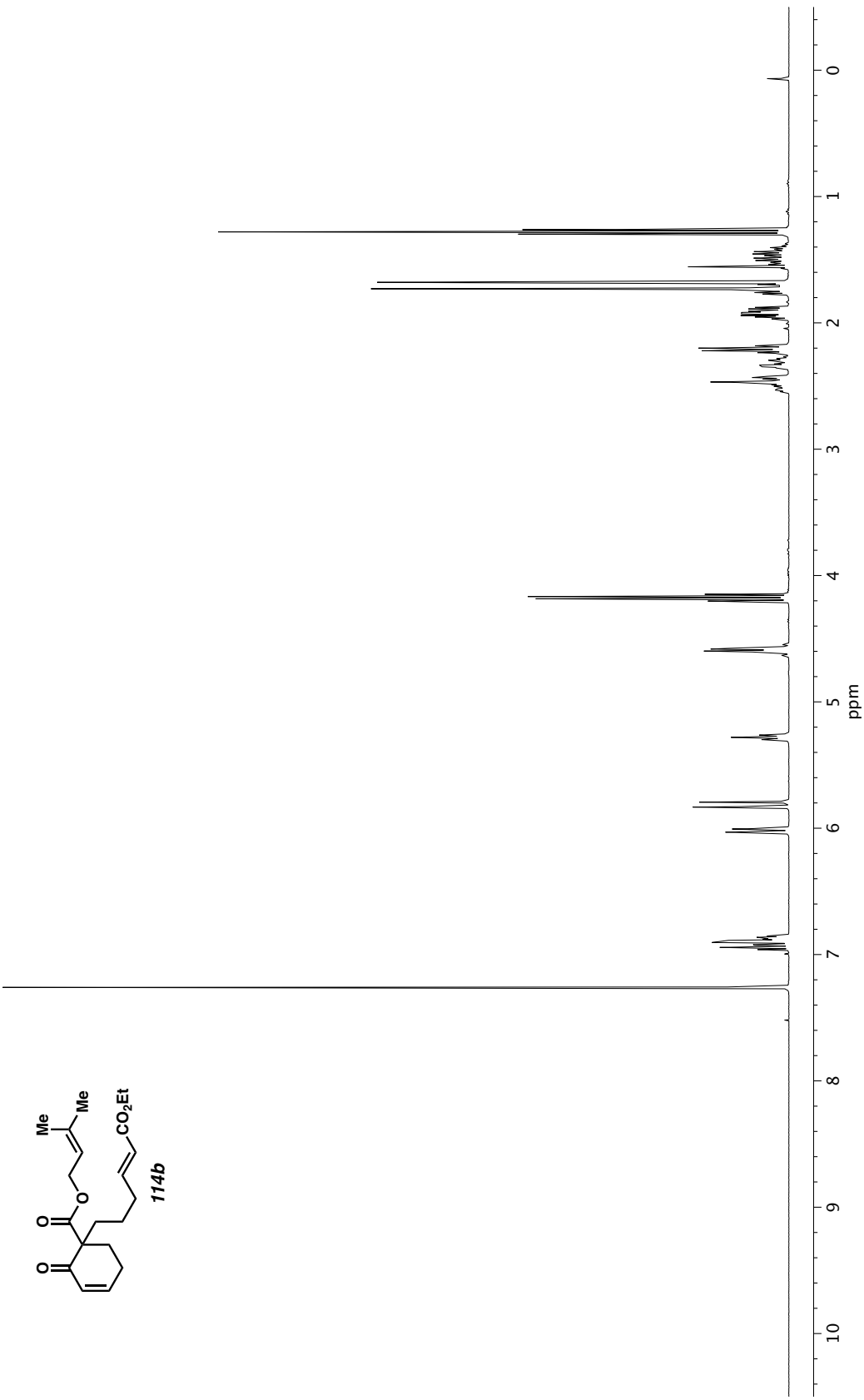

Figure A1.83. *^1H NMR (400 MHz, $CDCl_3$) of compound* ***114b.***

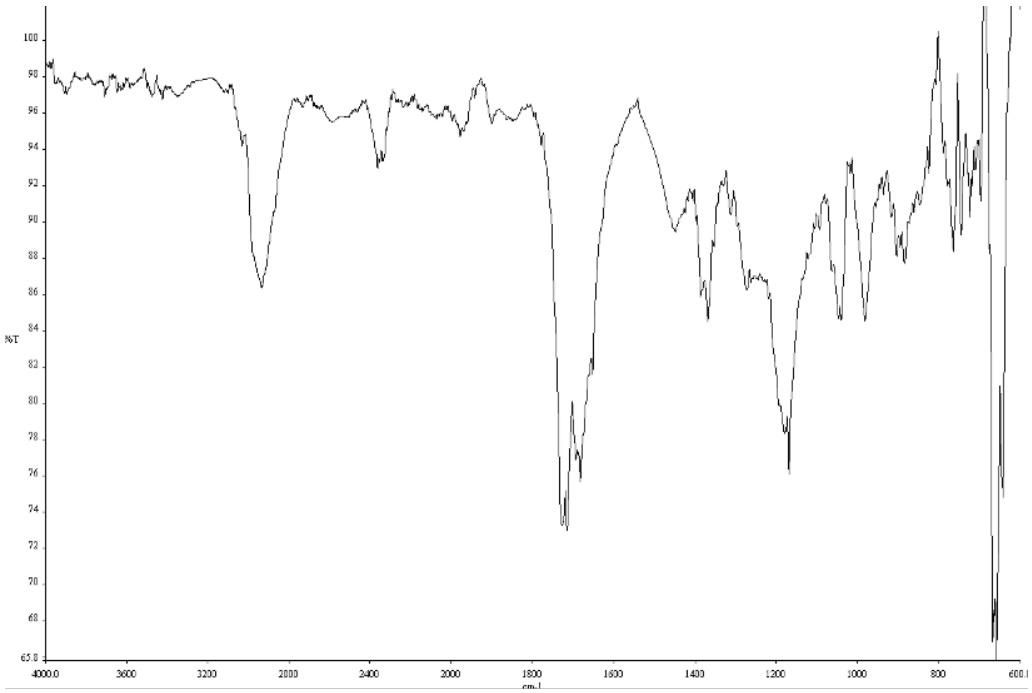

Figure A1.84. *Infrared spectrum (Thin Film, NaCl) of compound* ***114b.***

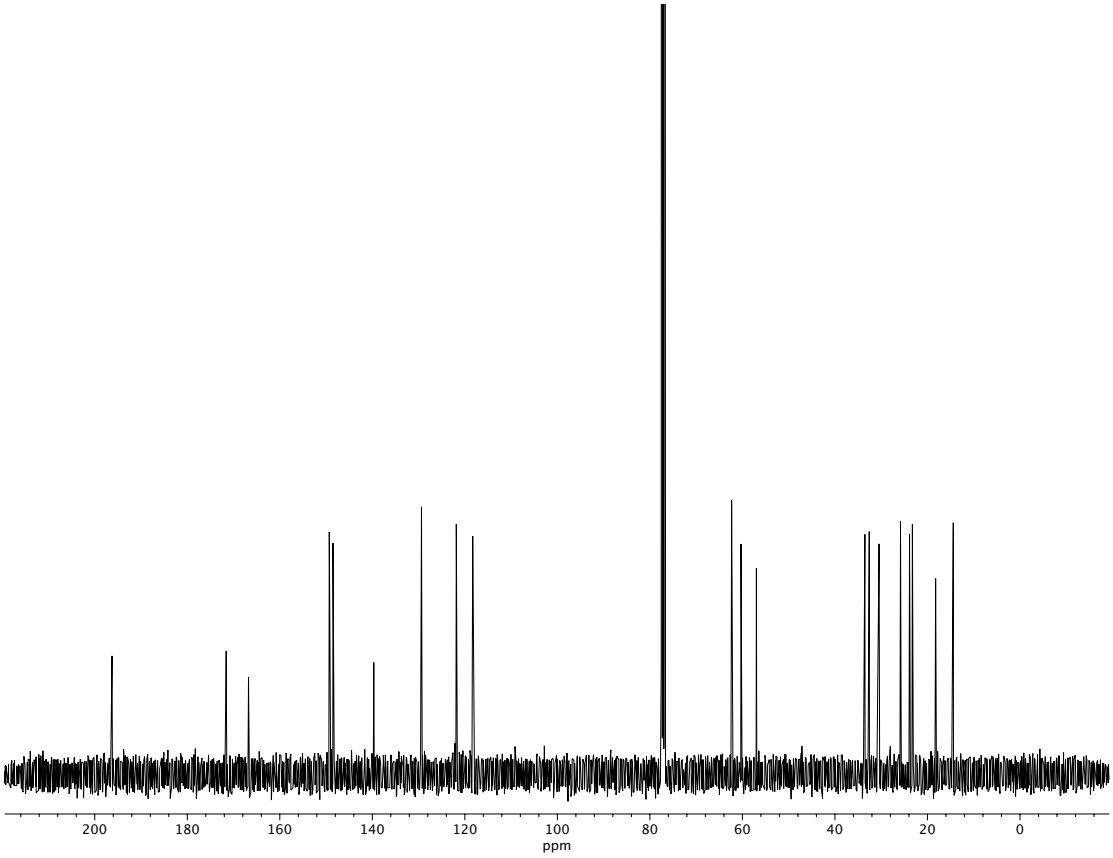

Figure A1.85. *^{13}C NMR (100 MHz, $CDCl_3$) of compound* ***114b.***

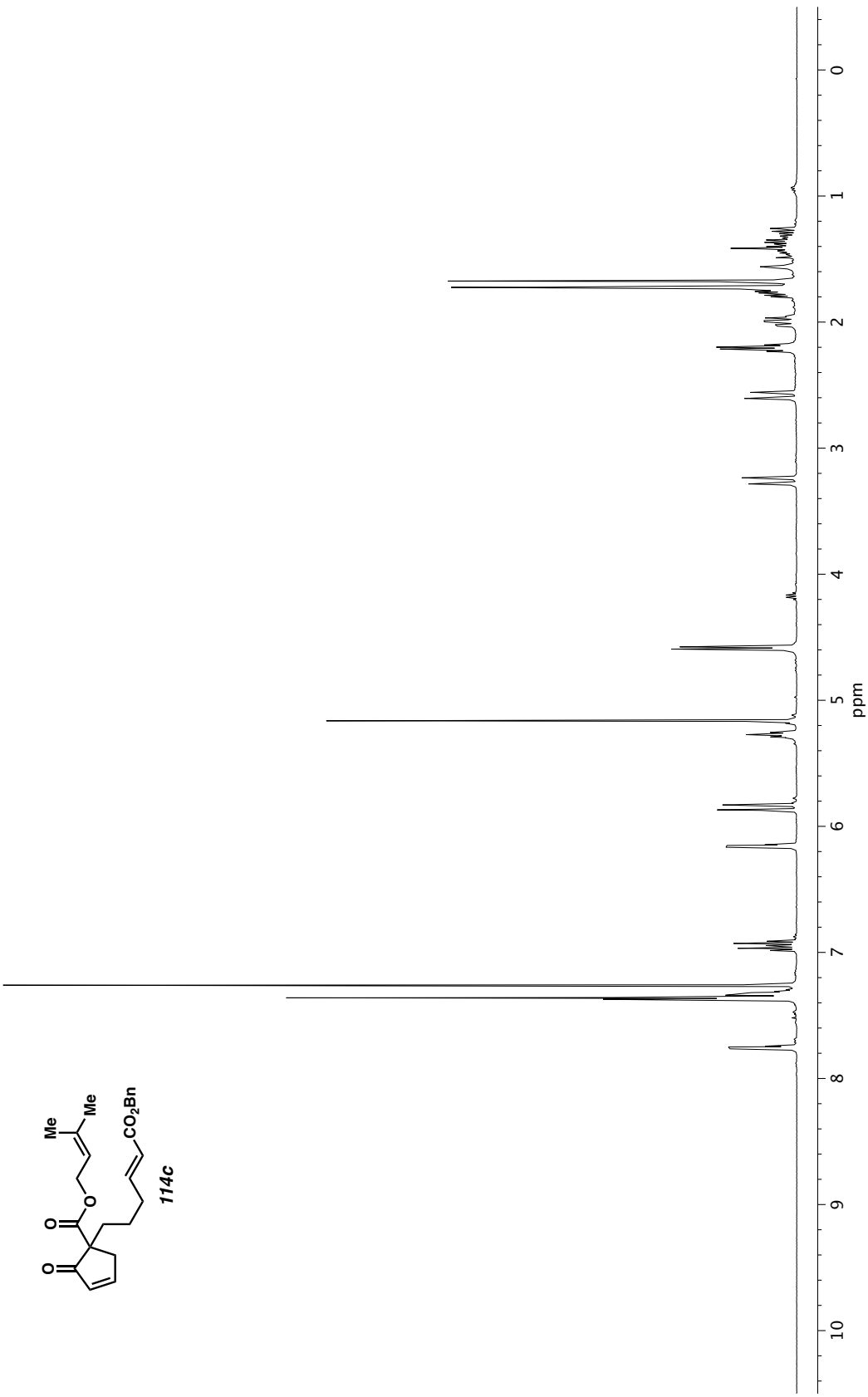

Figure A1.86. *^1H NMR (400 MHz, $CDCl_3$) of compound* ***114c.***

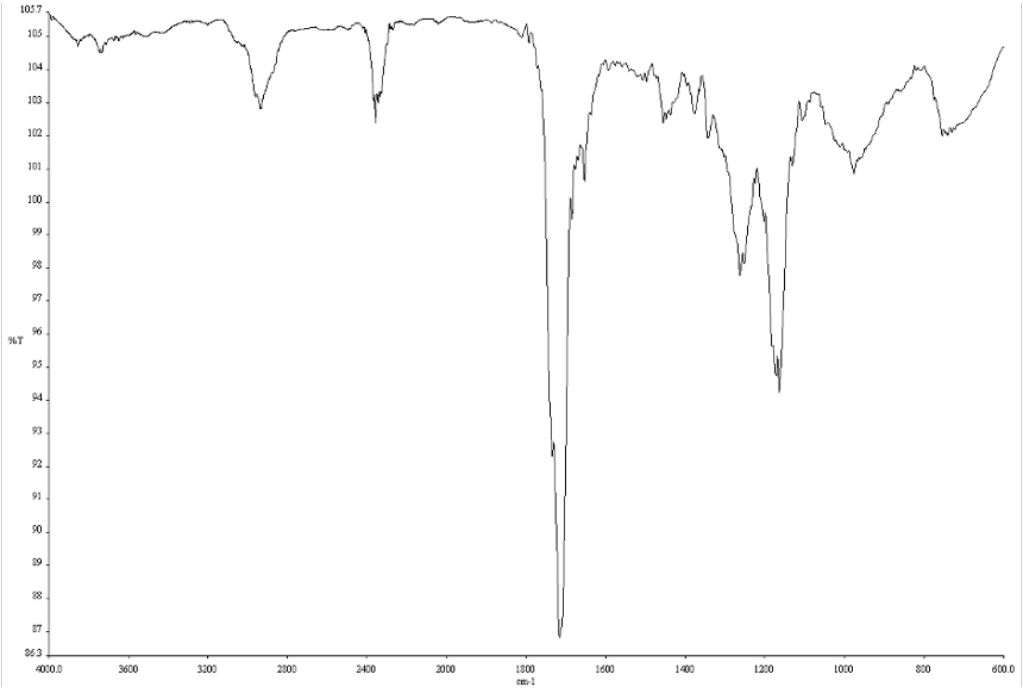

Figure A1.87. *Infrared spectrum (Thin Film, NaCl) of compound* ***114c.***

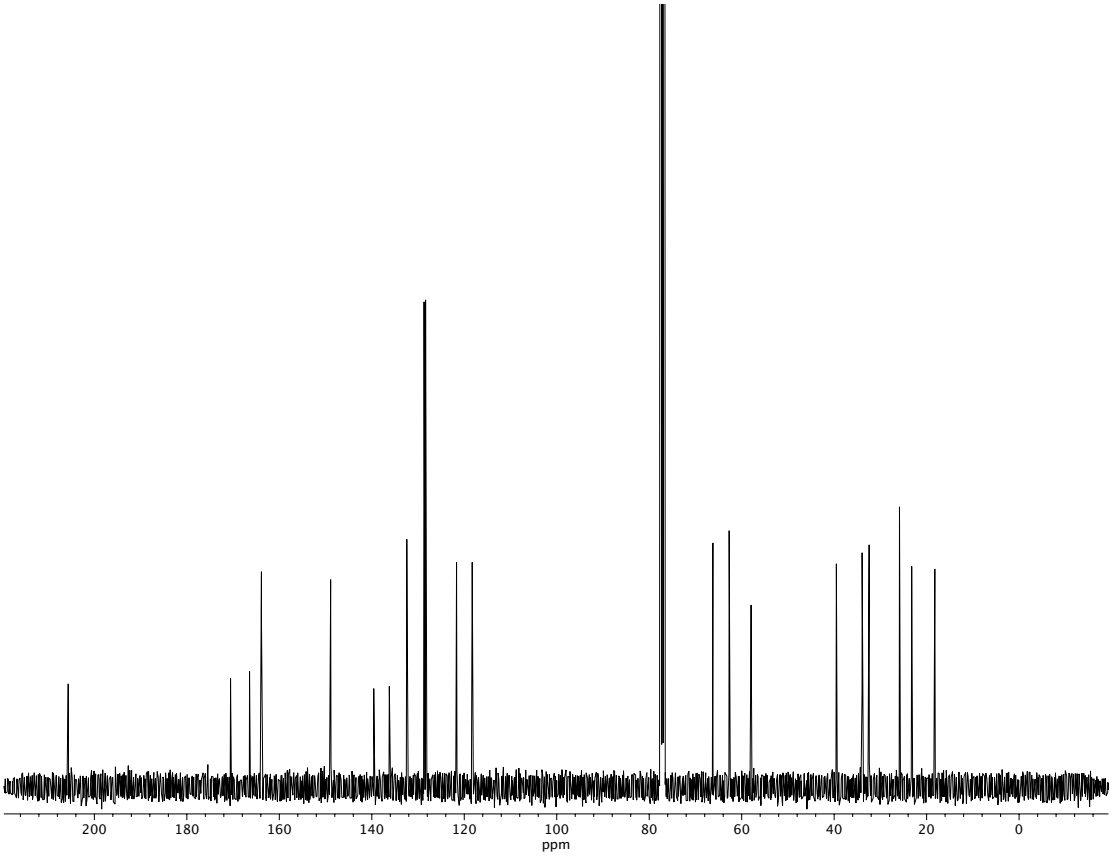

Figure A1.88. *^{13}C NMR (100 MHz, $CDCl_3$) of compound* ***114c.***

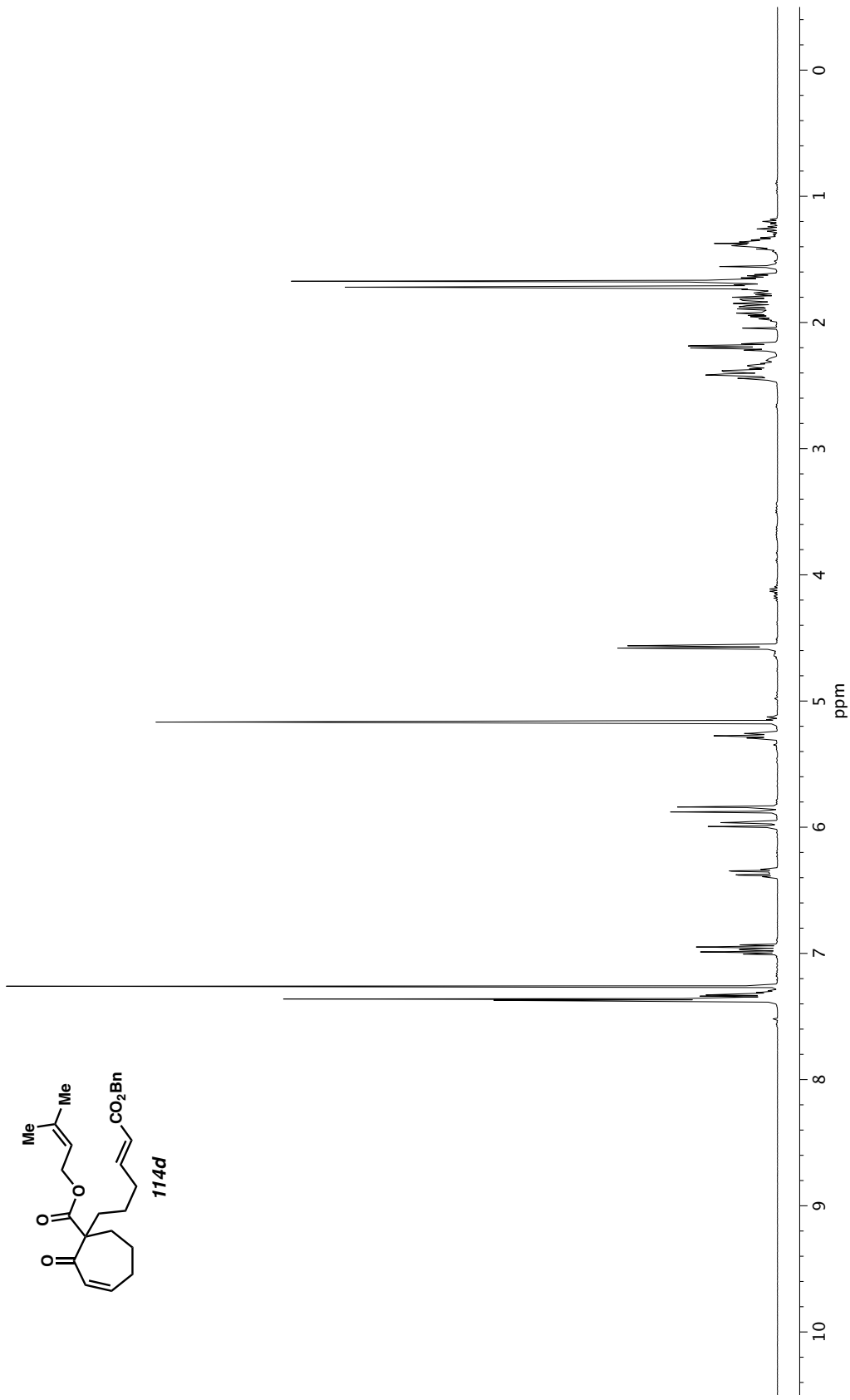

Figure A1.89. *^1H NMR (400 MHz, $CDCl_3$) of compound* ***114d.***

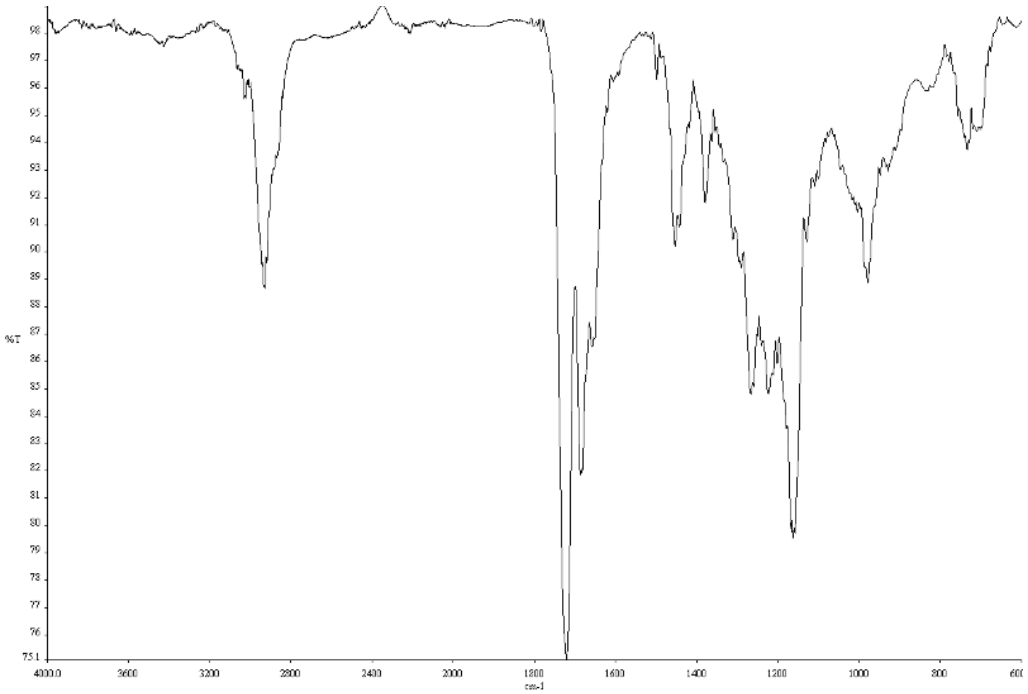

Figure A1.90. *Infrared spectrum (Thin Film, NaCl) of compound* ***114d.***

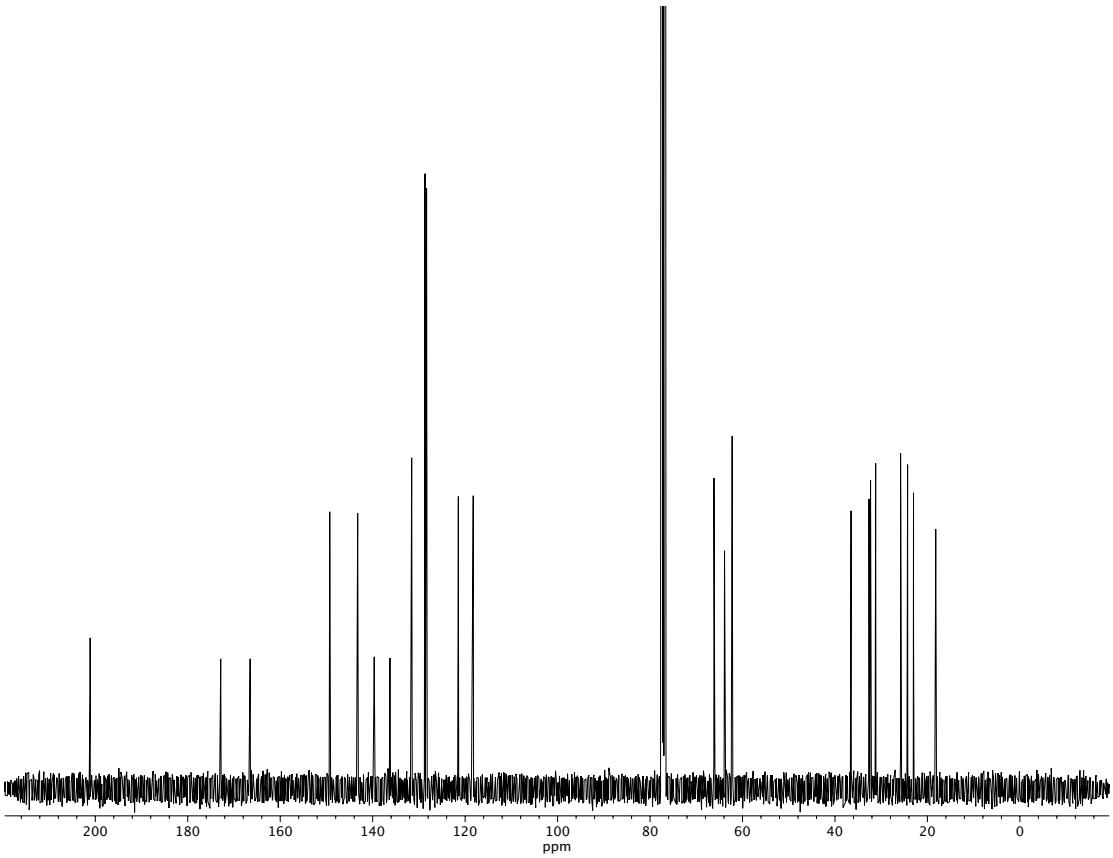

Figure A1.91. *^{13}C NMR (100 MHz, $CDCl_3$) of compound* ***114d.***

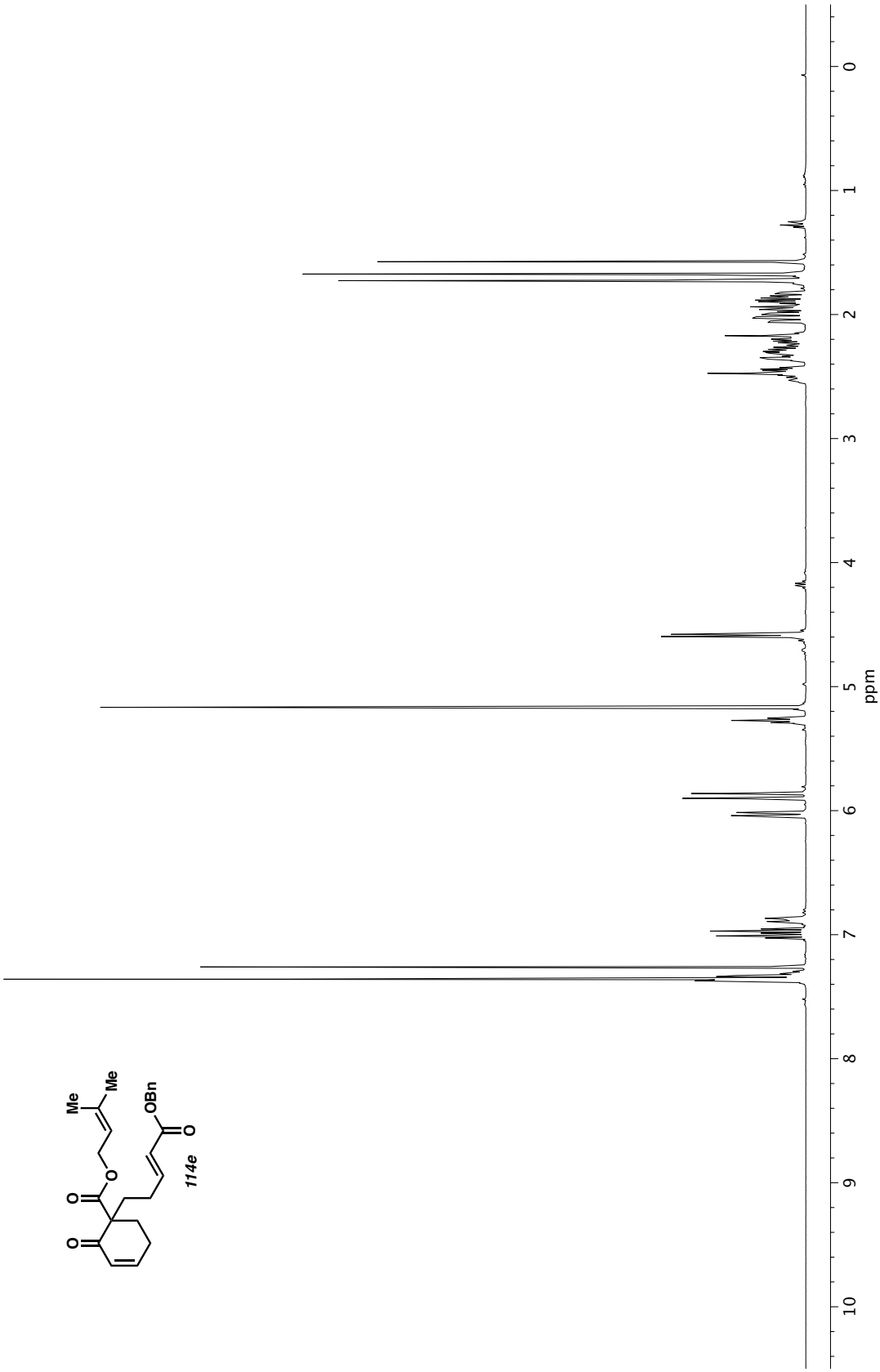

Figure A1.92. *^1H NMR (400 MHz, $CDCl_3$) of compound* ***114e.***

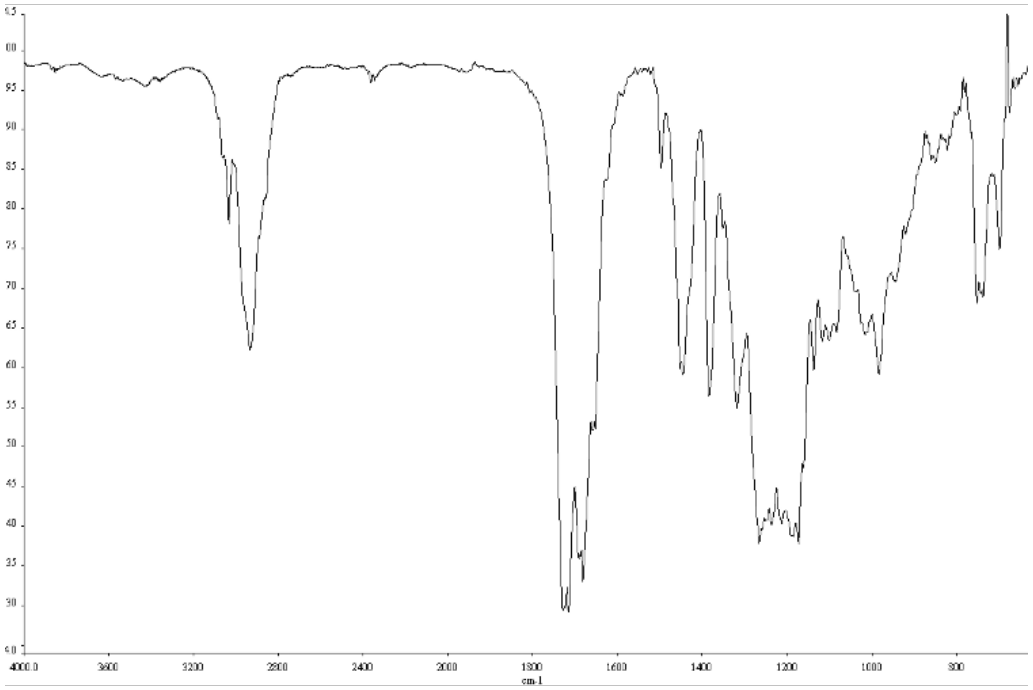

Figure A1.93. *Infrared spectrum (Thin Film, NaCl) of compound* ***114e.***

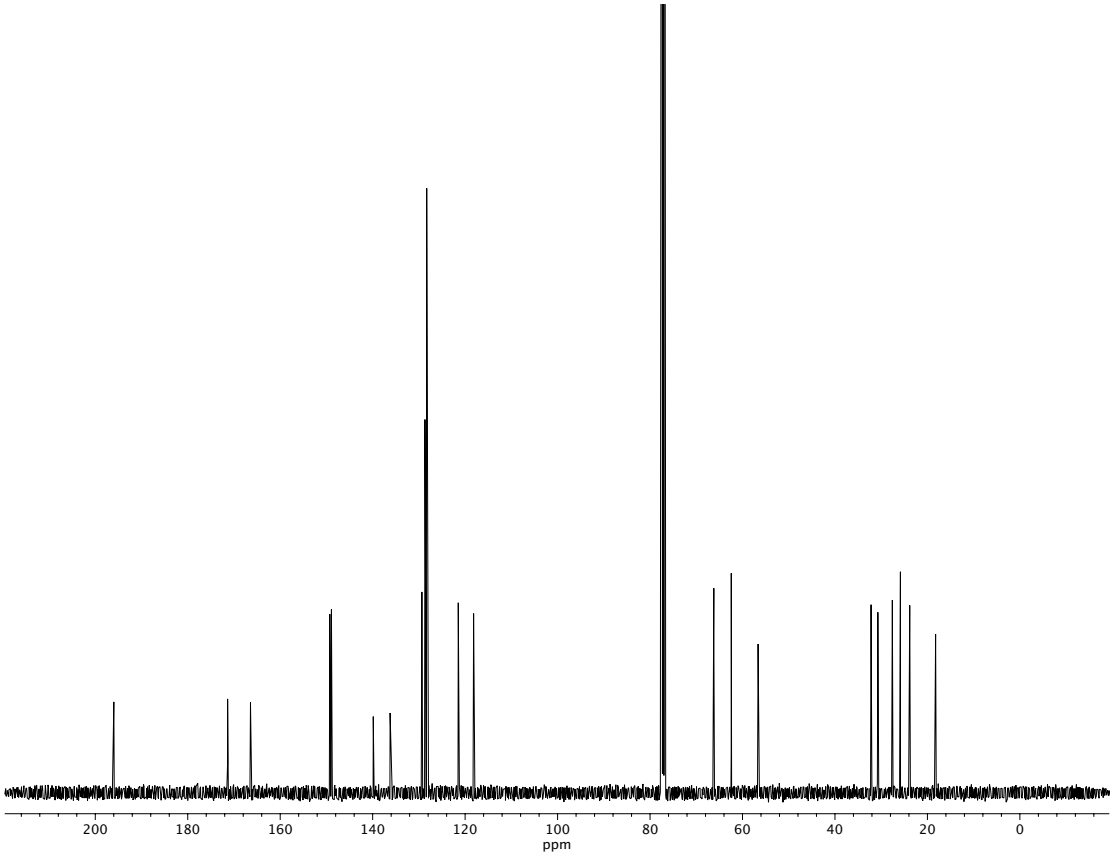

Figure A1.94. *^{13}C NMR (100 MHz, $CDCl_3$) of compound* ***114e.***

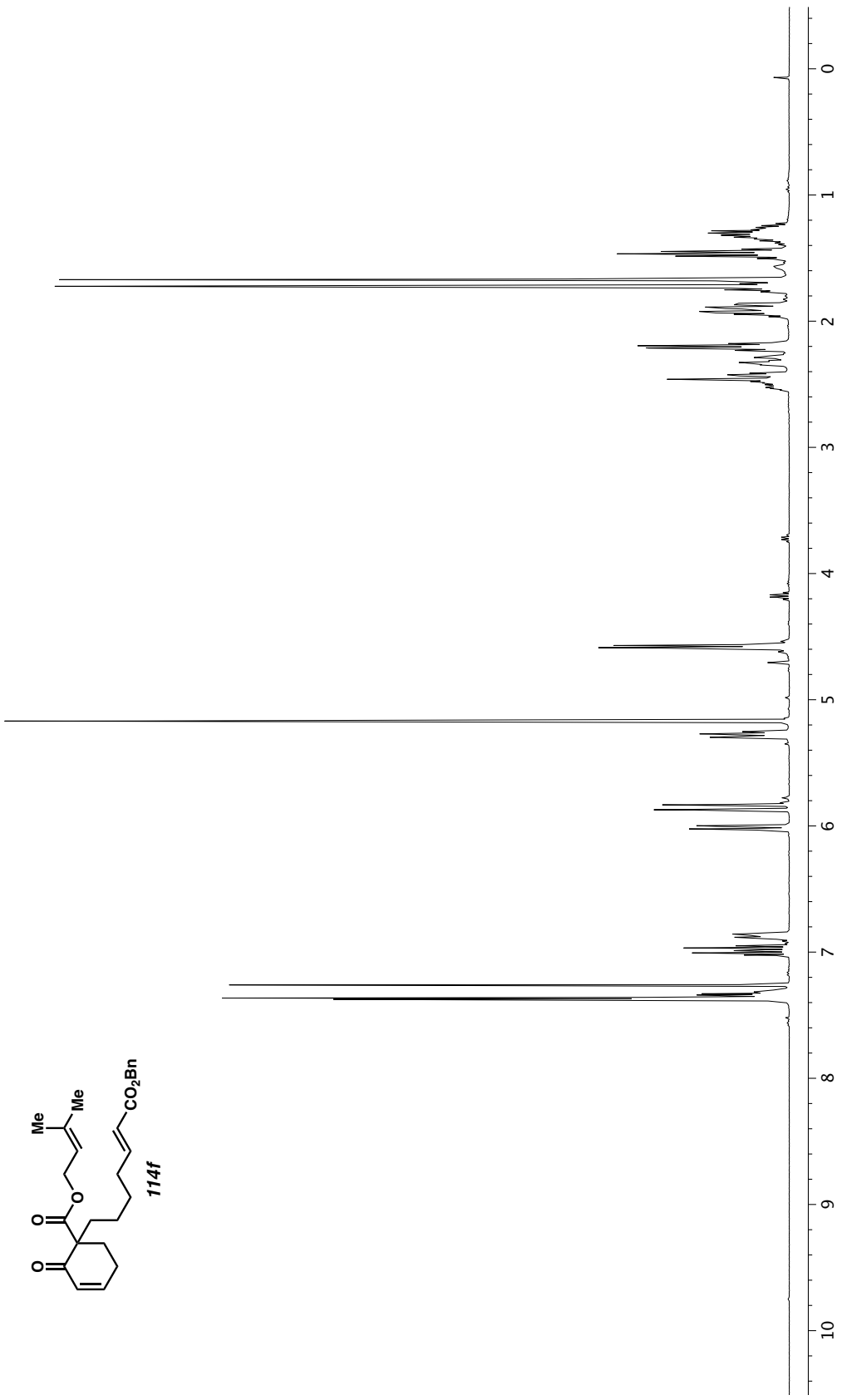

Figure A1.95. *^1H NMR (400 MHz, $CDCl_3$) of compound* ***114f.***

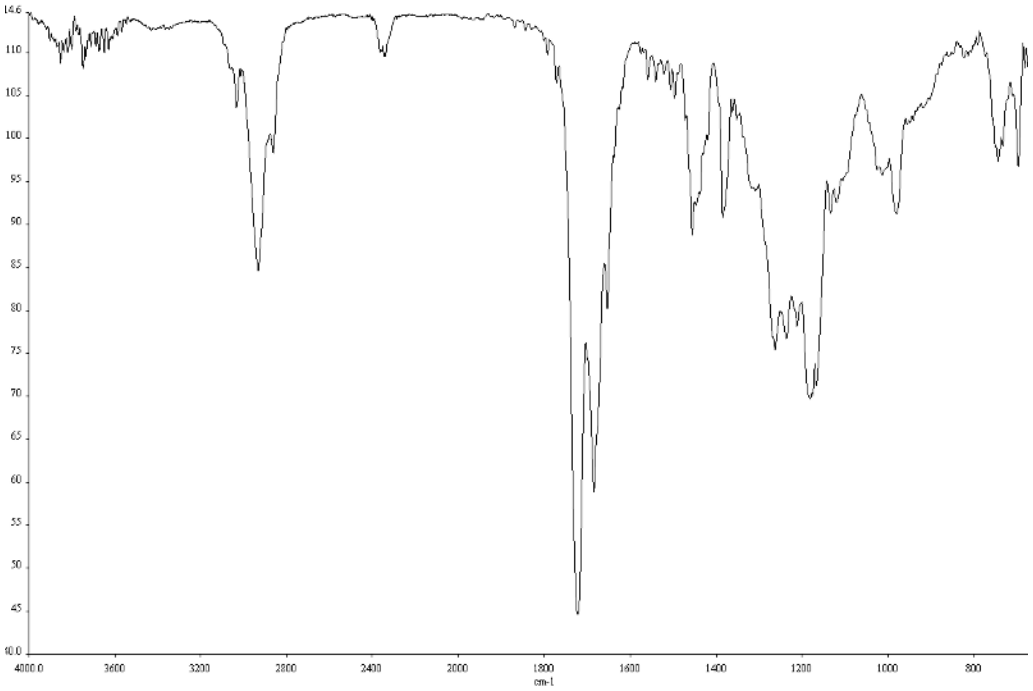

Figure A1.96. *Infrared spectrum (Thin Film, NaCl) of compound* ***114f.***

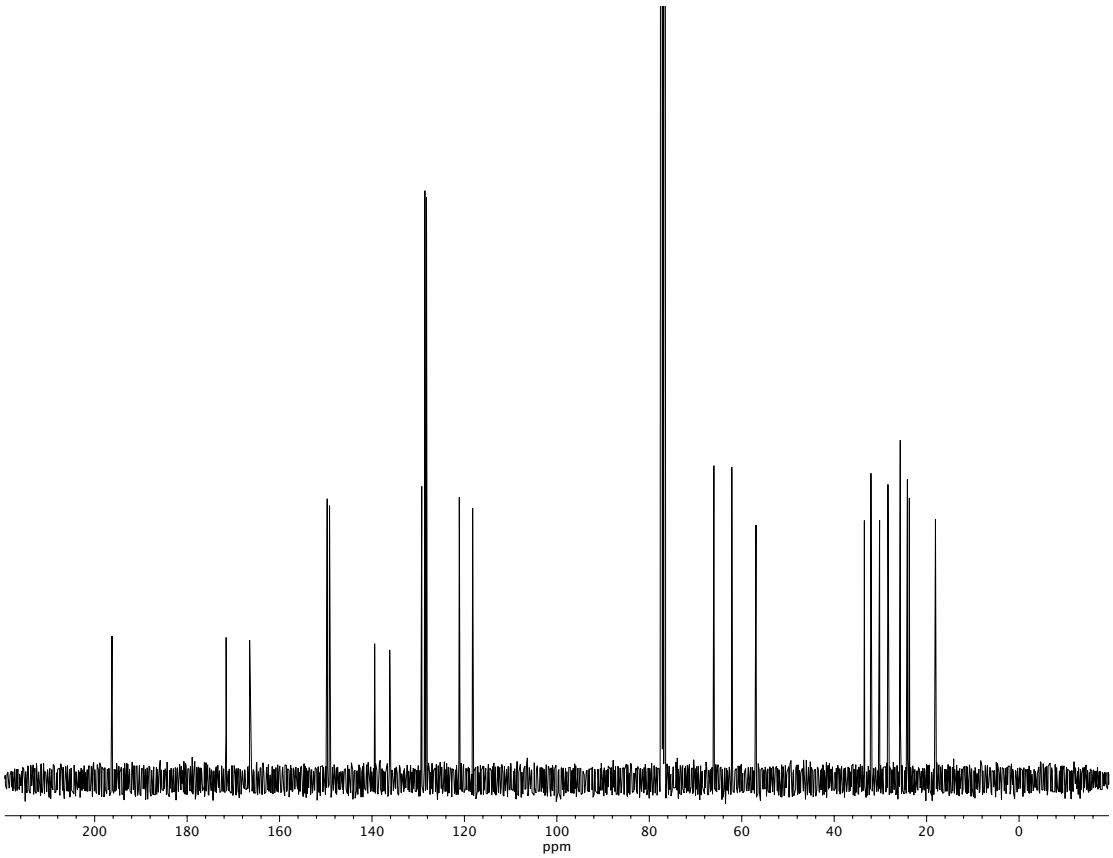

Figure A1.97. *^{13}C NMR (100 MHz, $CDCl_3$) of compound* ***114f.***

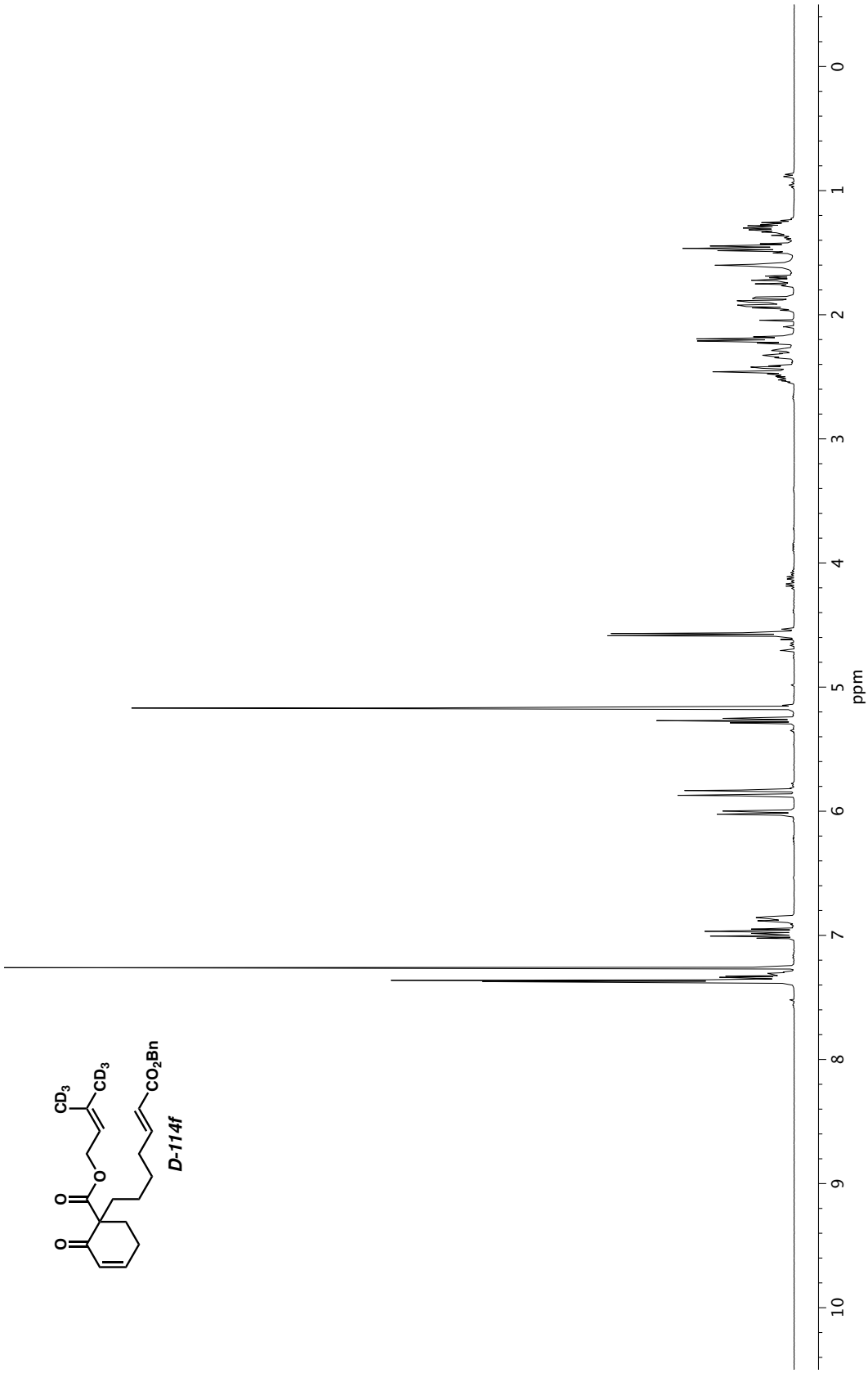

Figure A1.98. *^1H NMR (400 MHz, $CDCl_3$) of compound* ***D-114f.***

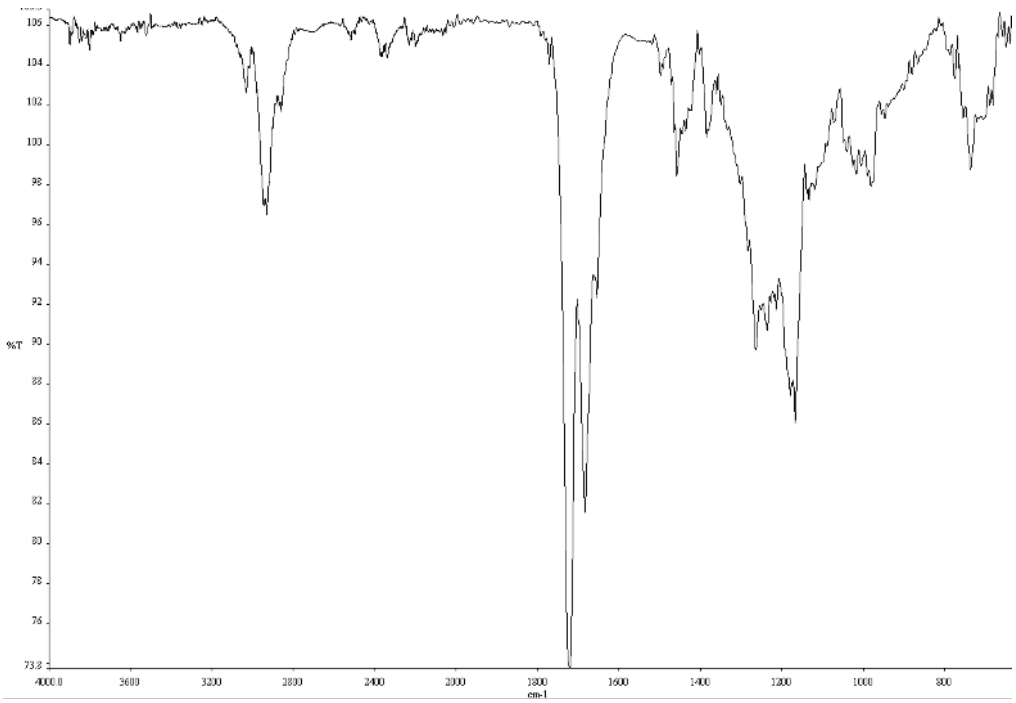

Figure A1.99. *Infrared spectrum (Thin Film, NaCl) of compound* ***D-114f.***

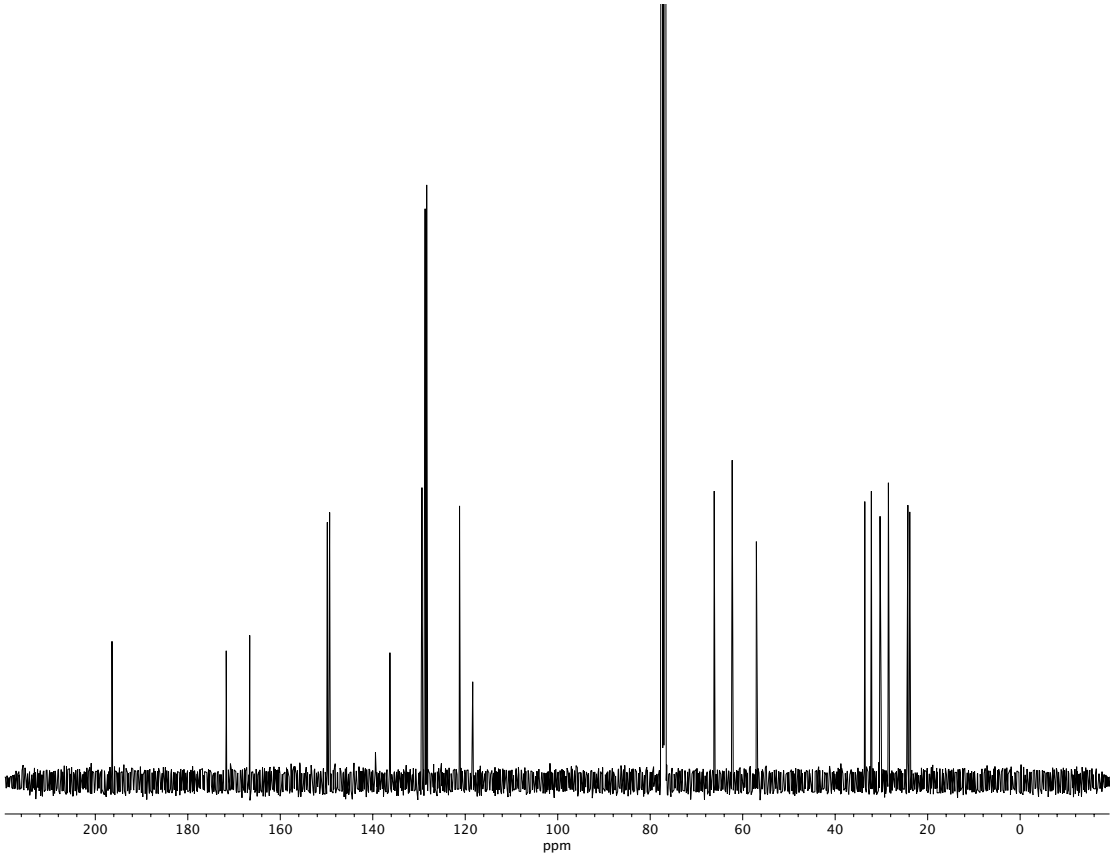

Figure A1.100. *^{13}C NMR (100 MHz, $CDCl_3$) of compound* ***D-114f.***

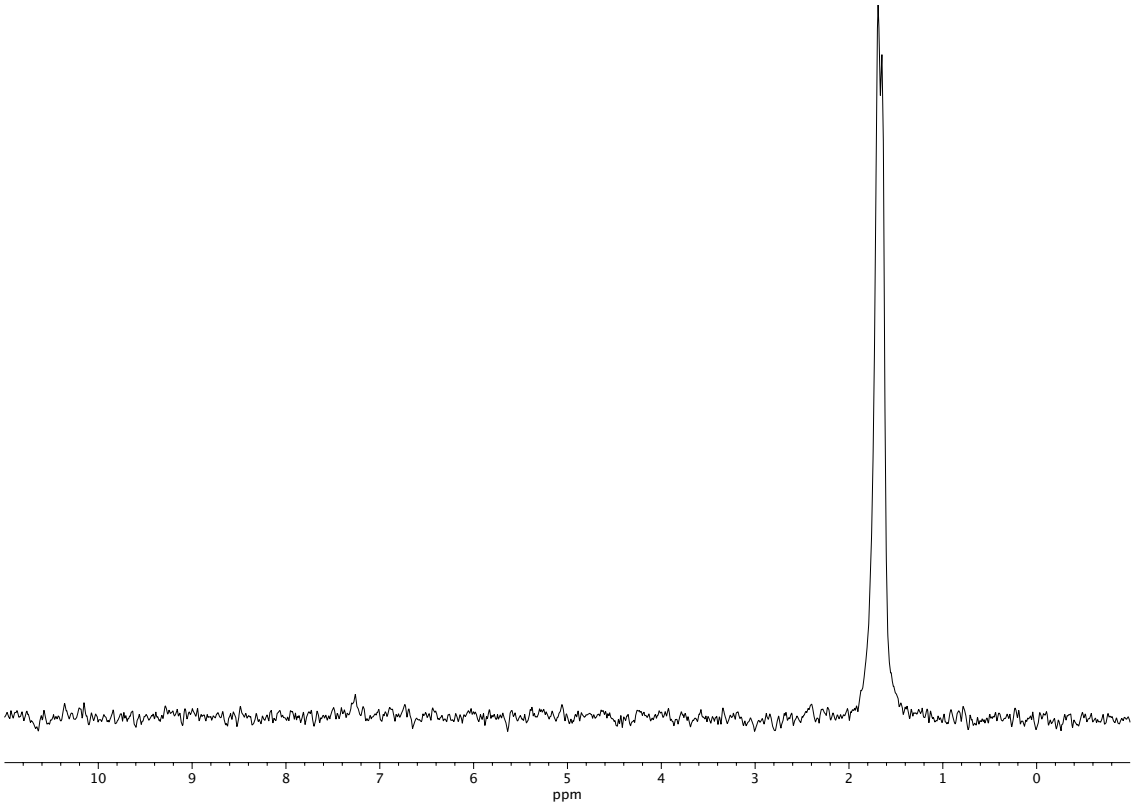

Figure A1.101. *^{2}H NMR (61 MHz, $CDCl_3$) of compound* ***D-114f.***

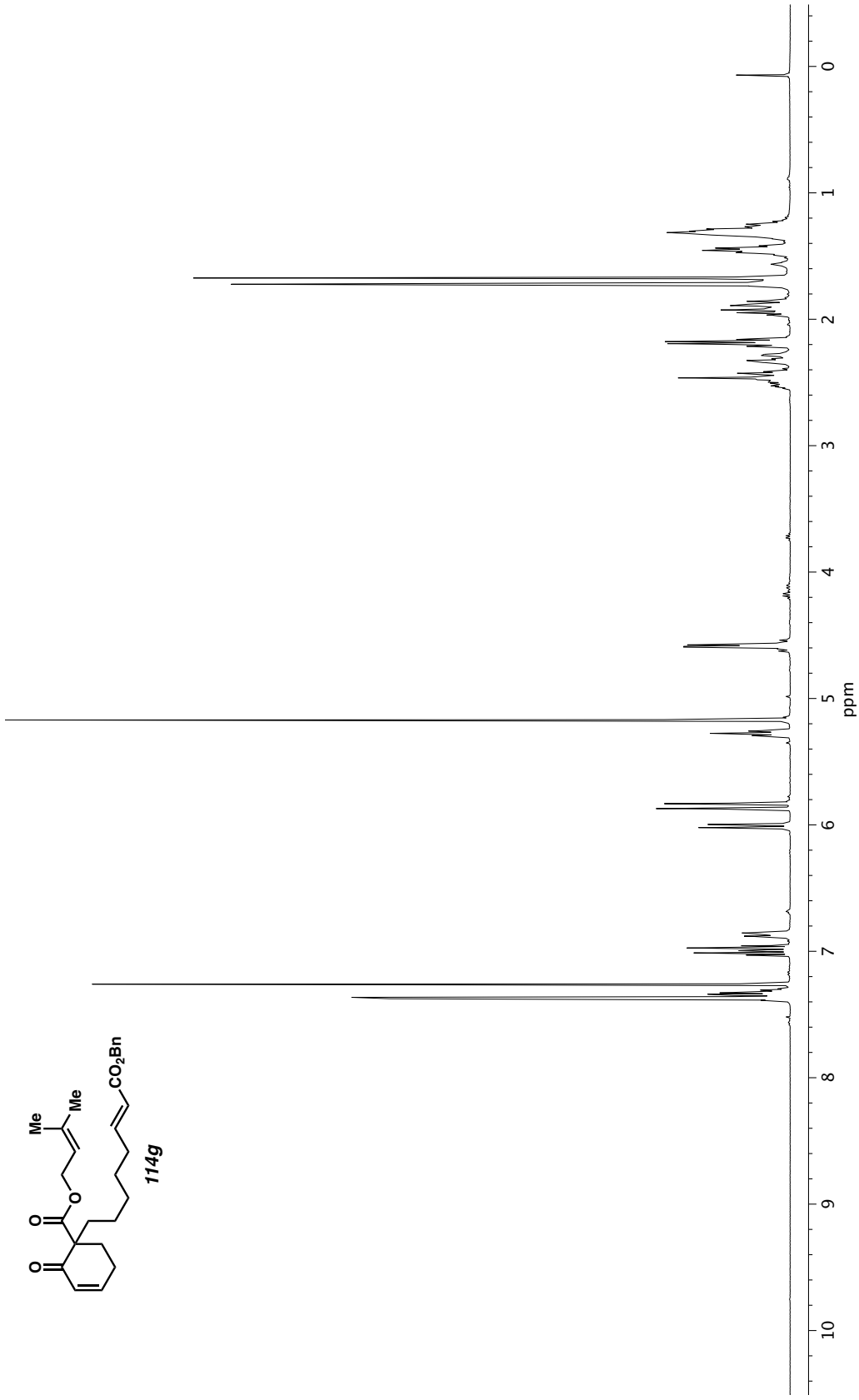

Figure A1.102. *^1H NMR (400 MHz, $CDCl_3$) of compound* ***114g.***

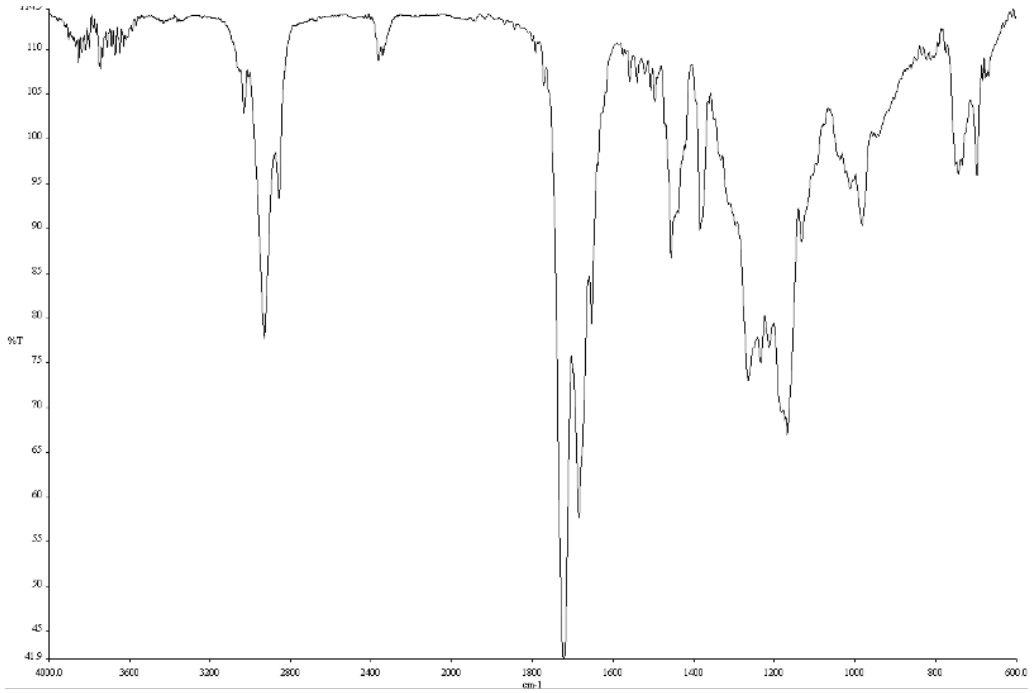

Figure A1.103. *Infrared spectrum (Thin Film, NaCl) of compound* ***114g.***

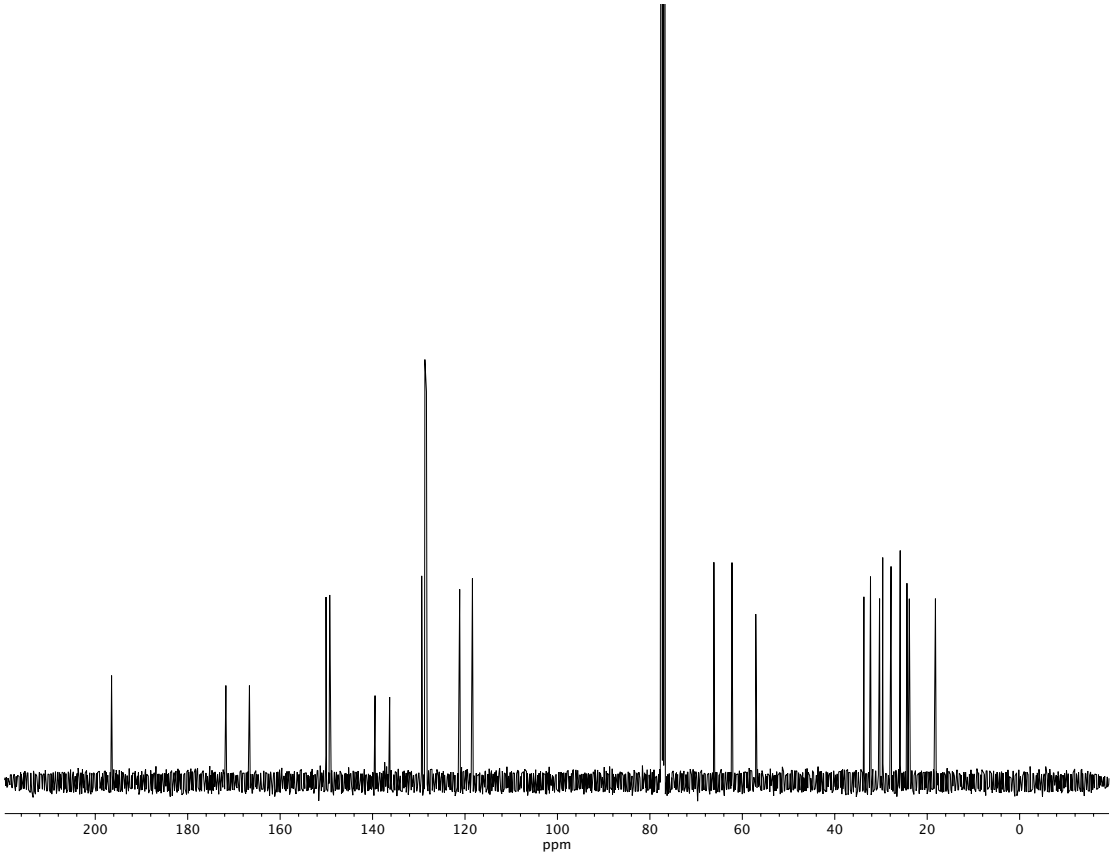

Figure A1.104. *^{13}C NMR (100 MHz, $CDCl_3$) of compound* ***114g.***

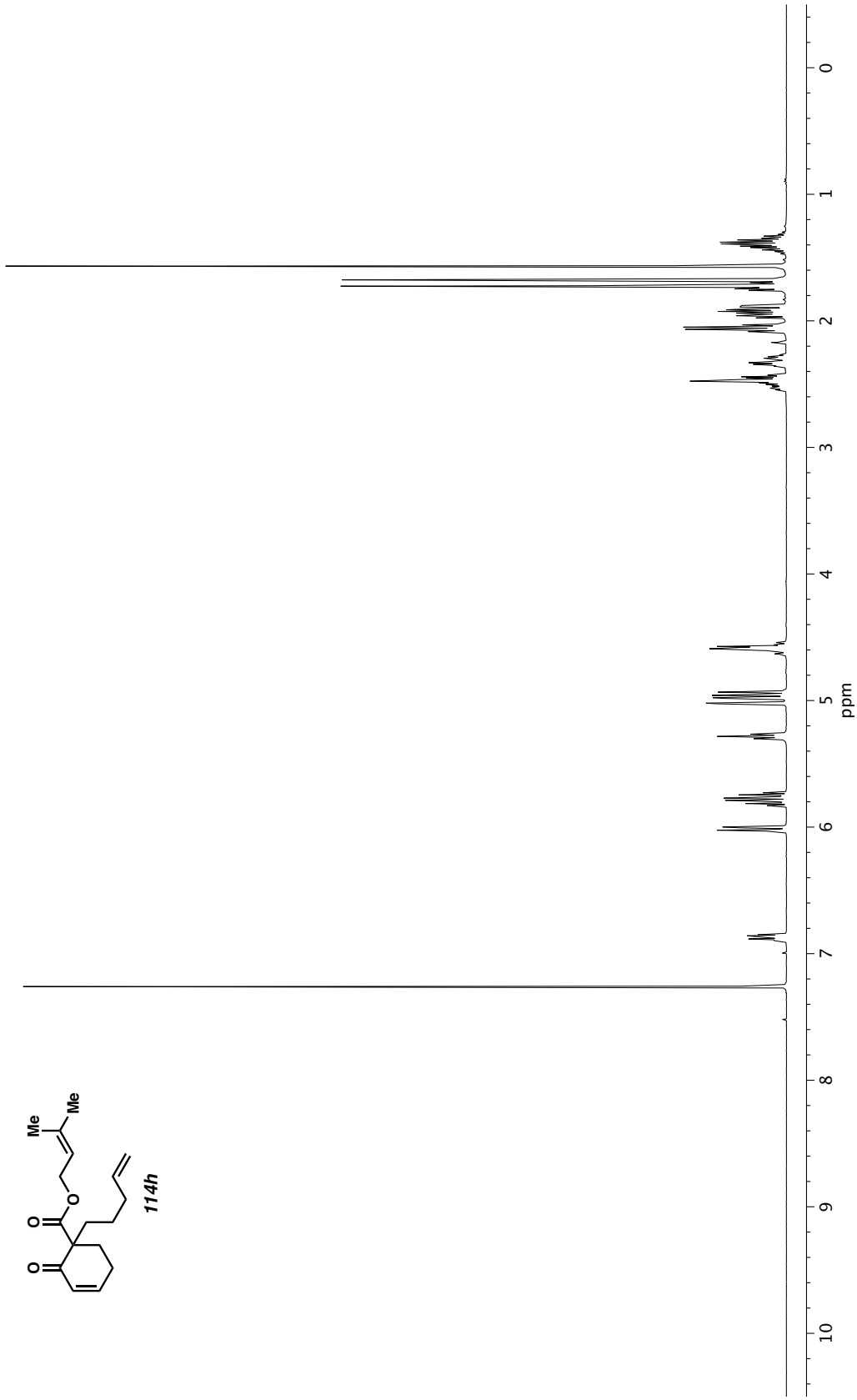

Figure A1.105. *^{1}H NMR (400 MHz, $CDCl_3$) of compound* ***114h.***

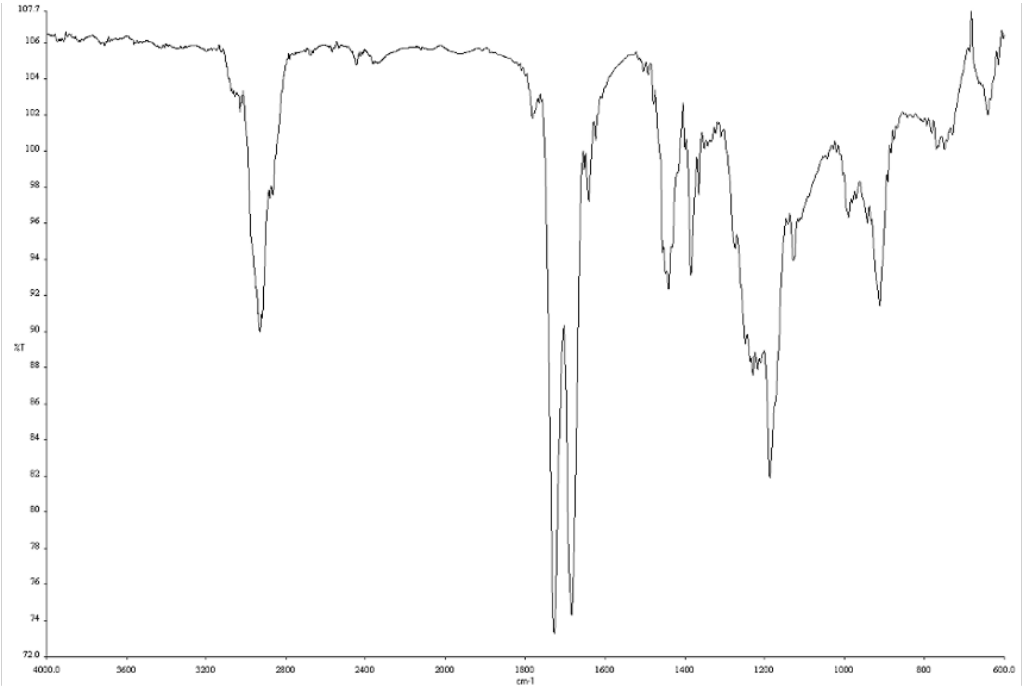

Figure A1.106. *Infrared spectrum (Thin Film, NaCl) of compound* ***114h.***

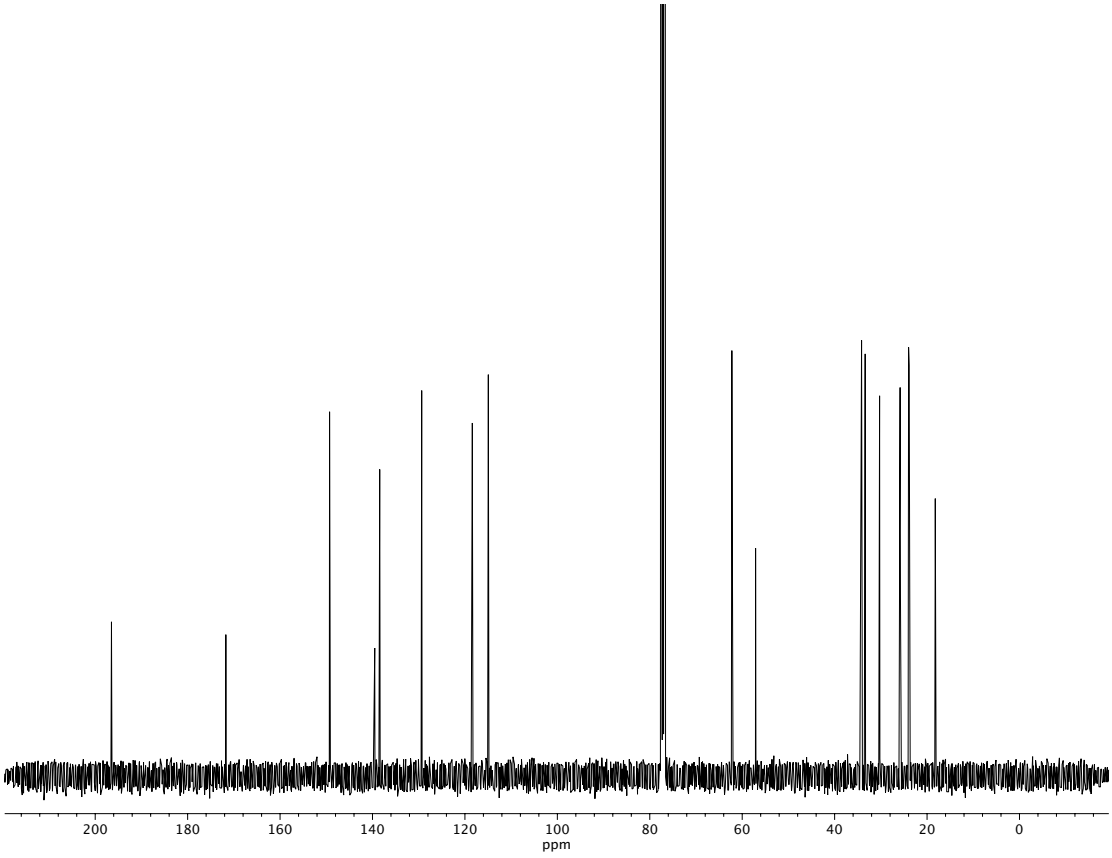

Figure A1.107. *^{13}C NMR (100 MHz, $CDCl_3$) of compound* ***114h.***

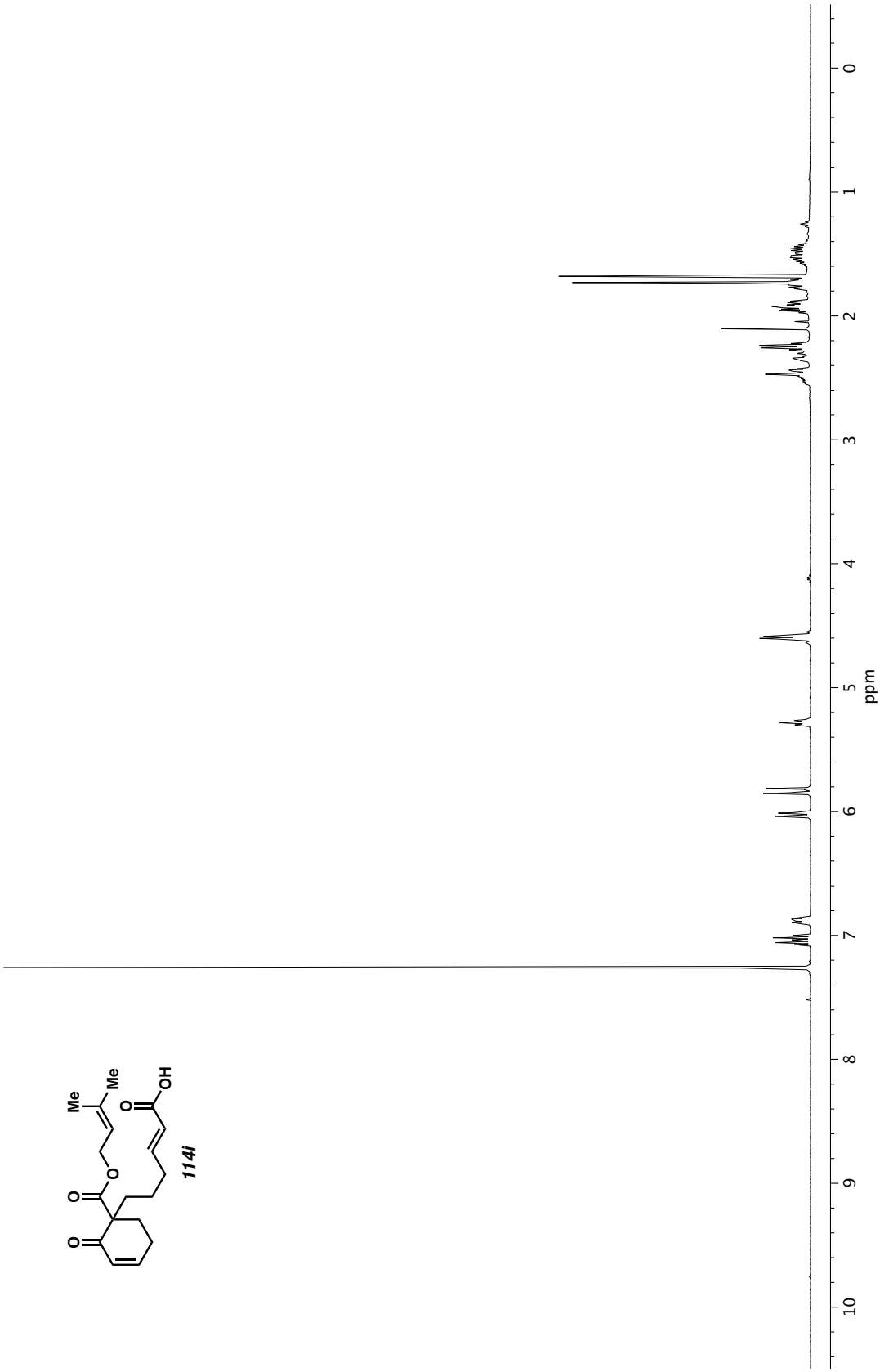

Figure A1.108. *^{1}H NMR (400 MHz, $CDCl_3$) of compound* ***114i.***

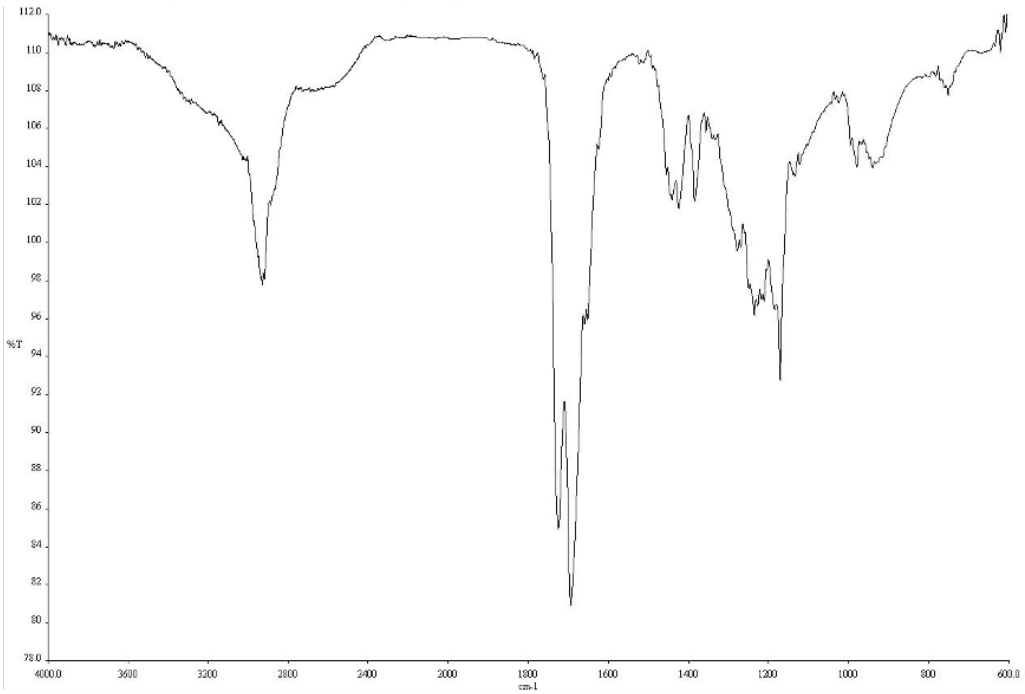

Figure A1.109. *Infrared spectrum (Thin Film, NaCl) of compound* ***114i.***

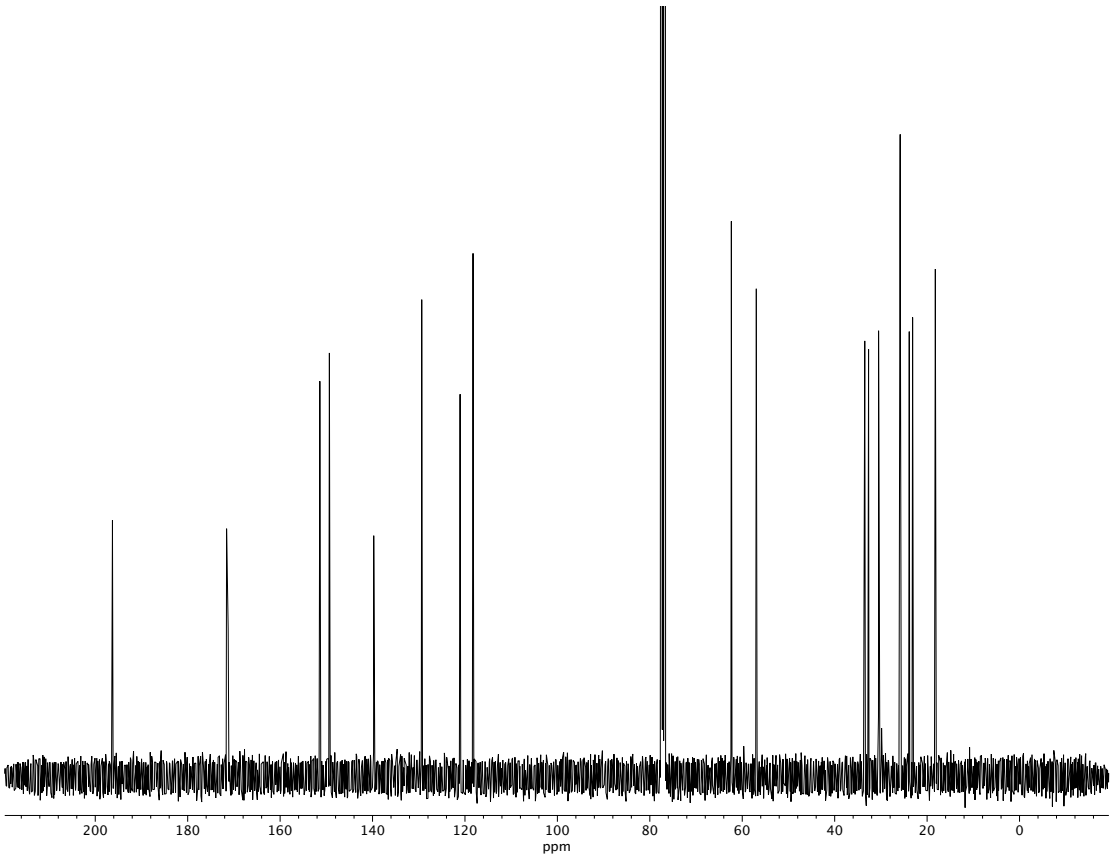

Figure A1.110. *^{13}C NMR (100 MHz, $CDCl_3$) of compound* ***114i.***

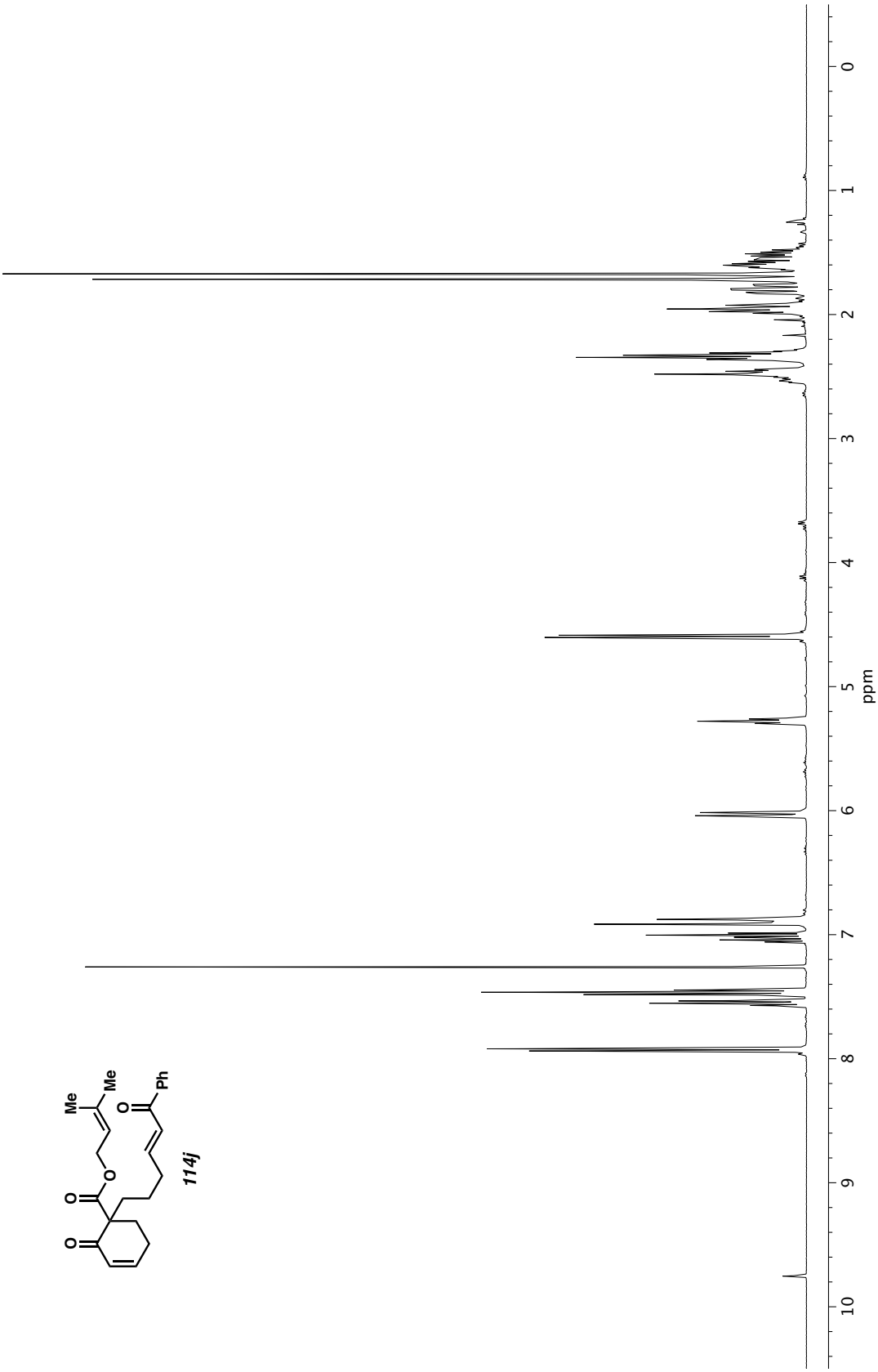

Figure A1.111. *^1H NMR (400 MHz, $CDCl_3$) of compound* ***114j.***

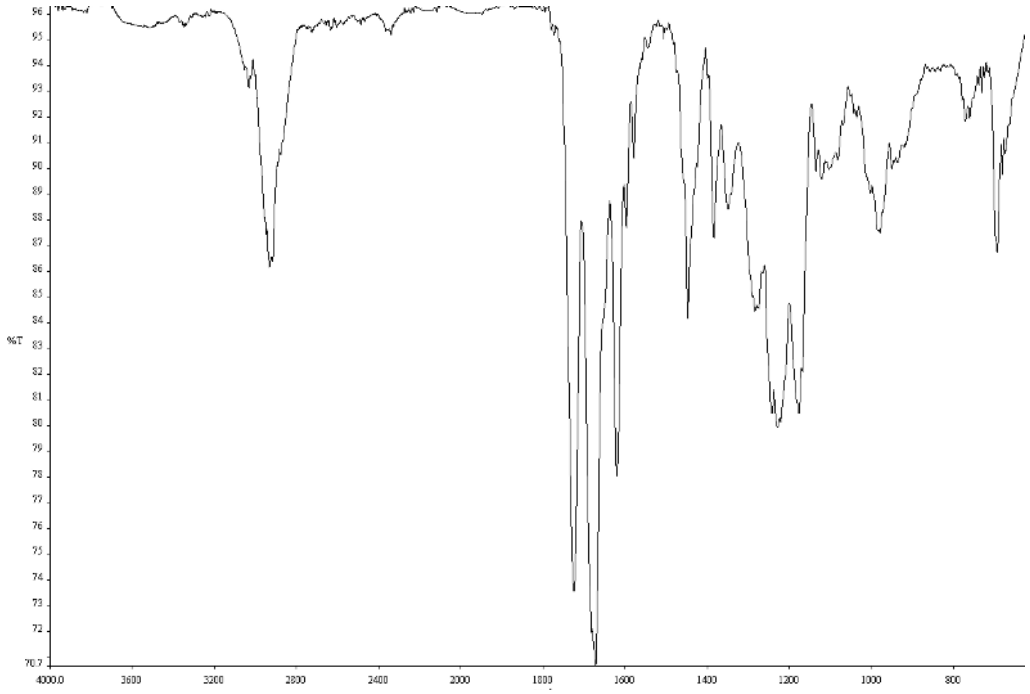

Figure A1.112. *Infrared spectrum (Thin Film, NaCl) of compound* ***114j.***

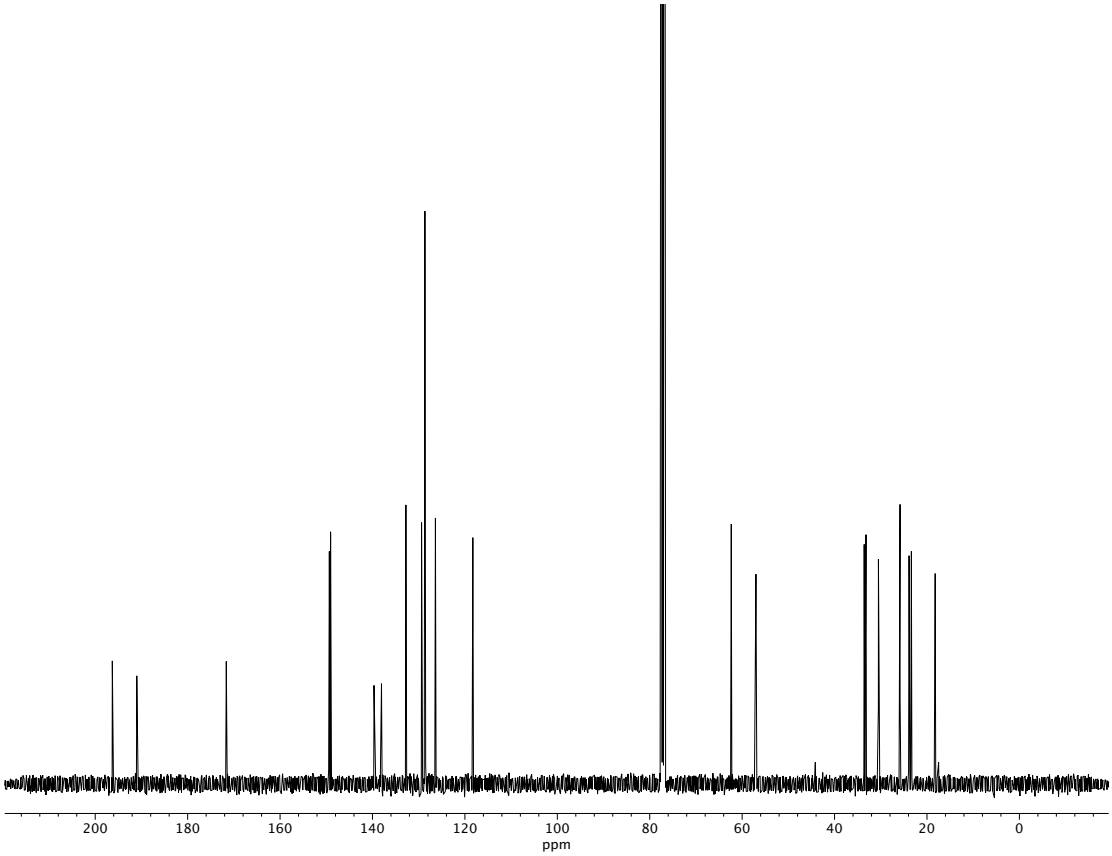

Figure A1.113. *^{13}C NMR (100 MHz, $CDCl_3$) of compound* ***114j.***

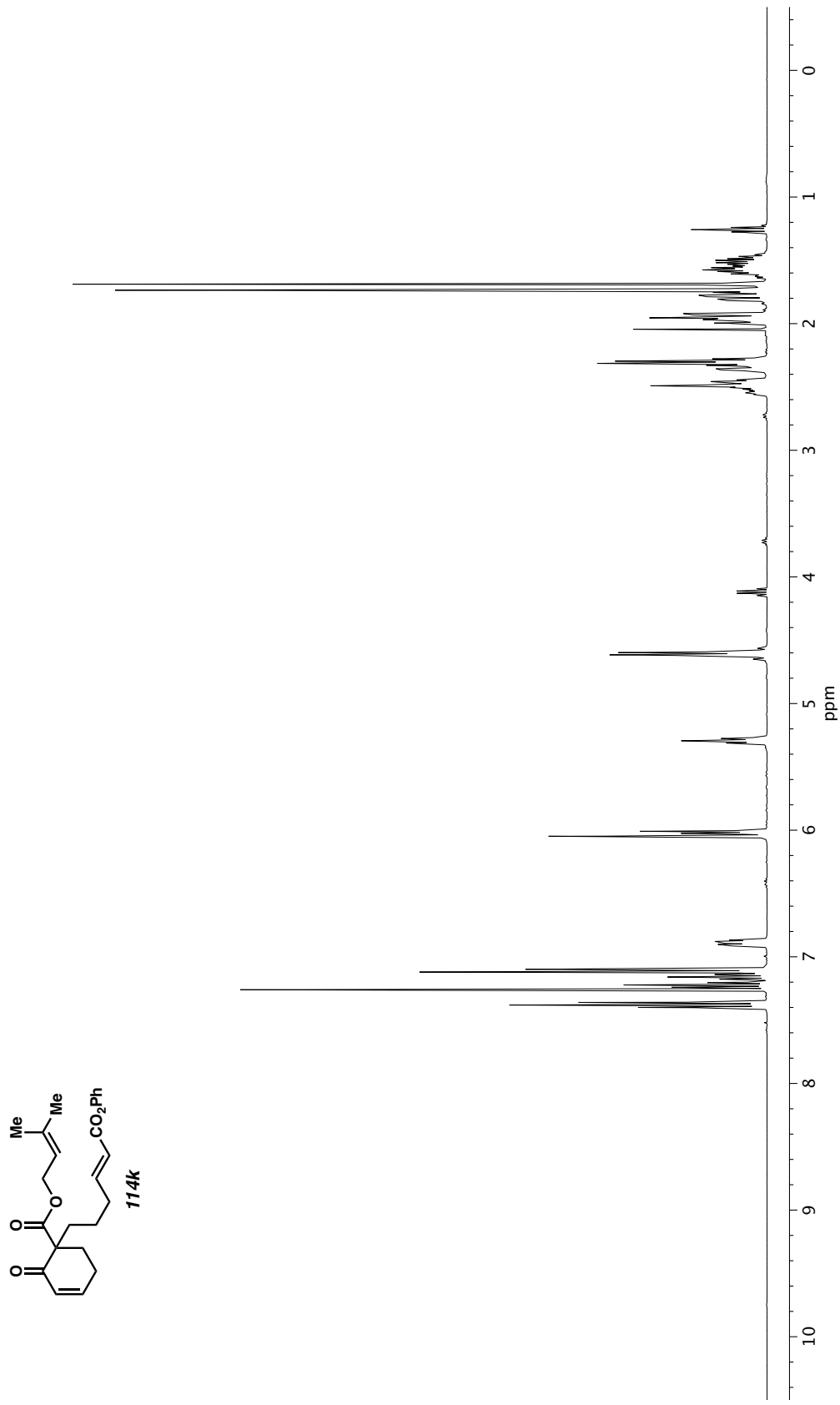

Figure A1.114. *^{1}H NMR (400 MHz, $CDCl_3$) of compound* ***114k.***

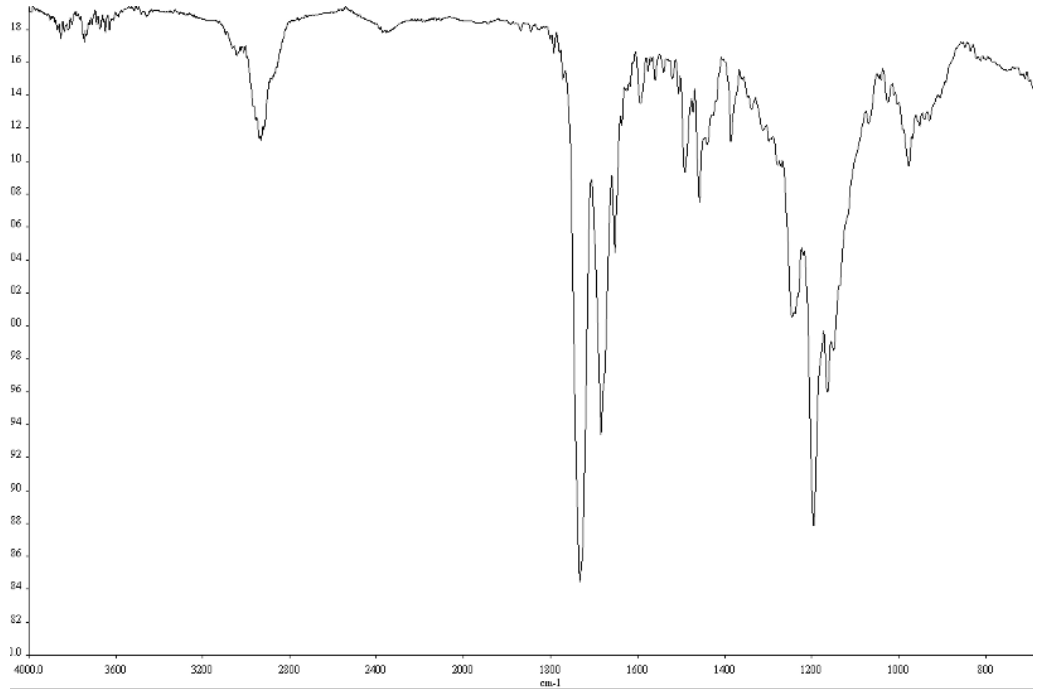

Figure A1.115. *Infrared spectrum (Thin Film, NaCl) of compound* ***114k.***

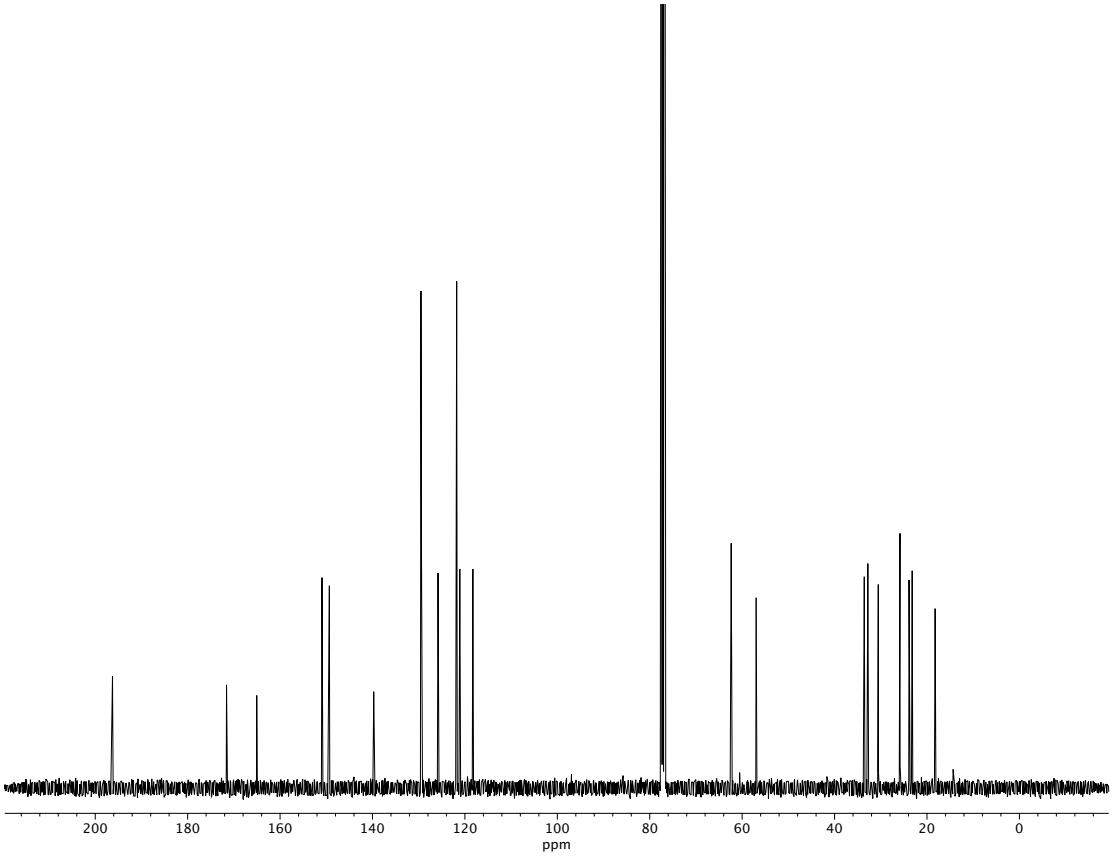

Figure A1.116. *^{13}C NMR (100 MHz, $CDCl_3$) of compound* ***114k.***

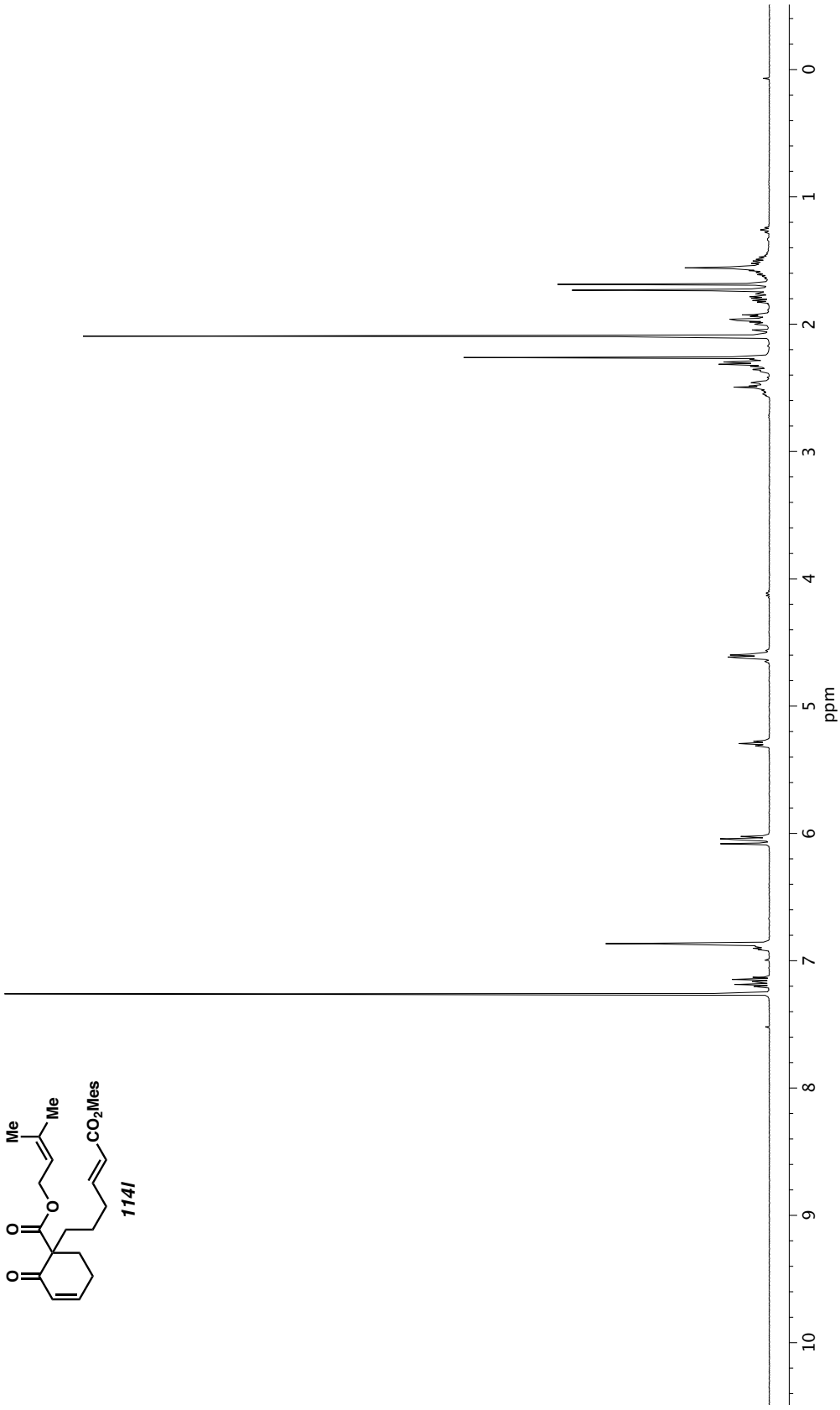

Figure A1.117. *^{1}H NMR (400 MHz, $CDCl_3$) of compound* ***114l.***

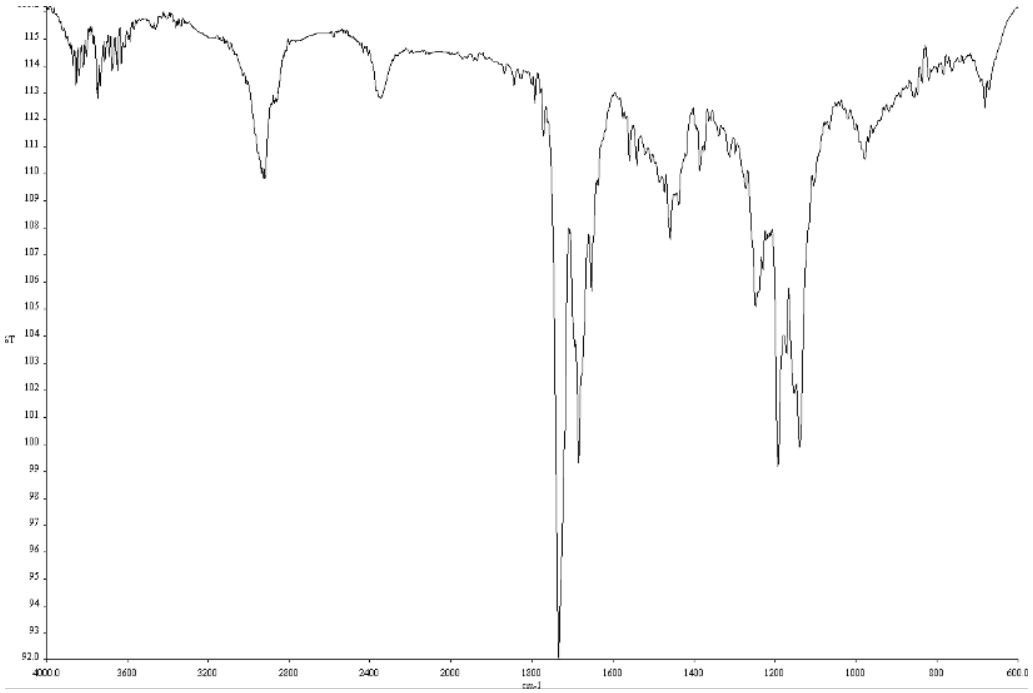

Figure A1.118. *Infrared spectrum (Thin Film, NaCl) of compound* ***114l.***

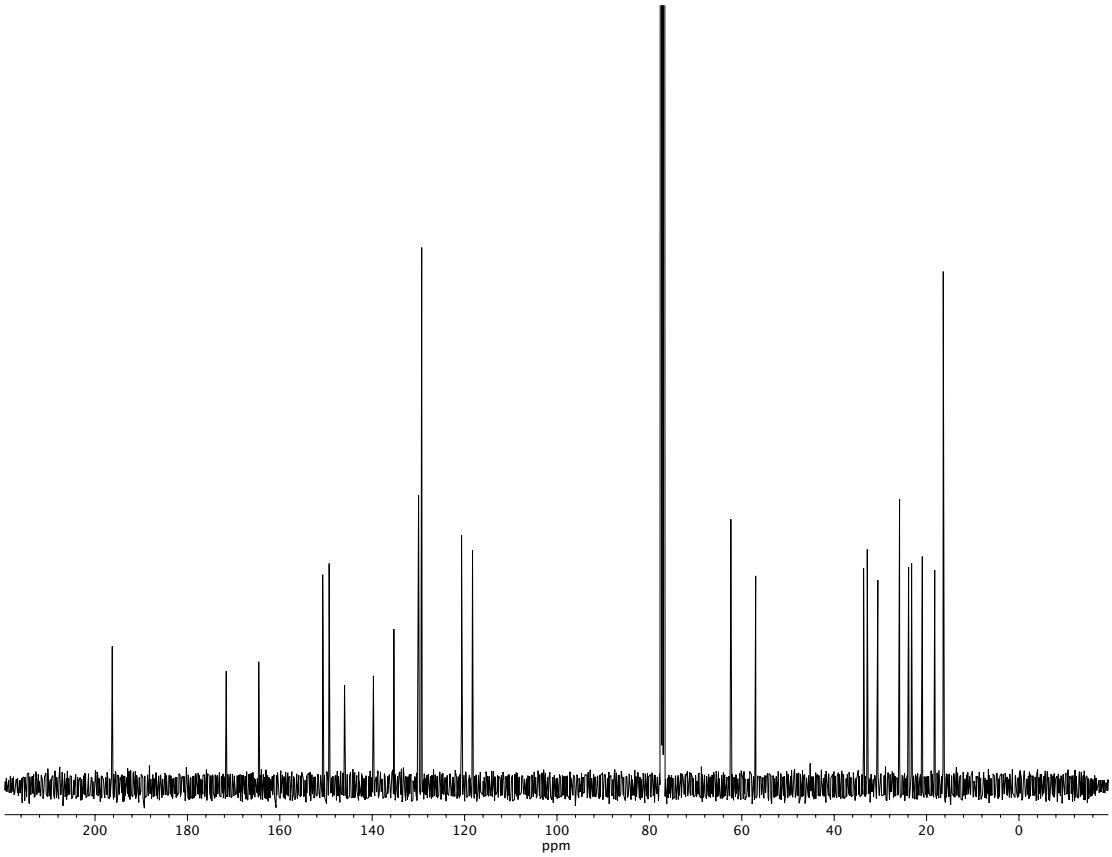

Figure A1.119. *^{13}C NMR (100 MHz, $CDCl_3$) of compound* ***114l.***

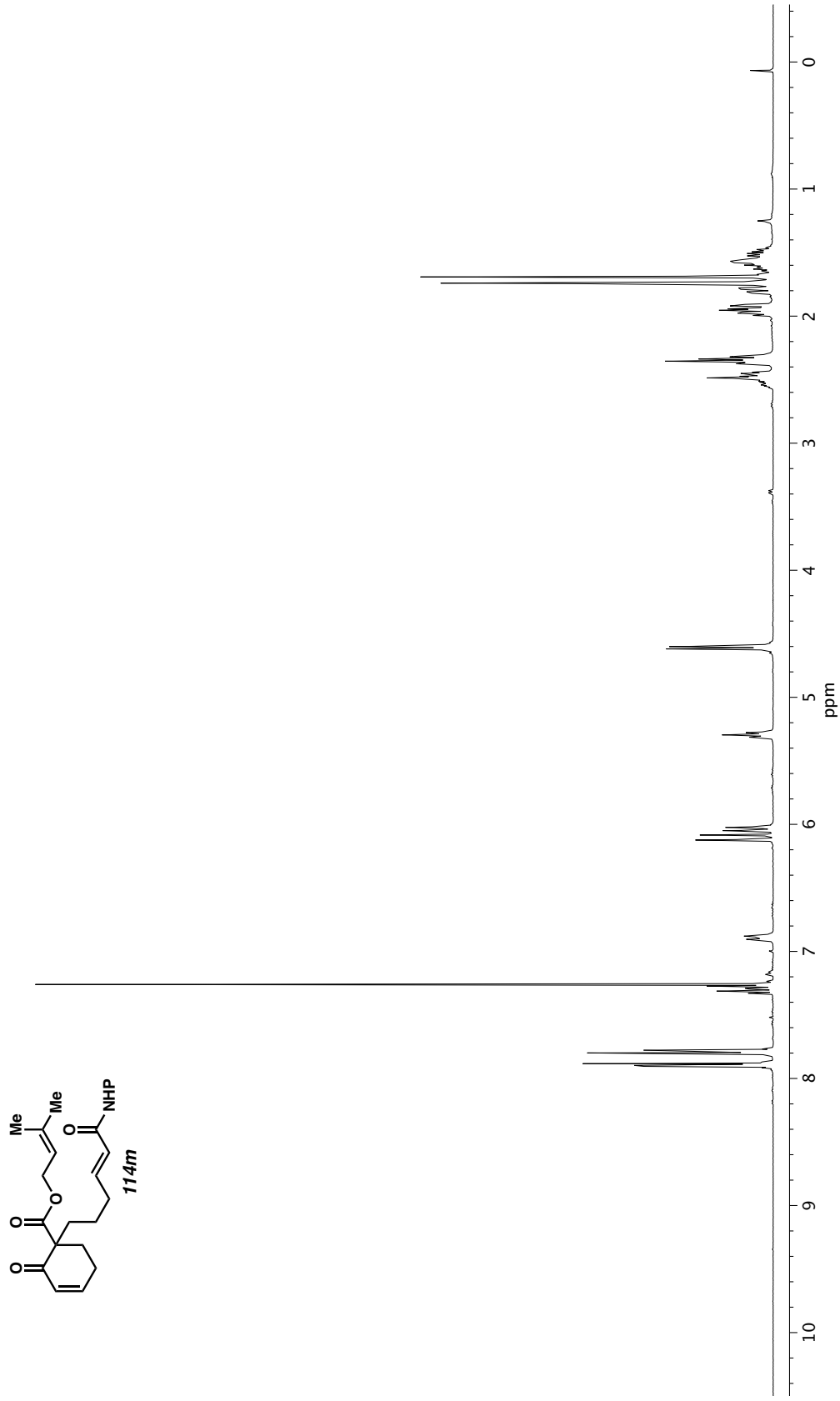

Figure A1.120. *^1H NMR (400 MHz, $CDCl_3$) of compound* ***114m.***

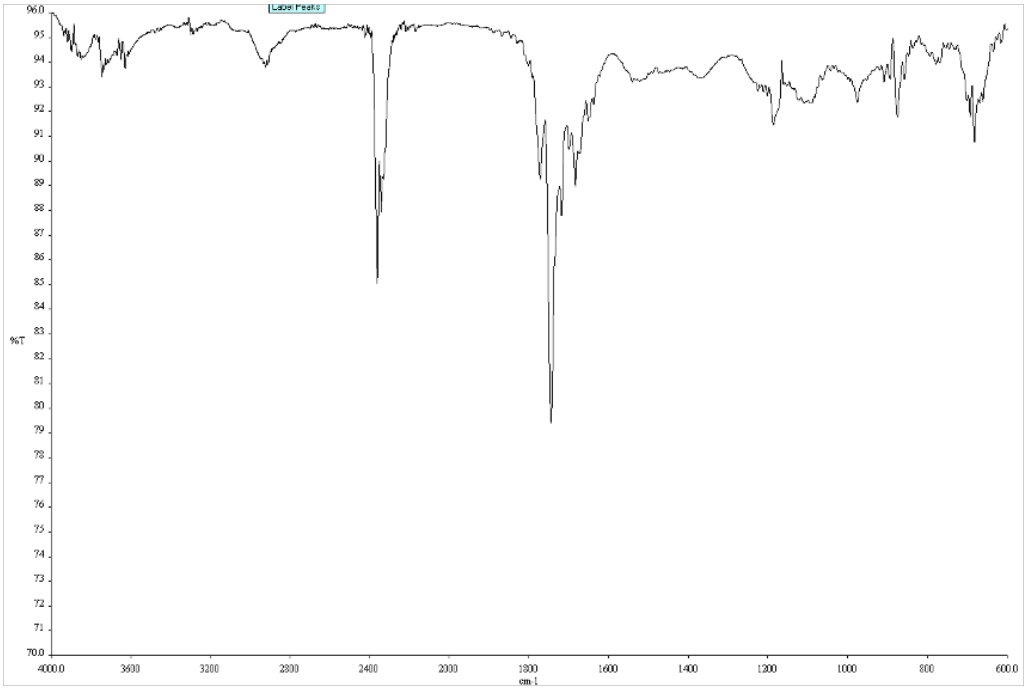

Figure A1.121. *Infrared spectrum (Thin Film, NaCl) of compound* ***114m.***

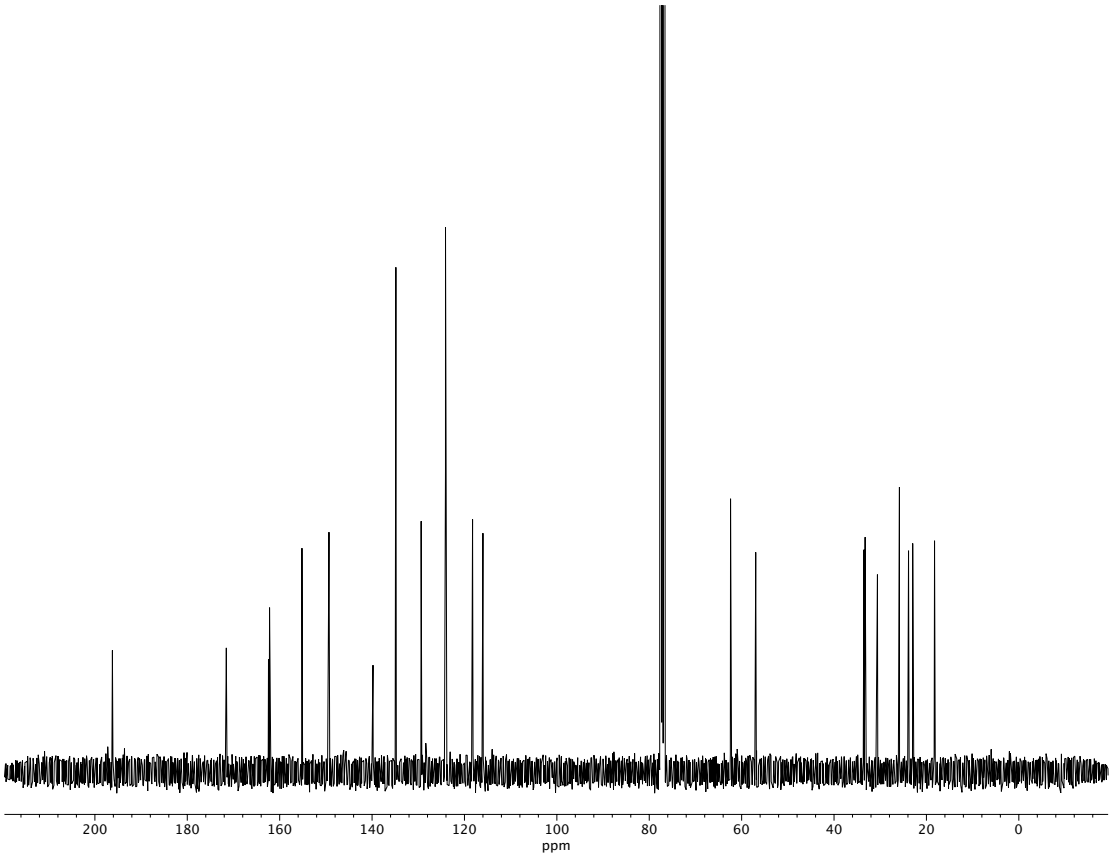

Figure A1.122. *^{13}C NMR (100 MHz, $CDCl_3$) of compound* ***114m.***

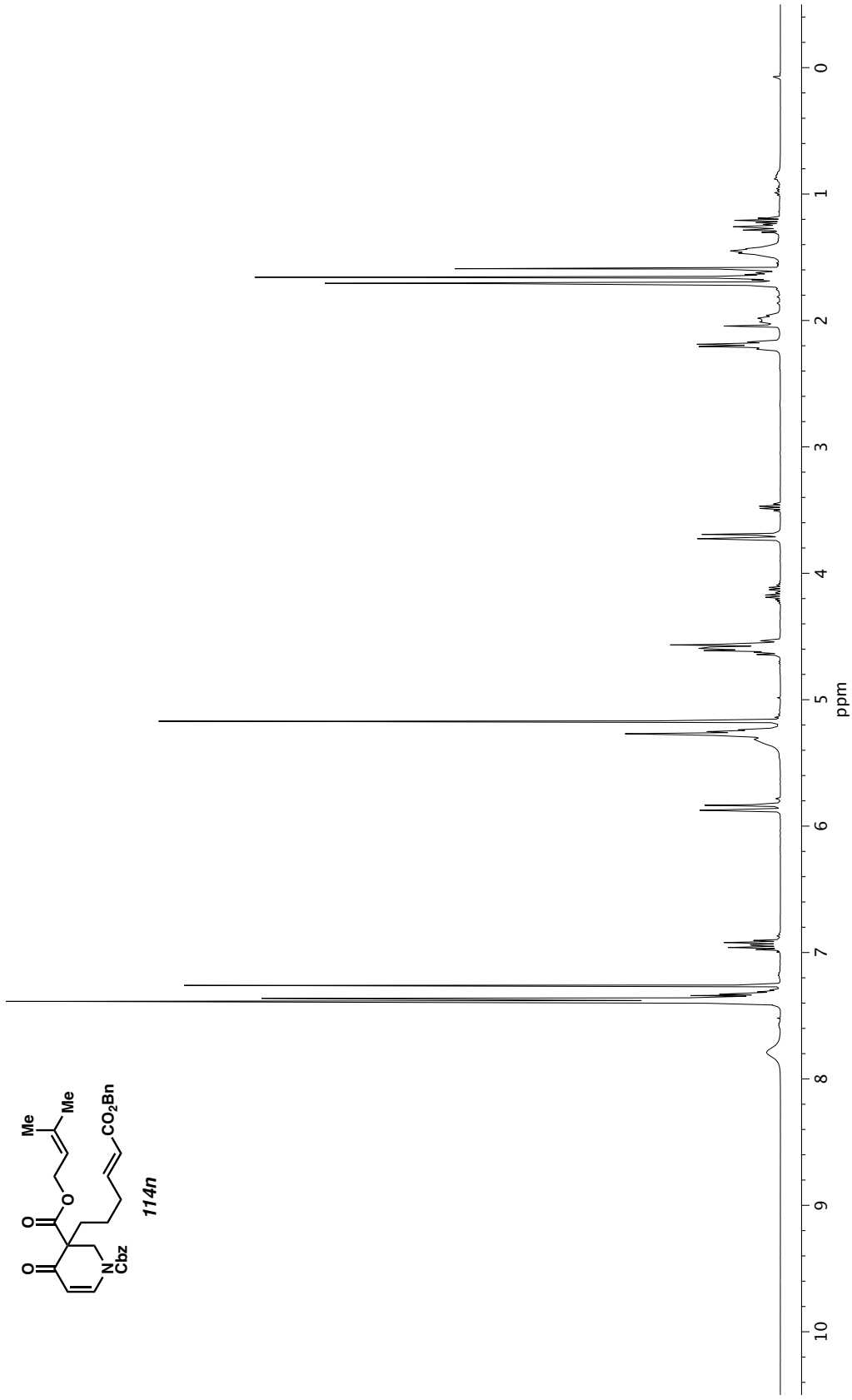

Figure A1.123. *^{1}H NMR (400 MHz, $CDCl_3$) of compound* ***114n.***

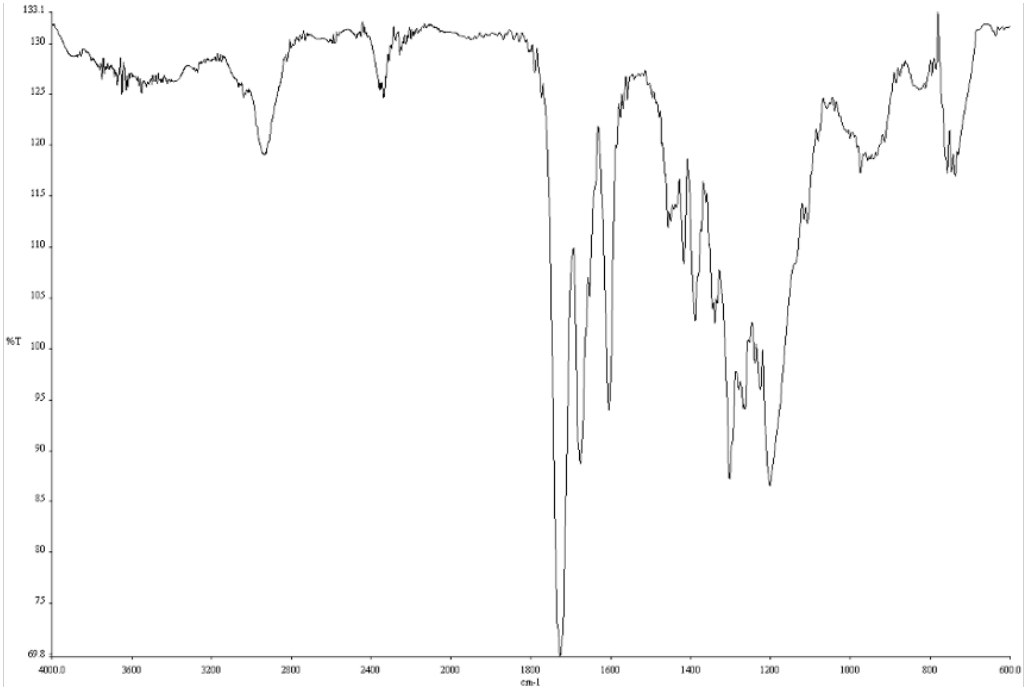

Figure A1.124. *Infrared spectrum (Thin Film, NaCl) of compound* ***114n.***

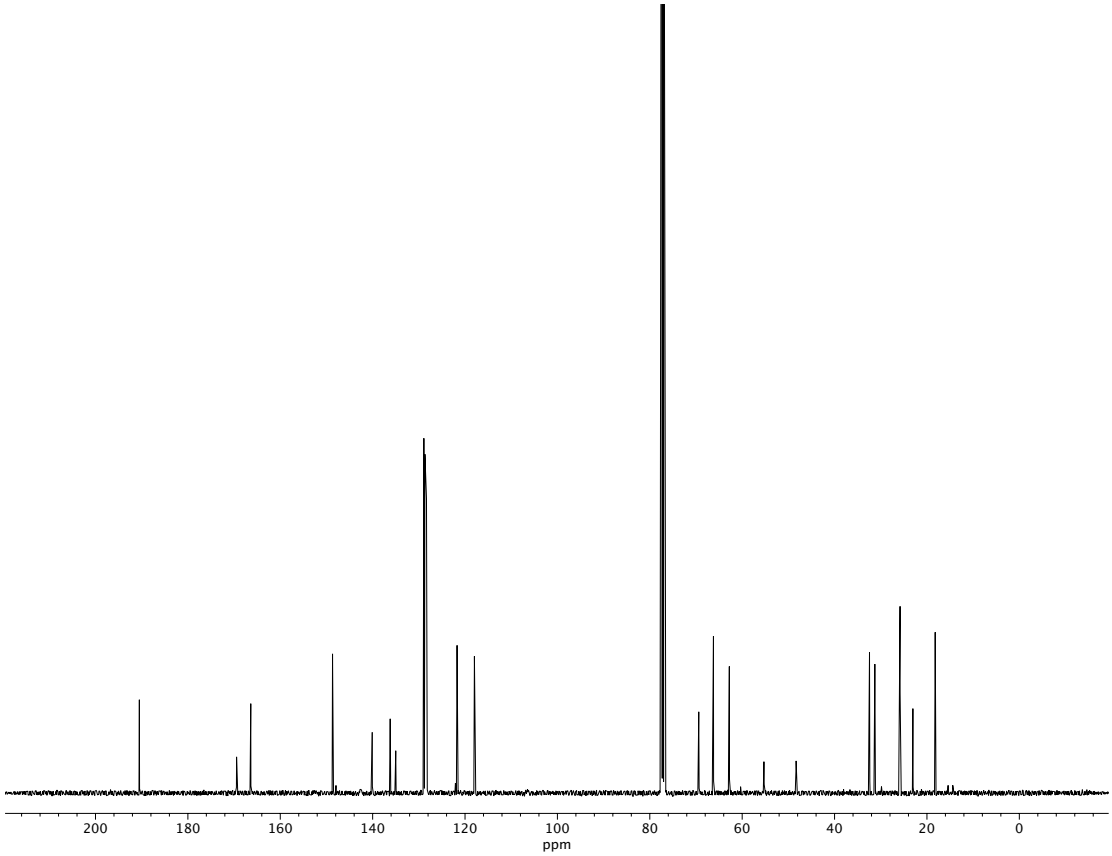

Figure A1.125. *^{13}C NMR (100 MHz, $CDCl_3$) of compound* ***114n.***

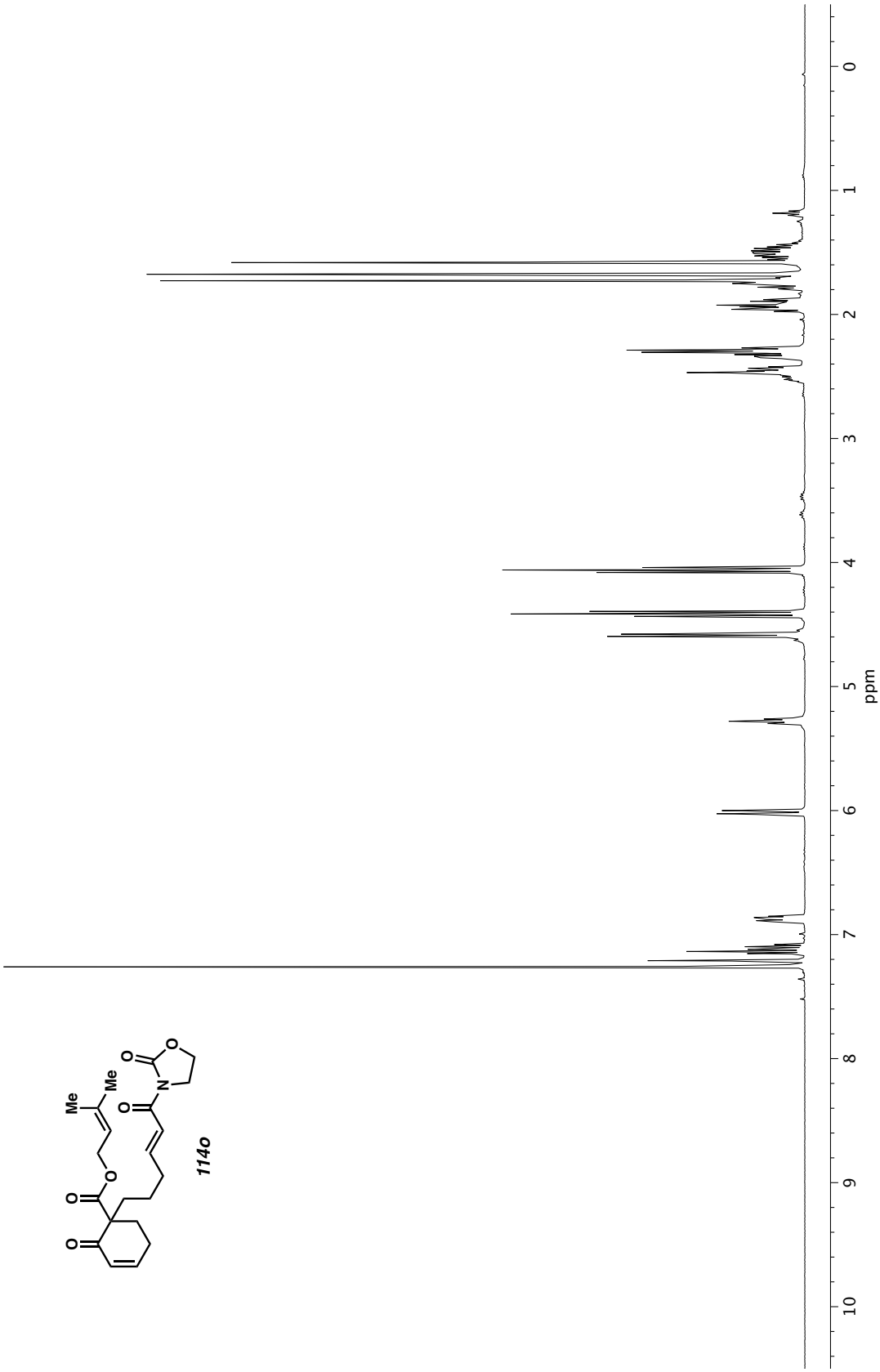

Figure A1.126. *^{1}H NMR (400 MHz, $CDCl_3$) of compound* ***114o.***

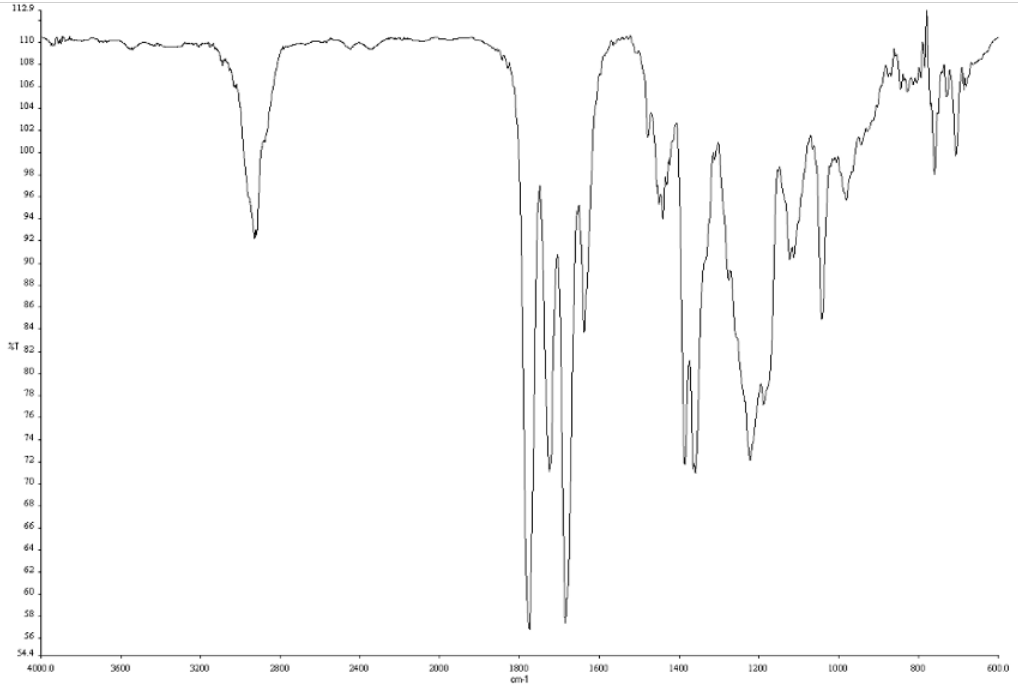

Figure A1.127. *Infrared spectrum (Thin Film, NaCl) of compound* ***114o.***

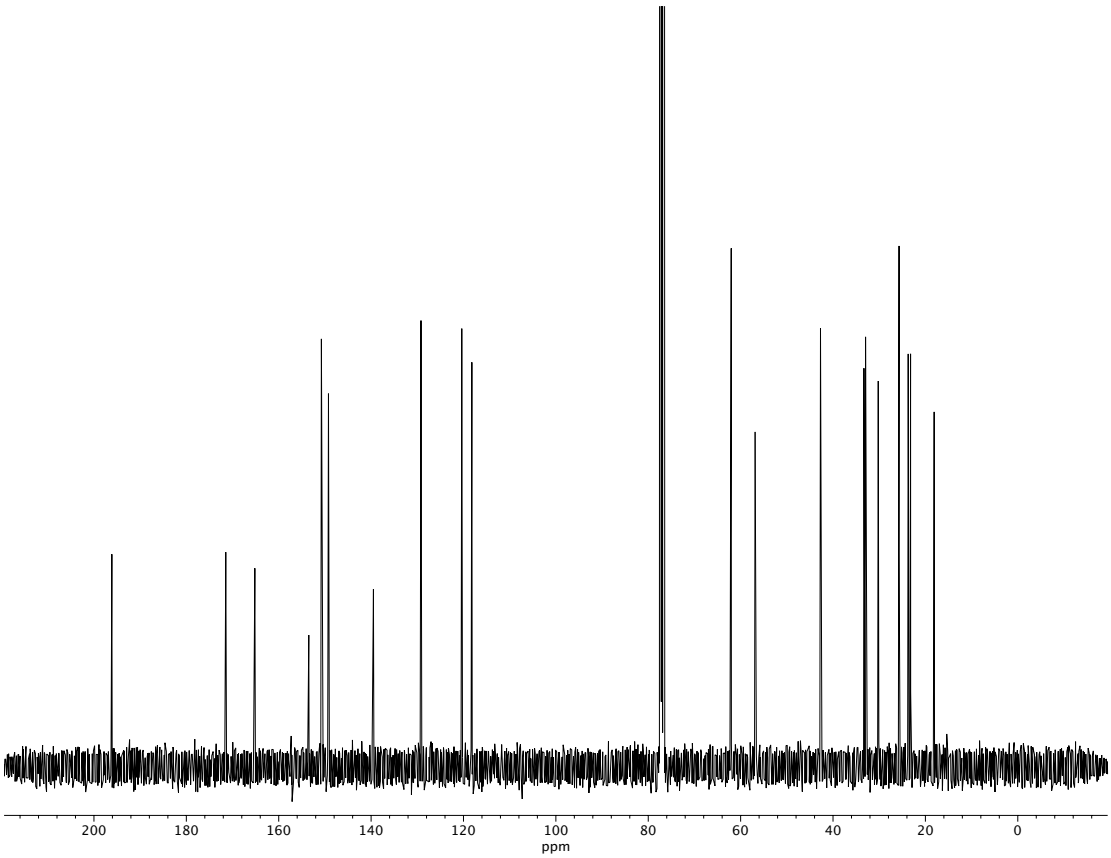

Figure A1.128. *^{13}C NMR (100 MHz, $CDCl_3$) of compound* ***114o.***

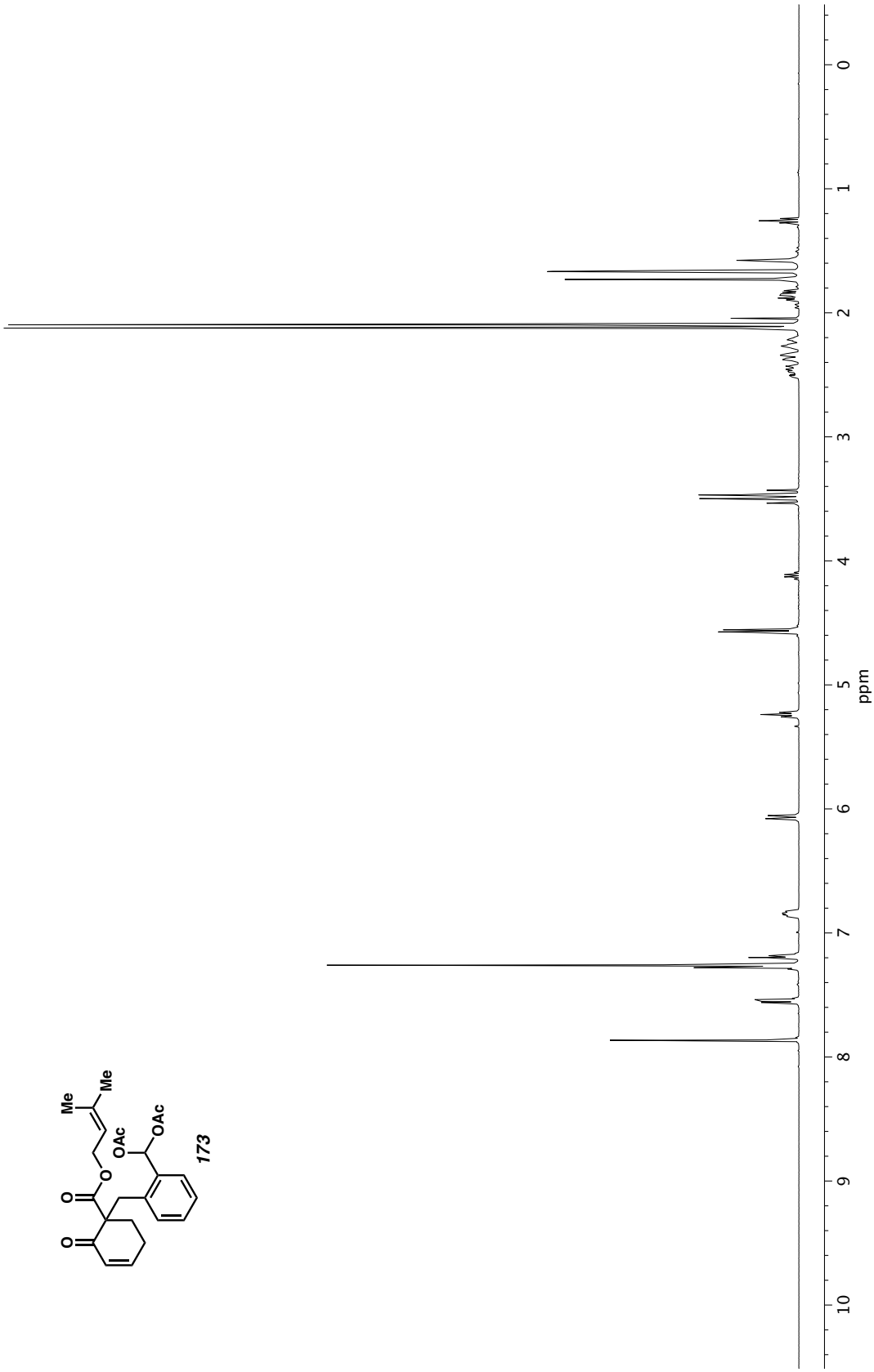

Figure A1.129. *^{1}H NMR (400 MHz, $CDCl_3$) of compound* ***173.***

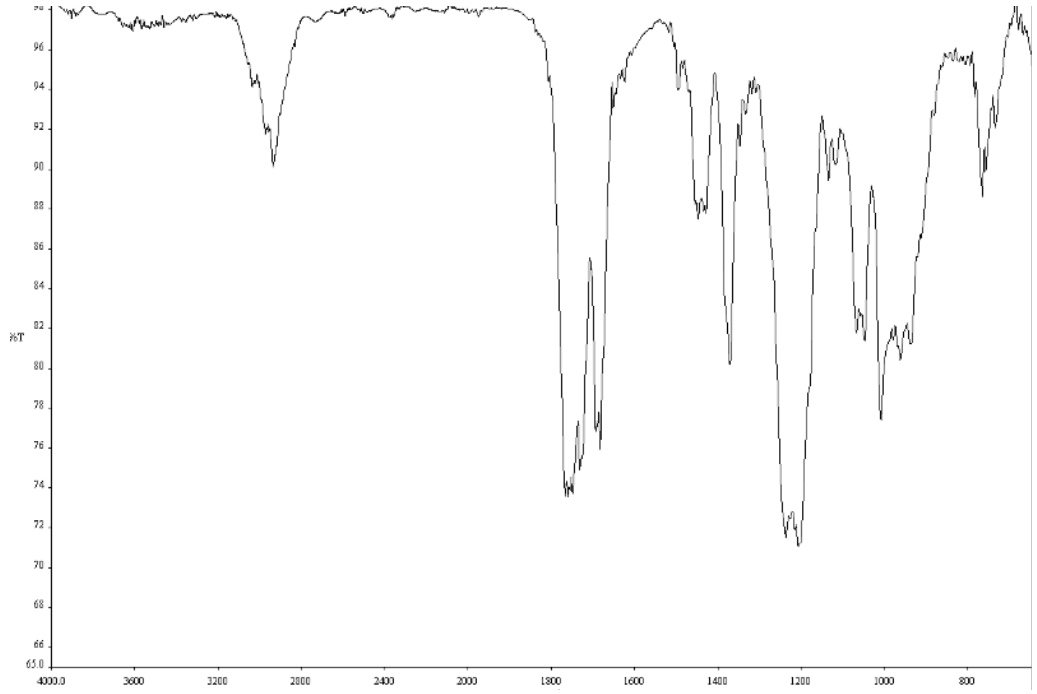

Figure A1.130. *Infrared spectrum (Thin Film, NaCl) of compound* ***173.***

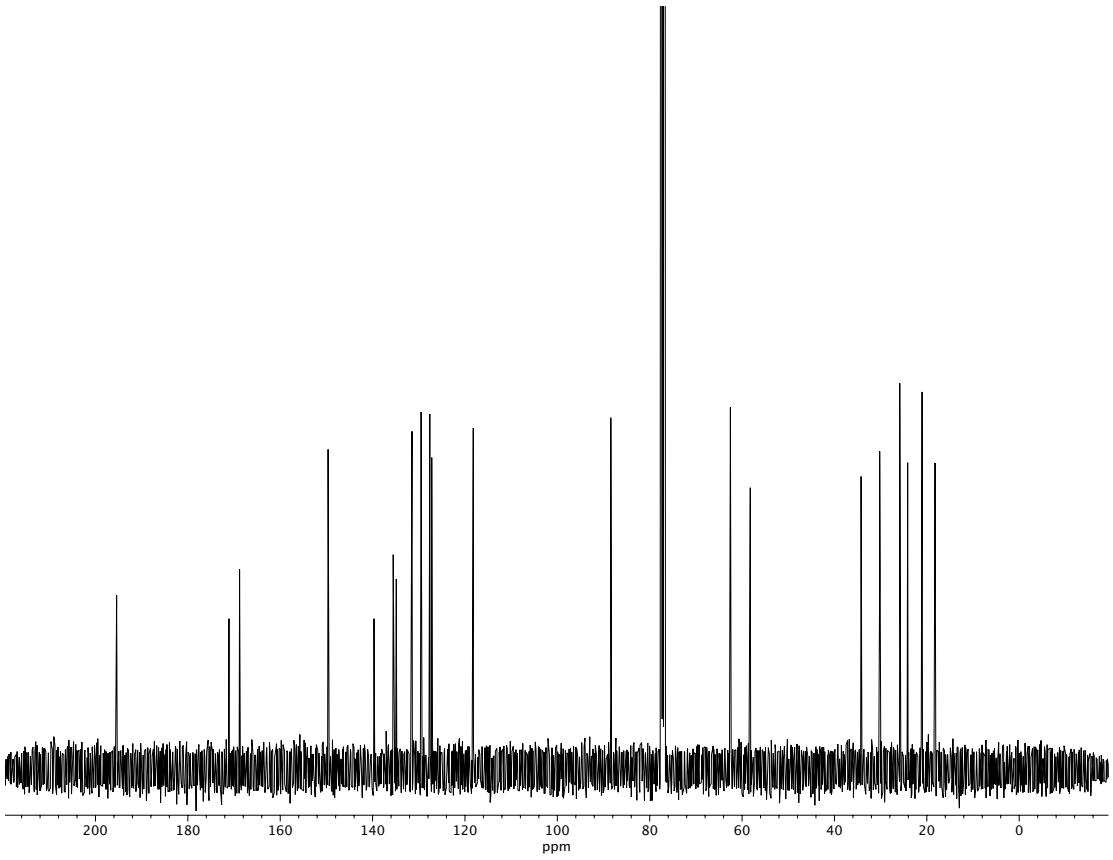

Figure A1.131. *^{13}C NMR (100 MHz, $CDCl_3$) of compound* ***173.***

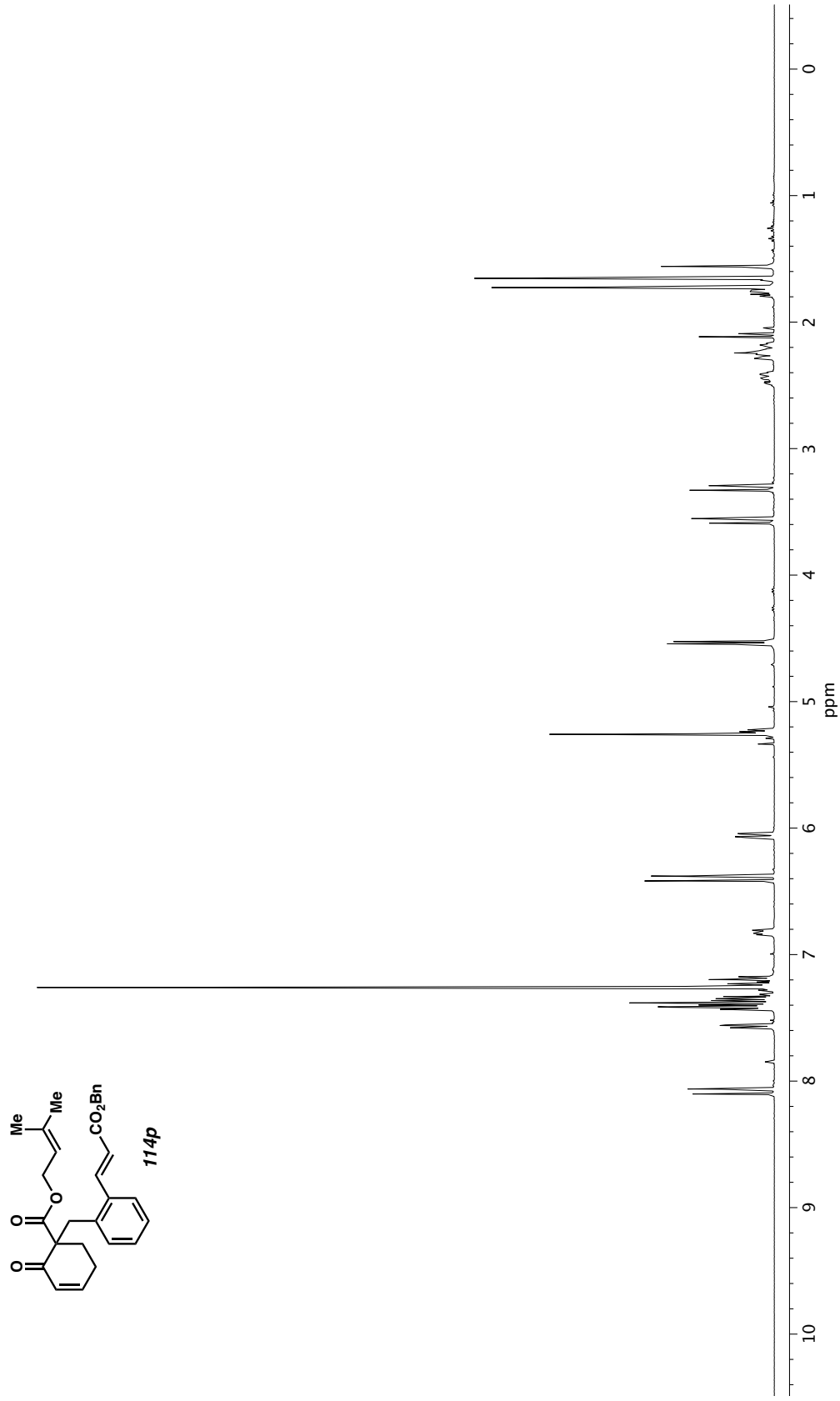

Figure A1.132. *^1H NMR (400 MHz, $CDCl_3$) of compound* ***114p.***

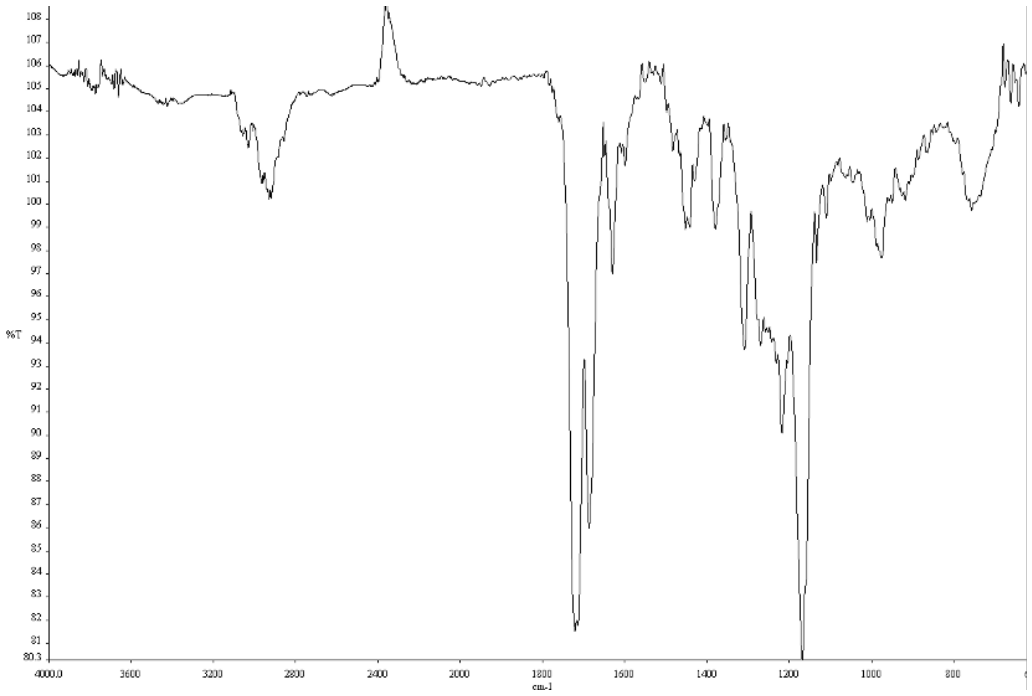

Figure A1.133. *Infrared spectrum (Thin Film, NaCl) of compound* ***114p.***

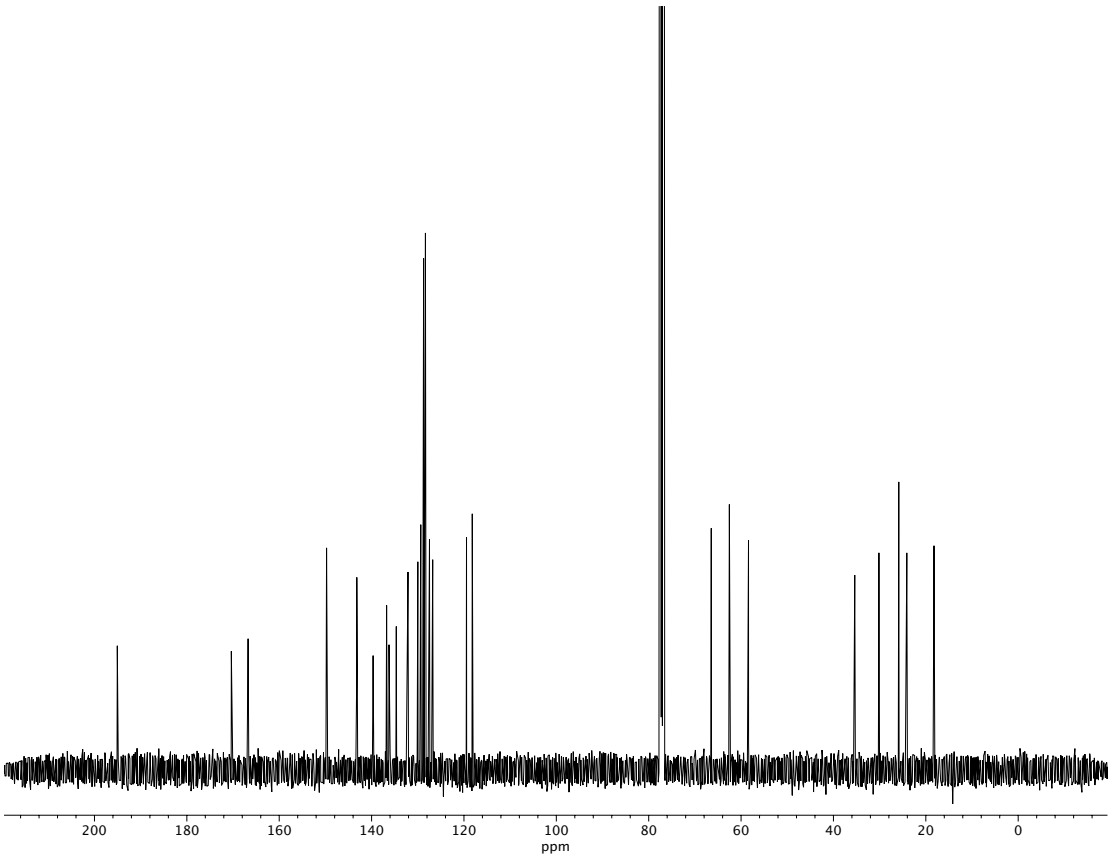

Figure A1.134. *^{13}C NMR (100 MHz, $CDCl_3$) of compound* ***114p.***

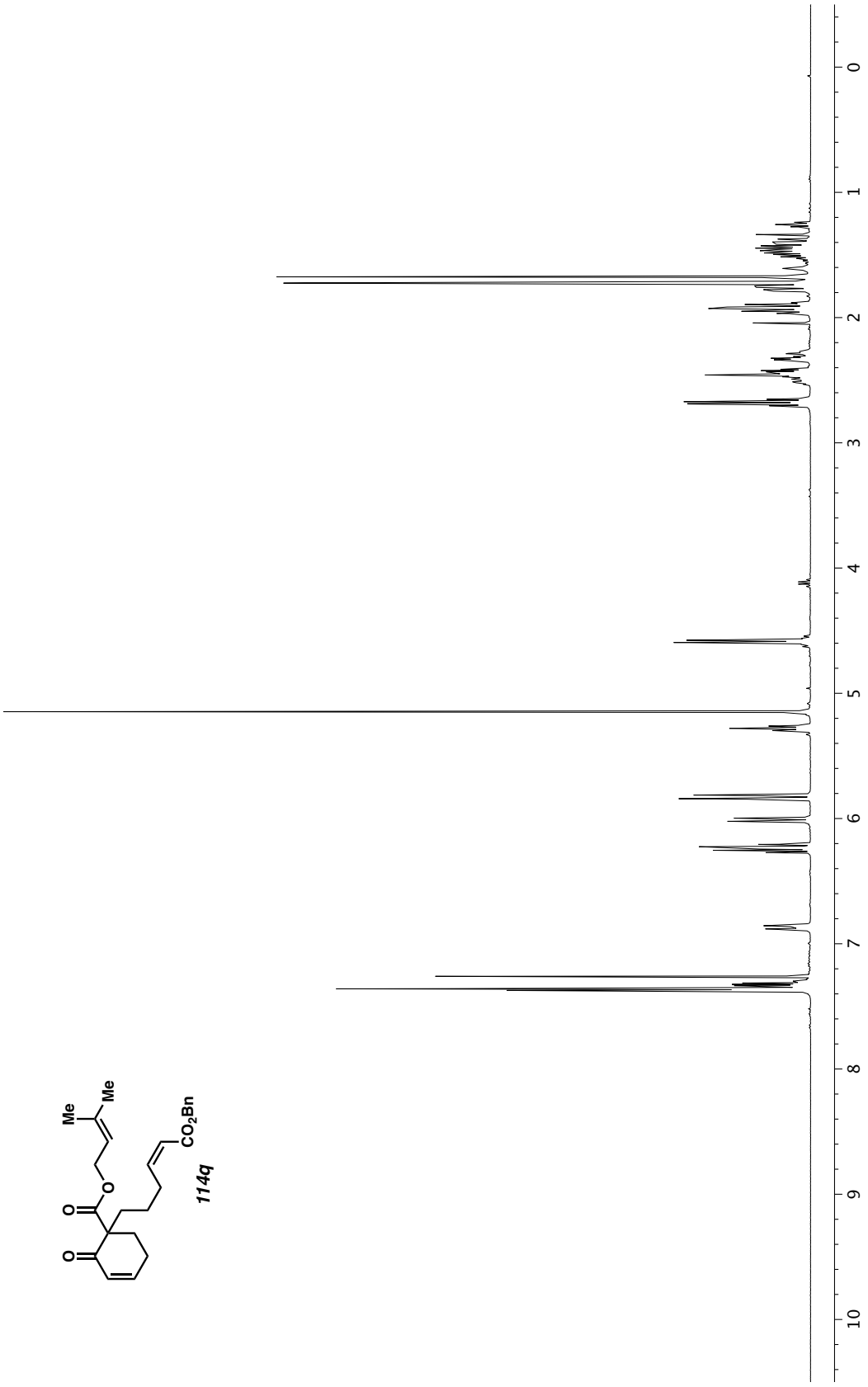

Figure A1.135. *^1H NMR (400 MHz, $CDCl_3$) of compound* ***114q.***

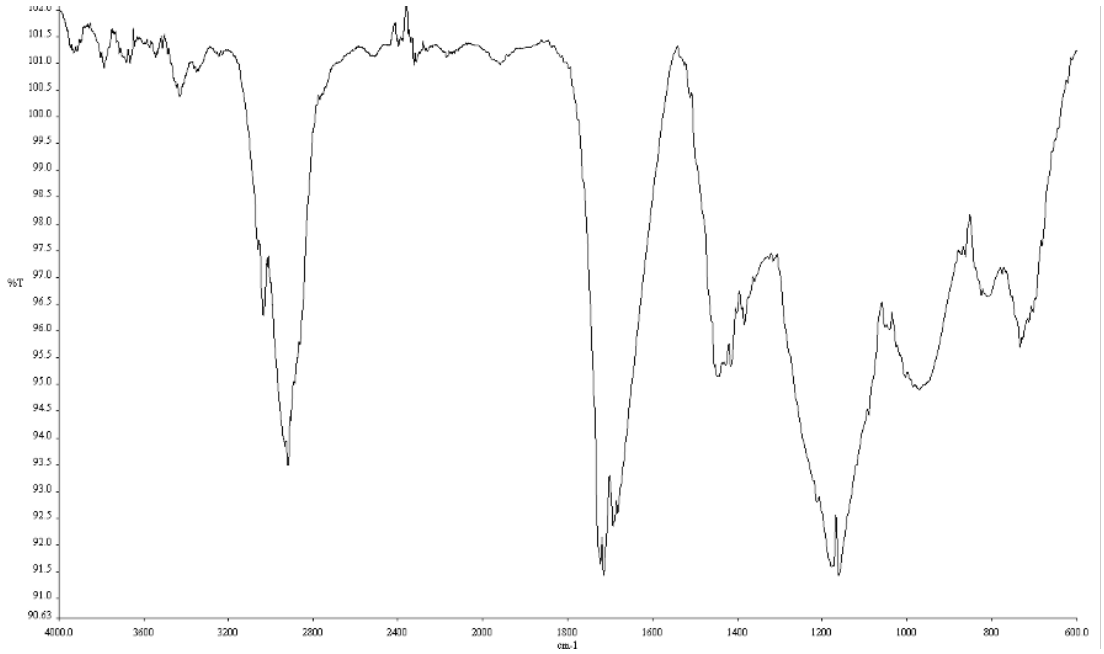

Figure A1.136. *Infrared spectrum (Thin Film, NaCl) of compound* ***114q.***

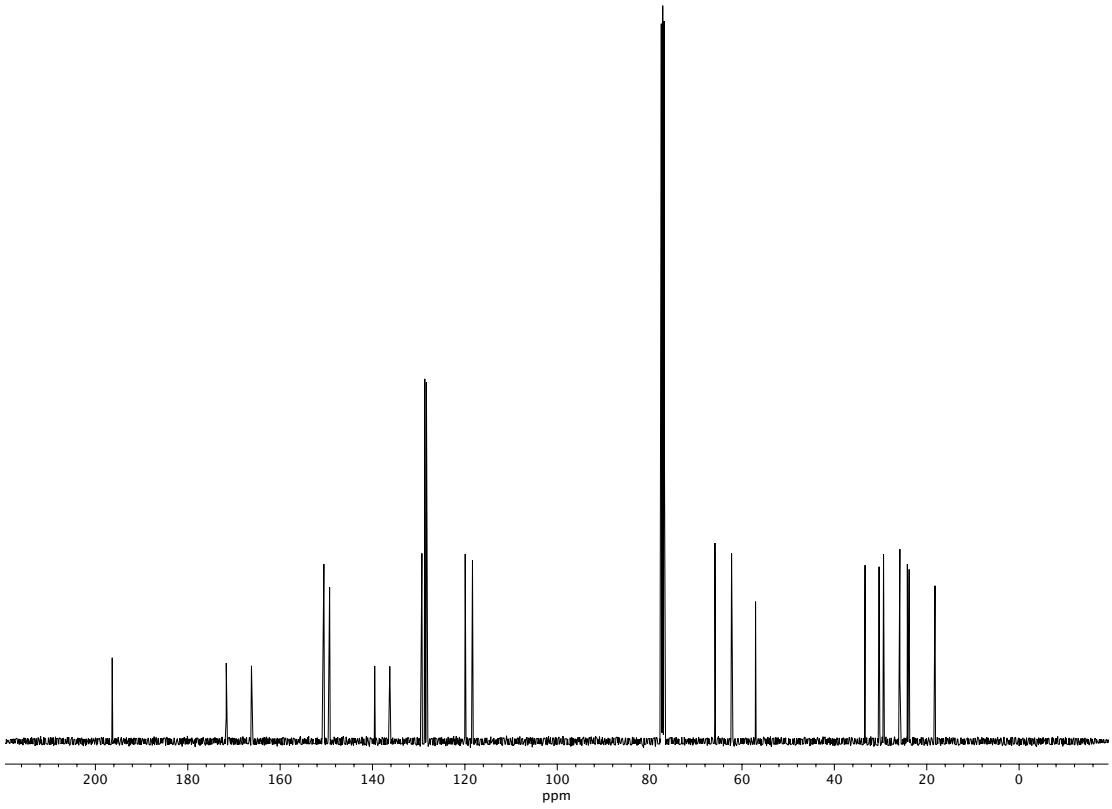

Figure A1.137. *^{13}C NMR (100 MHz, $CDCl_3$) of compound* ***114q.***

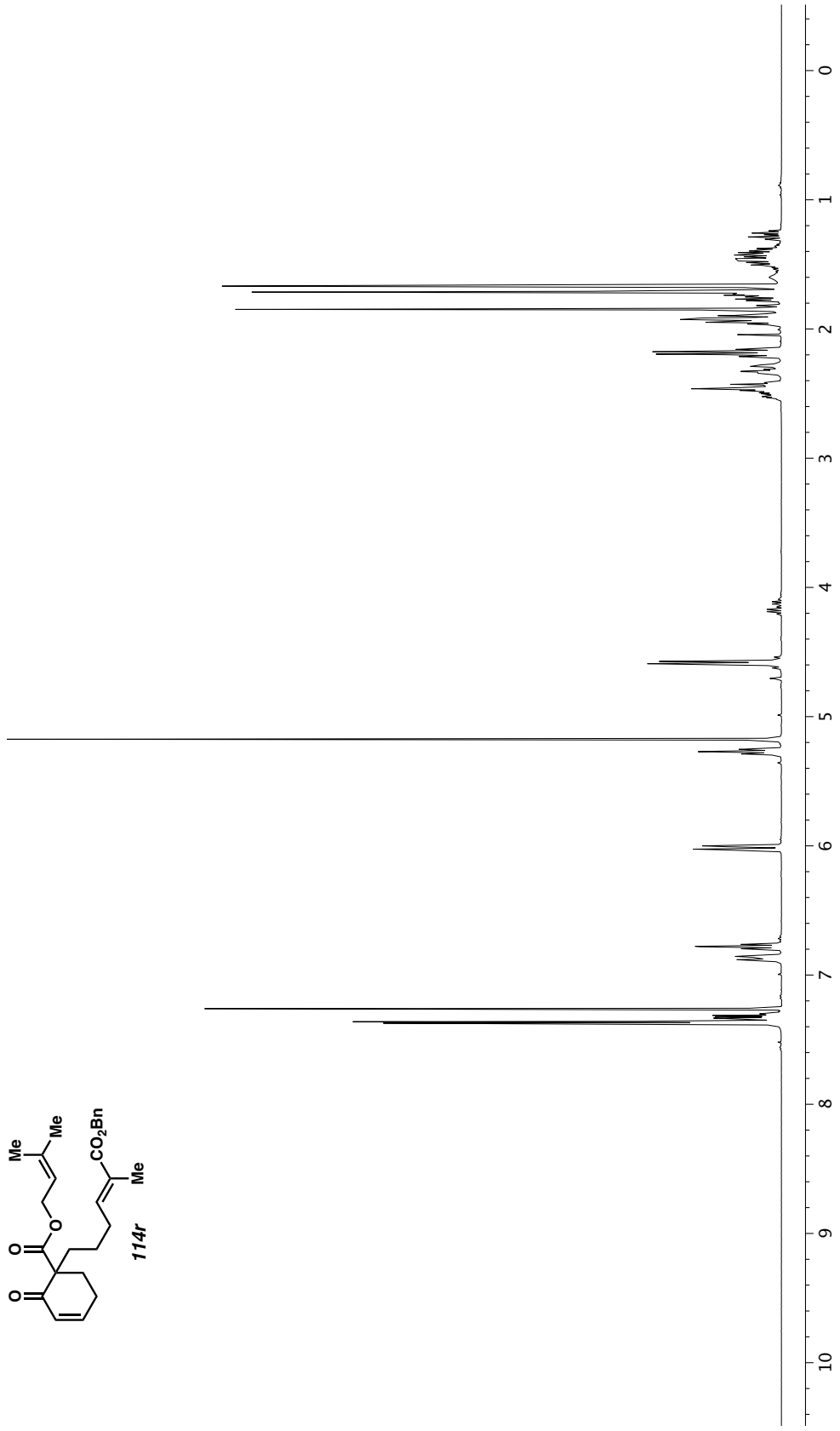

Figure A1.138. *^{1}H NMR (400 MHz, $CDCl_3$) of compound* ***114r.***

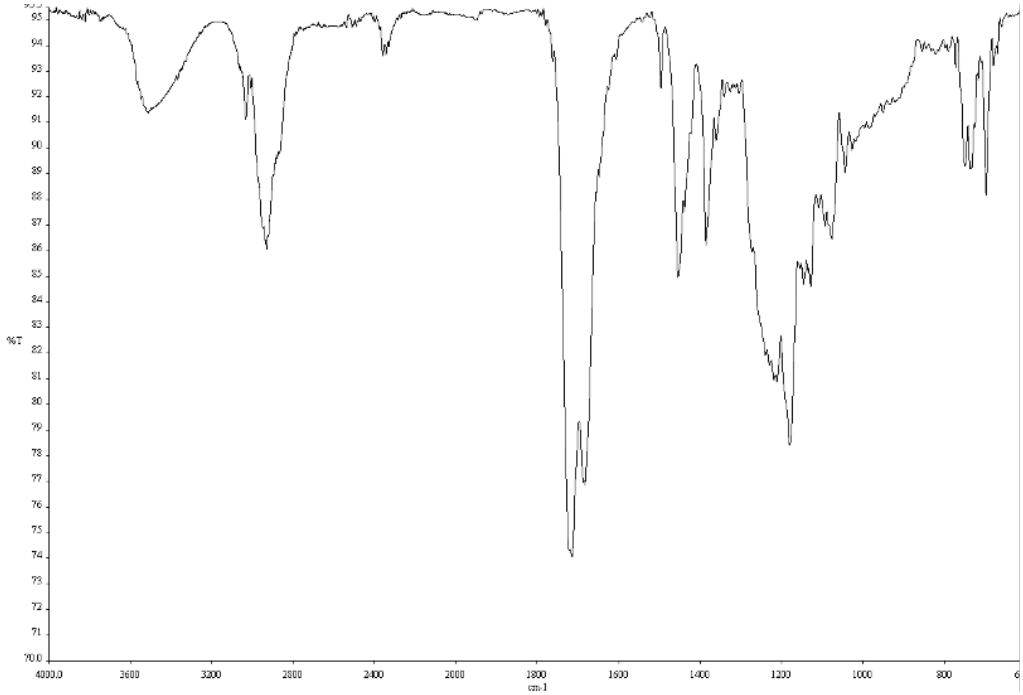

Figure A1.139. *Infrared spectrum (Thin Film, NaCl) of compound* ***114r.***

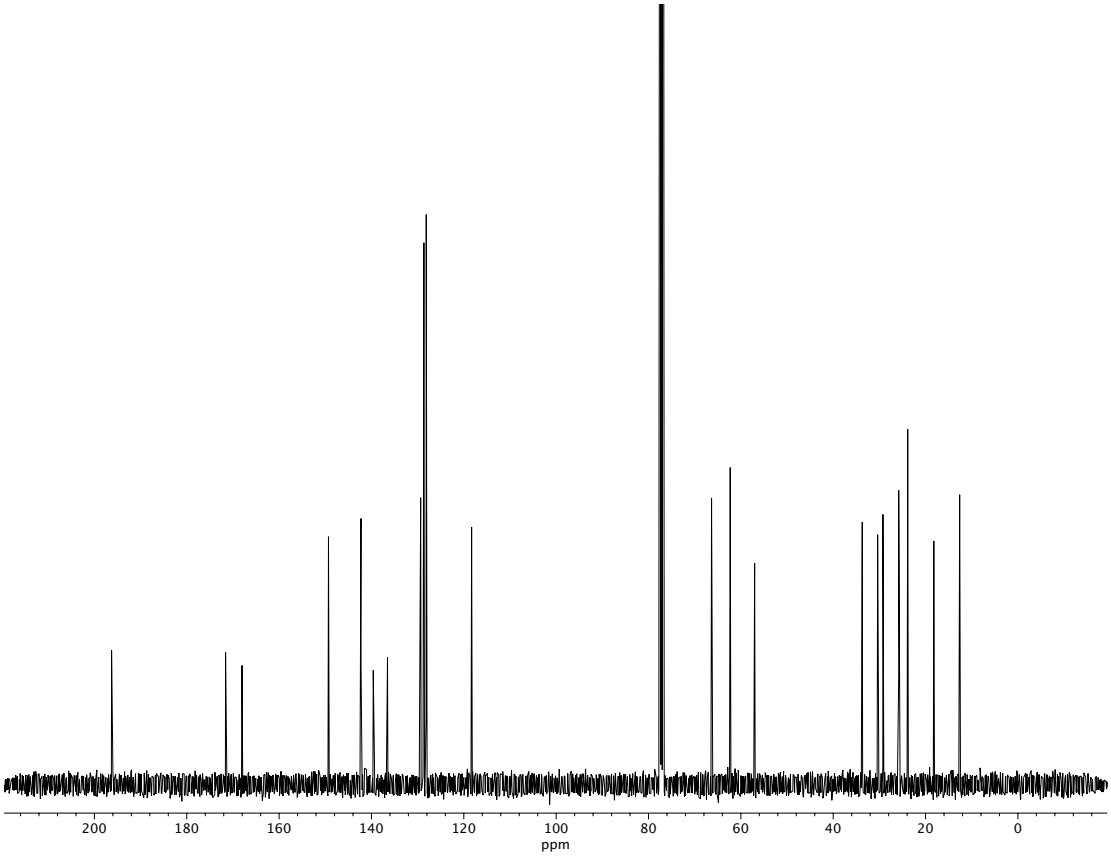

Figure A1.140. *^{13}C NMR (100 MHz, $CDCl_3$) of compound* ***114r.***

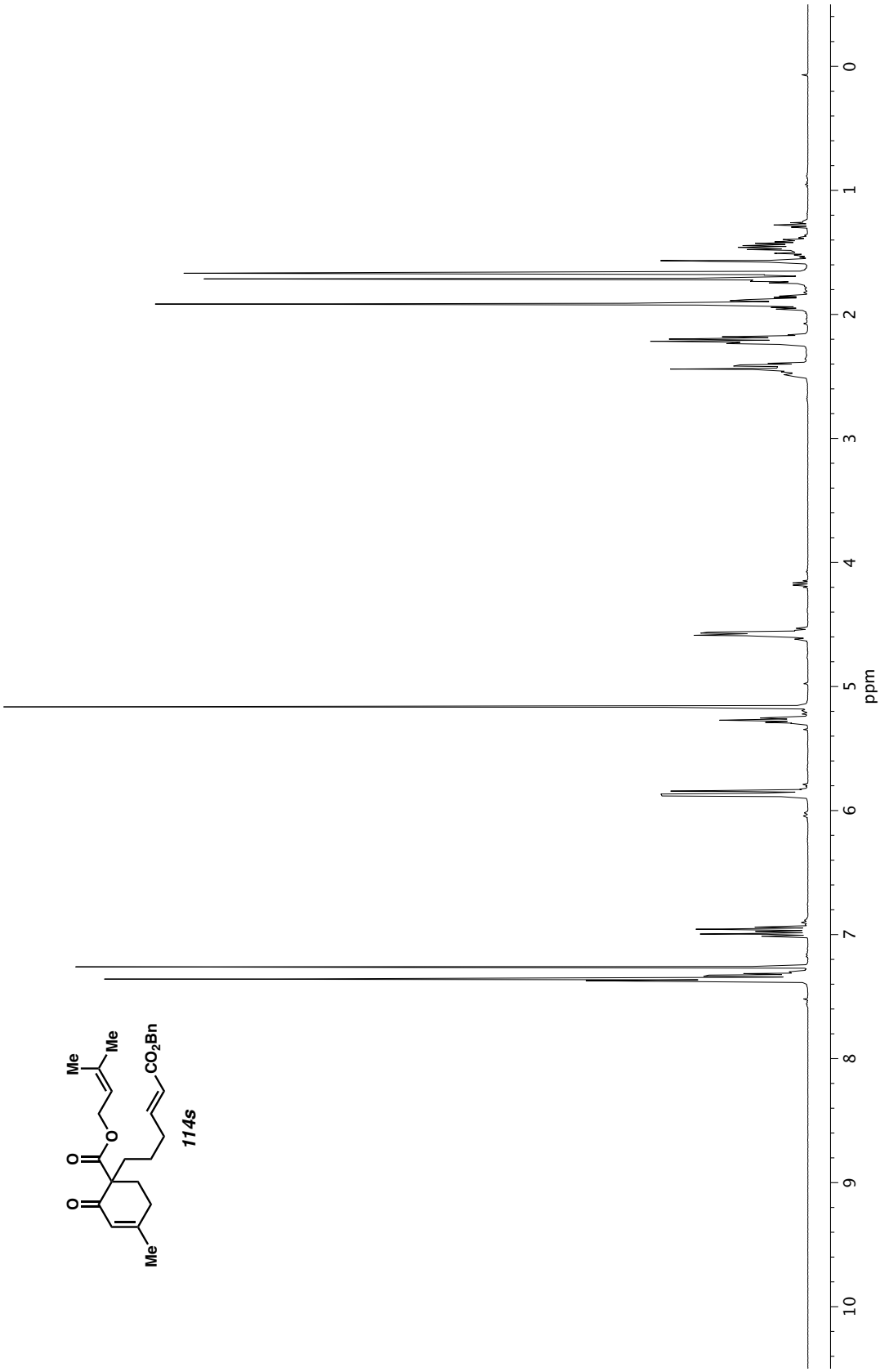

Figure A1.141. *^1H NMR (400 MHz, $CDCl_3$) of compound* ***114s.***

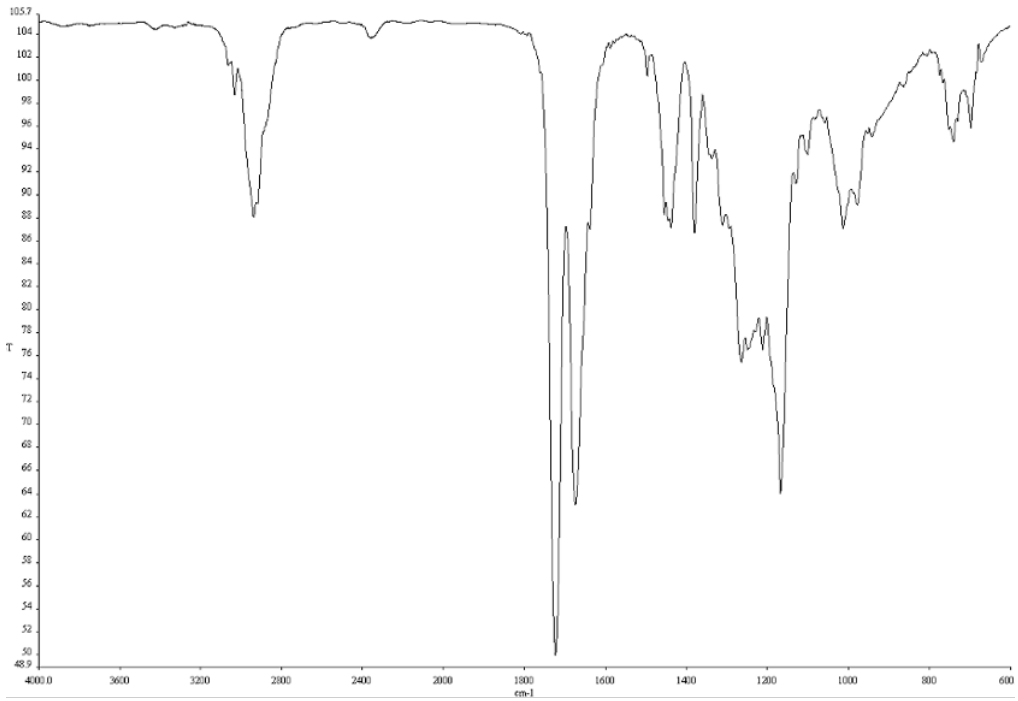

Figure A1.142. *Infrared spectrum (Thin Film, NaCl) of compound* ***114s.***

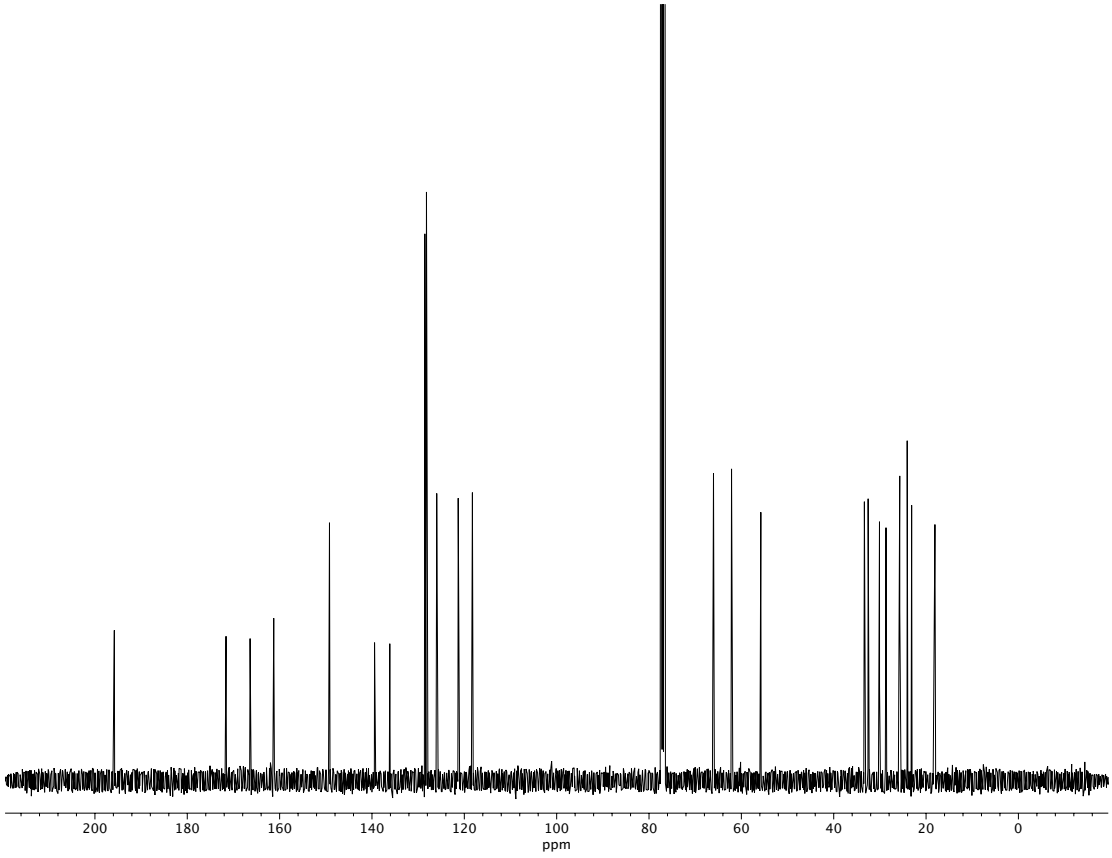

Figure A1.143. *^{13}C NMR (100 MHz, $CDCl_3$) of compound* ***114s.***

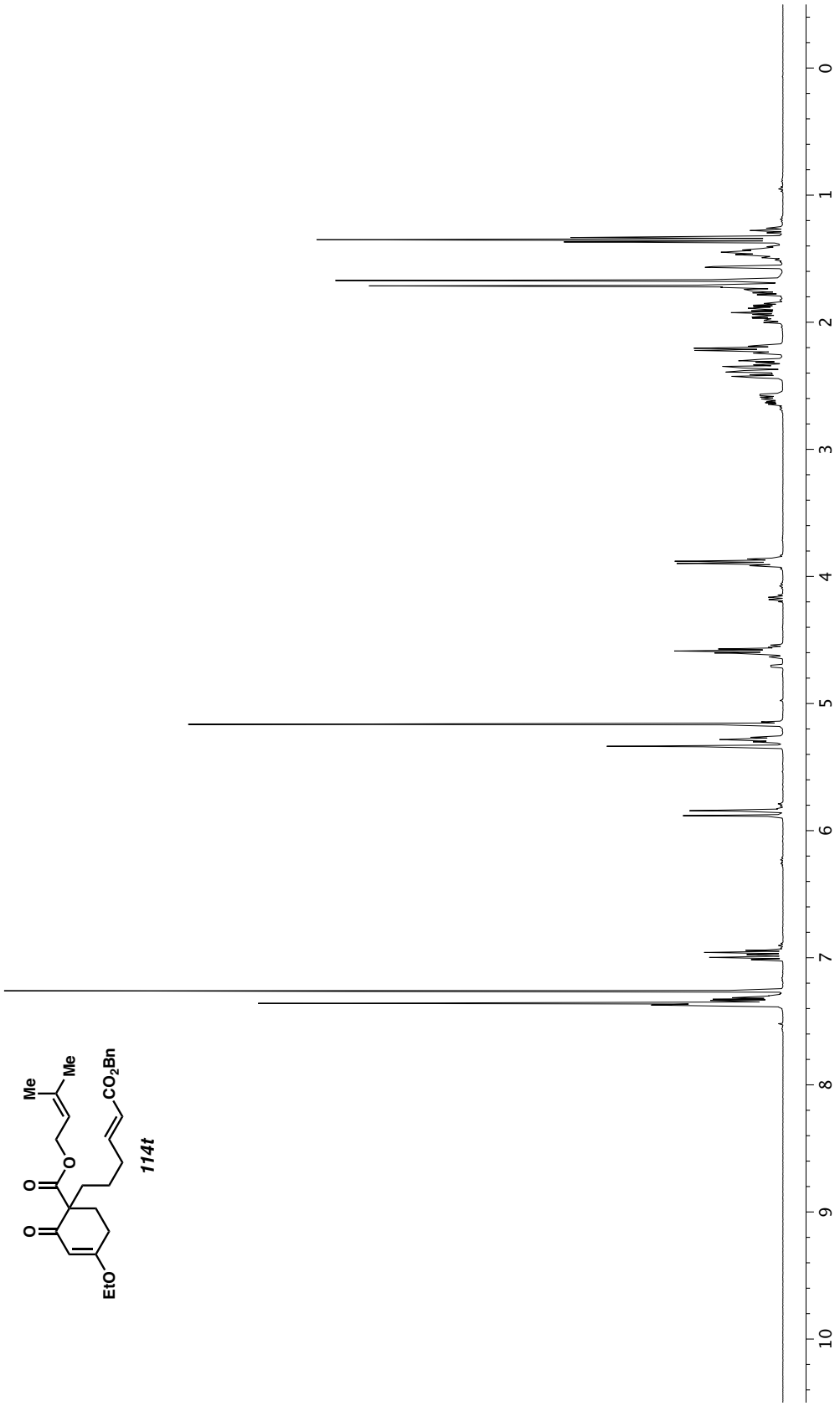

Figure A1.144. *^1H NMR (400 MHz, $CDCl_3$) of compound* ***114t.***

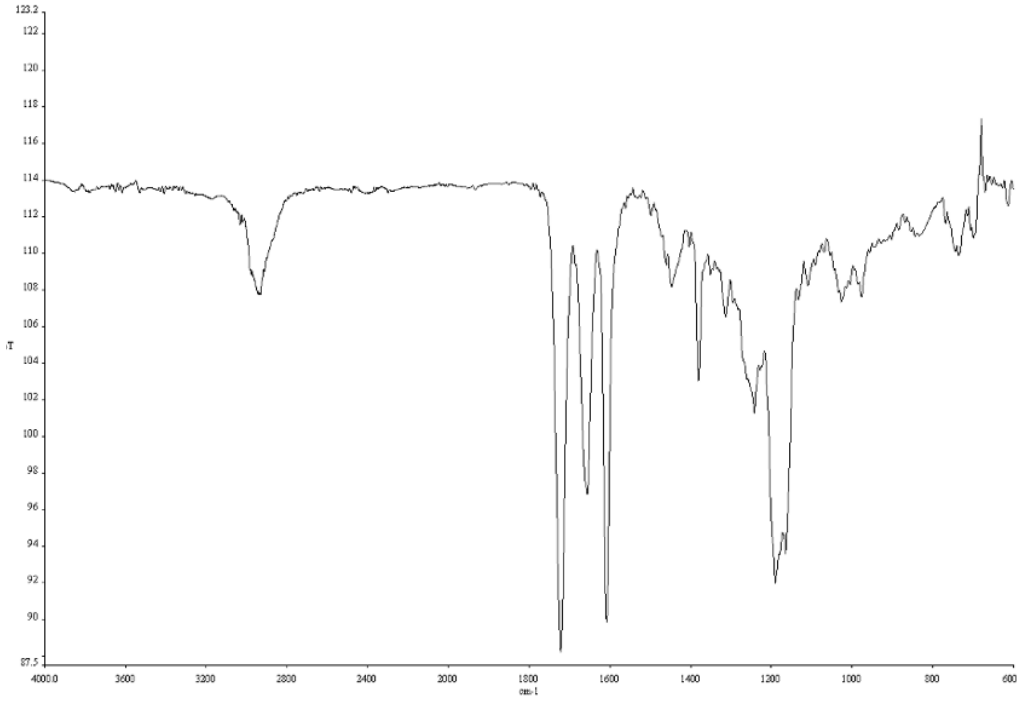

Figure A1.145. *Infrared spectrum (Thin Film, NaCl) of compound* ***114t.***

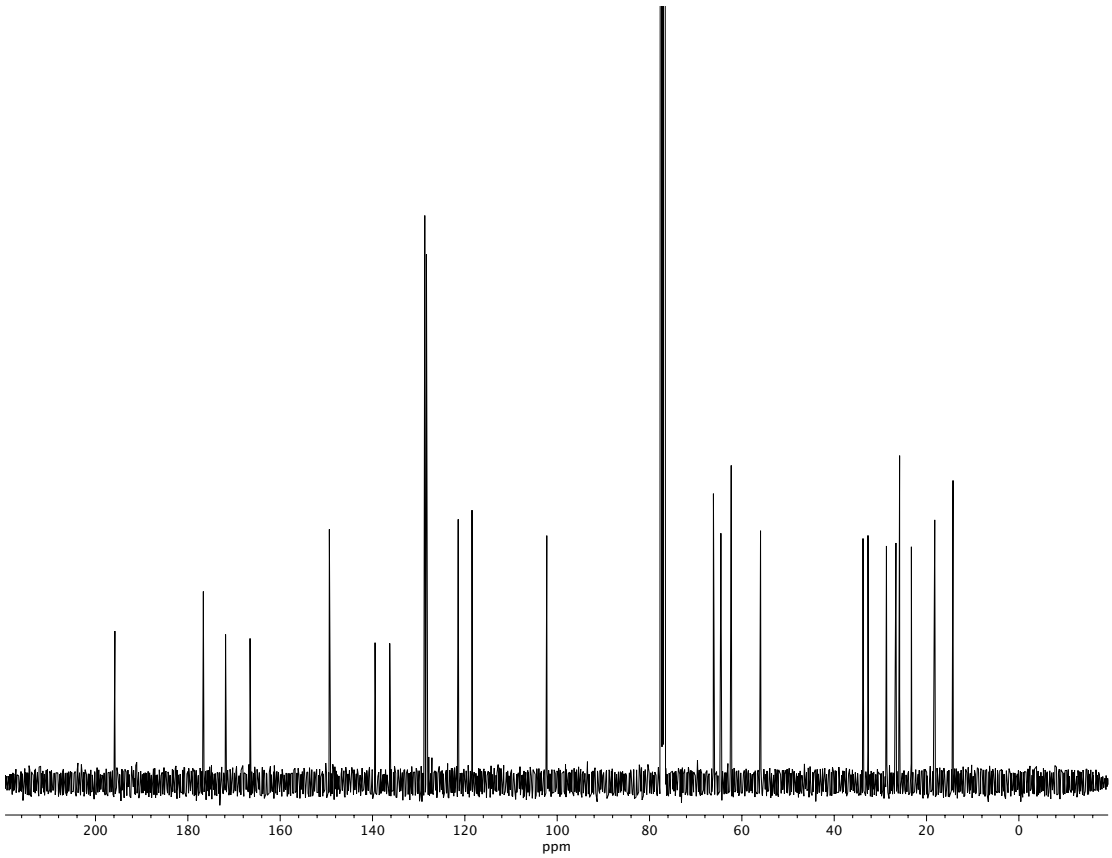

Figure A1.146. *^{13}C NMR (100 MHz, $CDCl_3$) of compound* ***114t.***

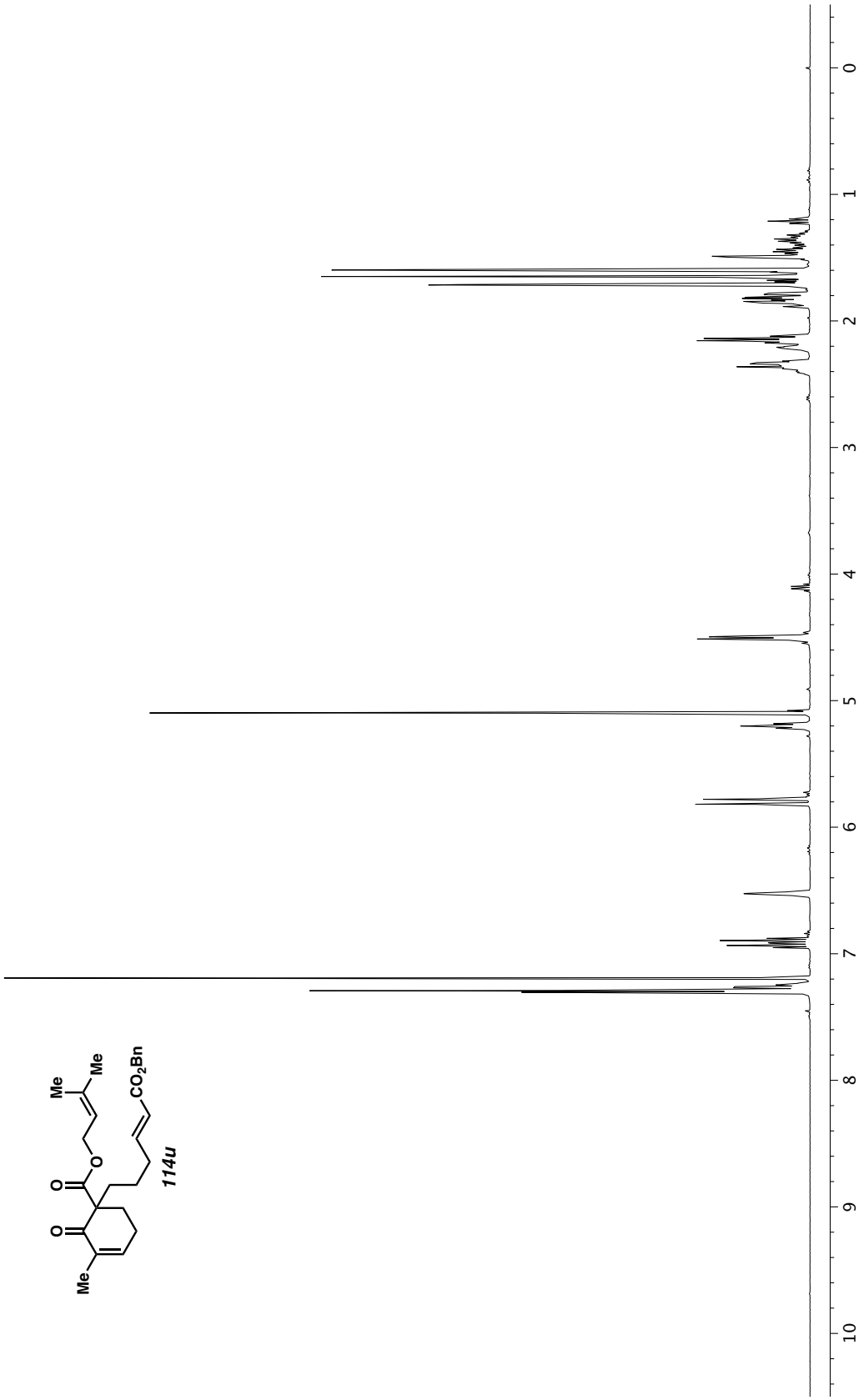

Figure A1.147. *^1H NMR (400 MHz, $CDCl_3$) of compound* ***114u.***

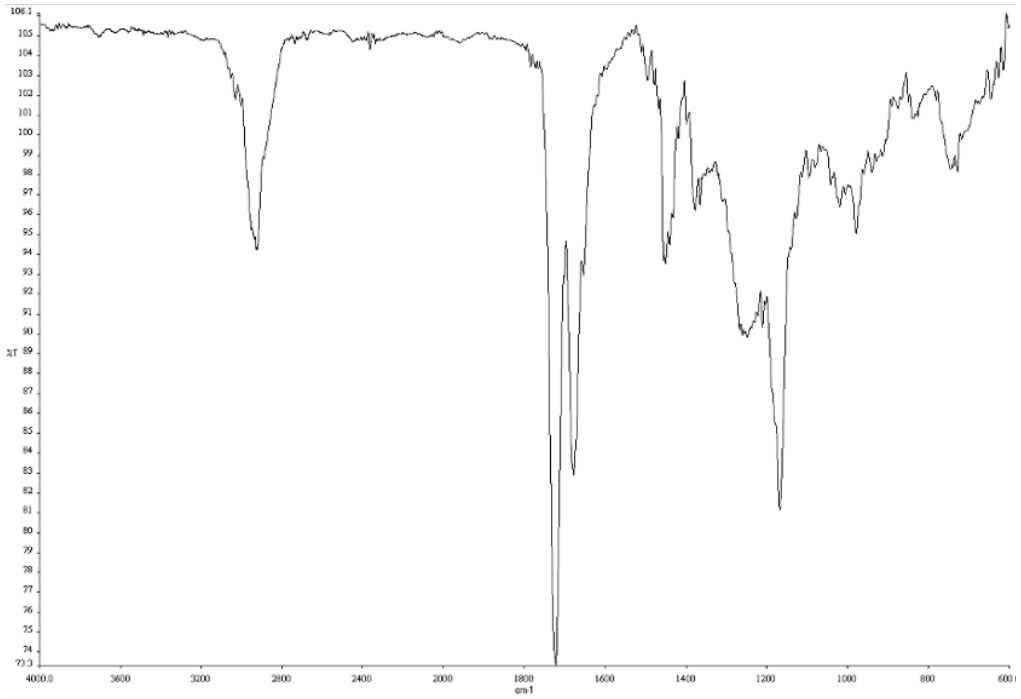

Figure A1.148. *Infrared spectrum (Thin Film, NaCl) of compound* ***114u.***

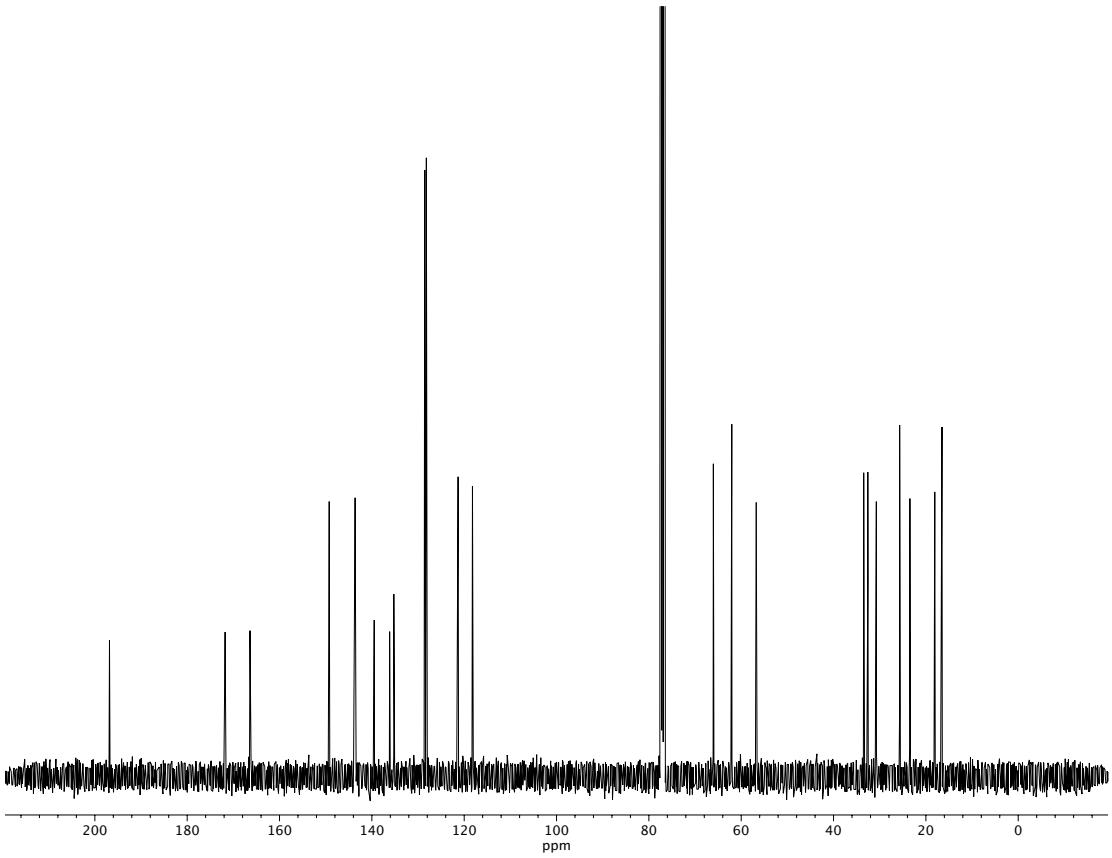

Figure A1.149. *^{13}C NMR (100 MHz, $CDCl_3$) of compound* ***114u.***

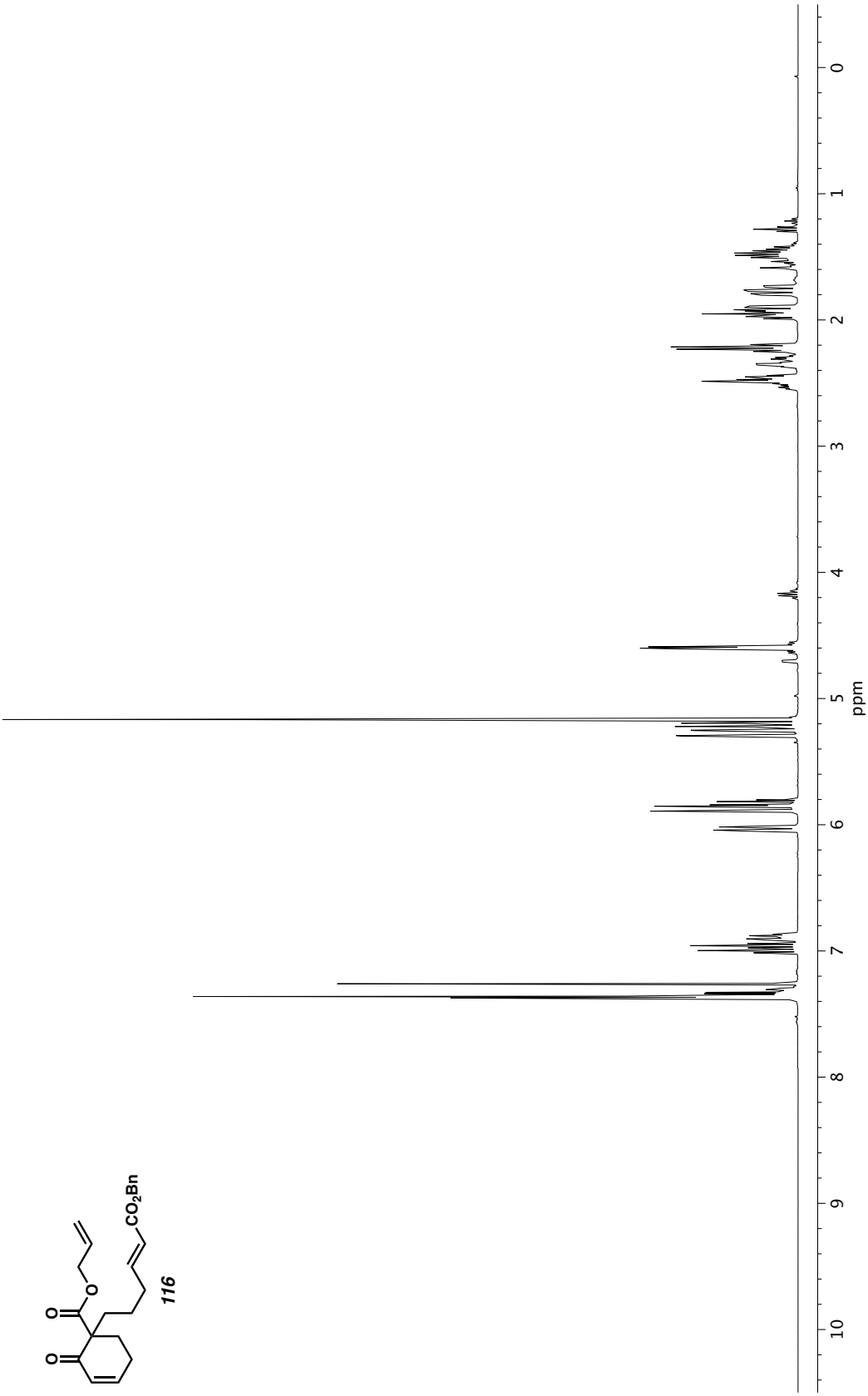

Figure A1.150. *^{1}H NMR (400 MHz, $CDCl_3$) of compound* ***116.***

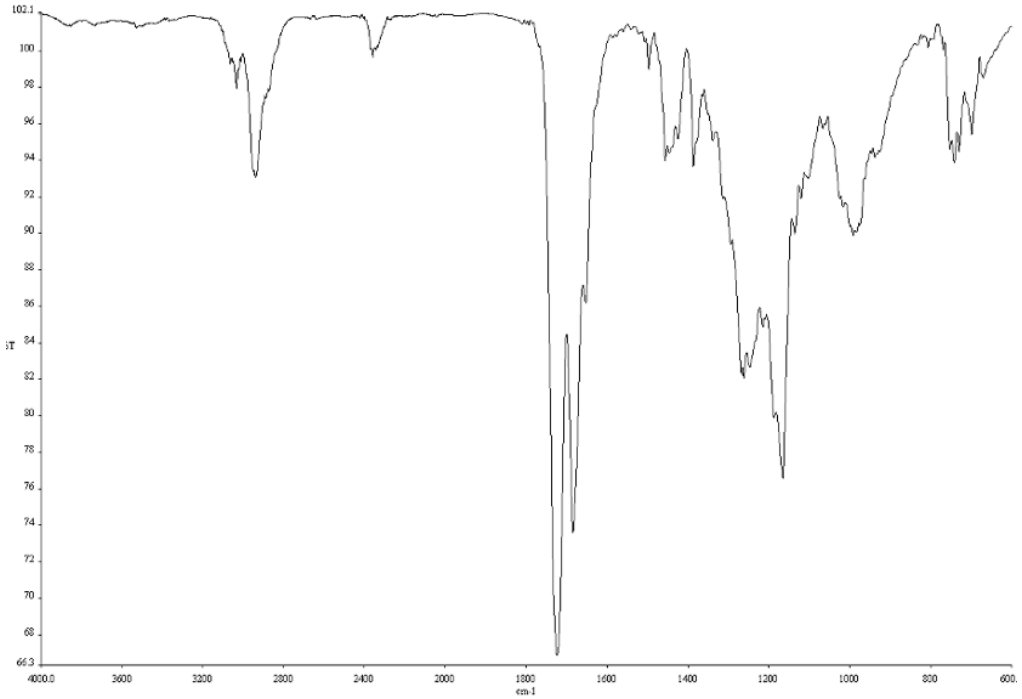

Figure A1.151. *Infrared spectrum (Thin Film, NaCl) of compound* ***116.***

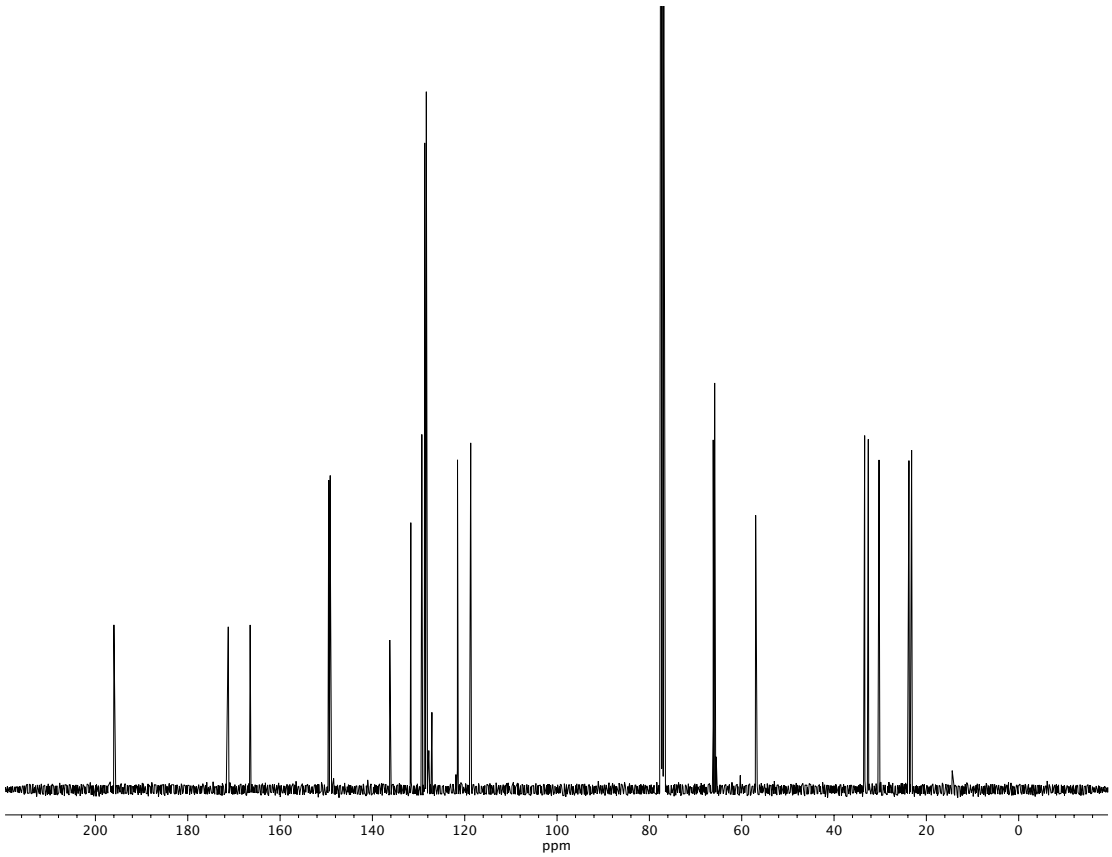

Figure A1.152. *^{13}C NMR (100 MHz, $CDCl_3$) of compound* ***116.***

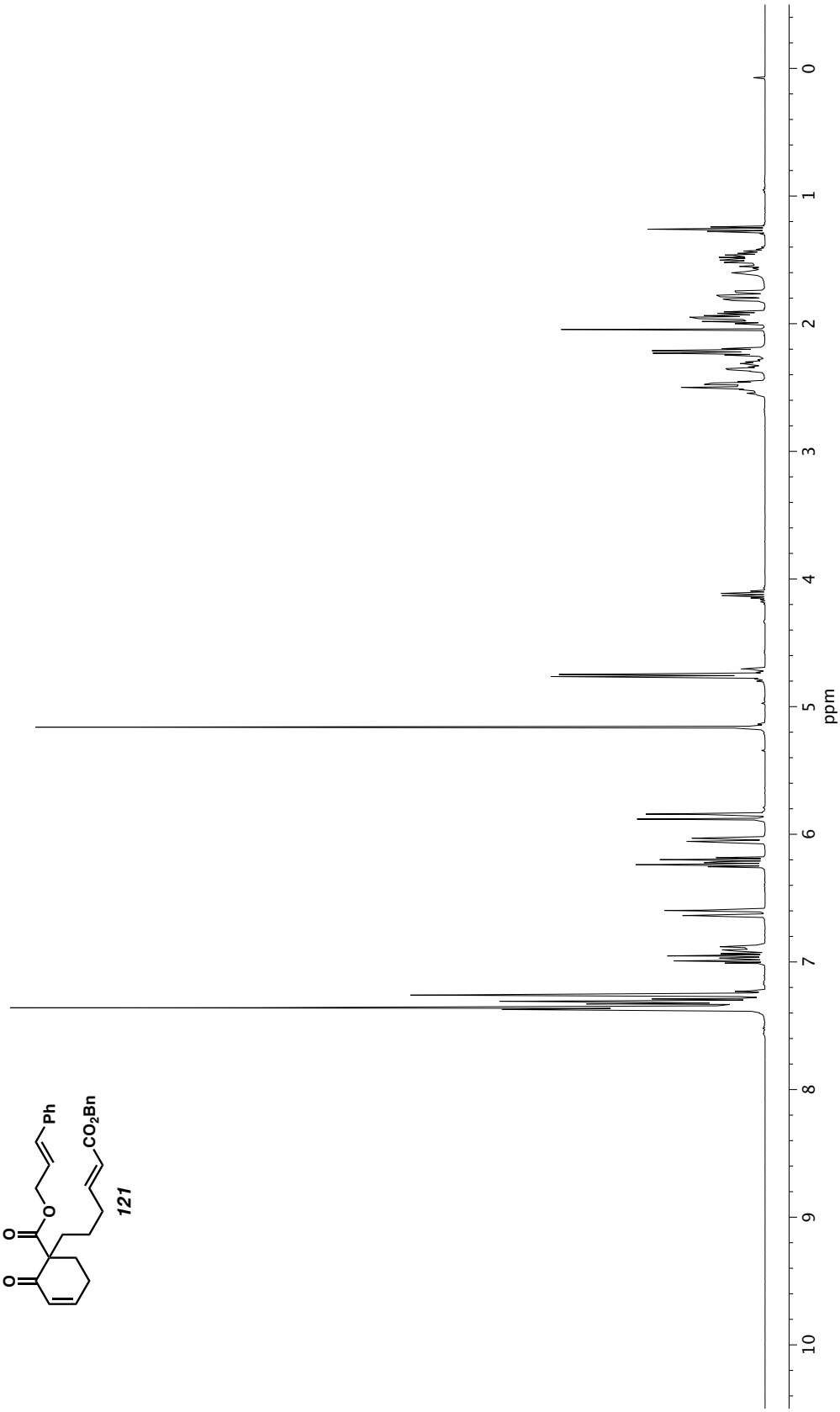

Figure A1.153. *^1H NMR (400 MHz, $CDCl_3$) of compound* ***121.***

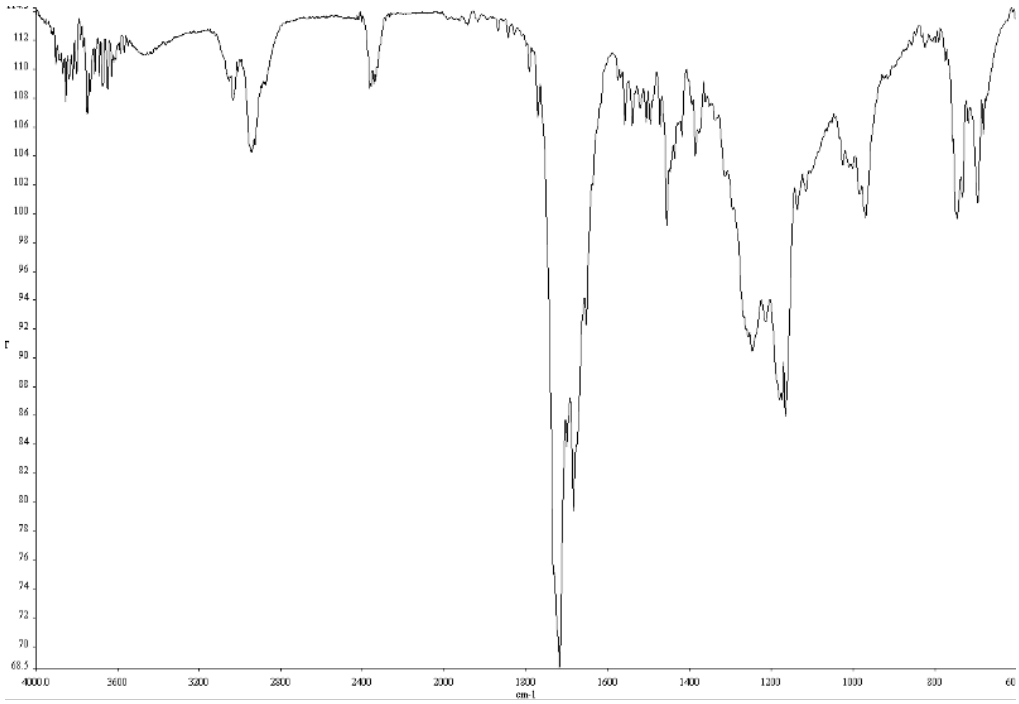

Figure A1.154. *Infrared spectrum (Thin Film, NaCl) of compound* ***121.***

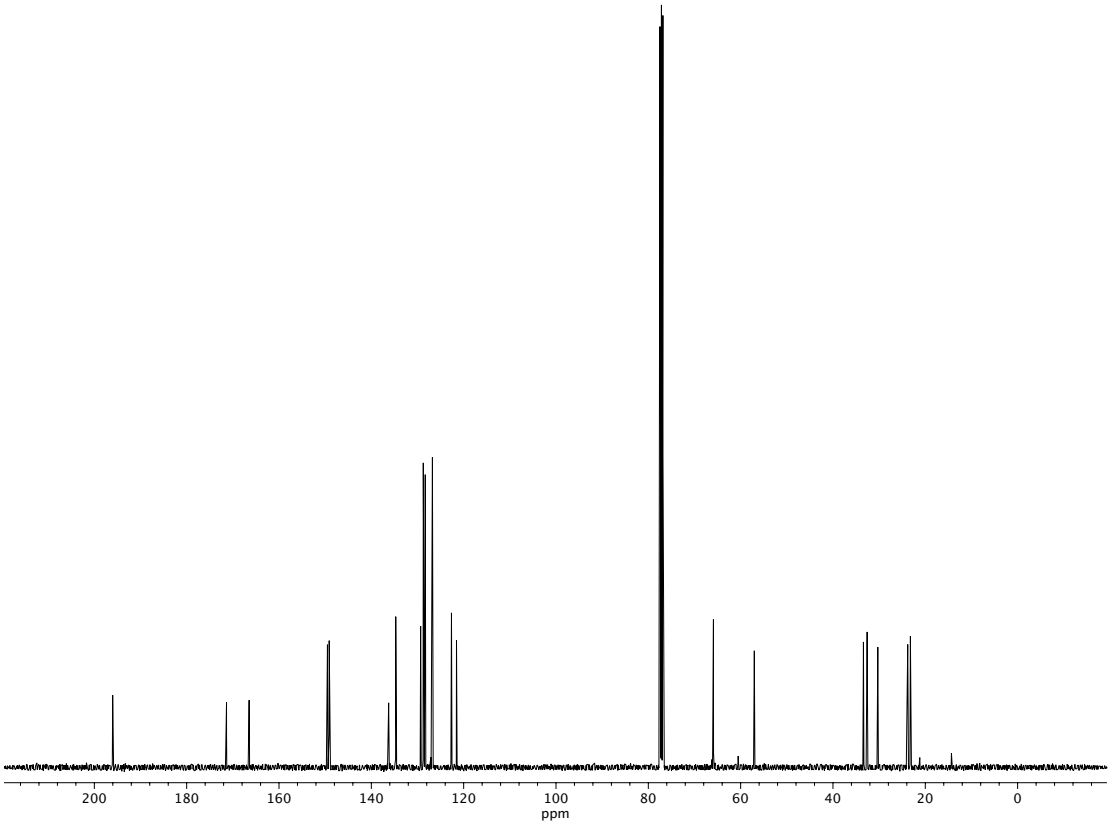

Figure A1.155. *^{13}C NMR (100 MHz, $CDCl_3$) of compound* ***121.***

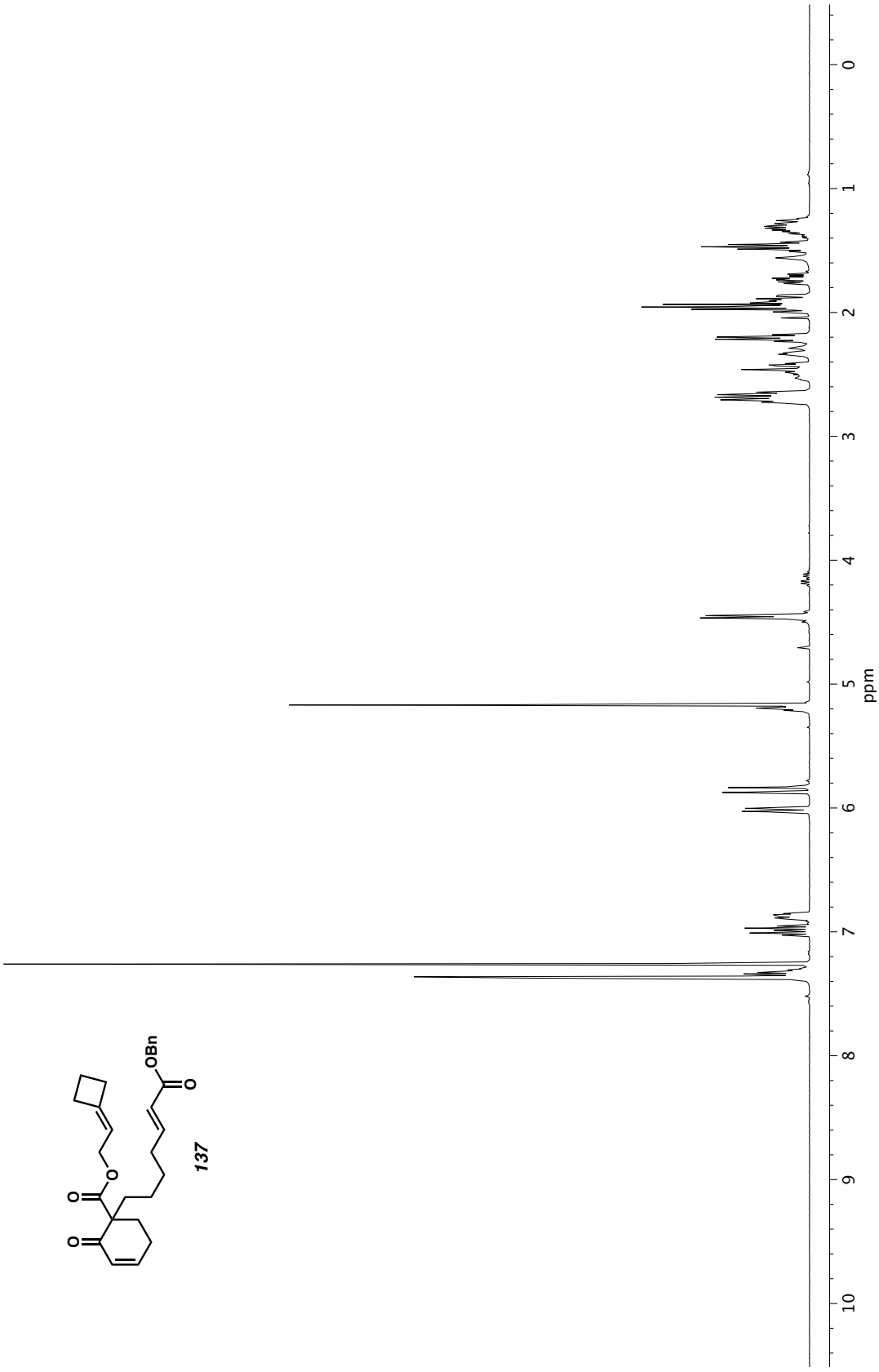

Figure A1.156. *^1H NMR (400 MHz, $CDCl_3$) of compound* ***137.***

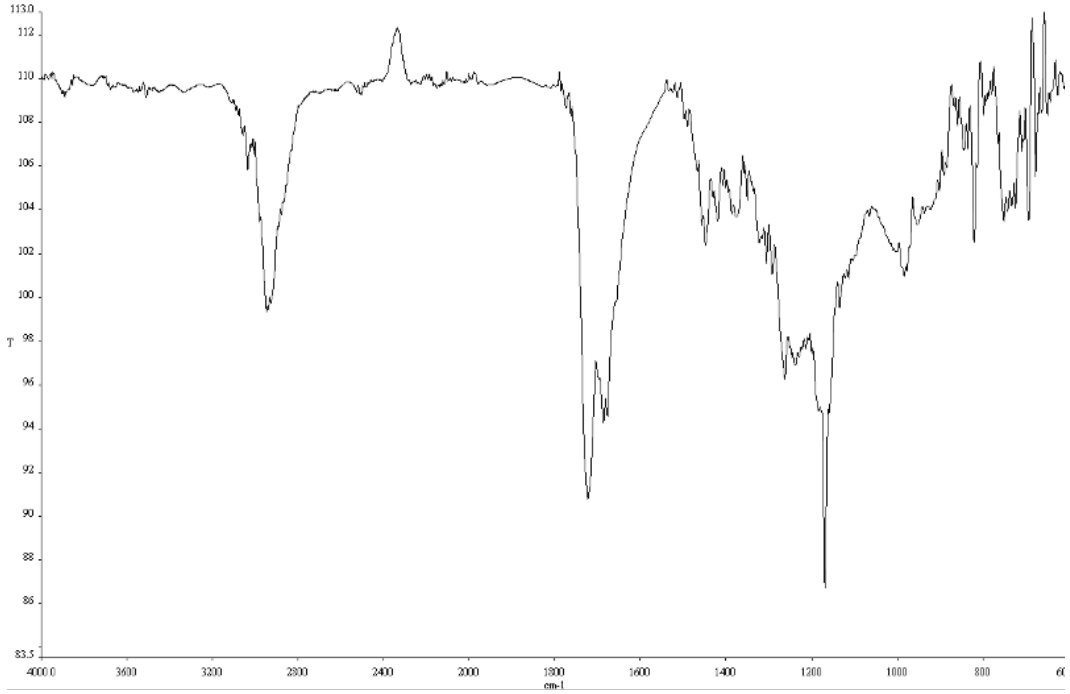

Figure A1.157. *Infrared spectrum (Thin Film, NaCl) of compound* ***137.***

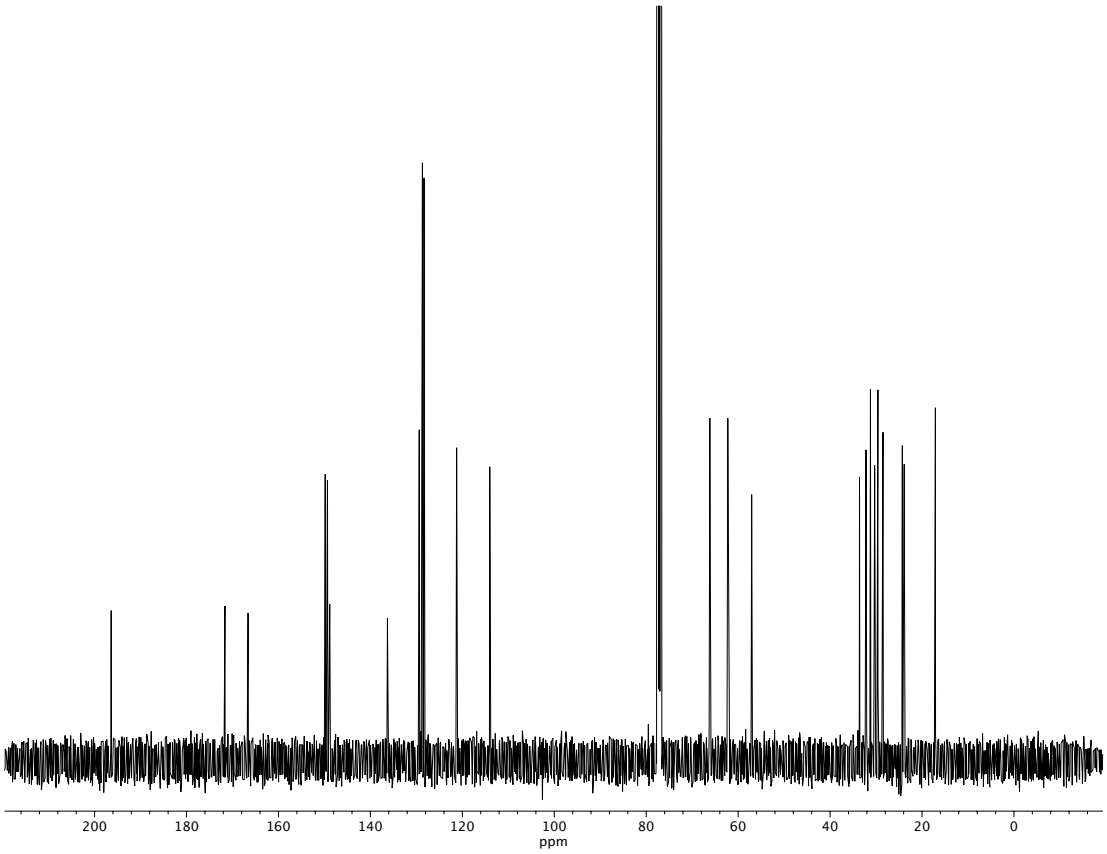

Figure A1.158. *^{13}C NMR (100 MHz, $CDCl_3$) of compound* ***137.***

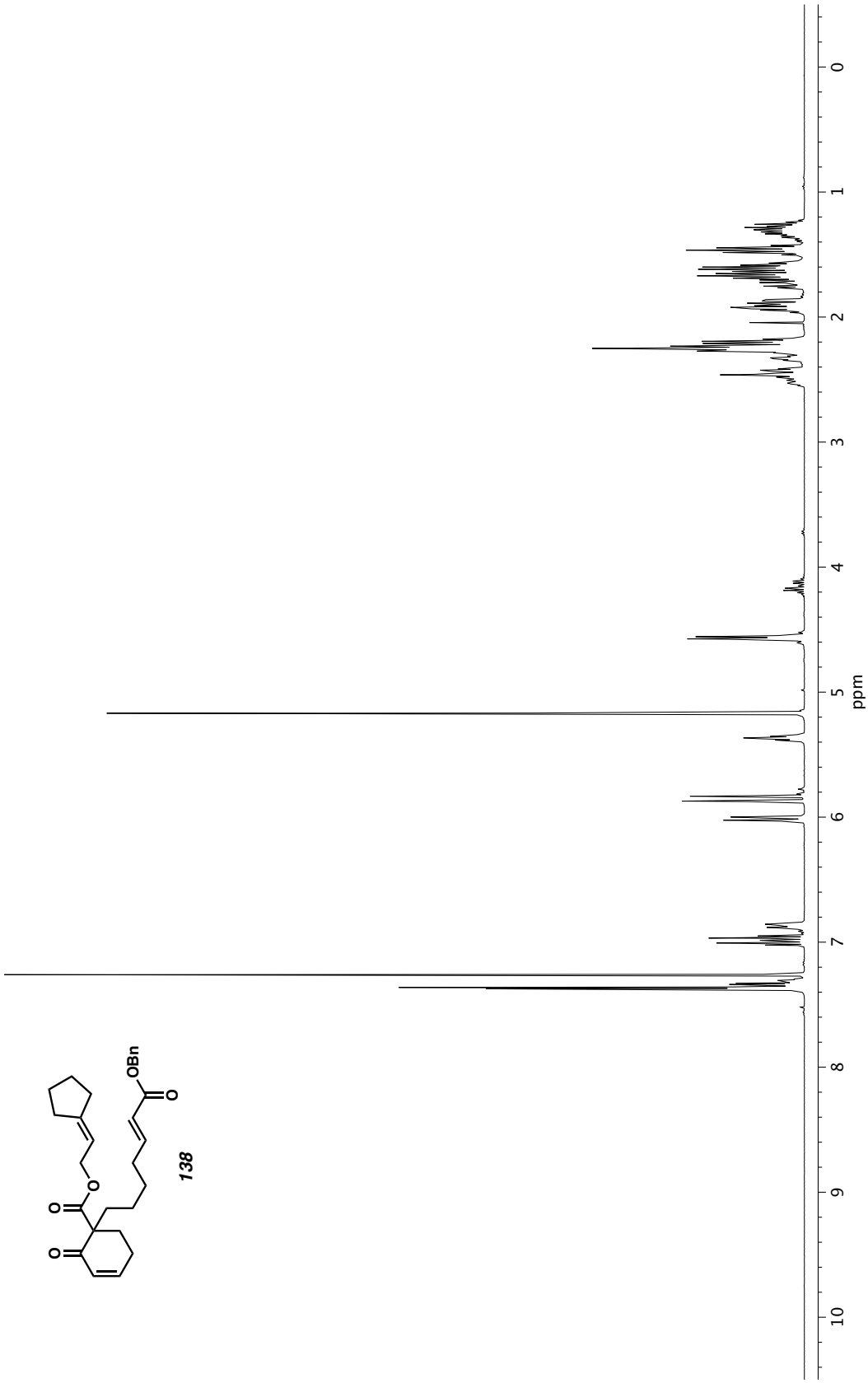

Figure A1.159. *^1H NMR (400 MHz, $CDCl_3$) of compound* ***138.***

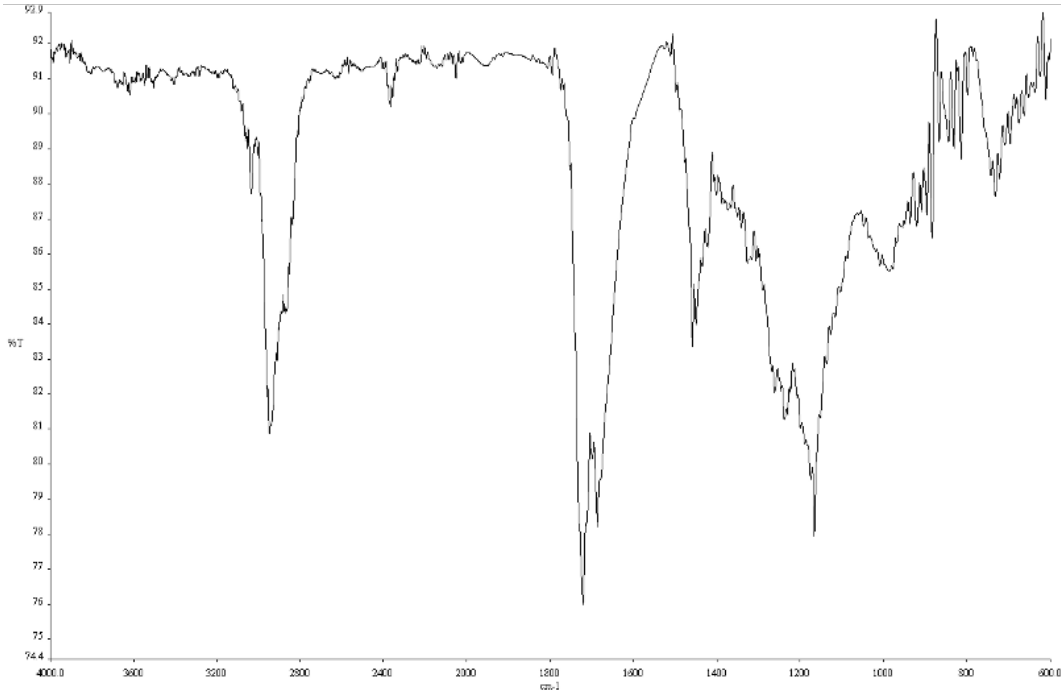

Figure A1.160. *Infrared spectrum (Thin Film, NaCl) of compound* ***138.***

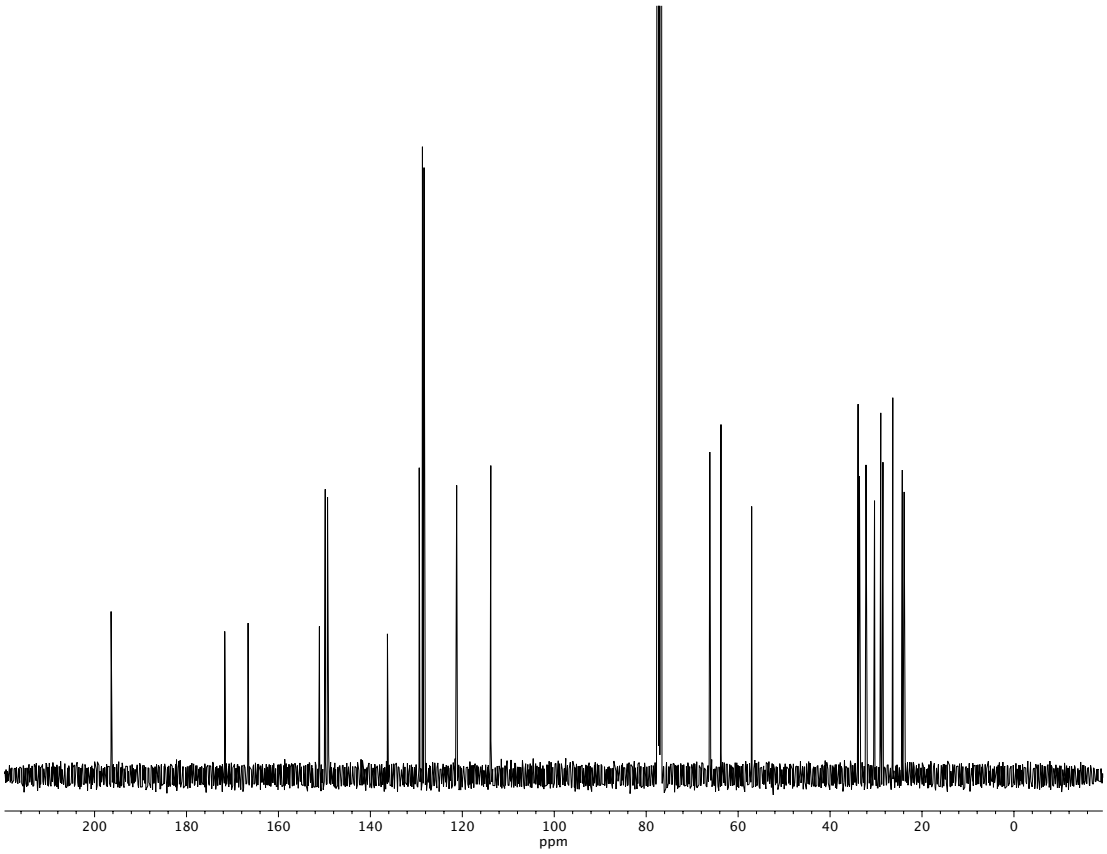

Figure A1.161. *^{13}C NMR (100 MHz, $CDCl_3$) of compound* ***138.***

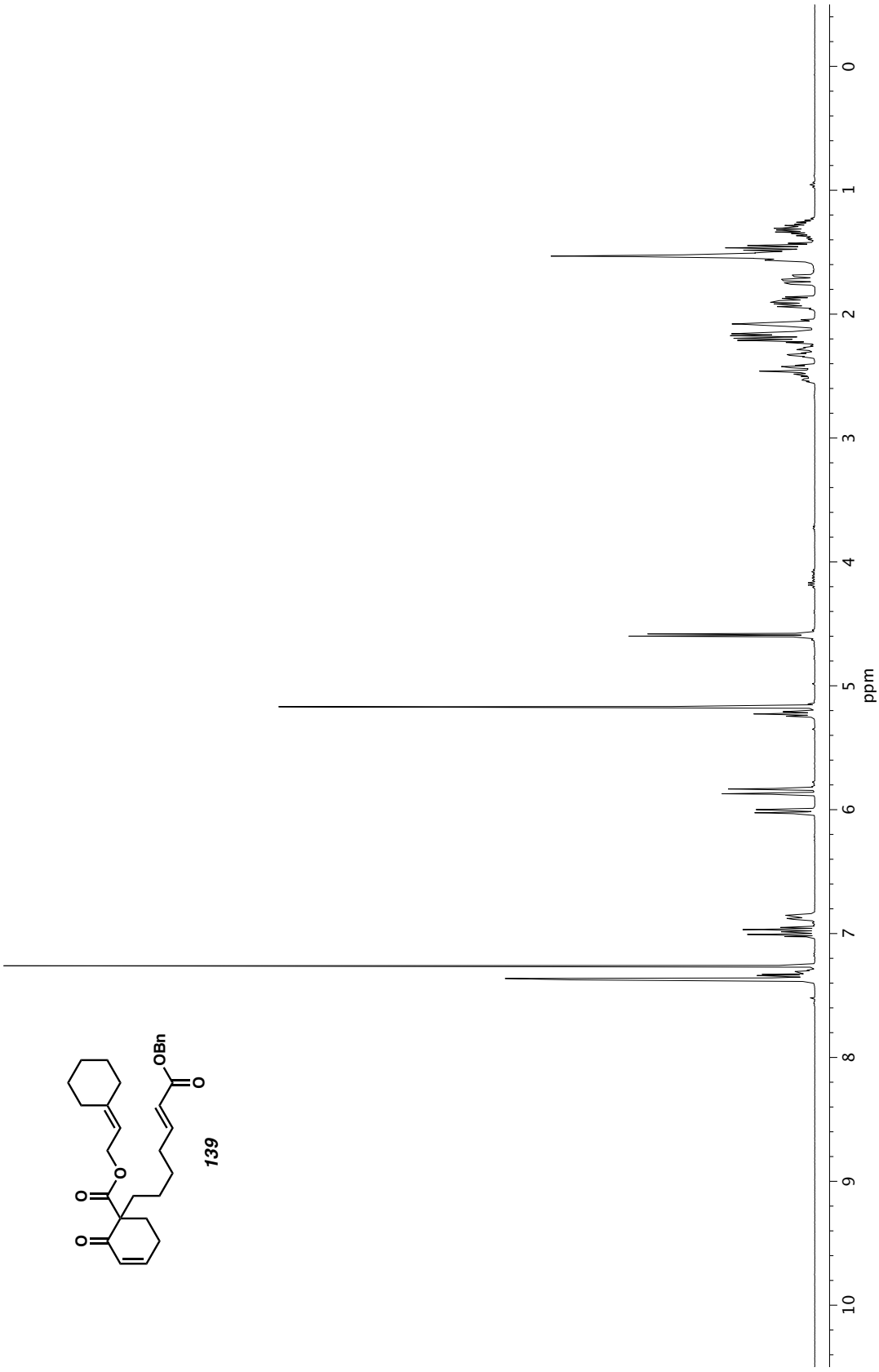

Figure A1.162. *^1H NMR (400 MHz, $CDCl_3$) of compound* ***139.***

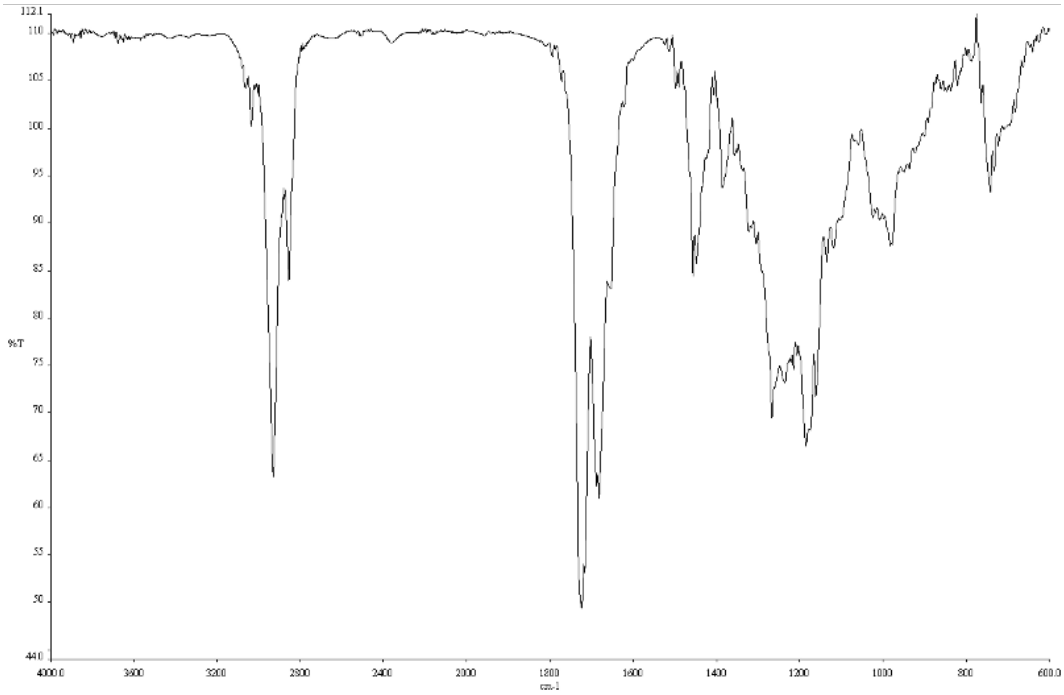

Figure A1.163. *Infrared spectrum (Thin Film, NaCl) of compound* ***139.***

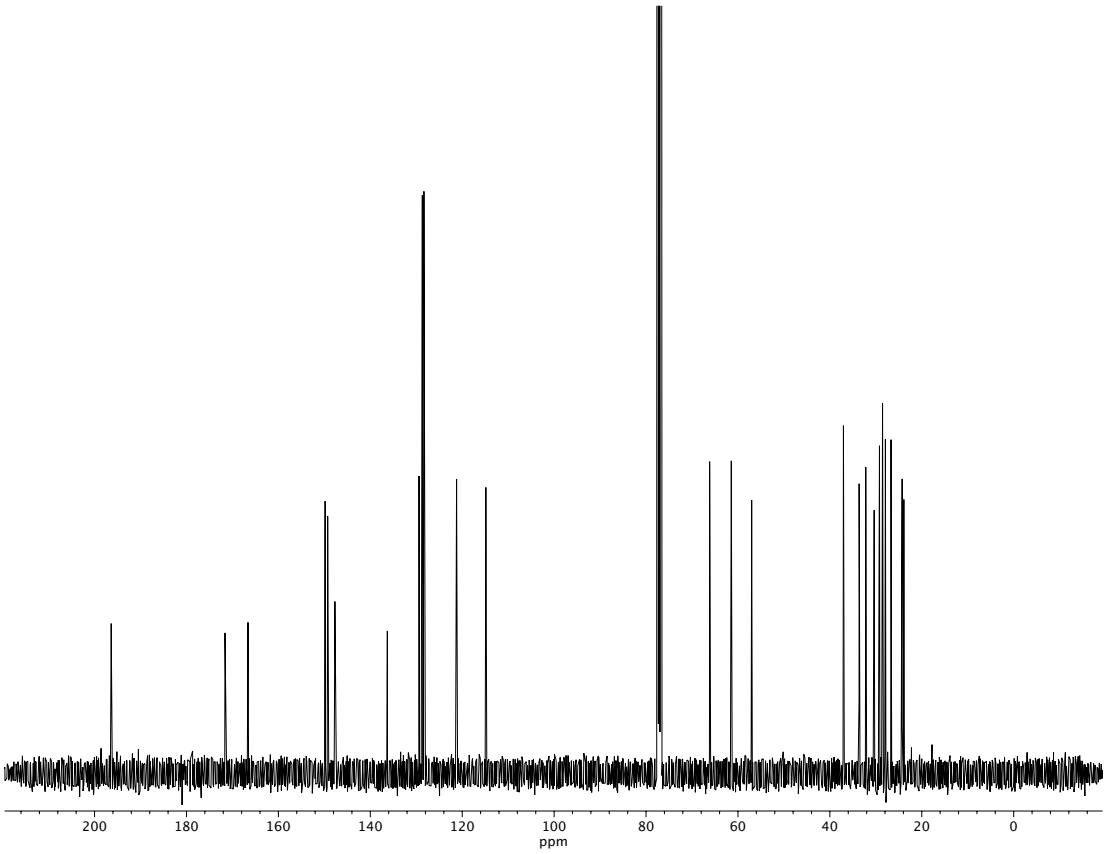

Figure A1.164. *^{13}C NMR (100 MHz, $CDCl_3$) of compound* ***139.***

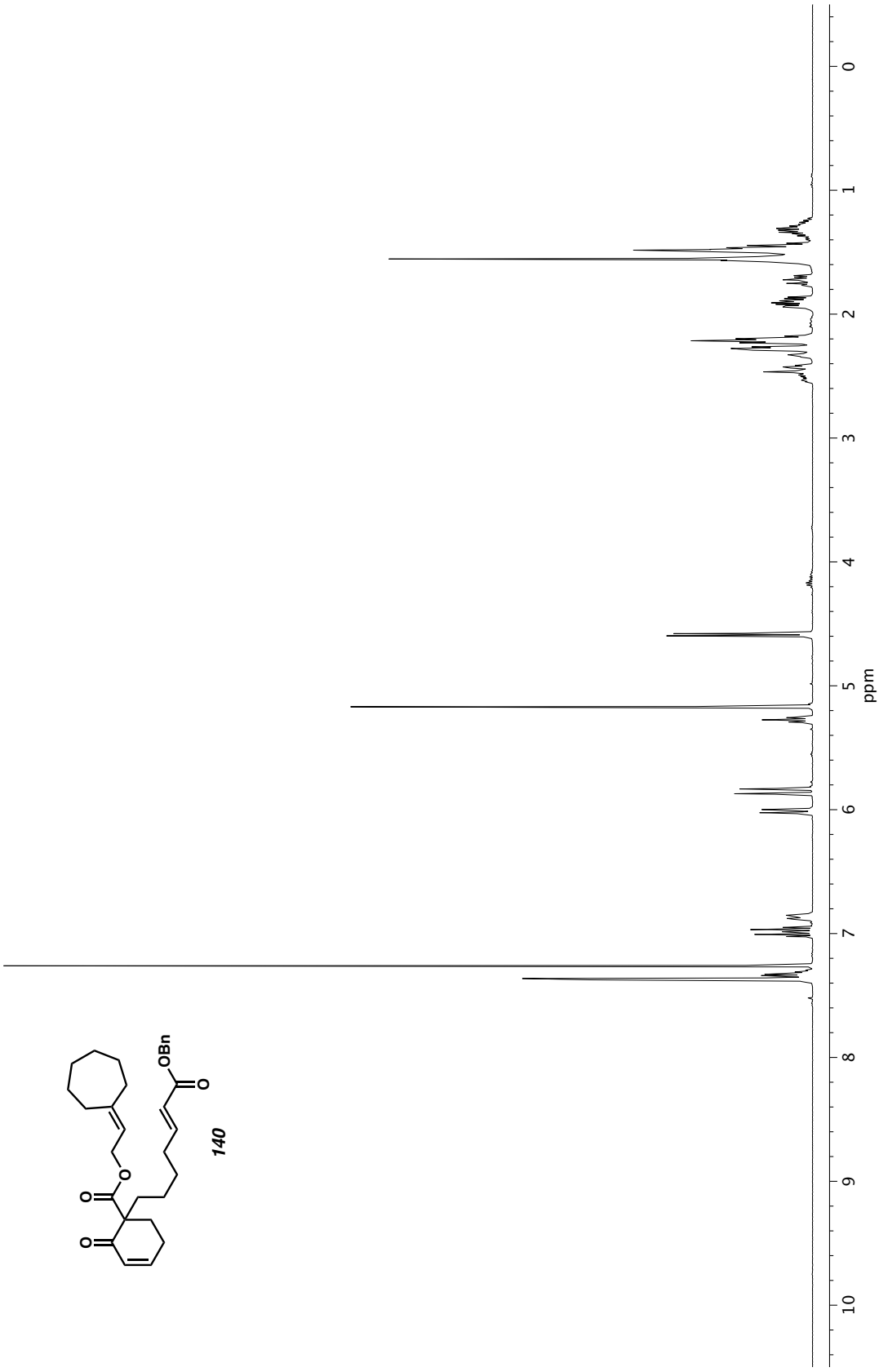

Figure A1.165. *^1H NMR (400 MHz, $CDCl_3$) of compound* ***140.***

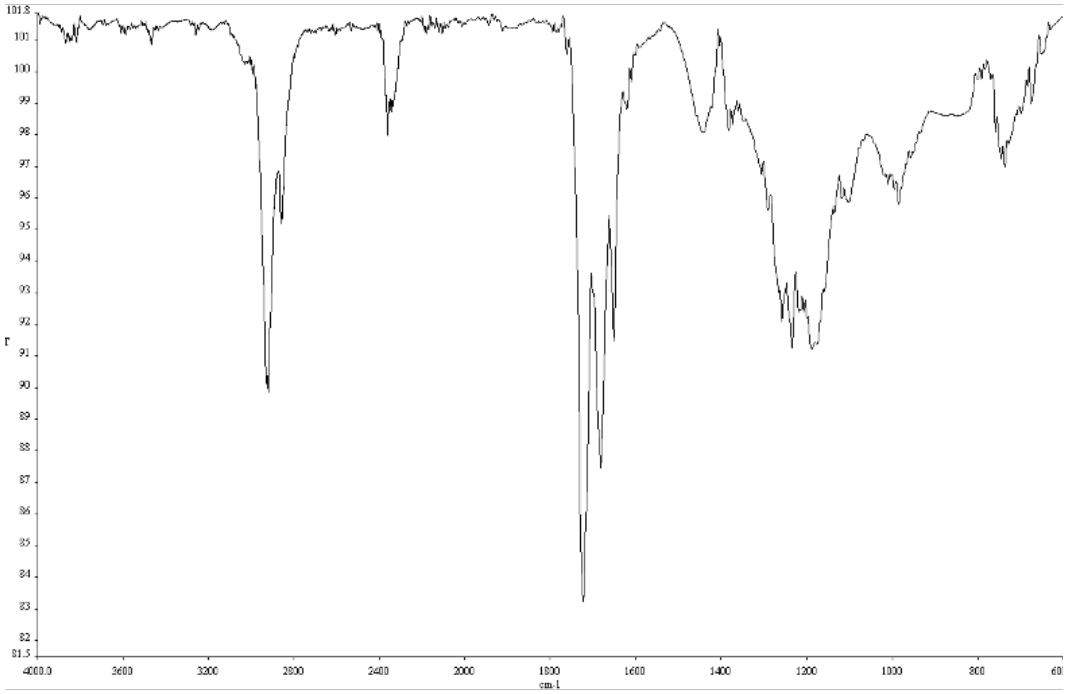

Figure A1.166. *Infrared spectrum (Thin Film, NaCl) of compound* ***140.***

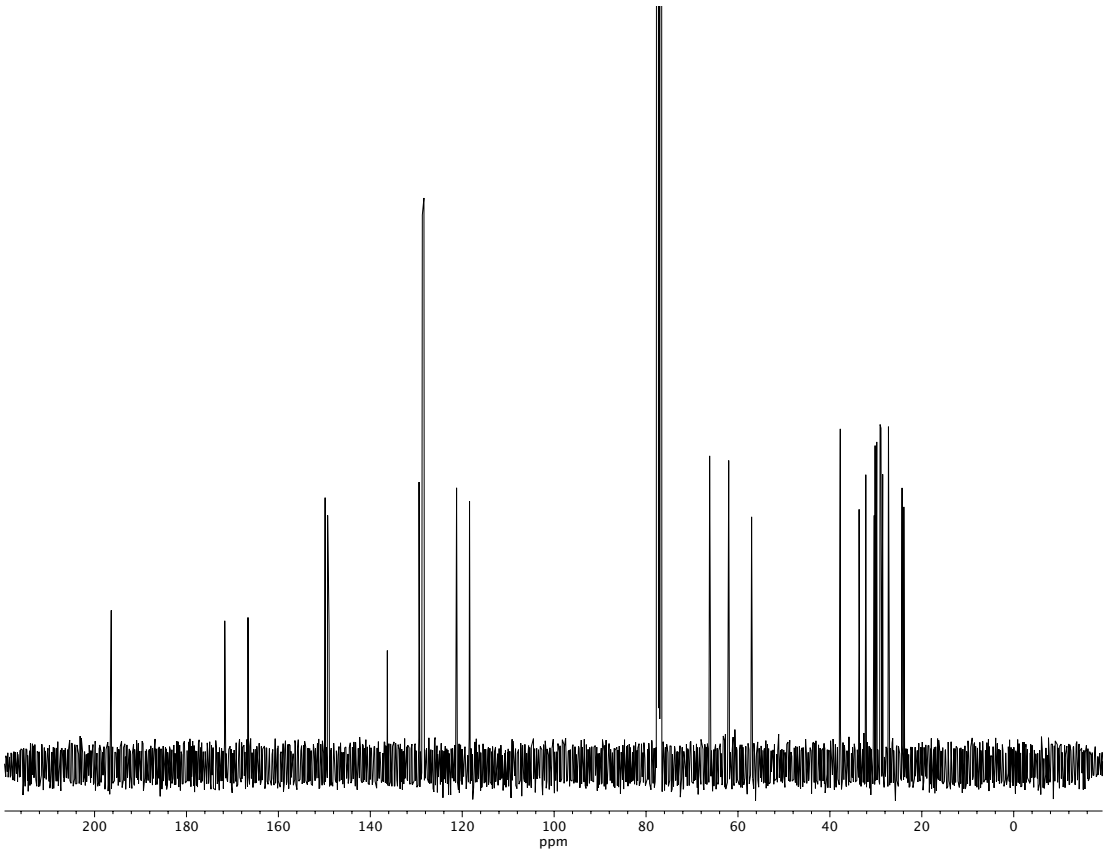

Figure A1.167. *^{13}C NMR (100 MHz, $CDCl_3$) of compound* ***140.***

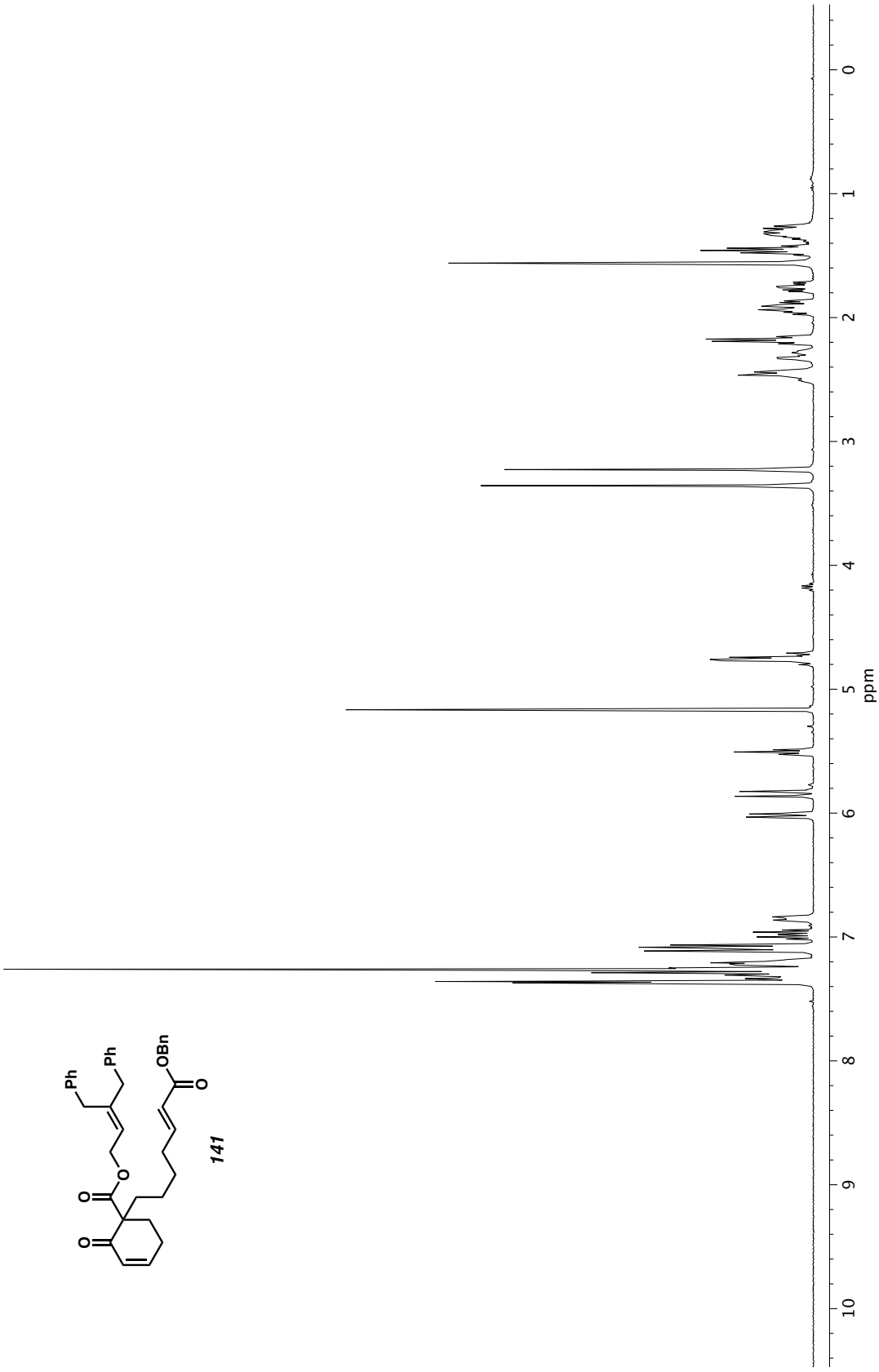

Figure A1.168. *^1H NMR (400 MHz, $CDCl_3$) of compound* ***141.***

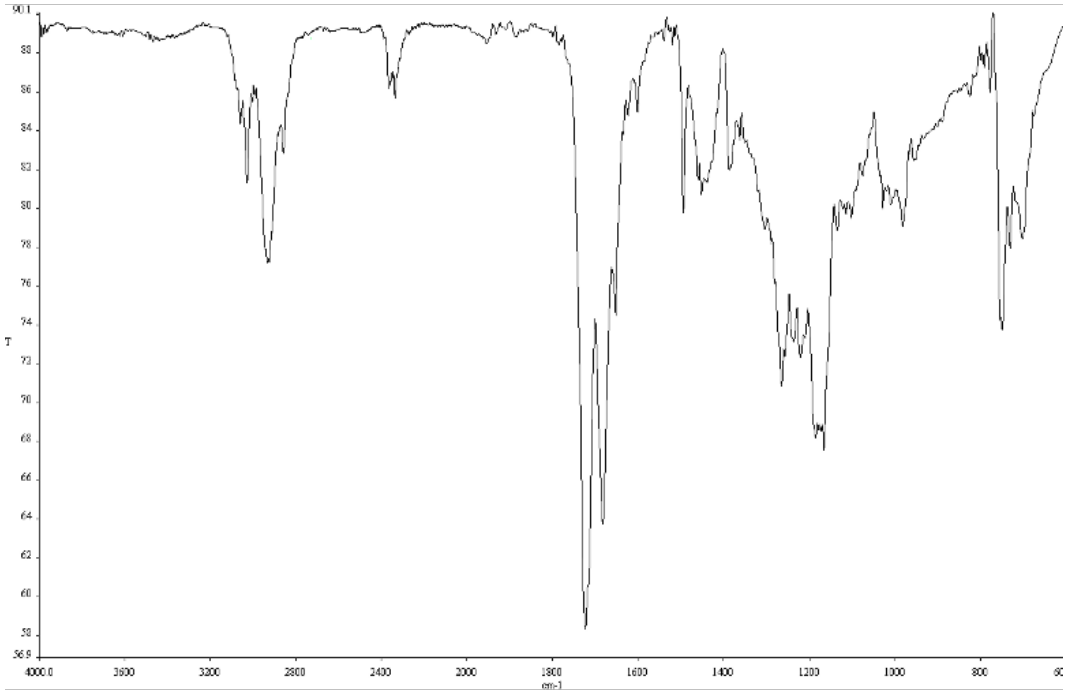

Figure A1.169. *Infrared spectrum (Thin Film, NaCl) of compound* ***141.***

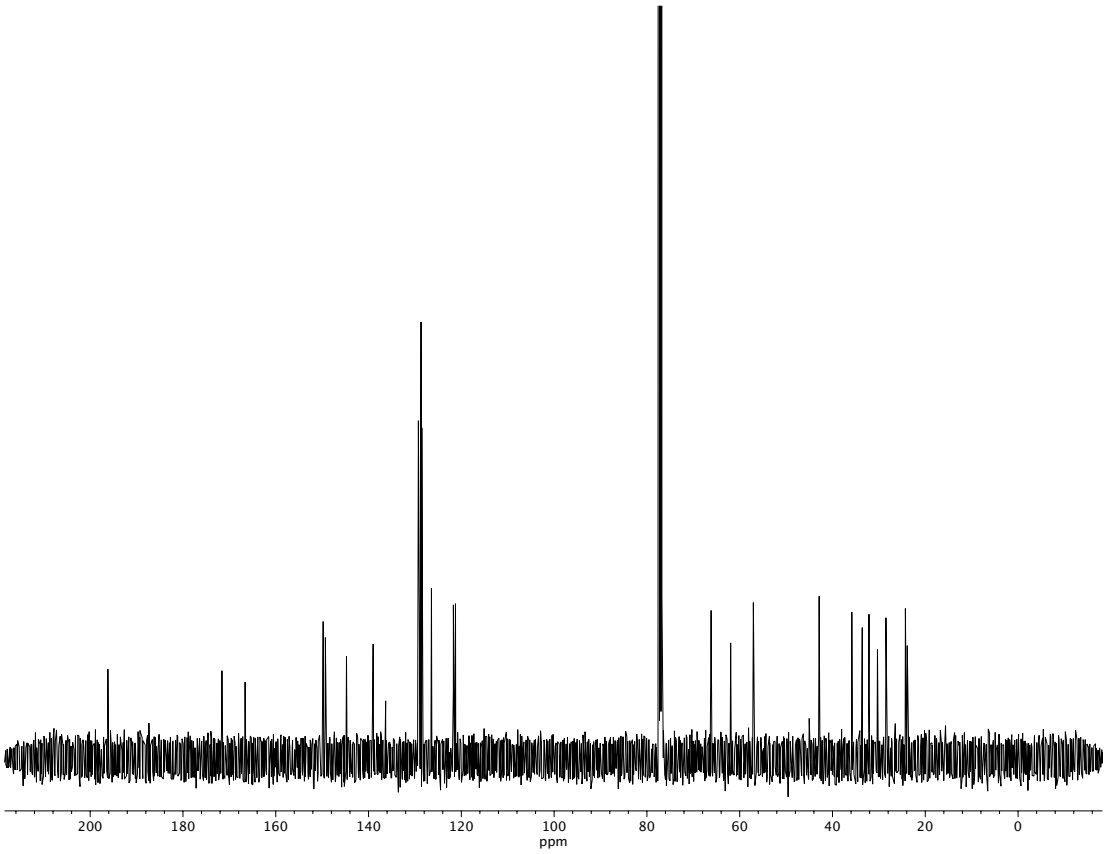

Figure A1.170. *^{13}C NMR (100 MHz, $CDCl_3$) of compound* ***141.***

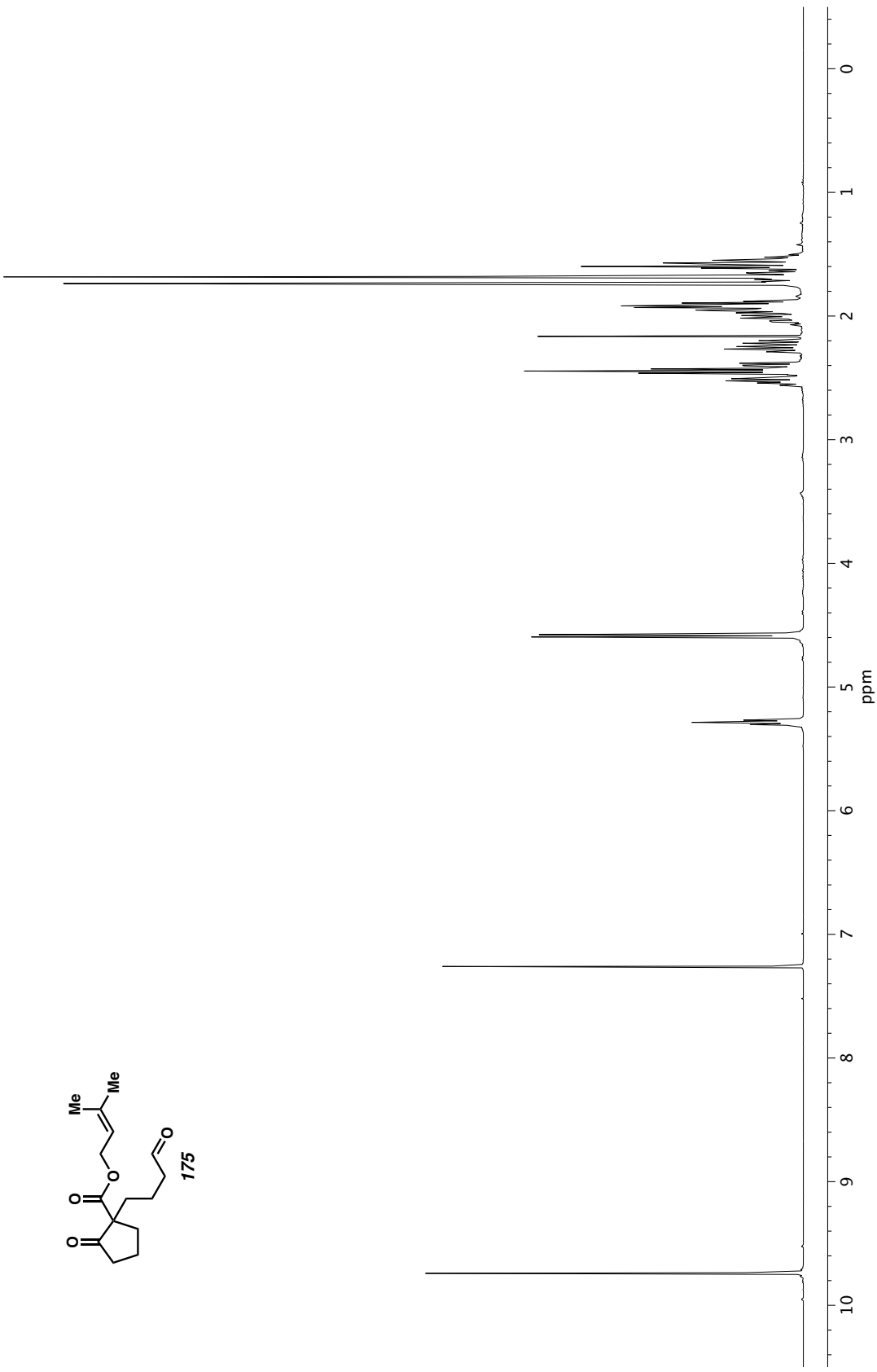

Figure A1.171. *^{1}H NMR (400 MHz, $CDCl_3$) of compound* ***175.***

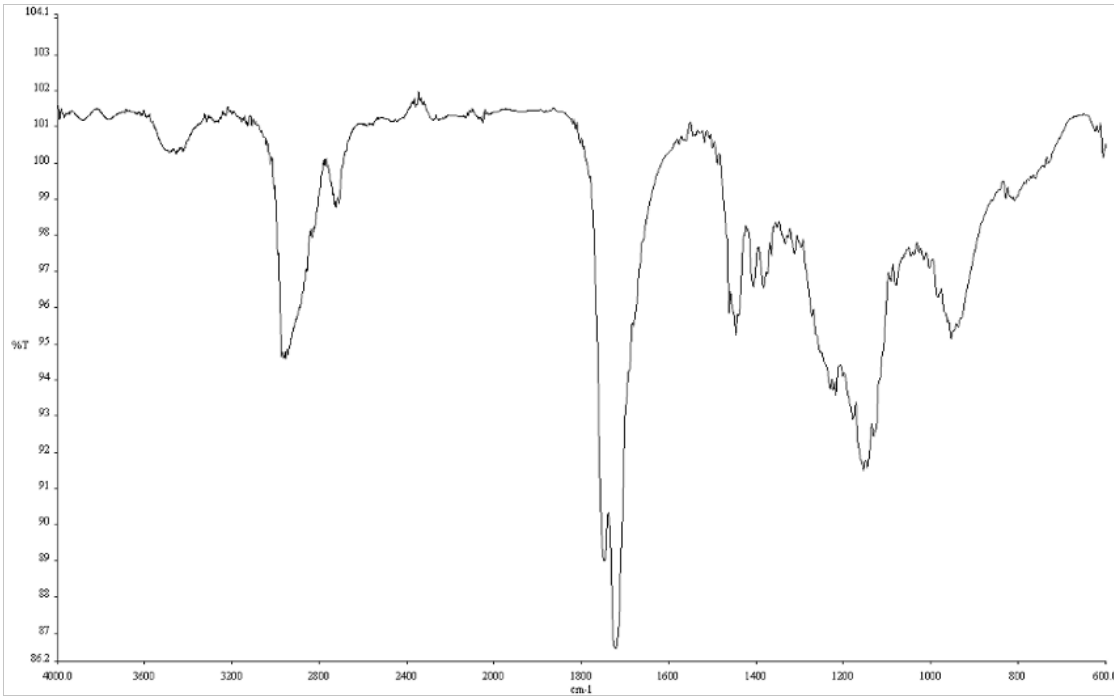

Figure A1.172. *Infrared spectrum (Thin Film, NaCl) of compound* ***175.***

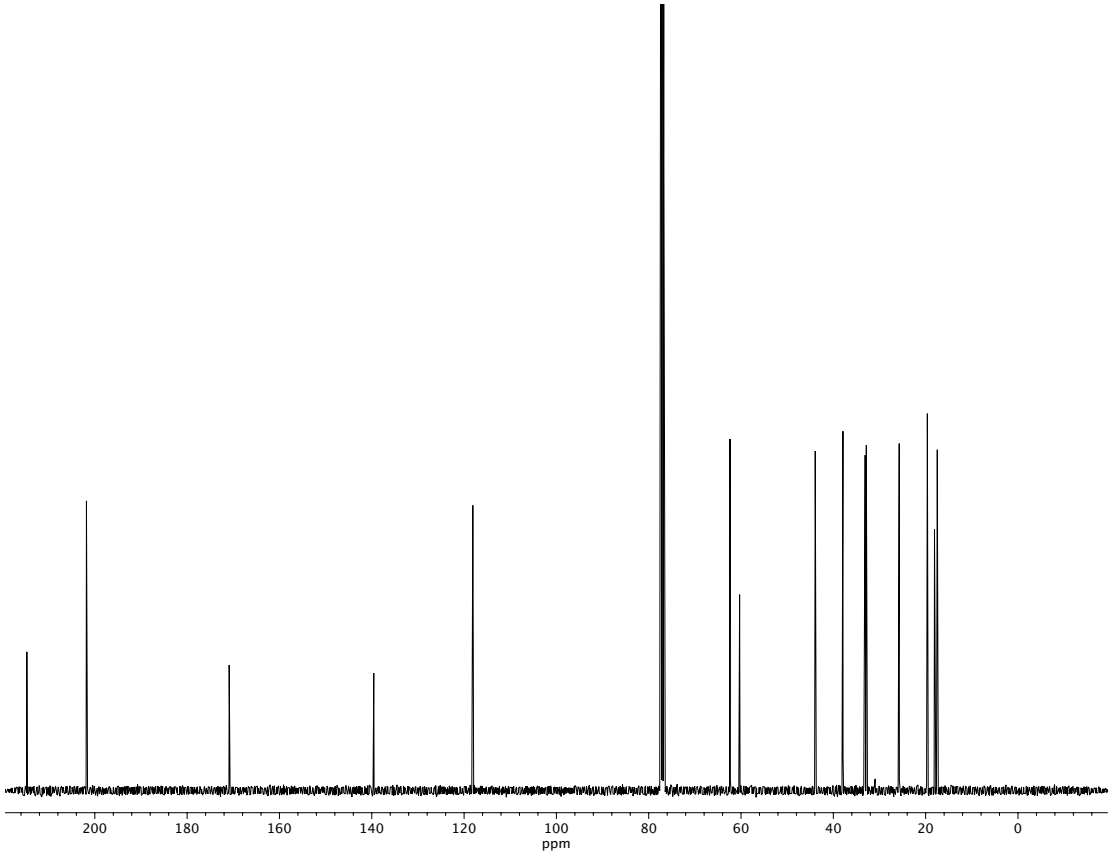

Figure A1.173. *^{13}C NMR (100 MHz, $CDCl_3$) of compound* ***175.***

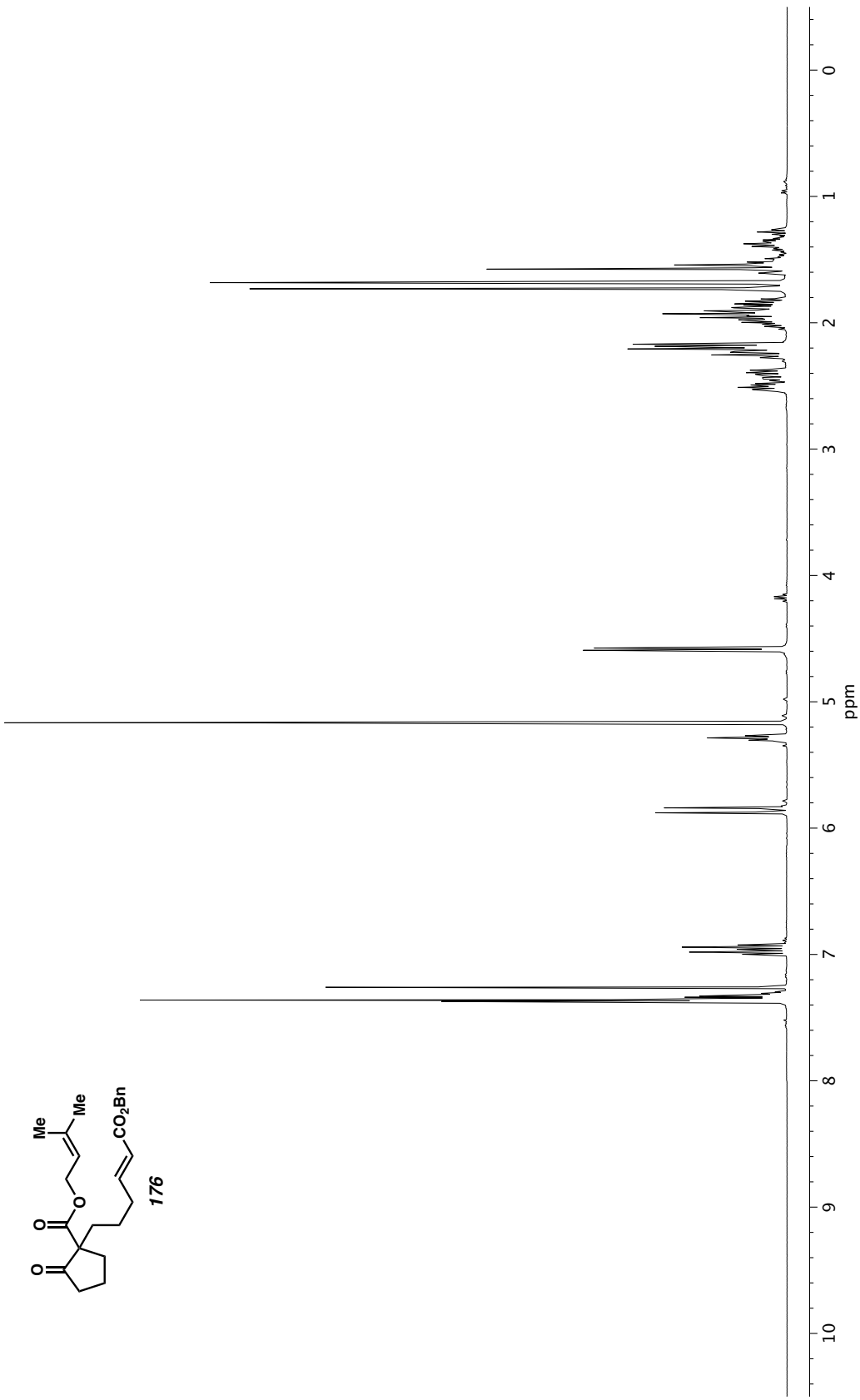

Figure A1.174. *^{1}H NMR (400 MHz, $CDCl_3$) of compound* ***176.***

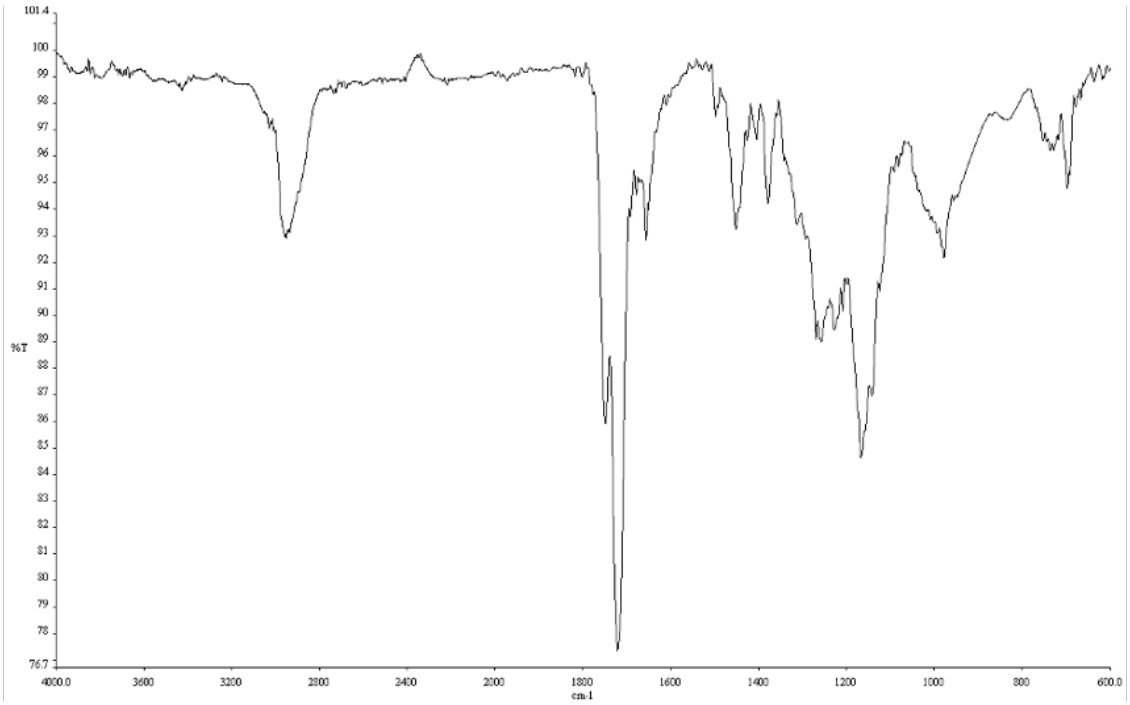

Figure A1.175. *Infrared spectrum (Thin Film, NaCl) of compound* ***176.***

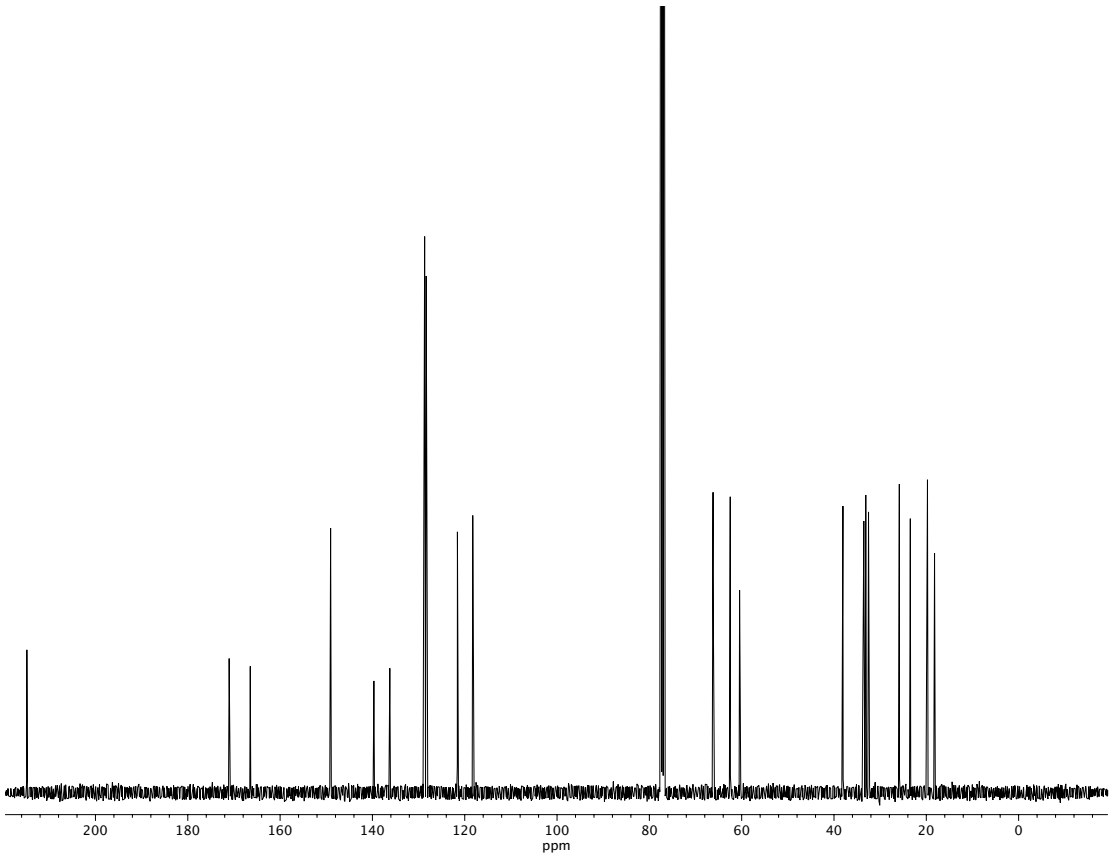

Figure A1.176. *^{13}C NMR (100 MHz, $CDCl_3$) of compound* ***176.***

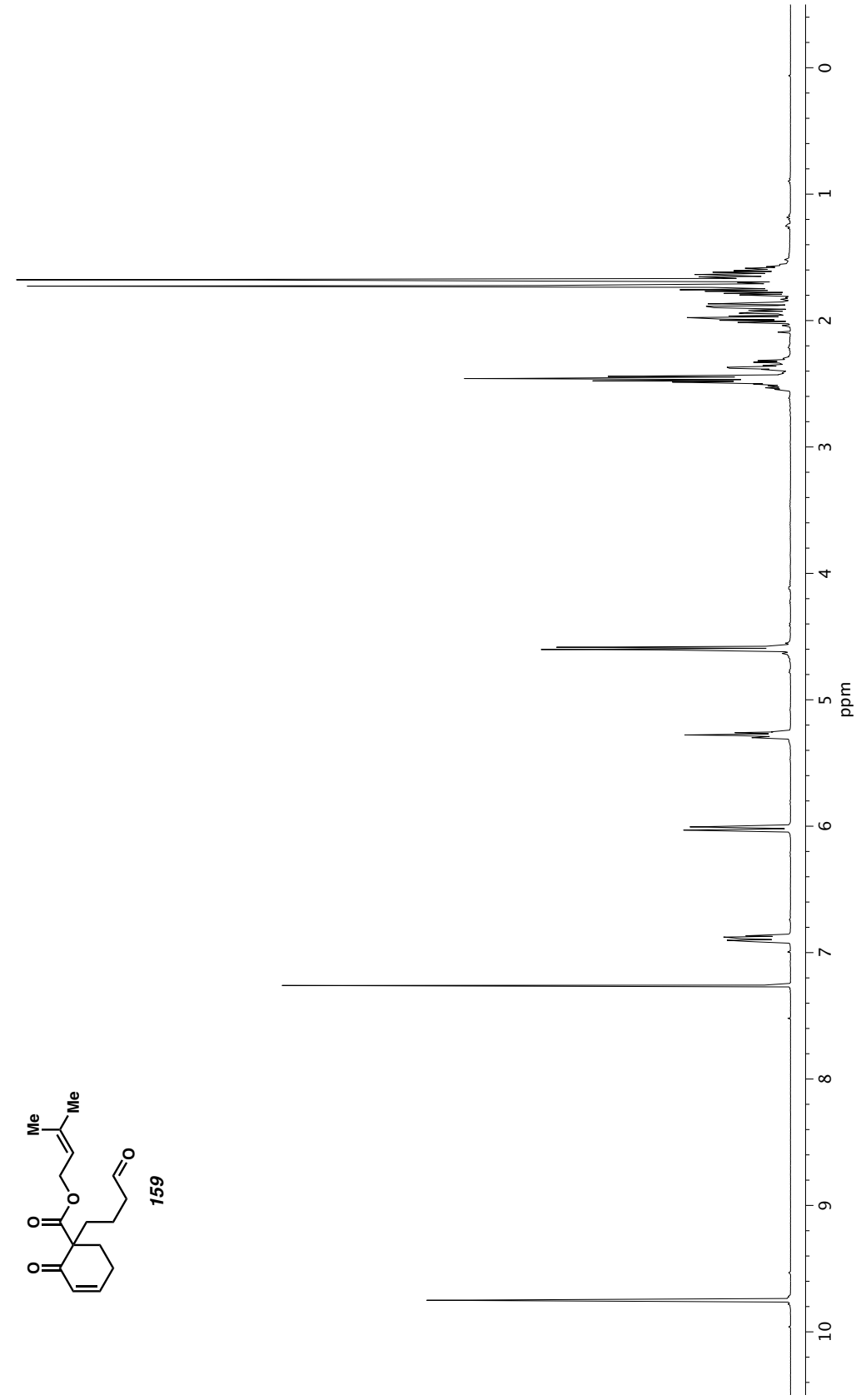

Figure A1.177. *^{1}H NMR (400 MHz, $CDCl_3$) of compound* ***159.***

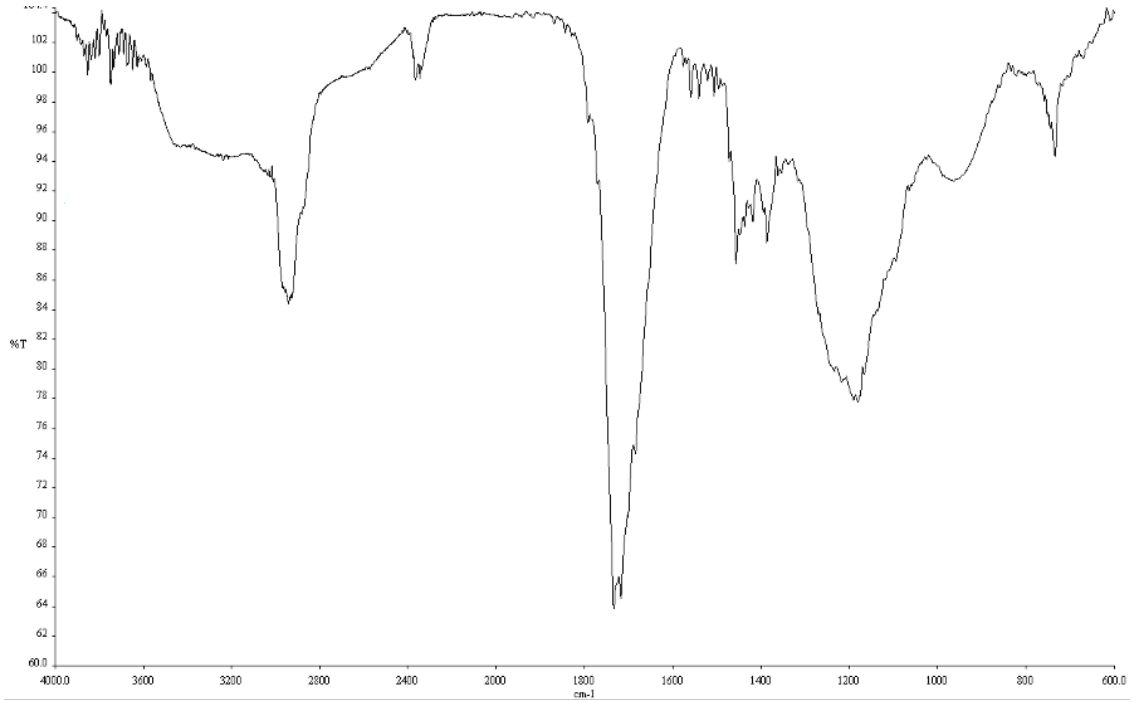

Figure A1.178. *Infrared spectrum (Thin Film, NaCl) of compound* ***159.***

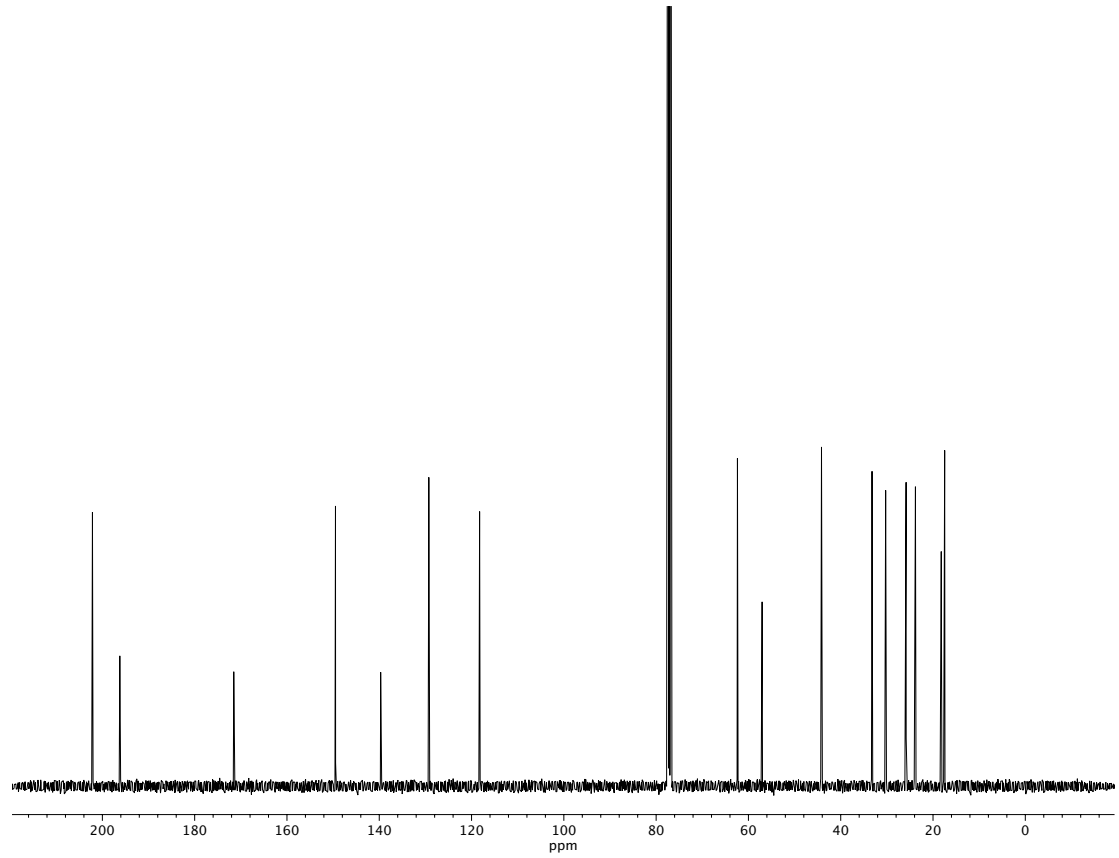

Figure A1.179. *^{13}C NMR (100 MHz, $CDCl_3$) of compound* ***159.***

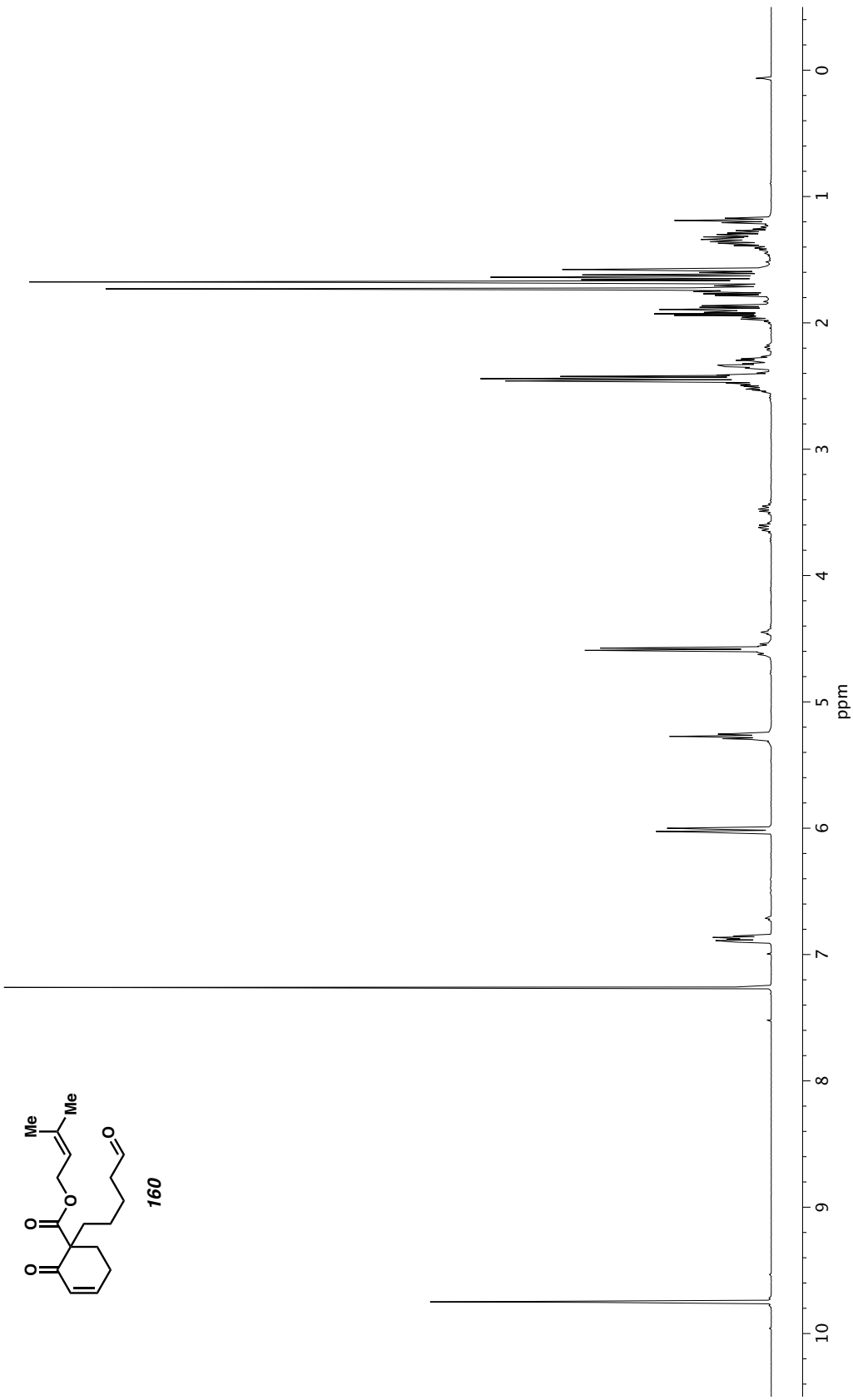

Figure A1.180. *^1H NMR (400 MHz, $CDCl_3$) of compound* ***160.***

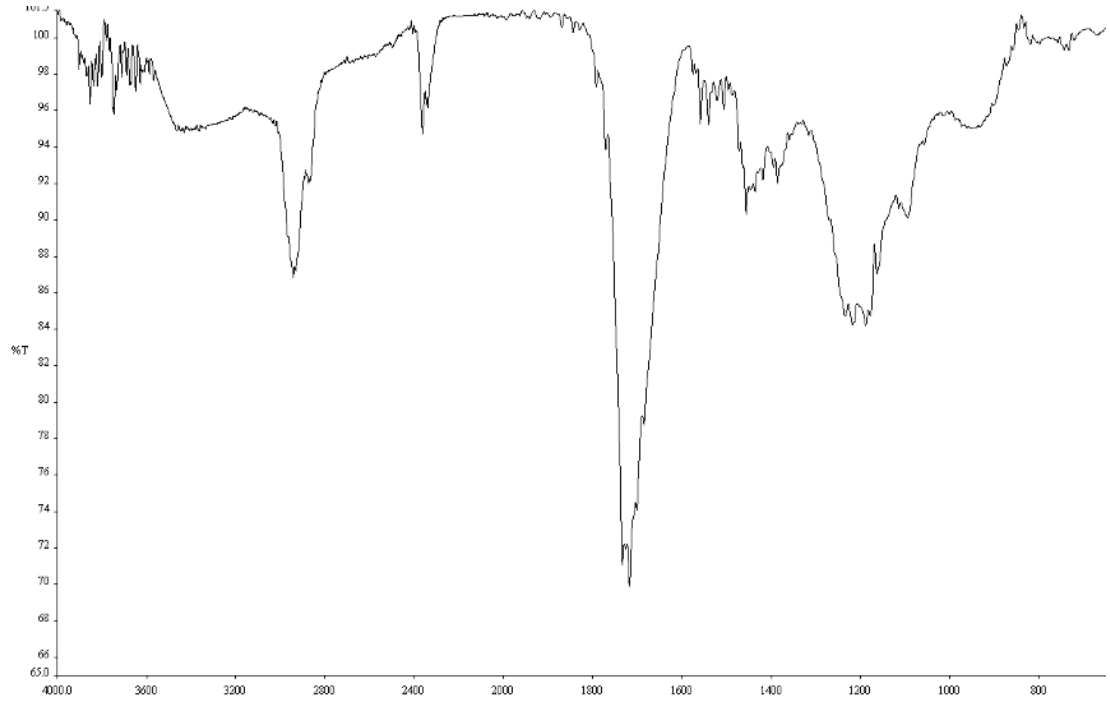

Figure A1.181. *Infrared spectrum (Thin Film, NaCl) of compound* ***160.***

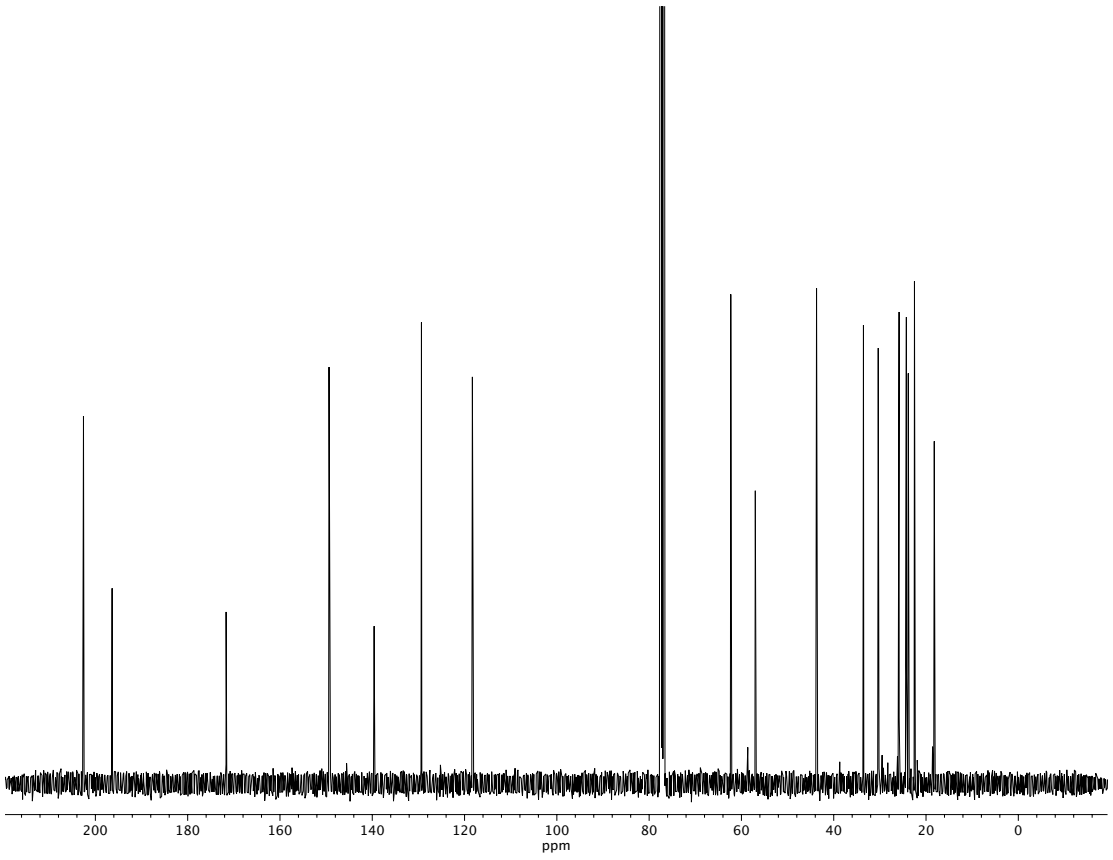

Figure A1.182. *^{13}C NMR (100 MHz, $CDCl_3$) of compound* ***160.***

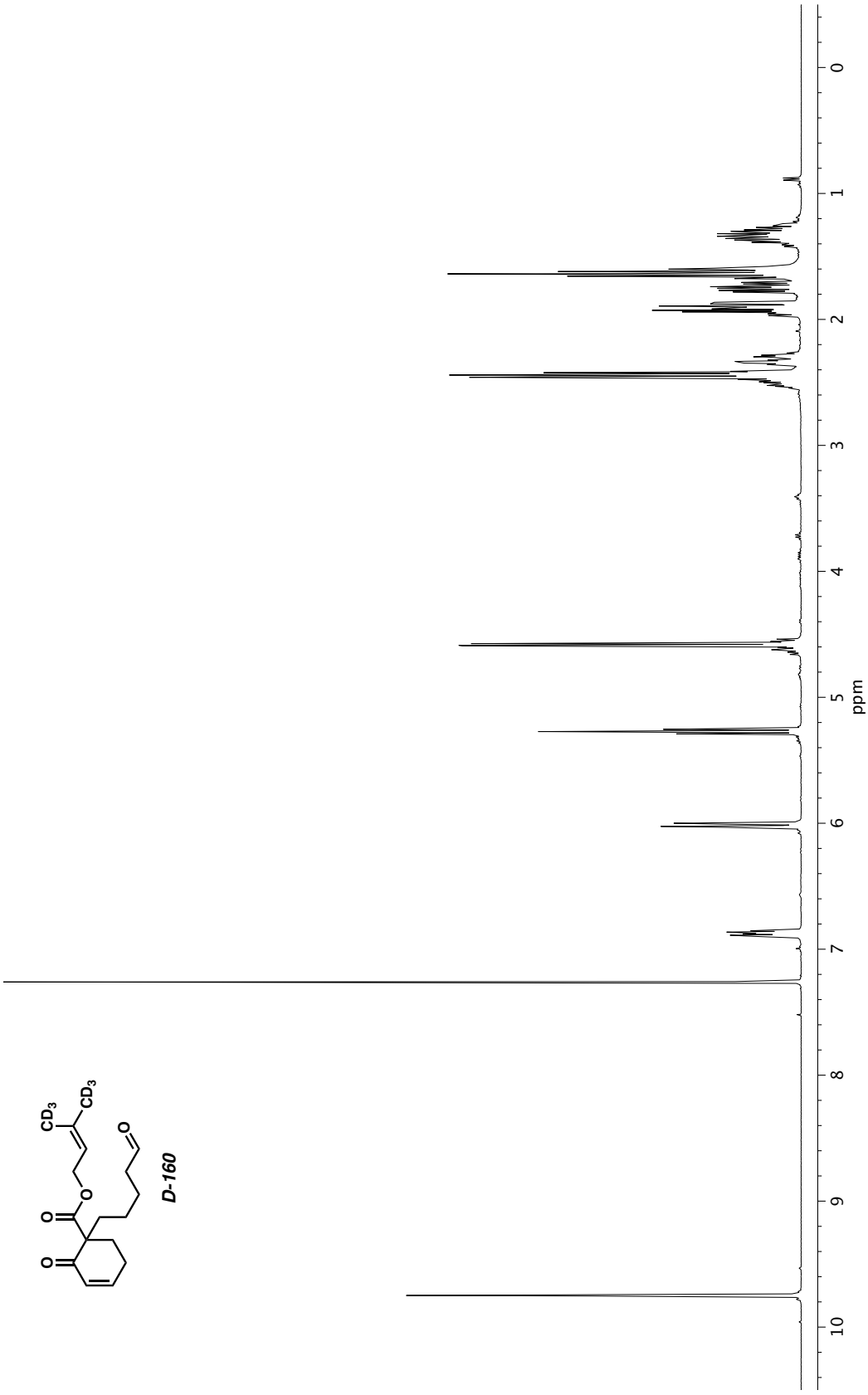

Figure A1.183. *^1H NMR (400 MHz, $CDCl_3$) of compound* ***D-160.***

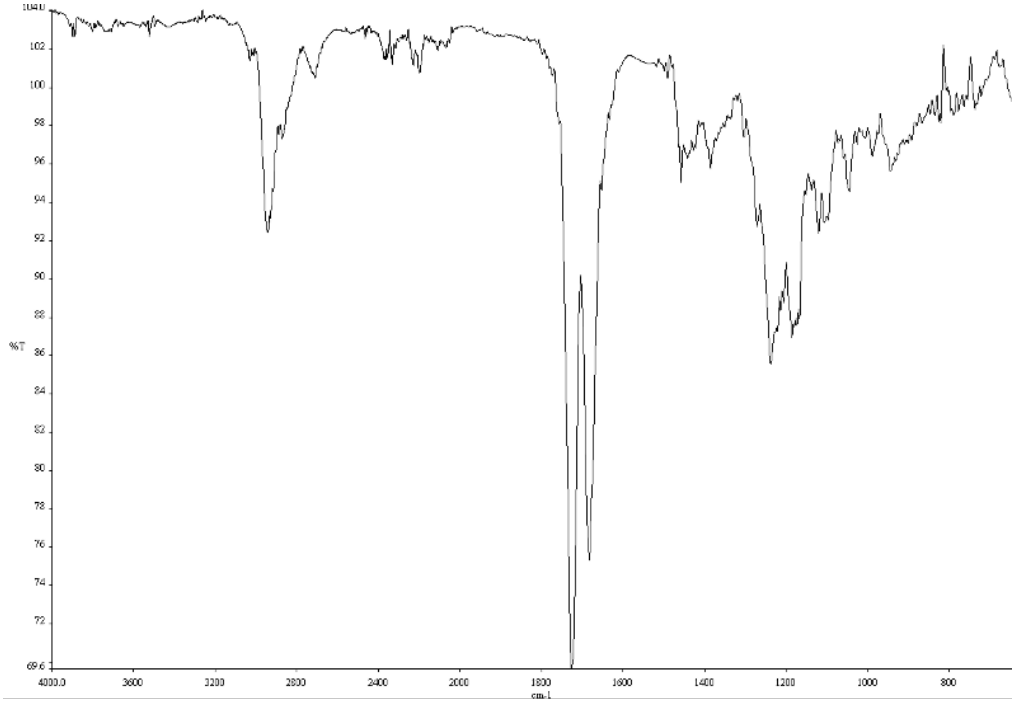

Figure A1.184. *Infrared spectrum (Thin Film, NaCl) of compound* ***D-160.***

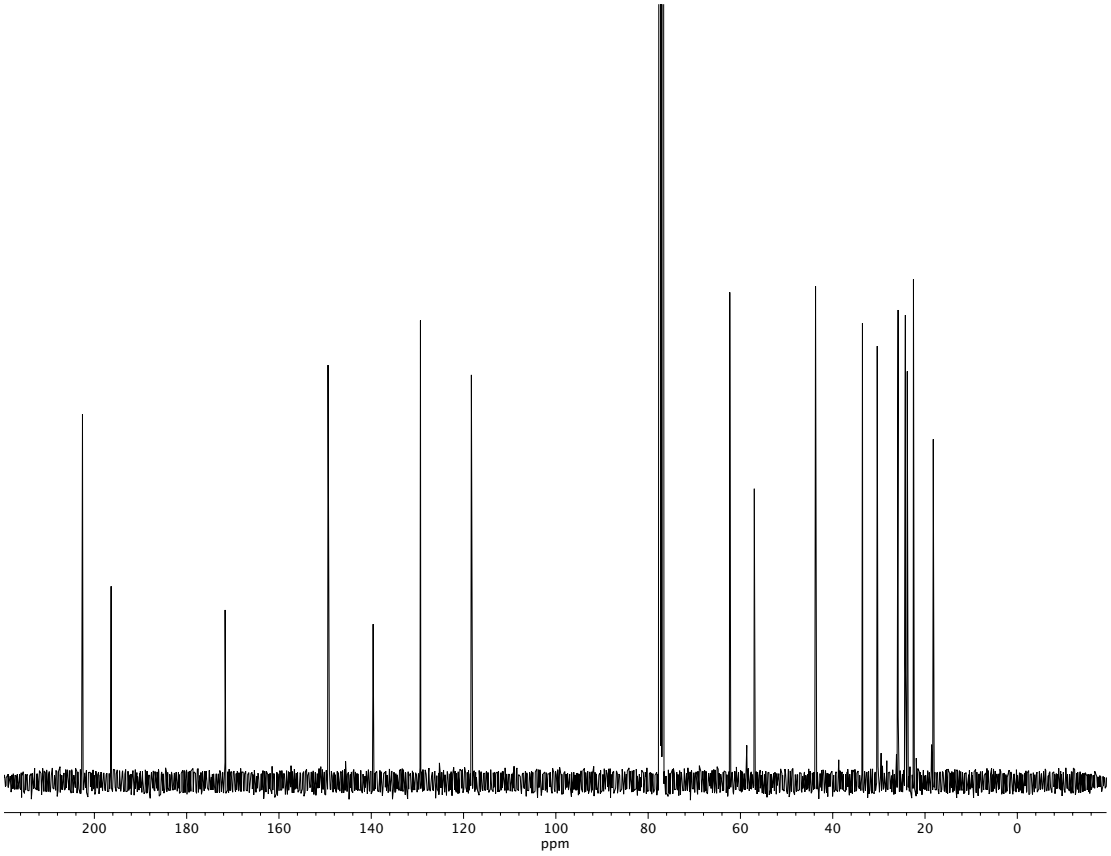

Figure A1.185. *^{13}C NMR (100 MHz, $CDCl_3$) of compound* ***D-160.***

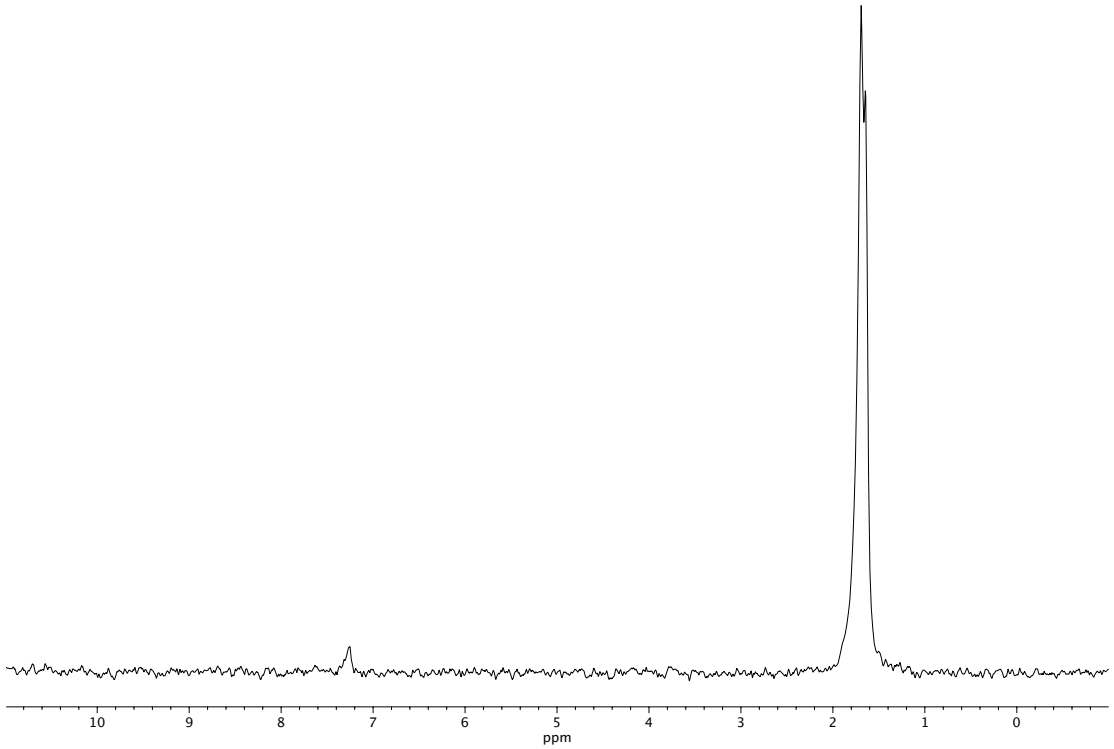

Figure A1.186. *^{2}H NMR (61 MHz, $CHCl_3$) of compound* ***D-160.***

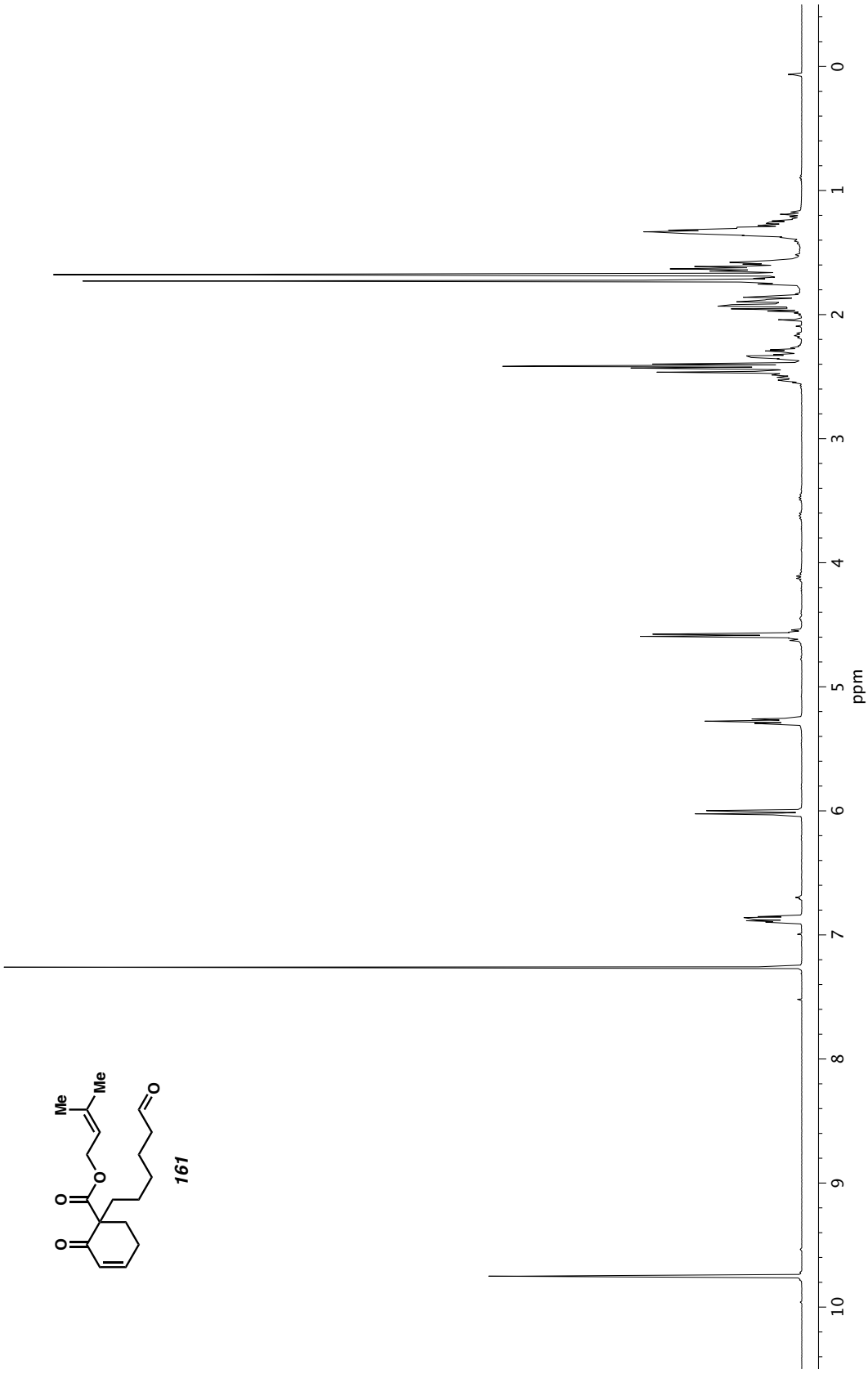

Figure A1.187. *^1H NMR (400 MHz, $CDCl_3$) of compound* ***161.***

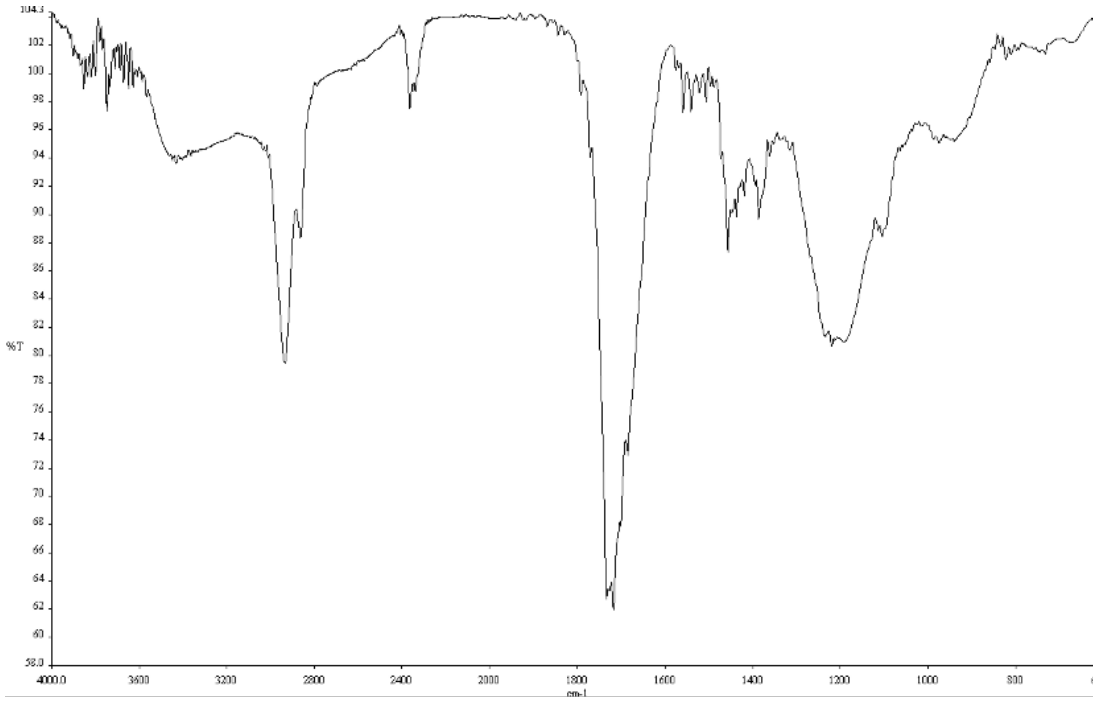

Figure A1.188. *Infrared spectrum (Thin Film, NaCl) of compound* ***161.***

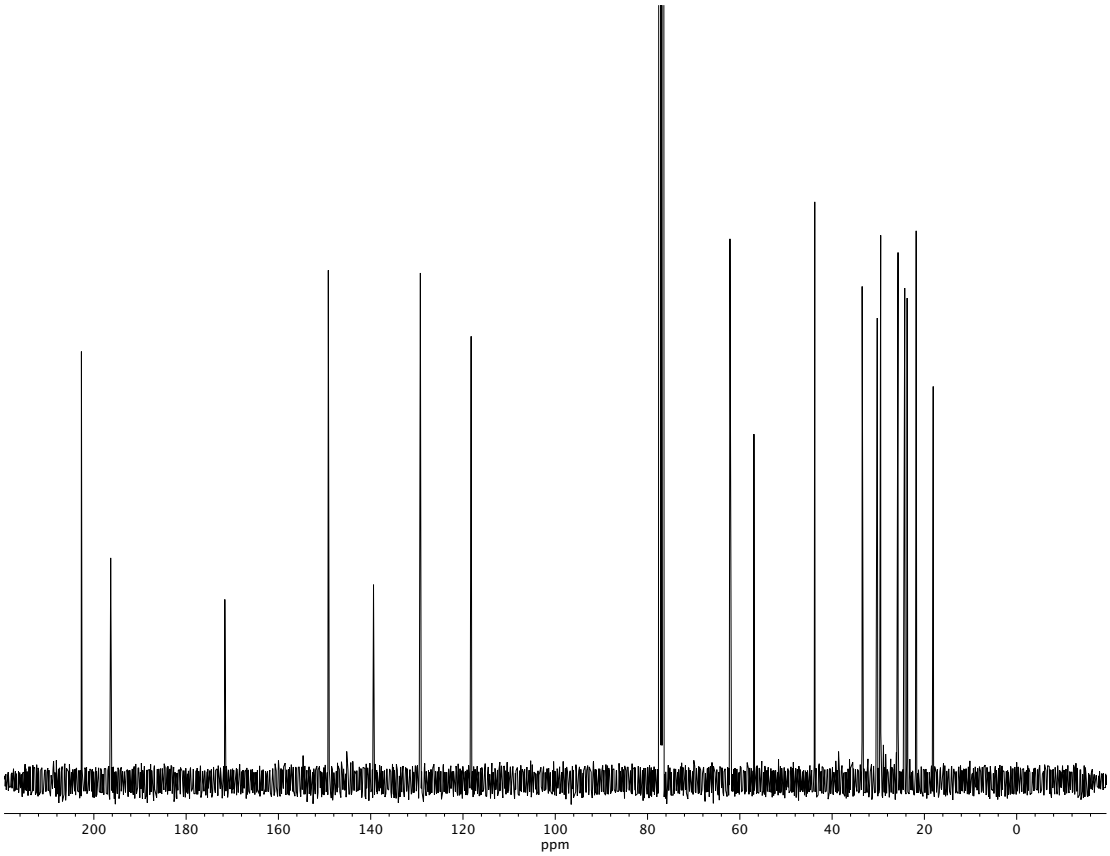

Figure A1.189. *^{13}C NMR (100 MHz, $CDCl_3$) of compound* ***161.***

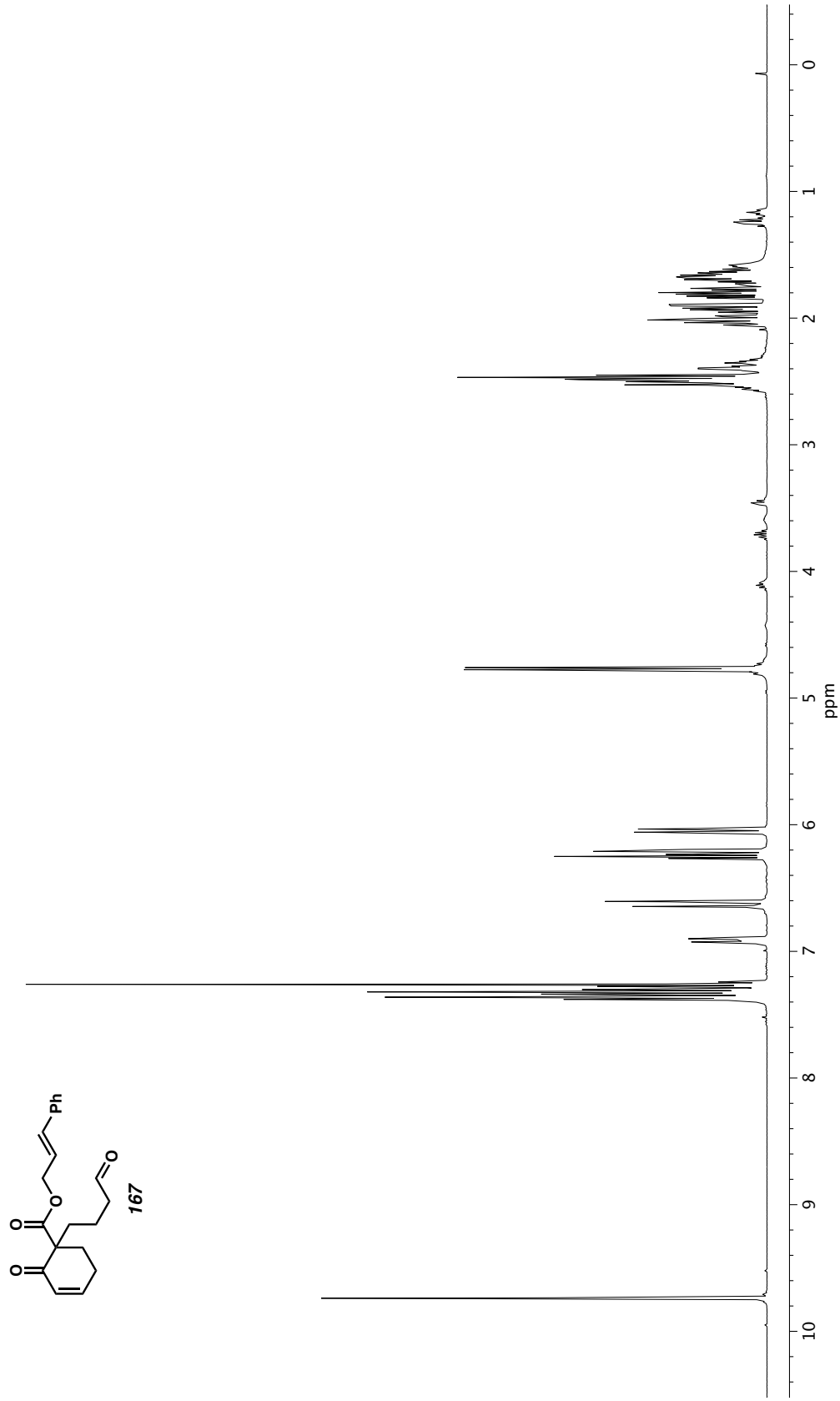

Figure A1.190. *^1H NMR (400 MHz, $CDCl_3$) of compound* ***167.***

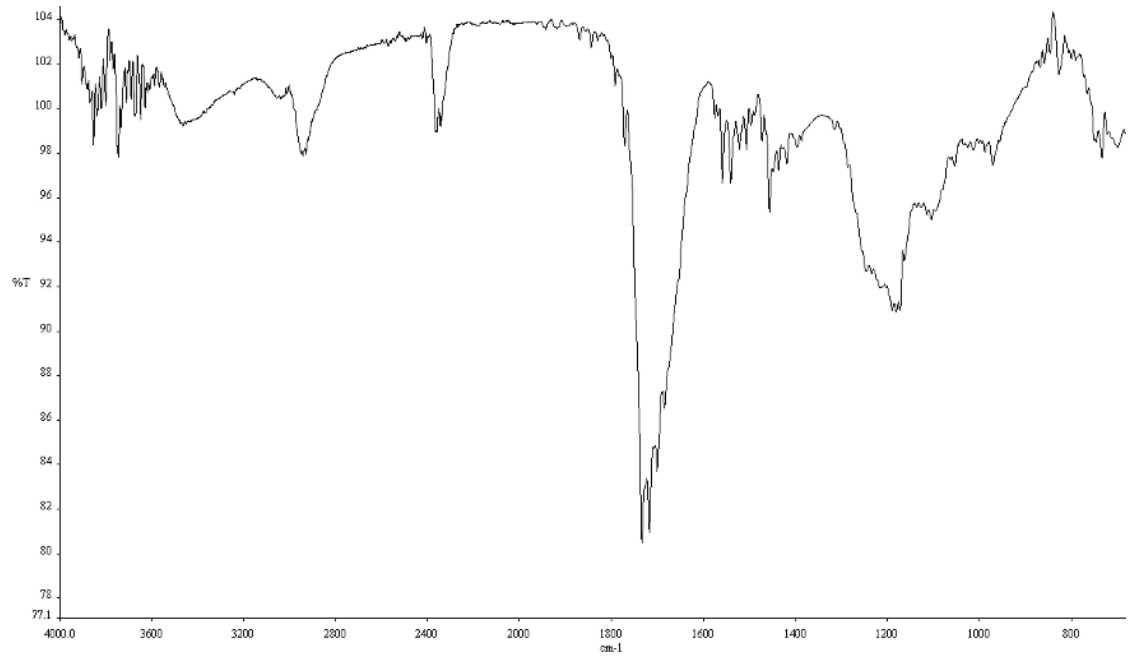

Figure A1.191. *Infrared spectrum (Thin Film, NaCl) of compound* ***167.***

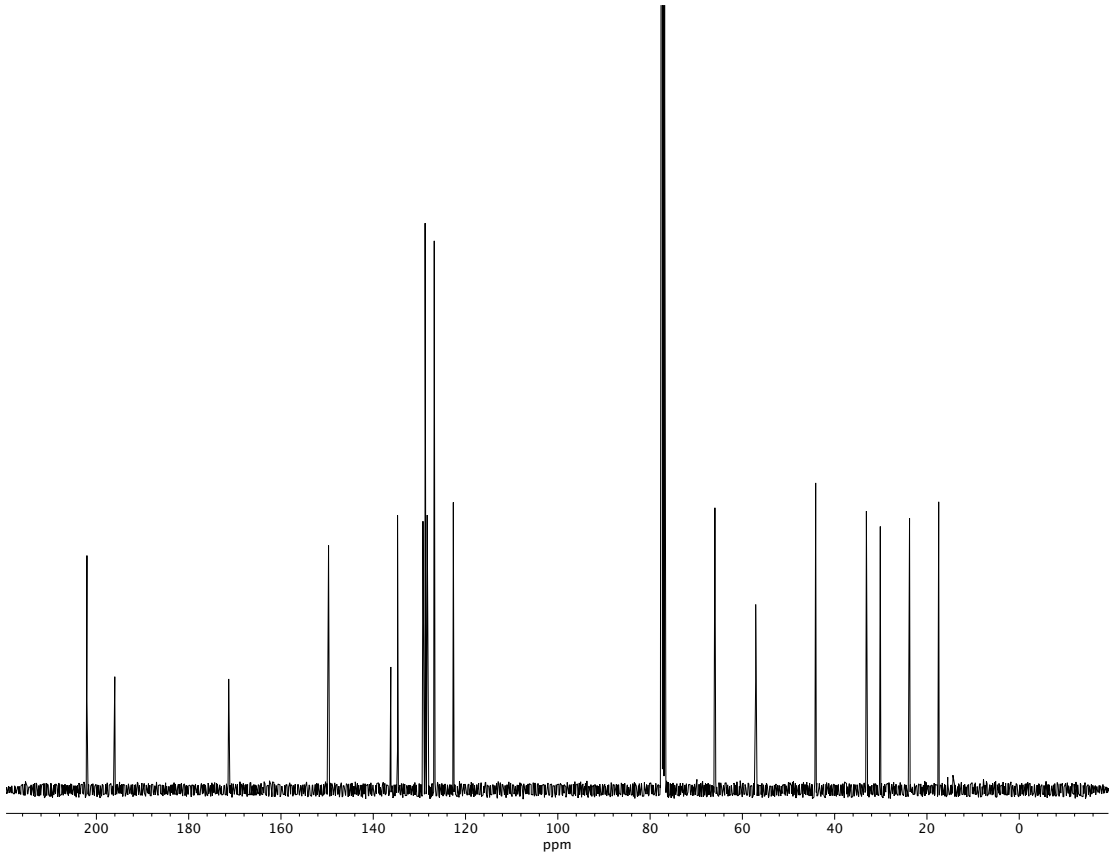

Figure A1.192. *^{13}C NMR (100 MHz, $CDCl_3$) of compound* ***167.***

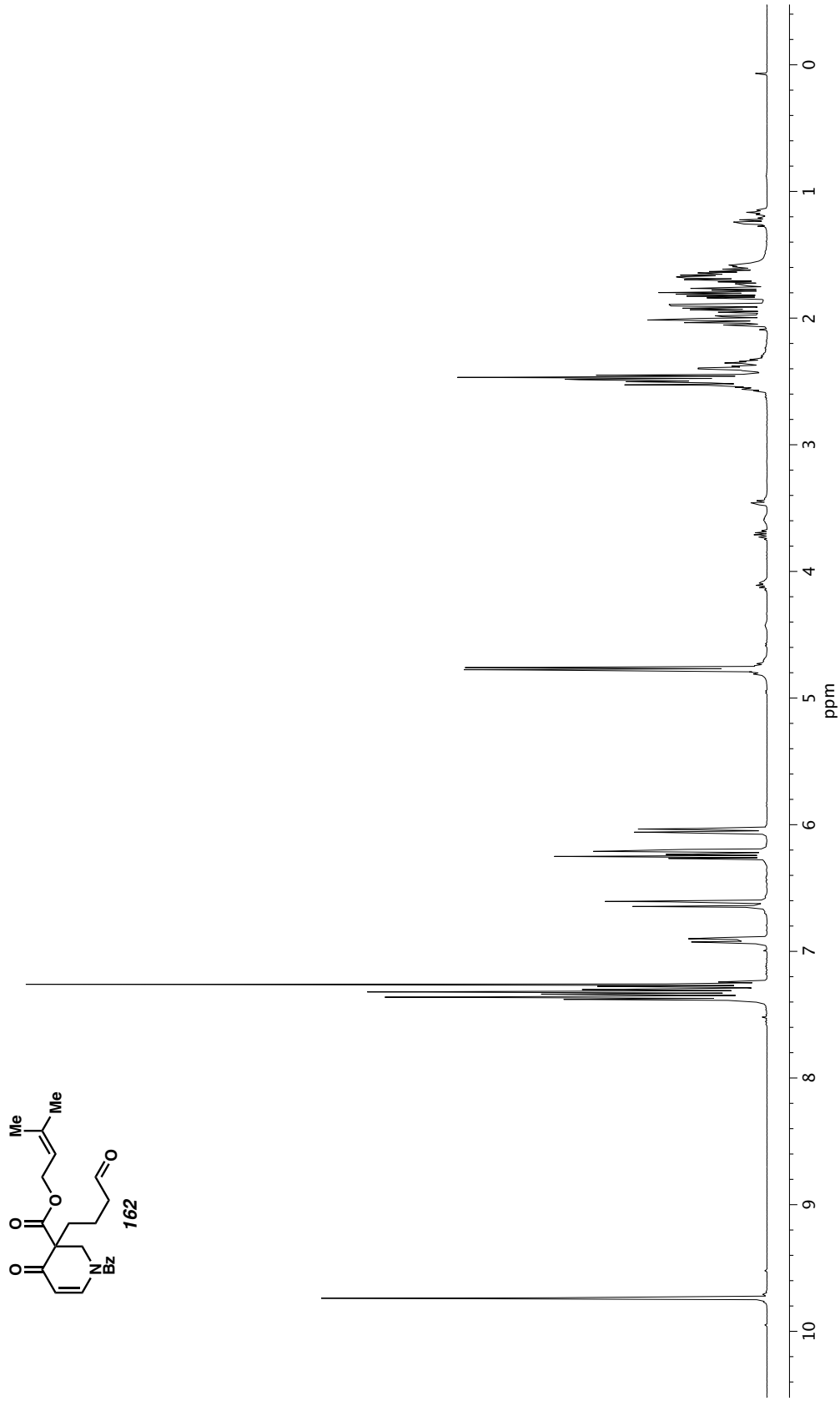

Figure A1.193. *^1H NMR (400 MHz, $CDCl_3$) of compound* ***162.***

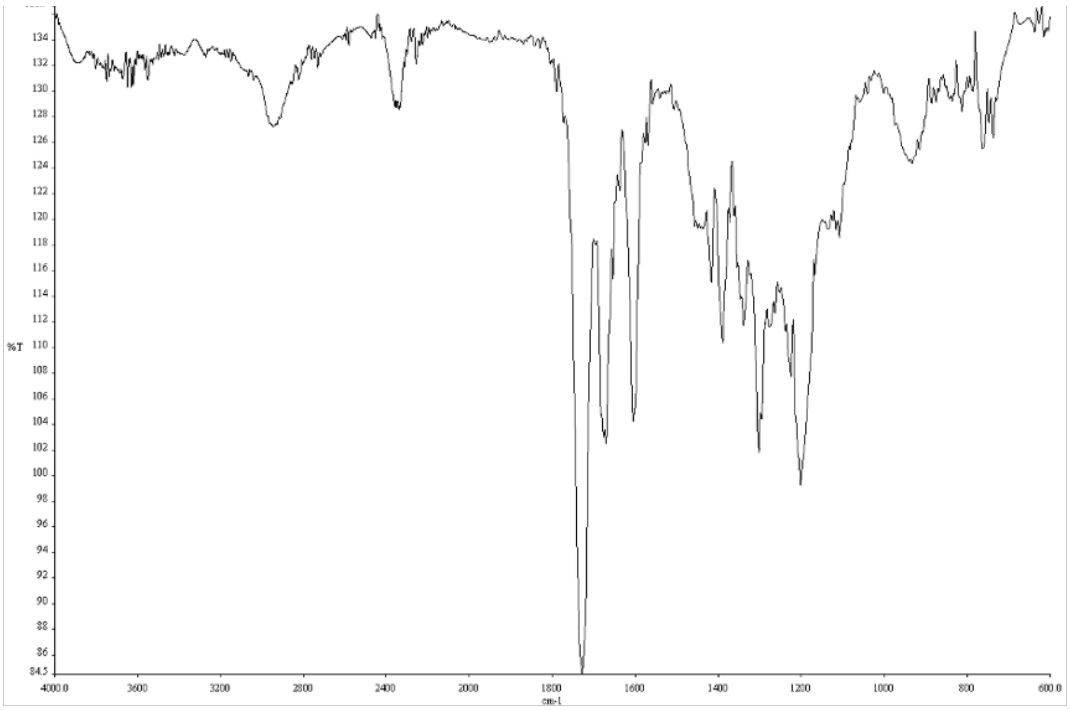

Figure A1.194. *Infrared spectrum (Thin Film, NaCl) of compound* ***162.***

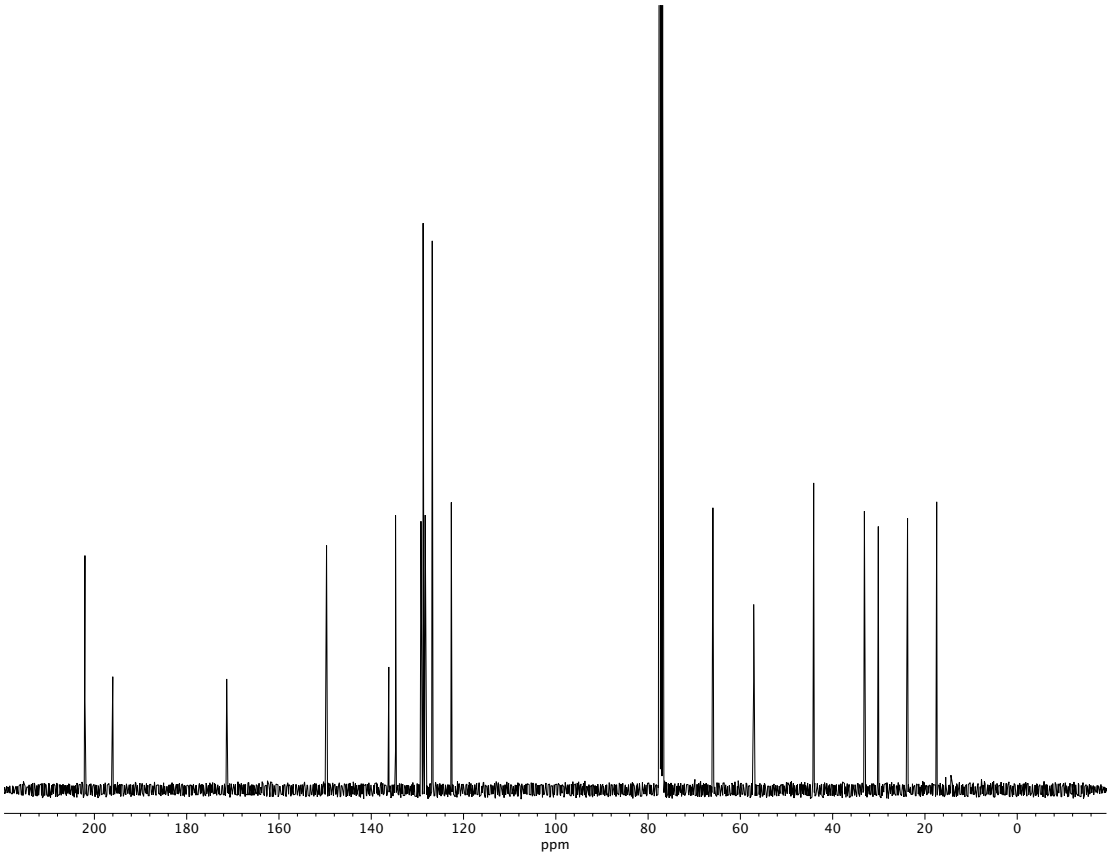

Figure A1.195. *^{13}C NMR (100 MHz, $CDCl_3$) of compound* ***162.***

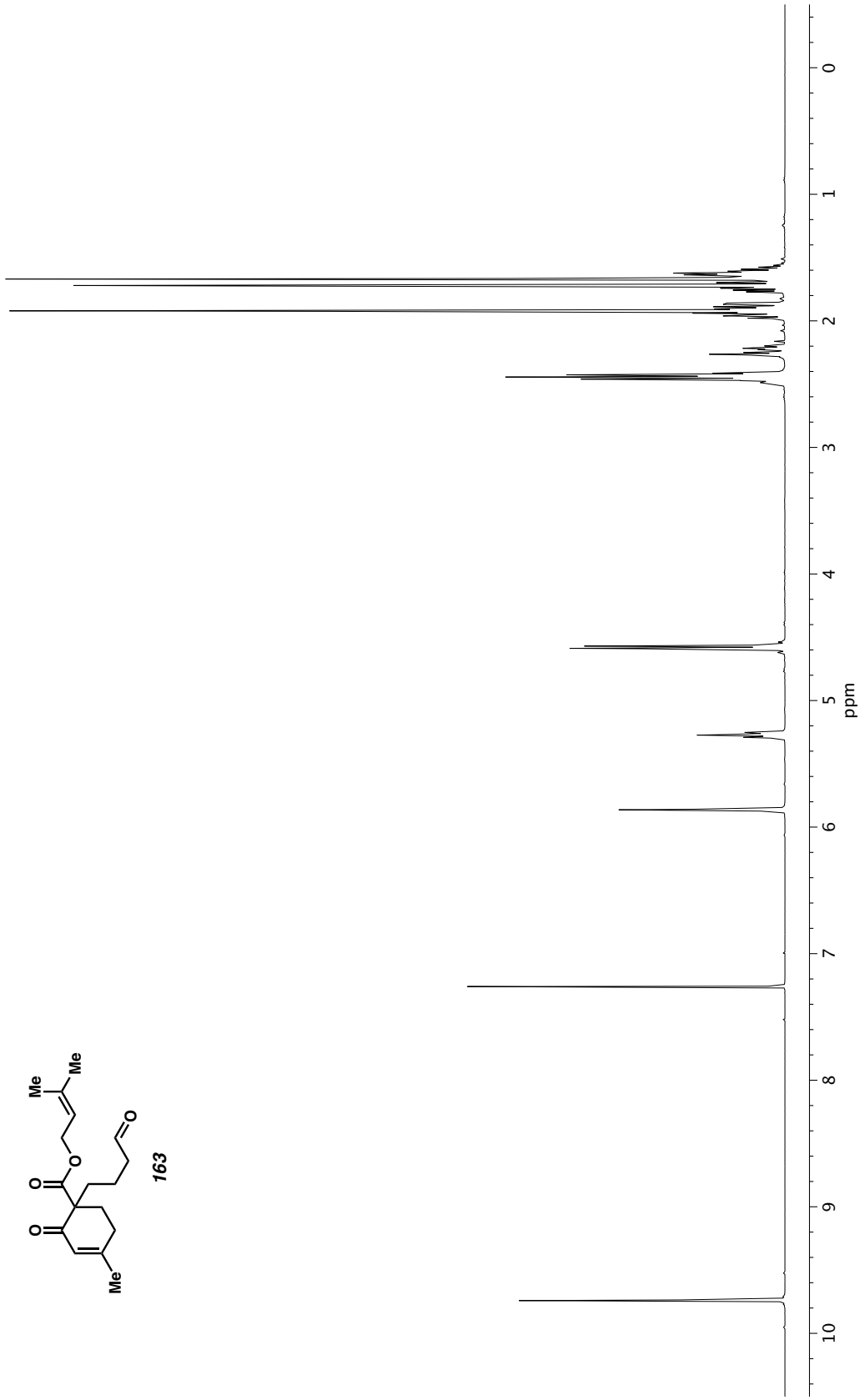

Figure A1.196. *^{1}H NMR (400 MHz, $CDCl_3$) of compound* ***163.***

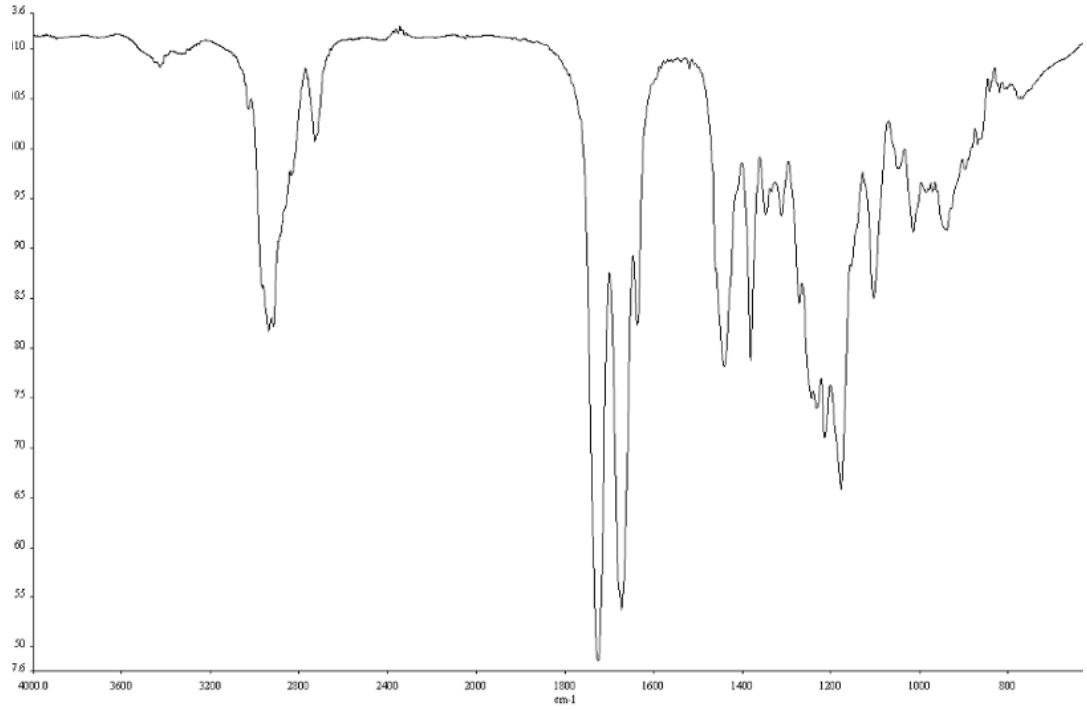

Figure A1.197. *Infrared spectrum (Thin Film, NaCl) of compound* ***163.***

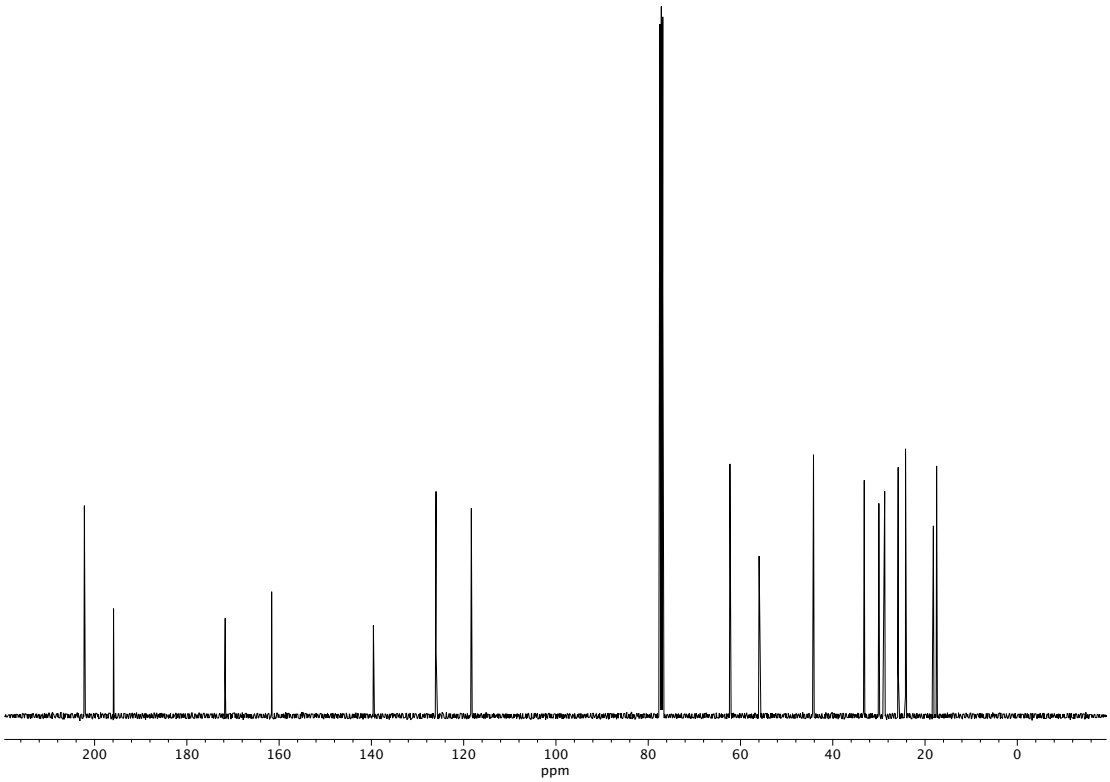

Figure A1.198. *^{13}C NMR (100 MHz, $CDCl_3$) of compound* ***163.***

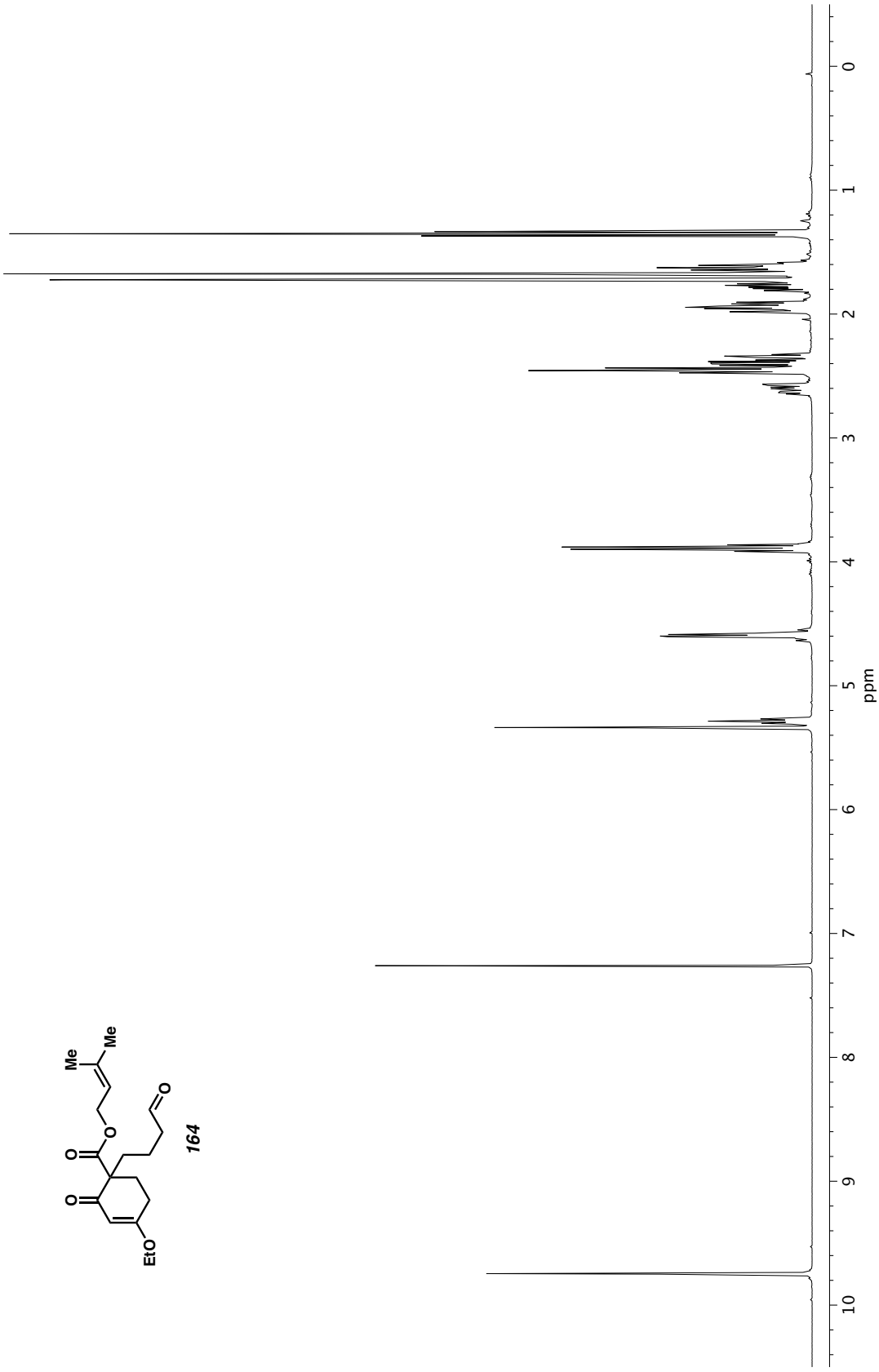

Figure A1.199. *^{1}H NMR (400 MHz, $CDCl_3$) of compound* ***164.***

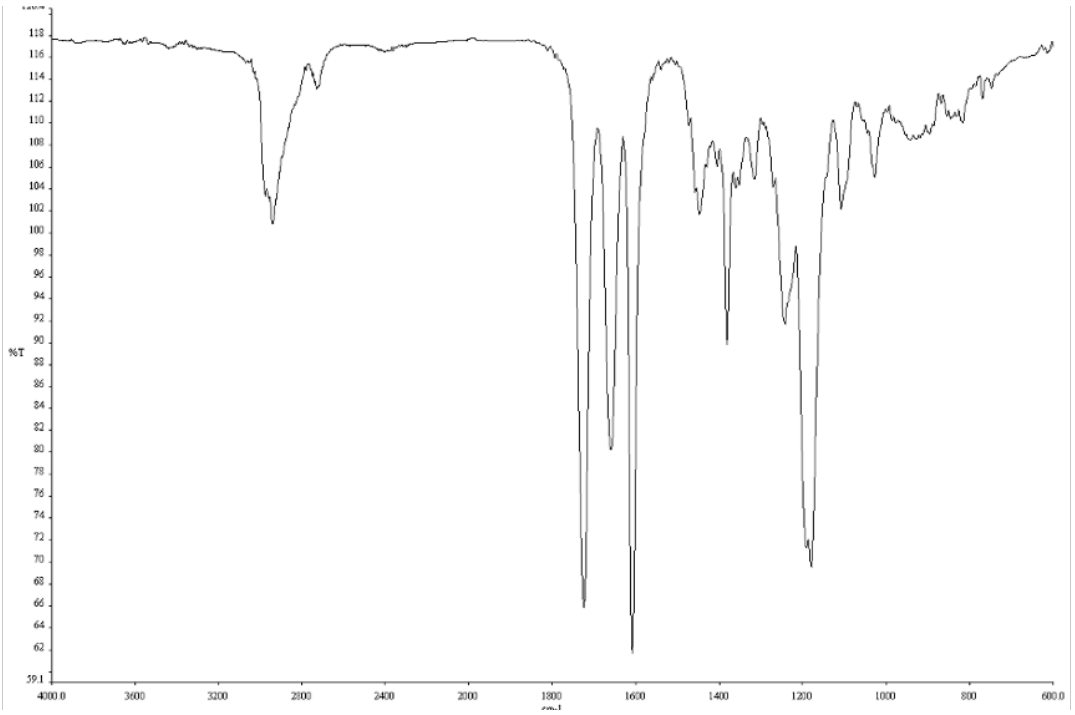

Figure A1.200. *Infrared spectrum (Thin Film, NaCl) of compound* ***164.***

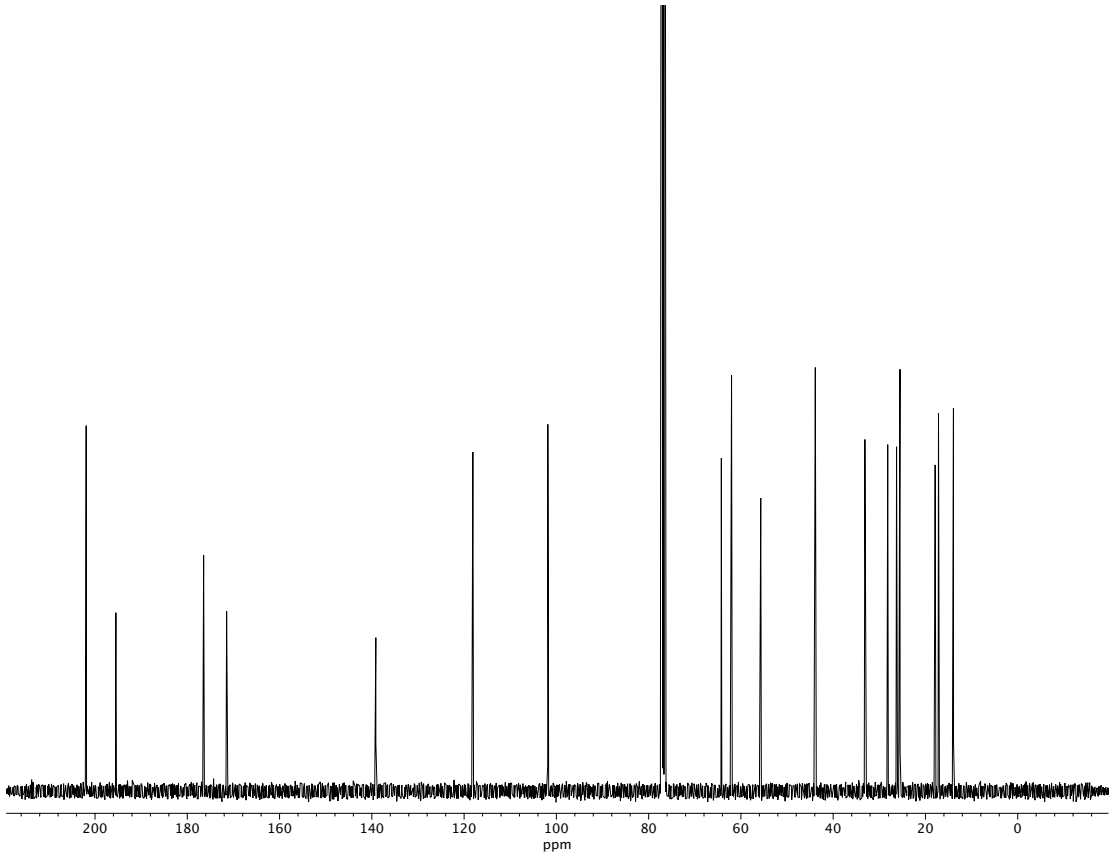

Figure A1.201. *^{13}C NMR (100 MHz, $CDCl_3$) of compound* ***164.***

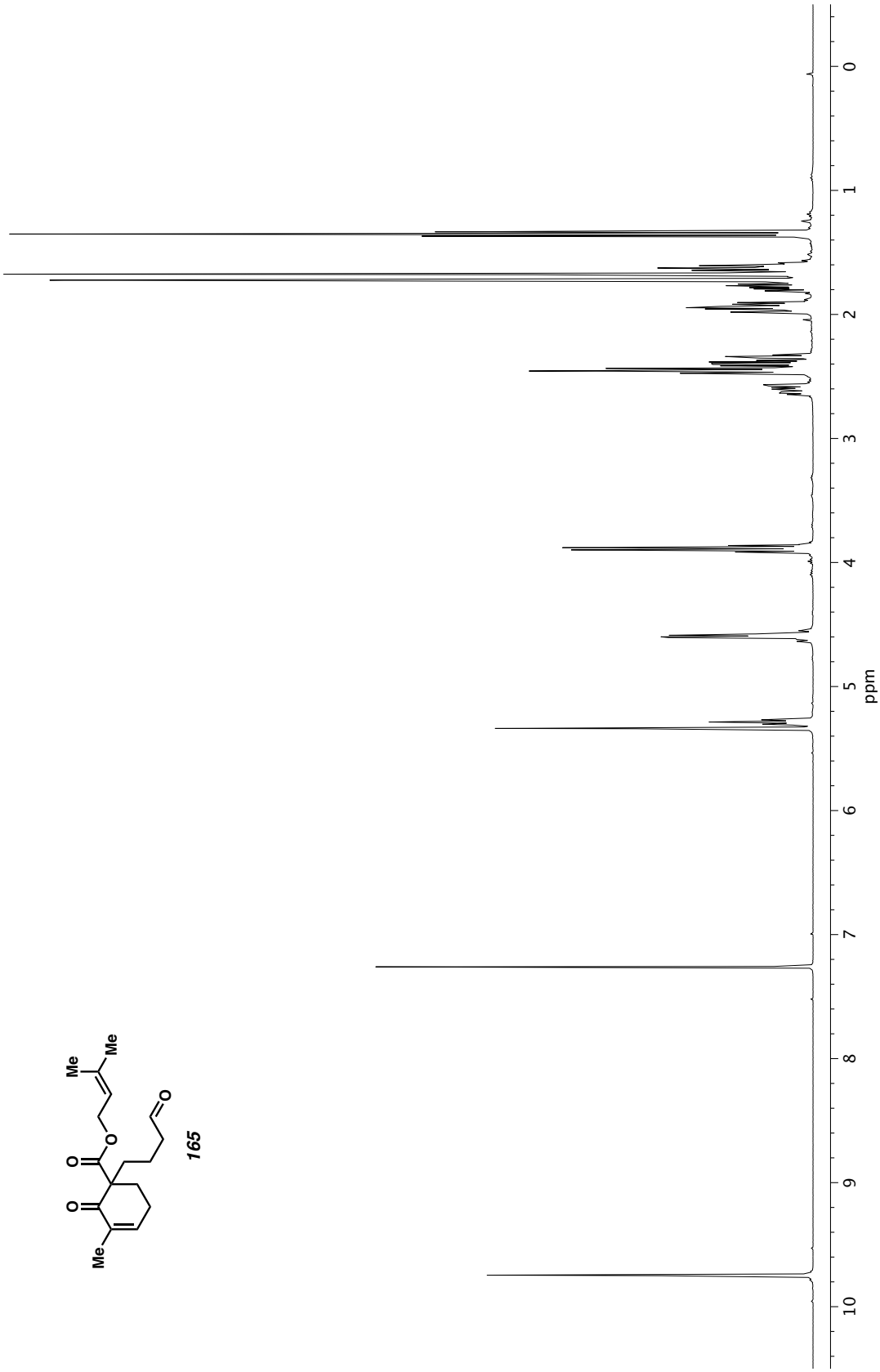

Figure A1.202. *^1H NMR (400 MHz, $CDCl_3$) of compound* ***165.***

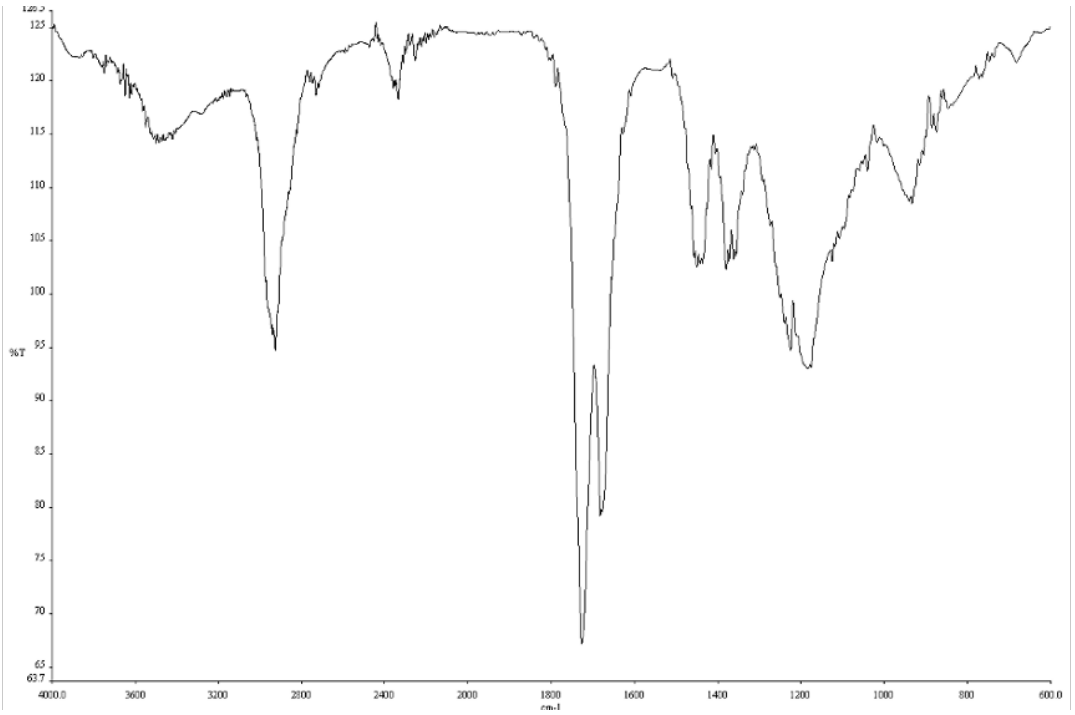

Figure A1.203. *Infrared spectrum (Thin Film, NaCl) of compound* ***165.***

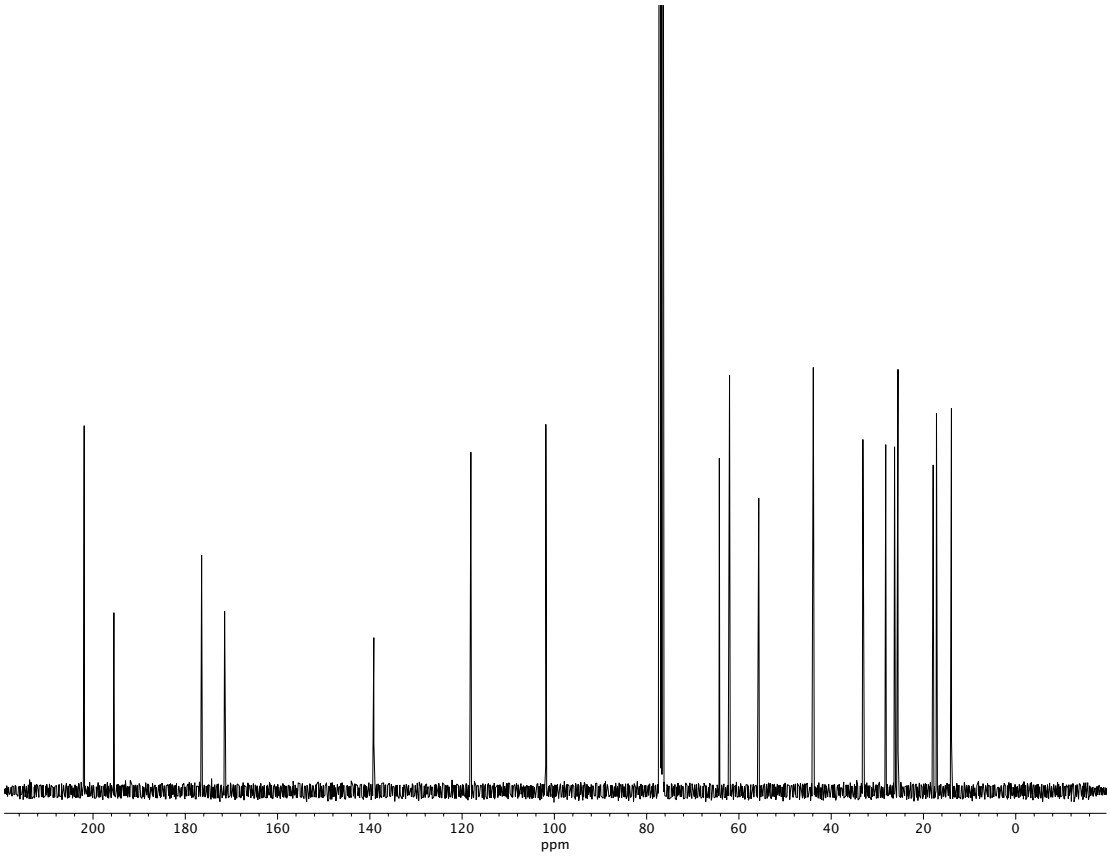

Figure A1.204. *^{13}C NMR (100 MHz, $CDCl_3$) of compound* ***165.***

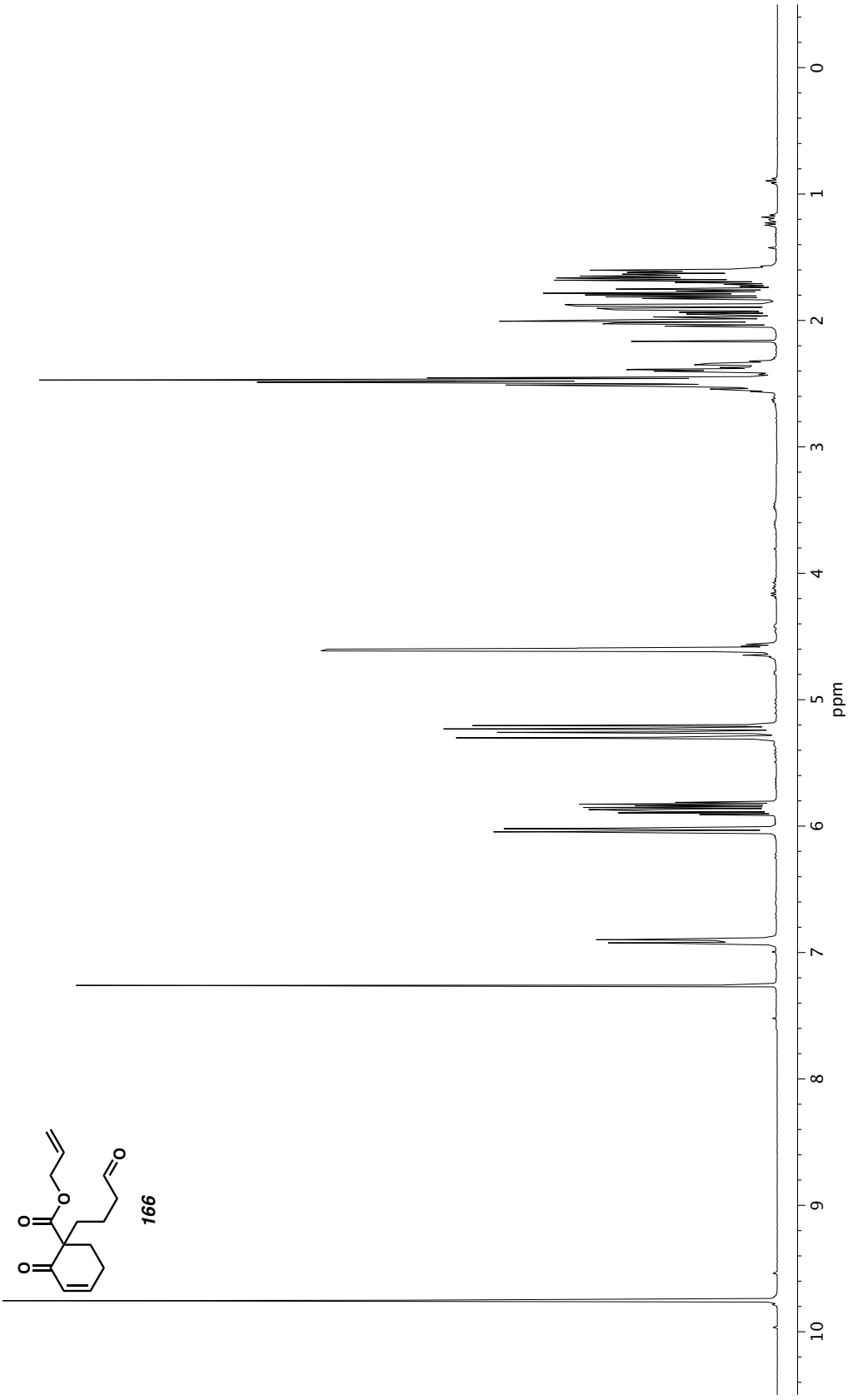

Figure A1.205. *^1H NMR (400 MHz, $CDCl_3$) of compound* ***166.***

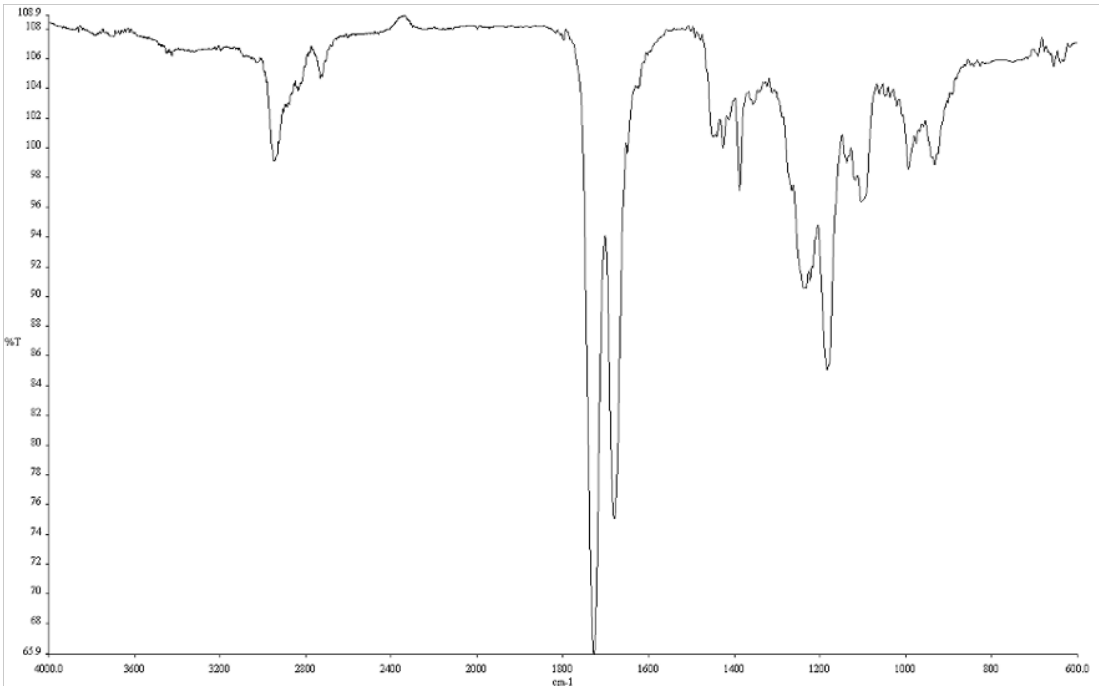

Figure A1.206. *Infrared spectrum (Thin Film, NaCl) of compound* ***166.***

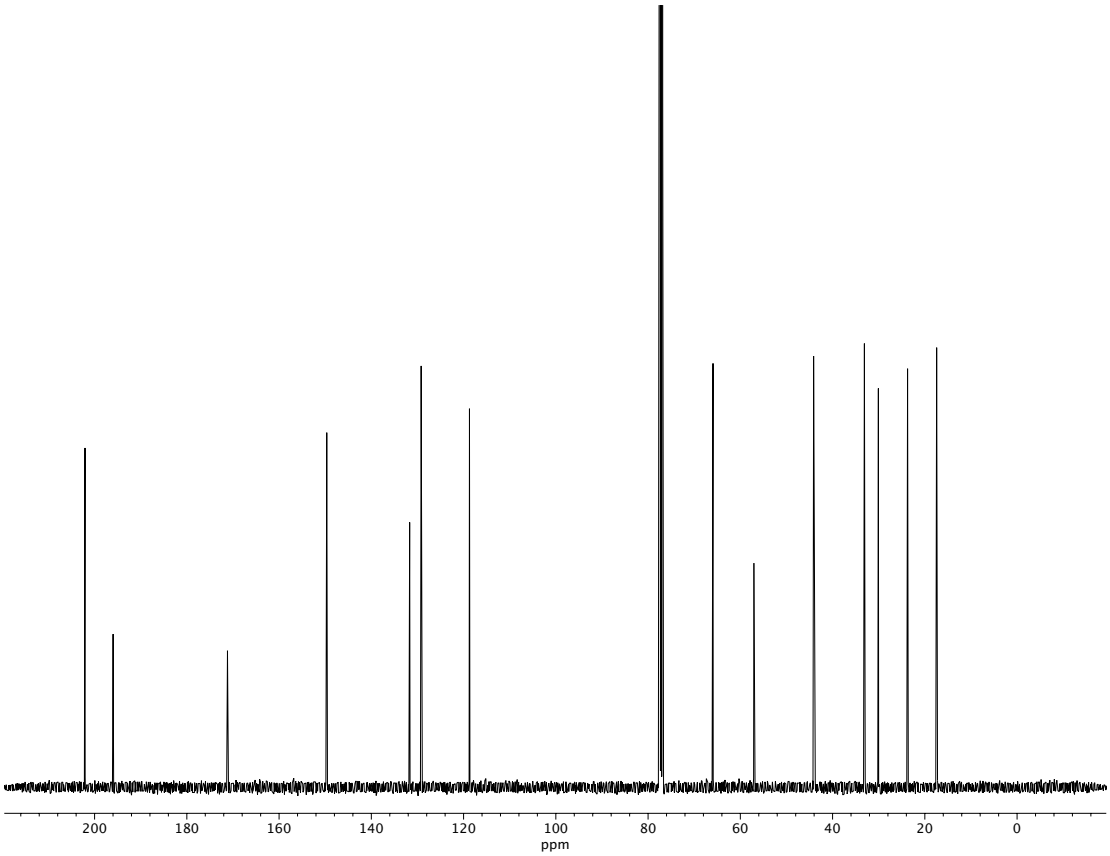

Figure A1.207. *^{13}C NMR (100 MHz, $CDCl_3$) of compound* ***166.***

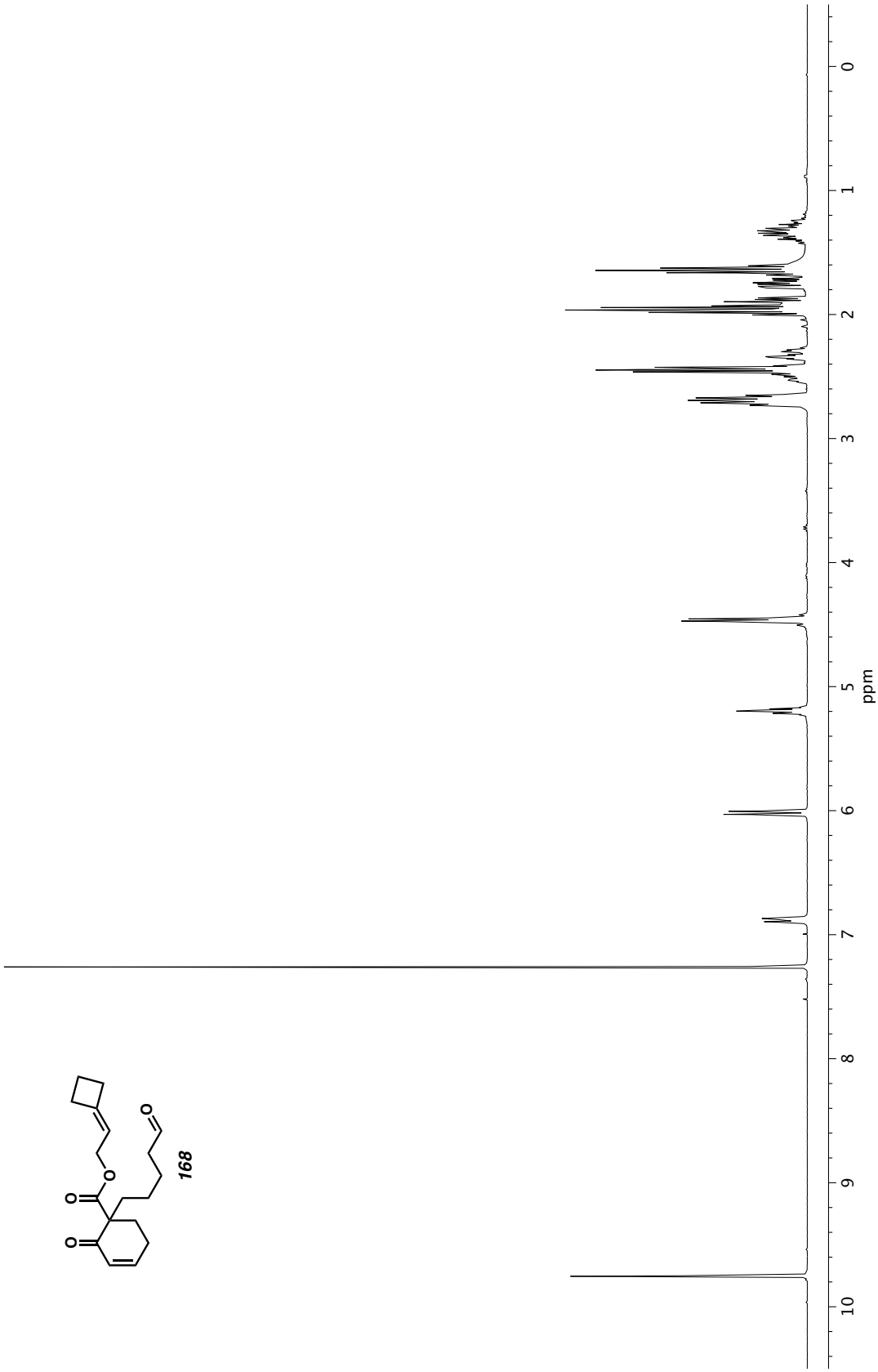

Figure A1.208. *^1H NMR (400 MHz, $CDCl_3$) of compound* ***168.***

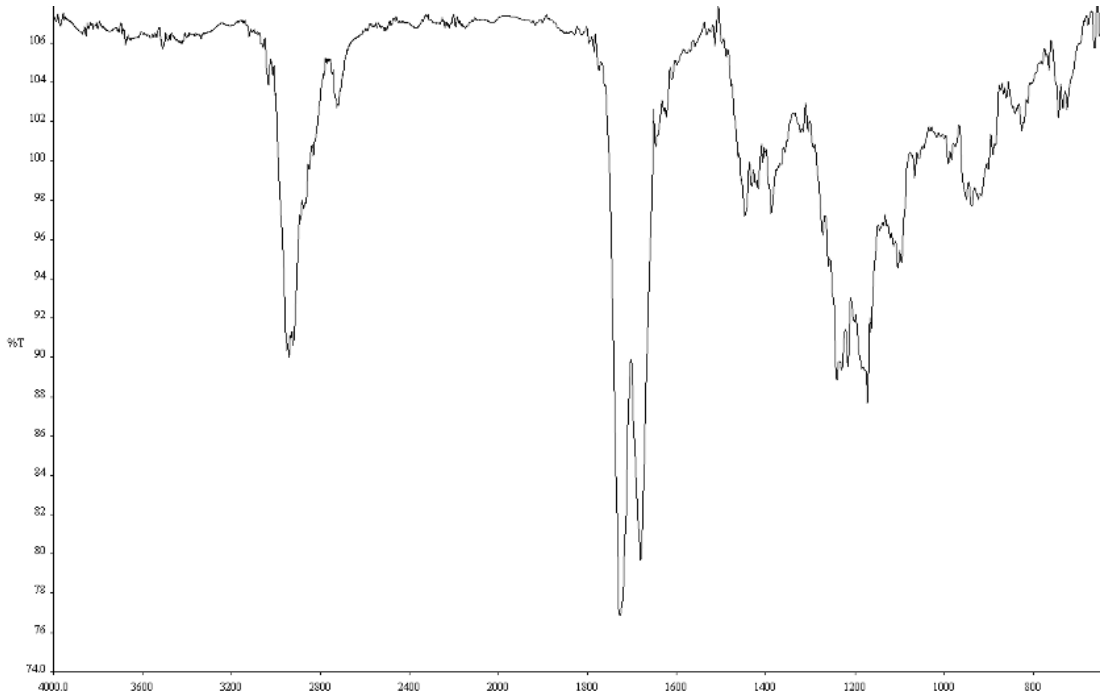

Figure A1.209. *Infrared spectrum (Thin Film, NaCl) of compound* ***168.***

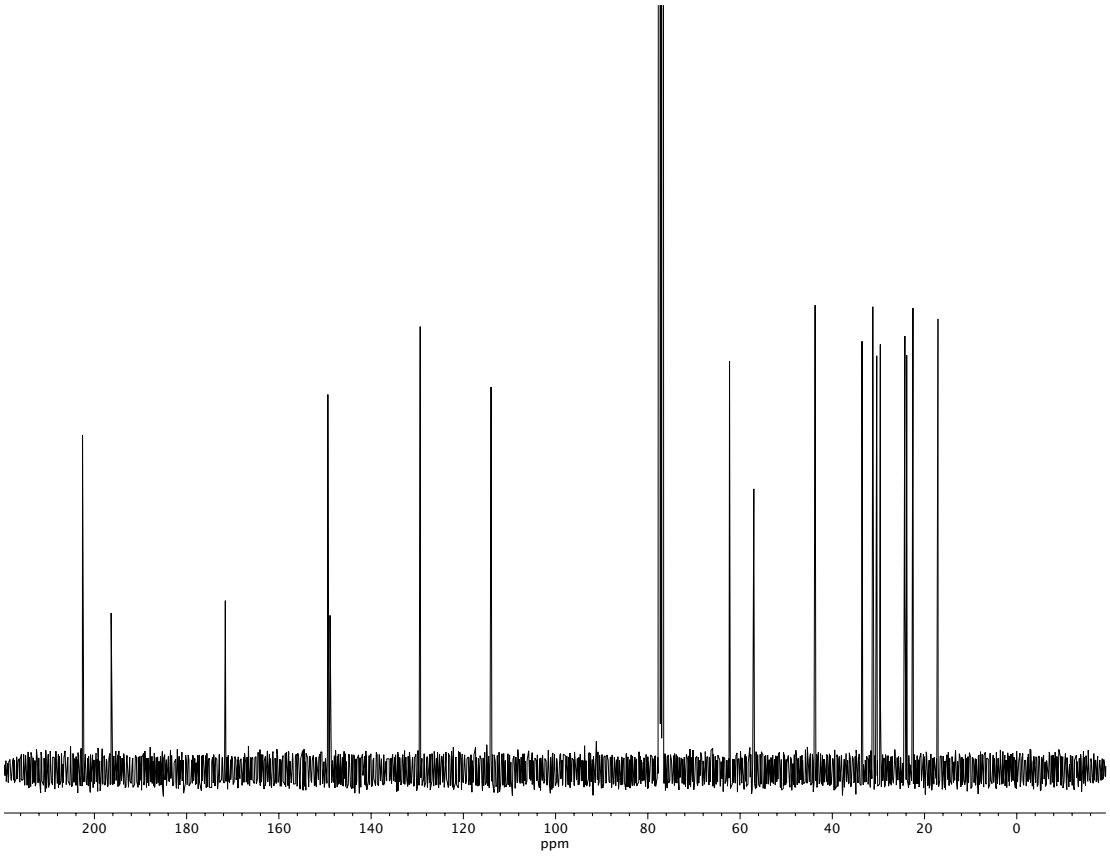

Figure A1.210. *^{13}C NMR (100 MHz, $CDCl_3$) of compound* ***168.***

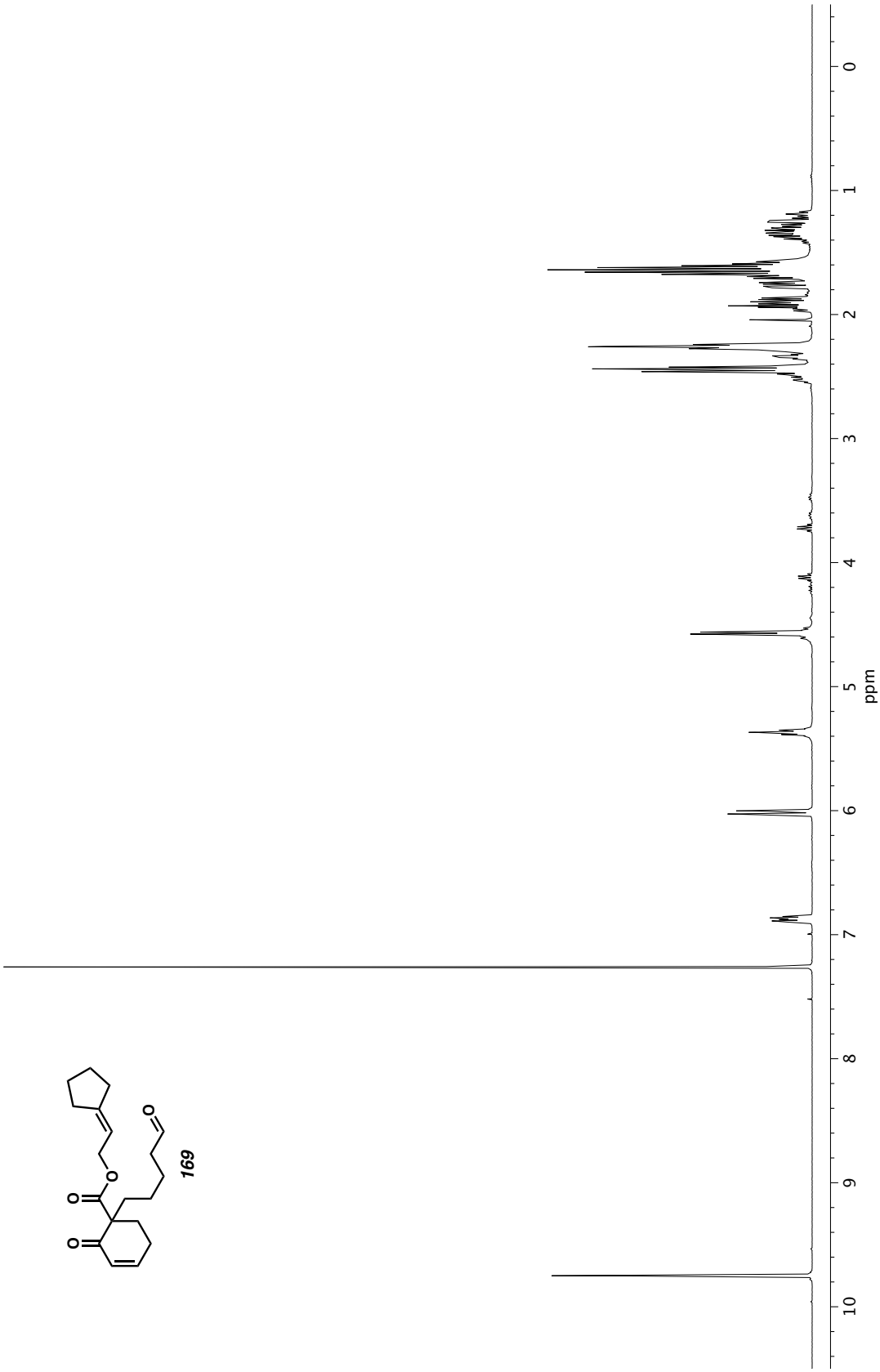

Figure A1.211. *^1H NMR (400 MHz, $CDCl_3$) of compound* ***169.***

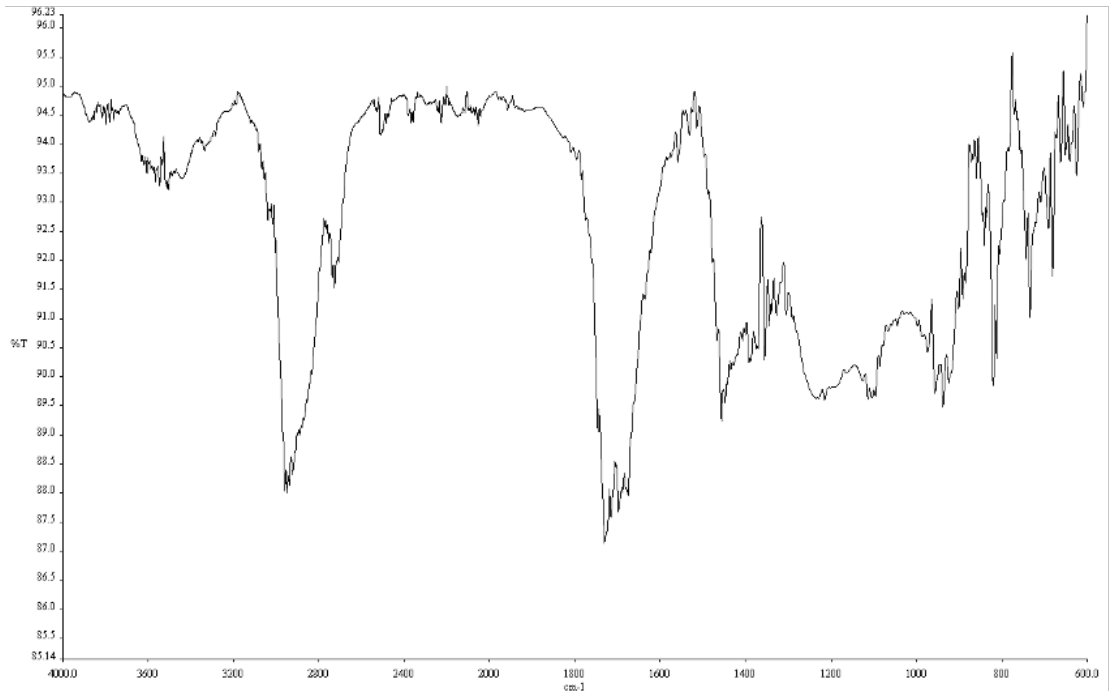

Figure A1.212. *Infrared spectrum (Thin Film, NaCl) of compound* ***169.***

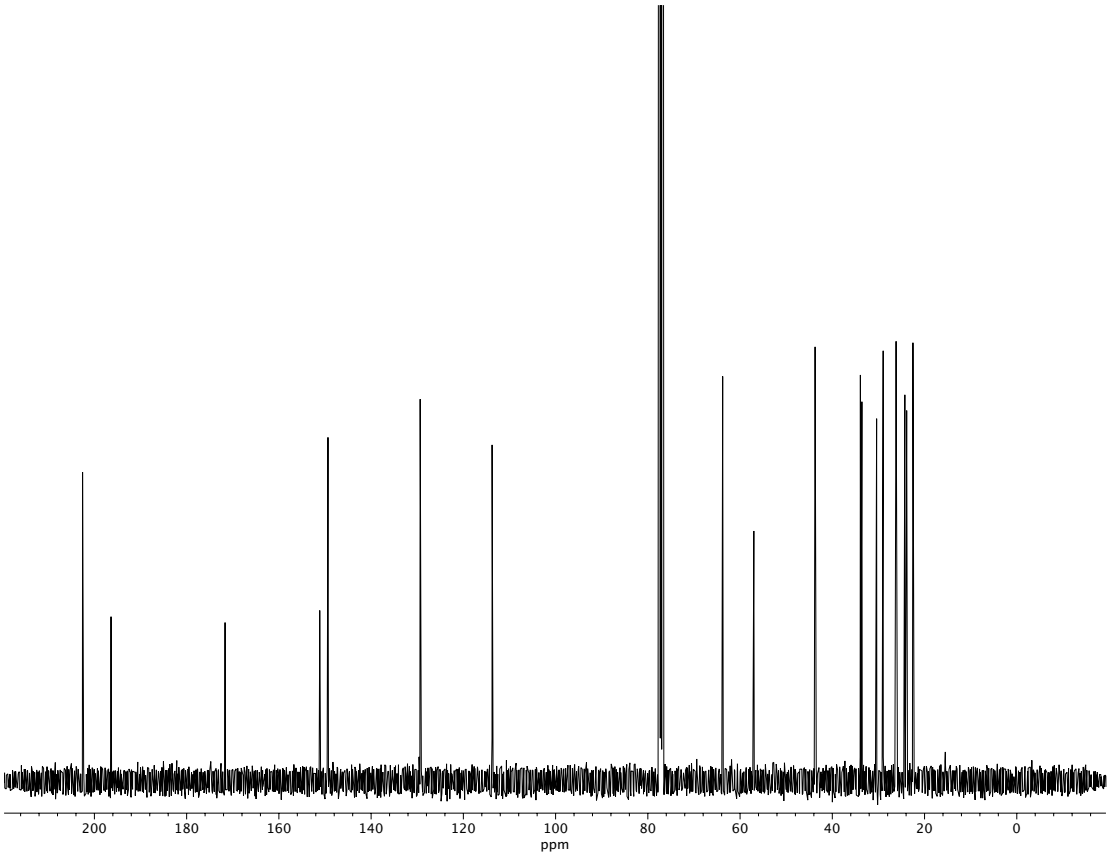

Figure A1.213. *^{13}C NMR (100 MHz, $CDCl_3$) of compound* ***169.***

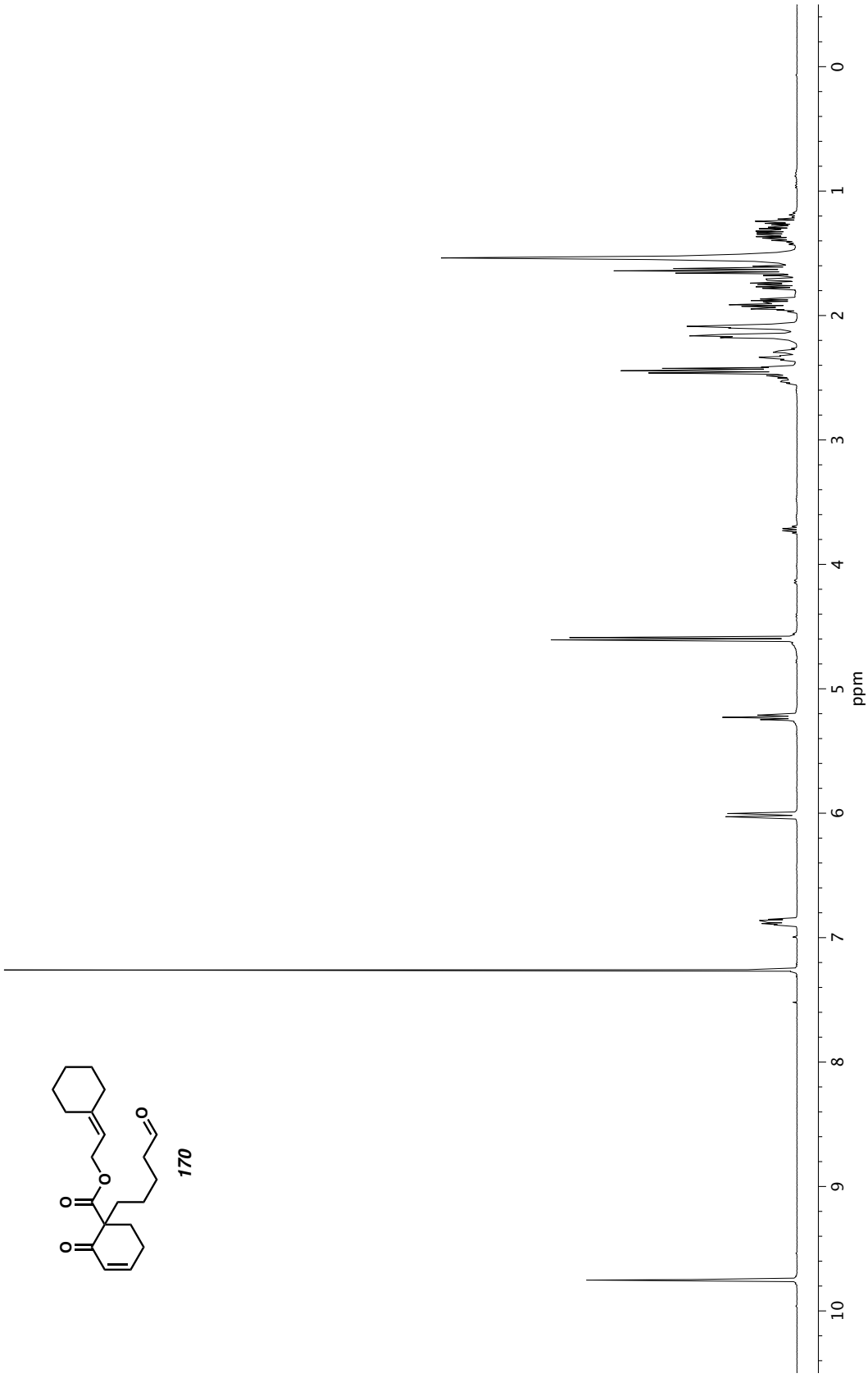

Figure A1.214. *^1H NMR (400 MHz, $CDCl_3$) of compound* ***170.***

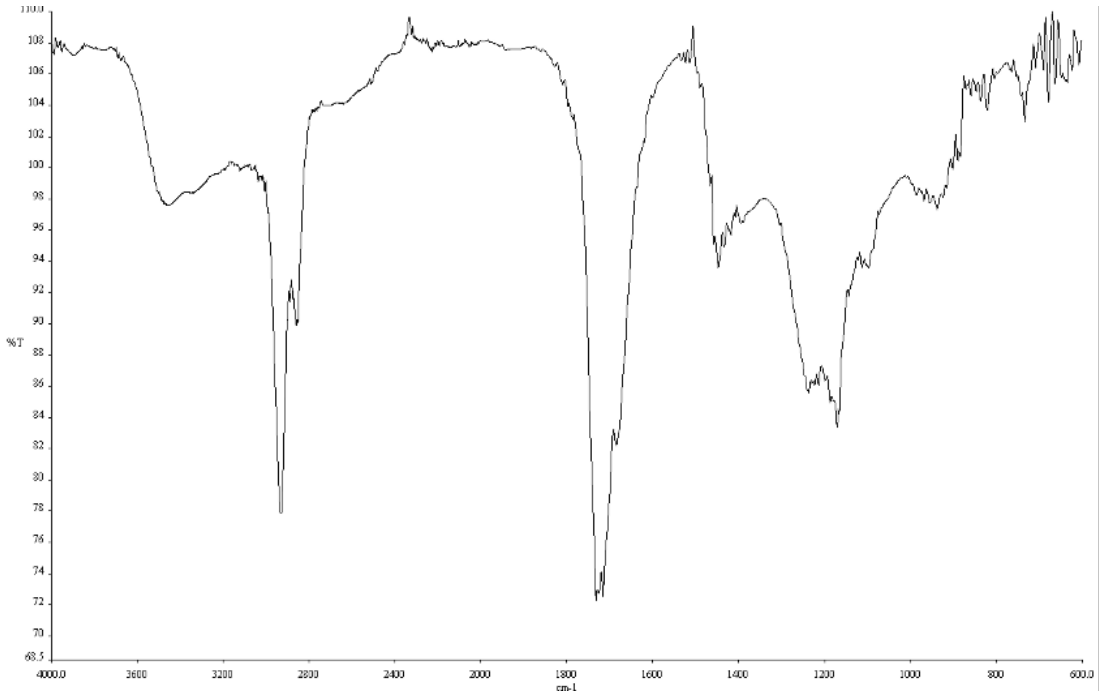

Figure A1.215. *Infrared spectrum (Thin Film, NaCl) of compound* ***170.***

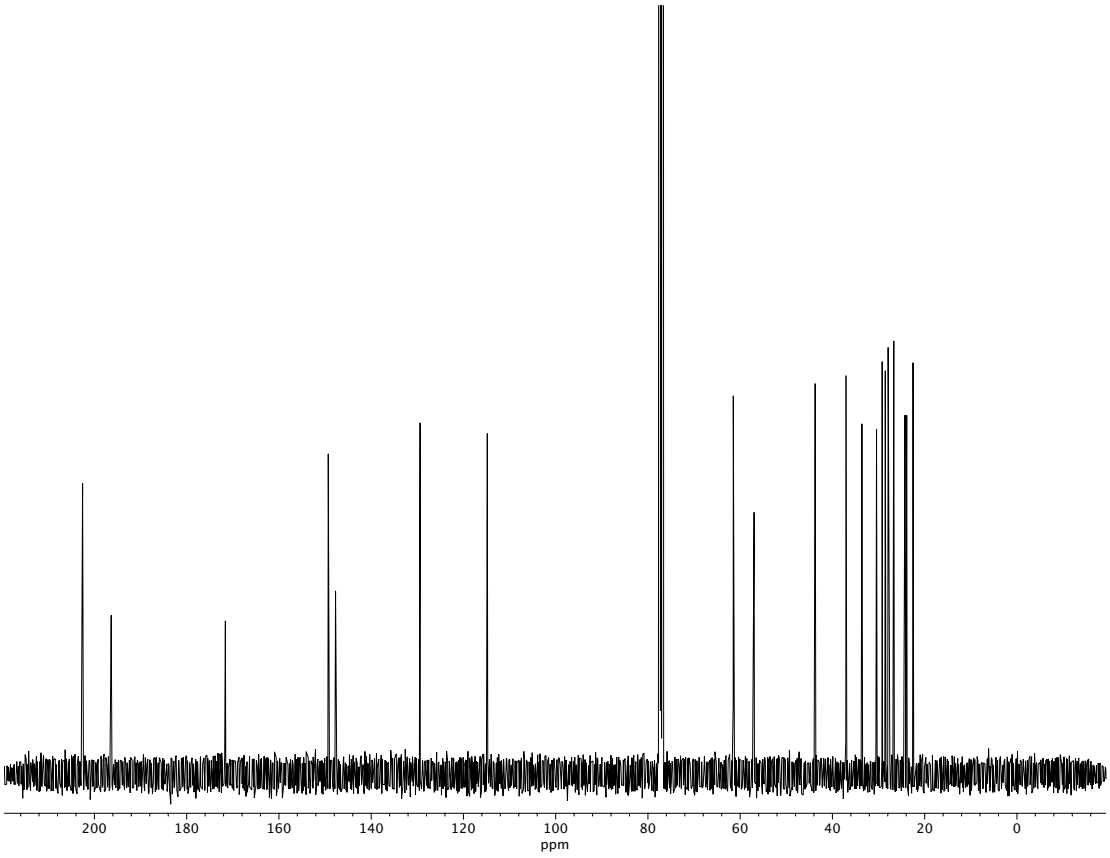

Figure A1.216. *^{13}C NMR (100 MHz, $CDCl_3$) of compound* ***170.***

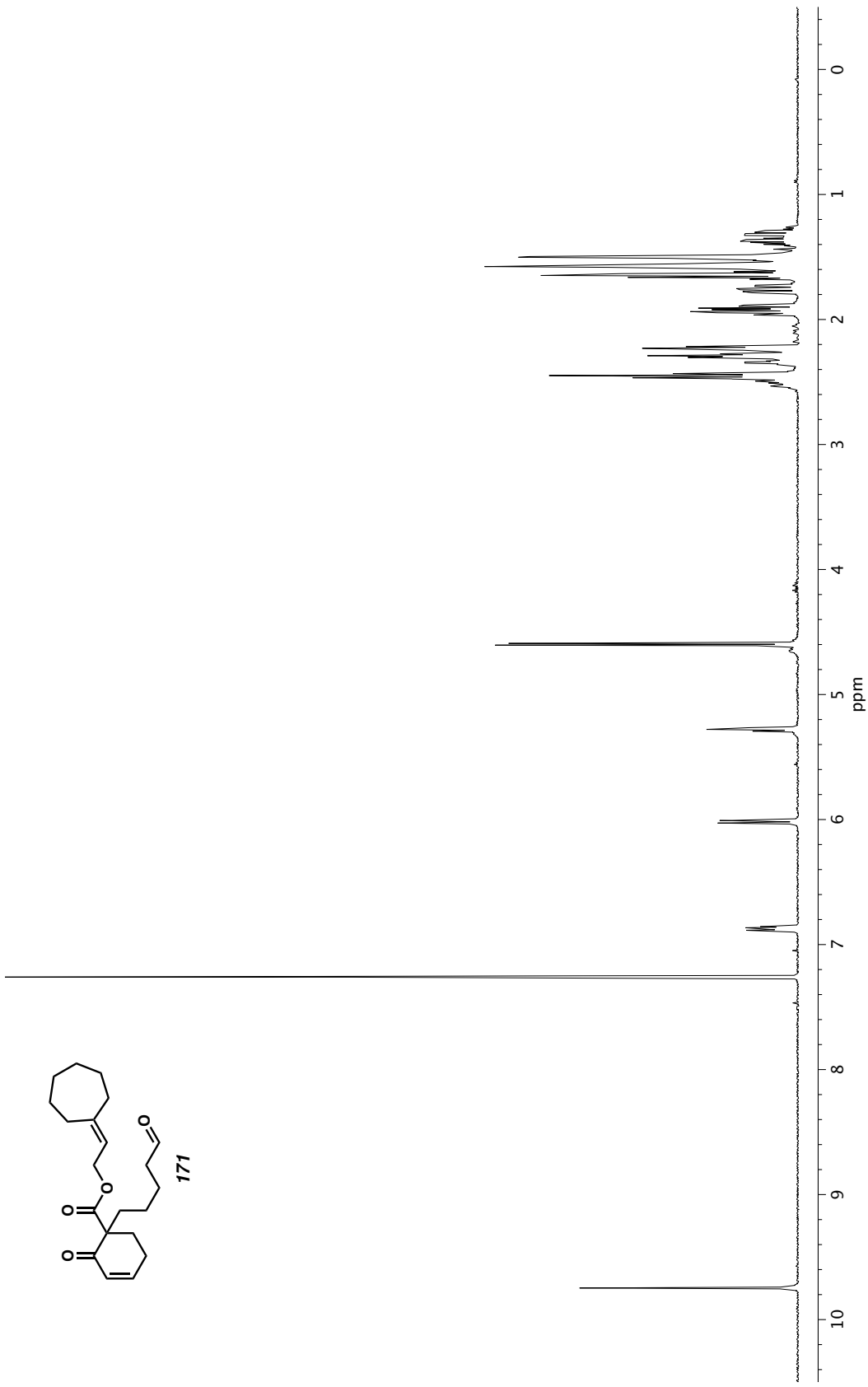

Figure A1.217. *^1H NMR (400 MHz, $CDCl_3$) of compound* ***171.***

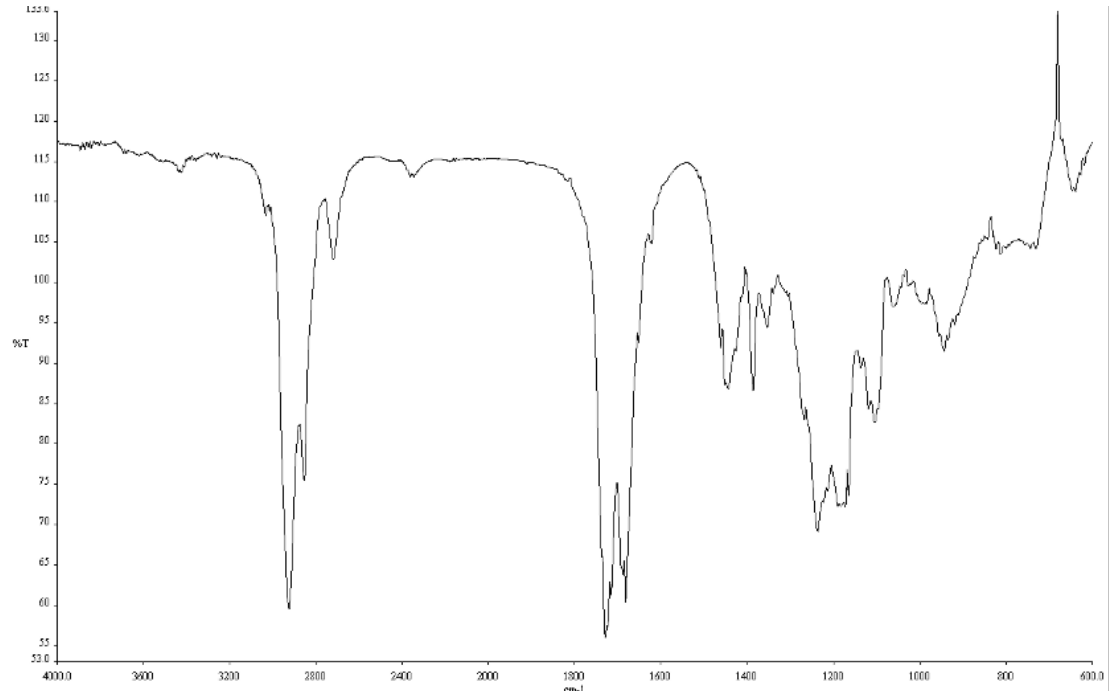

Figure A1.218. *Infrared spectrum (Thin Film, NaCl) of compound* ***171.***

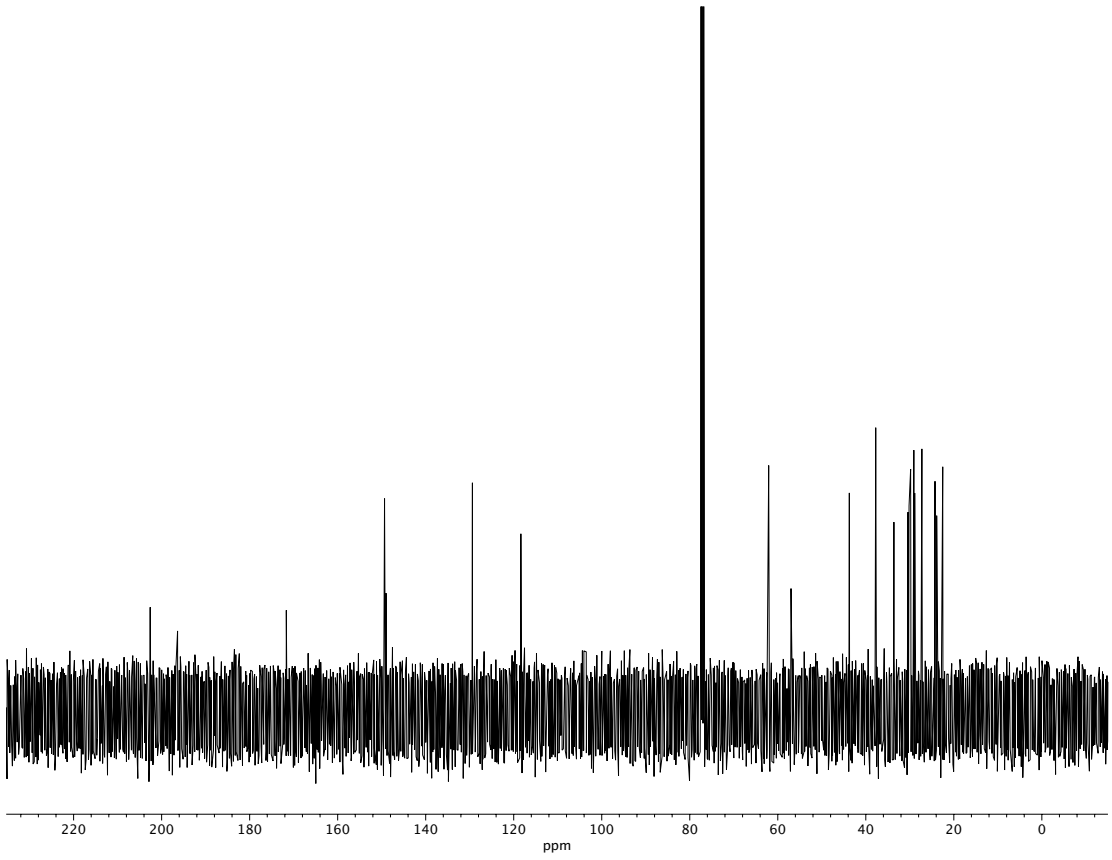

Figure A1.219. *^{13}C NMR (100 MHz, $CDCl_3$) of compound* ***171.***

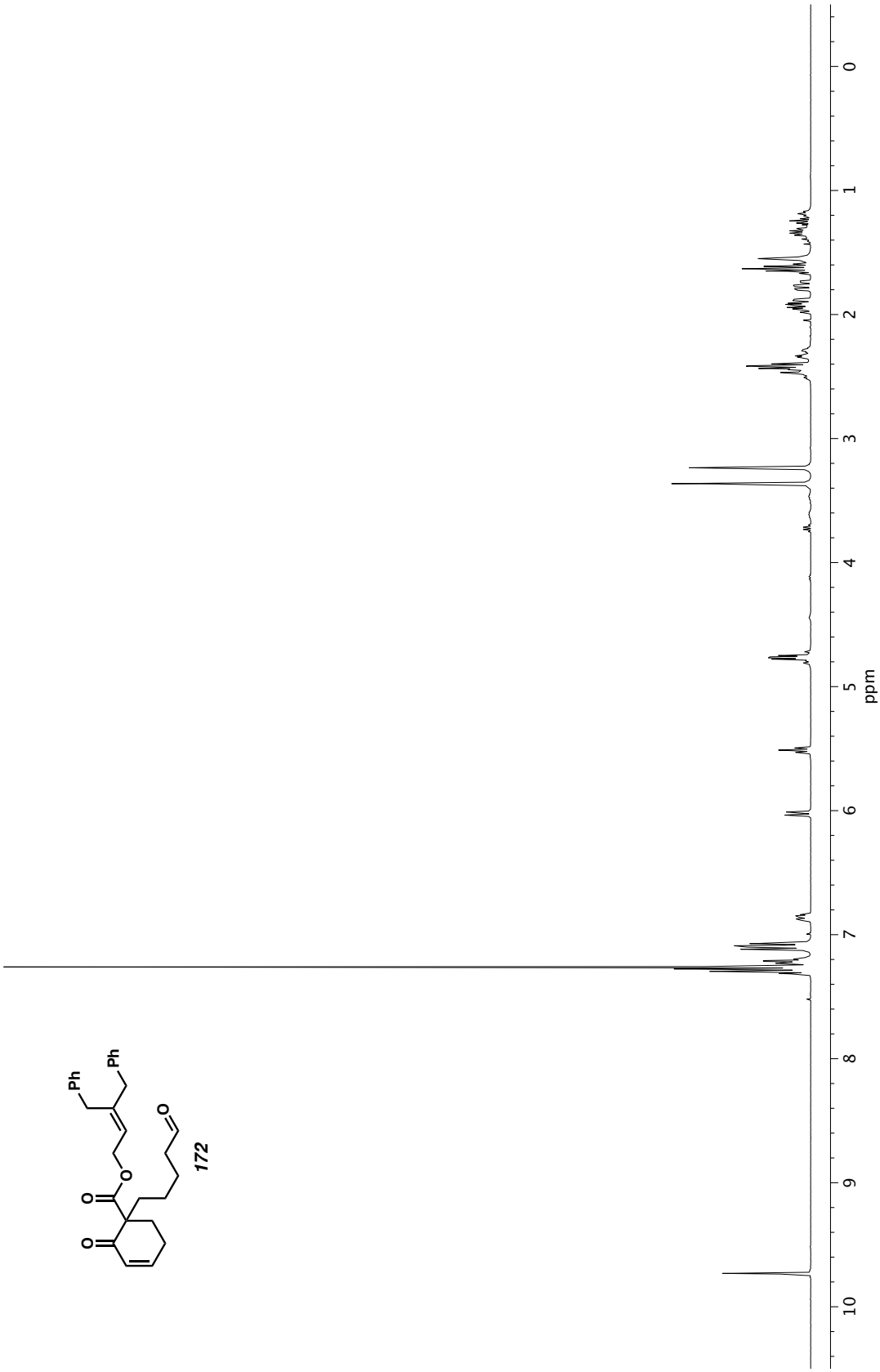

Figure A1.220. *^1H NMR (400 MHz, $CDCl_3$) of compound* ***172.***

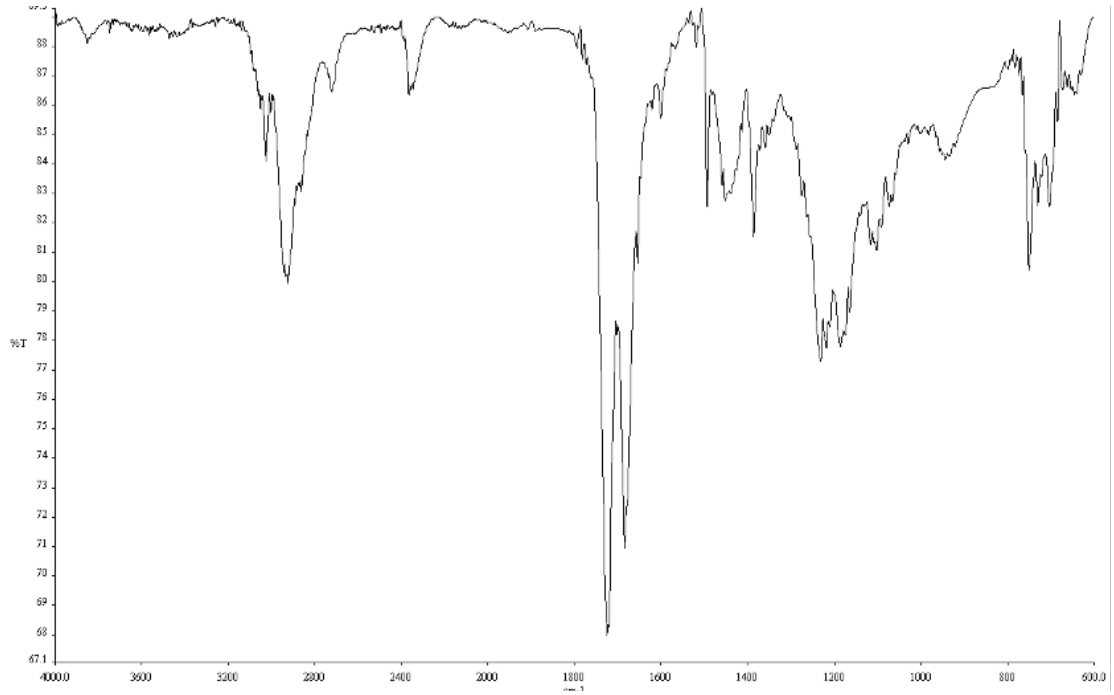

Figure A1.221. *Infrared spectrum (Thin Film, NaCl) of compound* ***172.***

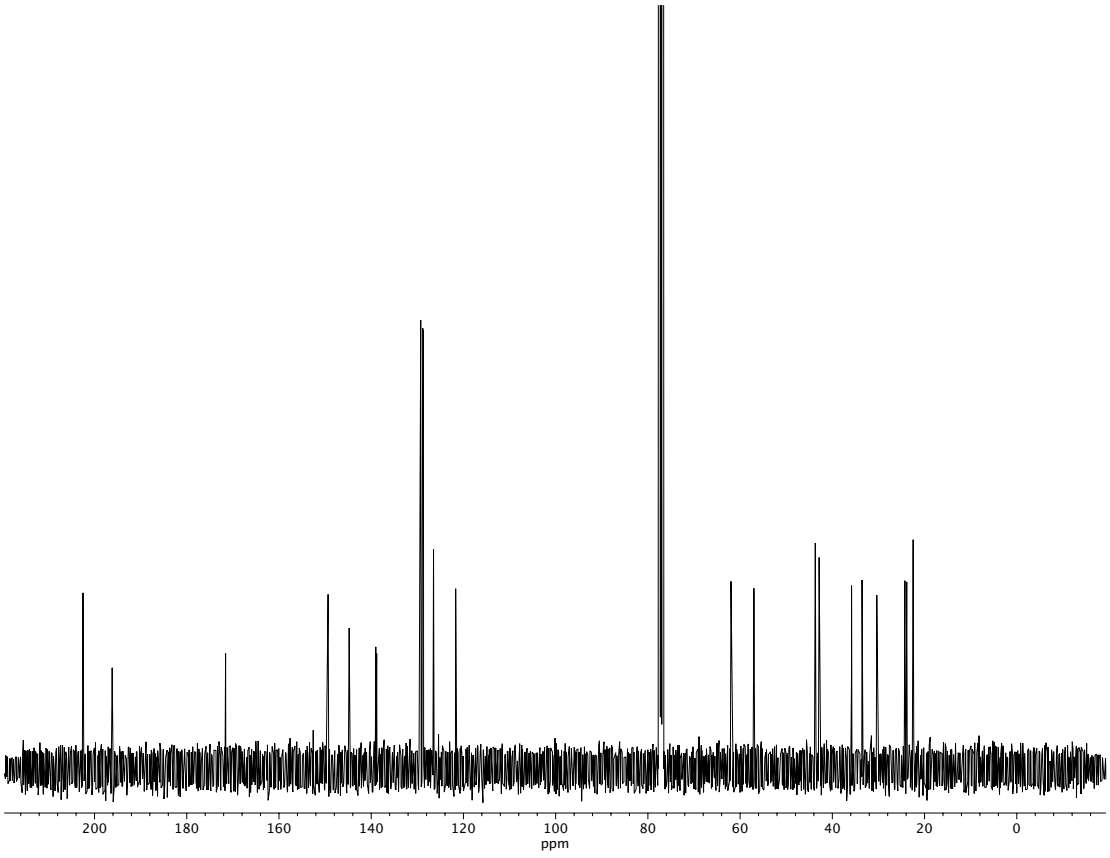

Figure A1.222. *^{13}C NMR (100 MHz, $CDCl_3$) of compound* ***172.***

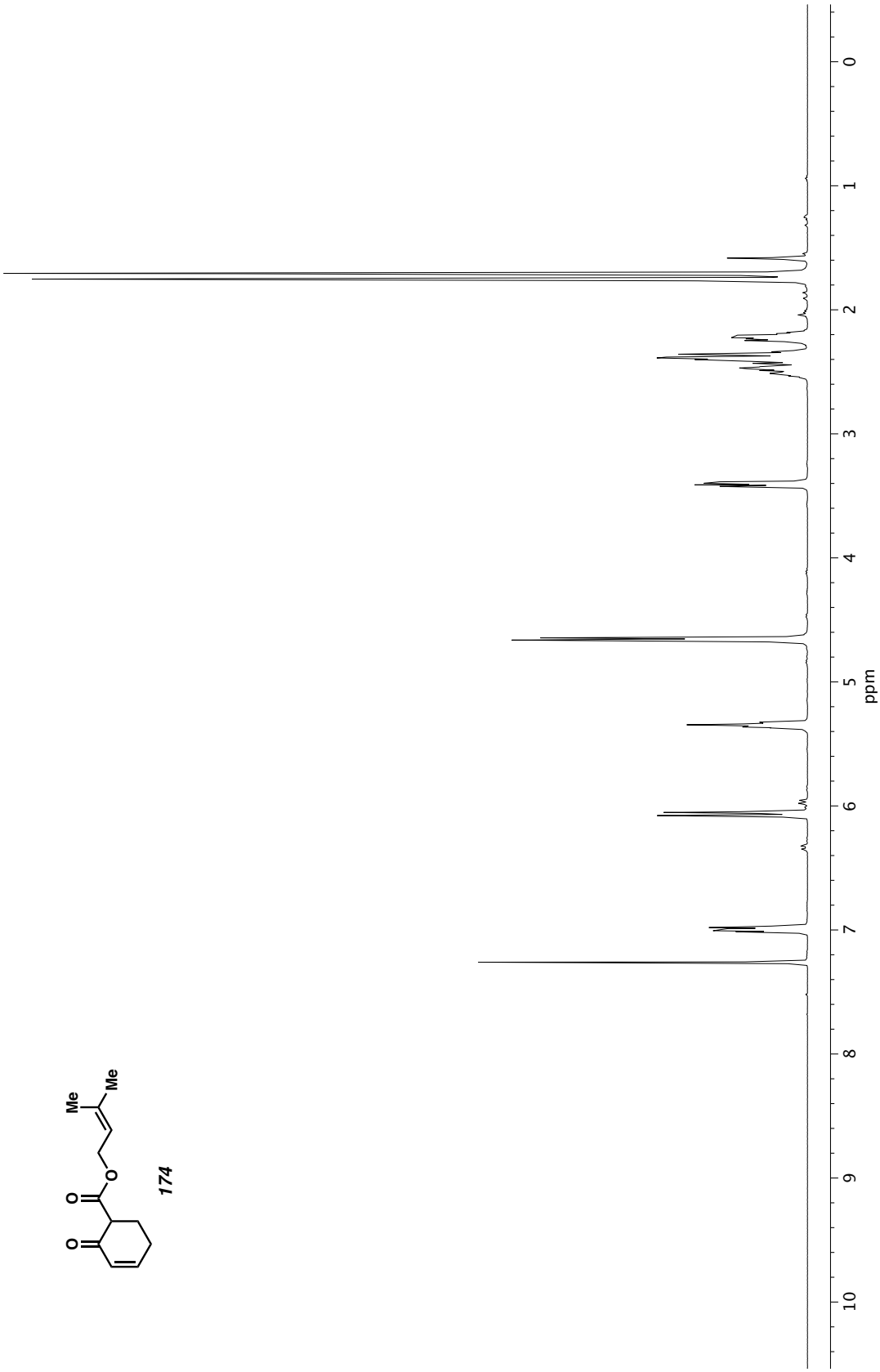

Figure A1.223. *^1H NMR (400 MHz, $CDCl_3$) of compound* ***174.***

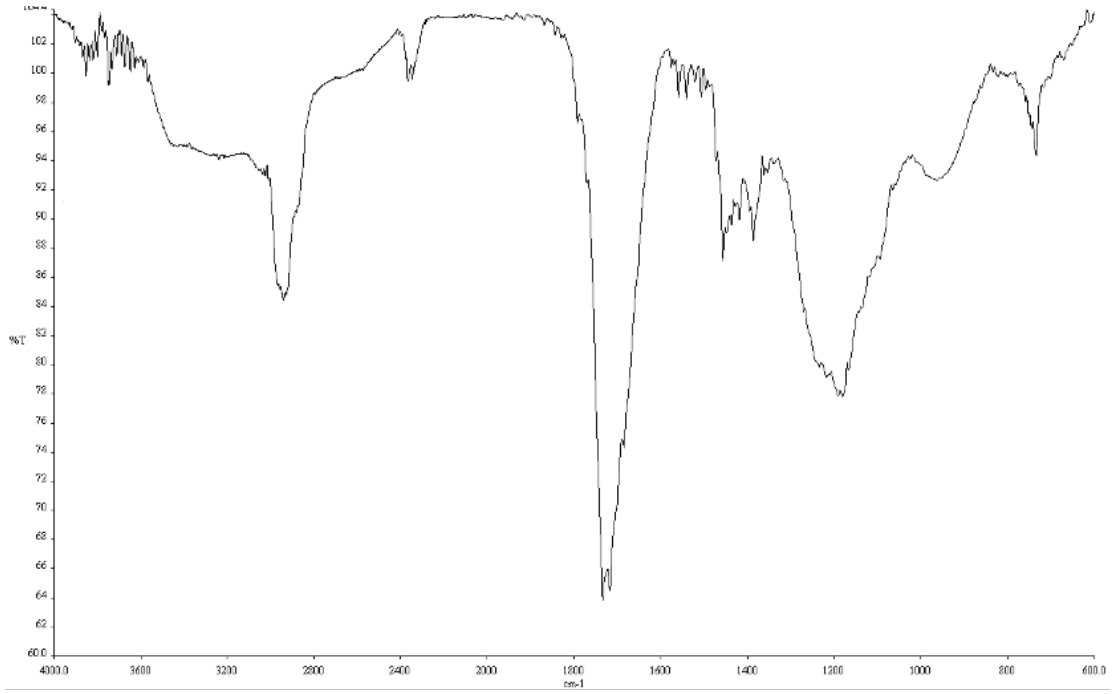

Figure A1.224. *Infrared spectrum (Thin Film, NaCl) of compound* ***174.***

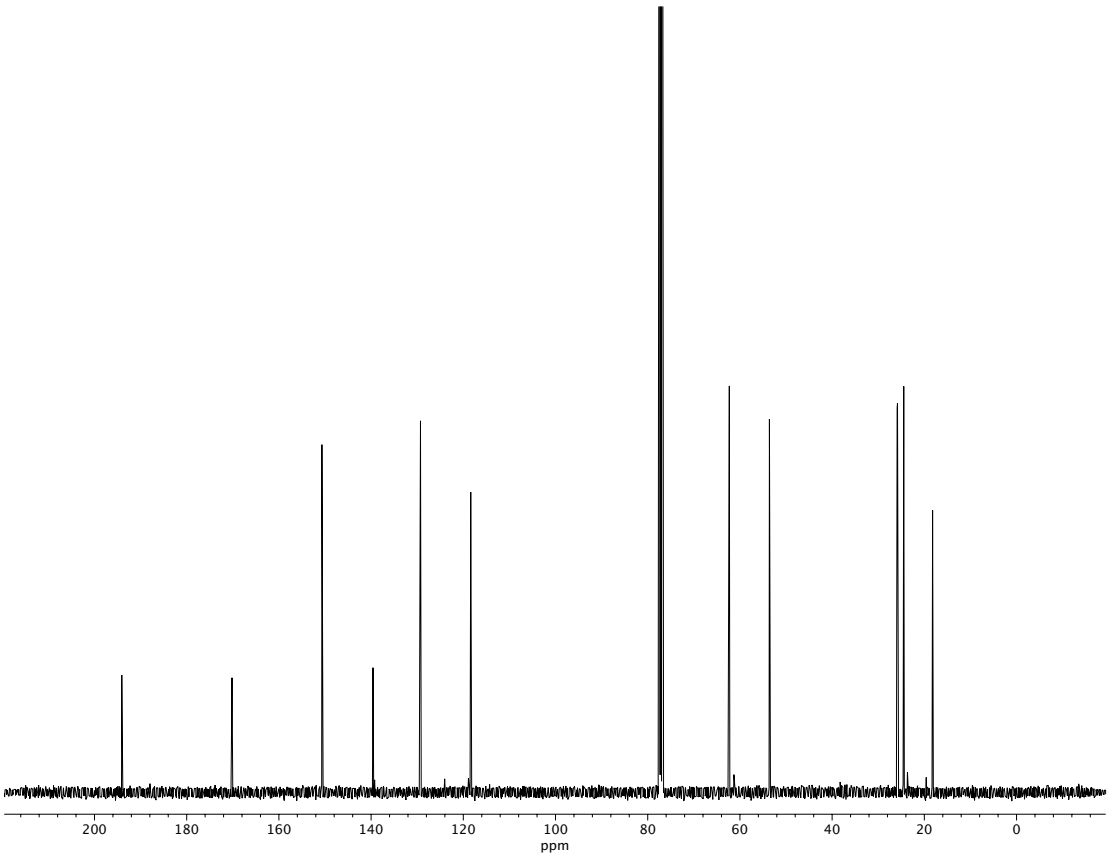

Figure A1.225. *^{13}C NMR (100 MHz, $CDCl_3$) of compound* ***174.***

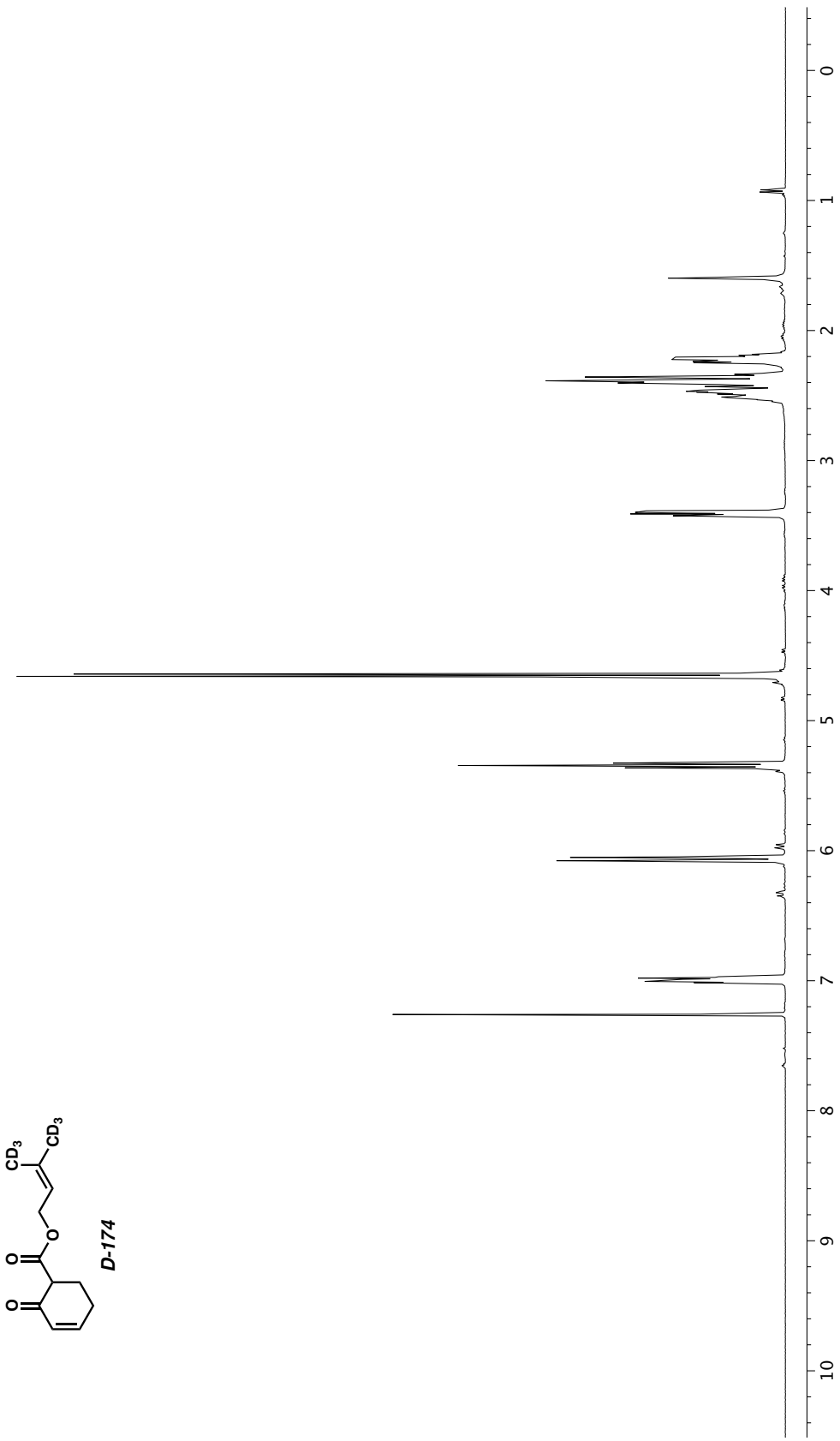

Figure A1.226. *^1H NMR (400 MHz, $CDCl_3$) of compound* ***D-174.***

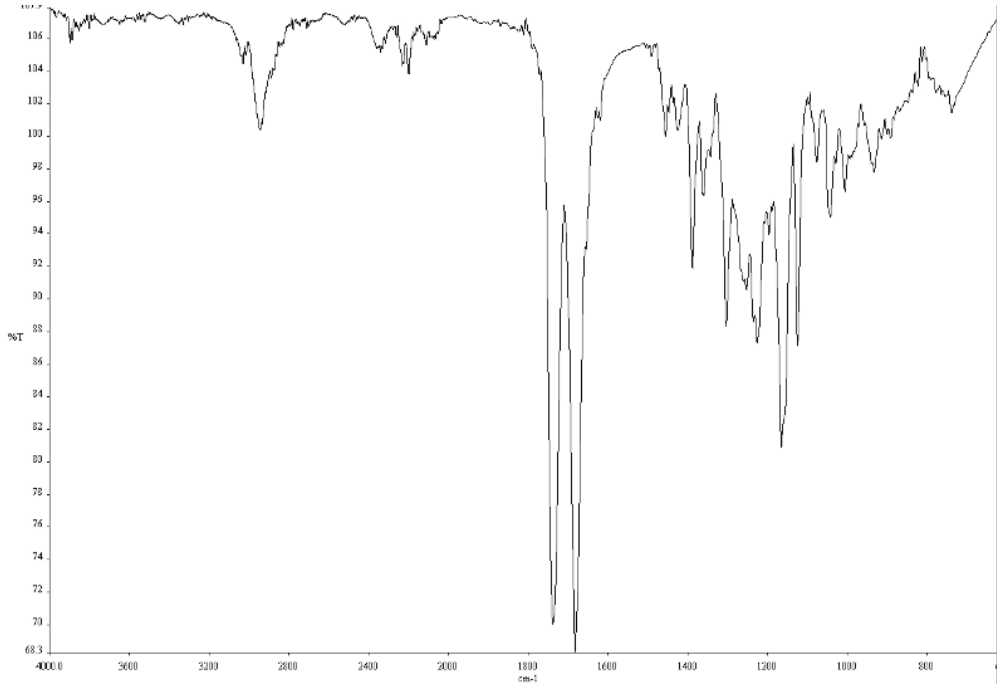

Figure A1.227. *Infrared spectrum (Thin Film, NaCl) of compound* ***D-174.***

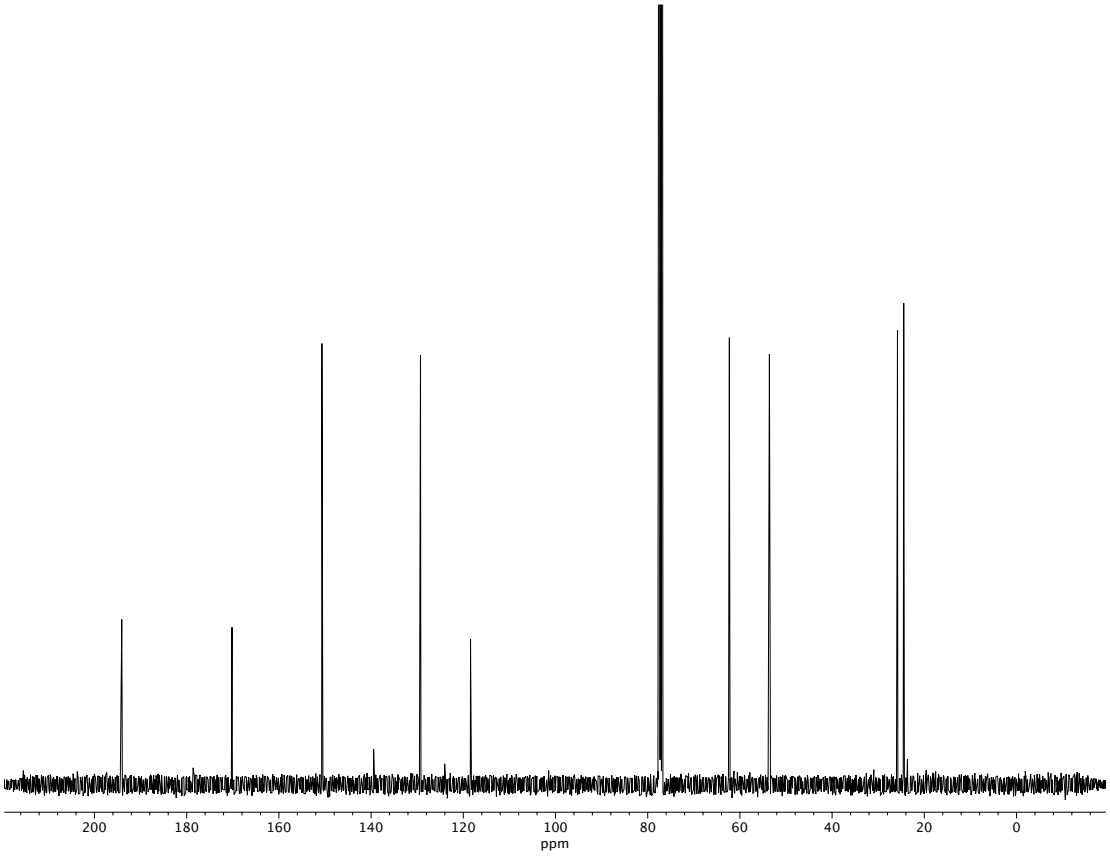

Figure A1.228. *^{13}C NMR (100 MHz, $CDCl_3$) of compound* ***D-174.***

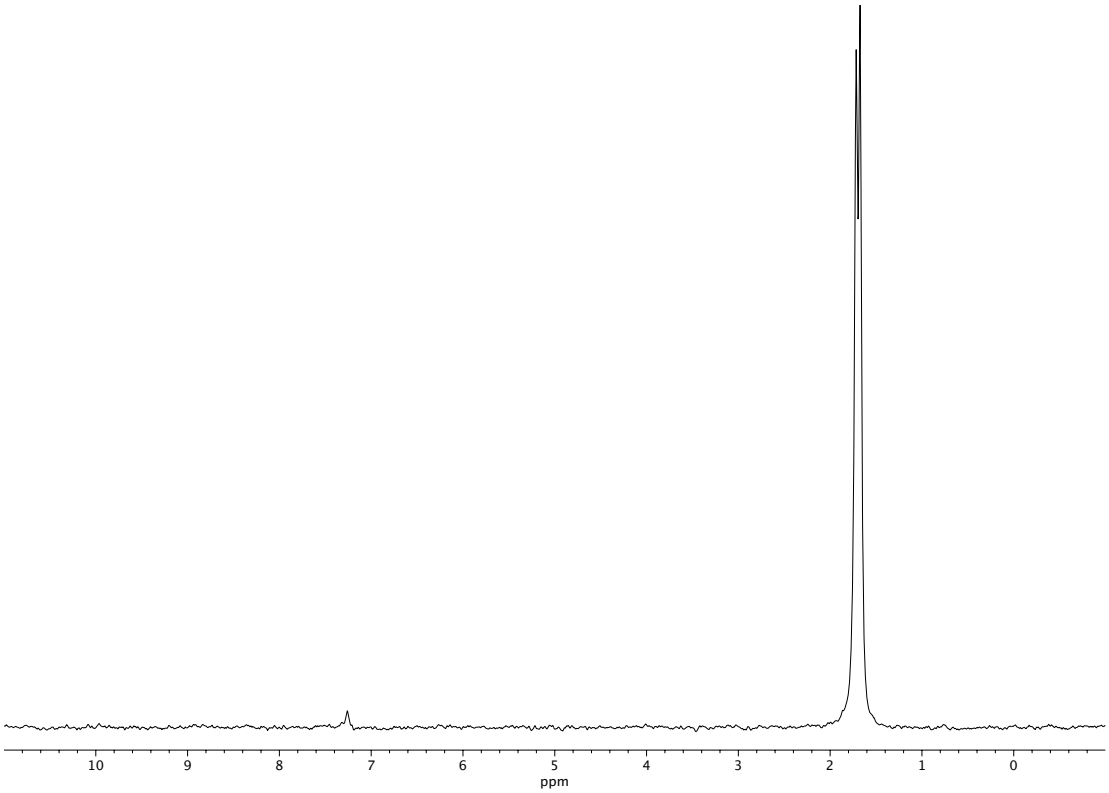

Figure A1.229. *^{2}H NMR (61 MHz, $CHCl_3$) of compound* ***D-174.***

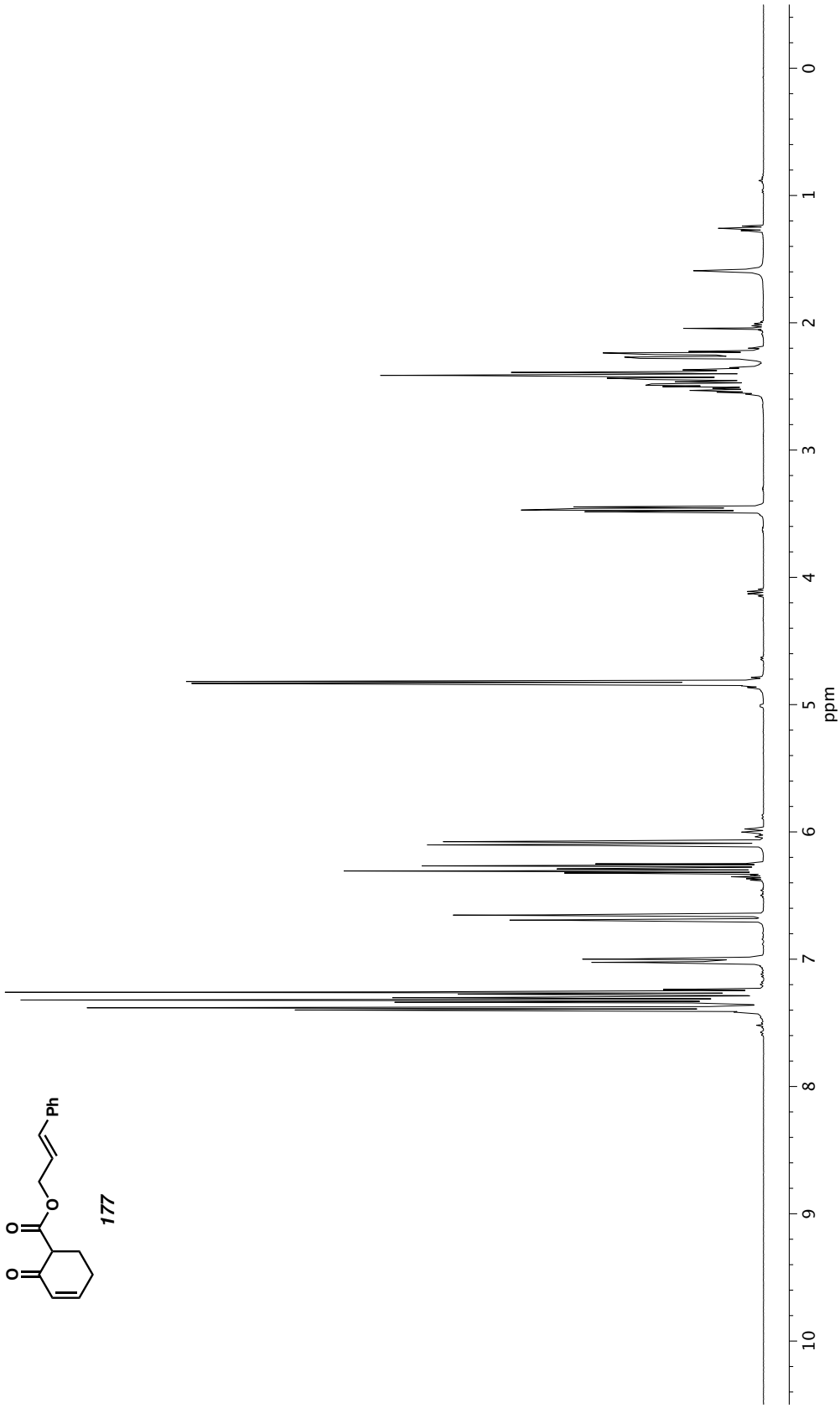

Figure A1.230. *^1H NMR (400 MHz, $CDCl_3$) of compound* ***177.***

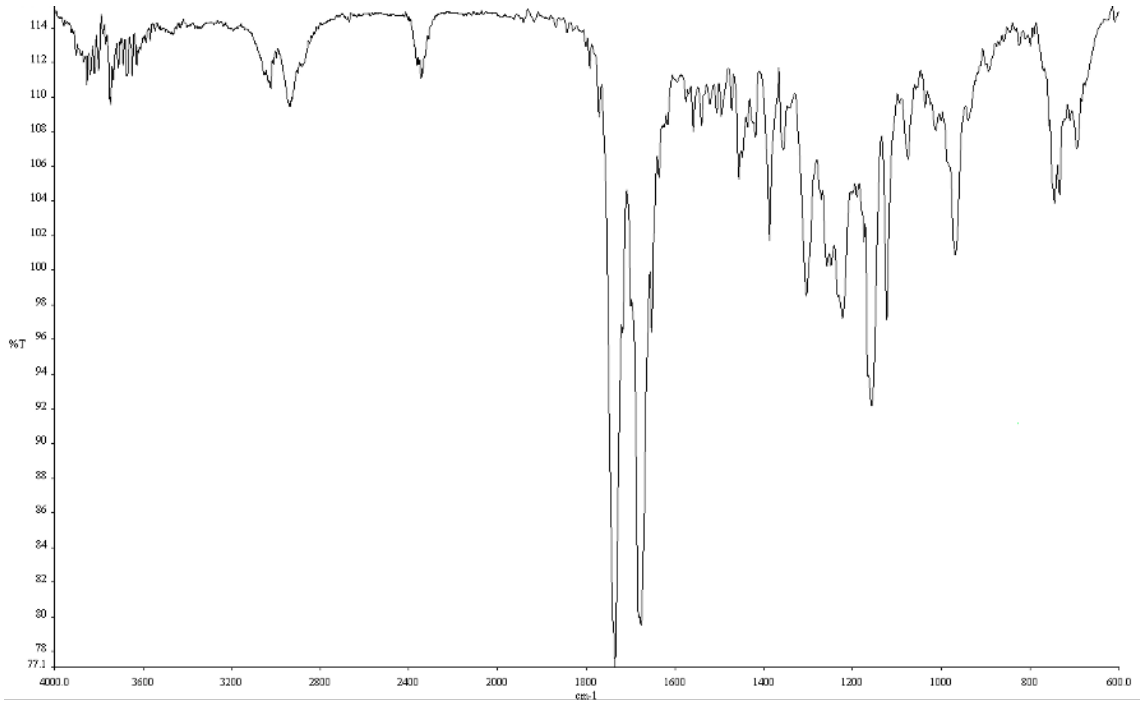

Figure A1.231. *Infrared spectrum (Thin Film, NaCl) of compound* ***177.***

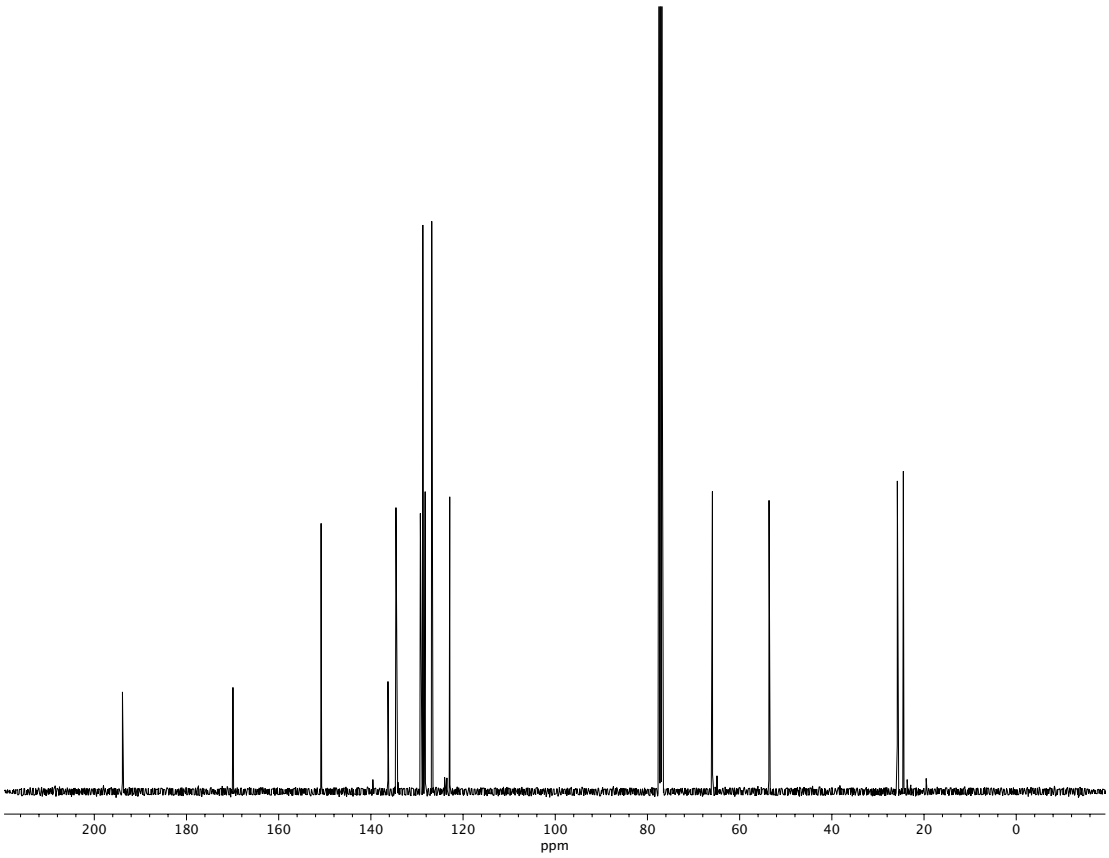

Figure A1.232. *^{13}C NMR (100 MHz, $CDCl_3$) of compound* ***177.***

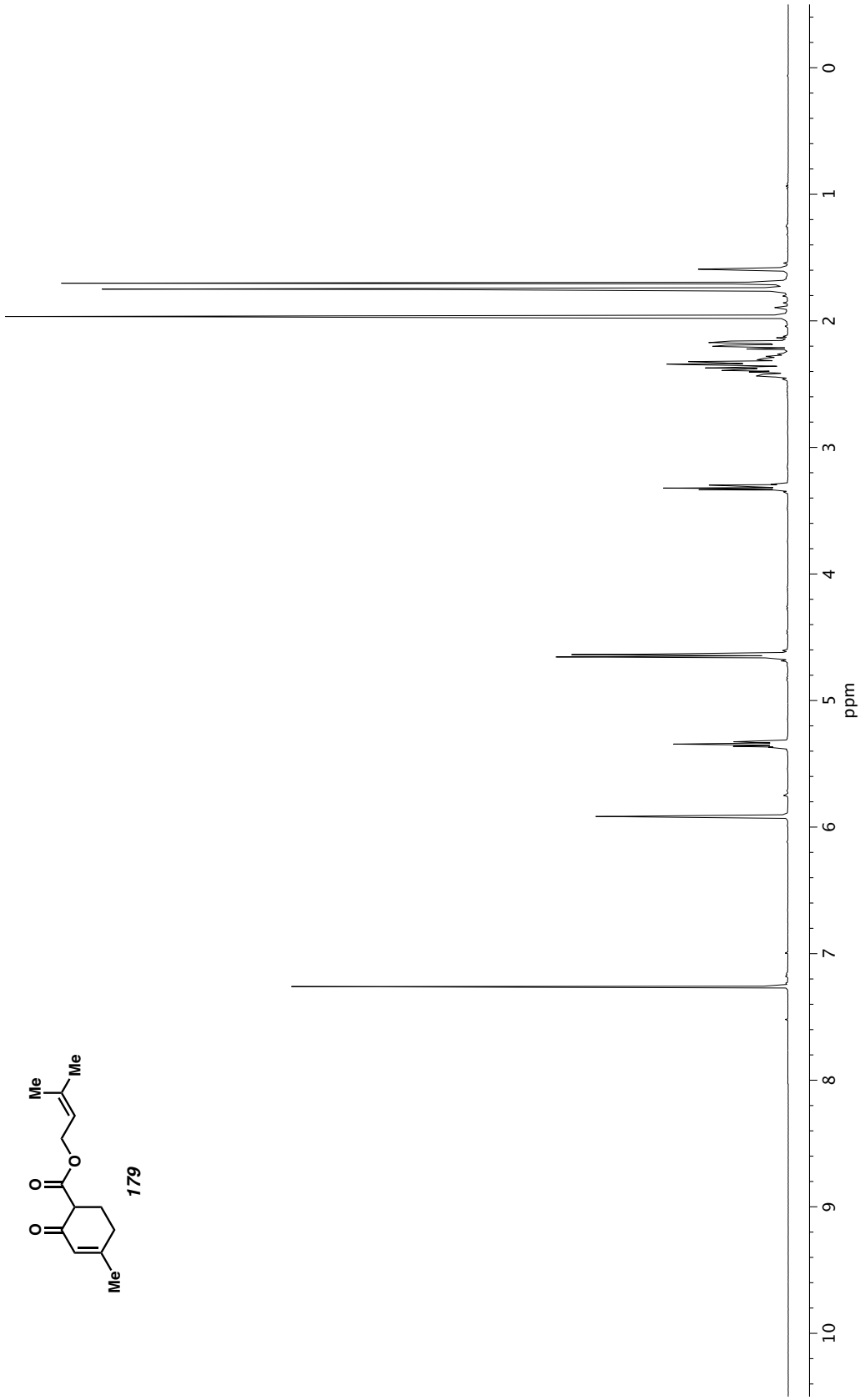

Figure A1.233. *^{1}H NMR (400 MHz, $CDCl_3$) of compound* ***179.***

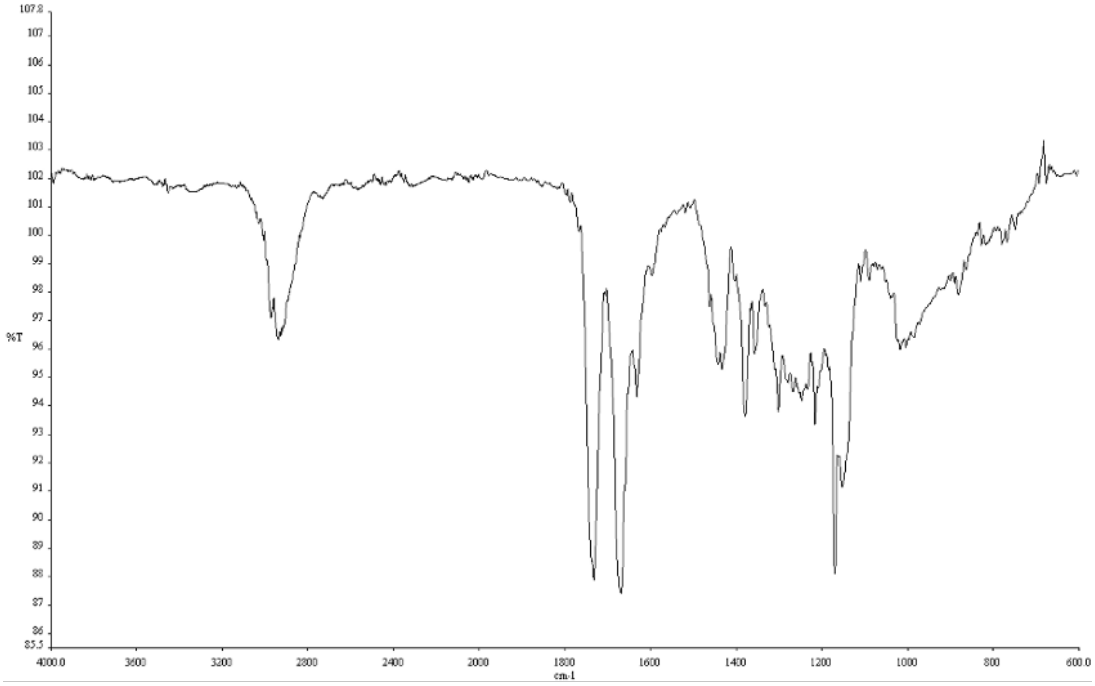

Figure A1.234. *Infrared spectrum (Thin Film, NaCl) of compound* ***179.***

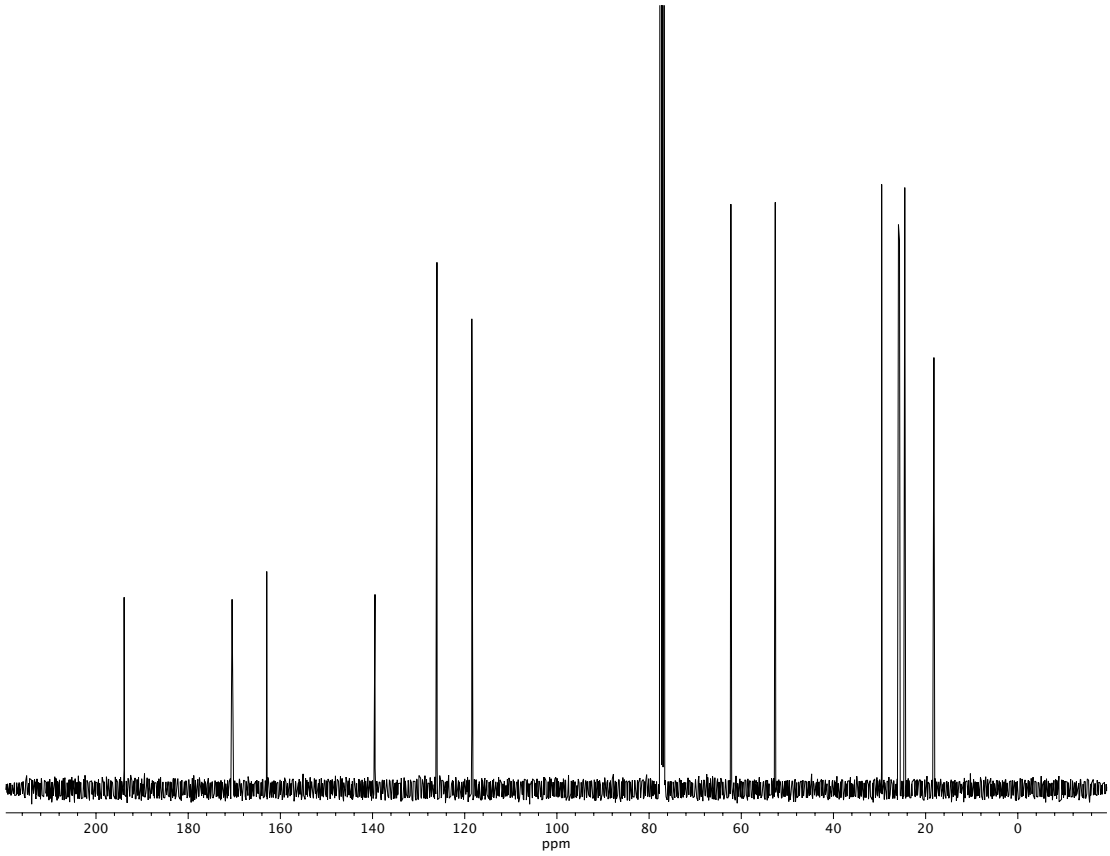

Figure A1.235. *^{13}C NMR (100 MHz, $CDCl_3$) of compound* ***179.***

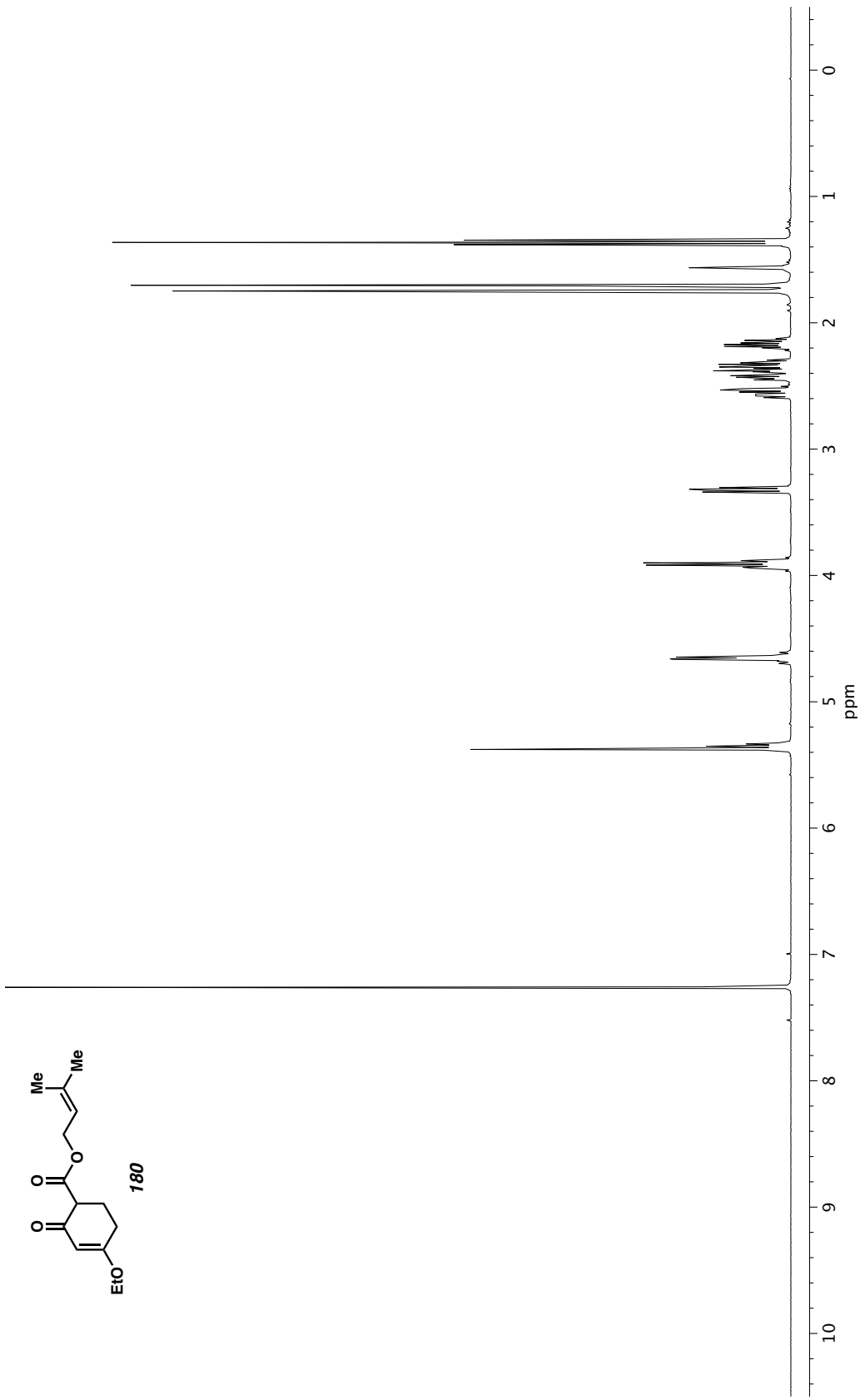

Figure A1.236. *^{1}H NMR (400 MHz, $CDCl_3$) of compound* ***180.***

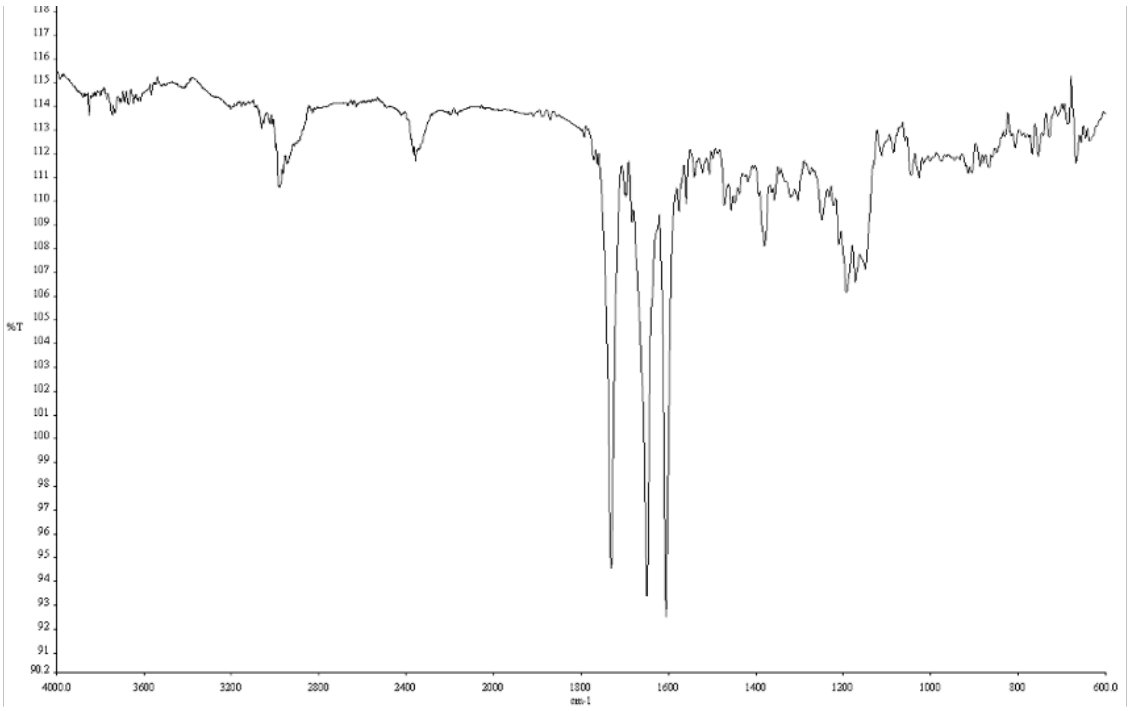

Figure A1.237. *Infrared spectrum (Thin Film, NaCl) of compound* ***180.***

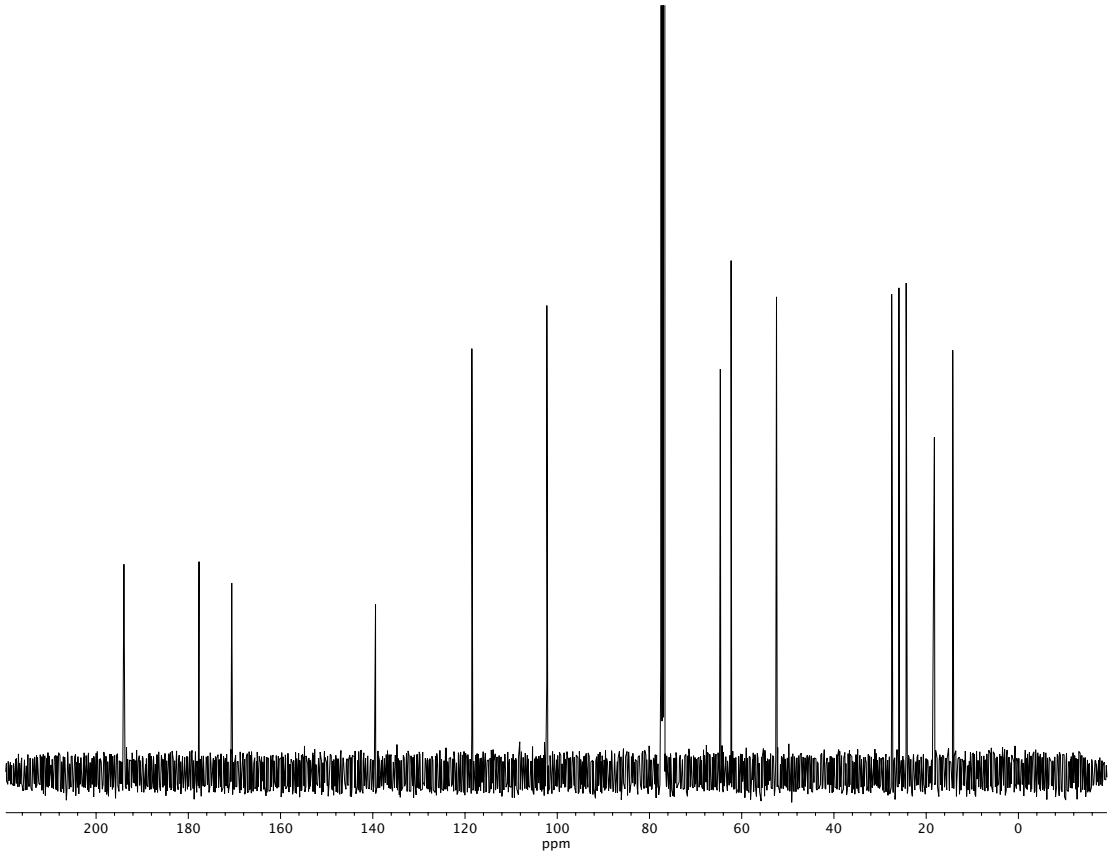

Figure A1.238. *^{13}C NMR (100 MHz, $CDCl_3$) of compound* ***180.***

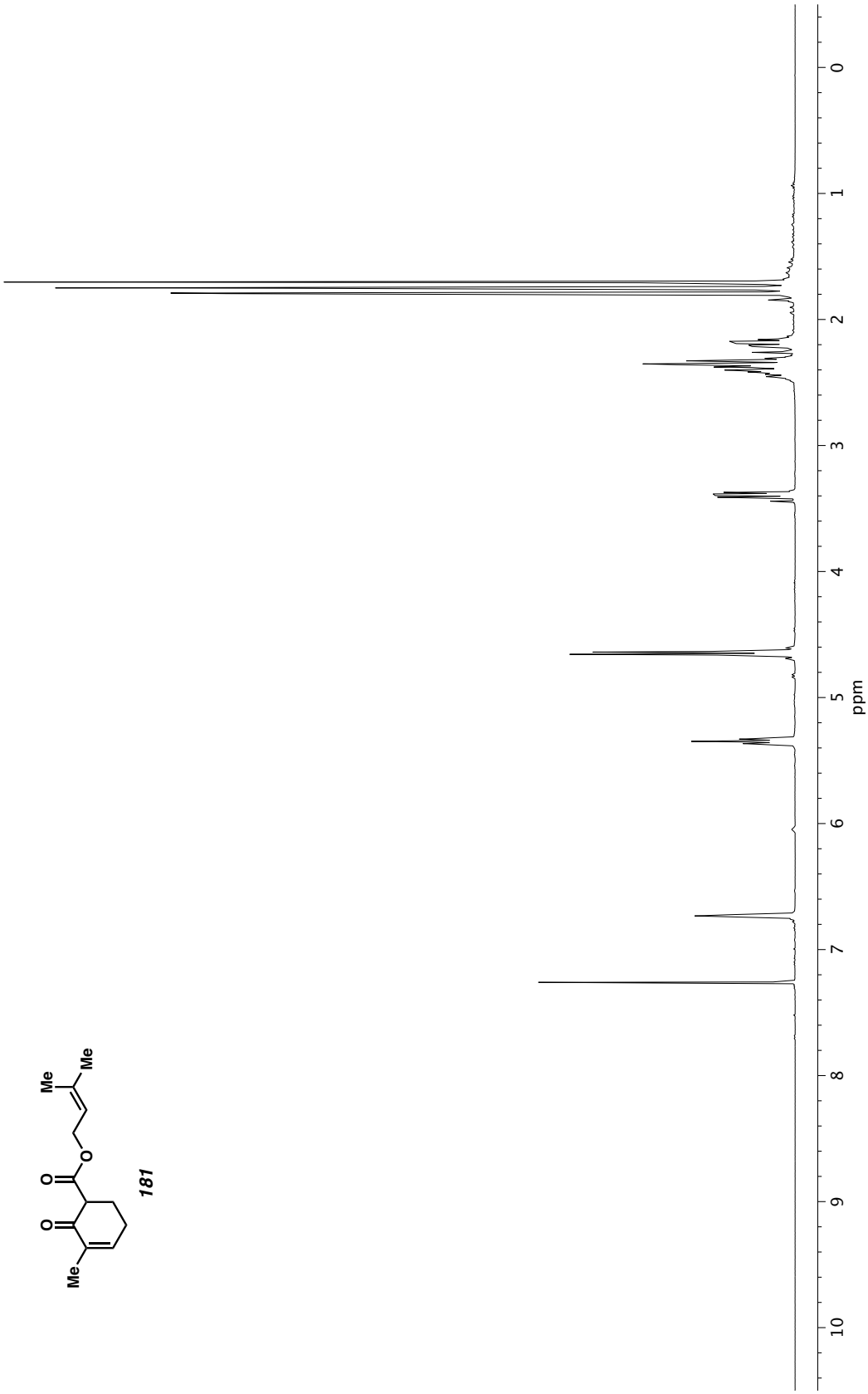

Figure A1.239. *^1H NMR (400 MHz, $CDCl_3$) of compound* ***181.***

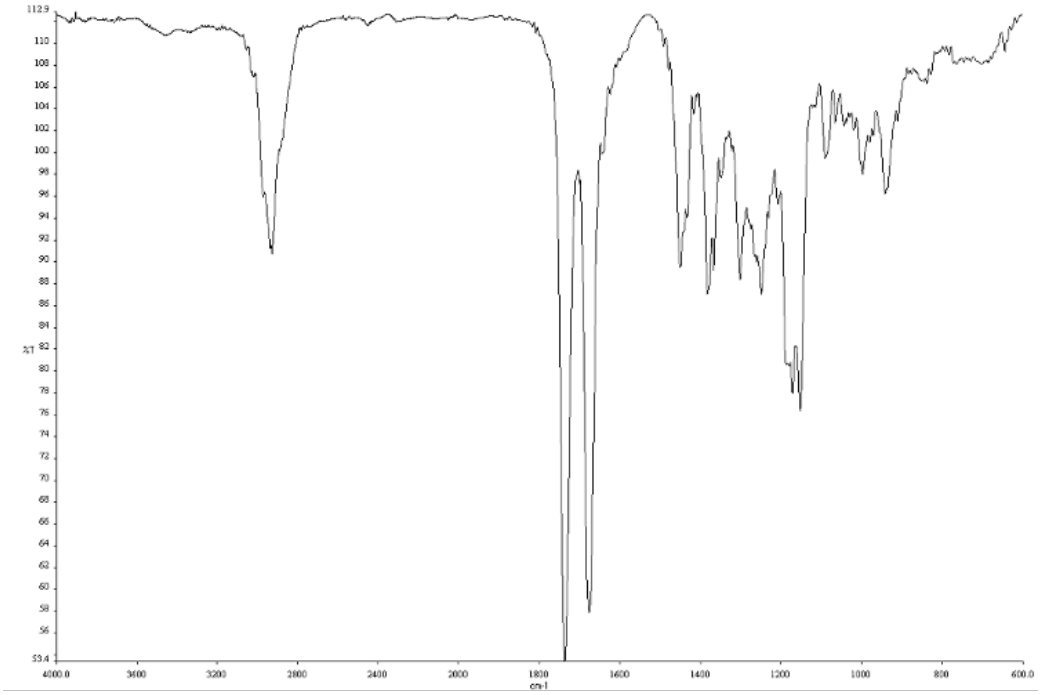

Figure A1.240. *Infrared spectrum (Thin Film, NaCl) of compound* ***181.***

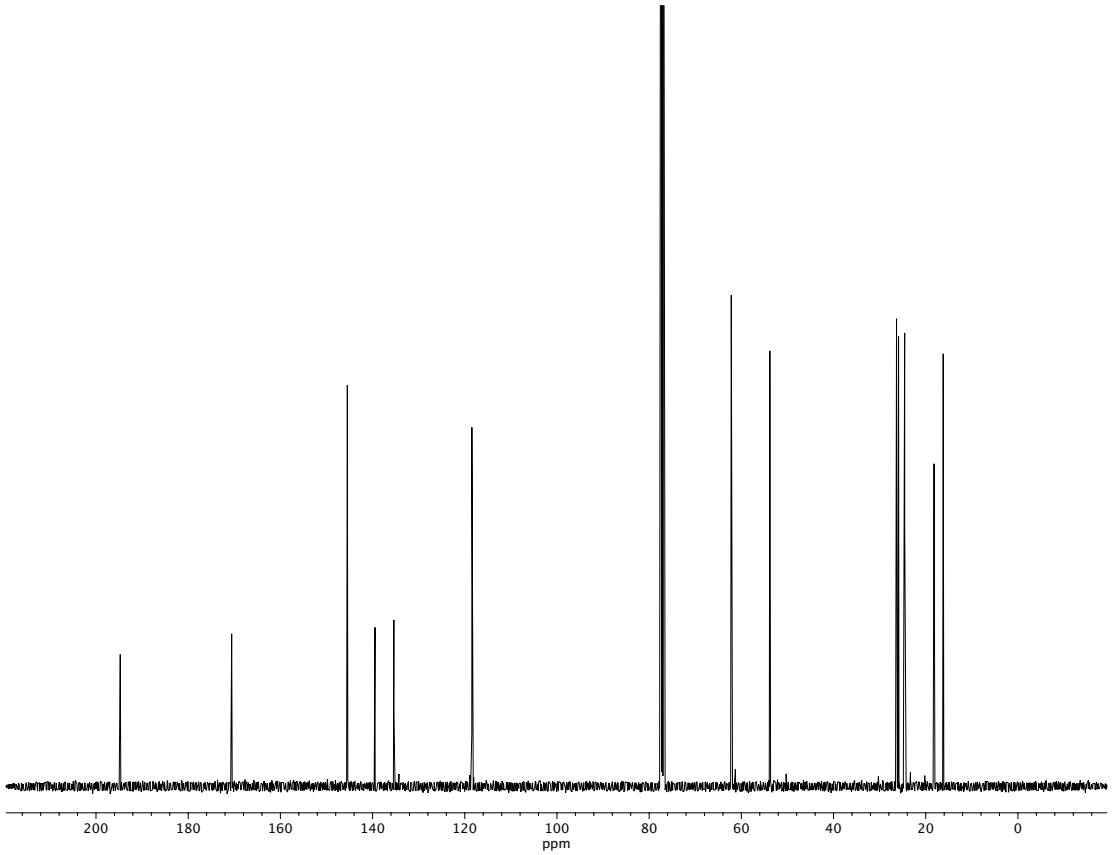

Figure A1.241. *^{13}C NMR (100 MHz, $CDCl_3$) of compound* ***181.***

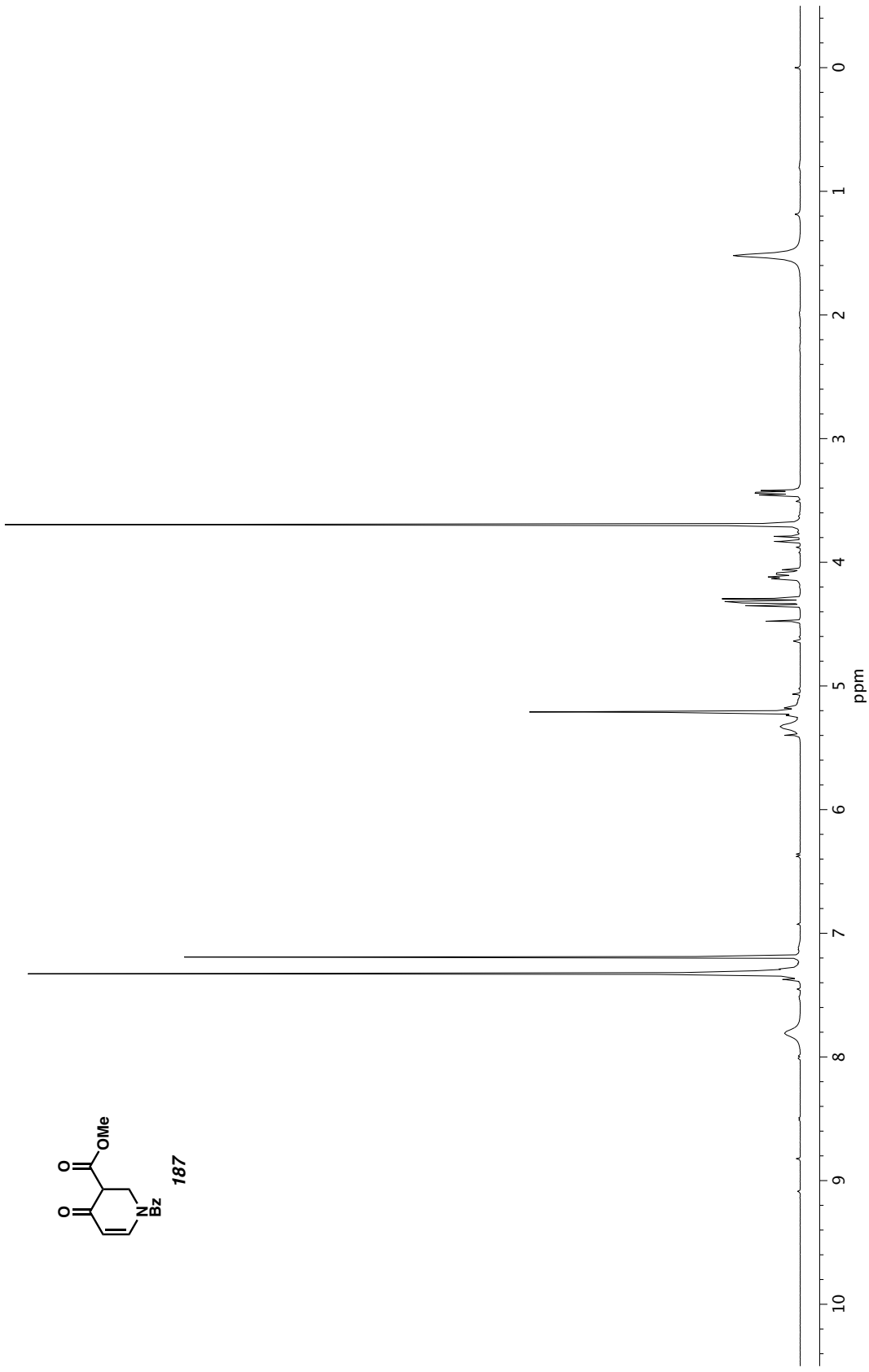

Figure A1.242. *^1H NMR (400 MHz, $CDCl_3$) of compound* ***187.***

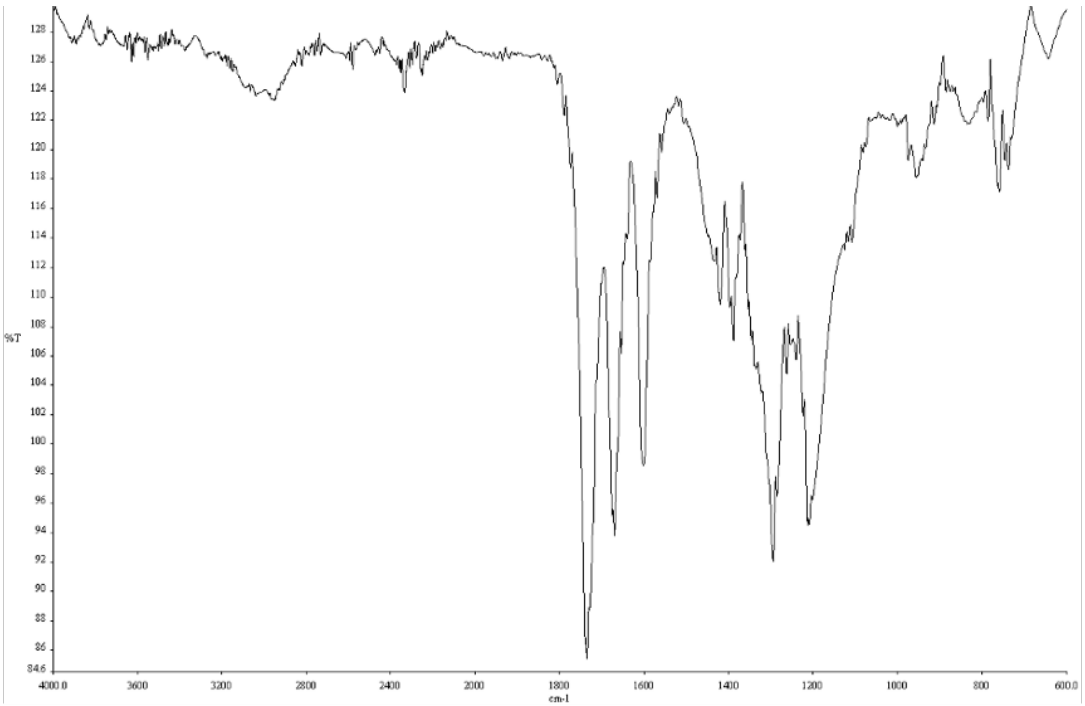

Figure A1.243. *Infrared spectrum (Thin Film, NaCl) of compound* ***187.***

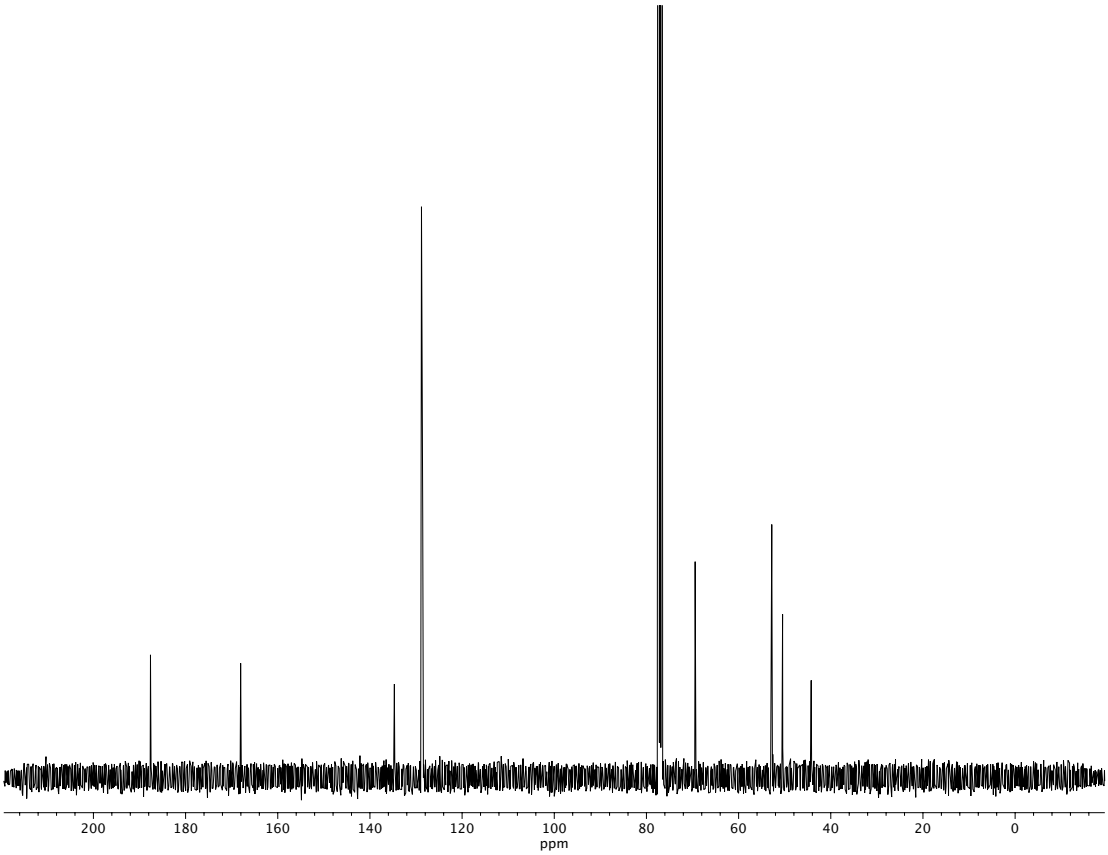

Figure A1.244. *^{13}C NMR (100 MHz, $CDCl_3$) of compound* ***187.***

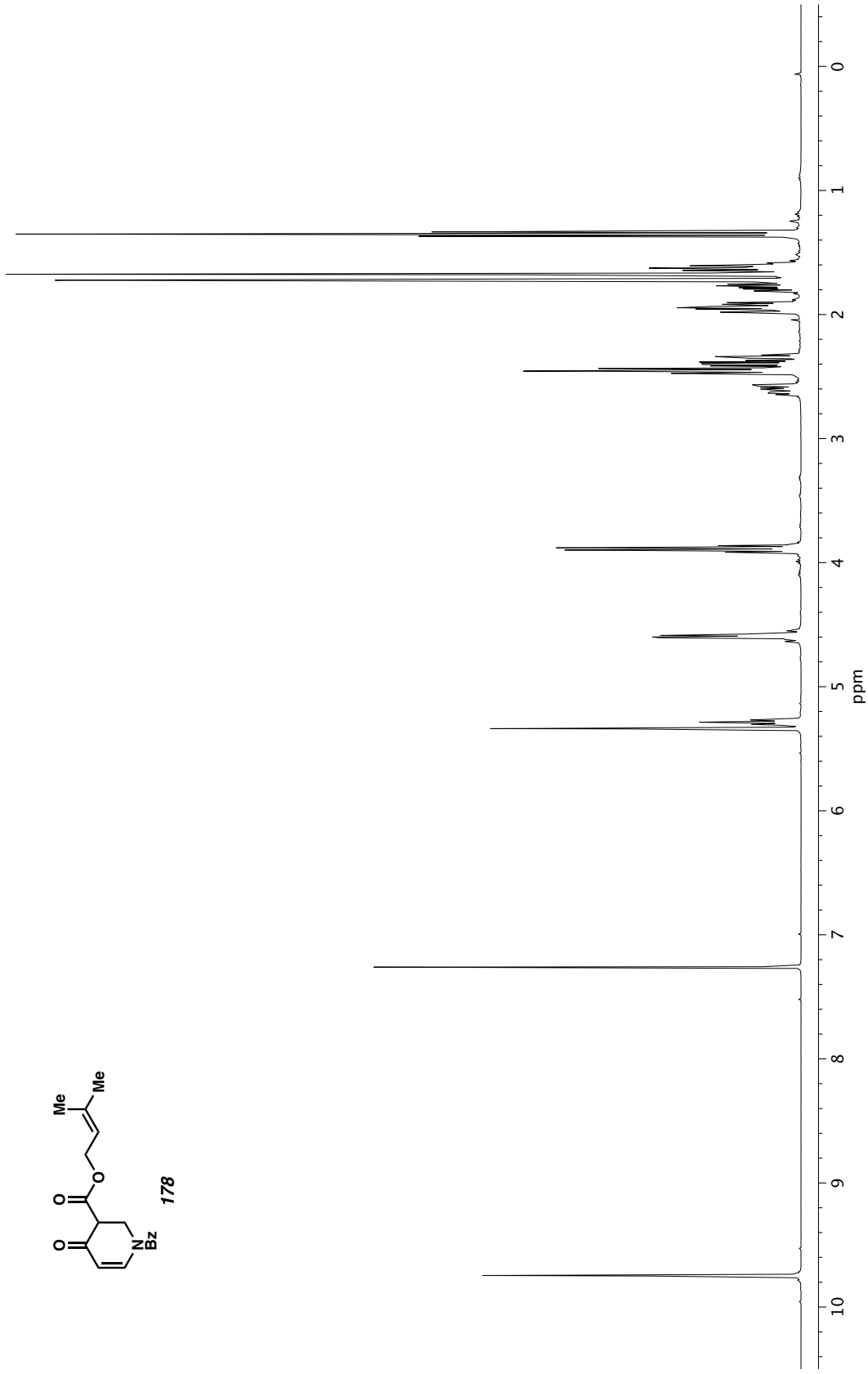

Figure A1.245. *^{1}H NMR (400 MHz, $CDCl_3$) of compound* ***178.***

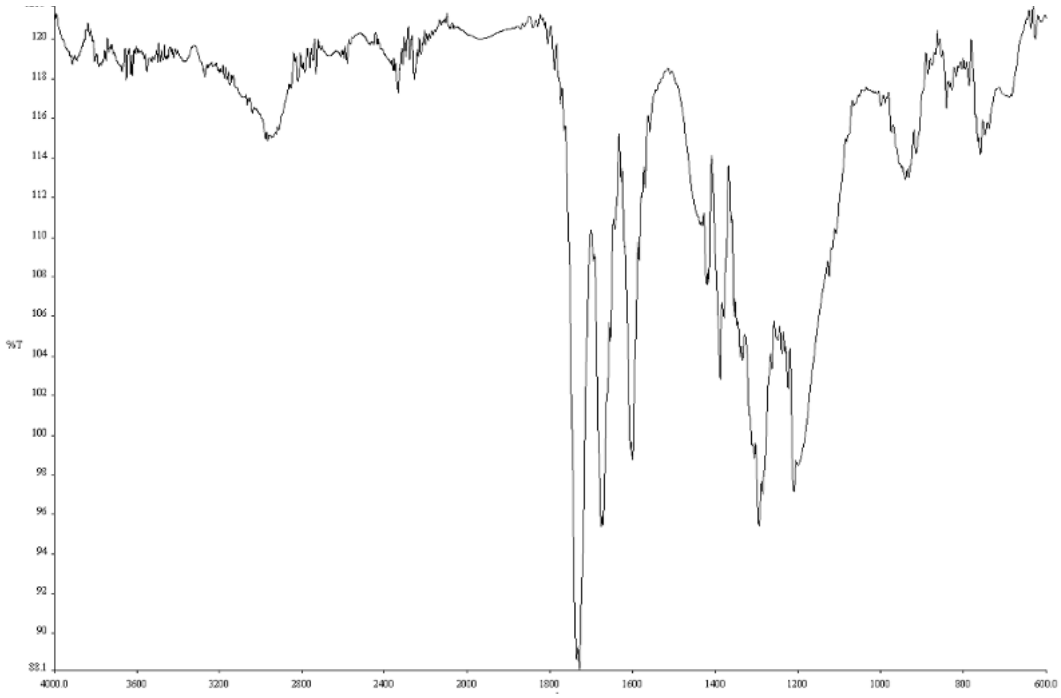

Figure A1.246. *Infrared spectrum (Thin Film, NaCl) of compound* ***178.***

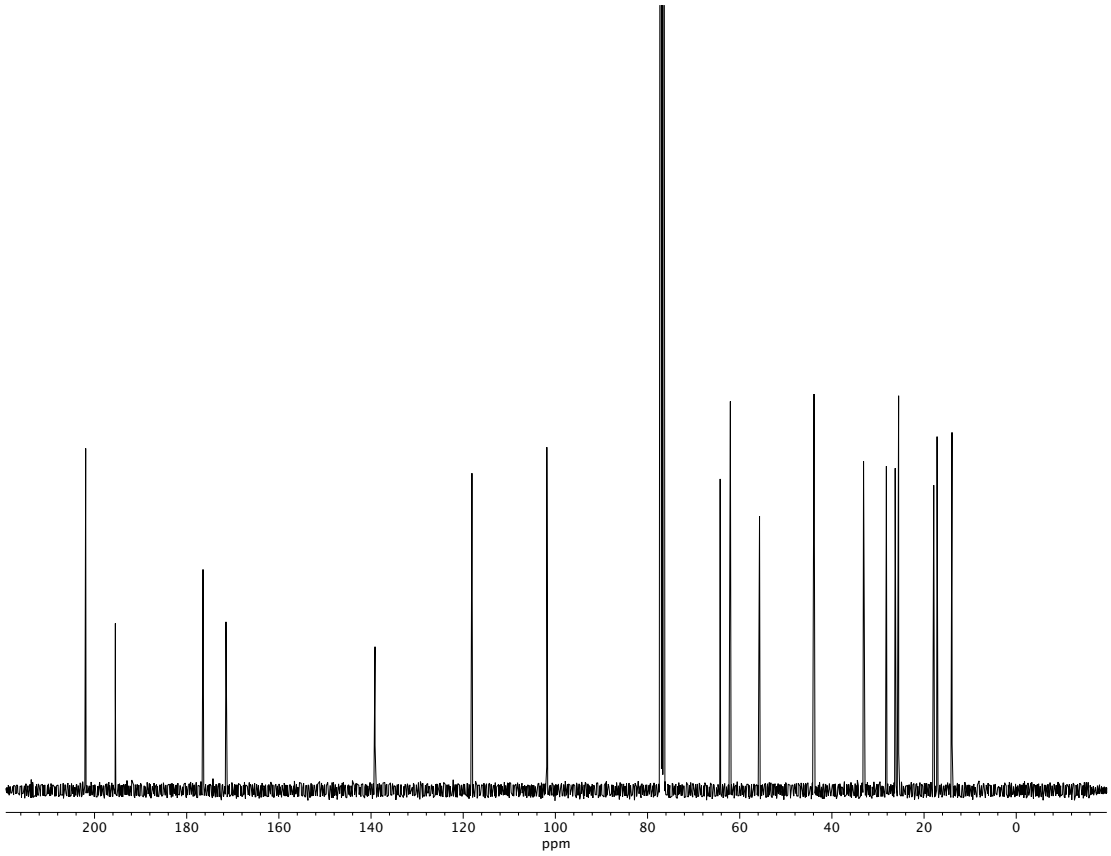

Figure A1.247. *^{13}C NMR (100 MHz, $CDCl_3$) of compound* ***178.***

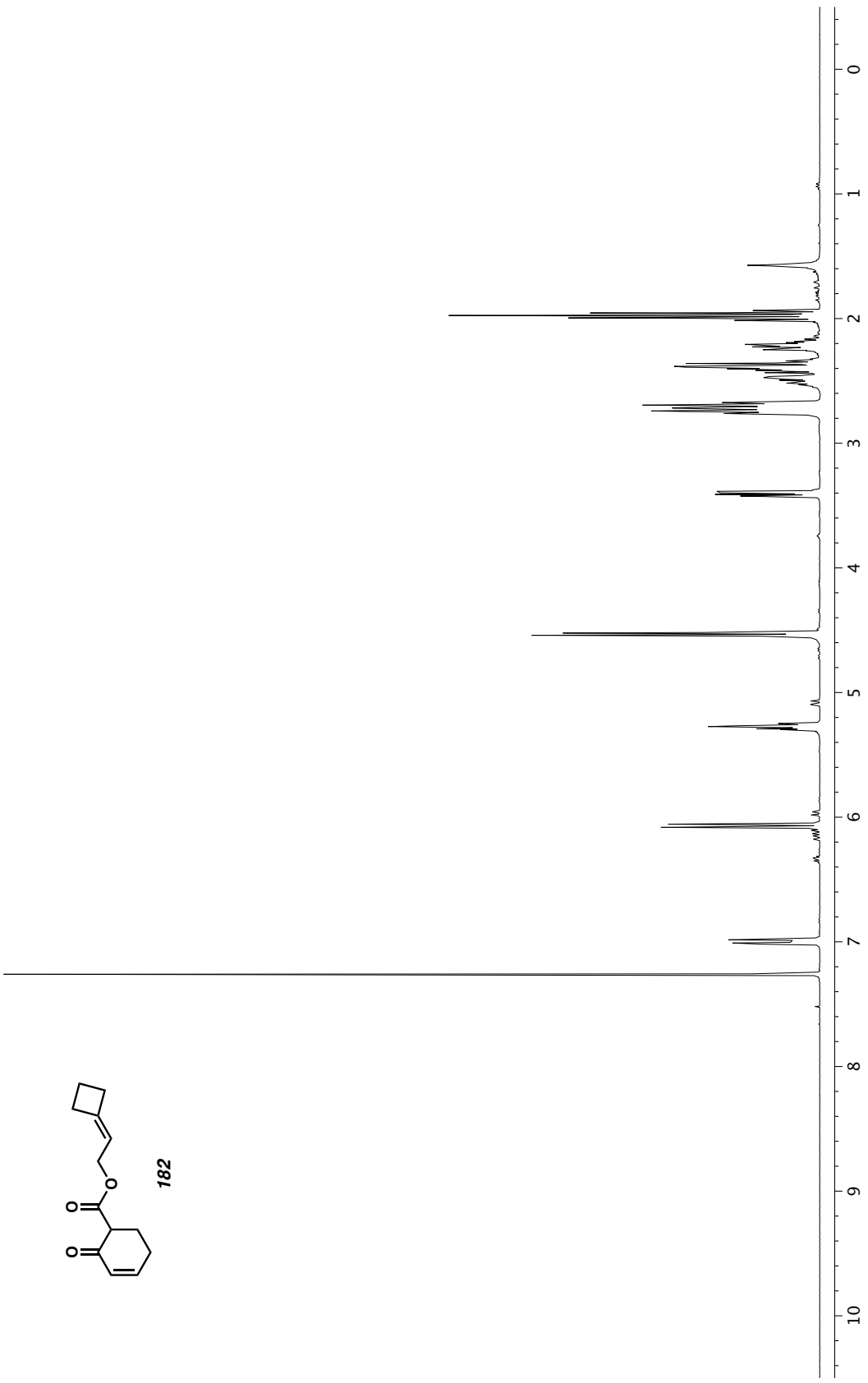

Figure A1.248. *^1H NMR (400 MHz, $CDCl_3$) of compound* ***182.***

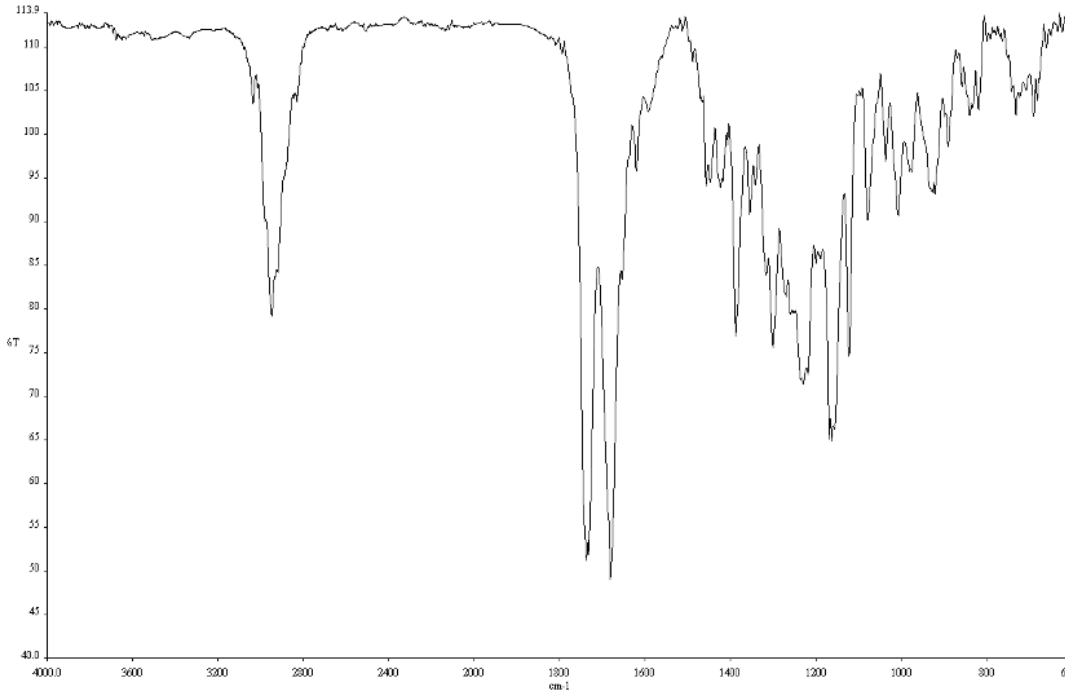

Figure A1.249. *Infrared spectrum (Thin Film, NaCl) of compound* ***182.***

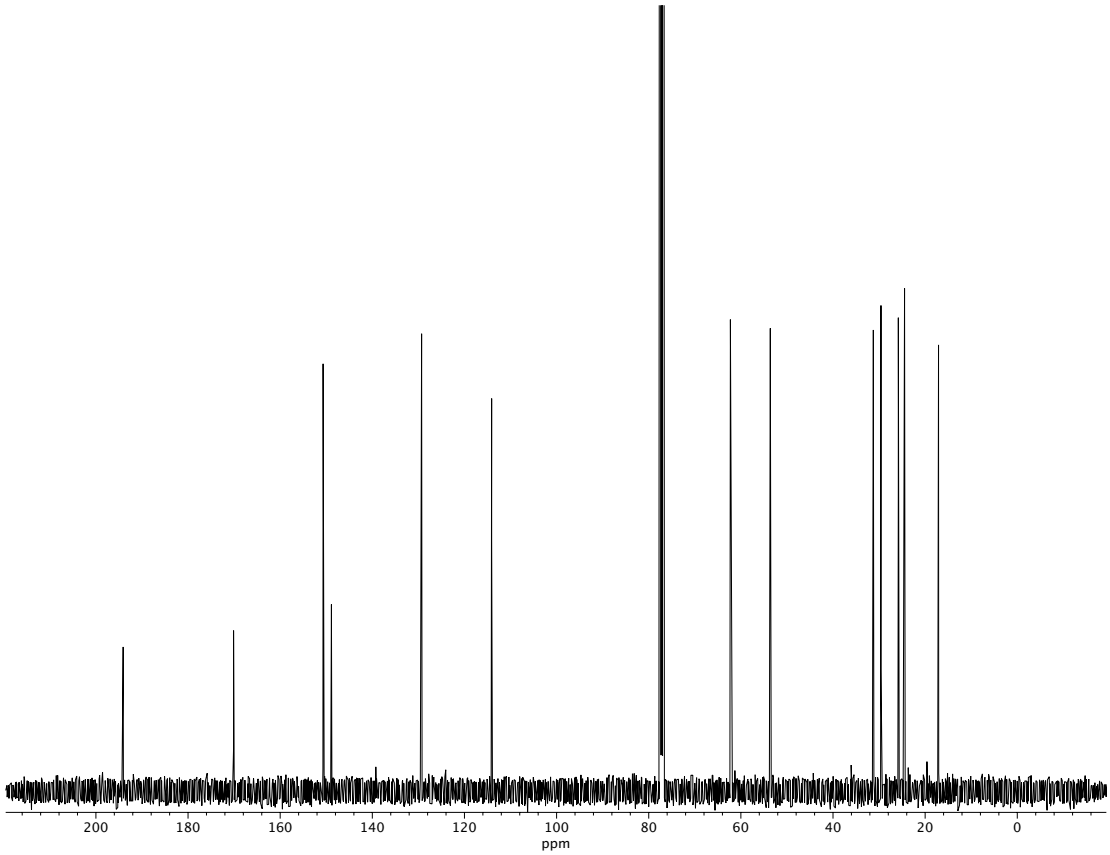

Figure A1.250. *^{13}C NMR (100 MHz, $CDCl_3$) of compound* ***182.***

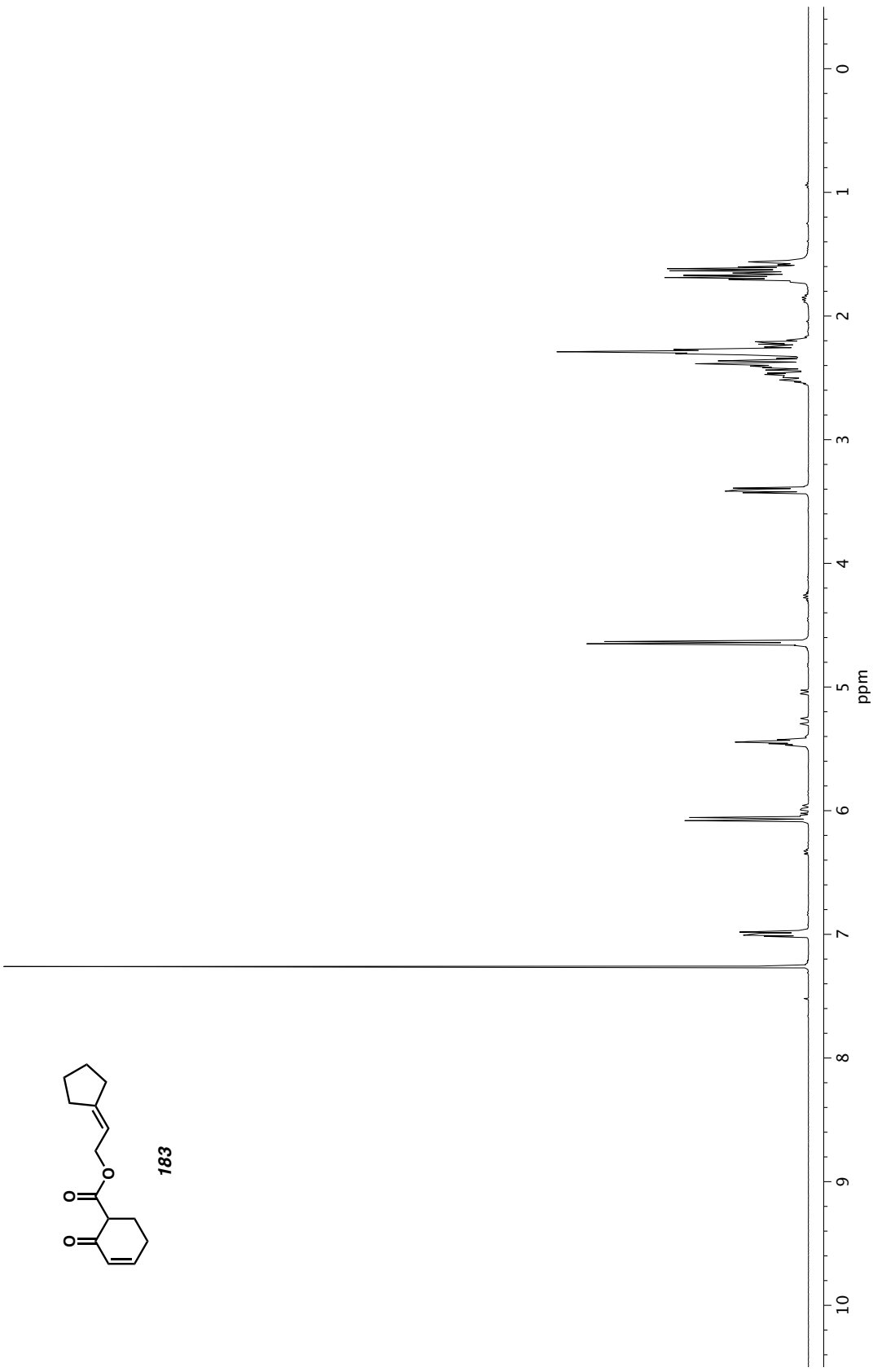

Figure A1.251. *^1H NMR (400 MHz, $CDCl_3$) of compound* ***183.***

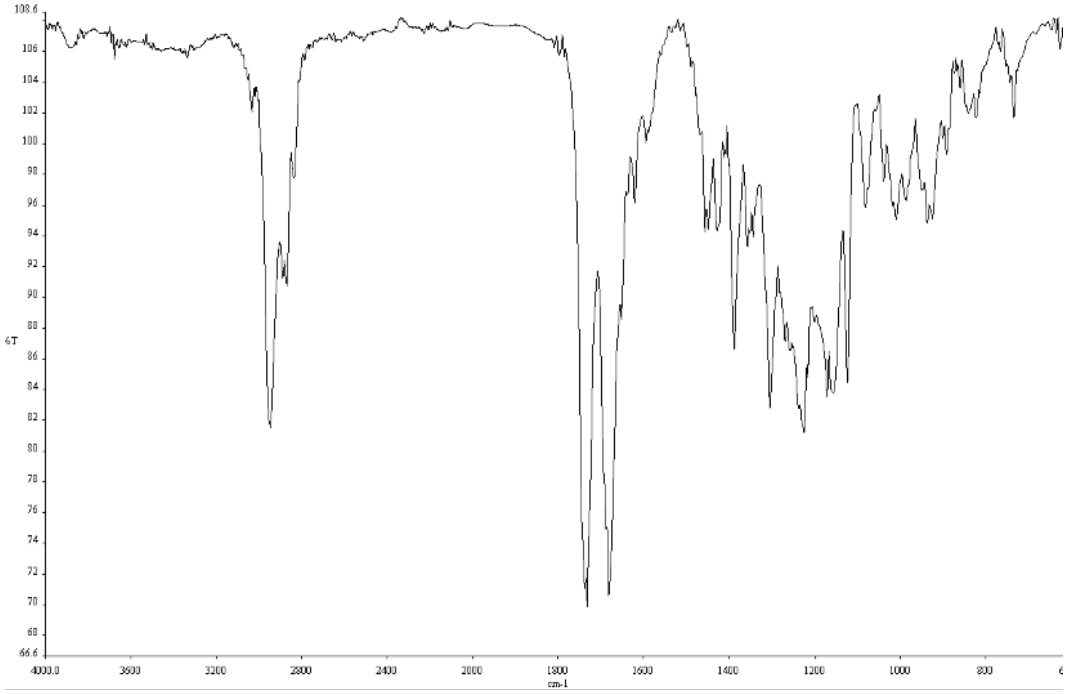

Figure A1.252. *Infrared spectrum (Thin Film, NaCl) of compound* ***183.***

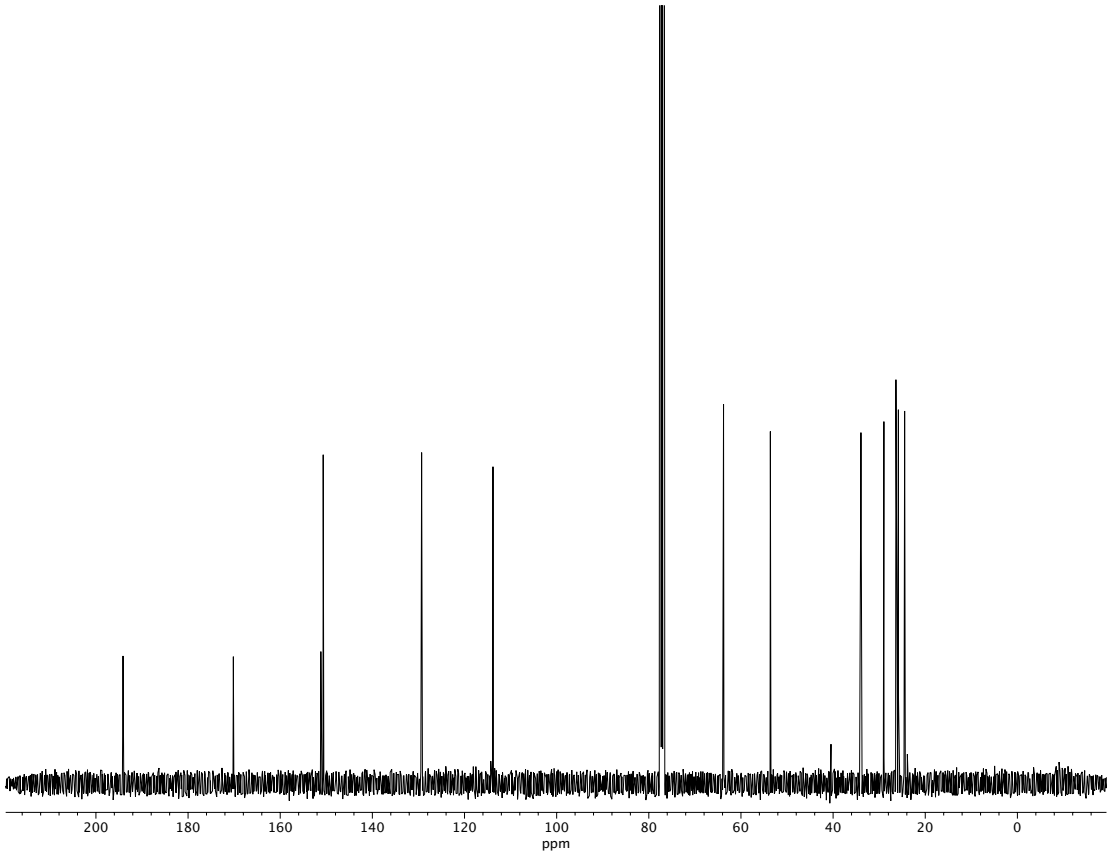

Figure A1.253. *^{13}C NMR (100 MHz, $CDCl_3$) of compound* ***183.***

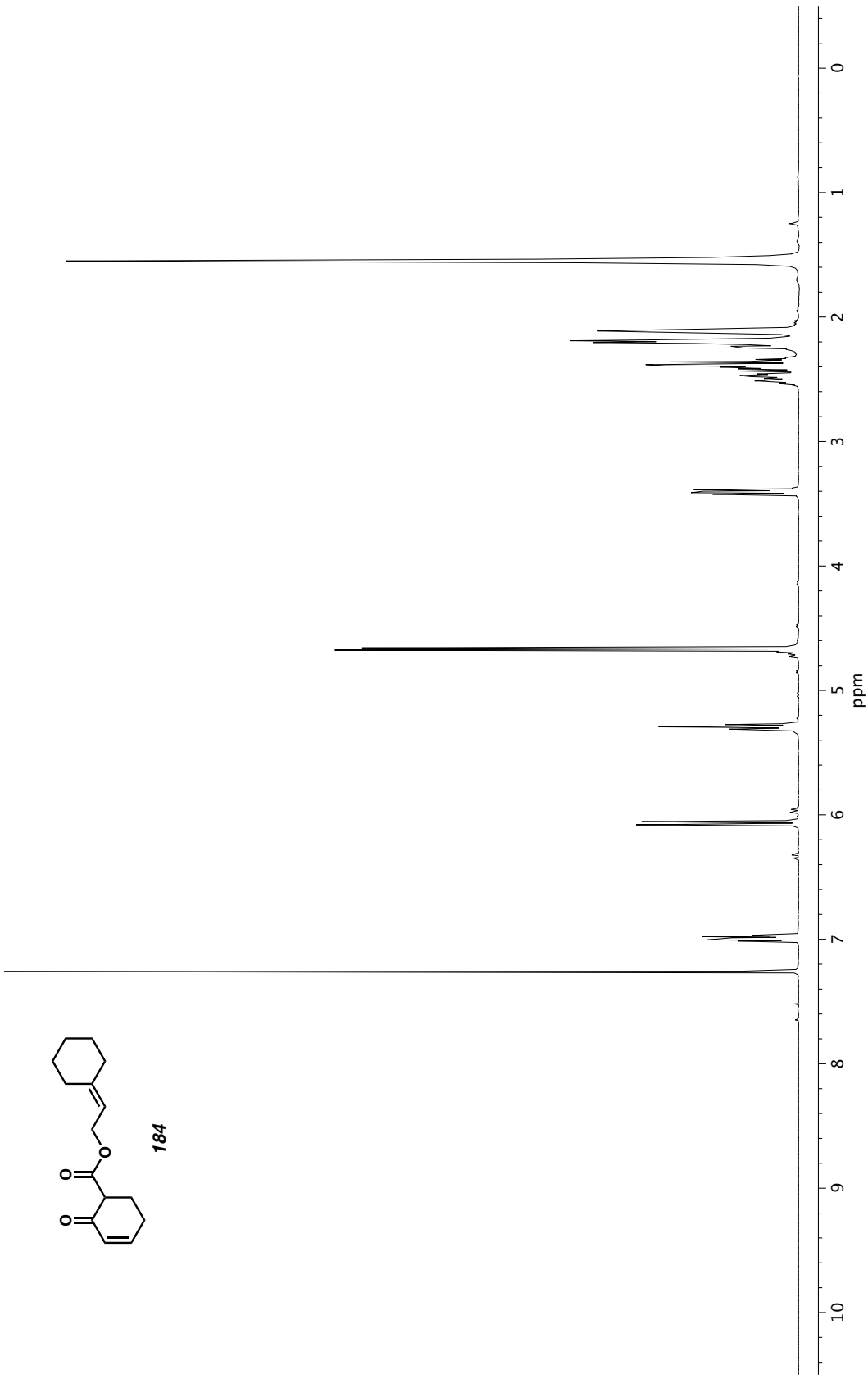

Figure A1.254. *^1H NMR (400 MHz, $CDCl_3$) of compound* ***184.***

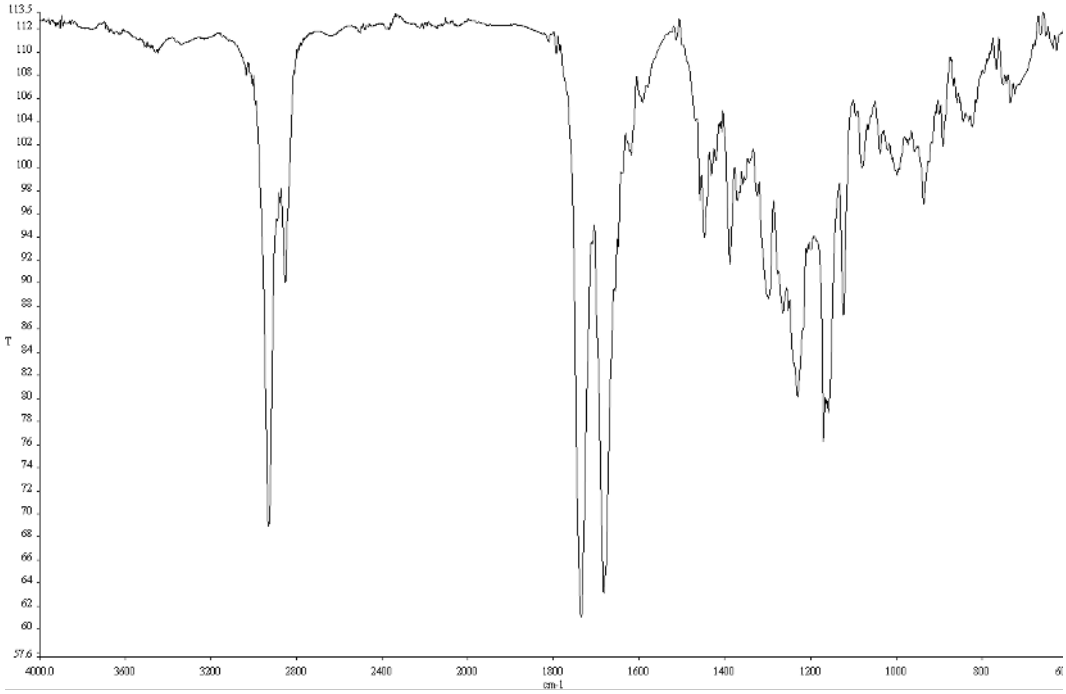

Figure A1.255. *Infrared spectrum (Thin Film, NaCl) of compound* ***184.***

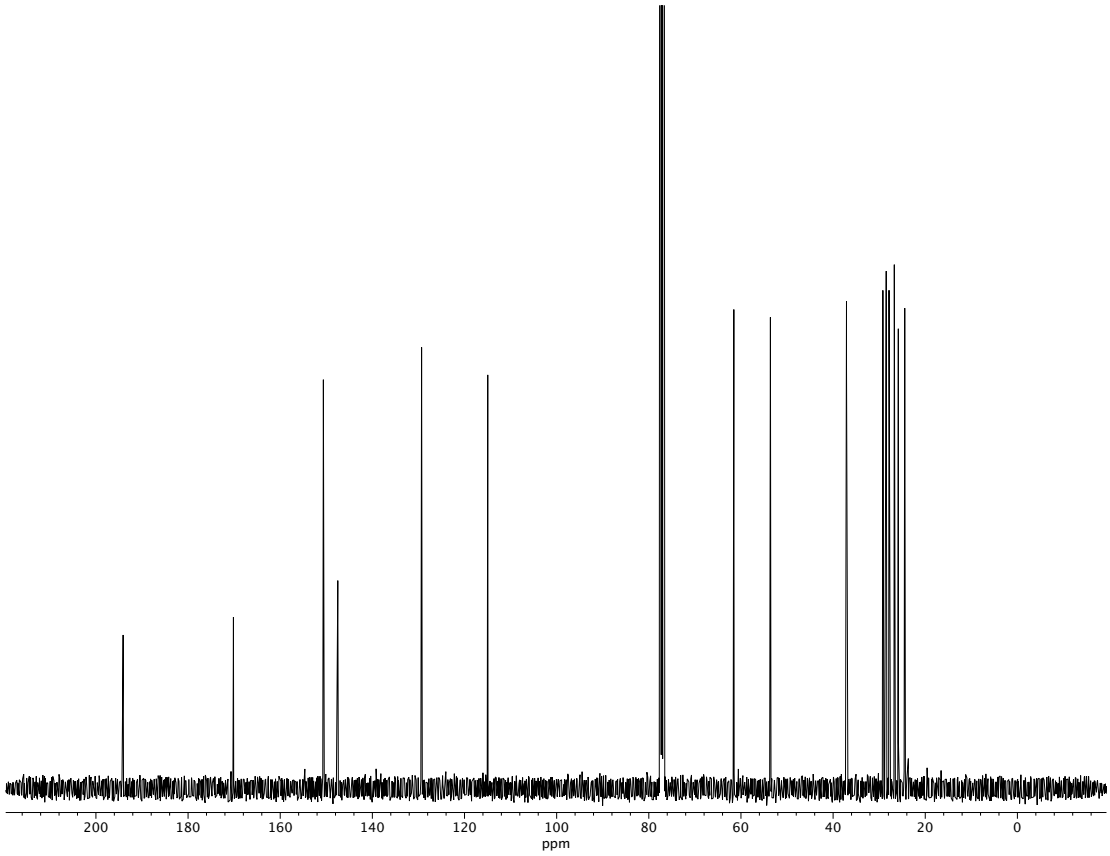

Figure A1.256. *^{13}C NMR (100 MHz, $CDCl_3$) of compound* ***184.***

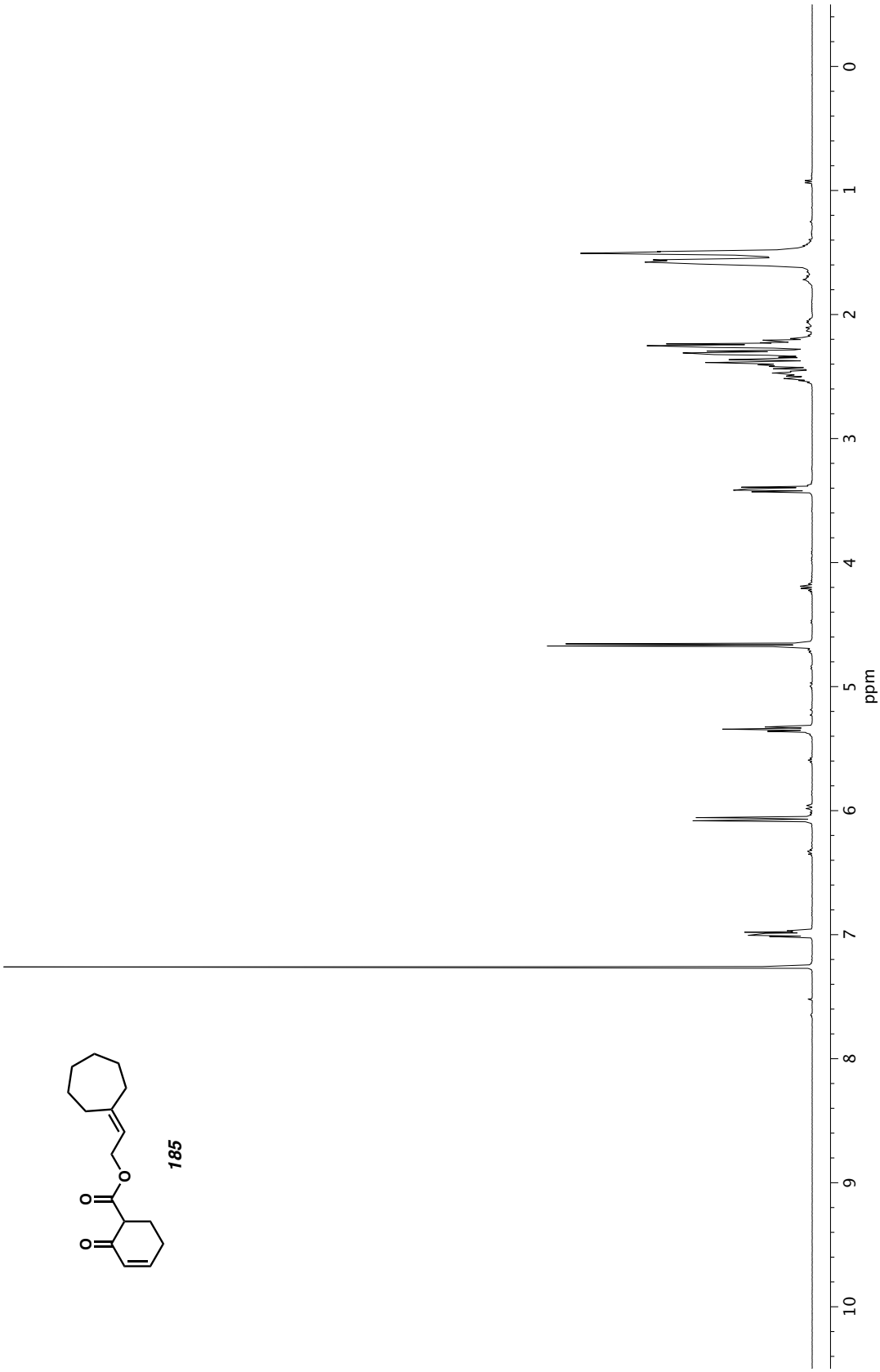

Figure A1.257. *^1H NMR (400 MHz, $CDCl_3$) of compound* ***185.***

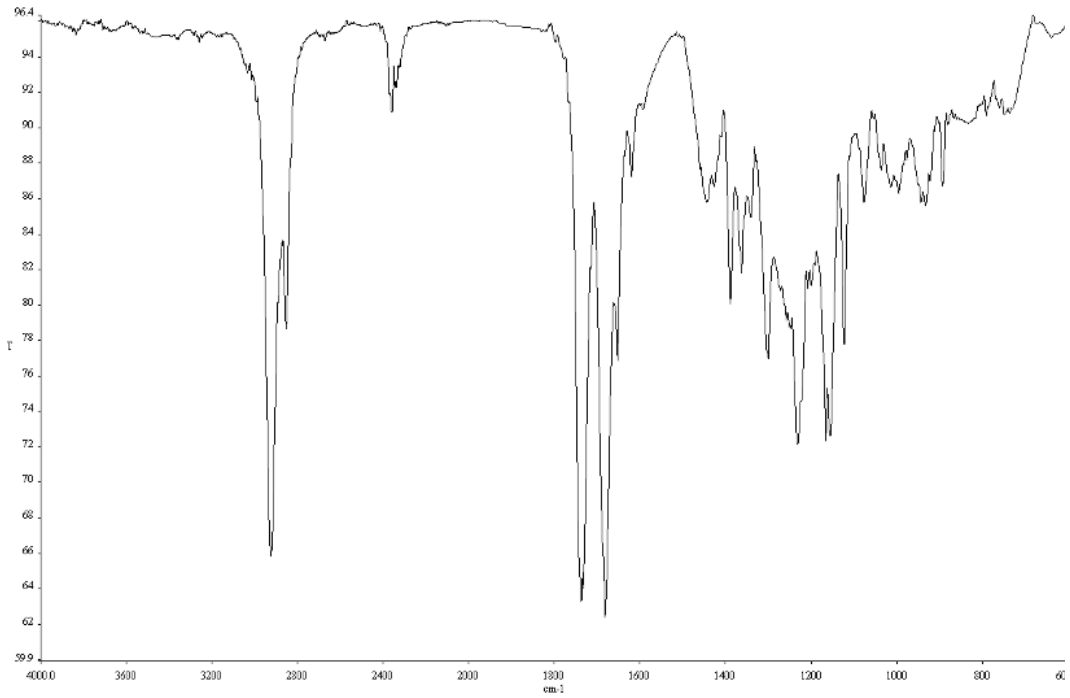

Figure A1.258. *Infrared spectrum (Thin Film, NaCl) of compound* ***185.***

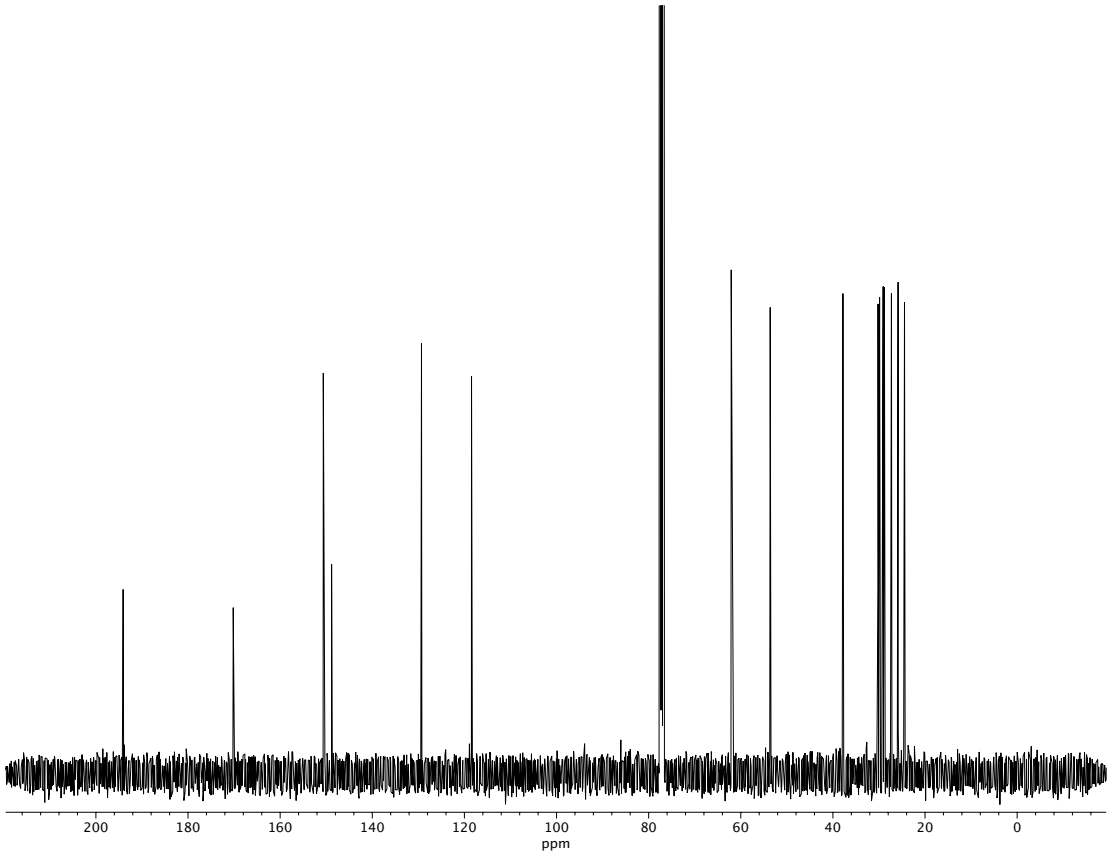

Figure A1.259. *^{13}C NMR (100 MHz, $CDCl_3$) of compound* ***185.***

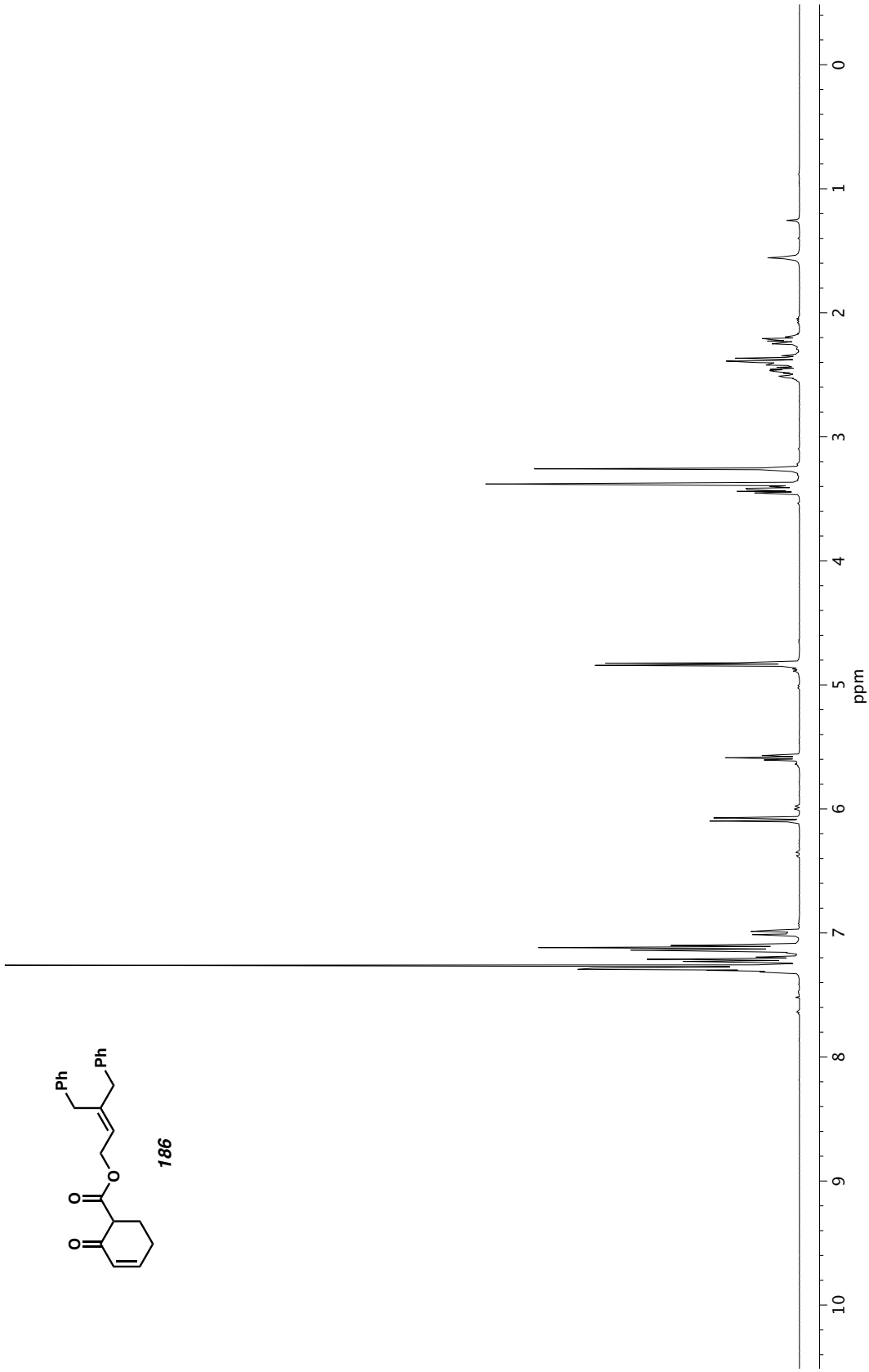

Figure A1.260. *^1H NMR (400 MHz, $CDCl_3$) of compound* ***186.***

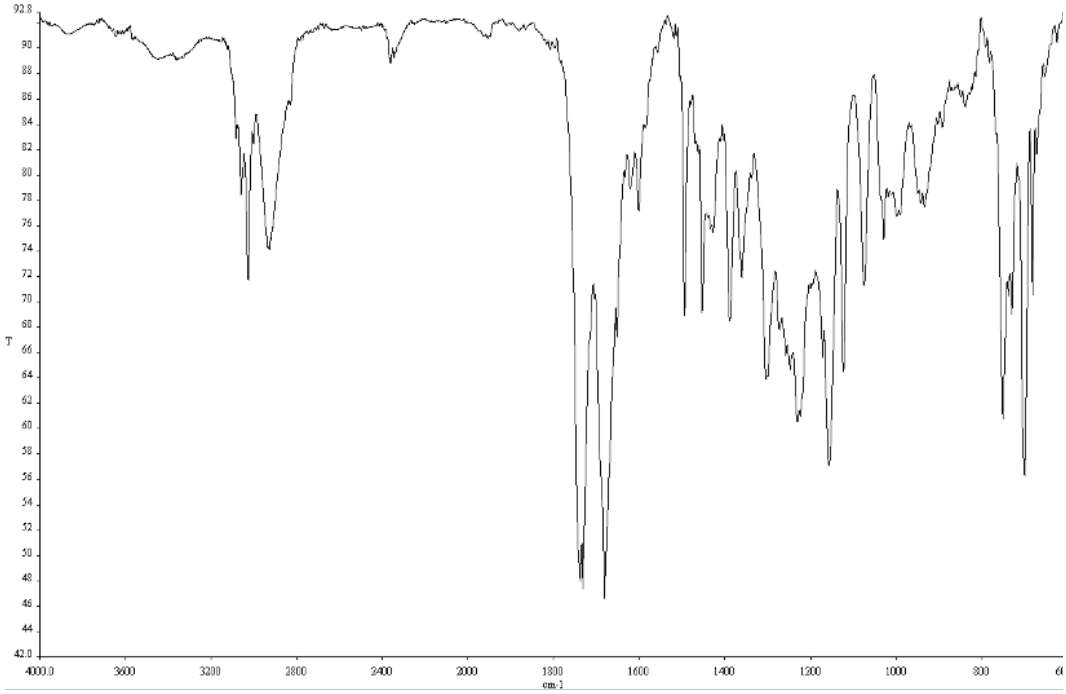

Figure A1.261. *Infrared spectrum (Thin Film, NaCl) of compound* ***186.***

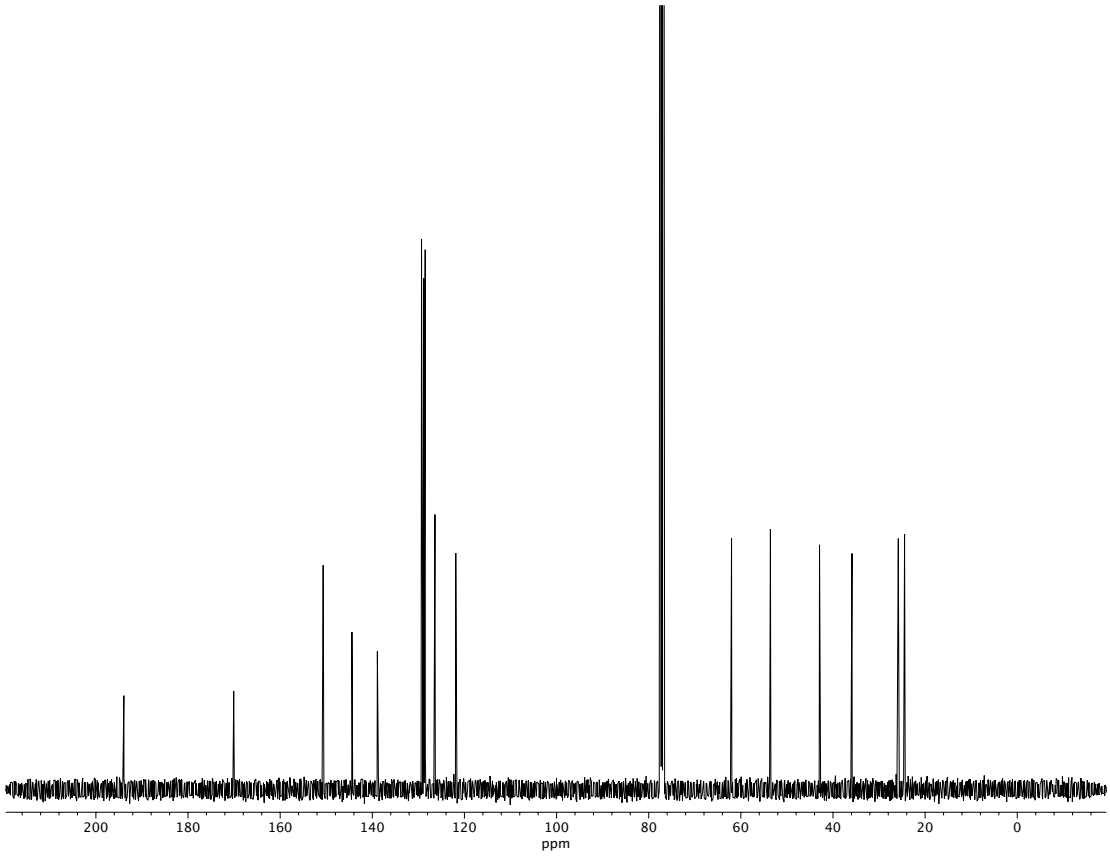

Figure A1.262. *^{13}C NMR (100 MHz, $CDCl_3$) of compound* ***186.***

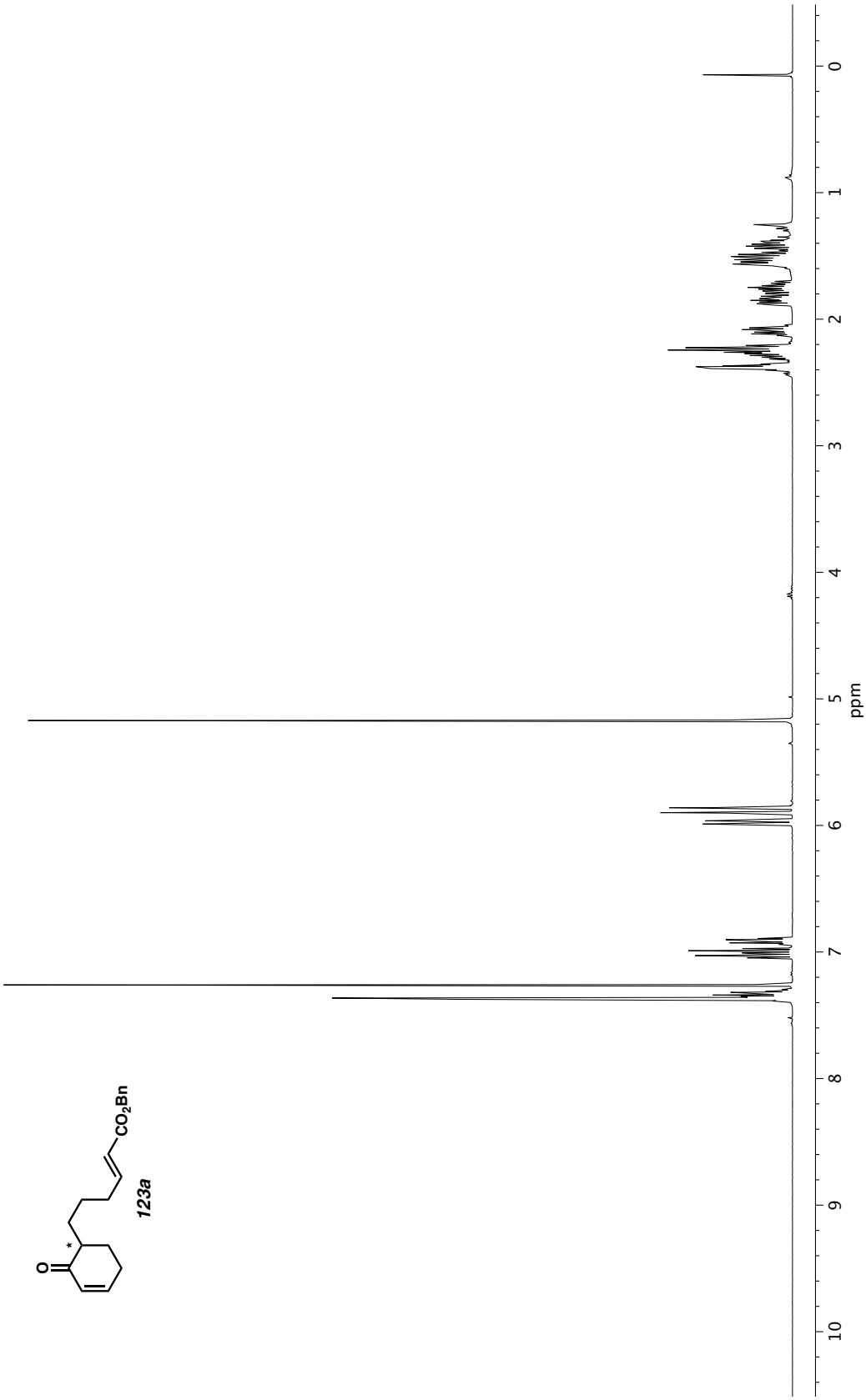

Figure A1.263. *^{1}H NMR (400 MHz, $CDCl_3$) of compound* ***123a.***

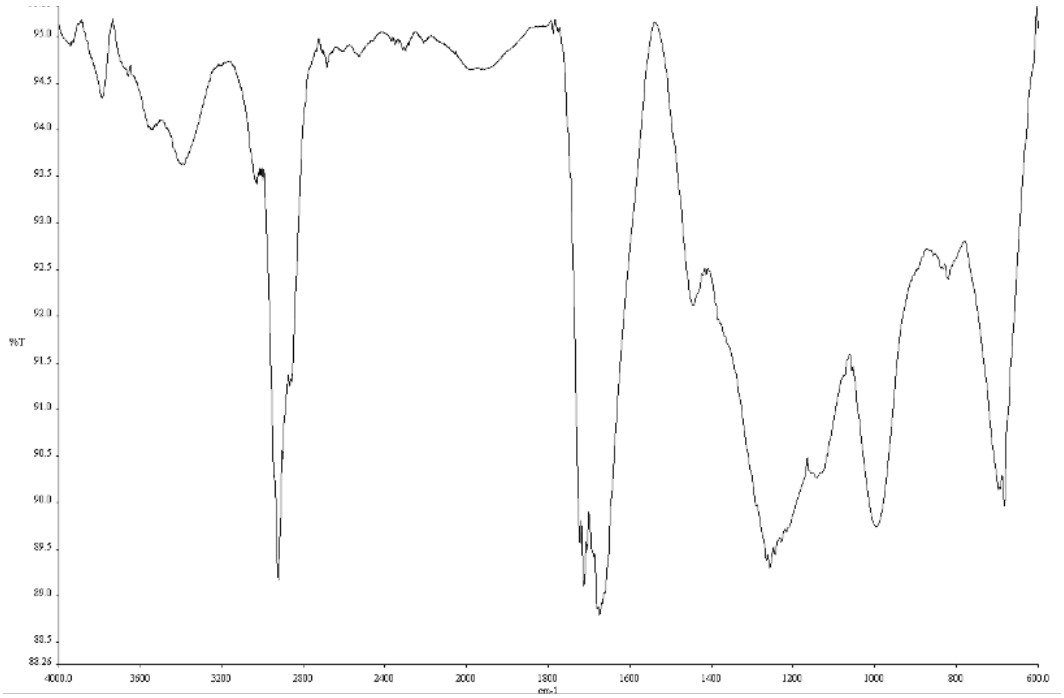

Figure A1.264. *Infrared spectrum (Thin Film, NaCl) of compound* ***123a.***

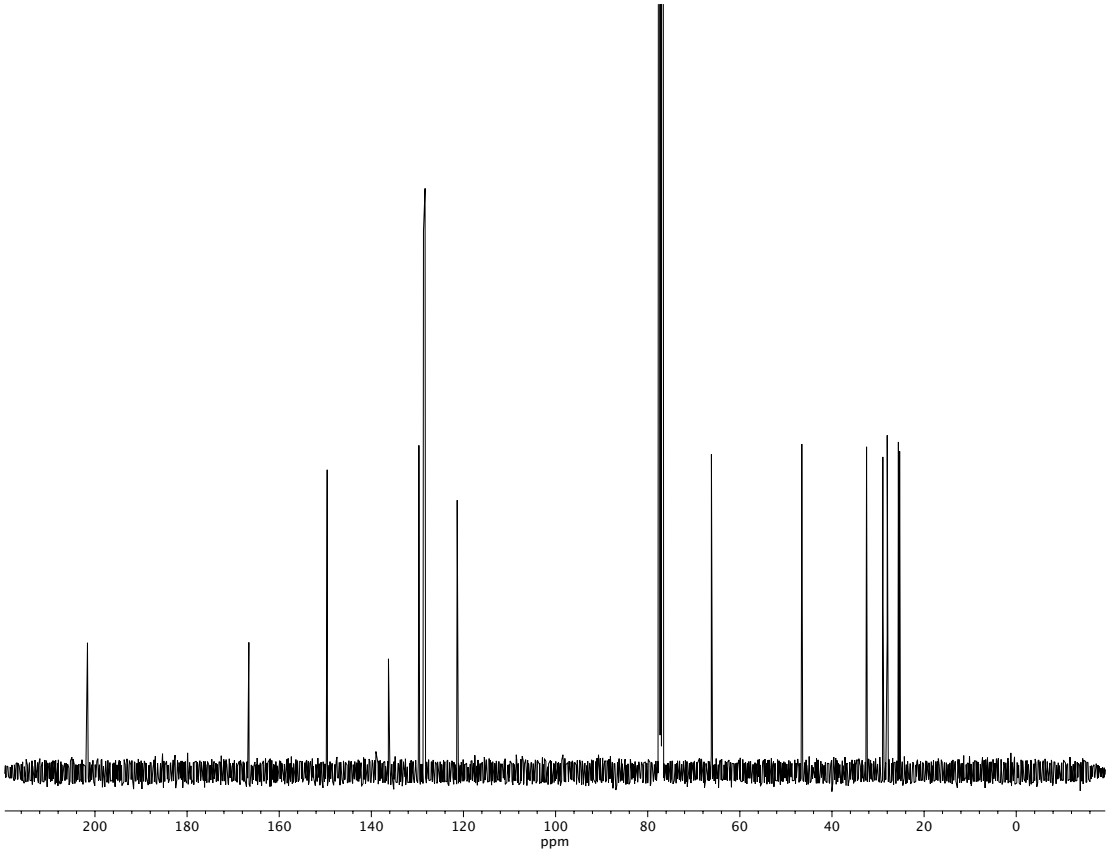

Figure A1.265. *^{13}C NMR (100 MHz, $CDCl_3$) of compound* ***123a.***

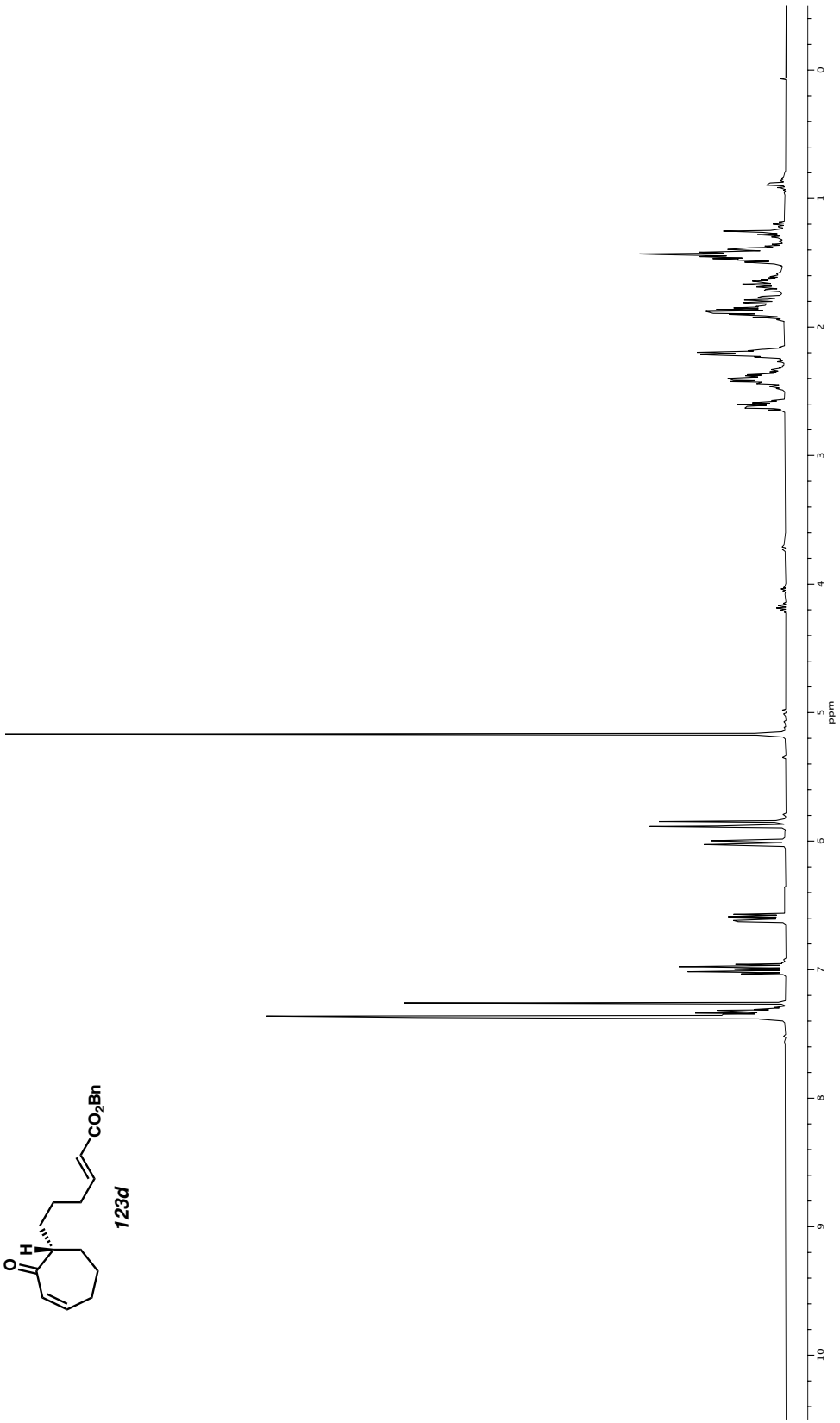

Figure A1.266. *^1H NMR (400 MHz, $CDCl_3$) of compound* ***123d.***

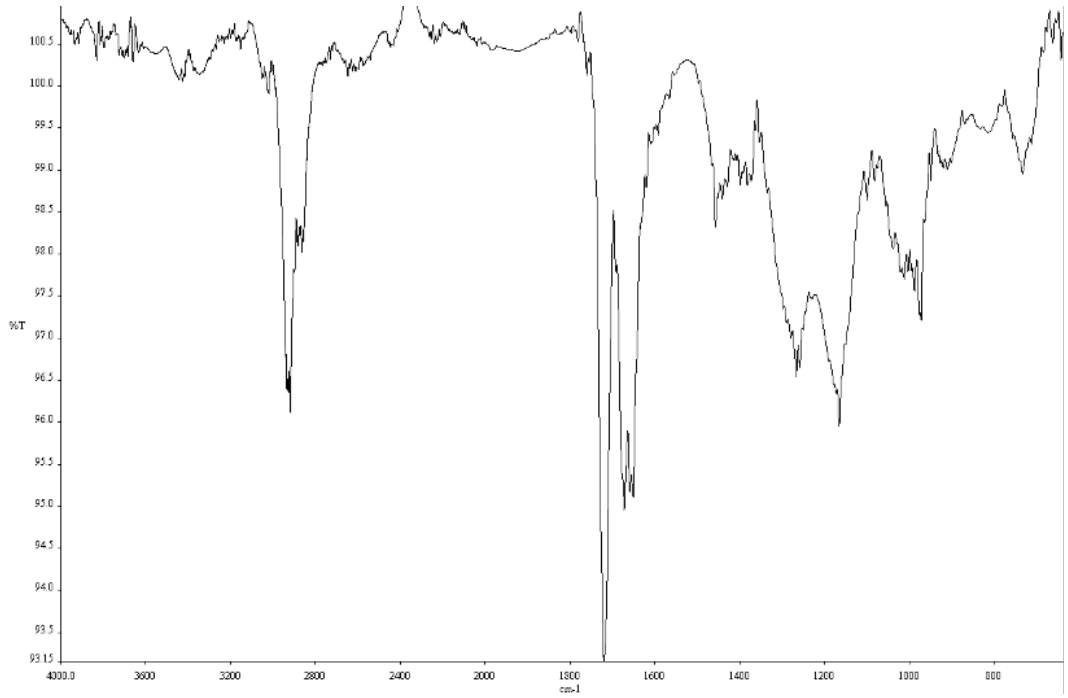

Figure A1.267. *Infrared spectrum (Thin Film, NaCl) of compound* ***123d.***

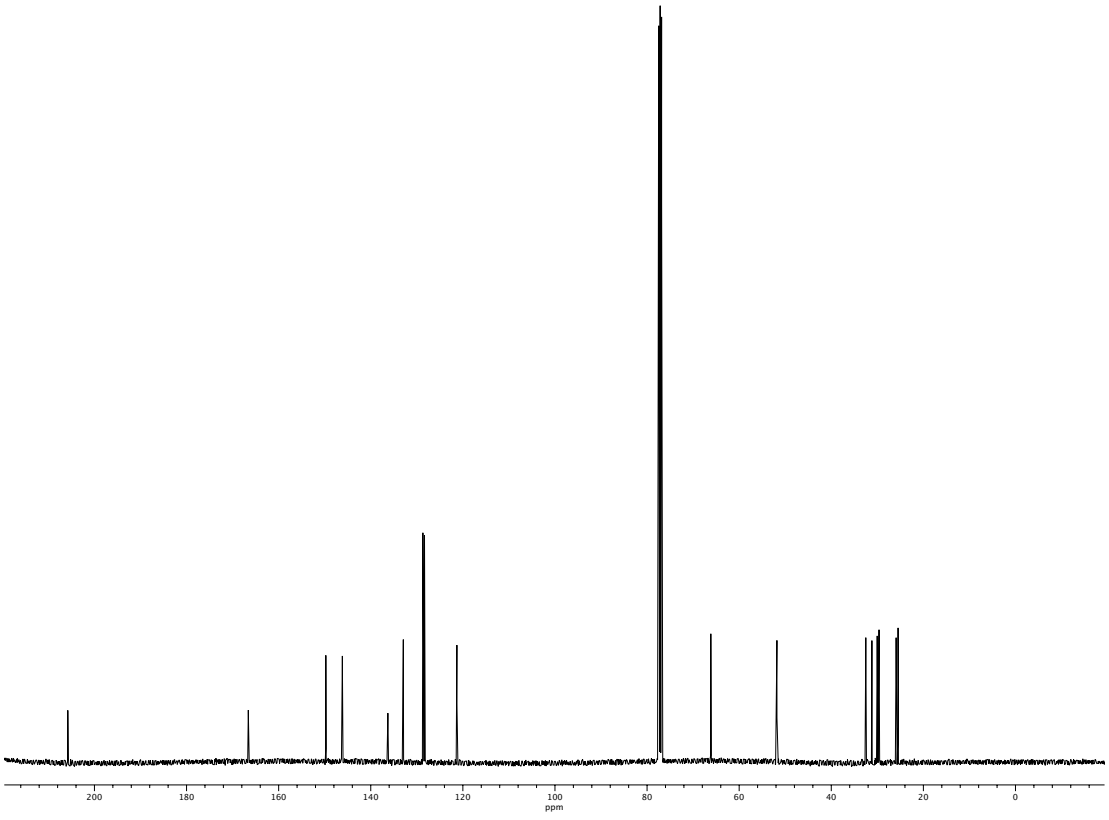

Figure A1.268. *^{13}C NMR (100 MHz, $CDCl_3$) of compound* ***123d.***

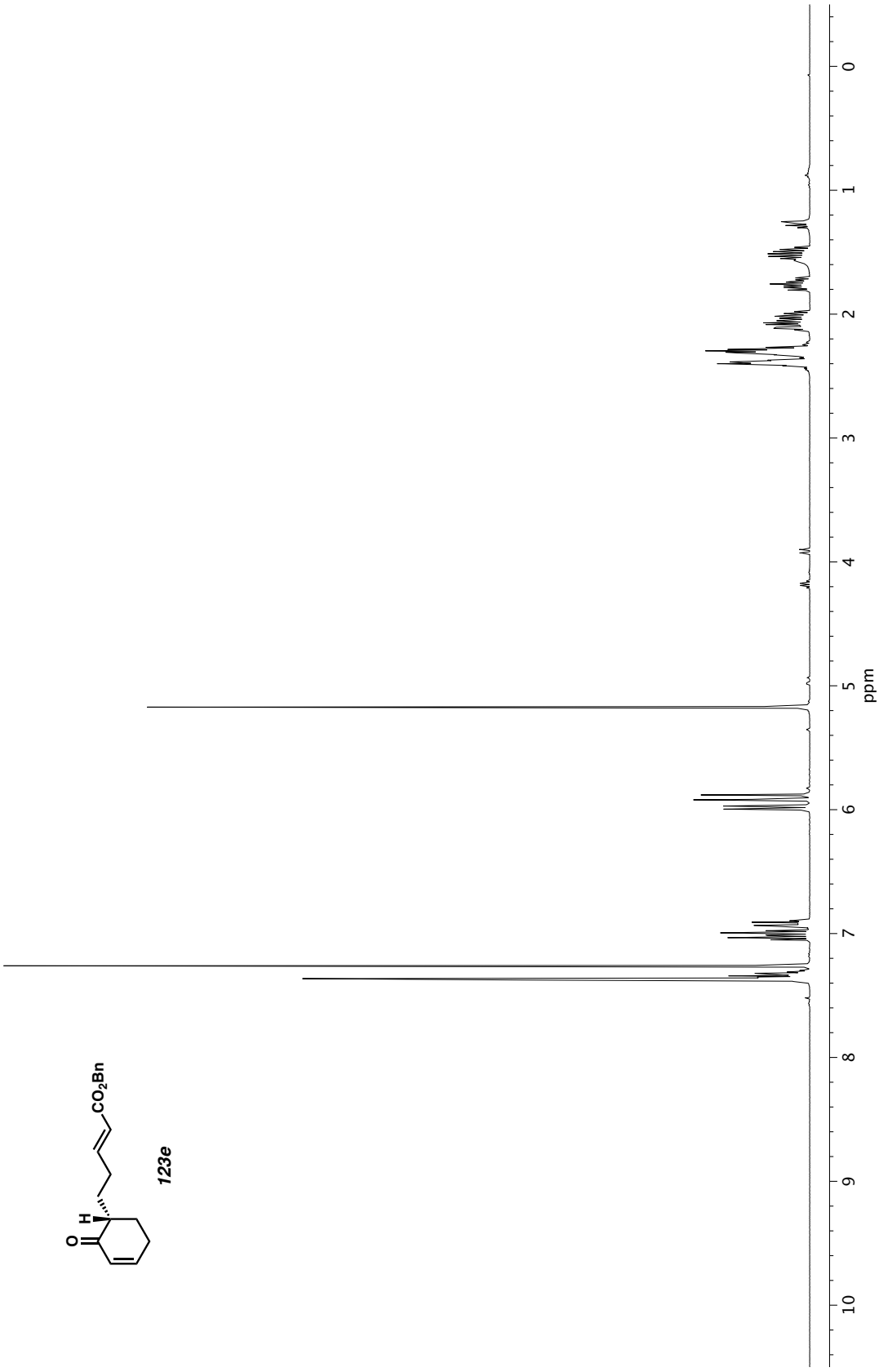

Figure A1.269. *^1H NMR (400 MHz, $CDCl_3$) of compound* ***123e.***

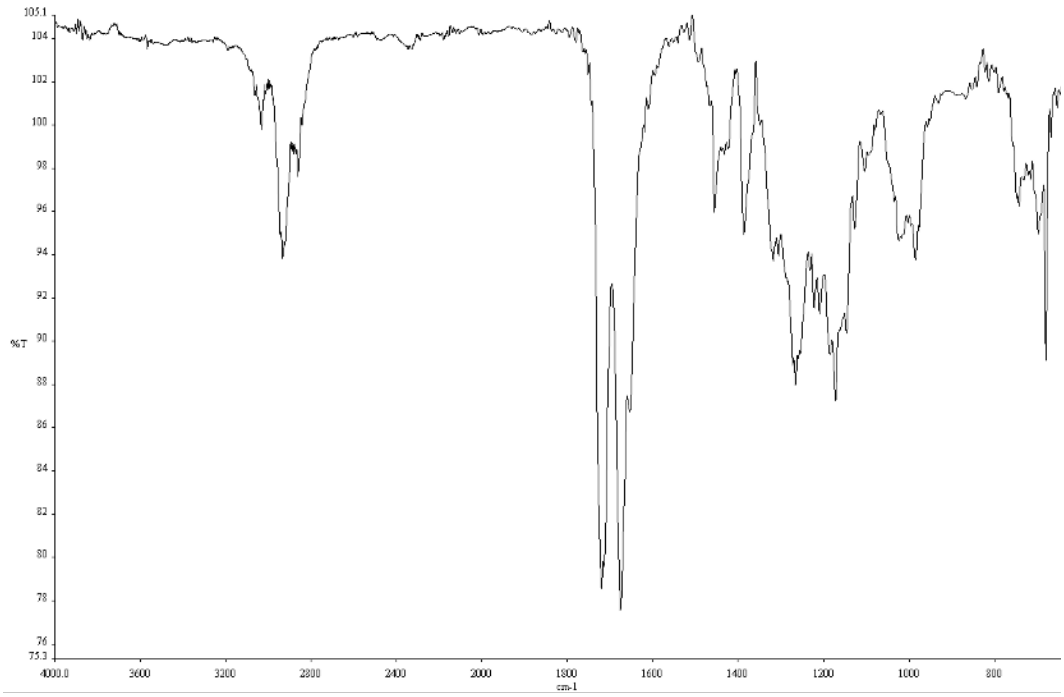

Figure A1.270. *Infrared spectrum (Thin Film, NaCl) of compound* ***123e.***

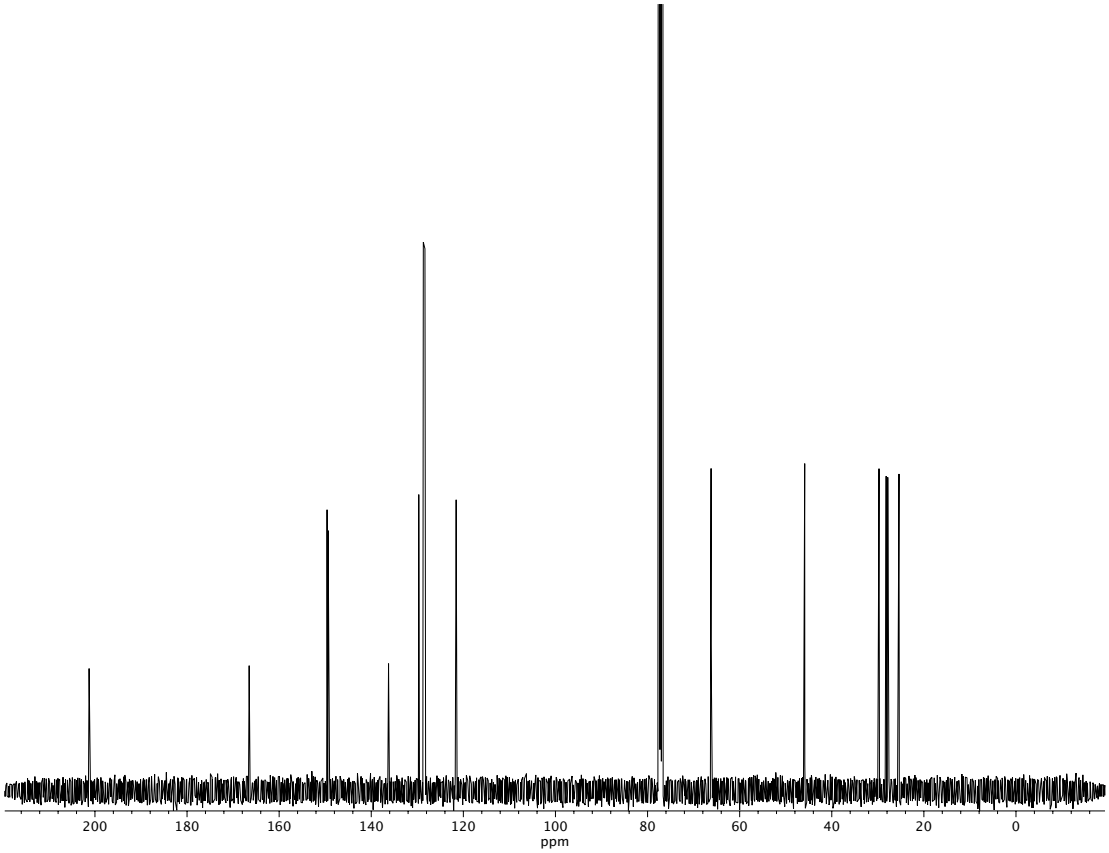

Figure A1.271. *^{13}C NMR (100 MHz, $CDCl_3$) of compound* ***123e.***

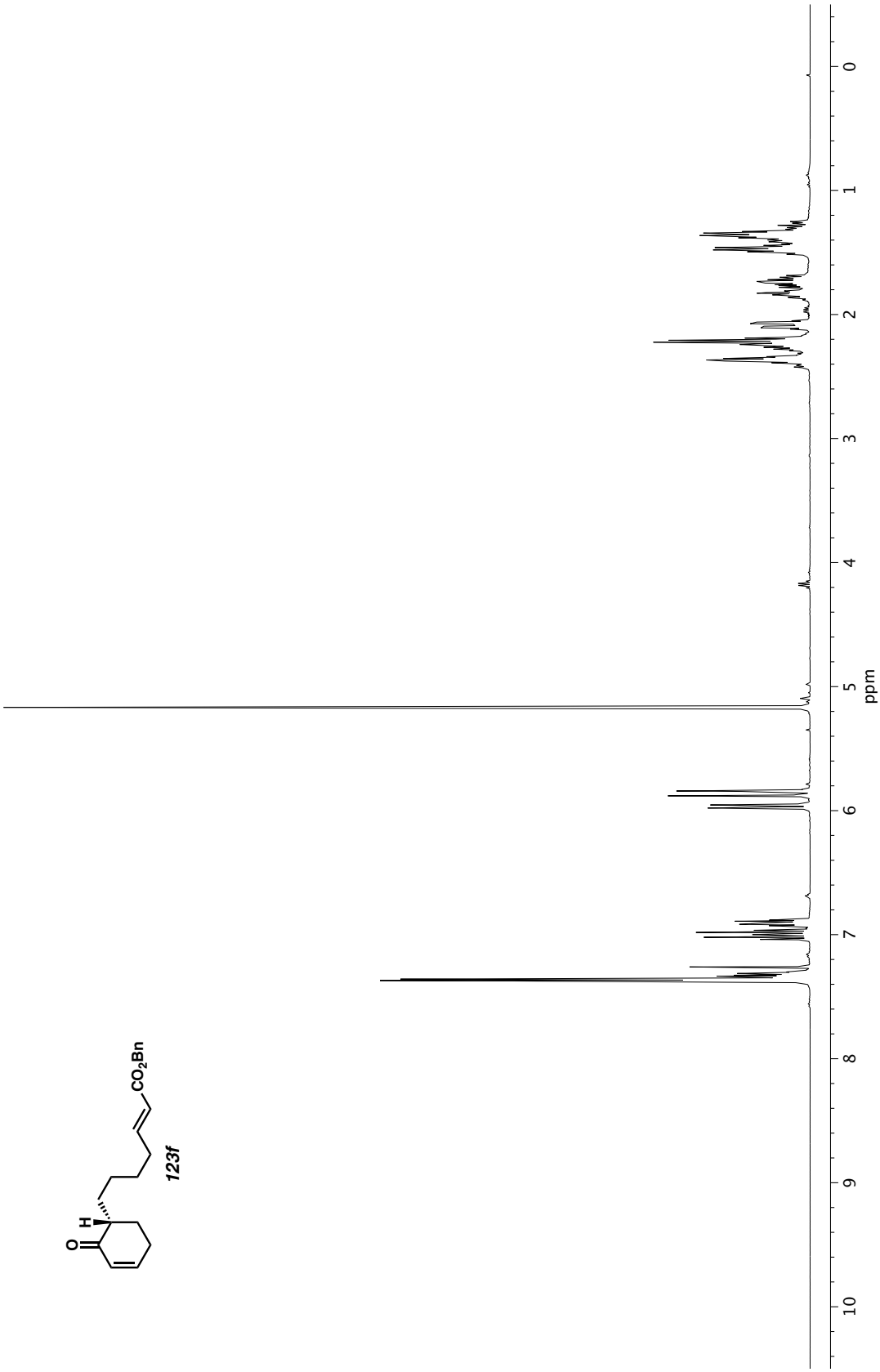

Figure A1.272. *^1H NMR (400 MHz, $CDCl_3$) of compound* ***123f.***

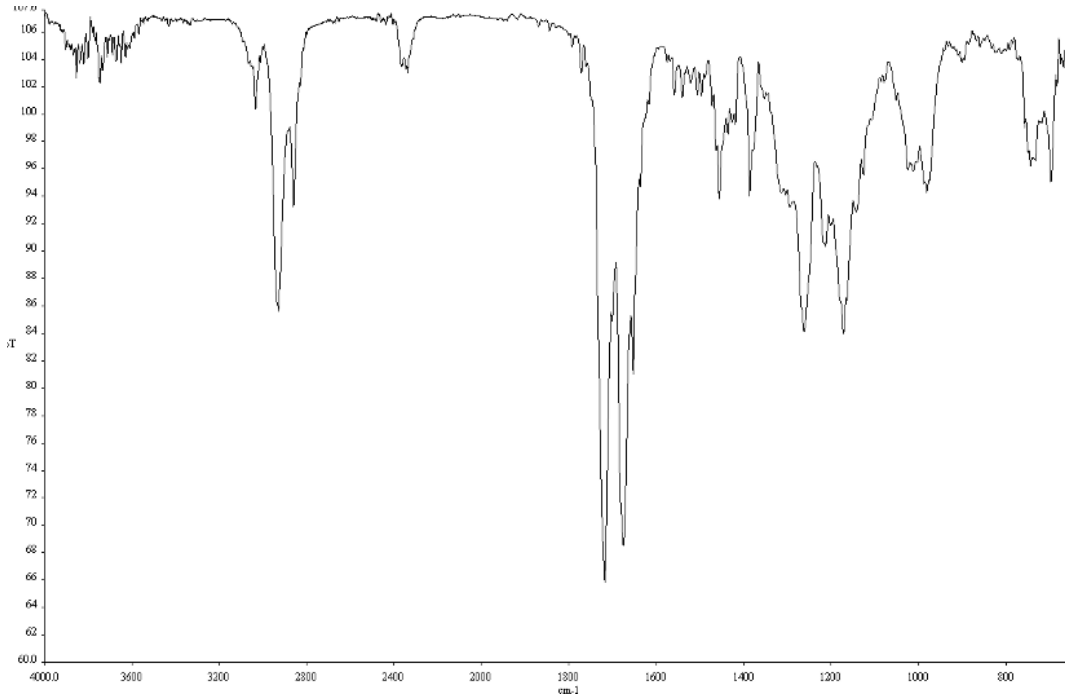

Figure A1.273. *Infrared spectrum (Thin Film, NaCl) of compound* ***123f.***

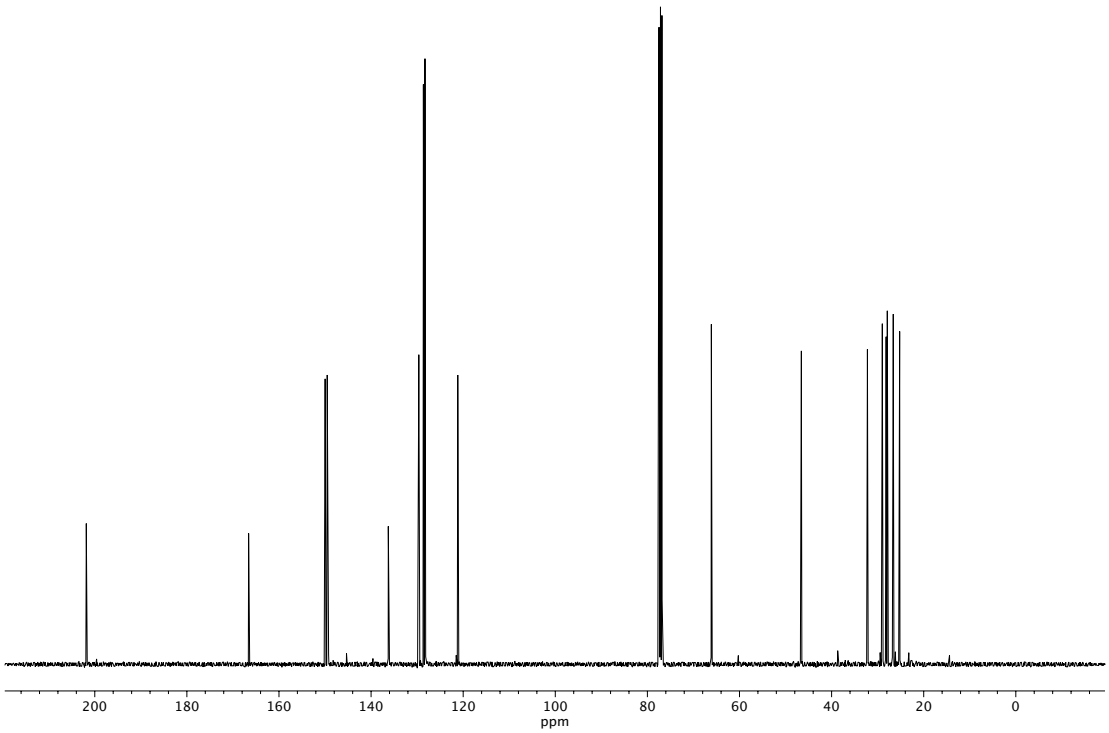

Figure A1.274. *^{13}C NMR (100 MHz, $CDCl_3$) of compound* ***123f.***

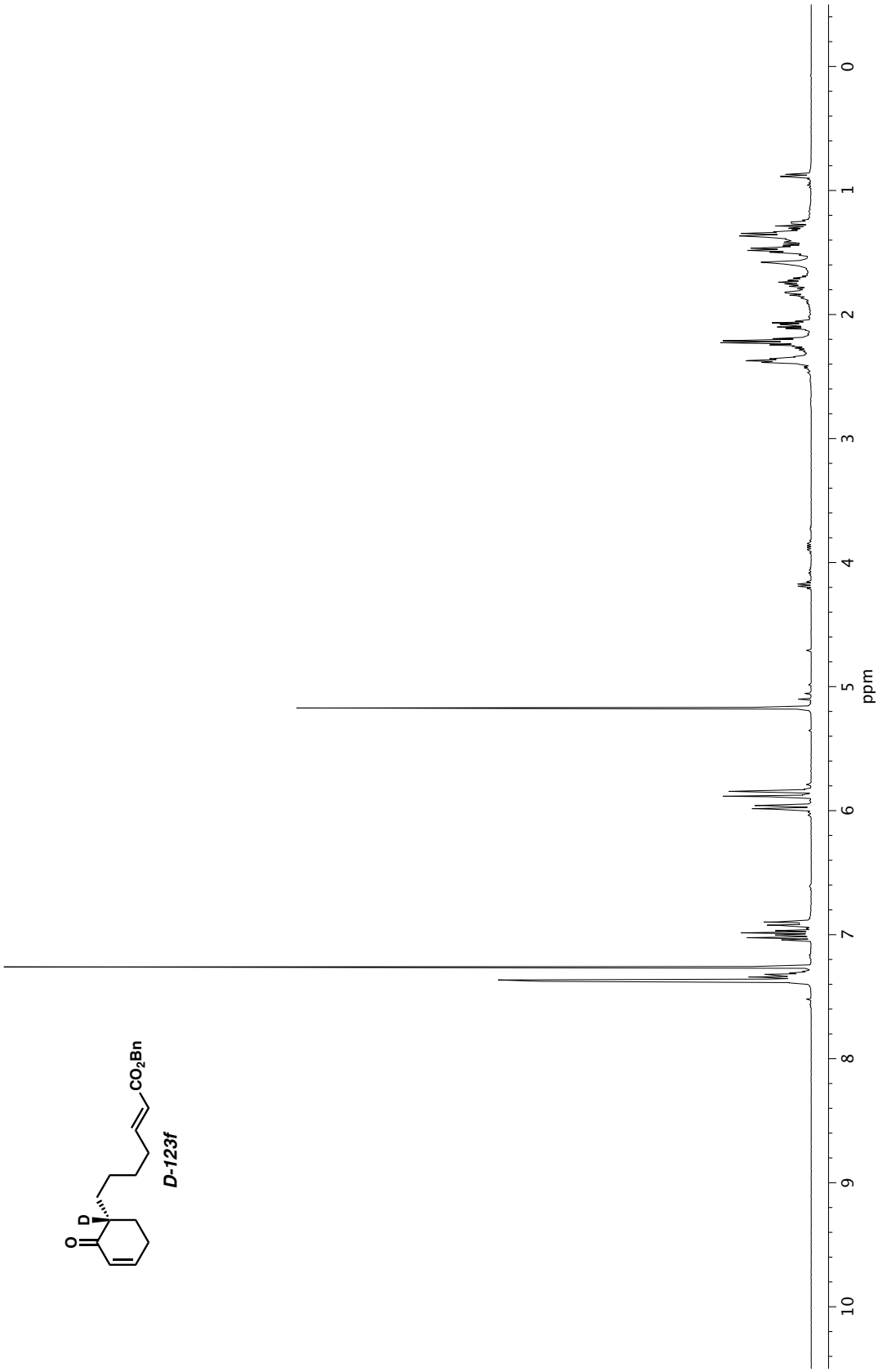

Figure A1.275. *^1H NMR (400 MHz, $CDCl_3$) of compound* ***D-123f.***

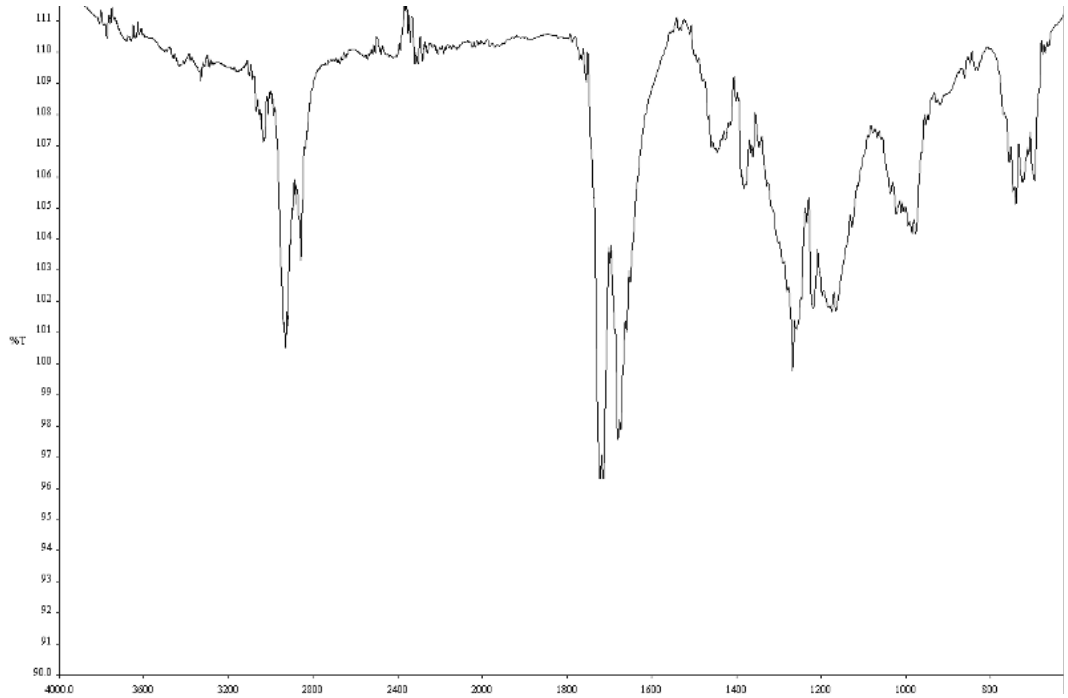

Figure A1.276. *Infrared spectrum (Thin Film, NaCl) of compound* ***D-123f.***

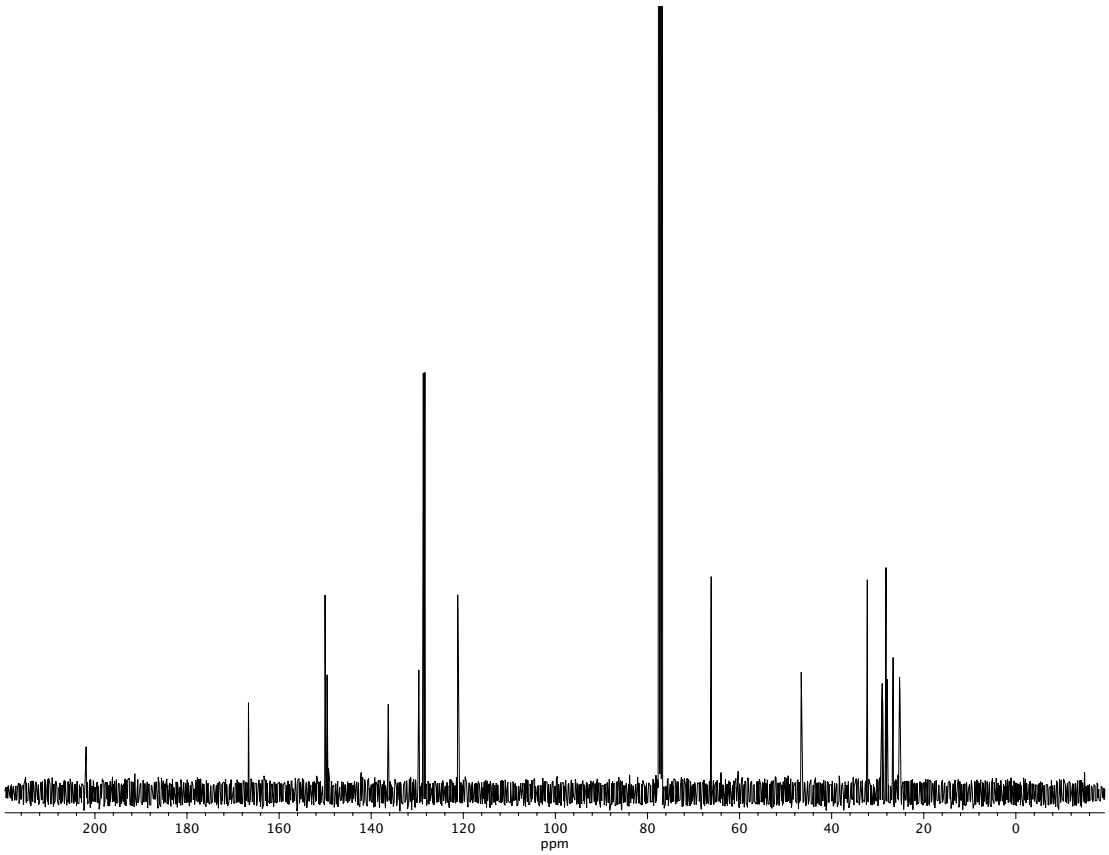

Figure A1.277. *^{13}C NMR (100 MHz, $CDCl_3$) of compound* ***D-123f.***

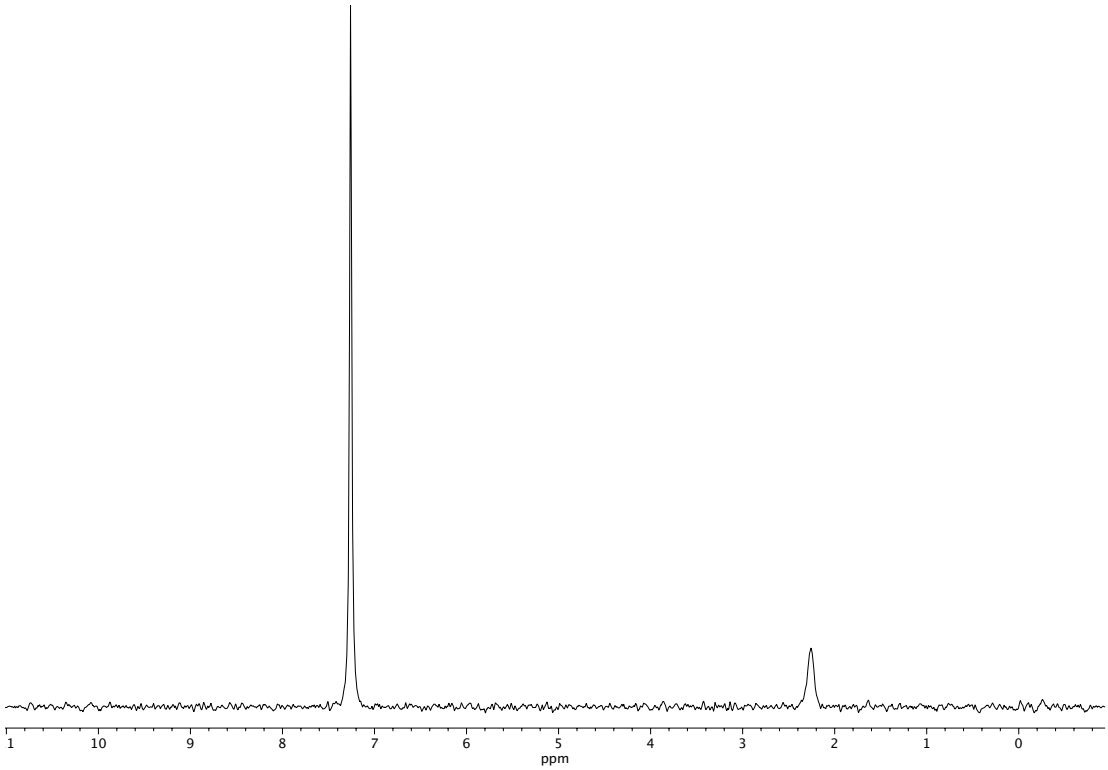

Figure A1.278. *^{2}H NMR (61 MHz, $CHCl_3$) of compound* ***D-123f.***

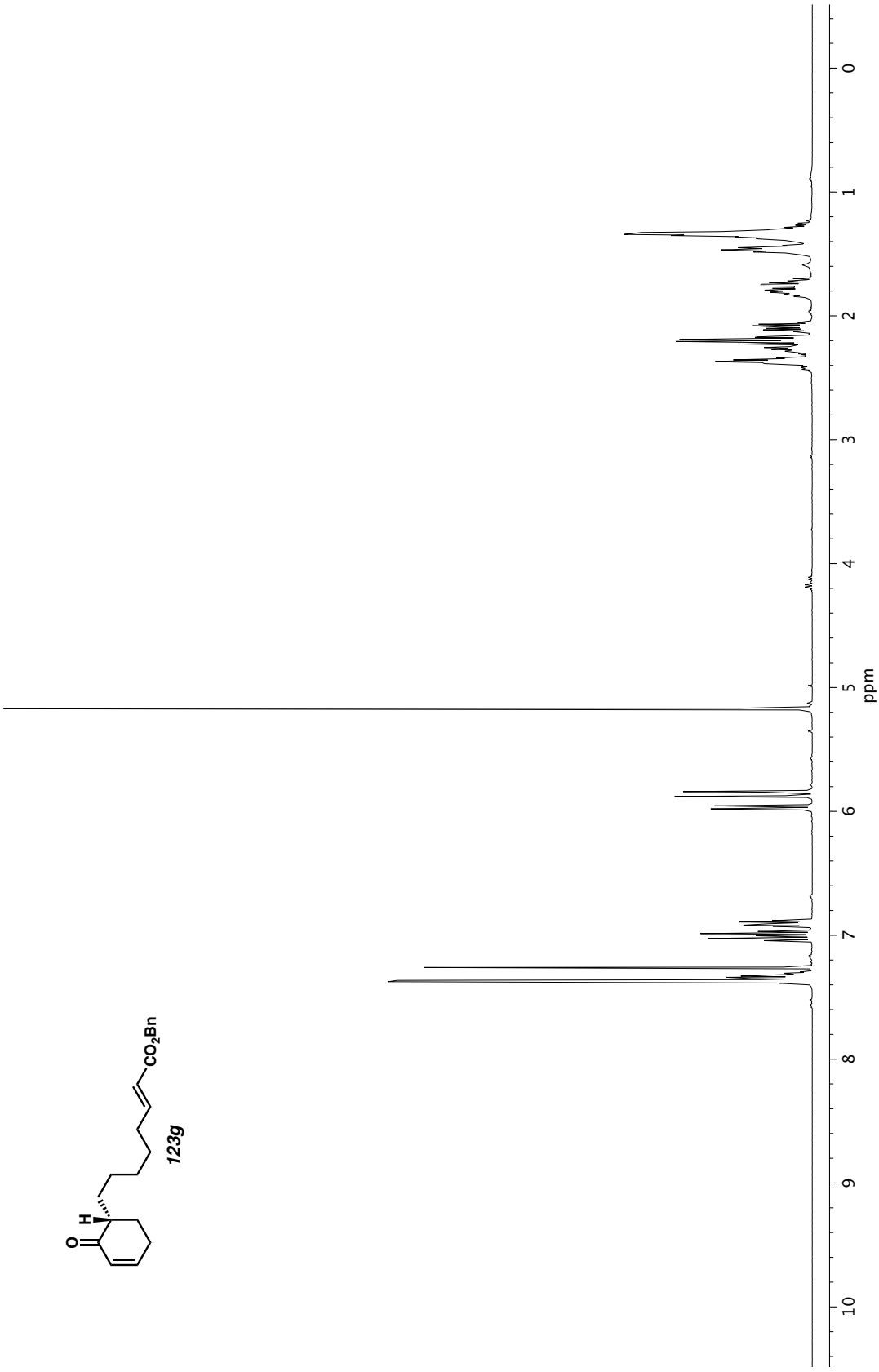

Figure A1.279. *^1H NMR (400 MHz, $CDCl_3$) of compound* ***123g.***

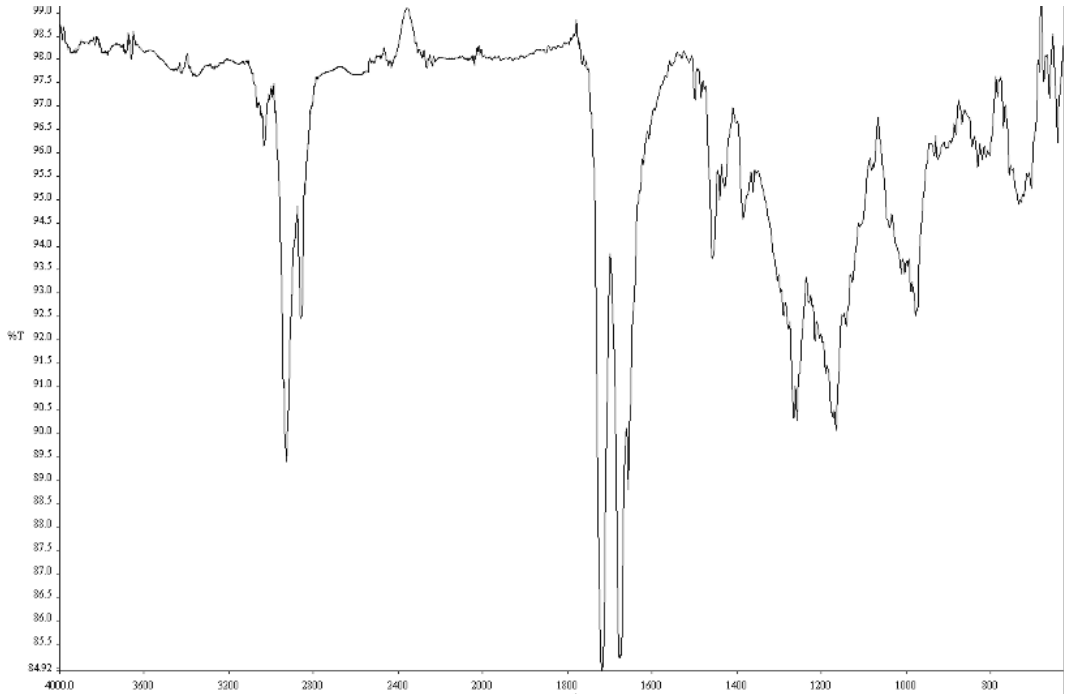

Figure A1.280. *Infrared spectrum (Thin Film, NaCl) of compound* ***123g.***

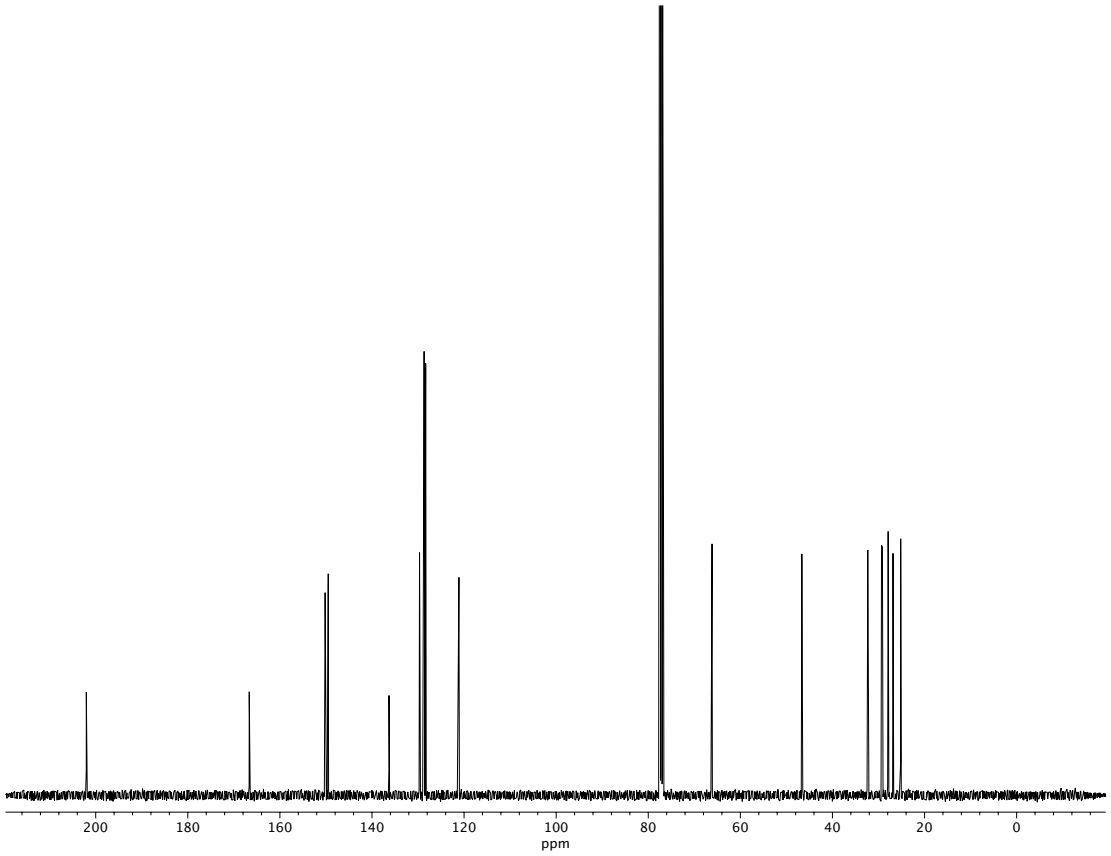

Figure A1.281. *^{13}C NMR (100 MHz, $CDCl_3$) of compound* ***123g.***

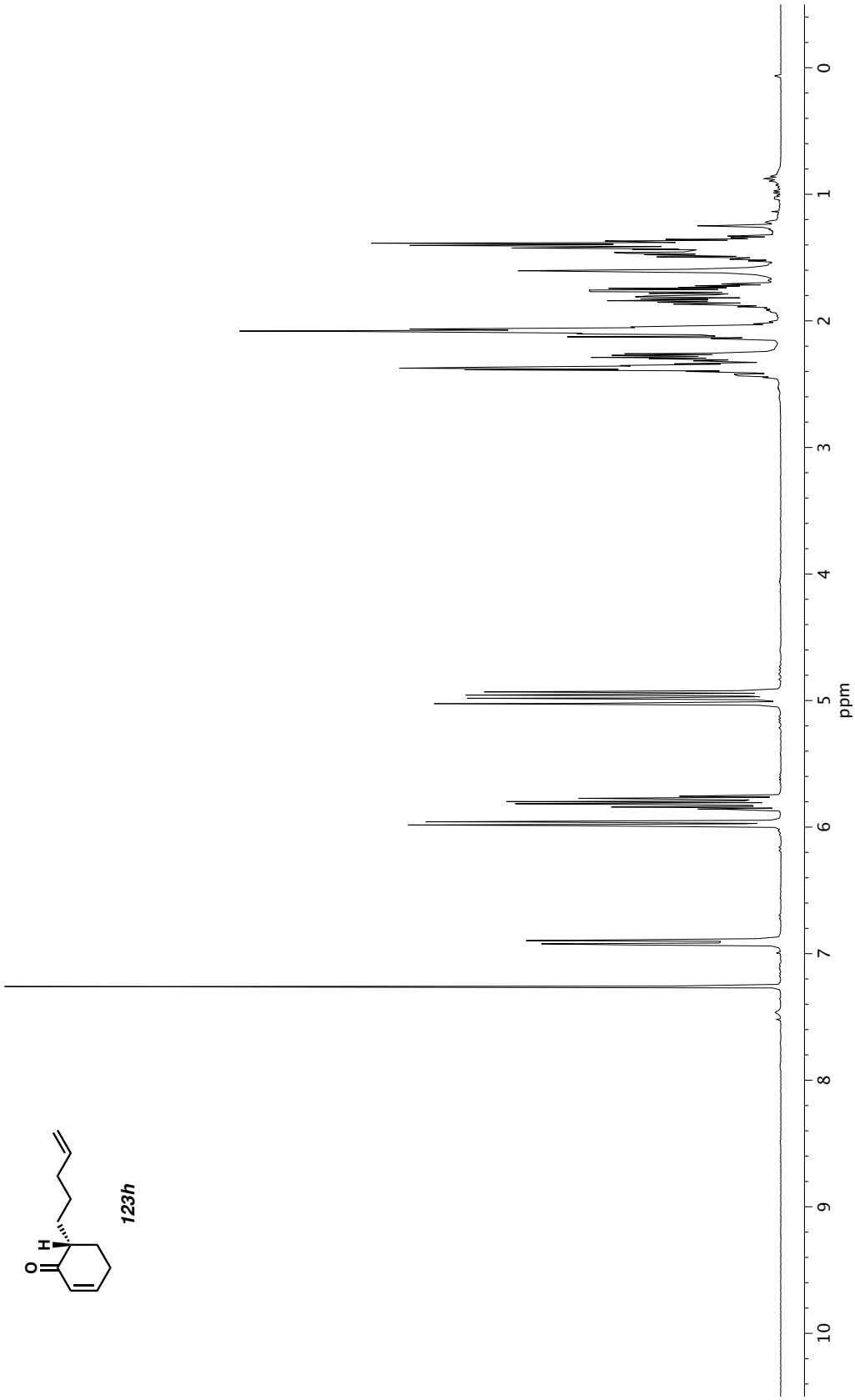

Figure A1.282. *^{1}H NMR (400 MHz, $CDCl_3$) of compound* ***123h.***

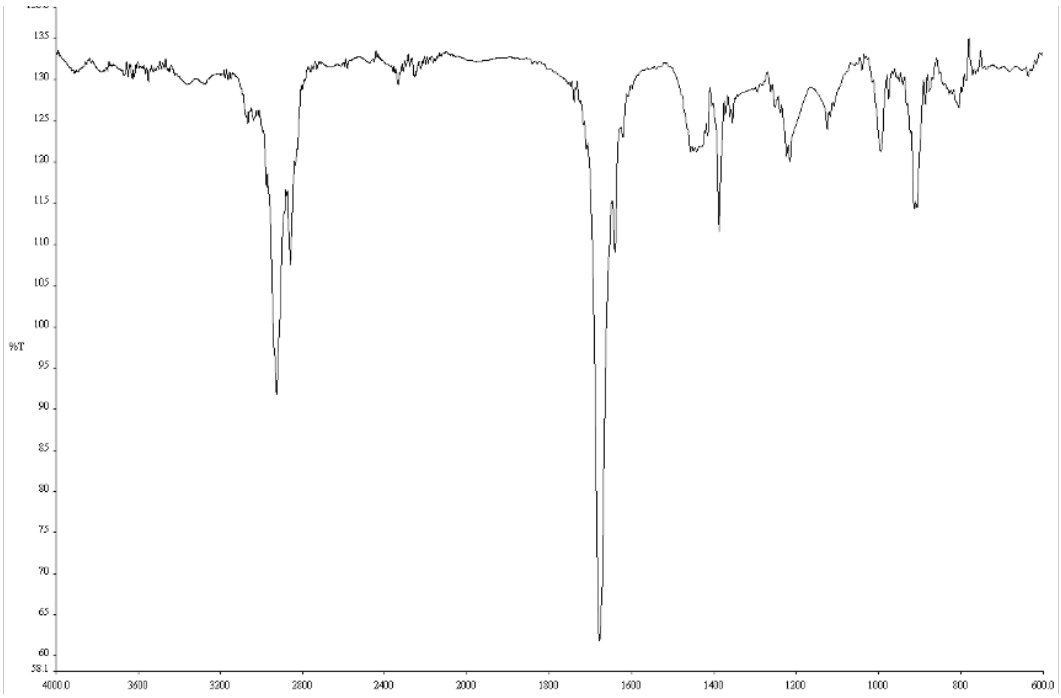

Figure A1.283. *Infrared spectrum (Thin Film, NaCl) of compound* ***123h.***

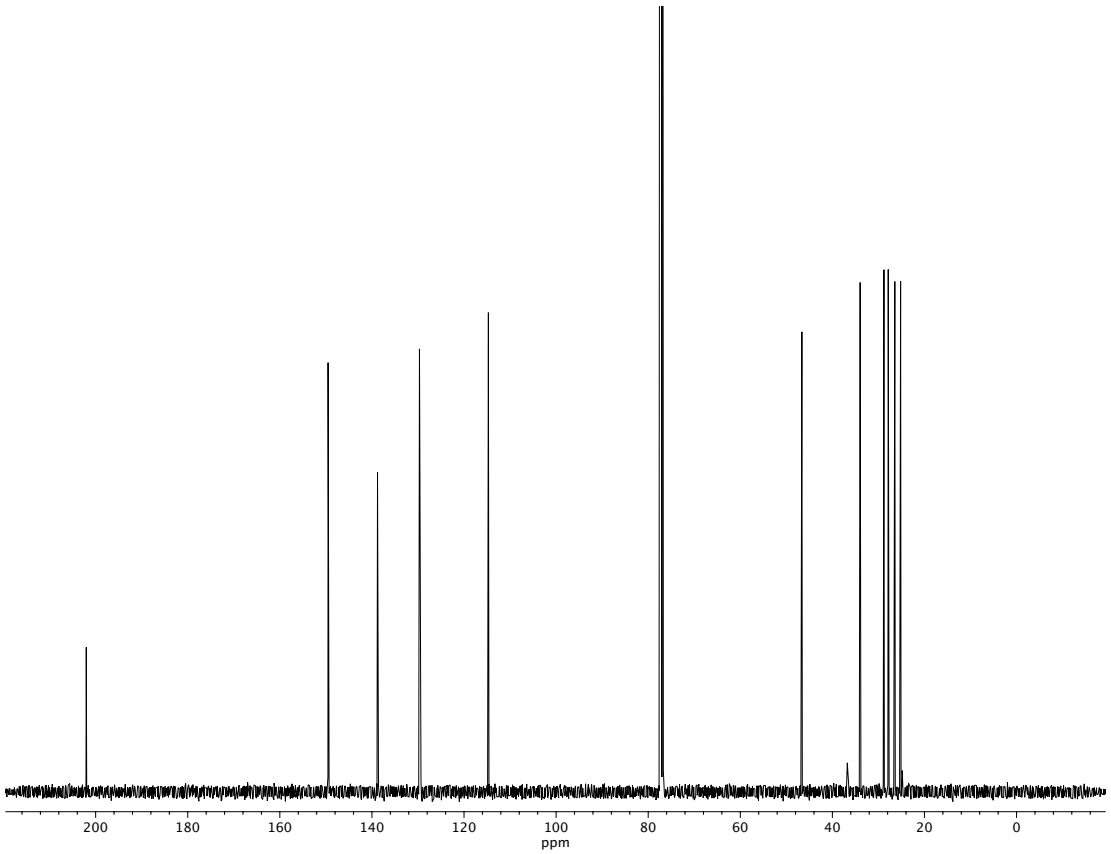

Figure A1.284. *^{13}C NMR (100 MHz, $CDCl_3$) of compound* ***123h.***

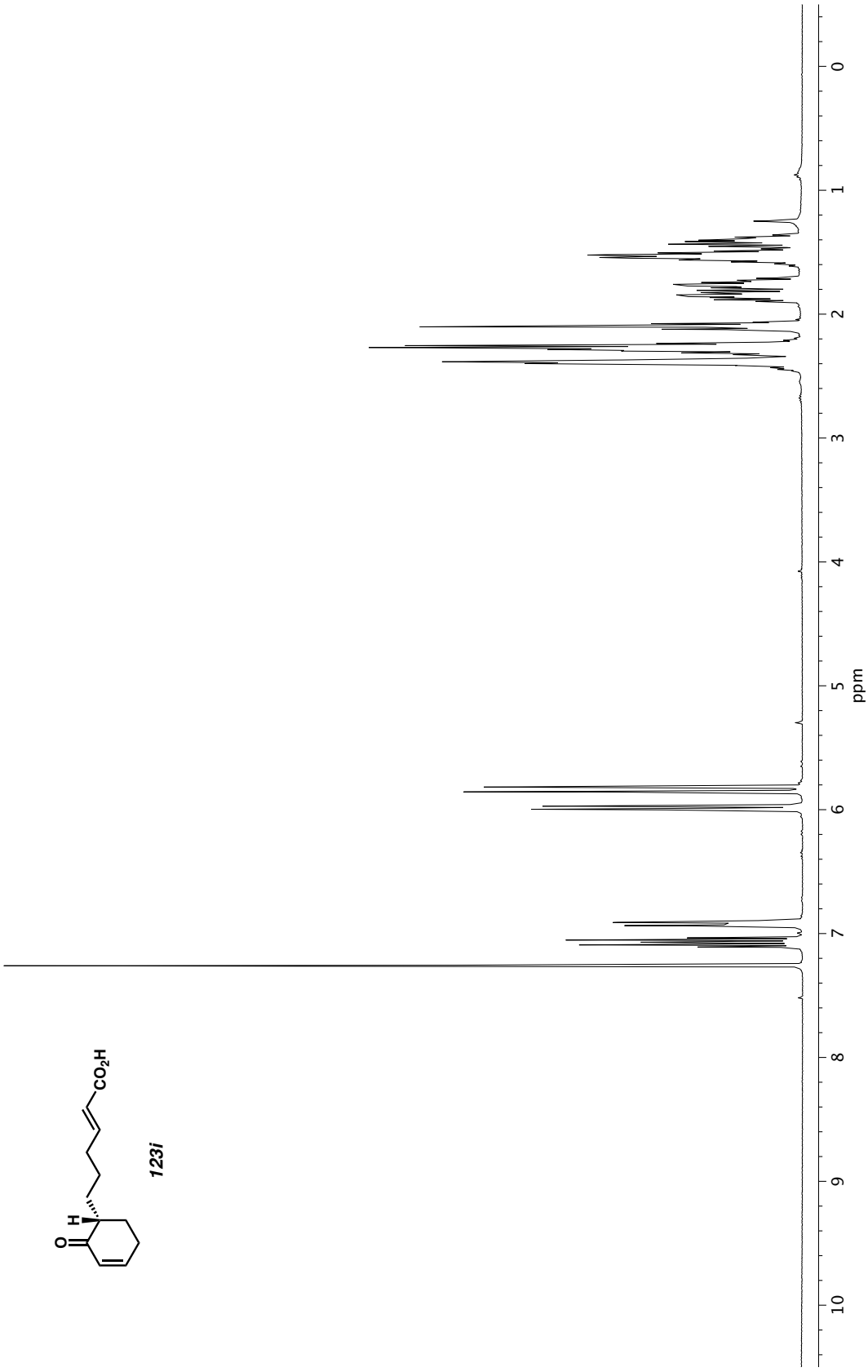

Figure A1.285. *^1H NMR (400 MHz, $CDCl_3$) of compound* ***123i.***

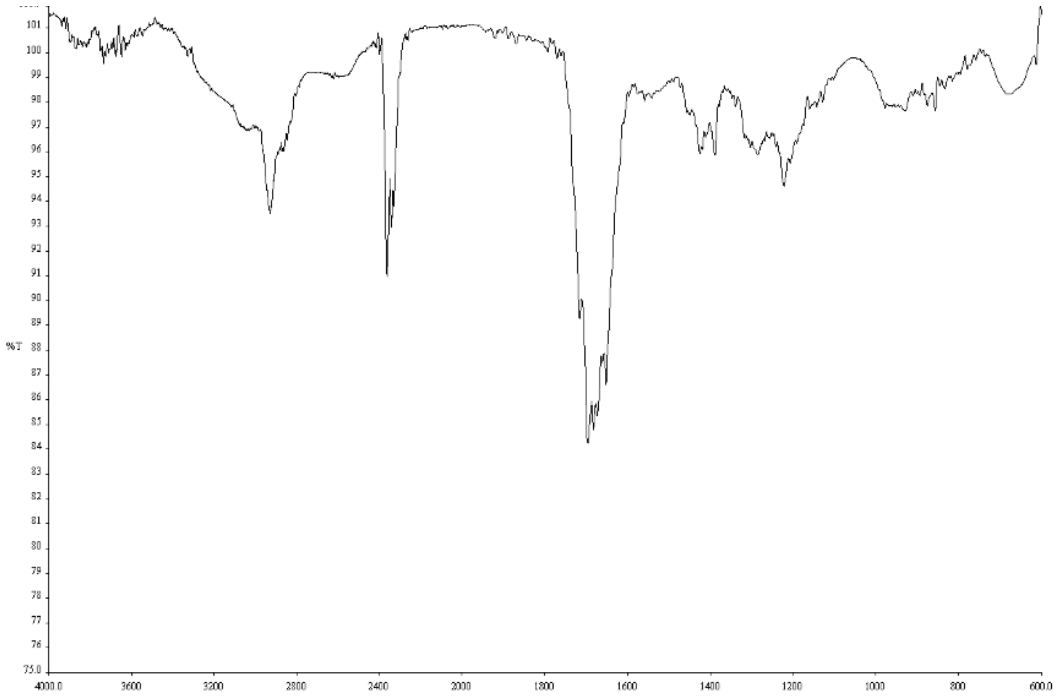

Figure A1.286. *Infrared spectrum (Thin Film, NaCl) of compound* ***123i.***

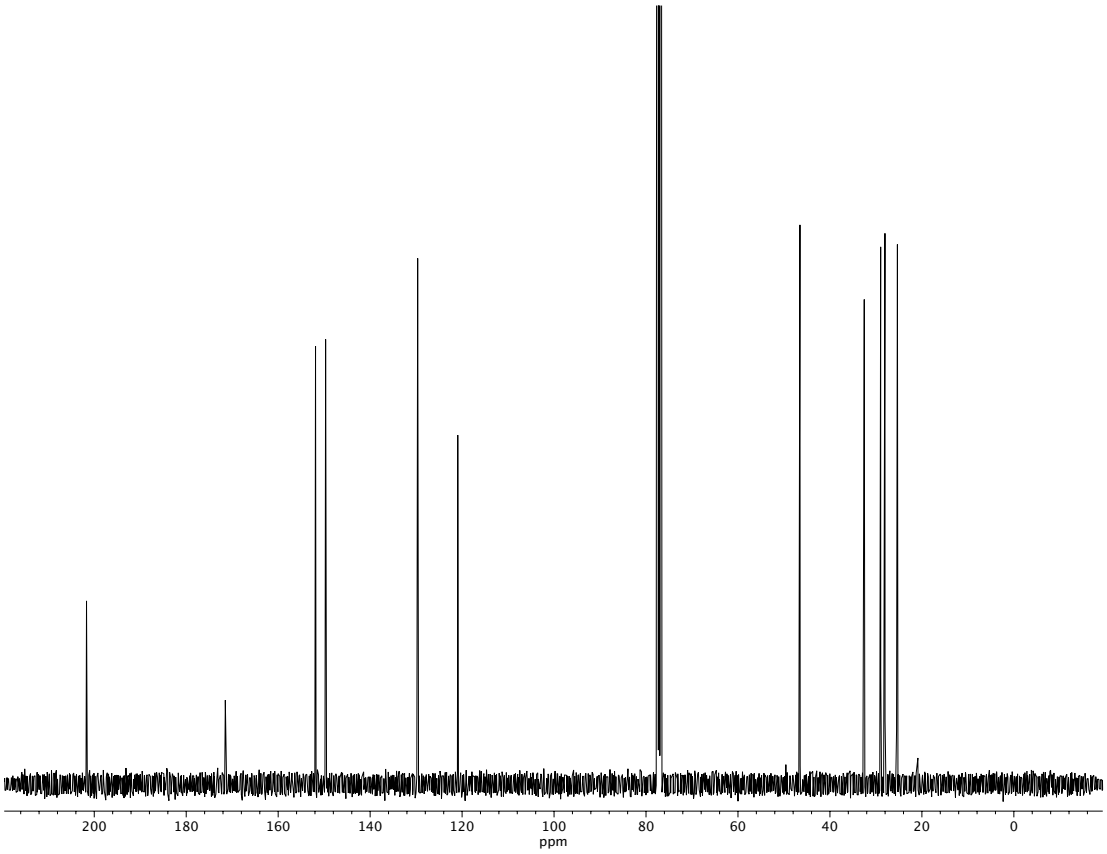

Figure A1.287. *^{13}C NMR (100 MHz, $CDCl_3$) of compound* ***123i.***

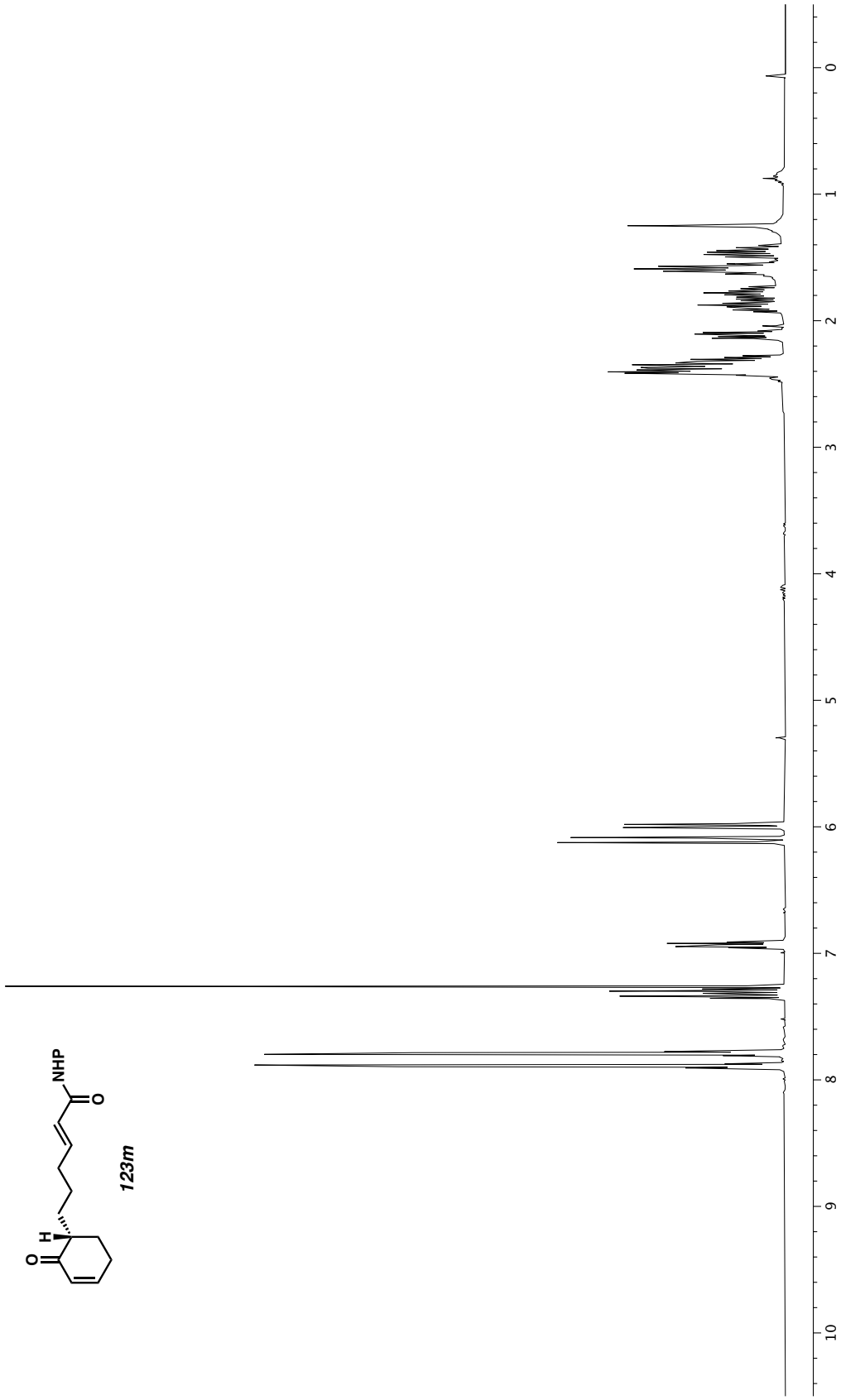

Figure A1.288. *^1H NMR (400 MHz, $CDCl_3$) of compound* ***123m.***

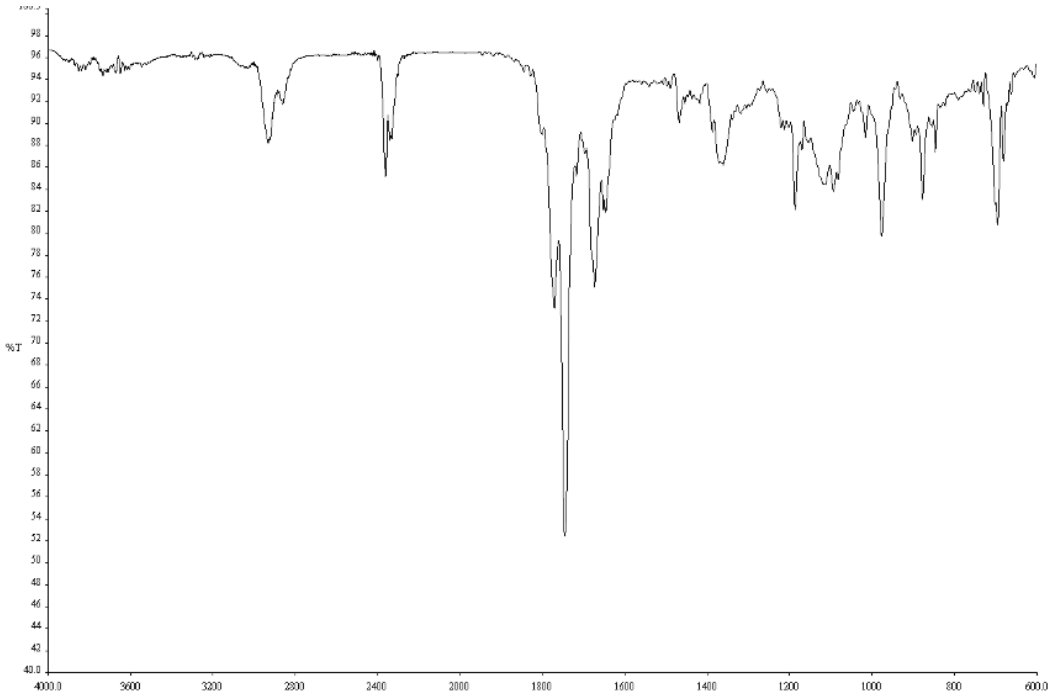

Figure A1.289. *Infrared spectrum (Thin Film, NaCl) of compound* ***123m.***

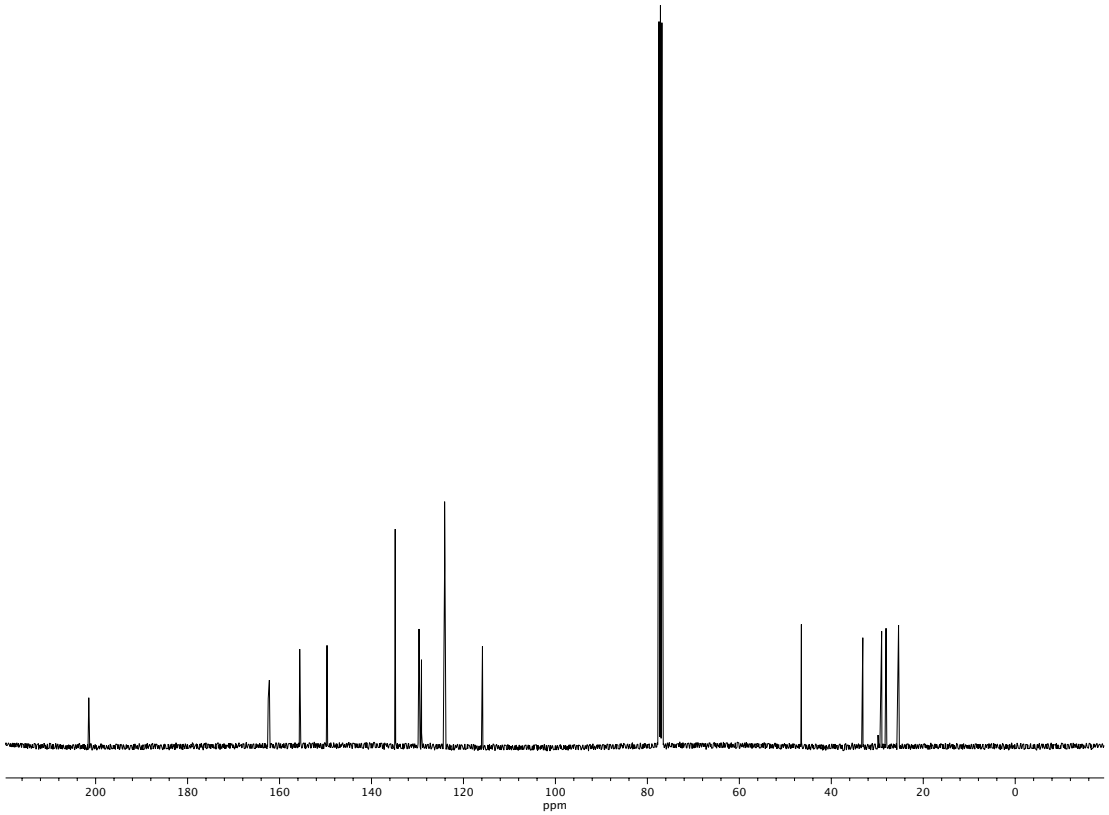

Figure A1.290. *^{13}C NMR (100 MHz, $CDCl_3$) of compound* ***123m.***

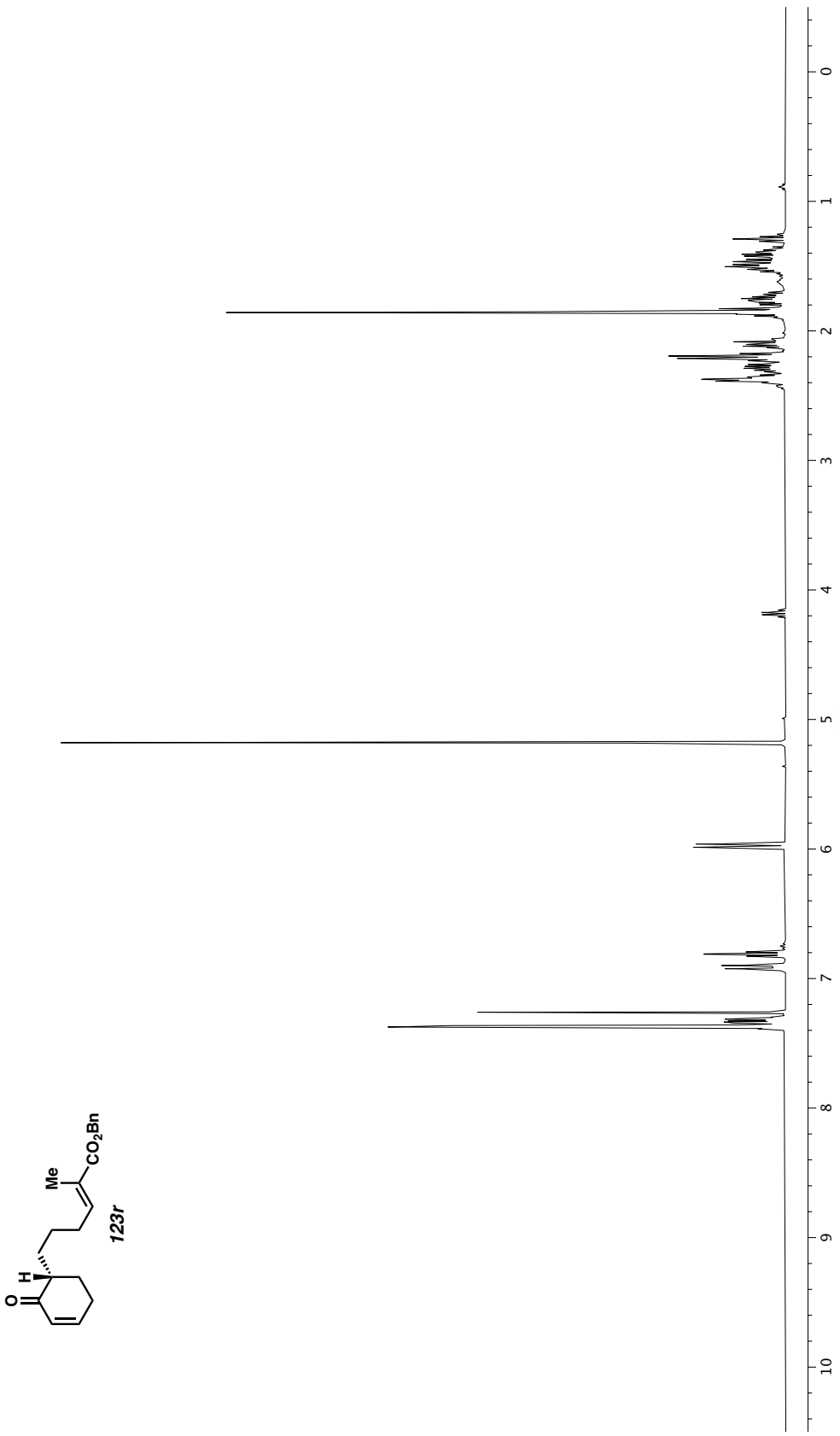

Figure A1.291. *^{1}H NMR (400 MHz, $CDCl_3$) of compound* ***123r.***

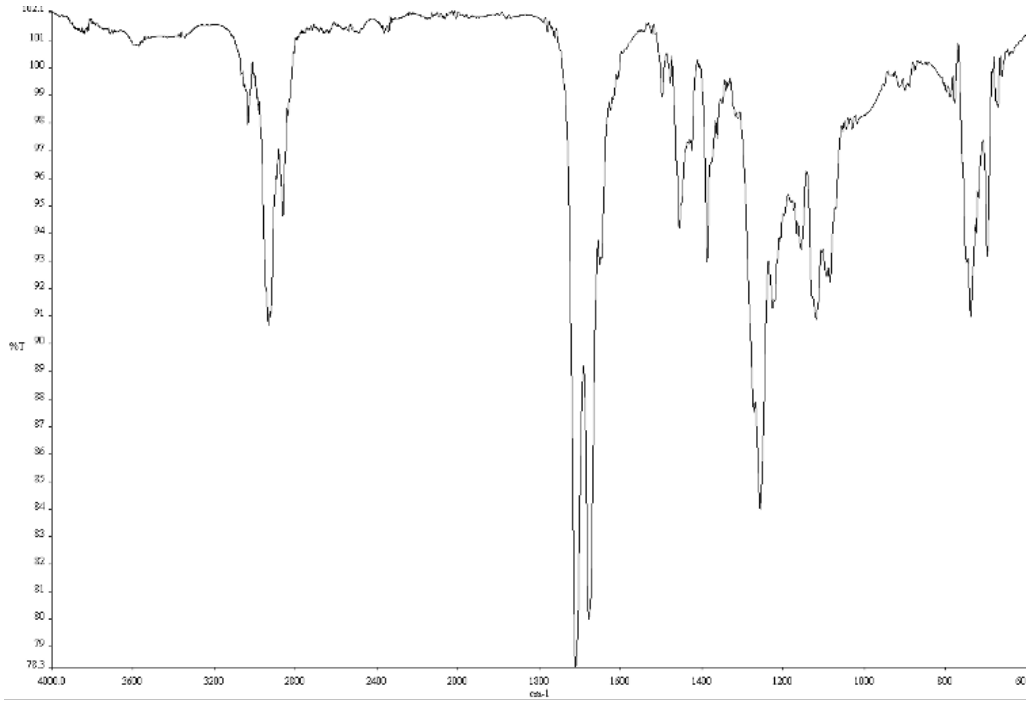

Figure A1.292. *Infrared spectrum (Thin Film, NaCl) of compound* ***123r.***

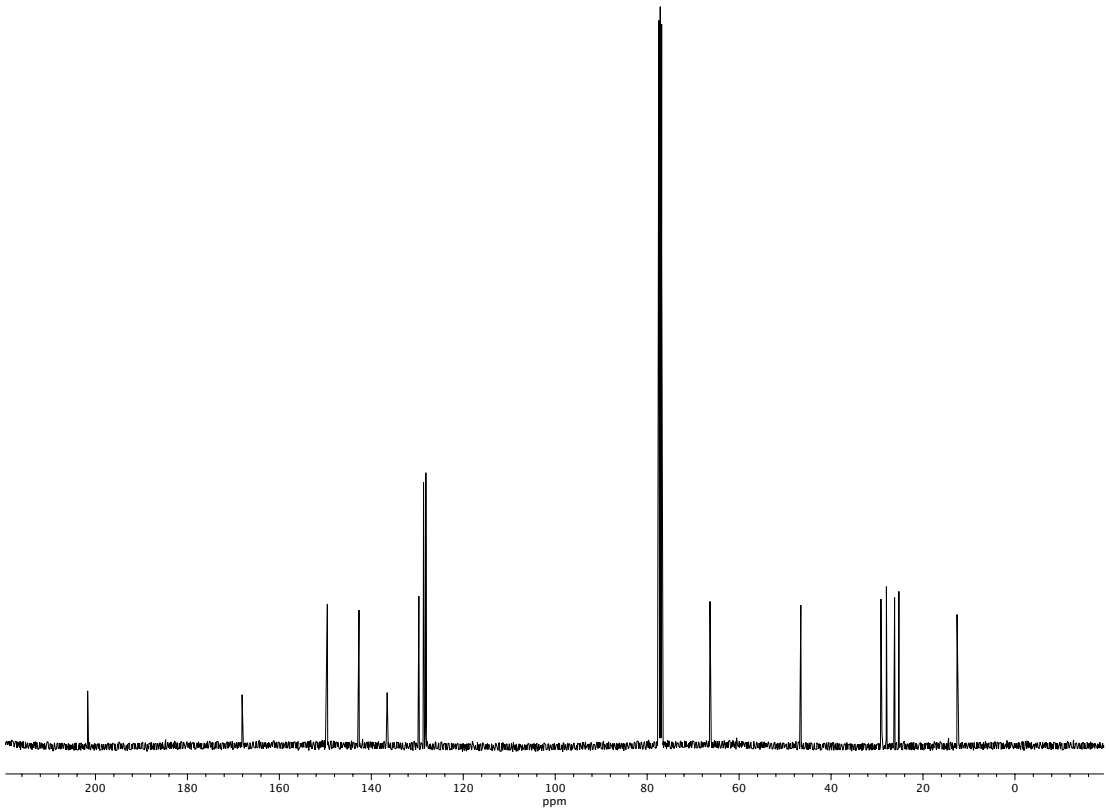

Figure A1.293. *^{13}C NMR (100 MHz, $CDCl_3$) of compound* ***123r.***

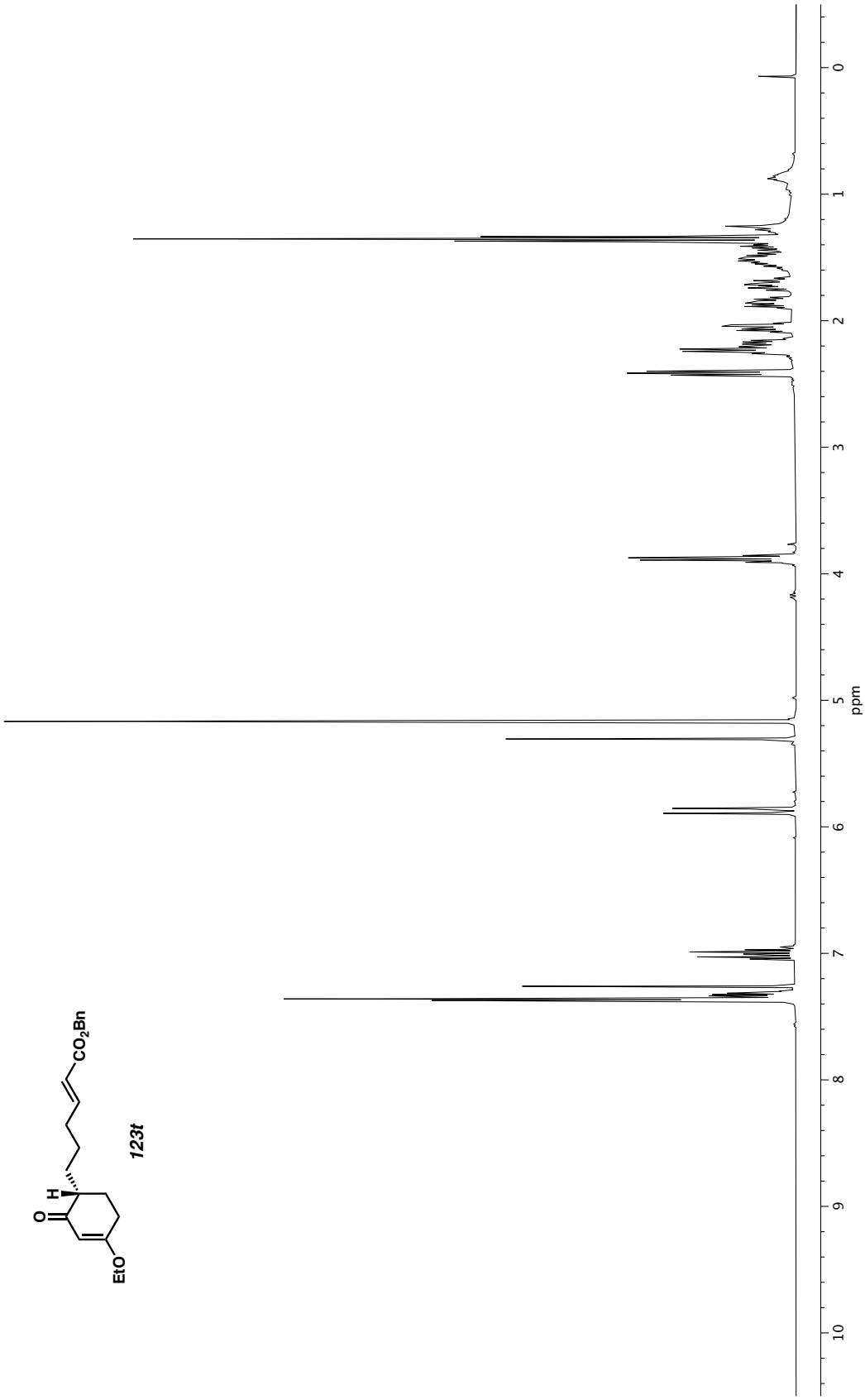

Figure A1.294. *^1H NMR (400 MHz, $CDCl_3$) of compound* ***123t.***

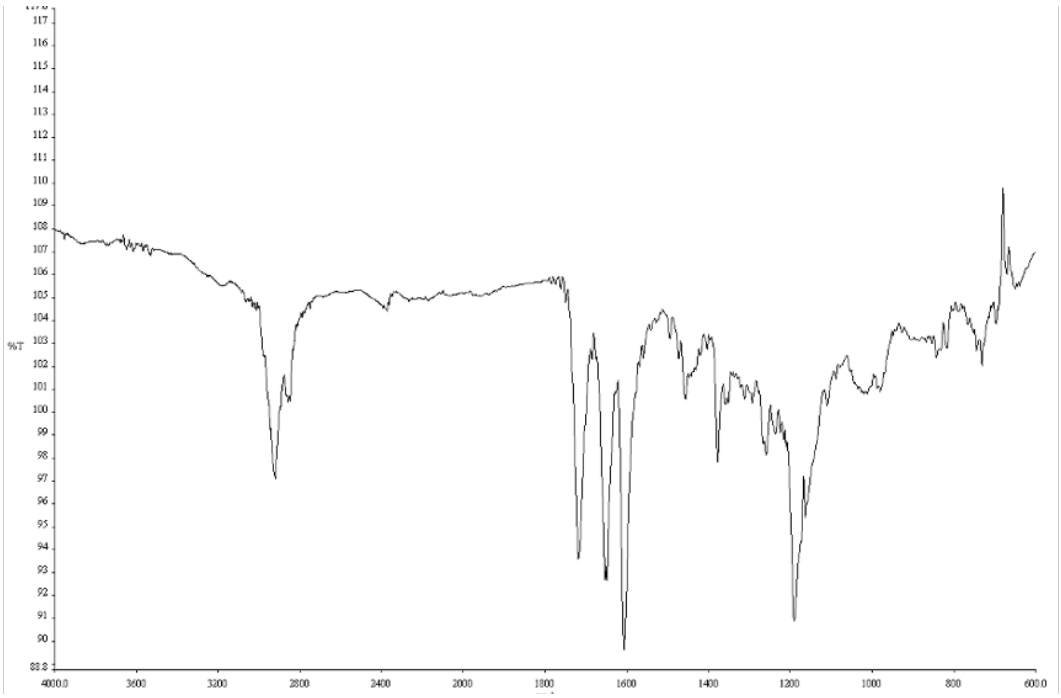

Figure A1.295. *Infrared spectrum (Thin Film, NaCl) of compound* ***123t.***

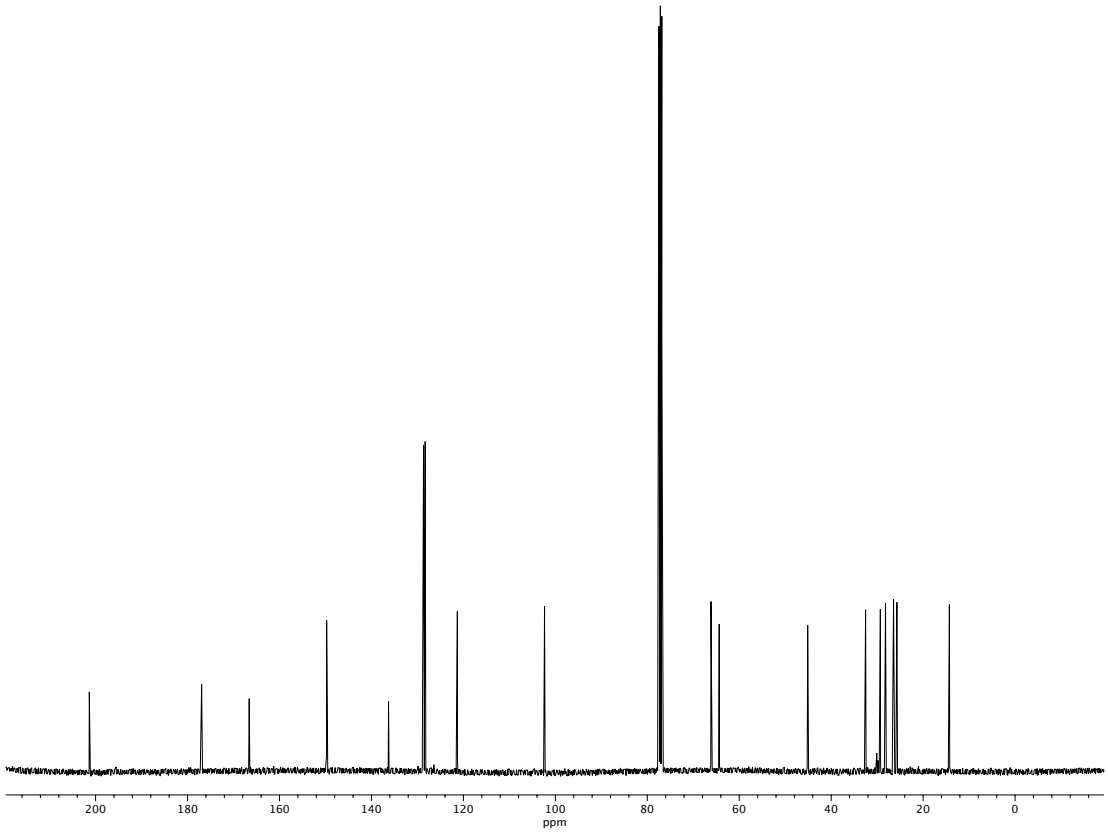

Figure A1.296. *^{13}C NMR (100 MHz, $CDCl_3$) of compound* ***123t.***

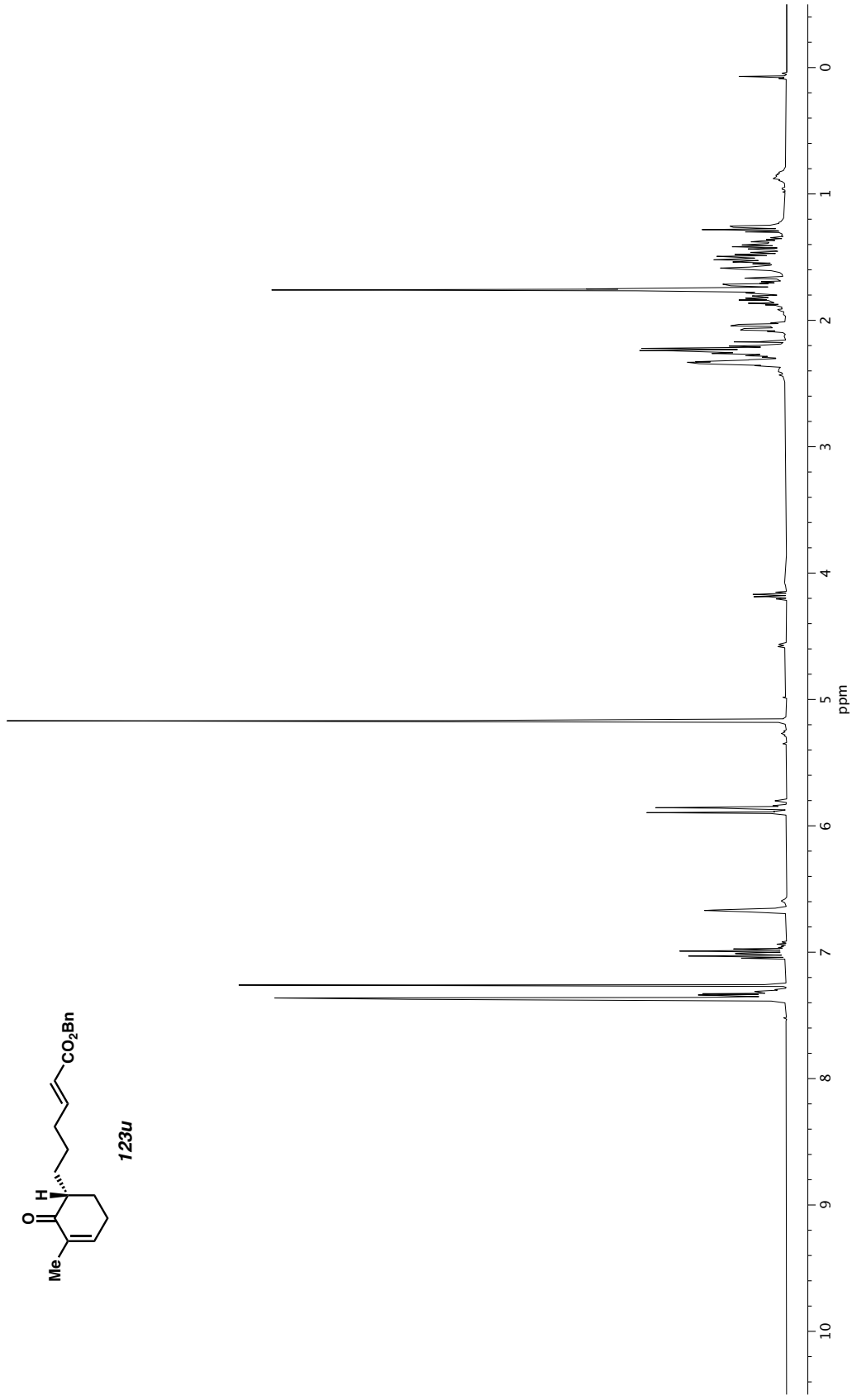

Figure A1.297. *^1H NMR (400 MHz, $CDCl_3$) of compound* ***123u.***

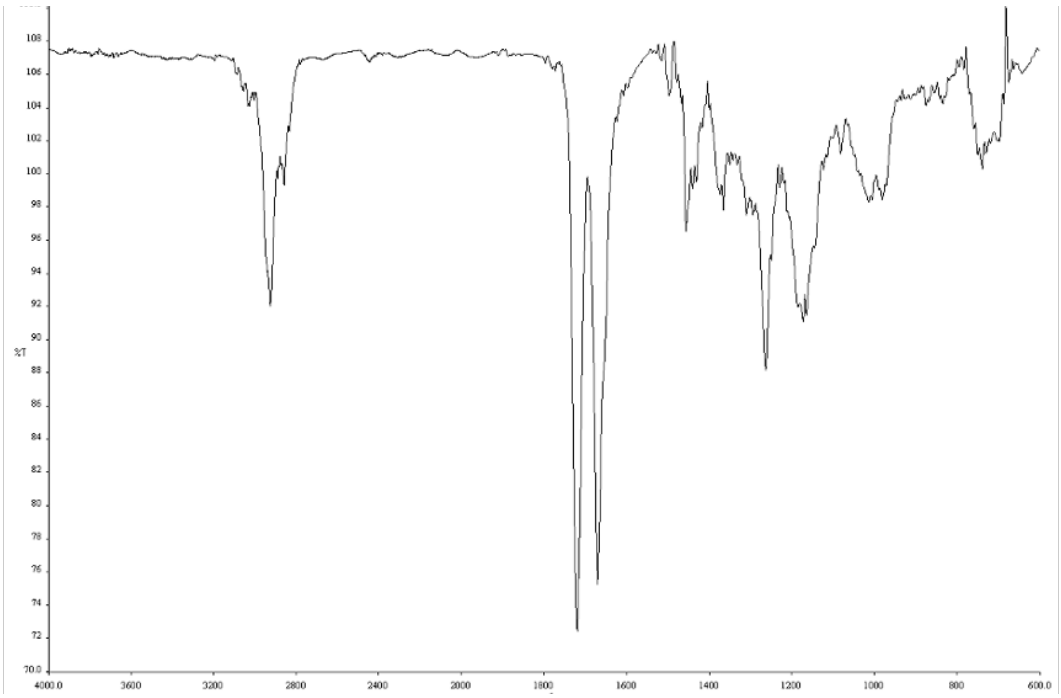

Figure A1.298. *Infrared spectrum (Thin Film, NaCl) of compound* ***123u.***

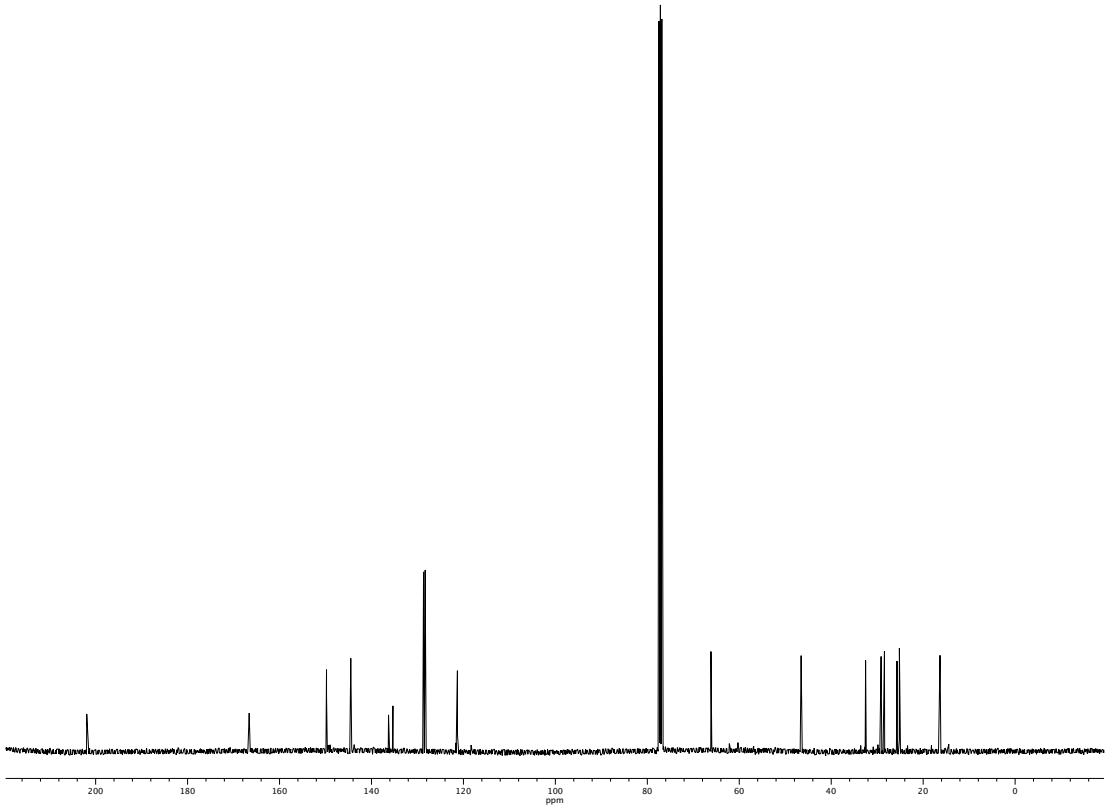

Figure A1.299. *^{13}C NMR (100 MHz, $CDCl_3$) of compound* ***123u.***

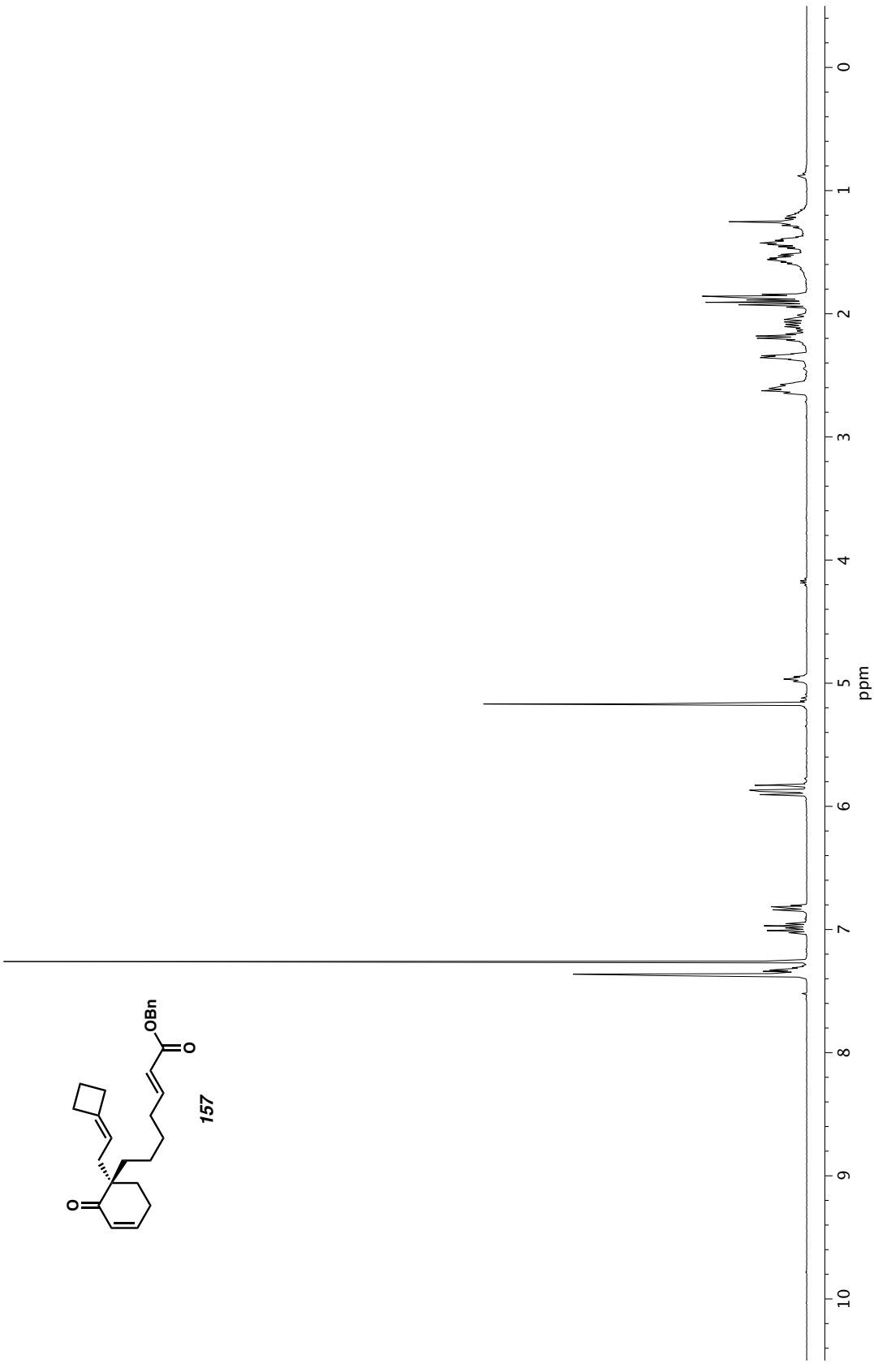

Figure A1.300. *^1H NMR (400 MHz, $CDCl_3$) of compound* ***157.***

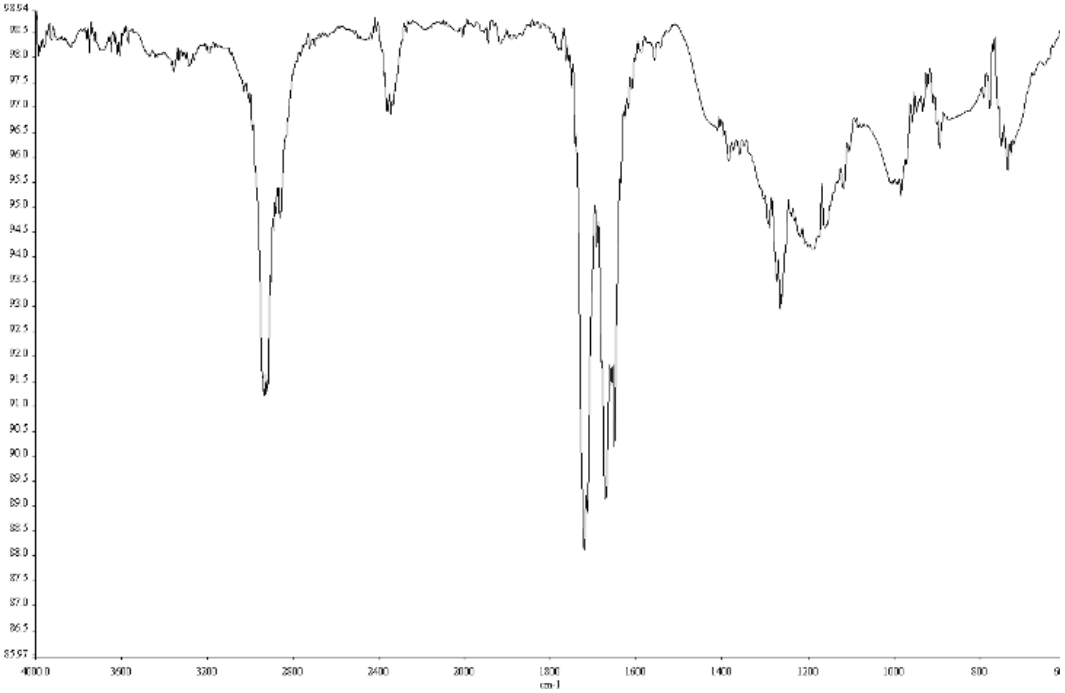

Figure A1.301. *Infrared spectrum (Thin Film, NaCl) of compound* ***157.***

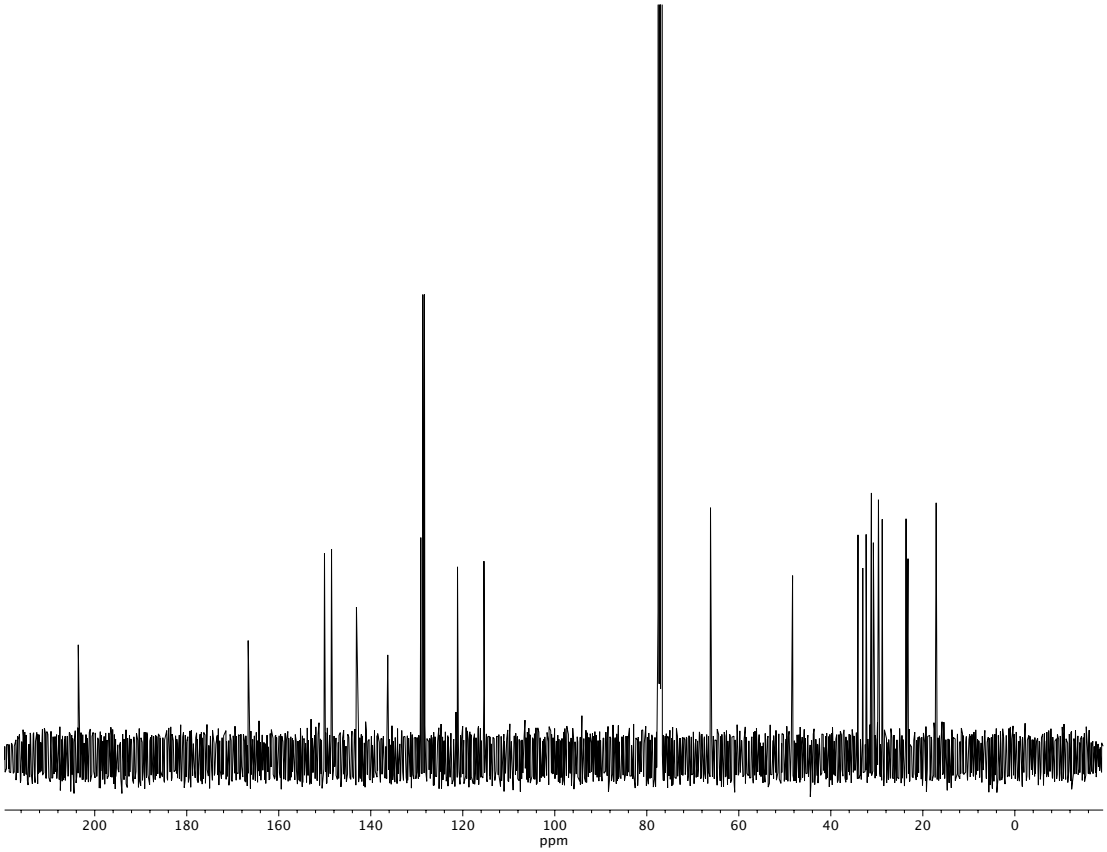

Figure A1.302. *^{13}C NMR (100 MHz, $CDCl_3$) of compound* ***157.***

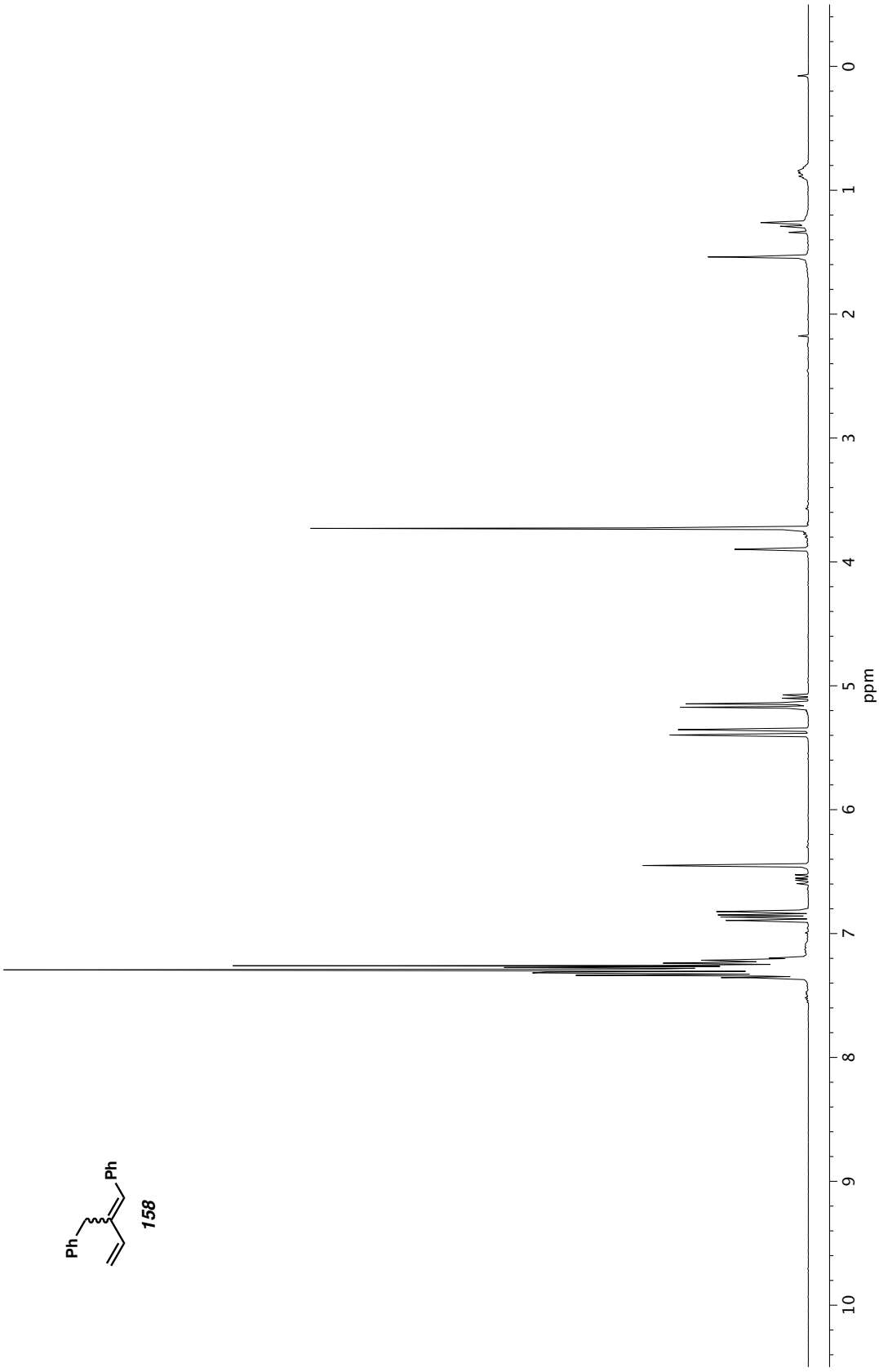

Figure A1.303. *^1H NMR (400 MHz, $CDCl_3$) of compound* ***158.***

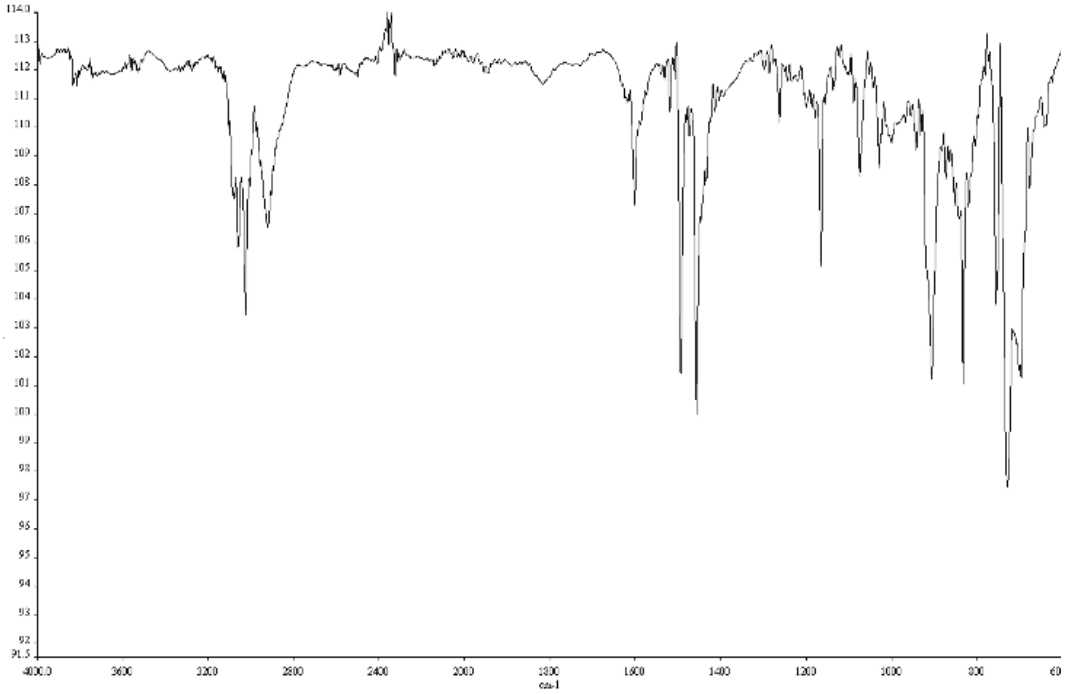

Figure A1.304. *Infrared spectrum (Thin Film, NaCl) of compound* ***158.***

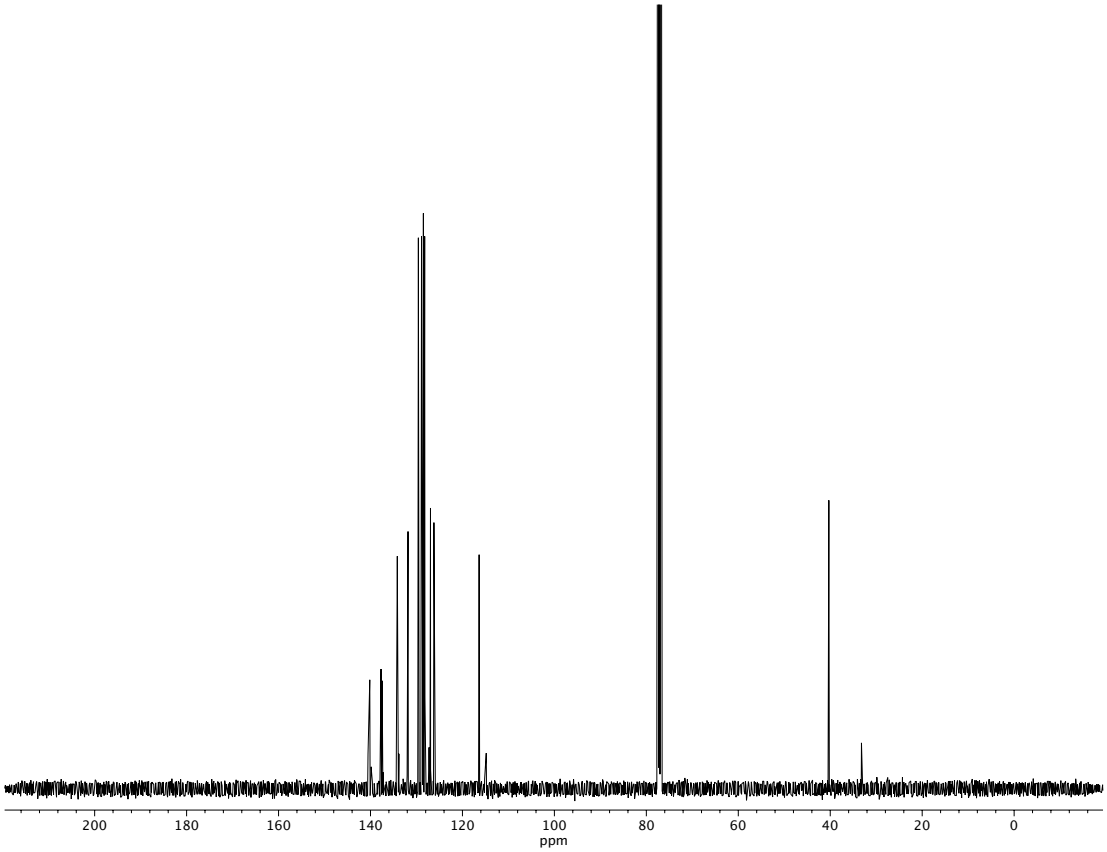

Figure A1.305. *^{13}C NMR (100 MHz, $CDCl_3$) of compound* ***158.***

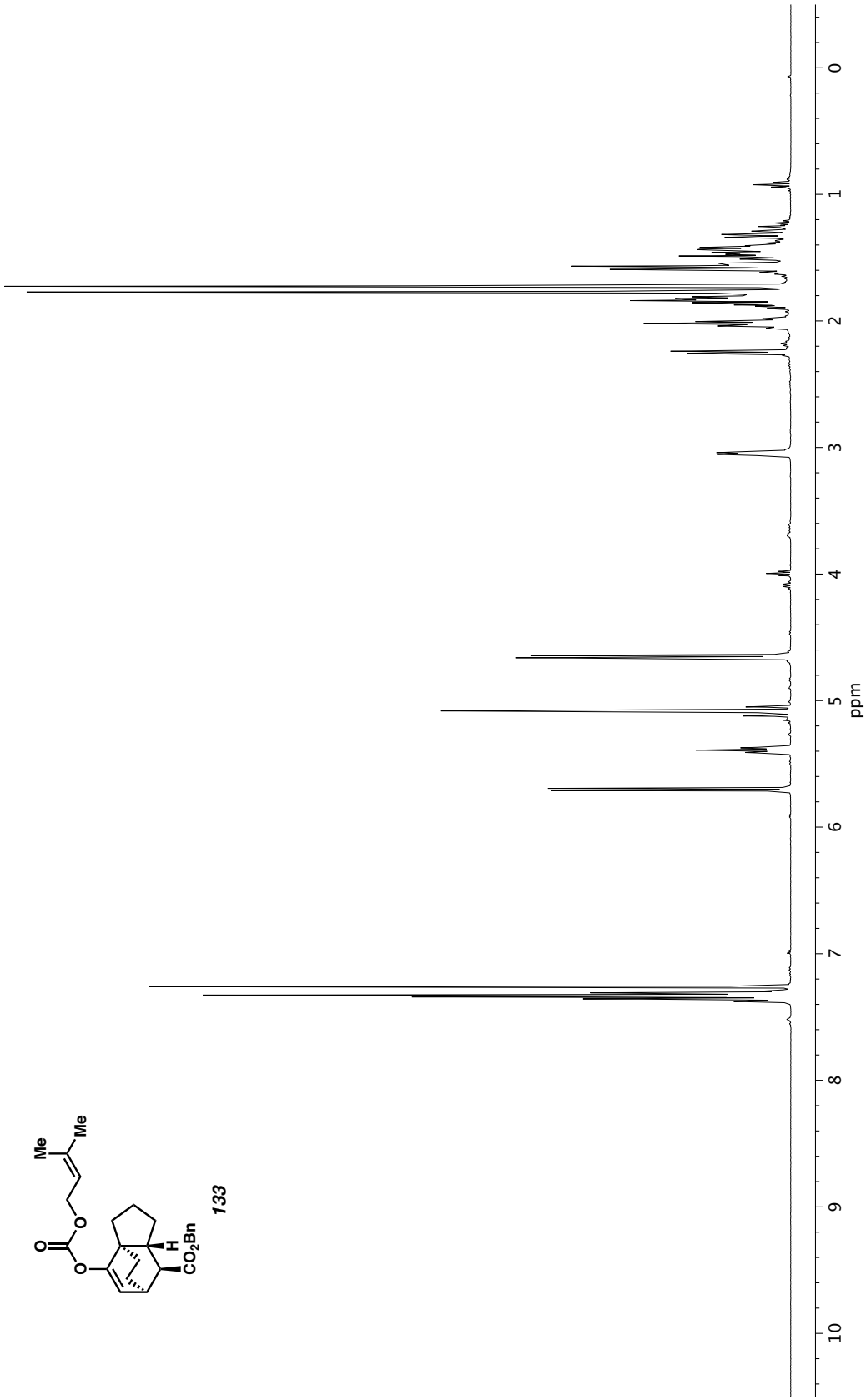

Figure A1.306. *^1H NMR (400 MHz, $CDCl_3$) of compound* ***133.***

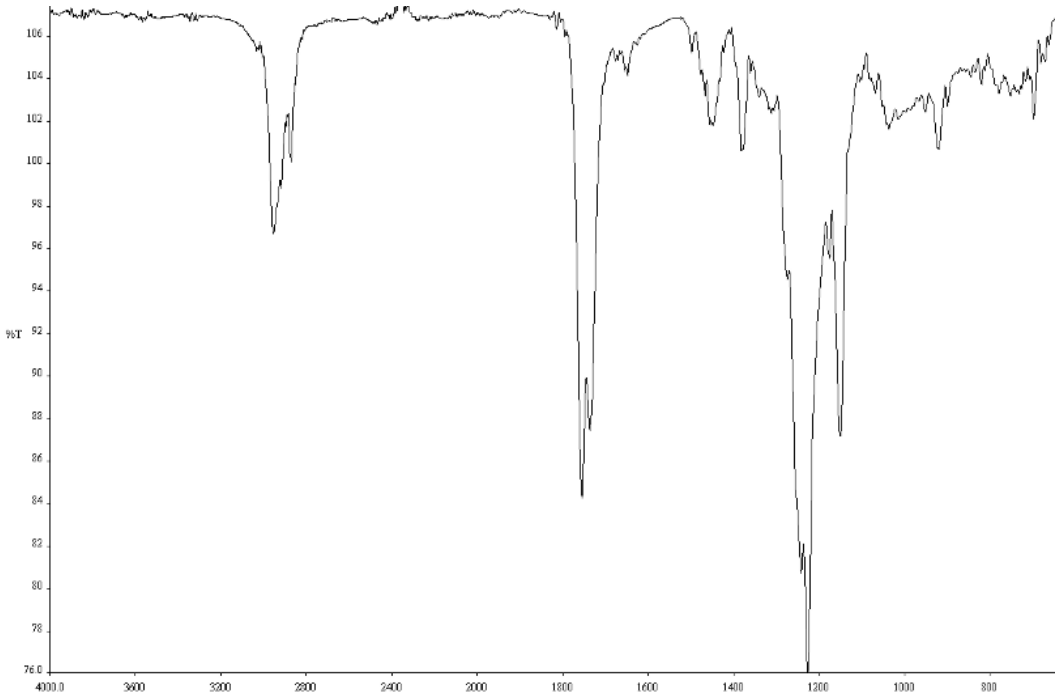

Figure A1.307. *Infrared spectrum (Thin Film, NaCl) of compound* ***133.***

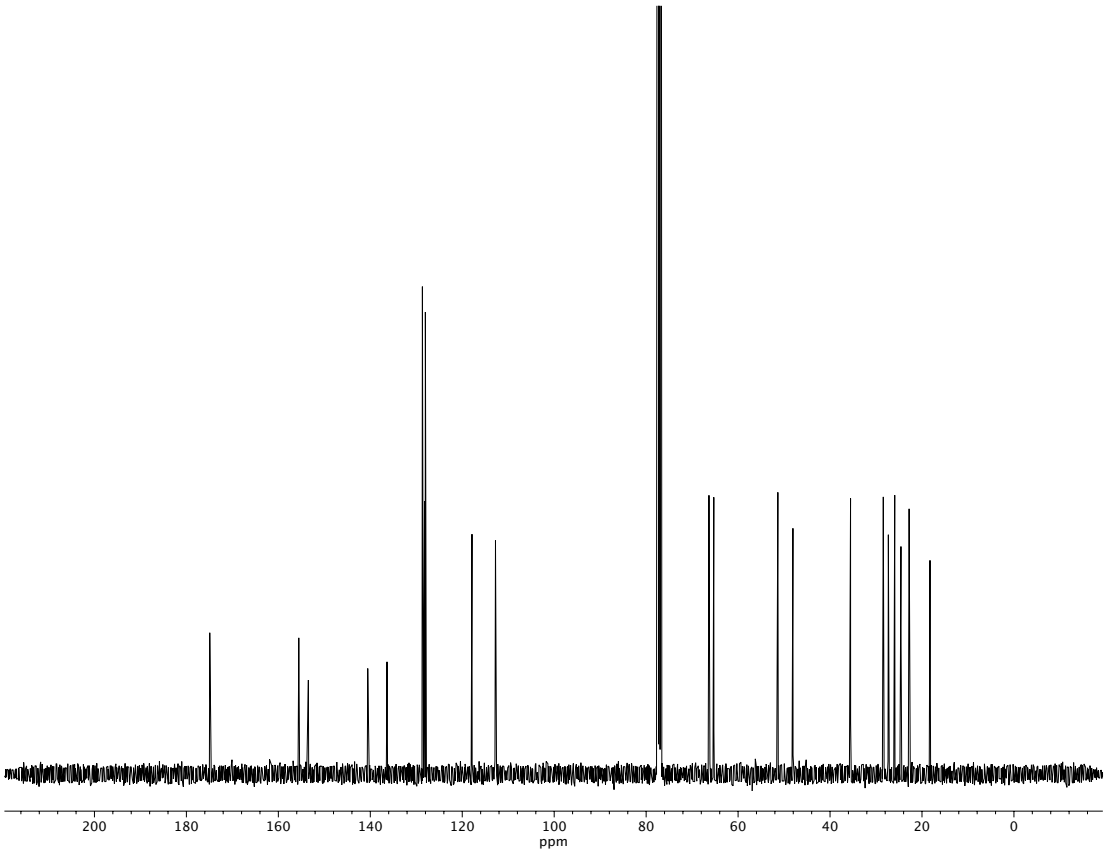

Figure A1.308. *^{13}C NMR (100 MHz, $CDCl_3$) of compound* ***133.***

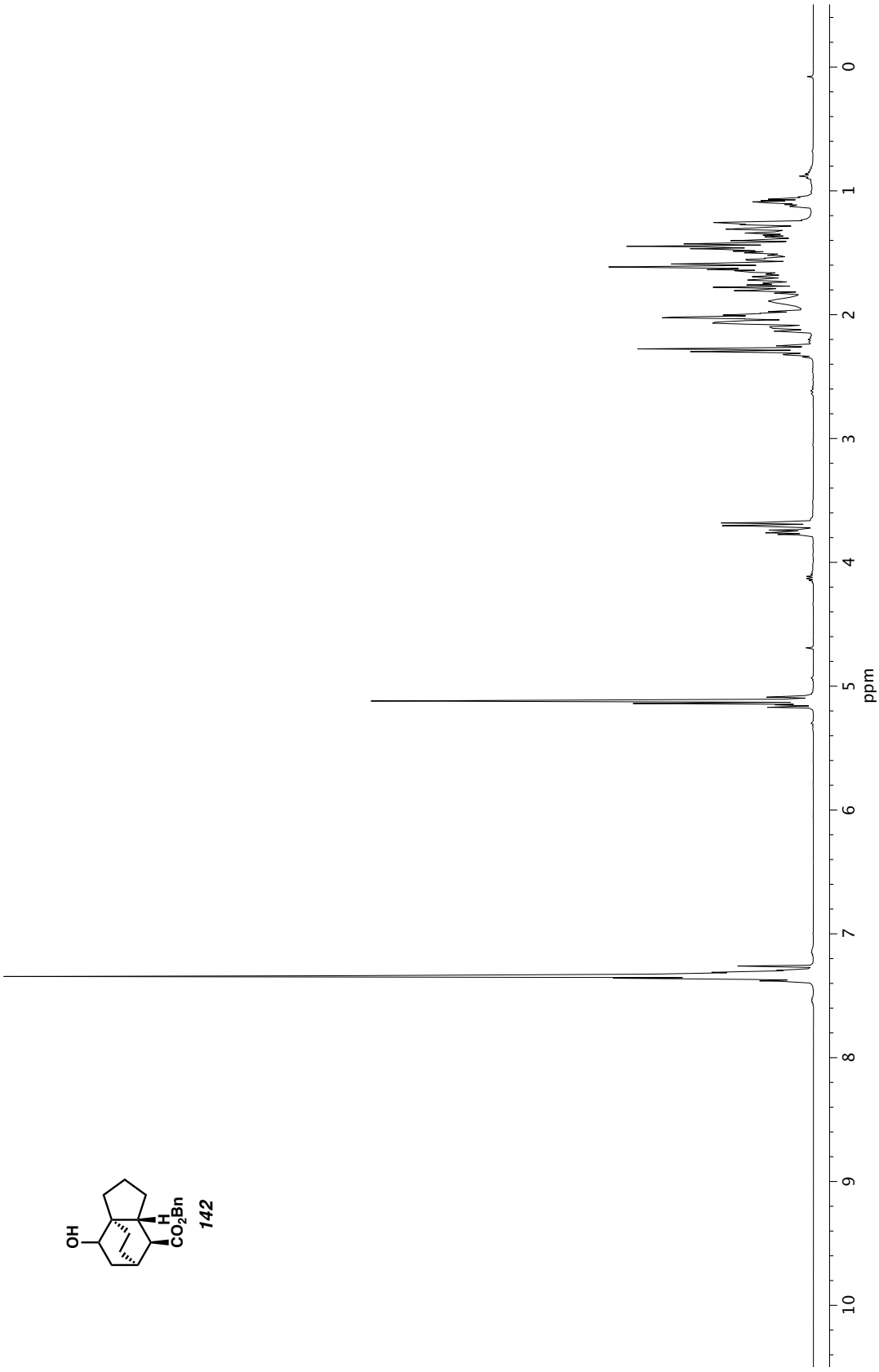

Figure A1.309. *^1H NMR (400 MHz, $CDCl_3$) of compound* ***142.***

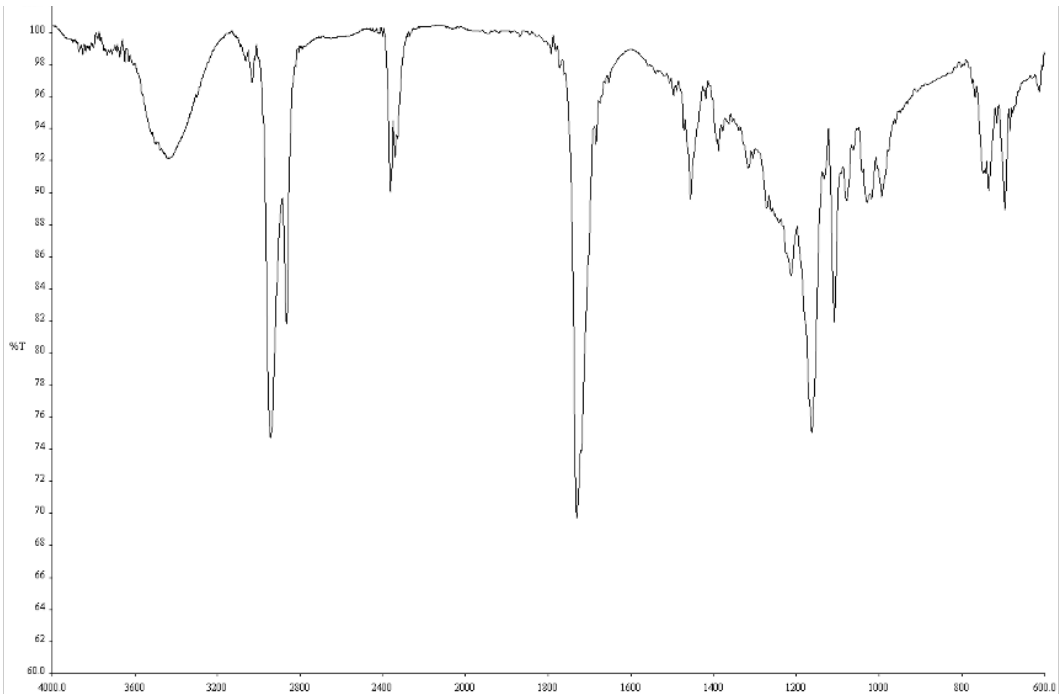

Figure A1.310. *Infrared spectrum (Thin Film, NaCl) of compound* ***142.***

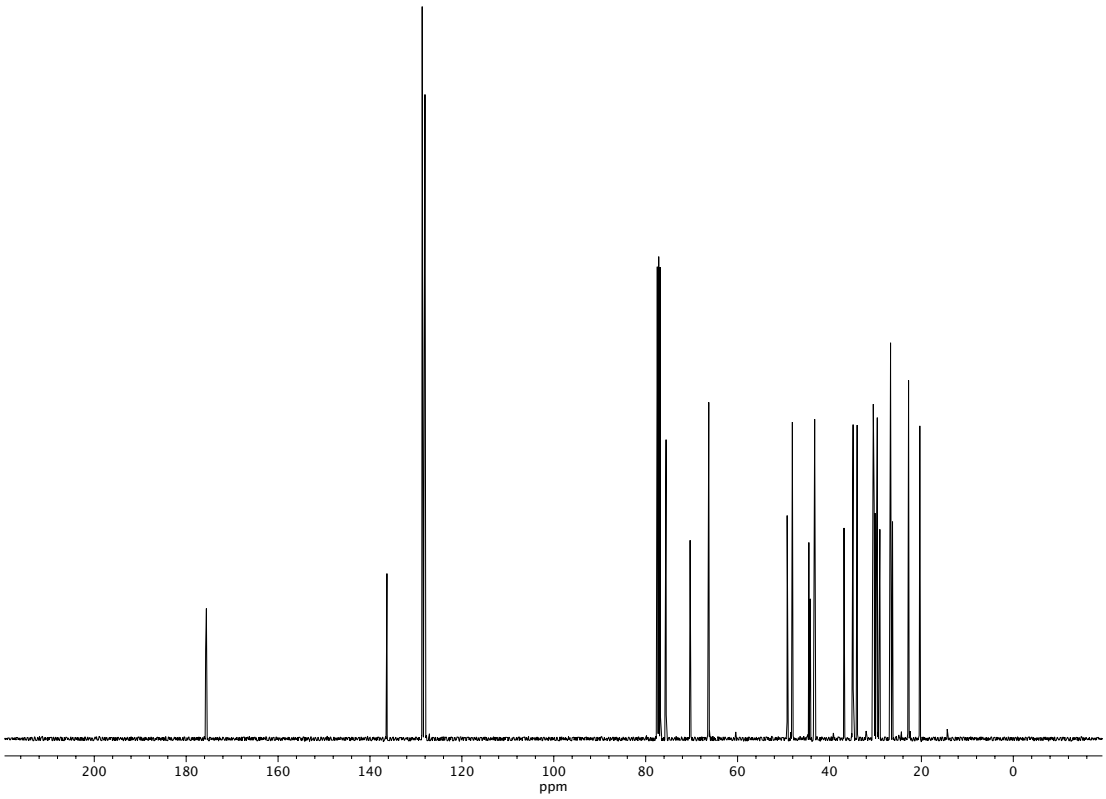

Figure A1.311. *^{13}C NMR (100 MHz, $CDCl_3$) of compound* ***142.***

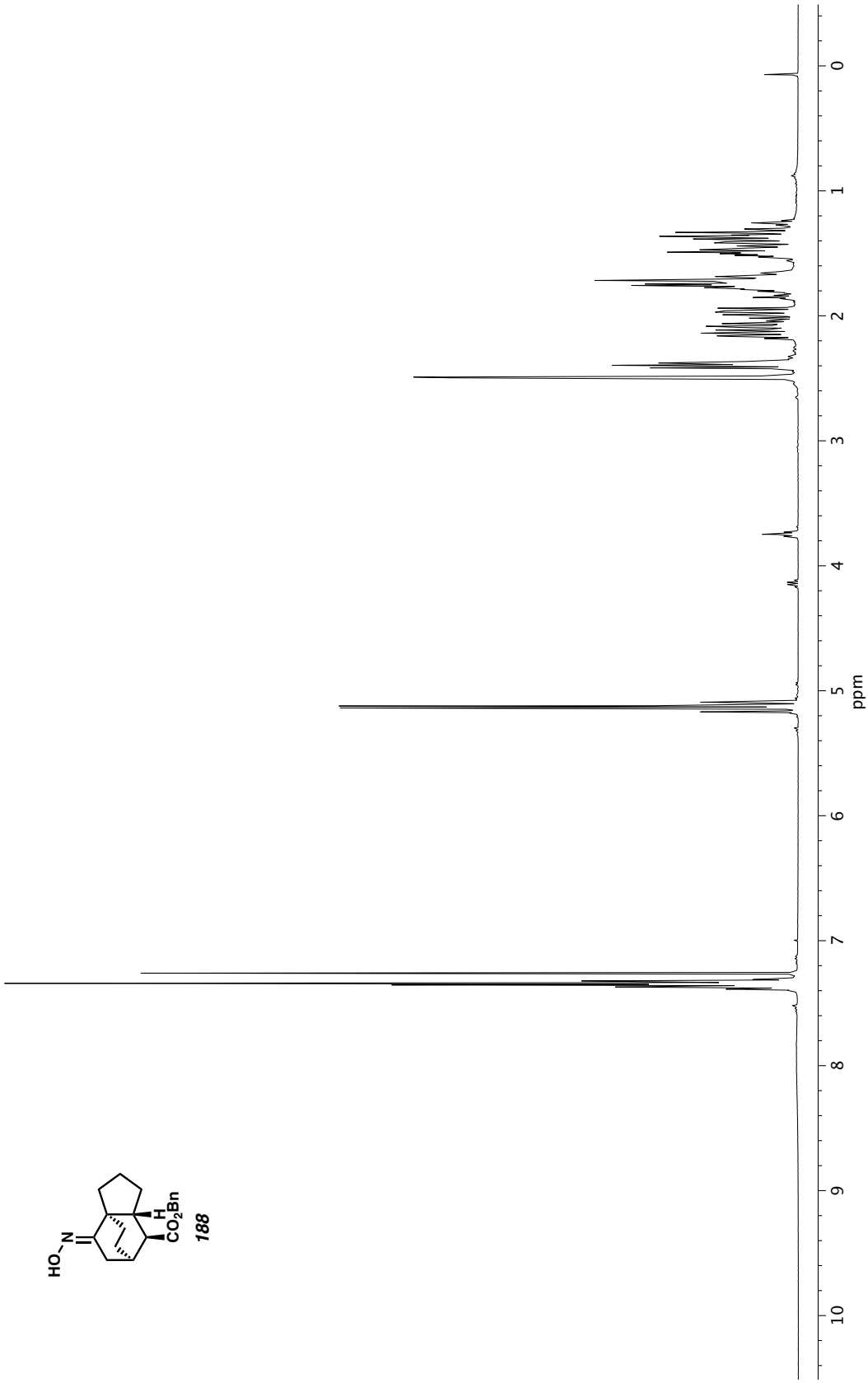

Figure A1.312. *^1H NMR (400 MHz, $CDCl_3$) of compound* ***188.***

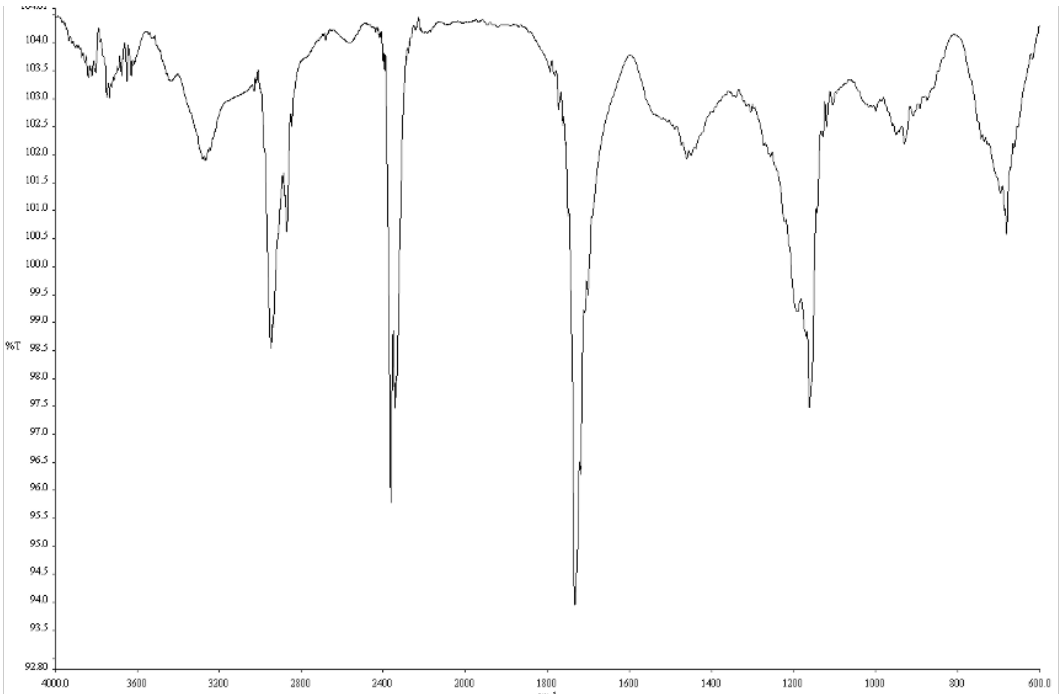

Figure A1.313. *Infrared spectrum (Thin Film, NaCl) of compound* ***188.***

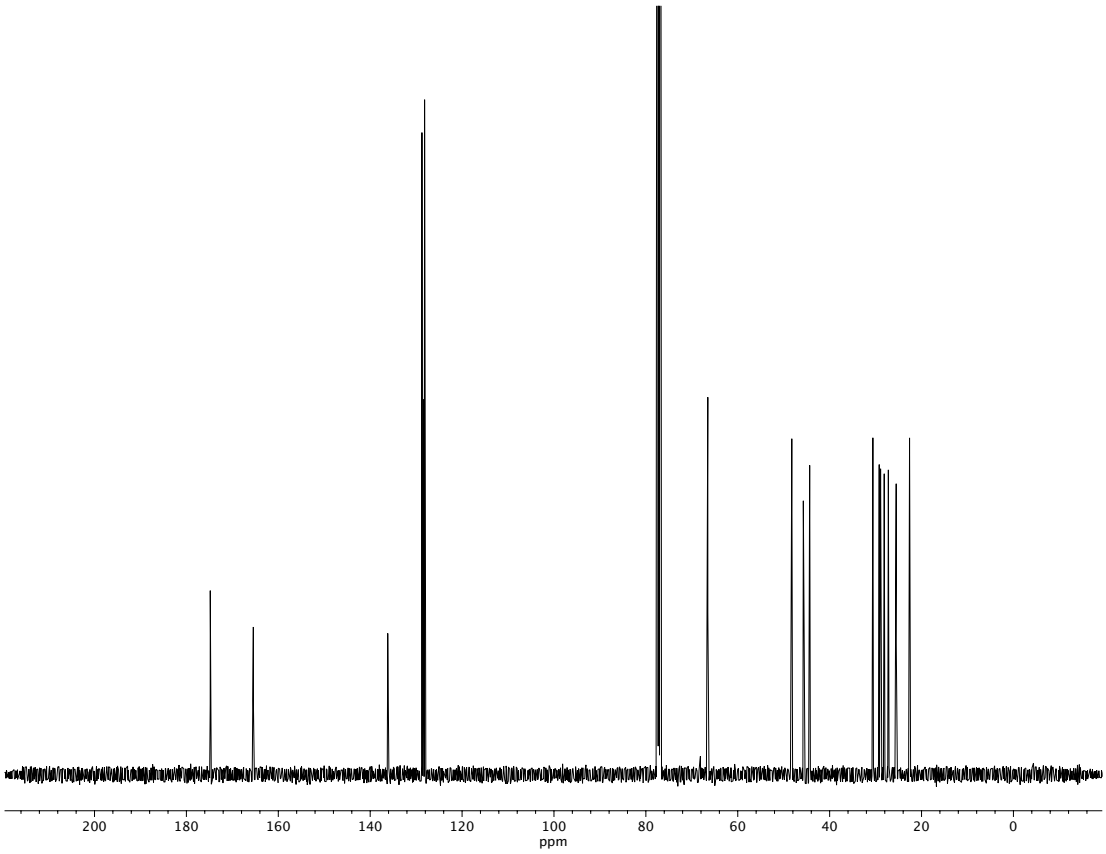

Figure A1.314. *^{13}C NMR (100 MHz, $CDCl_3$) of compound* ***188.***

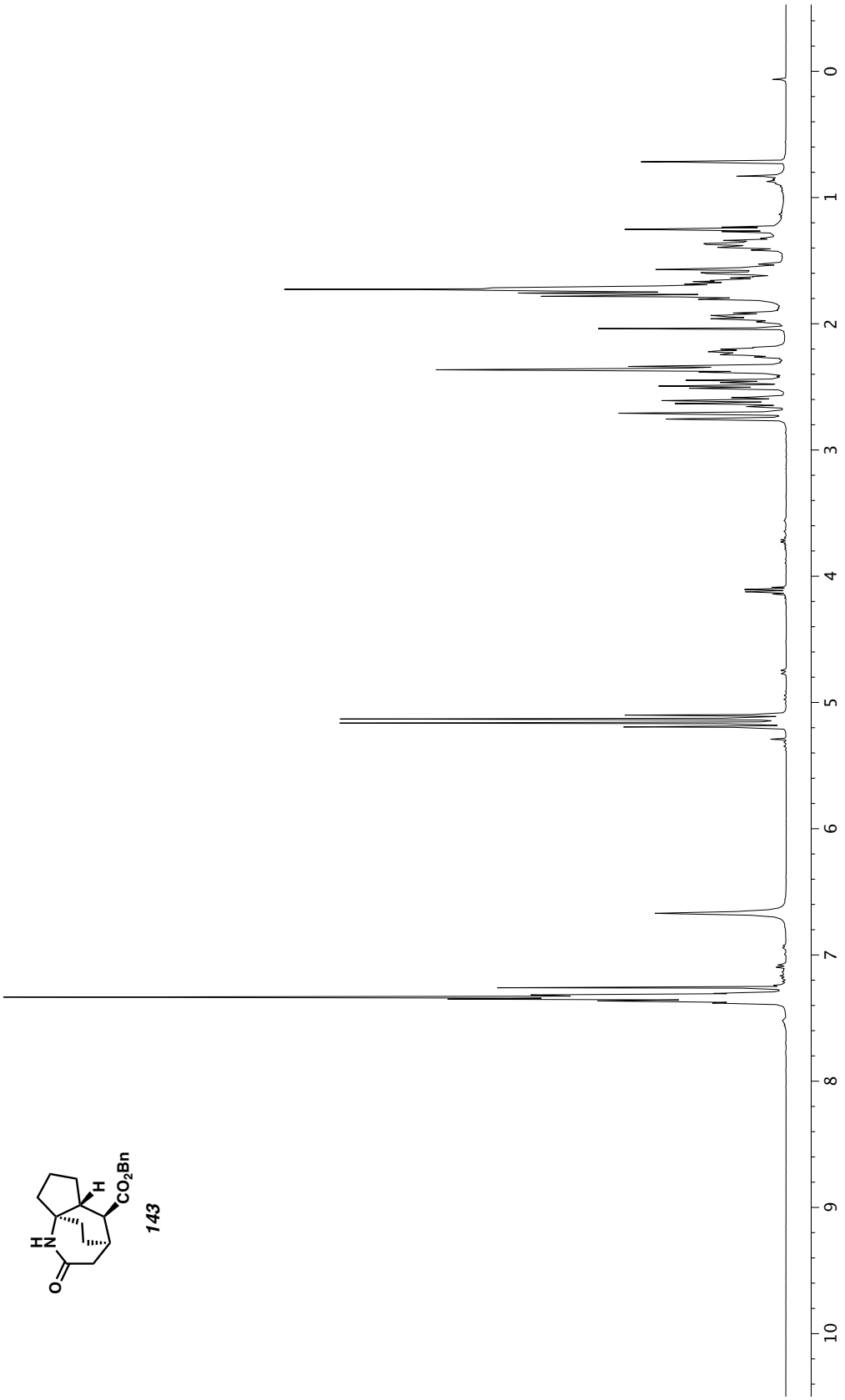

Figure A1.315. *^1H NMR (400 MHz, $CDCl_3$) of compound* ***143.***

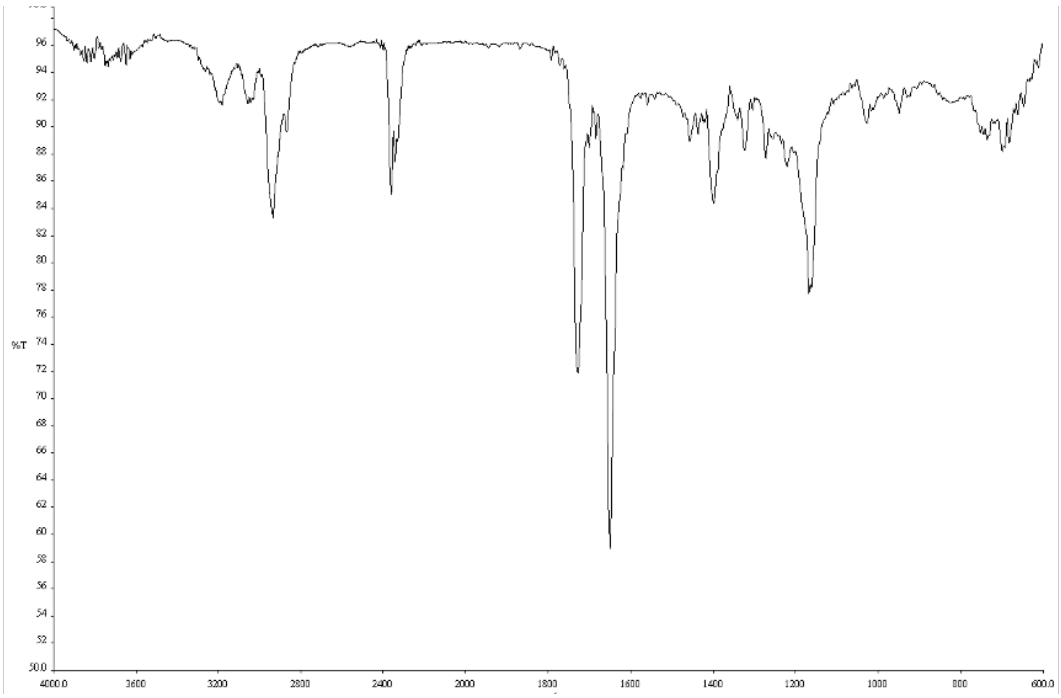

Figure A1.316. *Infrared spectrum (Thin Film, NaCl) of compound* ***143.***

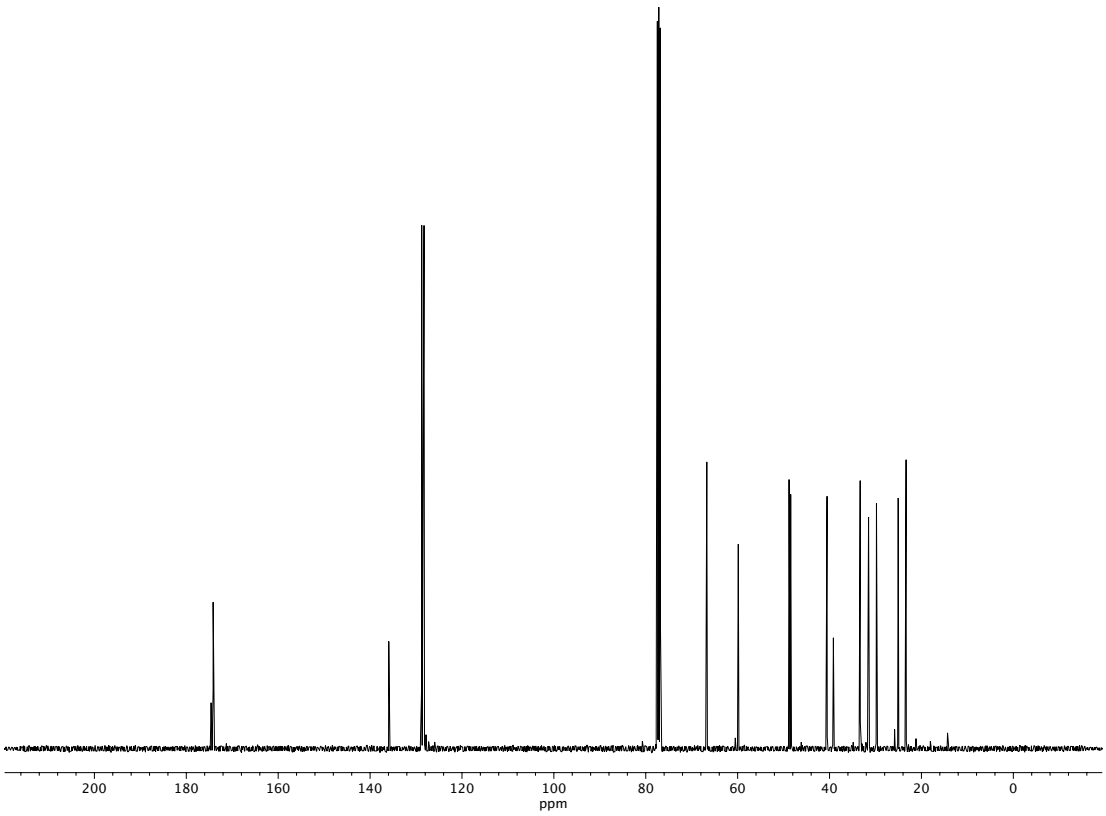

Figure A1.317. *^{13}C NMR (100 MHz, $CDCl_3$) of compound* ***143.***

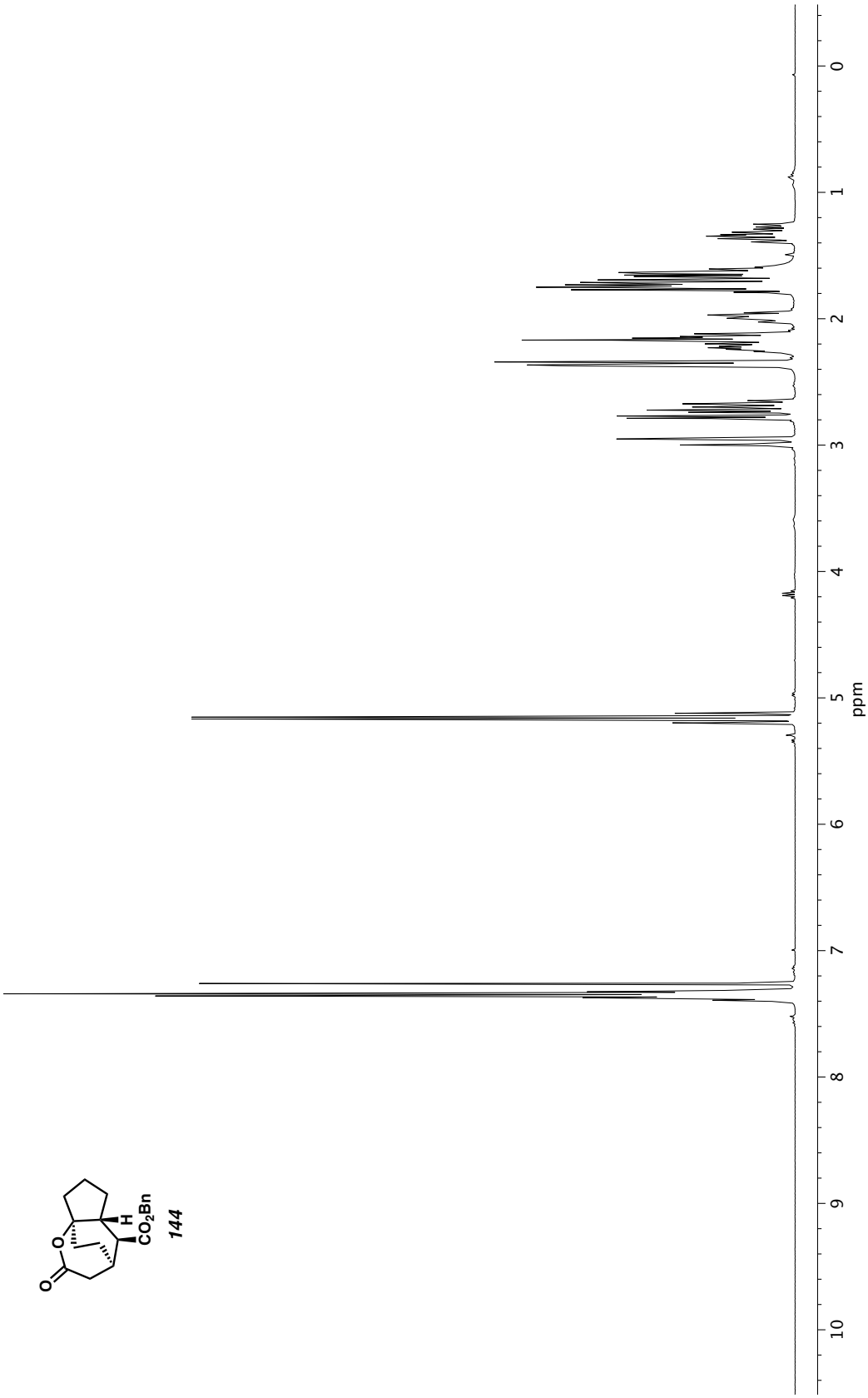

Figure A1.318. *^{1}H NMR (400 MHz, $CDCl_3$) of compound* ***144.***

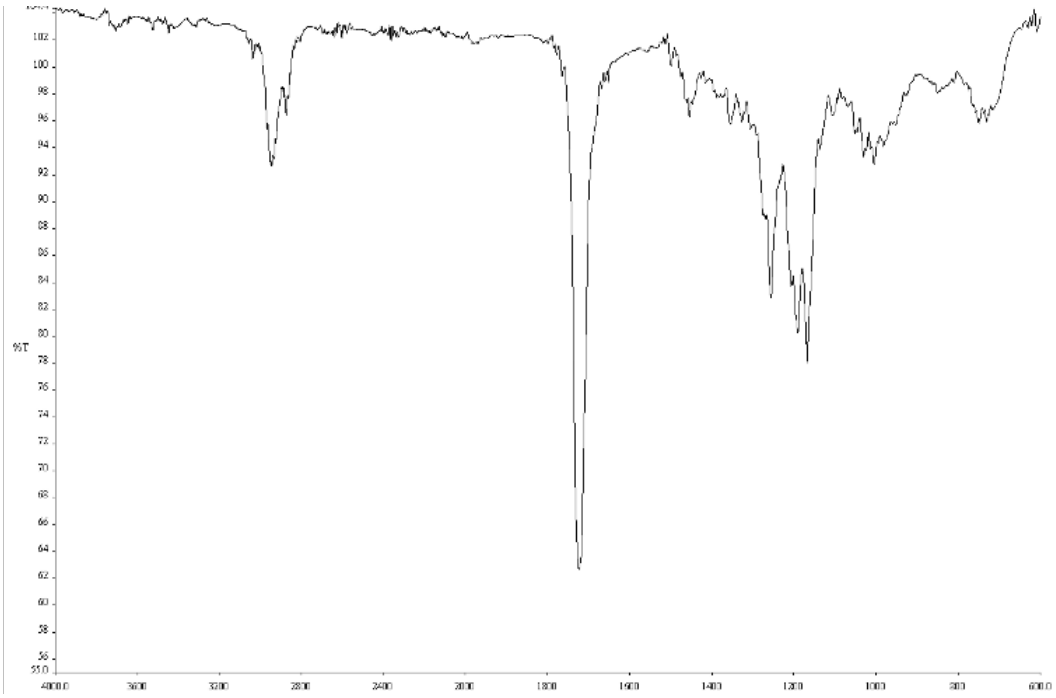

Figure A1.319. *Infrared spectrum (Thin Film, NaCl) of compound* ***144.***

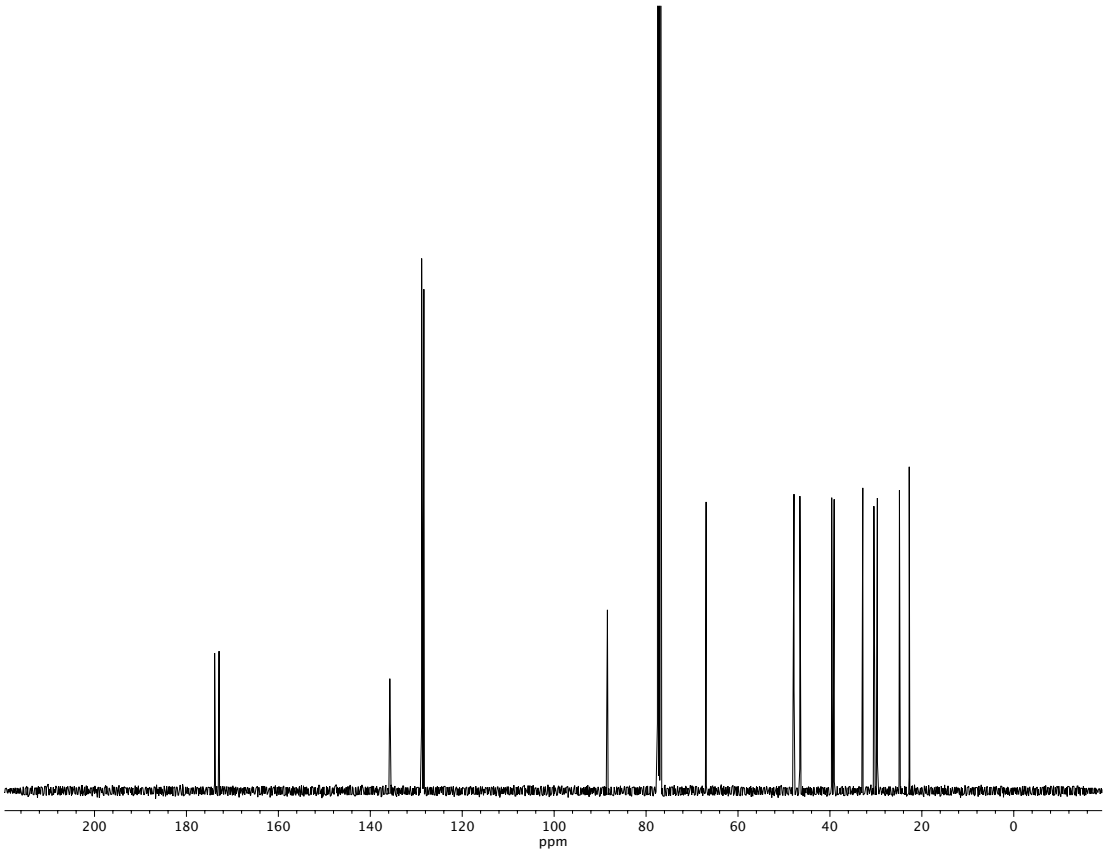

Figure A1.320. *^{13}C NMR (100 MHz, $CDCl_3$) of compound* ***144.***

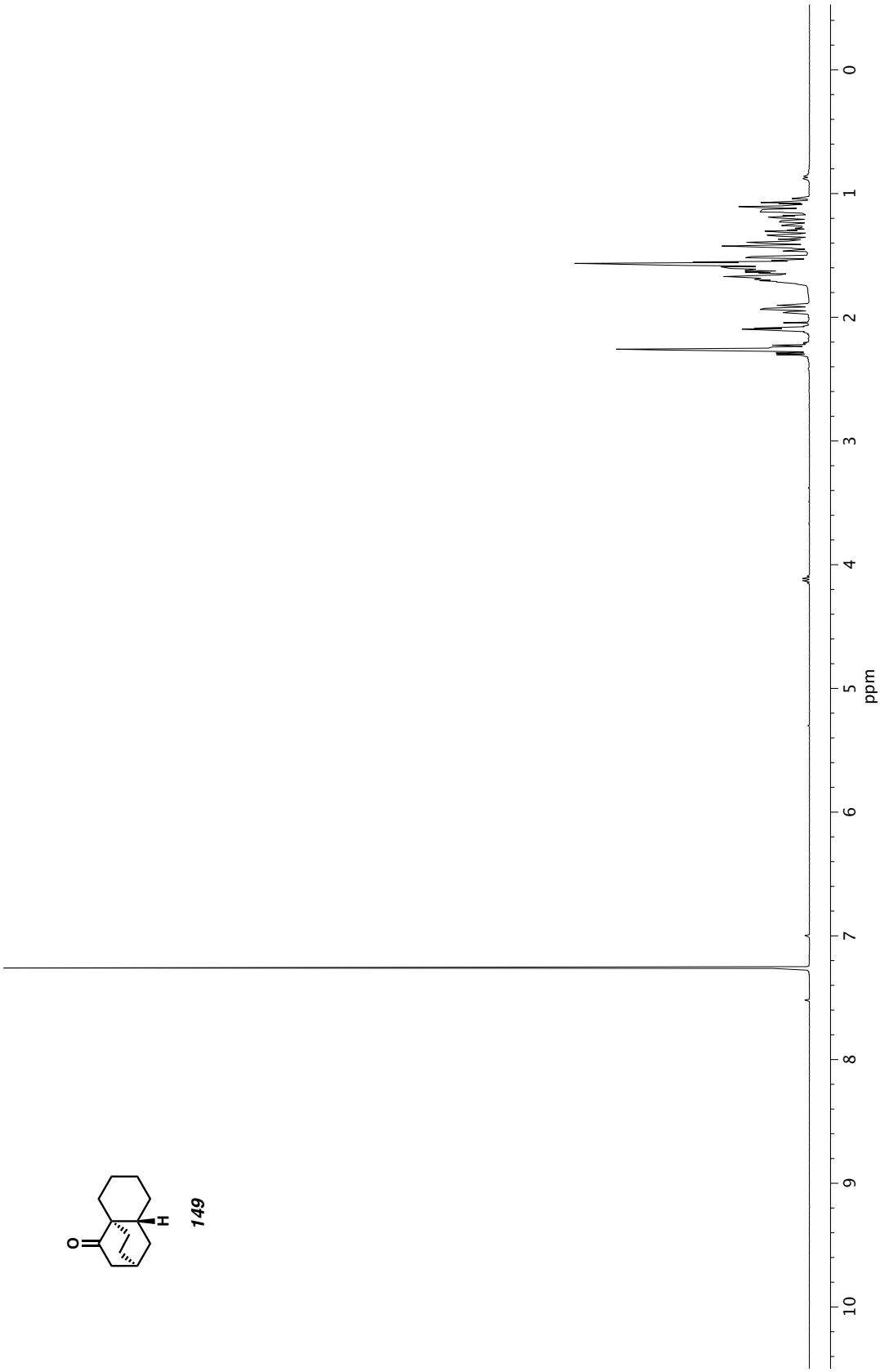

Figure A1.321. *^{1}H NMR (400 MHz, $CDCl_3$) of compound* ***149.***

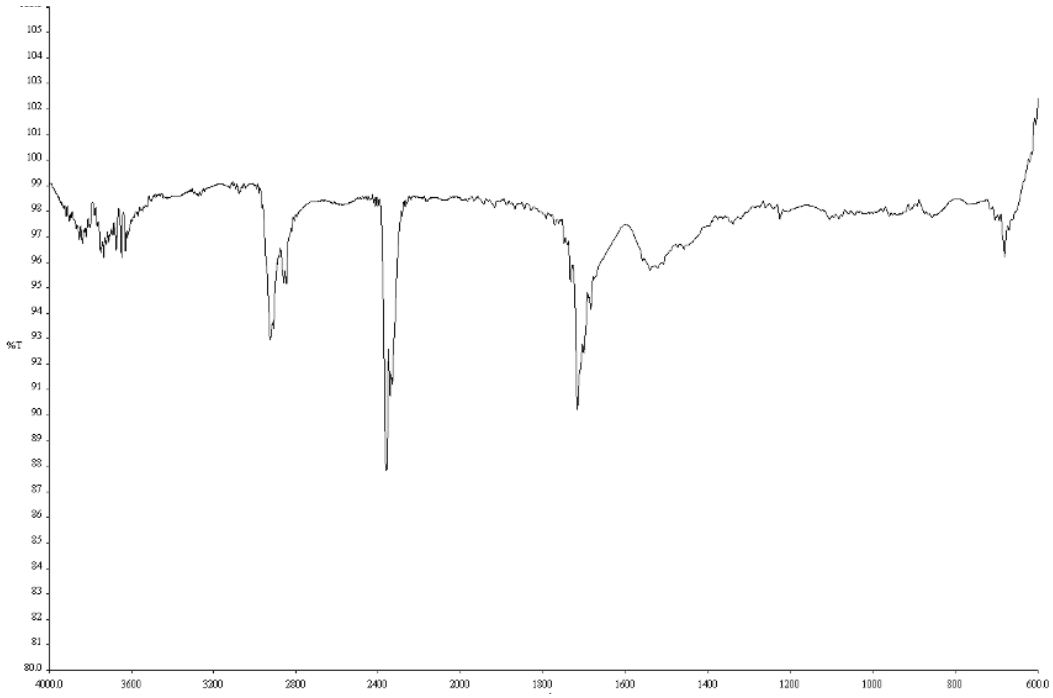

Figure A1.322. *Infrared spectrum (Thin Film, NaCl) of compound* ***149.***

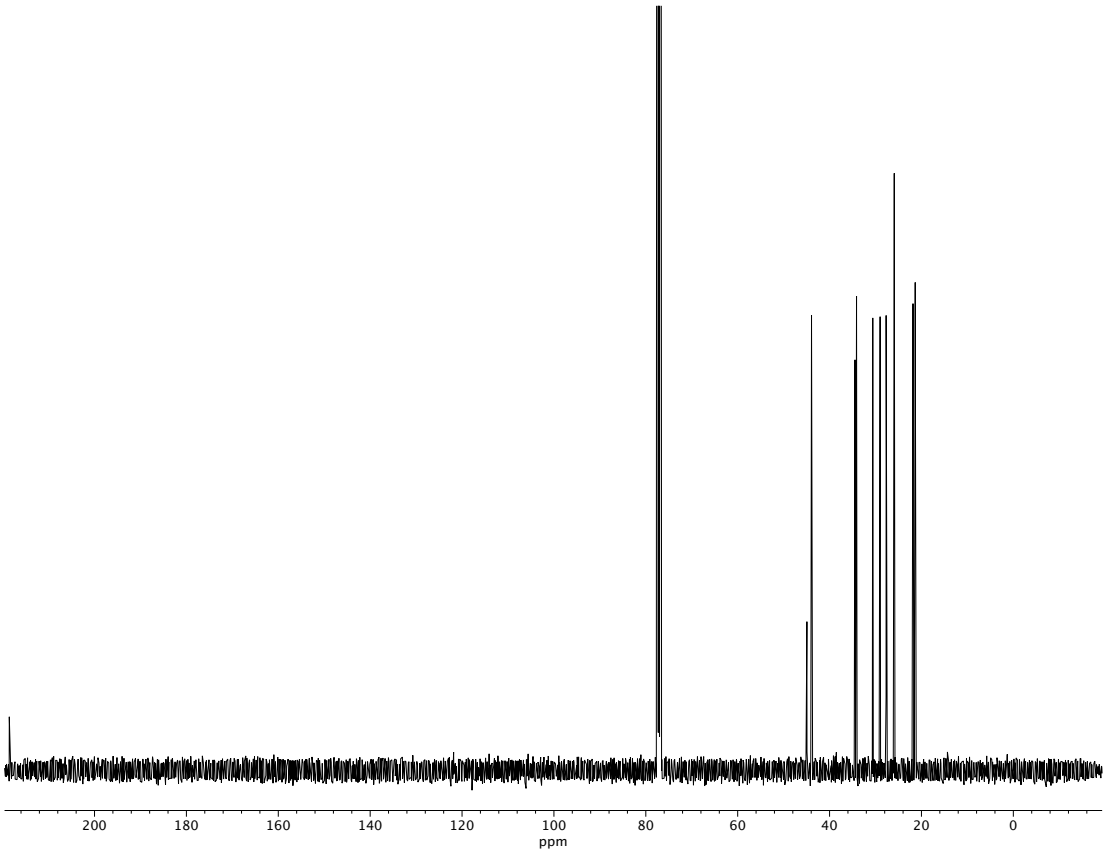

Figure A1.323. *^{13}C NMR (100 MHz, $CDCl_3$) of compound* ***149.***

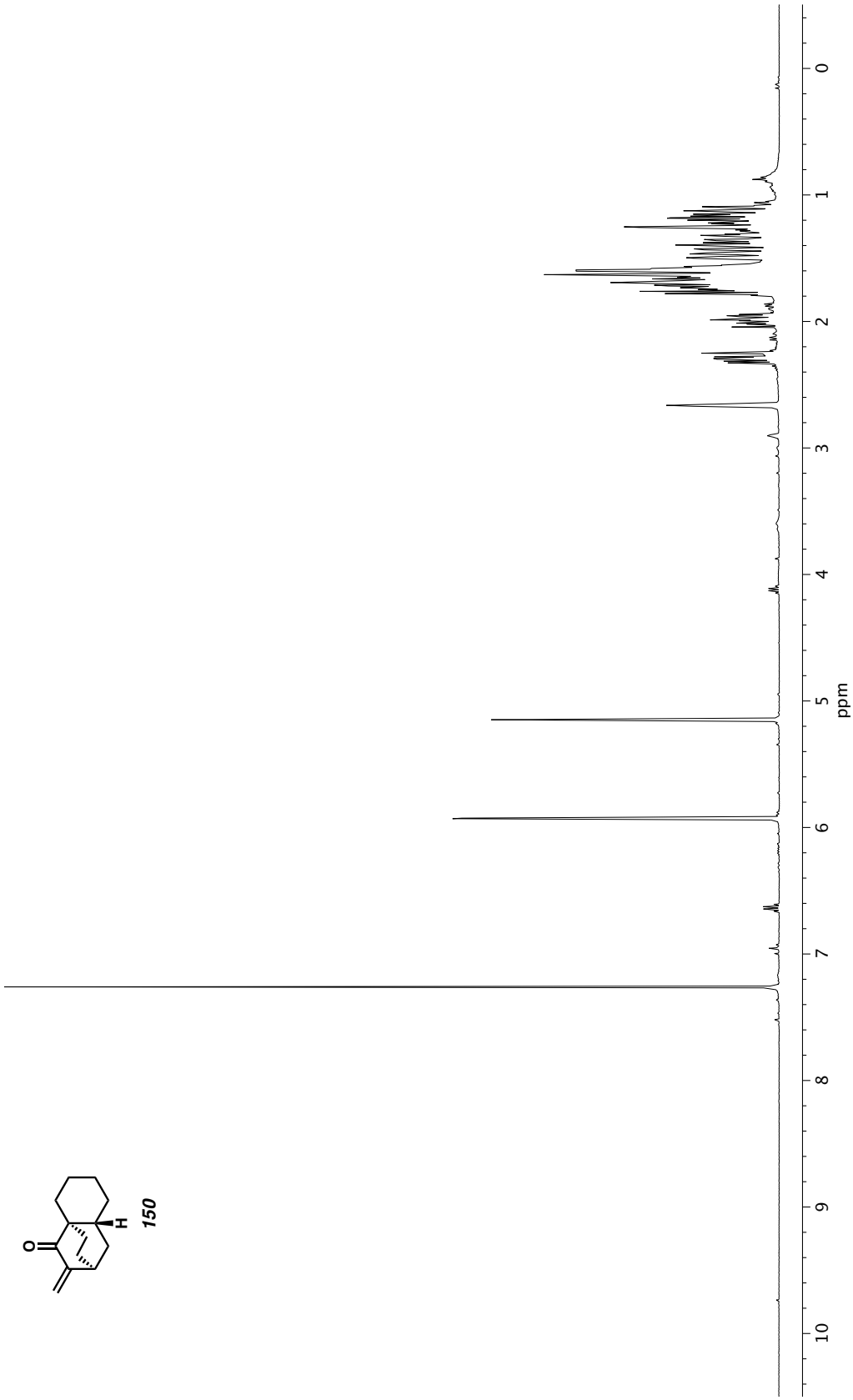

Figure A1.324. *^1H NMR (400 MHz, $CDCl_3$) of compound* ***150.***

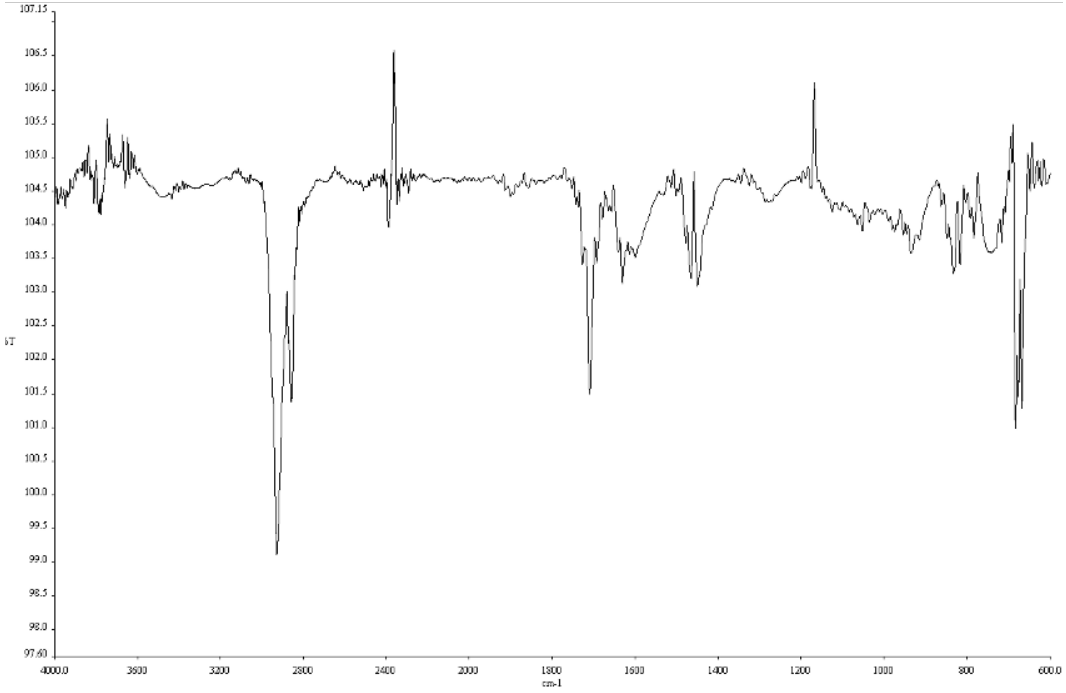

Figure A1.325. *Infrared spectrum (Thin Film, NaCl) of compound* ***150.***

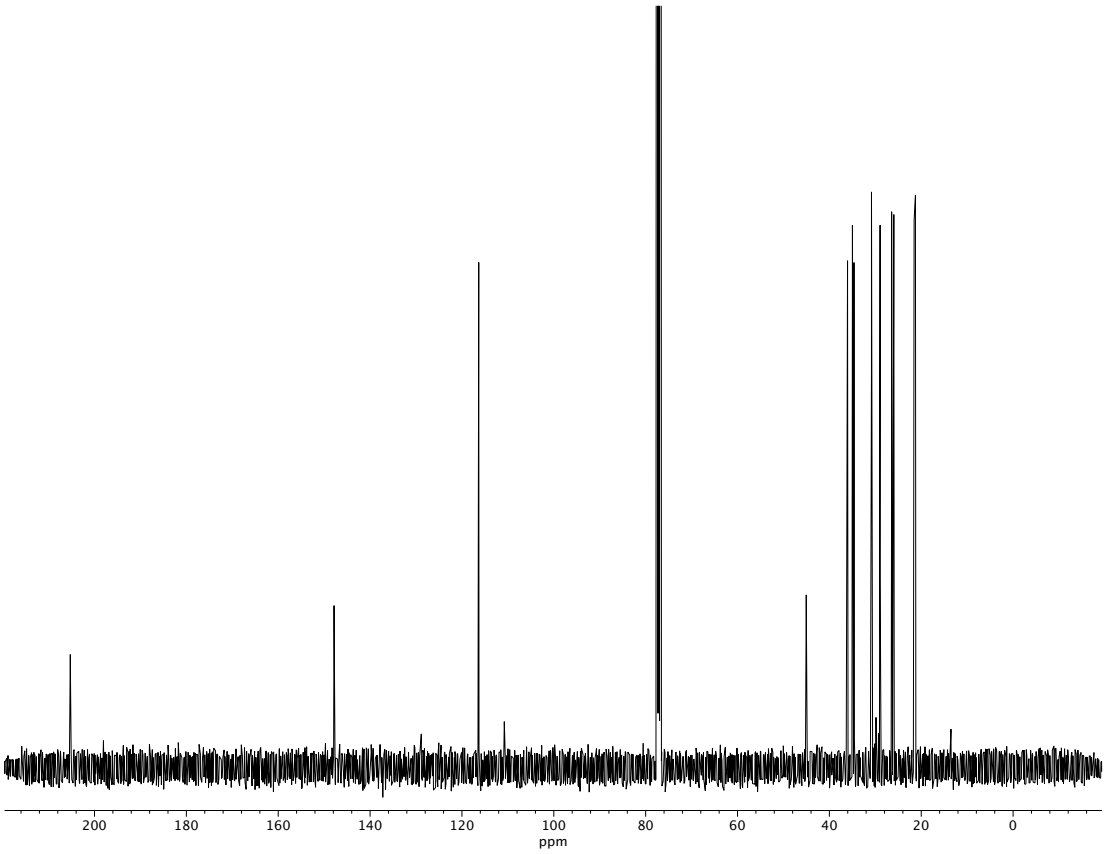

Figure A1.326. *^{13}C NMR (100 MHz, $CDCl_3$) of compound* ***150.***

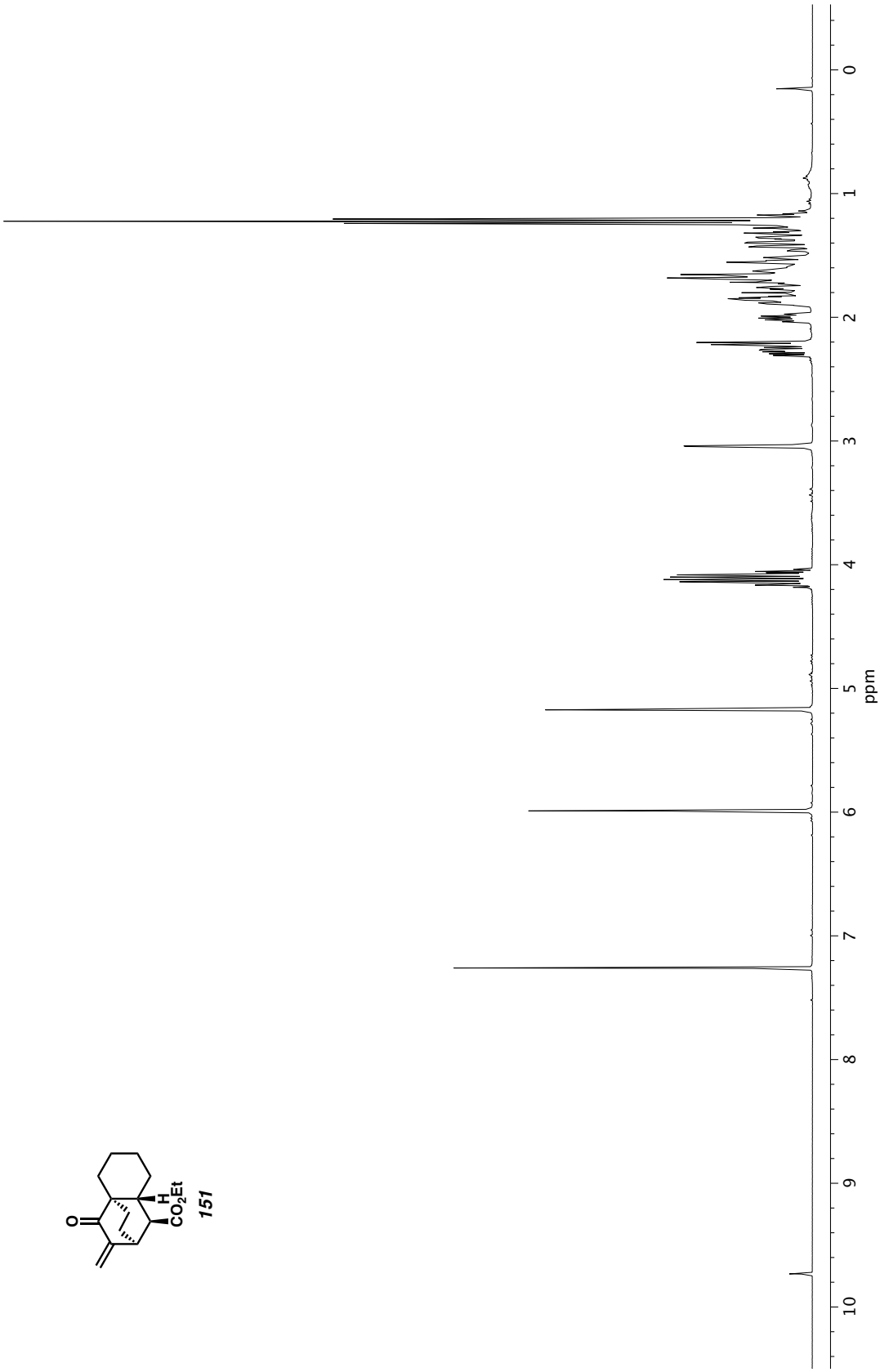

Figure A1.327. *^{1}H NMR (400 MHz, $CDCl_3$) of compound* ***151.***

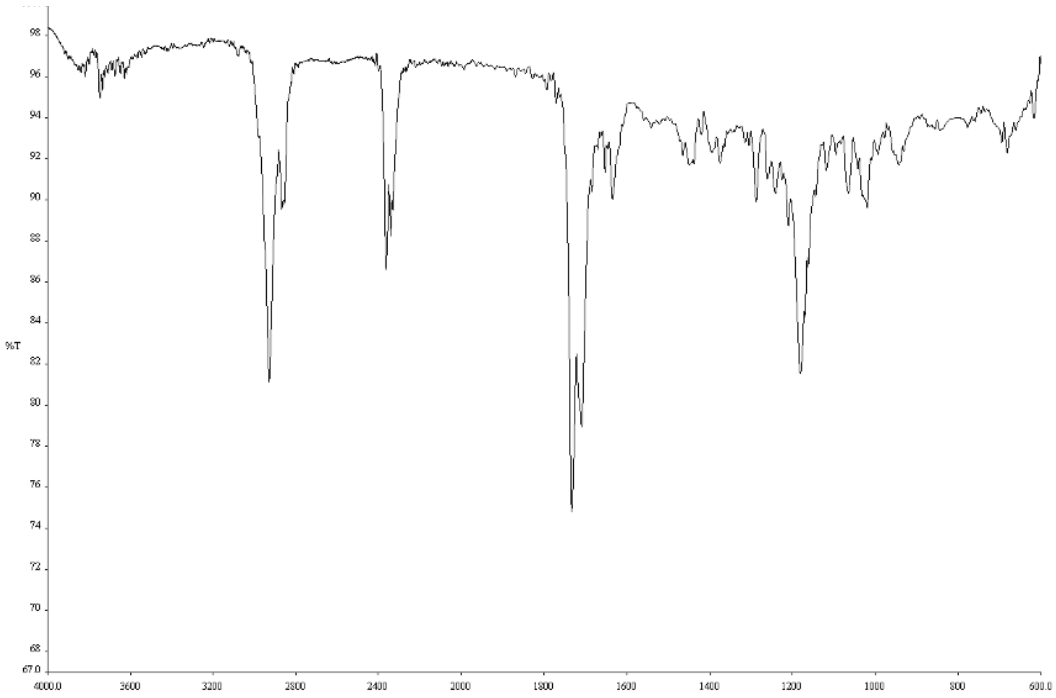

Figure A1.328. *Infrared spectrum (Thin Film, NaCl) of compound* ***151.***

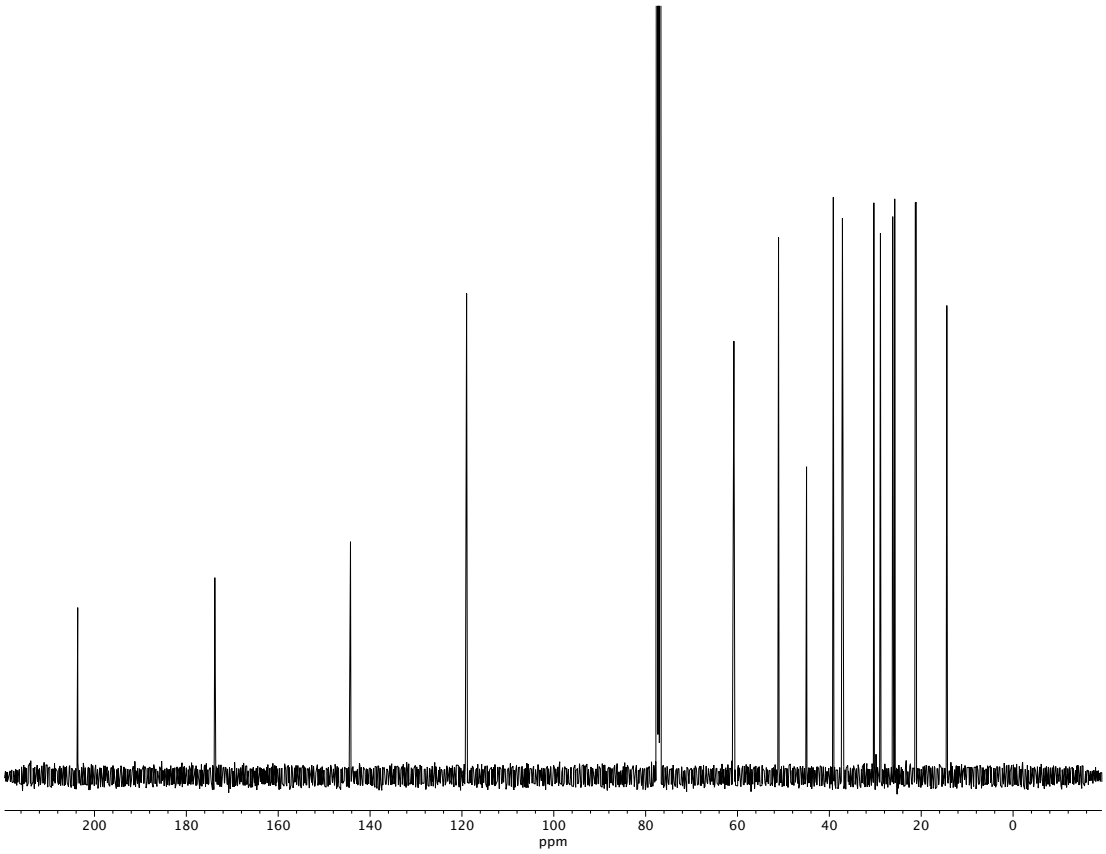

Figure A1.329. *^{13}C NMR (100 MHz, $CDCl_3$) of compound* ***151.***

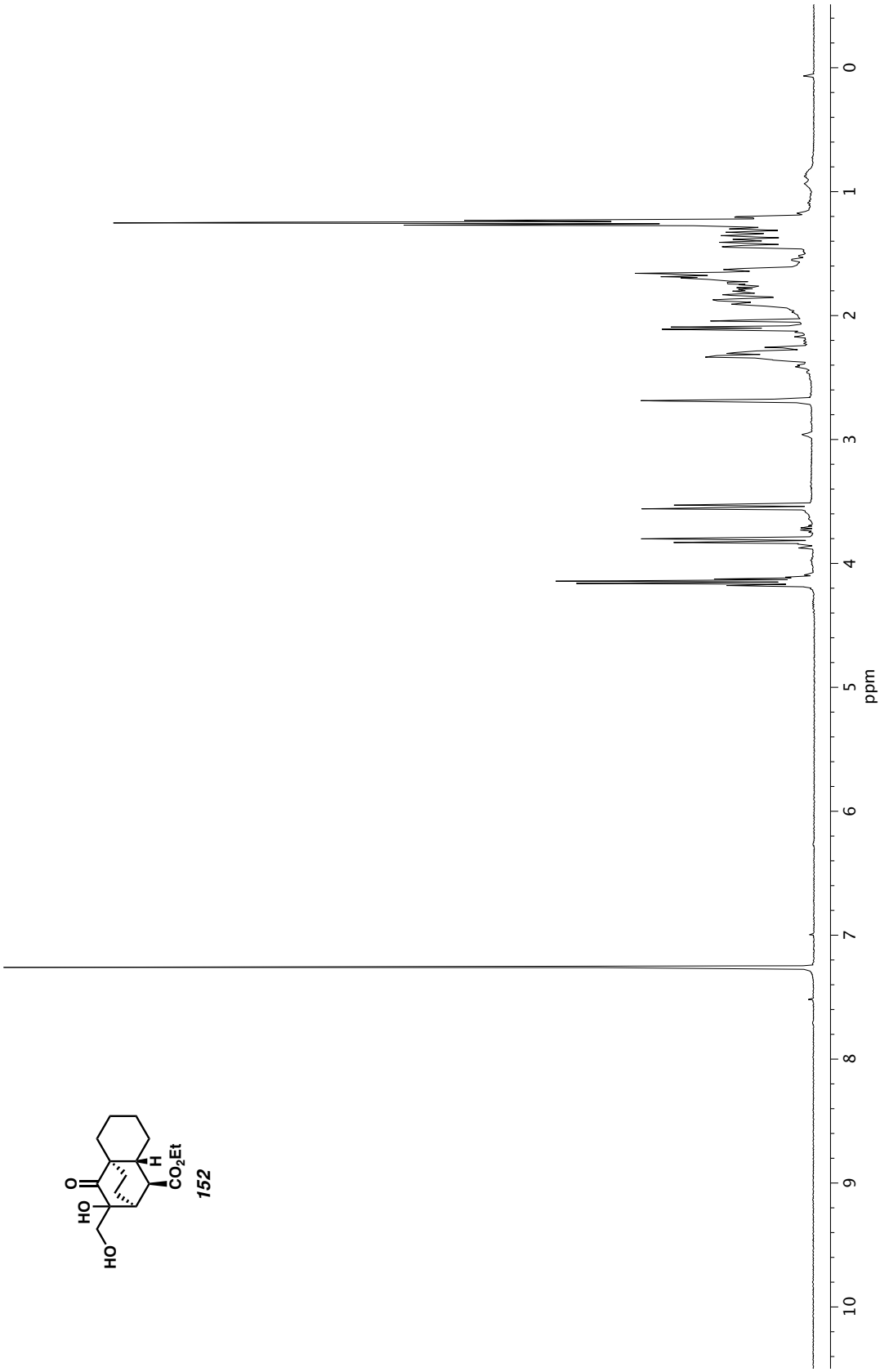

Figure A1.330. *^{1}H NMR (400 MHz, $CDCl_3$) of compound* ***152.***

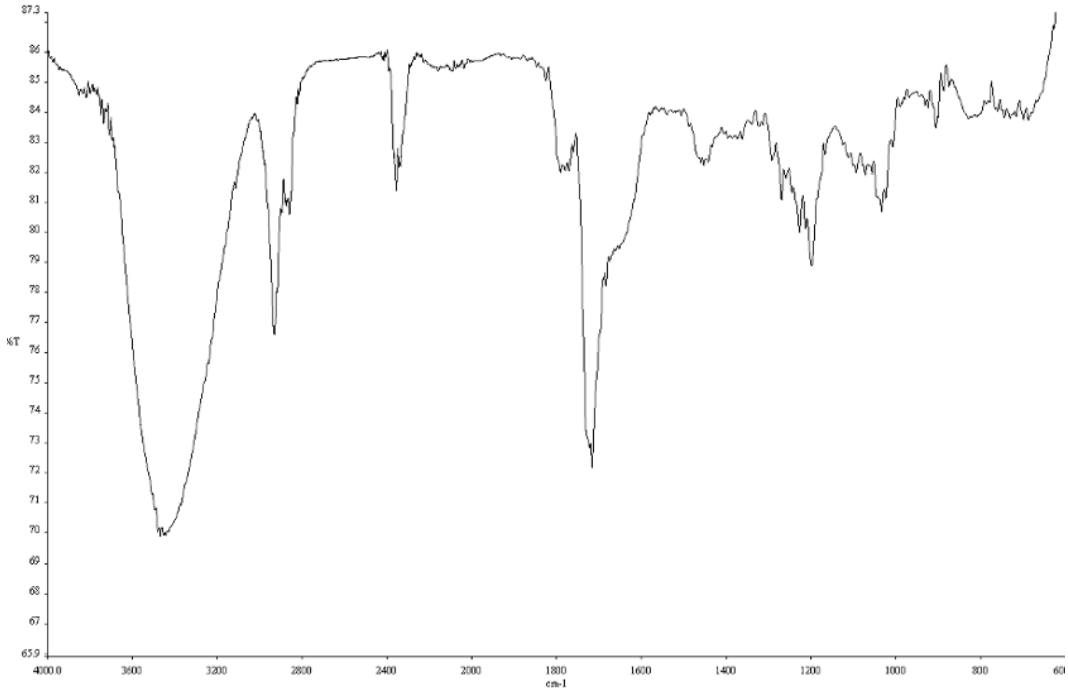

Figure A1.331. *Infrared spectrum (Thin Film, NaCl) of compound* ***152.***

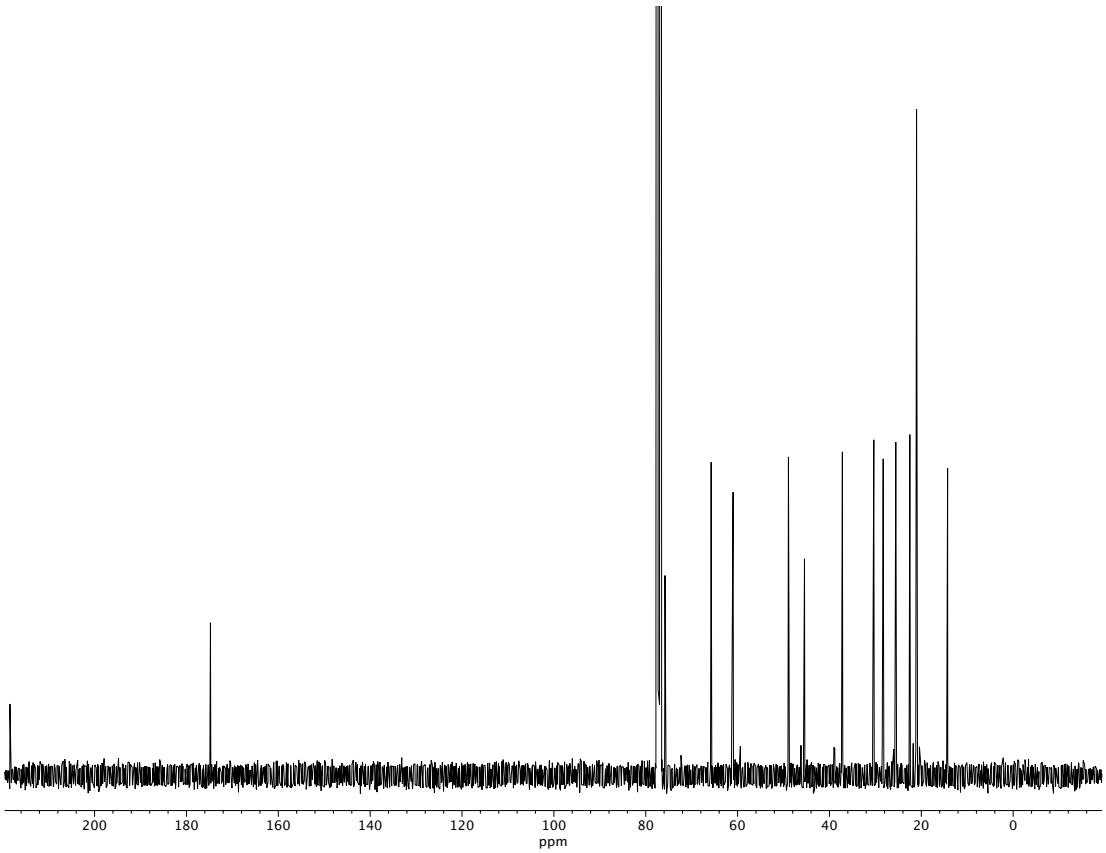

Figure A1.332. *^{13}C NMR (100 MHz, $CDCl_3$) of compound* ***152.***

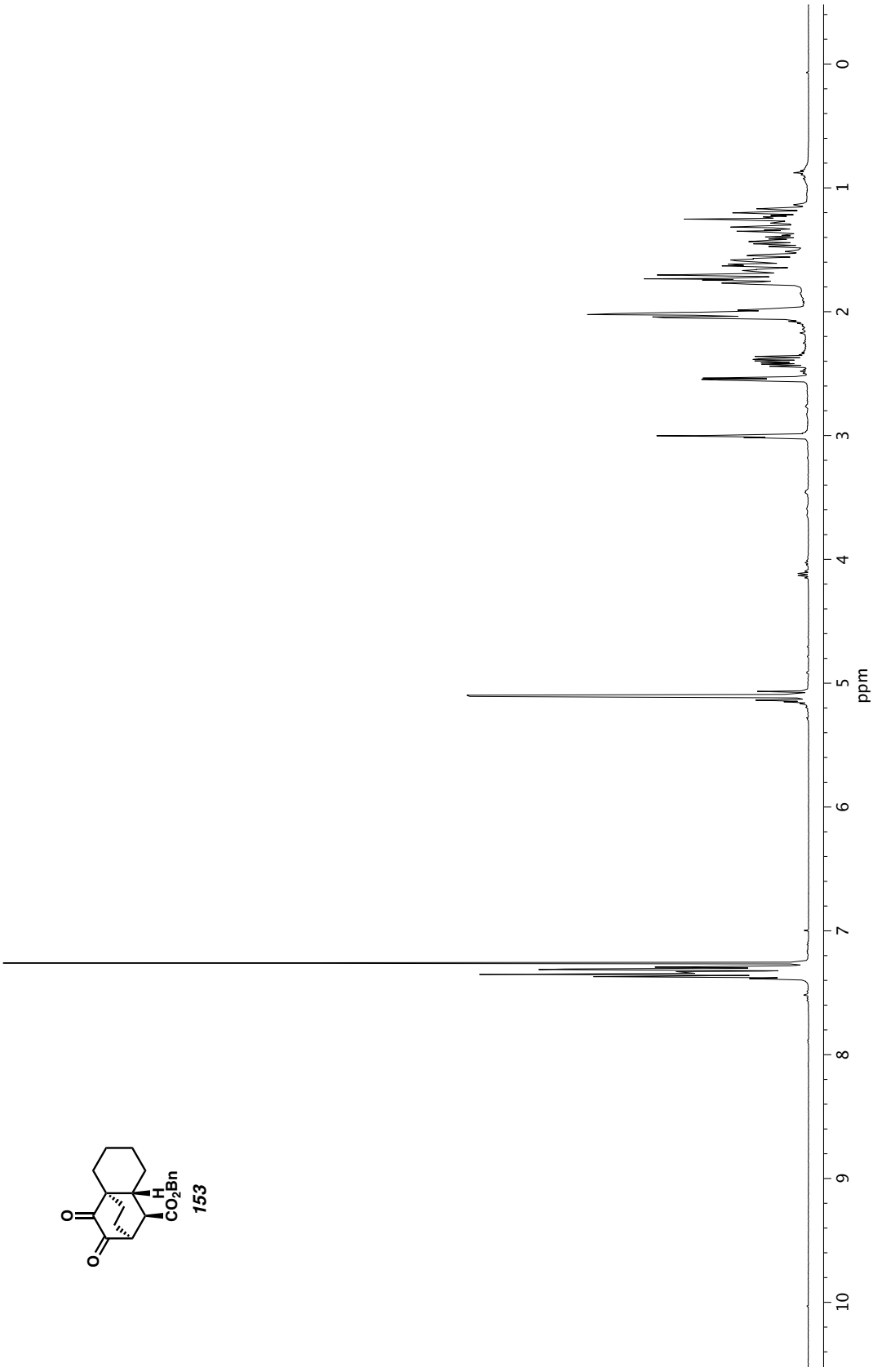

Figure A1.333. *^1H NMR (400 MHz, $CDCl_3$) of compound* ***153.***

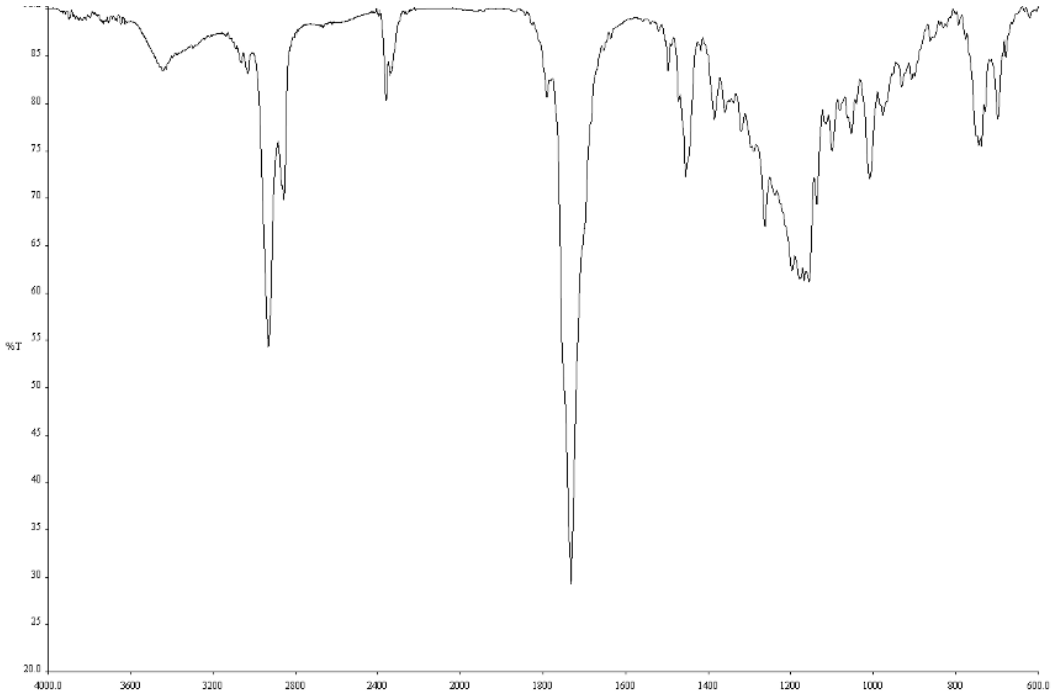

Figure A1.334. *Infrared spectrum (Thin Film, NaCl) of compound* ***153.***

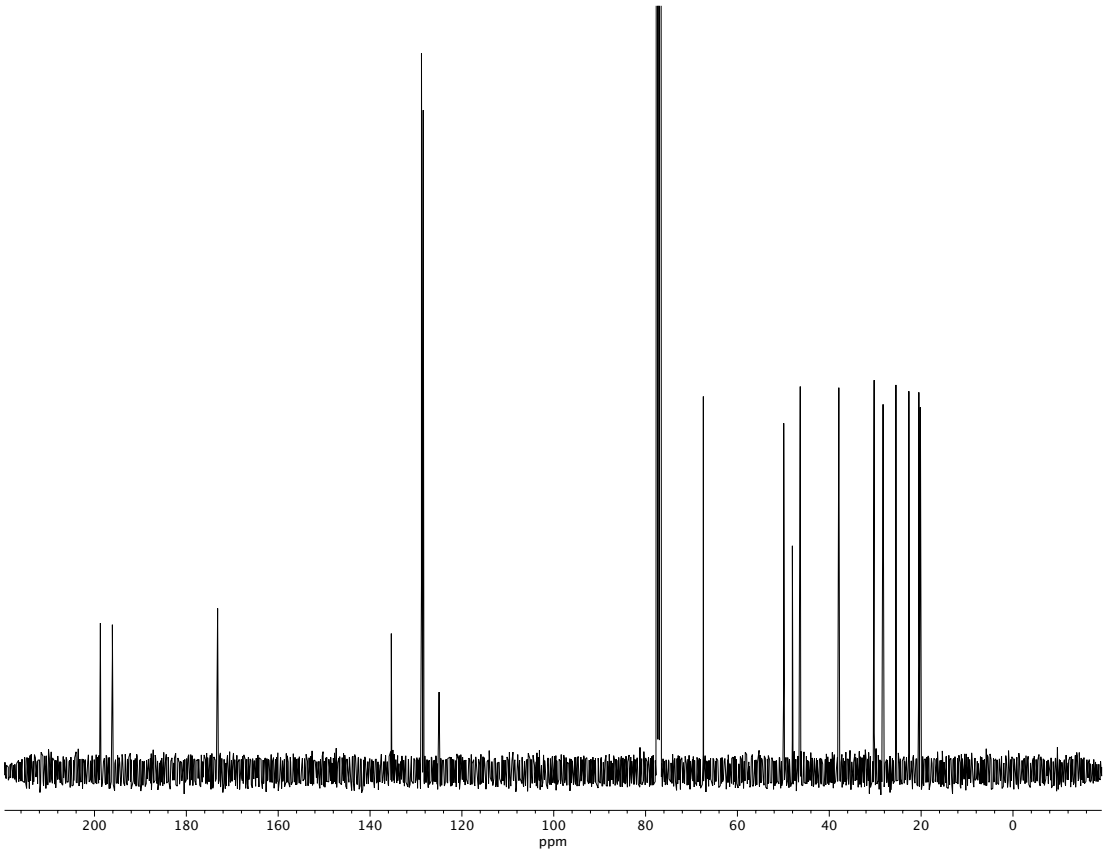

Figure A1.335. *^{13}C NMR (100 MHz, $CDCl_3$) of compound* ***153.***

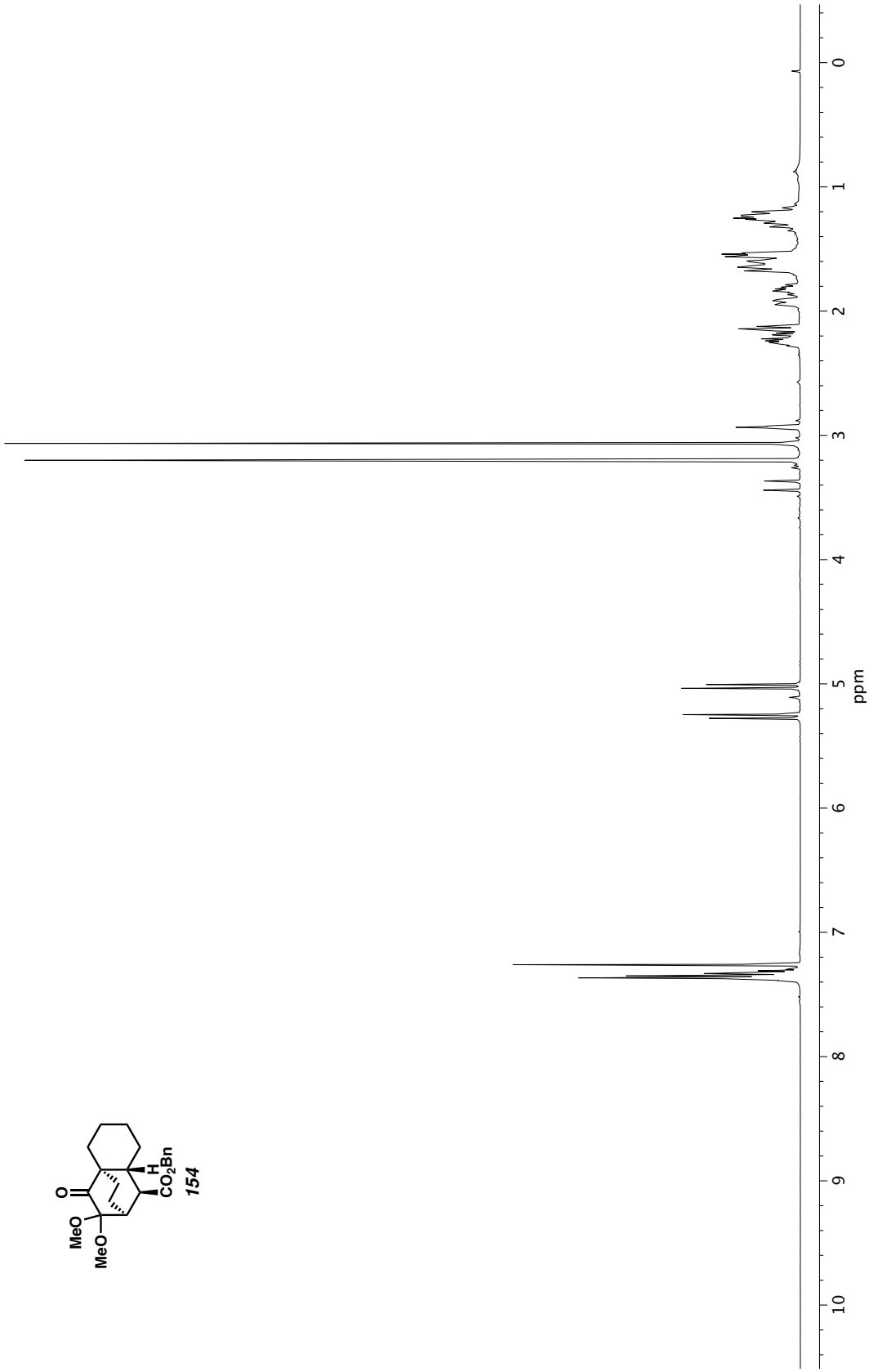

Figure A1.336. *^1H NMR (400 MHz, $CDCl_3$) of compound* ***154.***

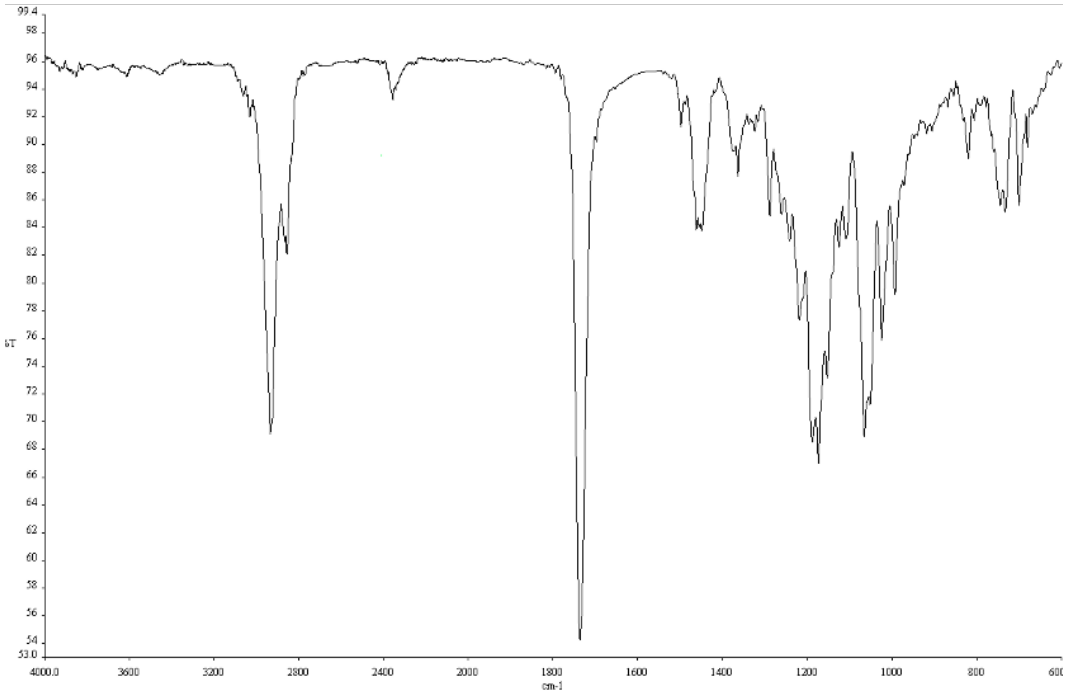

Figure A1.337. *Infrared spectrum (Thin Film, NaCl) of compound* ***154.***

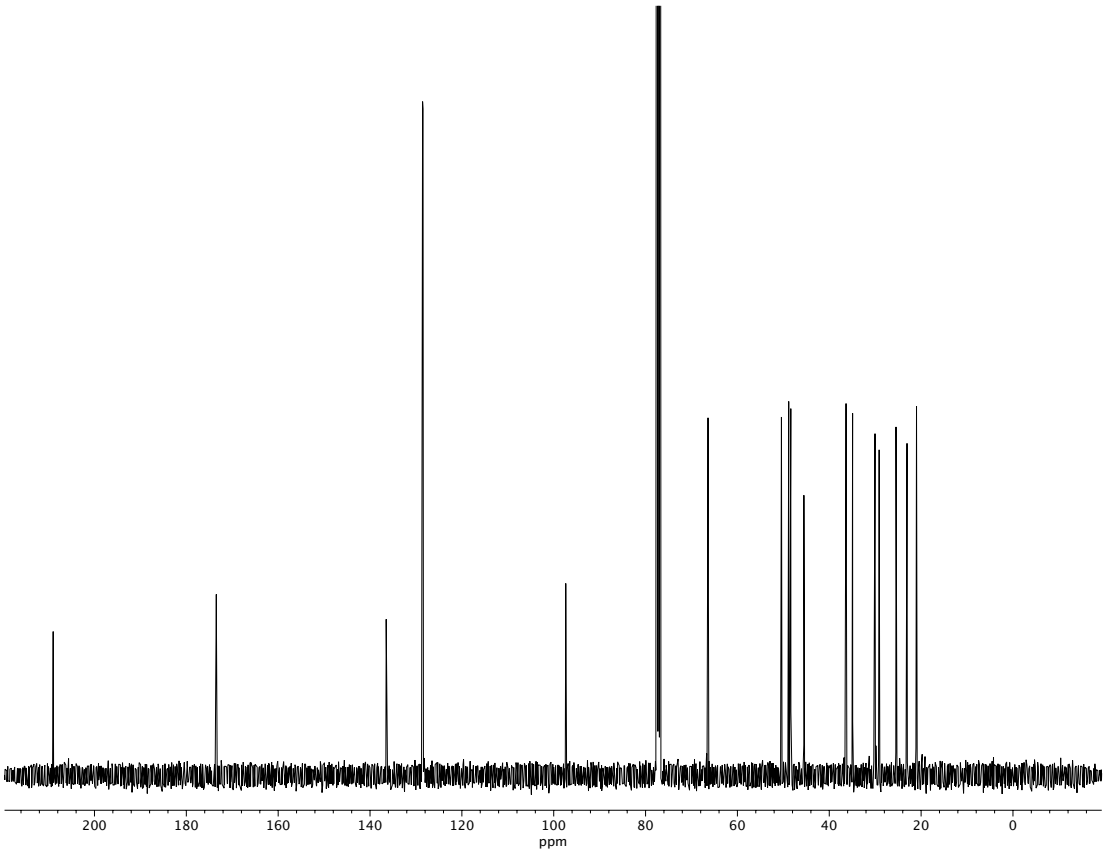

Figure A1.338. *^{13}C NMR (100 MHz, $CDCl_3$) of compound* ***154.***

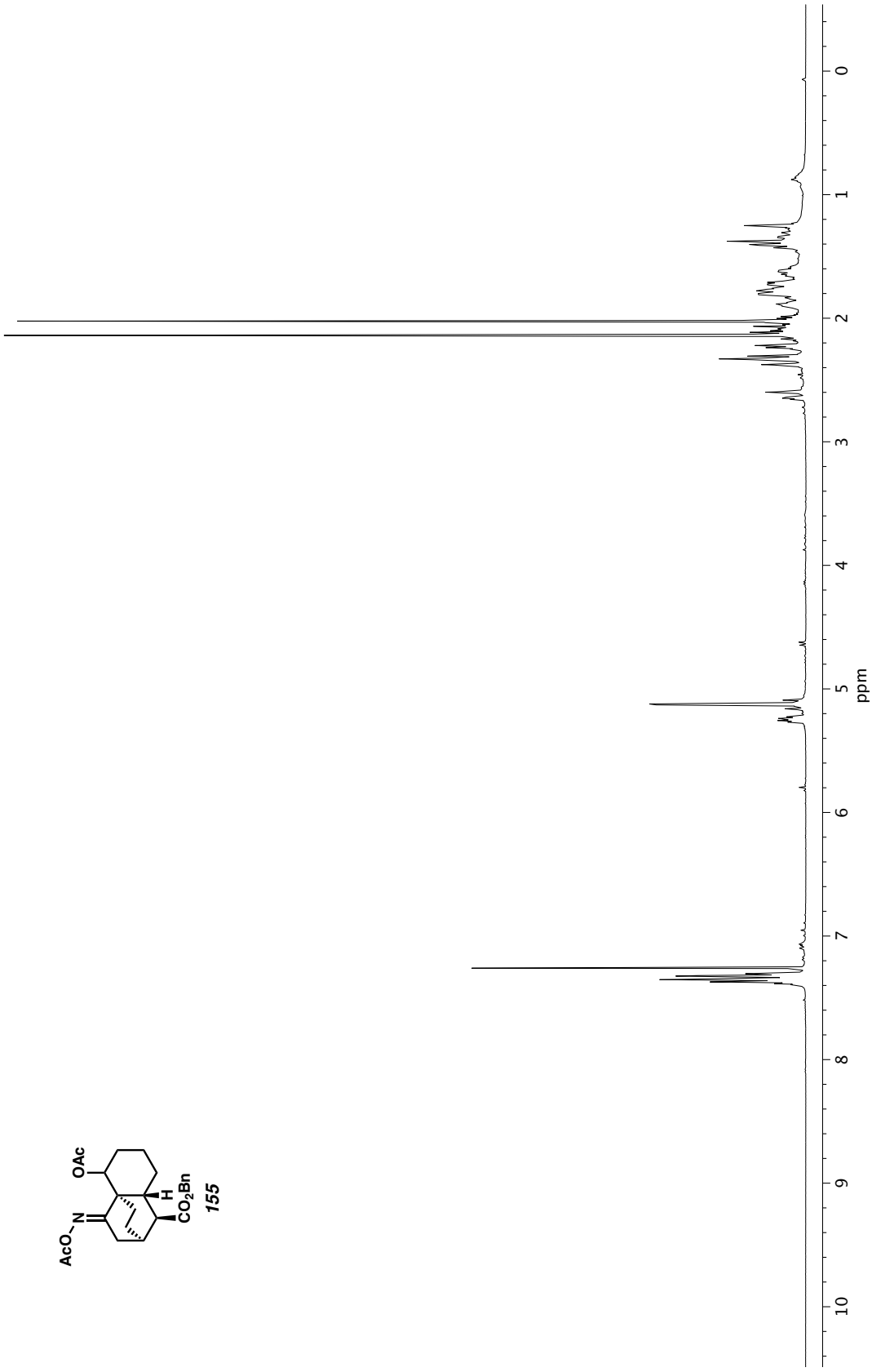

Figure A1.339. *^{1}H NMR (400 MHz, $CDCl_3$) of compound* ***155.***

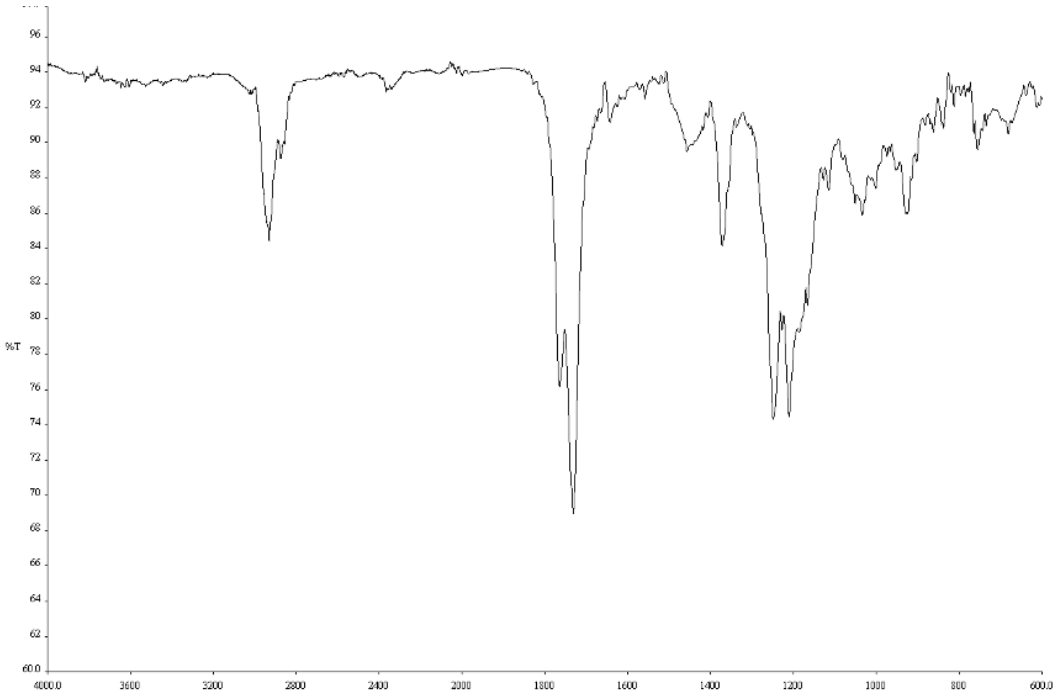

Figure A1.340. *Infrared spectrum (Thin Film, NaCl) of compound* ***155.***

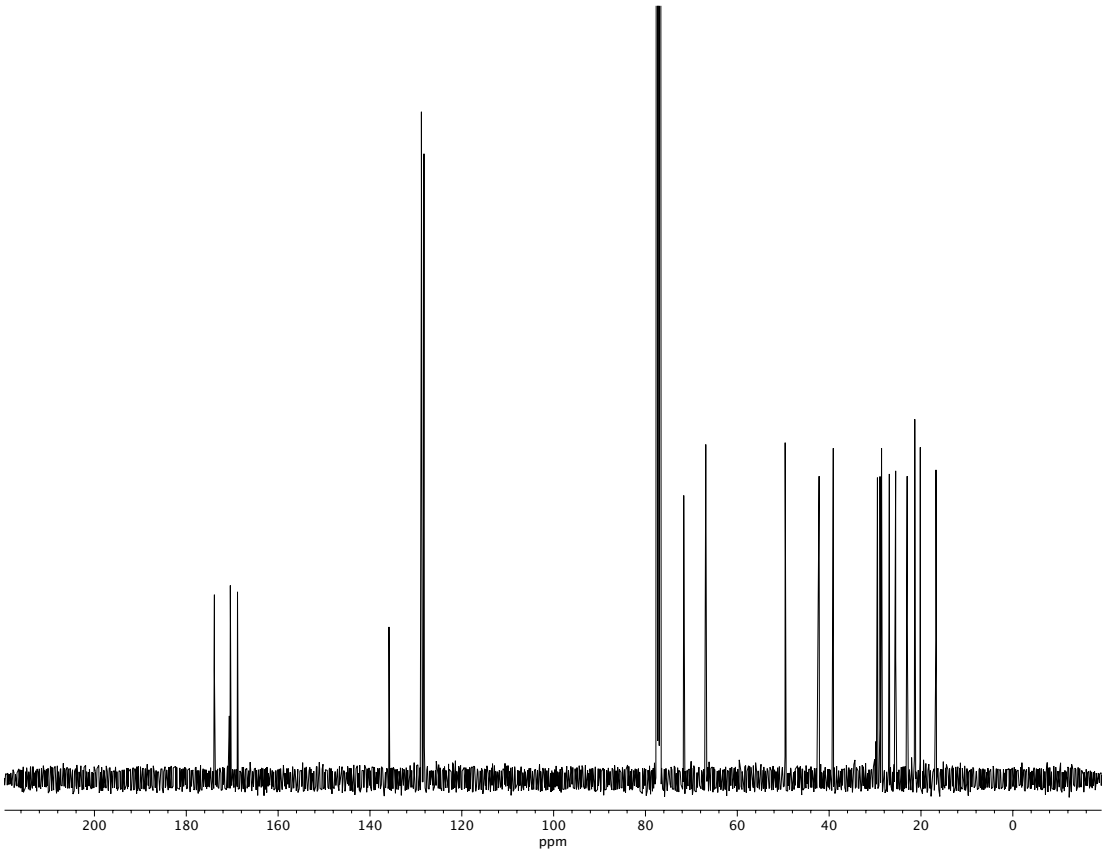

Figure A1.341. *^{13}C NMR (100 MHz, $CDCl_3$) of compound* ***155.***

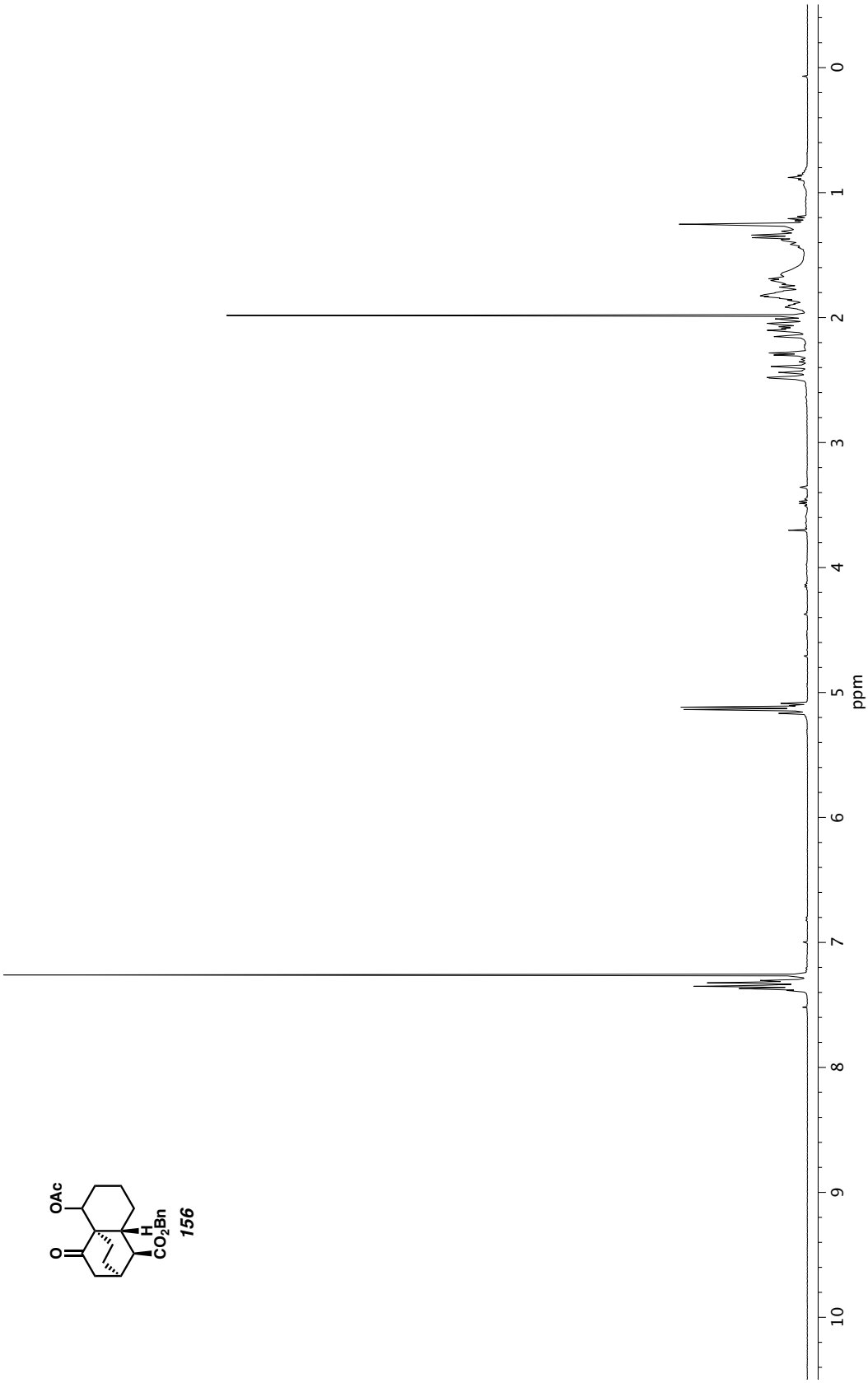

Figure A1.342. *^{1}H NMR (400 MHz, $CDCl_3$) of compound* ***156.***

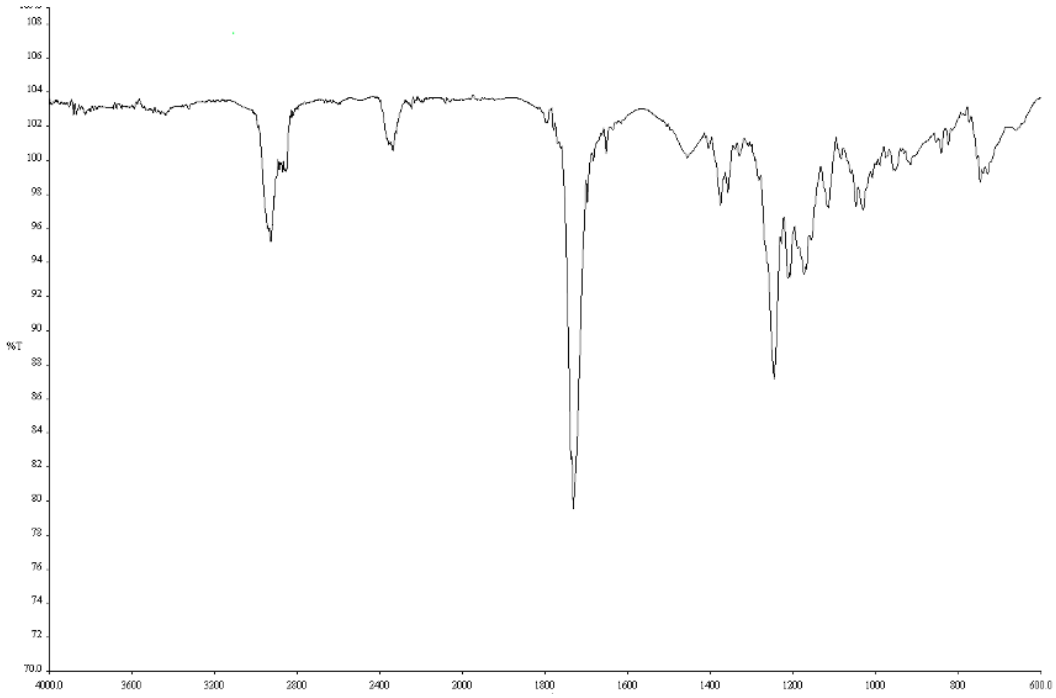

Figure A1.343. *Infrared spectrum (Thin Film, NaCl) of compound* ***156.***

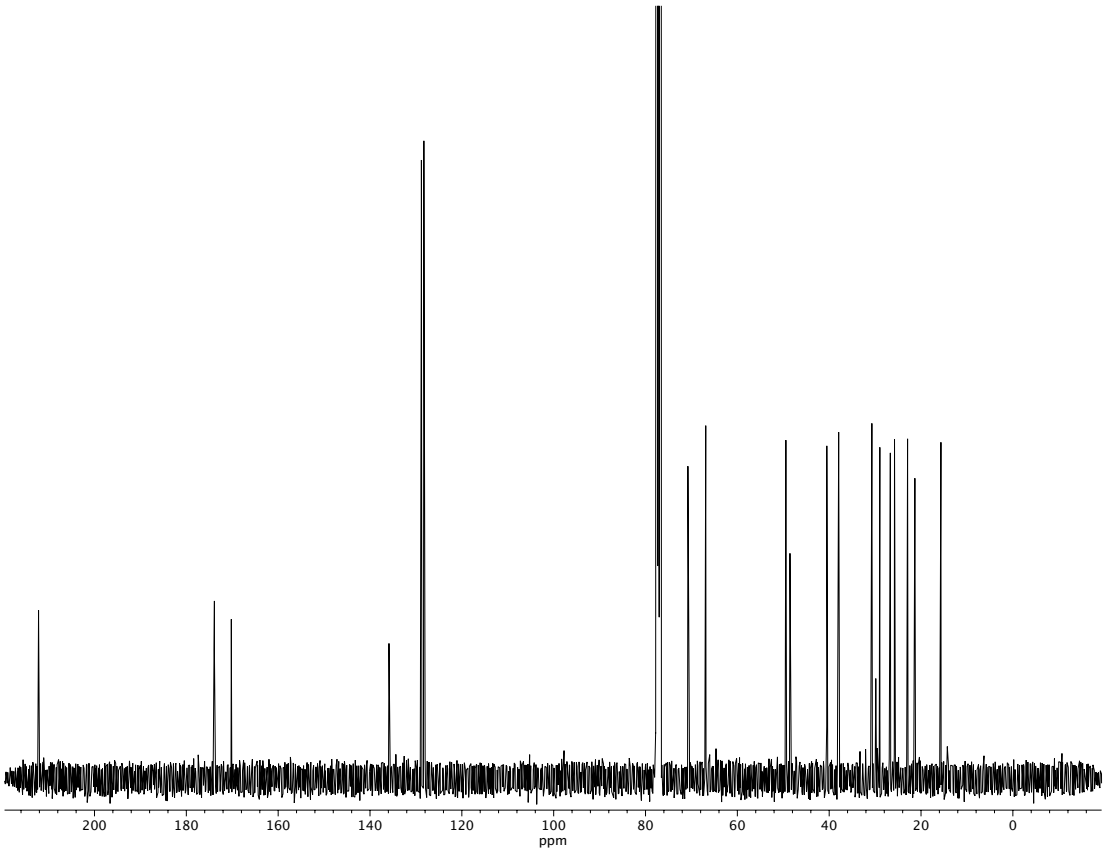

Figure A1.344. *^{13}C NMR (100 MHz, $CDCl_3$) of compound* ***156.***

CHAPTER 3

Asymmetric Michael Spirocyclization of Pd Enolates†

3.1 INTRODUCTION

The enantio- and diastereoselective construction of spirocycles bearing all-carbon quaternary centers remains a persistent challenge in synthetic organic chemistry.[1] The prevalence of these motifs in complex natural products and other medicinally relevant molecules necessitates the development of new stereoselective reactions that can form these ring systems effectively.[2] The enantioselective Pd-catalyzed decarboxylative allylic alkylation reaction has proven to be a valuable tool for the construction of sterically congested all-carbon quaternary centers from racemic or prochiral starting materials.[3, 4] Following extensive experimental and computational mechanistic studies, we have become interested in employing the chiral *O*-bound Pd enolate implicated in these transformations in the context of other reactions beyond allylic alkylation.[5]

Recently, our group reported a Pd-catalyzed decarboxylative [4+2] cycloaddition of Pd dienolates with tethered dienophiles (**TS2**), resulting in the formation of tricyclic scaffolds in high yield and good enantio- and diastereoselectivities (Figure 3.1A).[6] In 1989 Tsuji and coworkers reported a nonenantioselective Pd-catalyzed Michael spirocyclization reaction, which depending on conditions, could favor formation of either protonolysis

†This research was performed in collaboration with Chen, P.-J.; Bissenali, S.; Portions of this chapter have been reproduced with permission from Stoltz, et al. *ACS Catal.* **2025**, *15*, 12231–12237. © 2025 American Chemical Society.

product **194** or allylated product **195** (Figure 3.1B).[7] The diastereomeric outcome, mechanism of catalyst turnover, and broader scope beyond a 5/5 spirane were not discussed.

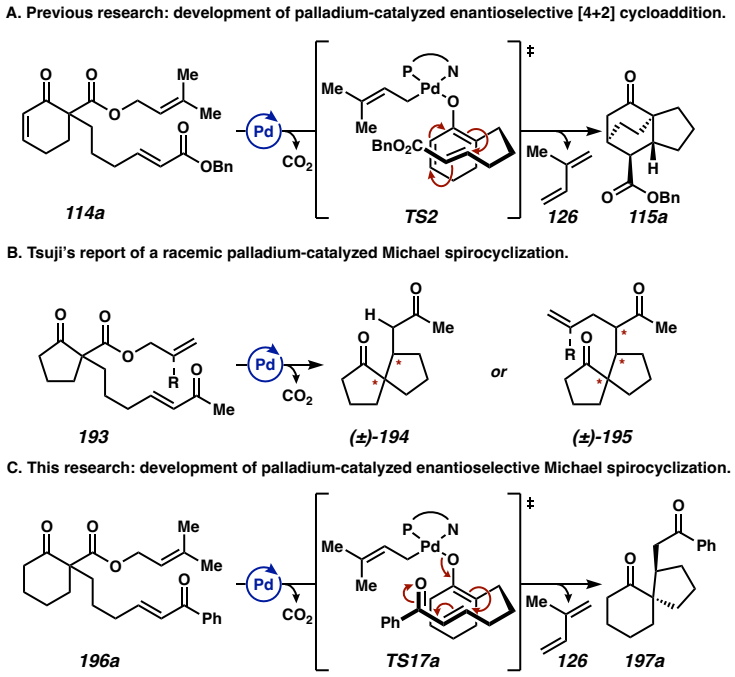

Figure 3.1 *(A) Pd-catalyzed enantioselective [4+2] cycloaddition. (B) Racemic Pd-catalyzed Michael spirocyclization reported by Tsuji et al. (C) Development of a new Pd-catalyzed enantio- and diastereoselective Michael spirocyclization.*

Inspired by these findings, we sought to develop an enantio- and diastereoselective spirocyclization that could efficiently forge vicinal quaternary and tertiary stereocenters (Figure 3.1C). We envisioned that enantioselectivity could be induced in a similar manner to the previously studied [4+2] cycloaddition.[5, 6] On the other hand, the development of Michael cyclizations can be challenging due to the various diastereoselectivity considerations, in contrast to the well-established (albeit not all encompassing) endo rule of Diels–Alder reactions.[8, 9] For these reasons, generating stereoenriched spiranes through

a Pd-catalyzed Michael cyclization via an unstabilized enolate would represent a significant advance, complementary to other approaches.[10]

3.2 RESULTS AND DISCUSSION

Designing the reaction substrate, we proposed applying our previously developed prenyl β-ketoester technology to achieve additive-free catalyst turnover.[6] Consequently, we synthesized the corresponding racemic substrate **196a** with a tethered phenyl enone as a Michael acceptor to evaluate reaction conditions. We found that performing the reaction at 0.025 mmol scale with $Pd_2(dba)_3$ (2.5 mol %) and *(S)*-$(CF_3)_3$-*t*-BuPHOX ligand (6.5 mol %) in toluene (0.1 M) at 40 ºC for 16 hours is optimal, affording **197a** in 89% ^{1}H NMR yield, 93% ee, and >20:1 dr (Table 3.1, entry 1). The reaction proceeds similarly in THF albeit with slightly diminished yield and selectivity (entry 2). At 21 °C the conversion is reduced, although the enantioselectivity is marginally higher (entry 3).[11] Raising reaction temperature to 60 ºC proves detrimental to both yield and selectivity (entry 4). Employing the more electron-rich *(S)*-*t*-BuPHOX results in similar selectivity but lower yield (entry 5). Further dilution of the reaction is inconsequential (entry 6). When the reaction is performed at a 0.1 mmol scale, the isolated yield and ee are comparable to what is observed on smaller scale (entry 7). The absolute configuration of **197a** was assigned via an X-ray crystal structure (Figure 3.2A, XRD).

Table 3.1 *Optimization of reaction conditions.*[a]

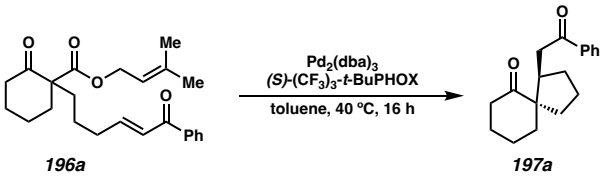

196a *197a*

entry	variation from standard conditions	yield (%)[b]	ee (%)
1	none	89%	93%
2	THF	83%	89%
3	21 °C	56%[c]	95%
4	60 °C	75%	92%
5	*(S)*-*t*-BuPHOX	76%	93%
6	0.05 M	83%	94%
7	0.1 mmol scale	81%[d]	94%

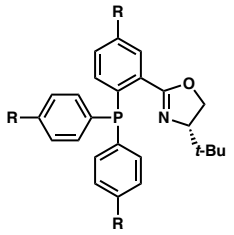

R = CF_3; *(S)*-$(CF_3)_3$-*t*-BuPHOX

R = H; *(S)*-*t*-BuPHOX

[a]Conditions: 0.025 mmol **196a**, 2.5 mol % $Pd_2(dba)_3$, 6.5 mol % ligand, in 0.25 mL of solvent (0.1 M). [b]Yields determined by ^{1}H NMR with respect to 1,3,5-trimethoxybenzene as internal standard.[12] [c]Incomplete conversion was observed.[11] [d]Isolated yield on 0.1 mmol scale.

With optimal conditions in hand, we began exploring the generality of this transformation (Figure 3.2B). The phenyl enone can be replaced with a methyl enone to form spirocycle **197b** in good yield and similar selectivity. Gratifyingly, reactions of both substrates can also be scaled to 1.0 mmol, resulting in slightly improved yields with maintained selectivities. 5/5 spirocycles can be accessed (**197c** and **197d**), albeit in slightly lowered enantioselectivity. In addition, 7/5 systems can also be formed (**197e** and **197f**). Spirolactam **197g** is formed in modest yield and lowered enantioselectivity, and tetralone-derived spirocycles are generated in slightly diminished dr and low ee (**197h d1** and **197h d2**, 12:1 dr based on crude NMR).[13] When Z-enone **198** is employed, the same diastereomer of product (**197a**) is obtained in modest yield with similar selectivity.[14]

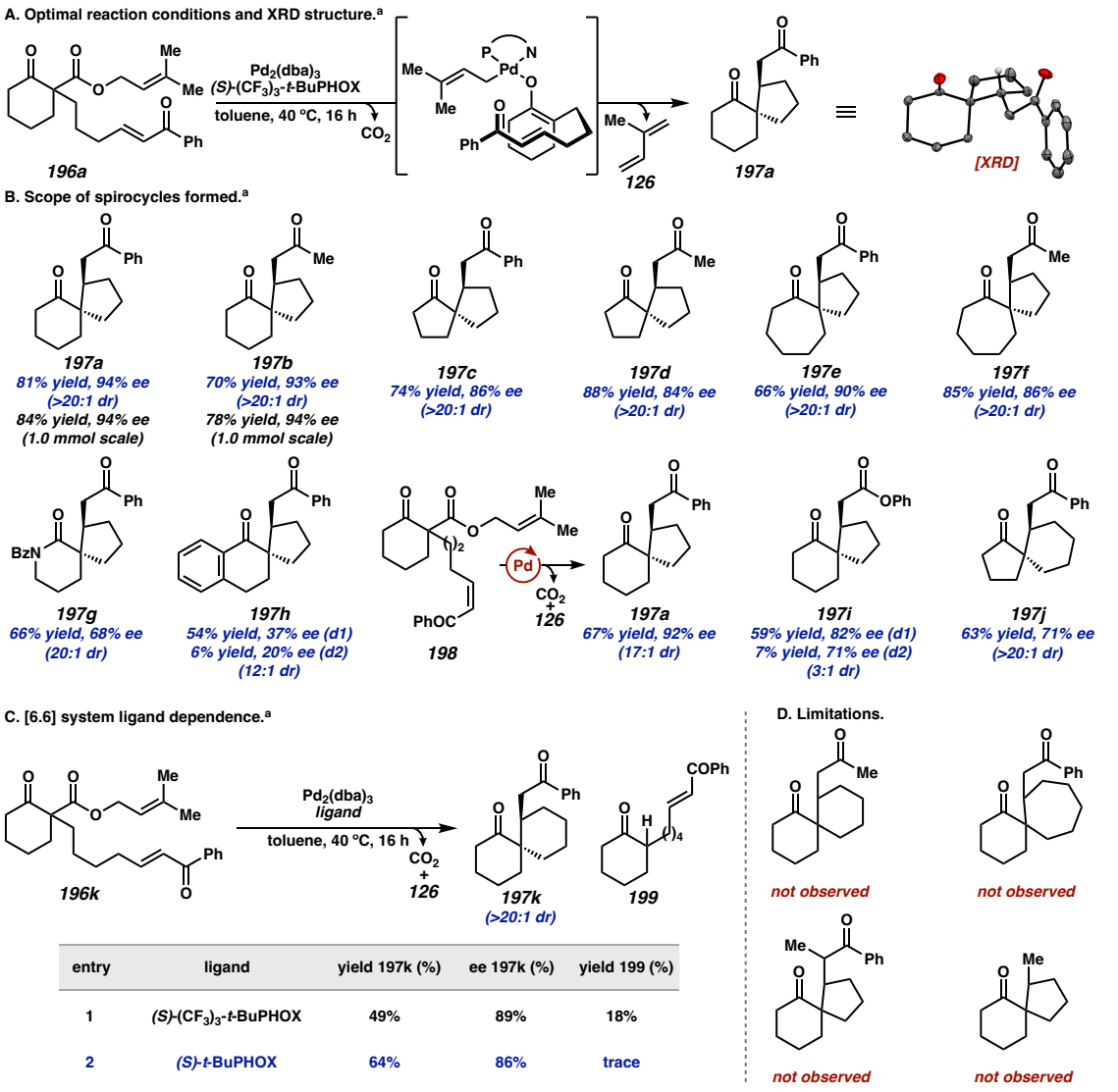

entry	ligand	yield 197k (%)	ee 197k (%)	yield 199 (%)
1	*(S)*-$(CF_3)_3$-*t*-BuPHOX	49%	89%	18%
2	*(S)*-*t*-BuPHOX	64%	86%	trace

Figure 3.2 *(A) Generic reaction scheme and XRD structure. (B) Scope of spirocycles formed via Michael spirocyclization reaction. (C) Ligand-dependent product distribution for 6/6 system (D) Limitations of this transformation.*

[a] Conditions: 0.1 mmol 7, 2.5 mol % Pd2(dba)3, 6.5 mol % ligand, in 0.25 mL of solvent (0.1 M). Isolated yields reported followed by dr's based on NMR ratios of unpurified reaction mixtures.

Employing a phenyl enoate, diastereoselectivity is greatly eroded (**197i d1** and **197i d2**, 3:1 dr based on crude NMR)[13], while moderate levels of enantioselectivity are

maintained. The 5/6 system (derived from a cyclopentanone starting material) forms in modestly lower yield and ee (**197j**). Interestingly, when employing the optimal ligand toward the 6/6 system (Figure 2C, entry 1, **196k** → **197k**), some undesired protonation of the initial Pd-enolate occurs, generating **199**. This can be suppressed however, by employing the more electron-rich *(S)-t*-BuPHOX ligand (entry 2). There were several systems investigated in which appreciable amounts of spirocycle are not clearly observed (Figure 2D). In these cases, direct protonation of the initial Pd-enolate is observed as the major product.

Inspired by Tsuji's enone difunctionalization (**195**, Figure 3.1B), we investigated whether it would be possible to selectively form a stereotriad by employing a cinnamyl β-ketoester (**200a**, Figure 3.3A).[7] We found that employing the same catalytic conditions with **200a** resulted in formation of the desired difunctionalized spirocycle **201a**, isolated as a single diastereomer in 44% yield.[15] The absolute configuration was confirmed via X-ray crystallography (Figure 3.3A, XRD). Additionally, the corresponding 6/6 spirane (**201b**) was also formed under the same conditions. Through this cascade transformation, racemic cinnamyl β-ketoesters were transformed to spirocycles bearing vicinal stereotriads. Further studies on these systems are currently underway.

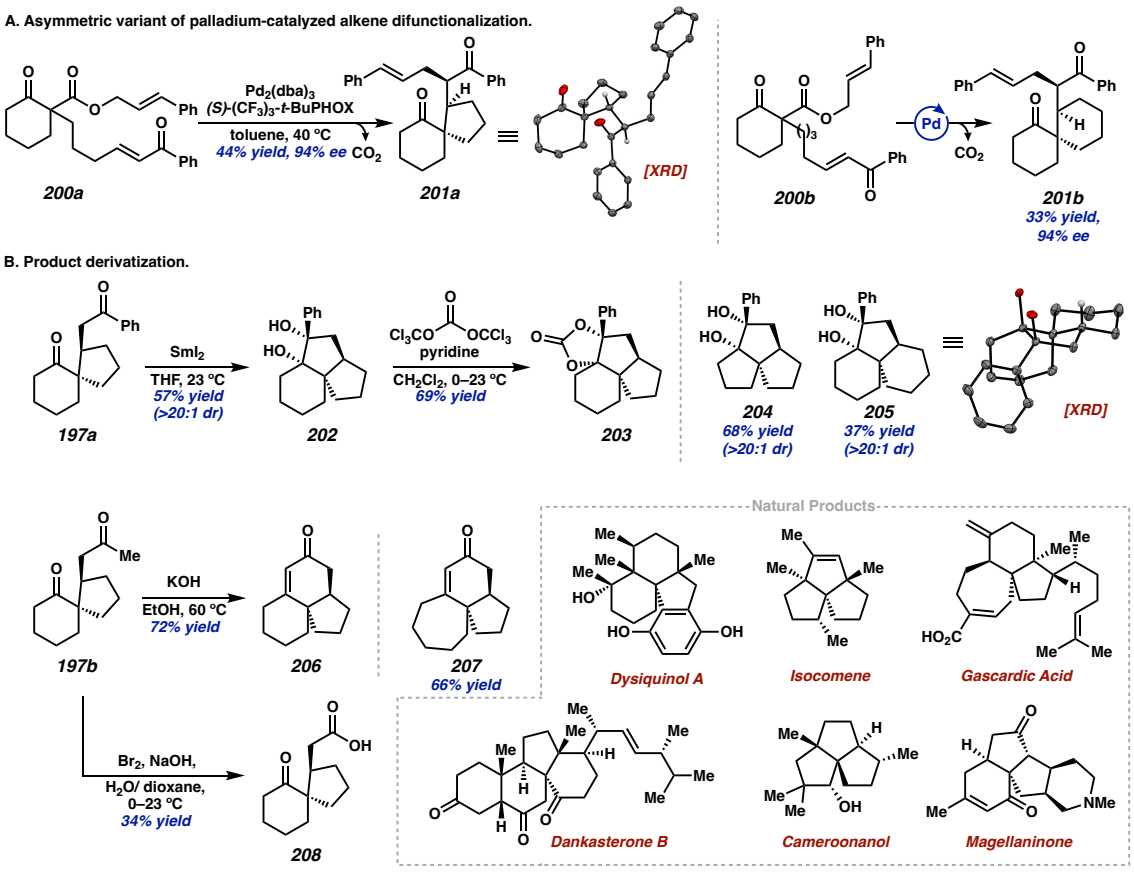

Figure 3.3 *(A) Application of this reaction system to asymmetric enone difunctionalization. (B) Product derivatizations toward versatile functional groups and diverse tricycles.*

With a diverse range of Michael adducts bearing dicarbonyls in hand, we sought to explore the utility of these scaffolds (Figure 3.3B). Treatment of spirane **197a** with stoichiometric samarium diiodide generates pinacol product **202**.[16] The *cis* diol is formed in this process, as suggested by the successful formation of cyclic carbonate **203** upon subjection of **202** to triphosgene and pyridine. In addition to the 6/5/5 system (**202**), 5/5/5 and 6/5/6 angular ring systems (**204** and **205**) are also accessible using this method with the latter's structure (**205**) confirmed via XRD. These ring systems bear four contiguous

stereocenters, three of which are fully substituted. Additionally, an aldol condensation was performed on methyl ketone **197b**, resulting in tricyclic enone **206**. This allows for differentiation of the carbonyls and access to the corresponding 6/6/5 (**206**) and (from **197f**) 7/6/5 (**207**) angular ring systems. Lastly, methyl ketone **197b** can be converted to the corresponding carboxylic acid **208** through a haloform reaction, providing two orthogonal functionalities. These carbocyclic ring systems are found in numerous natural products such as isocomene, dysiquinol A, gascardic acid, and others.[2, 17]

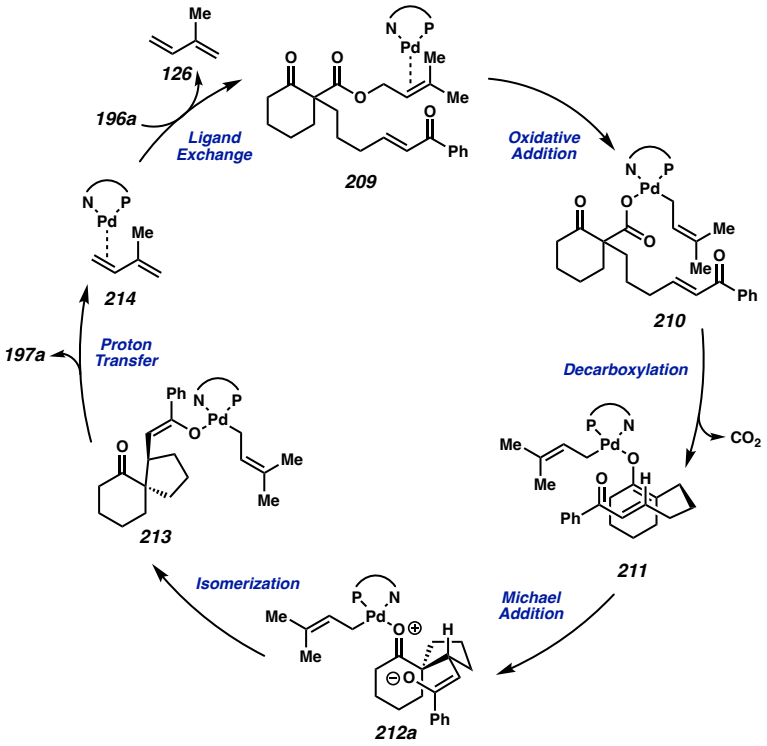

Figure 3.4 *Proposed catalytic cycle.*

Interested in the utility of this Michael spirocyclization, we sought to further understand the mechanism through which it proceeds by proposing a potential catalytic cycle. Using previous studies[4–6] as a starting point, we propose that the mechanism begins with oxidative addition to prenyl β-ketoester **209** to generate Pd-carboxylate **210** (Figure

3.4). Subsequent decarboxylation generates *O*-bound Pd enolate **211**, which can undergo intramolecular Michael spirocyclization to provide enolate **212a**. Following this, isomerization might occur to form *O*-bound Pd enolate **213** before a proton transfer liberates product **197a** and concomitantly generates isoprene bound to Pd(0) (**214**). Upon ligand exchange with another equivalent of substrate (**196a**), catalyst turnover can be achieved.

Intrigued by the Michael spirocyclization proposed in this cycle and the influence of our chiral ligand in this process, we opted to investigate potential Michael addition transition states leading to four possible stereoisomers **212a–d** through DFT calculations (Figure 3.5). Computations were performed at the PBE0-D4/def2-TZVPP (Pd), ma-def2-TZVPP (O), def2-TZVPP/CPCM(PhMe)//PBE0-D4/def2-TZVP (Pd), ma-def2-SVP (O), def2-SVP level of theory as it has proven to be a robust method in our prior studies of similar Pd systems[4] (see experimental section for more details).

Notably, the minimum energy transition structure to each product features an *s*-cis geometry of the Michael acceptor, resulting in Z-enolate geometries of intermediates **212a–d**. The lowest energy transition state **TS17a** features *syn* alignment of the Michael acceptor tether relative to the *t*-Bu substituent of the PHOX ligand, and the electrophile approaches from the more sterically accessible *external* face of the enolate. These characteristics are consistent with observations in our previously studied allylic alkylation and Diels–Alder transformations.[4, 6] In comparison, **TS17b** requires the dienophile tether be placed *anti* to the *t*-Bu group of the PHOX ligand to prevent steric clashing that would result from *internal* electrophile approach (see experimental section for more details). As

such, interaction of the tether and the ligand backbone in **TS17b** leads to a distortion of 15.8º at the Pd–O–C bond angle (∢) relative to **TS17a**, reflecting an increased level of steric congestion that contributes to an increased energy barrier of 9.0 kcal/mol (ΔΔG = 1.6 kcal/mol).

Steric interactions between the phenyl ketone of the Michael acceptor and the ligand backbone in **TS17c** lead to a distorted dihedral angle (ϕc) of 45º between the planes of the carbonyl and the phenyl ring. The *internal* electrophile approach in **TS17d** results in steric clash with the Pd complex, which is reflected by the shortened interatomic distance ($d_{9,10}$ = 2.57 Å) between the ligand aryl group and the prenyl moiety. These undesired interactions contribute to the increased 8.4 and 9.4 kcal/mol energy barriers in **TS17c** and **TS17d**, respectively. These computational studies predict **212a** to be the major stereoisomer, which aligns with the experimentally observed product. The calculated 1.6 kcal/mol preference for **TS17a** over **TS17b** is in good agreement with experimentally observed 94% ee (which corresponds to a 2.1 kcal/mol difference in energy barriers). Further computational and experimental investigations related to the mechanism of catalyst turnover and the reversibility of the Michael addition are currently underway and will be reported in due course.

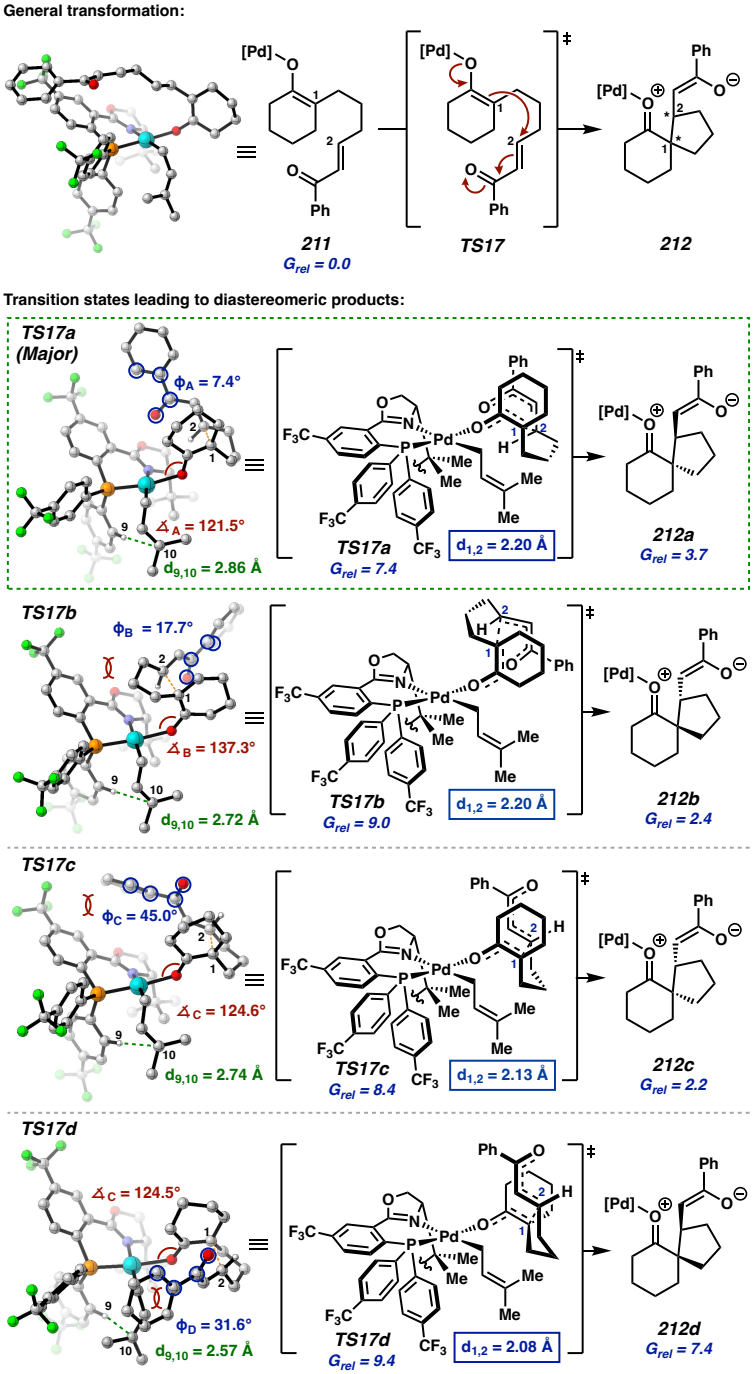

Figure 3.5 *Computational evaluation of the four possible Michael addition transition states leading to the formation of stereoisomers at the PBE0-D4/def2-TZVPP (Pd),*

ma-def2-TZVPP (O), def2-TZVPP/CPCM(PhMe)//PBE0-D4/def2-TZVP (Pd), ma-def2-SVP (O), def2-SVP level of theory.

3.3 CONCLUSIONS

In summary, we report an asymmetric Pd-catalyzed Michael spirocyclization reaction that allows for the efficient construction of vicinal quaternary and tertiary stereodiads. This reaction provides access to a broad scope of bicyclic scaffolds in good yield, dr, and ee. The diversification of these products toward complex tricycles relevant to natural product synthesis is also disclosed. Furthermore, our mechanistic understanding allowed for the development of a cinnamyl-based cascade reaction that generates a third stereocenter. We evaluated a stereochemical model of the Michael addition transition states, which suggest that the stereoselectivity of C–C bond formation could be governed by the Michael acceptor's conformation, placement of the Michael acceptor tether relative to the *t*-Bu substituent of the PHOX ligand, and the bias toward external versus internal approach of the electrophile.

By applying the rational design framework previously established,[5, 6] we were able to expand the utility of Pd enolates through their application in a highly stereoselective Michael spirocyclization. We envision this discovery will expedite the synthesis of stereochemically complex and medicinally relevant polycyclic scaffolds. The insights gained from this study broaden our knowledge regarding the stereochemical interactions of different enolate substrates with the Pd–PHOX catalyst system, which will be leveraged to accelerate the future development of synthetically useful asymmetric transformations.

3.4 EXPERIMENTAL SECTION

3.4.1 Materials and methods.

Unless otherwise stated, reactions were performed in flame-dried glassware under a nitrogen atmosphere using dry, deoxygenated solvents. Solvents were dried by passage through an activated alumina column under argon. Reaction progress was monitored by thin-layer chromatography (TLC) or Agilent 1290 UHPLC-MS. TLC was performed using E. Merck silica gel 60 F254 precoated glass plates (0.25 mm) and visualized by UV fluorescence quenching, $KMnO_4$ staining, or *p*-anisaldehyde staining. Silicycle Silia*Flash*® P60 Academic Silica gel (particle size 40–63 nm) was used for flash chromatography. The absolute configurations of **197a**, **197b**, **201a** and **205** were determined by X-ray crystallography, and all other products were assigned by analogy. Reagents were purchased from commercial sources and used as received unless otherwise stated. Ligands were prepared according to literature procedures.[18] HG-II was graciously provided by Umicore.

Instrumentation and Analysis:

^{1}H NMR spectra were recorded on Varian Inova 600 MHz and Bruker 400 MHz spectrometers and are reported relative to residual non-deuterated solvent $CHCl_3$ (δ 7.26 ppm) or C_6H_6 (δ 7.16 ppm). ^{13}C NMR spectra were recorded on a Bruker 400 MHz spectrometer (100 MHz) and are reported relative to solvent $CDCl_3$ (δ 77.16 ppm) or C_6D_6 (δ 128.06 ppm). Data for ^{1}H NMR are reported as follows: chemical shift (δ ppm) (multiplicity, coupling constant (Hz), integration). Multiplicities are reported as the peaks appear as follows: s = singlet, d = doublet, t = triplet, q = quartet, p = pentet, sept = septuplet, m = multiplet, br s = broad singlet, br d = broad doublet. Some reported spectra include

minor impurities of water (δ 1.56 ppm), ethyl acetate (δ 4.12, 2.05, 1.26 ppm), methylene chloride (δ 5.30 ppm), acetone (δ 2.17 ppm), grease (δ 1.26, 0.86 ppm), and/or silicon grease (δ 0.07 ppm), which do not impact product assignments. Data for ^{13}C NMR are reported in terms of chemical shifts (δ ppm). IR spectra were obtained by use of a Perkin Elmer Spectrum BXII spectrometer or Nicolet 6700 FTIR spectrometer using thin films deposited on NaCl plates and reported in frequency of absorption (cm^{-1}). Optical rotations were measured with a Jasco P-2000 polarimeter operating on the sodium D-line (589 nm), using a 100 mm path-length cell. Analytical SFC and SFC-MS studies were performed with an Agilent 1260 Infinity II G6125B SFC-MS supercritical CO_2 analytical chromatography system utilizing Chiralpak (IC-3, AD-3, ID-3, IF-3, IG-3, IH-3) or Chiralcel (OD-3, OJ-3) columns (4.6 mm x 25 cm) obtained from Daicel Chemical Industries, Ltd.[19] High resolution mass spectra (HRMS) were obtained from the Caltech Mass Spectral Facility using a JEOL JMS-T2000GC AccuTOFTM GC-Alpha High Resolution Mass Spectrometer in field ionization (FI+) or field desorption (FD+) mode, or an Agilent 6230 Series TOF with an Agilent Jet Stream ion source in electrospray ionization (ESI+). Low-temperature diffraction data (ϕ-and ω-scans) were collected on a Bruker AXS D8 VENTURE KAPPA diffractometer coupled to a PHOTON II CPAD detector with Cu K_α radiation (λ = 1.54178 Å) from an IμS micro-source for the structure of compound V25038. The structure was solved by direct methods using SHELXS[20] and refined against F^2 on all data by full-matrix least squares with SHELXL-2019[21] using established refinement techniques.[22] All non-hydrogen atoms were refined anisotropically. All hydrogen atoms were included into the model at geometrically calculated positions and

refined using a riding model. The isotropic displacement parameters of all hydrogen atoms were fixed to 1.2 times the *U* value of the atoms they are linked to (1.5 times for methyl groups).

List of Abbreviations:

ee – enantiomeric excess, dr – diastereomeric ratio, SFC – supercritical fluid chromatography, HPLC – high-performance liquid chromatography, TLC – thin-layer chromatography, IPA – isopropanol, EtOAc – ethyl acetate.

3.4.2 Experimental procedures and spectroscopic data.

Pd-Catalyzed Decarboxylative Michael Cyclization:

General Procedure A: Asymmetric Pd-Catalyzed Decarboxylative Michael Cyclization

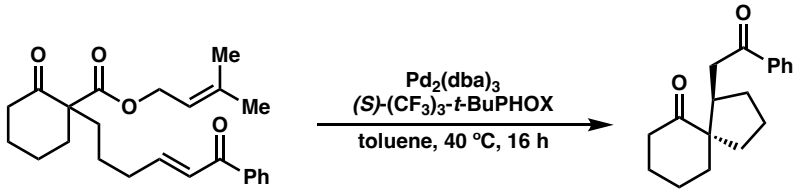

196 ***197***

In a nitrogen filled glovebox, an oven-dried 4 mL vial was charged with a stir bar, $Pd_2(dba)_3$ (2.3 mg, 0.0025 mmol, 2.5 mol %), *(S)*-$(CF_3)_3$-*t*-BuPHOX (3.8 mg, 0.0065 mmol, 6.5 mol %), and toluene (0.6 mL). The catalyst solution was stirred at 23 ºC for 20 min. A solution of substrate **196** (0.1 mmol, 1 equiv) in toluene (0.4 mL) was added to the catalyst solution. The resulting mixture was sealed, pumped out of the glovebox, and then heated to 40 ºC for 16 h. The solution was then cooled to 23 ºC and concentrated under reduced pressure. The crude mixture was purified by silica gel flash column chromatography to yield **197**.

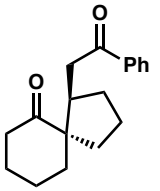

197a

(1*R*,5*S*)-1-(2-oxo-2-phenylethyl)spiro[4.5]decan-6-one (197a)

Prepared from **196a** following General Procedure A. Purification by flash column chromatography (0–60% Et_2O/hexanes) afforded the title compound as a white crystalline solid (21.9 mg, 0.081 mmol, 81% yield, 94% ee). Absolute and relative stereochemistry were assigned by X-ray crystallography (vide infra).

^{1}H NMR (600 MHz, $CDCl_3$): δ 8.12 – 8.07 (m, 2H), 7.58 – 7.53 (m, 1H), 7.51 – 7.45 (m, 2H), 3.21 (dd, *J* = 14.0, 3.6 Hz, 1H), 3.01 – 2.92 (m, 1H), 2.52 (dd, *J* = 13.9, 11.2 Hz, 1H), 2.47 – 2.38 (m, 2H), 2.07 – 2.00 (m, 1H), 1.99 – 1.92 (m, 1H), 1.89 – 1.82 (m, 1H), 1.82 – 1.55 (m, 8H), 1.38 – 1.30 (m, 1H).

^{13}C NMR (100 MHz, $CDCl_3$): δ 214.3, 200.8, 136.9, 133.1, 128.71, 128.69, 58.8, 40.5, 40.2, 39.9, 34.9, 31.5, 29.3, 27.3, 21.8, 21.7.

IR (Neat Film, NaCl): 2938, 2862, 1699, 1684, 1448, 1279, 1213, 1128 cm^{-1}.

HRMS (ESI+): *m/z* calc'd for $C_{18}H_{23}O_2$ $[M+H]^+$: 271.1693, found 271.1681.

Optical Rotation: $[\alpha]_D^{23}$ –23.9 (c = 0.69, $CHCl_3$).

SFC conditions: 20% IPA, 2.5 mL/min, Chiralpak IC-3 column, λ = 254 nm, t_R (min): minor = 6.99, major = 8.67

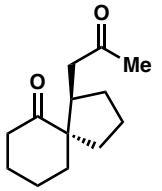

197b

(1*R*,5*S*)-1-(2-oxopropyl)spiro[4.5]decan-6-one (197b)

Prepared from **196b** following General Procedure A. Purification by flash column chromatography (0–60% Et_2O/hexanes) afforded the title compound as a pale yellow crystalline solid (14.5 mg, 0.070 mmol, 70% yield, 93% ee). Absolute and relative stereochemistry were assigned by X-ray crystallography (vide infra).

^{1}H NMR (400 MHz, $CDCl_3$): δ 2.95 – 2.79 (m, 1H), 2.49 (dd, *J* = 14.9, 4.2 Hz, 1H), 2.44 – 2.31 (m, 2H), 2.21 – 2.10 (m, 4H), 2.04 – 1.95 (m, 1H), 1.94 – 1.81 (m, 2H), 1.80 – 1.71 (m, 2H), 1.71 – 1.45 (m, 6H), 1.27 – 1.14 (m, 1H).

^{13}C NMR (100 MHz, $CDCl_3$): δ 214.0, 209.2, 58.3, 45.0, 40.3, 38.8, 35.1, 31.5, 30.0, 29.7, 27.1, 21.9, 21.7.

IR (Neat Film, NaCl): 2941, 2864, 1701, 1447, 1355, 1164, 1129 cm^{-1}.

HRMS (ESI+): *m/z* calc'd for $C_{13}H_{21}O_2$ $[M+H]^+$: 209.1536, found 209.1526.

Optical Rotation: $[\alpha]_D^{23}$ –5.3 (c = 0.49, $CHCl_3$).

SFC conditions: 30% IPA, 2.5 mL/min, Chiralpak IC-3 column, MSD1 TIC[19], t_R (min): major = 3.39, minor = 3.98

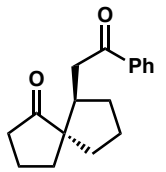

197c

(5*R*,6*R*)-6-(2-oxo-2-phenylethyl)spiro[4.4]nonan-1-one (197c)

Prepared from **196c** following General Procedure A. Purification by flash column chromatography (0–60% Et_2O/hexanes) afforded the title compound as a colorless oil (18.9 mg, 0.074 mmol, 74% yield, 86% ee).

^{1}H NMR (400 MHz, $CDCl_3$): δ 7.96 – 7.88 (m, 2H), 7.58 – 7.51 (m, 1H), 7.49 – 7.42 (m, 2H), 2.98 – 2.83 (m, 2H), 2.82 – 2.69 (m, 1H), 2.42 – 2.30 (m, 1H), 2.29 – 2.15 (m, 1H), 2.10 – 2.01 (m, 1H), 2.00 – 1.92 (m, 1H), 1.92 – 1.78 (m, 2H), 1.77 – 1.65 (m, 4H), 1.63 – 1.51 (m, 1H), 1.41 – 1.29 (m, 1H).

^{13}C NMR (100 MHz, $CDCl_3$): δ 222.9, 199.8, 136.9, 133.2, 128.8, 128.3, 58.8, 41.2, 40.5, 38.0, 37.8, 32.2, 31.5, 23.1, 19.6.

IR (Neat Film, NaCl): 2955, 2870, 1729, 1683, 1596, 1448, 1213, 1157 cm^{-1}.

HRMS (ESI+): *m/z* calc'd for $C_{17}H_{20}O_2Na$ $[M+Na]^+$: 279.1356, found 279.1345.

Optical Rotation: $[\alpha]_D^{23}$ +44.9 (c = 0.74, $CHCl_3$).

SFC conditions: 20% IPA, 2.5 mL/min, Chiralpak IC-3 column, λ = 254 nm, t_R (min): minor = 7.78, major = 10.03

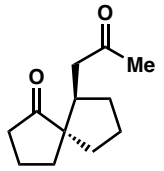

197d

(5*R*,6*R*)-6-(2-oxopropyl)spiro[4.4]nonan-1-one (197d)

Prepared from **196d** following General Procedure A. Purification by flash column chromatography (0–60% Et_2O/hexanes) afforded the title compound as a colorless oil (17.1 mg, 0.088 mmol, 88% yield, 84% ee).

^{1}H NMR (400 MHz, $CDCl_3$): δ 2.64 – 2.51 (m, 1H), 2.42 – 2.23 (m, 3H), 2.19 – 2.07 (m, 4H), 2.06 – 1.97 (m, 1H), 1.97 – 1.87 (m, 1H), 1.85 – 1.73 (m, 2H), 1.73 – 1.60 (m, 4H), 1.59 – 1.47 (m, 1H), 1.30 – 1.13 (m, 1H).

^{13}C NMR (100 MHz, $CDCl_3$): δ 222.9, 208.5, 58.7, 45.6, 40.6, 37.9, 37.7, 32.1, 31.2, 29.9, 22.9, 19.5.

IR (Neat Film, NaCl): 2955, 2872, 1730, 1406, 1357, 1158 cm^{-1}.

HRMS (ESI+): *m/z* calc'd for $C_{12}H_{19}O_2$ $[M+H]^+$: 195.1380, found 195.1370.

Optical Rotation: $[\alpha]_D^{23}$ +66.6 (c = 0.59, $CHCl_3$).

SFC conditions: 25% IPA, 2.5 mL/min, Chiralpak IC-3 column, MSD1 TIC[19], t_R (min): major = 4.16, minor = 4.78

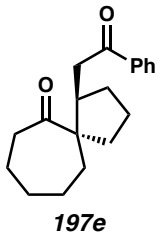

197e

(1*R*,5*S*)-1-(2-oxo-2-phenylethyl)spiro[4.6]undecan-6-one (197e)

Prepared from **196e** following General Procedure A. Purification by flash column chromatography (0–60% Et_2O/hexanes) afforded the title compound as a colorless oil (18.7 mg, 0.066 mmol, 66% yield, 90% ee).

^{1}H NMR (400 MHz, $CDCl_3$): δ 8.06 – 7.99 (m, 2H), 7.60 – 7.52 (m, 1H), 7.51 – 7.43 (m, 2H), 3.25 (dd, *J* = 14.5, 4.3 Hz, 1H), 2.85 – 2.72 (m, 1H), 2.67 – 2.52 (m, 3H), 2.01 – 1.79 (m, 3H), 1.78 – 1.55 (m, 9H), 1.54 – 1.46 (m, 1H), 1.44 – 1.30 (m, 1H).

^{13}C NMR (100 MHz, $CDCl_3$): δ 217.2, 200.3, 136.9, 133.1, 128.7, 128.5, 60.7, 42.7, 42.7, 40.3, 37.5, 31.5, 31.0, 30.2, 26.4, 25.8, 22.2.

IR (Neat Film, NaCl): 2931, 2858, 1686, 1596, 1579, 1448, 1287, 1215 cm^{-1}.

HRMS (ESI+): *m/z* calc'd for $C_{19}H_{25}O_2$ $[M+H]^+$: 285.1849, found 285.1841.

Optical Rotation: $[\alpha]_D^{23}$ +16.2 (c = 1.56, $CHCl_3$).

SFC conditions: 20% IPA, 2.5 mL/min, Chiralpak IC-3 column, λ = 254 nm, t_R (min): major = 10.28, minor = 11.76

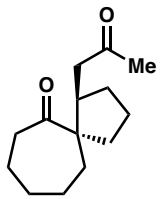

197f

(1*R*,5*S*)-1-(2-oxopropyl)spiro[4.6]undecan-6-one (197f)

Prepared from **196f** following General Procedure A. Purification by flash column chromatography (0–60% Et_2O/hexanes) afforded the title compound as a colorless oil (18.8 mg, 0.085 mmol, 85% yield, 86% ee).

^{1}H NMR (400 MHz, $CDCl_3$): δ 2.70 – 2.46 (m, 4H), 2.23 (dd, *J* = 15.2, 9.9 Hz, 1H), 2.14 (s, 3H), 2.02 – 1.85 (m, 2H), 1.81 – 1.72 (m, 1H), 1.72 – 1.44 (m, 10H), 1.30 – 1.17 (m, 1H).

^{13}C NMR (100 MHz, $CDCl_3$): δ 217.1, 208.7, 60.5, 45.3, 42.7, 42.1, 37.1, 31.3, 31.0, 30.6, 30.0, 26.3, 25.7, 22.3.

IR (Neat Film, NaCl): 2931, 2858, 1713, 1697, 1453, 1354, 1159 cm^{-1}.

HRMS (ESI+): *m/z* calc'd for $C_{14}H_{23}O_2$ $[M+H]^+$: 223.1693, found 223.1683.

Optical Rotation: $[\alpha]_D^{23}$ +30.9 (c = 0.73, $CHCl_3$).

SFC conditions: 30% IPA, 2.5 mL/min, Chiralpak IC-3 column, MSD1 TIC[19], t_R (min): major = 3.90, minor = 6.06

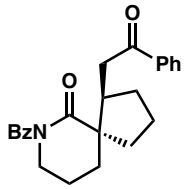

197g

(1*R*,5*R*)-7-benzoyl-1-(2-oxo-2-phenylethyl)-7-azaspiro[4.5]decan-6-one (197g)

Prepared from **196g** following General Procedure A. Purification by flash column chromatography (0–80% Et_2O/hexanes) afforded the title compound as a white foam (24.6 mg, 0.066 mmol, 66% yield, 68% ee).

^{1}H NMR (600 MHz, $CDCl_3$): δ 7.93 – 7.89 (m, 2H), 7.59 – 7.55 (m, 2H), 7.54 – 7.50 (m, 1H), 7.47 – 7.40 (m, 3H), 7.37 (t, *J* = 7.7 Hz, 2H), 3.96 (dtd, *J* = 12.7, 4.5, 1.7 Hz, 1H), 3.70 (ddd, *J* = 12.7, 10.9, 4.8 Hz, 1H), 3.19 – 3.11 (m, 1H), 3.06 (dd, *J* = 15.0, 5.2 Hz, 1H), 2.80 (dd, *J* = 15.0, 9.6 Hz, 1H), 2.11 – 1.93 (m, 5H), 1.89 – 1.82 (m, 1H), 1.80 – 1.71 (m, 3H), 1.40 – 1.32 (m, 1H).

^{13}C NMR (100 MHz, $CDCl_3$): δ 199.6, 178.5, 175.5, 136.8, 136.8, 133.1, 131.4, 128.7, 128.3, 128.3, 127.6, 53.8, 46.5, 41.9, 39.7, 38.4, 29.9, 27.4, 22.3, 20.1.

IR (Neat Film, NaCl): 3059, 2951, 2872, 1681, 1597, 1475, 1448, 1386, 1277, 1169, 1151 cm^{-1}.

HRMS (ESI+): *m/z* calc'd for $C_{24}H_{26}NO_3$ $[M+H]^+$: 376.1907, found 376.1907.

Optical Rotation: $[\alpha]_D^{23}$ +51.6 (c = 2.05, $CHCl_3$).

SFC conditions: 40% IPA, 2.5 mL/min, Chiralpak IC-3 column, λ = 254 nm, t_R (min): minor = 5.93, major = 9.07

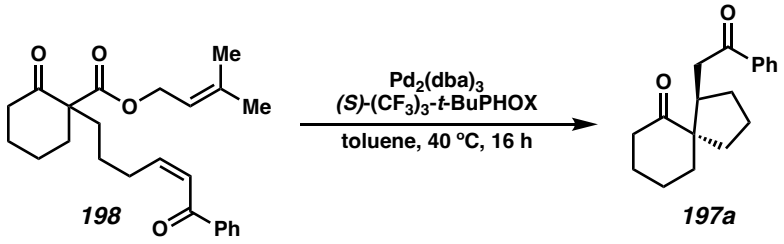

(1*R*,5*S*)-1-(2-oxo-2-phenylethyl)spiro[4.5]decan-6-one (197a)

Prepared from **198** following General Procedure A. Purification by flash column chromatography (0–55% Et_2O/hexanes) afforded the title compound as a colorless oil (18.2 mg, 0.067 mmol, 67% yield, 92% ee).

Note: see NMR, IR, HRMS, Optical Rotation data in reaction of 196a to 197a earlier in SI.

SFC conditions: 20% IPA, 2.5 mL/min, Chiralpak IC-3 column, λ = 254 nm, t_R (min): minor = 6.82, major = 8.44

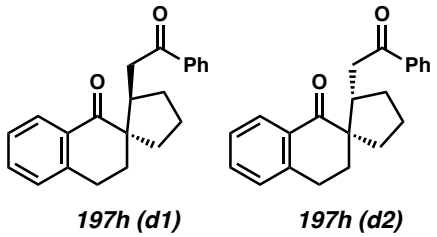

(1*R*,2*R*)-2-(2-oxo-2-phenylethyl)-3',4'-dihydro-1'*H*-spiro[cyclopentane-1,2'-naphthalen]-1'-one (197h, *d1* and *d2*)

Prepared from **196h** following General Procedure A. Crude analysis by ^{1}H NMR affords a 12:1 ratio of *d1* to *d2*. The diastereomers were subsequently separated by flash column chromatography (0–60% Et_2O/hexanes) to afford the *d1* as a colorless oil (17.3 mg, 0.054 mmol, 54% yield, 37% ee) and *d2* as a colorless oil (1.9 mg, 0.006 mmol, 6% yield, 20% ee). The absolute configuration of 8h *d1* is assigned by analogy to **197a**. The relative configuration of **197h *d2*** is assigned by comparison to ^{1}H NMR of **197h *d1***, the absolute configuration is not determined.

197h (*d1*):

^{1}H NMR (400 MHz, $CDCl_3$): δ 8.08 (dd, *J* = 7.8, 1.4 Hz, 1H), 8.05 – 7.97 (m, 2H), 7.60 – 7.52 (m, 1H), 7.51 – 7.43 (m, 3H), 7.32 (t, *J* = 7.6 Hz, 1H), 7.24 (d, *J* = 7.8 Hz, 1H), 3.40 – 3.29 (m, 1H), 3.21 – 3.09 (m, 2H), 3.00 – 2.89 (m, 1H), 2.68 (dd, *J* = 14.5, 10.6 Hz, 1H), 2.14 – 1.89 (m, 4H), 1.82 – 1.68 (m, 2H), 1.68 – 1.60 (m, 1H), 1.50 – 1.35 (m, 1H).

^{13}C NMR (100 MHz, $CDCl_3$): δ 201.3, 200.2, 143.3, 136.9, 133.3, 133.1, 132.6, 128.8, 128.7, 128.5, 128.1, 126.8, 55.1, 40.8, 40.0, 33.6, 29.8, 27.1, 25.8, 22.5.

IR (Neat Film, NaCl): 3061, 2933, 2868, 1679, 1597, 1448, 1288, 1224 cm^{-1}.

HRMS (ESI+): *m/z* calc'd for $C_{22}H_{23}O_2$ $[M+H]^+$: 319.1693, found 319.1687.

Optical Rotation: $[\alpha]_D^{23}$ –9.7 (c = 1.44, $CHCl_3$).

SFC conditions: 25% IPA, 2.5 mL/min, Chiralpak IC-3 column, λ = 210 nm, t_R (min): major = 8.97, minor = 10.37

197h (*d2*):

^{1}H NMR (400 MHz, $CDCl_3$): δ 8.04 (dd, *J* = 7.9, 1.5 Hz, 1H), 7.94 – 7.80 (m, 2H), 7.55 – 7.36 (m, 4H), 7.36 – 7.28 (m, 1H), 7.24 – 7.19 (m, 1H), 3.27 (dd, *J* = 17.1, 10.0 Hz, 1H), 3.04 (t, *J* = 6.2 Hz, 2H), 2.84 (dd, *J* = 17.1, 3.5 Hz, 1H), 2.58 – 2.46 (m, 1H), 2.34 – 2.21 (m, 2H), 2.20 – 2.08 (m, 1H), 1.94 (dt, *J* = 13.5, 5.3 Hz, 1H), 1.84 – 1.62 (m, 4H).

^{13}C NMR (100 MHz, $CDCl_3$): δ 201.7, 200.2, 143.6, 137.4, 133.3, 133.0, 132.6, 128.8, 128.6, 128.2, 127.8, 126.8, 55.7, 44.6, 40.2, 36.0, 35.3, 32.8, 27.0, 22.8.

Note: A grease signal is observed in the ^{1}H and ^{13}C spectra.

IR (Neat Film, NaCl): 2922, 2851, 1681, 1598, 1448, 1279, 1219 cm^{-1}.

HRMS (FD+): *m/z* calc'd for $C_{22}H_{22}O_2$ $[M]^{+\cdot}$: 318.16143, found 318.16025.

Note: The optical rotation measurement for this compound had a standard deviation greater than its magnitude (3.76) and is therefore unreliable.

Optical Rotation: $[\alpha]_D^{23}$ +0.04 (c = 0.16, $CHCl_3$).

SFC conditions: 25% IPA, 2.5 mL/min, Chiralpak IC-3 column, λ = 210 nm, t_R (min): minor = 3.85, major = 4.15

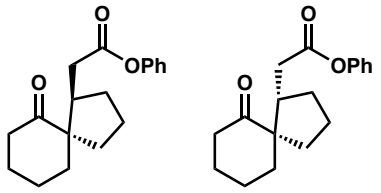

197i (d1) ***197i (d2)***

phenyl 2-((1*R*,5*S*)-6-oxospiro[4.5]decan-1-yl)acetate (197i, *d1* and *d2*)

Prepared from **196i** following General Procedure A. Crude analysis by ^{1}H NMR affords a 3:1 ratio of *d1* to *d2*. The diastereomers were subsequently separated by flash column chromatography (0–60% Et_2O/hexanes) to afford the *d1* as a colorless oil (16.9 mg, 0.059 mmol, 59% yield, 82% ee) and, after subsequent preparative TLC purification (5% Et_2O,

47.5% toluene, 47.5% hexanes) *d2* as a colorless oil (1.9 mg, 0.007 mmol, 7% yield, 71% ee). The absolute configuration of **197i *d1*** is assigned by analogy to **197a**. The relative configuration of **197i *d2*** is assigned by comparison to ^{1}H NMR of **197i *d1***, the absolute configuration is not determined.

197i (*d1*):

^{1}H NMR (400 MHz, $CDCl_3$): δ 7.42 – 7.32 (m, 2H), 7.25 – 7.16 (m, 1H), 7.14 – 7.06 (m, 2H), 3.12 – 3.00 (m, 1H), 2.64 (dd, *J* = 14.6, 5.4 Hz, 1H), 2.49 – 2.28 (m, 3H), 2.09 – 1.85 (m, 3H), 1.83 – 1.54 (m, 8H), 1.49 – 1.35 (m, 1H).

^{13}C NMR (100 MHz, $CDCl_3$): δ 213.5, 171.6, 150.8, 129.4, 125.7, 121.7, 58.1, 40.0, 39.4, 35.3, 35.3, 31.5, 29.9, 26.9, 21.8, 21.7.

IR (Neat Film, NaCl): 2938, 2865, 1757, 1702, 1593, 1492, 1455, 1230, 1195, 1126 cm^{-1}.

HRMS (ESI+): *m/z* calc'd for $C_{18}H_{23}O_3$ $[M+H]^+$: 287.1642, found 287.1629.

Optical Rotation: $[\alpha]_D^{23}$ +5.0 (c = 1.41, $CHCl_3$).

SFC conditions: 20% IPA, 2.5 mL/min, Chiralpak OD-3 column, λ = 210 nm, t_R (min): major = 2.80, minor = 2.99

197i (*d2*):

^{1}H NMR (600 MHz, $CDCl_3$): δ 7.37 (t, *J* = 7.8 Hz, 2H), 7.22 (t, *J* = 7.4 Hz, 1H), 7.10 – 7.03 (m, 2H), 2.80 (dd, *J* = 15.9, 10.6 Hz, 1H), 2.61 – 2.45 (m, 2H), 2.29 (dt, *J* = 14.9, 5.6 Hz, 1H), 2.25 – 2.15 (m, 2H), 2.13 – 2.03 (m, 1H), 1.96 (ddd, *J* = 13.7, 9.8, 3.8 Hz, 1H), 1.92 – 1.80 (m, 2H), 1.79 – 1.64 (m, 5H), 1.63 – 1.58 (m, 1H), 1.53 – 1.47 (m, 1H).

^{13}C NMR (100 MHz, $CDCl_3$): δ 213.9, 172.2, 150.8, 129.4, 125.7, 121.6, 59.3, 44.6, 40.4, 38.2, 36.3, 35.3, 30.3, 26.5, 22.6, 21.5.

IR (Neat Film, NaCl): 2925, 2855, 1756, 1697, 1592, 1492, 1197, 1126 cm^{-1}.

HRMS (FD+): *m/z* calc'd for $C_{18}H_{22}O_3$ $[M]^{+\cdot}$: 286.15635, 286.15495 found.

Optical Rotation: $[\alpha]_D^{23}$ –7.9 (c = 0.16 $CHCl_3$).

SFC conditions: 10% IPA, 2.5 mL/min, Chiralpak OD-3 column, λ = 210 nm, t_R (min): major = 3.99, minor = 4.23

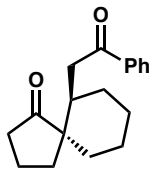

197j

(5*R*,6*R*)-6-(2-oxo-2-phenylethyl)spiro[4.5]decan-1-one (197j)

Prepared from **196j** following General Procedure A. Purification by flash column chromatography (0–60% Et_2O/hexanes) afforded the title compound as a colorless oil (16.9 mg, 0.063 mmol, 63% yield, 71% ee).

^{1}H NMR (400 MHz, $CDCl_3$): δ 7.99 – 7.88 (m, 2H), 7.59 – 7.51 (m, 1H), 7.50 – 7.42 (m, 2H), 2.70 (dd, *J* = 13.6, 2.9 Hz, 1H), 2.57 – 2.32 (m, 3H), 2.23 – 2.11 (m, 1H), 2.06 – 1.83 (m, 4H), 1.72 – 1.51 (m, 4H), 1.43 – 1.18 (m, 3H), 1.13 – 0.99 (m, 1H).

^{13}C NMR (100 MHz, $CDCl_3$): δ 223.9, 199.6, 136.7, 133.2, 128.7, 128.6, 54.0, 42.1, 38.9, 38.1, 33.4, 28.4, 27.7, 25.7, 21.8, 19.1.

IR (Neat Film, NaCl): 2929, 2854, 1728, 1683, 1447, 1291, 1209 cm^{-1}.

HRMS (ESI+): *m/z* calc'd for $C_{18}H_{23}O_2$ $[M+H]^+$: 271.1693, found 271.1681.

Note: The optical rotation measurement for this compound had a standard deviation greater than its magnitude (0.73) and is therefore unreliable.

Optical Rotation: $[\alpha]_D^{23}$ –0.38 (c = 0.97, $CHCl_3$).

SFC conditions: 20% IPA, 2.5 mL/min, Chiralpak IC-3 column, λ = 230 nm, t_R (min): minor = 4.95, major = 8.16

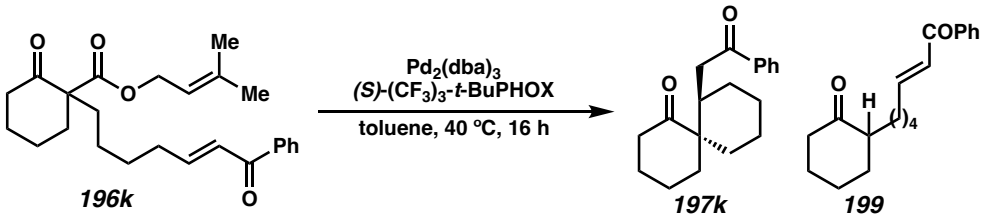

(6*R*,7*R*)-7-(2-oxo-2-phenylethyl)spiro[5.5]undecan-1-one (197k) and (*E*)-2-(7-oxo-7-phenylhept-5-en-1-yl)cyclohexan-1-one (199)

Prepared from **196k** following General Procedure A. Purification by flash column chromatography (0–60% Et_2O/hexanes) afforded the compound **197k** as a colorless oil (13.8 mg, 0.049 mmol, 49% yield, 89% ee) and compound **199** as a colorless oil (5.1 mg, 0.018 mmol, 18% yield).

197k:

^{1}H NMR (400 MHz, $CDCl_3$): δ 8.16 – 8.07 (m, 2H), 7.58 – 7.52 (m, 1H), 7.51 – 7.44 (m, 2H), 3.03 (dd, *J* = 14.1, 2.5 Hz, 1H), 2.69 (tt, *J* = 11.1, 3.2 Hz, 1H), 2.60 – 2.41 (m, 2H), 2.37 – 2.26 (m, 1H), 2.19 – 1.96 (m, 3H), 1.82 – 1.70 (m, 2H), 1.70 – 1.59 (m, 2H), 1.59 – 1.46 (m, 4H), 1.28 – 1.08 (m, 3H).

^{13}C NMR (100 MHz, $CDCl_3$): δ 215.9, 200.7, 137.1, 133.0, 128.7, 128.6, 52.2, 41.8, 38.7, 36.8, 33.1, 27.2, 26.6, 26.4, 25.4, 20.8, 20.3.

IR (Neat Film, NaCl): 2931, 2858, 1697, 1596, 1447, 1287, 1126 cm^{-1}.

HRMS (ESI+): *m/z* calc'd for $C_{19}H_{25}O_2$ $[M+H]^+$: 285.1849, found 285.1841.

Optical Rotation: $[\alpha]_D^{23}$ –2.5 (c = 0.425, $CHCl_3$).

SFC conditions: 20% IPA, 2.5 mL/min, Chiralpak IC-3 column, λ = 210 nm, t_R (min): minor = 7.13, major = 11.24

199:

^{1}H NMR (400 MHz, $CDCl_3$): δ 7.96 – 7.90 (m, 2H), 7.59 – 7.52 (m, 1H), 7.51 – 7.43 (m, 2H), 7.05 (dt, *J* = 15.3, 6.9 Hz, 1H), 6.87 (dt, *J* = 15.4, 1.4 Hz, 1H), 2.44 – 2.21 (m, 5H), 2.15 – 1.97 (m, 2H), 1.92 – 1.75 (m, 2H), 1.73 – 1.62 (m, 2H), 1.57 – 1.48 (m, 2H), 1.41 – 1.29 (m, 3H), 1.27 – 1.16 (m, 1H).

^{13}C NMR (100 MHz, $CDCl_3$): δ 213.5, 191.1, 150.0, 138.1, 132.7, 128.7, 128.7, 126.1, 50.8, 42.2, 34.1, 32.9, 29.3, 28.5, 28.2, 27.0, 25.1.

IR (Neat Film, NaCl): 2931, 2857, 1707, 1669, 1618, 1447, 1338, 1286, 1224, 1128 cm^{-1}.

HRMS (ESI+): *m/z* calc'd for $C_{19}H_{25}O_2$ $[M+H]^+$: 285,1849, found 285.1835.

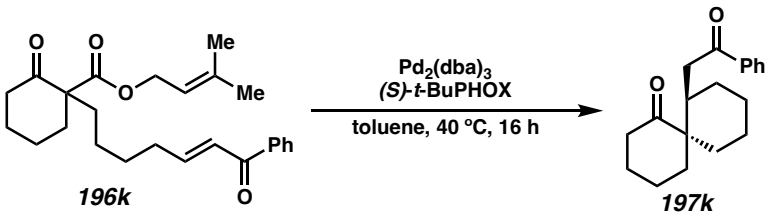

(6*R*,7*R*)-7-(2-oxo-2-phenylethyl)spiro[5.5]undecan-1-one (197k)

In a nitrogen filled glovebox, an oven-dried 4 mL vial was charged with a stir bar, $Pd_2(dba)_3$ (2.3 mg, 0.0025 mmol, 2.5 mol %), *(S)-t*-BuPHOX (2.5 mg, 0.0065 mmol, 6.5 mol %), and toluene (0.6 mL). The catalyst solution was stirred at 23 ºC for 20 min. A solution of

substrate **196k** (0.1 mmol, 1 equiv) in toluene (0.4 mL) was added to the catalyst solution. The resulting mixture was sealed, pumped out of the glovebox, and then heated to 40 ºC for 16 h. The solution was then cooled to 23 ºC and concentrated under reduced pressure. Purification by flash column chromatography (0–60% Et_2O/hexanes) afforded the compound **197k** as a colorless oil (18.3 mg, 0.064 mmol, 64% yield, 86% ee).

Note: see NMR, IR, HRMS, Optical Rotation data in reaction of 196k to 197k and 199 earlier in SI.

SFC conditions: 20% IPA, 2.5 mL/min, Chiralpak IC-3 column, λ = 210 nm, t_R (min): minor = 7.23, major = 11.41

Protonated Byproducts:

General Procedure B: Undesired Pd-Catalyzed Decarboxylative Protonation

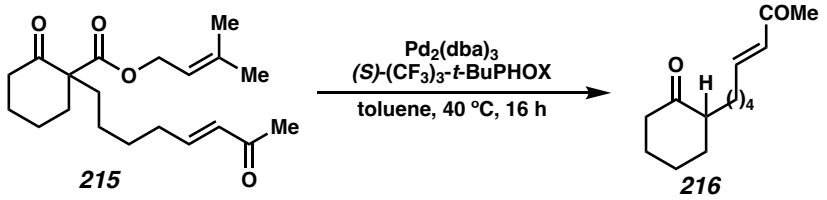

In a nitrogen filled glovebox, an oven-dried 4 mL vial was charged with a stir bar, $Pd_2(dba)_3$ (2.3 mg, 0.0025 mmol, 2.5 mol %), *(S)*-$(CF_3)_3$-*t*-BuPHOX (3.8 mg, 0.0065 mmol, 6.5 mol %), and toluene (0.6 mL). The catalyst solution was stirred at 23 ºC for 20 min. A solution of substrate **215** (0.1 mmol, 1 equiv) in toluene (0.4 mL) was added to the catalyst solution. The resulting mixture was sealed, pumped out of the glovebox, and then heated to 40 ºC for 16 h. The solution was then cooled to 23 ºC and concentrated under reduced pressure. The crude reaction mixture was loaded directly onto a flash column and the product (**216**) was isolated by silica gel flash column chromatography.

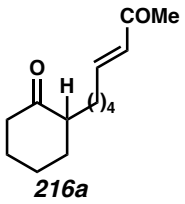

216a

(*E*)-2-(7-oxooct-5-en-1-yl)cyclohexan-1-one (216a)

Prepared from **215a** following General Procedure B. Purification by flash column chromatography (0–60% Et_2O/hexanes) afforded the title compound as a colorless oil (13.8 mg, 0.062 mmol, 62% yield).

^{1}H NMR (400 MHz, $CDCl_3$): δ 6.78 (dt, *J* = 15.9, 6.8 Hz, 1H), 6.05 (dt, *J* = 16.0, 1.5 Hz, 1H), 2.43 – 2.34 (m, 1H), 2.33 – 2.16 (m, 7H), 2.14 – 1.96 (m, 2H), 1.91 – 1.71 (m, 2H), 1.70 – 1.57 (m, 2H), 1.54 – 1.41 (m, 2H), 1.39 – 1.13 (m, 4H).

^{13}C NMR (100 MHz, $CDCl_3$): δ 213.4, 198.9, 148.5, 131.5, 50.8, 42.2, 34.1, 32.5, 29.3, 28.4, 28.2, 27.0, 26.9, 25.1.

IR (Neat Film, NaCl): 2931, 2858, 1707, 1673, 1625, 1430, 1360, 1253, 1127 cm^{-1}.

HRMS (ESI+): *m/z* calc'd for $C_{14}H_{22}O_2$ $[M+H]^+$: 223.1693, found 223.1686.

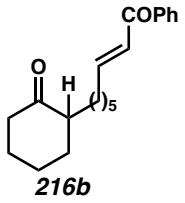

216b

(*E*)-2-(8-oxo-8-phenyloct-6-en-1-yl)cyclohexan-1-one (216b)

Prepared from **215b** following General Procedure B. Purification by flash column chromatography (0–60% Et_2O/hexanes) afforded the title compound as a colorless oil (17.7 mg, 0.059 mmol, 59% yield).

^{1}H NMR (400 MHz, $CDCl_3$): δ 7.97 – 7.88 (m, 2H), 7.59 – 7.51 (m, 1H), 7.49 – 7.42 (m, 2H), 7.05 (dt, *J* = 15.5, 6.9 Hz, 1H), 6.87 (dt, *J* = 15.4, 1.4 Hz, 1H), 2.46 – 2.18 (m, 5H), 2.16 – 1.94 (m, 2H), 1.92 – 1.58 (m, 4H), 1.57 – 1.47 (m, 2H), 1.44 – 1.11 (m, 6H).

Note: 2 carbon signals appear to be coincident.

^{13}C NMR (100 MHz, $CDCl_3$): δ 213.6, 191.1, 150.1, 138.1, 132.7, 128.7, 128.6, 126.1, 50.8, 42.1, 34.1, 32.9, 29.5, 29.5, 28.2, 27.1, 25.0.

IR (Neat Film, NaCl): 2930, 2856, 1708, 1669, 1619, 1447, 1338, 1282, 1222, 1127 cm^{-1}.

HRMS (ESI+): *m/z* calc'd for $C_{20}H_{26}O_2$ $[M+H]^+$: 299.2006, found 299.2002.

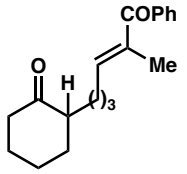

216c

(*E*)-2-(8-oxo-8-phenyloct-6-en-1-yl)cyclohexan-1-one (216c)

Prepared from **215c** following General Procedure B. Purification by flash column chromatography (0–60% Et_2O/hexanes) afforded the title compound as a colorless oil (13.4 mg, 0.047 mmol, 47% yield).

^{1}H NMR (600 MHz, $CDCl_3$): δ 7.62 (d, *J* = 7.6 Hz, 2H), 7.49 (t, *J* = 7.4 Hz, 1H), 7.41 (t, *J* = 7.6 Hz, 2H), 6.28 (t, *J* = 7.4 Hz, 1H), 2.42 – 2.34 (m, 1H), 2.33 – 2.23 (m, 4H), 2.11 –

2.01 (m, 2H), 1.96 (s, 3H), 1.89 – 1.76 (m, 2H), 1.70 – 1.61 (m, 2H), 1.47 – 1.33 (m, 3H), 1.24 – 1.17 (m, 1H).

^{13}C NMR (100 MHz, $CDCl_3$): δ 213.2, 199.2, 146.6, 138.9, 136.7, 131.5, 129.4, 128.2, 50.7, 42.2, 34.2, 29.5, 29.5, 28.2, 26.5, 25.1, 12.6.

IR (Neat Film, NaCl): 2929, 2856, 1707, 1646, 1446, 1284, 1167 cm^{-1}.

HRMS (ESI+): *m/z* calc'd for $C_{19}H_{25}O_2$ $[M+H]^+$: 285.1849, found 285.1841.

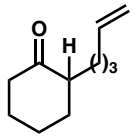

216d

2-(pent-4-en-1-yl)cyclohexan-1-one (216d)

Prepared from **215d** following General Procedure B. Purification by flash column chromatography (0–60% Et_2O/hexanes) afforded the title compound as a colorless oil (5.4 mg, 0.032 mmol, 32% yield).

^{1}H NMR (400 MHz, $CDCl_3$): δ 5.80 (ddt, *J* = 16.9, 10.2, 6.6 Hz, 1H), 5.06 – 4.88 (m, 2H), 2.44 – 2.35 (m, 1H), 2.34 – 2.20 (m, 2H), 2.16 – 1.94 (m, 3H), 1.90 – 1.73 (m, 2H), 1.66 (tddd, *J* = 14.0, 11.6, 7.7, 5.2 Hz, 2H), 1.45 – 1.31 (m, 3H), 1.28 – 1.14 (m, 1H).

Note: 2 carbon signals appear to be coincident.

^{13}C NMR (100 MHz, $CDCl_3$): δ 213.6, 138.9, 114.6, 50.8, 42.2, 34.0, 29.1, 28.2, 26.7, 25.0.

IR (Neat Film, NaCl): 2931, 2859, 1710, 1639, 1447, 1125 cm^{-1}.

HRMS (FI+): *m/z* calc'd for $C_{11}H_{18}O$ $[M]^{+\cdot}$: 166.13522, found 166.13526.

Pd-Catalyzed Decarboxylative Alkene Difunctionalization:

General Procedure C: Asymmetric Pd-Catalyzed Decarboxylative Alkene Difunctionalization

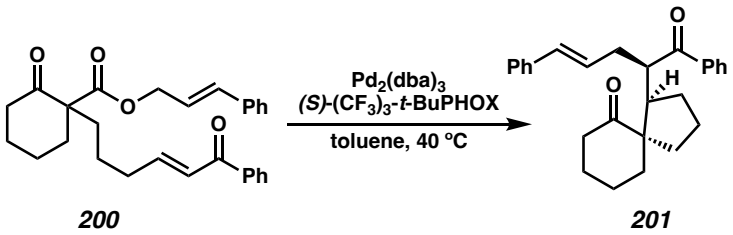

200 ***201***

In a nitrogen filled glovebox, an oven-dried 4 mL vial was charged with a stir bar, $Pd_2(dba)_3$ (2.3 mg, 0.0025 mmol, 2.5 mol %), *(S)*-$(CF_3)_3$-*t*-BuPHOX (3.8 mg, 0.0065 mmol, 6.5 mol %), and toluene (0.6 mL). The catalyst solution was stirred at 23 ºC for 20 min. A solution of substrate **200** (0.1 mmol, 1 equiv) in toluene (0.4 mL) was added to the catalyst solution. The resulting mixture was sealed, pumped out of the glovebox, and then heated to 40 ºC for 16 h. The solution was then cooled to 23 ºC and concentrated under reduced pressure. The crude reaction mixture was purified via preparative TLC to yield product **201**.

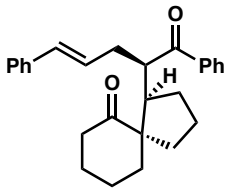

201a

(1*R*,5*S*)-1-((*R*,*E*)-1-oxo-1,5-diphenylpent-4-en-2-yl)spiro[4.5]decan-6-one (201a)

Prepared from **200a** following General Procedure C. Purification by preparative TLC (10% Et_2O, 45% toluene, 4% hexanes) afforded the title compound as a white crystalline solid (16.9 mg, 0.044 mmol, 44% yield, 94% ee). Absolute and relative stereochemistry were assigned by X-ray crystallography (vide infra).

^{1}H NMR (600 MHz, $CDCl_3$): δ 7.93 (dd, *J* = 7.6, 1.6 Hz, 2H), 7.55 – 7.50 (m, 1H), 7.44 (t, *J* = 7.7 Hz, 2H), 7.24 – 7.10 (m, 5H), 6.31 (d, *J* = 15.7 Hz, 1H), 6.02 (dt, *J* = 15.2, 7.3 Hz, 1H), 3.55 (ddd, *J* = 9.2, 7.5, 3.6 Hz, 1H), 3.14 (dt, *J* = 10.4, 7.5 Hz, 1H), 2.76 (dddd, *J* = 14.3, 9.1, 7.1, 1.4 Hz, 1H), 2.53 – 2.44 (m, 1H), 2.40 – 2.24 (m, 2H), 2.07 – 1.95 (m, 1H), 1.87 – 1.79 (m, 1H), 1.79 – 1.72 (m, 3H), 1.72 – 1.47 (m, 6H), 1.37 – 1.27 (m, 1H).

^{13}C NMR (100 MHz, $CDCl_3$): δ 213.2, 203.6, 138.0, 137.5, 132.8, 131.9, 128.7, 128.7, 128.5, 127.6, 127.2, 126.2, 58.3, 47.4, 44.2, 39.4, 38.5, 34.6, 33.0, 28.7, 25.4, 22.7, 21.6.

IR (Neat Film, NaCl): 2932, 2858, 1697, 1681, 1596, 1493, 1446, 1221 cm^{-1}.

HRMS (ESI+): *m/z* calc'd for $C_{27}H_{31}O_2$ $[M+H]^+$: 387.2319, found 387.2319.

Optical Rotation: $[\alpha]_D^{23}$ –10.7 (c = 0.53, $CHCl_3$).

SFC conditions: 30% IPA, 2.5 mL/min, Chiralpak AD-3 column, λ = 254 nm, t_R (min): major = 5.07, minor = 6.14

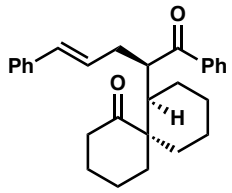

201b

(6*R*,7*R*)-7-((*R*,*E*)-1-oxo-1,5-diphenylpent-4-en-2-yl)spiro[5.5]undecan-1-one (201b)

Prepared from **200b** following General Procedure C. Purification by preparative TLC (5% Et_2O, 47.5% toluene, 47.5% hexanes) afforded the title compound as a colorless oil (13.3 mg, 0.033 mmol, 33% yield, 94% ee).

^{1}H NMR (400 MHz, $CDCl_3$): δ 7.96 – 7.89 (m, 2H), 7.56 – 7.48 (m, 1H), 7.46 – 7.39 (m, 2H), 7.23 – 7.16 (m, 2H), 7.15 – 7.05 (m, 3H), 6.30 (dd, *J* = 15.8, 1.6 Hz, 1H), 5.93 (dt, *J*

= 15.7, 7.2 Hz, 1H), 3.48 (ddd, *J* = 10.9, 3.4, 2.3 Hz, 1H), 2.70 (dddd, *J* = 14.1, 10.9, 7.1, 1.4 Hz, 1H), 2.56 – 2.39 (m, 3H), 2.34 – 2.16 (m, 2H), 2.11 – 1.90 (m, 3H), 1.82 – 1.62 (m, 5H), 1.55 – 1.36 (m, 3H), 1.31 – 1.20 (m, 1H), 1.13 (td, *J* = 12.6, 4.9 Hz, 1H).

^{13}C NMR (100 MHz, $CDCl_3$): δ 215.2, 205.1, 138.1, 137.5, 132.7, 131.4, 128.9, 128.6, 128.5, 128.4, 127.1, 126.1, 54.1, 47.3, 40.7, 38.5, 33.8, 33.5, 28.5, 26.1, 26.0, 22.8, 21.1, 20.3.

IR (Neat Film, NaCl): 2929, 2855, 1698, 1673, 1596, 1446, 1222 cm^{-1}.

HRMS (ESI+): *m/z* calc'd for $C_{28}H_{33}O_2$ $[M+H]^+$: 401.2475, found 401.2471.

Optical Rotation: $[\alpha]_D^{23}$ –18.2 (c = 0.23, $CHCl_3$).

SFC conditions: 30% IPA, 2.5 mL/min, Chiralpak AD-3 column, λ = 254 nm, t_R (min): minor = 5.29, minor = 6.18

Preparation of Enone Starting Materials:

General Procedure D: Horner–Wadsworth–Emmons Olefination

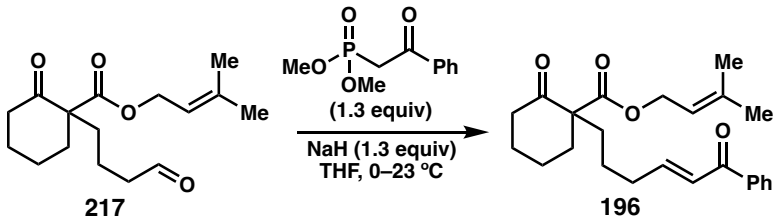

To a suspension of NaH (60% by weight in mineral oil, 1.3 equiv) in THF (0.65 M) at 23 ºC was added dropwise a solution of the corresponding phosphonate ester (1.3 equiv) in THF (1.3 M). *Note: Caution, hydrogen evolution occurs.* This is stirred at 23 ºC for 30 minutes before cooling to 0 ºC. To this reaction was then added a solution of aldehyde **217** (1.0 equiv) in THF (0.35 M) dropwise. The reaction is gradually warmed to 23 ºC. Upon complete consumption of starting material by TLC, the reaction mixture was cooled to 0

ºC, diluted with a saturated solution of $NaHCO_3$, and extracted with EtOAc (3x). The combined organic layers were dried over Na_2SO_4, filtered, and concentrated under reduced pressure. Product **196** was purified by silica gel flash column chromatography.

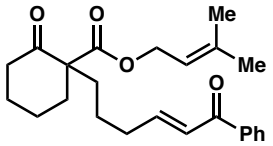

196a

3-methylbut-2-en-1-yl (*E*)-2-oxo-1-(6-oxo-6-phenylhex-4-en-1-yl)cyclohexane-1-carboxylate (196a)

Prepared from **217a** and dimethyl (2-oxo-2-phenylethyl)phosphonate[23] following General Procedure D. Purification by flash column chromatography (0–50% EtOAc/hexanes) afforded the title compound as a colorless oil (1.41 g, 3.68 mmol, 64% yield).

^{1}H NMR (400 MHz, $CDCl_3$): δ 7.96 – 7.89 (m, 2H), 7.58 – 7.51 (m, 1H), 7.50 – 7.42 (m, 2H), 7.01 (dt, *J* = 15.5, 6.7 Hz, 1H), 6.88 (d, *J* = 15.4 Hz, 1H), 5.31 (tt, *J* = 7.3, 1.4 Hz, 1H), 4.70 – 4.55 (m, 2H), 2.57 – 2.37 (m, 3H), 2.37 – 2.22 (m, 2H), 2.01 (ddq, *J* = 12.4, 6.3, 3.2 Hz, 1H), 1.91 (td, *J* = 12.2, 3.1 Hz, 1H), 1.71 (dd, *J* = 12.7, 1.3 Hz, 7H), 1.67 – 1.48 (m, 4H), 1.48 – 1.32 (m, 2H).

^{13}C NMR (100 MHz, $CDCl_3$): δ 208.1, 191.0, 172.1, 149.2, 140.1, 138.1, 132.7, 128.7, 128.6, 126.3, 118.1, 62.2, 60.9, 41.3, 36.6, 34.6, 33.2, 27.8, 25.8, 23.1, 22.8, 18.2.

IR (Neat Film, NaCl): 2937, 2864, 1712, 1670, 1620, 1447, 1340, 1289, 1208, 1173, 1135 cm^{-1}.

HRMS (ESI+): *m/z* calc'd for $C_{24}H_{30}O_4Na$ $[M+Na]^+$: 405.2036, found 405.2045

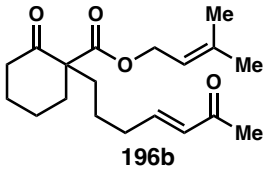

196b

3-methylbut-2-en-1-yl (*E*)-2-oxo-1-(6-oxohept-4-en-1-yl)cyclohexane-1-carboxylate (196b)

Prepared from **217a** and dimethyl acetylmethylphosphonate following General Procedure D. Purification by flash column chromatography (0–50% EtOAc/hexanes) afforded the title compound as a colorless oil (406 mg, 1.27 mmol, 71% yield).

^{1}H NMR (400 MHz, $CDCl_3$): δ 6.76 (dt, *J* = 16.0, 6.8 Hz, 1H), 6.06 (dt, *J* = 16.0, 1.6 Hz, 1H), 5.37 – 5.27 (m, 1H), 4.69 – 4.57 (m, 2H), 2.55 – 2.37 (m, 3H), 2.27 – 2.17 (m, 4H), 2.06 – 1.95 (m, 1H), 1.86 (td, *J* = 12.6, 3.6 Hz, 1H), 1.79 – 1.72 (m, 4H), 1.70 (s, 3H), 1.69 – 1.27 (m, 7H).

^{13}C NMR (100 MHz, $CDCl_3$): δ 208.1, 198.8, 172.1, 147.8, 140.2, 131.7, 118.1, 62.2, 60.9, 41.3, 36.6, 34.5, 32.8, 27.8, 27.0, 25.9, 23.1, 22.8, 18.2.

IR (Neat Film, NaCl): 2937, 2865, 1708, 1675, 1625, 1438, 1362, 1253, 1207, 1173, 1135 cm^{-1}.

HRMS (ESI+): *m/z* calc'd for $C_{19}H_{28}O_4Na$ $[M+Na]^+$: 343.1880, found 343.1884.

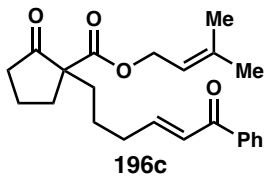

196c

3-methylbut-2-en-1-yl (*E*)-2-oxo-1-(6-oxo-6-phenylhex-4-en-1-yl)cyclopentane-1-carboxylate (196c)

Prepared from **217b** and dimethyl (2-oxo-2-phenylethyl)phosphonate[23] following General Procedure D. Purification by flash column chromatography (0–50% EtOAc/hexanes) afforded the title compound as a colorless oil (631 mg, 2.37 mmol, 47% yield).

^{1}H NMR (400 MHz, $CDCl_3$): δ 8.00 – 7.84 (m, 2H), 7.60 – 7.51 (m, 1H), 7.51 – 7.41 (m, 2H), 7.01 (dt, *J* = 15.4, 6.7 Hz, 1H), 6.88 (dt, *J* = 15.4, 1.4 Hz, 1H), 5.33 – 5.23 (m, 1H), 4.60 (d, *J* = 7.1 Hz, 2H), 2.58 – 2.49 (m, 1H), 2.48 – 2.37 (m, 1H), 2.37 – 2.17 (m, 3H), 2.09 – 1.83 (m, 4H), 1.73 (s, 3H), 1.70 – 1.57 (m, 5H), 1.52 – 1.38 (m, 1H).

^{13}C NMR (100 MHz, $CDCl_3$): δ 214.9, 190.9, 171.1, 148.9, 139.7, 138.0, 132.8, 128.7, 128.7, 126.4, 118.3, 62.5, 60.5, 38.1, 33.6, 33.2, 33.1, 25.9, 23.6, 19.8, 18.2.

IR (Neat Film, NaCl): 2961, 1749, 1718, 1670, 1618, 1447, 1379, 1284, 1224, 1159 cm^{-1}.

HRMS (ESI+): *m/z* calc'd for $C_{23}H_{28}O_4Na$ $[M+Na]^+$: 391.1880, found 391.1879.

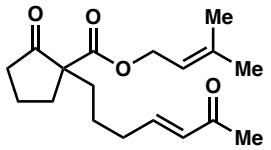

196d

3-methylbut-2-en-1-yl (*E*)-2-oxo-1-(6-oxohept-4-en-1-yl)cyclopentane-1-carboxylate (196d)

Prepared from **217b** and dimethyl acetylmethylphosphonate following General Procedure D. Purification by flash column chromatography (0–50% EtOAc/hexanes) afforded the title compound as a colorless oil (120 mg, 0.390 mmol, 52% yield).

^{1}H NMR (400 MHz, $CDCl_3$): δ 6.75 (dt, *J* = 15.9, 6.8 Hz, 1H), 6.06 (dt, *J* = 16.1, 1.6 Hz, 1H), 5.34 – 5.24 (m, 1H), 4.59 (d, *J* = 7.1 Hz, 2H), 2.57 – 2.36 (m, 2H), 2.30 – 2.15 (m, 6H), 2.08 – 1.81 (m, 4H), 1.74 (s, 3H), 1.69 (s, 3H), 1.64 – 1.57 (m, 1H), 1.56 – 1.48 (m, 1H), 1.39 (qdd, *J* = 11.9, 8.2, 4.5 Hz, 1H).

^{13}C NMR (100 MHz, $CDCl_3$): δ 214.9, 198.7, 171.1, 147.4, 139.7, 131.8, 118.2, 62.5, 60.4, 38.1, 33.5, 33.2, 32.7, 27.1, 25.9, 23.6, 19.8, 18.2.

IR (Neat Film, NaCl): 2962, 1750, 1718, 1675, 1626, 1448, 1362, 1253, 1225, 1161 cm^{-1}.

HRMS (ESI+): *m/z* calc'd for $C_{18}H_{26}O_4Na$ $[M+Na]^+$: 329.1723, found 329.1722.

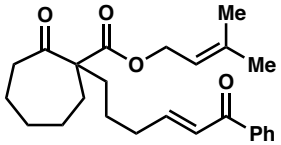

196e

3-methylbut-2-en-1-yl (*E*)-2-oxo-1-(6-oxo-6-phenylhex-4-en-1-yl)cycloheptane-1-carboxylate (196e)

Prepared from **217c** and dimethyl (2-oxo-2-phenylethyl)phosphonate[23] following General Procedure D. Purification by flash column chromatography (0–50% EtOAc/hexanes) afforded the title compound as a colorless oil (494 mg, 1.24 mmol, 73% yield).

^{1}H NMR (400 MHz, $CDCl_3$): δ 7.97 – 7.87 (m, 2H), 7.59 – 7.52 (m, 1H), 7.51 – 7.42 (m, 2H), 7.01 (dt, *J* = 15.5, 6.7 Hz, 1H), 6.88 (dt, *J* = 15.4, 1.3 Hz, 1H), 5.38 – 5.23 (m, 1H), 4.71 – 4.54 (m, 2H), 2.71 – 2.59 (m, 1H), 2.50 – 2.41 (m, 1H), 2.38 – 2.23 (m, 2H), 2.21 – 2.10 (m, 1H), 2.08 – 1.96 (m, 1H), 1.80 – 1.71 (m, 5H), 1.71 – 1.58 (m, 7H), 1.56 – 1.37 (m, 4H).

^{13}C NMR (100 MHz, $CDCl_3$): δ 209.6, 191.0, 172.6, 149.2, 139.9, 138.1, 132.8, 128.7, 128.7, 126.4, 118.2, 62.9, 62.1, 42.3, 35.3, 33.2, 33.2, 29.9, 25.8, 25.6, 25.0, 23.5, 18.2.

IR (Neat Film, NaCl): 2932, 2860, 1707, 1670, 1619, 1447, 1377, 1344, 1286, 1222, 1165 cm^{-1}.

HRMS (ESI+): *m/z* calc'd for $C_{25}H_{32}O_4Na$ $[M+Na]^+$: 419.2193, found 419.2194.

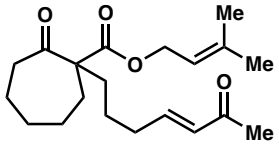

196f

3-methylbut-2-en-1-yl (*E*)-2-oxo-1-(6-oxohept-4-en-1-yl)cycloheptane-1-carboxylate (196f)

Prepared from **217c** and dimethyl acetylmethylphosphonate following General Procedure D. Purification by flash column chromatography (0–50% EtOAc/hexanes) afforded the title compound as a colorless oil (409 mg, 1.22 mmol, 72% yield).

^{1}H NMR (400 MHz, $CDCl_3$): δ 6.76 (dt, *J* = 16.0, 6.8 Hz, 1H), 6.06 (dt, *J* = 16.0, 1.5 Hz, 1H), 5.38 – 5.24 (m, 1H), 4.69 – 4.53 (m, 2H), 2.74 – 2.54 (m, 1H), 2.52 – 2.38 (m, 1H), 2.30 – 2.06 (m, 6H), 2.05 – 1.90 (m, 1H), 1.83 – 1.72 (m, 4H), 1.70 (d, *J* = 1.4 Hz, 4H), 1.66 – 1.49 (m, 5H), 1.49 – 1.31 (m, 3H).

^{13}C NMR (100 MHz, $CDCl_3$): δ 209.6, 198.8, 172.5, 147.7, 139.9, 131.7, 118.2, 62.8, 62.1, 42.3, 35.2, 33.2, 32.9, 29.9, 27.0, 25.8, 25.6, 25.0, 23.5, 18.2.

IR (Neat Film, NaCl): 2930, 2862, 1707, 1675, 1626, 1445, 1359, 1253, 1219, 1166 cm^{-1}.

HRMS (ESI+): *m/z* calc'd for $C_{20}H_{30}O_4Na$ $[M+Na]^+$: 357.2036, found 357.2041.

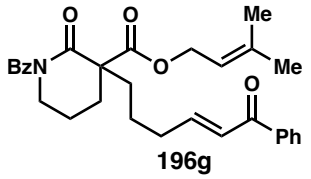

196g

3-methylbut-2-en-1-yl (*E*)-1-benzoyl-2-oxo-3-(6-oxo-6-phenylhex-4-en-1-yl)piperidine-3-carboxylate (196g)

Prepared from **217d** and dimethyl (2-oxo-2-phenylethyl)phosphonate[23] following General Procedure D. Purification by flash column chromatography (0–50% EtOAc/hexanes) afforded the title compound as a colorless oil (317 mg, 0.650 mmol, 61% yield).

^{1}H NMR (400 MHz, $CDCl_3$): δ 7.96 – 7.84 (m, 2H), 7.78 – 7.70 (m, 2H), 7.59 – 7.51 (m, 1H), 7.50 – 7.40 (m, 3H), 7.40 – 7.33 (m, 2H), 6.97 (dt, *J* = 15.5, 6.6 Hz, 1H), 6.85 (dt, *J* = 15.4, 1.4 Hz, 1H), 5.49 – 5.35 (m, 1H), 4.81 – 4.64 (m, 2H), 3.90 – 3.70 (m, 2H), 2.51 – 2.39 (m, 1H), 2.28 (q, *J* = 7.2 Hz, 2H), 2.04 – 1.82 (m, 5H), 1.79 (s, 3H), 1.75 (s, 3H), 1.70 – 1.60 (m, 1H), 1.51 – 1.37 (m, 1H).

^{13}C NMR (100 MHz, $CDCl_3$): δ 190.9, 175.1, 172.3, 172.2, 148.8, 140.7, 138.0, 136.0, 132.8, 131.8, 128.7, 128.6, 128.3, 128.2, 126.4, 117.8, 63.0, 56.7, 46.6, 35.4, 33.0, 30.9, 26.0, 23.5, 20.5, 18.3.

IR (Neat Film, NaCl): 2937, 1724, 1701, 1676, 1618, 1447, 1386, 1348, 1277, 1189, 1166, 1149 cm^{-1}.

HRMS (ESI+): *m/z* calc'd for $C_{30}H_{33}NO_5Na$ $[M+Na]^+$: 510.2251, found 510.2264.

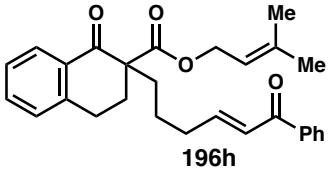

196h

3-methylbut-2-en-1-yl (*E*)-1-oxo-2-(6-oxo-6-phenylhex-4-en-1-yl)-1,2,3,4-tetrahydronaphthalene-2-carboxylate (196h)

Prepared from **217e** and dimethyl (2-oxo-2-phenylethyl)phosphonate[23] following General Procedure D. Purification by flash column chromatography (0–50% EtOAc/hexanes) afforded the title compound as a colorless oil (248 mg, 0.576 mmol, 58% yield).

^{1}H NMR (400 MHz, $CDCl_3$): δ 8.04 (dd, *J* = 7.9, 1.4 Hz, 1H), 7.97 – 7.88 (m, 2H), 7.59 – 7.51 (m, 1H), 7.50 – 7.42 (m, 3H), 7.31 (t, *J* = 7.6 Hz, 1H), 7.20 (d, *J* = 7.7 Hz, 1H), 7.04 (dt, *J* = 15.5, 6.6 Hz, 1H), 6.91 (dt, *J* = 15.3, 1.4 Hz, 1H), 5.26 – 5.14 (m, 1H), 4.63 – 4.49 (m, 2H), 3.07 (ddd, *J* = 15.5, 10.4, 4.7 Hz, 1H), 2.91 (dt, *J* = 17.4, 4.9 Hz, 1H), 2.56 (dt, *J* = 13.7, 4.9 Hz, 1H), 2.36 (q, *J* = 7.5 Hz, 2H), 2.22 – 2.09 (m, 1H), 2.07 – 1.88 (m, 2H), 1.80 – 1.64 (m, 4H), 1.63 – 1.56 (m, 4H).

^{13}C NMR (100 MHz, $CDCl_3$): δ 195.6, 191.0, 172.0, 149.1, 143.1, 139.9, 138.1, 133.5, 132.8, 132.3, 128.8, 128.7, 128.7, 128.2, 126.9, 126.4, 118.2, 62.3, 57.6, 33.9, 33.3, 31.1, 26.1, 25.8, 23.5, 18.1.

IR (Neat Film, NaCl): 2931, 1725, 1685, 1670, 1618, 1599, 1447, 1351,1292,1230, 1174 cm^{-1}.

HRMS (ESI+): *m/z* calc'd for $C_{28}H_{30}O_4Na$ $[M+Na]^+$: 453.2036, found 453.2035.

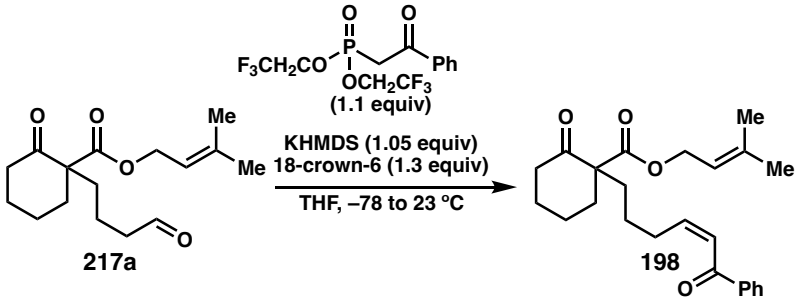

3-methylbut-2-en-1-yl (*Z*)-2-oxo-1-(6-oxo-6-phenylhex-4-en-1-yl)cyclohexane-1-carboxylate (198)

An oven dried 100 mL round bottom flask was charged with 18-crown-6 (610 mg, 2.31 mmol, 1.3 equiv). To this a solution of bis(2,2,2-trifluoroethyl) (2-oxo-2-phenylethyl)phosphonate[24] (714 mg, 1.96 mmol, 1.1 equiv) in THF (10 mL, 0.2 M) was added. This was cooled to –78 ºC for 10 minutes before a solution of KHMDS (373 mg, 1.87 mmol, 1.05 equiv) in THF (2 mL, 0.9 M) was added dropwise. The solution was stirred for 20 minutes at –78 ºC before a solution of **217a** (500 mg, 1.78 mmol, 1.0 equiv) in THF (10 mL, 0.18 M) was added dropwise. The reaction was warmed gradually to 23 ºC. Upon complete consumption of starting material by TLC, the reaction mixture was cooled to 0 ºC, diluted with a saturated solution of NH_4Cl (20 mL), and extracted with Et_2O (3x). The combined organic layers were dried over Na_2SO_4, filtered, and concentrated under reduced pressure. The crude reaction mixture was purified by silica gel flash column chromatography (15% Et_2O/hexanes) to afford **198** as a colorless oil (101 mg, 0.264 mmol, 15% yield).

^{1}H NMR (400 MHz, $CDCl_3$): δ 7.91 – 7.84 (m, 2H), 7.13 – 7.02 (m, 3H), 6.53 (dt, *J* = 11.5, 1.7 Hz, 1H), 6.05 (dt, *J* = 11.6, 7.4 Hz, 1H), 5.31 (tdt, *J* = 7.2, 2.9, 1.4 Hz, 1H), 4.55

(d, *J* = 7.2 Hz, 2H), 2.82 – 2.65 (m, 2H), 2.48 – 2.26 (m, 3H), 2.14 – 2.01 (m, 1H), 1.75 – 1.46 (m, 8H), 1.44 (s, 3H), 1.37 – 1.06 (m, 3H).

^{13}C NMR (100 MHz, C_6D_6): δ 206.2, 191.0, 172.1, 148.7, 139.4, 139.2, 132.4, 128.6, 128.6, 124.8, 119.0, 61.8, 61.1, 41.2, 36.4, 34.9, 30.5, 27.7, 25.6, 24.6, 22.9, 17.9.

*Note: It was noted that upon standing in basified (K_2CO_3) or neutral deuterochloroform, Z-enone **198** isomerizes to **196a**.*

IR (Neat Film, NaCl): 2938, 2865, 1711, 1664, 1610, 1448, 1227, 1174, 1134 cm^{-1}.

HRMS (ESI+): *m/z* calc'd for $C_{24}H_{34}NO_4$ $[M+NH_4]^+$: 400.2482, found 400.2490.

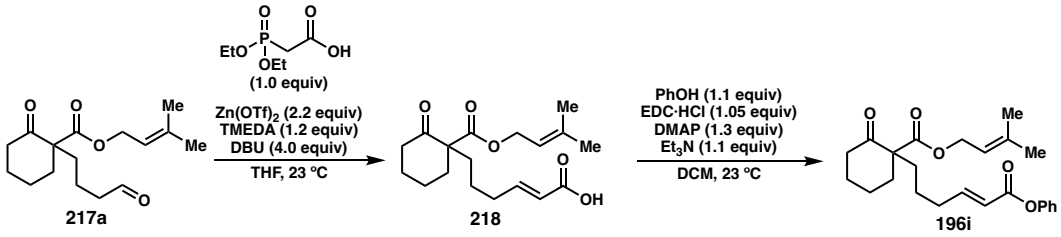

(*E*)-6-(1-(((3-methylbut-2-en-1-yl)oxy)carbonyl)-2-oxocyclohexyl)hex-2-enoic acid (218)

To a flame dried 50 mL round bottom flask was added zinc triflate (2.09 g, 5.74 mmol, 2.2 equiv) followed by THF (9.5 mL, 0.6 M). 2-(diethoxyphosphoryl)acetic acid was then added (0.42 mL, 2.61 mmol, 1.0 equiv) followed by TMEDA (0.47 mL, 3.13 mmol, 1.2 equiv) and DBU (1.56 mL, 10.4 mmol, 4.0 equiv). To this a solution of **217a** (805 mg, 2.87 mmol, 1.1 equiv) in THF (6.6 mL, 0.43 M) was added dropwise. Upon complete consumption of starting material by TLC, the reaction was diluted with 1 M HCl (27 mL), extracted with CH_2Cl_2 (3x). The combined organic layers were dried over Na_2SO_4, filtered, and concentrated under reduced pressure. The crude reaction mixture was purified by silica

gel flash column chromatography (0–50% EtOAc/hexanes) to afford **218** as an amorphous white solid (610 mg, 1.89 mmol, 72% yield).

^{1}H NMR (400 MHz, $CDCl_3$): δ 7.06 (dt, *J* = 15.6, 6.8 Hz, 1H), 5.84 (dt, *J* = 15.7, 1.6 Hz, 1H), 5.38 – 5.30 (m, 1H), 4.66 (d, *J* = 7.3 Hz, 2H), 2.59 – 2.40 (m, 3H), 2.33 – 2.18 (m, 2H), 2.08 – 1.97 (m, 1H), 1.90 (td, *J* = 12.5, 3.5 Hz, 1H), 1.83 – 1.72 (m, 7H), 1.72 – 1.23 (m, 6H).

*Note: OH proton not observed for **218** in ^{1}H NMR.*

^{13}C NMR (100 MHz, $CDCl_3$): δ 208.1, 172.1, 171.2, 151.6, 140.2, 120.9, 118.1, 62.2, 60.9, 41.3, 36.6, 34.5, 32.6, 27.8, 25.8, 22.9, 22.8, 18.2.

IR (Neat Film, NaCl): 2937, 2865, 1711, 1653, 1437, 1275, 1208, 1168 cm^{-1}.

HRMS (ESI+): *m/z* calc'd for $C_{18}H_{25}O_5$ $[M–H]^-$: 321.1707, found 321.1710.

3-methylbut-2-en-1-yl (*E*)-2-oxo-1-(6-oxo-6-phenoxyhex-4-en-1-yl)cyclohexane-1-carboxylate (196i)

To a flame dried scint vial was added **218** (220 mg, 0.68 mmol, 1.0 equiv), phenol (70.6 mg, 0.75 mmol, 1.1 equiv), EDC·HCl (144 mg, 0.75 mmol, 1.1 equiv), followed by CH_2Cl_2 (3.4 mL, 0.2 M). Following this, Et_3N (0.10 mL, 0.75 mmol, 1.1 equiv) and DMAP (8.3 mg, 0.068 mmol, 0.1 equiv) were added successively. Upon complete consumption of starting material by TLC, the reaction was diluted with CH_2Cl_2, followed by a 1 M HCl (4 mL) rinse, and sat. $NaHCO_3$ solution (4 mL) rinse, and then rinsed with brine. The combined organic layers were dried over Na_2SO_4, filtered, and concentrated under reduced pressure. The crude reaction mixture was purified by silica gel flash column

chromatography (0–35% Et_2O/hexanes) to afford **196i** as an amorphous white solid (144 mg, 0.36 mmol, 53% yield).

^{1}H NMR (400 MHz, $CDCl_3$): δ 7.42 – 7.34 (m, 2H), 7.25 – 7.19 (m, 1H), 7.17 – 7.07 (m, 3H), 6.02 (dt, *J* = 15.7, 1.6 Hz, 1H), 5.37 – 5.29 (m, 1H), 4.65 (d, *J* = 6.7 Hz, 2H), 2.58 – 2.38 (m, 3H), 2.34 – 2.20 (m, 2H), 2.07 – 1.97 (m, 1H), 1.91 (td, *J* = 12.5, 3.4 Hz, 1H), 1.80 – 1.71 (m, 7H), 1.70 – 1.57 (m, 3H), 1.55 – 1.32 (m, 3H).

^{13}C NMR (100 MHz, $CDCl_3$): δ 208.1, 172.1, 165.1, 151.1, 150.9, 140.2, 129.5, 125.8, 121.8, 121.0, 118.1, 62.2, 60.9, 41.3, 36.6, 34.5, 32.8, 27.8, 25.8, 23.0, 22.8, 18.2.

IR (Neat Film, NaCl): 2938, 2864, 1734, 1711, 1651, 1593, 1491, 1450, 1310, 1243, 1197 cm^{-1}.

HRMS (ESI+): *m/z* calc'd for $C_{24}H_{34}NO_5$ $[M+NH_4]^+$: 416.2431, found 416.2433.

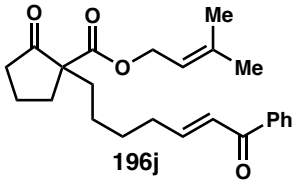

196j

3-methylbut-2-en-1-yl (*E*)-2-oxo-1-(7-oxo-7-phenylhept-5-en-1-yl)cyclopentane-1-carboxylate (196j)

Prepared from **217f** and dimethyl (2-oxo-2-phenylethyl)phosphonate[23] following General Procedure D. Purification by flash column chromatography (0–50% EtOAc/hexanes) afforded the title compound as a colorless oil (392 mg, 1.03 mmol, 58% yield).

^{1}H NMR (400 MHz, $CDCl_3$): δ 7.96 – 7.88 (m, 2H), 7.59 – 7.53 (m, 1H), 7.51 – 7.41 (m, 2H), 7.03 (dt, *J* = 15.4, 6.8 Hz, 1H), 6.87 (dt, *J* = 15.4, 1.4 Hz, 1H), 5.34 – 5.22 (m, 1H), 4.58 (dt, *J* = 7.2, 1.0 Hz, 2H), 2.57 – 2.48 (m, 1H), 2.47 – 2.37 (m, 1H), 2.36 – 2.16 (m,

3H), 2.07 – 1.82 (m, 4H), 1.73 (s, 3H), 1.68 (s, 3H), 1.64 – 1.47 (m, 3H), 1.46 – 1.34 (m, 1H), 1.33 – 1.20 (m, 1H).

^{13}C NMR (100 MHz, $CDCl_3$): δ 215.1, 191.0, 171.2, 149.5, 139.5, 138.1, 132.8, 128.7, 128.7, 126.2, 118.3, 62.5, 60.6, 38.1, 33.7, 33.0, 32.6, 28.6, 25.9, 24.6, 19.8, 18.2.

IR (Neat Film, NaCl): 2930, 2859, 1750, 1719, 1670, 1618, 1597, 1447, 1335, 1278, 1223, 1166 cm^{-1}.

HRMS (ESI+): *m/z* calc'd for $C_{24}H_{30}O_4Na$ $[M+Na]^+$: 405.2036, found 405.2043.

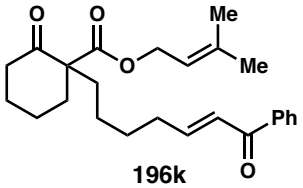

196k

3-methylbut-2-en-1-yl (*E*)-2-oxo-1-(7-oxo-7-phenylhept-5-en-1-yl)cyclohexane-1-carboxylate (196k)

Prepared from **217g** and dimethyl (2-oxo-2-phenylethyl)phosphonate[23] following General Procedure D. Purification by flash column chromatography (0–50% EtOAc/hexanes) afforded the title compound as a colorless oil (273 mg, 0.69 mmol, 69% yield).

^{1}H NMR (400 MHz, $CDCl_3$): δ 7.95 – 7.89 (m, 2H), 7.59 – 7.52 (m, 1H), 7.50 – 7.43 (m, 2H), 7.03 (dt, *J* = 15.4, 6.8 Hz, 1H), 6.87 (dt, *J* = 15.4, 1.4 Hz, 1H), 5.34 – 5.26 (m, 1H), 4.67 – 4.55 (m, 2H), 2.56 – 2.37 (m, 3H), 2.36 – 2.23 (m, 2H), 2.07 – 1.95 (m, 1H), 1.94 – 1.80 (m, 1H), 1.77 – 1.68 (m, 7H), 1.67 – 1.59 (m, 2H), 1.57 – 1.47 (m, 3H), 1.46 – 1.37 (m, 1H), 1.36 – 1.21 (m, 2H).

^{13}C NMR (100 MHz, $CDCl_3$): δ 208.2, 191.1, 172.2, 149.7, 140.0, 138.1, 132.7, 128.69, 128.65, 126.2, 118.2, 62.1, 61.0, 41.3, 36.4, 34.7, 32.7, 28.7, 27.8, 25.8, 24.1, 22.8, 18.2.

IR (Neat Film, NaCl): 2929, 2854, 1728, 1683, 1596, 1447, 1291, 1209, 1185, 1160 cm^{-1}.

HRMS (ESI+): *m/z* calc'd for $C_{25}H_{32}O_4Na$ $[M+Na]^+$: 419.2193, found 419.2201.

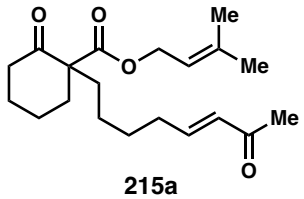

215a

3-methylbut-2-en-1-yl (*E*)-2-oxo-1-(7-oxooct-5-en-1-yl)cyclohexane-1-carboxylate (215a)

Prepared from **217g** and acetylmethylphosphonate following General Procedure D. Purification by flash column chromatography (0–50% EtOAc/hexanes) afforded the title compound as a colorless oil (222 mg, 0.66 mmol, 68% yield).

^{1}H NMR (400 MHz, $CDCl_3$): δ 6.77 (dt, *J* = 15.9, 6.9 Hz, 1H), 6.05 (dt, *J* = 16.0, 1.5 Hz, 1H), 5.35 – 5.26 (m, 1H), 4.69 – 4.55 (m, 2H), 2.54 – 2.35 (m, 3H), 2.26 – 2.15 (m, 5H), 2.06 – 1.95 (m, 1H), 1.85 (ddd, *J* = 13.6, 12.2, 4.7 Hz, 1H), 1.78 – 1.67 (m, 7H), 1.67 – 1.36 (m, 6H), 1.35 – 1.13 (m, 2H).

^{13}C NMR (100 MHz, $CDCl_3$): δ 208.2, 198.9, 172.2, 148.3, 140.0, 131.5, 118.1, 62.1, 61.0, 41.3, 36.4, 34.6, 32.4, 28.6, 27.8, 27.0, 25.8, 24.1, 22.8, 18.2.

IR (Neat Film, NaCl): 2938, 2863, 1709, 1674, 1626, 1449, 1361, 1309, 1253, 1208, 1170, 1135, 1100 cm^{-1}.

HRMS (ESI+): *m/z* calc'd for $C_{20}H_{30}O_4Na$ $[M+Na]^+$: 357.2036, found 357.2035.

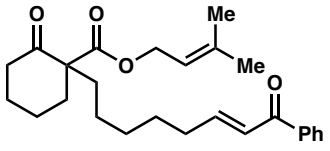

215b

3-methylbut-2-en-1-yl (*E*)-2-oxo-1-(8-oxo-8-phenyloct-6-en-1-yl)cyclohexane-1-carboxylate (215b)

Prepared from **217h** and dimethyl (2-oxo-2-phenylethyl)phosphonate[23] following General Procedure D. Purification by flash column chromatography (0–50% EtOAc/hexanes) afforded the title compound as a colorless oil (493 mg, 1.20 mmol, 74% yield).

^{1}H NMR (400 MHz, $CDCl_3$): δ 7.97 – 7.89 (m, 2H), 7.59 – 7.51 (m, 1H), 7.50 – 7.42 (m, 2H), 7.04 (dt, *J* = 15.4, 6.9 Hz, 1H), 6.86 (dt, *J* = 15.4, 1.4 Hz, 1H), 5.36 – 5.25 (m, 1H), 4.68 – 4.56 (m, 2H), 2.56 – 2.36 (m, 3H), 2.33 – 2.24 (m, 2H), 2.03 – 1.93 (m, 1H), 1.86 (ddd, *J* = 13.5, 12.0, 4.5 Hz, 1H), 1.78 – 1.68 (m, 7H), 1.67 – 1.47 (m, 5H), 1.46 – 1.30 (m, 3H), 1.29 – 1.13 (m, 2H).

^{13}C NMR (100 MHz, $CDCl_3$): δ 208.3, 191.1, 172.2, 150.0, 139.9, 138.2, 132.7, 128.7, 128.6, 126.1, 118.2, 62.1, 61.0, 41.3, 36.4, 34.8, 32.9, 29.7, 28.1, 27.8, 25.9, 24.1, 22.8, 18.2.

IR (Neat Film, NaCl): 2935, 2859, 1710, 1670, 1618, 1447, 1378, 1340, 1279, 1221, 1167 cm^{-1}.

HRMS (ESI+): *m/z* calc'd for $C_{26}H_{34}O_4Na$ $[M+Na]^+$: 433.2349, found 433.2360.

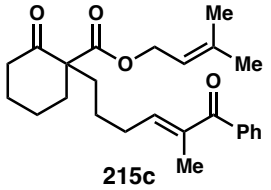

215c

3-methylbut-2-en-1-yl (*E*)-1-(5-methyl-6-oxo-6-phenylhex-4-en-1-yl)-2-oxocyclohexane-1-carboxylate (215c)

Prepared from **217a** and dimethyl (1-oxo-1-phenylpropan-2-yl)phosphonate[25] following General Procedure D. Purification by flash column chromatography (20% Et_2O/hexanes) afforded the title compound as a colorless oil (72.4 mg, 0.18 mmol, 26% yield).

^{1}H NMR (400 MHz, $CDCl_3$): δ 7.64 – 7.59 (m, 2H), 7.52 – 7.46 (m, 1H), 7.44 – 7.38 (m, 2H), 6.24 (td, *J* = 7.3, 1.4 Hz, 1H), 5.33 – 5.23 (m, 1H), 4.68 – 4.52 (m, 2H), 2.54 – 2.35 (m, 3H), 2.31 – 2.22 (m, 2H), 2.05 – 1.93 (m, 4H), 1.93 – 1.82 (m, 1H), 1.79 – 1.66 (m, 8H), 1.66 – 1.57 (m, 2H), 1.48 – 1.36 (m, 2H), 1.35 – 1.22 (m, 1H).

^{13}C NMR (100 MHz, $CDCl_3$): δ 208.1, 199.1, 172.1, 146.1, 140.1, 138.8, 136.9, 131.5, 129.5, 128.2, 118.1, 62.2, 60.9, 41.3, 36.6, 34.8, 29.6, 27.8, 25.8, 23.7, 22.8, 18.2, 12.7.

IR (Neat Film, NaCl): 2938, 2864, 1711, 1647, 1445, 1381, 1280, 1208, 1185 cm^{-1}.

HRMS (ESI+): *m/z* calc'd for $C_{25}H_{32}O_4Na$ $[M+Na]^+$: 419.2193, found 419.2203.

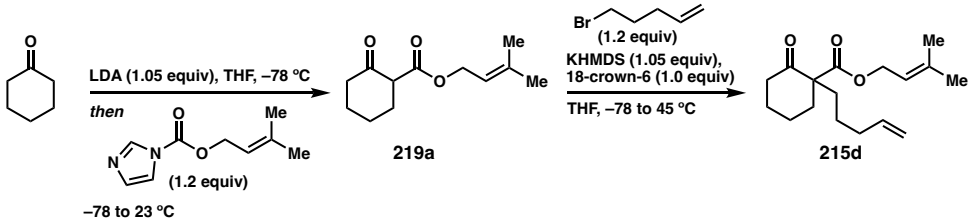

3-methylbut-2-en-1-yl 2-oxo-1-(pent-4-en-1-yl)cyclohexane-1-carboxylate (215d)

To a flame dried 250 mL round bottom flask was added *i*Pr_2NH (4.6 mL, 33 mmol, 1.1 equiv) followed by THF (17 mL, 1.9 M) before the solution was cooled to 0 °C. To this,

n-BuLi (2.5 M in hexanes, 12.6 mL, 31.5 mmol, 1.05 equiv) was added dropwise before the solution was allowed to stir at 0 °C for 15 minutes. To this, a solution of cyclohexanone (3.1 mL, 30 mmol, 1.0 equiv) in THF (24 mL, 1.25 M) was added dropwise before the solution was allowed to stir at 0 °C for 30 minutes. The solution was then cooled to –78 °C, and a solution of 3-methylbut-2-en-1-yl 1*H*-imidazole-1-carboxylate[26] (6.48 g, 36 mmol, 1.2 equiv) in THF (9 mL, 4 M) was added dropwise. The reaction was warmed gradually to 23 °C. Upon complete consumption of starting material by TLC, the reaction was cooled to 0 °C, the pH was adjusted to 1.0 using 1 M HCl, and the mixture was extracted with EtOAc (3x). The combined organic layers were rinsed with brine, dried over Na_2SO_4, filtered, and concentrated under reduced pressure. The crude reaction mixture was purified by silica gel flash column chromatography (0–20% EtOAc/hexanes) to afford **219a** as a mixture of tautomers (4.18 g, 19.9 mmol, 66% yield), which was used directly in the next step.

To a flame dried 250 mL round bottom flask was added KHMDS (796 mg, 4.0 mmol, 1.05 equiv), and 18-crown-6 (1.00 g, 3.8 mmol, 1.0 equiv) followed by THF (20 mL, 0.19 M) before the solution was cooled to –78 °C. A solution of β-ketoester **219a** (884 mg, 3.8 mmol, 1.0 equiv) in THF (10 mL, 0.38 M) was added dropwise at –78 °C. The solution was stirred at this temperature for 15 minutes before 5-bromopent-1-ene was added neat (0.54 mL, 4.6 mmol, 1.2 equiv). The reaction was then warmed to 45 °C. Upon complete consumption of starting material by TLC, the reaction was cooled to 0 °C, and diluted with EtOAc (10 mL), followed by a saturated solution of NH_4Cl (20 mL). This mixture was then extracted with EtOAc (3x). The combined organic layers were rinsed with brine, dried over

Na_2SO_4, filtered, and concentrated under reduced pressure. The crude reaction mixture was purified by silica gel flash column chromatography (0–20% EtOAc/hexanes) to afford **215d** as a colorless oil (601 mg, 2.16 mmol, 57% yield).

^{1}H NMR (400 MHz, $CDCl_3$): δ 5.77 (ddt, *J* = 16.9, 10.2, 6.6 Hz, 1H), 5.37 – 5.24 (m, 1H), 5.04 – 4.89 (m, 2H), 4.62 (d, *J* = 7.3 Hz, 2H), 2.56 – 2.35 (m, 3H), 2.08 – 1.94 (m, 3H), 1.86 (ddd, *J* = 13.7, 12.3, 4.6 Hz, 1H), 1.78 – 1.47 (m, 10H), 1.46 – 1.19 (m, 3H).

^{13}C NMR (100 MHz, $CDCl_3$): δ 208.2, 172.2, 140.0, 138.5, 118.2, 114.8, 62.1, 61.0, 41.3, 36.4, 34.4, 34.2, 27.8, 25.8, 23.7, 22.8, 18.2.

IR (Neat Film, NaCl): 2938, 2864, 1713, 1639, 1449, 1379, 1339, 1308, 1210, 1186, 1143 cm^{-1}.

HRMS (ESI+): *m/z* calc'd for $C_{17}H_{26}O_3Na$ $[M+Na]^+$: 301.1774, found 301.1761.

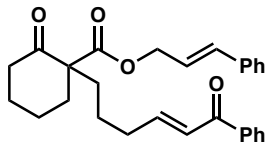

200a

cinnamyl 2-oxo-1-((*E*)-6-oxo-6-phenylhex-4-en-1-yl)cyclohexane-1-carboxylate (200a)

Prepared from **217i** and dimethyl (2-oxo-2-phenylethyl)phosphonate[23] following General Procedure D. Purification by flash column chromatography (0–50% EtOAc/hexanes) afforded the title compound as a colorless oil (533 mg, 1.24 mmol, 81% yield).

^{1}H NMR (400 MHz, $CDCl_3$): δ 7.95 – 7.87 (m, 2H), 7.58 – 7.51 (m, 1H), 7.49 – 7.42 (m, 2H), 7.40 – 7.34 (m, 2H), 7.33 – 7.27 (m, 2H), 7.26 – 7.21 (m, 1H), 7.00 (dt, *J* = 15.4, 6.7 Hz, 1H), 6.86 (dt, *J* = 15.4, 1.4 Hz, 1H), 6.71 – 6.62 (m, 1H), 6.26 (dt, *J* = 15.9, 6.6 Hz,

1H), 4.87 – 4.73 (m, 2H), 2.59 – 2.39 (m, 3H), 2.38 – 2.23 (m, 2H), 2.08 – 1.87 (m, 2H), 1.82 – 1.57 (m, 4H), 1.55 – 1.36 (m, 3H).

^{13}C NMR (100 MHz, $CDCl_3$): δ 207.9, 191.0, 171.9, 149.0, 138.1, 136.1, 135.4, 132.7, 128.8, 128.7, 128.6, 128.4, 126.8, 126.3, 122.4, 66.0, 61.0, 41.3, 36.4, 34.5, 33.2, 27.7, 23.2, 22.8.

IR (Neat Film, NaCl): 2942, 2865, 1711, 1669, 1619, 1448, 1339, 1288, 1218, 1170, 1135, 1101 cm^{-1}.

HRMS (ESI+): *m/z* calc'd for $C_{28}H_{30}O_4Na$ $[M+Na]^+$: 453.2036, found 453.2031.

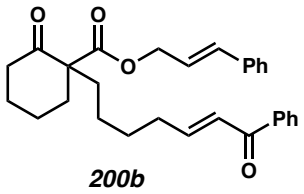

200b

cinnamyl 2-oxo-1-((*E*)-7-oxo-7-phenylhept-5-en-1-yl)cyclohexane-1-carboxylate (200b)

Prepared from **217j** and dimethyl (2-oxo-2-phenylethyl)phosphonate[23] following General Procedure D. Purification by flash column chromatography (0–50% EtOAc/hexanes) afforded the title compound as a colorless oil (504 mg, 1.13 mmol, 76% yield).

^{1}H NMR (400 MHz, $CDCl_3$): δ 7.95 – 7.87 (m, 2H), 7.59 – 7.51 (m, 1H), 7.50 – 7.41 (m, 2H), 7.39 – 7.35 (m, 2H), 7.35 – 7.29 (m, 2H), 7.30 – 7.23 (m, 1H), 7.00 (dt, *J* = 15.4, 6.8 Hz, 1H), 6.82 (dt, *J* = 15.4, 1.5 Hz, 1H), 6.65 (dt, *J* = 15.8, 1.4 Hz, 1H), 6.25 (dt, *J* = 15.8, 6.5 Hz, 1H), 4.78 (dd, *J* = 6.6, 1.3 Hz, 2H), 2.59 – 2.50 (m, 1H), 2.49 – 2.38 (m, 2H), 2.34

– 2.20 (m, 2H), 2.05 – 1.87 (m, 2H), 1.81 – 1.59 (m, 4H), 1.57 – 1.41 (m, 3H), 1.38 – 1.20 (m, 2H).

^{13}C NMR (100 MHz, $CDCl_3$): δ 208.0, 191.0, 172.0, 149.6, 138.1, 136.1, 135.3, 132.7, 128.8, 128.7, 128.6, 128.4, 126.8, 126.1, 122.5, 65.8, 61.1, 41.3, 36.3, 34.6, 32.7, 28.6, 27.7, 24.1, 22.7.

IR (Neat Film, NaCl): 2939, 2862, 1711, 1668, 1620, 1578, 1495, 1447, 1338, 1284, 1214, 1168 cm^{-1}.

HRMS (ESI+): *m/z* calc'd for $C_{29}H_{32}O_4$ $[M+Na]^+$: 467.2193, found 467.2200.

Preparation of Aldehyde Precursors:

General Procedure E: Acylation, Alkylation of Carbonyls and Hydrolysis of Acetals

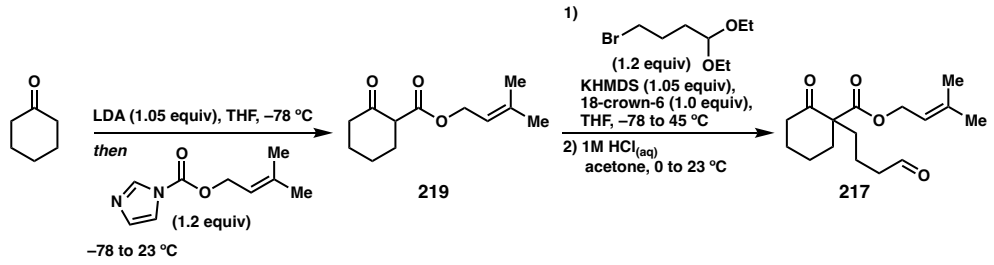

To a flame dried 250 mL round bottom flask was added *i*Pr_2NH (1.1 equiv) followed by THF (1.9 M) before the solution was cooled to 0 °C. To this, *n*-BuLi (2.5 M in hexanes, 1.05 equiv) was added dropwise before the solution was allowed to stir at 0 °C for 15 minutes. To this, a solution of the appropriate carbonyl compound (1.0 equiv) in THF (1.25 M) was added dropwise before the solution was allowed to stir at 0 °C for 30 minutes. The solution was then cooled to –78 °C, before a solution of 3-methylbut-2-en-1-yl 1*H*-imidazole-1-carboxylate[26] (1.2 equiv) in THF (4 M) was added dropwise. The reaction was warmed gradually to 23 °C. Upon complete consumption of starting material

by TLC, the reaction was cooled to 0 °C, the pH was adjusted to 1.0 using 1 M HCl and the mixture was extracted with EtOAc (3x). The combined organic layers were rinsed with brine, dried over Na_2SO_4, filtered, and concentrated under reduced pressure. The crude reaction mixture was purified by silica gel flash column chromatography to afford **219** as a mixture of tautomers, which was used directly in the next step.

To a flame dried 250 mL round bottom flask was added KHMDS (1.05 equiv), and 18-crown-6 (1.0 equiv) followed by THF (0.19 M) before the solution was cooled to –78 °C. A solution of β-ketoester **219** (1.0 equiv) in THF (0.38 M) was added dropwise at –78 °C. The solution was stirred at this temperature for 15 minutes before the appropriate alkyl bromide was added neat (1.2 equiv). The reaction was then warmed to 45 °C. Upon complete consumption of starting material by TLC, the reaction was cooled to 0 °C, and diluted with EtOAc followed by a saturated solution of NH_4Cl. This mixture was then extracted with EtOAc (3x). The combined organic layers were rinsed with brine, dried over Na_2SO_4, filtered, and concentrated under reduced pressure to afford the corresponding diethyl acetal which was used directly in the next step. A round bottom flask was charged with the corresponding diethyl acetal as a solution in acetone (0.5 M) before being cooled to 0 °C, and 1 M HCl was added (in a 2:1 volume ratio of 1 M HCl:acetone). The reaction was gradually warmed to 23 °C. Upon complete consumption of starting material by TLC, the reaction was diluted with EtOAc, extracted with EtOAc (3x), rinsed with brine, dried with Na_2SO_4, filtered, and concentrated under reduced pressure. The crude reaction mixture was purified by silica gel flash column chromatography to afford **217**. *Note: Yields*

are reported based on alkylation and hydrolysis sequence. This is done because the corresponding β-keto esters were sometimes used to prepare multiple substrates.

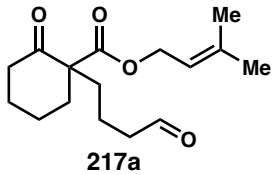

217a

3-methylbut-2-en-1-yl 2-oxo-1-(4-oxobutyl)cyclohexane-1-carboxylate (217a)

Prepared from cyclohexanone and 4-bromo-1,1-diethoxybutane[27] according to General Procedure E. Purification by flash column chromatography (0–60% EtOAc/hexanes) afforded the title compound as a colorless oil (715 mg, 2.55 mmol, 43% yield).

^{1}H NMR (400 MHz, $CDCl_3$): δ 9.73 (t, *J* = 1.6 Hz, 1H), 5.36 – 5.28 (m, 1H), 4.70 – 4.57 (m, 2H), 2.56 – 2.37 (m, 5H), 2.05 – 1.95 (m, 1H), 1.91 – 1.79 (m, 1H), 1.79 – 1.73 (m, 4H), 1.71 (s, 3H), 1.69 – 1.49 (m, 5H), 1.49 – 1.39 (m, 1H).

^{13}C NMR (100 MHz, $CDCl_3$): δ 208.0, 202.2, 172.0, 140.2, 118.1, 62.3, 60.9, 44.2, 41.2, 36.4, 34.3, 27.8, 25.8, 22.7, 18.2, 17.3.

IR (Neat Film, NaCl): 2939, 2866, 1713, 1450, 1380, 1211, 1179, 1137, 1096 cm^{-1}.

HRMS (ESI+): *m/z* calc'd for $C_{16}H_{24}O_4Na$ $[M+Na]^+$: 303.1567, found 393.1564.

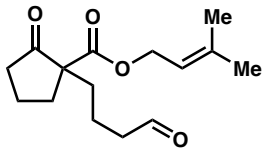

217b

3-methylbut-2-en-1-yl 2-oxo-1-(5-oxopentyl)cyclopentane-1-carboxylate (217b)

Prepared from cyclopentanone and 4-bromo-1,1-diethoxybutane[27] according to General Procedure E. Purification by flash column chromatography (0–50% EtOAc/hexanes) afforded the title compound as a colorless oil (631 mg, 2.37 mmol, 47% yield).

^{1}H NMR (400 MHz, $CDCl_3$): δ 9.75 (t, *J* = 1.4 Hz, 1H), 5.35 – 5.24 (m, 1H), 4.63 – 4.54 (m, 2H), 2.60 – 2.35 (m, 4H), 2.32 – 2.17 (m, 1H), 2.09 – 1.84 (m, 4H), 1.74 (s, 3H), 1.72 – 1.49 (m, 6H).

^{13}C NMR (100 MHz, $CDCl_3$): δ 214.9, 201.9, 171.0, 139.7, 118.2, 62.5, 60.4, 44.1, 38.1, 33.3, 33.0, 25.9, 19.8, 18.2, 17.6.

IR (Neat Film, NaCl): 2960, 1748, 1719, 1448, 1380, 1335, 1157 cm^{-1}.

HRMS (ESI+): *m/z* calc'd for $C_{15}H_{22}O_4Na$ $[M+Na]^+$: 289.1410, found 289.1408.

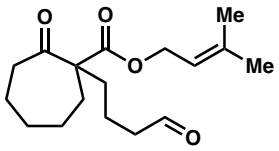

217c

3-methylbut-2-en-1-yl 2-oxo-1-(4-oxobutyl)cycloheptane-1-carboxylate (217c)

Prepared from cycloheptanone and 4-bromo-1,1-diethoxybutane[27] according to General Procedure E. Purification by flash column chromatography (0–50% EtOAc/hexanes) afforded the title compound as a colorless oil (1.34 g, 4.56 mmol, 57% yield).

^{1}H NMR (400 MHz, $CDCl_3$): δ 9.73 (t, *J* = 1.6 Hz, 1H), 5.37 – 5.24 (m, 1H), 4.62 (dd, *J* = 7.3, 3.1 Hz, 2H), 2.71 – 2.56 (m, 1H), 2.52 – 2.34 (m, 3H), 2.22 – 2.06 (m, 1H), 2.06 – 1.87 (m, 1H), 1.83 – 1.72 (m, 5H), 1.72 – 1.49 (m, 10H), 1.48 – 1.35 (m, 1H).

^{13}C NMR (100 MHz, $CDCl_3$): δ 209.6, 202.2, 172.4, 139.9, 118.2, 62.8, 62.2, 44.2, 42.3, 34.9, 33.0, 29.9, 25.8, 25.6, 25.0, 18.2, 17.6.

IR (Neat Film, NaCl): 2931, 2862, 1708, 1457, 1379, 1220, 1168 cm^{-1}.

HRMS (ESI+): *m/z* calc'd for $C_{17}H_{26}O_4Na$ $[M+Na]^+$: 317.1723, found 317.1719.

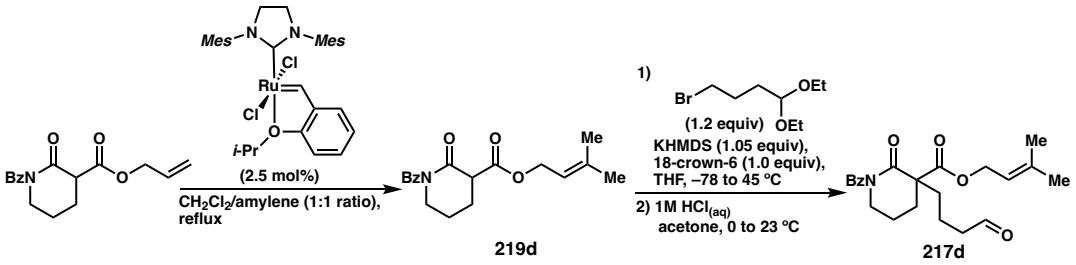

3-methylbut-2-en-1-yl 1-benzoyl-2-oxo-3-(4-oxobutyl)piperidine-3-carboxylate (217d)

To a flame dried 2-neck 250 mL round bottom flask equipped with a reflux condenser was added HG-II (54.5 mg, 0.09 mmol, 0.025 equiv). Allyl 1-benzoyl-2-oxopiperidine-3-carboxylate[28] (1.00 g, 3.5 mmol, 1.0 equiv) was added as a solution in CH_2Cl_2 (35 mL, 0.1 M) followed by amylene (35 mL, 1:1 volume ratio with CH_2Cl_2). The reaction mixture was heated to reflux and monitored via NMR. Upon complete consumption of allyl 1-benzoyl-2-oxopiperidine-3-carboxylate, the reaction was cooled to 23 °C and concentrated under reduced pressure. The crude reaction mixture was purified by silica gel flash column chromatography (0–50% EtOAc/hexanes) to afford **219d** (953 mg, 3.02 mmol, 87% yield), which was used directly in the next step.

To a flame dried 100 mL round bottom flask was added KHMDS (622 mg, 3.1 mmol, 1.05 equiv), and 18-crown-6 (784 mg, 3.0 mmol, 1.0 equiv) followed by THF (15 mL, 0.2 M) before the solution was cooled to –78 °C. A solution of β-ketoester **219d** (936 mg, 3.0 mmol, 1.0 equiv) in THF (7.5 mL, 0.4 M) was added dropwise at –78 °C. The solution was stirred at this temperature for 15 minutes before 4-bromo-1,1-diethoxybutane[27] was added neat (801 mg, 3.6 mmol, 1.2 equiv). The reaction was then warmed to 45 °C. Upon

complete consumption of starting material by TLC, the reaction was cooled to 0 °C, and diluted with EtOAc (10 mL) followed by a saturated solution of NH_4Cl (20 mL). This mixture was then extracted with EtOAc (3x). The combined organic layers were rinsed with brine, dried over Na_2SO_4, filtered, and concentrated under reduced pressure to afford the corresponding diethyl acetal which was used directly in the next step. A 50 mL round bottom flask was charged with the corresponding diethyl acetal as a solution in acetone (6 mL, 0.5 M) before being cooled to 0 °C, and 1 M HCl was added (in a 1:1 volume ratio of 1 M HCl:acetone). The reaction was gradually warmed to 23 °C. Upon complete consumption of starting material by TLC, the reaction was diluted with EtOAc, extracted with EtOAc (3x), rinsed with brine, dried with Na_2SO_4, filtered, and concentrated under reduced pressure. The crude reaction mixture was purified by silica gel flash column chromatography (0–50% EtOAc/hexanes) to afford **217d** as a colorless oil (409 mg, 1.06 mmol, 36% yield).

^{1}H NMR (400 MHz, $CDCl_3$): δ 9.71 (t, *J* = 1.4 Hz, 1H), 7.78 – 7.68 (m, 2H), 7.51 – 7.43 (m, 1H), 7.41 – 7.34 (m, 2H), 5.47 – 5.38 (m, 1H), 4.81 – 4.65 (m, 2H), 3.88 – 3.69 (m, 2H), 2.54 – 2.30 (m, 3H), 2.07 – 1.95 (m, 2H), 1.93 – 1.85 (m, 2H), 1.84 – 1.79 (m, 3H), 1.79 – 1.69 (m, 4H), 1.67 – 1.43 (m, 2H).

^{13}C NMR (100 MHz, $CDCl_3$): δ 201.9, 175.1, 172.1, 172.1, 140.7, 136.0, 131.8, 128.2, 128.2, 117.8, 63.0, 56.7, 46.6, 44.0, 35.0, 30.7, 26.0, 20.5, 18.3, 17.5.

IR (Neat Film, NaCl): 2941, 1718, 1684, 1448, 1387, 1272, 1190, 1148 cm^{-1}.

HRMS (ESI+): *m/z* calc'd for $C_{22}H_{27}NO_5Na$ $[M+Na]^+$: 408.1781, found 408.1786.

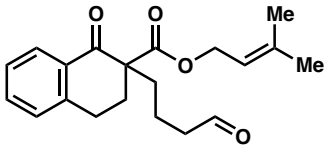

217e

3-methylbut-2-en-1-yl 1-oxo-2-(4-oxobutyl)-1,2,3,4-tetrahydronaphthalene-2-carboxylate (217e)

Prepared from 1-tetralone and 4-bromo-1,1-diethoxybutane[27] according to General Procedure E. Purification by flash column chromatography (0–50% EtOAc/hexanes) afforded the title compound as a colorless oil (531 mg, 1.62 mmol, 20% yield).

^{1}H NMR (400 MHz, $CDCl_3$): δ 9.76 (t, *J* = 1.5 Hz, 1H), 8.03 (dd, *J* = 7.9, 1.5 Hz, 1H), 7.46 (td, *J* = 7.5, 1.4 Hz, 1H), 7.30 (t, *J* = 7.6 Hz, 1H), 7.21 (d, *J* = 7.7 Hz, 1H), 5.26 – 5.17 (m, 1H), 4.64 – 4.49 (m, 2H), 3.07 (ddd, *J* = 17.4, 10.1, 4.7 Hz, 1H), 2.93 (dt, *J* = 17.4, 5.0 Hz, 1H), 2.57 (dt, *J* = 13.8, 5.0 Hz, 1H), 2.48 (t, *J* = 7.1 Hz, 2H), 2.23 – 2.11 (m, 1H), 2.03 – 1.86 (m, 2H), 1.86 – 1.72 (m, 1H), 1.72 – 1.62 (m, 4H), 1.58 (s, 3H).

^{13}C NMR (100 MHz, $CDCl_3$): δ 202.2, 195.6, 171.9, 143.2, 139.9, 133.6, 132.2, 128.8, 128.2, 126.9, 118.2, 62.4, 57.6, 44.2, 33.5, 30.9, 26.1, 25.8, 18.1, 17.7.

IR (Neat Film, NaCl): 2935, 2724, 1724, 1687, 1600, 1453, 1453, 1379, 1294, 1231, 1184, 1096 cm^{-1}.

HRMS (ESI+): *m/z* calc'd for $C_{20}H_{24}O_4Na$ $[M+Na]^+$: 351.1567, found 351.1571.

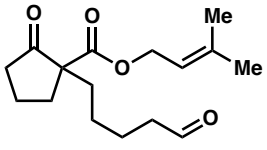

217f

3-methylbut-2-en-1-yl 2-oxo-1-(5-oxopentyl)cyclopentane-1-carboxylate (217f)

Prepared from cyclopentanone and 5-bromo-1,1-diethoxypentane[27] according to General Procedure E. Purification by flash column chromatography (0–40% EtOAc/hexanes) afforded the title compound as a colorless oil (886 mg, 3.16 mmol, 63% yield).

^{1}H NMR (400 MHz, $CDCl_3$): δ 9.75 (t, *J* = 1.7 Hz, 1H), 5.34 – 5.23 (m, 1H), 4.62 – 4.53 (m, 2H), 2.56 – 2.36 (m, 4H), 2.29 – 2.17 (m, 1H), 2.07 – 1.80 (m, 4H), 1.74 (s, 3H), 1.69 (s, 3H), 1.67 – 1.53 (m, 3H), 1.44 – 1.32 (m, 1H), 1.31 – 1.18 (m, 1H).

^{13}C NMR (100 MHz, $CDCl_3$): δ 215.0, 202.4, 171.1, 139.6, 118.3, 62.5, 60.5, 43.7, 38.1, 33.6, 33.1, 25.9, 24.5, 22.4, 19.8, 18.2.

IR (Neat Film, NaCl): 2947, 2725, 1748, 1722, 1451, 1380, 1224, 1159, 1127 cm^{-1}.

HRMS (ESI+): *m/z* calc'd for $C_{16}H_{24}O_4Na$ $[M+Na]^+$: 303.1567, found 303.1571.

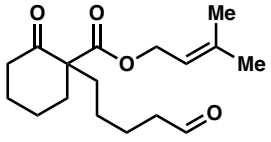

217g

3-methylbut-2-en-1-yl 2-oxo-1-(5-oxopentyl)cyclohexane-1-carboxylate (217g)

Prepared from cyclohexanone and 5-bromo-1,1-diethoxypentane[27] according to General Procedure E. Purification by flash column chromatography (0–60% EtOAc/hexanes) afforded the title compound as a colorless oil (617 mg, 2.10 mmol, 44% yield).

^{1}H NMR (400 MHz, $CDCl_3$): δ 9.74 (t, *J* = 1.7 Hz, 1H), 5.35 – 5.25 (m, 1H), 4.70 – 4.53 (m, 2H), 2.56 – 2.33 (m, 5H), 2.05 – 1.95 (m, 1H), 1.92 – 1.80 (m, 1H), 1.74 (s, 3H), 1.73 – 1.67 (m, 4H), 1.66 – 1.48 (m, 5H), 1.47 – 1.35 (m, 1H), 1.34 – 1.14 (m, 2H).

^{13}C NMR (100 MHz, $CDCl_3$): δ 208.2, 202.6, 172.1, 140.0, 118.1, 62.2, 60.9, 43.8, 41.3, 36.4, 34.6, 27.8, 25.8, 24.0, 22.7, 22.5, 18.2.

IR (Neat Film, NaCl): 2939, 2865, 2724, 1712, 1449, 1380, 1297, 1173, 1136, 1097 cm^{-1}.

HRMS (ESI+): *m/z* calc'd for $C_{17}H_{26}O_4Na$ $[M+Na]^+$: 317.1723, found 317.1719.

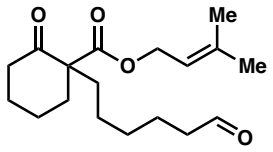

217h

3-methylbut-2-en-1-yl 2-oxo-1-(6-oxohexyl)cyclohexane-1-carboxylate (217h)

Prepared from cyclohexanone and 6-bromo-1,1-diethoxyhexane[27] according to General Procedure E. Purification by flash column chromatography (0–60% EtOAc/hexanes) afforded the title compound as a colorless oil (515 mg, 1.67 mmol, 44% yield).

^{1}H NMR (400 MHz, $CDCl_3$): δ 9.75 (t, *J* = 1.8 Hz, 1H), 5.40 – 5.23 (m, 1H), 4.70 – 4.54 (m, 2H), 2.57 – 2.32 (m, 5H), 2.06 – 1.95 (m, 1H), 1.85 (ddd, *J* = 13.3, 12.1, 4.1 Hz, 1H), 1.79 – 1.67 (m, 7H), 1.67 – 1.56 (m, 4H), 1.54 – 1.37 (m, 2H), 1.36 – 1.11 (m, 4H).

^{13}C NMR (100 MHz, $CDCl_3$): δ 208.3, 202.8, 172.2, 140.0, 118.2, 62.1, 61.0, 43.9, 41.3, 36.5, 34.7, 29.6, 27.8, 25.9, 24.1, 22.8, 21.9, 18.2.

IR (Neat Film, NaCl): 2936, 2862, 2720, 1712, 1450, 1380, 1270, 1200, 1170, 1136, 1098 cm^{-1}.

HRMS (ESI+): *m/z* calc'd for $C_{18}H_{28}O_4Na$ $[M+Na]^+$: 331.1880, found 331.1880.

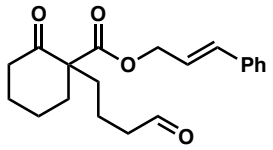

217i

cinnamyl 2-oxo-1-(4-oxobutyl)cyclohexane-1-carboxylate (217i)

Prepared from cyclohexanone, cinnamyl 1*H*-imidazole-1-carboxylate (in place of 3-methylbut-2-en-1-yl 1*H*-imidazole-1-carboxylate), and 4-bromo-1,1-diethoxybutane[27] according to General Procedure E. Purification by flash column chromatography (0–60% EtOAc/hexanes) afforded the title compound as a colorless oil (1.81 g, 5.50 mmol, 37% yield).

^{1}H NMR (400 MHz, $CDCl_3$): δ 9.77 – 9.65 (m, 1H), 7.41 – 7.36 (m, 2H), 7.36 – 7.30 (m, 2H), 7.30 – 7.26 (m, 1H), 6.67 (d, *J* = 15.8 Hz, 1H), 6.27 (dtd, *J* = 15.9, 6.6, 0.8 Hz, 1H), 4.87 – 4.74 (m, 2H), 2.59 – 2.36 (m, 5H), 2.04 – 1.96 (m, 1H), 1.92 – 1.82 (m, 1H), 1.82 – 1.43 (m, 7H).

^{13}C NMR (100 MHz, $CDCl_3$): δ 207.8, 202.1, 171.8, 136.1, 135.4, 128.8, 128.4, 126.8, 122.4, 66.0, 61.0, 44.1, 41.2, 36.2, 34.2, 27.7, 22.7, 17.3.

IR (Neat Film, NaCl): 2944, 2866, 1713, 1495, 1450, 1242, 1206, 1178, 1137, 1098 cm^{-1}.

HRMS (ESI+): *m/z* calc'd for $C_{20}H_{24}O_4Na$ $[M+Na]^+$: 351.1567, found 351.1562.

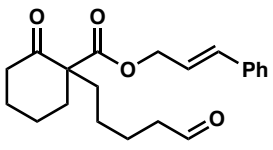

217j

cinnamyl 2-oxo-1-(5-oxopentyl)cyclohexane-1-carboxylate (217j)

Prepared from cyclohexanone, cinnamyl 1*H*-imidazole-1-carboxylate (in place of 3-methylbut-2-en-1-yl 1*H*-imidazole-1-carboxylate), and 5-bromo-1,1-diethoxypentane[27] according to General Procedure E. Purification by flash column chromatography (0–60% EtOAc/hexanes) afforded the title compound as a colorless oil (767 mg, 2.24 mmol, 45% yield).

^{1}H NMR (600 MHz, $CDCl_3$): δ 9.69 (t, *J* = 1.7 Hz, 1H), 7.41 – 7.36 (m, 2H), 7.36 – 7.31 (m, 2H), 7.30 – 7.26 (m, 1H), 6.66 (dd, *J* = 15.9, 1.6 Hz, 1H), 6.26 (dt, *J* = 15.9, 6.6 Hz, 1H), 4.79 (dd, *J* = 6.6, 1.3 Hz, 2H), 2.56 – 2.41 (m, 3H), 2.40 – 2.31 (m, 2H), 2.04 – 1.96 (m, 1H), 1.90 (ddd, *J* = 13.5, 12.2, 4.6 Hz, 1H), 1.80 – 1.72 (m, 1H), 1.71 – 1.53 (m, 5H), 1.46 (ddd, *J* = 13.6, 12.0, 4.2 Hz, 1H), 1.34 – 1.18 (m, 2H).

^{13}C NMR (100 MHz, $CDCl_3$): δ 207.9, 202.5, 171.9, 136.1, 135.4, 128.8, 128.5, 126.8, 122.4, 65.9, 61.0, 43.7, 41.3, 36.3, 34.6, 27.7, 24.1, 22.7, 22.5.

IR (Neat Film, NaCl): 2944, 2865, 1713, 1495, 1451, 1240, 1310, 1240, 1206, 1174, 1135, 1098 cm^{-1}.

HRMS (ESI+): *m/z* calc'd for $C_{21}H_{26}O_4Na$ $[M+Na]^+$: 365.1723, found 365.1721.

Product Derivatizations:

General Procedure F: Samarium Mediated Pinacol Coupling[29]

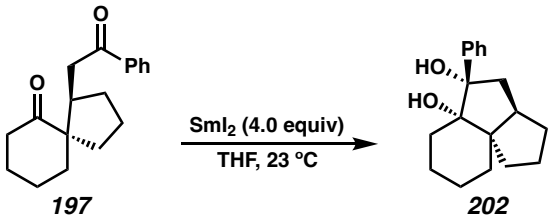

197 ***202***

To a flame dried round bottom flask was added a solution of SmI_2 (0.1 M in THF, 4.0 equiv), followed by a solution of the corresponding diketone (1.0 equiv) in THF (0.1

M). Upon complete consumption of starting material by TLC, the reaction was diluted with Et_2O, followed by further dilution with a saturated aqueous solution of $NaHCO_3$. The mixture was extracted with Et_2O (3x), rinsed with brine, dried with Na_2SO_4, filtered, and concentrated under reduced pressure. The crude reaction mixture was purified by silica gel flash column chromatography or preparative TLC to afford the corresponding diol.

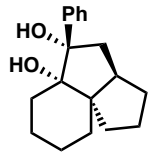

202

(3a*R*,5*S*,5a*S*,9a*S*)-5-phenyldecahydro-5a*H*-cyclopenta[*c*]indene-5,5a-diol (202)

Prepared from diketone **197a** according to General Procedure F. Purification by flash column chromatography (0–40% Et_2O/hexanes) afforded the title compound as a colorless oil (23 mg, 0.084 mmol, 56% yield). Structure assigned via 1D ^1H and ^{13}C NMR, 2D NMR studies (see below), and comparison with compounds found in the literature. Cis configuration was assigned via carbonate formation[29] (see **203** below).

^1H NMR (400 MHz, $CDCl_3$): δ 7.64 – 7.58 (m, 2H), 7.38 – 7.31 (m, 2H), 7.29 – 7.22 (m, 1H), 4.12 (s, 1H), 2.73 (s, 1H), 2.65 – 2.47 (m, 2H), 2.12 – 1.94 (m, 2H), 1.72 – 1.58 (m, 3H), 1.55 – 1.47 (m, 1H), 1.41 – 1.11 (m, 7H), 1.07 – 0.96 (m, 1H), 0.12 – -0.05 (m, 1H).

^{13}C NMR (100 MHz, $CDCl_3$): δ 144.3, 127.9, 127.6, 127.2, 90.7, 79.3, 58.6, 47.0, 37.6, 35.3, 26.4, 25.7, 25.0, 22.3, 21.9, 20.8.

IR (Neat Film, NaCl): 3307, 2946, 2871, 1494, 1445, 1394, 1221, 1050, 1019 cm^{-1}.

HRMS (FD+): *m/z* calc'd for $C_{18}H_{24}O_2$ $[M]^{+\cdot}$: 272.17708, found 272.17608.

Optical Rotation: $[\alpha]_D^{23}$ –30.0 (c = 1.53, $CHCl_3$).

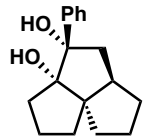

204

(3a*S*,4*S*,5a*R*,8a*R*)-4-phenyloctahydrocyclopenta[*c*]pentalene-3a,4(1*H*)-diol (204)

Prepared from diketone **197c** according to General Procedure F. Purification by preparative TLC (40% Et_2O/hexanes) afforded the title compound as a colorless oil (7.0 mg, 0.027 mmol, 68% yield).

^{1}H NMR (400 MHz, $CDCl_3$): δ 7.49 – 7.42 (m, 2H), 7.38 – 7.31 (m, 2H), 7.31 – 7.27 (m, 1H), 3.29 (s, 1H), 3.12 (s, 1H), 2.52 – 2.36 (m, 1H), 2.16 (dd, *J* = 13.5, 12.1 Hz, 1H), 2.12 – 2.02 (m, 1H), 2.01 – 1.88 (m, 1H), 1.82 (dd, *J* = 12.2, 4.5 Hz, 1H), 1.72 – 1.58 (m, 2H), 1.57 – 1.48 (m, 2H), 1.47 – 1.35 (m, 2H), 1.34 – 1.21 (m, 3H), 1.16 – 1.01 (m, 1H).

^{13}C NMR (100 MHz, $CDCl_3$): δ 144.5, 128.3, 127.6, 126.5, 90.0, 87.3, 64.3, 47.4, 39.5, 35.9, 34.0, 31.1, 26.6, 22.6, 22.1.

Note: A grease and water signal are observed in the ^{1}H and ^{13}C spectra.

IR (Neat Film, NaCl): 3334, 2953, 2873, 1446, 1376, 1128, 1100, 1046 cm^{-1}.

HRMS (FD+): *m/z* calc'd for $C_{17}H_{22}O_2$ $[M]^{+\cdot}$: 258.16143, found 258.16203.

Optical Rotation: $[\alpha]_D^{23}$ –36.0 (c = 0.58, $CHCl_3$).

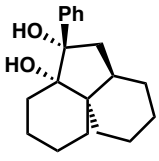

205

(4a*S*,5*S*,6a*R*,10a*R*)-5-phenyldecahydrobenzo[*c*]indene-4a,5(5*H*)-diol (205)

Prepared from diketone **197k** according to General Procedure F. Purification by preparative TLC (40% Et_2O/hexanes) afforded the title compound as a colorless crystalline solid (5.2 mg, 0.018 mmol, 37% yield). Absolute and relative stereochemistry were assigned by X-ray crystallography (vide infra).

^{1}H NMR (400 MHz, $CDCl_3$): δ 7.64 – 7.55 (m, 2H), 7.38 – 7.30 (m, 2H), 7.30 – 7.21 (m, 1H), 3.92 (s, 1H), 2.77 (s, 1H), 2.58 (t, *J* = 13.4 Hz, 1H), 2.20 – 2.05 (m, 1H), 1.82 – 1.66 (m, 4H), 1.61 (dd, *J* = 11.6, 2.9 Hz, 1H), 1.55 – 1.43 (m, 3H), 1.43 – 1.14 (m, 6H), 1.13 – 0.96 (m, 2H), 0.20 – 0.02 (m, 1H).

^{13}C NMR (100 MHz, $CDCl_3$): δ 144.6, 127.9, 127.6, 127.2, 83.7, 83.2, 46.6, 42.2, 41.7, 34.1, 28.2, 26.3, 24.7, 22.2, 21.4, 20.9, 19.2.

IR (Neat Film, NaCl): 3310, 2924, 2857, 1495, 1444, 1391, 1143, 1038, 1028 cm^{-1}.

HRMS (FD+): *m/z* calc'd for $C_{19}H_{26}O_2$ $[M]^{+\cdot}$: 286.19273, found 286.19351.

Optical Rotation: $[\alpha]_D^{23}$ –27.4 (c = 0.43, $CHCl_3$).

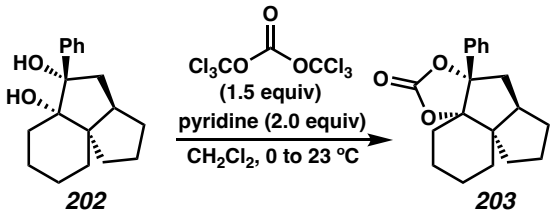

(3a*S*,4a*R*,7a*S*,11a*S*)-3a-phenyldecahydrocyclopenta[3,3a]indeno[1,7a-*d*][1,3]dioxol-2-onediol (203)

To a flame dried 2-dram vial was added a solution of diol **202** (5.0 mg, 0.02 mmol, 1.0 equiv) in CH_2Cl_2 (0.02 M, 1.0 mL) then the solution was cooled to 0 °C. Pyridine (3 μL, 0.04 mmol, 2.0 equiv) was added before a solution of triphosgene (8.9 mg, 0.03 mmol, 1.5 equiv) in CH_2Cl_2 (0.06 M, 0.5 mL) was added dropwise at 0 °C. *Note: serious caution must*

be taken when working with triphosgene due to its high toxicity. Review MSDS information before using. Upon complete consumption of starting material by TLC, the reaction was diluted with saturated aqueous NH_4Cl, extracted with Et_2O (3x), rinsed with 1 M HCl, saturated aqueous $NaHCO_3$, and brine. Following this the organic layer was dried with Na_2SO_4, filtered, and concentrated under reduced pressure. Purification of the crude compound via flash column chromatography (0–50% Et_2O/hexanes) afforded the title compound as a colorless oil (4.1 mg, 0.014 mmol, 69% yield). Successful formation of the carbonate (assigned via ^1H and ^{13}C NMR) is consistent with **202** being the cis-diol. This is due to the high degree of ring strain associated with the corresponding trans-fused [3.3.0] ring system.[29]

^{1}H NMR (400 MHz, $CDCl_3$): δ 7.54 – 7.48 (m, 2H), 7.46 – 7.34 (m, 3H), 2.59 (t, *J* = 13.6 Hz, 1H), 2.48 – 2.36 (m, 1H), 2.19 – 2.03 (m, 3H), 1.76 – 1.65 (m, 2H), 1.64 – 1.56 (m, 2H), 1.54 – 1.30 (m, 4H), 1.29 – 1.15 (m, 3H), 0.36 – 0.20 (m, 1H).

Note: A grease and water signal are observed in the ^1H spectrum.

^{13}C NMR (100 MHz, $CDCl_3$): δ 154.9, 136.4, 129.0, 128.5, 127.0, 102.4, 91.7, 58.2, 47.1, 35.2, 30.3, 26.6, 25.9, 25.2, 22.3, 21.0, 20.4.

IR (Neat Film, NaCl): 2948, 2877, 1794, 1447, 1298, 1272, 1241, 1060 cm^{-1}.

HRMS (FD+): *m/z* calc'd for $C_{19}H_{22}O_3$ $[M]^{+\cdot}$: 298.15635, found 298.15641.

Optical Rotation: $[\alpha]_D^{23}$ –12.2 (c = 0.34, $CHCl_3$).

General Procedure G: Aldol Condensation[30]

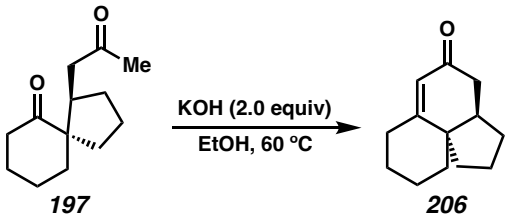

197 ***206***

To a flame dried round bottom flask was added a solution of KOH (2.3 equiv) in EtOH (0.14 M) followed by a solution of the corresponding ketone (1.0 equiv) in EtOH (0.1 M). The reaction was heated to 60 °C. Upon complete consumption of starting material by TLC, the reaction was quenched with AcOH (2.3 equiv) and concentrated under reduced pressure. The crude reaction mixture was purified by silica gel flash column chromatography to afford the corresponding enone.

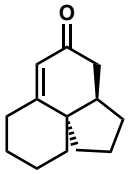

206

(3a*R*,10a*S*)-2,3,3a,4,7,8,9,10-octahydrocyclopenta[*d*]naphthalen-5(1*H*)-one (206)

Prepared from diketone **197b** according to General Procedure G. Purification by flash column chromatography (0–45% Et_2O/hexanes) afforded the title compound as a colorless oil (13.1 mg, 0.069 mmol, 72% yield).

^{1}H NMR (400 MHz, $CDCl_3$): δ 5.77 (s, 1H), 2.42 (dd, *J* = 16.5, 3.7 Hz, 1H), 2.35 – 2.15 (m, 3H), 2.15 – 1.94 (m, 3H), 1.83 – 1.67 (m, 5H), 1.62 – 1.53 (m, 1H), 1.51 – 1.27 (m, 4H).

^{13}C NMR (100 MHz, $CDCl_3$): δ 200.6, 175.7, 123.2, 48.4, 44.8, 37.9, 35.1, 32.3, 31.7, 30.6, 26.2, 21.9, 20.0.

IR (Neat Film, NaCl): 2937, 2870, 1668, 1607, 1445, 1369, 1277, 1250, 1213, 1164, 1133, 1101 cm^{-1}.

HRMS (FI+): *m/z* calc'd for $C_{13}H_{18}O$ $[M]^{+\cdot}$: 190.13522, found 190.13552.

Optical Rotation: $[\alpha]_D^{23}$ +127.5 (c = 1.09, $CHCl_3$).

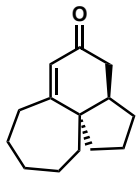

207

(3a*R*,11a*S*)-2,3,3a,4,8,9,10,11-octahydro-1*H*-cyclohepta[*d*]inden-5(7*H*)-one (207)

Prepared from diketone **197f** according to General Procedure G. Purification by preparative TLC (30% Et_2O/hexanes) afforded the title compound as a colorless oil (6.1 mg, 0.030 mmol, 66% yield).

^{1}H NMR (400 MHz, $CDCl_3$): δ 5.71 (s, 1H), 2.63 – 2.52 (m, 1H), 2.45 (dd, *J* = 17.6, 4.8 Hz, 1H), 2.39 – 2.27 (m, 2H), 2.19 – 1.99 (m, 2H), 1.87 – 1.53 (m, 8H), 1.53 – 1.36 (m, 3H), 1.32 – 1.15 (m, 2H).

^{13}C NMR (100 MHz, $CDCl_3$): δ 201.4, 174.0, 127.1, 49.4, 47.7, 38.2, 34.9, 30.7, 30.7, 26.6, 26.3, 26.2, 25.5, 20.5.

Note: A grease and water signal are observed in the ^{1}H and ^{13}C spectra.

IR (Neat Film, NaCl): 2929, 2870, 1665, 1600, 1443, 1368, 1283, 1254 cm^{-1}.

HRMS (FI+): *m/z* calc'd for $C_{13}H_{18}O$ $[M]^{+\cdot}$: 204.15087, found 204.15113.

Optical Rotation: $[\alpha]_D^{23}$ +41.7 (c = 0.51, $CHCl_3$).

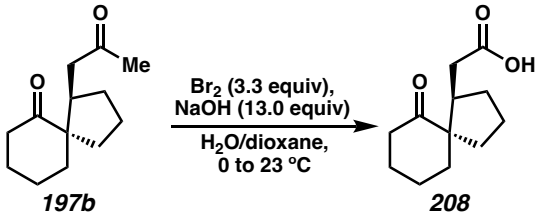

197b *208*

2-((1*R*,5*S*)-6-oxospiro[4.5]decan-1-yl)acetic acid (208)

To a dried 2-dram vial was added a solution of diketone **197b** (20 mg, 0.096 mmol, 1.0 equiv) in 1,4-dioxane (0.1 M, 1.0 mL) and water (0.5 M, 0.2 mL) before being cooled to 0 °C. A solution of NaOBr in water was then prepared: NaOH (50 mg, 1.25 mmol, 13.0 equiv) was dissolved in water (2.6 M, 0.48 mL) and cooled to 0 °C. Bromine (16.5 μL, 0.32 mmol, 3.3 equiv) was then added dropwise at 0 °C. The NaOBr solution was then added dropwise to the solution of **197b** at 0 °C. The reaction was allowed to gradually warm to 23 °C. Upon complete consumption of starting material by TLC, the reaction was diluted with 2 mL of water and then quenched by slow addition of concentrated HCl (until pH was 1.0). The mixture was then extracted with EtOAc (3x), rinsed with brine, dried with Na_2SO_4, filtered, and concentrated under reduced pressure. Purification of the crude mixture via preparative TLC purification (79% Et_2O, 20% hexanes, 1% AcOH) afforded the title compound as a white solid (6.9 mg, 0.033 mmol, 34% yield).

^{1}H NMR (400 MHz, $CDCl_3$): δ 2.95 – 2.82 (m, 1H), 2.50 – 2.35 (m, 3H), 2.11 (dd, *J* = 15.0, 10.4 Hz, 1H), 2.04 – 1.92 (m, 2H), 1.92 – 1.80 (m, 1H), 1.80 – 1.48 (m, 8H), 1.39 – 1.26 (m, 1H).

^{13}C NMR (100 MHz, $CDCl_3$): δ 213.9, 178.6, 58.3, 40.1, 39.3, 35.1, 35.0, 31.7, 29.9, 27.1, 21.8, 21.8.

IR (Neat Film, NaCl): 3021, 2941, 2865, 1705, 1444, 1420, 1281, 1235, 1164, 1129 cm^{-1}.

HRMS (FD+): *m/z* calc'd for $C_{12}H_{18}O_3$ $[M]^{+\cdot}$: 210.12505, found 210.12518.

Optical Rotation: $[\alpha]_D^{23}$ +7.7 (c = 0.58, $CHCl_3$).

3.4.3 Quantum Mechanics Calculations:

General Notes

All quantum mechanics calculations were carried out with the ORCA program.[31] Geometry optimizations, harmonic frequency calculations, and single-point energy evaluations were carried out with density functional theory (DFT). The PBE0 hybrid functional[32] paired with Becke–Johnson damped D4 dispersion corrections[33], henceforth referred to as PBE0-D4, was used in this study. For geometry optimization and harmonic frequency calculations, Pd is described by the def2-TZVP all electron basis set[34] and the ECP28MWB small-core (18 explicit valence electrons) quasi-relativistic pseudopotential,[35] while C, H, N, and P are assigned the def2-SVP basis. Diffuse functions are added to oxygen (ma-def2-SVP). Herein, we refer to this composite basis set as BS1. This combination of functional and basis set was chosen as it has been shown to be reliable in prior benchmarking studies of similar systems, and has subsequently been employed to study various Pd-catalyzed reactions reported by our group and has remained robust, providing results in good agreement with experimental observations.[36] Geometry optimization and harmonic frequency calculations were carried out with the CPCM implicit solvation model for toluene (PhMe, ε = 2.4). For all calculations employing CPCM, surface charges are described by the improved Gaussian charge scheme of Neese and coworkers

with a scaled Van der Waals cavity (α = 1.2).[37] All Hessians were computed analytically. Stationary points are characterized by the correct number of imaginary vibrational modes (zero for minima and one for saddle points). Intrinsic reaction coordinate (IRC) analysis confirms the nature of transition states.[38] Cartesian coordinates of all optimized structures are included as ".xyz" files, available online in a compressed zip file format.

Electronic energies are further refined with single-point calculations employing the PBE0-D4 functional[39] and the def2-TZVPP basis set on all atoms (with the ECP28MWB pseudopotential for Pd) with additional diffuse functions on O (ma-def2-TZVPP). This mixed basis is henceforth referred to as BS2. Solvation was accounted for with CPCM as mentioned above (PhMe, ε = 2.4). Final Gibbs free energies were obtained by applying thermodynamic corrections to the calculated electronic energies. Thermodynamic corrections from harmonic frequency calculations employ the quasi-ridged rotor harmonic oscillator approach to correct for the breakdown of the harmonic oscillator approximation at low vibrational frequencies.[40] The translational (S_{trans}) and rotational entropy (S_{rot}) contributions to the Gibbs free energy calculated for a complex in condensed phase are *ca.* 40–60% of the values obtained assuming an ideal gas.[41] As suggested in the literature, S_{trans} and S_{rot} obtained by ideal gas treatment are scaled by a factor of 0.5 to obtain the final condensed phase values.[42] Hence, the final Gibbs free energy at 313.15 K is calculated as:

$$G^*_{solv} = E^{BS2}_{el,solv} + ZPE + E_{trans} + E_{rot} + E_{vib} + k_b - T\left(S_{el} + S_{vib} + \frac{1}{2}S_{trans} + \frac{1}{2}S_{rot}\right)$$

The resolution of identity (RI) and Chain-of-Spheres (COS) approximations are employed for efficient evaluation of Coulomb and exchange integrals, respectively.[43] The def2/J auxiliary basis[44] is employed for all atoms except oxygen, for which a suitable auxiliary

was obtained via the automatic generation algorithm in the ORCA program (keyword: *AutoAux*). [45] Very fine grid settings are employed in all calculations (optimization/frequency calculations: DefGrid2, single point calculations: DefGrid3).

Conformer searching was carried out for each stationary point individually using the meta-dynamics-based CREST program (using GNF-FF) from the Grimme group.[46] Duplicate conformers were removed, low energy conformers were subsequently optimized, and energies were evaluated at the cheaper PBE0-D4/def2-TZVPP (Pd), ma-def2-TZVPP (O), def2-TZVPP/CPCM(PhMe)//PBE-D4/def2-TZVP (Pd), ma-def2-SV(P) (O), def2-SV(P) level of theory. The final low energy conformers were further optimized at the level of theory mentioned prior, and the free energies and the optimized structures of the lowest-energy conformers are reported. It is assumed that interconversion of conformers of a single stationary point proceeds with a low barrier compared to bond formation and breakage processes and is inconsequential to the evaluation of reaction pathways.

Comparison of Michael Addition Transition State Barriers:

Explicit conformer searching for rotation about the Pd–O–C–C(enolate) dihedral was performed for the Michael addition transition states (Figure 3.6). A strong preference for placement of the enolate electrophile tether *syn* to the ligand *t*-Bu group is observed for transition states to form *S* stereocenters at the spirocyclic quaternary carbon (Figure S1 **TS17a** and **TS17c**). This arrangement not only avoids undesired steric interactions of the rather bulky cyclohexyl group and the ligand *t*-Bu group but also places the *Re* face in the more sterically accessible orientation, external of the Pd complex.

In contrast, to form the *R* spirocyclic stereocenters in products **212b** and **212d**, either internal electrophile approach to the sterically hindered *Si* face of the enolate or positioning the bulky cyclohexyl group *syn* to the ligand *t*-Bu substituent is required. These destabilizing steric interactions contribute to the increase in energy barriers of **TS17b**, **TS17d**, **TS19**, and **TS21**. Between **TS17b** and **TS19**, steric clash resulting from internal electrophile approach outweighs preference for placement of electrophile tether *syn* to the ligand *t*-Bu group, leading to **TS17b** being the lower energy conformer. On the other hand, these two steric interactions cause energy increase of similar magnitudes in both **TS17d** and **TS21**.

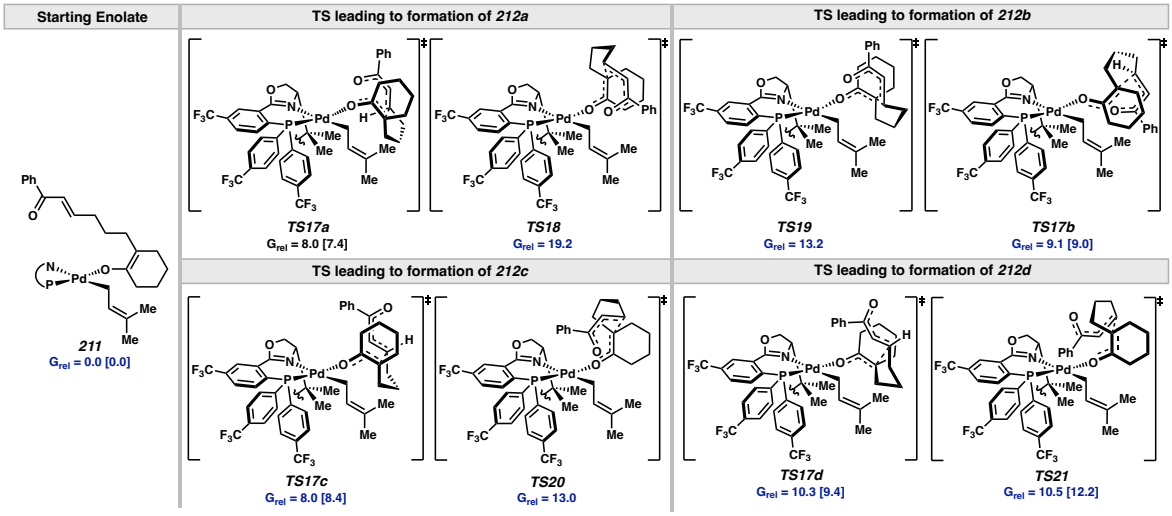

Figure 3.6 *Relative free energies for transition states explored for the Michael addition process. Gibbs free energies in kcal/mol computed at the PBE0-D4/BS2/CPCM(PhMe)//PBE-D4/def2-TZVP (Pd), ma-def2-SV(P) (O), def2-SV(P) level of theory, and in brackets are energies calculated at the PBE0-D4/BS2/CPCM(PhMe)//PBE0-D4/BS1/CPCM(PhMe) level of theory at 313.15 K.*

The major stereoisomer predicted based on these calculations is consistent with the major stereoisomer observed in all compounds which were structurally elucidated via x-ray crystallography (**197a**, **197b**, **201a**, **205**). Although additional computational and experimental evidence would be required to explain other observations regarding distinct substrate classes, we hypothesize that more general insights can potentially be taken from this stereochemical model. For instance, N-benzoyl lactam **197g** is modestly enantioselective but has good diastereoselectivity. Looking at **TS17a**, we imagine that the N-benzoyl moiety might have a destabilizing steric interaction with our ligand, potentially raising the energy of that transition state and thus decreasing the energy gap with the transition state leading to formation of the enantiomeric product. Tetralone **197h** has good diastereoselectivity but poor enantioselectivity for both diastereomers. Electronically and sterically, tetralones are a unique substrate class and it is speculated that this fused aryl ring could influence the energies of many of the transition structures investigated. In addition, phenyl ester **197i** is formed in poor diastereoselectivity with decent levels of enantioselectivity, which is potentially due to altered geometrical elements (i.e. enolate conformation) and steric interactions with the ligand.

Computed Energies for Intermediates Post Michael Addition:

As apically bound enolate intermediate **212a** is an unusual and high-energy intermediate, we propose that following its formation, isomerization to lower-energy Pd intermediates can occur. In addition to intermediates **213** and **224** (Figure 3.9), various Pd intermediates were explored and are shown in Figure 3.7.

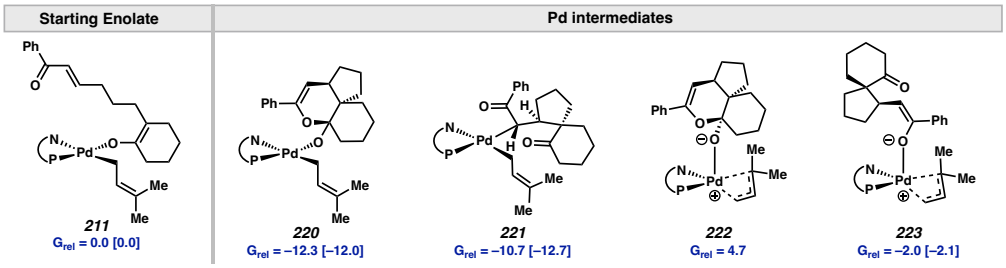

Figure 3.7 *Relative free energies for Pd intermediates explored. Gibbs free energies in kcal/mol computed at the PBE0-D4/BS2/CPCM(PhMe)//PBE-D4/def2-TZVP (Pd), ma-def2-SV(P) (O), def2-SV(P) level of theory, and in brackets are energies calculated at the PBE0-D4/BS2/CPCM(PhMe)//PBE0-D4/BS1/CPCM(PhMe) level of theory at 313.15 K.*

Investigation of the Mechanism of Proton Transfer:

We hypothesized that in analogy to previously investigated systems,[36] catalyst turnover can be achieved through the proton transfer from the prenyl group to a Pd enolate and the concomitant reduction of Pd. We therefore sampled the inner-sphere, outer-sphere, and N-detached inner-sphere proton transfer transition states (Figure 3.8) analogous to the lowest energy pathways of each type of mechanism observed in previously investigated systems.[Error! Bookmark not defined.] Proton transfer to both *Si* and *Re* face of the enolates were sampled for the N-detached inner-sphere pathway.

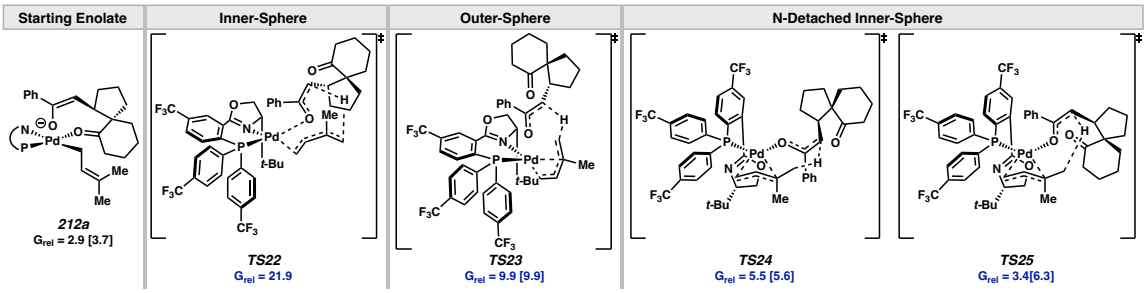

Figure 3.8 *Relative free energies for proton transfer pathways studied. Gibbs free energies in kcal/mol computed at the PBE0-D4/BS2/CPCM(PhMe)//PBE-D4/def2-TZVP (Pd), ma-def2-SV(P) (O), def2-SV(P) level of theory, and in brackets are energies calculated at the PBE0-D4/BS2/CPCM(PhMe)//PBE0-D4/BS1/CPCM(PhMe) level of theory at 313.15 K. The lowest-energy conformer for TS25 at the PBE0-D4/BS2/CPCM(PhMe)//PBE-D4/def2-TZVP (Pd), ma-def2-SV(P) (O), def2-SV(P) level of theory failed to converge in geometry optimization at the PBE0-D4/BS2/CPCM(PhMe)//PBE0-D4/BS1/CPCM(PhMe) level of theory (due to a small imaginary mode corresponding to CF_3 rotation that we were unable to eliminate), and therefore the TS25 energy shown in brackets is of a different conformer.*

Preliminary Computational Investigation of the Thermodynamics of the Reaction Post Decarboxylation:

We propose that simultaneous control of vicinal stereocenters can occur either via an irreversible Michael addition or a reversible C–C bond formation coupled to a subsequent irreversible process. We began by investigating the energetics of the Michael

addition (Figure S4). Computationally, we found that the Michael addition of Pd enolate **211** to form spirocycle **212a** proceeds with a $\Delta G^{\ddagger}$ of 7.4 kcal/mol. Further isomerization of Pd-bound ketone **212a** to Pd enolate **213** releases an additional 16.2 kcal/mol of energy (Figure 3.9), leading to an overall exothermic process with a ΔG of –12.5 kcal/mol from intermediate **211**. The reverse process displays a 19.9 kcal/mol energy barrier, which is likely still achievable at the reaction temperature. Hence, we began to study select potential mechanisms for the subsequent proton transfer process. Among the pathways studied (Figure S3), an *N*-detached inner-sphere pathway was found to be the most energetically favorable, with $\Delta G^{\ddagger}$ of 5.6 kcal/mol and ΔG of –9.5 kcal/mol. However, further computational investigation of the isomerizations of Pd intermediates **212a**, **213**, and **224** (along with all corresponding stereoisomers such as **212b**–**d**, etc.) is required to determine whether these isomerizations are important to understanding the thermodynamics/kinetics of the overall reaction. These areas are currently being investigated by our group and will be reported in due course.

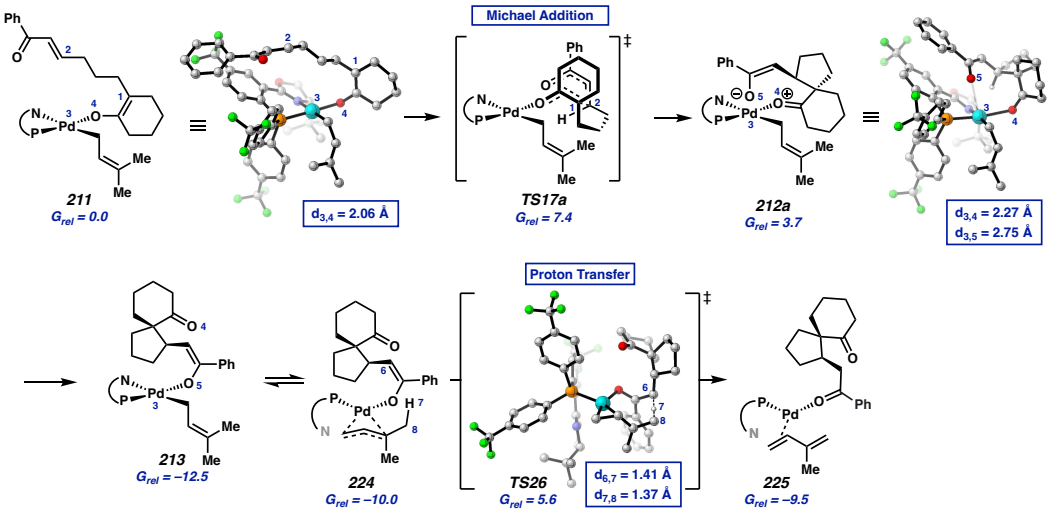

Figure 3.9 *Proposed reaction pathway for Michael addition and proton transfer and the computed relative energies of relevant intermediates and transition states. Gibbs free energies in kcal/mol computed at the PBE0-D4/BS2/CPCM(PhMe)//PBE0-D4/BS1/CPCM(PhMe) level of theory at 313.15 K.*

3.4.4 2D NMR Analysis of Select Compounds:

Compound **202**

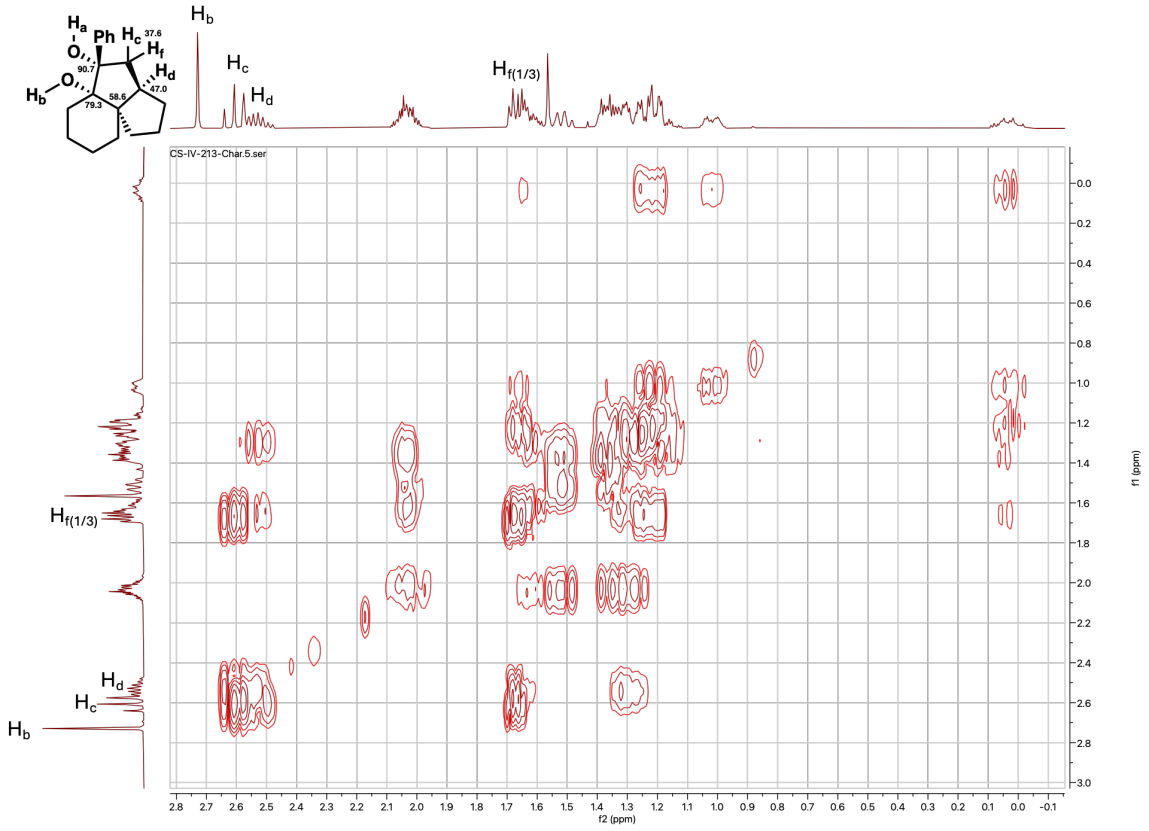

Figure 3.10 *^{1}H–^{1}H COSY NMR spectrum of* ***202*** *(400 MHz, $CDCl_3$)*

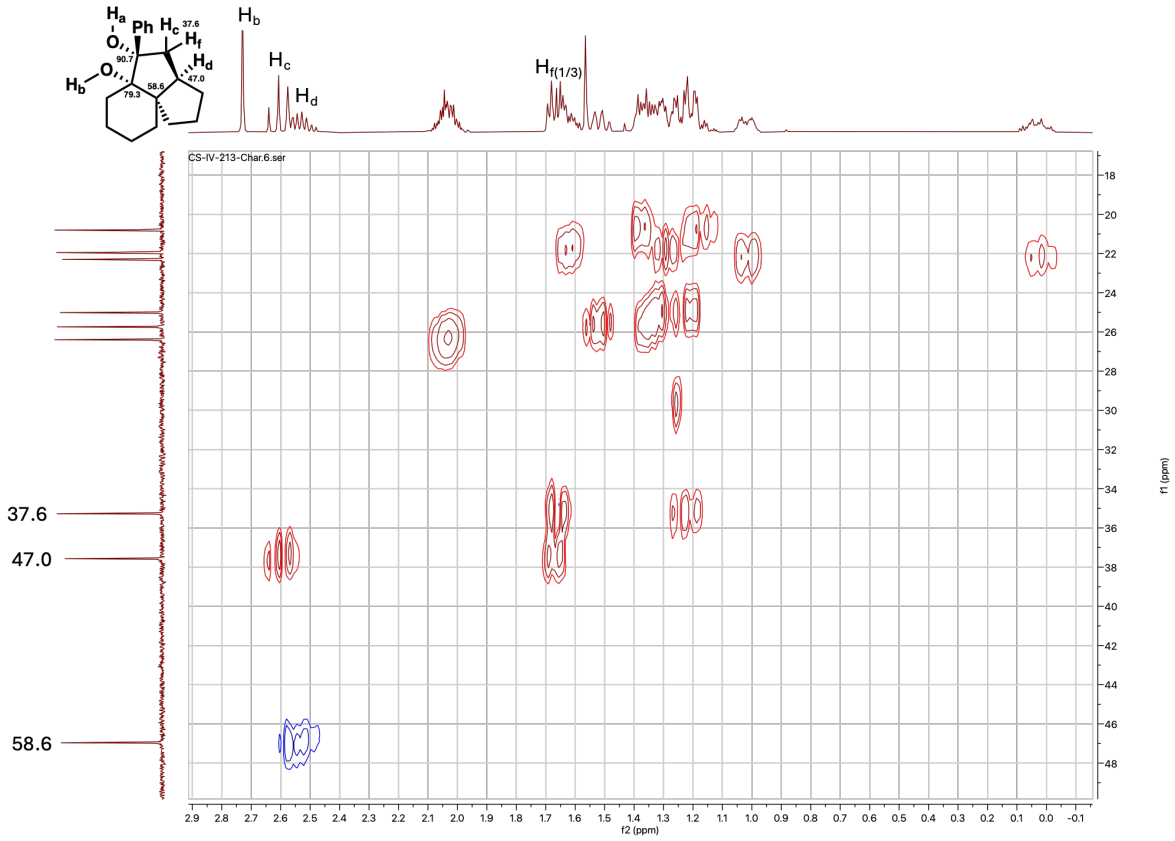

Figure 3.11 *^{1}H–^{13}C HSQC NMR spectrum of* ***202*** *(400 MHz, $CDCl_3$)*

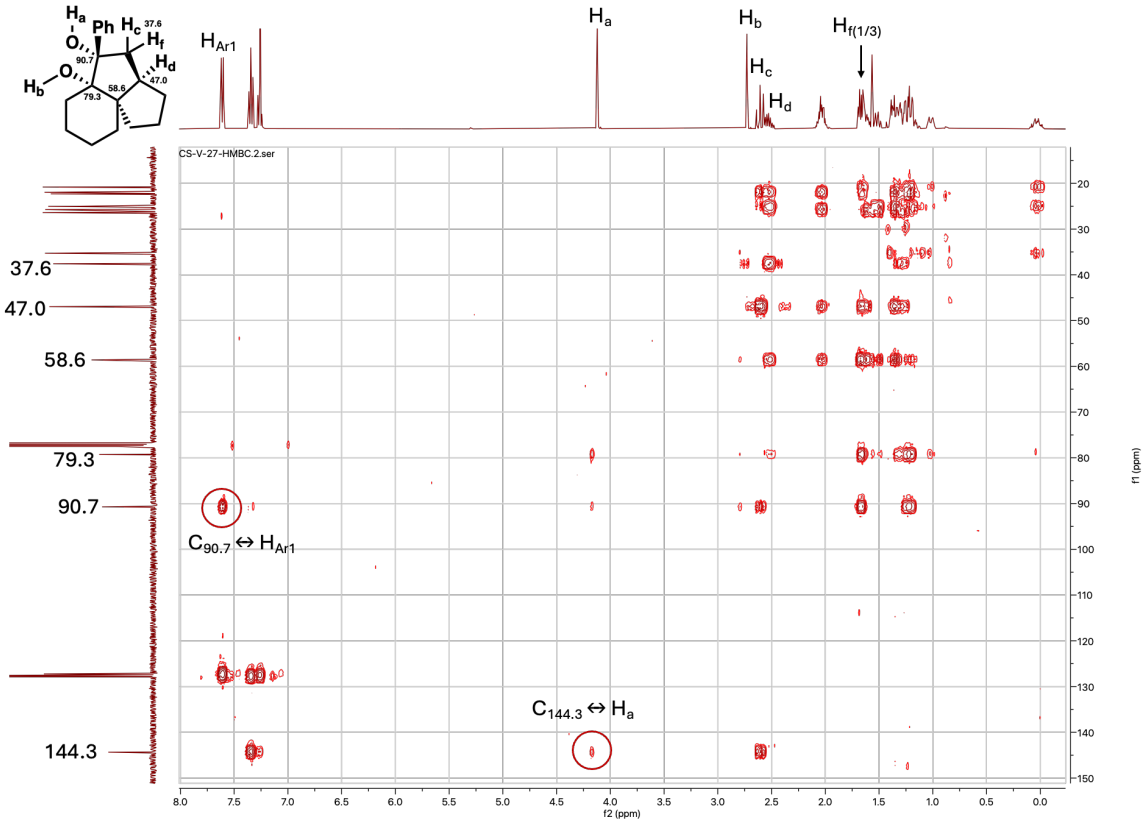

Figure 3.12 *^{1}H–^{13}C HMBC NMR spectrum of* ***202*** *(400 MHz, $CDCl_3$)*

Compound **206**

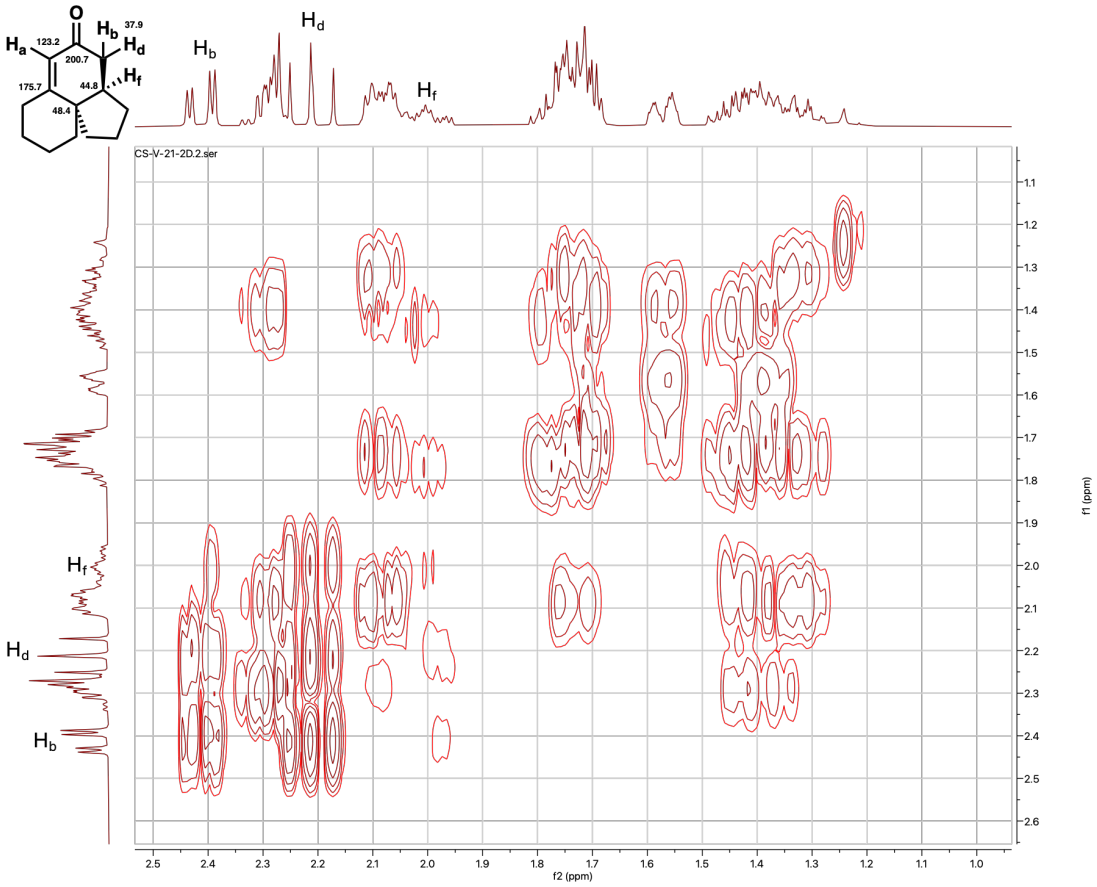

Figure 3.13 *^{1}H–^{1}H COSY NMR spectrum of* ***206*** *(400 MHz, $CDCl_3$)*

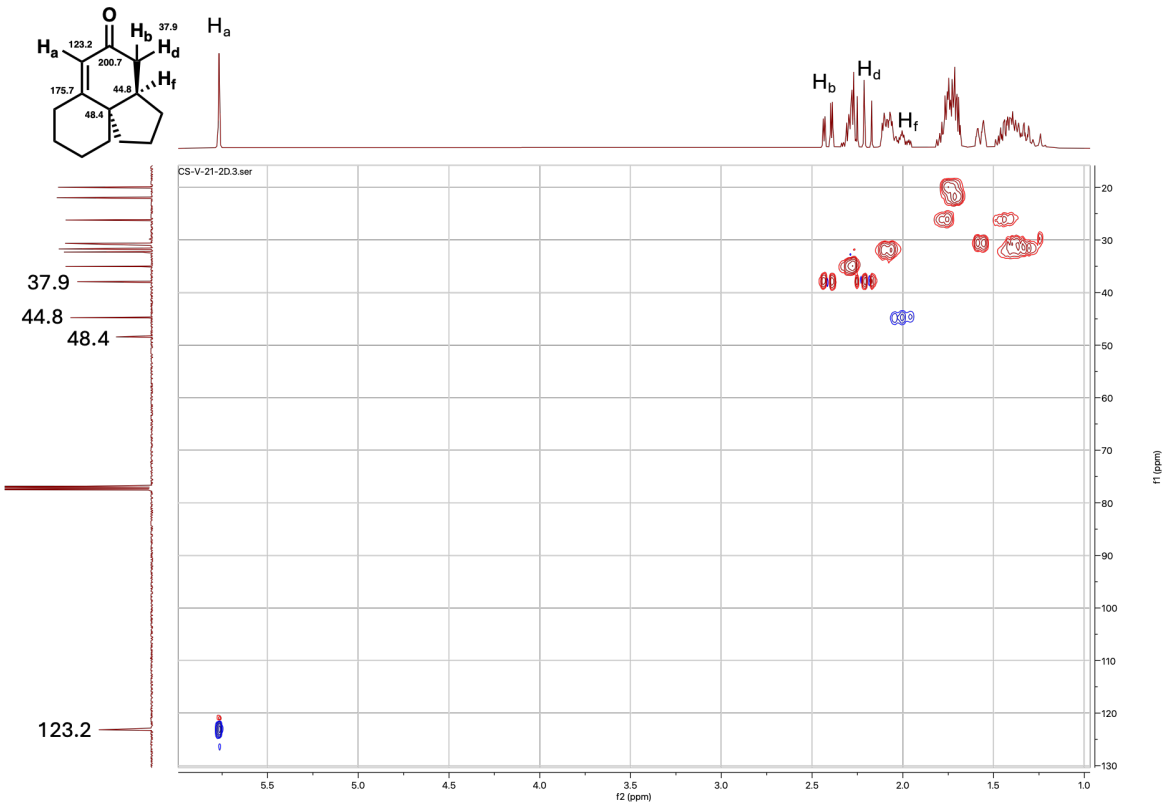

Figure 3.14 *^{1}H–^{13}C HSQC NMR spectrum of* ***206*** *(400 MHz, $CDCl_3$)*

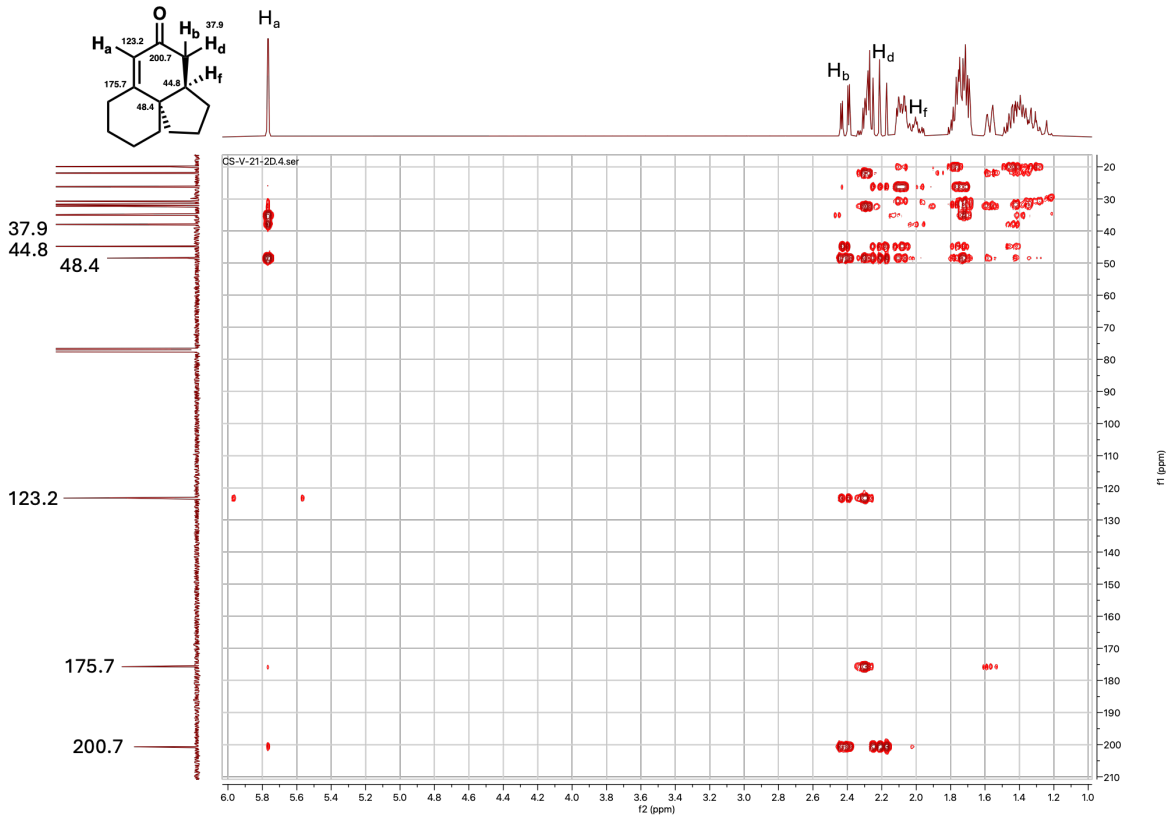

Figure 3.15 *^{1}H–^{13}C HMBC NMR spectrum of* ***206*** *(400 MHz, $CDCl_3$)*

3.4.5 Preliminary Experimental Mechanistic Investigations:

^{31}P NMR Studies and ^{1}H Time course:

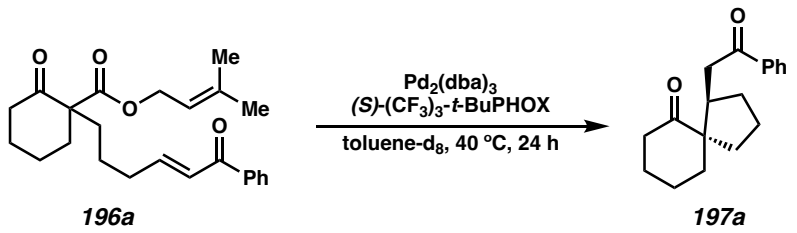

196a ***197a***

NMR Sample preparation ^{31}P NMR monitoring and ^{1}H time course:

In a nitrogen filled glovebox, an oven-dried 4 mL vial was charged with a stir bar, $Pd_2(dba)_3$ (1.4 mg, 0.0015 mmol, 2.5 mol %), *(S)*-$(CF_3)_3$-*t*-BuPHOX (2.3 mg, 0.0039 mmol, 6.5 mol %), and toluene-d_8 (0.8 mL). The catalyst solution was stirred at 23 ºC for 20 min. A solution of substrate **196a** (0.06 mmol, 1 equiv) in toluene-d_8 (0.2 mL) was prepared and added to an NMR tube with a threaded top. To this solution was added 0.4 mL of the catalyst solution before the tube was sealed with a Teflon-lined lid and brought to the NMR instrument. At 25 ºC, initial ^{31}P and ^{1}H NMRs were taken of this mixture followed by additional ^{31}P and ^{1}H NMR spectra taken upon heating to 40 ºC. ^{1}H NMR spectra were taken (at 40 ºC) every 5 minutes for 1 hour followed by an additional ^{31}P NMR spectrum. ^{1}H NMR spectra were then taken (at 40 ºC) every 5 minutes for an additional ~4 hours. The reaction was then heated overnight at 40 ºC in an oil bath. A final ^{31}P and ^{1}H NMRs were taken at 25 ºC following completion of the reaction (after 24 hours). Purification by flash column chromatography (0–60% Et_2O/hexanes) afforded the title compound as a white crystalline solid (9.1 mg, 0.034 mmol, 56% yield, 93% ee). The full characterization for this material is above.

In a separate NMR tube, the remaining 0.4 mL of catalyst solution prepared above were added followed by 0.2 mL of toluene- d_8. At 25 ºC, ^{31}P and ^{1}H NMR were taken of this mixture.

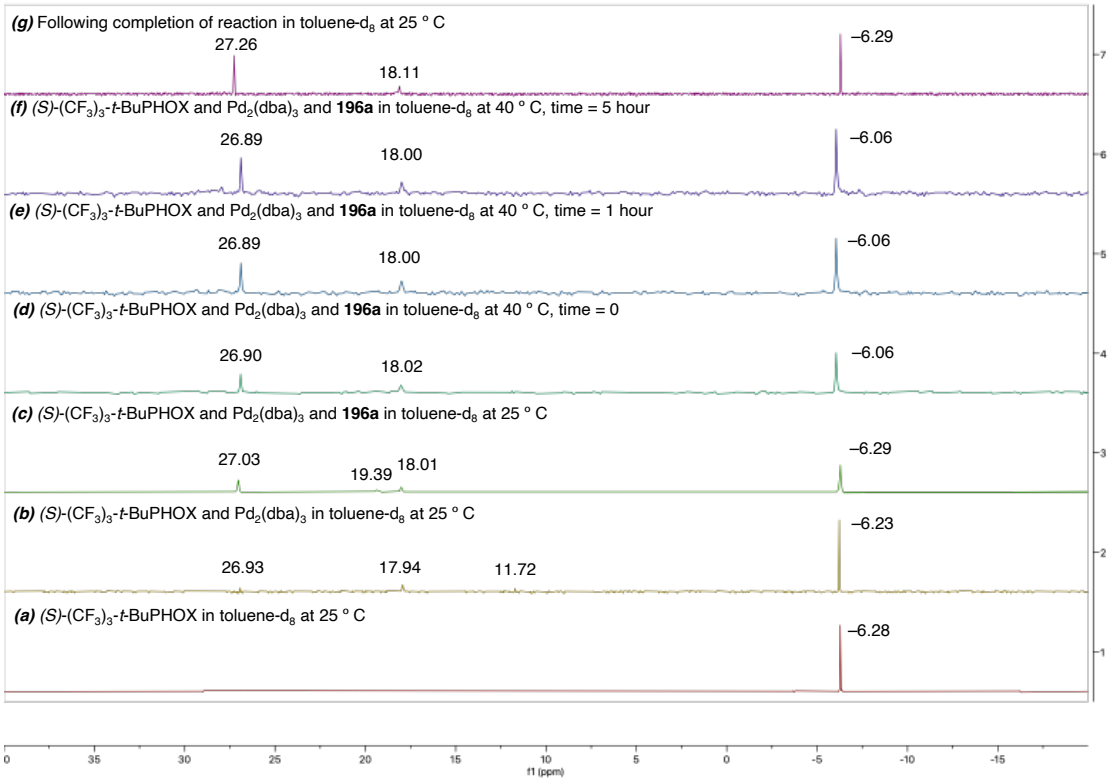

Figure 3.16 *^{31}P spectra of various relevant mixtures (400 MHz, toluene-d_8).*

This displays the peaks observed in the ^{31}P NMR spectra of various species and reaction mixtures throughout the course of the reaction (Figure 3.16). Apparently, *(S)*-$(CF_3)_3$-*t*-BuPHOX alone in toluene-d_8 appears at –6.28 ppm as a sharp singlet (spectrum a). Upon formation of the precatalyst solution a similar peak is observed (at –6.23 ppm) which is logical considering the excess stoichiometry of ligand (spectrum b). A peak with a similar chemical shift is observed throughout the duration of the experiment. Three new species are observed at 11.72, 17.94, and 26.93 ppm respectively. Following addition of

substrate **196a** and at 25 ºC, the peak around 11.72 ppm is no longer observable although a new broad peak is observed at 19.39 ppm (spectrum c). When this mixture is heated to 40 ºC the signal believed to correspond to free ligand shifts modestly to –6.06 ppm whereas the two species around 18.02 and 26.90 ppm persist (spectrum d). At 40 ºC and over 5 hours the relative intensity of the species around 26.89 ppm appears to grow in slightly (spectra e and f). Following completion of the reaction at 40 ºC it was cooled to 25 ºC to give spectrum g which shows three similar signals as previous spectra. Further experimentation is required to elucidate the structures of these species and determine their relevance to catalysis. This is an active area of investigation in our group and will be reported in due course.

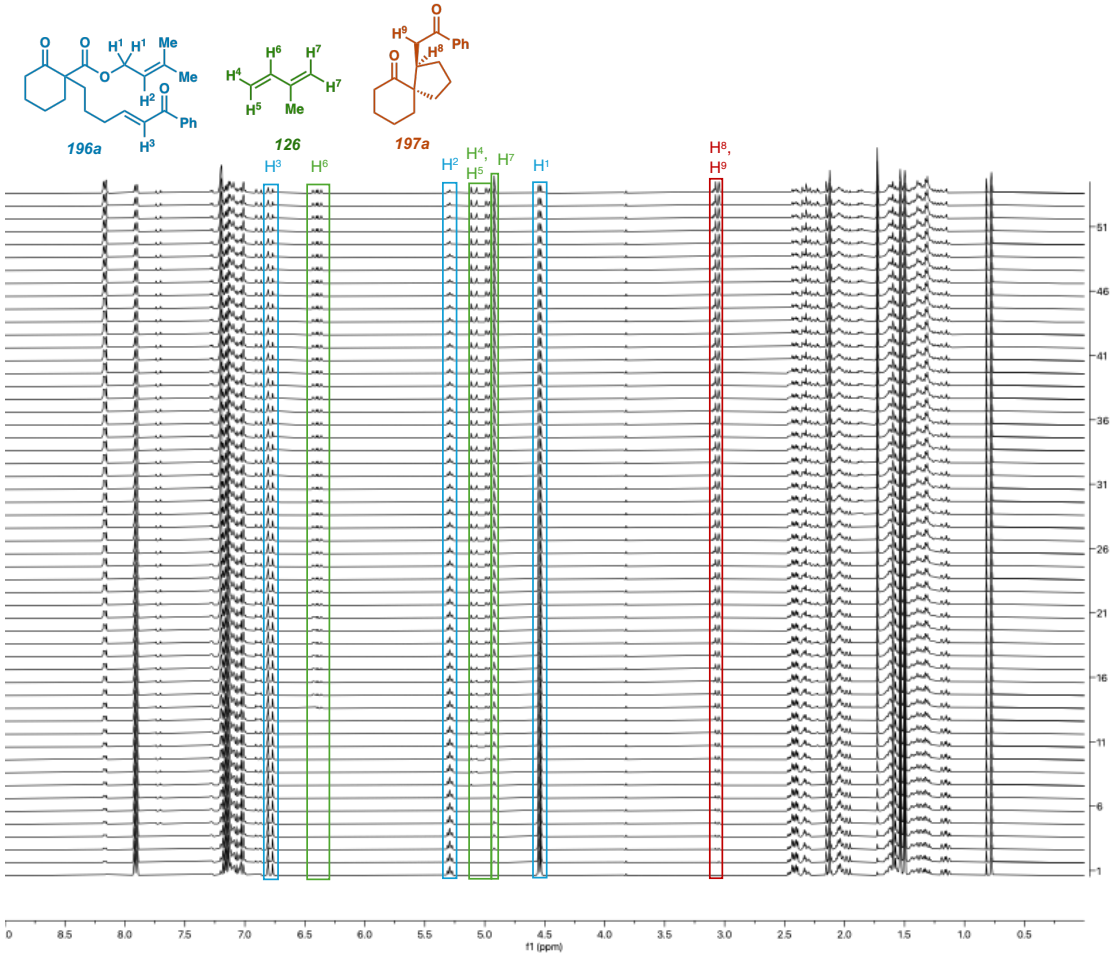

Figure 3.17 *^{1}H spectra timecourse over ~ 5 hours (400 MHz, toluene-d_8).*

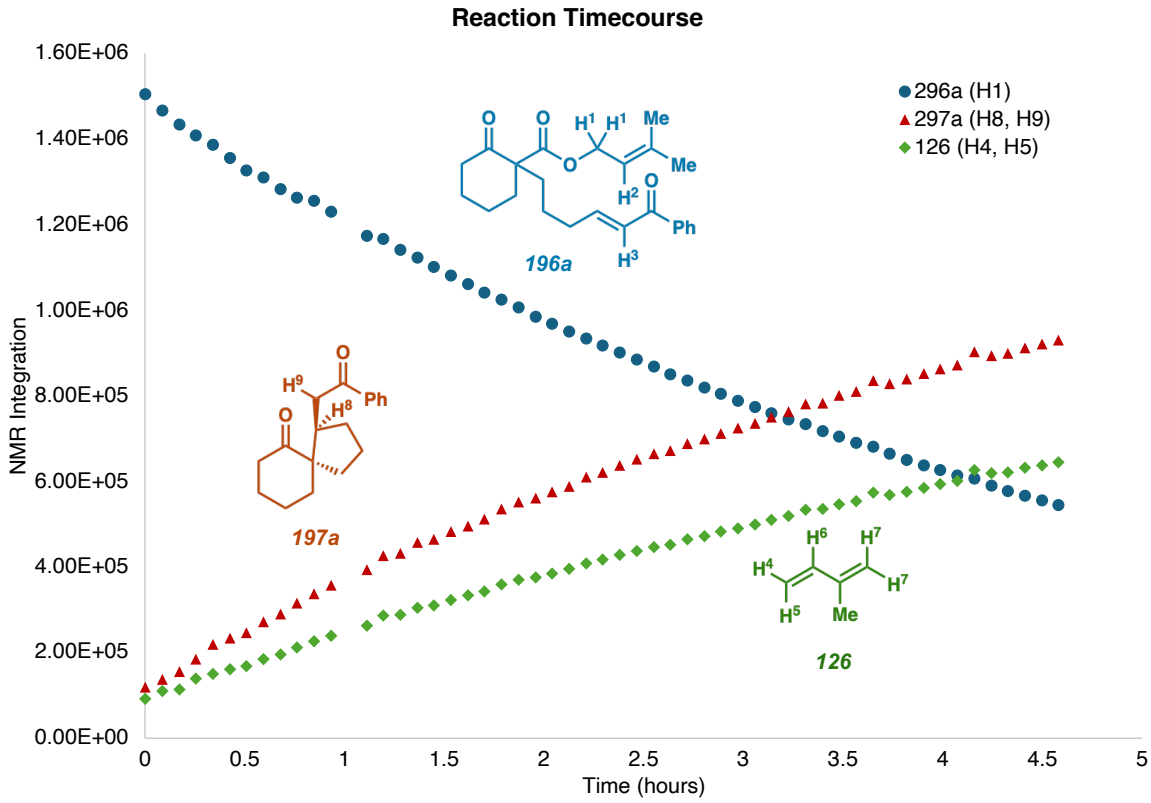

Figure 3.18 *^{1}H NMR timecourse plot of integration vs time.*

These data (presented in Figure 3.17 and 3.18) display the evolution of products from this reaction over time as monitored by proton NMR. These data present the time points at 40 ºC that were taken approximately every 5 minutes. It is worth noting that minimal conversion does occur at 25 ºC, although it is quite sluggish. A set of two protons was selected for each of the three major species involved during the course of this reaction. For **196a**, the allylic protons H1 were utilized. For **197a**, the methine H8 and one of the protons α to the phenyl ketone, H9, was used. Finally, for isoprene two vinylic protons, H4 and H5 were used. The deflated integration of isoprene's vinylic protons might be due to it evaporating into the headspace during the reaction (boiling point = 34 ºC). Further studies

related to elucidating the mechanism of this reaction and its kinetic profile are currently ongoing.

3.5 REFERENCES AND NOTES

(1) (a) Ding, A.; Meazza, M.; Guo, H.; Yang, J. W.; Rios, R. New development in the enantioselective synthesis of spiro compounds. *Chem. Soc. Rev.* **2018**, *47*, 5946–5996. (b) Rios, R. Enantioselective Methodologies for the Synthesis of Spiro Compounds. *Chem. Soc. Rev.* **2012**, *41*, 1060–1074. (c) Franz, A. K.; Hanhan, N. V.; Ball-Jones, N. R. Asymmetric Catalysis for the Synthesis of Spirocyclic Compounds. *ACS Catal.* **2013**, *3*, 540–553.

(2) (a) Hiesinger, K.; Dar'in, D.; Proschak, E.; Krasavin, M. Spirocyclic Scaffolds in Medicinal Chemistry. *J. Med. Chem.* **2021**, *64*, 150–183. (b) Chupakhin, E.; Babich, O.; Prosekov, A.; Asyakina, L.; Krasavin, M. Spirocyclic Motifs in Natural Products. *Molecules* **2019**, *24*, 4165. (c) Smith, L. K.; Baxendale, I. R. Total Syntheses of Natural Products Containing Spirocarbocycles. *Org. Biomol. Chem.* **2015**, *13*, 9907–9933. (d) Trost, B. M.; Brennan, M. K. Asymmetric Syntheses of Oxindole and Indole Spirocyclic Alkaloid Natural Products. *Synthesis* **2009**, *18*, 3003–3025. (e) White, D. E.; Stewart, I. C.; Grubbs, R. H.; Stoltz, B. M. The Catalytic Asymmetric Total Synthesis of Elatol. *J. Am. Chem. Soc.* **2008**, *130*, 810–811.

(3) (a) Tsuji, J.; Takahashi, H.; Morikawa, M. Organic Syntheses by Means of Noble Metal Compounds XVII. Reaction of π-Allylpalladium Chloride with Nucleophiles. *Tetrahedron Lett.* **1965**, *6*, 4387–4388. (b) Tsuji, J. New General Synthetic

Methods Involving π-Allypalladium Complexes as Intermediates and Neutral Reaction Conditions. *Tetrahedron* **1986**, *42*, 4361–4401. (c) Tsuji, J. The Tsuji–Trost Reaction and Related Carbon–Carbon Bond Formation Reactions: Overview of the Palladium–Catalyzed Carbon–Carbon Bond Formation via π-Allylpalladium and Propargylpalladium Intermediates. In *Handbook of Organopalladium Chemistry in Organic Synthesis*; Negishi, E.-i., Meijere, A., Eds.; John Wiley & Sons: New York, 2002; Vol. 2, pp 1669–1687. (d) Tsuji, J. Development of β-keto Ester and Malonate Chemistry. Palladium-catalyzed New Reactions of their Allylic Esters. *Proc. Japan Acad.* **2004**, *80*, 349–358. (e) Trost, B. M.; Jiang, C. Catalytic Enantioselective Construction of All-Carbon Quaternary Stereocenters. *Synthesis* **2006**, *3*, 369–396. (f) Corey, E. J.; Guzman-Perez, A. The Catalytic Enantioselective Construction of Molecules with Quaternary Carbon Stereocenters. *Angew. Chem. Int. Ed.* **1998**, *37*, 388–401. (g) Weaver, J. D.; Recio, A.; Grenning, A. J.; Tunge, J. A. Transition Metal-Catalyzed Decarboxylative Allylation and Benzylation Reactions. *Chem. Rev.* **2011**, *111*, 1846–1913. (h) Overman, L. E.; Quasdorf, K. W. Catalytic Enantioselective Synthesis of Quaternary Carbon Stereocentres. *Nature* **2014**, *516*, 181–191.

(4) (a) Behenna, D. C.; Stoltz, B. M. The Enantioselective Tsuji Allylation. *J. Am. Chem. Soc.* **2004**, *126*, 15044–15045. (b) Mohr, J. T.; Behenna, D. C.; Harned, A. M.; Stoltz, B. M. Deracemization of Quaternary Stereocenters by Pd-Catalyzed Enantioconvergent Decarboxylative Allylation of Racemic β-Ketoesters. *Angew. Chem. Int. Ed.* **2005**, *44*, 6924–6927. (c) Keith, J. A.; Behenna, D. C.; Mohr, J. T.;

Ma, S.; Marinescu, S. C.; Oxgaard, J.; Stoltz, B. M.; Goddard, W. A. The Inner-Sphere Process in the Enantioselective Tsuji Allylation Reaction with (S)-t-Bu-phosphinooxazoline Ligands. *J. Am. Chem. Soc.* **2007**, *129*, 11876–11877. (d) Sherden, N. H.; Behenna, D. C.; Virgil, S. C.; Stoltz, B. M. Unusual Allylpalladium Carboxylate Complexes: Identification of the Resting State of Catalytic Enantioselective Decarboxylative Allylic Alkylation Reactions of Ketones. *Angew. Chem. Int. Ed.* **2009**, *48*, 6840–6843. (e) Behenna, D. C.; Mohr, J. T.; Sherden, N. H.; Marinescu, S. C.; Harned, A. M.; Tani, K.; Seto, M.; Ma, S.; Novák, Z.; Krout, M. R.; McFadden, R. M.; Roizen, J. L.; Enquist, J. A.; White, D. E.; Levine, S. R.; Petrova, K. V.; Iwashita, A.; Virgil, S. C.; Stoltz, B. M. Enantioselective Decarboxylative Alkylation Reactions: Catalyst Development, Substrate Scope, and Mechanistic Studies. *Chem. Eur. J.* **2011**, *17*, 14199–14223. (f) Keith, J. A.; Behenna, D. C.; Sherden, N.; Mohr, J. T.; Ma, S.; Marinescu, S.; Nielsen, R. J.; Oxgaard, J.; Stoltz, B. M.; Goddard, W. A. The Reaction Mechanism of the Enantioselective Tsuji Allylation: Inner-Sphere and Outer-Sphere Pathways, Internal Rearrangements, and Asymmetric C−C Bond Formation. *J. Am. Chem. Soc.* **2012**, *134*, 19050–19060. (g) Liu, Y.; Han, S.-J.; Liu, W.-B.; Stoltz, B. M. Catalytic Enantioselective Construction of Quaternary Stereocenters: Assembly of Key Building Blocks for the Synthesis of Biologically Active Molecules. *Acc. Chem. Res.* **2015**, *48*, 740–751. (h) Cusumano, A. Q.; Stoltz, B. M.; Goddard, W. A. Reaction Mechanism, Origins of Enantioselectivity, and Reactivity Trends in Asymmetric Allylic Alkylation: A Comprehensive Quantum Mechanics

Investigation of a C(sp^3)−C(sp^3) Cross-Coupling. *J. Am. Chem. Soc.* **2020**, *142*, 13917–13933. (i) Cusumano, A. Q.; Goddard, W. A.; Stoltz, B. M. The Transition Metal Catalyzed [π2s + π2s + σ2s + σ2s] Pericyclic Reaction: Woodward−Hoffmann Rules, Aromaticity, and Electron Flow. *J. Am. Chem. Soc.* **2020**, *142*, 19033–19039. (j) Cusumano, A. Q.; Zhang, T.; Goddard, W. A.; Stoltz, B. M. Origins of Enhanced Enantioselectivity in the Pd-Catalyzed Decarboxylative Allylic Alkylation of *N*-Benzoyl Lactams. *Catalysts* **2023**, *13*, 1258. (k) McPherson, K. E.; Croatt, M. P.; Morehead, A. T.; Sargent, A. L. DFT Mechanistic Investigation of an Enantioselective Tsuji−Trost Allylation Reaction. *Organometallics* **2018**, *37*, 3791–3802.

(5) (a) Mohr, J. T.; Nishimata, T.; Behenna, D. C.; Stoltz, B. M. Catalytic Enantioselective Decarboxylative Protonation. *J. Am. Chem. Soc.* **2006**, *128*, 11348–11349. (b) Marinescu, S. C.; Nishimata, T.; Mohr, J. T.; Stoltz, B. M. Homogeneous Pd-Catalyzed Enantioselective Decarboxylative Protonation. *Org. Lett.* **2008**, *10*, 1039–1042. (c) Streuff, J.; White, D. E.; Virgil, S. C.; Stoltz, B. M. A Palladium-Catalysed Enolate Alkylation Cascade for the Formation of Adjacent Quaternary and Tertiary Stereocentres. *Nat. Chem.* **2010**, *2*, 192–196. (d) Nakamura, H.; Shim, J.-G.; Yamamoto, Y. Amphiphilic Catalytic Allylating Reagent, Bis-π-allylpalladium Complex. *J. Am. Chem. Soc.* **1997**, *119*, 8113–8114. (e) Patil, N. T.; Huo, Z.; Yamamoto, Y. Palladium-Catalyzed Decarboxylative Aza-Michael Addition-Allylation Reactions between Allyl Carbamates and Activated Olefins. Generation of Quaternary Carbon Adjacent to Secondary Amine Carbon

Center. *J. Org. Chem.* **2006**, *71*, 6991–6995. (f) Fulton, T. J.; Wu, B.; Alexy, E. J.; Zhang, H.; Stoltz, B. M. Palladium-catalyzed α,β-Dehydrogenation of Acyclic Ester Equivalents Promoted by a Novel Electron Deficient Phosphinooxazoline Ligand. *Tetrahedron* **2019**, *75*, 4104–4109. (g) Inanaga, K.; Wollenburg, M.; Bachman, S.; Hafeman, N. J.; Stoltz, B. M. Catalytic Enantioselective Synthesis of Carbocyclic and Heterocyclic Spiranes via a Decarboxylative Aldol Cyclization. *Chem. Sci.* **2020**, *11*, 7390–7395. (h) Barbor, J. P.; Flesch, K. N.; Chan, M.; Ang, H. R.; Stoltz, B. M. An Enantioselective Spirocyclization of Pd-Enolates and Isocyanates. *Angew. Chem. Int. Ed.* **2025**, e202502583. (i) Sodeoka, M.; Hamashima, Y. Development of Catalytic Enantioselective Reactions via Palladium Enolates as Key Intermediates. *Bull. Chem. Soc. Jpn.* **2005**, *78*, 941–956.

(6) (a) Flesch, K. N.; Cusumano, A. Q.; Chen, P.-J.; Strong, C. S.; Sardini, S. R.; Du, Y. E.; Bartberger, M. D.; Goddard, W. A.; Stoltz, B. M. Divergent Catalysis: Catalytic Asymmetric [4+2] Cycloaddition of Palladium Enolates. *J. Am. Chem. Soc.* **2023**, *145*, 11301–11310. (b) Chen, P.-J.; Cusumano, A. Q.; Flesch, K. N.; Strong, C. S.; Goddard, W. A.; Stoltz, B. M. Molecular Dynamics Investigations of Dienolate [4 + 2] Reactions. *J. Am. Chem. Soc.* **2024**, *145*, 12758–12765.

(7) Nokami, J.; Watanabe, H.; Mandai, T.; Kawada, M.; Tsuji, J. The Palladium-catalyzed Michael Addition of the Ketone Enolates Generated by the Decarboxylation of Allyl-β-keto Carboxylates Under Neutral Conditions. *Tetrahedron Lett.* **1989**, *30*, 4829–4832.

(8) (a) Martin, J. G.; Hill, R. K. Stereochemistry of the Diels–Alder Reaction. *Chem. Rev,* **1961**, *61*, 537–562. (b) Fernández, I.; Bickelhaupt, F. M. Origin of the "Endo Rule" in Diels–Alder Reactions. *J. Comput. Chem.* **2014**, *35*, 371–376.

(9) (a) Little, R. D.; Masjedizadeh, M. R.; Wallquist, O.; McLoughlin, J. I. The Intramolecular Michael Reaction. *Organic Reactions* **1995**, 315–552. (b) Kwan, E. E.; Evans, D. A. Intermolecular Michael Reactions: A Computational Investigation. *Org. Lett.* **2010**, *12*, 5124–5127. (c) Kwan, E. E.; Scheerer, J. R.; Evans, D. A. The Stereochemical Course of Intramolecular Michael Reactions. *J. Org. Chem.* **2013**, *78*, 175–203. (d) Oare, D. A.; Heathcock, C. A. Stereochemistry of the Base-Promoted Michael Addition Reaction. In *Topics in Stereochemistry*; Eliel, E. L., Wilen, S. H., Eds.; John Wiley & Sons: New York, 1989; Vol. 19, pp 227−408. (e) Reznikov, A. N.; Klimochkin, Y. N. Recent Developments in Highly Stereoselective Michael Addition Reactions Catalyzed by Metal Complexes. *Synthesis* **2020**, *52*, 781–795.

(10) (a) Kohnke, P.; Zhang, L. Gold(I)-Catalyzed Desymmetrization of Homopropargylic Alcohols *via* Cycloisomerization: Enantioselective Synthesis of Cyclopentenes Featuring a Quaternary Chiral Center. *Angew. Chem. Int. Ed.* **2024**, e20241192. (b) Gayen, P.; Sar, S.; Ghorai, P. Stereodivergent Synthesis of Spiroaminals via Chiral Bifunctional Hydrogen Bonding Organocatalysis. *Angew. Chem. Int. Ed.* **2024**, e202404106. (c) Li, M.; Scheeff, S.; Chen, J.; Johnston, R. C.; Rizzo, A.; Krenske, E. H.; Chiu, P. Diastereo- and Enantioselective Construction of Stereochemical Arrays Exploiting Non-Classical Hydrogen Bonding in

Enolborates. *Chem. Eur. J.* **2024**, *30*, e202401485. (d) Gayen, P.; Ghorai, P. Organocatalytic Asymmetric Construction of Spirooxazines via Chemoselective Cascade Addition of *N*-Substituted Hydroxylamine with Keto-bis-enone. *Org. Lett.* **2024**, *26*, 6185–6190. (e) Zhang, S.-J.; Zhang, J.; Zhou, Q.-Q.; Dong, L.; Chen, Y.-C. Aminocatalytic Asymmetric exo-Diels Alder Reaction with Methiodide Salts of Mannich Bases and 2,4-Dienals to Construct Chiral Spirocycles. *Org. Lett*. **2013**, *15*, 968–971. (f) Lai, J.; Reid, J. P. A Bulky Imidodiphosphorimidate Brønsted Acid Enables Highly Enantioselective Prins-semipinacol Rearrangements. *ACS Catal.* **2024**, *14*, 8518–8527. (g) Huang, D.; Olivieri, D.; Sun, Y.; Zhang, P.; Newhouse, T. R. Nickel-Catalyzed Difunctionalization of Unactivated Alkenes Initiated by Unstabilized Enolates. *J. Am. Chem. Soc.* **2019**, *141*, 16249–16254. (h) Zheng, C.; Wang, L.; Li, J.; Wang, L.; Wang, D. Z. Ortho-Dearomatization of Phenols Creating All-Carbon Spiro-Bicycles. *Org. Lett.* **2013**, *15*, 4046–4049. (i) Boddaert, T.; Coquerel, Y.; Rodriguez, J. Combination of Rearrangement with Metallic and Organic Catalyses – a Step- and Atom-Economical Approach to α-Spirolactones and -lactams. *Eur. J. Org. Chem.* **2011**, 5061–5070. (j) Desmaële, D.; Zouhiri, F.; d'Angelo, J. The Asymmetric Michael Reaction Involving Chiral Imines: Use of Acrylonitrile as Acceptor and Subsequent Functionalization of the Adducts. *Tetrahedron Asymmetry* **1994**, *5*, 1645–1648. (k) d'Angelo, J.; Ferroud, C. An Efficient Asymmetric Spiroannulation Process. *Tetrahedron Lett.* **1989**, *30*, 6511–6514. (l) Midya, A.; Khalse, L. D.; Ghorai, P. Organocatalytic Enantioselective Intramolecular Michael Addition by In Situ Generated Aminoisobenzofulvenes:

Construction of Spiro Quaternary Carbon Stereocenters. *Chem. Eur. J.* **2023**, *29*, e202301563. (m) Sha, C.-K.; Hsu, C.-W.; Chen, Y.-T.; Cheng, S.-Y. 1,5-Hydrogen Atom Transfer/Radical Cyclization of Cycloalkanones Bearing a β-Iodo α,β-Unsaturated Ester or Nitrile Side Chain. *Tetrahedron Lett.* **2000**, *41*, 9865–9869. (n) Zhu, Z.; Hu, Q.; Fu, Y.; Tong, Y.; Zhou, Z. Design and Evolution of an Enzyme for the Asymmetric Michael Addition of Cyclic Ketones to Nitroolefins by Enamine Catalysis. *Angew. Chem. Int. Ed.* **2024**, e 202404312. (o) Le Dréau, M.-A.; Desmaële, D.; Dumas, F.; d'Angelo, J. A New Access to Homoerythrina Alkaloids. *J. Org. Chem.* **1993**, *58*, 2933–2935. (p) Boddaert, T.; Conquerel, Y.; Rodriguez, J. Organocatalytic Activity of N-Heterocyclic Carbenes in the Michael Addition of 1,3-Dicarbonyl Compounds: Application to a Stereoselective Spirocyclization Sequence. *Adv. Synth. Catal.* **2009**, *351*, 1744–1748. (q) Guevara-Pulido, J. O.; Andrés, J. M.; Ávila, D. P.; Pedrosa, R. Enantioselective Synthesis of Seven-membered Carbo- and Heterocyles by Organocatalyzed Intramolecular Michael Addition. *RSC Adv.* **2016**, *6*, 30166–30169. (r) Takasu, K.; Ueno, M.; Ihara, M. Auxiliary Induced Asymmetric Michael-aldol Reaction Under Kinetic and Thermodynamic Conditions. *Tetrahedron Lett.* **2000**, *41*, 2145–2148. (s) Azuma, T.; Takemoto, Y.; Takasu, K. Formal (3+3) Cycloaddition of Silyl Enol Ethers Catalyzed by Trifric Imide: Domino Michael Addition–Claisen Condensation Accompanied with Isomerization of Silyl Enol Ethers. *Chem. Pharm. Bull.* **2011**, *59*, 1190–1193. (t) Nocket, A. J.; Feng, Y.; Weinreb, S. M. Construction of the Myrioneuron Alkaloids: A Total Synthesis of (±)-Myrioneurinol. *J. Org. Chem.*

2015, *80*, 1116–1129. (u) Nocket, A. J.; Weinreb, S. M. Total Synthesis of the Tetracyclic Antimalarial Alkaloid ()-Myrioneurinol. *Angew. Chem. Int. Ed.* **2014**, *53*, 14162–14165. (v) Jousse, C.; Mainguy, D.; Desmaële, D. Six-Membered Annulation Reaction by Sequential η^3Allylpalladium Alkylation-Michael Addition. *Tetrahedron Lett.* **1998**, *39*, 1349–1352. (w) Mayol-Llinàs, J.; Farnaby, W.; Nelson, A. Modular Synthesis of Thirty Lead-Like Scaffolds Suitable for CNS Drug Discovery. *Chem. Commun.* **2017**, *53*, 12345–12348. (x) Shikari, A.; Sharma, M.; Bhattacharyya, K.; Pan, S. C. Organocatalytic Dearomative Spirocyclization Reaction of Enone- Tethered *α*-and *β*-Naphthols and Dearomatization Reaction of In Situ Generated Nitro-Olefin-Tethered *α*-Naphthols. *J. Org. Chem.* **2024**, *89*, 9769–9782. (y) Snider, B. B.; Vo, N. H.; Foxman, B. M. Mn(III)-Based Oxidative Fragmentation-Cyclization Reactions of Unsaturated Cyclobutanols. *J. Org. Chem.* **1993**, *58*, 7228–7237. (z) Xu, Q.; Ning, L.; Xu, W.; Lin, L.; Feng, X. Synthesis of *γ*-Butyrolactones with Chiral Quaternary−Tertiary Stereocenters via Catalytic Asymmetric Mukaiyama−Michael Addition. *Org. Lett.* **2024**, *26*, 9665–9670.

(11) 31% remaining starting material was also observed via ^{1}H NMR with respect to 1,3,5-trimethoxybenzene as internal standard.

(12) Significant quantities of prematurely protonated byproduct were not observed in entries with lower NMR yields.

(13) The configuration of the corresponding major diastereomers “d1” are assigned by analogy to related substrates. The absolute configuration of the minor diastereomer is unassigned. The dr’s reported are based on integration in the crude NMR spectra.

The isolated yields do not reflect these ratios due to challenging isolations of diastereopure compounds.

(14) It was noted that upon standing in basified or neutral deuterochloroform, Z-enone **198** isomerizes to **196a**.

(15) In an NMR experiment, 60% yield of **201a** is observed via ^{1}H NMR with respect to 1,3,5-trimethoxybenzene as internal standard. The rest of the mass balance is primarily what has been tentatively assigned as a mixture of diastereomers corresponding to the branched constitutional isomer. That said, at this stage we cannot confidently provide a crude dr for **201a** or **201b** value based on the crude profile.

(16) Kawato, Y.; Takahashi, N.; Kumagai, N.; Shibasaki, M. Catalytic Asymmetric Conjugate Addition of α-Cyanoketones for the Construction of a Quaternary Stereogenic Center. *Org. Lett.* **2010**, *12*, 1484–1487.

(17) (a) Sun, Y.; Huang, X.; Ren, J.; Wang, Z. Highly Efficient Construction of Angular Polycycles. *Nat. Commun.* **2024**, *15*, 9206. (b) Salahi, F.; Yao, C.; Norton, J. R.; Snyder, S. A. The Synthesis of Diverse Terpene Architectures from Phenols. *Nat. Synth.* **2022**, *1*, 313–321. (c) Pirrung, M. C. Total Synthesis of (±)-Isocomene. *J. Am. Chem. Soc.* **1979**, *101*, 7130–7131. (d) Jiao, W.-H.; Shi, G.-H.; Xu, T.-T.; Chen, G.-D.; Gu, B.-B.; Wang, Z.; Peng, S.; Wang, S.-P.; Li, J.; Han, B.-N.; Zhang, W.; Lin, H-W. Dysiherbols A−C and Dysideanone E, Cytotoxic and NF-κB Inhibitory Tetracyclic Meroterpenes from a Dysidea sp. Marine Sponge. *J. Nat. Prod.* **2016**, *79*, 406–411. (e) Boeckman, R. K.; Blum, D. M.; Arthur, S. D. A Total Synthesis

of Gascardic Acid. *J. Am. Chem. Soc.* **1979**, *101*, 5060–5062. (f) Davies, H. M. L.; Dai, X.; Long, M. S. Combined C-H Activation/Cope Rearrangement as a Strategic Reaction in Organic Synthesis: Total Synthesis of (-)-Colombiasin A and (-)-Elisapterosin B. *J. Am. Chem. Soc.* **2006**, *128*, 2485–2490. (g) Davis, C. E.; Duffy, B. C.; Coates, R. M. Total Synthesis of (±)-Cameroonanol. *Org. Lett.* **2000**, *2*, 2717–2719. (h) Amagata, T.; Doi, M.; Tohgo, M.; Minoura, K.; Numata, A. Dankasterone, a New Class of Cytotoxic Steroid Produced by a Gymnascella Species from a Marine Sponge. *Chem. Commun.* **1999**, 1321–1322. (i) Loyola, L. A.; Morales, G.; Castillo, M. Alkaloids of Lycopodium Magellanicum. *Phytochemistry* **1979**, *18*, 1721–1723.

(18) (a) Krout, M. R.; Mohr, J. T.; Stoltz, B. M. Preparation of (*S*)-*tert*-ButylPHOX (Oxazole, 4-(1,1-dimethylethyl)-2-[2-(diphenylphosphino)phenyl]-4,5- dihydro-(4*S*)-). *Org. Synth.* **2009**, *86*, 181–193. (b) McDougal, N. T.; Streuff, J.; Mukherjee, H.; Virgil, S. C.; Stoltz, B. M. Rapid synthesis of an electron-deficient *t*-BuPHOX ligand: cross-coupling of aryl bromides with secondary phosphine oxides. *Tetrahedron Lett*. **2010**, *51*, 5550–5554.

(19) Wagen, C. C.; McMinn, S. E.; Kwan, E. E.; Jacobsen, E. N. Screening for Generality in Asymmetric Catalysis. *Nature*, **2022**, *610*, 680–686.

(20) Sheldrick, G. M. *Acta Cryst.* **1990**, A46, 467–473.

(21) Sheldrick, G. M. *Acta Cryst.* **2015**, C71, 3–8.

(22) Müller, P. *Crystallography Reviews* **2009**, *15*, 57–83.

(23) Milburn, R. R; McRae, K.; Chan, Johann, Tedrow, J.; Larsen, R.; Faul, M. A practical preparation of aryl β-ketophosphonates. *Tetrahedron Lett.* **2009**, *50*, 870–872.

(24) Sano, S.; Okubo, Y.; Hanada, A.; Nakao, M.; Kitaike, S.; Nagao, Y.; Nakegawa, H. Reinvestigation of the Synthesis of Isoliquiritigenin: Application of Horner–Wadsworth–Emmons Reaction and Claisen–Schmidt Condensation. *Chem. Pharm. Bull.* **2011**, *59*, 885–888.

(25) Murai, M.; Nakamura, M.; Takai, K. Rhenium-Catalyzed Synthesis of 2H-1,2-Oxaphosphorin 2-Oxides via the Regio- and Stereoselective Addition Reaction of β-Keto Phosphonates with Alkynes. *Org. Lett.* **2014**, *16*, 5784–5787.

(26) Trost, B. M.; Xu, J. The O-Acylation of Ketone Enolates by Allyl 1H-Imidazole-1-carboxylate Mediated with Boron Trifluoride Etherates–A Convenient Procedure for the Synthesis of Substituted Allyl Enol Carbonates. *J. Org. Chem.* **2007**, *72*, 9372–9375.

(27) Inanaga, K.; Wollenburg, M.; Bachman, S.; Hafeman, N. J.; Stoltz, B. M. Catalytic Enantioselective Synthesis of Carbocyclic and Heterocyclic Spiranes via a Decarboxylative Aldol Cyclization. *Chem. Sci.* **2020**, *11*, 7390–7395.

(28) Behenna, D. C.; Liu, Y.; Yurino, T.; Kim, J.; White, D. E.; Virgil, S. C.; Stoltz, B. M. Enantioselective Construction of Quaternary N-heterocycles by Palladium-Catalysed Decarboxylative Allylic Alkylation of Lactams. *Nat. Chem.* **2012**, *4*, 130–133.

(29) Kawato, Y.; Takahashi, N.; Kumagai, N.; Shibasaki, M. Catalytic Asymmetric Conjugate Addition of α-Cyanoketones for the Construction of a Quaternary Stereogenic Center. *Org. Lett.* **2010**, *12*, 1484–1487.

(30) Behenna, D. C.; Mohr, J. T.; Sherden N. H.; Marinescu, S. C., Harned, A. M.; Tani, K.; Seto, M.; Ma, S.; Novák, Z.; Krout, M. R.; McFadden, R. M.; Roizen, J. L.; Enquist jr.; J. A.; White, D. E.; Levine, S. R.; Petrova, K. V.; Iwashita, A.; Virgil, S. C.; Stoltz, B. M. Enantioselective Decarboxylative Alkylation Reactions: Catalyst Development, Substrate Scope, and Mechanistic Studies. *Chem. Eur. J.* **2011**, *17*, 14199–14223.

(31) (a) Neese, F. Software Update: The ORCA Program System, Version 5.0. *Wiley Interdiscip. Rev.: Comput. Mol. Sci.* **2022,** *12*, No. e1606. (b) Neese, F. The ORCA Program System. *Wiley Interdiscip. Rev.: Comput. Mol. Sci.* **2012**, *2*, 73−78.

(32) Adamo, C.; Barone, V. Toward Reliable Density Functional Methods without Adjustable Parameters: The PBE0 Model. *J. Chem. Phys.* **1999**, *110*, 6158−6170.

(33) (a) Caldeweyher, E.; Ehlert, S.; Hansen, A.; Neugebauer, H.; Spicher, S.; Bannwarth, C.; Grimme, S. A Generally Applicable Atomic-Charge Dependent London Dispersion Correction. *J. Chem. Phys.* **2019**, *150* (15), 154122. (b) Caldeweyher, E.; Bannwarth, C.; Grimme, S. Extension of the D3 Dispersion Coefficient Model. *J. Chem. Phys.* **2017**, *147*, 034112.

(34) Weigend, F.; Ahlrichs, R. Balanced Basis Sets of Split Valence, Triple Zeta Valence and Quadruple Zeta Valence Quality for H to Rn: Design and Assessment of Accuracy. *Phys. Chem. Chem. Phys.* **2005**, *7*, 3297–3305.

(35) Peterson, K. A.; Figgen, D.; Goll, E.; Stoll, H.; Dolg, M. Systematically Convergent Basis Sets with Relativistic Pseudopotentials. II. Small-Core Pseudopotentials and Correlation Consistent Basis Sets for the Post- *d* Group 16–18 Elements. *The Journal of Chemical Physics* **2003**, *119*, 11113–11123.

(36) (a) Cusumano, A. Q.; Goddard, W. A. I.; Stoltz, B. M. The Transition Metal Catalyzed [π2s + π2s + s2s + s2s] Pericyclic Reaction: Woodward–Hoffmann Rules, Aromaticity, and Electron Flow. *J. Am. Chem. Soc.* **2020**, *142*, 19033–19039. (b) Cusumano, A. Q.; Stoltz, B. M.; Goddard, W. A. Reaction Mechanism, Origins of Enantioselectivity, and Reactivity Trends in Asymmetric Allylic Alkylation: A Comprehensive Quantum Mechanics Investigation of a $C(sp^3)$–$C(sp^3)$ Cross-Coupling. *J. Am. Chem. Soc.* **2020**, *142*, 13917–13933. (c) Flesch, K. N.; Cusumano, A. Q.; Chen, P.-J.; Strong, C. S.; Sardini, S. R.; Du, Y. E.; Bartberger, M. D.; Goddard, W. A.; Stoltz, B. M. Divergent Catalysis: Catalytic Asymmetric [4+2] Cycloaddition of Palladium Enolates. *J. Am. Chem. Soc.* **2023**, *145*, 11301–11310.

(37) Garcia-Ratés, M.; Neese, F. Effect of the Solute Cavity on the Solvation Energy and Its Derivatives within the Framework of the Gaussian Charge Scheme. *J. Comput. Chem.* **2020**, *41*, 922–939.

(38) Ishida, K.; Morokuma, K.; Komornicki, A. The Intrinsic Reaction Coordinate. An Ab Initio Calculation for HNC→HCN and H−+CH4→CH4+H−. *J. Chem. Phys.* **1977**, *66 (5)*, 2153−2156.

(39) Zhao, Y.; Truhlar, D. G. The M06 Suite of Density Functionals for Main Group Thermochemistry, Thermochemical Kinetics, Noncovalent Interactions, Excited

States, and Transition Elements: Two New Functionals and Systematic Testing of Four M06-Class Functionals and 12 Other Functionals. *Theor Chem Account* **2008**, *120* (1), 215–241.

(40) Grimme, S. Supramolecular Binding Thermodynamics by Dispersion-Corrected Density Functional Theory. *Chem. Eur. J.* **2012**, *18*, 9955–9964.

(41) Izato, Y.; Matsugi, A.; Koshi, M.; Miyake, A. A Simple Heuristic Approach to Estimate the Thermochemistry of Condensed-Phase Molecules Based on the Polarizable Continuum Model. *Phys. Chem. Chem. Phys.* **2019**, *21*, 18920–18929.

(42) Finkelstein, A. V.; Janin, J. The Price of Lost Freedom: Entropy of Bimolecular Complex Formation. *Protein Engineering, Design and Selection* **1989**, *3*, 1–3.

(43) Neese, F.; Wennmohs, F.; Hansen, A.; Becker, U. Efficient, Approximate and Parallel Hartree-Fock and Hybrid DFT Calculations. A 'Chain-of-Spheres' Algorithm for the Hartree-Fock Exchange. *Chemical Physics* **2009**, *356*, 98–109.

(44) Weigend, F. Accurate Coulomb-Fitting Basis Sets for H to Rn. *Phys. Chem. Chem. Phys.* **2006**, *8*, 1057–1065.

(45) Stoychev, G. L.; Auer, A. A.; Neese, F. Automatic Generation of Auxiliary Basis Sets. *J. Chem. Theory Comput.* **2017**, *13*, 554–562.

(46) Grimme, S. Exploration of Chemical Compound, Conformer, and Reaction Space with Meta-Dynamics Simulations Based on Tight-Binding Quantum Chemical Calculations. *J. Chem. Theory Comput.* **2019**, *15*, 2847–2862.

APPENDIX 2

Spectra Relevant to Chapter 3:

Asymmetric Michael Spirocyclization of Pd Enolates

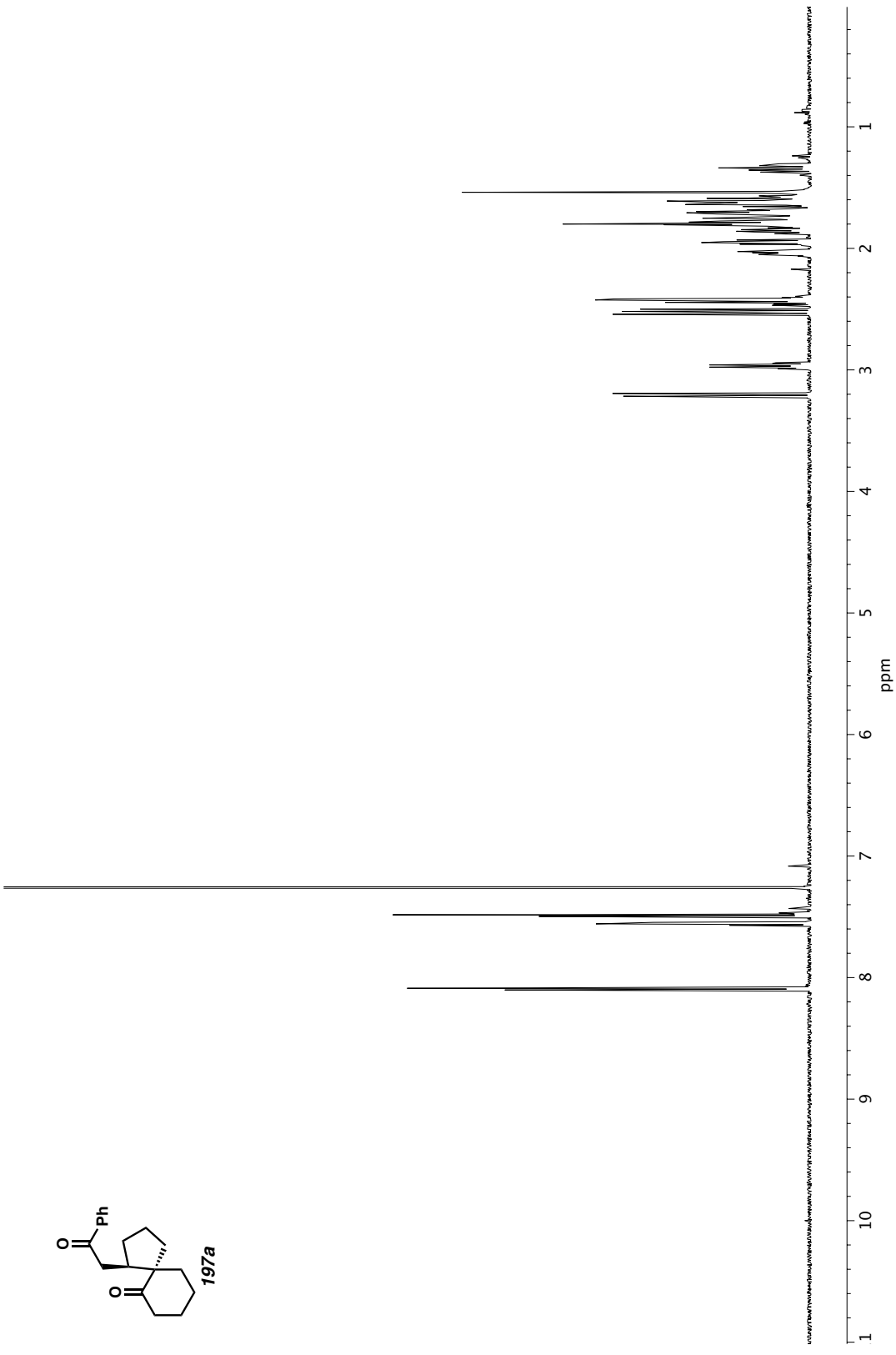

Figure A2.1. *^1H NMR (600 MHz, $CDCl_3$) of compound* ***197a.***

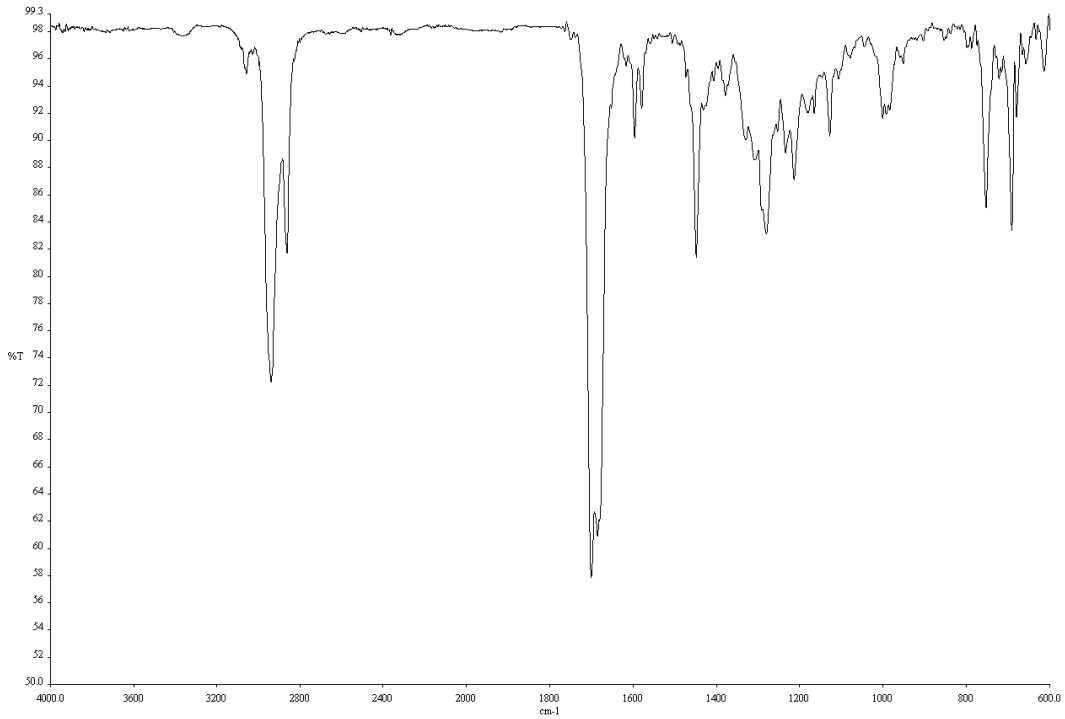

Figure A2.2. *Infrared spectrum (Thin Film, NaCl) of compound* ***197a.***

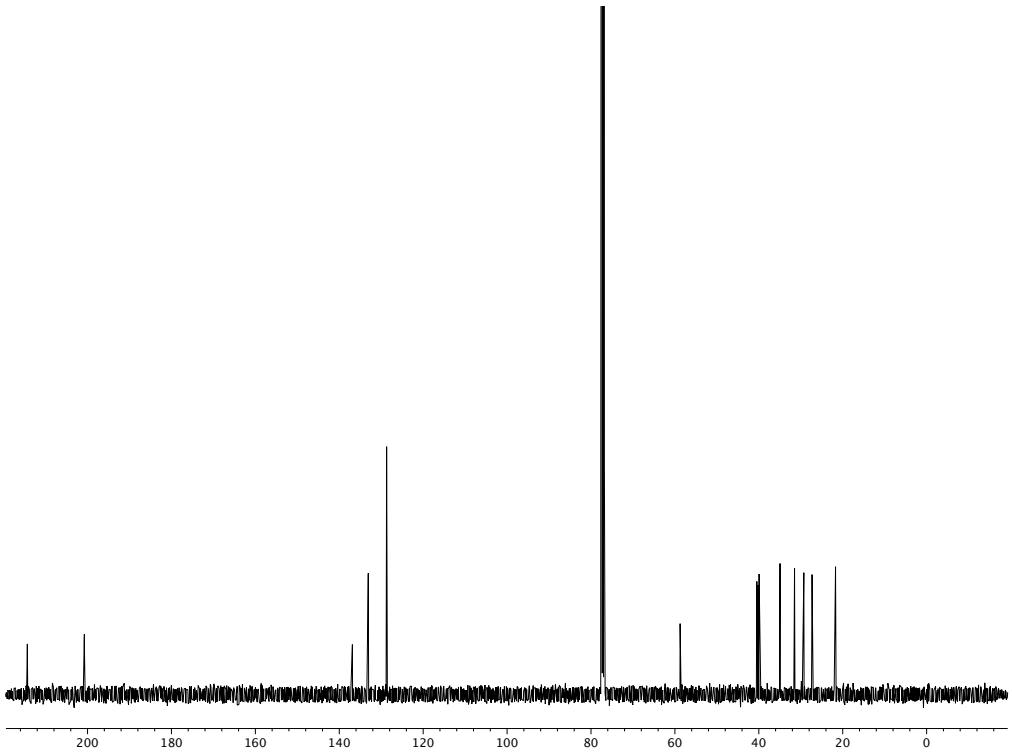

Figure A2.3. *^{13}C NMR (100 MHz, $CDCl_3$) of compound* ***197a.***

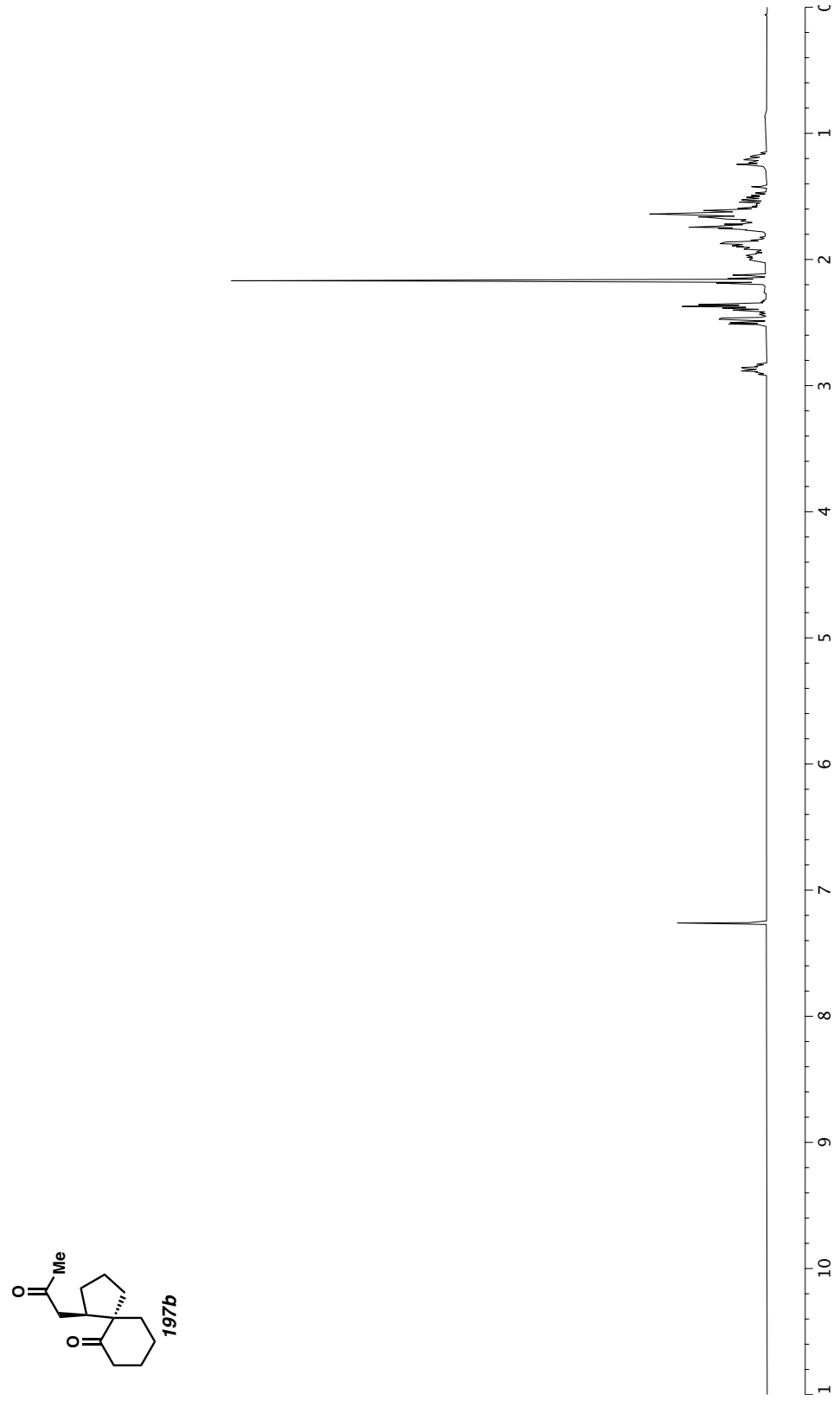

Figure A2.4. *^1H NMR (400 MHz, $CDCl_3$) of compound* ***197b.***

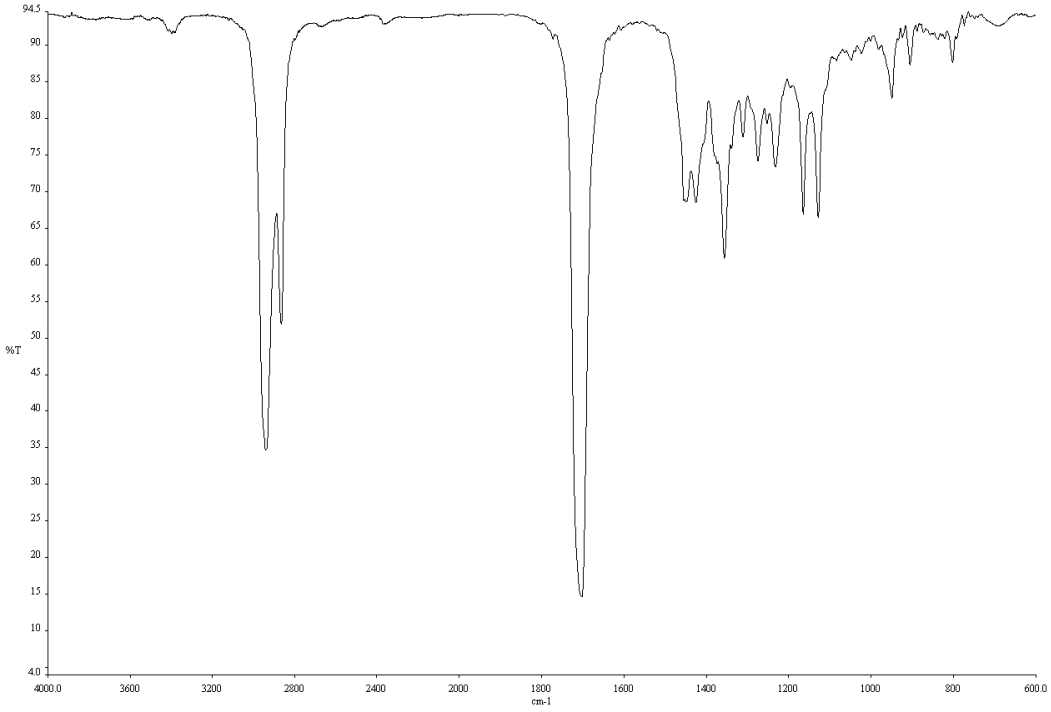

Figure A2.5. *Infrared spectrum (Thin Film, NaCl) of compound* ***197b.***

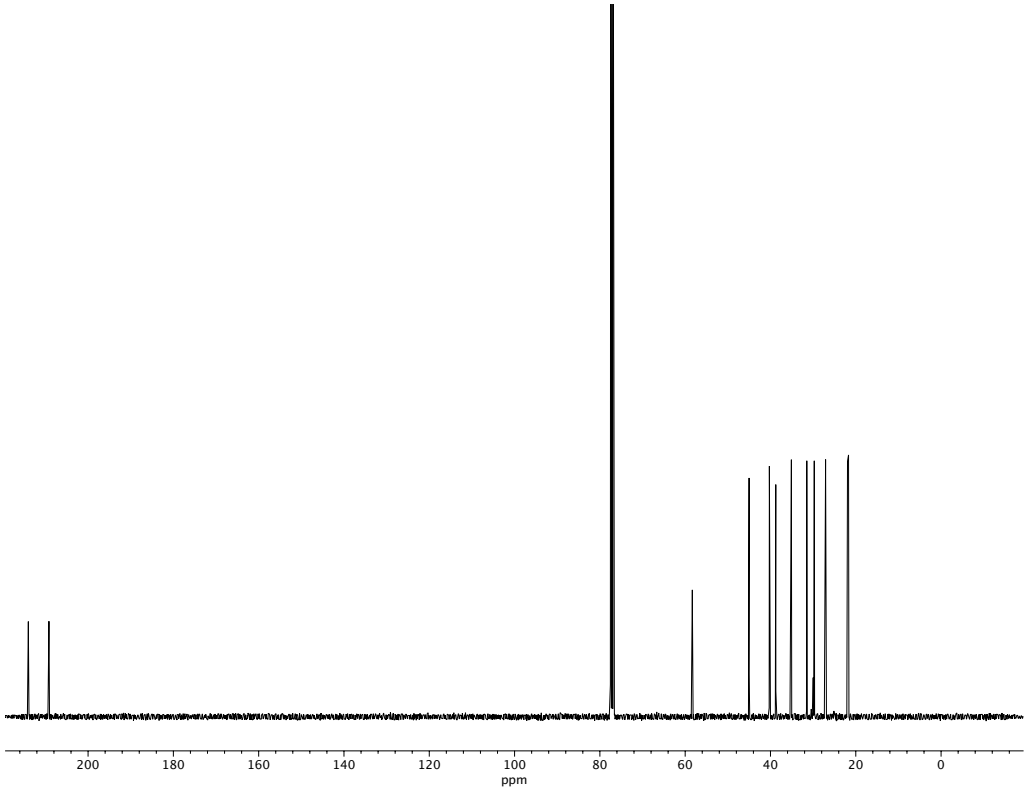

Figure A2.6. *^{13}C NMR (100 MHz, $CDCl_3$) of compound* ***197b.***

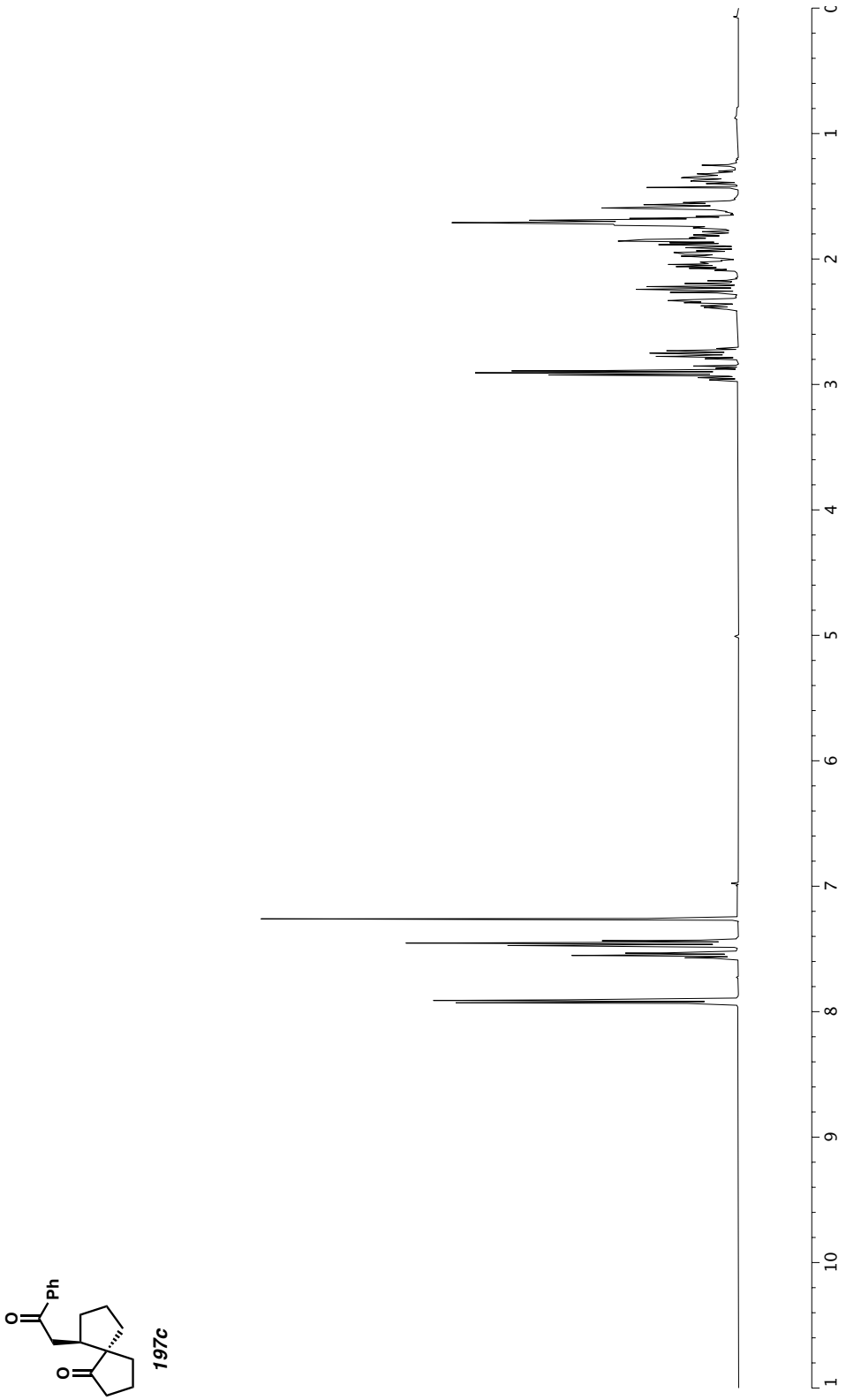

Figure A2.7. *^1H NMR (400 MHz, $CDCl_3$) of compound* ***197c.***

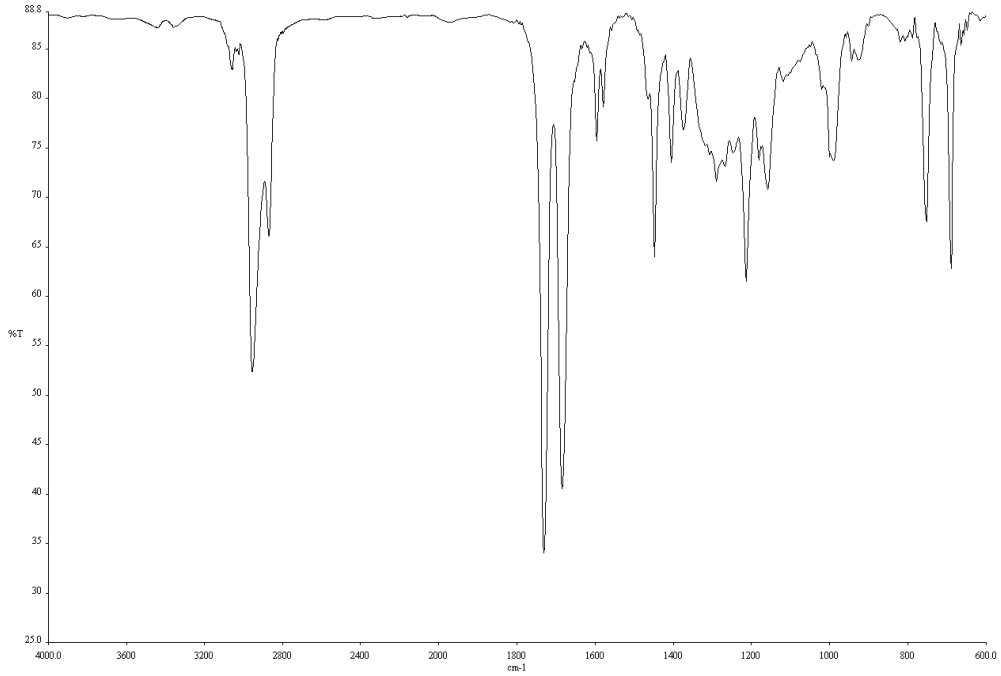

Figure A2.8. *Infrared spectrum (Thin Film, NaCl) of compound* ***197c.***

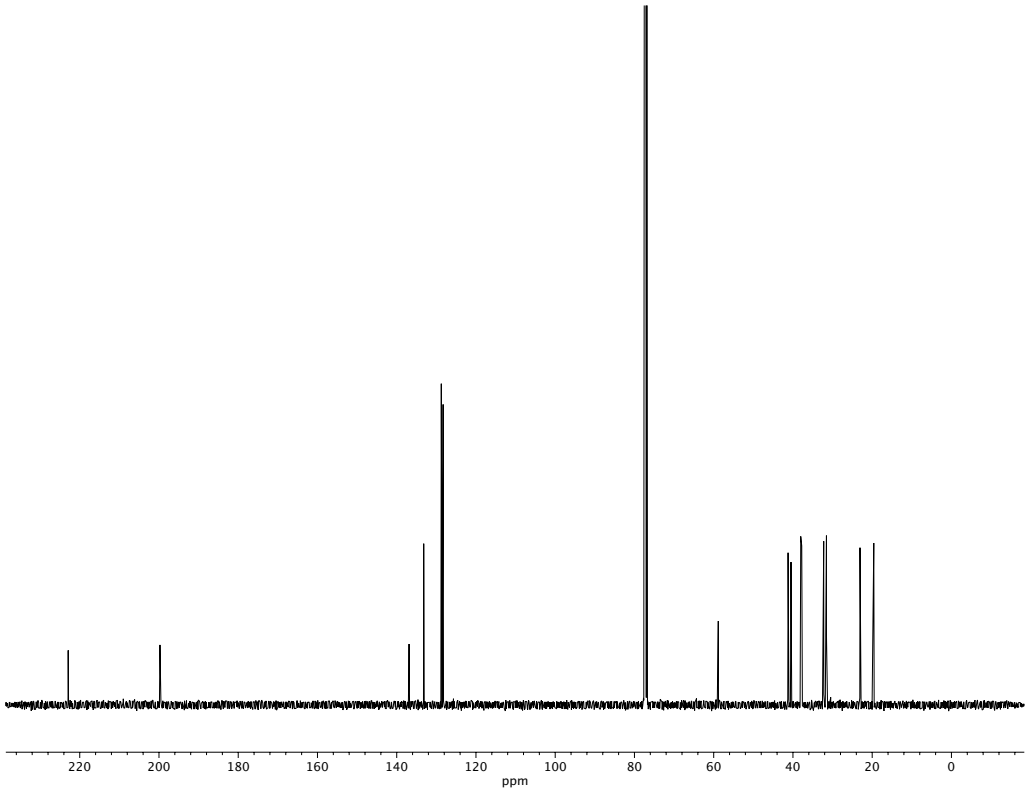

Figure A2.9. *^{13}C NMR (100 MHz, $CDCl_3$) of compound* ***197c.***

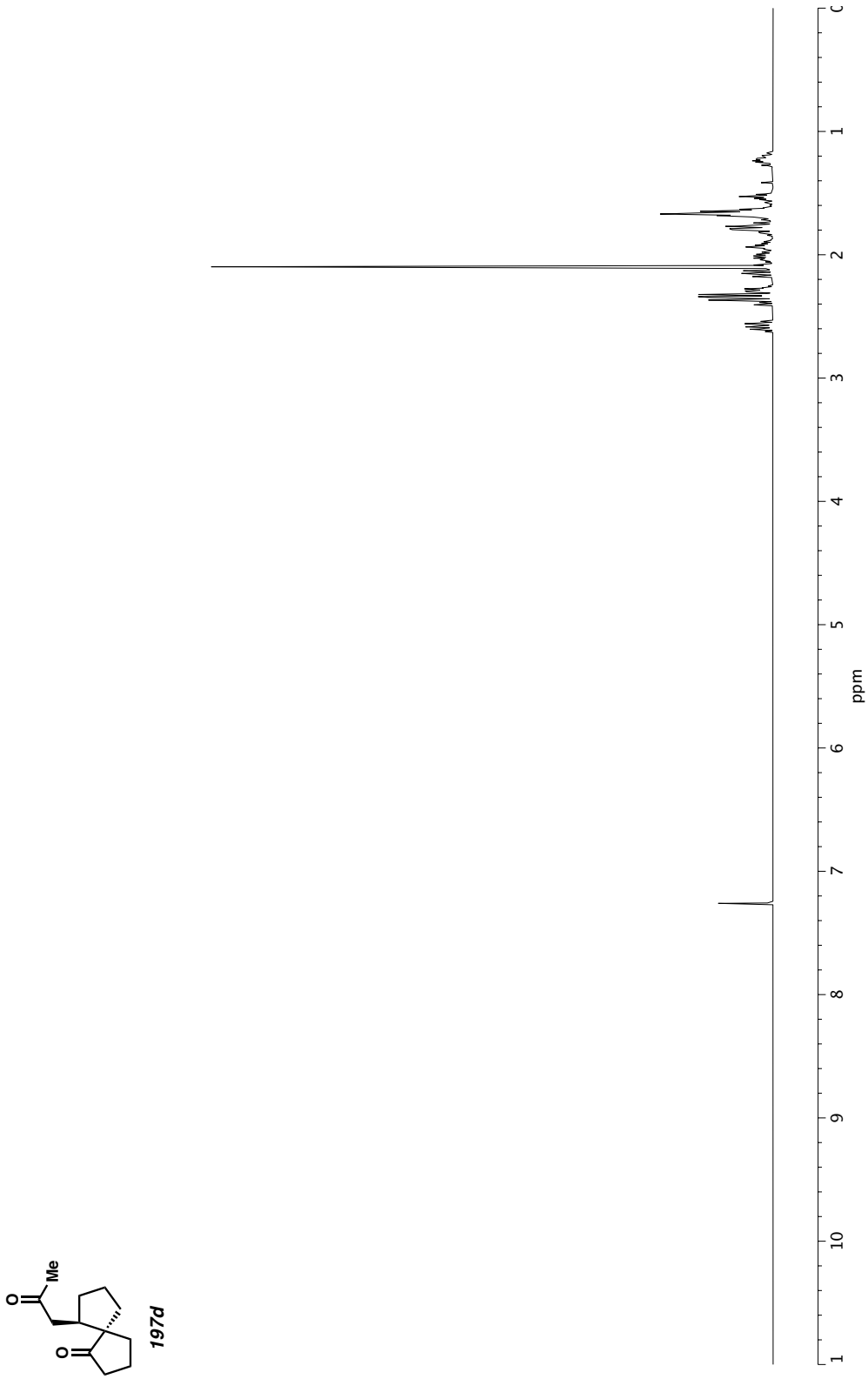

Figure A2.10. *^1H NMR (400 MHz, $CDCl_3$) of compound* ***197d.***

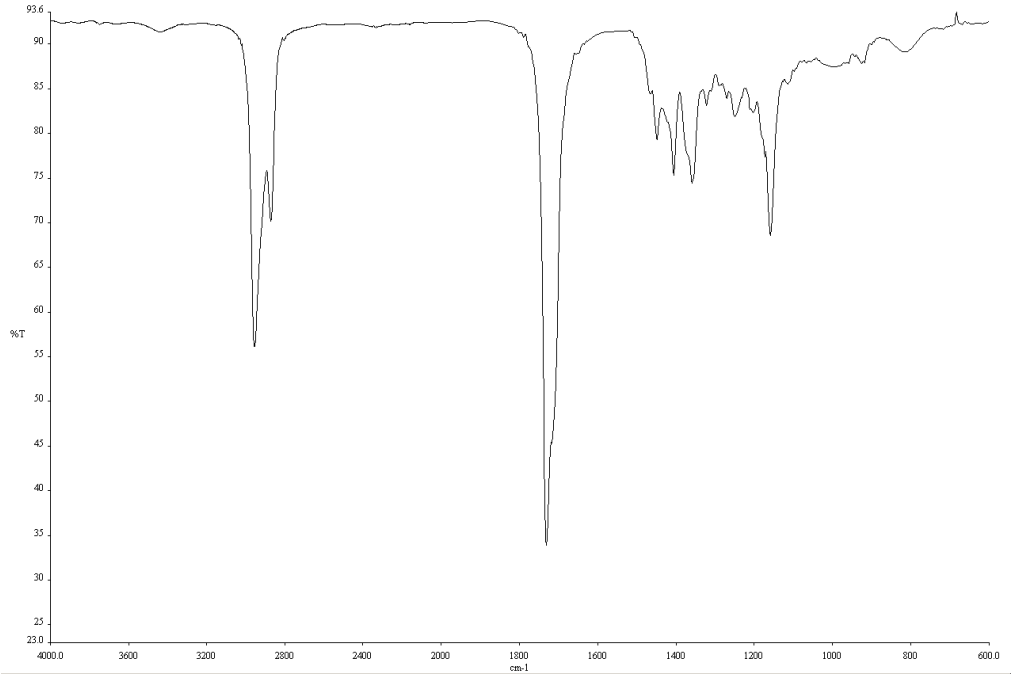

Figure A2.11. *Infrared spectrum (Thin Film, NaCl) of compound* ***197d.***

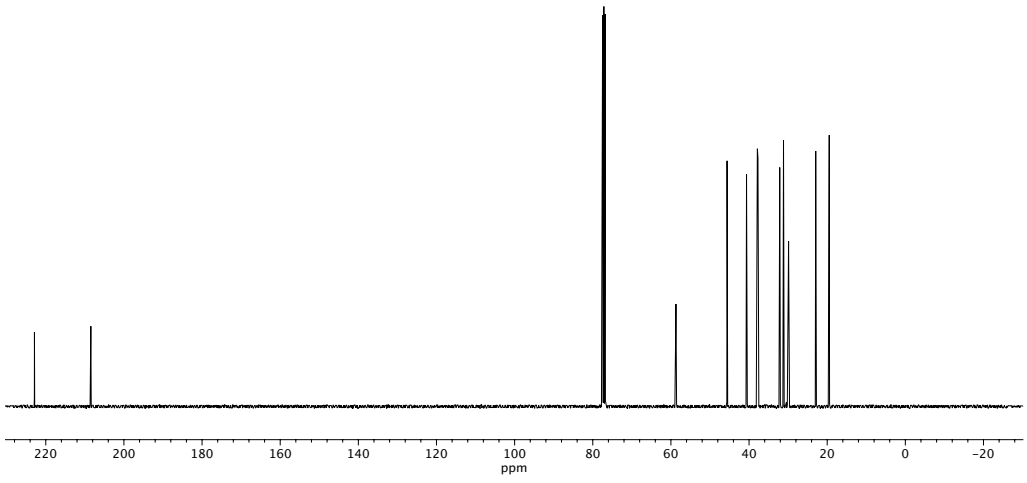

Figure A2.12. *^{13}C NMR (100 MHz, $CDCl_3$) of compound* ***197d.***

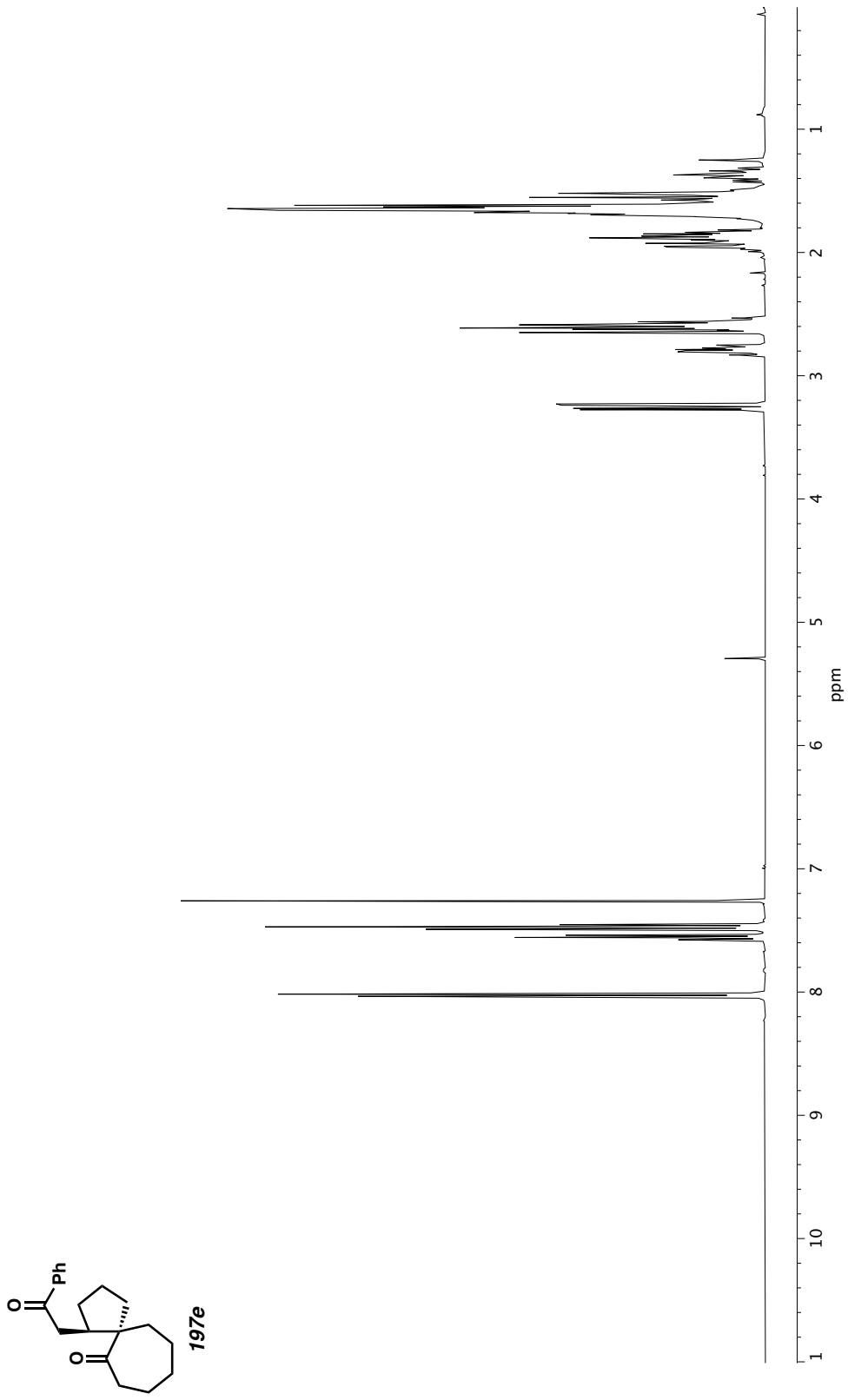

Figure A2.13. *^1H NMR (400 MHz, $CDCl_3$) of compound* ***197e.***

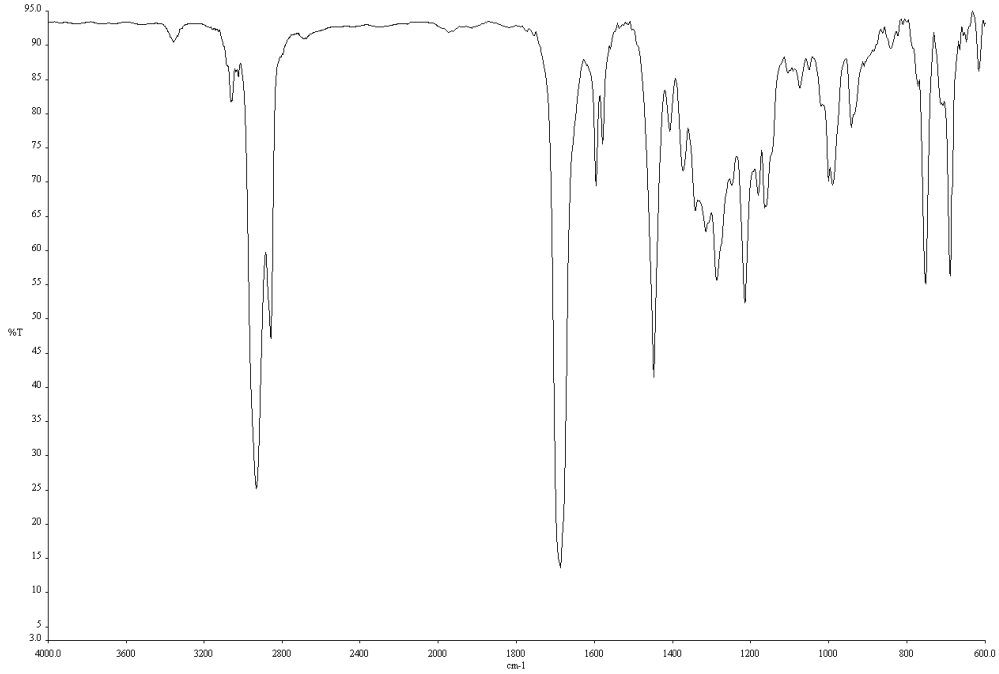

Figure A2.14. *Infrared spectrum (Thin Film, NaCl) of compound* ***197e.***

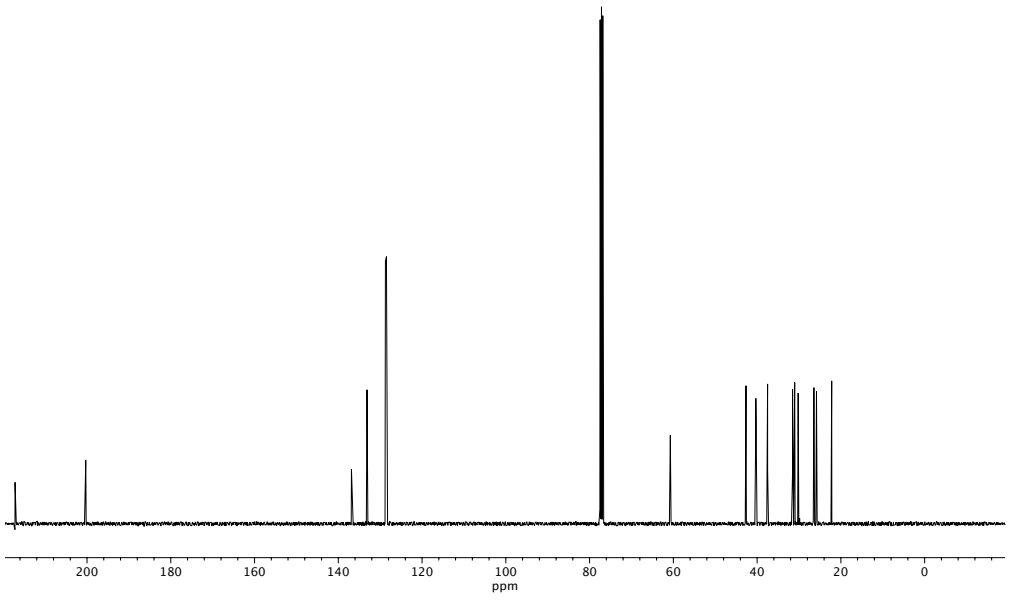

Figure A2.15. *^{13}C NMR (100 MHz, $CDCl_3$) of compound* ***197e.***

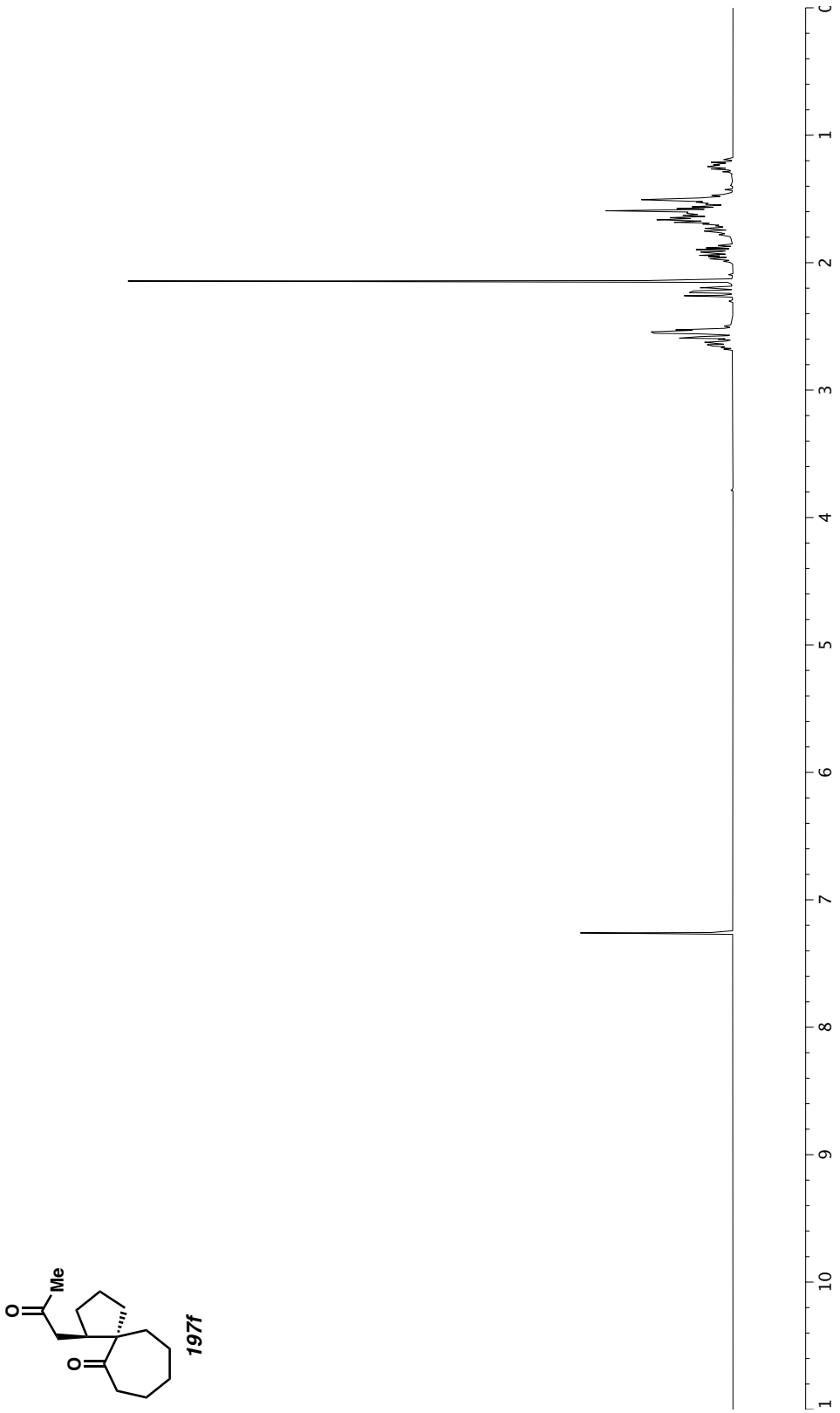

Figure A2.16. *^1H NMR (400 MHz, $CDCl_3$) of* ***compound 197f.***

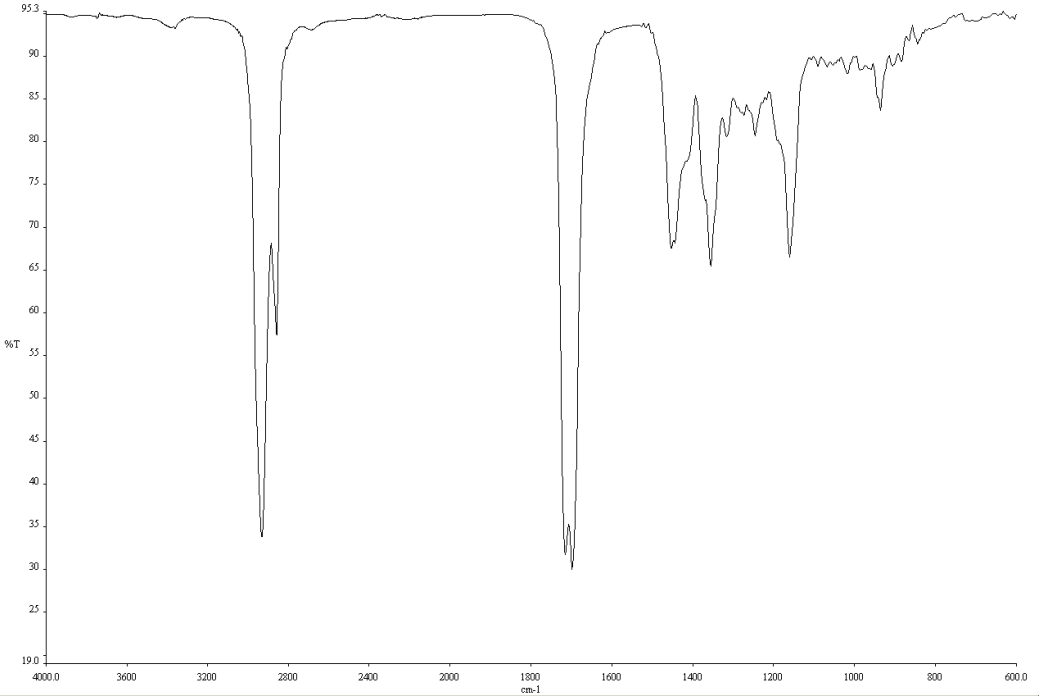

Figure A2.17. *Infrared spectrum (Thin Film, NaCl) of compound* ***197f.***

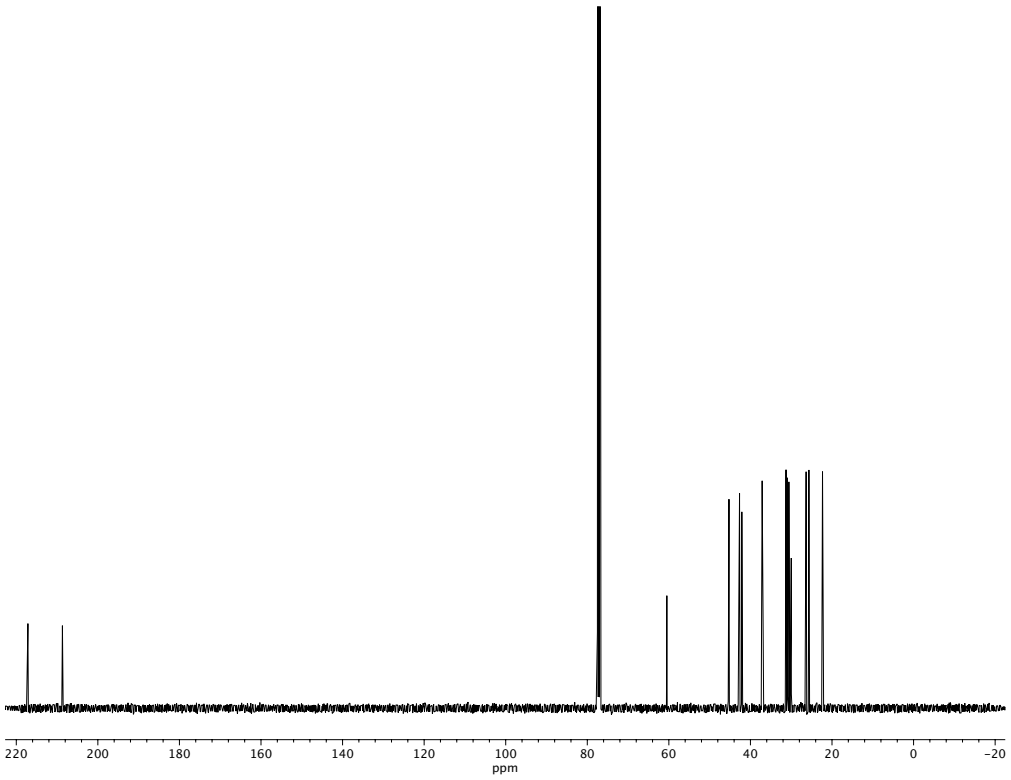

Figure A2.18. *^{13}C NMR (100 MHz, $CDCl_3$) of compound* ***197f.***

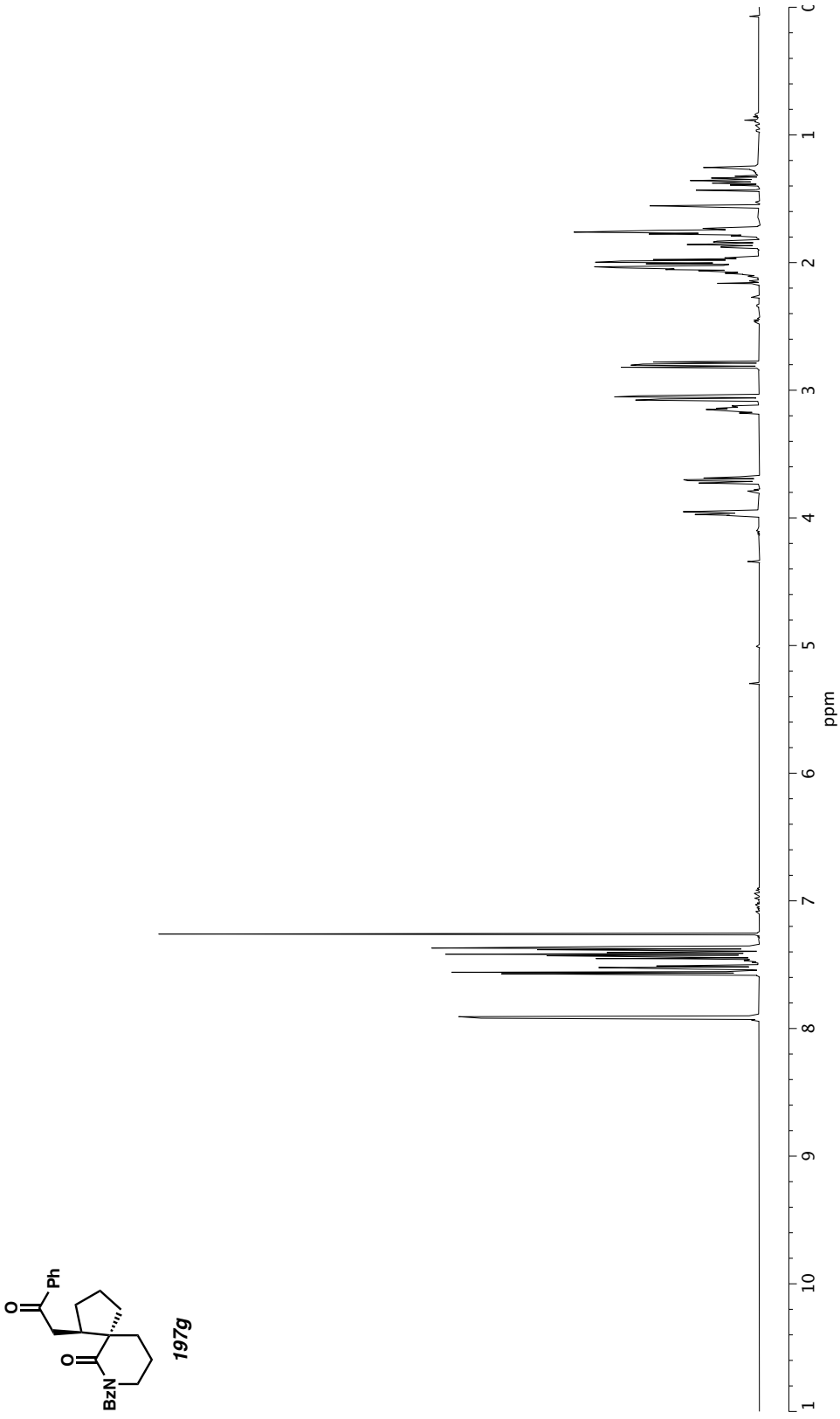

Figure A2.19. *^1H NMR (400 MHz, $CDCl_3$) of compound* ***197g.***

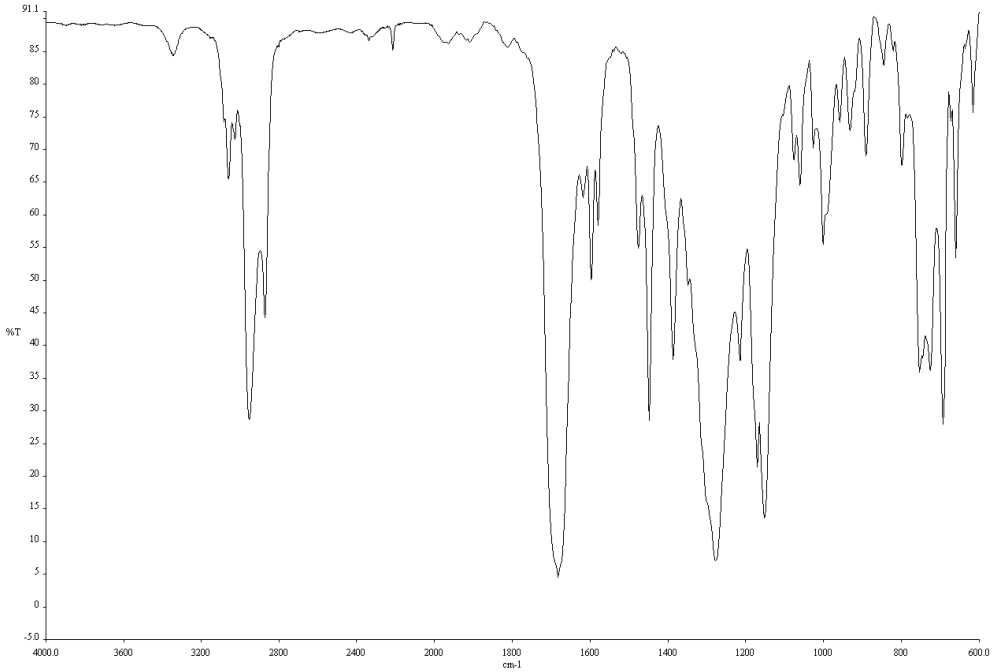

Figure A2.20. *Infrared spectrum (Thin Film, NaCl) of compound* ***197g.***

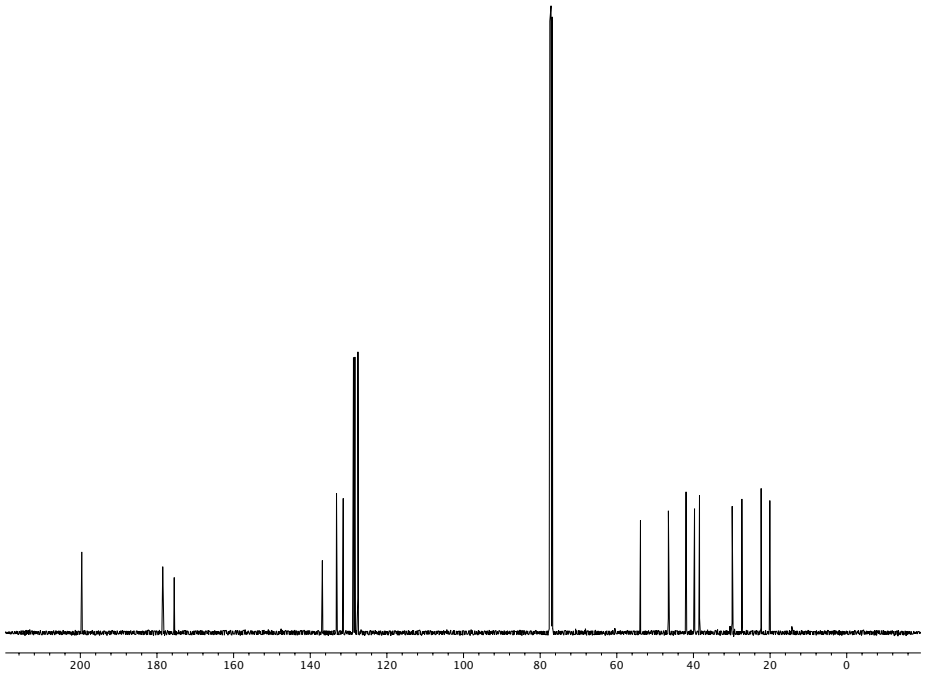

Figure A2.21. *^{13}C NMR (100 MHz, $CDCl_3$) of compound* ***197g.***

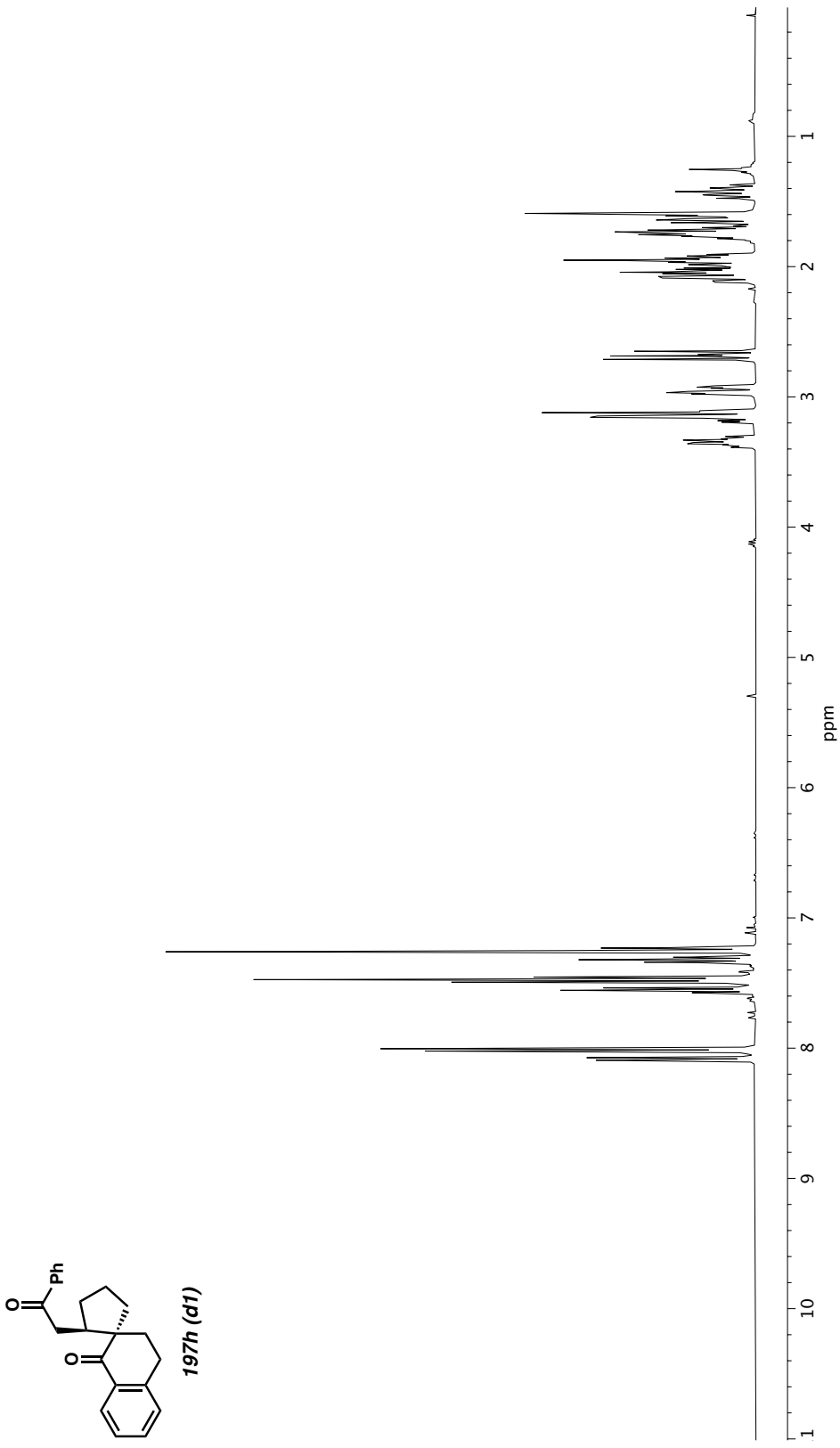

Figure A2.22. *^1H NMR (400 MHz, $CDCl_3$) of compound* ***197h (d1).***

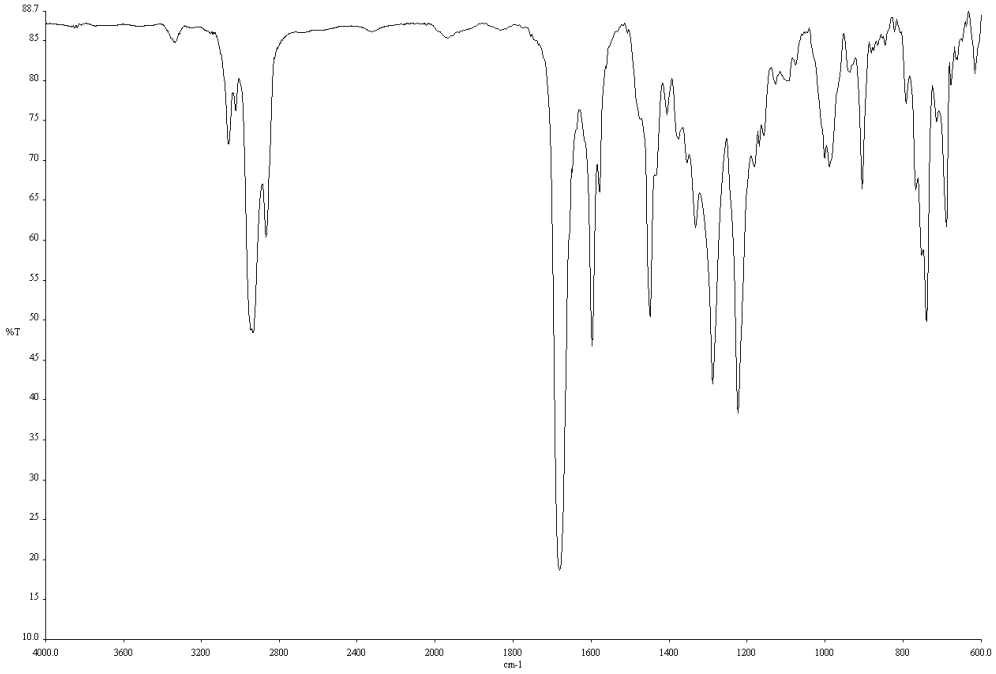

Figure A2.23. *Infrared spectrum (Thin Film, NaCl) of compound* ***197h (d1).***

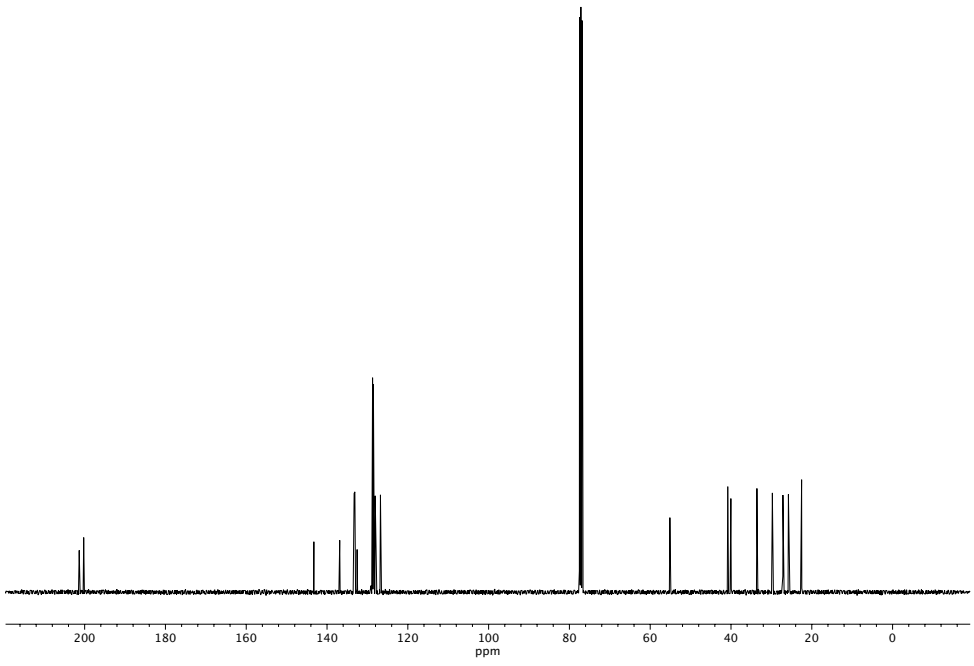

Figure A2.24. *^{13}C NMR (100 MHz, $CDCl_3$) of compound 197h* ***(d1).***

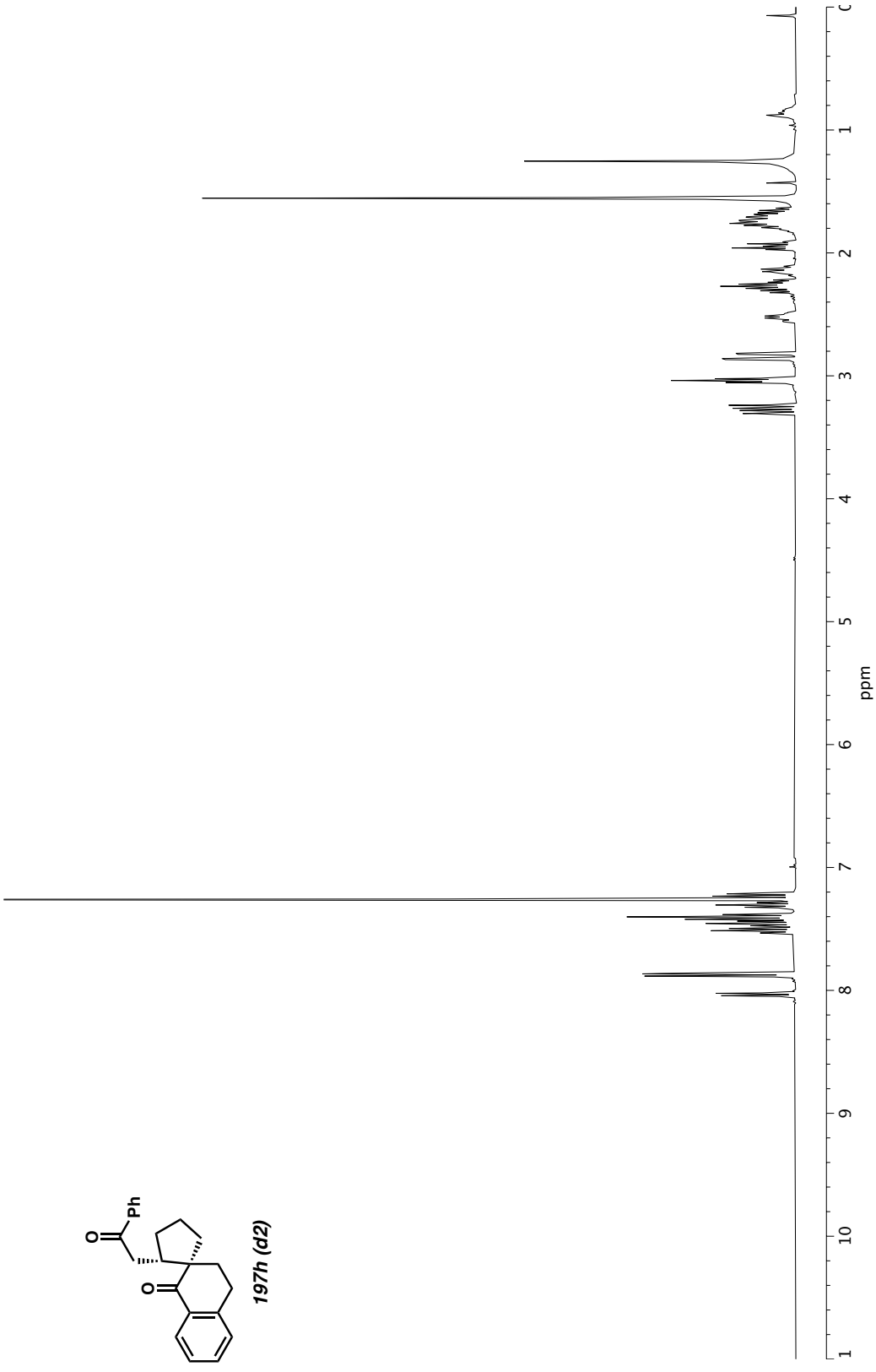

Figure A2.25. *^1H NMR (400 MHz, $CDCl_3$) of compound* ***197h (d2).***

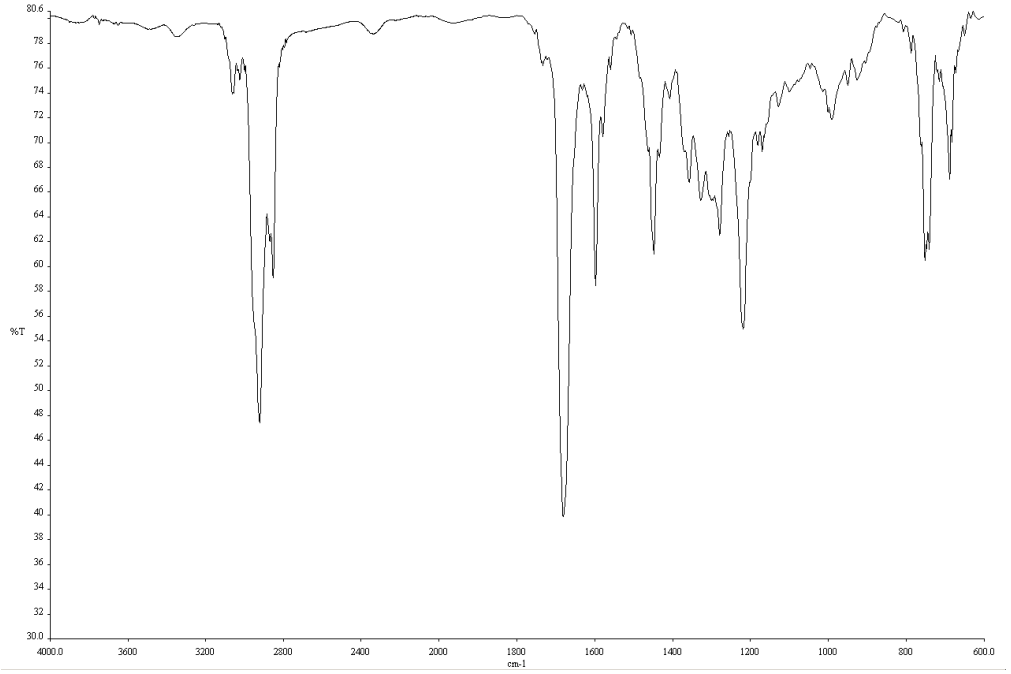

Figure A2.26. *Infrared spectrum (Thin Film, NaCl) of compound* ***197h (d2).***

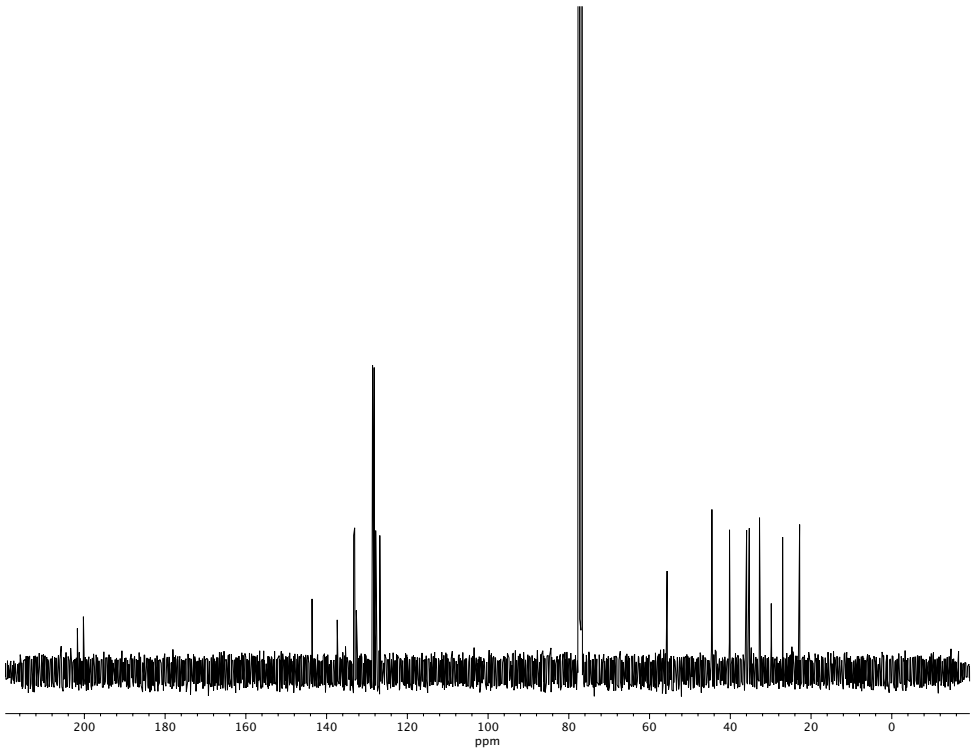

Figure A2.27. *^{13}C NMR (100 MHz, $CDCl_3$) of compound* ***197h (d2).***

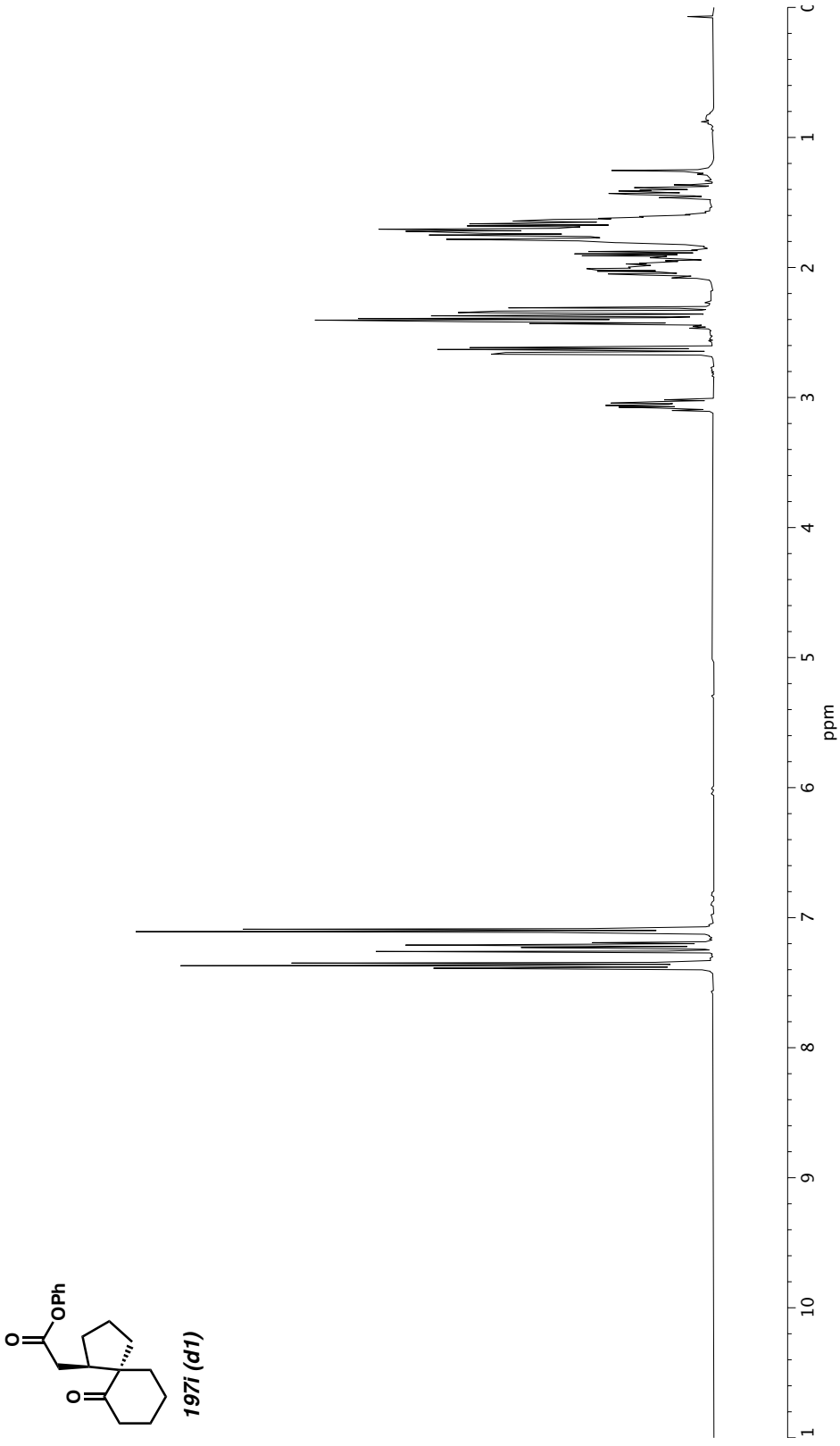

Figure A2.28. *^1H NMR (400 MHz, $CDCl_3$) of compound* ***197i (d1).***

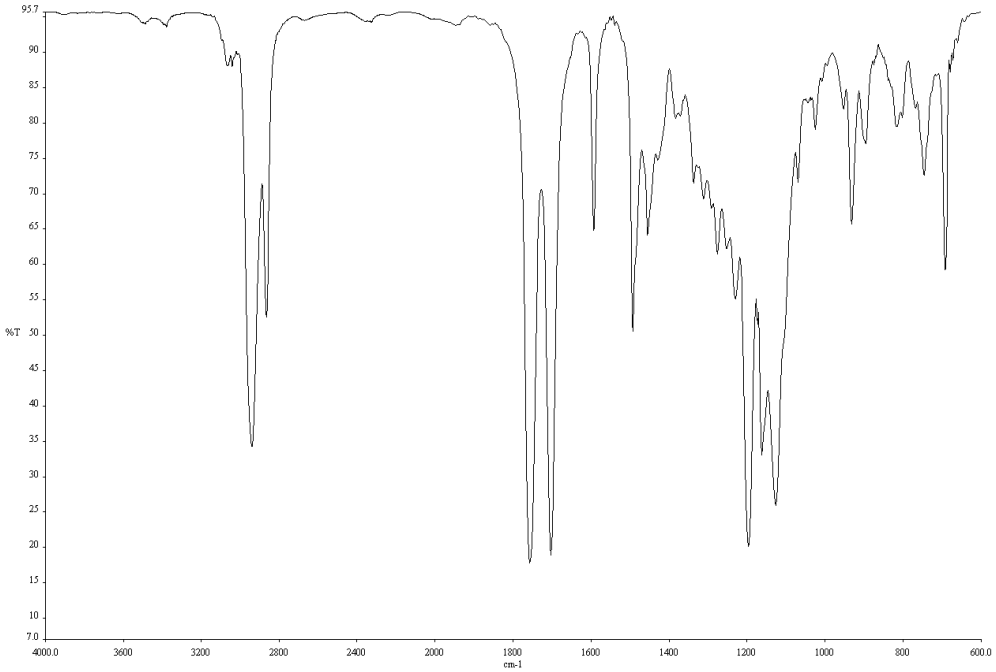

Figure A2.29. *Infrared spectrum (Thin Film, NaCl) of compound* ***197i (d1).***

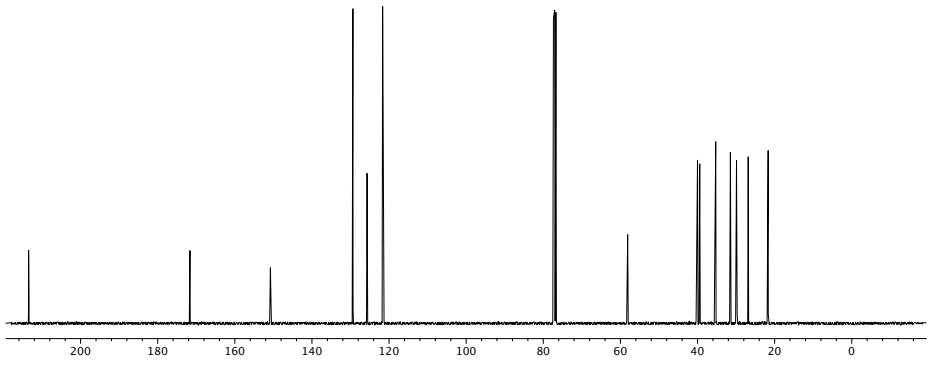

Figure A2.30. *^{13}C NMR (100 MHz, $CDCl_3$) of compound* ***197i (d1).***

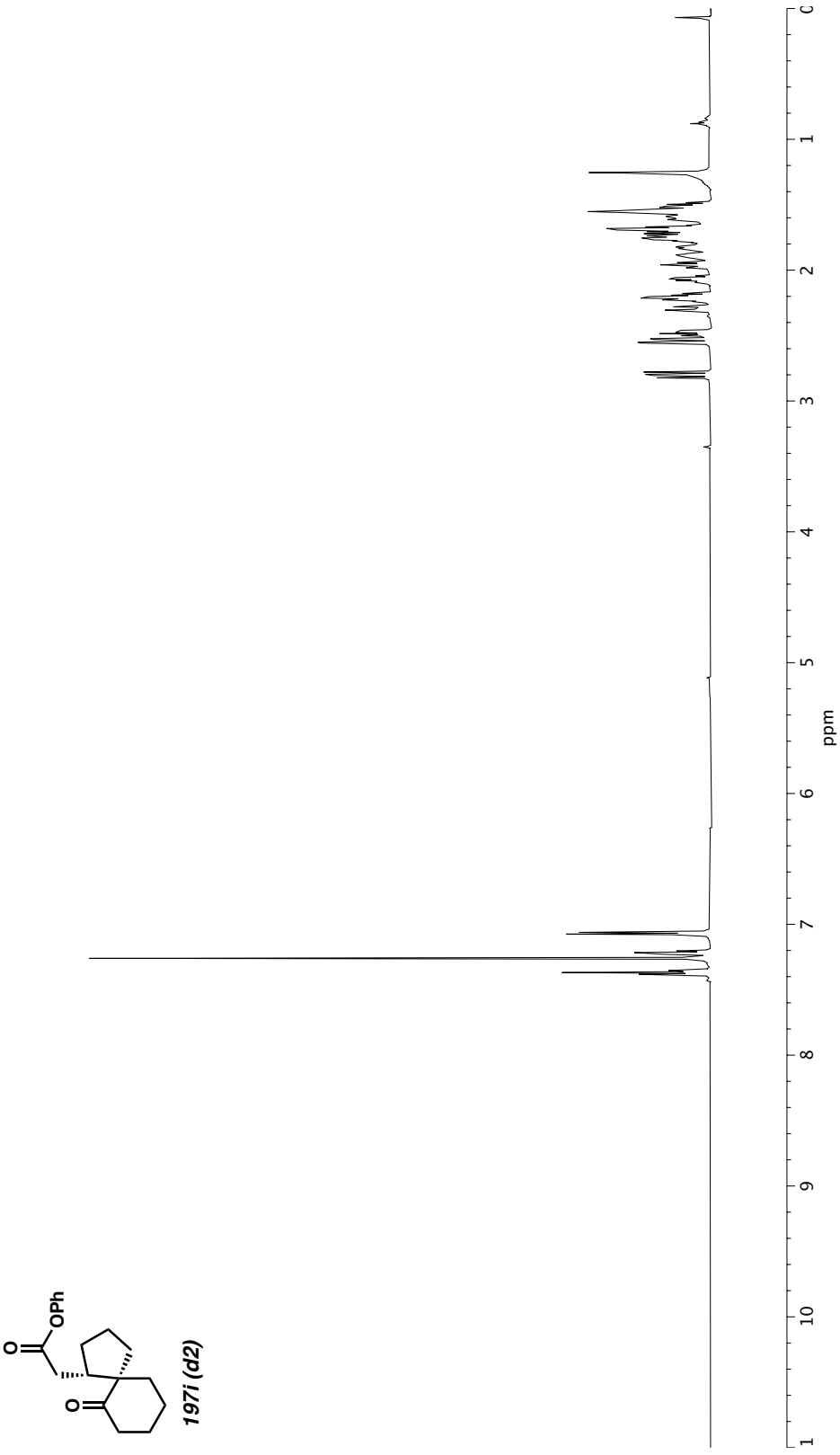

Figure A2.31. *^1H NMR (600 MHz, $CDCl_3$) of compound* ***197i (d2).***

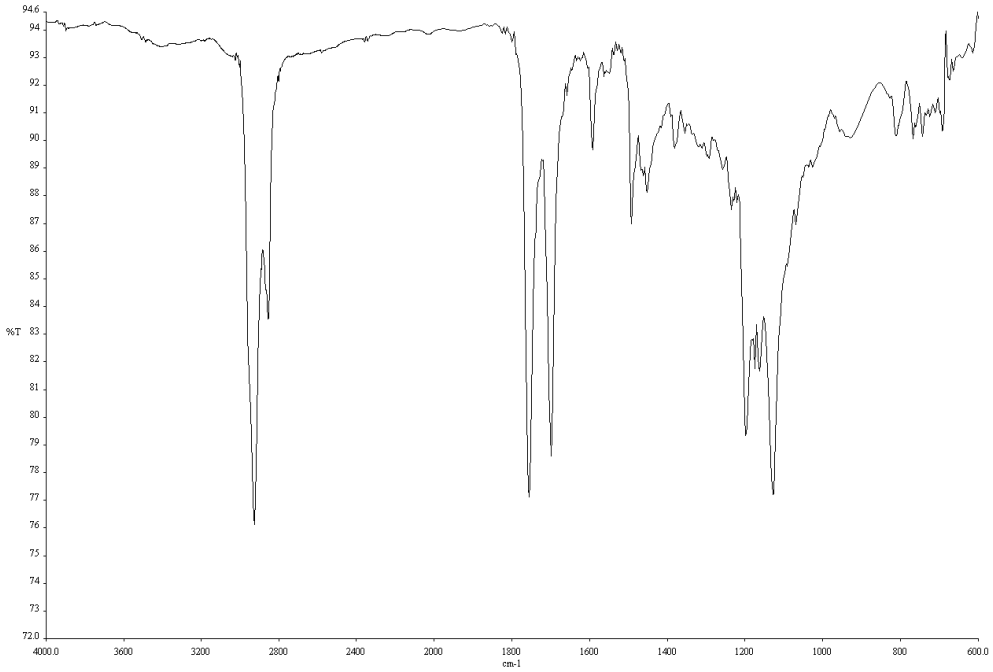

Figure A2.32. *Infrared spectrum (Thin Film, NaCl) of compound* ***197i (d2).***

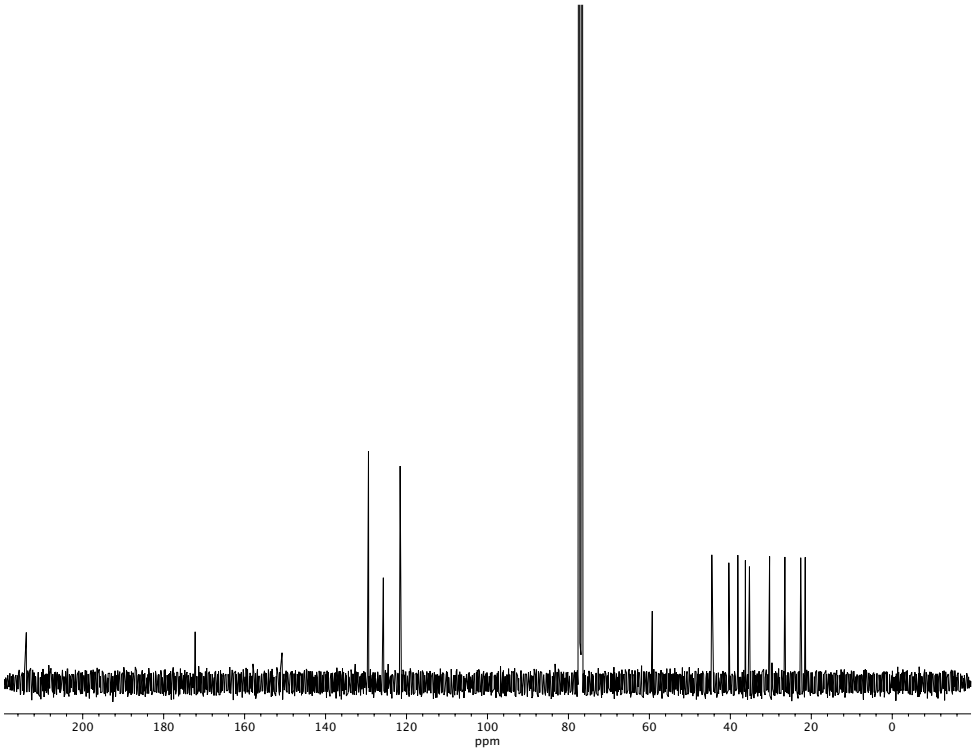

Figure A2.33. *^{13}C NMR (100 MHz, $CDCl_3$) of compound* ***197i (d2).***

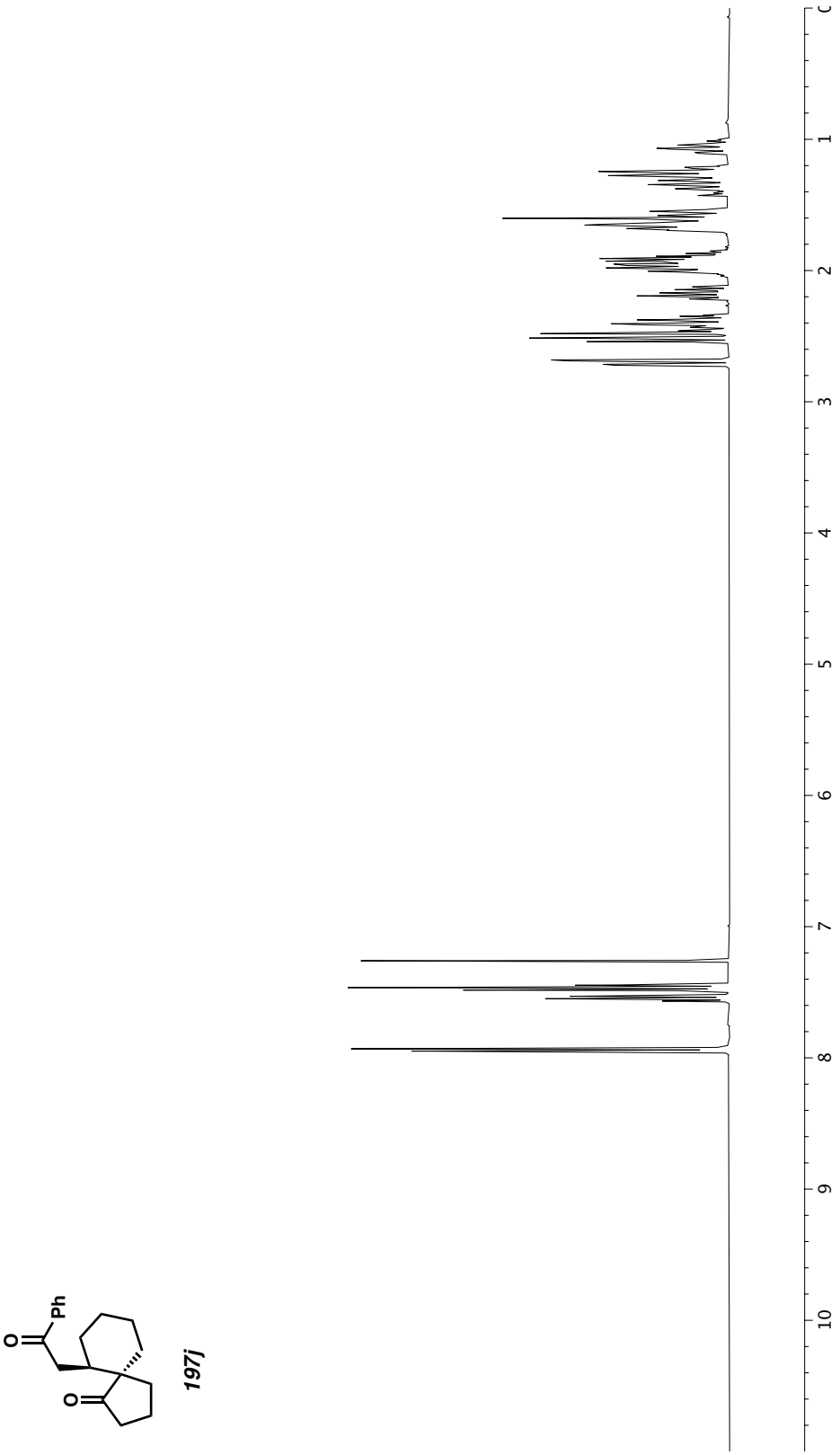

Figure A2.34. *^1H NMR (600 MHz, $CDCl_3$) of compound* ***197j.***

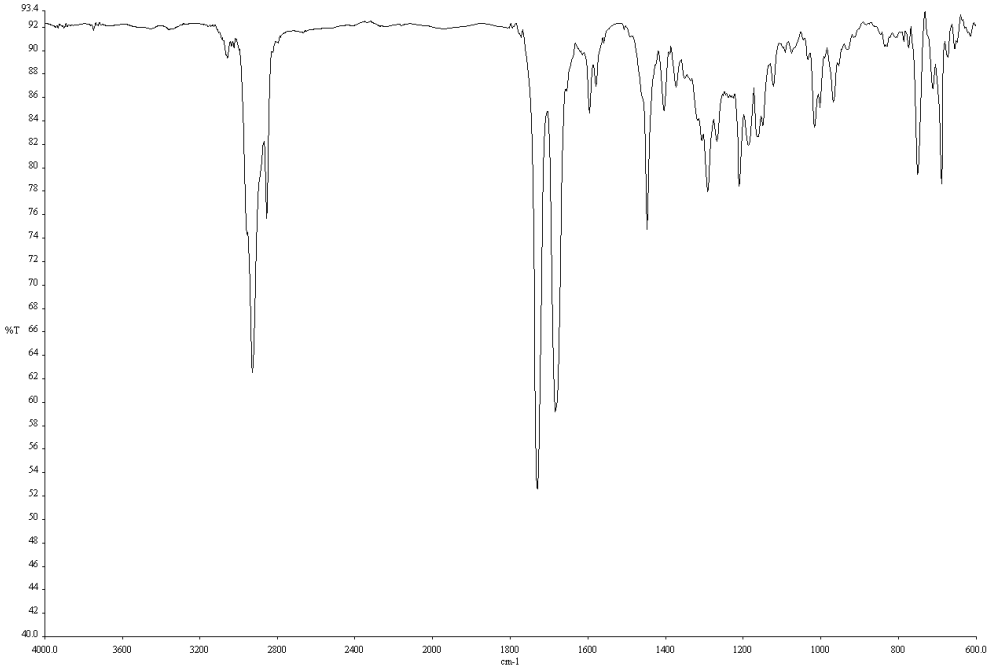

Figure A2.35. *Infrared spectrum (Thin Film, NaCl) of compound* ***197j.***

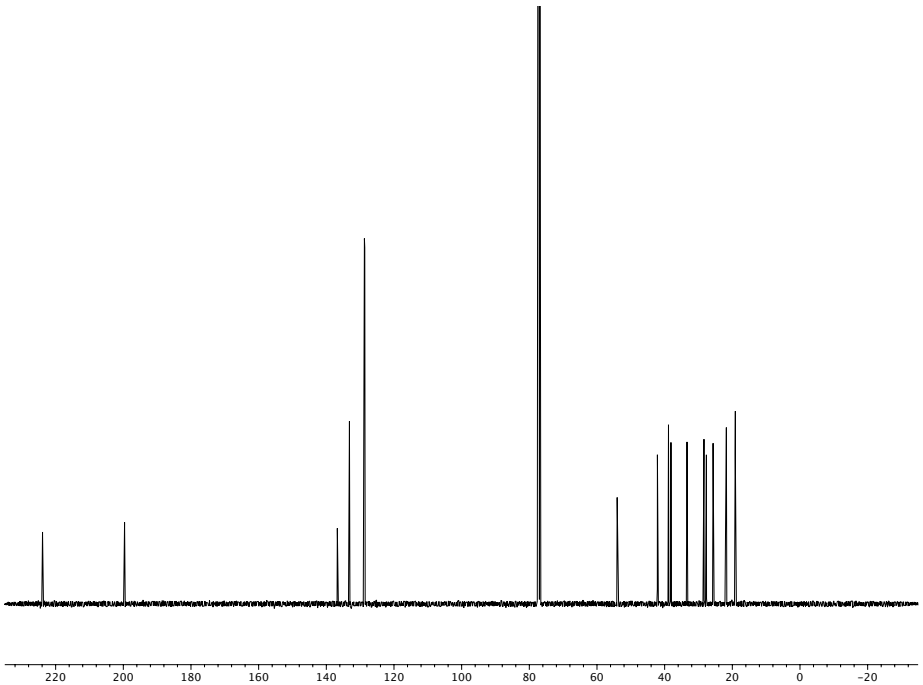

Figure A2.36. *^{13}C NMR (100 MHz, $CDCl_3$) of compound* ***197j.***

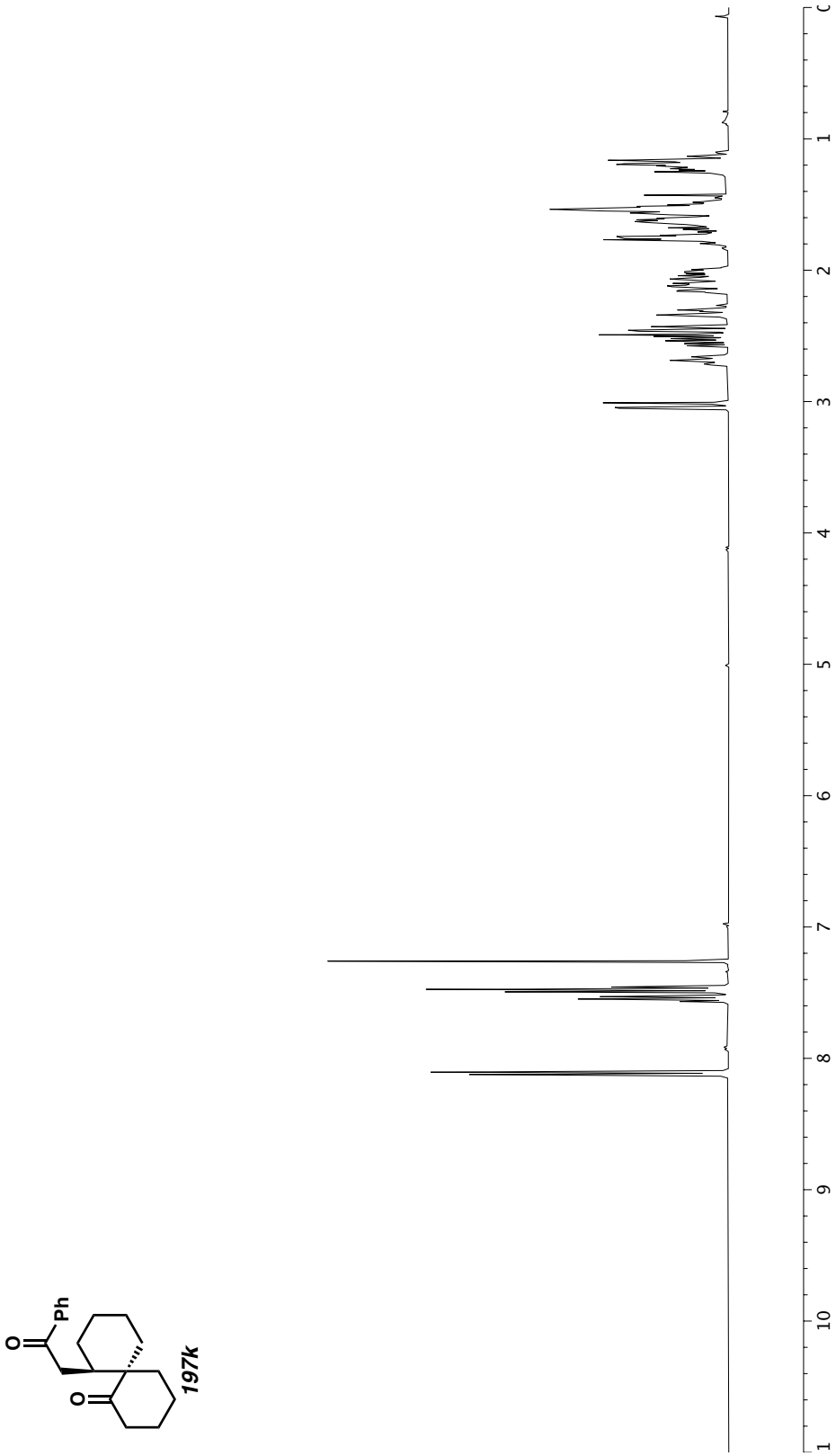

Figure A2.37. *^1H NMR (400 MHz, $CDCl_3$) of compound* ***197k.***

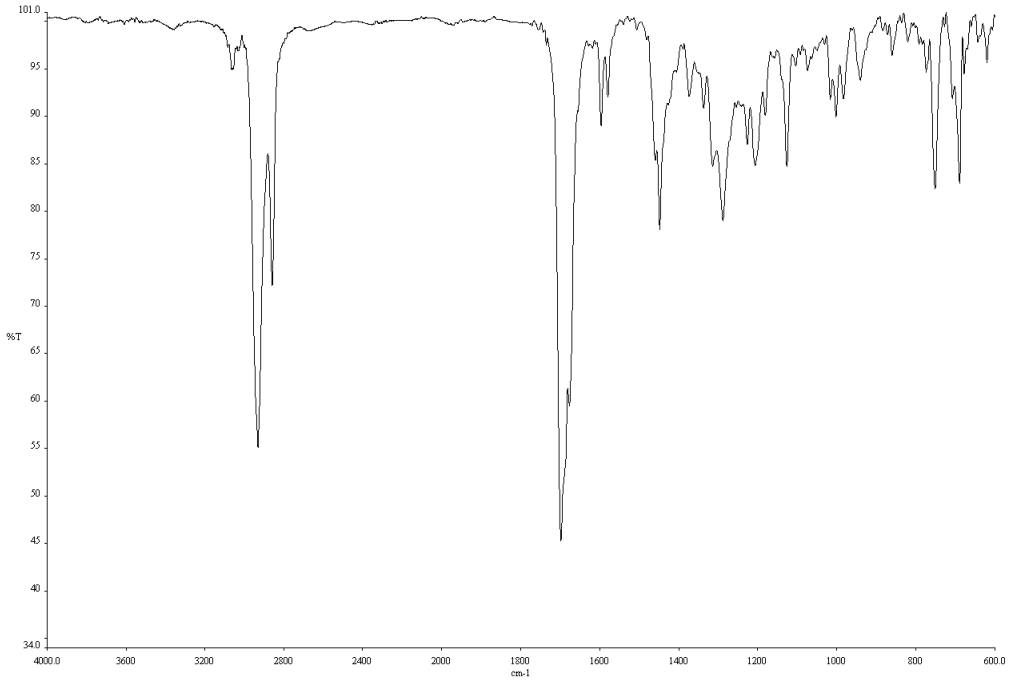

Figure A2.38. *Infrared spectrum (Thin Film, NaCl) of compound* ***197k.***

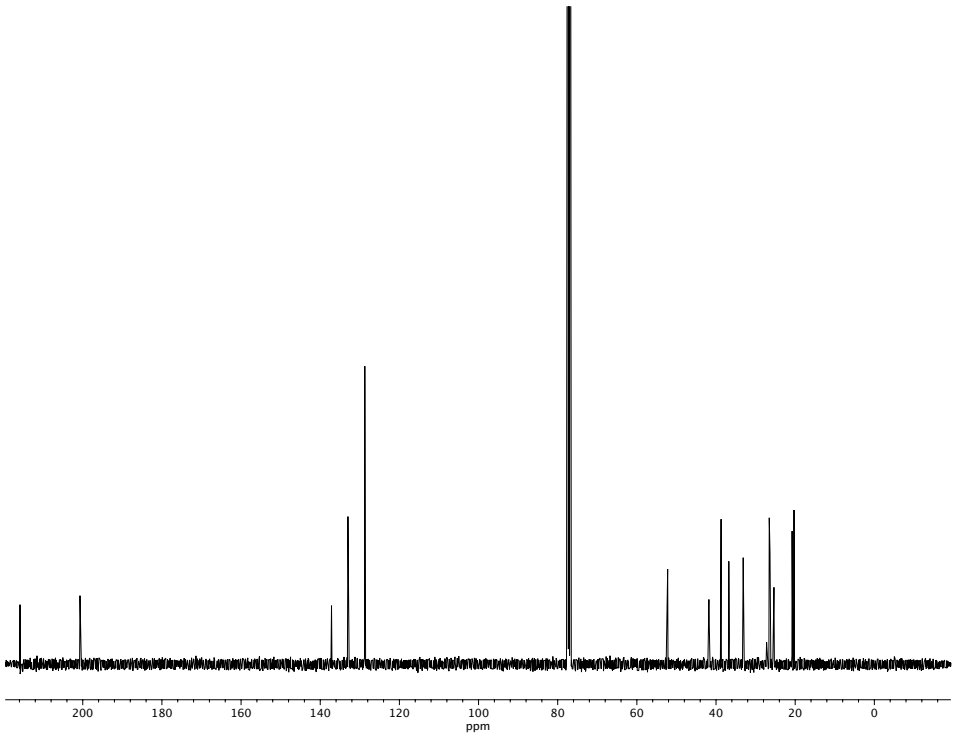

Figure A2.39. *^{13}C NMR (100 MHz, $CDCl_3$) of compound* ***197k.***

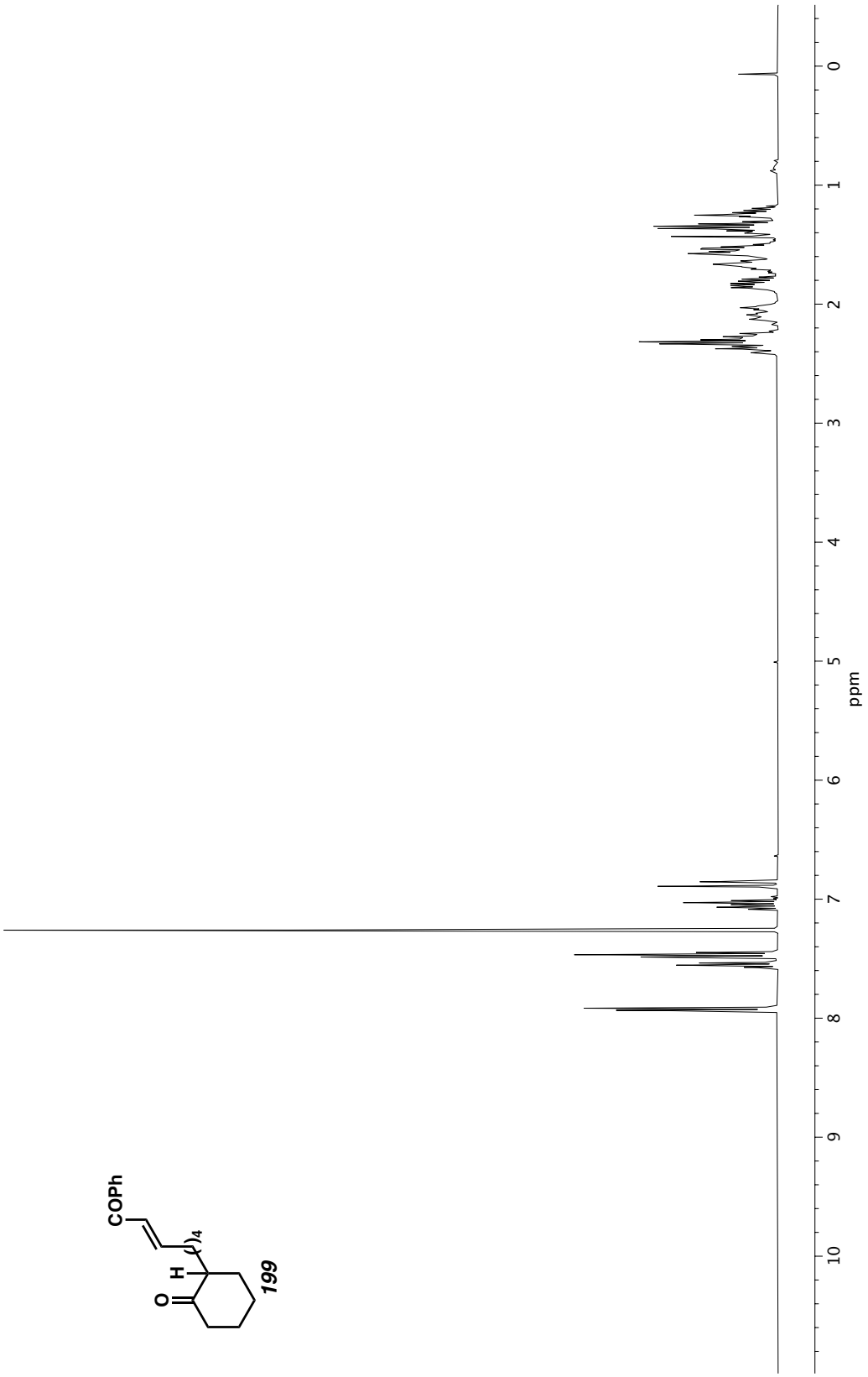

Figure A2.40. *^1H NMR (400 MHz, $CDCl_3$) of compound* ***199.***

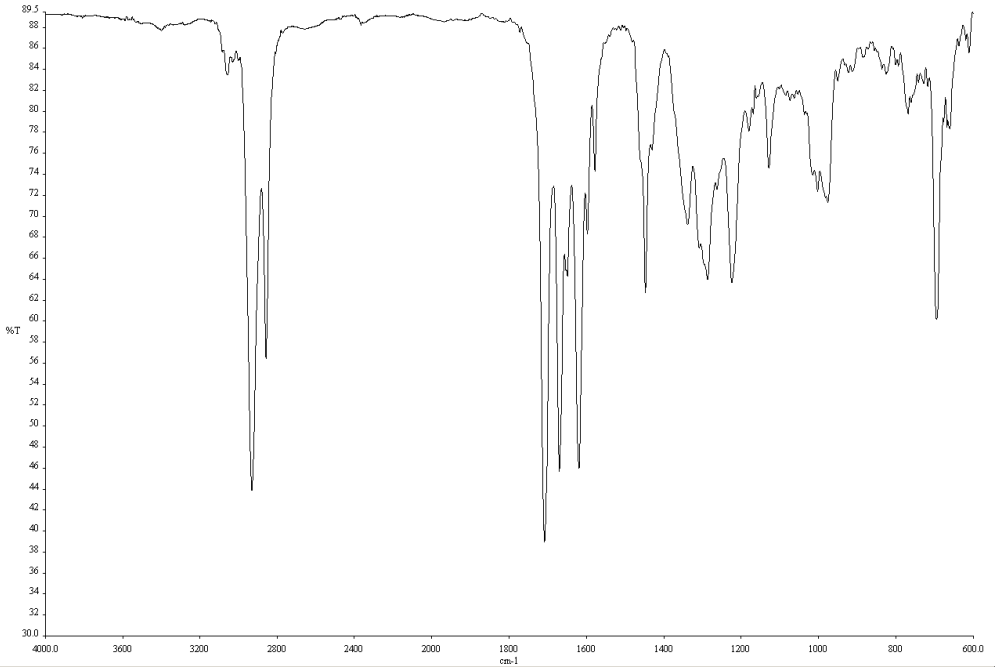

Figure A2.41. *Infrared spectrum (Thin Film, NaCl) of compound* ***199.***

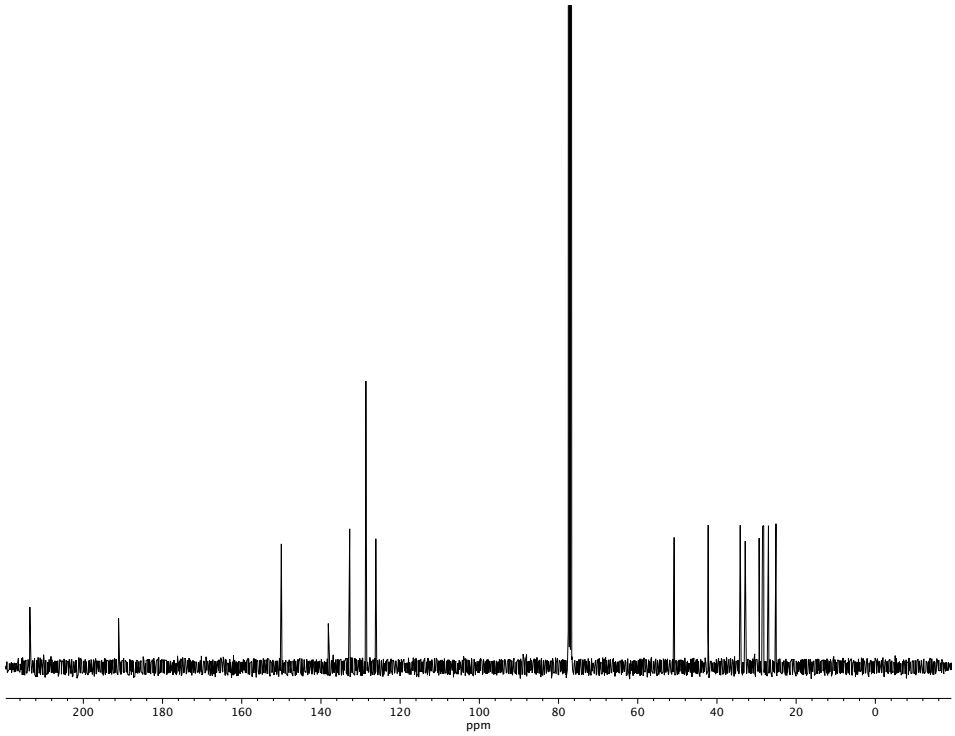

Figure A2.42. *^{13}C NMR (100 MHz, $CDCl_3$) of compound* ***199.***

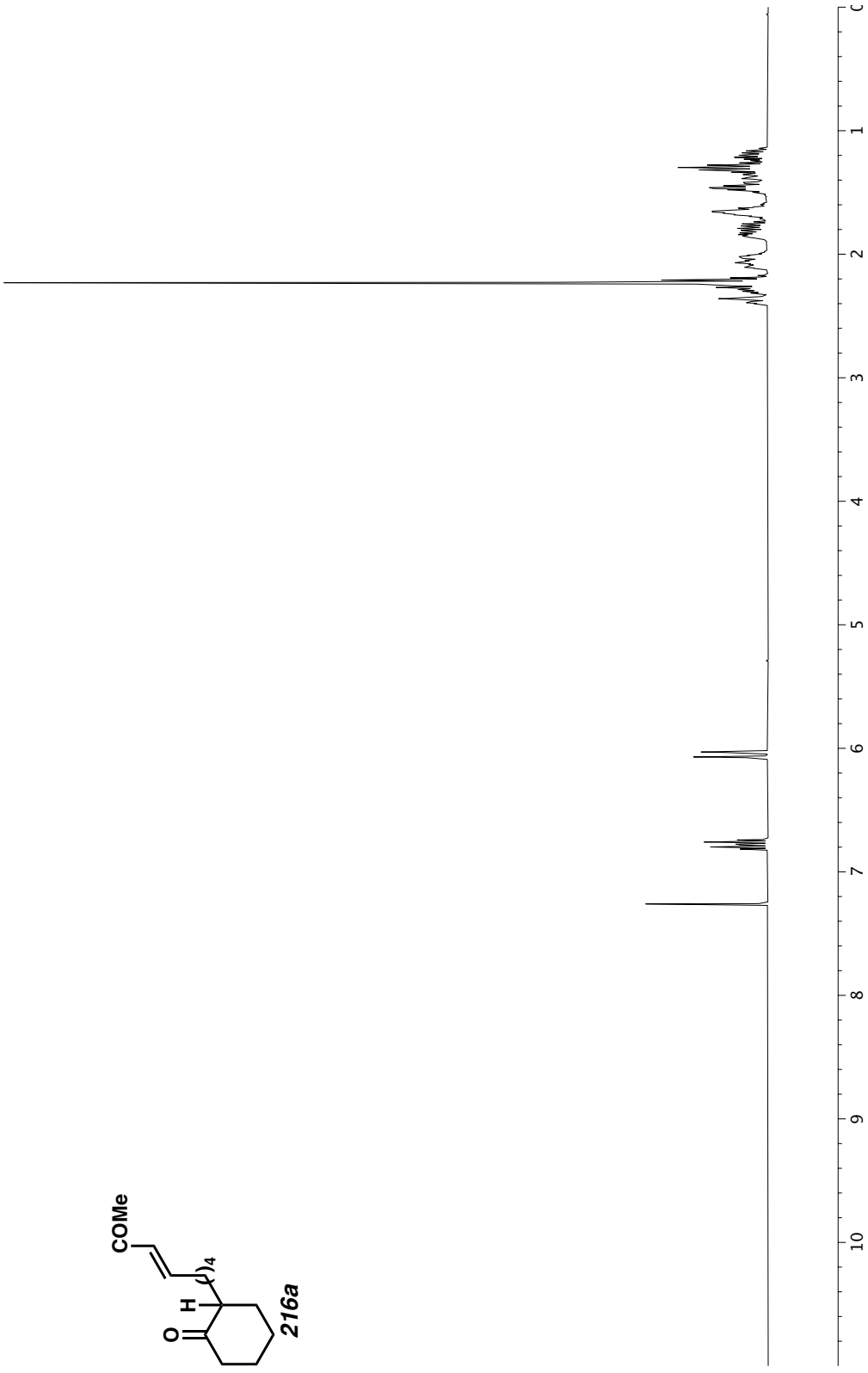

Figure A2.43. *^1H NMR (400 MHz, $CDCl_3$) of compound* ***216a.***

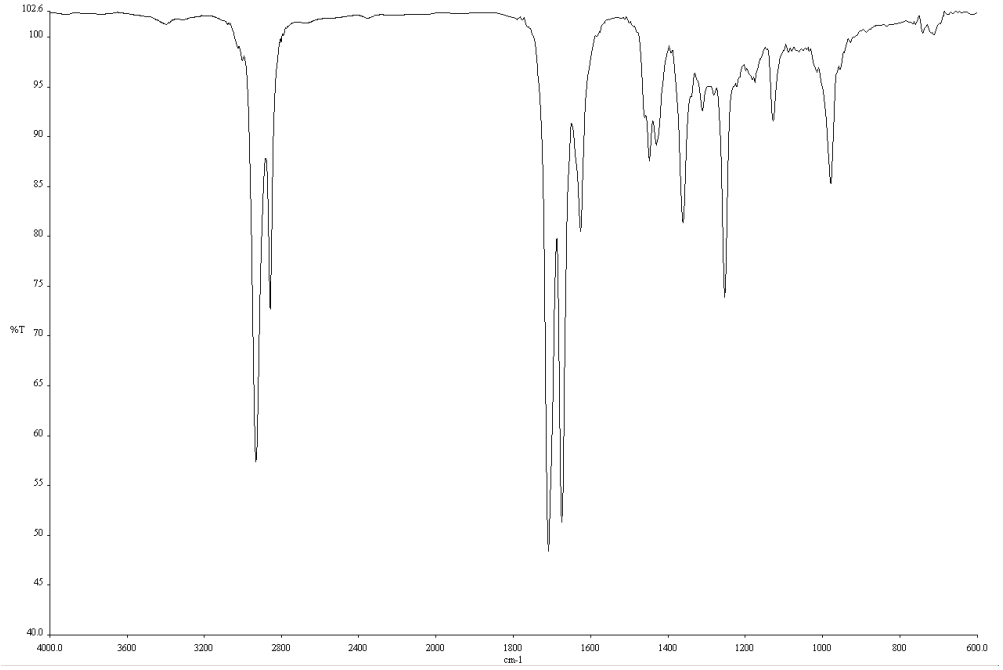

Figure A2.44. *Infrared spectrum (Thin Film, NaCl) of compound* ***216a.***

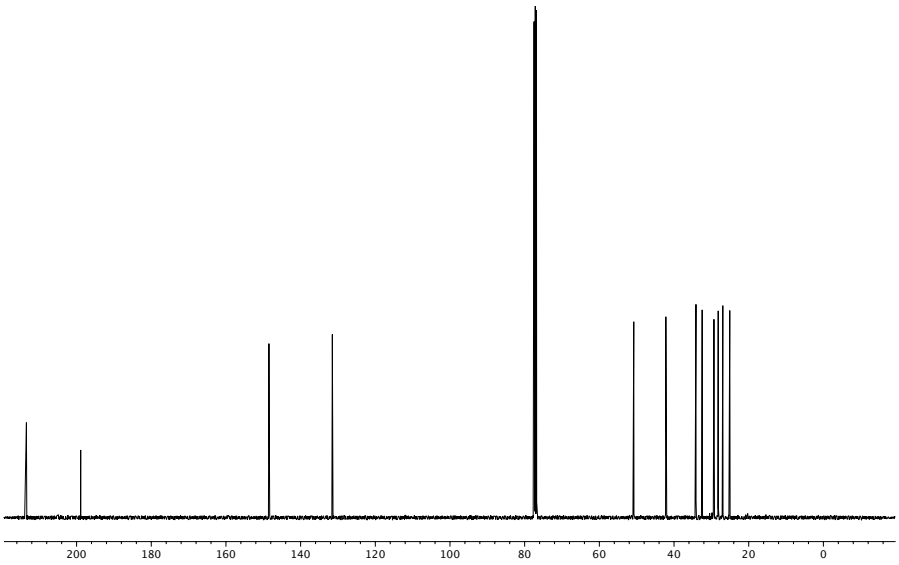

Figure A2.45. *^{13}C NMR (100 MHz, $CDCl_3$) of compound* ***216a.***

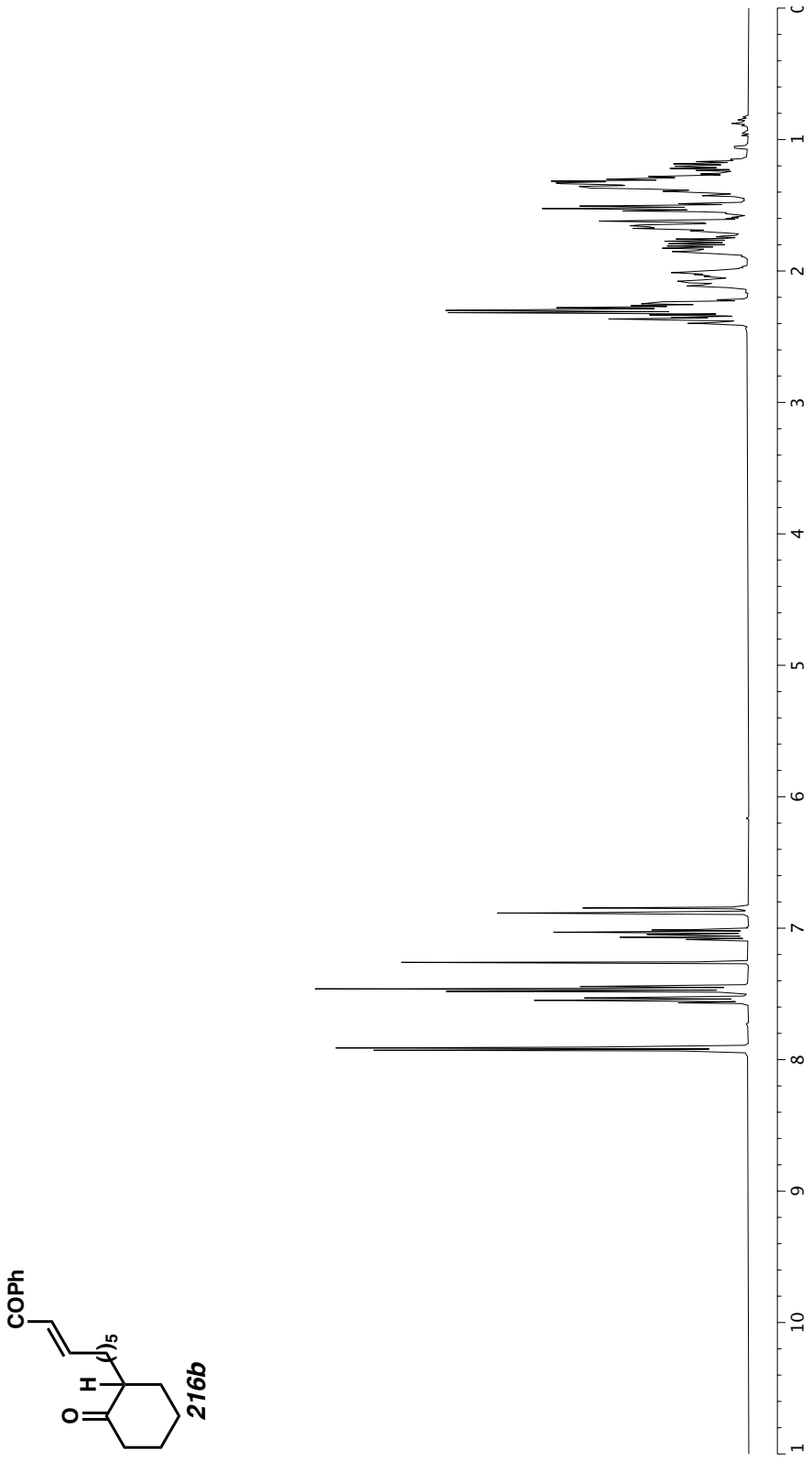

Figure A2.46. *^1H NMR (400 MHz, $CDCl_3$) of compound* ***216b.***

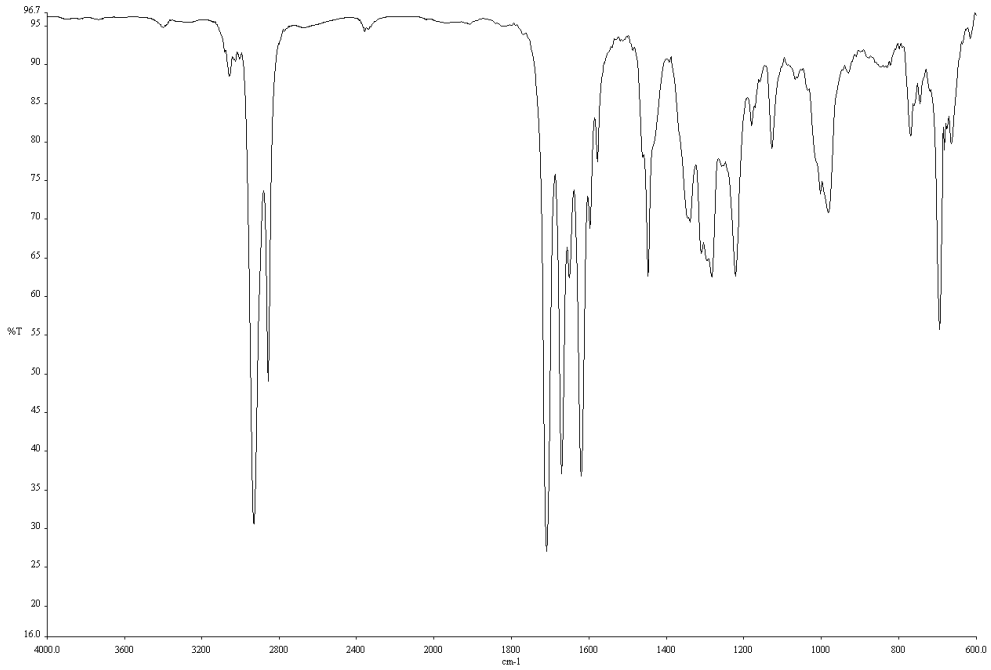

Figure A2.47. *Infrared spectrum (Thin Film, NaCl) of compound* ***216b.***

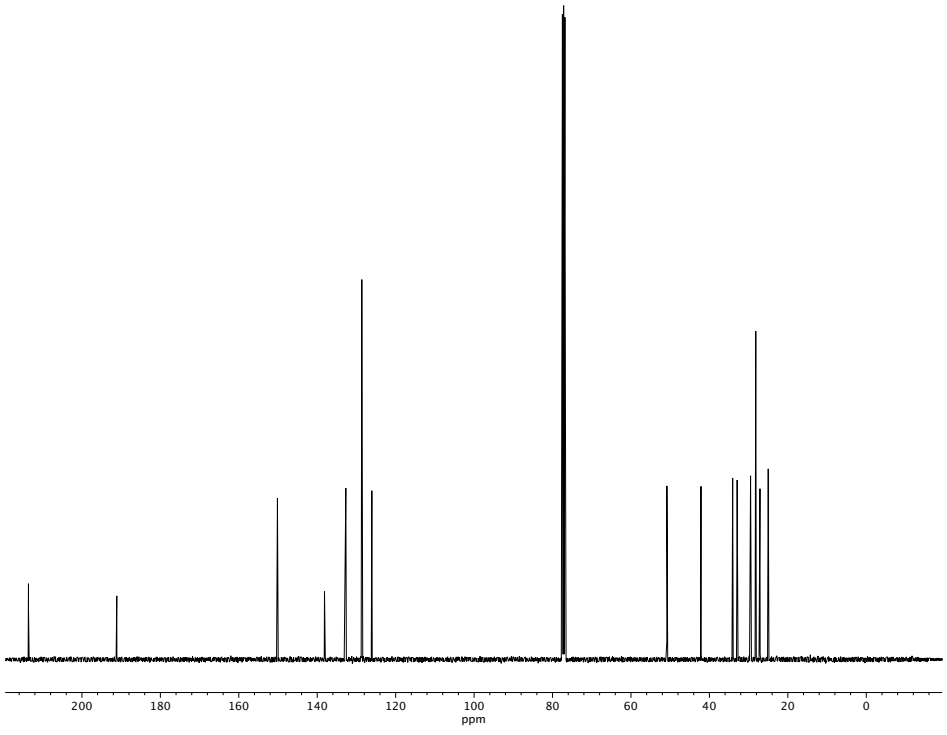

Figure A2.48. *^{13}C NMR (100 MHz, $CDCl_3$) of compound* ***216b.***

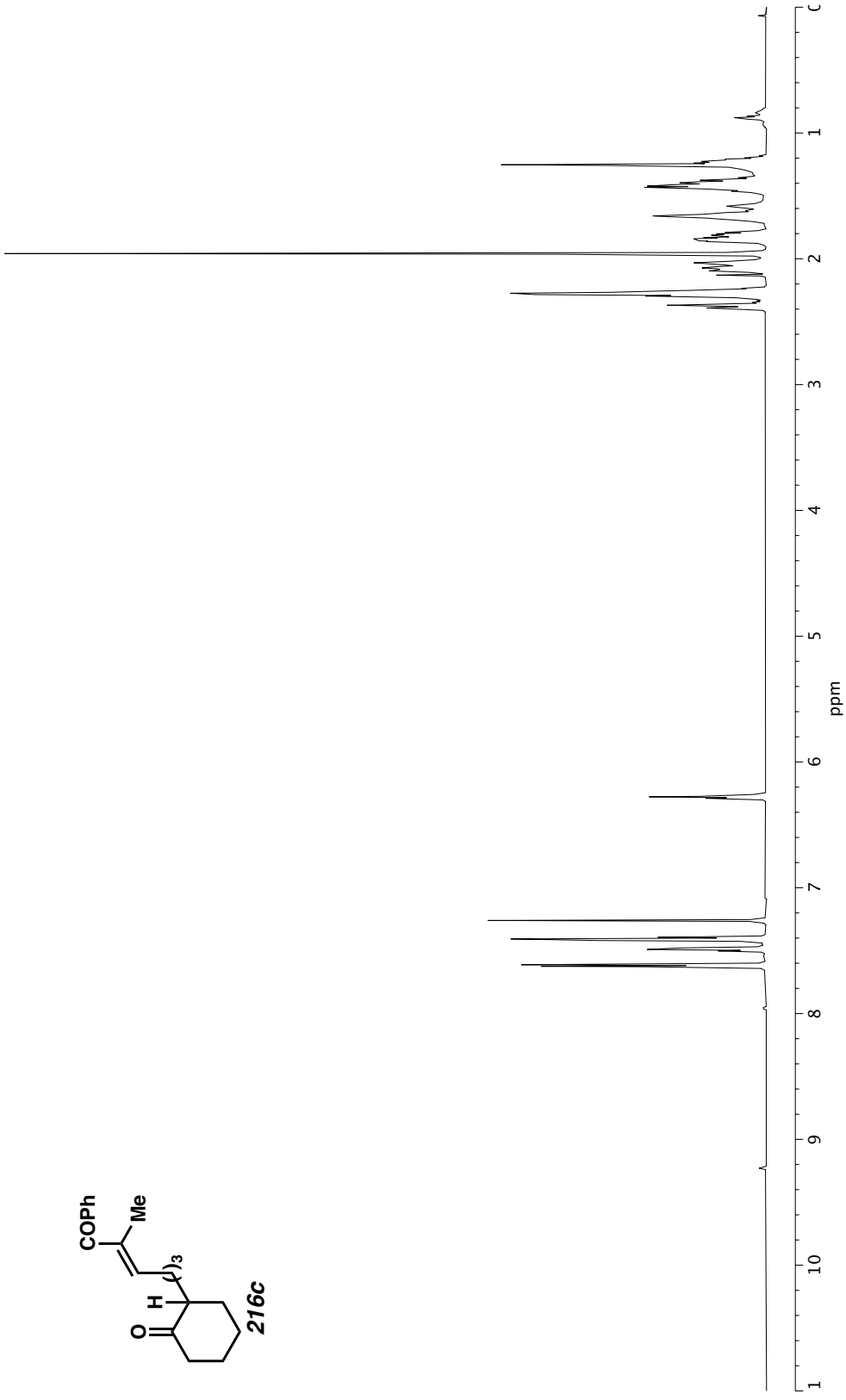

Figure A2.49. *^1H NMR (400 MHz, $CDCl_3$) of compound 216c.*

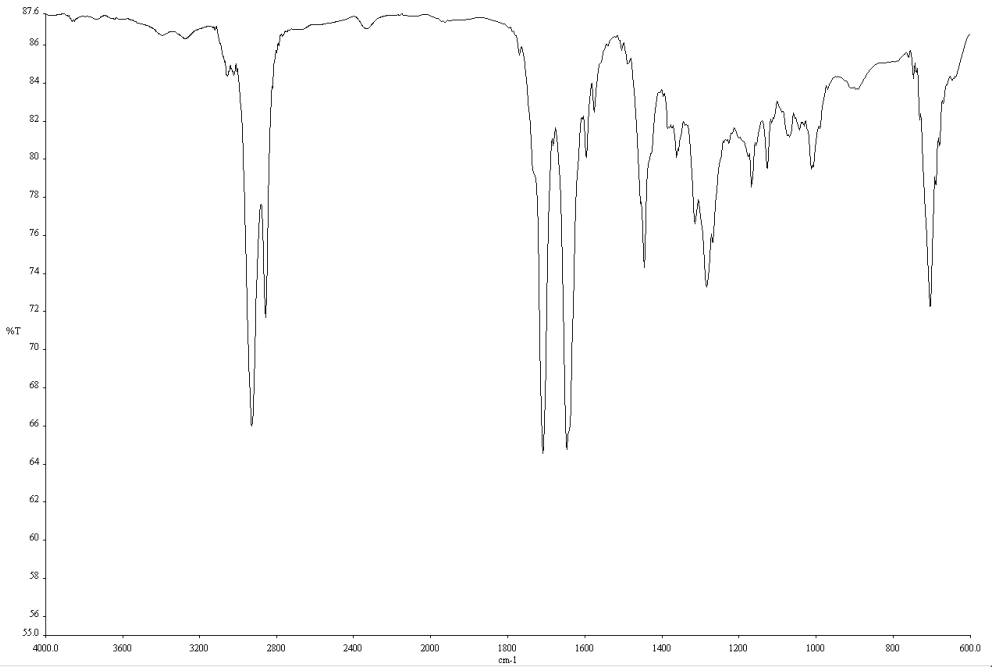

Figure A2.50. *Infrared spectrum (Thin Film, NaCl) of compound* ***216c.***

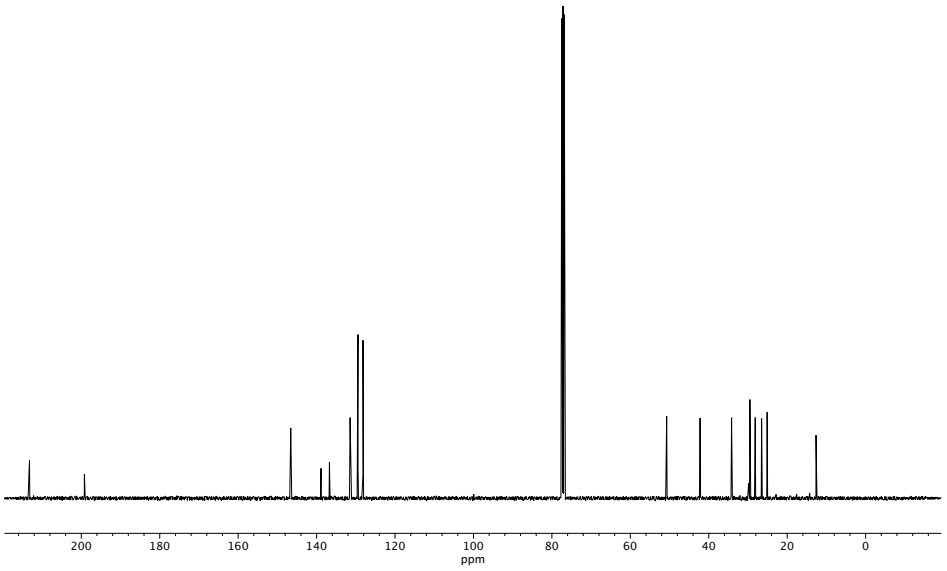

Figure A2.51. *^{13}C NMR (100 MHz, $CDCl_3$) of compound* ***216c.***

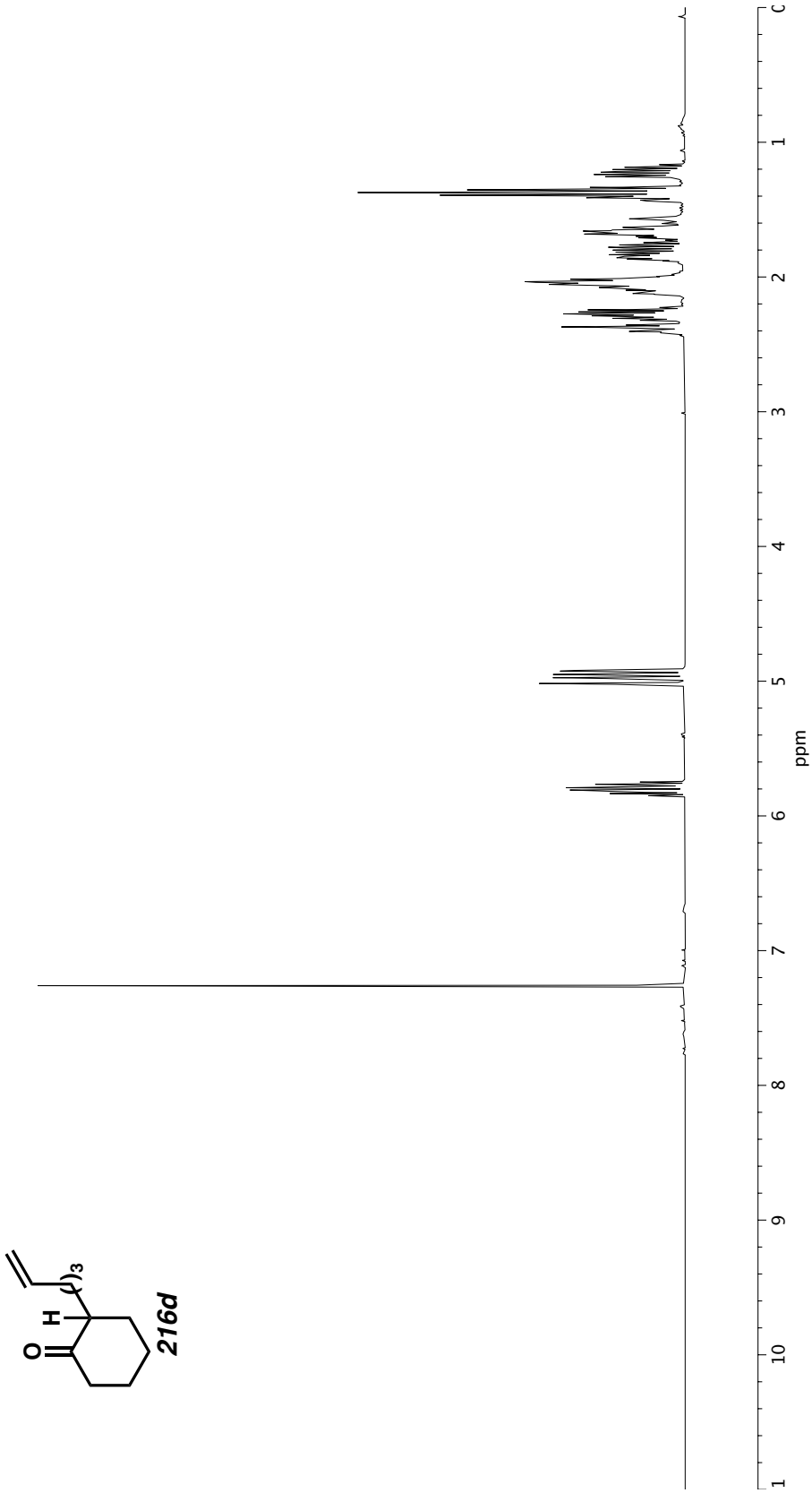

Figure A2.52. *^{1}H NMR (600 MHz, $CDCl_3$) of compound* ***216d.***

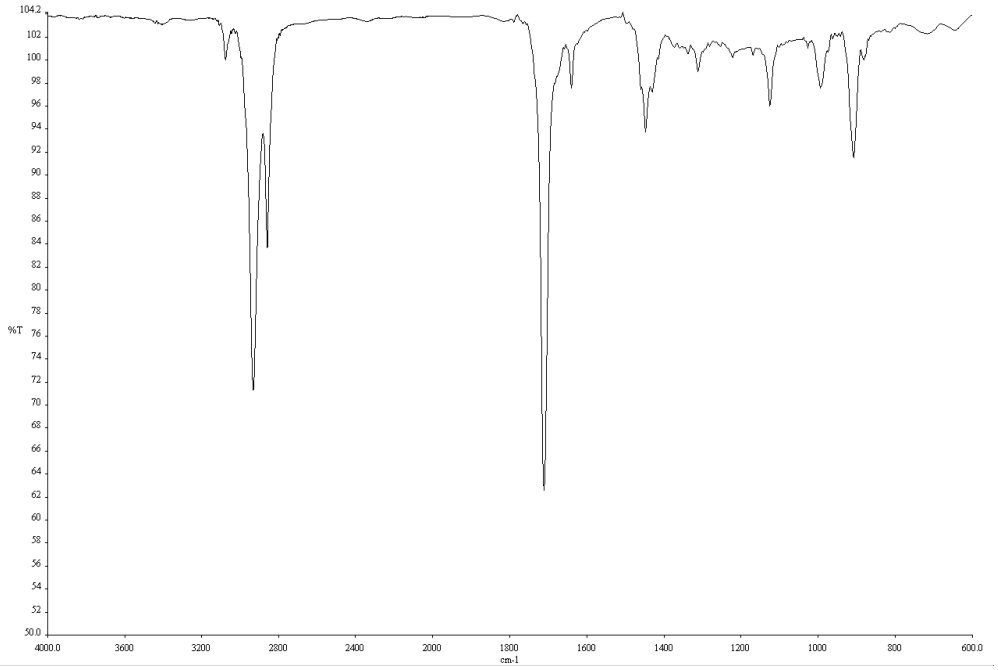

Figure A2.53. *Infrared spectrum (Thin Film, NaCl) of compound* ***216d.***

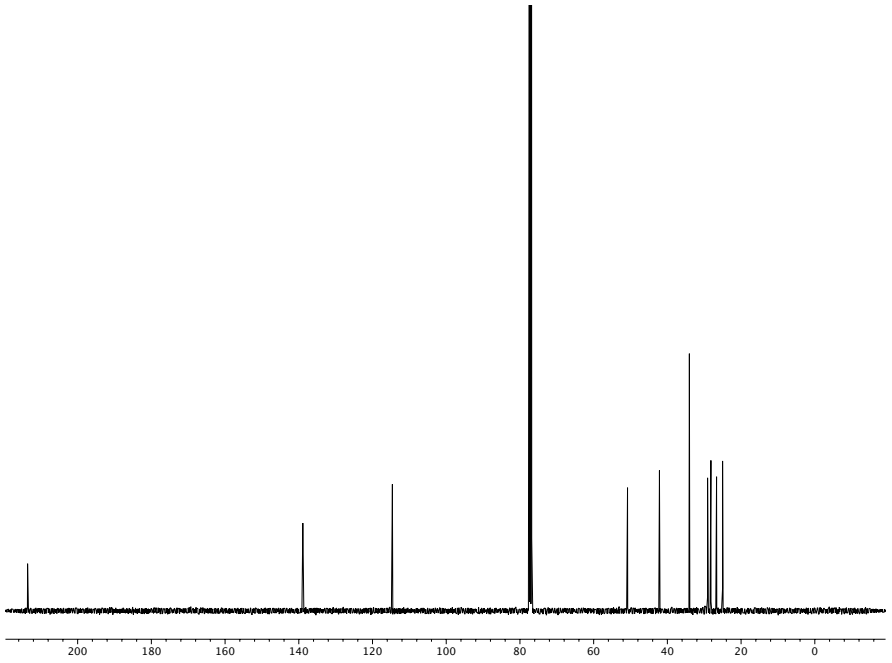

Figure A2.54. *^{13}C NMR (100 MHz, $CDCl_3$) of compound* ***216d.***

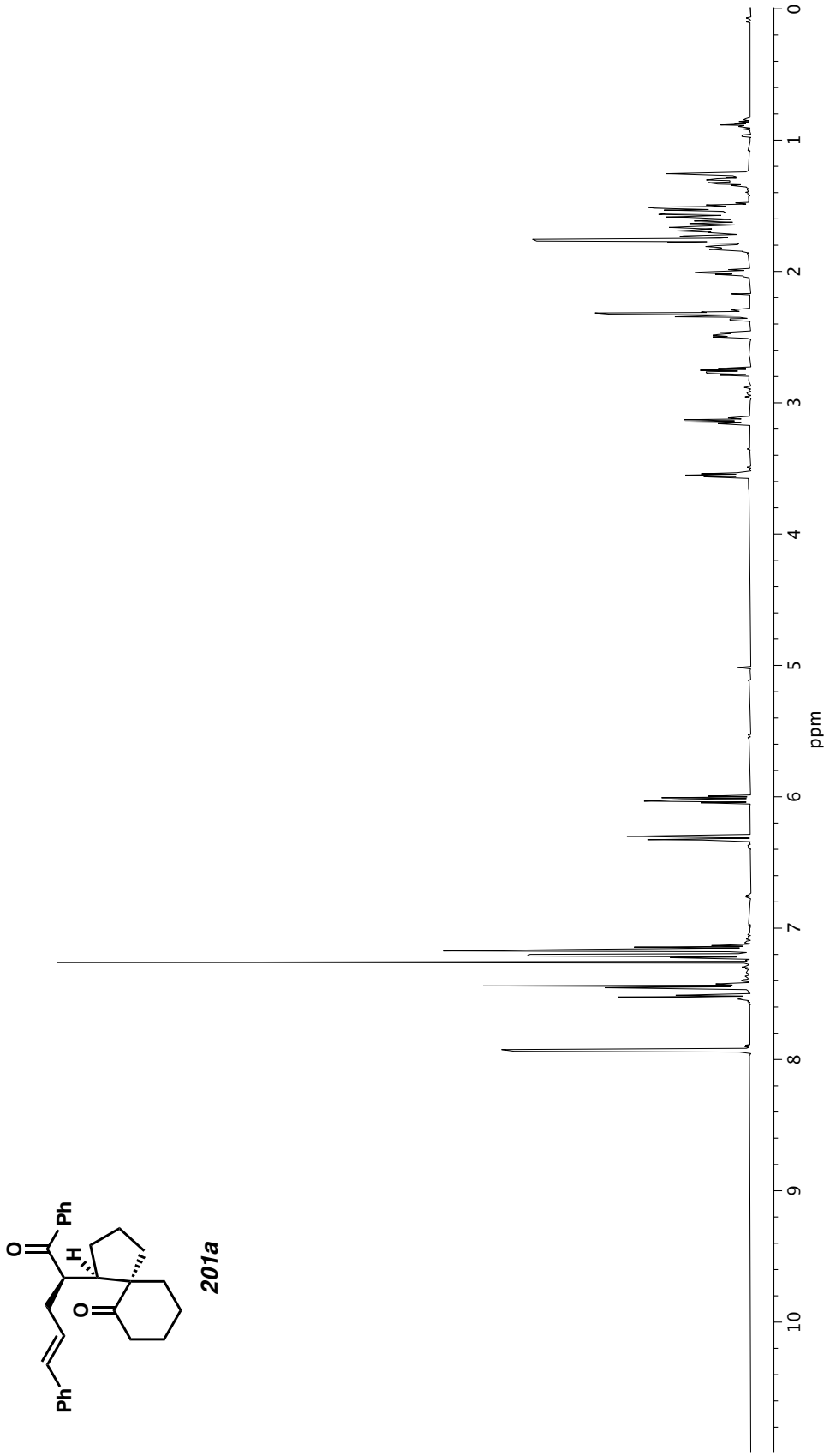

Figure A2.55. *^1H NMR (600 MHz, $CDCl_3$) of compound* ***201a.***

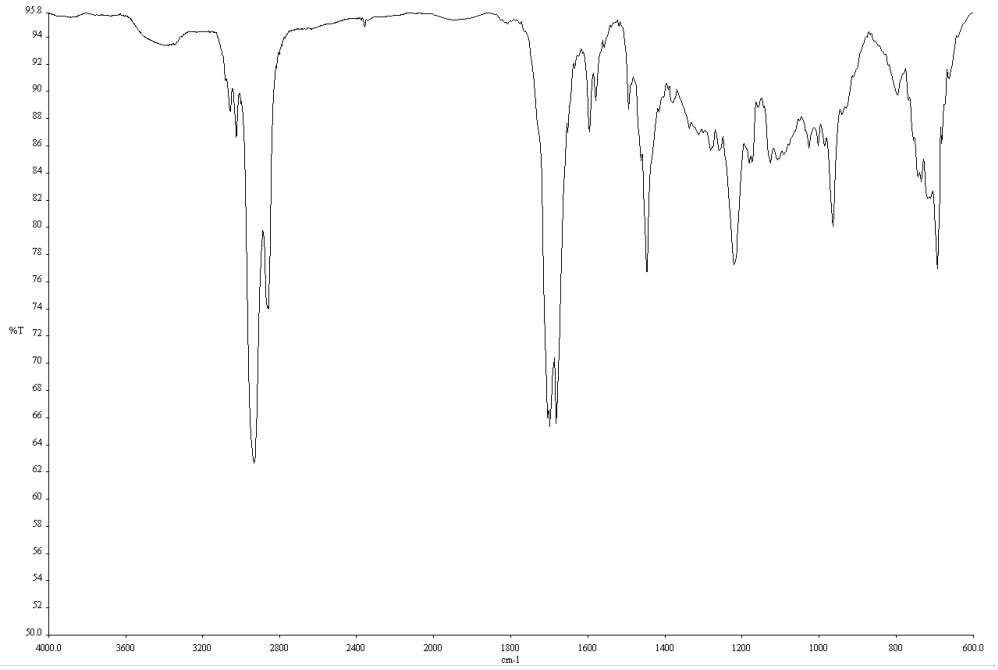

Figure A2.56. *Infrared spectrum (Thin Film, NaCl) of compound* ***201a.***

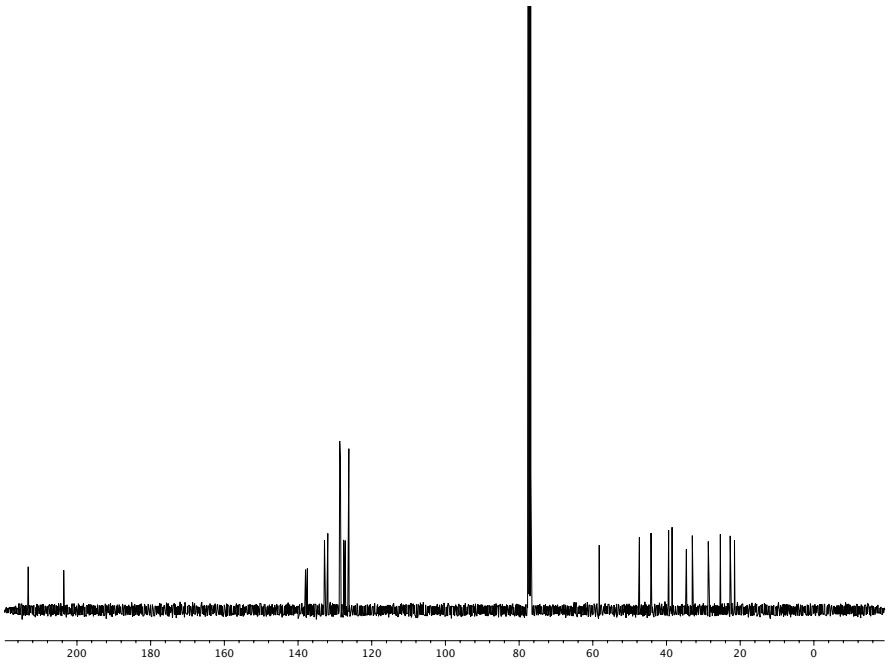

Figure A2.57. *^{13}C NMR (100 MHz, $CDCl_3$) of compound* ***201a.***

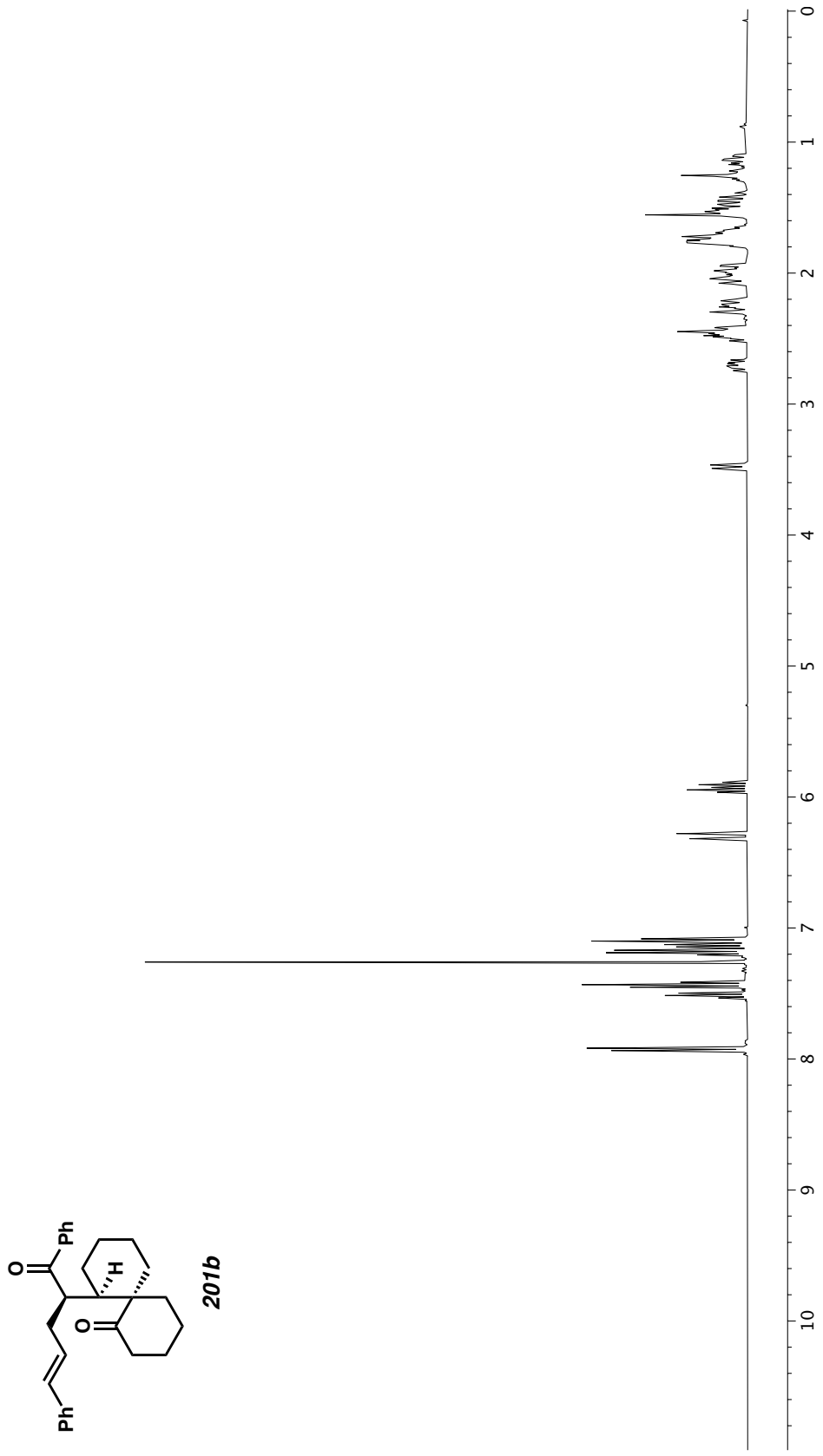

Figure A2.58. *^1H NMR (400 MHz, $CDCl_3$) of compound* ***201b.***

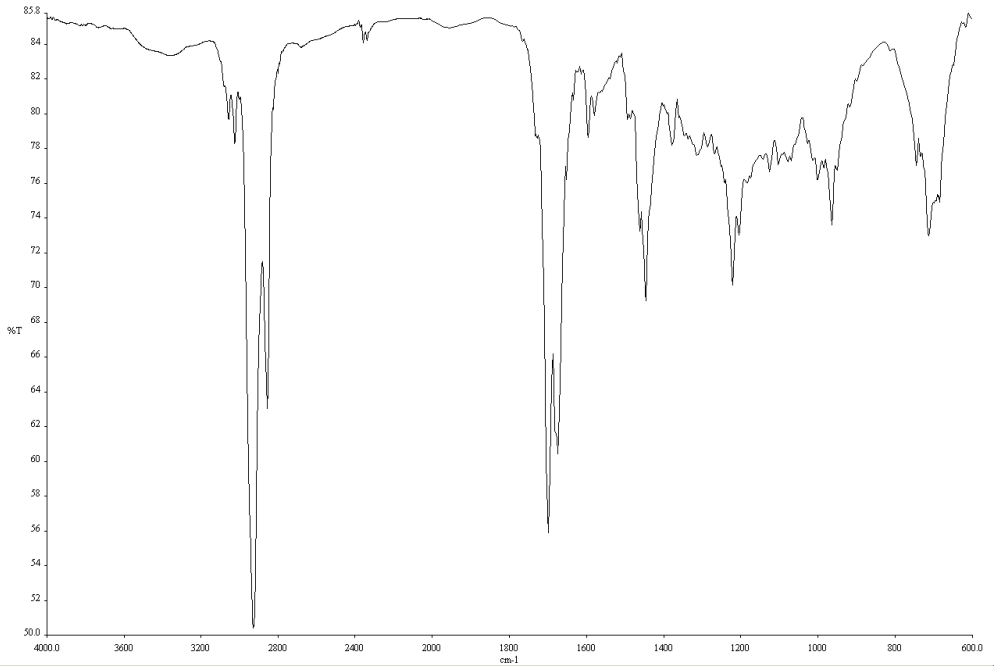

Figure A2.59. *Infrared spectrum (Thin Film, NaCl) of compound* ***201b.***

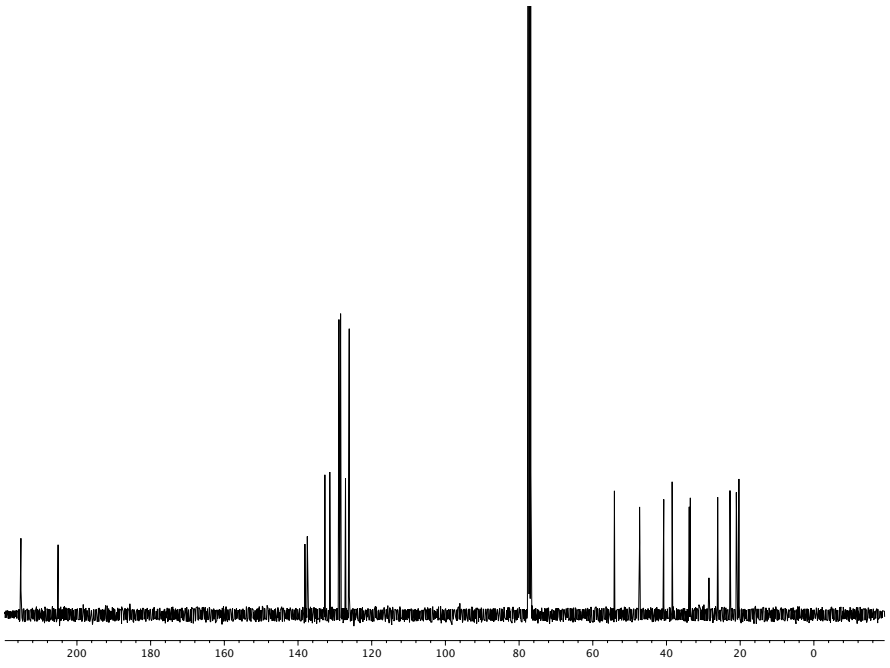

Figure A2.60. *^{13}C NMR (100 MHz, $CDCl_3$) of compound* ***201b.***

Figure A2.61. *^1H NMR (400 MHz, $CDCl_3$) of compound* ***196a.***

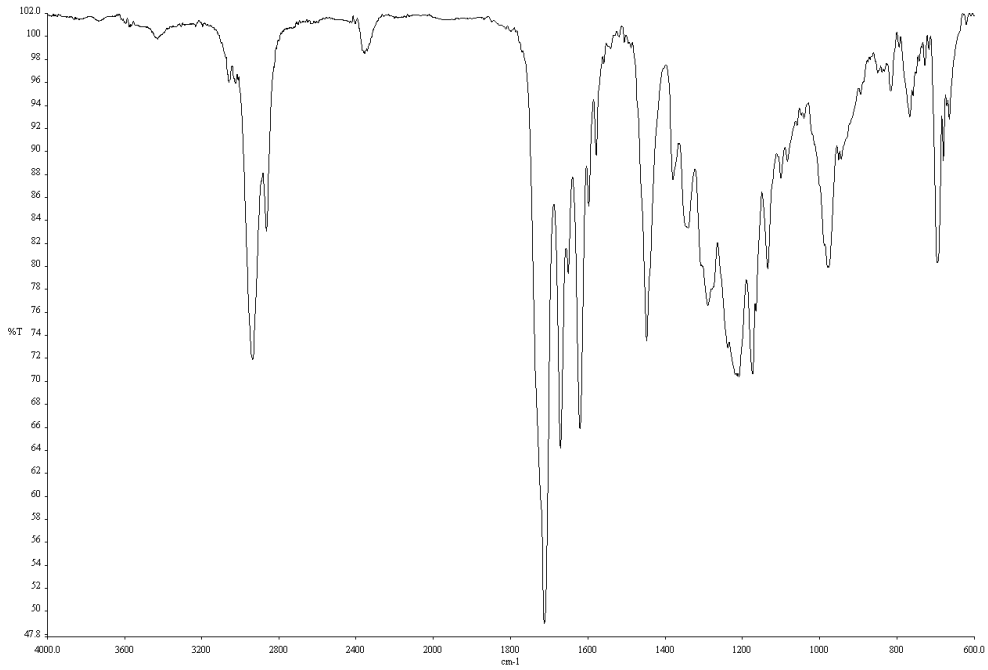

Figure A2.62. *Infrared spectrum (Thin Film, NaCl) of compound* ***196a.***

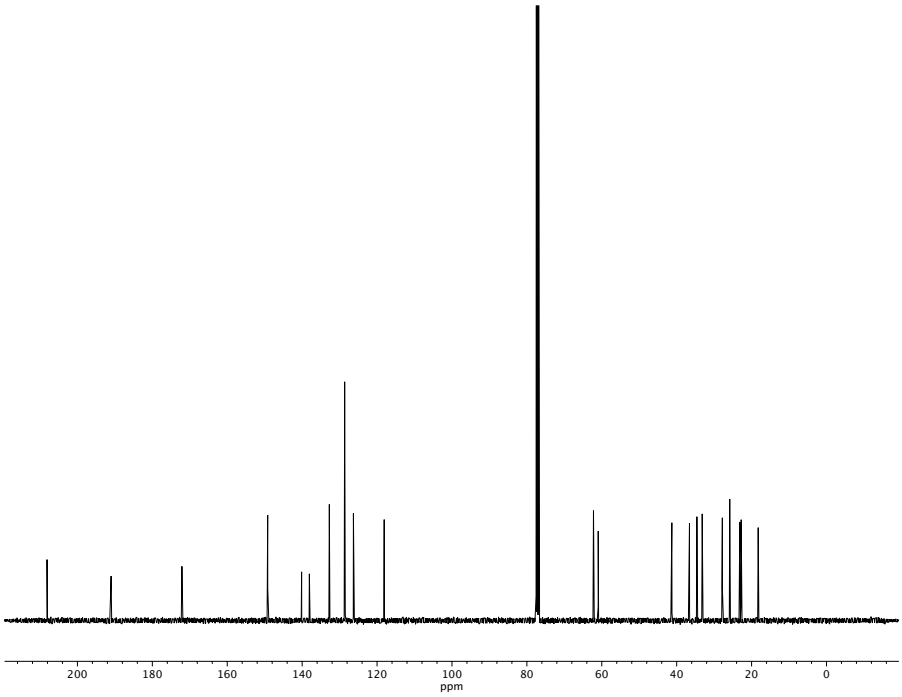

Figure A2.63. *^{13}C NMR (100 MHz, $CDCl_3$) of compound* ***196a.***

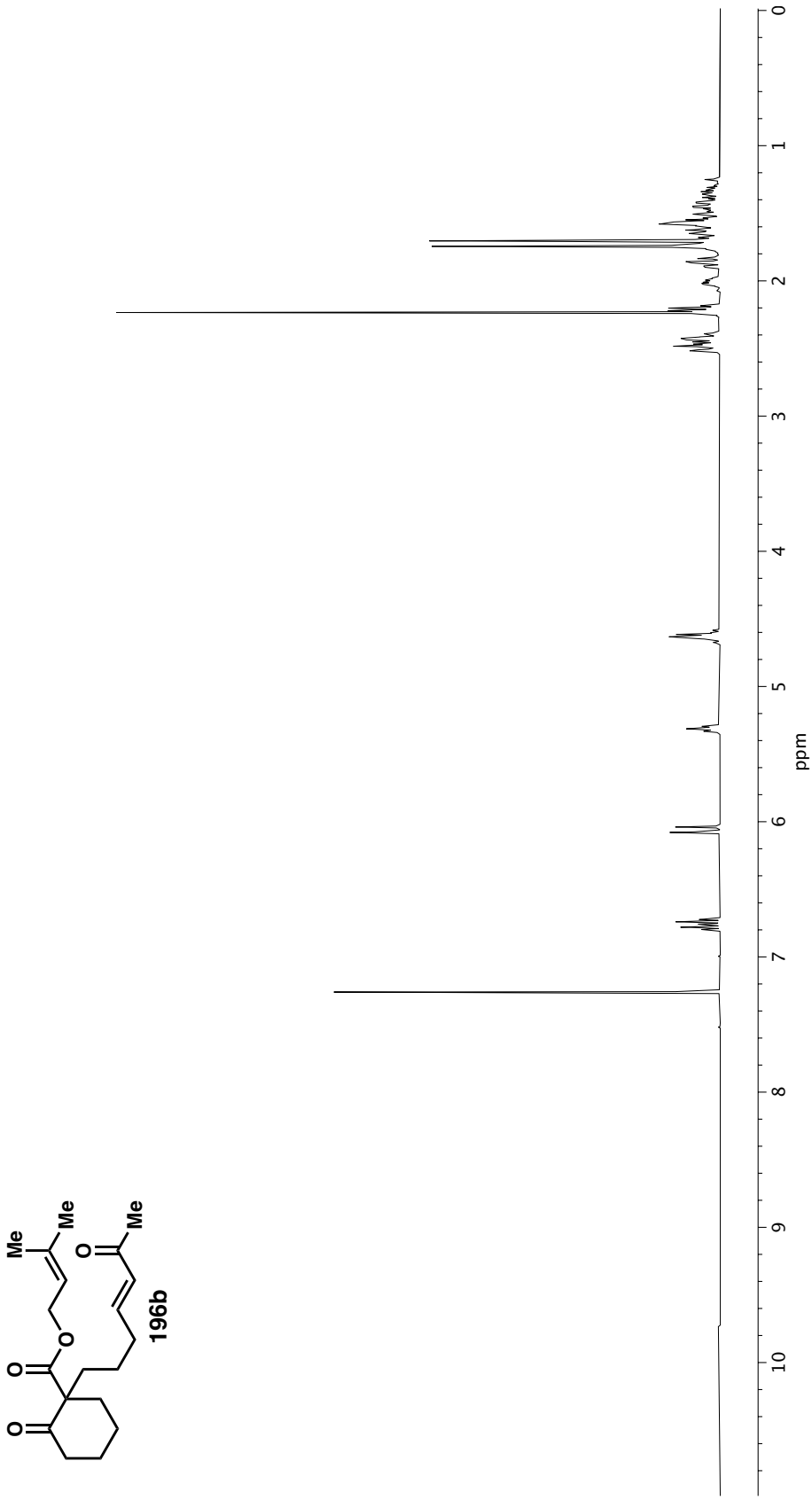

Figure A2.64. *^1H NMR (400 MHz, $CDCl_3$) of compound* ***196b.***

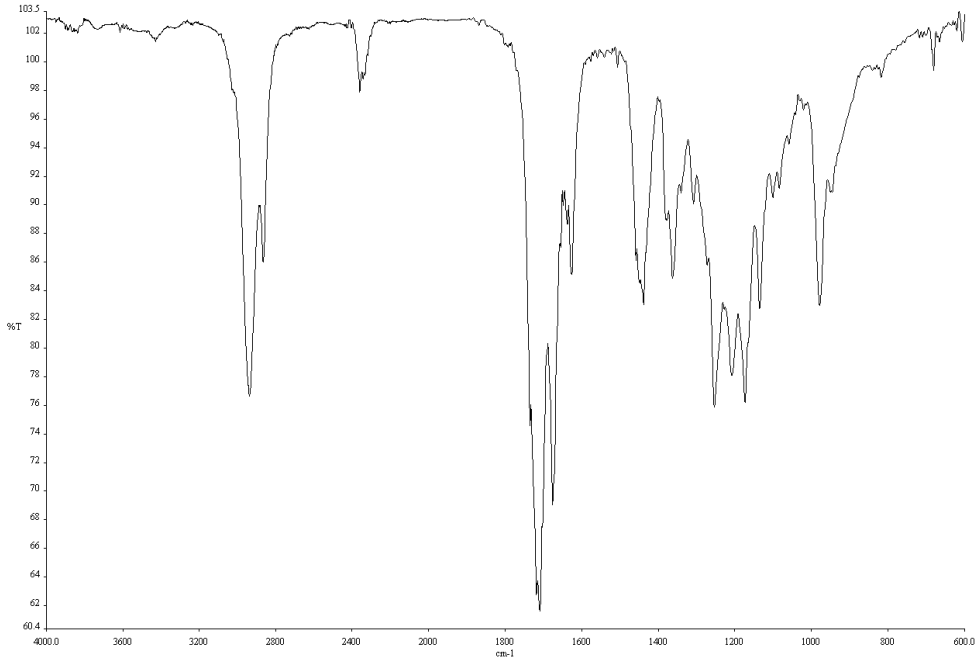

Figure A2.65. *Infrared spectrum (Thin Film, NaCl) of compound* ***196b.***

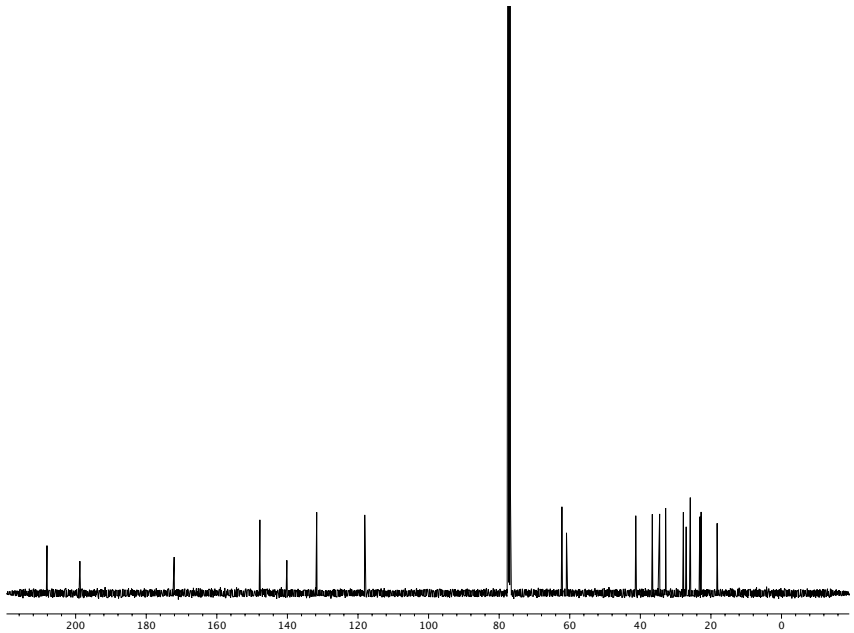

Figure A2.66. *^{13}C NMR (100 MHz, $CDCl_3$) of compound* ***196b.***

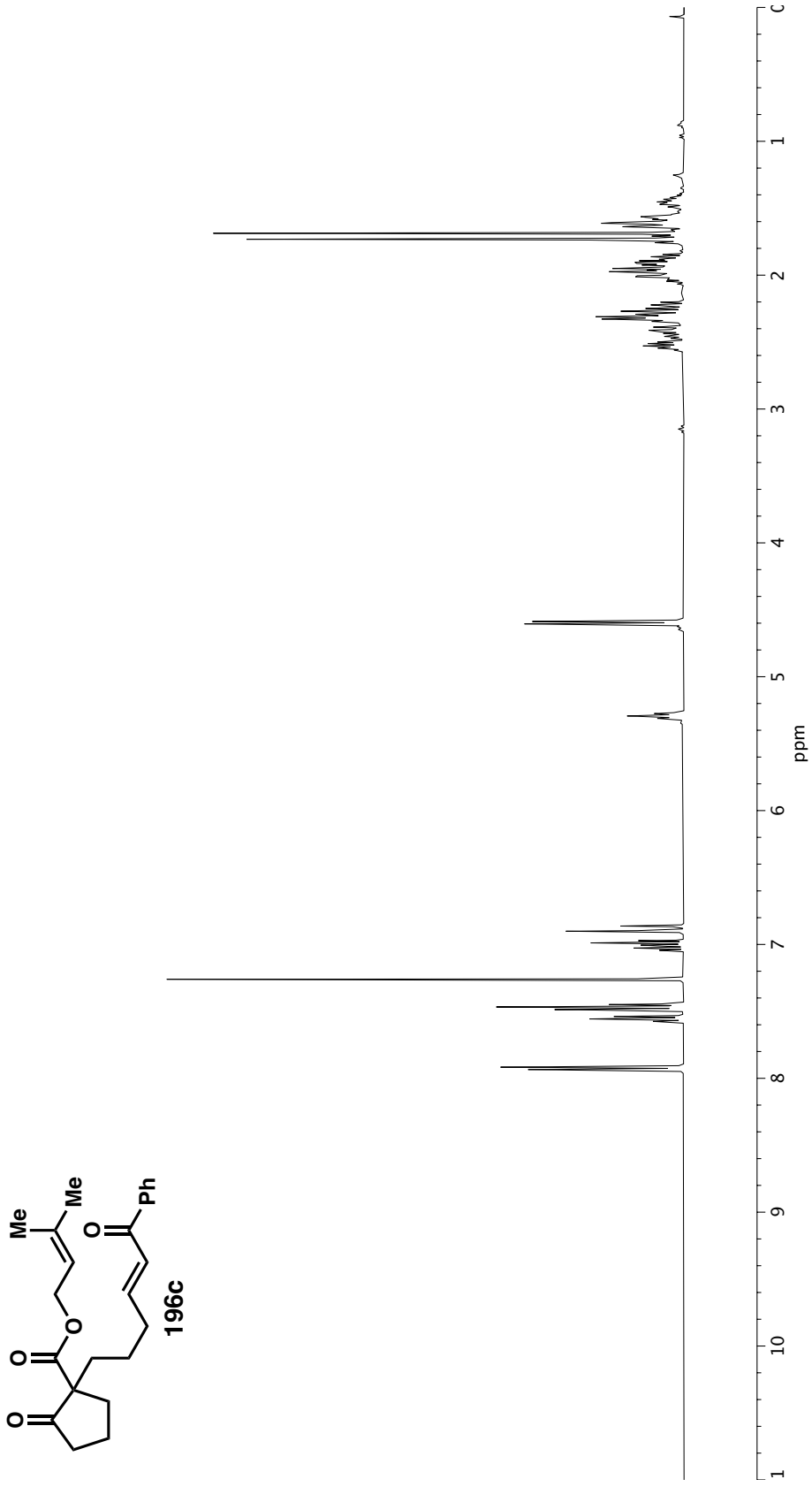

Figure A2.67. *^1H NMR (400 MHz, $CDCl_3$) of compound* ***196c.***

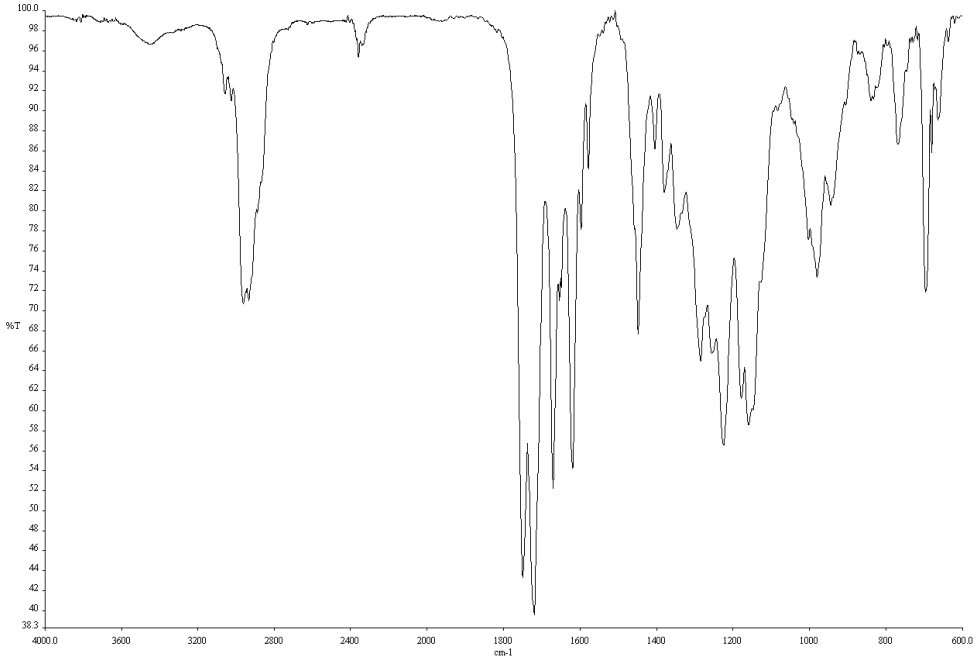

Figure A2.68. *Infrared spectrum (Thin Film, NaCl) of compound* ***196c.***

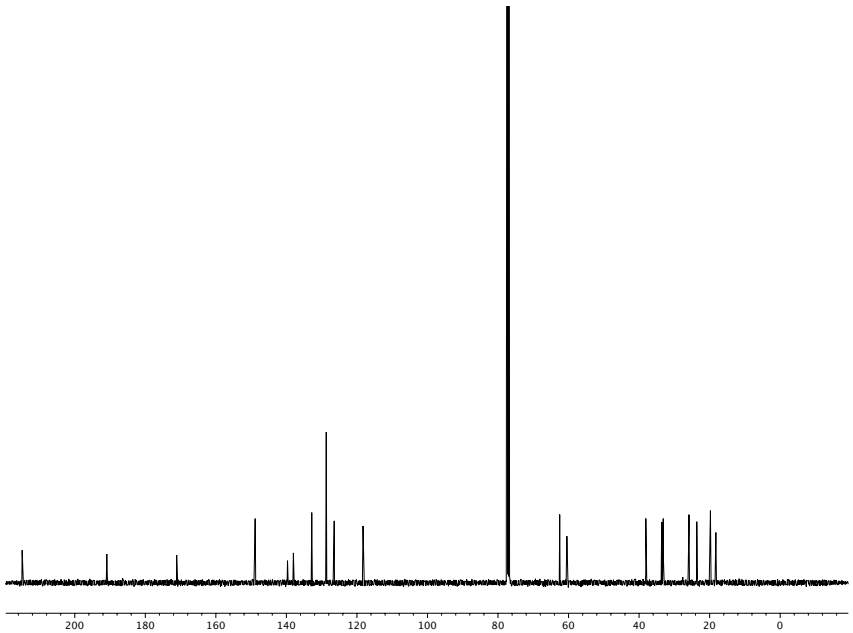

Figure A2.69. *^{13}C NMR (100 MHz, $CDCl_3$) of compound* ***196c.***

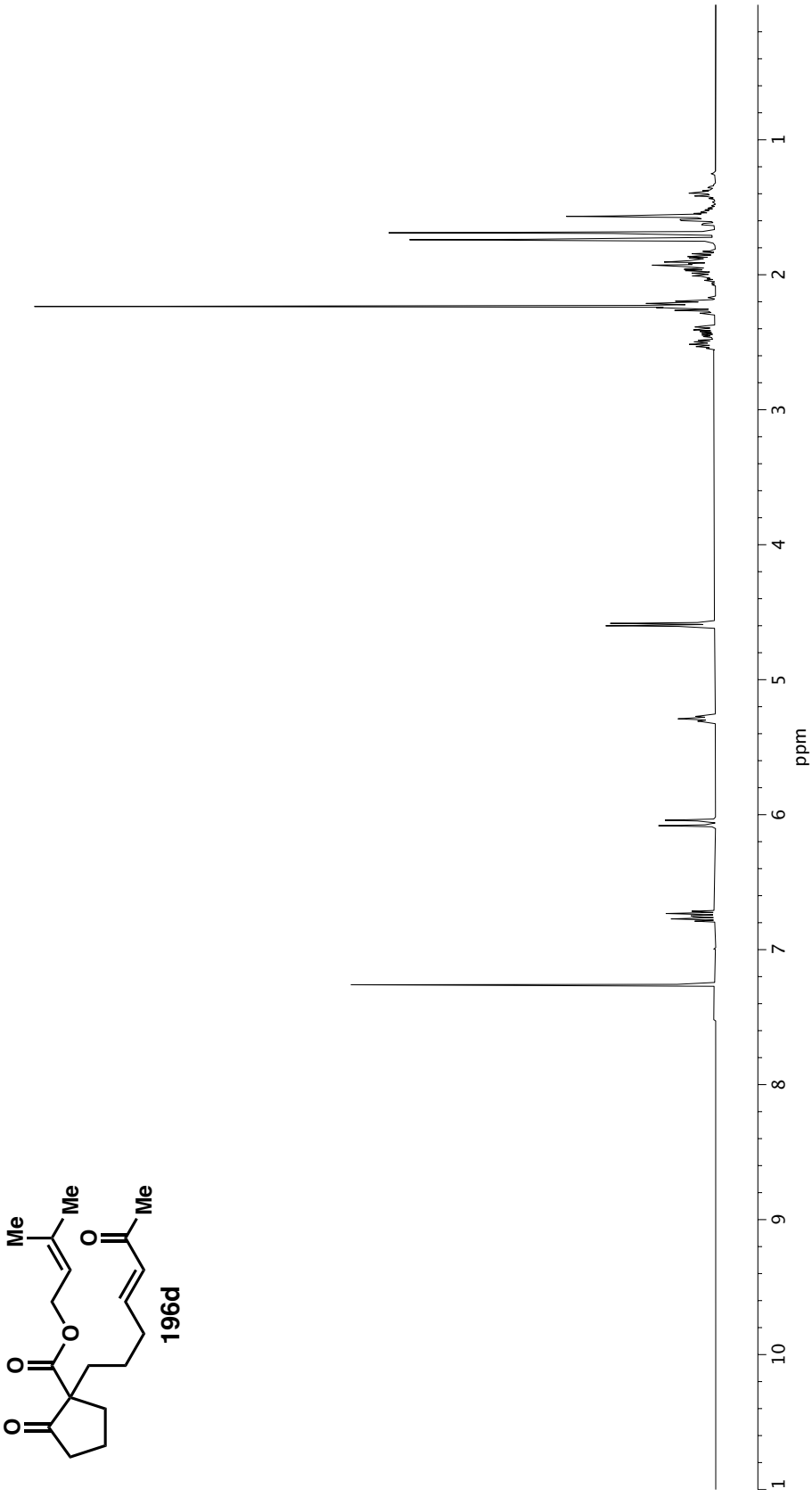

Figure A2.70. *^1H NMR (400 MHz, $CDCl_3$) of compound* ***196d.***

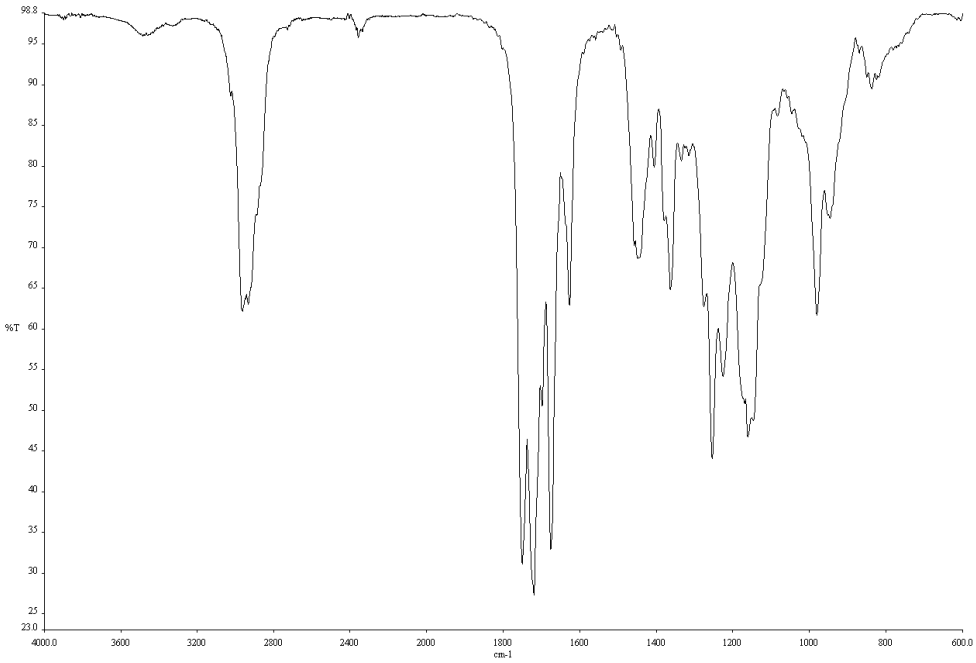

Figure A2.71. *Infrared spectrum (Thin Film, NaCl) of compound* ***196d.***

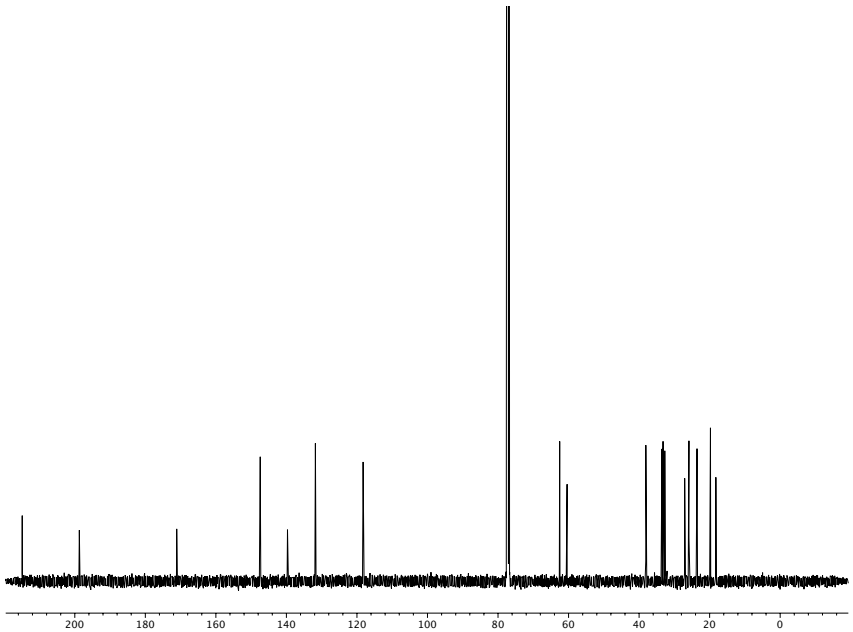

Figure A2.72. *^{13}C NMR (100 MHz, $CDCl_3$) of compound* ***196d.***

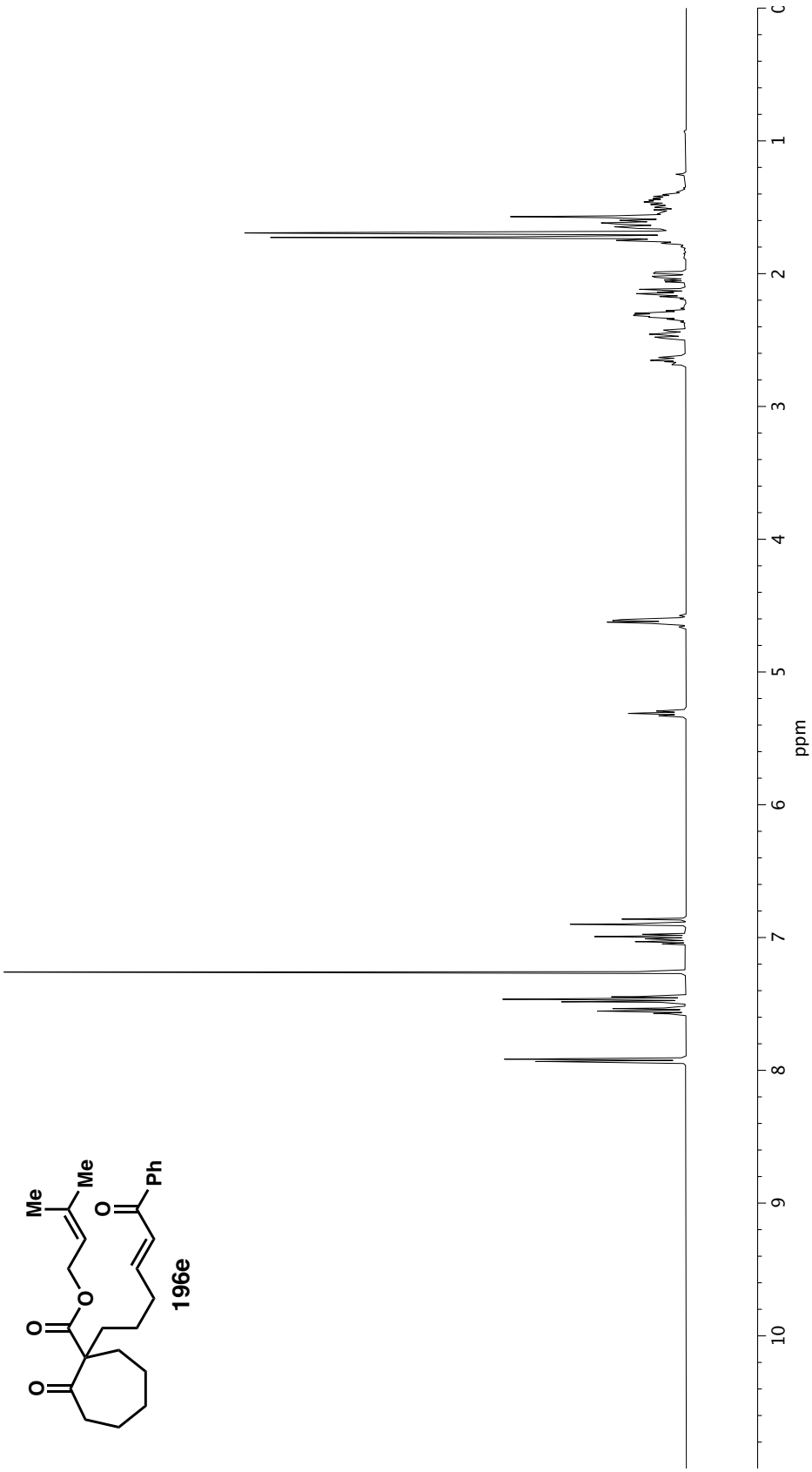

Figure A2.73. *^1H NMR (400 MHz, $CDCl_3$) of compound* ***196e.***

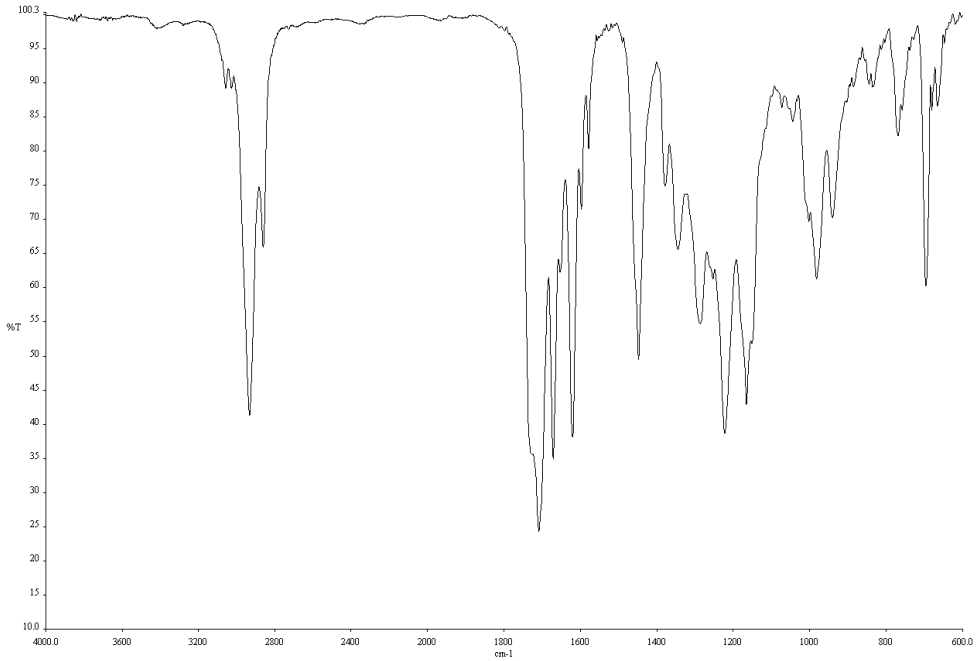

Figure A2.74. *Infrared spectrum (Thin Film, NaCl) of compound* ***196e.***

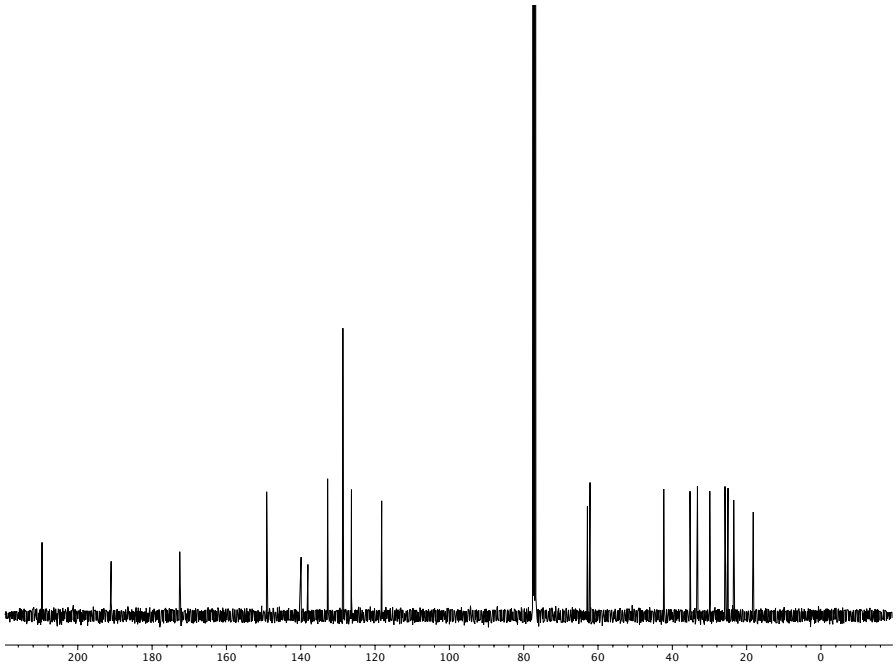

Figure A2.75. *^{13}C NMR (100 MHz, $CDCl_3$) of compound* ***196e.***

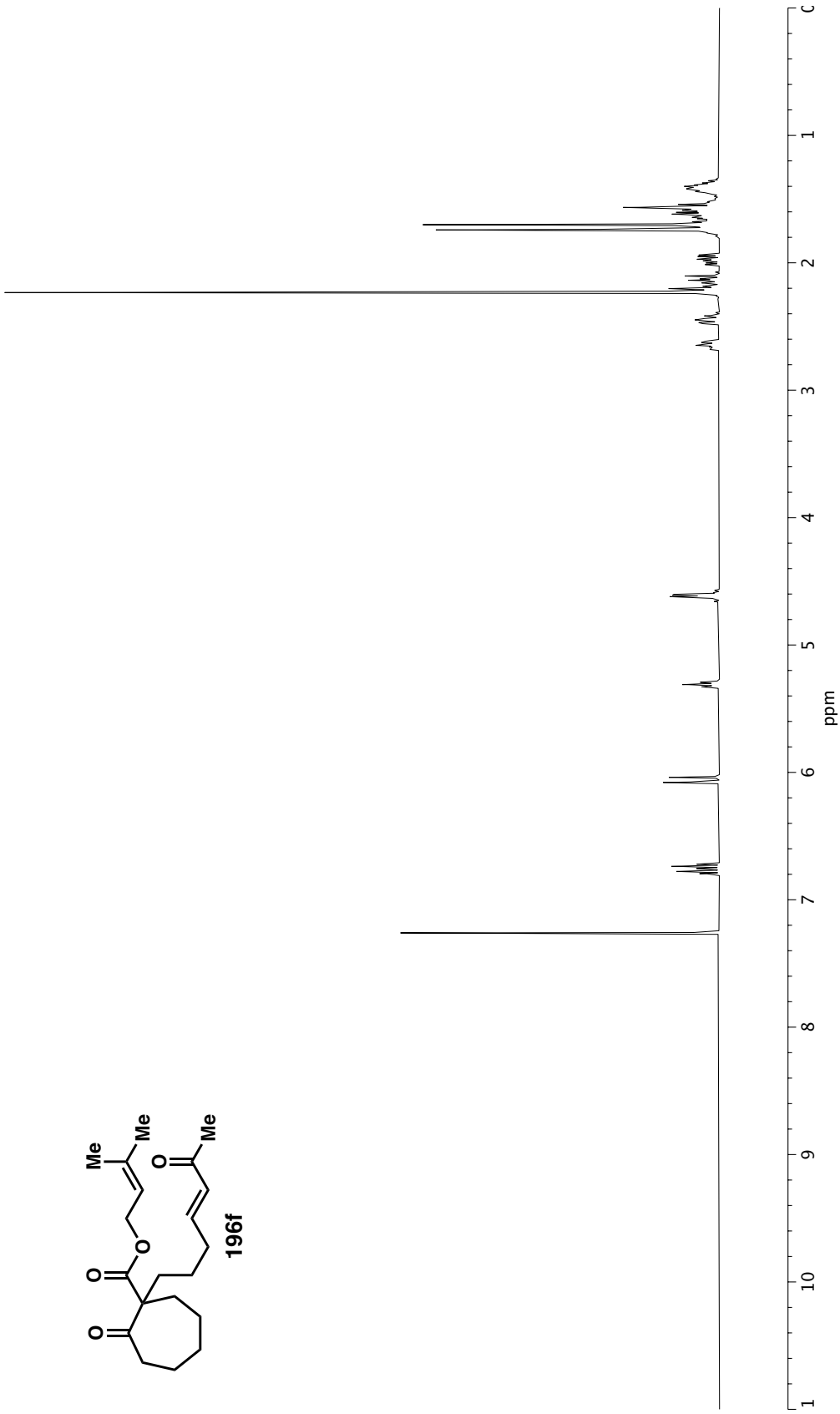

Figure A2.76. *^1H NMR (400 MHz, $CDCl_3$) of compound* ***196f.***

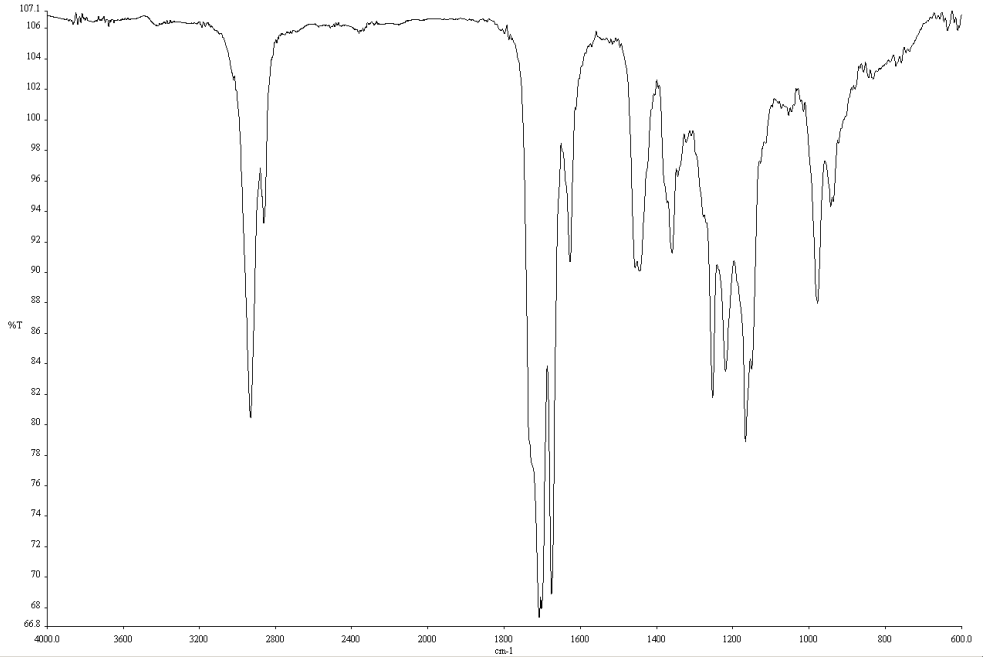

Figure A2.77. *Infrared spectrum (Thin Film, NaCl) of compound* ***196f.***

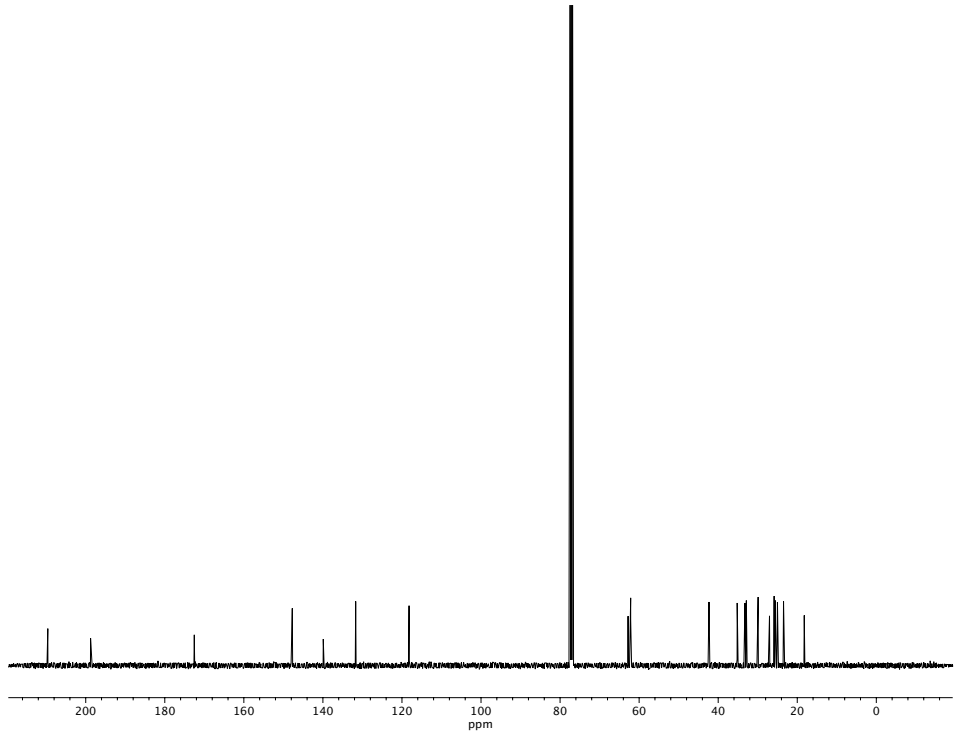

Figure A2.78. *^{13}C NMR (100 MHz, $CDCl_3$) of compound* ***196f.***

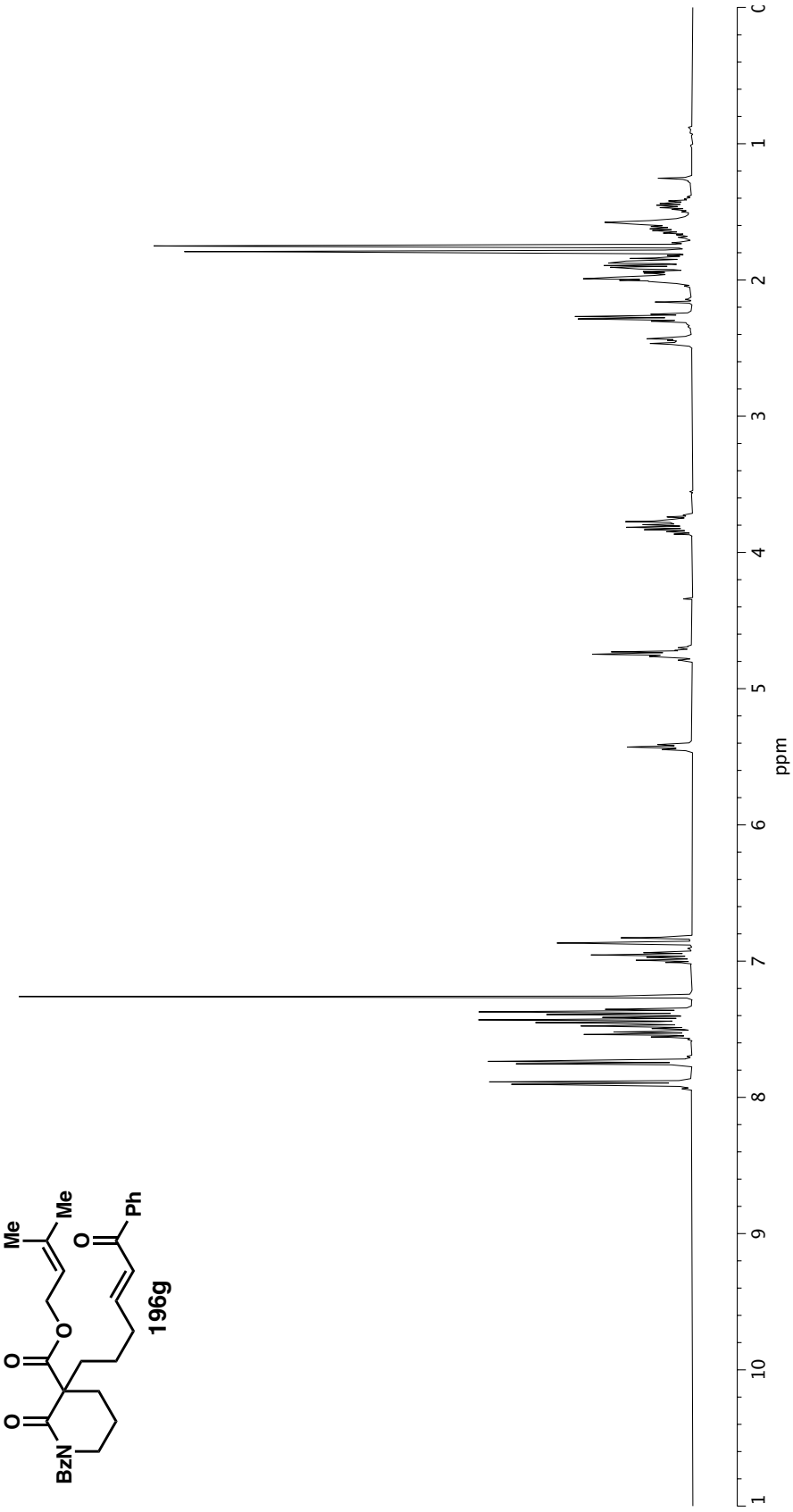

Figure A2.79. *^1H NMR (400 MHz, $CDCl_3$) of compound* ***196g.***

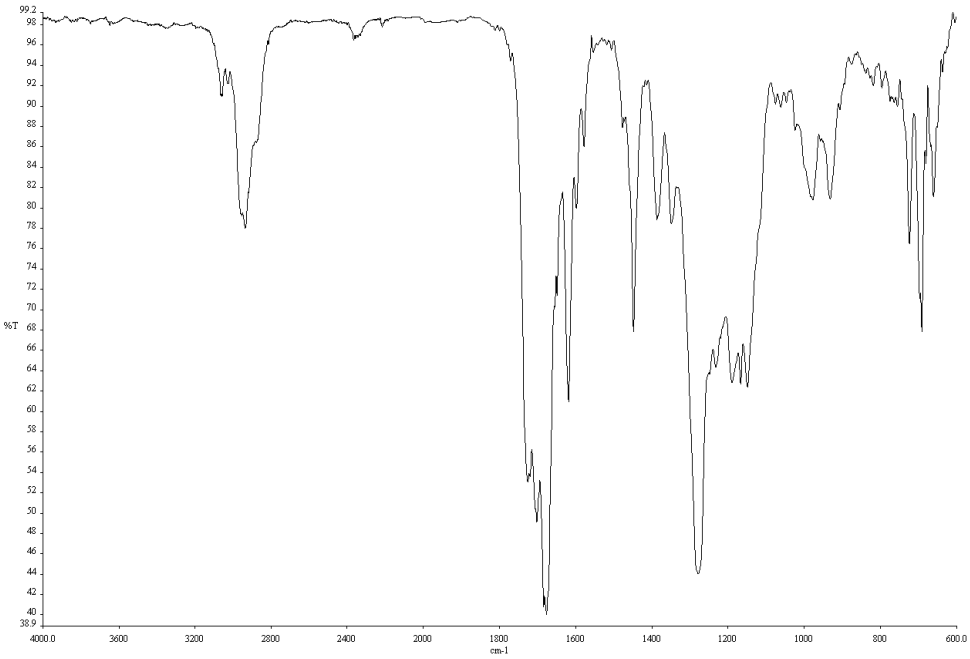

Figure A2.80. *Infrared spectrum (Thin Film, NaCl) of compound* ***196g.***

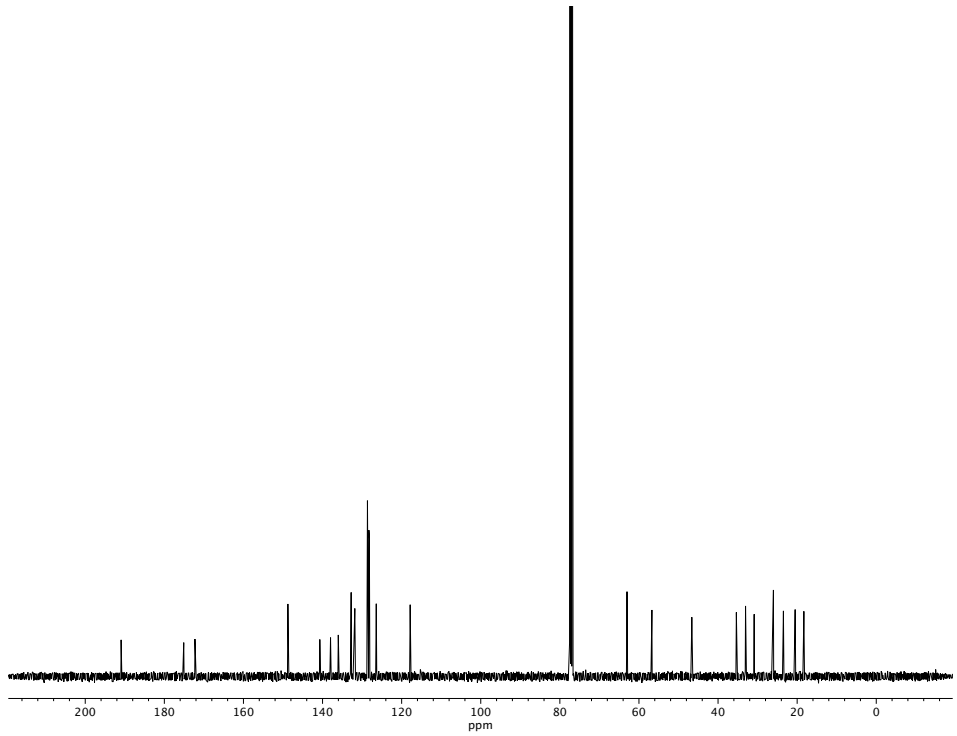

Figure A2.81. *^{13}C NMR (100 MHz, $CDCl_3$) of compound* ***196g.***

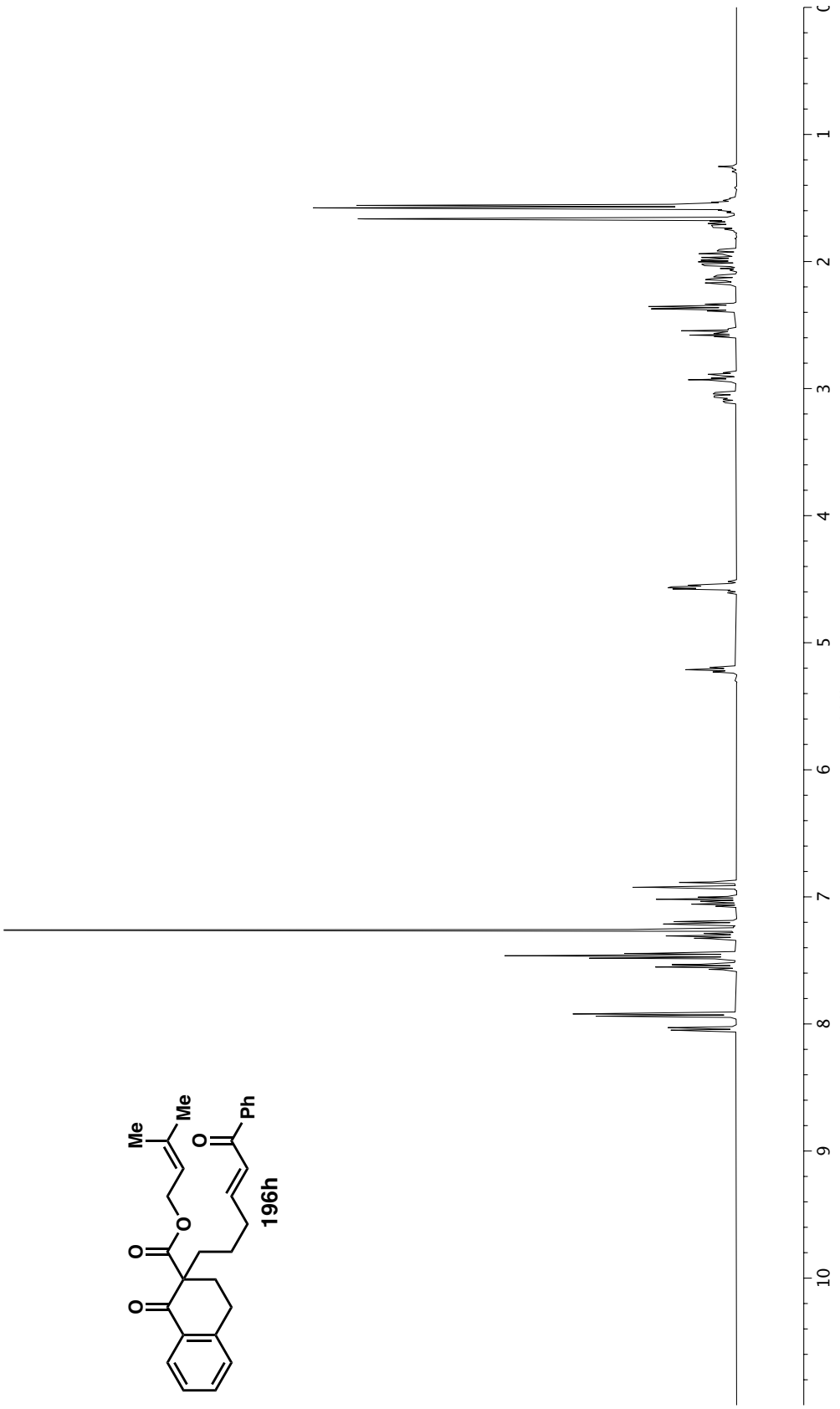

Figure A2.82. *^1H NMR (400 MHz, $CDCl_3$) of compound* ***196h.***

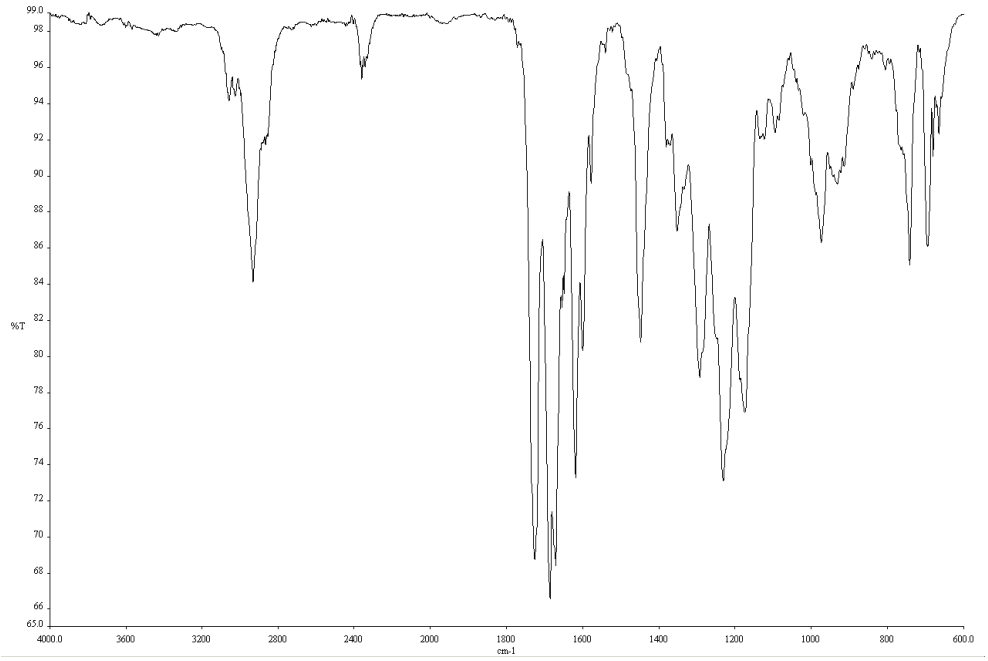

Figure A2.83. *Infrared spectrum (Thin Film, NaCl) of compound* ***196h.***

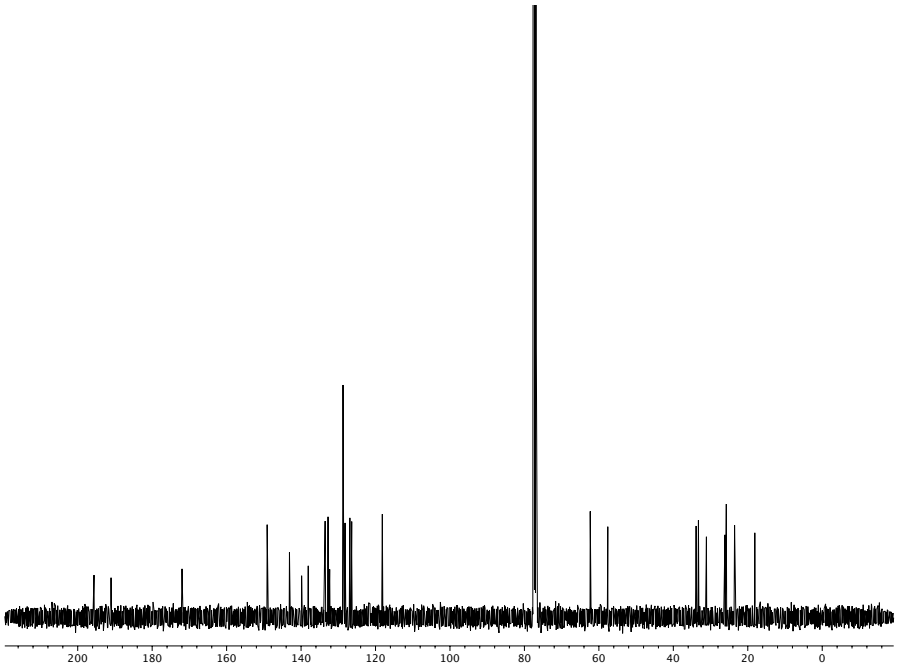

Figure A2.84. *^{13}C NMR (100 MHz, $CDCl_3$) of compound* ***196h.***

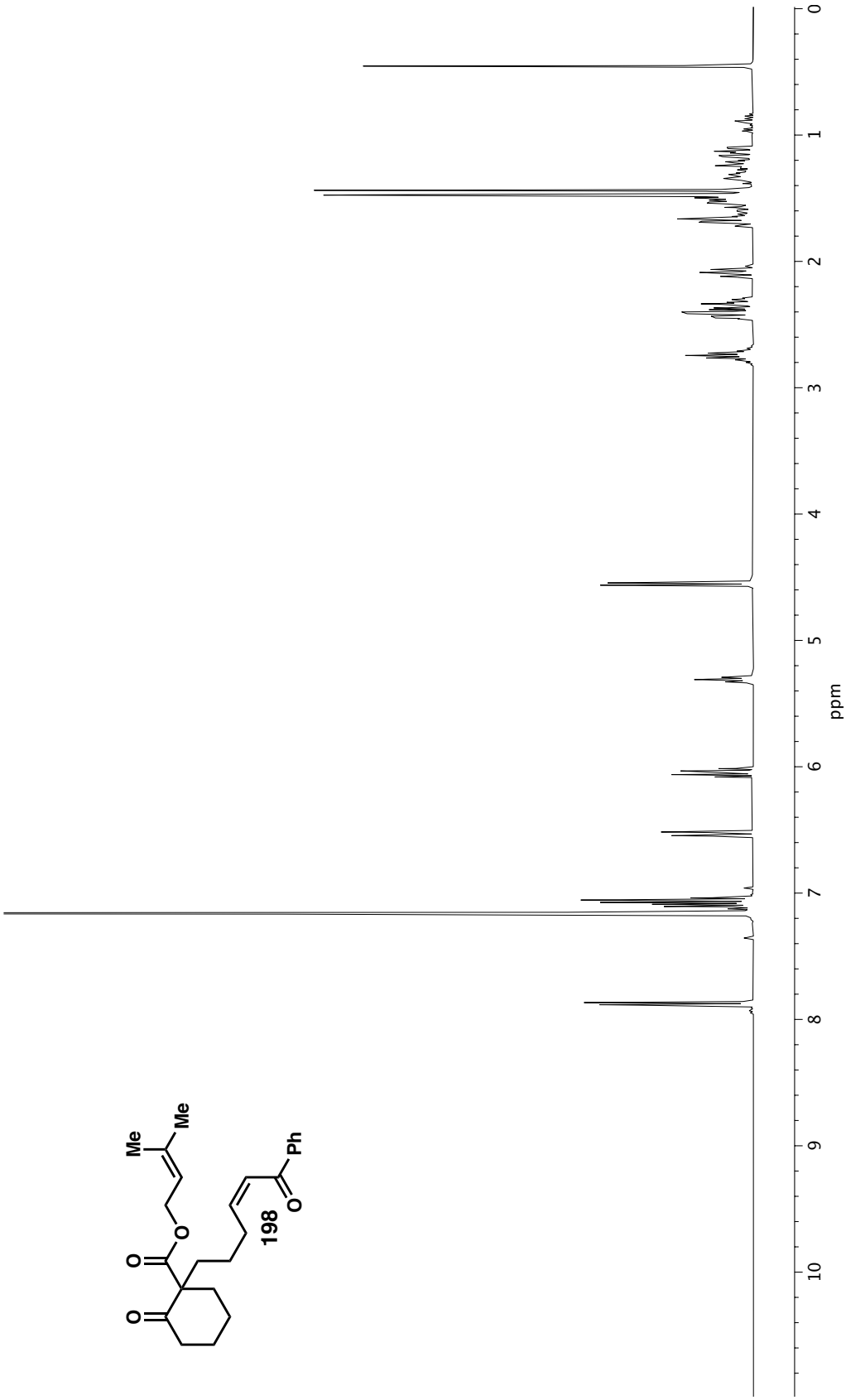

Figure A2.85. *^1H NMR (400 MHz, C_6D_6) of compound* ***198.***

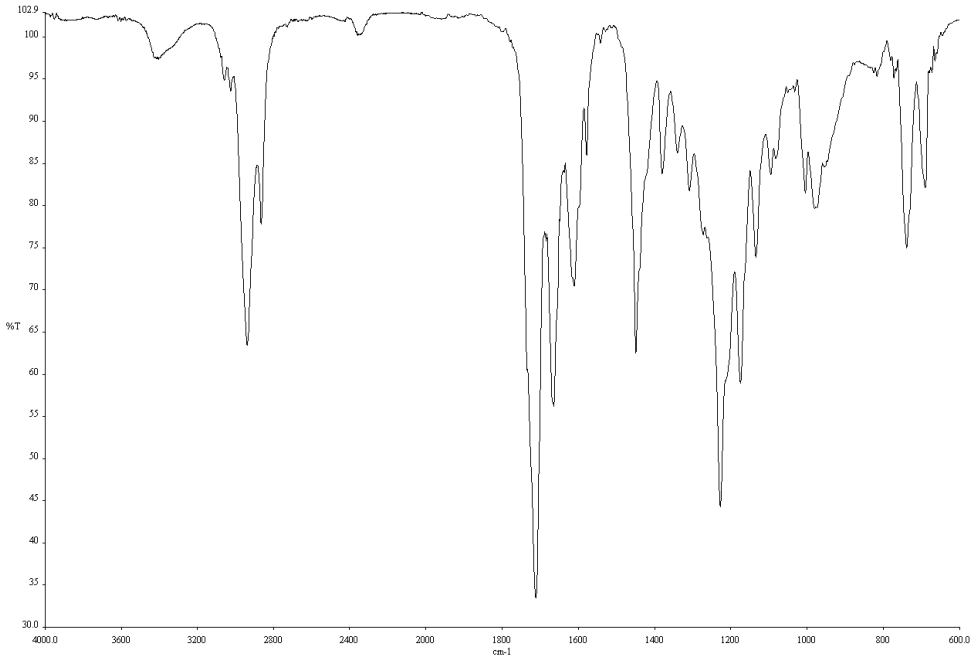

Figure A2.86. *Infrared spectrum (Thin Film, NaCl) of compound* ***198.***

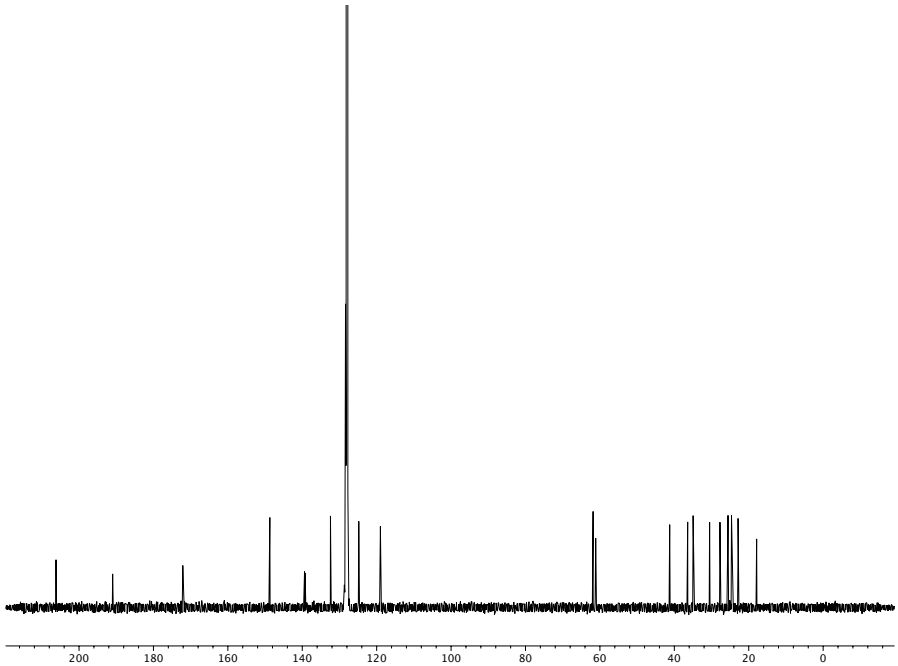

Figure A2.87. *^{13}C NMR (100 MHz, C_6D_6) of compound* ***198.***

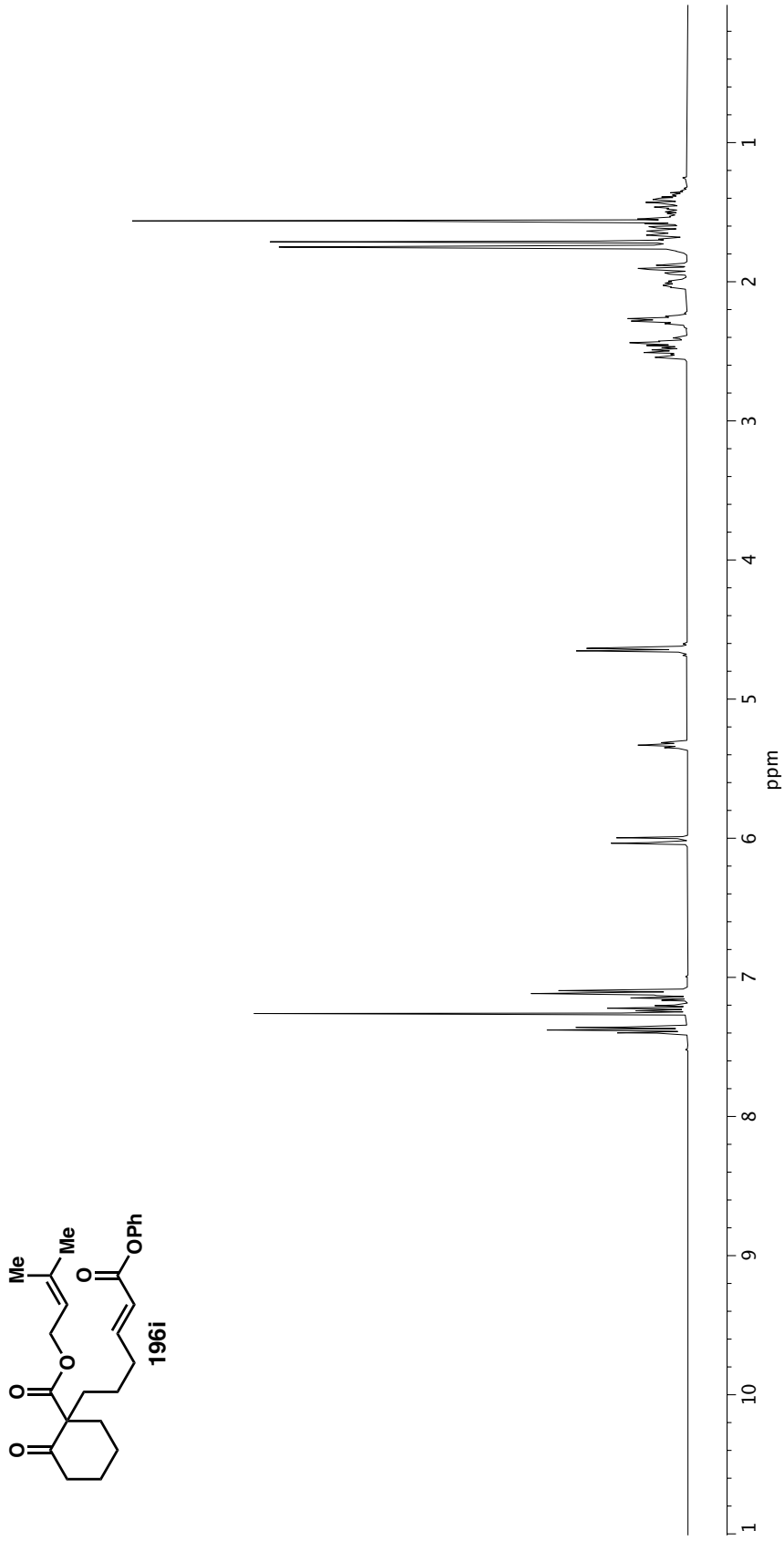

Figure A2.88. *^1H NMR (400 MHz, $CDCl_3$) of compound* ***196i.***

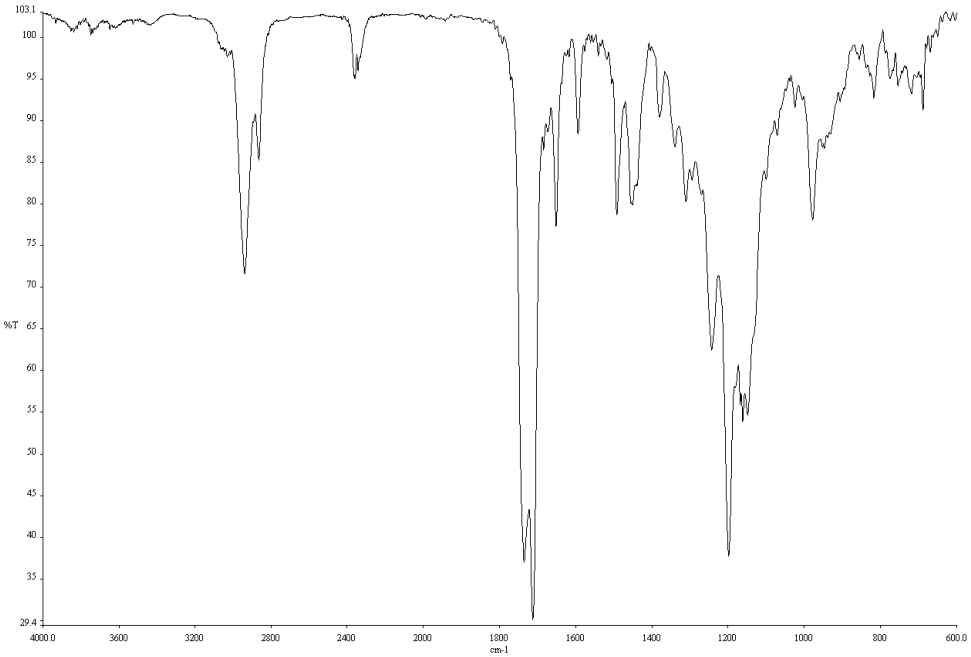

Figure A2.89. *Infrared spectrum (Thin Film, NaCl) of compound* ***196i.***

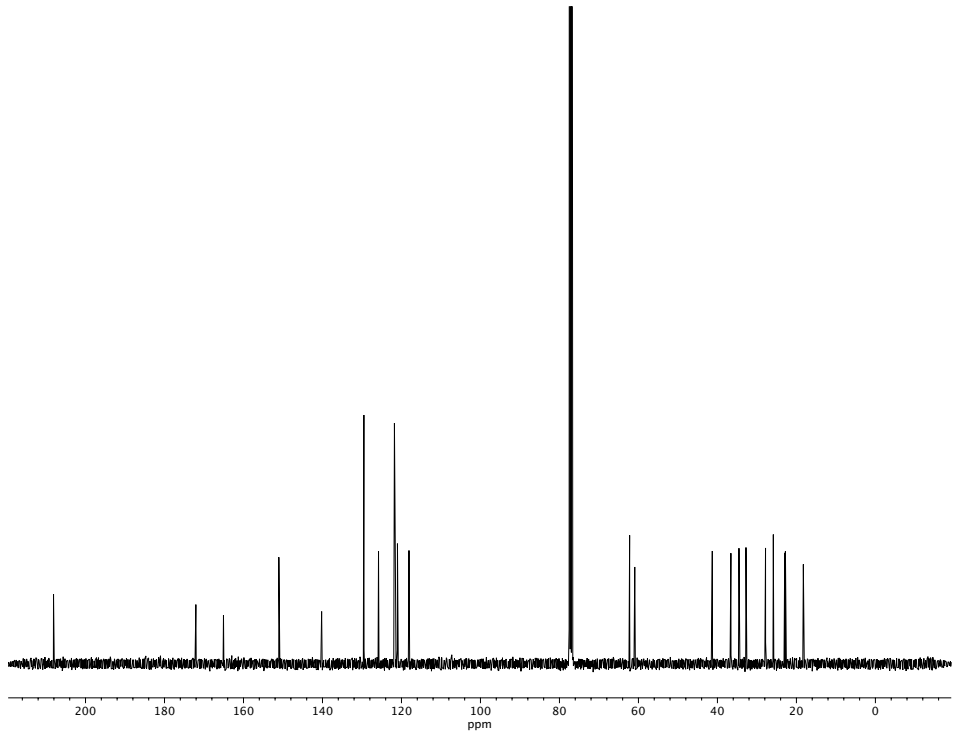

Figure A2.90. *^{13}C NMR (100 MHz, $CDCl_3$) of compound* ***196i.***

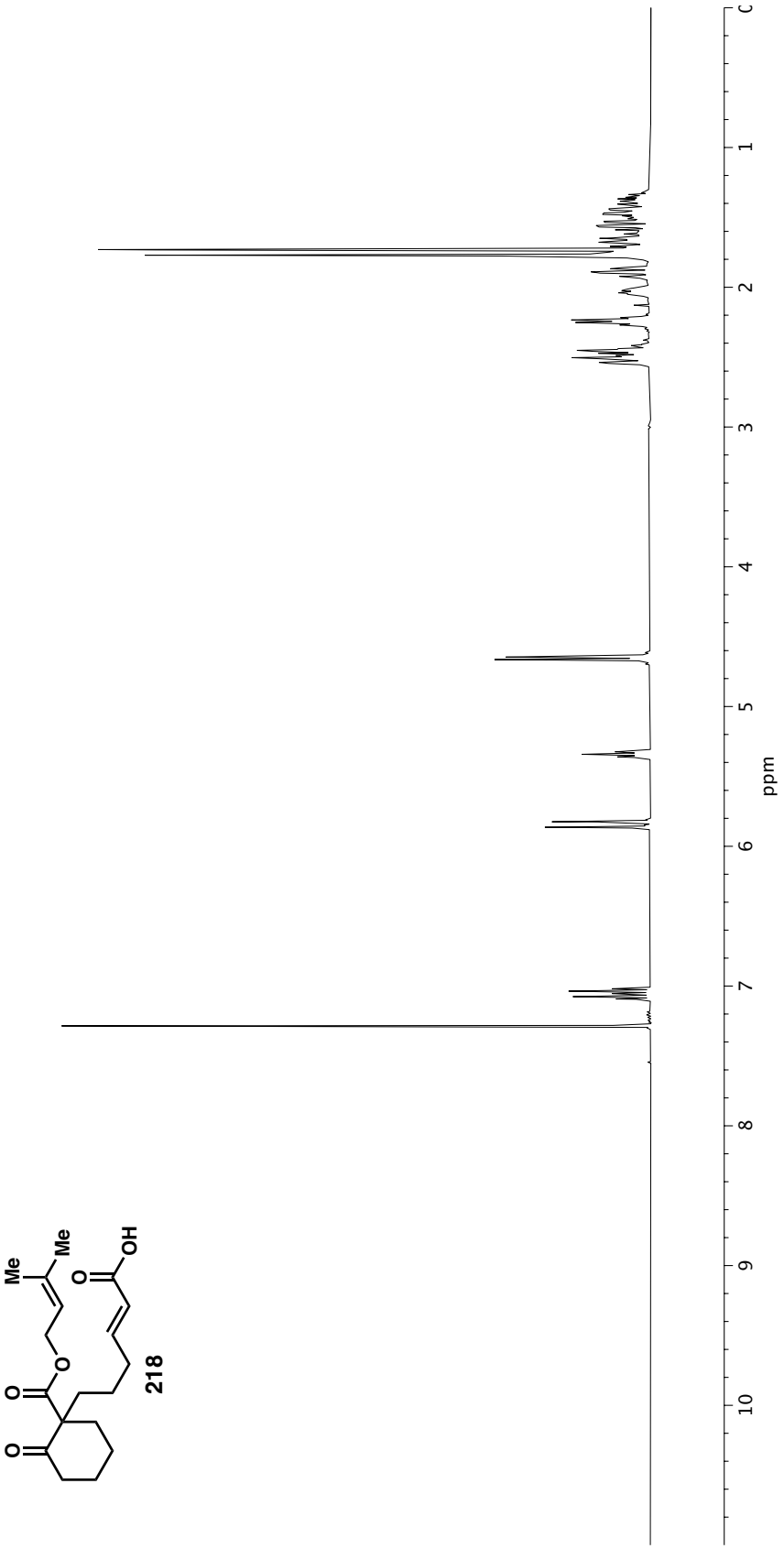

Figure A2.91. *^1H NMR (400 MHz, $CDCl_3$) of compound* ***218.***

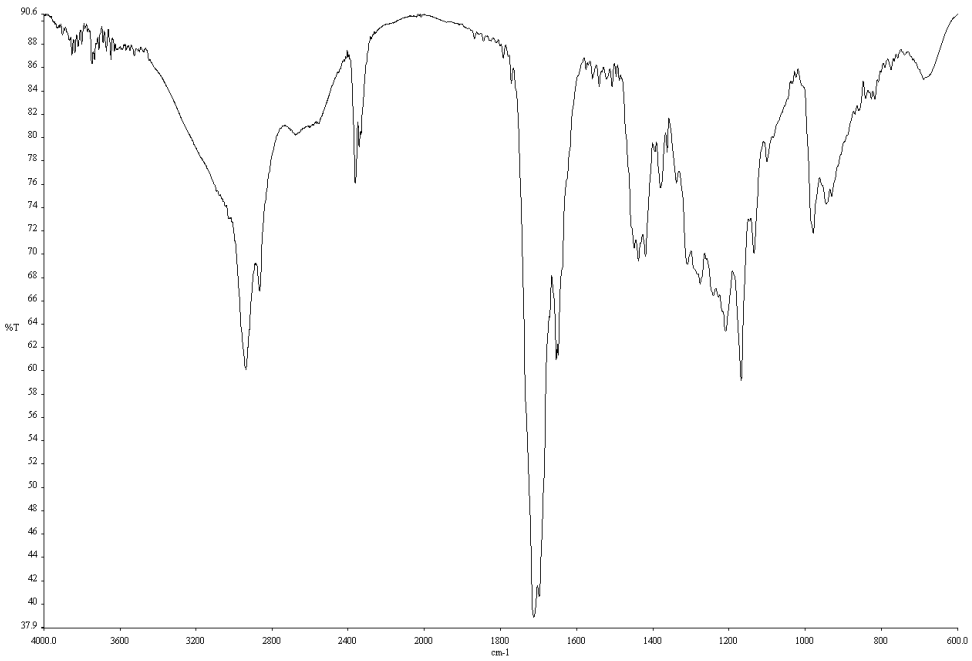

Figure A2.92. *Infrared spectrum (Thin Film, NaCl) of compound* ***218.***

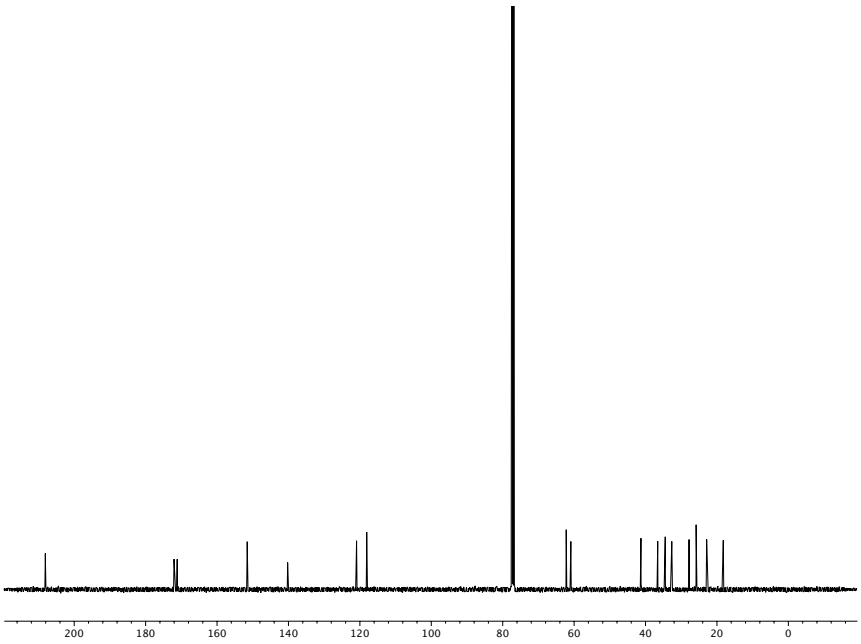

Figure A2.93. *^{13}C NMR (100 MHz, $CDCl_3$) of compound* ***218.***

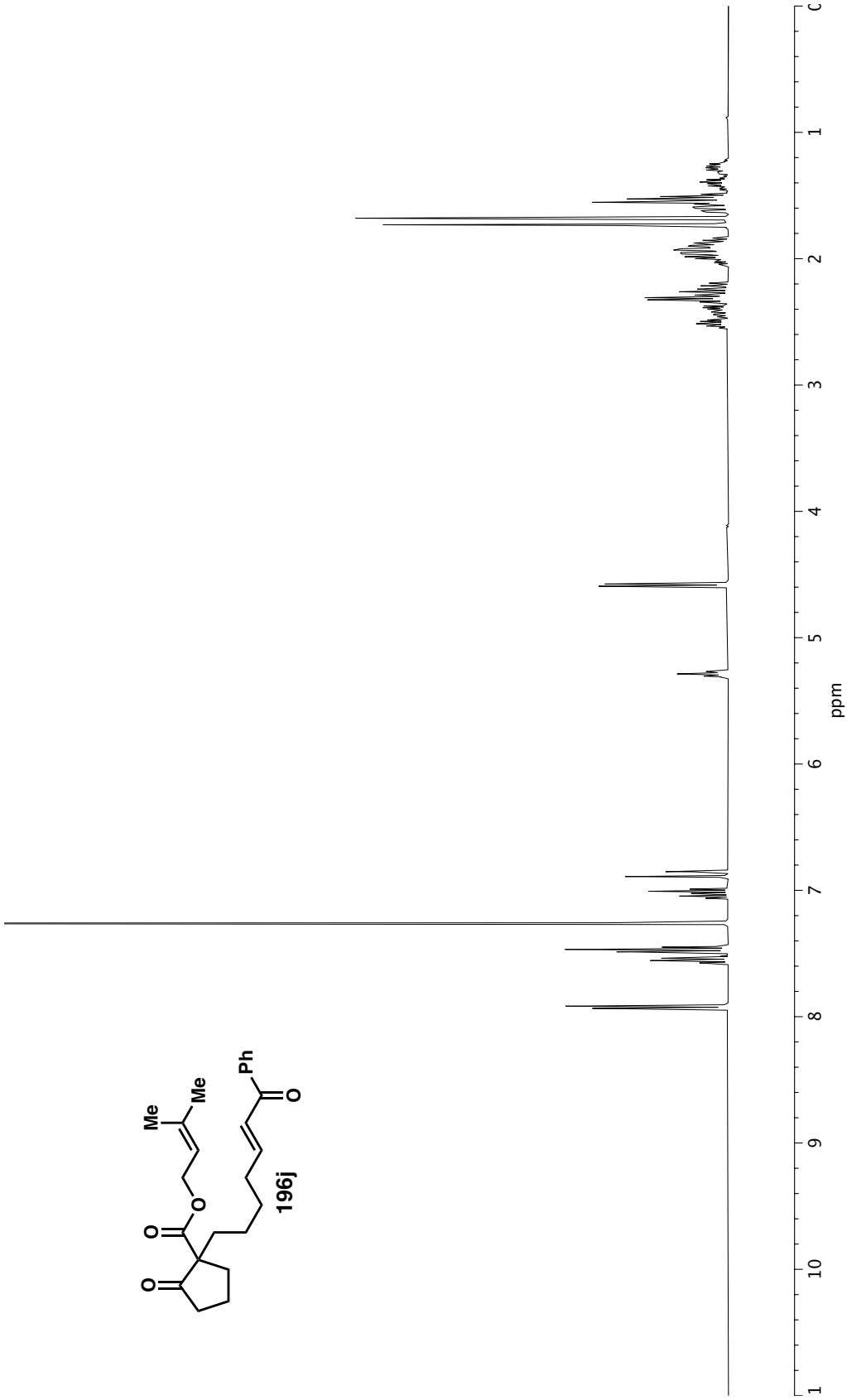

Figure A2.94. *^1H NMR (400 MHz, $CDCl_3$) of compound* ***196j.***

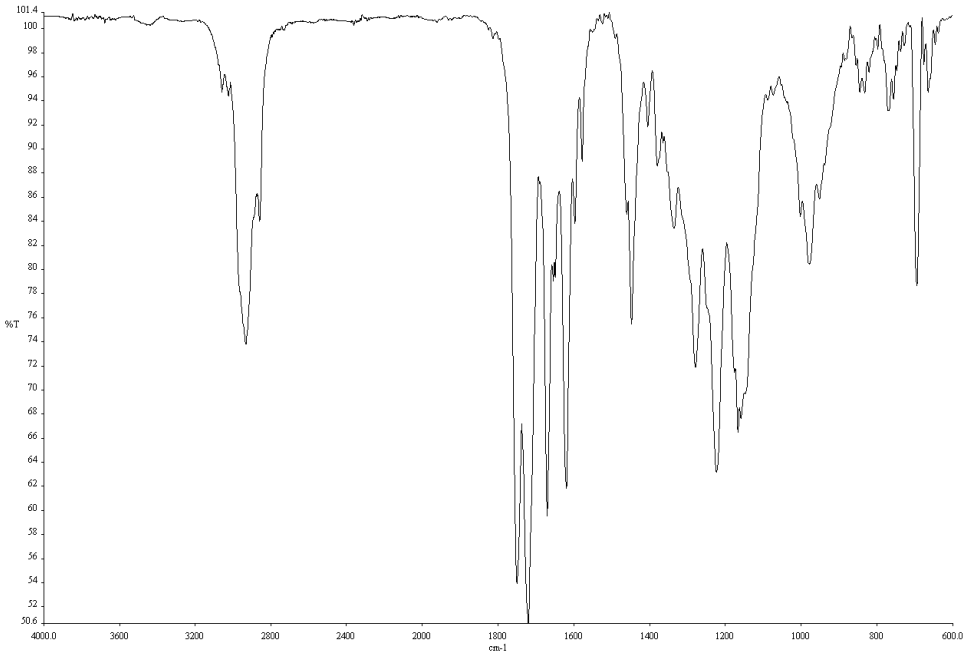

Figure A2.95. *Infrared spectrum (Thin Film, NaCl) of compound* ***196j.***

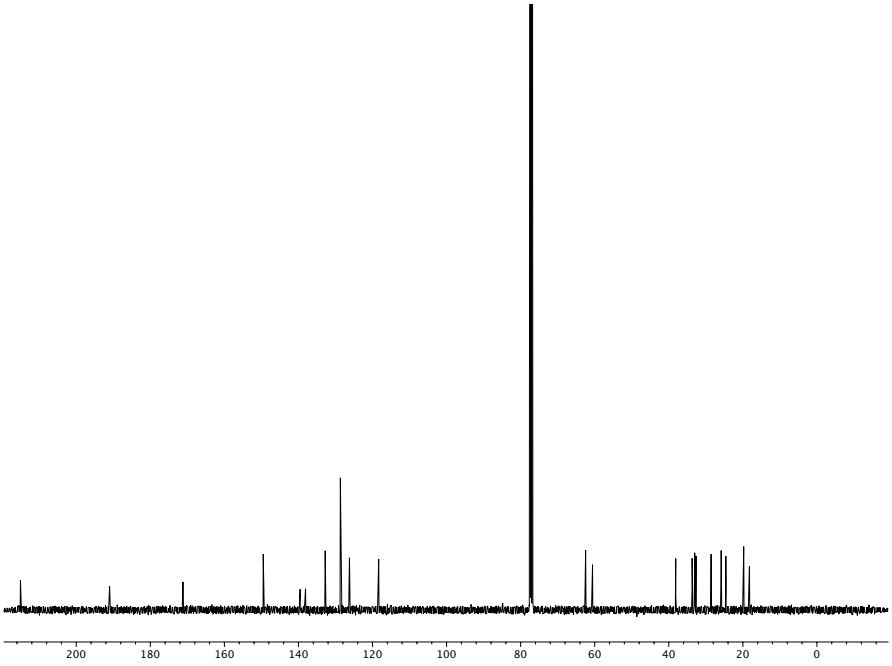

Figure A2.96. *^{13}C NMR (100 MHz, $CDCl_3$) of compound* ***196j.***

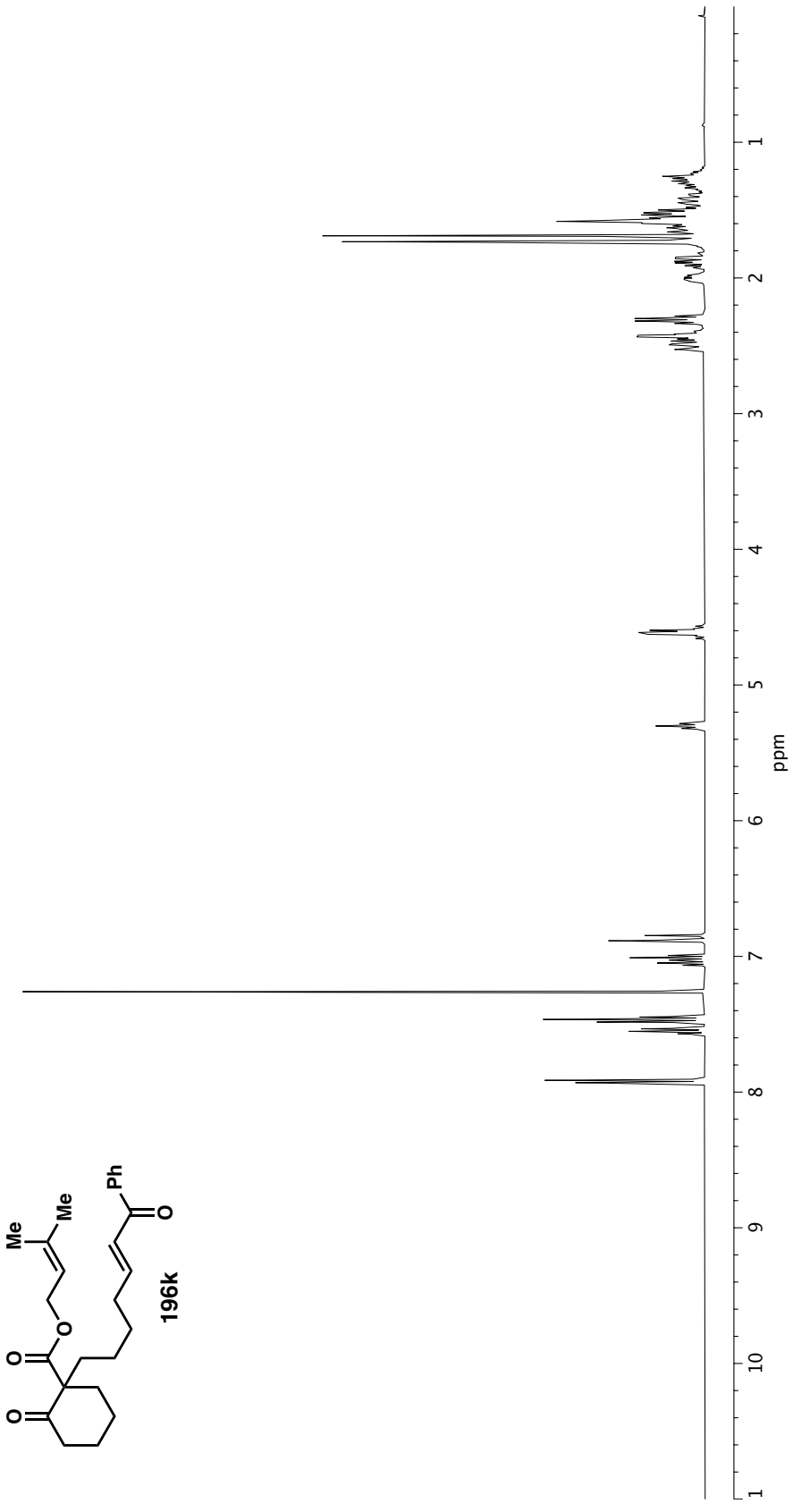

Figure A2.97. *^1H NMR (400 MHz, $CDCl_3$) of compound* ***196k.***

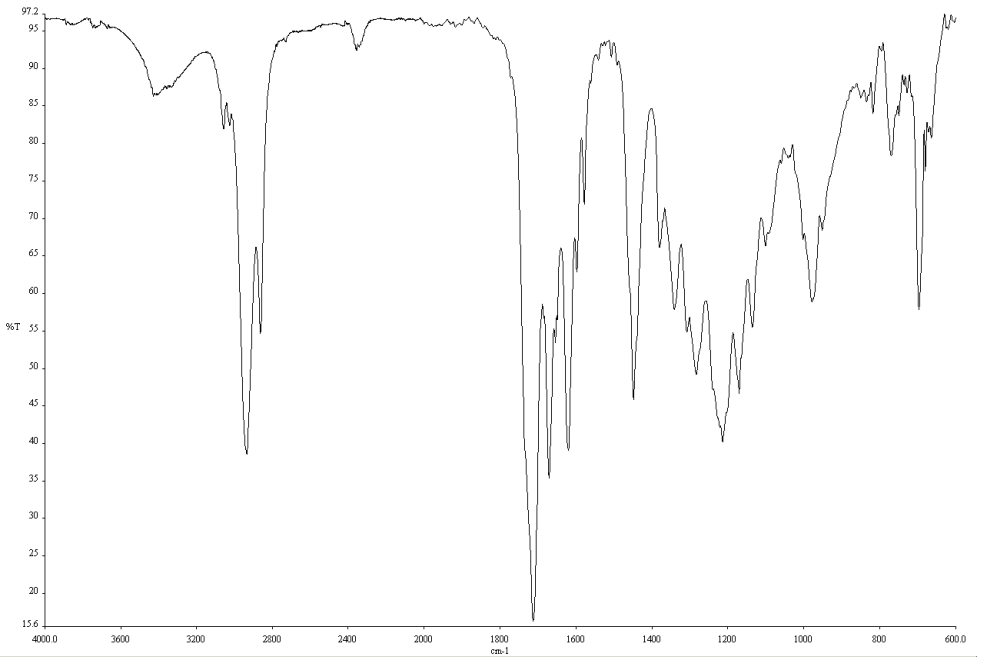

Figure A2.98. *Infrared spectrum (Thin Film, NaCl) of compound* ***196k.***

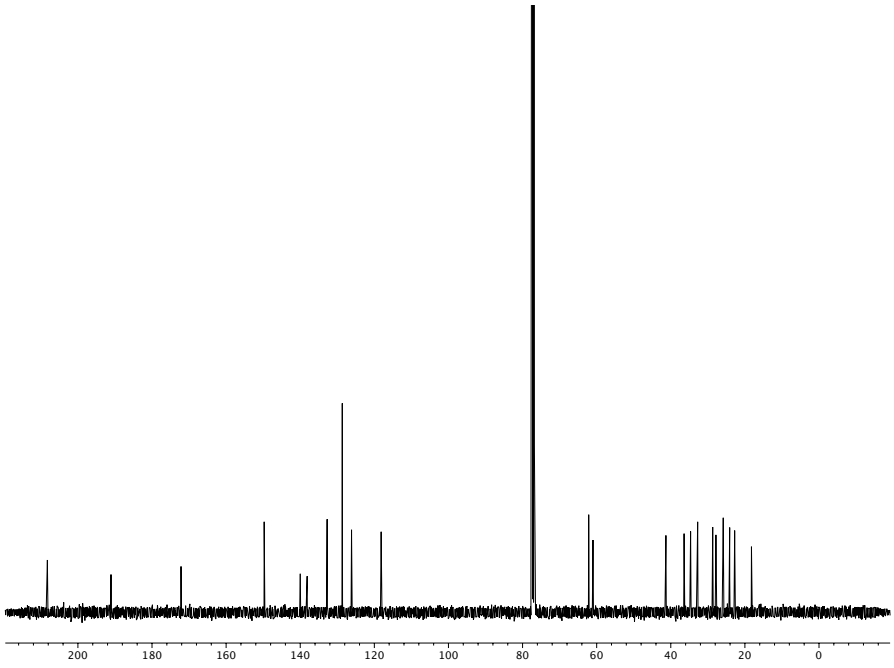

Figure A2.99. *^{13}C NMR (100 MHz, $CDCl_3$) of compound* ***196k.***

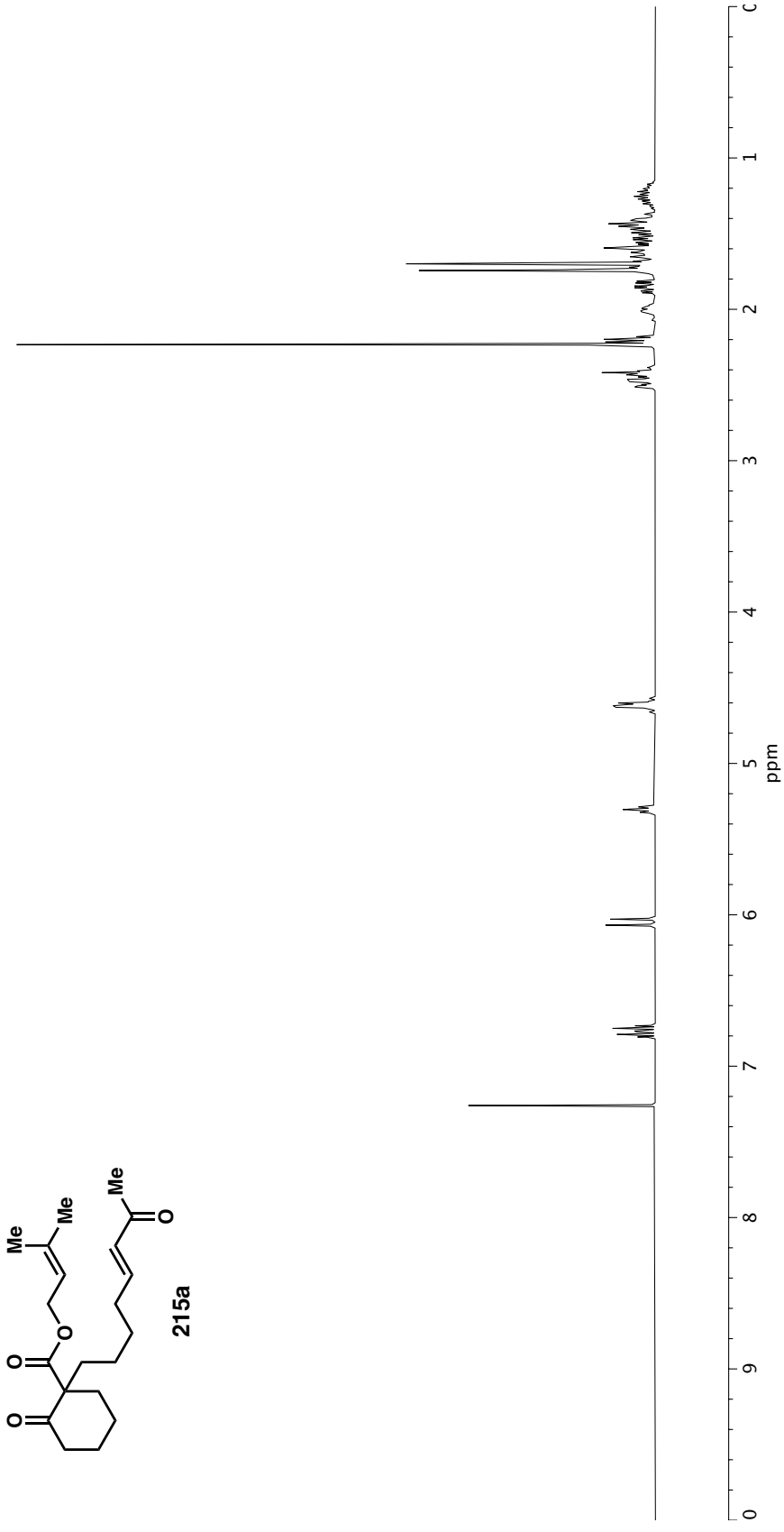

Figure A2.100. *^{1}H NMR (400 MHz, $CDCl_3$) of compound* ***215a.***

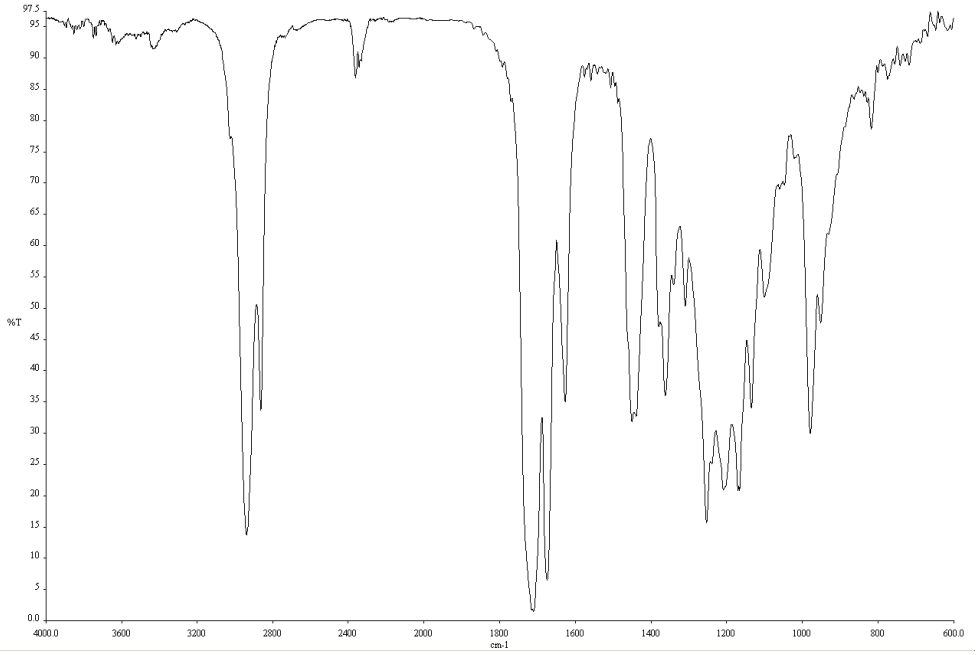

Figure A2.101. *Infrared spectrum (Thin Film, NaCl) of compound* ***215a.***

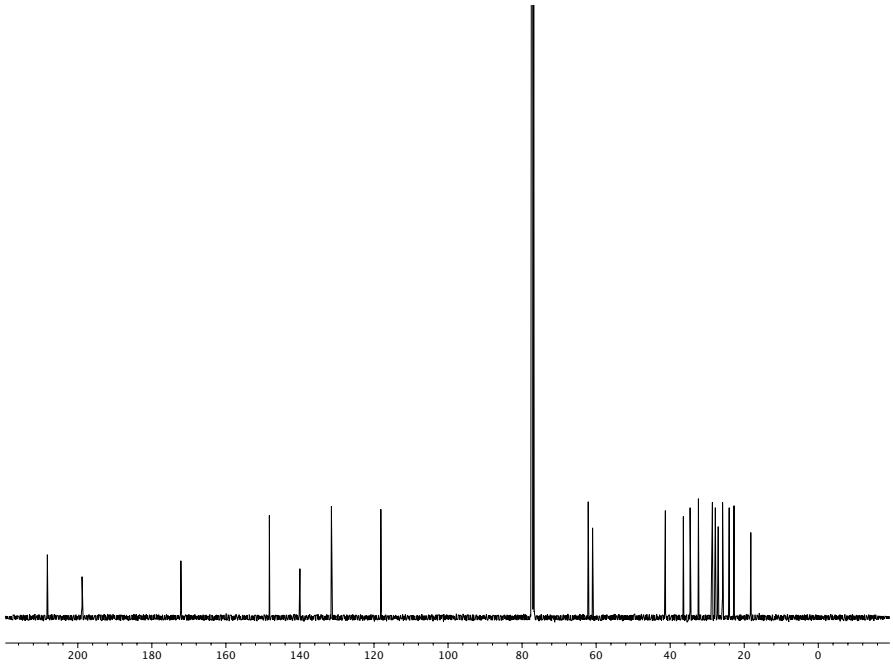

Figure A2.102. *^{13}C NMR (100 MHz, $CDCl_3$) of compound* ***215a.***

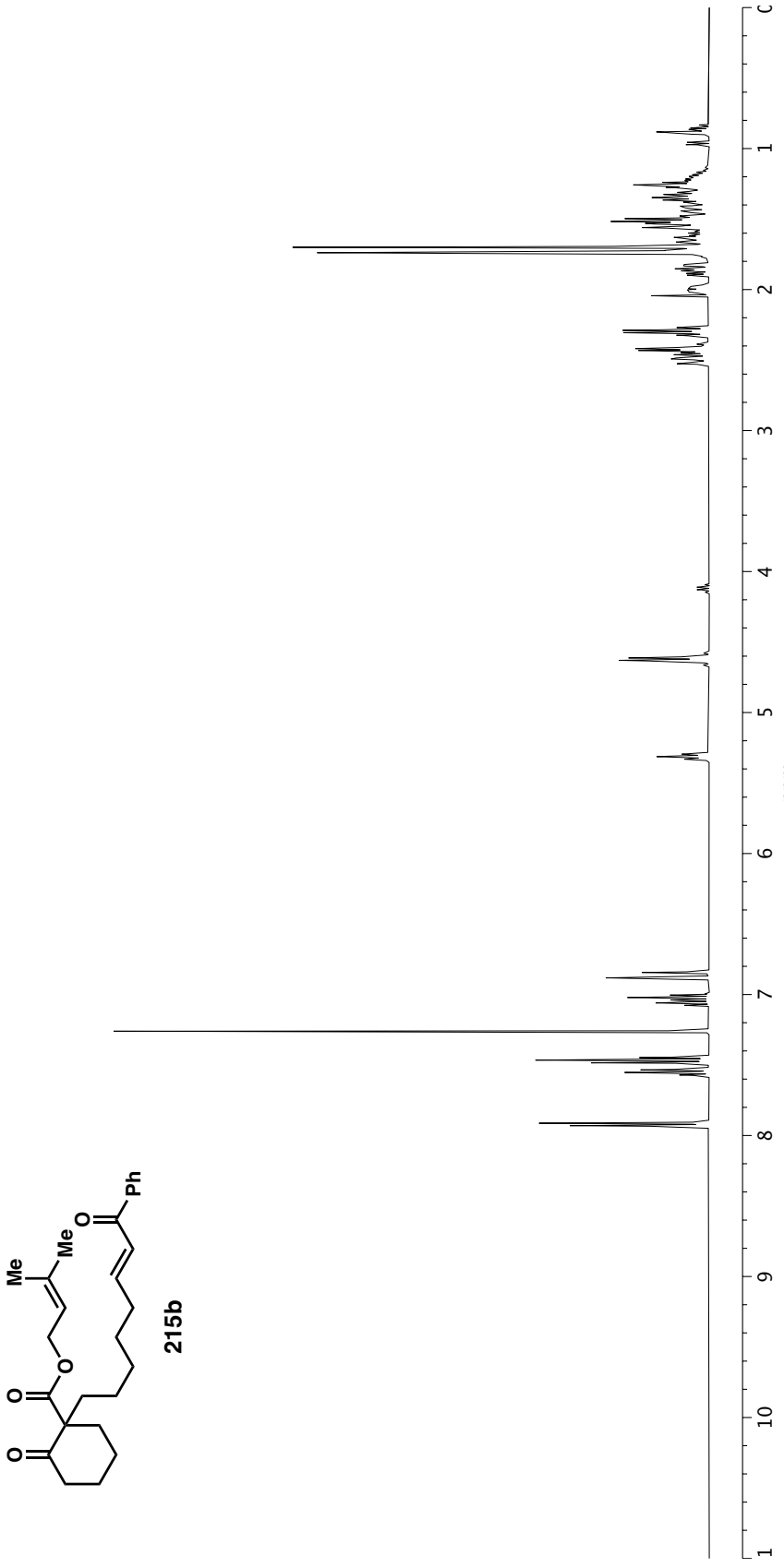

Figure A2.103. *^1H NMR (400 MHz, $CDCl_3$) of compound* ***215b.***

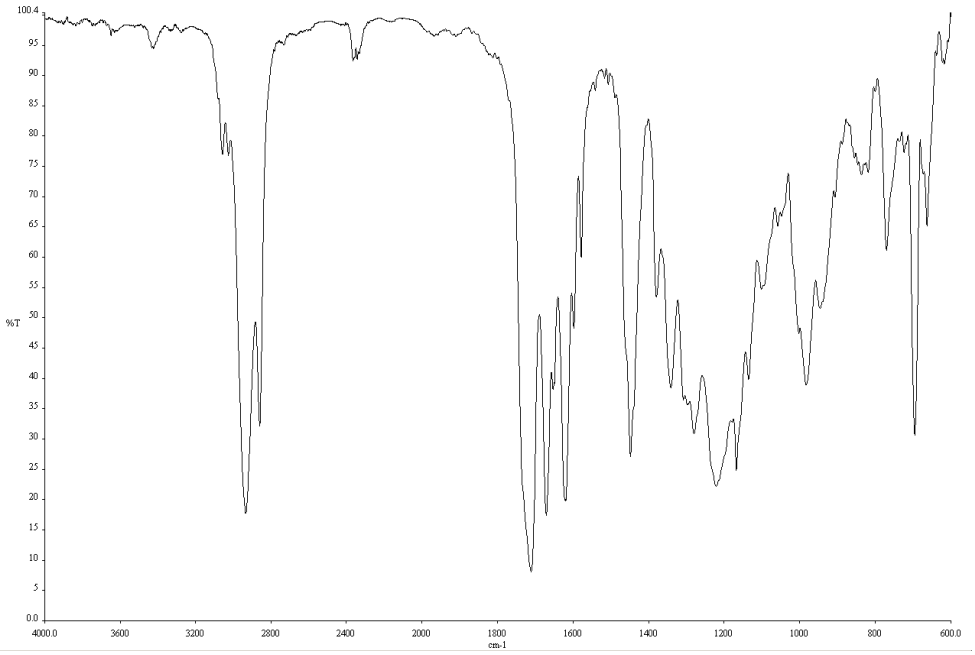

Figure A2.104. *Infrared spectrum (Thin Film, NaCl) of compound* ***215b.***

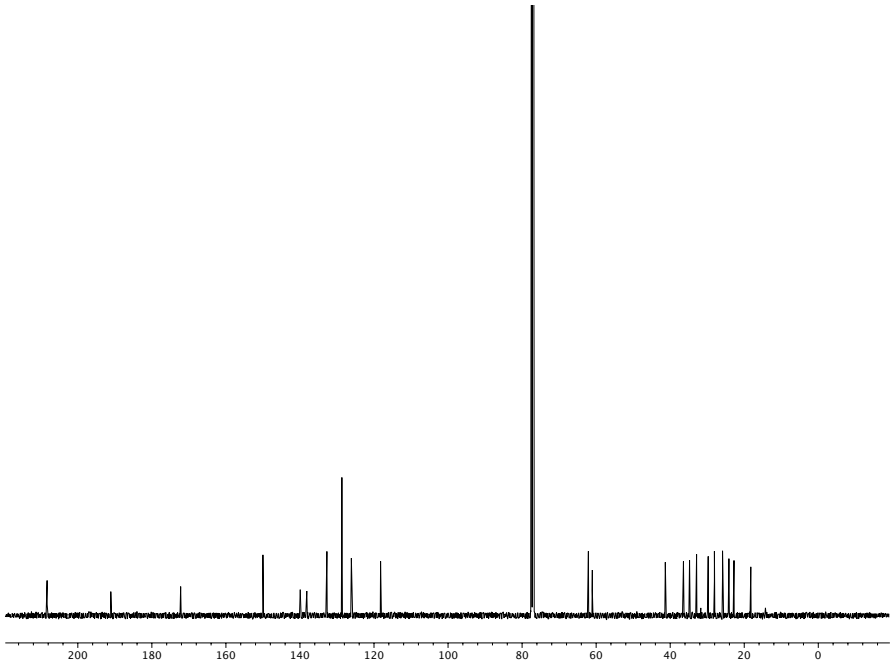

Figure A2.105. *^{13}C NMR (100 MHz, $CDCl_3$) of compound* ***215b.***

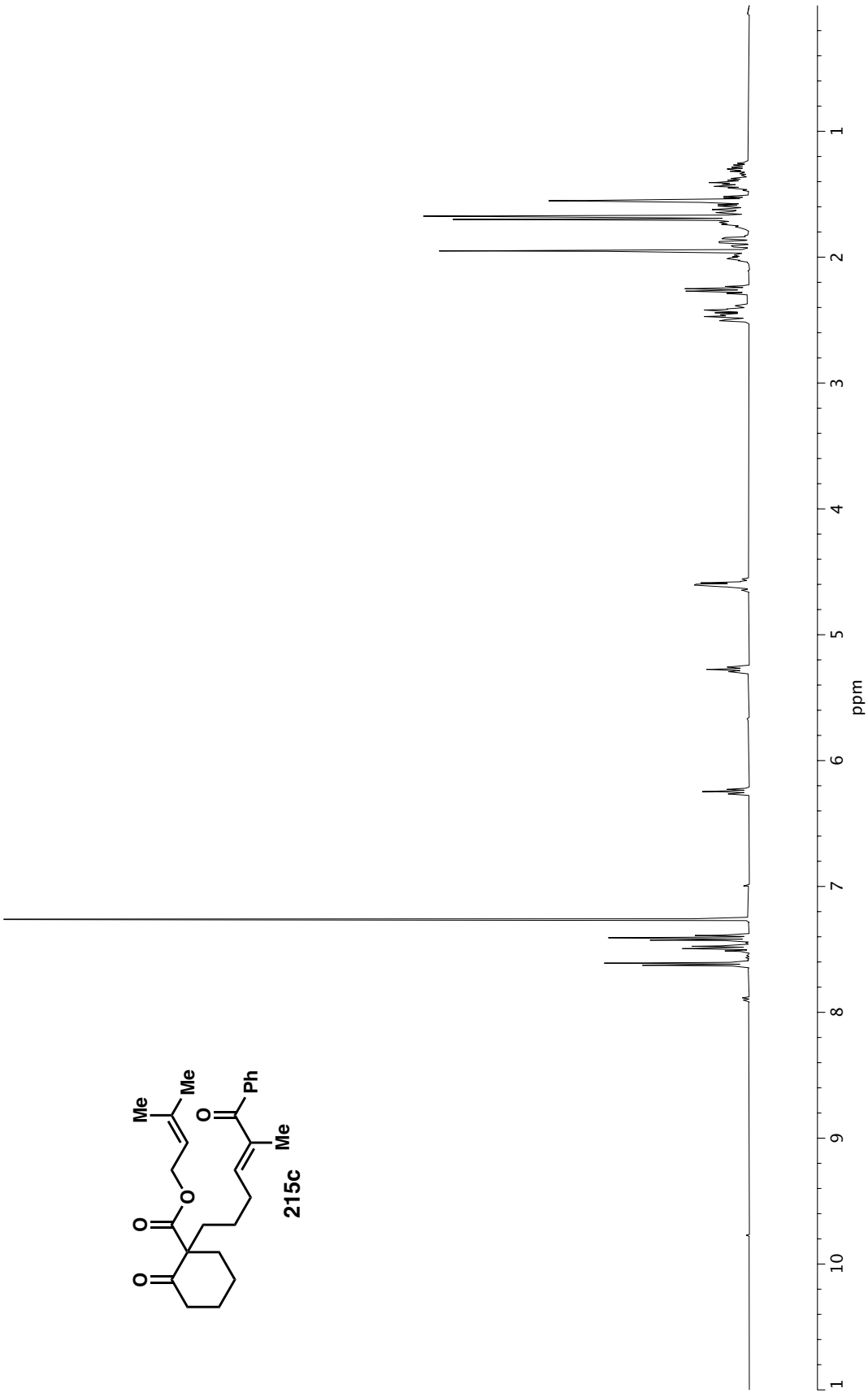

Figure A2.106. *^1H NMR (400 MHz, $CDCl_3$) of compound* ***215c.***

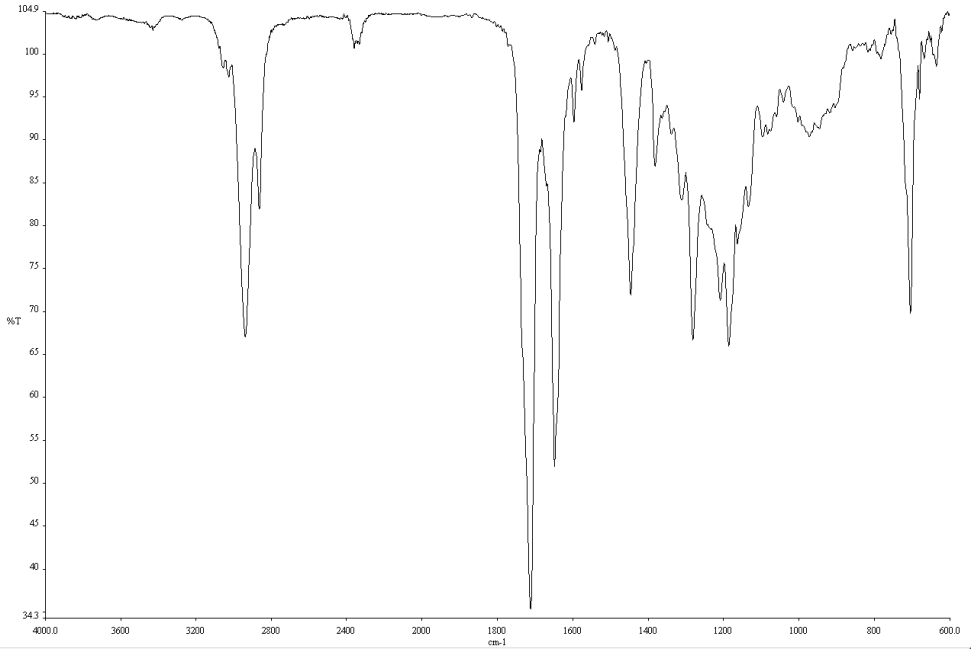

Figure A2.107. *Infrared spectrum (Thin Film, NaCl) of compound* ***215c.***

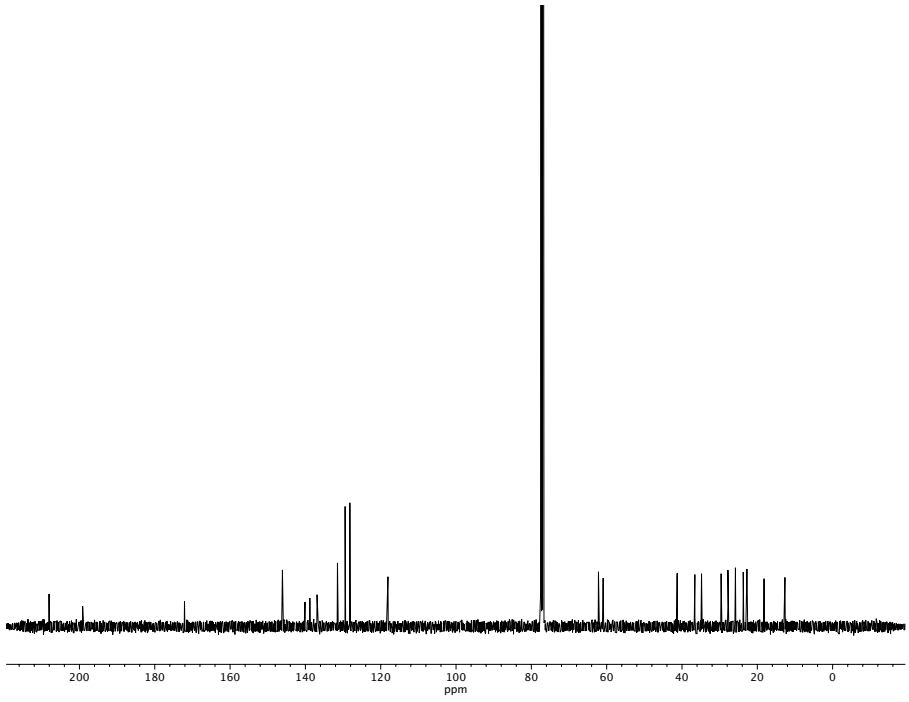

Figure A2.108. *^{13}C NMR (100 MHz, $CDCl_3$) of compound* ***215c.***

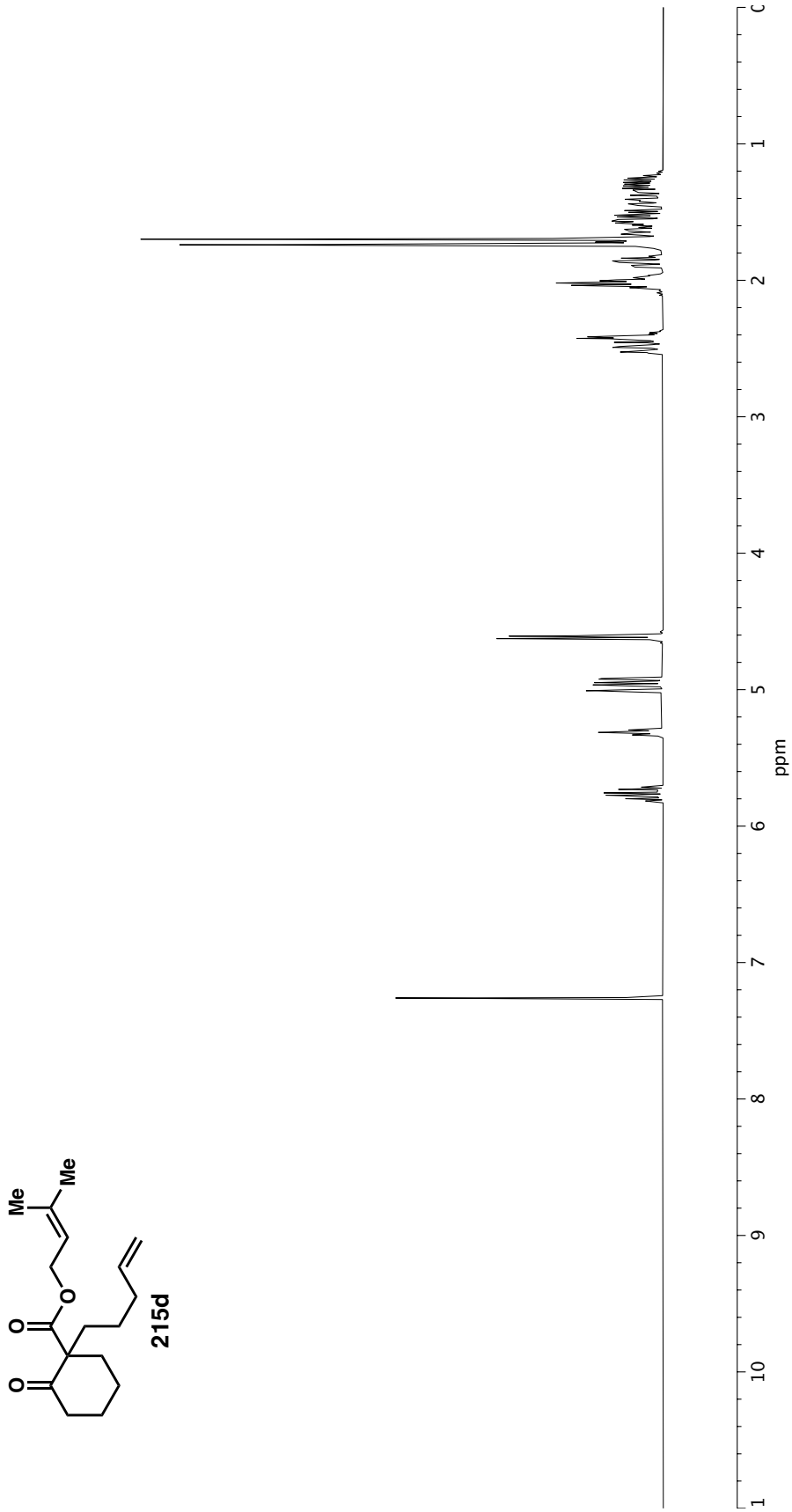

Figure A2.109. *^1H NMR (400 MHz, $CDCl_3$) of compound* ***215d.***

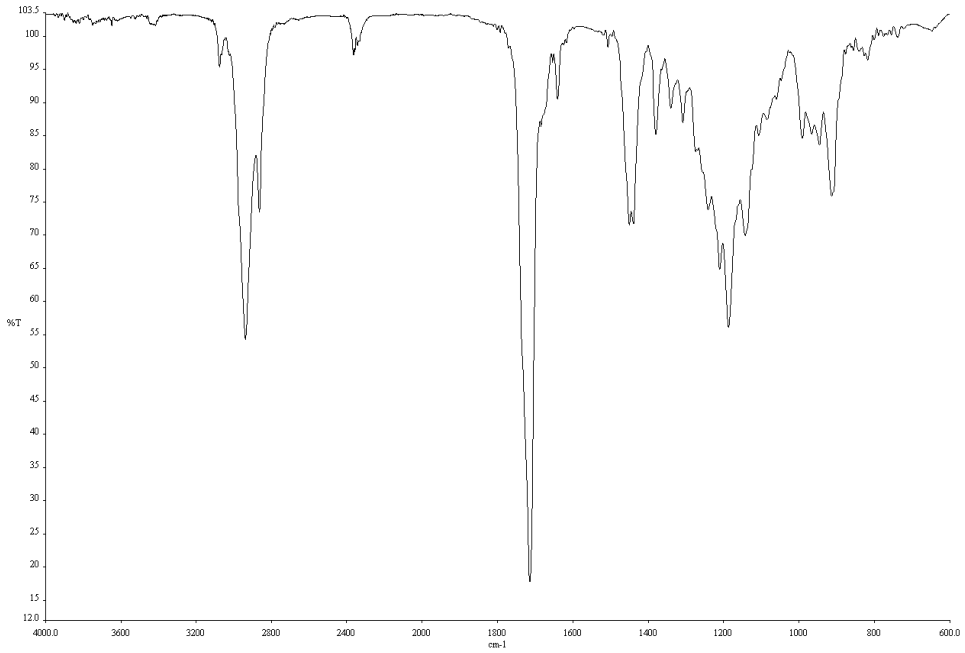

Figure A2.110. *Infrared spectrum (Thin Film, NaCl) of compound* ***215d.***

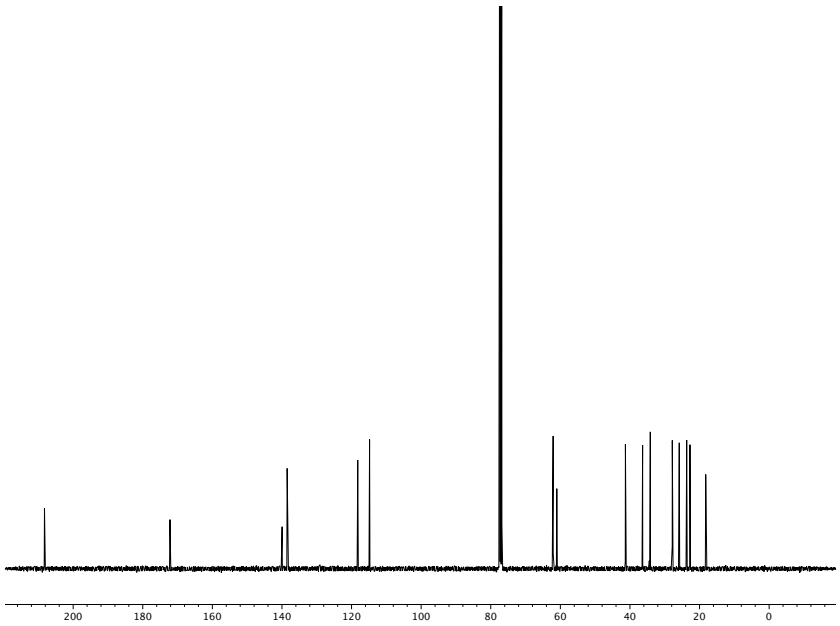

Figure A2.111. *^{13}C NMR (100 MHz, $CDCl_3$) of compound* ***215d.***

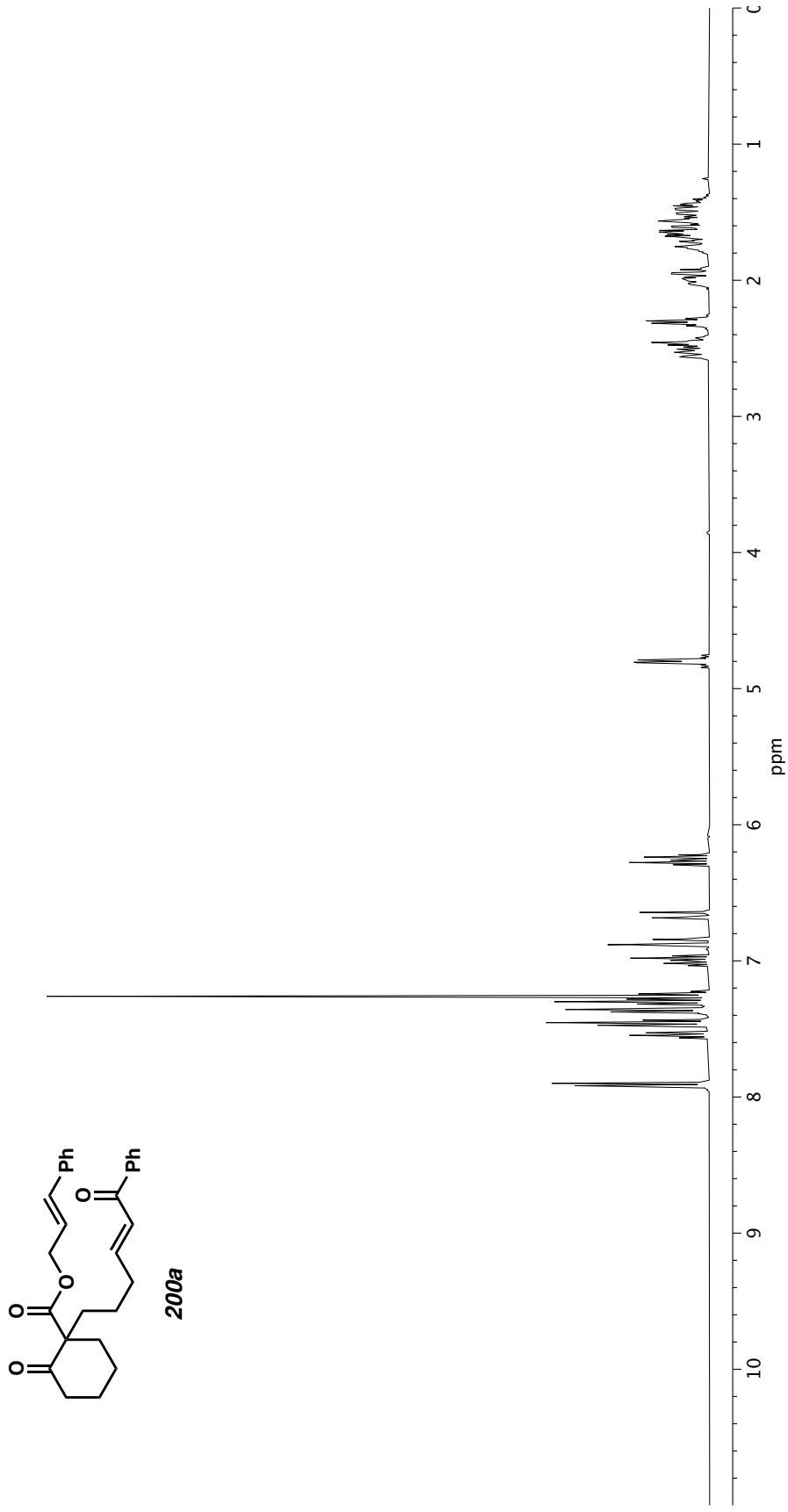

Figure A2.112. *^1H NMR (400 MHz, $CDCl_3$) of compound* ***200a.***

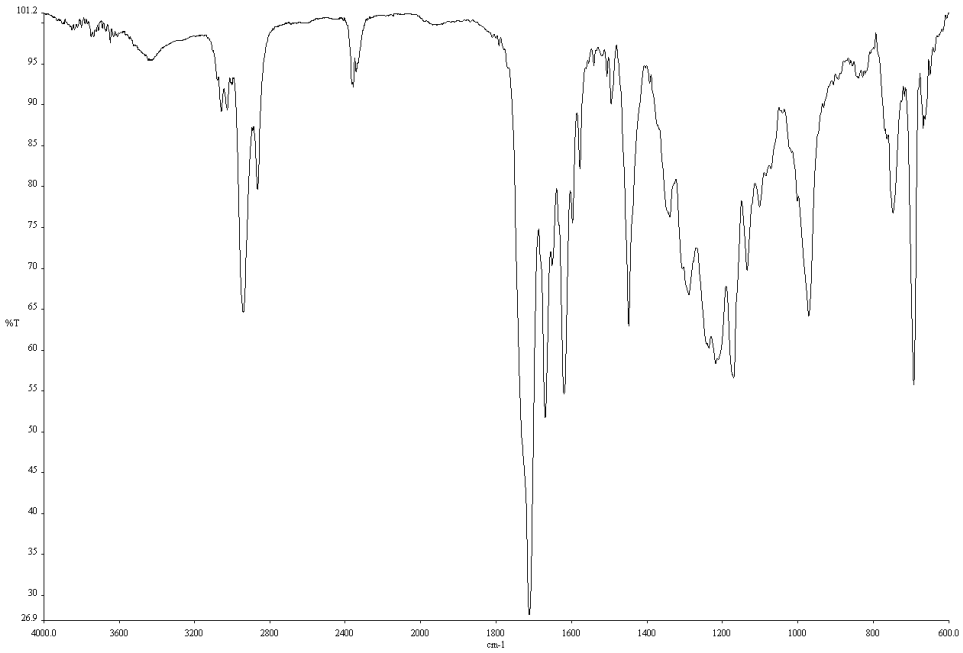

Figure A2.113. *Infrared spectrum (Thin Film, NaCl) of compound* ***200a.***

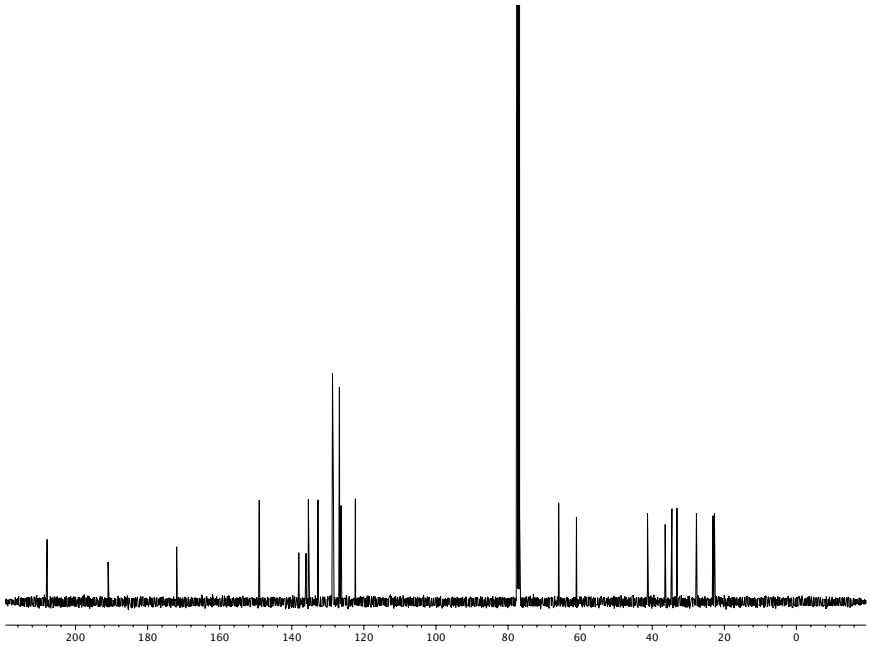

Figure A2.114. *^{13}C NMR (100 MHz, $CDCl_3$) of compound* ***200a.***

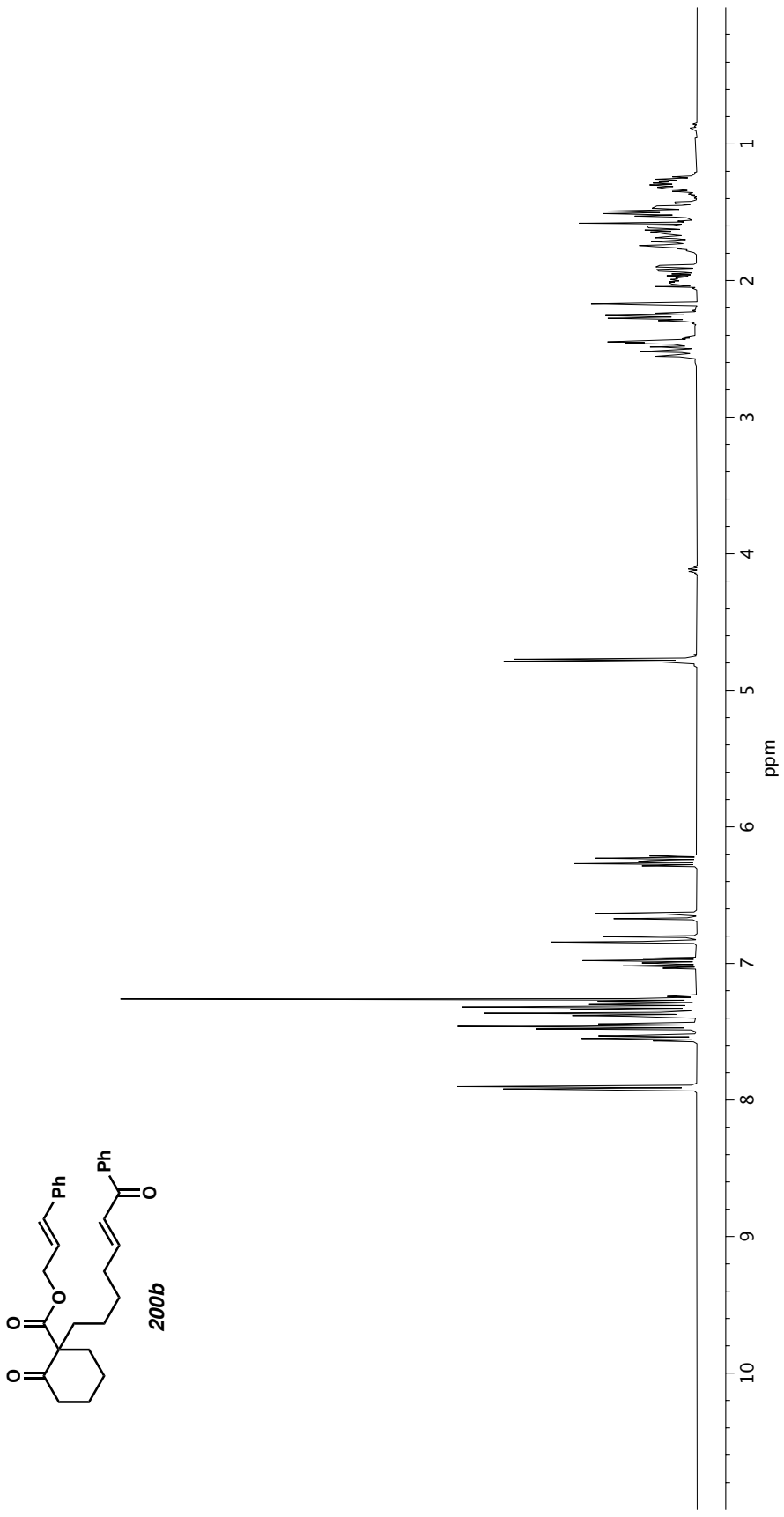

Figure A2.115. *^1H NMR (400 MHz, $CDCl_3$) of compound* ***200b.***

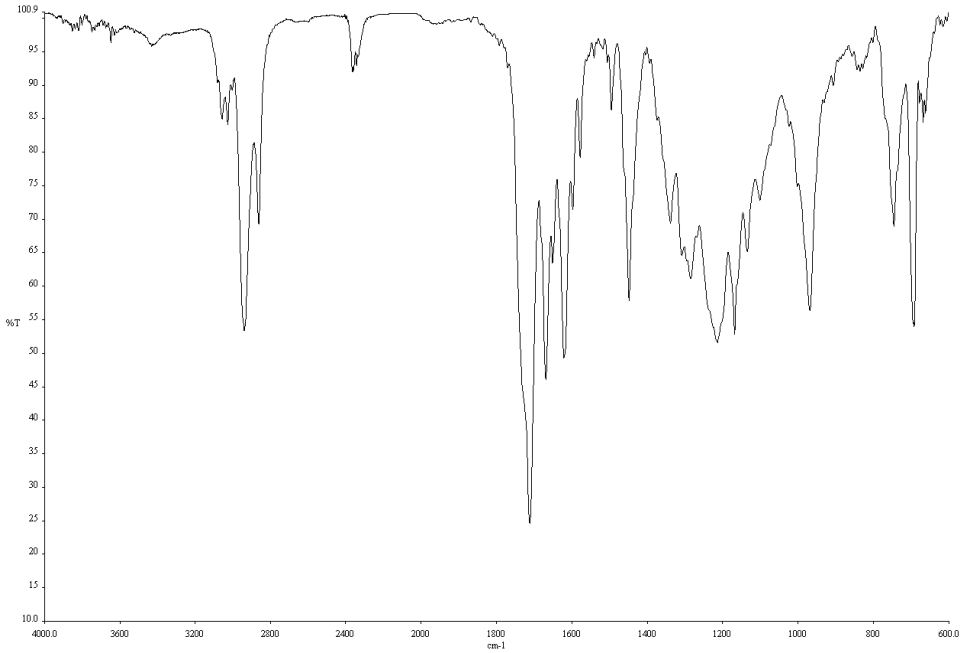

Figure A2.116. *Infrared spectrum (Thin Film, NaCl) of compound* ***200b.***

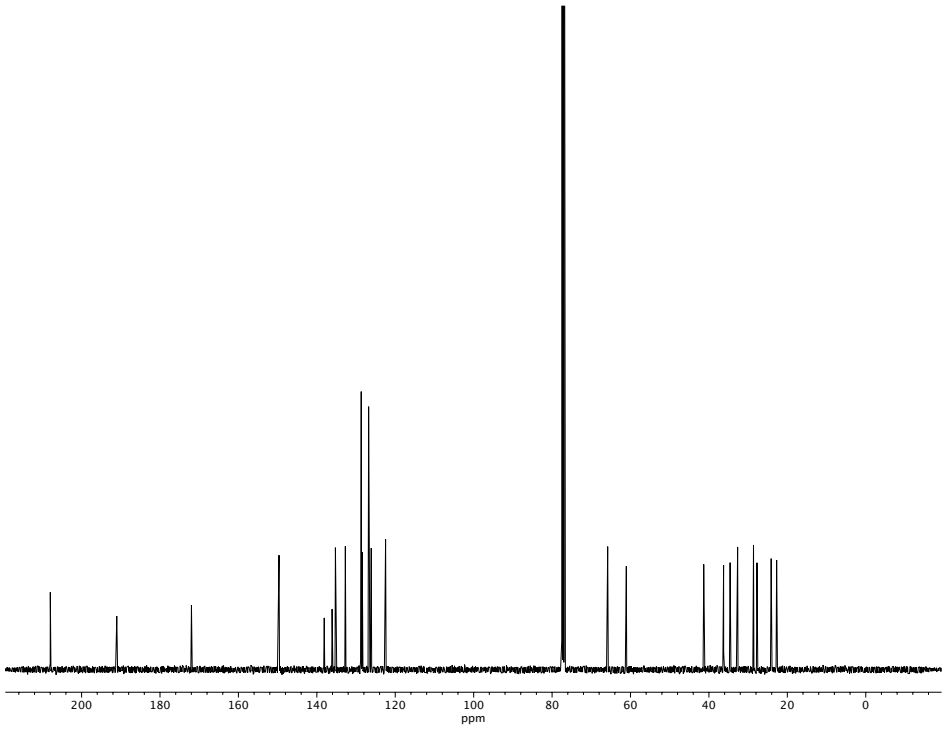

Figure A2.117. *^{13}C NMR (100 MHz, $CDCl_3$) of compound* ***200b.***

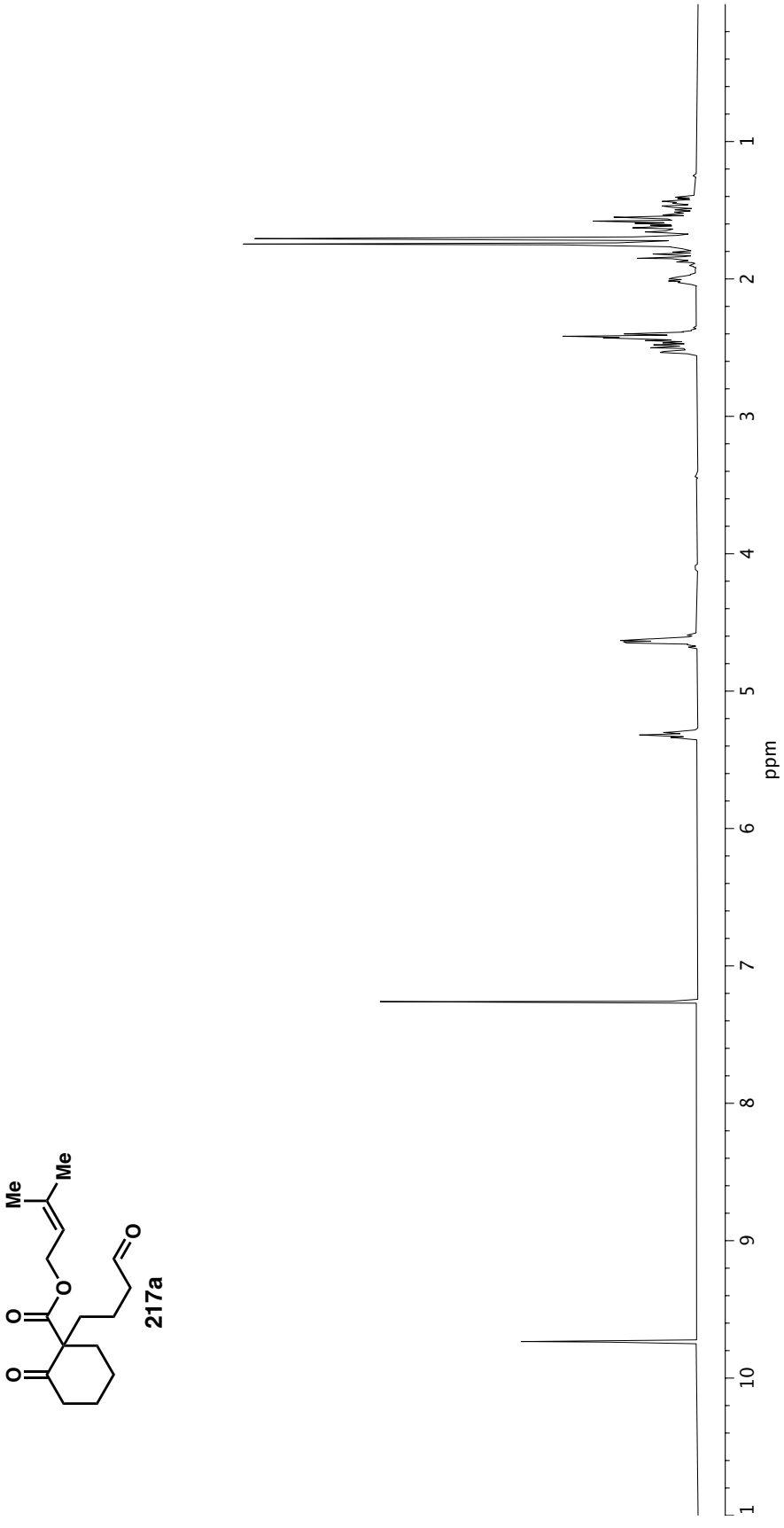

Figure A2.118. *^{1}H NMR (400 MHz, $CDCl_3$) of compound* ***217a.***

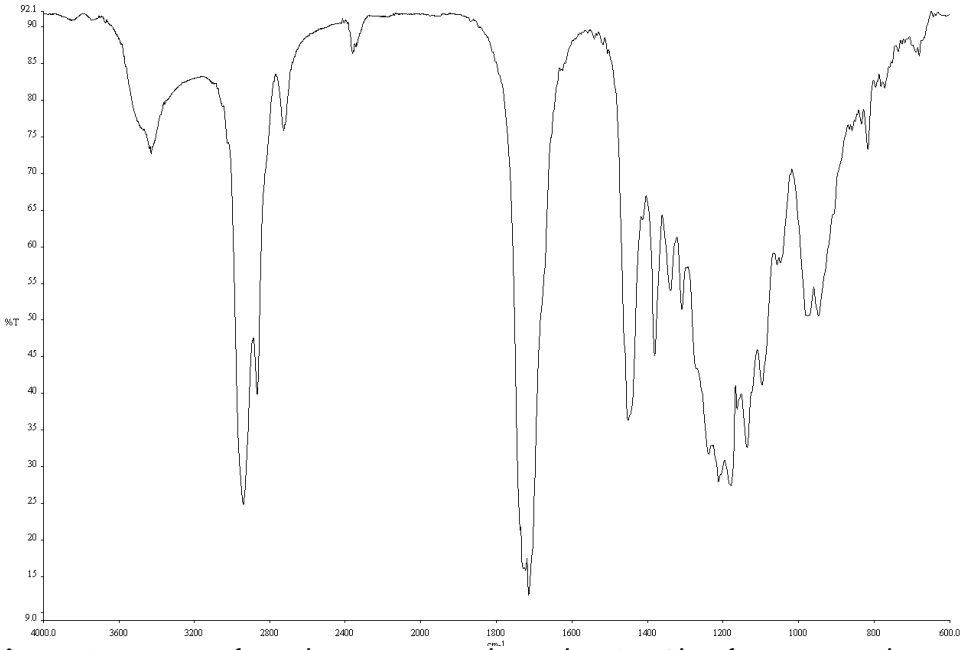

Figure A2.119. *Infrared spectrum (Thin Film, NaCl) of compound* ***217a.***

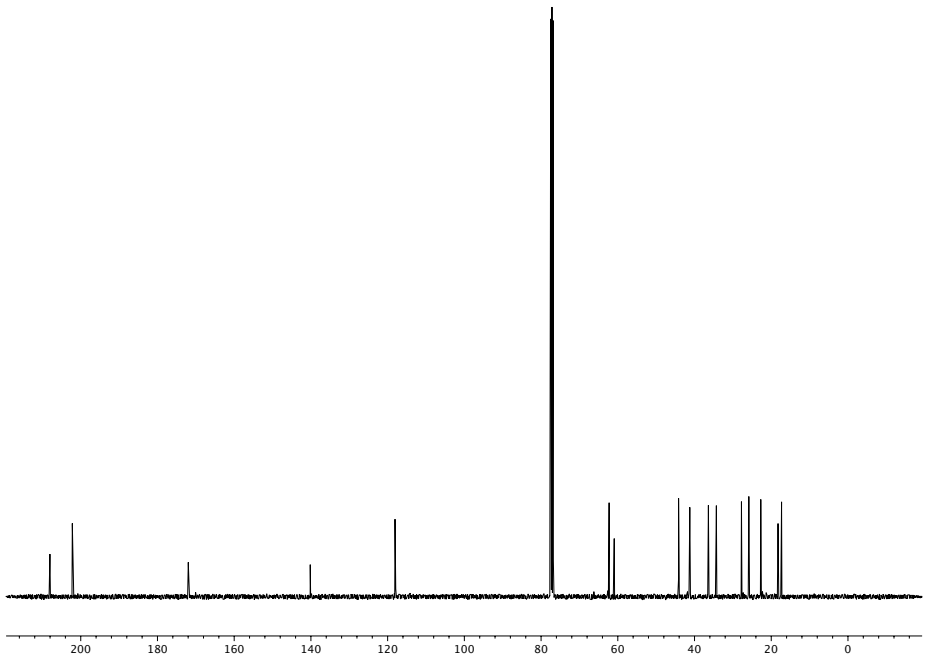

Figure A2.120. *^{13}C NMR (100 MHz, $CDCl_3$) of compound* ***217a.***

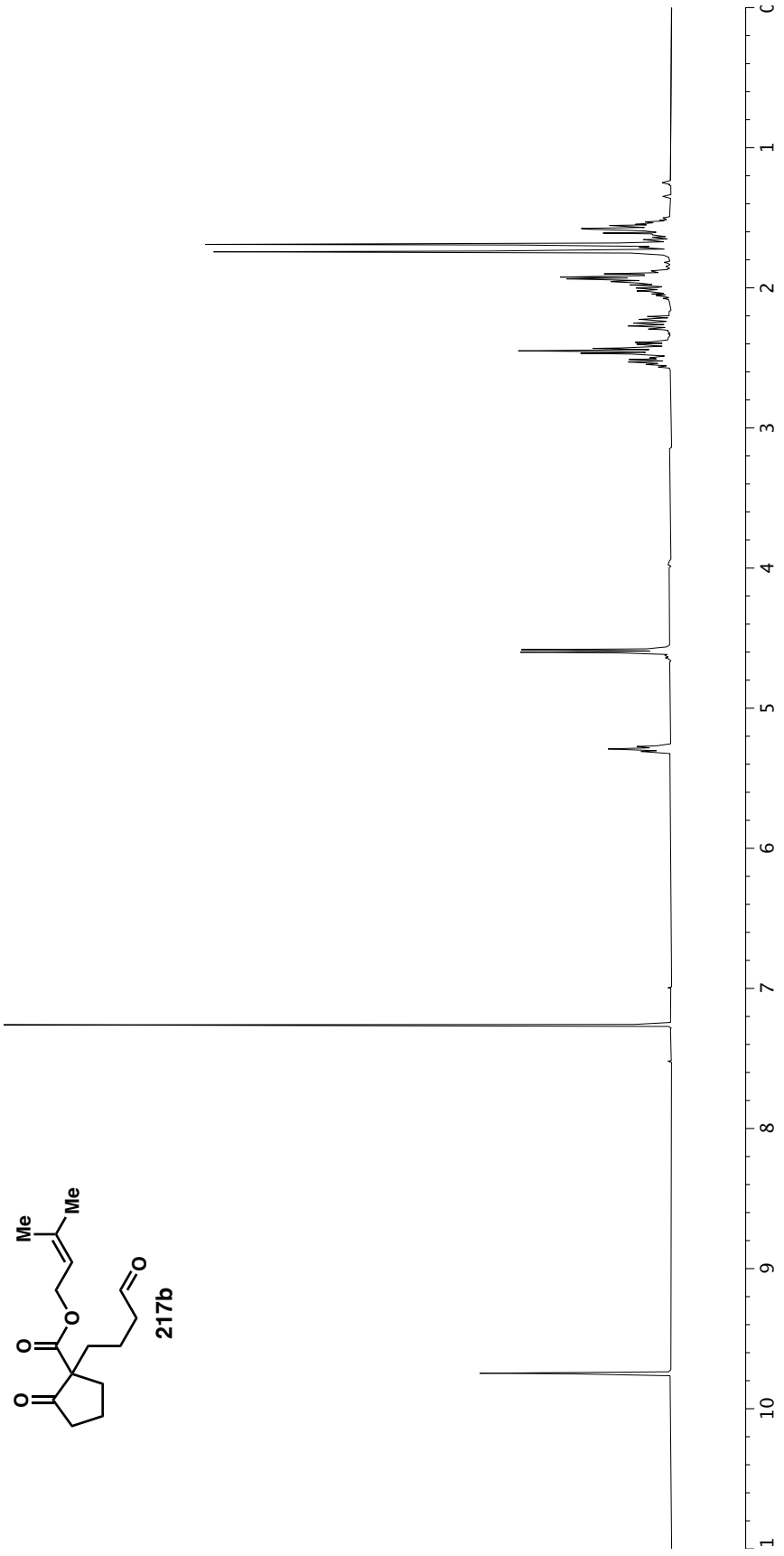

Figure A2.121. *^1H NMR (400 MHz, $CDCl_3$) of compound* ***217b.***

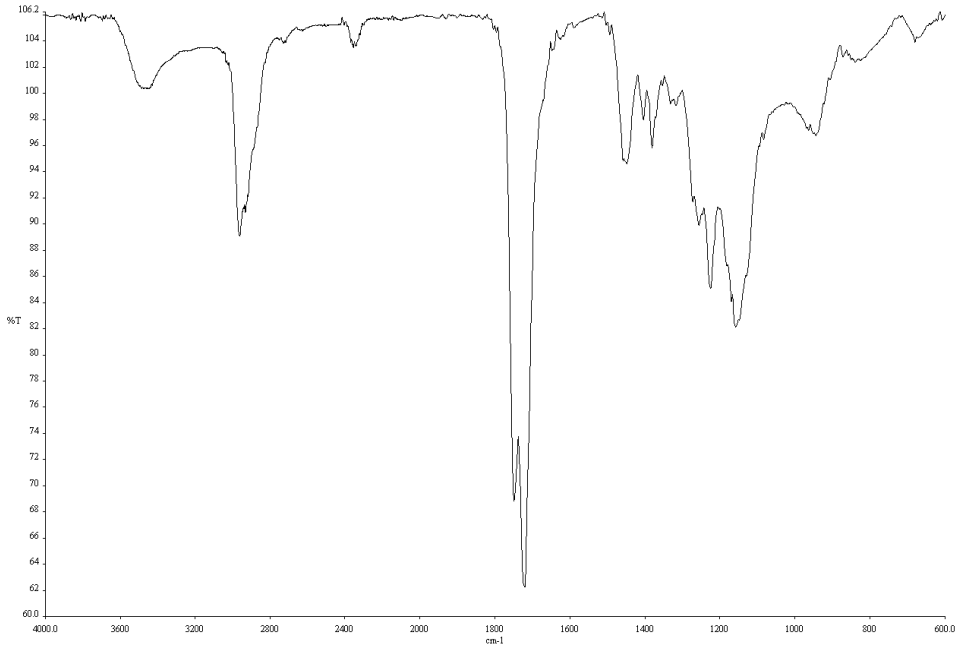

Figure A2.122. *Infrared spectrum (Thin Film, NaCl) of compound* ***217b.***

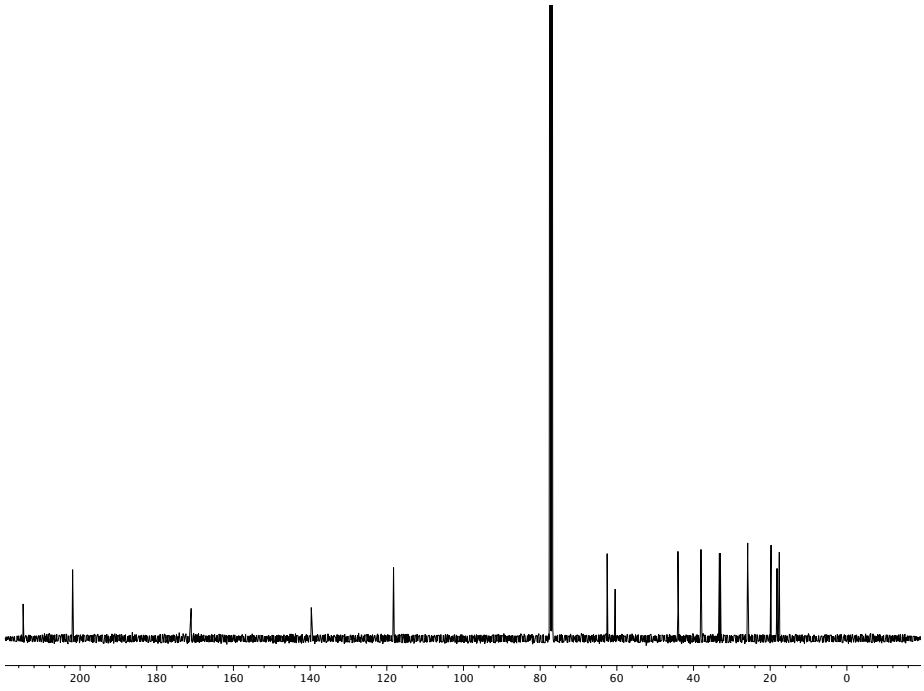

Figure A2.123. *^{13}C NMR (100 MHz, $CDCl_3$) of compound* ***217b.***

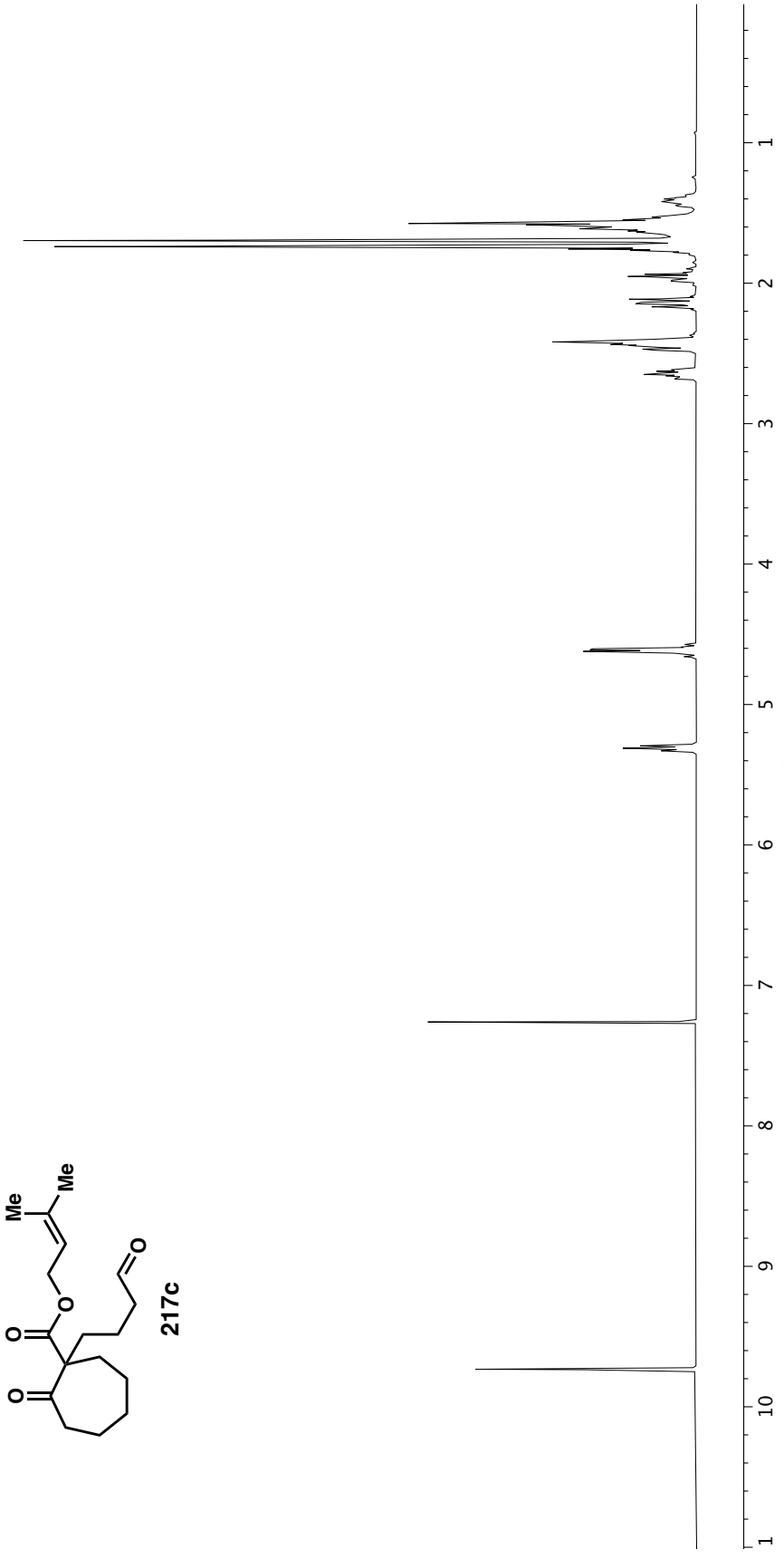

Figure A2.124. *^1H NMR (400 MHz, $CDCl_3$) of compound* ***217c.***

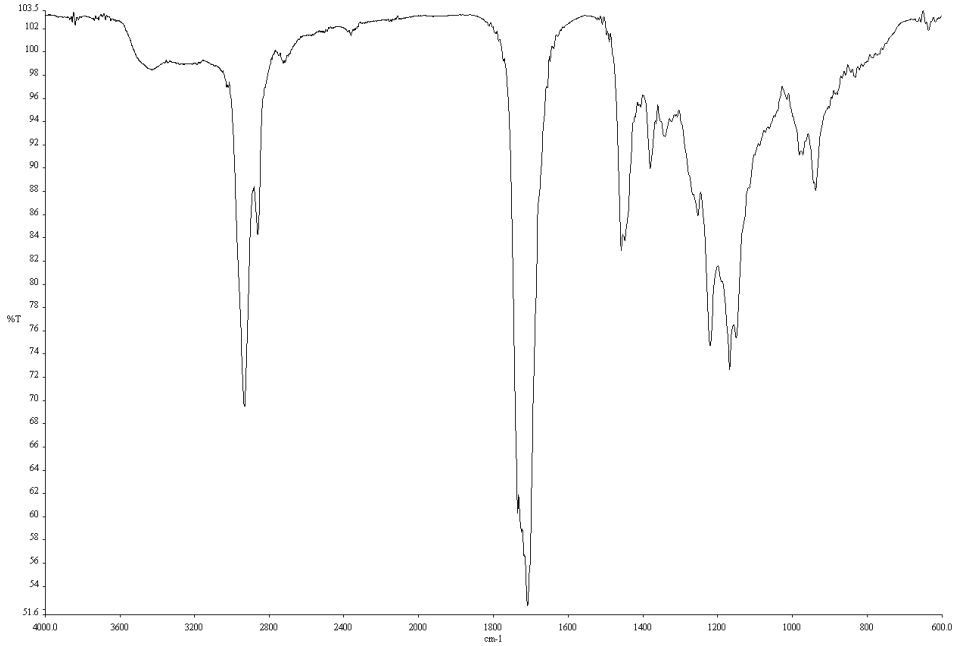

Figure A2.125. *Infrared spectrum (Thin Film, NaCl) of compound* ***217c.***

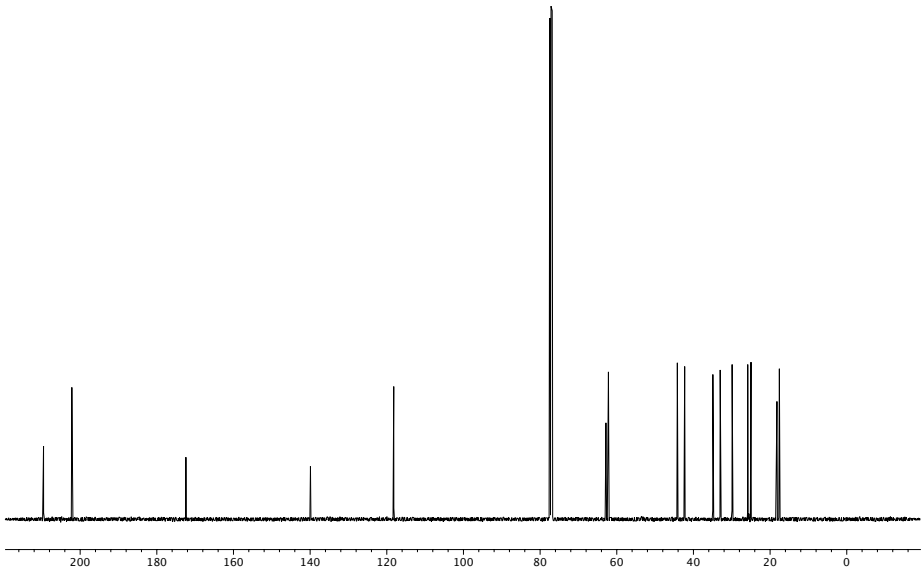

Figure A2.126. *^{13}C NMR (100 MHz, $CDCl_3$) of compound* ***217c.***

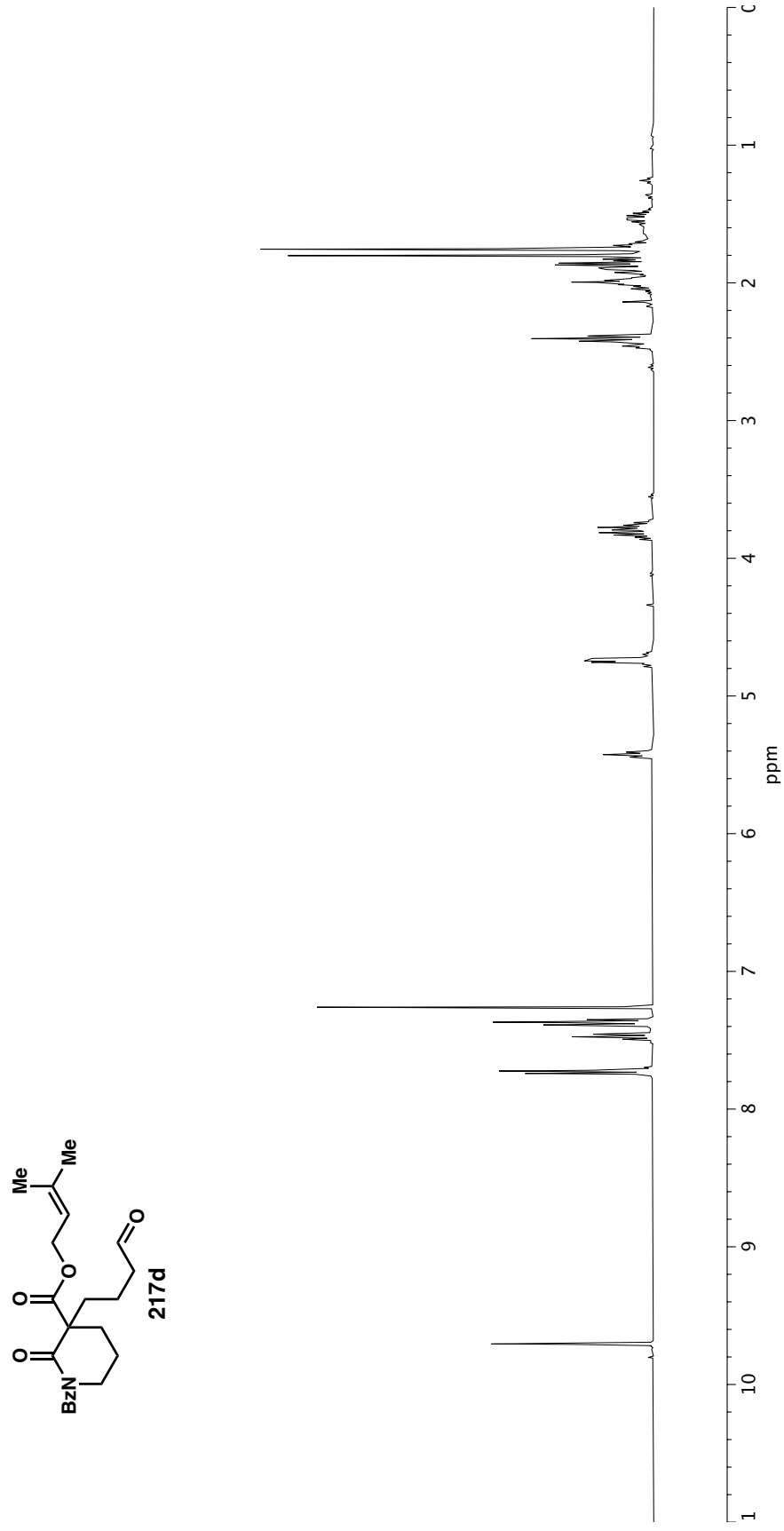

Figure A2.127. *^1H NMR (400 MHz, $CDCl_3$) of compound* ***217d.***

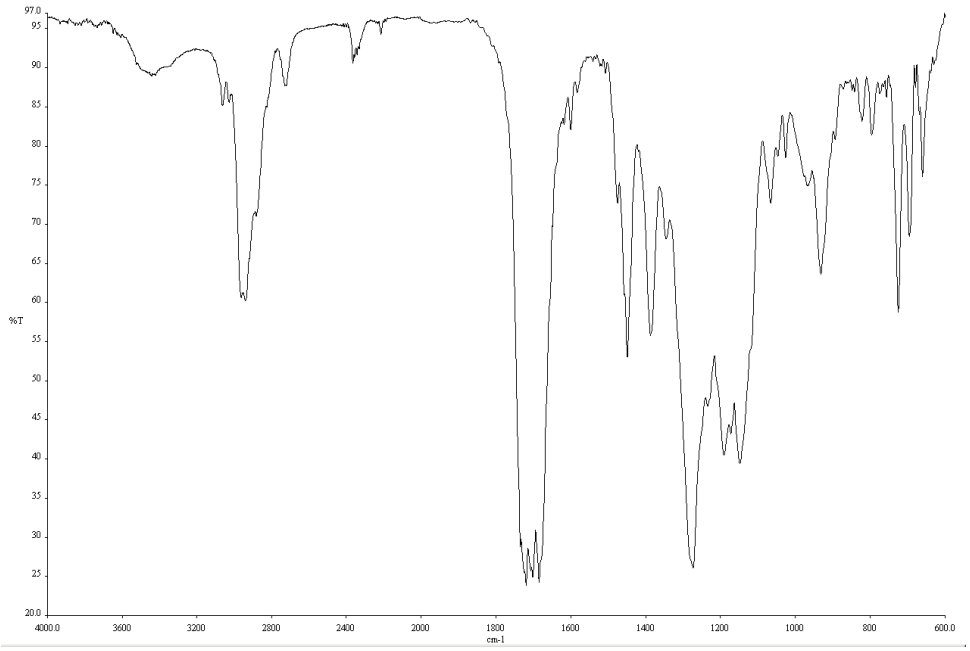

Figure A2.128. *Infrared spectrum (Thin Film, NaCl) of compound* ***217d.***

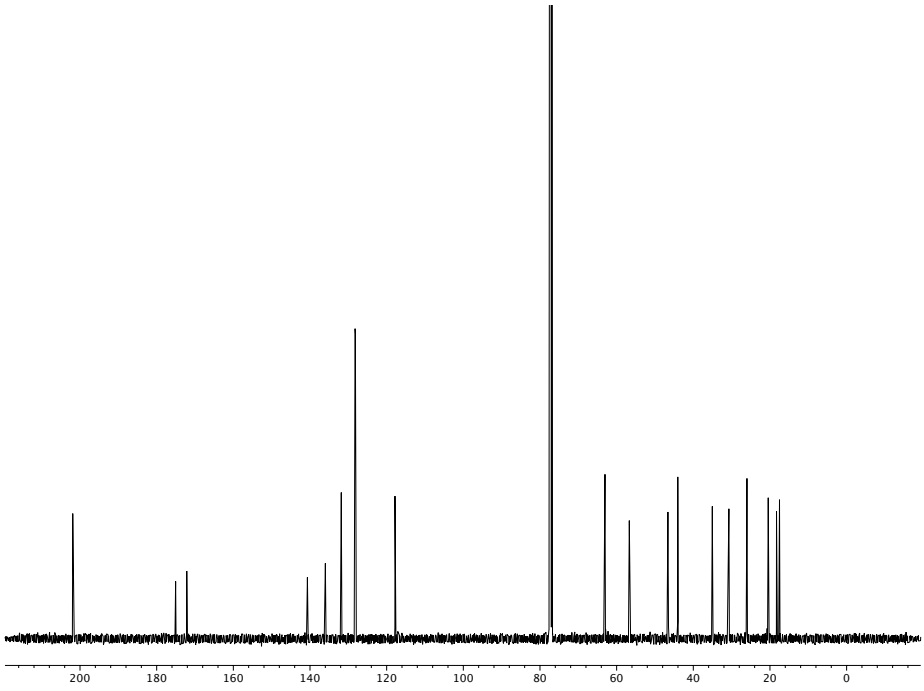

Figure A2.129. *^{13}C NMR (100 MHz, $CDCl_3$) of compound* ***217d.***

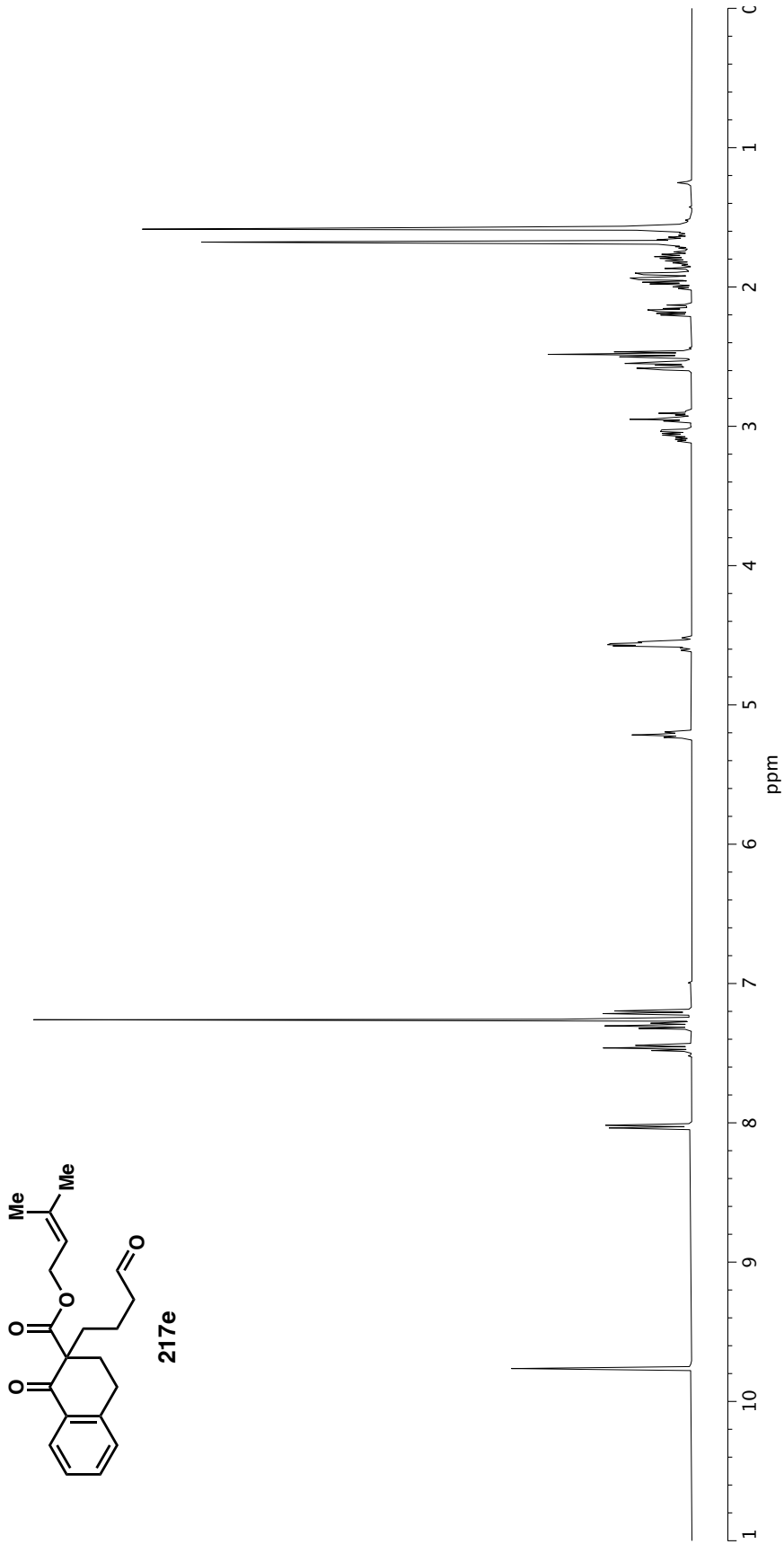

Figure A2.130. *^{1}H NMR (400 MHz, $CDCl_3$) of compound* ***217e.***

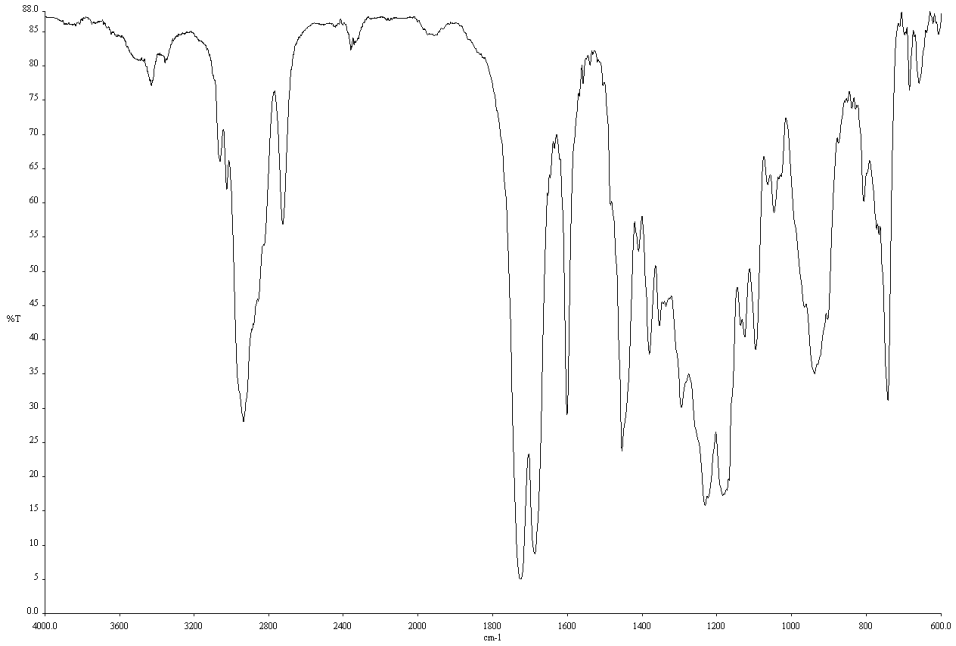

Figure A2.131. *Infrared spectrum (Thin Film, NaCl) of compound* ***217e.***

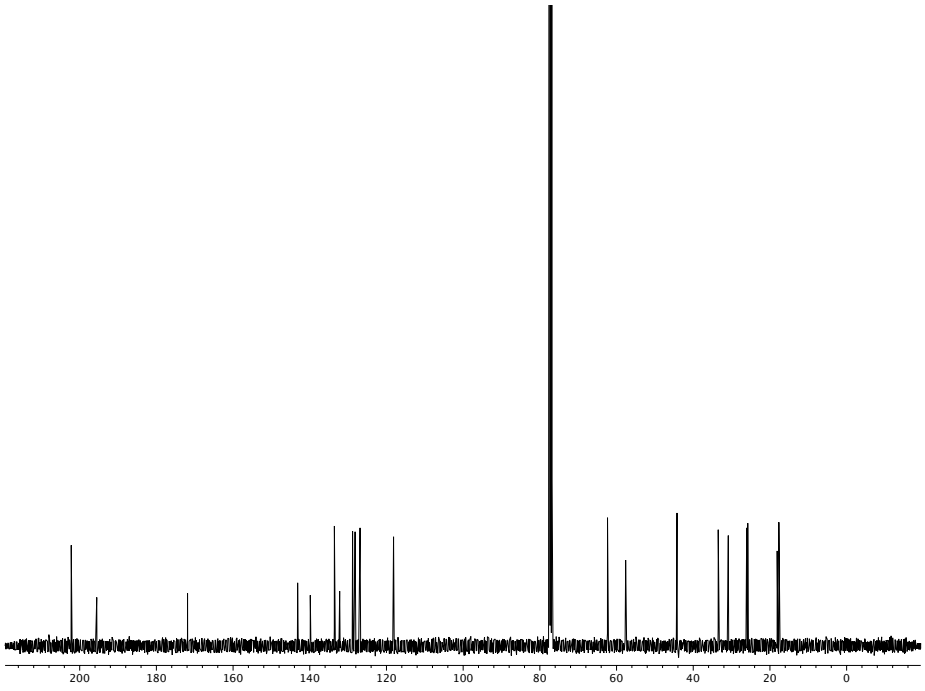

Figure A2.132. *^{13}C NMR (100 MHz, $CDCl_3$) of compound* ***217e.***

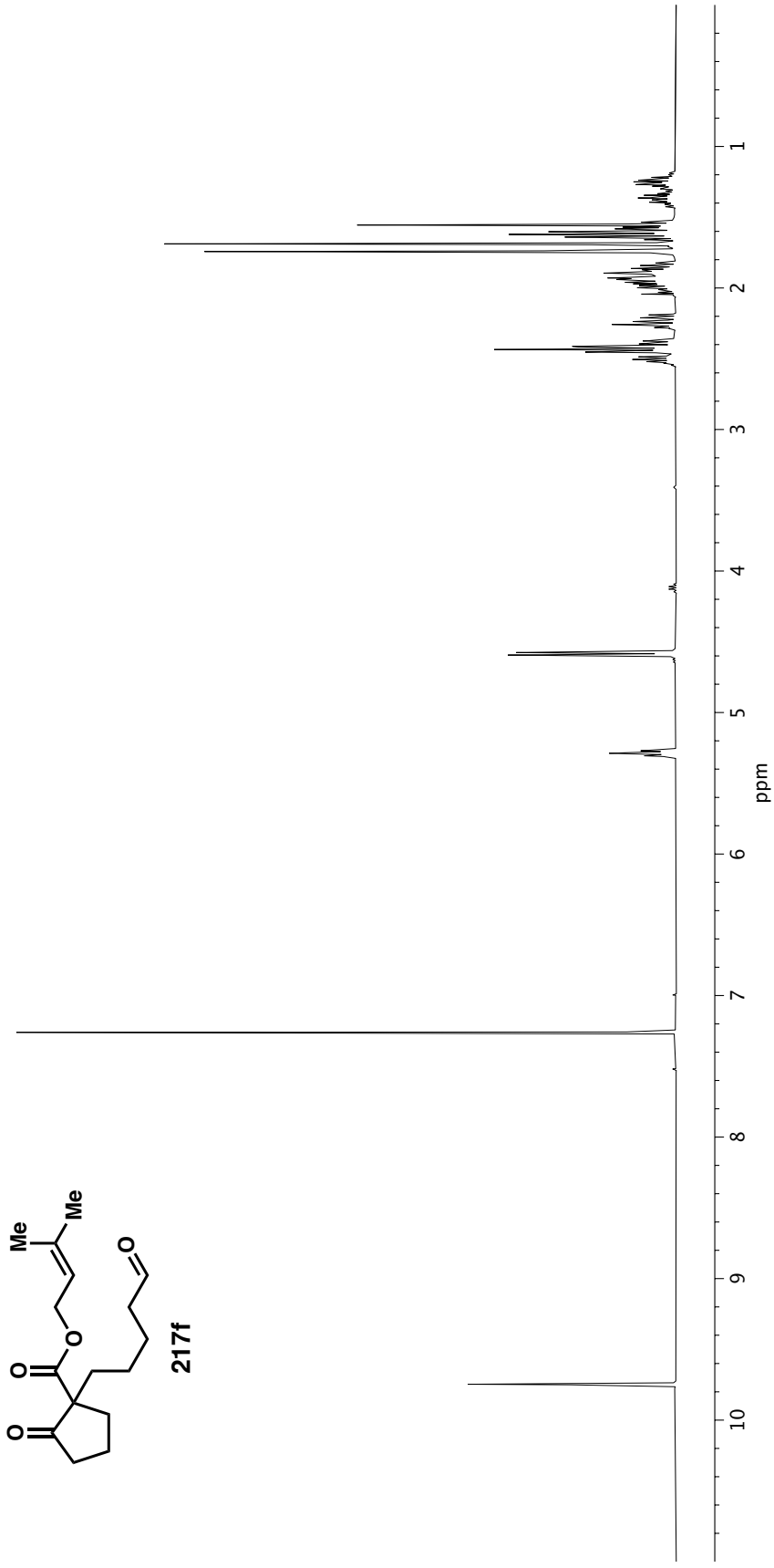

Figure A2.133. *^1H NMR (400 MHz, $CDCl_3$) of compound* ***217f.***

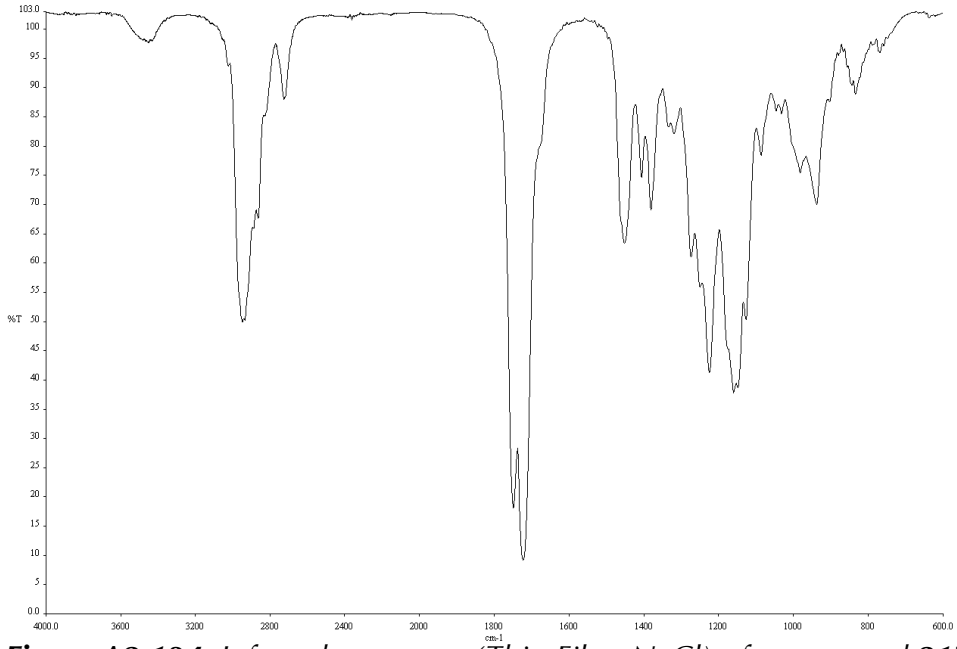

Figure A2.134. *Infrared spectrum (Thin Film, NaCl) of compound* ***217f.***

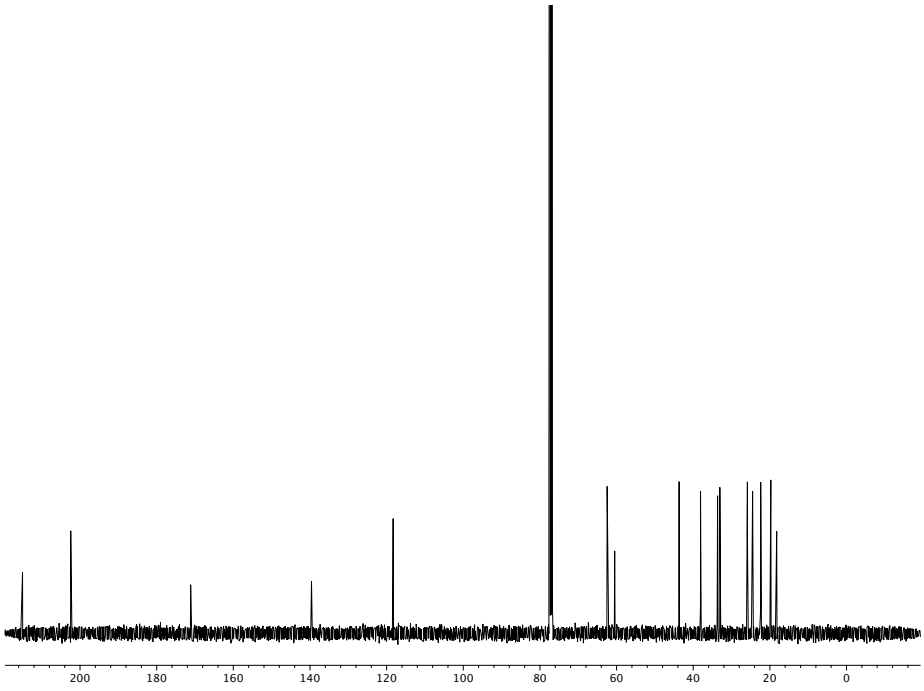

Figure A2.135. *^{13}C NMR (100 MHz, $CDCl_3$) of compound* ***217f.***

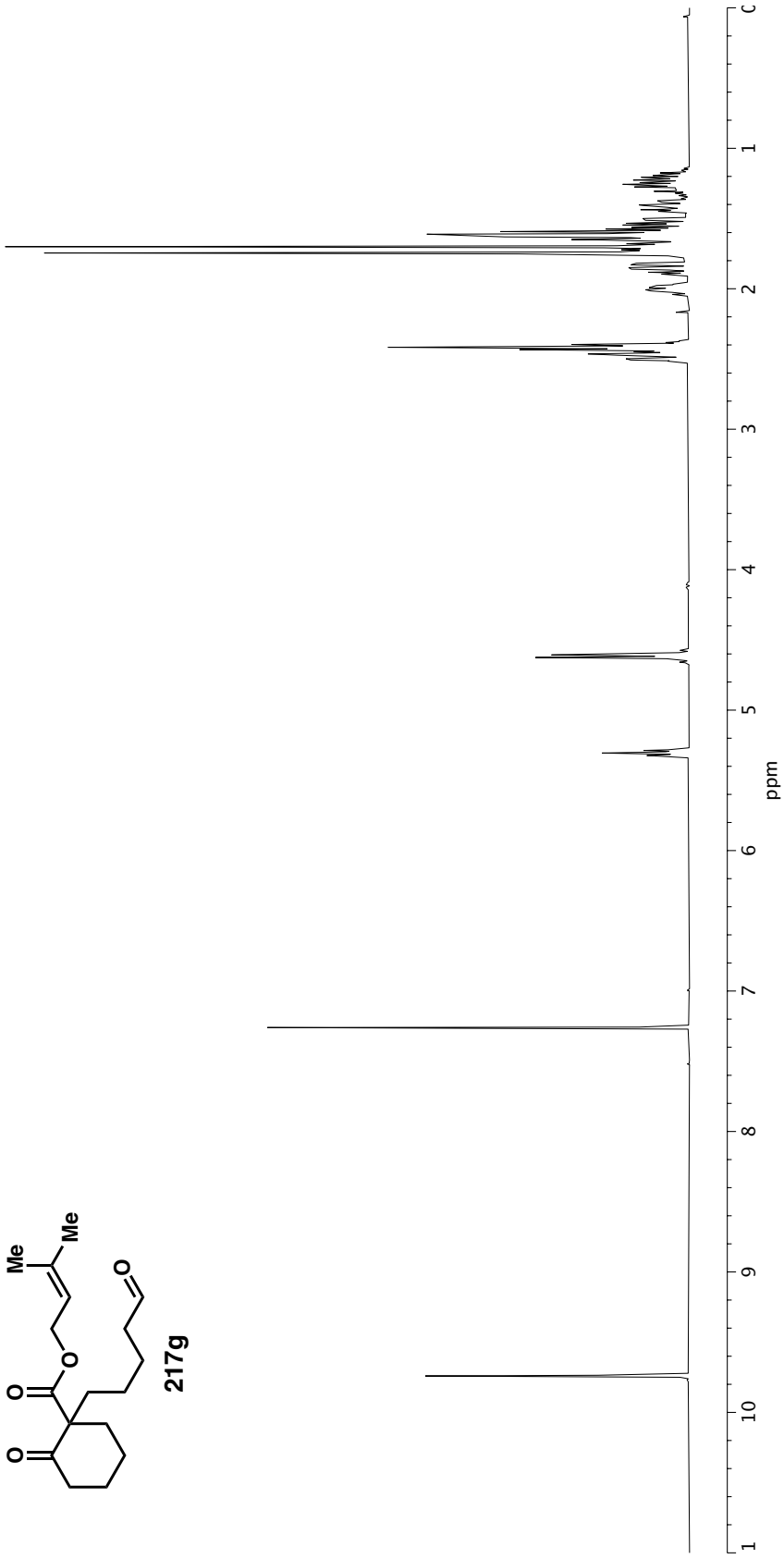

Figure A2.136. *^1H NMR (400 MHz, $CDCl_3$) of compound* ***217g.***

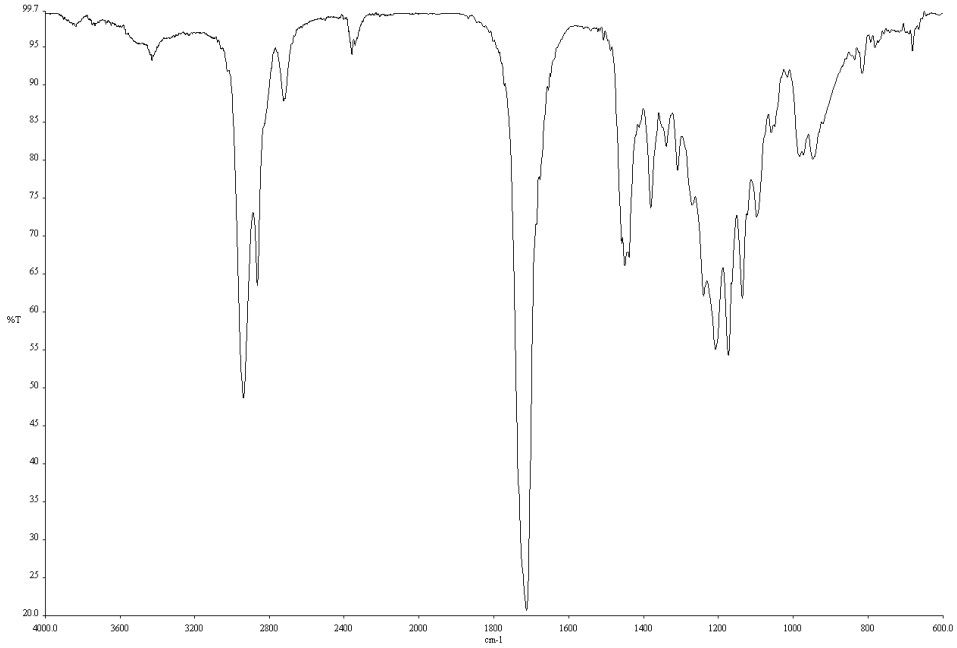

Figure A2.137. *Infrared spectrum (Thin Film, NaCl) of compound* ***217g.***

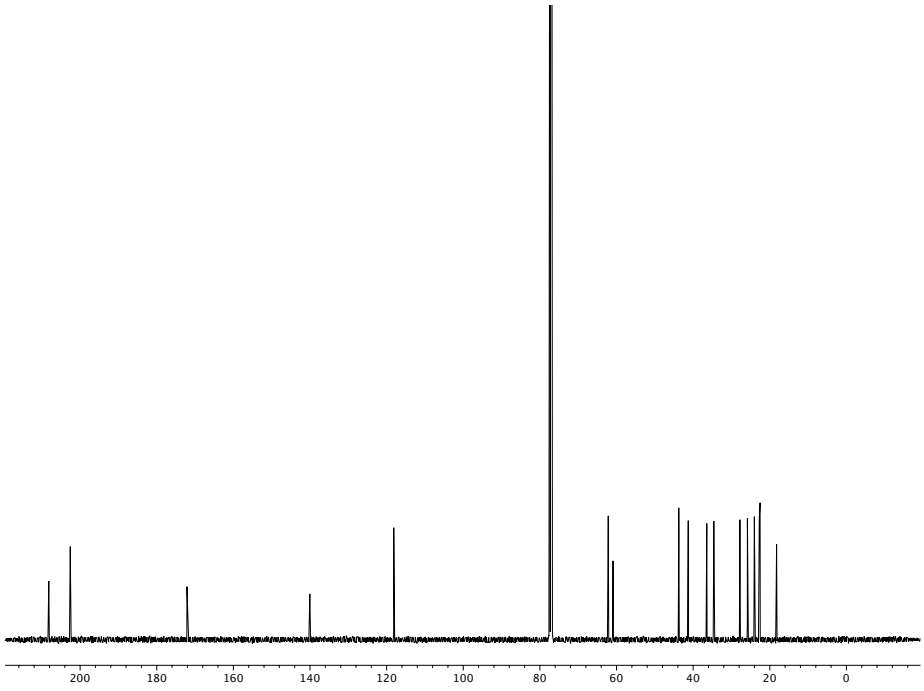

Figure A2.138. *^{13}C NMR (100 MHz, $CDCl_3$) of compound* ***217g.***

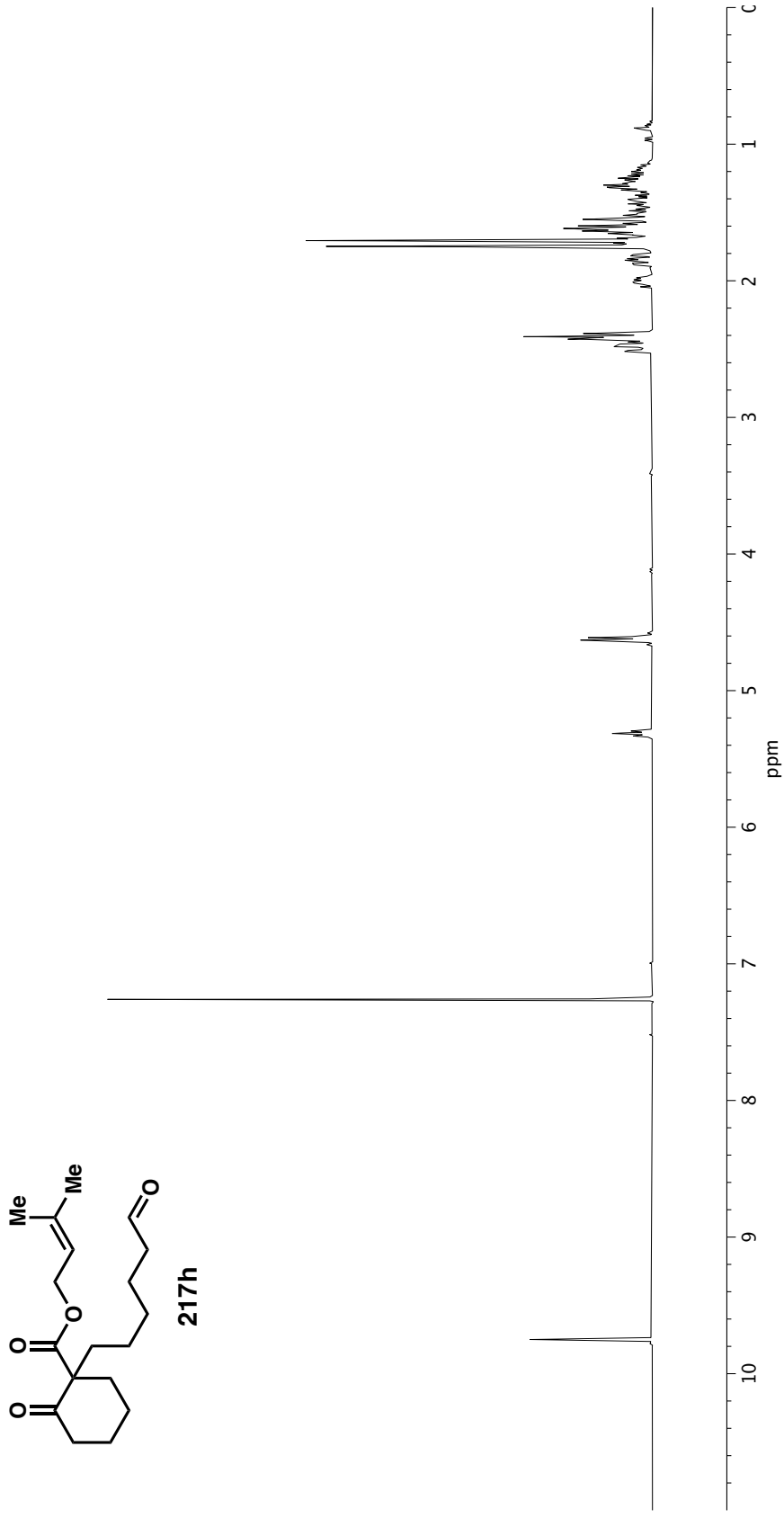

Figure A2.139. *^1H NMR (400 MHz, $CDCl_3$) of compound* ***217h.***

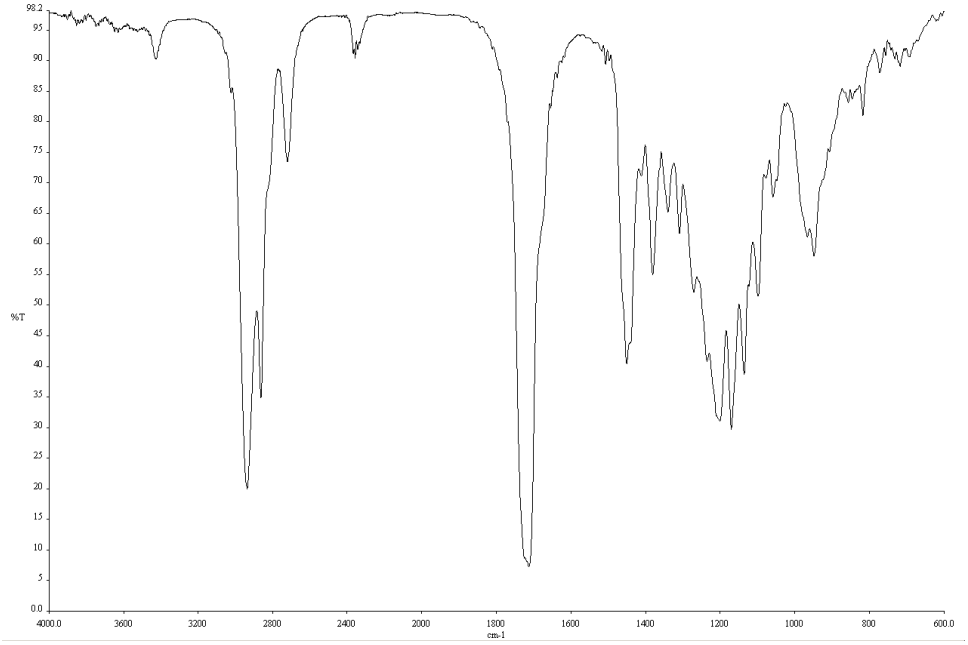

Figure A2.140. *Infrared spectrum (Thin Film, NaCl) of compound* ***217h.***

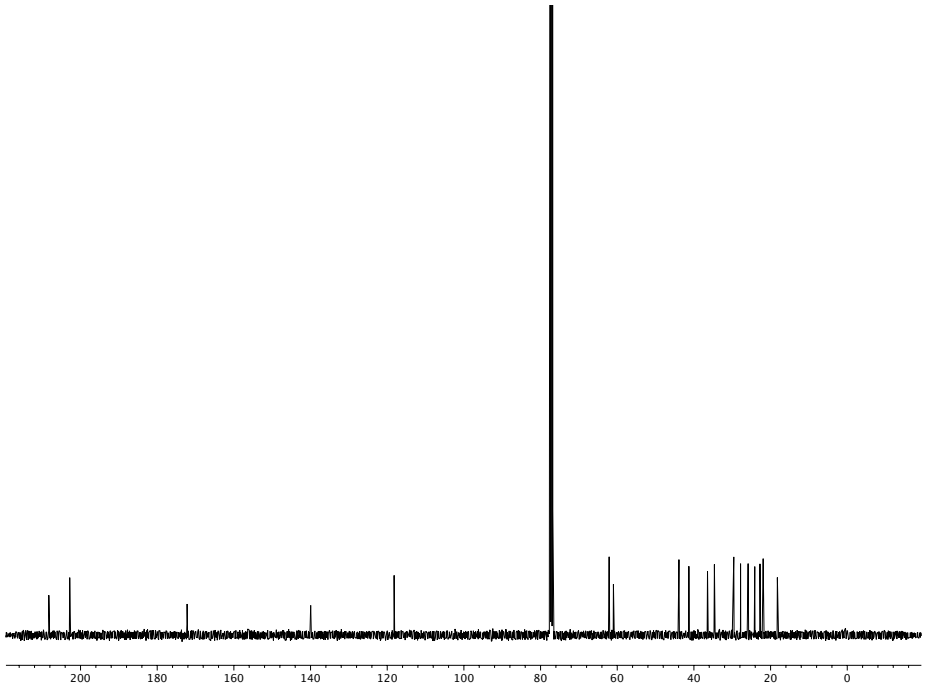

Figure A2.141. *^{13}C NMR (100 MHz, $CDCl_3$) of compound* ***217h.***

Figure A2.142. *^1H NMR (400 MHz, $CDCl_3$) of compound* ***217i.***

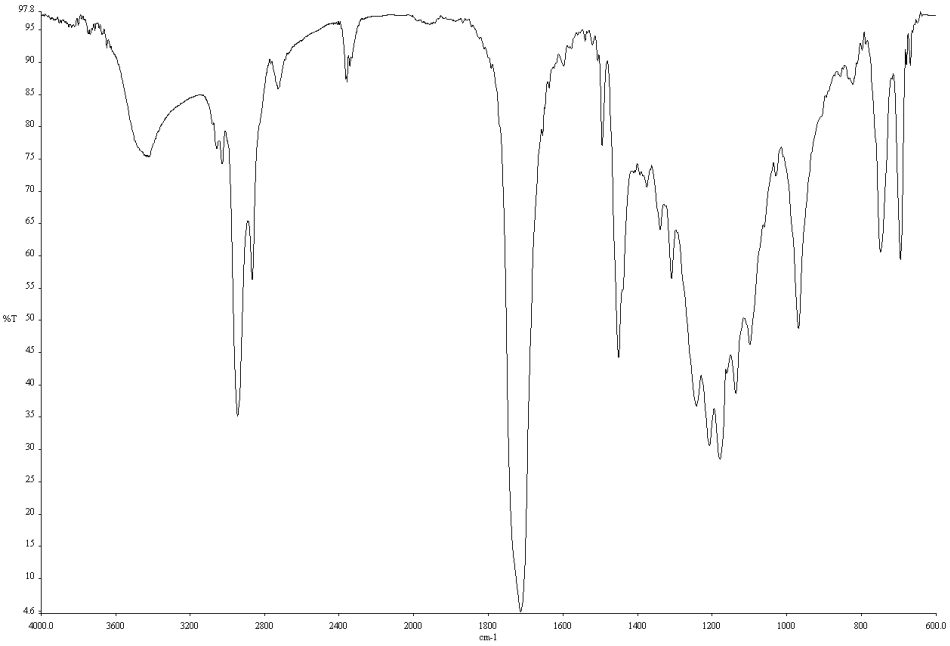

Figure A2.143. *Infrared spectrum (Thin Film, NaCl) of compound* ***217i.***

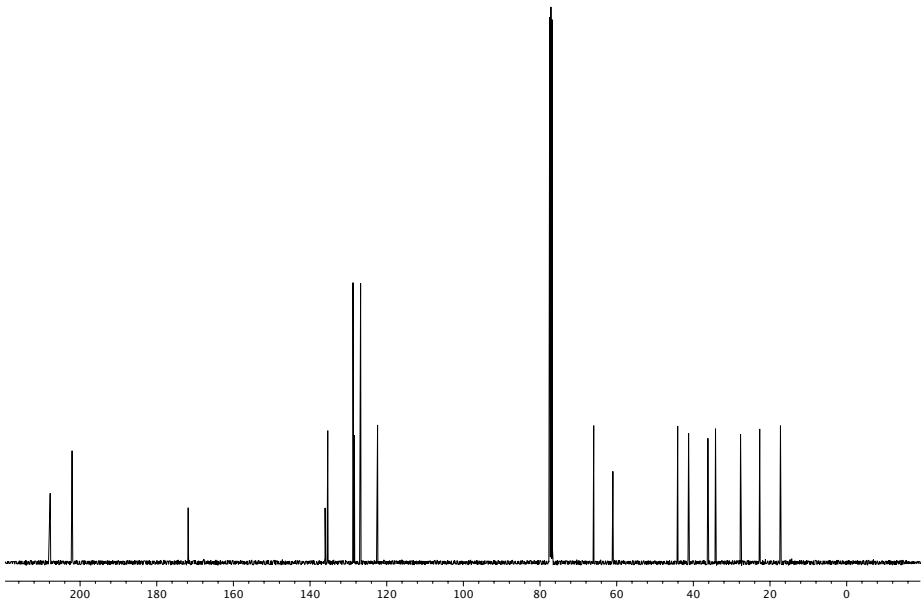

Figure A2.144. *^{13}C NMR (100 MHz, $CDCl_3$) of compound* ***217i.***

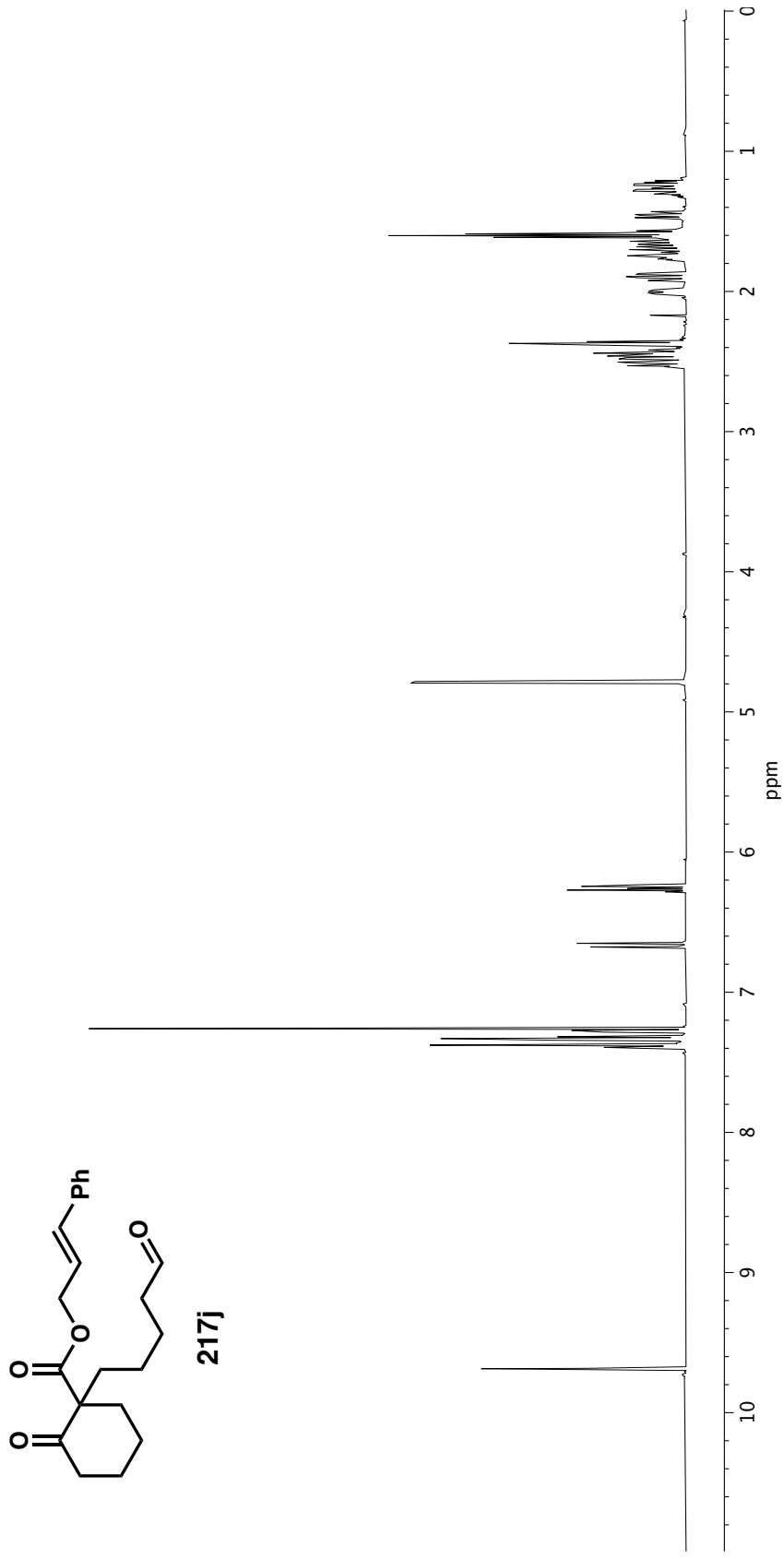

Figure A2.145. *^1H NMR (600 MHz, $CDCl_3$) of compound* ***217j.***

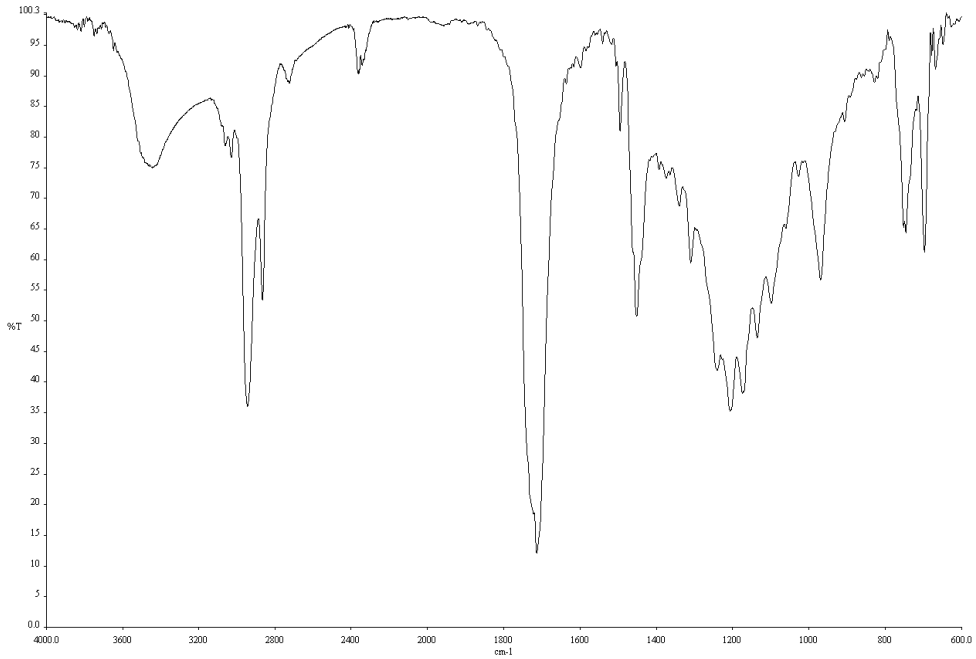

Figure A2.146. *Infrared spectrum (Thin Film, NaCl) of compound* ***217j.***

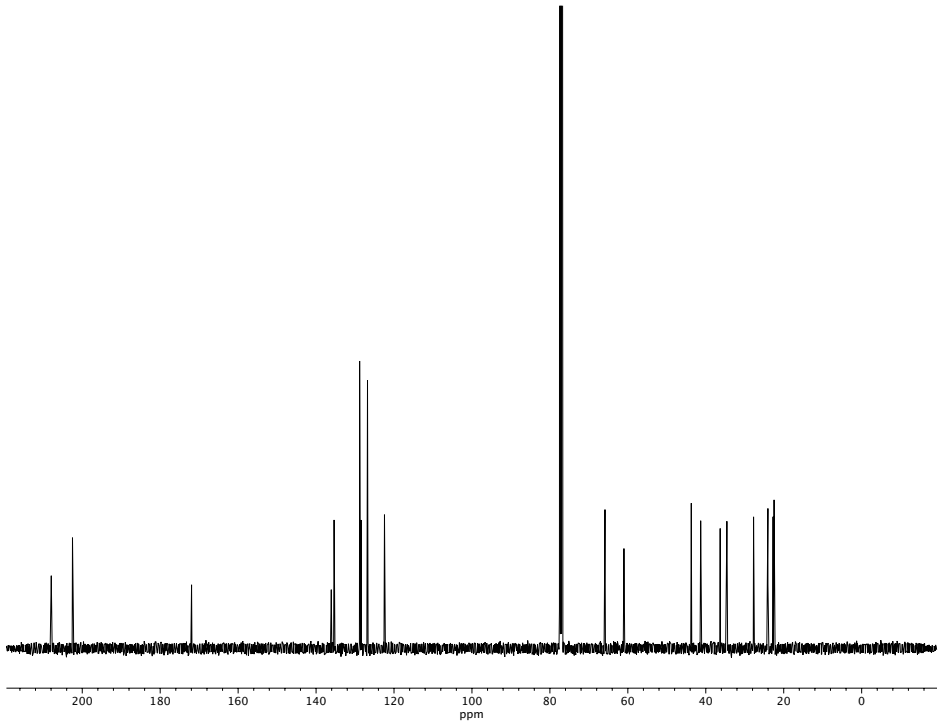

Figure A2.147. *^{13}C NMR (100 MHz, $CDCl_3$) of compound* ***217j.***

Figure A2.148. *^1H NMR (400 MHz, $CDCl_3$) of compound* ***202.***

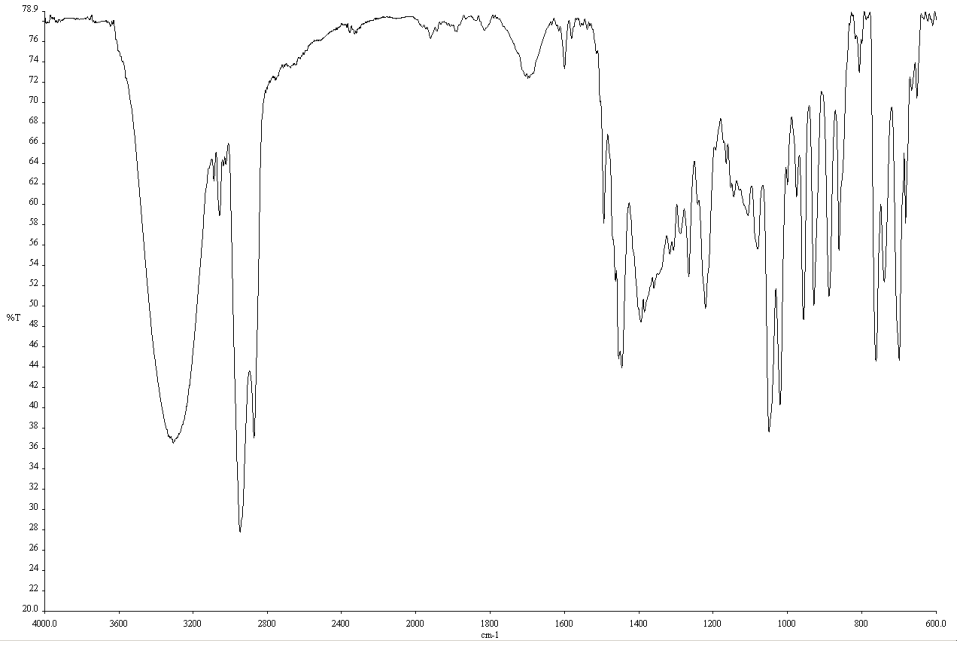

Figure A2.149. *Infrared spectrum (Thin Film, NaCl) of compound* ***202.***

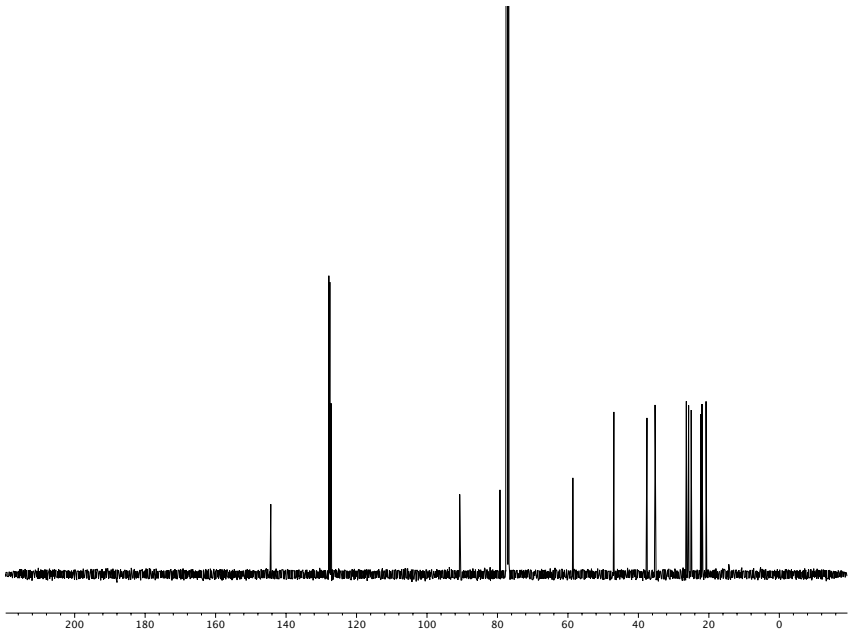

Figure A2.150. *^{13}C NMR (100 MHz, $CDCl_3$) of compound* ***202.***

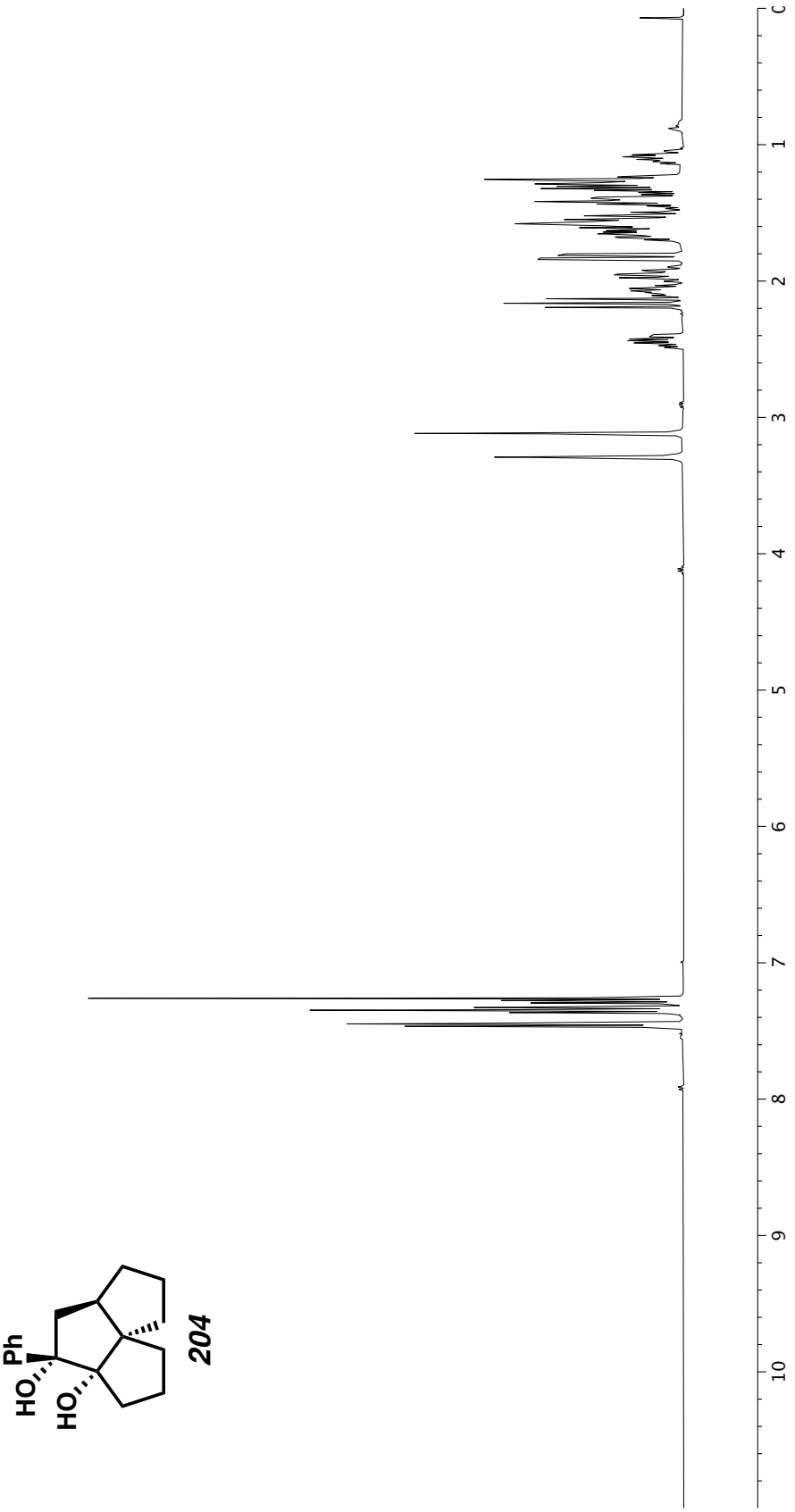

Figure A2.151. *^{1}H NMR (400 MHz, $CDCl_3$) of compound* ***204.***

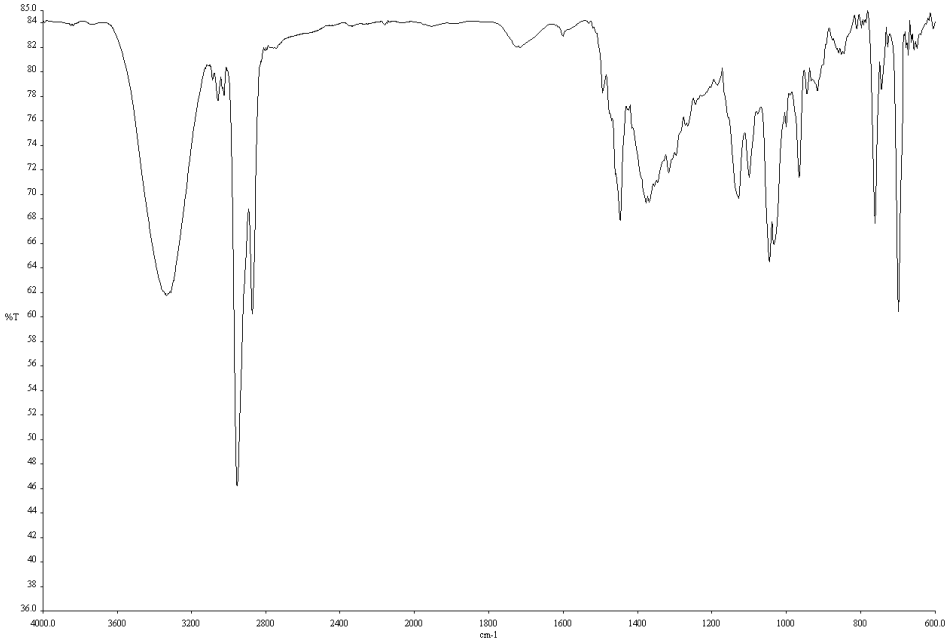

Figure A2.152. *Infrared spectrum (Thin Film, NaCl) of compound* ***204.***

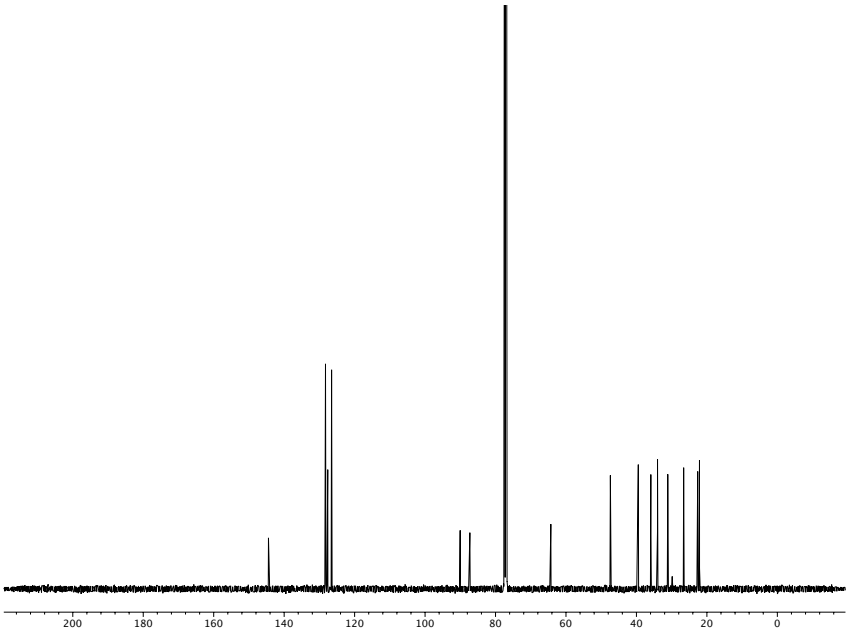

Figure A2.153. *^{13}C NMR (100 MHz, $CDCl_3$) of compound* ***204.***

Figure A2.154. *^{1}H NMR (400 MHz, $CDCl_3$) of compound* ***205.***

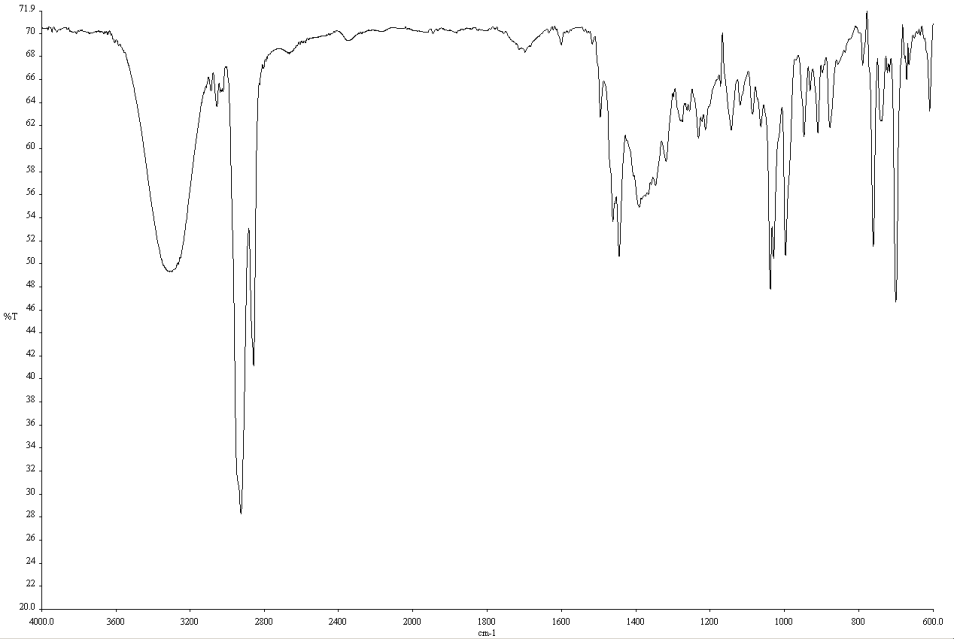

Figure A2.155. *Infrared spectrum (Thin Film, NaCl) of compound* ***205.***

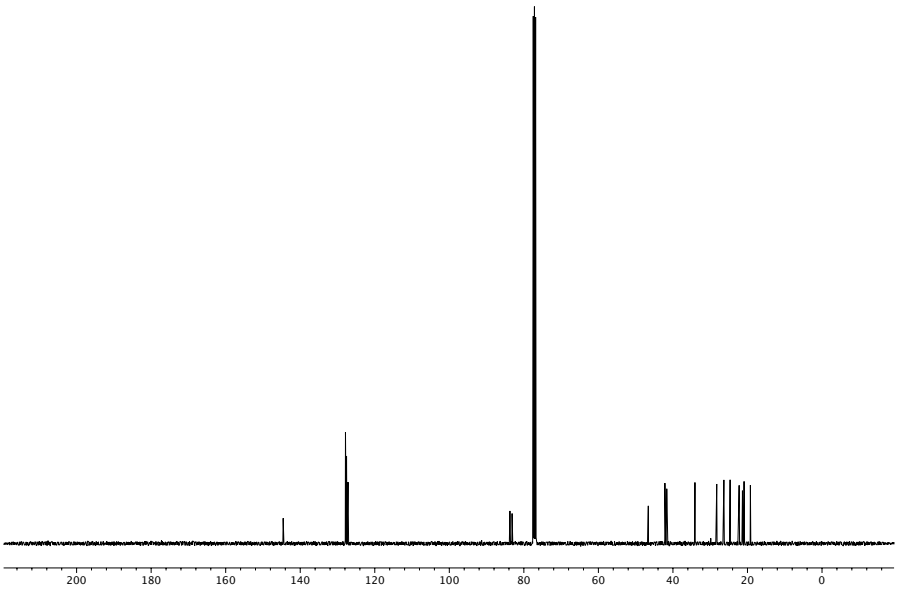

Figure A2.156. *^{13}C NMR (100 MHz, $CDCl_3$) of compound* ***205.***

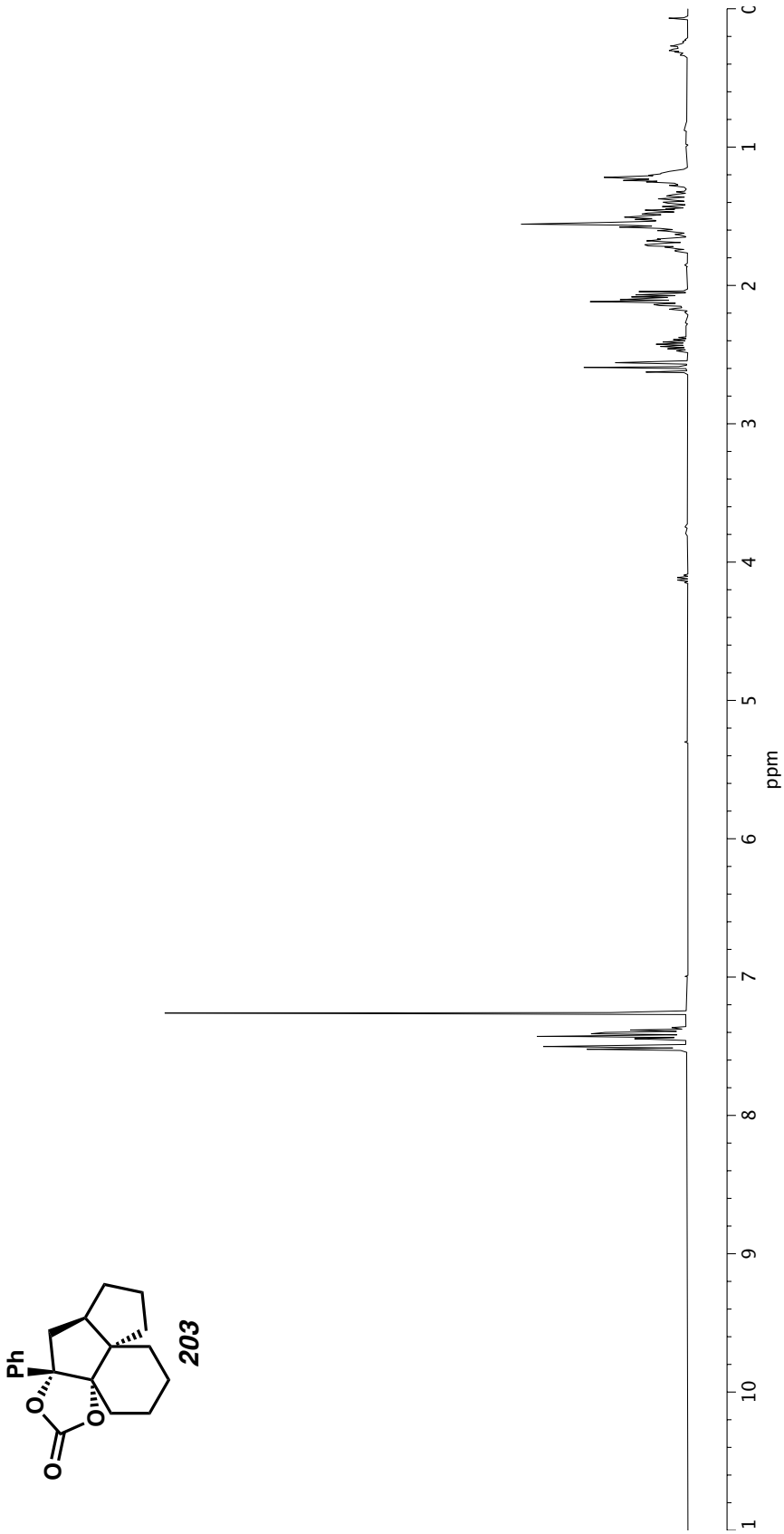

Figure A2.157. *^1H NMR (400 MHz, $CDCl_3$) of compound* ***203.***

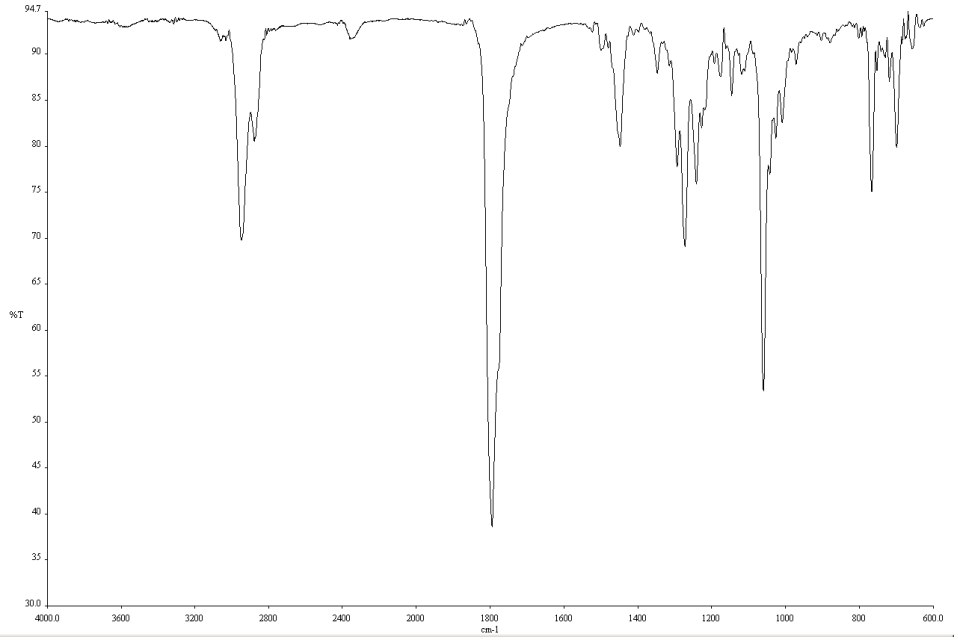

Figure A2.158. *Infrared spectrum (Thin Film, NaCl) of compound* ***203.***

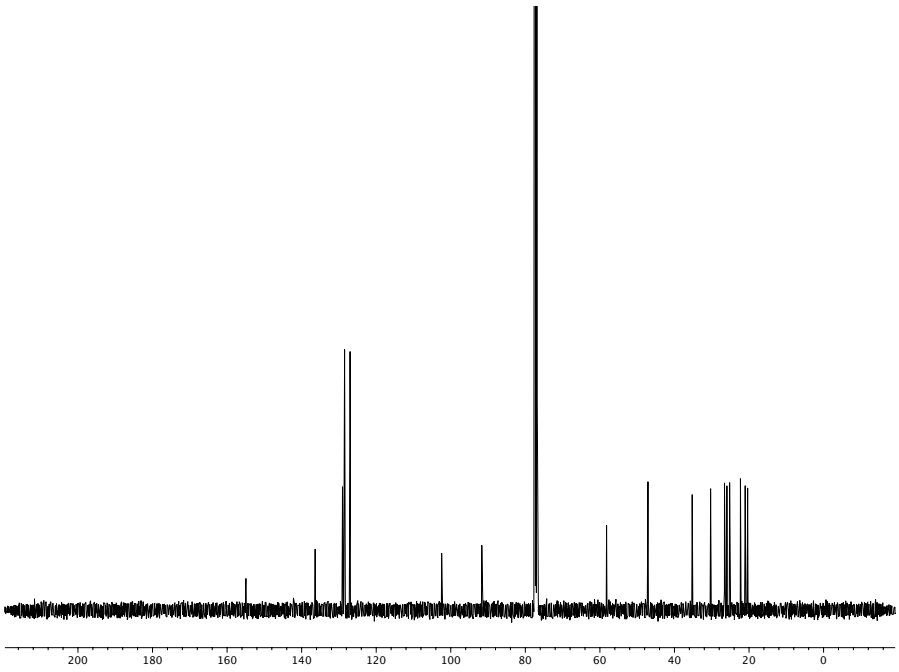

Figure A2.159. *^{13}C NMR (100 MHz, $CDCl_3$) of compound* ***203.***

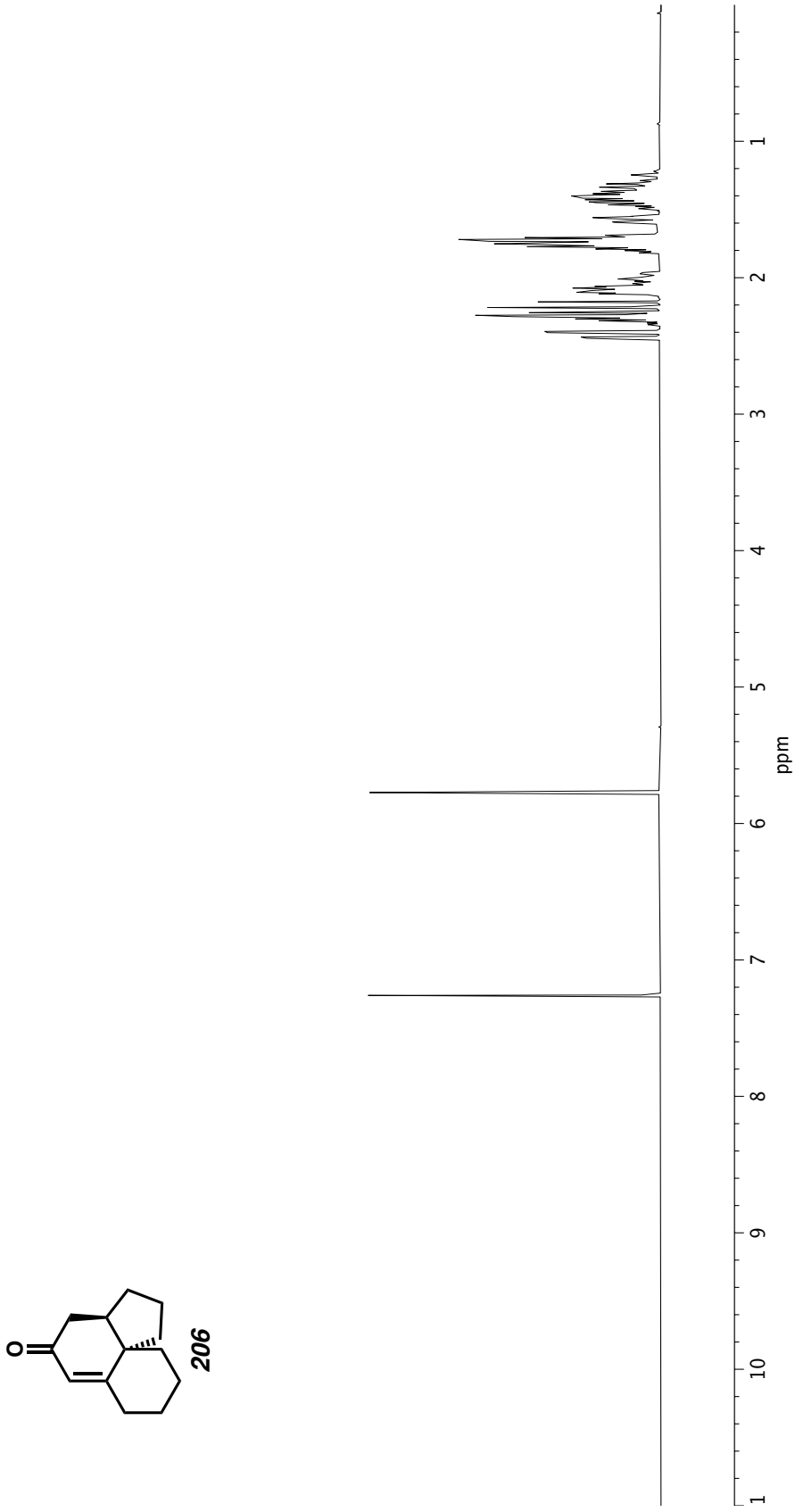

Figure A2.160. *^1H NMR (400 MHz, $CDCl_3$) of compound* ***206.***

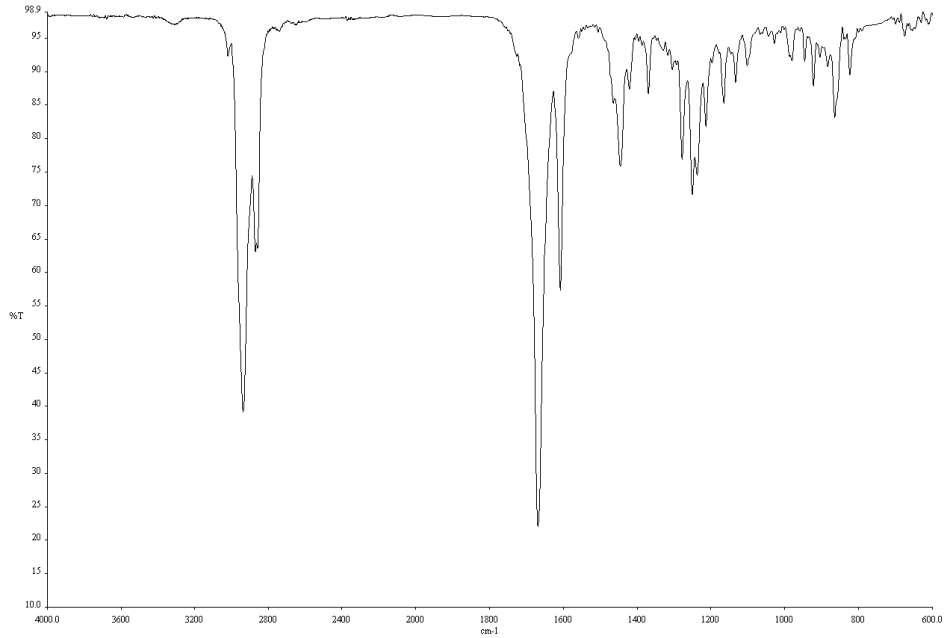

Figure A2.161. *Infrared spectrum (Thin Film, NaCl) of compound* ***206.***

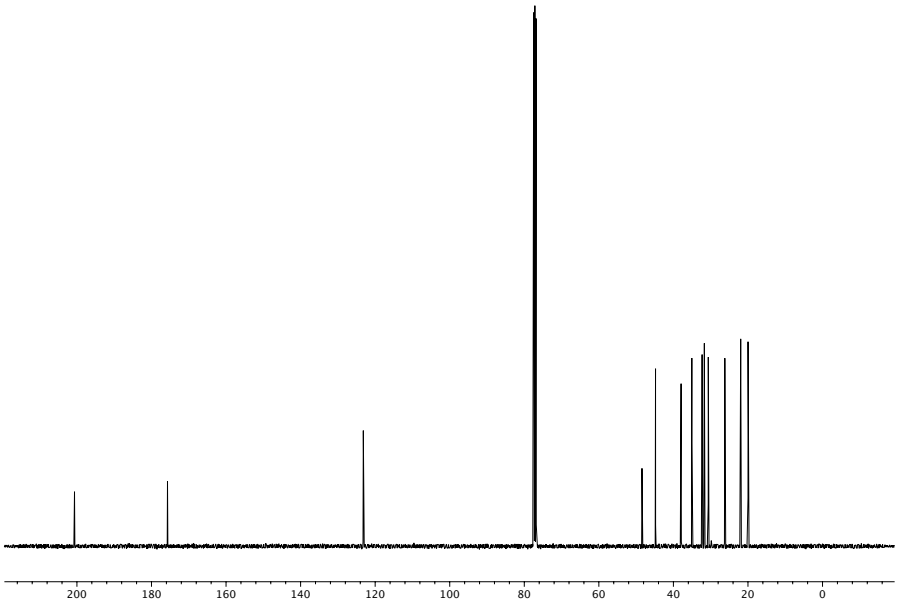

Figure A2.162. *^{13}C NMR (100 MHz, $CDCl_3$) of compound* ***206.***

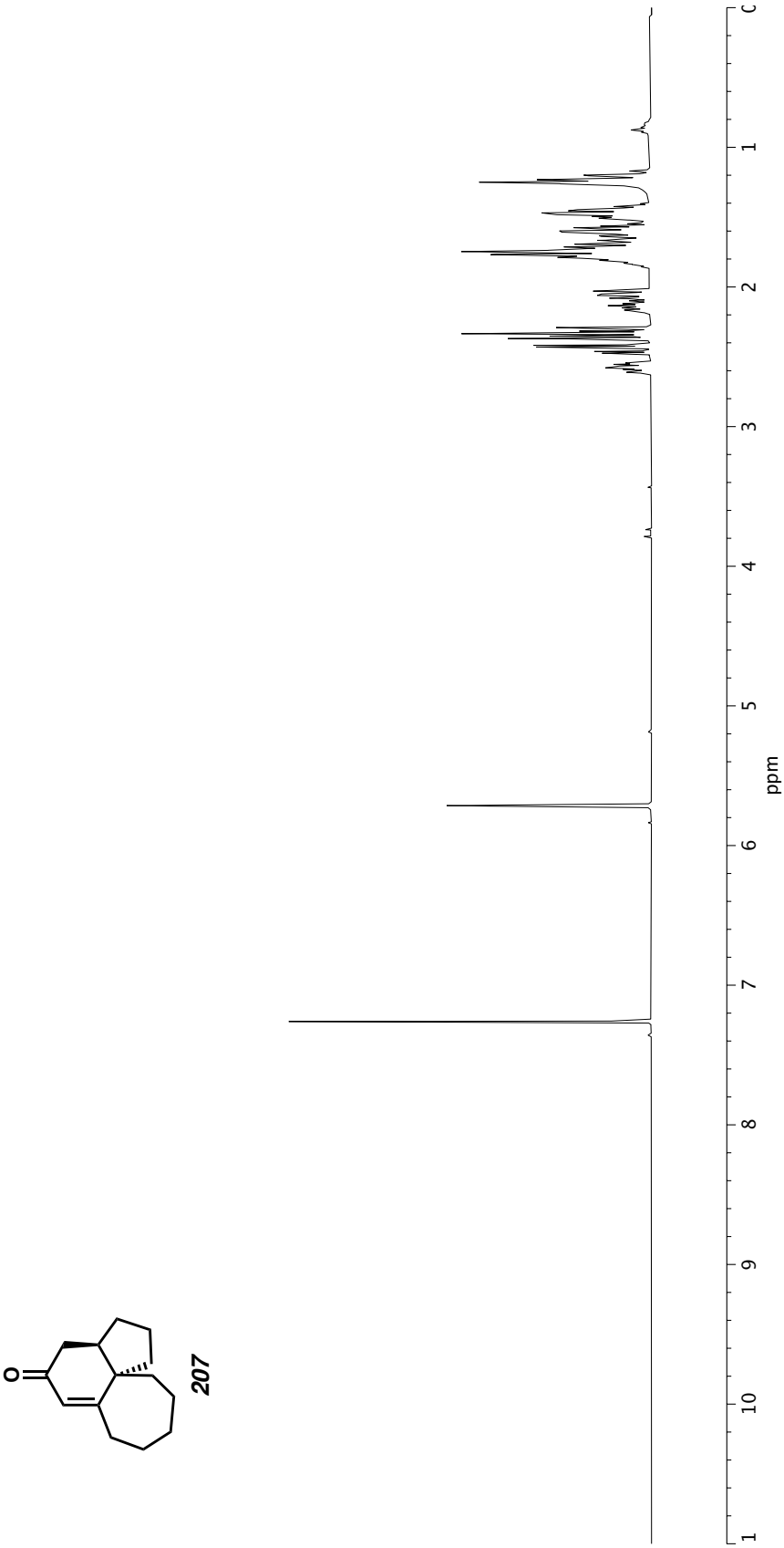

Figure A2.163. *^1H NMR (400 MHz, $CDCl_3$) of compound* ***207.***

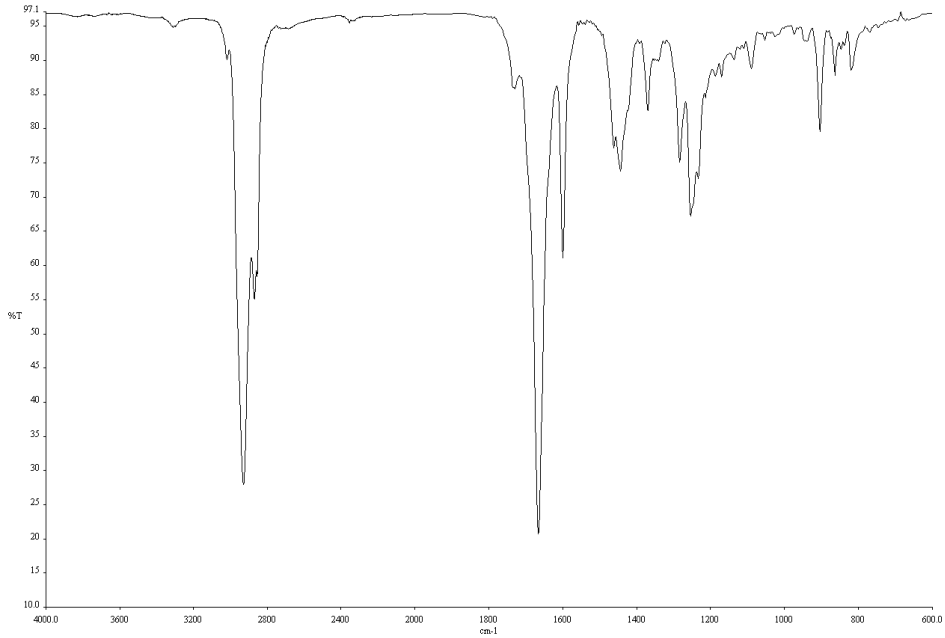

Figure A2.164. *Infrared spectrum (Thin Film, NaCl) of compound* ***207.***

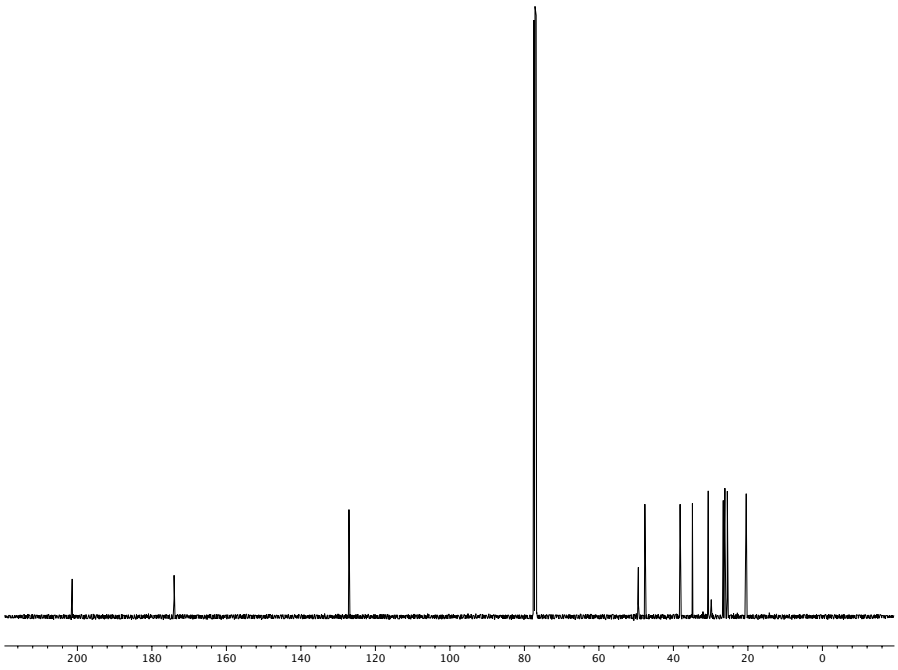

Figure A2.165. *^{13}C NMR (100 MHz, $CDCl_3$) of compound* ***207.***

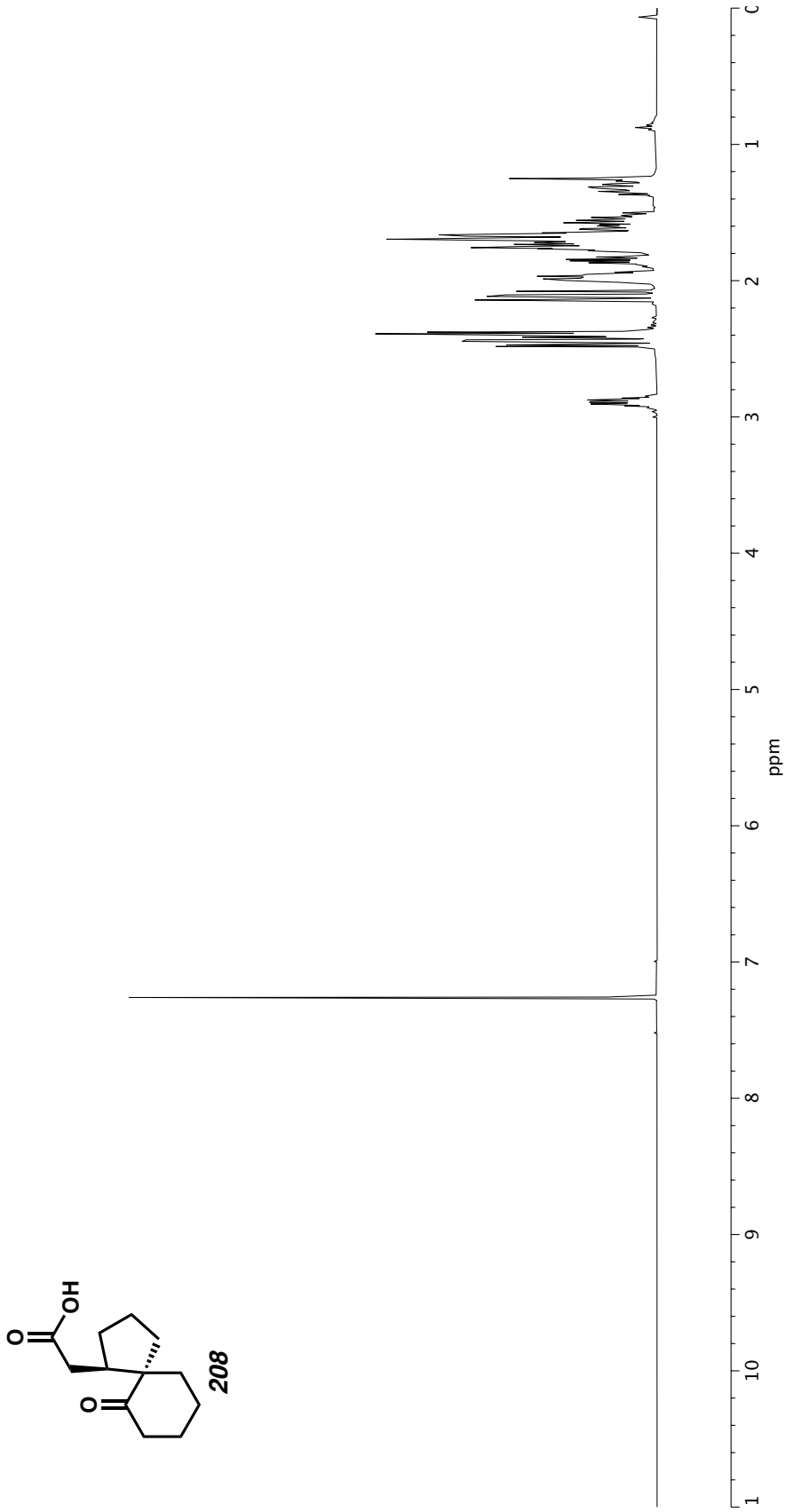

Figure A2.166. *^{1}H NMR (400 MHz, $CDCl_3$) of compound* ***208.***

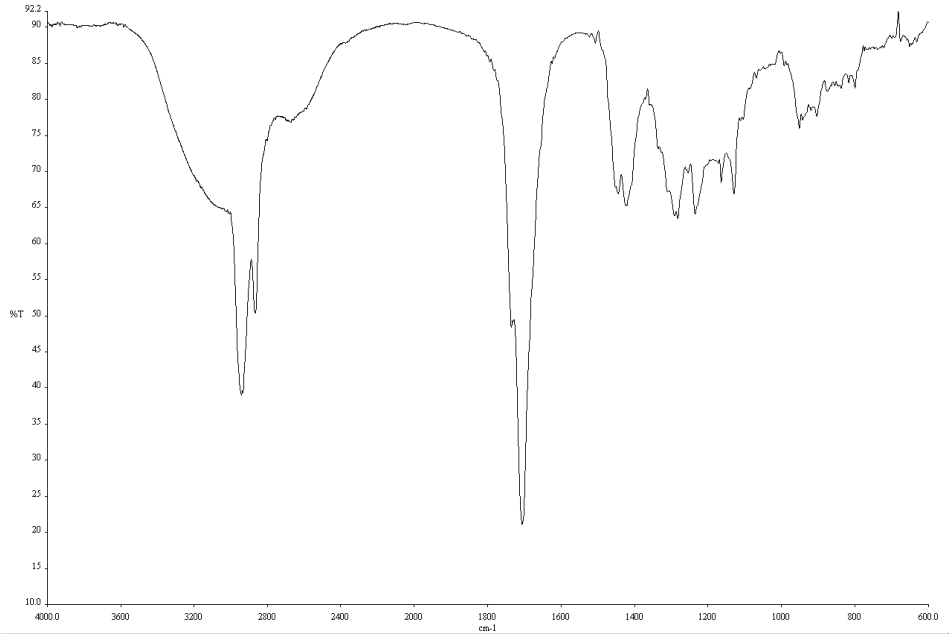

Figure A2.167. *Infrared spectrum (Thin Film, NaCl) of compound* ***208.***

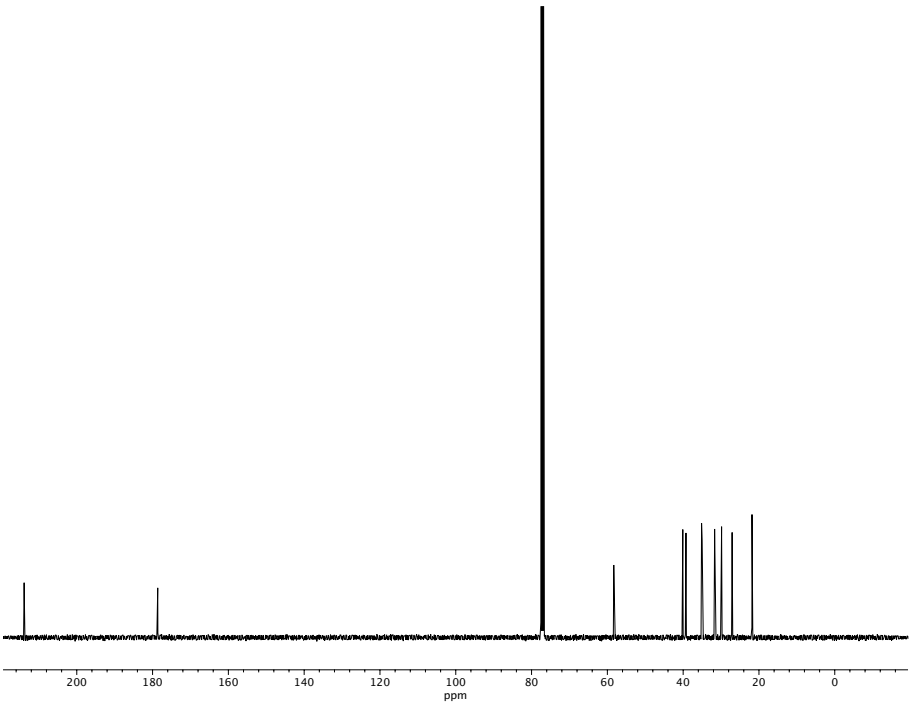

Figure A2.168. *^{13}C NMR (100 MHz, $CDCl_3$) of compound* ***208.***

APPENDIX 3

X-Ray Crystallography Reports Relevant to Chapter 3:

Asymmetric Michael Spirocyclization of Pd Enolates

A3.1 GENERAL EXPERIMENTAL

X-Ray crystallographic analysis was obtained from the Caltech X-Ray Crystallography Facility using a Bruker AXS D8 VENTURE KAPPA diffractometer.

A3.2 CRYSTAL STRUCTURE ANALYSIS OF PRODUCT 197A (V25038)

Spirocycle **197a** was crystalized by layering pentane onto a saturated solution of **197a** in Et_2O at 23 °C to provide crystalline needles suitable for X-ray analysis.

Compound V25038 (CCDC 2421482) crystallizes in the monoclinic space group $P2_1$ with two molecules in the asymmetric unit. Absolute configuration was assigned via Flack (Flack = 0.0(2)) and Parsons (Parsons = –0.14(9)) parameters. Bayesian Statistics further confirmed the absolute stereochemistry: P2(true) = 1.000, P3(true) = 1.000, P3(rac-twin) = 0.7×10^{-5}, and P3(false) = 0.7×10^{-17}.

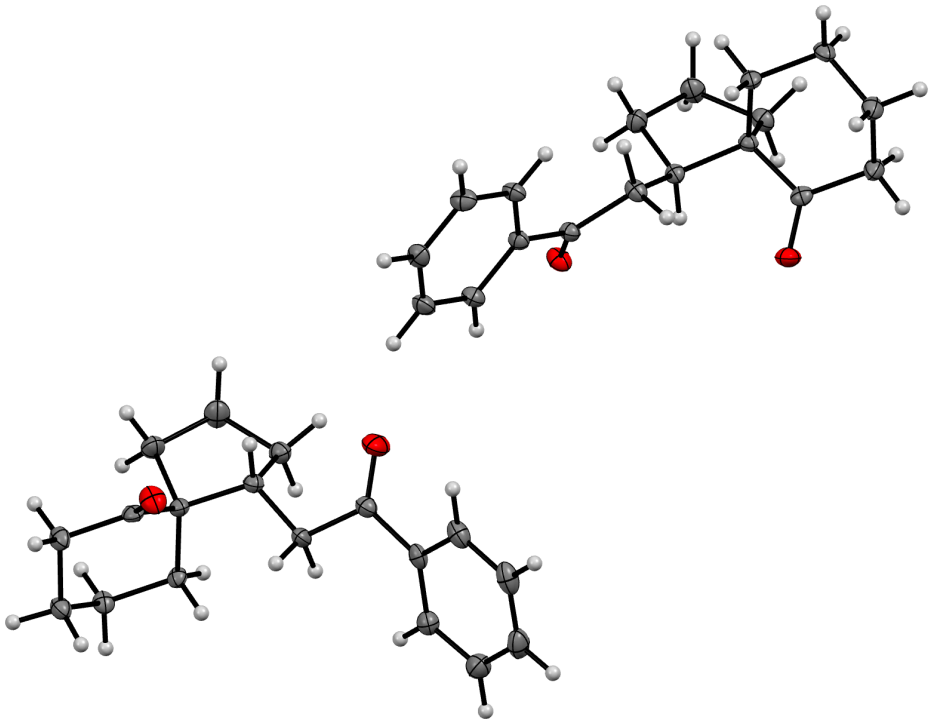

Figure A3.2.1 *X-Ray Coordinates of Compound* ***197a*** *(V25038)*

Table A3.2.1 *Crystal data and structure refinement for V25038.*

Identification code	V25038	
Empirical formula	C18 H22 O2	
Formula weight	270.35	
Temperature	100(2) K	
Wavelength	1.54178 Å	
Crystal system	Monoclinic	
Space group	$P2_1$	
Unit cell dimensions	a = 5.9068(7) Å	a= 90°.
	b = 15.569(2) Å	b= 95.830(9)°.
	c = 15.9353(19) Å	g = 90°.
Volume	1457.9(3) $Å^3$	
Z	4	
Density (calculated)	1.232 Mg/m^3	
Absorption coefficient	0.615 mm^{-1}	
F(000)	584	
Crystal size	0.200 x 0.050 x 0.050 mm^3	
Theta range for data collection	2.787 to 74.590°.	
Index ranges	-7<=h<=7, -19<=k<=19, -19<=l<=19	
Reflections collected	37754	
Independent reflections	5928 [R(int) = 0.0777]	
Completeness to theta = 67.679°	100.0 %	
Absorption correction	Semi-empirical from equivalents	
Max. and min. transmission	0.7538 and 0.5453	
Refinement method	Full-matrix least-squares on F^2	
Data / restraints / parameters	5928 / 1 / 361	
Goodness-of-fit on F^2	1.019	
Final R indices [I>2sigma(I)]	R1 = 0.0470, wR2 = 0.1204	
R indices (all data)	R1 = 0.0502, wR2 = 0.1243	
Absolute structure parameter (Flack)	0.0(2)	
Absolute structure parameter (Parsons)	–0.14(9)	
Extinction coefficient	n/a	
Largest diff. peak and hole	0.184 and -0.225 $e.Å^{-3}$	

Table A3.2.2 *Atomic coordinates (x 10^4) and equivalent isotropic displacement parameters ($Å^2$x 10^3) for V25038. U(eq) is defined as one third of the trace of the orthogonalized U^{ij} tensor.*

	x	y	z	U(eq)
O(1)	8508(3)	8282(1)	9038(1)	24(1)
C(1)	7524(4)	8967(2)	8976(2)	16(1)
C(2)	8233(4)	9702(2)	9567(2)	21(1)
C(3)	6181(5)	10074(2)	9961(2)	23(1)
C(4)	4326(4)	10332(2)	9272(2)	20(1)
C(5)	3576(4)	9563(2)	8713(2)	18(1)
C(6)	5562(4)	9140(2)	8302(2)	15(1)
C(7)	6385(5)	9725(2)	7607(2)	20(1)
C(8)	4659(5)	9567(2)	6824(2)	25(1)
C(9)	3538(5)	8694(2)	6969(2)	21(1)
C(10)	4843(4)	8330(2)	7778(2)	15(1)
C(11)	3515(5)	7648(2)	8206(2)	18(1)
C(12)	3238(4)	6817(2)	7696(2)	16(1)
O(2)	4370(3)	6680(1)	7115(1)	22(1)
C(13)	1592(4)	6152(2)	7944(2)	16(1)
C(14)	1914(5)	5294(2)	7715(2)	19(1)
C(15)	380(5)	4668(2)	7906(2)	22(1)
C(16)	-1508(5)	4893(2)	8317(2)	21(1)
C(17)	-1828(5)	5738(2)	8548(2)	21(1)
C(18)	-286(4)	6368(2)	8372(2)	18(1)
O(3)	-381(3)	980(1)	5999(1)	26(1)
C(21)	291(4)	912(2)	5305(2)	18(1)
C(22)	-483(4)	180(2)	4719(2)	21(1)
C(23)	1581(5)	-318(2)	4456(2)	21(1)
C(24)	3222(5)	291(2)	4076(2)	19(1)
C(25)	3977(4)	1017(2)	4690(2)	16(1)

C(26)	1961(4)	1540(2)	4976(2)	16(1)
C(27)	743(5)	2066(2)	4224(2)	25(1)
C(28)	1758(6)	2967(2)	4286(2)	28(1)
C(29)	3510(4)	2978(2)	5068(2)	20(1)
C(30)	2717(4)	2256(2)	5618(2)	17(1)
C(31)	4459(5)	2003(2)	6348(2)	20(1)
C(32)	4685(5)	2658(2)	7058(2)	18(1)
O(4)	3478(4)	3285(1)	7058(1)	31(1)
C(33)	6420(5)	2481(2)	7794(2)	19(1)
C(34)	6013(5)	2791(2)	8591(2)	24(1)
C(35)	7596(6)	2652(2)	9280(2)	29(1)
C(36)	9609(6)	2225(2)	9190(2)	29(1)
C(37)	10029(5)	1915(2)	8401(2)	27(1)
C(38)	8432(5)	2035(2)	7707(2)	21(1)

Table A3.2.3 *Bond lengths [Å] and angles [°] for V25038.*

O(1)-C(1)	1.215(3)
C(1)-C(2)	1.513(4)
C(1)-C(6)	1.522(3)
C(2)-C(3)	1.534(4)
C(2)-H(2A)	0.9900
C(2)-H(2B)	0.9900
C(3)-C(4)	1.524(4)
C(3)-H(3A)	0.9900
C(3)-H(3B)	0.9900
C(4)-C(5)	1.531(4)
C(4)-H(4A)	0.9900
C(4)-H(4B)	0.9900
C(5)-C(6)	1.548(3)
C(5)-H(5A)	0.9900

C(5)-H(5B)	0.9900
C(6)-C(10)	1.548(3)
C(6)-C(7)	1.550(4)
C(7)-C(8)	1.548(4)
C(7)-H(7A)	0.9900
C(7)-H(7B)	0.9900
C(8)-C(9)	1.539(4)
C(8)-H(8A)	0.9900
C(8)-H(8B)	0.9900
C(9)-C(10)	1.541(4)
C(9)-H(9A)	0.9900
C(9)-H(9B)	0.9900
C(10)-C(11)	1.522(3)
C(10)-H(10)	1.0000
C(11)-C(12)	1.527(3)
C(11)-H(11A)	0.9900
C(11)-H(11B)	0.9900
C(12)-O(2)	1.215(3)
C(12)-C(13)	1.500(3)
C(13)-C(18)	1.401(4)
C(13)-C(14)	1.403(4)
C(14)-C(15)	1.386(4)
C(14)-H(14)	0.9500
C(15)-C(16)	1.394(4)
C(15)-H(15)	0.9500
C(16)-C(17)	1.385(4)
C(16)-H(16)	0.9500
C(17)-C(18)	1.385(4)
C(17)-H(17)	0.9500
C(18)-H(18)	0.9500
O(3)-C(21)	1.216(3)
C(21)-C(22)	1.515(4)
C(21)-C(26)	1.519(4)
C(22)-C(23)	1.539(4)

C(22)-H(22A)	0.9900
C(22)-H(22B)	0.9900
C(23)-C(24)	1.526(4)
C(23)-H(23A)	0.9900
C(23)-H(23B)	0.9900
C(24)-C(25)	1.532(4)
C(24)-H(24A)	0.9900
C(24)-H(24B)	0.9900
C(25)-C(26)	1.549(3)
C(25)-H(25A)	0.9900
C(25)-H(25B)	0.9900
C(26)-C(30)	1.548(4)
C(26)-C(27)	1.565(4)
C(27)-C(28)	1.526(4)
C(27)-H(27A)	0.9900
C(27)-H(27B)	0.9900
C(28)-C(29)	1.537(4)
C(28)-H(28A)	0.9900
C(28)-H(28B)	0.9900
C(29)-C(30)	1.528(4)
C(29)-H(29A)	0.9900
C(29)-H(29B)	0.9900
C(30)-C(31)	1.525(4)
C(30)-H(30)	1.0000
C(31)-C(32)	1.519(4)
C(31)-H(31A)	0.9900
C(31)-H(31B)	0.9900
C(32)-O(4)	1.209(4)
C(32)-C(33)	1.503(4)
C(33)-C(38)	1.395(4)
C(33)-C(34)	1.403(4)
C(34)-C(35)	1.385(5)
C(34)-H(34)	0.9500
C(35)-C(36)	1.383(5)

C(35)-H(35)	0.9500
C(36)-C(37)	1.392(4)
C(36)-H(36)	0.9500
C(37)-C(38)	1.391(4)
C(37)-H(37)	0.9500
C(38)-H(38)	0.9500

O(1)-C(1)-C(2)	120.9(2)
O(1)-C(1)-C(6)	122.4(2)
C(2)-C(1)-C(6)	116.7(2)
C(1)-C(2)-C(3)	111.1(2)
C(1)-C(2)-H(2A)	109.4
C(3)-C(2)-H(2A)	109.4
C(1)-C(2)-H(2B)	109.4
C(3)-C(2)-H(2B)	109.4
H(2A)-C(2)-H(2B)	108.0
C(4)-C(3)-C(2)	110.1(2)
C(4)-C(3)-H(3A)	109.6
C(2)-C(3)-H(3A)	109.6
C(4)-C(3)-H(3B)	109.6
C(2)-C(3)-H(3B)	109.6
H(3A)-C(3)-H(3B)	108.1
C(3)-C(4)-C(5)	111.0(2)
C(3)-C(4)-H(4A)	109.4
C(5)-C(4)-H(4A)	109.4
C(3)-C(4)-H(4B)	109.4
C(5)-C(4)-H(4B)	109.4
H(4A)-C(4)-H(4B)	108.0
C(4)-C(5)-C(6)	113.1(2)
C(4)-C(5)-H(5A)	109.0
C(6)-C(5)-H(5A)	109.0
C(4)-C(5)-H(5B)	109.0
C(6)-C(5)-H(5B)	109.0
H(5A)-C(5)-H(5B)	107.8

C(1)-C(6)-C(5)	109.4(2)
C(1)-C(6)-C(10)	112.6(2)
C(5)-C(6)-C(10)	113.4(2)
C(1)-C(6)-C(7)	109.7(2)
C(5)-C(6)-C(7)	111.0(2)
C(10)-C(6)-C(7)	100.50(19)
C(8)-C(7)-C(6)	104.7(2)
C(8)-C(7)-H(7A)	110.8
C(6)-C(7)-H(7A)	110.8
C(8)-C(7)-H(7B)	110.8
C(6)-C(7)-H(7B)	110.8
H(7A)-C(7)-H(7B)	108.9
C(9)-C(8)-C(7)	106.1(2)
C(9)-C(8)-H(8A)	110.5
C(7)-C(8)-H(8A)	110.5
C(9)-C(8)-H(8B)	110.5
C(7)-C(8)-H(8B)	110.5
H(8A)-C(8)-H(8B)	108.7
C(8)-C(9)-C(10)	105.4(2)
C(8)-C(9)-H(9A)	110.7
C(10)-C(9)-H(9A)	110.7
C(8)-C(9)-H(9B)	110.7
C(10)-C(9)-H(9B)	110.7
H(9A)-C(9)-H(9B)	108.8
C(11)-C(10)-C(9)	113.3(2)
C(11)-C(10)-C(6)	116.9(2)
C(9)-C(10)-C(6)	103.7(2)
C(11)-C(10)-H(10)	107.5
C(9)-C(10)-H(10)	107.5
C(6)-C(10)-H(10)	107.5
C(10)-C(11)-C(12)	112.6(2)
C(10)-C(11)-H(11A)	109.1
C(12)-C(11)-H(11A)	109.1
C(10)-C(11)-H(11B)	109.1

C(12)-C(11)-H(11B)	109.1
H(11A)-C(11)-H(11B)	107.8
O(2)-C(12)-C(13)	120.1(2)
O(2)-C(12)-C(11)	121.1(2)
C(13)-C(12)-C(11)	118.8(2)
C(18)-C(13)-C(14)	119.3(2)
C(18)-C(13)-C(12)	122.0(2)
C(14)-C(13)-C(12)	118.7(2)
C(15)-C(14)-C(13)	120.3(2)
C(15)-C(14)-H(14)	119.9
C(13)-C(14)-H(14)	119.9
C(14)-C(15)-C(16)	119.9(2)
C(14)-C(15)-H(15)	120.1
C(16)-C(15)-H(15)	120.1
C(17)-C(16)-C(15)	120.0(2)
C(17)-C(16)-H(16)	120.0
C(15)-C(16)-H(16)	120.0
C(16)-C(17)-C(18)	120.6(2)
C(16)-C(17)-H(17)	119.7
C(18)-C(17)-H(17)	119.7
C(17)-C(18)-C(13)	119.8(2)
C(17)-C(18)-H(18)	120.1
C(13)-C(18)-H(18)	120.1
O(3)-C(21)-C(22)	121.3(2)
O(3)-C(21)-C(26)	122.8(2)
C(22)-C(21)-C(26)	115.9(2)
C(21)-C(22)-C(23)	110.4(2)
C(21)-C(22)-H(22A)	109.6
C(23)-C(22)-H(22A)	109.6
C(21)-C(22)-H(22B)	109.6
C(23)-C(22)-H(22B)	109.6
H(22A)-C(22)-H(22B)	108.1
C(24)-C(23)-C(22)	110.4(2)
C(24)-C(23)-H(23A)	109.6

C(22)-C(23)-H(23A)	109.6
C(24)-C(23)-H(23B)	109.6
C(22)-C(23)-H(23B)	109.6
H(23A)-C(23)-H(23B)	108.1
C(23)-C(24)-C(25)	111.1(2)
C(23)-C(24)-H(24A)	109.4
C(25)-C(24)-H(24A)	109.4
C(23)-C(24)-H(24B)	109.4
C(25)-C(24)-H(24B)	109.4
H(24A)-C(24)-H(24B)	108.0
C(24)-C(25)-C(26)	113.2(2)
C(24)-C(25)-H(25A)	108.9
C(26)-C(25)-H(25A)	108.9
C(24)-C(25)-H(25B)	108.9
C(26)-C(25)-H(25B)	108.9
H(25A)-C(25)-H(25B)	107.8
C(21)-C(26)-C(30)	112.9(2)
C(21)-C(26)-C(25)	108.0(2)
C(30)-C(26)-C(25)	113.2(2)
C(21)-C(26)-C(27)	109.7(2)
C(30)-C(26)-C(27)	102.0(2)
C(25)-C(26)-C(27)	110.9(2)
C(28)-C(27)-C(26)	106.6(2)
C(28)-C(27)-H(27A)	110.4
C(26)-C(27)-H(27A)	110.4
C(28)-C(27)-H(27B)	110.4
C(26)-C(27)-H(27B)	110.4
H(27A)-C(27)-H(27B)	108.6
C(27)-C(28)-C(29)	106.8(2)
C(27)-C(28)-H(28A)	110.4
C(29)-C(28)-H(28A)	110.4
C(27)-C(28)-H(28B)	110.4
C(29)-C(28)-H(28B)	110.4
H(28A)-C(28)-H(28B)	108.6

C(30)-C(29)-C(28)	103.7(2)
C(30)-C(29)-H(29A)	111.0
C(28)-C(29)-H(29A)	111.0
C(30)-C(29)-H(29B)	111.0
C(28)-C(29)-H(29B)	111.0
H(29A)-C(29)-H(29B)	109.0
C(31)-C(30)-C(29)	113.9(2)
C(31)-C(30)-C(26)	116.4(2)
C(29)-C(30)-C(26)	103.6(2)
C(31)-C(30)-H(30)	107.5
C(29)-C(30)-H(30)	107.5
C(26)-C(30)-H(30)	107.5
C(32)-C(31)-C(30)	113.3(2)
C(32)-C(31)-H(31A)	108.9
C(30)-C(31)-H(31A)	108.9
C(32)-C(31)-H(31B)	108.9
C(30)-C(31)-H(31B)	108.9
H(31A)-C(31)-H(31B)	107.7
O(4)-C(32)-C(33)	120.2(2)
O(4)-C(32)-C(31)	122.4(3)
C(33)-C(32)-C(31)	117.3(2)
C(38)-C(33)-C(34)	119.2(3)
C(38)-C(33)-C(32)	122.3(2)
C(34)-C(33)-C(32)	118.5(3)
C(35)-C(34)-C(33)	120.0(3)
C(35)-C(34)-H(34)	120.0
C(33)-C(34)-H(34)	120.0
C(36)-C(35)-C(34)	120.8(3)
C(36)-C(35)-H(35)	119.6
C(34)-C(35)-H(35)	119.6
C(35)-C(36)-C(37)	119.7(3)
C(35)-C(36)-H(36)	120.2
C(37)-C(36)-H(36)	120.2
C(38)-C(37)-C(36)	120.2(3)

C(38)-C(37)-H(37)	119.9
C(36)-C(37)-H(37)	119.9
C(37)-C(38)-C(33)	120.2(3)
C(37)-C(38)-H(38)	119.9
C(33)-C(38)-H(38)	119.9

Symmetry transformations used to generate equivalent atoms:

Table A3.2.4 *Anisotropic displacement parameters ($Å^2$x 10^3) for V25038. The anisotropic displacement factor exponent takes the form: $-2p^2[h^2 a^{*2}U^{11} + ... + 2 h k a^* b^* U^{12}]$*

	U^{11}	U^{22}	U^{33}	U^{23}	U^{13}	U^{12}
O(1)	23(1)	22(1)	26(1)	-2(1)	0(1)	9(1)
C(1)	13(1)	20(1)	17(1)	1(1)	5(1)	1(1)
C(2)	16(1)	24(1)	23(1)	-7(1)	0(1)	1(1)
C(3)	18(1)	25(1)	24(1)	-9(1)	3(1)	1(1)
C(4)	16(1)	16(1)	28(1)	-6(1)	6(1)	2(1)
C(5)	13(1)	19(1)	23(1)	-3(1)	3(1)	2(1)
C(6)	13(1)	13(1)	18(1)	-1(1)	4(1)	0(1)
C(7)	22(1)	18(1)	22(1)	2(1)	5(1)	-2(1)
C(8)	33(2)	21(1)	20(1)	3(1)	-1(1)	-1(1)
C(9)	22(1)	21(1)	19(1)	-1(1)	-2(1)	-1(1)
C(10)	14(1)	16(1)	17(1)	-1(1)	4(1)	-1(1)
C(11)	19(1)	16(1)	21(1)	-2(1)	9(1)	-2(1)
C(12)	16(1)	14(1)	18(1)	0(1)	3(1)	1(1)
O(2)	23(1)	20(1)	23(1)	-4(1)	11(1)	-1(1)
C(13)	17(1)	14(1)	17(1)	1(1)	3(1)	0(1)
C(14)	21(1)	17(1)	20(1)	-1(1)	4(1)	2(1)

C(15)	25(1)	14(1)	25(1)	0(1)	2(1)	2(1)
C(16)	22(1)	17(1)	25(1)	5(1)	2(1)	-4(1)
C(17)	19(1)	22(1)	24(1)	4(1)	8(1)	1(1)
C(18)	20(1)	13(1)	21(1)	1(1)	5(1)	2(1)
O(3)	25(1)	30(1)	27(1)	-5(1)	14(1)	-3(1)
C(21)	11(1)	17(1)	24(1)	-1(1)	4(1)	3(1)
C(22)	16(1)	20(1)	28(1)	-4(1)	6(1)	-4(1)
C(23)	20(1)	18(1)	26(1)	-5(1)	5(1)	-1(1)
C(24)	17(1)	21(1)	20(1)	-4(1)	6(1)	-1(1)
C(25)	12(1)	18(1)	18(1)	-2(1)	3(1)	-1(1)
C(26)	13(1)	15(1)	20(1)	0(1)	1(1)	2(1)
C(27)	24(1)	21(1)	29(2)	4(1)	-6(1)	1(1)
C(28)	34(2)	25(2)	25(1)	7(1)	-3(1)	-4(1)
C(29)	18(1)	17(1)	26(1)	1(1)	2(1)	-1(1)
C(30)	15(1)	15(1)	20(1)	-1(1)	2(1)	1(1)
C(31)	22(1)	15(1)	21(1)	-4(1)	-3(1)	4(1)
C(32)	19(1)	16(1)	21(1)	-1(1)	4(1)	1(1)
O(4)	33(1)	28(1)	31(1)	-10(1)	0(1)	12(1)
C(33)	24(1)	15(1)	19(1)	-2(1)	3(1)	-6(1)
C(34)	29(1)	19(1)	23(1)	-5(1)	9(1)	-5(1)
C(35)	40(2)	25(2)	20(1)	-4(1)	4(1)	-10(1)
C(36)	36(2)	26(1)	22(1)	-1(1)	-6(1)	-6(1)
C(37)	26(1)	25(1)	29(2)	1(1)	-1(1)	0(1)
C(38)	22(1)	20(1)	21(1)	-1(1)	2(1)	-2(1)

Table A3.2.5 *Hydrogen coordinates (x 10^4) and isotropic displacement parameters ($Å^2$x 10^3) for V25038.*

	x	y	z	U(eq)
H(2A)	8949	10159	9252	25
H(2B)	9374	9495	10020	25
H(3A)	5577	9641	10335	27
H(3B)	6663	10583	10307	27
H(4A)	4905	10792	8921	24
H(4B)	3001	10562	9534	24
H(5A)	2406	9755	8263	22
H(5B)	2868	9129	9058	22
H(7A)	6378	10336	7779	24
H(7B)	7944	9566	7488	24
H(8A)	3500	10029	6768	30
H(8B)	5446	9552	6305	30
H(9A)	3673	8306	6485	25
H(9B)	1906	8769	7044	25
H(10)	6261	8053	7613	19
H(11A)	1991	7876	8290	22
H(11B)	4314	7520	8768	22
H(14)	3189	5142	7428	23
H(15)	614	4086	7757	26
H(16)	-2576	4466	8439	26
H(17)	-3116	5888	8829	26
H(18)	-502	6945	8543	22
H(22A)	-1384	410	4211	25
H(22B)	-1470	-213	5007	25
H(23A)	2374	-609	4955	25
H(23B)	1058	-764	4038	25

H(24A)	2469	539	3547	23
H(24B)	4574	-34	3935	23
H(25A)	4995	1410	4416	19
H(25B)	4861	769	5193	19
H(27A)	1008	1797	3680	30
H(27B)	-917	2088	4266	30
H(28A)	552	3398	4344	34
H(28B)	2503	3103	3773	34
H(29A)	5062	2864	4911	24
H(29B)	3503	3537	5362	24
H(30)	1328	2464	5865	20
H(31A)	4013	1443	6576	24
H(31B)	5960	1927	6132	24
H(34)	4651	3097	8659	28
H(35)	7296	2853	9821	34
H(36)	10699	2143	9664	34
H(37)	11410	1621	8336	32
H(38)	8713	1813	7172	26

Table A3.2.6 *Torsion angles [°] for V25038.*

O(1)-C(1)-C(2)-C(3)	-129.1(3)
C(6)-C(1)-C(2)-C(3)	51.8(3)
C(1)-C(2)-C(3)-C(4)	-54.6(3)
C(2)-C(3)-C(4)-C(5)	58.1(3)
C(3)-C(4)-C(5)-C(6)	-57.0(3)
O(1)-C(1)-C(6)-C(5)	132.6(3)
C(2)-C(1)-C(6)-C(5)	-48.3(3)
O(1)-C(1)-C(6)-C(10)	5.6(3)
C(2)-C(1)-C(6)-C(10)	-175.4(2)

O(1)-C(1)-C(6)-C(7)	-105.5(3)
C(2)-C(1)-C(6)-C(7)	73.6(3)
C(4)-C(5)-C(6)-C(1)	50.0(3)
C(4)-C(5)-C(6)-C(10)	176.6(2)
C(4)-C(5)-C(6)-C(7)	-71.1(3)
C(1)-C(6)-C(7)-C(8)	158.5(2)
C(5)-C(6)-C(7)-C(8)	-80.6(3)
C(10)-C(6)-C(7)-C(8)	39.7(2)
C(6)-C(7)-C(8)-C(9)	-21.0(3)
C(7)-C(8)-C(9)-C(10)	-6.3(3)
C(8)-C(9)-C(10)-C(11)	159.1(2)
C(8)-C(9)-C(10)-C(6)	31.4(3)
C(1)-C(6)-C(10)-C(11)	74.2(3)
C(5)-C(6)-C(10)-C(11)	-50.6(3)
C(7)-C(6)-C(10)-C(11)	-169.1(2)
C(1)-C(6)-C(10)-C(9)	-160.3(2)
C(5)-C(6)-C(10)-C(9)	74.8(3)
C(7)-C(6)-C(10)-C(9)	-43.7(2)
C(9)-C(10)-C(11)-C(12)	69.1(3)
C(6)-C(10)-C(11)-C(12)	-170.3(2)
C(10)-C(11)-C(12)-O(2)	14.1(4)
C(10)-C(11)-C(12)-C(13)	-168.0(2)
O(2)-C(12)-C(13)-C(18)	-156.3(3)
C(11)-C(12)-C(13)-C(18)	25.7(4)
O(2)-C(12)-C(13)-C(14)	21.7(4)
C(11)-C(12)-C(13)-C(14)	-156.2(2)
C(18)-C(13)-C(14)-C(15)	0.5(4)
C(12)-C(13)-C(14)-C(15)	-177.6(2)
C(13)-C(14)-C(15)-C(16)	0.8(4)
C(14)-C(15)-C(16)-C(17)	-1.2(4)
C(15)-C(16)-C(17)-C(18)	0.1(4)
C(16)-C(17)-C(18)-C(13)	1.2(4)
C(14)-C(13)-C(18)-C(17)	-1.5(4)
C(12)-C(13)-C(18)-C(17)	176.5(2)

O(3)-C(21)-C(22)-C(23)	-124.2(3)
C(26)-C(21)-C(22)-C(23)	55.0(3)
C(21)-C(22)-C(23)-C(24)	-54.6(3)
C(22)-C(23)-C(24)-C(25)	56.4(3)
C(23)-C(24)-C(25)-C(26)	-56.7(3)
O(3)-C(21)-C(26)-C(30)	0.7(4)
C(22)-C(21)-C(26)-C(30)	-178.6(2)
O(3)-C(21)-C(26)-C(25)	126.6(3)
C(22)-C(21)-C(26)-C(25)	-52.6(3)
O(3)-C(21)-C(26)-C(27)	-112.4(3)
C(22)-C(21)-C(26)-C(27)	68.4(3)
C(24)-C(25)-C(26)-C(21)	52.5(3)
C(24)-C(25)-C(26)-C(30)	178.2(2)
C(24)-C(25)-C(26)-C(27)	-67.7(3)
C(21)-C(26)-C(27)-C(28)	144.9(2)
C(30)-C(26)-C(27)-C(28)	25.0(3)
C(25)-C(26)-C(27)-C(28)	-95.9(3)
C(26)-C(27)-C(28)-C(29)	-1.0(3)
C(27)-C(28)-C(29)-C(30)	-23.9(3)
C(28)-C(29)-C(30)-C(31)	167.4(2)
C(28)-C(29)-C(30)-C(26)	39.9(3)
C(21)-C(26)-C(30)-C(31)	76.6(3)
C(25)-C(26)-C(30)-C(31)	-46.6(3)
C(27)-C(26)-C(30)-C(31)	-165.8(2)
C(21)-C(26)-C(30)-C(29)	-157.5(2)
C(25)-C(26)-C(30)-C(29)	79.4(3)
C(27)-C(26)-C(30)-C(29)	-39.9(2)
C(29)-C(30)-C(31)-C(32)	73.7(3)
C(26)-C(30)-C(31)-C(32)	-165.8(2)
C(30)-C(31)-C(32)-O(4)	4.7(4)
C(30)-C(31)-C(32)-C(33)	-177.9(2)
O(4)-C(32)-C(33)-C(38)	-151.3(3)
C(31)-C(32)-C(33)-C(38)	31.3(4)
O(4)-C(32)-C(33)-C(34)	27.3(4)

C(31)-C(32)-C(33)-C(34)	-150.1(3)
C(38)-C(33)-C(34)-C(35)	-0.2(4)
C(32)-C(33)-C(34)-C(35)	-178.8(2)
C(33)-C(34)-C(35)-C(36)	1.4(4)
C(34)-C(35)-C(36)-C(37)	-1.3(5)
C(35)-C(36)-C(37)-C(38)	0.0(5)
C(36)-C(37)-C(38)-C(33)	1.2(4)
C(34)-C(33)-C(38)-C(37)	-1.1(4)
C(32)-C(33)-C(38)-C(37)	177.5(3)

Symmetry transformations used to generate equivalent atoms:

A3.3 CRYSTAL STRUCTURE ANALYSIS OF PRODUCT 197B (V25125)

Spirocycle **197b** was crystalized by layering pentane onto a saturated solution of **197b** in diethyl ether at 23 °C to provide crystalline blocks suitable for X-ray analysis.

Compound V25125 (CCDC 2444207) crystallizes in the orthorhombic space group $P2_12_12_1$ with one molecule in the asymmetric unit. One carbon atom and the associated hydrogen atoms were disordered over two positions. Absolute configuration was assigned via Flack (Flack = -0.06(5)) parameter.

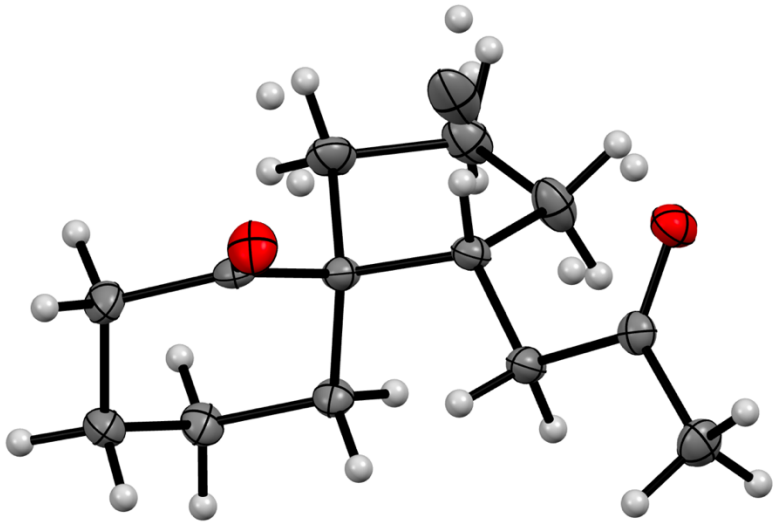

Figure A3.3.1 *X-Ray Coordinates of Compound* ***197b*** *(V25125)*

Table A3.3.1 *Crystal data and structure refinement for V25125.*

Identification code	V25125
Empirical formula	C13 H20 O2
Formula weight	208.29
Temperature	100(2) K
Wavelength	1.54178 Å
Crystal system	Orthorhombic

Space group	$P2_12_12_1$	
Unit cell dimensions	a = 6.0311(6) Å	a= 90°.
	b = 13.5742(13) Å	b= 90°.
	c = 14.2929(13) Å	g = 90°.
Volume	1170.12(19) $Å^3$	
Z	4	
Density (calculated)	1.182 Mg/m^3	
Absorption coefficient	0.612 mm^{-1}	
F(000)	456	
Crystal size	0.400 x 0.150 x 0.100 mm^3	
Theta range for data collection	4.492 to 74.468°.	
Index ranges	-7<=h<=7, -16<=k<=16, -17<=l<=17	
Reflections collected	17358	
Independent reflections	2402 [R(int) = 0.0414]	
Completeness to theta = 67.679°	100.0 %	
Absorption correction	Semi-empirical from equivalents	
Max. and min. transmission	0.7538 and 0.6398	
Refinement method	Full-matrix least-squares on F^2	
Data / restraints / parameters	2402 / 47 / 147	
Goodness-of-fit on F^2	1.051	
Final R indices [I>2sigma(I)]	R1 = 0.0287, wR2 = 0.0751	
R indices (all data)	R1 = 0.0296, wR2 = 0.0753	
Absolute structure parameter	-0.06(5)	
Extinction coefficient	n/a	
Largest diff. peak and hole	0.158 and -0.155 $e.Å^{-3}$	

Table A3.3.2 *Atomic coordinates (x 10^4) and equivalent isotropic displacement parameters ($Å^2$x 10^3) for V25125. U(eq) is defined as one third of the trace of the orthogonalized U^{ij} tensor.*

	x	y	z	U(eq)
C(1)	7886(2)	6404(1)	2188(1)	19(1)
O(1)	8477(2)	6891(1)	2857(1)	29(1)
C(2)	8676(2)	6636(1)	1208(1)	24(1)
C(3)	6709(2)	6745(1)	534(1)	22(1)
C(4)	5266(3)	5827(1)	562(1)	22(1)
C(5)	4436(2)	5629(1)	1557(1)	19(1)
C(6)	6323(2)	5527(1)	2284(1)	17(1)
C(7)	5457(2)	5403(1)	3294(1)	17(1)
C(11)	3665(2)	6123(1)	3598(1)	19(1)
C(12)	3251(2)	6139(1)	4640(1)	19(1)
O(2)	4340(2)	5656(1)	5185(1)	25(1)
C(13)	1393(3)	6799(1)	4967(1)	26(1)
C(8)	4755(3)	4316(1)	3349(1)	28(1)
C(9)	6153(8)	3759(2)	2645(2)	27(1)
C(9A)	7050(30)	3850(8)	2883(10)	36(3)
C(10)	7624(3)	4548(1)	2147(1)	26(1)

Table A3.3.3 *Bond lengths [Å] and angles [°] for V25125.*

C(1)-O(1)	1.2155(18)
C(1)-C(2)	1.5130(19)
C(1)-C(6)	1.5243(18)
C(2)-C(3)	1.535(2)

C(2)-H(2A)	0.9900
C(2)-H(2B)	0.9900
C(3)-C(4)	1.522(2)
C(3)-H(3A)	0.9900
C(3)-H(3B)	0.9900
C(4)-C(5)	1.5322(19)
C(4)-H(4A)	0.9900
C(4)-H(4B)	0.9900
C(5)-C(6)	1.5477(17)
C(5)-H(5A)	0.9900
C(5)-H(5B)	0.9900
C(6)-C(7)	1.5436(17)
C(6)-C(10)	1.5549(18)
C(7)-C(11)	1.5199(18)
C(7)-C(8)	1.5378(18)
C(7)-H(7)	1.0000
C(11)-C(12)	1.5110(18)
C(11)-H(11A)	0.9900
C(11)-H(11B)	0.9900
C(12)-O(2)	1.2119(18)
C(12)-C(13)	1.5082(19)
C(13)-H(13A)	0.9800
C(13)-H(13B)	0.9800
C(13)-H(13C)	0.9800
C(8)-C(9)	1.515(3)
C(8)-C(9A)	1.661(11)
C(8)-H(8A)	0.9900
C(8)-H(8B)	0.9900
C(8)-H(8C)	0.9900
C(8)-H(8D)	0.9900
C(9)-C(10)	1.563(3)
C(9)-H(9A)	0.9900
C(9)-H(9B)	0.9900
C(9A)-C(10)	1.458(9)

C(9A)-H(9A1)	0.9900
C(9A)-H(9A2)	0.9900
C(10)-H(10A)	0.9900
C(10)-H(10B)	0.9900
C(10)-H(10C)	0.9900
C(10)-H(10D)	0.9900

O(1)-C(1)-C(2)	121.42(12)
O(1)-C(1)-C(6)	122.41(13)
C(2)-C(1)-C(6)	116.17(11)
C(1)-C(2)-C(3)	110.95(12)
C(1)-C(2)-H(2A)	109.4
C(3)-C(2)-H(2A)	109.4
C(1)-C(2)-H(2B)	109.4
C(3)-C(2)-H(2B)	109.4
H(2A)-C(2)-H(2B)	108.0
C(4)-C(3)-C(2)	110.28(12)
C(4)-C(3)-H(3A)	109.6
C(2)-C(3)-H(3A)	109.6
C(4)-C(3)-H(3B)	109.6
C(2)-C(3)-H(3B)	109.6
H(3A)-C(3)-H(3B)	108.1
C(3)-C(4)-C(5)	110.73(11)
C(3)-C(4)-H(4A)	109.5
C(5)-C(4)-H(4A)	109.5
C(3)-C(4)-H(4B)	109.5
C(5)-C(4)-H(4B)	109.5
H(4A)-C(4)-H(4B)	108.1
C(4)-C(5)-C(6)	113.53(11)
C(4)-C(5)-H(5A)	108.9
C(6)-C(5)-H(5A)	108.9
C(4)-C(5)-H(5B)	108.9
C(6)-C(5)-H(5B)	108.9
H(5A)-C(5)-H(5B)	107.7

C(1)-C(6)-C(7)	112.23(11)
C(1)-C(6)-C(5)	108.90(11)
C(7)-C(6)-C(5)	112.86(11)
C(1)-C(6)-C(10)	110.09(11)
C(7)-C(6)-C(10)	101.32(11)
C(5)-C(6)-C(10)	111.29(11)
C(11)-C(7)-C(8)	114.01(12)
C(11)-C(7)-C(6)	115.98(11)
C(8)-C(7)-C(6)	104.21(11)
C(11)-C(7)-H(7)	107.4
C(8)-C(7)-H(7)	107.4
C(6)-C(7)-H(7)	107.4
C(12)-C(11)-C(7)	114.14(11)
C(12)-C(11)-H(11A)	108.7
C(7)-C(11)-H(11A)	108.7
C(12)-C(11)-H(11B)	108.7
C(7)-C(11)-H(11B)	108.7
H(11A)-C(11)-H(11B)	107.6
O(2)-C(12)-C(13)	121.69(13)
O(2)-C(12)-C(11)	122.42(13)
C(13)-C(12)-C(11)	115.90(12)
C(12)-C(13)-H(13A)	109.5
C(12)-C(13)-H(13B)	109.5
H(13A)-C(13)-H(13B)	109.5
C(12)-C(13)-H(13C)	109.5
H(13A)-C(13)-H(13C)	109.5
H(13B)-C(13)-H(13C)	109.5
C(9)-C(8)-C(7)	106.95(16)
C(7)-C(8)-C(9A)	96.6(5)
C(9)-C(8)-H(8A)	110.3
C(7)-C(8)-H(8A)	110.3
C(9)-C(8)-H(8B)	110.3
C(7)-C(8)-H(8B)	110.3
H(8A)-C(8)-H(8B)	108.6

C(7)-C(8)-H(8C)	112.4
C(9A)-C(8)-H(8C)	112.4
C(7)-C(8)-H(8D)	112.4
C(9A)-C(8)-H(8D)	112.4
H(8C)-C(8)-H(8D)	110.0
C(8)-C(9)-C(10)	106.06(18)
C(8)-C(9)-H(9A)	110.5
C(10)-C(9)-H(9A)	110.5
C(8)-C(9)-H(9B)	110.5
C(10)-C(9)-H(9B)	110.5
H(9A)-C(9)-H(9B)	108.7
C(10)-C(9A)-C(8)	103.9(6)
C(10)-C(9A)-H(9A1)	111.0
C(8)-C(9A)-H(9A1)	111.0
C(10)-C(9A)-H(9A2)	111.0
C(8)-C(9A)-H(9A2)	111.0
H(9A1)-C(9A)-H(9A2)	109.0
C(9A)-C(10)-C(6)	110.1(4)
C(6)-C(10)-C(9)	103.98(16)
C(6)-C(10)-H(10A)	111.0
C(9)-C(10)-H(10A)	111.0
C(6)-C(10)-H(10B)	111.0
C(9)-C(10)-H(10B)	111.0
H(10A)-C(10)-H(10B)	109.0
C(9A)-C(10)-H(10C)	109.6
C(6)-C(10)-H(10C)	109.6
C(9A)-C(10)-H(10D)	109.6
C(6)-C(10)-H(10D)	109.6
H(10C)-C(10)-H(10D)	108.1

Symmetry transformations used to generate equivalent atoms:

Table A3.3.4 *Anisotropic displacement parameters ($Å^2 x\ 10^3$) for V25125. The anisotropic displacement factor exponent takes the form: $-2p^2[\ h^2\ a^{*2}U^{11} + \ldots + 2\ h\ k\ a^*\ b^*\ U^{12}]$*

	U^{11}	U^{22}	U^{33}	U^{23}	U^{13}	U^{12}
C(1)	13(1)	24(1)	21(1)	2(1)	-4(1)	2(1)
O(1)	27(1)	35(1)	24(1)	-3(1)	-5(1)	-9(1)
C(2)	17(1)	30(1)	24(1)	4(1)	0(1)	-3(1)
C(3)	22(1)	25(1)	19(1)	4(1)	-1(1)	1(1)
C(4)	23(1)	28(1)	16(1)	-1(1)	-3(1)	-2(1)
C(5)	17(1)	23(1)	17(1)	-1(1)	-3(1)	-1(1)
C(6)	15(1)	18(1)	17(1)	0(1)	-1(1)	3(1)
C(7)	18(1)	18(1)	16(1)	2(1)	-2(1)	2(1)
C(11)	20(1)	21(1)	17(1)	2(1)	0(1)	4(1)
C(12)	20(1)	18(1)	20(1)	-1(1)	0(1)	-3(1)
O(2)	29(1)	28(1)	19(1)	2(1)	-2(1)	3(1)
C(13)	27(1)	26(1)	25(1)	-2(1)	6(1)	4(1)
C(8)	41(1)	18(1)	23(1)	2(1)	5(1)	0(1)
C(9)	38(2)	20(1)	24(1)	0(1)	1(1)	5(1)
C(9A)	57(7)	20(4)	30(5)	1(4)	16(5)	16(4)
C(10)	27(1)	24(1)	27(1)	0(1)	2(1)	10(1)

Table A3.3.5 *Hydrogen coordinates (x 10^4) and isotropic displacement parameters ($Å^2$x 10^3) for V25125.*

	x	y	z	U(eq)
H(2A)	9660	6101	986	28
H(2B)	9544	7255	1216	28
H(3A)	5815	7327	714	27
H(3B)	7266	6850	-110	27
H(4A)	6133	5253	339	26
H(4B)	3982	5914	138	26
H(5A)	3547	5016	1557	23
H(5B)	3449	6176	1750	23
H(7)	6747	5493	3725	21
H(11A)	4093	6793	3393	23
H(11B)	2265	5950	3276	23
H(13A)	-27	6456	4890	39
H(13B)	1385	7405	4594	39
H(13C)	1612	6964	5628	39
H(8A)	5011	4055	3987	33
H(8B)	3161	4246	3198	33
H(8C)	3423	4174	2968	33
H(8D)	4518	4093	4001	33
H(9A)	5196	3417	2186	33
H(9B)	7092	3264	2964	33
H(9A1)	8248	3806	3355	43
H(9A2)	6774	3187	2621	43
H(10A)	9109	4587	2440	31
H(10B)	7799	4394	1474	31
H(10C)	7259	4262	1529	31
H(10D)	9237	4682	2163	31

Table A3.3.6 *Torsion angles [°] for V25125.*

O(1)-C(1)-C(2)-C(3)	-127.07(14)
C(6)-C(1)-C(2)-C(3)	53.10(16)
C(1)-C(2)-C(3)-C(4)	-55.29(16)
C(2)-C(3)-C(4)-C(5)	57.61(16)
C(3)-C(4)-C(5)-C(6)	-56.67(15)
O(1)-C(1)-C(6)-C(7)	4.99(18)
C(2)-C(1)-C(6)-C(7)	-175.18(11)
O(1)-C(1)-C(6)-C(5)	130.69(14)
C(2)-C(1)-C(6)-C(5)	-49.49(14)
O(1)-C(1)-C(6)-C(10)	-107.04(15)
C(2)-C(1)-C(6)-C(10)	72.78(14)
C(4)-C(5)-C(6)-C(1)	50.52(15)
C(4)-C(5)-C(6)-C(7)	175.86(11)
C(4)-C(5)-C(6)-C(10)	-71.02(15)
C(1)-C(6)-C(7)-C(11)	75.92(14)
C(5)-C(6)-C(7)-C(11)	-47.59(16)
C(10)-C(6)-C(7)-C(11)	-166.68(12)
C(1)-C(6)-C(7)-C(8)	-157.90(11)
C(5)-C(6)-C(7)-C(8)	78.59(14)
C(10)-C(6)-C(7)-C(8)	-40.50(13)
C(8)-C(7)-C(11)-C(12)	72.66(16)
C(6)-C(7)-C(11)-C(12)	-166.28(11)
C(7)-C(11)-C(12)-O(2)	3.6(2)
C(7)-C(11)-C(12)-C(13)	-176.48(12)
C(11)-C(7)-C(8)-C(9)	154.3(2)
C(6)-C(7)-C(8)-C(9)	26.9(2)
C(11)-C(7)-C(8)-C(9A)	175.4(7)
C(6)-C(7)-C(8)-C(9A)	48.0(7)
C(7)-C(8)-C(9)-C(10)	-2.2(3)
C(7)-C(8)-C(9A)-C(10)	-38.5(12)
C(8)-C(9A)-C(10)-C(6)	15.4(14)

C(1)-C(6)-C(10)-C(9A)	133.0(10)
C(7)-C(6)-C(10)-C(9A)	14.0(10)
C(5)-C(6)-C(10)-C(9A)	-106.2(10)
C(1)-C(6)-C(10)-C(9)	157.9(2)
C(7)-C(6)-C(10)-C(9)	39.0(2)
C(5)-C(6)-C(10)-C(9)	-81.2(2)
C(8)-C(9)-C(10)-C(6)	-23.1(3)

Symmetry transformations used to generate equivalent atoms:

A3.4 CRYSTAL STRUCTURE ANALYSIS OF PRODUCT 201A (V24254)

Spirocycle **201a** was crystalized by layering pentane onto a saturated solution of **201a** in benzene at 23 °C to provide crystalline blocks suitable for X-ray analysis.

Compound V24254 (CCDC 2421483) crystallizes in the orthorhombic space group $P2_12_12_1$ with one molecule in the asymmetric unit. Absolute configuration was assigned via Flack (Flack = 0.01(9)) parameter.

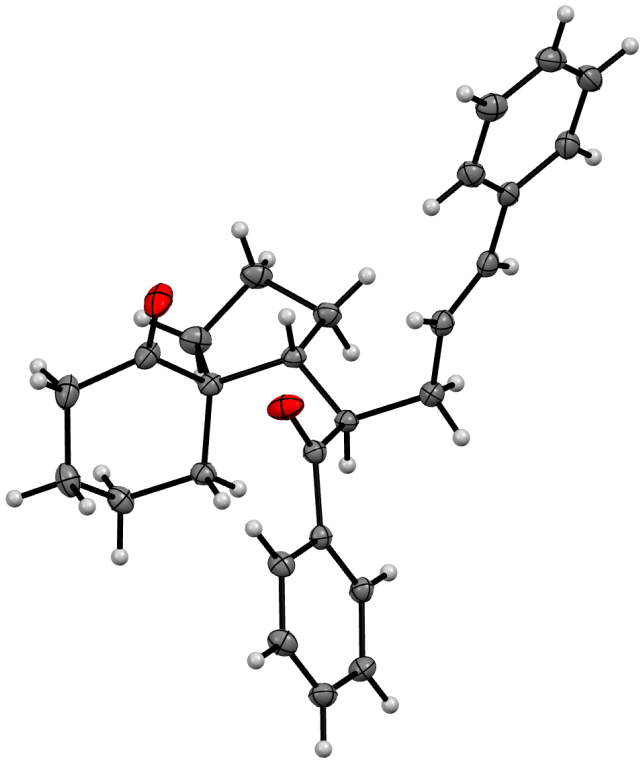

Figure A3.4.1 *X-Ray Coordinates of Compound* ***201a*** *(V24254)*

Table A3.4.1 *Crystal data and structure refinement for V24254.*

Identification code	V24254	
Empirical formula	C27 H30 O2	
Formula weight	386.51	
Temperature	100(2) K	
Wavelength	1.54178 Å	
Crystal system	Orthorhombic	
Space group	$P2_12_12_1$	
Unit cell dimensions	a = 8.3129(6) Å	a= 90°.
	b = 14.2383(15) Å	b= 90°.
	c = 17.763(2) Å	g = 90°.
Volume	2102.4(4) $Å^3$	
Z	4	
Density (calculated)	1.221 Mg/m^3	
Absorption coefficient	0.581 mm^{-1}	
F(000)	832	
Crystal size	0.200 x 0.100 x 0.100 mm^3	
Theta range for data collection	3.979 to 74.369°.	
Index ranges	-10<=h<=10, -17<=k<=17, -22<=l<=22	
Reflections collected	37667	
Independent reflections	4303 [R(int) = 0.0447]	
Completeness to theta = 67.679°	100.0 %	
Absorption correction	Semi-empirical from equivalents	
Max. and min. transmission	0.7538 and 0.6890	
Refinement method	Full-matrix least-squares on F^2	
Data / restraints / parameters	4303 / 0 / 262	
Goodness-of-fit on F^2	1.070	
Final R indices [I>2sigma(I)]	R1 = 0.0292, wR2 = 0.0703	
R indices (all data)	R1 = 0.0312, wR2 = 0.0720	
Absolute structure parameter	0.01(9)	
Extinction coefficient	n/a	
Largest diff. peak and hole	0.186 and -0.160 $e.Å^{-3}$	

Table A3.4.2 *Atomic coordinates (x 10^4) and equivalent isotropic displacement parameters ($Å^2$x 10^3) for V24254. U(eq) is defined as one third of the trace of the orthogonalized U^{ij} tensor.*

	x	y	z	U(eq)
O(1)	1331(2)	2536(1)	1678(1)	34(1)
C(1)	569(2)	3260(1)	1732(1)	22(1)
C(2)	239(2)	3847(1)	1036(1)	29(1)
C(3)	229(2)	4904(1)	1177(1)	26(1)
C(4)	-868(2)	5135(1)	1834(1)	22(1)
C(5)	-240(2)	4649(1)	2541(1)	19(1)
C(6)	-206(2)	3565(1)	2473(1)	17(1)
C(7)	-1973(2)	3176(1)	2445(1)	25(1)
C(8)	-1971(2)	2304(1)	2944(1)	25(1)
C(9)	-841(2)	2593(1)	3579(1)	22(1)
C(10)	576(2)	3053(1)	3166(1)	17(1)
C(11)	1633(2)	3674(1)	3668(1)	17(1)
C(21)	3139(2)	3996(1)	3245(1)	18(1)
O(2)	3831(2)	3457(1)	2822(1)	28(1)
C(22)	3782(2)	4969(1)	3365(1)	17(1)
C(23)	5022(2)	5272(1)	2890(1)	20(1)
C(24)	5640(2)	6173(1)	2954(1)	23(1)
C(25)	5022(2)	6783(1)	3491(1)	23(1)
C(26)	3798(2)	6488(1)	3965(1)	22(1)
C(27)	3173(2)	5584(1)	3905(1)	19(1)
C(12)	2171(2)	3183(1)	4407(1)	21(1)
C(13)	3016(2)	2259(1)	4312(1)	21(1)
C(14)	2624(2)	1501(1)	4713(1)	21(1)
C(15)	3431(2)	580(1)	4725(1)	21(1)
C(16)	2981(2)	-72(1)	5277(1)	24(1)
C(17)	3707(2)	-955(1)	5314(1)	28(1)
C(18)	4869(2)	-1200(1)	4792(1)	27(1)

C(19)	5315(2)	-564(1)	4235(1)	27(1)
C(20)	4617(2)	320(1)	4208(1)	23(1)

Table A3.4.3 *Bond lengths [Å] and angles [°] for V24254.*

O(1)-C(1)	1.215(2)
C(1)-C(2)	1.517(2)
C(1)-C(6)	1.528(2)
C(2)-C(3)	1.526(3)
C(2)-H(2A)	0.9900
C(2)-H(2B)	0.9900
C(3)-C(4)	1.517(2)
C(3)-H(3A)	0.9900
C(3)-H(3B)	0.9900
C(4)-C(5)	1.526(2)
C(4)-H(4A)	0.9900
C(4)-H(4B)	0.9900
C(5)-C(6)	1.549(2)
C(5)-H(5A)	0.9900
C(5)-H(5B)	0.9900
C(6)-C(10)	1.571(2)
C(6)-C(7)	1.571(2)
C(7)-C(8)	1.525(2)
C(7)-H(7A)	0.9900
C(7)-H(7B)	0.9900
C(8)-C(9)	1.523(2)
C(8)-H(8A)	0.9900
C(8)-H(8B)	0.9900
C(9)-C(10)	1.534(2)
C(9)-H(9A)	0.9900

C(9)-H(9B)	0.9900
C(10)-C(11)	1.532(2)
C(10)-H(10)	1.0000
C(11)-C(21)	1.530(2)
C(11)-C(12)	1.553(2)
C(11)-H(11)	1.0000
C(21)-O(2)	1.218(2)
C(21)-C(22)	1.501(2)
C(22)-C(27)	1.395(2)
C(22)-C(23)	1.400(2)
C(23)-C(24)	1.387(2)
C(23)-H(23)	0.9500
C(24)-C(25)	1.388(2)
C(24)-H(24)	0.9500
C(25)-C(26)	1.386(3)
C(25)-H(25)	0.9500
C(26)-C(27)	1.392(2)
C(26)-H(26)	0.9500
C(27)-H(27)	0.9500
C(12)-C(13)	1.501(2)
C(12)-H(12A)	0.9900
C(12)-H(12B)	0.9900
C(13)-C(14)	1.334(2)
C(13)-H(13)	0.9500
C(14)-C(15)	1.473(2)
C(14)-H(14)	0.9500
C(15)-C(20)	1.398(3)
C(15)-C(16)	1.401(2)
C(16)-C(17)	1.395(3)
C(16)-H(16)	0.9500
C(17)-C(18)	1.384(3)
C(17)-H(17)	0.9500
C(18)-C(19)	1.392(3)
C(18)-H(18)	0.9500

C(19)-C(20)	1.386(2)
C(19)-H(19)	0.9500
C(20)-H(20)	0.9500

O(1)-C(1)-C(2)	119.87(15)
O(1)-C(1)-C(6)	121.90(16)
C(2)-C(1)-C(6)	118.01(14)
C(1)-C(2)-C(3)	114.22(15)
C(1)-C(2)-H(2A)	108.7
C(3)-C(2)-H(2A)	108.7
C(1)-C(2)-H(2B)	108.7
C(3)-C(2)-H(2B)	108.7
H(2A)-C(2)-H(2B)	107.6
C(4)-C(3)-C(2)	110.05(15)
C(4)-C(3)-H(3A)	109.7
C(2)-C(3)-H(3A)	109.7
C(4)-C(3)-H(3B)	109.7
C(2)-C(3)-H(3B)	109.7
H(3A)-C(3)-H(3B)	108.2
C(3)-C(4)-C(5)	109.24(13)
C(3)-C(4)-H(4A)	109.8
C(5)-C(4)-H(4A)	109.8
C(3)-C(4)-H(4B)	109.8
C(5)-C(4)-H(4B)	109.8
H(4A)-C(4)-H(4B)	108.3
C(4)-C(5)-C(6)	113.17(14)
C(4)-C(5)-H(5A)	108.9
C(6)-C(5)-H(5A)	108.9
C(4)-C(5)-H(5B)	108.9
C(6)-C(5)-H(5B)	108.9
H(5A)-C(5)-H(5B)	107.8
C(1)-C(6)-C(5)	110.95(14)
C(1)-C(6)-C(10)	111.66(13)
C(5)-C(6)-C(10)	114.13(13)

C(1)-C(6)-C(7)	105.48(13)
C(5)-C(6)-C(7)	109.67(13)
C(10)-C(6)-C(7)	104.38(13)
C(8)-C(7)-C(6)	105.49(13)
C(8)-C(7)-H(7A)	110.6
C(6)-C(7)-H(7A)	110.6
C(8)-C(7)-H(7B)	110.6
C(6)-C(7)-H(7B)	110.6
H(7A)-C(7)-H(7B)	108.8
C(9)-C(8)-C(7)	102.20(14)
C(9)-C(8)-H(8A)	111.3
C(7)-C(8)-H(8A)	111.3
C(9)-C(8)-H(8B)	111.3
C(7)-C(8)-H(8B)	111.3
H(8A)-C(8)-H(8B)	109.2
C(8)-C(9)-C(10)	103.60(13)
C(8)-C(9)-H(9A)	111.0
C(10)-C(9)-H(9A)	111.0
C(8)-C(9)-H(9B)	111.0
C(10)-C(9)-H(9B)	111.0
H(9A)-C(9)-H(9B)	109.0
C(11)-C(10)-C(9)	114.13(13)
C(11)-C(10)-C(6)	115.17(12)
C(9)-C(10)-C(6)	104.78(13)
C(11)-C(10)-H(10)	107.5
C(9)-C(10)-H(10)	107.5
C(6)-C(10)-H(10)	107.5
C(21)-C(11)-C(10)	110.92(13)
C(21)-C(11)-C(12)	108.29(13)
C(10)-C(11)-C(12)	113.40(13)
C(21)-C(11)-H(11)	108.0
C(10)-C(11)-H(11)	108.0
C(12)-C(11)-H(11)	108.0
O(2)-C(21)-C(22)	120.00(15)

O(2)-C(21)-C(11)	120.07(14)
C(22)-C(21)-C(11)	119.93(13)
C(27)-C(22)-C(23)	119.22(14)
C(27)-C(22)-C(21)	123.25(15)
C(23)-C(22)-C(21)	117.50(14)
C(24)-C(23)-C(22)	120.56(15)
C(24)-C(23)-H(23)	119.7
C(22)-C(23)-H(23)	119.7
C(23)-C(24)-C(25)	119.86(16)
C(23)-C(24)-H(24)	120.1
C(25)-C(24)-H(24)	120.1
C(26)-C(25)-C(24)	119.99(16)
C(26)-C(25)-H(25)	120.0
C(24)-C(25)-H(25)	120.0
C(25)-C(26)-C(27)	120.53(15)
C(25)-C(26)-H(26)	119.7
C(27)-C(26)-H(26)	119.7
C(26)-C(27)-C(22)	119.85(15)
C(26)-C(27)-H(27)	120.1
C(22)-C(27)-H(27)	120.1
C(13)-C(12)-C(11)	115.78(13)
C(13)-C(12)-H(12A)	108.3
C(11)-C(12)-H(12A)	108.3
C(13)-C(12)-H(12B)	108.3
C(11)-C(12)-H(12B)	108.3
H(12A)-C(12)-H(12B)	107.4
C(14)-C(13)-C(12)	122.37(16)
C(14)-C(13)-H(13)	118.8
C(12)-C(13)-H(13)	118.8
C(13)-C(14)-C(15)	128.06(16)
C(13)-C(14)-H(14)	116.0
C(15)-C(14)-H(14)	116.0
C(20)-C(15)-C(16)	118.20(16)
C(20)-C(15)-C(14)	123.24(15)

C(16)-C(15)-C(14)	118.56(16)
C(17)-C(16)-C(15)	120.98(17)
C(17)-C(16)-H(16)	119.5
C(15)-C(16)-H(16)	119.5
C(18)-C(17)-C(16)	119.82(17)
C(18)-C(17)-H(17)	120.1
C(16)-C(17)-H(17)	120.1
C(17)-C(18)-C(19)	119.87(17)
C(17)-C(18)-H(18)	120.1
C(19)-C(18)-H(18)	120.1
C(20)-C(19)-C(18)	120.29(18)
C(20)-C(19)-H(19)	119.9
C(18)-C(19)-H(19)	119.9
C(19)-C(20)-C(15)	120.83(16)
C(19)-C(20)-H(20)	119.6
C(15)-C(20)-H(20)	119.6

Symmetry transformations used to generate equivalent atoms:

Table A3.4.4 *Anisotropic displacement parameters ($Å^2$x 10^3) for V24254. The anisotropic displacement factor exponent takes the form: $-2p^2[h^2 a^{*2}U^{11} + ... + 2 h k a^* b^* U^{12}]$*

	U^{11}	U^{22}	U^{33}	U^{23}	U^{13}	U^{12}
O(1)	43(1)	35(1)	25(1)	-10(1)	-5(1)	20(1)
C(1)	21(1)	25(1)	21(1)	-6(1)	-4(1)	4(1)
C(2)	33(1)	37(1)	17(1)	-3(1)	-3(1)	7(1)
C(3)	22(1)	33(1)	23(1)	6(1)	-1(1)	5(1)
C(4)	18(1)	23(1)	26(1)	4(1)	-1(1)	3(1)
C(5)	19(1)	16(1)	20(1)	-1(1)	-1(1)	3(1)

C(6)	15(1)	17(1)	19(1)	-2(1)	-1(1)	3(1)
C(7)	17(1)	24(1)	35(1)	0(1)	-4(1)	-1(1)
C(8)	21(1)	22(1)	33(1)	1(1)	-2(1)	-4(1)
C(9)	23(1)	20(1)	24(1)	0(1)	2(1)	-3(1)
C(10)	17(1)	14(1)	19(1)	-1(1)	-1(1)	2(1)
C(11)	18(1)	14(1)	18(1)	0(1)	-1(1)	1(1)
C(21)	17(1)	17(1)	19(1)	0(1)	-2(1)	1(1)
O(2)	26(1)	23(1)	35(1)	-9(1)	10(1)	-2(1)
C(22)	15(1)	18(1)	18(1)	0(1)	-3(1)	1(1)
C(23)	17(1)	20(1)	22(1)	1(1)	2(1)	3(1)
C(24)	19(1)	23(1)	27(1)	3(1)	3(1)	-2(1)
C(25)	24(1)	18(1)	27(1)	0(1)	-3(1)	-2(1)
C(26)	26(1)	20(1)	21(1)	-4(1)	-1(1)	0(1)
C(27)	21(1)	20(1)	17(1)	-1(1)	2(1)	-2(1)
C(12)	25(1)	19(1)	19(1)	-1(1)	-2(1)	-1(1)
C(13)	22(1)	22(1)	19(1)	-1(1)	-4(1)	1(1)
C(14)	22(1)	24(1)	16(1)	-2(1)	-4(1)	-1(1)
C(15)	22(1)	21(1)	19(1)	1(1)	-8(1)	-4(1)
C(16)	28(1)	26(1)	19(1)	2(1)	-4(1)	-2(1)
C(17)	35(1)	22(1)	27(1)	6(1)	-8(1)	-5(1)
C(18)	28(1)	19(1)	35(1)	0(1)	-11(1)	0(1)
C(19)	22(1)	25(1)	33(1)	-2(1)	-4(1)	-1(1)
C(20)	22(1)	22(1)	25(1)	2(1)	-2(1)	-4(1)

Table A3.4.5 *Hydrogen coordinates (x 10^4) and isotropic displacement parameters ($Å^2$x 10^3) for V24254.*

	x	y	z	U(eq)
H(2A)	-817	3661	826	35

H(2B)	1068	3703	653	35
H(3A)	1335	5121	1289	31
H(3B)	-151	5235	720	31
H(4A)	-1975	4917	1724	27
H(4B)	-898	5822	1913	27
H(5A)	-929	4826	2973	22
H(5B)	862	4877	2647	22
H(7A)	-2741	3649	2638	30
H(7B)	-2277	3011	1922	30
H(8A)	-3063	2164	3137	30
H(8B)	-1556	1749	2670	30
H(9A)	-482	2039	3871	26
H(9B)	-1369	3044	3923	26
H(10)	1270	2537	2965	20
H(11)	998	4245	3806	20
H(23)	5444	4856	2521	24
H(24)	6484	6373	2631	28
H(25)	5438	7402	3534	27
H(26)	3382	6906	4334	27
H(27)	2333	5387	4232	23
H(12A)	2895	3614	4683	25
H(12B)	1208	3082	4724	25
H(13)	3861	2212	3954	25
H(14)	1710	1562	5031	25
H(16)	2169	88	5631	29
H(17)	3404	-1386	5697	34
H(18)	5362	-1801	4814	33
H(19)	6100	-736	3872	32
H(20)	4949	754	3833	28

Table A3.4.6 *Torsion angles [°] for V24254.*

O(1)-C(1)-C(2)-C(3)	-145.22(18)
C(6)-C(1)-C(2)-C(3)	40.1(2)
C(1)-C(2)-C(3)-C(4)	-51.0(2)
C(2)-C(3)-C(4)-C(5)	61.25(18)
C(3)-C(4)-C(5)-C(6)	-61.33(18)
O(1)-C(1)-C(6)-C(5)	148.18(17)
C(2)-C(1)-C(6)-C(5)	-37.3(2)
O(1)-C(1)-C(6)-C(10)	19.6(2)
C(2)-C(1)-C(6)-C(10)	-165.80(15)
O(1)-C(1)-C(6)-C(7)	-93.14(19)
C(2)-C(1)-C(6)-C(7)	81.42(18)
C(4)-C(5)-C(6)-C(1)	47.77(18)
C(4)-C(5)-C(6)-C(10)	174.96(13)
C(4)-C(5)-C(6)-C(7)	-68.35(18)
C(1)-C(6)-C(7)-C(8)	102.34(16)
C(5)-C(6)-C(7)-C(8)	-138.12(15)
C(10)-C(6)-C(7)-C(8)	-15.46(17)
C(6)-C(7)-C(8)-C(9)	37.04(17)
C(7)-C(8)-C(9)-C(10)	-44.80(17)
C(8)-C(9)-C(10)-C(11)	161.94(13)
C(8)-C(9)-C(10)-C(6)	35.06(16)
C(1)-C(6)-C(10)-C(11)	108.41(15)
C(5)-C(6)-C(10)-C(11)	-18.42(19)
C(7)-C(6)-C(10)-C(11)	-138.12(14)
C(1)-C(6)-C(10)-C(9)	-125.36(14)
C(5)-C(6)-C(10)-C(9)	107.81(15)
C(7)-C(6)-C(10)-C(9)	-11.89(15)
C(9)-C(10)-C(11)-C(21)	172.19(13)
C(6)-C(10)-C(11)-C(21)	-66.53(17)
C(9)-C(10)-C(11)-C(12)	50.08(18)
C(6)-C(10)-C(11)-C(12)	171.36(13)

C(10)-C(11)-C(21)-O(2)	-38.8(2)
C(12)-C(11)-C(21)-O(2)	86.24(18)
C(10)-C(11)-C(21)-C(22)	142.37(13)
C(12)-C(11)-C(21)-C(22)	-92.58(16)
O(2)-C(21)-C(22)-C(27)	-172.12(16)
C(11)-C(21)-C(22)-C(27)	6.7(2)
O(2)-C(21)-C(22)-C(23)	9.8(2)
C(11)-C(21)-C(22)-C(23)	-171.36(14)
C(27)-C(22)-C(23)-C(24)	-0.1(2)
C(21)-C(22)-C(23)-C(24)	178.06(15)
C(22)-C(23)-C(24)-C(25)	-0.2(2)
C(23)-C(24)-C(25)-C(26)	0.4(3)
C(24)-C(25)-C(26)-C(27)	-0.3(3)
C(25)-C(26)-C(27)-C(22)	0.0(3)
C(23)-C(22)-C(27)-C(26)	0.2(2)
C(21)-C(22)-C(27)-C(26)	-177.86(15)
C(21)-C(11)-C(12)-C(13)	-68.62(17)
C(10)-C(11)-C(12)-C(13)	54.95(19)
C(11)-C(12)-C(13)-C(14)	-132.36(17)
C(12)-C(13)-C(14)-C(15)	-174.46(15)
C(13)-C(14)-C(15)-C(20)	-10.8(3)
C(13)-C(14)-C(15)-C(16)	169.78(17)
C(20)-C(15)-C(16)-C(17)	0.6(2)
C(14)-C(15)-C(16)-C(17)	-179.92(16)
C(15)-C(16)-C(17)-C(18)	-1.2(3)
C(16)-C(17)-C(18)-C(19)	0.4(3)
C(17)-C(18)-C(19)-C(20)	1.0(3)
C(18)-C(19)-C(20)-C(15)	-1.6(3)
C(16)-C(15)-C(20)-C(19)	0.8(2)
C(14)-C(15)-C(20)-C(19)	-178.69(16)

Symmetry transformations used to generate equivalent atoms:

A3.5 CRYSTAL STRUCTURE ANALYSIS OF PRODUCT 205 (V25146)

Pinacol **205** was crystalized by layering pentane onto a saturated solution of **205** in diethyl ether at 23 °C to provide crystalline blocks suitable for X-ray analysis.

Compound V25146 (CCDC 2444208) crystallizes in the orthorhombic space group $P2_12_12_1$ with one molecule in the asymmetric unit. The coordinates for the hydrogen atoms bound to O1 and O2 were located in the difference Fourier synthesis and refined semi-freely with the help of a restraint on the O-H distance (0.84(4) Å). Absolute configuration was assigned via Flack (Flack = 0.08(5)) parameter.

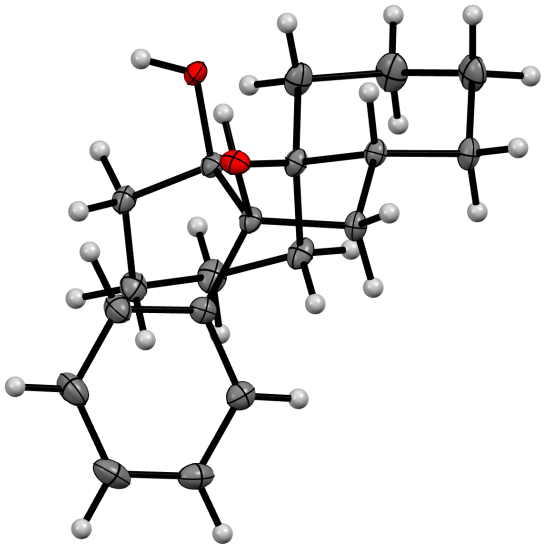

Figure A3.5.1 *X-Ray Coordinates of Compound* ***205*** *(V25146)*

Table A3.5.1 *Crystal data and structure refinement for V25146.*

Identification code	V25146	
Empirical formula	C19 H26 O2	
Formula weight	286.40	
Temperature	100(2) K	
Wavelength	1.54178 Å	
Crystal system	Orthorhombic	
Space group	$P2_12_12_1$	
Unit cell dimensions	a = 7.4117(6) Å	a= 90°.
	b = 8.4258(9) Å	b= 90°.
	c = 24.689(3) Å	g = 90°.
Volume	1541.8(3) $Å^3$	
Z	4	
Density (calculated)	1.234 Mg/m^3	
Absorption coefficient	0.605 mm^{-1}	
F(000)	624	
Crystal size	0.200 x 0.200 x 0.150 mm^3	
Theta range for data collection	3.580 to 74.555°.	
Index ranges	-9<=h<=9, -10<=k<=9, -30<=l<=30	
Reflections collected	24262	
Independent reflections	3148 [R(int) = 0.0479]	
Completeness to theta = 67.679°	100.0 %	
Absorption correction	Semi-empirical from equivalents	
Max. and min. transmission	0.7538 and 0.6822	
Refinement method	Full-matrix least-squares on F^2	
Data / restraints / parameters	3148 / 0 / 196	
Goodness-of-fit on F^2	1.065	
Final R indices [I>2sigma(I)]	R1 = 0.0280, wR2 = 0.0694	
R indices (all data)	R1 = 0.0287, wR2 = 0.0697	
Absolute structure parameter	0.08(5)	
Extinction coefficient	n/a	
Largest diff. peak and hole	0.174 and -0.205 $e.Å^{-3}$	

Table A3.5.2 *Atomic coordinates (x 10^4) and equivalent isotropic displacement parameters ($Å^2$x 10^3) for V25146. U(eq) is defined as one third of the trace of the orthogonalized U^{ij} tensor.*

	x	y	z	U(eq)
C(1)	4966(2)	6727(2)	5938(1)	13(1)
O(1)	3972(2)	7531(1)	5518(1)	15(1)
C(14)	4440(2)	4984(2)	5896(1)	14(1)
C(15)	4248(2)	4297(2)	5384(1)	19(1)
C(16)	3711(3)	2728(2)	5324(1)	25(1)
C(17)	3370(2)	1795(2)	5776(1)	25(1)
C(18)	3584(2)	2450(2)	6287(1)	22(1)
C(19)	4110(2)	4024(2)	6347(1)	17(1)
C(2)	7108(2)	7110(2)	5839(1)	13(1)
O(2)	7142(1)	8365(1)	5444(1)	15(1)
C(3)	8314(2)	5767(2)	5630(1)	16(1)
C(4)	8823(2)	4490(2)	6045(1)	19(1)
C(5)	9566(2)	5270(2)	6556(1)	20(1)
C(6)	8202(2)	6446(2)	6786(1)	17(1)
C(7)	7736(2)	7816(2)	6390(1)	14(1)
C(8)	9299(2)	9008(2)	6348(1)	20(1)
C(9)	9585(2)	9887(2)	6890(1)	26(1)
C(10)	7849(2)	10662(2)	7102(1)	24(1)
C(11)	6260(2)	9498(2)	7125(1)	17(1)
C(12)	6040(2)	8733(2)	6569(1)	14(1)
C(13)	4512(2)	7547(2)	6484(1)	14(1)

Table A3.5.3 *Bond lengths [Å] and angles [°] for V25146.*

C(1)-O(1)	1.4407(16)
C(1)-C(14)	1.5230(19)
C(1)-C(13)	1.5524(18)
C(1)-C(2)	1.638(2)
O(1)-H(1O)	0.79(2)
C(14)-C(19)	1.397(2)
C(14)-C(15)	1.398(2)
C(15)-C(16)	1.389(2)
C(15)-H(15)	0.9500
C(16)-C(17)	1.390(2)
C(16)-H(16)	0.9500
C(17)-C(18)	1.385(2)
C(17)-H(17)	0.9500
C(18)-C(19)	1.390(2)
C(18)-H(18)	0.9500
C(19)-H(19)	0.9500
C(2)-O(2)	1.4386(16)
C(2)-C(3)	1.5310(19)
C(2)-C(7)	1.5563(18)
O(2)-H(2O)	0.83(2)
C(3)-C(4)	1.5327(19)
C(3)-H(3A)	0.9900
C(3)-H(3B)	0.9900
C(4)-C(5)	1.526(2)
C(4)-H(4A)	0.9900
C(4)-H(4B)	0.9900
C(5)-C(6)	1.525(2)
C(5)-H(5A)	0.9900
C(5)-H(5B)	0.9900
C(6)-C(7)	1.5515(19)
C(6)-H(6A)	0.9900

C(6)-H(6B)	0.9900
C(7)-C(8)	1.536(2)
C(7)-C(12)	1.5399(19)
C(8)-C(9)	1.544(2)
C(8)-H(8A)	0.9900
C(8)-H(8B)	0.9900
C(9)-C(10)	1.536(2)
C(9)-H(9A)	0.9900
C(9)-H(9B)	0.9900
C(10)-C(11)	1.534(2)
C(10)-H(10A)	0.9900
C(10)-H(10B)	0.9900
C(11)-C(12)	1.5251(18)
C(11)-H(11A)	0.9900
C(11)-H(11B)	0.9900
C(12)-C(13)	1.525(2)
C(12)-H(12)	1.0000
C(13)-H(13A)	0.9900
C(13)-H(13B)	0.9900

O(1)-C(1)-C(14)	105.93(11)
O(1)-C(1)-C(13)	107.70(11)
C(14)-C(1)-C(13)	115.59(12)
O(1)-C(1)-C(2)	107.26(10)
C(14)-C(1)-C(2)	115.37(11)
C(13)-C(1)-C(2)	104.55(11)
C(1)-O(1)-H(1O)	105.5(15)
C(19)-C(14)-C(15)	117.56(13)
C(19)-C(14)-C(1)	123.36(13)
C(15)-C(14)-C(1)	119.07(13)
C(16)-C(15)-C(14)	121.37(14)
C(16)-C(15)-H(15)	119.3
C(14)-C(15)-H(15)	119.3
C(15)-C(16)-C(17)	120.28(15)

C(15)-C(16)-H(16)	119.9
C(17)-C(16)-H(16)	119.9
C(18)-C(17)-C(16)	119.07(14)
C(18)-C(17)-H(17)	120.5
C(16)-C(17)-H(17)	120.5
C(17)-C(18)-C(19)	120.59(15)
C(17)-C(18)-H(18)	119.7
C(19)-C(18)-H(18)	119.7
C(18)-C(19)-C(14)	121.12(14)
C(18)-C(19)-H(19)	119.4
C(14)-C(19)-H(19)	119.4
O(2)-C(2)-C(3)	107.76(11)
O(2)-C(2)-C(7)	107.79(11)
C(3)-C(2)-C(7)	113.73(12)
O(2)-C(2)-C(1)	105.19(10)
C(3)-C(2)-C(1)	118.05(12)
C(7)-C(2)-C(1)	103.64(10)
C(2)-O(2)-H(2O)	111.4(14)
C(2)-C(3)-C(4)	115.94(12)
C(2)-C(3)-H(3A)	108.3
C(4)-C(3)-H(3A)	108.3
C(2)-C(3)-H(3B)	108.3
C(4)-C(3)-H(3B)	108.3
H(3A)-C(3)-H(3B)	107.4
C(5)-C(4)-C(3)	109.78(12)
C(5)-C(4)-H(4A)	109.7
C(3)-C(4)-H(4A)	109.7
C(5)-C(4)-H(4B)	109.7
C(3)-C(4)-H(4B)	109.7
H(4A)-C(4)-H(4B)	108.2
C(6)-C(5)-C(4)	110.39(12)
C(6)-C(5)-H(5A)	109.6
C(4)-C(5)-H(5A)	109.6
C(6)-C(5)-H(5B)	109.6

C(4)-C(5)-H(5B)	109.6
H(5A)-C(5)-H(5B)	108.1
C(5)-C(6)-C(7)	113.36(12)
C(5)-C(6)-H(6A)	108.9
C(7)-C(6)-H(6A)	108.9
C(5)-C(6)-H(6B)	108.9
C(7)-C(6)-H(6B)	108.9
H(6A)-C(6)-H(6B)	107.7
C(8)-C(7)-C(12)	107.88(12)
C(8)-C(7)-C(6)	111.20(11)
C(12)-C(7)-C(6)	111.98(11)
C(8)-C(7)-C(2)	114.59(11)
C(12)-C(7)-C(2)	101.44(11)
C(6)-C(7)-C(2)	109.39(11)
C(7)-C(8)-C(9)	111.00(12)
C(7)-C(8)-H(8A)	109.4
C(9)-C(8)-H(8A)	109.4
C(7)-C(8)-H(8B)	109.4
C(9)-C(8)-H(8B)	109.4
H(8A)-C(8)-H(8B)	108.0
C(10)-C(9)-C(8)	112.63(13)
C(10)-C(9)-H(9A)	109.1
C(8)-C(9)-H(9A)	109.1
C(10)-C(9)-H(9B)	109.1
C(8)-C(9)-H(9B)	109.1
H(9A)-C(9)-H(9B)	107.8
C(11)-C(10)-C(9)	112.56(13)
C(11)-C(10)-H(10A)	109.1
C(9)-C(10)-H(10A)	109.1
C(11)-C(10)-H(10B)	109.1
C(9)-C(10)-H(10B)	109.1
H(10A)-C(10)-H(10B)	107.8
C(12)-C(11)-C(10)	108.62(12)
C(12)-C(11)-H(11A)	110.0

C(10)-C(11)-H(11A)	110.0
C(12)-C(11)-H(11B)	110.0
C(10)-C(11)-H(11B)	110.0
H(11A)-C(11)-H(11B)	108.3
C(11)-C(12)-C(13)	118.70(12)
C(11)-C(12)-C(7)	112.50(11)
C(13)-C(12)-C(7)	103.77(11)
C(11)-C(12)-H(12)	107.1
C(13)-C(12)-H(12)	107.1
C(7)-C(12)-H(12)	107.1
C(12)-C(13)-C(1)	104.50(11)
C(12)-C(13)-H(13A)	110.9
C(1)-C(13)-H(13A)	110.9
C(12)-C(13)-H(13B)	110.9
C(1)-C(13)-H(13B)	110.9
H(13A)-C(13)-H(13B)	108.9

Symmetry transformations used to generate equivalent atoms:

Table A3.5.4 *Anisotropic displacement parameters ($Å^2$x 10^3) for V25146. The anisotropic displacement factor exponent takes the form: $-2p^2[h^2 a^{*2}U^{11} + ... + 2 h k a^* b^* U^{12}]$*

	U^{11}	U^{22}	U^{33}	U^{23}	U^{13}	U^{12}
C(1)	13(1)	16(1)	10(1)	0(1)	-1(1)	2(1)
O(1)	17(1)	14(1)	15(1)	3(1)	-6(1)	0(1)
C(14)	11(1)	15(1)	16(1)	0(1)	-1(1)	1(1)
C(15)	24(1)	16(1)	18(1)	-1(1)	-3(1)	2(1)
C(16)	32(1)	17(1)	26(1)	-6(1)	-5(1)	1(1)

C(17)	24(1)	13(1)	39(1)	0(1)	-2(1)	-1(1)
C(18)	18(1)	19(1)	28(1)	8(1)	2(1)	1(1)
C(19)	14(1)	20(1)	18(1)	2(1)	0(1)	2(1)
C(2)	14(1)	15(1)	10(1)	1(1)	0(1)	1(1)
O(2)	19(1)	16(1)	10(1)	1(1)	4(1)	2(1)
C(3)	16(1)	19(1)	13(1)	0(1)	2(1)	3(1)
C(4)	19(1)	19(1)	19(1)	1(1)	1(1)	6(1)
C(5)	17(1)	25(1)	18(1)	2(1)	-2(1)	8(1)
C(6)	15(1)	24(1)	12(1)	2(1)	-2(1)	4(1)
C(7)	12(1)	19(1)	11(1)	0(1)	0(1)	1(1)
C(8)	14(1)	27(1)	18(1)	-4(1)	1(1)	-4(1)
C(9)	19(1)	35(1)	24(1)	-9(1)	-2(1)	-9(1)
C(10)	26(1)	27(1)	19(1)	-9(1)	-2(1)	-4(1)
C(11)	17(1)	22(1)	13(1)	-4(1)	0(1)	1(1)
C(12)	12(1)	17(1)	11(1)	-1(1)	-1(1)	1(1)
C(13)	12(1)	18(1)	12(1)	-3(1)	0(1)	1(1)

Table A3.5.5 *Hydrogen coordinates (x 10^4) and isotropic displacement parameters ($Å^2$x 10^3) for V25146.*

	x	y	z	U(eq)
H(1O)	4660(30)	8130(30)	5386(8)	18
H(15)	4490	4916	5071	23
H(16)	3576	2290	4971	30
H(17)	2995	723	5736	30
H(18)	3370	1817	6599	26
H(19)	4247	4454	6700	21
H(2O)	7670(30)	8090(20)	5164(8)	18

H(3A)	9440	6241	5487	19
H(3B)	7692	5246	5323	19
H(4A)	7746	3849	6136	23
H(4B)	9744	3773	5888	23
H(5A)	9834	4445	6830	24
H(5B)	10704	5831	6470	24
H(6A)	8692	6903	7125	21
H(6B)	7079	5869	6878	21
H(8A)	9033	9788	6059	24
H(8B)	10419	8439	6248	24
H(9A)	10038	9126	7163	31
H(9B)	10516	10717	6840	31
H(10A)	8072	11088	7470	28
H(10B)	7525	11564	6864	28
H(11A)	6493	8671	7401	21
H(11B)	5142	10068	7226	21
H(12)	5857	9612	6302	16
H(13A)	3333	8097	6464	17
H(13B)	4473	6763	6782	17

Table A3.5.6 *Torsion angles [°] for V25146.*

O(1)-C(1)-C(14)-C(19)	-138.81(14)
C(13)-C(1)-C(14)-C(19)	-19.65(19)
C(2)-C(1)-C(14)-C(19)	102.72(15)
O(1)-C(1)-C(14)-C(15)	40.32(17)
C(13)-C(1)-C(14)-C(15)	159.48(13)
C(2)-C(1)-C(14)-C(15)	-78.15(16)
C(19)-C(14)-C(15)-C(16)	1.4(2)
C(1)-C(14)-C(15)-C(16)	-177.79(14)
C(14)-C(15)-C(16)-C(17)	-0.7(3)

C(15)-C(16)-C(17)-C(18)	-0.4(3)
C(16)-C(17)-C(18)-C(19)	0.8(2)
C(17)-C(18)-C(19)-C(14)	-0.2(2)
C(15)-C(14)-C(19)-C(18)	-0.9(2)
C(1)-C(14)-C(19)-C(18)	178.20(13)
O(1)-C(1)-C(2)-O(2)	11.89(14)
C(14)-C(1)-C(2)-O(2)	129.62(11)
C(13)-C(1)-C(2)-O(2)	-102.29(12)
O(1)-C(1)-C(2)-C(3)	-108.30(13)
C(14)-C(1)-C(2)-C(3)	9.43(17)
C(13)-C(1)-C(2)-C(3)	137.53(12)
O(1)-C(1)-C(2)-C(7)	124.94(11)
C(14)-C(1)-C(2)-C(7)	-117.33(13)
C(13)-C(1)-C(2)-C(7)	10.76(13)
O(2)-C(2)-C(3)-C(4)	166.10(12)
C(7)-C(2)-C(3)-C(4)	46.68(17)
C(1)-C(2)-C(3)-C(4)	-75.06(16)
C(2)-C(3)-C(4)-C(5)	-50.84(17)
C(3)-C(4)-C(5)-C(6)	56.35(16)
C(4)-C(5)-C(6)-C(7)	-60.91(17)
C(5)-C(6)-C(7)-C(8)	-73.43(16)
C(5)-C(6)-C(7)-C(12)	165.79(12)
C(5)-C(6)-C(7)-C(2)	54.15(15)
O(2)-C(2)-C(7)-C(8)	-39.64(16)
C(3)-C(2)-C(7)-C(8)	79.77(16)
C(1)-C(2)-C(7)-C(8)	-150.80(11)
O(2)-C(2)-C(7)-C(12)	76.29(12)
C(3)-C(2)-C(7)-C(12)	-164.31(12)
C(1)-C(2)-C(7)-C(12)	-34.87(13)
O(2)-C(2)-C(7)-C(6)	-165.29(11)
C(3)-C(2)-C(7)-C(6)	-45.88(15)
C(1)-C(2)-C(7)-C(6)	83.55(13)
C(12)-C(7)-C(8)-C(9)	56.76(16)
C(6)-C(7)-C(8)-C(9)	-66.40(16)

C(2)-C(7)-C(8)-C(9)	168.90(13)
C(7)-C(8)-C(9)-C(10)	-53.29(19)
C(8)-C(9)-C(10)-C(11)	51.7(2)
C(9)-C(10)-C(11)-C(12)	-53.55(17)
C(10)-C(11)-C(12)-C(13)	-178.67(13)
C(10)-C(11)-C(12)-C(7)	59.97(16)
C(8)-C(7)-C(12)-C(11)	-62.00(15)
C(6)-C(7)-C(12)-C(11)	60.69(15)
C(2)-C(7)-C(12)-C(11)	177.24(11)
C(8)-C(7)-C(12)-C(13)	168.46(11)
C(6)-C(7)-C(12)-C(13)	-68.85(13)
C(2)-C(7)-C(12)-C(13)	47.70(13)
C(11)-C(12)-C(13)-C(1)	-166.74(12)
C(7)-C(12)-C(13)-C(1)	-41.06(13)
O(1)-C(1)-C(13)-C(12)	-95.90(13)
C(14)-C(1)-C(13)-C(12)	145.92(12)
C(2)-C(1)-C(13)-C(12)	17.96(13)

Symmetry transformations used to generate equivalent atoms:

Table A3.5.7 *Hydrogen bonds for V25146 [Å and °].*

D-H...A	d(D-H)	d(H...A)	d(D...A)	<(DHA)
O(1)-H(1O)...O(2)	0.79(2)	1.85(2)	2.4591(15)	132.6(19)
O(2)-H(2O)...O(1)#1	0.83(2)	2.01(2)	2.8384(14)	179(2)

Symmetry transformations used to generate equivalent atoms:
#1 x+1/2,-y+3/2,-z+1

Chapter 4 and Appendices 4–5 are under embargo.

APPENDIX 6

Notebook Cross-Reference for New Compounds

Table A6.1. *Notebook cross-reference for Chapter 2.*

Compound	Notebook Ref.
114a	AQC3-189
114b	AQC5-245
114c	KNF-2-145
114d	AQC4-33
114e	CS-I-153
114f	AQC4-274
114g	AQC3-213
114h	KNF-2-219
114i	RC-I-99
114j	AQC4-109
114k	AQC3-263
114l	AQC3-277
114m	RC-I-75
114n	KNF-3-033
114o	KNF-2-207
114p	AQC4-55
114q	AQC3-281
114r	AQC4-67
114s	KNF-1-287
114t	KNF-2-157
114u	ED-2-043
115a	AQC3-291
115b	AQC5-251
115c	KNF-2-151
115d	AQC4-35_p1
115f	AQC4-19_p1
115j	AQC4-117
115k	AQC3-265B_p4
115k'	AQC3-265B_p3
115k"	AQC3-265B_p1
115l	AQC3-287
115m	RC-I-181A
115m'	RC-I-181A
115n	KNF-3-043-B
115o	KNF-2-221A
115p	AQC4-61

Compound	Notebook Ref.
115o'	KNF-2-221B
115p'	AQC4-181_p2
115q	AQC3-275_p2
115r	AQC4-69_p1
115s	KNF-1-295
115t	KNF-2-161_A
115t'	KNF-2-161_B
115u	KNF-2-229_C
116	KNF-1-289
118	KNF-1-293
121	AQC3-137
123a	AQC3-229
123d	AQC4-35-p2
123e	CS-I-163
123f	AQC4-19_p2
123g	AQC4-21
123h	KNF-3-031
123i	RC-I-119A
123m	RC-1-181A
123r	AQC4-69-p2
123t	KNF-2-161-C
123u	KNF-2-229-D
133	AQC4-75
137	CS-I-225
138	CS-I-223
139	CS-I-183
140	CS-I-271
141	CS-I-257
142	RC-I-111
143	RC-I-129
144	CS-I-51
149	RC-II-35
150	RC-II-39
151	RC-II-41
152	KNF-3-177
153	RC-I-301

154	RC-II-67
155	RC-II-65
156	RC-II-77
157	CS-I-229
158	CS-I-279
159	AQC3-187
160	AQC3-201
161	AQC3-203
162	KNF-3-029
163	KNF-1-283
164	KNF-2-155
165	KNF-2-277
166	KNF-1-275-B
167	AQC3-129
168	CS-I-217
169	CS-I-215
170	CS-I-179
171	CS-I-267
172	CS-I-249
173	AQC4-159
174	AQC3-183
175	KNF-2-121
176	KNF-2-123
177	AQC3-117
178	KNF-2-155
179	KNF-1-279
180	KNF-2-147
181	ED-2-035
182	CS-I-207
183	CS-I-203
184	CS-I-175
185	CS-I-253
186	CS-I-237
187	KNF-2-283
188	RC-I-113
D-114f	AQC4-143

D-15f	AQC4-153_p1
D-123f	AQC4-153_p2
D-160	AQC4-139
D-174	AQC4-133

Table A6.2. *Notebook cross-reference for Chapter 3.*

Compound	Notebook Ref.
196a	CS-IV-23
196b	CS-IV-99
196c	SAN-I-17
196d	CS-IV-239
196e	CS-IV-109
196f	CS-V-67
196g	CS-IV-91
196h	SAN-I-27
196i	CS-IV-295
196j	CS-V-49
196k	CS-IV-53
197a	CS-IV-45
197b	CS-IV-105-A
197c	SAN-I-21
197d	CS-IV-243-A
197e	CS-IV-115-A
197f	CS-V-79-A
197g	CS-IV-97-A
197h (d1)	CS-IV-85-A-F.20
197h (d2)	CS-IV-85-A-F.10
197i (d1)	CS-IV-301-F.24
197i (d2)	CS-V-15-C-PTLC
197j	CS-V-53
197k	CS-IV-85-C
198	CS-IV-297
199	CS-IV-57-F.32
200a	CS-IV-195
200b	CS-IV-223
201a	CS-IV-203-A-PTLC-a
201b	CS-IV-233-A-PTLC-a
202	CS-V-27
203	CS-V-33
204	CS-V-47

Compound	Notebook Ref.
205	CS-V-51
206	CS-V-21
207	CS-V-81
208	CS-V-41
215a	CS-IV-293
215b	CS-IV-139
215c	CS-IV-241
215d	CS-IV-127
216a	CS-IV-299-F.34
216b	CS-IV-143-A
216c	CS-IV-245-A
216d	CS-IV-143-D
217a	CS-IV-19
217b	SAN-I-15
217c	SAN-I-33
217d	CS-IV-83
217e	SAN-I-25
217f	CS-V-45
217g	CS-IV-49
217h	CS-IV-135
217i	CS-IV-189
217j	CS-IV-211
218	CS-IV-285

Table A6.3. *Notebook cross-reference for Chapter 4.*

Compound	Notebook Ref.
269	CSS-5-063
271	CSS-3-281
272	KJG-5-083
273	KJG-5-085 (Duff route)
274	KJG-5-095
275	CSS-4-173
267	CSS-4-231
277	CSS-4-141
278	CSS-4-149
273	CSS-5-265 (*ortho*-aldol route)
279	KJG-8-225
280	KJG-7-237
281	KJG-7-241
266	KJG-7-243
282	KJG-10-171
283	KJG-9-237
284	CSS-5-127
295	KJG-9-243
295a	KJG-10-031
290	KJG-9-253
298	KJG-9-279
299	KJG-9-281
300	KJG-9-283
301	KJG-10-067
305	KJG-11-059

ABOUT THE AUTHOR

Christian Santiago Strong was born in San Antonio, Texas on November 14th, 1998, to Isabel and John Strong. After spending ages 1–15 north of Dallas, his family moved south to the Rio Grande Valley to take care of his octogenarian grandparents. There he attended the Science Academy of South Texas, where he developed a strong interest in chemistry which was further bolstered by a summer internship at the University of Texas, Rio Grande Valley (UTRGV) in the synthetic chemistry lab of Prof. Shizue Mito.

In the fall of 2017, Christian began attending the University of Texas at San Antonio (UTSA) as a chemical engineer. During his sophomore year, he was fortunate to take organic chemistry with Prof. Doug Frantz who inspired Christian to consider pursuing a career in synthetic chemistry. In the Frantz lab, he studied the preparation of acidic derivatives of dibenzylideneacetone and their application in Pd catalysis. Christian graduated from UTSA in 2021 with a B.S. degree in Chemical Engineering.

Upon completion of his undergraduate studies, Christian moved to Pasadena to pursue graduate research at the California Institute of Technology under the advisory of Prof. Brian Stoltz. His research has centered around the development of enantioselective reactions of Pd enolates and progress toward the synthesis of mitomycin B. In the summer 2025, Christian participated in the Manabiya Exchange at Hokkaido University in the lab of Prof. Hajime Ito where he was mentored by Prof. Koji Kubota on the mechanochemical activation of small molecules. Upon completion of his Ph.D., Christian will pursue his interest in the chemistry of the p-block as a postdoctoral fellow in the lab of Prof. Alexander Radosevich at MIT.